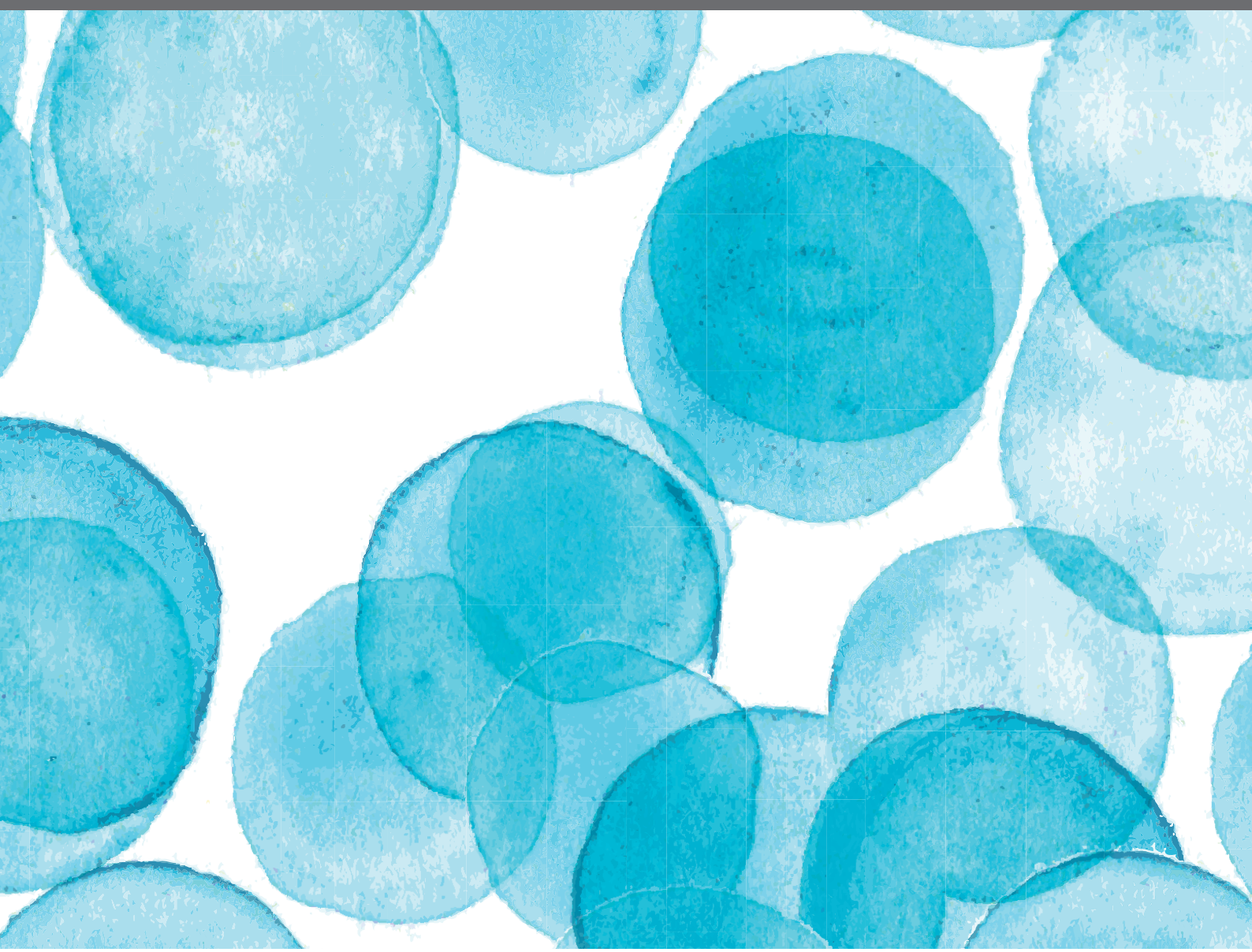
FUNGAL SYSTEMATICS AND BIOGEOGRAPHY

EDITED BY: Dhanushka Nadeeshan Wanasinghe,
Jadson Diogo Pereira Bezerra and Peter Edward Mortimer

PUBLISHED IN: Frontiers in Microbiology



frontiers Research Topics

Frontiers eBook Copyright Statement

The copyright in the text of individual articles in this eBook is the property of their respective authors or their respective institutions or funders. The copyright in graphics and images within each article may be subject to copyright of other parties. In both cases this is subject to a license granted to Frontiers.

The compilation of articles constituting this eBook is the property of Frontiers.

Each article within this eBook, and the eBook itself, are published under the most recent version of the Creative Commons CC-BY licence. The version current at the date of publication of this eBook is CC-BY 4.0. If the CC-BY licence is updated, the licence granted by Frontiers is automatically updated to the new version.

When exercising any right under the CC-BY licence, Frontiers must be attributed as the original publisher of the article or eBook, as applicable.

Authors have the responsibility of ensuring that any graphics or other materials which are the property of others may be included in the CC-BY licence, but this should be checked before relying on the CC-BY licence to reproduce those materials. Any copyright notices relating to those materials must be complied with.

Copyright and source acknowledgement notices may not be removed and must be displayed in any copy, derivative work or partial copy which includes the elements in question.

All copyright, and all rights therein, are protected by national and international copyright laws. The above represents a summary only. For further information please read Frontiers' Conditions for Website Use and Copyright Statement, and the applicable CC-BY licence.

ISSN 1664-8714
ISBN 978-2-88974-502-9
DOI 10.3389/978-2-88974-502-9

About Frontiers

Frontiers is more than just an open-access publisher of scholarly articles: it is a pioneering approach to the world of academia, radically improving the way scholarly research is managed. The grand vision of Frontiers is a world where all people have an equal opportunity to seek, share and generate knowledge. Frontiers provides immediate and permanent online open access to all its publications, but this alone is not enough to realize our grand goals.

Frontiers Journal Series

The Frontiers Journal Series is a multi-tier and interdisciplinary set of open-access, online journals, promising a paradigm shift from the current review, selection and dissemination processes in academic publishing. All Frontiers journals are driven by researchers for researchers; therefore, they constitute a service to the scholarly community. At the same time, the Frontiers Journal Series operates on a revolutionary invention, the tiered publishing system, initially addressing specific communities of scholars, and gradually climbing up to broader public understanding, thus serving the interests of the lay society, too.

Dedication to Quality

Each Frontiers article is a landmark of the highest quality, thanks to genuinely collaborative interactions between authors and review editors, who include some of the world's best academicians. Research must be certified by peers before entering a stream of knowledge that may eventually reach the public - and shape society; therefore, Frontiers only applies the most rigorous and unbiased reviews.
Frontiers revolutionizes research publishing by freely delivering the most outstanding research, evaluated with no bias from both the academic and social point of view. By applying the most advanced information technologies, Frontiers is catapulting scholarly publishing into a new generation.

What are Frontiers Research Topics?

Frontiers Research Topics are very popular trademarks of the Frontiers Journals Series: they are collections of at least ten articles, all centered on a particular subject. With their unique mix of varied contributions from Original Research to Review Articles, Frontiers Research Topics unify the most influential researchers, the latest key findings and historical advances in a hot research area! Find out more on how to host your own Frontiers Research Topic or contribute to one as an author by contacting the Frontiers Editorial Office: frontiersin.org/about/contact

FUNGAL SYSTEMATICS AND BIOGEOGRAPHY

Topic Editors:
Dhanushka Nadeeshan Wanasinghe, Key Laboratory for Plant Diversity and Biogeography of East Asia, Kunming Institute of Botany, Chinese Academy of Sciences, China
Jadson Diogo Pereira Bezerra, Universidade Federal de Goiás, Brazil
Peter Edward Mortimer, Kunming Institute of Botany, Chinese Academy of Sciences (CAS), China

Citation: Wanasinghe, D. N., Bezerra, J. D. P., Mortimer, P. E., eds. (2022). Fungal Systematics and Biogeography. Lausanne: Frontiers Media SA.
doi: 10.3389/978-2-88974-502-9

Table of Contents

06 ***Editorial: Fungal Systematics and Biogeography***
Dhanushka N. Wanasinghe, Peter E. Mortimer and Jadson D. P. Bezerra

10 ***Soil Fungal Community Composition, Not Assembly Process, Was Altered by Nitrogen Addition and Precipitation Changes at an Alpine Steppe***
Yuanming Xiao, Changbin Li, Yang Yang, Yunfeng Peng, Yuanhe Yang and Guoying Zhou

22 ***The Enigmatic Thelebolaceae (Thelebolales, Leotiomycetes): One New Genus* Solomyces *and Five New Species***
Zhiyuan Zhang, Chunbo Dong, Wanhao Chen, Quanrong Mou, Xiaoxiao Lu, Yanfeng Han, Jianzhong Huang and Zongqi Liang

37 ***Diversity and Geographic Distribution of Ligninolytic Fungi Associated With* Castanopsis sieboldii *Leaf Litter in Japan***
Takashi Osono, Shunsuke Matsuoka and Dai Hirose

46 ***Crop-Zone Weed Mycobiomes of the South-Western Australian Grain Belt***
Pippa J. Michael, Darcy Jones, Nicole White, James K. Hane, Michael Bunce and Mark Gibberd

54 ***Species Diversity With Comprehensive Annotations of Wood-Inhabiting Poroid and Corticioid Fungi in Uzbekistan***
Yusufjon Gafforov, Alexander Ordynets, Ewald Langer, Manzura Yarasheva, Adriana de Mello Gugliotta, Dmitry Schigel, Lorenzo Pecoraro, Yu Zhou, Lei Cai and Li-Wei Zhou

89 ***Bambusicolous* Arthrinium *Species in Guangdong Province, China***
Indunil C. Senanayake, Jayarama D. Bhat, Ratchadawan Cheewangkoon and Ning Xie

105 ***An Updated Global Species Diversity and Phylogeny in the Forest Pathogenic Genus* Heterobasidion *(Basidiomycota, Russulales)***
Yuan Yuan, Jia-Jia Chen, Kari Korhonen, Francis Martin and Yu-Cheng Dai

120 ***Three Novel Entomopathogenic Fungi From China and Thailand***
De-Ping Wei, Dhanushka N. Wanasinghe, Jian-Chu Xu, Chaiwat To-anun, Peter E. Mortimer, Kevin D. Hyde, Abdallah M. Elgorban, Sumedha Madawala, Nakarin Suwannarach, Samantha C. Karunarathna, Saowaluck Tibpromma and Saisamorn Lumyong

136 ***Species Diversity and Molecular Phylogeny of* Cyanosporus *(Polyporales, Basidiomycota)***
Shun Liu, Lu-Lu Shen, Yan Wang, Tai-Min Xu, Genevieve Gates and Bao-Kai Cui

159 ***Global Phylogeny and Taxonomy of the Wood-Decaying Fungal Genus* Phlebiopsis *(Polyporales, Basidiomycota)***
Ya-Nan Zhao, Shuang-Hui He, Karen K. Nakasone, K. L. Wasantha Kumara, Che-Chih Chen, Shi-Liang Liu, Hai-Xia Ma and Man-Rong Huang

179 ***Parametarhizium* (Clavicipitaceae) *gen. nov. With Two New Species as a Potential Biocontrol Agent Isolated From Forest Litters in Northeast China***
Siyu Gao, Wei Meng, Lixiang Zhang, Qun Yue, Xu Zheng and Lijian Xu

191 **Inonotus rickii** ***(Agaricomycetes, Hymenochaetaceae) in Brazilian Cerrado: Expanding Its Geographic Distribution and Host List***
Lucas Leonardo-Silva, Ahmed M. Abdel-Azeem and Solange Xavier-Santos

205 ***Fungal Diversity and Community Assembly of Ectomycorrhizal Fungi Associated With Five Pine Species in Inner Mongolia, China***
Yong-Long Wang, Xuan Zhang, Ying Xu, Busayo Joshua Babalola, Si-Min Xiang, Yan-Ling Zhao and Yong-Jun Fan

219 ***The Phylogenetic Relationship Revealed Three New Wood-Inhabiting Fungal Species From Genus*** **Trechispora**
Wei Zhao and Chang-Lin Zhao

230 ***Seed Banks as Incidental Fungi Banks: Fungal Endophyte Diversity in Stored Seeds of Banana Wild Relatives***
Rowena Hill, Theo Llewellyn, Elizabeth Downes, Joseph Oddy, Catriona MacIntosh, Simon Kallow, Bart Panis, John B. Dickie and Ester Gaya

250 ***Morpho-Phylo Taxonomy of Novel Dothideomycetous Fungi Associated With Dead Woody Twigs in Yunnan Province, China***
Peter E. Mortimer, Rajesh Jeewon, Jian-Chu Xu, Saisamorn Lumyong and Dhanushka N. Wanasinghe

268 ***Taxonomy and Phylogeny of the*** **Fomitopsis pinicola** ***Complex With Descriptions of Six New Species From East Asia***
Shun Liu, Mei-Ling Han, Tai-Min Xu, Yan Wang, Dong-Mei Wu and Bao-Kai Cui

287 ***Additions to the Genus*** **Arthrinium** ***(Apiosporaceae) From Bamboos in China***
Yao Feng, Jian-Kui (Jack) Liu, Chuan-Gen Lin, Ya-Ya Chen, Mei-Mei Xiang and Zuo-Yi Liu

310 ***An Unexpectedly High Number of New*** **Sutorius** ***(Boletaceae) Species From Northern and Northeastern Thailand***
Santhiti Vadthanarat, Roy E. Halling, Mario Amalfi, Saisamorn Lumyong and Olivier Raspé

337 ***New Glomeromycotan Taxa,*** **Dominikia glomerocarpica** ***sp. nov. and*** **Epigeocarpum crypticum** ***gen. nov. et sp. nov. From Brazil, and*** **Silvaspora** ***gen. nov. From New Caledonia***
Janusz Błaszkowski, Khadija Jobim, Piotr Niezgoda, Edward Meller, Ryszard Malinowski, Paweł Milczarski, Szymon Zubek, Franco Magurno, Leonardo Casieri, Wojciech Bierza, Tomasz Błaszkowski, Thomas Crossay and Bruno Tomio Goto

358 ***Biogeography and Ecology of Magnaporthales: A Case Study***
Jia-Wei Feng, Wei-Ting Liu, Jia-Jie Chen and Chu-Long Zhang

368 ***Reappraisal of*** **Immotthia** ***in Dictyosporiaceae, Pleosporales: Introducing*** **Immotthia bambusae** ***sp. nov. and*** **Pseudocyclothyriella clematidis** ***comb. et gen. nov. Based on Morphology and Phylogeny***
Hong-Bo Jiang, Rajesh Jeewon, Samantha C. Karunarathna, Chayanard Phukhamsakda, Mingkwan Doilom, Pattana Kakumyan, Nakarin Suwannarach, Rungtiwa Phookamsak and Saisamorn Lumyong

385 ***The Plant Family Asteraceae Is a Cache for Novel Fungal Diversity: Novel Species and Genera With Remarkable Ascospores in Leptosphaeriaceae***
Mingkwan Doilom, Kevin D. Hyde, Wei Dong, Chun-Fang Liao, Nakarin Suwannarach and Saisamorn Lumyong

400 ***Multigene Phylogeny and Morphology Reveal Three Novel Species and a Novel Record of* Agaricus *From Northern Thailand***
Chanyawat Jaichaliaw, Jaturong Kumla, Santhiti Vadthanarat, Nakarin Suwannarach and Saisamorn Lumyong

414 ***Genomic Analysis of* Sarcomyxa edulis *Reveals the Basis of Its Medicinal Properties and Evolutionary Relationships***
Fenghua Tian, Changtian Li and Yu Li

426 ***An Overview of 24 Years of Molecular Phylogenetic Studies in* Phallales (Basidiomycota) *With Notes on Systematics, Geographic Distribution, Lifestyle, and Edibility***
Gislaine C. S. Melanda, Alexandre G. S. Silva-Filho, Alexandre Rafael Lenz, Nelson Menolli Jr., Alexandro de Andrade de Lima, Renato Juciano Ferreira, Nathalia Mendonça de Assis, Tiara S. Cabral, María P. Martín and Iuri Goulart Baseia

frontiers in Microbiology

EDITORIAL
published: 25 January 2022
doi: 10.3389/fmicb.2021.827725

Editorial: Fungal Systematics and Biogeography

Dhanushka N. Wanasinghe[1,2]*, *Peter E. Mortimer*[1,2]* and *Jadson D. P. Bezerra*[3]

[1] Center for Mountain Futures, Kunming Institute of Botany, Chinese Academy of Sciences, Kunming, China, [2] Department of Economic Plants and Biotechnology, Yunnan Key Laboratory for Wild Plant Resources, Kunming Institute of Botany, Chinese Academy of Sciences, Kunming, China, [3] Setor de Micologia, Departamento de Biociências e Tecnologia, Instituto de Patologia Tropical e Saúde Pública (IPTSP), Universidade Federal de Goiás (UFG), Goiânia, Brazil

Keywords: taxonomic diversity, biogeographic distributions, molecular phylogeny, ecological roles, host-specificity

Editorial on the Research Topic

Fungal Systematics and Biogeography

According to best estimates, it is predicted that ∼2.2–3.8 million or more fungal species exist on Earth (Hawksworth and Lücking, 2017). Nevertheless, we know of only 146,000 (Bánki et al., 2021), suggesting that 96% of fungal species remain unknown. Owing to their abundance across all ecosystems, fungal taxa simply cannot be overlooked in any region (Wanasinghe et al., 2020). Most species of plant-associated fungi can be pathogens, endophytes, saprobes or epiphytes across a wide range of hosts in terrestrial as well as aquatic habitats (Põlme et al., 2020). Given the ubiquitous nature of fungi, additional taxonomic and ecological knowledge are prerequisites to understanding fungal biology and their environmental significance.

Fungi are experiencing considerable conversion pressures due to a variety of devastating activities, including the intensification of land use alongside growing human populations, environmental exploitation and pollution, invasive species and climate change challenges. Recent studies have shown that fungi are likely to be sensitive to environmental changes and global warming (Tedersoo et al., 2014; Casadevall et al., 2019; Nnadi and Carter, 2021). This may be triggering the extinction of a large number of species that cannot adapt fast enough to the rate of environmental change, imbuing the research community with a sense of urgency that future opportunities for study may not exist. If we are willing to confront these challenges and work to mitigate species loss, then a robust, updated fungal classification that enables clear taxonomic communication using extensive fungal sampling across different geographic regions will be needed (Hyde et al., 2020).

Past studies have shown that certain fungi form close relationships with plants through mutualistic or antagonistic interactions (van der Heijden et al., 2008). Based on these plant-fungi interactions, it is clear that fungi play a key role in shaping plant community compositions and distribution patterns along natural gradients. Numerous studies have attempted to document the biogeography of fungi at granular and regional scales. The findings of these studies indicate a high diversity of fungi in tropical regions, specifically in tropical forests, with a decline in diversity toward the northern latitudes (Tedersoo et al., 2014). Additional studies in fungal biogeography, adopting either regional or fine scale approaches as well as studies focusing on specific fungal groups, will further enrich our knowledge of the distribution of fungi. In support of this endeavor, we propose the Research Topic "*Fungal Systematics and Biogeography*" for both Reviews and Original Research manuscripts. In this Research Topic, we accepted 26 articles from authors on five continents with emphasis on Asian countries, based on taxonomic diversity, molecular phylogeny,

OPEN ACCESS

Edited by:
Martin G. Klotz, Washington State University, United States

Reviewed by:
Gustavo Henrique Goldman, University of São Paulo, Brazil

***Correspondence:**
Dhanushka N. Wanasinghe
dnadeeshan@gmail.com
Peter E. Mortimer
peter@mail.kib.ac.cn

Specialty section:
This article was submitted to Fungi and Their Interactions, a section of the journal Frontiers in Microbiology

Received: *02 December 2021*
Accepted: *31 December 2021*
Published: *25 January 2022*

Citation:
Wanasinghe DN, Mortimer PE and Bezerra JDP (2022) Editorial: Fungal Systematics and Biogeography. Front. Microbiol. 12:827725. doi: 10.3389/fmicb.2021.827725

ecological roles, biogeographic distributions, host-specificity and co-evolutionary relationships of fungi.

Micro fungi are less studied when compared to macro fungi, especially in poorly sampled regions like Yunnan Province, China. Mortimer et al. collected and investigated several micro-fungi in Yunnan province from dead woody twigs based on morpho-molecular approaches. The study of Mortimer et al. resulted in one new genus and four new species within Dothideomycetes (Ascomycota). Jiang et al. investigated bambusicolous fungi in southwest China and Thailand. *Immotthia* was for the first time established within Dictyosporiaceae (Dothideomycetes, Ascomycota) based on morphological and phylogenetic analyses, with a new *Immotthia* species. In addition, a new monotypic genus *Pseudocyclothyriella* was established to accommodate *Pseudocyclothyriella clematidis*, which is the latest synonym of *Pseudocoleophoma clematidis*. Both genera were investigated by detailed morphological characterizations of type materials and multi-gene phylogenetic analyses. Doilom et al. collected and recorded several Leptosphaeriaceae (Dothideomycetes, Ascomycota) species from Asteraceae in China. A new genus *Praeclarispora* and a new species *Sphaerellopsis artemisiae* sp. nov. were introduced within Leptosphaeriaceae based on ascospores morphology and multi-locus phylogenetic analysis. Studying species in Thelebolaceae (Leotiomycetes, Acomycota) is important because they can produce antifreeze proteins, ice-binding proteins and other secondary metabolites that are valuable for biotechnological exploitation. During an extensive diversity survey of microfungi in China, Zhang et al. introduced one new genus (Solomyces) and five new species belonging to the order Thelebolales.

Arthrinium (Sordariomycetes, Ascomycota) is a cosmopolitan genus characterized by basauxic conidiogenesis and apiospores on its asexual and sexual morphs, respectively. Senanayake et al. collected *Arthrinium*-like taxa from bamboo plants in Guangdong Province, China. Based on morphological characteristics and phylogenetic data, they introduced two new species and reported two new locality records of *Arthrinium*. Feng Y. et al. introduced four new species and seven existing species of *Arthrinium* obtained from 17 isolates from China. Among the known species, three sexual morphs and one asexual morph were recorded for the first time. All species were subjected to detailed morphological and phylogenetic analyses. Entomopathogenic fungi are ubiquitous in tropical rainforests and feature a high level of diversity. Wei et al. collected entomopathogenic fungi from forests in the Greater Mekong Subregion and introduced three new species to *Paraisaria* (Sordariomycetes, Ascomycota). Gao et al. identified and described a novel genus, *Parametarhizium* (Sordariomycetes, Ascomycota) with two new entomopathogenic species based on morphology and a multi-gene phylogenetic reconstruction. In addition, their potential as biocontrol agents was evaluated by applying a spore-based anti-insect assay against *Monolepta hieroglyphica* (Coleoptera). Magnaporthales (Sordariomycetes, Ascomycota) members can be pathogenic, saprobic or endophytic, mainly on monocotyledonous herbaceous plants. Their biogeography has received less attention. Feng J.-W. et al. described the biodiversity of endophytic Magnaporthales fungi from Poaceae across three latitudes in China and conducted a meta-analysis of the geography and ecology of Magnaporthales worldwide.

Wood-inhabiting fungi play an important role in wood degradation and nutrient recycling. During a survey of wood-inhabiting fungi in southern China, Zhao and Zhao introduced three species of *Trechispora* (Bartheletiomycetes, Basidiomycota) from rotten wood. Wood-inhabiting poroid and corticioid species are ecologically and economically important as decomposers, pathogens, and sources of food and medicines. Gafforov et al. provided the first comprehensive, thoroughly annotated checklist of species diversity of wood-inhabiting poroid and corticioid fungi in Uzbekistan. They compiled 790 fungal records collected from 1950 to 2020. Fungi play central roles in the decomposition of lignin and other recalcitrant compounds. Osono et al. investigated the diversity and geographic pattern of ligninolytic fungi on *Castanopsis sieboldii* (Fagaceae) in Japan. They showed that the ligninolytic activity of fungi on leaf litter was greater at sites with higher mean annual temperature and precipitation where the latitudes and longitudes are lower. Osono et al. suggest that not only the geographic location and climatic conditions but also the biogeographic patterns of distribution of ligninolytic fungi influence the decomposition of lignin in leaf litter.

Agaricus (Agaricomycetes, Basidiomycota) is a saprophytic mushroom genus with worldwide distribution and is commonly found in grasslands and forests. Jaichaliaw et al. conducted a survey of *Agaricus* species in northern Thailand and described three new species based on morphology coupled with multigene analyses of combined ITS, LSU and TEF sequences. Additionally, this study acts as a mini-review of *Agaricus* species in Thailand. *Sarcomyxa edulis* (Agaricomycetes, Basidiomycota) is an important edible and medicinal mushroom endemic to Northeastern China; however molecular-level information from the genome was lacking. Therefore, Tian et al. provided the *de novo* sequencing and assembly of the *Sarcomyxa edulis* genome using single-molecule real-time sequencing technology. *Sutorius* (Agaricomycetes, Basidiomycota) is a poroid genus that typically has chocolate brown to reddish brown or purplish brown basidiomata. Vadthanarat et al. conducted a survey on the diversity of boletes in Northern and Northeastern Thailand and accounted seven new species in *Sutorius*. *Inonotus rickii* (Agaricomycetes, Basidiomycota) is an important fungus that causes canker and white rot of various ornamental and wild trees in tropical and subtropical regions. Leonardo-Silva et al. broadly studied this fungus in the Cerrado biome of Brazilian Savanna and expanded the knowledge on its geographical distribution as well as its structural, physiological characteristics and associated hosts.

Heterobasidion (Bartheletiomycetes, Basidiomycota) species are among the most intensively studied polypores due to their economic significance as pathogens in coniferous forests of Europe and North America. Yuan et al. carried out both morphological and multi-gene phylogenetic analyses on *Heterobasidion* samples from Asia, Oceania, Europe and North America. Yuan et al. introduced three new species in *Heterobasidion* from Asia. *Cyanosporus* (Bartheletiomycetes, Basidiomycota) is a cosmopolitan brown-rot fungal genus,

recognizable by blue-tinted basidiocarps. Species in this genus were usually treated as belonging to the *Postia caesia* complex. In Liu, Shen et al. the phylogenetic analysis of *Cyanosporus* was carried out based on a combined ITS, LSU, SSU, mtSSU, RPB1, RPB2 and TEF dataset. Combining morphological characters and molecular evidence, Liu, Han et al. introduced five new species and fifteen new combinations in *Cyanosporus*. *Fomitopsis pinicola*-species complex (Bartheletiomycetes, Basidiomycota) has been intensively studied because of its economic importance in having anti-tumor, antifungal, antioxidant, immunomodulation and neuroprotective activities. Based on morphological characters and phylogenetic analysis of ITS, RPB2 and TEF genes, Liu, Han et al. introduced six new species in the *Fomitopsis pinicola*-complex. Phallales (Bartheletiomycetes, Basidiomycota) is represented by gasteroid fungi with expanded and sequestrate basidiomata that are commonly known as stinkhorns and false truffles. Melanda et al. provided an overview of Phallales diversity represented by selected DNA markers available in public databases. They also mapped the global geographic distribution of Phallales with available literature. Zhao et al. conducted an in-depth study of the phylogeny and taxonomy of the corticioid genus *Phlebiopsis* (Bartheletiomycetes, Basidiomycota). Zhao et al. demonstrated that *Phlebiopsis* is a strongly supported genus in Phanerochaetaceae, and two genera viz. *Australohydnum* and *Hjortstamia* were synonymized under *Phlebiopsis*. They proposed six new species and five new combinations in *Phlebiopsis*.

Błaszkowski et al. collected and examined new epigeous and semihypogeous glomerocarp-producing species belonging to Glomeromycota from Atlantic rain forest ecosystems of Northeast Brazil and New Caledonia. Błaszkowski et al. established two new genera namely *Epigeocarpum* and *Silvaspora*, and a new species within Glomeraceae (Glomeromycetes) based on evidence from morpho-molecular characterizations. Ectomycorrhizal (EM) fungal diversity, community composition and underlying assembly processes in Inner Mongolia, China (semiarid and cold-temperate) are critically neglected. Wang et al. extensively investigated the EM fungal community associated with pine species in the semiarid and cold temperate forests and showed that there is high diversity and distinctive community composition of EM fungi associated with natural pine species in Inner Mongolia.

On the Qinghai-Tibetan Plateau (QTP), the responses of soil microbial communities to chemical and biophysical changes are poorly studied. Xiao et al. explored the responses of soil fungal community composition, diversity, and community assembly processes to nitrogen addition and precipitation changes at an alpine steppe on the northeastern QTP. Xiao et al. showed that soil fungal community composition and diversity were altered significantly by nitrogen addition and precipitation change. The study suggested that soil fungal communities located on the alpine steppes of the QTP may significantly change under long-term global change scenarios in the future. Michael et al. identified the plant pathogens present in the phyllosphere of common weed species associated with cropping fields in Western Australia. This information on weed host-specific or region-specific association with pathogen species may become an increasingly important factor in developing new methods for crop disease management in the future. Seed banks are an important resource for biodiversity research, as they provide curated specimens spanning time and space. Hill et al. used both culture-dependent and culture-independent approaches to assess the diversity of endophytes in stored banana CWR (crop wild relatives) seeds and demonstrated that seed banks provide huge potential for research into fungal endophyte communities.

AUTHOR CONTRIBUTIONS

DW, PM, and JB drafted the editorial and contributed to editorial revision. All authors contributed to the article and approved the submitted version.

FUNDING

PM thanks the High-End Foreign Experts in the High-Level Talent 318 Recruitment Plan of Yunnan Province, 2021. DW would like to thank the CAS President's International Fellowship Initiative (No. 2021FYB0005), the National Science Foundation of China (NSFC) under the project code (32150410362), and the Postdoctoral Fund from Human Resources and Social Security Bureau of Yunnan Province.

ACKNOWLEDGMENTS

Austin G. Smith at World Agroforestry (ICRAF), Kunming Institute of Botany, China, is thanked for English editing.

REFERENCES

Bánki, O., Roskov, Y., Vandepitte, L., DeWalt, R. E., Remsen, D., Schalk, P., et al. (2021). *Catalogue of Life Checklist*. Catalogue of Life. doi: 10.48580/d4t2

Casadevall, A., Kontoyiannis, D. P., and Robert, V. (2019). On the emergence of *Candida auris*: climate change, azoles, swamps, and birds. *mBio* 10:e01397–19. doi: 10.1128/mBio.01397-19

Hawksworth, D. L., and Lücking, R. (2017). Fungal diversity revisited: 2.2 to 3.8 million species. *Microbiol. Spectr.* 5, FUNK-0052-2016. doi: 10.1128/microbiolspec.FUNK-0052-2016

Hyde, K. D., Jeewon, R., Chen, Y. J., Bhunjun, C. S., Calabon, M. S., Jiang H. B., et al. (2020). The numbers of fungi: is the descriptive curve flattening? *Fungal Divers.* 103, 219–271. doi: 10.1007/s13225-020-00458-2

Nnadi, N. E., and Carter, D. A. (2021). Climate change and the emergence of fungal pathogens. *PLoS Pathog.* 17:e1009503. doi: 10.1371/journal.ppat.1009503

Põlme, S., Abarenkov, K., Henrik Nilsson, R., Lindahl, B. D., Clemmensen, K. E., Kauserud, H., et al. (2020). FungalTraits: a user-friendly traits database of fungi and fungus-like stramenopiles. *Fungal Divers.* 105, 1–16. doi: 10.1007/s13225-020-00466-2

Tedersoo, L., Bahram, M., Põlme, S., Kõljalg, U., Yorou, N. S., Wijesundera, R., et al. (2014). Global diversity and geography

of soil fungi. *Science* 346, 1–10. doi: 10.1126/science.1256688

van der Heijden, M. G. A., Bardgett, R. D., and van Straalen, N. M. (2008). The unseen majority: soil microbes as drivers of plant diversity and productivity in terrestrial ecosystems. *Ecol. Lett.* 11, 296–310. doi: 10.1111/j.1461-0248.2007.01139.x

Wanasinghe, D. N., Wijayawardene, N. N., Xu, J., Cheewangkoon, R., and Mortimer, P. E. (2020). Taxonomic novelties in *Magnolia*-associated pleosporalean fungi in the Kunming Botanical Gardens (Yunnan, China). *PLoS One* 15:e0235855. doi: 10.1371/journal.pone.0235855

Conflict of Interest: The authors declare that the research was conducted in the absence of any commercial or financial relationships that could be construed as a potential conflict of interest.

Publisher's Note: All claims expressed in this article are solely those of the authors and do not necessarily represent those of their affiliated organizations, or those of the publisher, the editors and the reviewers. Any product that may be evaluated in this article, or claim that may be made by its manufacturer, is not guaranteed or endorsed by the publisher.

Copyright © 2022 Wanasinghe, Mortimer and Bezerra. This is an open-access article distributed under the terms of the Creative Commons Attribution License (CC BY). The use, distribution or reproduction in other forums is permitted, provided the original author(s) and the copyright owner(s) are credited and that the original publication in this journal is cited, in accordance with accepted academic practice. No use, distribution or reproduction is permitted which does not comply with these terms.

frontiers in Microbiology

ORIGINAL RESEARCH
published: 16 October 2020
doi: 10.3389/fmicb.2020.579072

Soil Fungal Community Composition, Not Assembly Process, Was Altered by Nitrogen Addition and Precipitation Changes at an Alpine Steppe

*Yuanming Xiao[1,2], Changbin Li[1,2], Yang Yang[1,2], Yunfeng Peng[3], Yuanhe Yang[3] and Guoying Zhou[1,4,5]**

[1] Northwest Institute of Plateau Biology, Chinese Academy of Sciences, Xining, China, [2] College of Life Sciences, University of Chinese Academy of Sciences, Beijing, China, [3] State Key Laboratory of Vegetation and Environmental Change, Institute of Botany, Chinese Academy of Sciences, Beijing, China, [4] Key Laboratory of Tibetan Medicine Research, Chinese Academy of Sciences, Xining, China, [5] Qinghai Key Laboratory of Qinghai-Tibetan Plateau Biological Resources, Xining, China

Global climate change and nitrogen deposition have been having broad impacts on microorganisms. On the Qinghai-Tibetan Plateau (QTP), the responses of soil microbial community assemblage and diversity to nitrogen deposition and changes in precipitation are poorly understood, especially in the alpine steppe. In this study, we conducted a field manipulative experiment of nitrogen deposition and precipitation amount in an alpine steppe on the northeastern QTP and investigated the responses of community composition, diversity, and community assemblage of soil fungi. Soil fungal community compositions were significantly altered under nitrogen addition, precipitation change, and their interaction, and positively related with soil moisture, soil pH, and plant species richness. However, they were negatively related to soil mineralizable N and soil available P content. Operational taxonomic units (OTU) richness and Chao 1 index decreased under nitrogen addition combined with precipitation reduction treatment, whereas the Shannon–Wiener index declined only under precipitation increment treatment. Convergent fungal community assembly processes were not acutely altered by both nitrogen addition and precipitation changes, indicating that environmental filtering was a dominant ecological process controlling fungal community assemblage. By elucidating the above questions, the study enhanced our ability to predict the responses of soil fungal communities to nitrogen deposition and precipitation changes at alpine steppes on the QTP in the future.

Keywords: soil fungi, phylogenetic community structure, community assembly, climate change, structural equation model

OPEN ACCESS

Edited by:
Jadson Diogo Pereira Bezerra, Universidade Federal de Goiás, Brazil

Reviewed by:
César Marín, Universidad de O'Higgins, Chile
Mark Anthony, ETH Zürich, Switzerland

***Correspondence:**
Guoying Zhou
zhougy@nwipb.cas.cn

Specialty section:
This article was submitted to Fungi and Their Interactions, a section of the journal Frontiers in Microbiology

Received: *01 July 2020*
Accepted: *18 September 2020*
Published: *16 October 2020*

Citation:
Xiao Y, Li C, Yang Y, Peng Y, Yang Y and Zhou G (2020) Soil Fungal Community Composition, Not Assembly Process, Was Altered by Nitrogen Addition and Precipitation Changes at an Alpine Steppe. Front. Microbiol. 11:579072. doi: 10.3389/fmicb.2020.579072

INTRODUCTION

Dominant ecological processes controlling soil microbial community assemblage have attracted extensive attention (Dini-Andreote et al., 2015). Evaluating the relative importance of deterministic and stochastic ecological processes in community assembly is a primary work for exploring community assembly (Dumbrell et al., 2010; Nemergut et al., 2013; Mori et al., 2015; Feng et al., 2018; Luo et al., 2019; Gao et al., 2020). For example, Beck et al. (2015) found

that the deterministic and stochastic ecological processes jointly controlled fungal community assembly. Global changes have broad and profound impacts on microbial communities (Hutchins et al., 2019); for example, Chen et al. (2017) revealed that nitrogen addition enhanced the role of deterministic processes (i.e., environmental filtering) during soil arbuscular mycorrhizal fungal community assemblage in a temperate steppe. The Qinghai-Tibetan Plateau (QTP) is the largest and highest plateau in the world (average elevation, >4,000 m; area, 2.5×10^6 km^2), and low temperature and strong evaporation are primary climatic features (Zheng and Zhao, 2017), which limit the rate of mineralization of soil organic matter and make this area more sensitive to global changes (e.g., nitrogen deposition and precipitation change). Soil fungi play important roles in accelerating biogeochemical cycles (Amend et al., 2015), maintaining the health of soil ecosystems (Frac et al., 2018), and regulating feedback between plants and soil (Semchenko et al., 2018) and are studied well in a global scale (Tedersoo et al., 2014; Davison et al., 2015), whereas it is still poorly understood on the QTP. Therefore, it is important that the responses of soil fungal diversity, community composition, and assemblage process to nitrogen deposition and precipitation change are explored on the QTP. Human activity-induced nitrogen deposition has triggered a lot of changes in ecological processes and environmental factors, such as soil available nitrogen, soil pH, availability of soil phosphorus, and negative effects on biodiversity (Serna-Chavez et al., 2013; Lu et al., 2014; Chen et al., 2017). Soil environmental variables strongly affected soil fungal communities (Shen et al., 2013; Wang et al., 2017; Cho et al., 2019). On the QTP, nitrogen deposition has been presenting an increasing trend gradually, ranging from 0.87 to 1.38 g N m^{-2} year^{-1} in the recent decade (Lü and Tian, 2007). Thus, soil fungi diversity might decline, and community composition might change significantly in the future. However, we still poorly understand how soil fungal diversity, community composition, and assemblage process respond to nitrogen deposition, and relationships between fungal community composition and soil environmental variables remain to be unclear. In addition to soil variables, plant diversity was also a factor affecting soil fungal community (Chen et al., 2017). Thus, examining relationships between soil fungal community and plant diversity is also important for comprehensively understanding the responses of soil fungal community to nitrogen deposition.

Precipitation changes also leave imprints on soil microbial community composition and assemblage (Leff et al., 2015; Zhang et al., 2017; Na et al., 2019). Wang et al. (2018) found that precipitation was a main driver for the distribution pattern and community structure of a soil fungal community at a temperate steppe in Inner Mongolia of China. Additionally, the negative effects of nitrogen deposition on biodiversity may be changed by the effects of elevated precipitation (Zhang et al., 2018). Precipitation has been occurring with an increasing trend gradually on the QTP (Yang, 2018), which might alleviate environmental drought pressure and then might benefit soil fungal diversity and community composition. However, the responses of soil fungal community composition, biodiversity, and assemblage process to the individual effect of precipitation change and interactions with nitrogen deposition are still poorly understood on the QTP. An alpine steppe is one of the main vegetation ecosystems on the QTP (Miehe et al., 2011; **Figure 1A**) and is more sensitive to climate change than other ecosystems (Zheng and Zhao, 2017). Therefore, alpine steppes are predicted to have stronger responses than other ecosystems to atmospheric nitrogen deposition and precipitation changes. In this study, nitrogen deposition and precipitation amounts were manipulated at an alpine steppe. High-throughput sequencing technology, beta diversity null modeling analysis (Powell et al., 2015), and co-occurrence network analysis (Barberán et al., 2012) were employed to investigate soil fungal community composition, diversity, and community assemblage process in response to nitrogen deposition and precipitation changes. The study examined the following questions: (1) whether soil fungal community composition and diversity were altered by nitrogen deposition, precipitation changes, and their interaction; (2) which environmental factors are significantly related with soil fungal community composition; (3) which ecological process, stochastic or deterministic process, played a dominant role in controlling soil fungal community assemblage and whether this dominant role was altered by nitrogen addition and precipitation changes. Through the examination of these questions, the study aimed to predict how the soil fungal community composition, diversity, and community assemblage processes will change under nitrogen deposition and precipitation changes in the future at an alpine steppe and to provide a theoretical basis for anthropogenic nitrogen source input and precipitation changes in alpine steppe management.

MATERIALS AND METHODS

Study Site and Experimental Design

The field experiment was performed in Gangcha County (37°18′N, 100°15′E), which is located in Qinghai Province in the northeast of the QTP, China (**Figure 1A**). The altitude, mean annual temperature, and mean annual precipitation were 3,286 m, 0.08°C, and 387 mm, respectively. Alpine steppes are the dominant vegetation and comprised *Stipa purpurea* Grisebach, *Poa crymophila* Keng, and *Leymus secalinus* (Georgi) Tzvelev. The soil was classified as calcium soil order, semidry calcium soil suborder, and chestnut soil (Li et al., 2019).

The field experiment was established in 2013 by manipulating nitrogen deposition and precipitation to simulate atmospheric nitrogen deposition and precipitation changes due to climate change in the alpine steppe (**Figure 1B**). The experiment included six treatments, namely, NP− (ambient N with 50% precipitation reduction), NP (ambient N with ambient precipitation), NP + (ambient N with 50% precipitation increment), N + P− (N addition with 50% precipitation reduction), N + P (N addition with ambient precipitation), and N + P + (N addition with 50% precipitation increment). Five replicates for each treatment were established; thus, a total of 30 plots of 3.3m × 2.7 m in area were randomly separated in a 5 × 6 block design and divided by 2 m-wide buffer zones. V-shaped, sunlight-pervious, concave polyvinyl

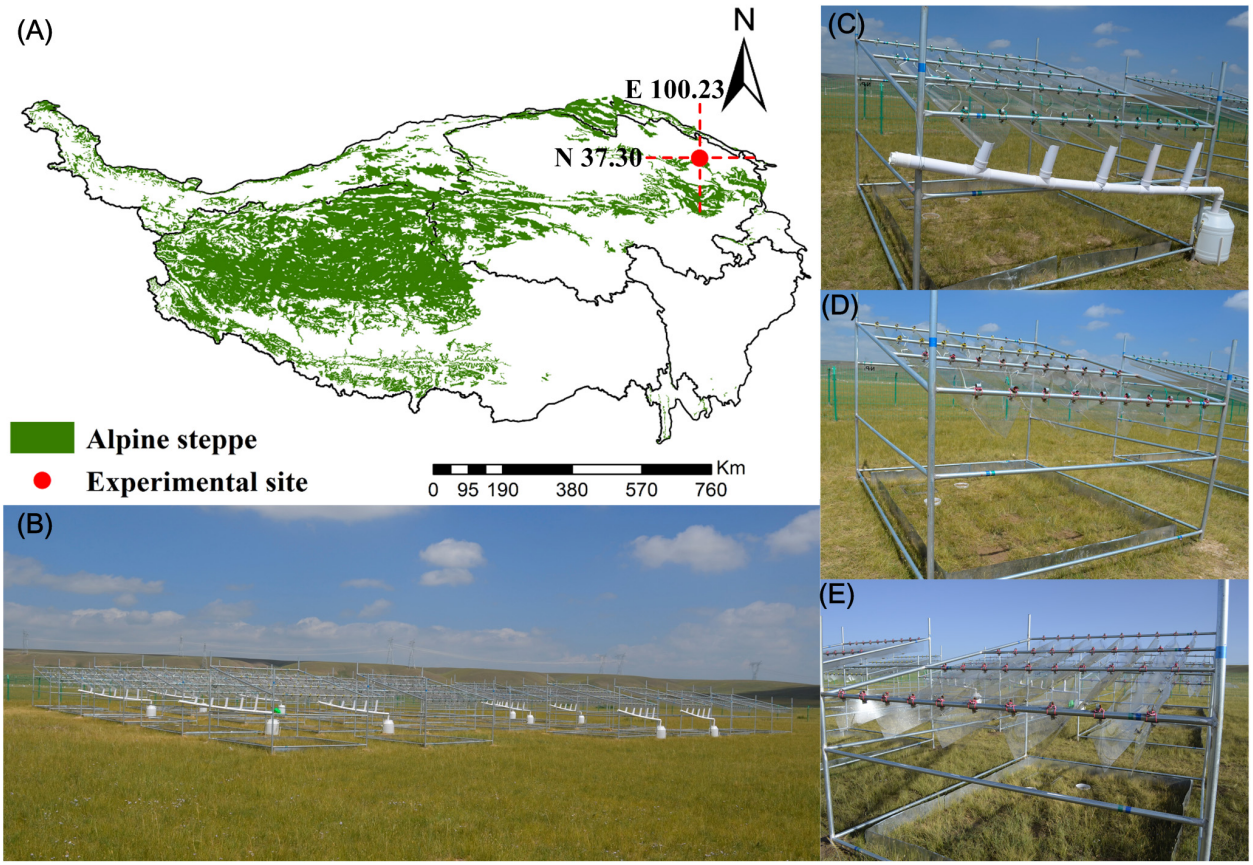


FIGURE 1 | Geographical location and photographs of the experimental site. **(A)** Geographical location; **(B)** overview of the experimental site; **(C)** 50% precipitation reduction treatment; **(D)** 50% precipitation addition treatment; **(E)** nitrogen addition treatment.

chloride (PVC) boards without slots, which were installed above treatments of 50% reduction in precipitation at a 15° angle, were used to collect precipitation (**Figure 1C**). This precipitation was then transferred (sprinkling evenly) to the treatments of 50% increase in precipitation. For precipitation increments and ambient precipitation treatments, V-shaped, sunlight-pervious, concave PVC boards with slots were established above these plots (Ma et al., 2017) (**Figures 1D,E**). NH_4NO_3 was fertilized in the plots to simulate atmospheric nitrogen deposition (10 g N m^{-2} $year^{-1}$). Although nitrogen deposition will go up to 40 g N m^{-2} $year^{-1}$ by 2050 (Zong et al., 2016), 8 g m^{-2} $year^{-1}$ has led to N saturation in the soil in our study area concurrently (Peng and Yang, 2016). NH_4NO_3 was dissolved in 1 L of distilled water and sprinkled evenly twice into the plots of nitrogen addition during the peak growing season (midmonth of June and July). Identical amounts of distilled water were sprayed uniformly on the ambient nitrogen addition plots (Li et al., 2019).

Plant Community Investigation and Soil Sampling

Species richness under the different treatments was investigated in August (peak of biomass) using a 1 m^2 quadrat and three replicates for each plot. The total species (non-repeat count) occurring in all three quadrats was used to represent the species richness for each plot. Numbers of each individual species were also recorded. Average relative abundance based on the three quadrats was calculated to represent abundance of each species. For soil sampling, five topsoil cores (0–10 cm) were randomly collected from each plot in August 2019 using a soil auger (diameter: 3.5 cm, depth: 15 cm) with sterilization. The five cores were mixed thoroughly using a 2.0 mm sieve to form a mixing sample without roots and debris, which was transported (at 4°C) to the laboratory within 24 h. Each mixing sample was divided into two parts; one was stored at −80°C for DNA extraction, and the other part was air-dried for analysis of soil physicochemical properties.

Soil Physicochemical Analyses

Soil samples were dried at 105°C for 48 h to a constant weight to assess soil moisture. Soil pH was determined using a pH meter in a liquid supernatant with a soil-to-water ratio of 1:2.5. Soil organic carbon (SOC) contents were analyzed using a dichromate oxidation-titration method. Soil mineralizable nitrogen (N) and soil available phosphorus (P) and potassium (K) contents were examined using the diffusion by alkali dissociation method, the ammonium molybdate method after extraction with $NaHCO_3$

solution, and the flame atomic absorption spectrometric method, respectively (Bao, 2005). Soil mineralizable nitrogen (N), available phosphorus (P), and available potassium (K) represent plant available N, P, and K contents in soil, respectively.

DNA Extraction, Sequencing, and Bioinformatics Analysis

An E.Z.N.A. Soil DNA Kit (Omega Bio-tek, Inc., Norcross, GA, United States) was used to extract soil genomic DNA from exactly 0.3 g of fresh soil according to the manufacturer's instructions; three replicates for each soil sample were established. The concentration and purity of the obtained DNA sample were determined using a NanoDrop 2000 spectrophotometer (Thermo Scientific, Wilmington, DE, United States). Primers ITS1F (5′-ACTTGGTCATTTAGAGGAAGTAA-3′) and ITS2 (5′-BGCTGCGTTCTTCATCGATGC-3′) were used to amplify fungal internal transcribed spacer-1 (ITS1) sequences (Adams et al., 2013). Details of the processes and reaction conditions for ITS1 amplification have been described in previous studies (Adams et al., 2013). Sequencing of DNA samples was conducted on an Illumina MiSeq PE300 instrument (Illumina, San Diego, United States) provided by Shanghai Majorbio Bio-Pharm Technology Co., Ltd.

Paired-ended sequence reads generated from the Illumina MiSeq PE300 were filtered by fastp (version 0.20.0; Chen et al., 2018) and merged using FLASH software (version 1.2.11; Magoč and Salzberg, 2011) with the following criteria: (i) 300 bp reads were truncated at any site receiving an average quality score of <20 over a 50 bp sliding window, and truncated reads shorter than 50 bp were discarded; reads containing ambiguous characters were also discarded, and samples were distinguished according to the barcode and primers; (ii) only overlapping sequences longer than 10 bp were assembled according to their overlapped sequence. The maximum mismatch ratio of the overlap region is 0.2. Reads that could not be assembled were discarded; (iii) the sequence direction was adjusted, with exact barcode matching and two-nucleotide mismatch in primer matching. A total of 1,862,202 (99.31%) sequences were obtained for the soil fungal community. Subsequently, operational taxonomic units (OTUs) were generated by clustering the sequences with 97% similarity using UPARSE (version 7.1; Edgar, 2013). The BLAST tool and UNITE database (version 8.0; Koljalg et al., 2013) was used to filter out potentially non-fungal taxa, and then the RDP Classifier version 2.2 (Wang et al., 2007) was used to annotate the most representative sequence of each OTU at a confidence threshold of 0.7. Finally, 3,423 OTUs, which were classified as 13 phyla, 45 classes, 101 orders, 220 families, and 416 genera, were detected across all samples. FUNGuild was used to match fungal functional profiles (Nguyen et al., 2016). All representative sequences in the study were deposited in the GenBank database with accession number PRJNA638547.

Diversity and Phylogenetic Structure of Soil Fungal Community

A rarefaction curve was used to evaluate sequencing depth (shown in **Supplementary Figure S1**). The OTU richness, Chao 1 index, and Shannon–Wiener index were used to assess alpha diversity of the soil fungal community. The Shannon–Wiener index evaluates species richness and evenness and is more sensitive to dominant species, whereas Chao 1 index is more sensitive to rare species. The R environment with the functions *chao1*() in the "fossil" package (Vavrek, 2011) and *rowSums*() and *diversity*() in the "vegan" package (Oksanen et al., 2019) was used to calculate the above diversity indices.

Abundance-based β-diversity null modeling analysis with community Bray–Curtis dissimilarity was used to detect soil fungal community assembly processes by evaluating the difference between "real" community and null modeling (neutral process) (Beck et al., 2015; Powell et al., 2015; Powell and Bennett, 2016). This difference was represented by effect size, which was calculated as follows (Mori et al., 2015):

$$\text{Effect size} = [\beta\text{-diversity}_{obs} - \text{mean}(\beta\text{-diversity}_{null})]/\beta\text{-diversity}_{sd}.$$

The $\beta\text{-diversity}_{obs}$ represented the observed value of a "real" community, and the mean ($\beta\text{-diversity}_{null}$) represented the mean of null β-diversity distribution. The $\beta\text{-diversity}_{sd}$ represented the standard deviation of null β-diversity distribution. To get the null β-diversity distribution, each OTU in the community was drawn 999 times with the same probability from the OTU pool, which was represented by all of the OTUs occurring in the study. If effect size (relative to neutral prediction) was significantly greater (divergence) or lesser (convergence) than zero, it indicates that the deterministic processes (i.e., interspecific competition or environmental filtering) play leading roles in community assembly. If there was no significant difference between effect size and zero (random), it indicates that neutral factors (for example, dispersal limitations and homogenizing dispersal) control community assembly (Beck et al., 2015; Powell et al., 2015; Powell and Bennett, 2016). The above calculation processes were performed in R (R Core Team, 2015).

Statistical Analysis

Two-way analysis of variance (ANOVA) was used to determine the effects of nitrogen addition, precipitation alteration, interactions of nitrogen addition and precipitation alteration, and blocking variable on soil environmental factors, plant species richness, and relative abundance of fungal taxon. Significant differences of soil environmental factors, plant species richness, and relative abundance of fungal taxon (**Supplementary Table S1**) between treatments were examined using Tukey's test at $P < 0.05$. To estimate the effects of treatments on soil fungal community composition, non-metric multidimensional scaling (NMDS) analysis was used to present visually the differences in soil fungal community composition. Additionally, permutational multivariate ANOVA (PERMANOVA) was conducted based on the Bray–Curtis distance matrix of community relative abundance using the *adonis*() function in the "vegan" package (Oksanen et al., 2019) to determine the effects of nitrogen addition, precipitation changes, nitrogen addition × precipitation changes, and random effect of block (blocking variable) on differences in soil fungal community composition. Spearman's correlation analysis using the *cor.test*() function was calculated to determine relationships between

fungal community composition and environmental factors, and the response variable was the first axes of the NMDS.

A co-occurrence network was used also to explore the co-occurrence patterns in the study (Barberán et al., 2012). Before analysis, low-abundance OTUs (relative abundance < 0.005%) were removed. The ***corr.test***() function in the "psych" package (Revelle, 2018) was used to calculate Spearman's correlation based on the relative abundance table of soil fungal community, and only Spearman's correlation coefficient > 0.6 or < −0.6 and $P < 0.05$ were included in the network (de Vries et al., 2018; Jiao et al., 2020). Gephi (version 0.9.2)[1] was used to visualize the co-occurrence network.

RESULTS

Soil Environmental Factors and Plant Community Characteristics

Significant differences in soil moisture, soil pH, SOC, plant available N, P in soil, and plant species richness, but not in plant available K content in soil, were detected across the treatments (**Table 1**). Specifically, soil moistures were significantly higher in the precipitation increment treatments than in the precipitation reduction treatments, but there were no significant differences with NP (control) treatment. In comparison with NP (control) treatment, the nitrogen addition with precipitation reduction (N + P−) treatment increased soil mineralizable N but reduced soil pH and plant species richness. SOC concentration was increased by nitrogen addition and was significantly higher than ambient nitrogen treatments. SOC was also the only environmental factor affected by the interaction of nitrogen addition and precipitation change. Soil available P content declined significantly under the nitrogen addition and precipitation increment (N + P +) treatment, but no significant differences were found with the NP (control) treatment (**Table 1**). Significant differences in plant community structure were also detected under different treatments (**Supplementary Figure S2**).

Soil Fungi Abundance, Community Composition, and Diversity

Relative abundances of soil fungi at the class level were significantly different across all the treatments (**Figure 2** and **Supplementary Table S1**). Among groups with a relative abundance > 10.0%, Agaricomycetes and Mortierellomycetes increased significantly under the precipitation increment treatments. In contrast, the abundance of Sordariomycetes declined under the precipitation increment treatments but increased significantly under nitrogen addition with precipitation reduction treatment (**Figure 2** and **Supplementary Table S1**). Significant differences in fungal community composition were also detected under nitrogen addition, precipitation change, and interactive effects of nitrogen addition and precipitation change (**Figure 3** and **Table 3**), in which precipitation change has the highest significant effect on community composition (**Table 3**).

Diversity analysis revealed that OTU richness and the Chao 1 index were lower under nitrogen addition combined with precipitation reduction (N + P−) than under control (NP) and other treatments (**Figures 4A,B**), and the Shannon–Wiener index declined as a result of ambient nitrogen with precipitation increment treatment (**Figure 4C**). Precipitation change has a significant effect on all three indices, while the interaction of nitrogen addition and precipitation change has a significant effect only on the Shannon–Wiener index (**Supplementary Table S3**).

Relationships Between Soil Fungal Community Composition and Soil Environmental Factors and Plant Species Richness

Spearman's correlation analysis revealed that fungal taxon compositions were related positively and significantly to soil moisture content, soil pH, and plant species richness but were

[1]https://gephi.org/

TABLE 1 | Soil environmental factors and plant species richness under nitrogen addition and precipitation changes.

Treatment	Soil moisture (%)	Soil pH	Soil organic C (g kg^{-1})	Soil mineralizable N (mg kg^{-1})	Soil available P (mg kg^{-1})	Soil available K (mg kg^{-1})	Plant species richness
NP −	13.37 ± 1.08c	7.98 ± 0.06b	17.46 ± 0.72b	265.00 ± 12.38ab	5.01 ± 0.21a	352.55 ± 43.83a	7.80 ± 0.66b
NP (Control)	17.07 ± 0.83ab	8.11 ± 0.08ab	16.85 ± 0.99b	265.20 ± 16.13ab	3.66 ± 0.68bc	316.80 ± 59.48a	11.40 ± 1.08a
NP +	19.33 ± 1.22a	8.17 ± 0.03a	19.13 ± 1.05ab	241.60 ± 10.22b	3.60 ± 0.27bc	311.59 ± 34.52a	13.60 ± 0.93a
N + P−	14.93 ± 0.39bc	7.75 ± 0.05c	20.18 ± 0.85a	286.80 ± 3.60a	4.82 ± 0.35ab	325.59 ± 29.85a	5.00 ± 0.45c
N + P	16.77 ± 1.30ab	7.99 ± 0.06b	21.07 ± 0.49a	238.20 ± 7.63b	4.35 ± 0.26ab	355.64 ± 50.86a	7.00 ± 0.71bc
N + P +	19.18 ± 0.70a	8.11 ± 0.03ab	18.86 ± 0.45ab	247.40 ± 16.55b	3.08 ± 0.40c	369.62 ± 15.31a	6.60 ± 1.08bc
Significance of							
N	0.718	**0.035**	**0.032**	0.959	0.981	0.461	**0.000**
P	**0.002**	**0.005**	0.981	**0.035**	**0.024**	0.993	**0.004**
N × P	0.661	0.266	**0.035**	0.099	0.355	0.702	0.061
Block	0.931	0.677	0.931	0.430	0.615	0.999	0.334

Data are mean ± SE (n = 5). Lowercase letters indicate significant differences (P < 0.05). Two-way analysis of variance was used to determine the effect of nitrogen addition (N), precipitation change (P), their interactions (N × P) on observations, and effects of block (Block). The significant differences of these variables between treatments were examined using Tukey's test at P < 0.05, and significant effects (P < 0.05) are highlighted in bold.

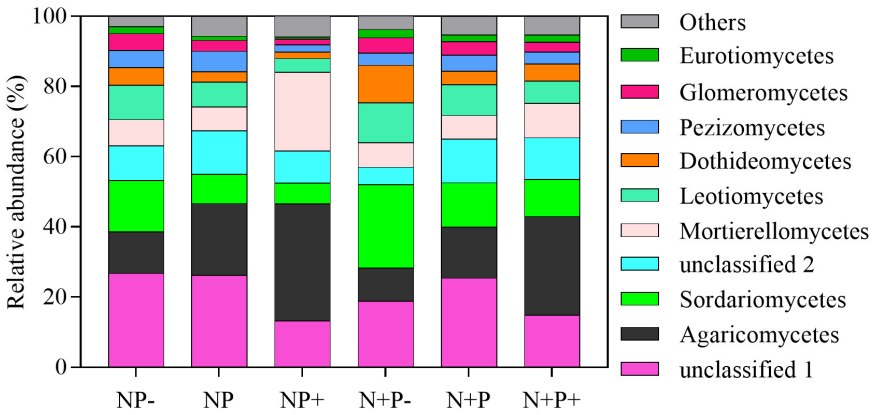


FIGURE 2 | Average relative abundances (%) of the top 10 fungal groups at the class level found at each treatment. Others present the sum of other classes of fungi outside the top 10 in this study. N (ambient N), N + (N addition), P (ambient precipitation), P + (50% added precipitation), and P− (50% reduction in precipitation).

negatively and significantly related to plant available N and P content in soil. There were no significant relationships detected with SOC and plant available K content in soil (**Table 2**).

Community Assembly of the Soil Fungal Community

Beta diversity null modeling analysis showed that an effect size lesser than zero across treatments (**Figure 4D**) indicated that deterministic ecological processes (i.e., environmental filtering) were more important than neutral processes in soil fungal community assembly. Compared to that under NP (control) treatment, the importance of environmental filtering was decreased under N + P− treatment (**Figure 4D**). The co-occurrence network analysis of fungi revealed that strong positive interactions among fungi OTUs were detected under all treatments (**Figure 5**), in which this positive interaction under NP + treatment was overwhelmingly stronger than all other treatments including NP (control) treatment. The mean of clustering coefficients was up to 0.639, which was higher in NP + treatment than in NP (control) treatment and was lesser in NP treatment than in other treatments (**Supplementary Table S4**). Other network parameters are shown in **Supplementary Table S4**.

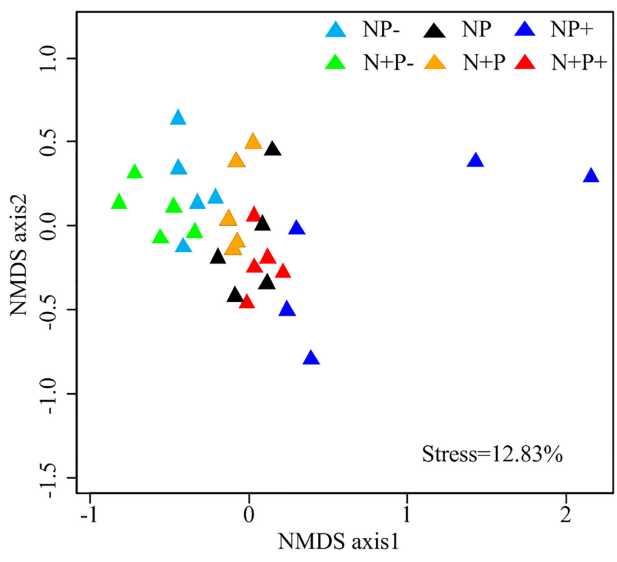


FIGURE 3 | Non-metric multidimensional scaling (NMDS) ordinations based on Bray–Curtis distance dissimilarity matrix of soil fungal Operational taxonomic unit (OTU) taxon composition.

DISCUSSION

Effects of Nitrogen Addition and Precipitation Changes on Relative Abundance and Diversity of Soil Fungi

Several studies have shown that both nitrogen addition and precipitation changes have significant impacts on the relative abundance and diversity of soil fungi (Leff et al., 2015; Chen et al., 2017; Zhang et al., 2018). Here, experimental results also indicated that the relative abundances of soil fungal taxa were altered significantly under nitrogen addition and precipitation alteration (**Figure 2** and **Supplementary Table S1**), suggesting that shifts in both nitrogen and precipitation may influence the ecological functions of soil fungal taxa in the alpine steppe ecosystem. Soil fungi play important roles in the interactions between plants and soil (Semchenko et al., 2018), especially in nutrient acquisition for plants (Bowles et al., 2018). Nitrogen addition and precipitation changes would induce changes in soil availability of nitrogen, soil moisture content, and soil pH (Serna-Chavez et al., 2013; Lu et al., 2014). These changes in soil environmental factors might decrease the importance of some fungal groups involved in nutrient absorption for plants (Leff et al., 2015) and result in alteration of the initial carbon allocation strategy of plants to fungi (Wei et al., 2013). The changes would motivate significant shifts in the relative abundance of soil fungi. In addition, significant changes in plant communities may be

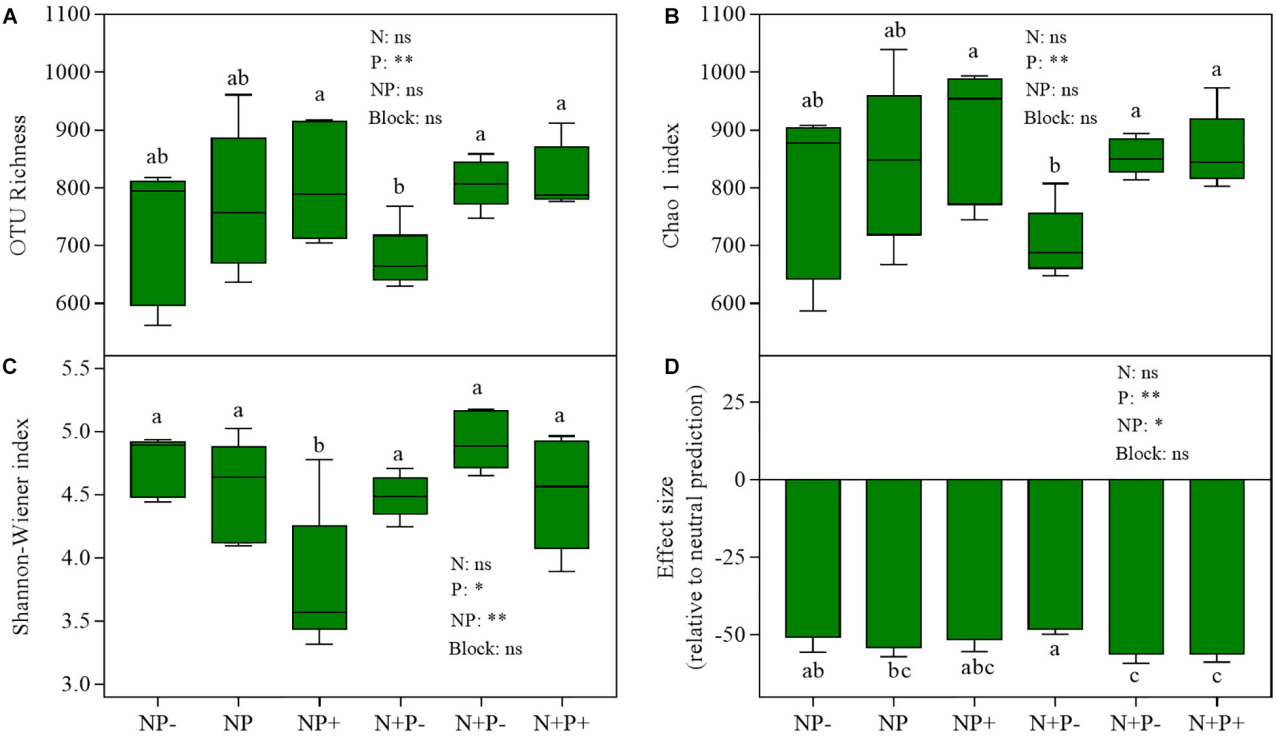


FIGURE 4 | Diversity and effect size relative to neutral prediction based on null model analysis of Bray–Curtis dissimilarity of soil fungal community across treatments. **(A)** OTU richness; **(B)** Chao 1 index; **(C)** Shannon–Wiener index; **(D)** effect size (relative to neutral prediction). Lowercase letters indicate significant differences ($P < 0.05$). Student's *t*-test was used to determine the difference between effect size of community assembly and zero, and significant differences of these diversity indicators between treatments were examined using Tukey's test at $P < 0.05$.

another explanation for shifts in the relative abundance of soil fungi (Qin et al., 2020), since plant community changes would trigger shifts in soil fungal trophic groups (e.g., pathogenic and saprophytic fungi) (Makiola et al., 2019).

The relative abundance analysis also revealed a dynamic shift in Agaricomycetes and Sordariomycetes, with one falling and the other rising with the increasing gradient in precipitation (**Figure 2**). Specifically, the precipitation increment increased the relative abundance of Agaricomycetes but caused a decrease in that of Sordariomycetes. Furthermore, the relative abundance of Sordariomycetes increased in drought conditions. These observations suggested that the two taxa may be related to soil moisture. Results of function prediction showed that Agaricomycetes was closely related to dung saprotroph and plant saprotroph, whereas Sordariomycetes was closely related to soil animal pathogen (**Figure 6**). A previous study showed that soil animal abundance increased with increasing soil moisture (Sylvain et al., 2014), suggesting that the precipitation reduction treatment might enhance the likelihood of soil animals being infected by pathogens in alpine steppes (Delgado-Baquerizo et al., 2020). However, a study conducted in a subtropical forest reported that the abundance of Agaricomycetes increased in drought conditions (He et al., 2017), which was not consistent with our results. Agaricomycetes contained more undefined function groups (**Figure 6A**). Therefore, the responses of Agaricomycetes to precipitation may vary in different habitats.

Negative effects of nitrogen deposition on biodiversity, including microbial diversity, have been routinely observed (McClean et al., 2011; Zeng et al., 2016). In this study, nitrogen addition only slightly decreased the diversity of the soil fungal community (**Figures 4A–C**). However, significant negative effects of nitrogen addition combined with precipitation reduction on OTU richness and Chao 1 index were detected

TABLE 2 | Spearman's correlation analysis between soil fungal community composition and soil environmental factors and plant species richness, and the response variable was the first axes of the non-metric multidimensional scaling (NMDS).

Explanatory factor	Operational taxonomic unit (OTU) community composition	
	r	*P*
Soil moisture	**0.5283**	**0.0027**
Soil pH	**0.4995**	**0.0049**
Soil organic C	−0.1275	0.5018
Soil available N	**−0.4425**	**0.0143**
Soil available P	**−0.4818**	**0.0070**
Soil available K	−0.2289	0.2238
Plant species richness	**0.5366**	**0.0022**

Significant correlations and P-values are in bold type.

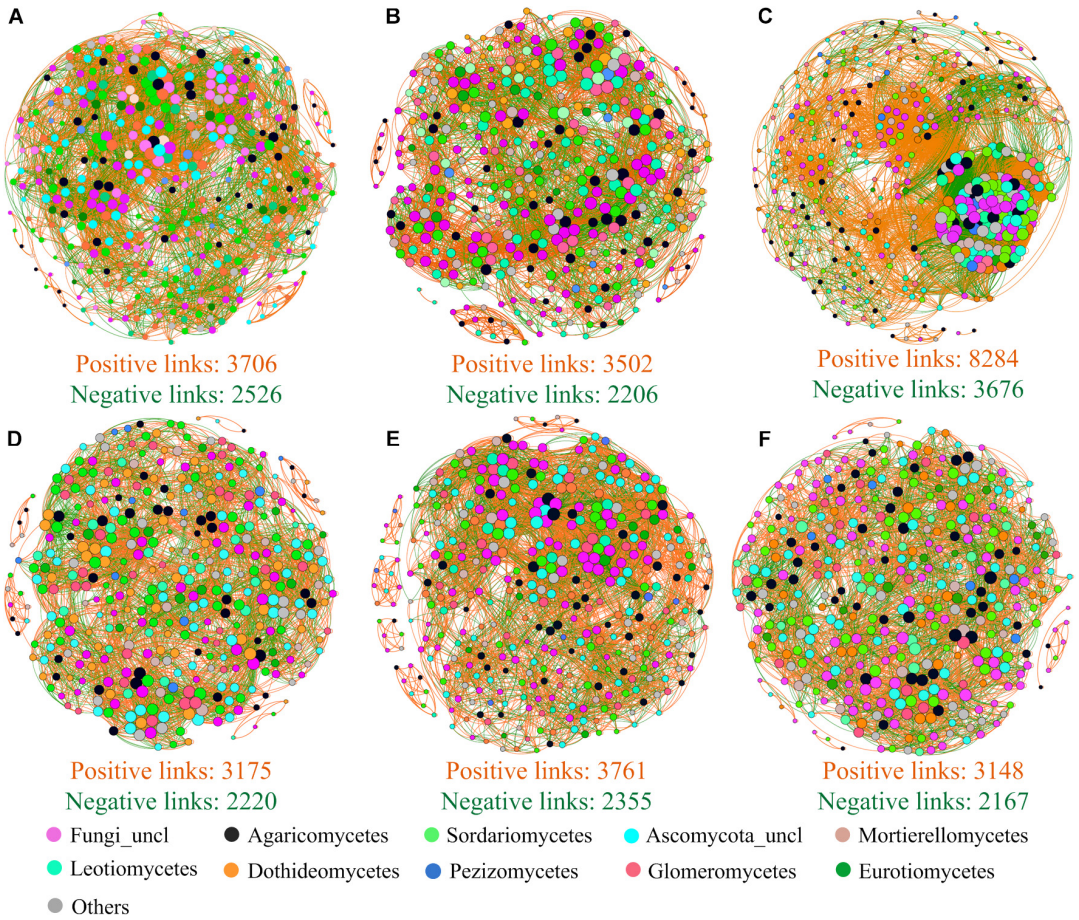


FIGURE 5 | Co-occurrence patterns of soil fungal taxon at OTU level for NP− treatment **(A)**, NP treatment **(B)**, NP + treatment **(C)**, N + P− treatment **(D)**, N + P **(E)**, and N + P + treatment **(F)**. The size of nodes was proportional to the link numbers of each node. Nodes in different colors are representative of the top 10 classes and other classes. Edges are shown with orange lines (positive interaction) and green lines (negative interaction). In each subfigure, only the top 400 OTUs and edges with Spearman's $\rho > 0.60$ or < -0.6 and $P < 0.05$ are shown.

(**Figures 4A,B**), suggesting that drought reinforces the negative effect of nitrogen addition on soil microbial diversity in the alpine steppe ecosystem. A previous study showed that nitrogen addition combined with elevated precipitation is beneficial for maintaining soil fungal diversity in the *Stipa baicalensis* temperate steppe (Zhang et al., 2018). Based on these observations, we speculated that, in the alpine steppe, drought had a stronger negative effect on microbial diversity than that of nitrogen addition. Moreover, only the Shannon–Wiener index decreased in precipitation addition, which may be related to the increase in the abundance of dominant soil fungal taxa under precipitation increment treatments (**Figure 2**).

Relationships Between Soil Fungal Community Composition and Environmental Factors Under Nitrogen Addition and Precipitation Alteration

Soil fungal community composition differed under nitrogen addition and precipitation change (**Figure 3** and **Table 3**), which evidenced the responses of soil microbial composition to nitrogen deposition and precipitation change in the alpine steppe and may be related with the remission of nitrogen and precipitation limitation on the QTP (Zheng and Zhao, 2017). Nitrogen deposition and precipitation change could induce changes in availability of soil nitrogen, moisture, and other soil variables (Serna-Chavez et al., 2013; Xu et al., 2015) and subsequently affected soil fungal community composition (Zhang Y. et al., 2016). This result also further highlighted the significance of this study.

The soil moisture was strongly positively related with soil fungal community composition (**Table 2**). Precipitation driving the distribution pattern and community structure of a soil fungal community was reported at a temperate steppe (Wang et al., 2018). On the QTP, precipitation change altered the availability of soil moisture at an alpine steppe (**Table 1**), which may be the main reason for our result. Nitrogen addition would alter the availability of soil nitrogen and induces shifts in plant available P content in soil (Deng et al., 2017; Li et al., 2020) and then changed soil nutrient conditions for

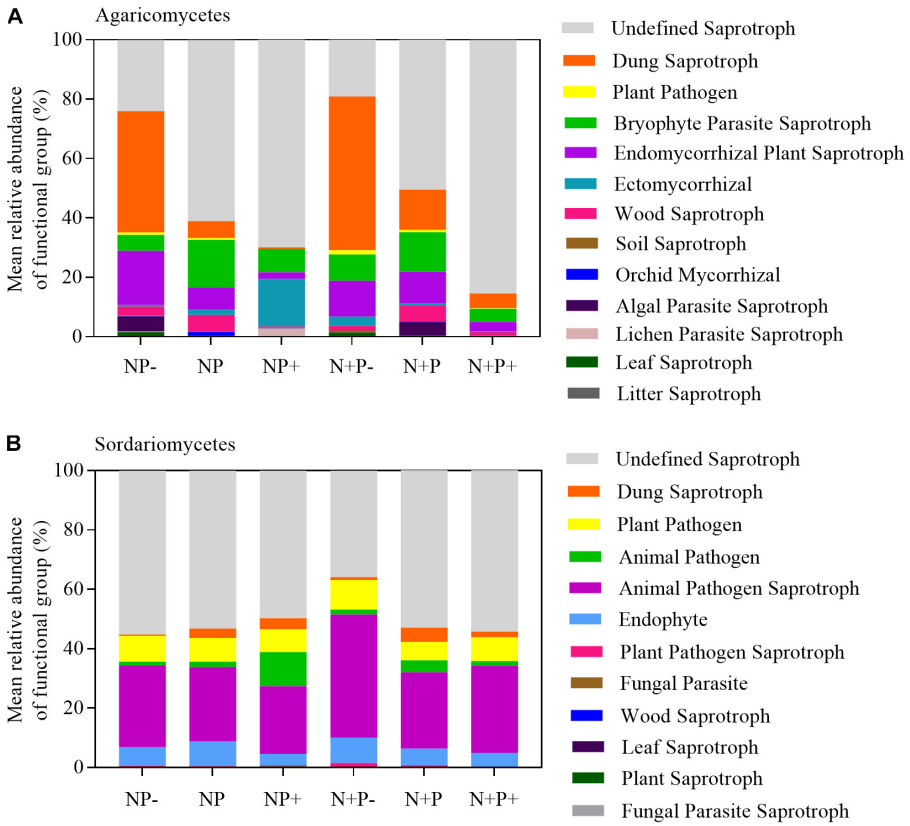


FIGURE 6 | Compositions of fungal functional group (guild) inferred by FUNGuild, Agaricomycetes **(A)** and Sordariomycetes **(B)**.

soil microbial community. These explained the significant correlation between soil fungal community composition and plant available N and P content in soil (**Table 2**). Soil pH was an important predictor for soil microbial community composition (Shen et al., 2013; Chen et al., 2017; Zhou et al., 2020) and played primary roles in community assemblage (Dumbrell et al., 2010; Wang et al., 2017; Tripathi et al., 2018; Cho et al., 2019). A significant positive relationship between soil pH and fungal community composition was also revealed (**Table 2**), which was consistent with previous studies. Change in plant species richness intuitively reflected plant community shift and also significantly related with fungal community composition, which could be explained by the shift in initial carbon allocation strategy of plants to fungi (Wei et al., 2013).

Mechanism of Soil Fungal Community Assemblage Under Nitrogen Addition and Precipitation Alteration

Beta diversity null modeling analysis has increasingly been employed to access the mechanism of community assemblage (Beck et al., 2015; Powell et al., 2015; Powell and Bennett, 2016). Here, the effect size of null modeling analysis showed that the soil fungal community was convergent across all treatments (**Figure 4D**), suggesting that deterministic ecological processes, which are largely environmental filtering, play primary and dominant roles in shaping the soil fungal community (Powell and Bennett, 2016). In addition to the N + P− treatment, non-significant differences between others and NP (control) treatment were revealed, suggesting that overall soil fungal community assembly processes may be relatively stable. A previous study has shown that fungal communities are more stable than other microbial groups under climate change (de Vries et al., 2018). The long formation period of alpine steppes may be another reason for a relatively stable process of soil fungal community assemblage under climate change scenarios, since ecosystem development strongly influences belowground biodiversity (Delgado-Baquerizo et al., 2019). The 7-year period

TABLE 3 | Results of permutational multivariate analysis of variance (PERMANOVA) for fungal community composition, and significant effects ($P < 0.05$) are highlighted in bold.

	Fungal community composition		
	***F* model**	**R^2**	***P*-value**
N	1.7505	0.0487	**0.016**
P	3.1996	0.1781	**0.001**
N × P	1.3753	0.0765	**0.045**
Block	1.2601	0.1403	0.062

of this field experiment was extremely short compared with the long period of alpine steppe formation in the QTP that may have led to a relatively stable process in soil fungal community assemblage. Similarly, a previous study reporting no significant responses of a fungal community to short-term changes in climate conditions (Zhang K. P. et al., 2016) supported our explanation. It should be noted that even though soil fungal communities were convergent across treatments, precipitation change and its interaction with nitrogen addition had significant effects on the community assembly process (**Supplementary Table S3**), which indicated that soil fungal community assembly processes may tend to neutralize processes under long-term nitrogen deposition and precipitation reduction in the future.

Co-occurrence network analysis is another powerful tool to explore the mechanism of microbial community assemblage (Barberán et al., 2012; Cardinale et al., 2015; Jiao et al., 2020). Here, stronger positive interactions between fungal OTUs were presented (**Figure 5**), suggesting a closer cooperation among fungal OTUs (Deng et al., 2012) and reflecting, to some extent, that soil fungi might tend to share similar soil niches. Interestingly, precipitation increment (NP +) treatment strongly enhances cluster degree than did control (NP) and other treatments (**Figure 5C**), which suggested that precipitation increment might trigger a soil ecological process and improve interactions of soil fungal taxon. The mean of clustering coefficients was up to 0.639, which indicated closer relationships between OTUs (Jiao et al., 2020). These speculations might support results that deterministic processes played more important roles in shaping soil fungal community at the alpine steppe on the QTP than neutral ecological processes. Although co-occurrence network analysis was used to infer biotic interactions, we acknowledged shortcomings of the network analysis due to difficulty in accurately detecting community assembly ecological processes (Carr et al., 2019). Therefore, incorporating more experiments or more sophisticated approaches into the research framework will be necessary in the future.

CONCLUSION

This study explored the responses of soil fungal community composition, diversity, and community assembly processes to nitrogen addition and precipitation changes at an alpine steppe on the northeastern Qinghai-Tibetan Plateau. Soil fungal community composition and diversity were altered significantly by nitrogen addition and precipitation change, while the convergent processes of fungal community assembly were also altered, even though the dominance of deterministic ecological processes was not changed. The study suggested that soil fungal communities at alpine steppes on the QTP may change a lot under long-term global change scenarios in the future. Future works investigating more comprehensive environmental factors and using more research methods simultaneously are essential to fully understand the construction of fungal communities in nature.

DATA AVAILABILITY STATEMENT

The datasets presented in this study can be found in online repositories. The names of the repository/repositories and accession number(s) can be found in the article/**Supplementary Material**.

AUTHOR CONTRIBUTIONS

YX, CL, and GZ designed the experiments. YX and GZ jointly wrote the manuscript. YY assisted with the field sampling. YP and YY participated in the discussions. All authors contributed to the article and approved the submitted version.

FUNDING

This work was jointly supported by the National Key Research and Development Program of China (2019YFC0507404), the Natural Science Foundation of Qinghai Province (2019-ZJ-910), and the International Exchange and Cooperation Project of Qinghai Province (2019-HZ-807).

SUPPLEMENTARY MATERIAL

The Supplementary Material for this article can be found online at: https://www.frontiersin.org/articles/10.3389/fmicb.2020.579072/full#supplementary-material

REFERENCES

Adams, R. I., Miletto, M., Taylor, J. W., and Bruns, T. D. (2013). Dispersal in microbes: fungi in indoor air are dominated by outdoor air and show dispersal limitation at short distances. *ISME J.* 7, 1460–1460. doi: 10.1038/ismej.2013.84

Amend, A. S., Matulich, K. L., and Martiny, J. B. H. (2015). Nitrogen addition, not initial phylogenetic diversity, increases litter decomposition by fungal communities. *Front. Microbiol.* 6:109. doi: 10.3389/fmicb.2015.00109

Bao, S. D. (2005). *Agricultural Chemical Analysis of Soil*. Beijing: China Agriculture Press.

Barberán, A., Bates, S. T., Casamayor, E. O., and Fierer, N. (2012). Using network analysis to explore co-occurrence patterns in soil microbial communities. *ISME J.* 6, 343–351. doi: 10.1038/ismej.2011.119

Beck, S., Powell, J. R., Drigo, B., Cairney, J. W. G., and Anderson, I. C. (2015). The role of stochasticity differs in the assembly of soil- and root-associated fungal communities. *Soil Biol. Biochem.* 80, 18–25. doi: 10.1016/j.soilbio.2014.09.010

Bowles, T. M., Jackson, L. E., and Cavagnaro, T. R. (2018). Mycorrhizal fungi enhance plant nutrient acquisition and modulate nitrogen loss with variable water regimes. *Glob. Chang. Biol.* 24, E171–E182. doi: 10.1111/gcb.13884

Cardinale, M., Grube, M., Erlacher, A., Quehenberger, J., and Berg, G. (2015). Bacterial networks and co-occurrence relationships in the lettuce root microbiota. *Environ. Microbiol.* 17, 239–252. doi: 10.1111/1462-2920.12686

Carr, A., Diener, C., Baliga, N. S., and Gibbons, S. M. (2019). Use and abuse of correlation analyses in microbial ecology. *ISME J.* 13, 2647–2655. doi: 10.1038/s41396-019-0459-z

Chen, S. F., Zhou, Y. Q., Chen, Y. R., and Gu, J. (2018). fastp: an ultra-fast all-in-one FASTQ preprocessor. *Bioinformatics* 34, 884–890. doi: 10.1093/bioinformatics/bty560

Chen, Y. L., Xu, Z. W., Xu, T. L., Veresoglou, S. D., Yang, G. W., and Chen, B. D. (2017). Nitrogen deposition and precipitation induced phylogenetic clustering of arbuscular mycorrhizal fungal communities. *Soil Biol. Biochem.* 115, 233–242. doi: 10.1016/j.soilbio.2017.08.024

Cho, H. J., Tripathi, B. M., Moroenyane, I., Takahashi, K., Kerfahi, D., Dong, K., et al. (2019). Soil pH rather than elevation determines bacterial phylogenetic community assembly on Mt. *Norikura. FEMS Microbiol. Ecol.* 95:fiy216. doi: 10.1093/femsec/fiy216

Davison, J., Moora, M., Opik, M., Adholeya, A., Ainsaar, L., Ba, A., et al. (2015). Global assessment of arbuscular mycorrhizal fungus diversity reveals very low endemism. *Science* 349, 970–973. doi: 10.1126/science.aab1161

de Vries, F. T., Griffiths, R. I., Bailey, M., Craig, H., Girlanda, M., and Gweon, H. S. (2018). Soil bacterial networks are less stable under drought than fungal networks. *Nat. Commun.* 9:3033. doi: 10.1038/s41467-018-05516-7

Delgado-Baquerizo, M., Bardgett, R. D., Vitousek, P. M., Maestre, F. T., Williams, M. A., and Fierer, N. (2019). Changes in belowground biodiversity during ecosystem development. *Proc. Natl. Acad. Sci. U.S.A.* 116, 6891–6896. doi: 10.1073/pnas.1818400116

Delgado-Baquerizo, M., Guerra, C. A., Cano-Diaz, C., Egidi, E., Wang, J. T., Eisenhauer, N., et al. (2020). The proportion of soil-borne pathogens increases with warming at the global scale. *Nat. Clim. Chang* 10, 550–554. doi: 10.1038/s41558-020-0759-3

Deng, Q., Hui, D. F., Dennis, S., and Reddy, K. C. (2017). Responses of terrestrial ecosystem phosphorus cycling to nitrogen addition: a meta-analysis. *Glob. Ecol. Biogeogr.* 26, 713–728. doi: 10.1111/geb.12576

Deng, Y., Jiang, Y. H., Yang, Y. F., He, Z. L., Luo, F., and Zhou, J. Z. (2012). Molecular ecological network analyses. *BMC Bioinformatics* 13:113. doi: 10.1186/1471-2105-13-113

Dini-Andreote, F., Stegen, J. C., van Elsas, J. D., and Salles, J. F. (2015). Disentangling mechanisms that mediate the balance between stochastic and deterministic processes in microbial succession. *Proc. Natl. Acad. Sci. U.S.A.* 112, E1326–E1332. doi: 10.1073/pnas.1414261112

Dumbrell, A. J., Nelson, M., Helgason, T., Dytham, C., and Fitter, A. H. (2010). Relative roles of niche and neutral processes in structuring a soil microbial community. *ISME J.* 4, 337–345. doi: 10.1038/ismej.2009.122

Edgar, R. C. (2013). UPARSE: highly accurate OTU sequences from microbial amplicon reads. *Nat. Methods* 10, 996–998. doi: 10.1038/Nmeth.2604

Feng, M. M., Adams, J. M., Fan, K. K., Shi, Y., Sun, R. B., and Chu, H. Y. (2018). Long-term fertilization influences community assembly processes of soil diazotrophs. *Soil Biol. Biochem.* 126, 151–158. doi: 10.1016/j.soilbio.2018.08.021

Frac, M., Hannula, S. E., Belka, M., and Jedryczka, M. (2018). Fungal biodiversity and their role in soil health. *Front. Microbiol.* 9:707. doi: 10.3389/fmicb.2018.00707

Gao, C., Montoya, L., Xu, L., Madera, M., Hollingsworth, J., and Taylor, J. W. (2020). Fungal community assembly in drought-stressed sorghum shows stochasticity, selection, and universal ecological dynamics. *Nat. Commun.* 11, 34–47. doi: 10.1038/s41467-019-13913-9

He, D., Shen, W. J., Eberwein, J., Zhao, Q., Ren, L. J., and Wu, Q. L. L. (2017). Diversity and co-occurrence network of soil fungi are more responsive than those of bacteria to shifts in precipitation seasonality in a subtropical forest. *Soil Biol. Biochem.* 115, 499–510. doi: 10.1016/j.soilbio.2017.09.023

Hutchins, D. A., Jansson, J. K., Remais, J. V., Rich, V. I., Singh, B. K., and Trivedi, P. (2019). Climate change microbiology - problems and perspectives. *Nat. Rev. Microbiol.* 17, 391–396. doi: 10.1038/s41579-019-0178-5

Jiao, S., Yang, Y. F., Xu, Y. Q., Zhang, J., and Lu, Y. H. (2020). Balance between community assembly processes mediates species coexistence in agricultural soil microbiomes across eastern China. *ISME J.* 14, 202–216. doi: 10.1038/s41396-019-0522-9

Koljalg, U., Nilsson, R. H., Abarenkov, K., Tedersoo, L., Taylor, A. F. S., Bahram, M., et al. (2013). Towards a unified paradigm for sequence-based identification of fungi. *Mol. Ecol.* 22, 5271–5277. doi: 10.1111/mec.12481

Leff, J. W., Jones, S. E., Prober, S. M., Barberan, A., Borer, E. T., and Fierer, N. (2015). Consistent responses of soil microbial communities to elevated nutrient inputs in grasslands across the globe. *Proc. Natl. Acad. Sci. U.S.A.* 112, 10967–10972. doi: 10.1073/pnas.1508382112

Li, C. B., Zheng, Z., Peng, Y. F., Nie, X. Q., Yang, L. C., Xiao, Y. M., et al. (2019). Precipitation and nitrogen addition enhance biomass allocation to aboveground in an alpine steppe. *Ecol. Evol.* 9, 12193–12201. doi: 10.1002/ece3.5706

Li, S., Dong, S. K., Shen, H., Xu, Y. D., Gao, X. X., Han, Y. H., et al. (2020). Nitrogen addition gradient can regulate the environmental filtering of soil potassium or phosphorus in shaping the community assembly of alpine meadow. *Ecol. Indic.* 109:105774. doi: 10.1016/j.ecolind.2019.105774

Lü, C. Q., and Tian, H. Q. (2007). Spatial and temporal patterns of nitrogen deposition in China: Synthesis of observational data. *J. Geophys. Res.* 112:D22S05. doi: 10.1029/2006jd007990

Lu, X. K., Mao, Q. G., Gilliam, F. S., Luo, Y. Q., and Mo, J. M. (2014). Nitrogen deposition contributes to soil acidification in tropical ecosystems. *Glob. Chang. Biol.* 20, 3790–3801. doi: 10.1111/gcb.12665

Luo, Z. M., Liu, J. X., Zhao, P. Y., Jia, T., Li, C., and Chai, B. F. (2019). Biogeographic patterns and assembly mechanisms of bacterial communities differ between habitat generalists and specialists across elevational gradients. *Front. Microbiol.* 10:169. doi: 10.3389/fmicb.2019.00169

Ma, Z. Y., Liu, H. Y., Mi, Z. R., Zhang, Z. H., Wang, Y. H., Xu, W., et al. (2017). Climate warming reduces the temporal stability of plant community biomass production. *Nat. Commun.* 8, 15378–15384. doi: 10.1038/ncomms15378

Magoč, T., and Salzberg, S. L. (2011). FLASH: fast length adjustment of short reads to improve genome assemblies. *Bioinformatics* 27, 2957–2963. doi: 10.1093/bioinformatics/btr507

Makiola, A., Dickie, I. A., Holdaway, R. J., Wood, J. R., Orwin, K. H., and Glare, T. R. (2019). Land use is a determinant of plant pathogen alpha- but not beta-diversity. *Mol. Ecol.* 28, 3786–3798. doi: 10.1111/mec.15177

McClean, C. J., van den Berg, L. J. L., Ashmore, M. R., and Preston, C. D. (2011). Atmospheric nitrogen deposition explains patterns of plant species loss. *Glob. Change Biol.* 17, 2882–2892. doi: 10.1111/j.1365-2486.2011.02462.x

Miehe, G., Miehe, S., Bach, K., Nolling, J., Hanspach, J., Reudenbach, C., et al. (2011). Plant communities of central Tibetan pastures in the Alpine Steppe/Kobresia pygmaea ecotone. *J. Arid. Environ.* 75, 711–723. doi: 10.1016/j.jaridenv.2011.03.001

Mori, A. S., Fujii, S., Kitagawa, R., and Koide, D. (2015). Null model approaches to evaluating the relative role of different assembly processes in shaping ecological communities. *Oecologia* 178, 261–273. doi: 10.1007/s00442-014-3170-9

Na, X. F., Yu, H. L., Wang, P., Zhu, W. W., Niu, Y. B., and Huang, J. Y. (2019). Vegetation biomass and soil moisture coregulate bacterial community succession under altered precipitation regimes in a desert steppe in northwestern China. *Soil Biol. Biochem.* 136:107520. doi: 10.1016/j.soilbio.2019.107520

Nemergut, D. R., Schmidt, S. K., Fukami, T., O'Neill, S. P., Bilinski, T. M., and Ferrenberg, S. (2013). Patterns and processes of microbial community assembly. *Microbiol. Rev.* 77, 342–356. doi: 10.1128/Mmbr.00051-12

Nguyen, N. H., Song, Z. W., Bates, S. T., Branco, S., Tedersoo, L., Menke, J., et al. (2016). FUNGuild: An open annotation tool for parsing fungal community datasets by ecological guild. *Fungal Ecol.* 20, 241–248. doi: 10.1016/j.funeco.2015.06.006

Oksanen, J., Blanchet, F. G., Friendly, M., Kindt, R., Legendre, P., McGlinn, D., et al. (2019). *vegan: Community Ecology Package. R Package Version 2.5-4*. Avaliable online at: https://CRAN.R-project.org/package=vegan (accessed January 9, 2019).

Peng, Y. F., and Yang, Y. H. (2016). Allometric biomass partitioning under nitrogen enrichment: Evidence from manipulative experiments around the world. *Sci. Rep.* 6:28918. doi: 10.1038/srep28918

Powell, J. R., and Bennett, A. E. (2016). Unpredictable assembly of arbuscular mycorrhizal fungal communities. *Pedobiologia* 59, 11–15. doi: 10.1016/j.pedobi.2015.12.001

Powell, J. R., Karunaratne, S., Campbell, C. D., Yao, H. Y., Robinson, L., and Singh, B. K. (2015). Deterministic processes vary during community assembly for ecologically dissimilar taxa. *Nat. Commun.* 6:8444. doi: 10.1038/ncomms9444

Qin, C., Zhu, K., Chiariello, N. R., Field, C. B., and Peay, K. G. (2020). Fire history and plant community composition outweigh decadal multi-factor global change as drivers of microbial composition in an annual grassland. *J. Ecol.* 108, 611–625. doi: 10.1111/1365-2745.13284

R Core Team (2015). *R: A Language and Environment for Statistical Computing*. Vienna: R Foundation for Statistical Computing.

Revelle, W. (2018). *psych: Procedures for Personality and Psychological Research*. Evanston, IL: Northwestern University.

Semchenko, M., Leff, J. W., Lozano, Y. M., Saar, S., Davison, J., and Bardgett, R. D. (2018). Fungal diversity regulates plant-soil feedbacks in temperate grassland. *Sci. Adv.* 4:eaau4578. doi: 10.1126/sciadv.aau4578

Serna-Chavez, H. M., Fierer, N., and van Bodegom, P. M. (2013). Global drivers and patterns of microbial abundance in soil. *Glob. Ecol. Biogeogr.* 22, 1162–1172. doi: 10.1111/geb.12070

Shen, C. C., Xiong, J. B., Zhang, H. Y., Feng, Y. Z., Lin, X. G., and Chu, H. Y. (2013). Soil pH drives the spatial distribution of bacterial communities along elevation on changbai mountain. *Soil Biol. Biochem.* 57, 204–211. doi: 10.1016/j.soilbio.2012.07.013

Sylvain, Z. A., Wall, D. H., Cherwin, K. L., Peters, D. P. C., Reichmann, L. G., and Sala, O. E. (2014). Soil animal responses to moisture availability are largely scale, not ecosystem dependent: insight from a cross-site study. *Glob. Chang Biol.* 20, 2631–2643. doi: 10.1111/gcb.12522

Tedersoo, L., Bahram, M., Polme, S., Koljalg, U., Yorou, N. S., Wijesundera, R., et al. (2014). Global diversity and geography of soil fungi. *Science* 346:1256688. doi: 10.1126/science.1256688

Tripathi, B. M., Stegen, J. C., Kim, M., Dong, K., Adams, J. M., and Lee, Y. K. (2018). Soil pH mediates the balance between stochastic and deterministic assembly of bacteria. *ISME J.* 12, 1072–1083. doi: 10.1038/s41396-018-0082-4

Vavrek, M. J. (2011). fossil: palaeoecological and palaeogeographical analysis tools. *Palaeontol. Electronica* 14:16.

Wang, D., Rui, Y. C., Ding, K., Cui, X. Y., Hao, Y. B., and Wang, Y. F. (2018). Precipitation drives the biogeographic distribution of soil fungal community in Inner Mongolian temperate grasslands. *J. Soils Sediments* 18, 222–228. doi: 10.1007/s11368-017-1727-z

Wang, Q., Garrity, G. M., Tiedje, J. M., and Cole, J. R. (2007). Naive bayesian classifier for rapid assignment of rRNA sequences into the new bacterial taxonomy. *Appl. Environ. Microbiol.* 73, 5261–5267. doi: 10.1128/Aem.00062-07

Wang, Y. S., Li, C. N., Kou, Y. P., Wang, J. J., Tu, B., Li, H., et al. (2017). Soil pH is a major driver of soil diazotrophic community assembly in qinghai-tibet alpine meadows. *Soil Biol. Biochem.* 115, 547–555. doi: 10.1016/j.soilbio.2017.09.024

Wei, C. Z., Yu, Q., Bai, E., Lu, X. T., Li, Q., and Han, X. G. (2013). Nitrogen deposition weakens plant-microbe interactions in grassland ecosystems. *Glob. Change Biol.* 19, 3688–3697. doi: 10.1111/gcb.12348

Xu, Z. W., Ren, H. Y., Cai, J. P., Wang, R. Z., He, P., Li, M. H., et al. (2015). Antithetical effects of nitrogen and water availability on community similarity of semiarid grasslands: evidence from a nine-year manipulation experiment. *Plant Soil* 397, 357–369. doi: 10.1007/s11104-015-2634-y

Yang, Y. H. (2018). Ecological processes in alpine ecosystems under changing environment. *J. Plant Ecol.* 42, 1–5. doi: 10.17521/cjpe.2018.0048

Zeng, J., Liu, X. J., Song, L., Lin, X. G., Zhang, H. Y., Shen, C. C., et al. (2016). Nitrogen fertilization directly affects soil bacterial diversity and indirectly affects bacterial community composition. *Soil Biol. Biochem.* 92, 41–49. doi: 10.1016/j.soilbio.2015.09.018

Zhang, H. F., Liu, H. M., Zhao, J. N., Wang, L. L., Li, G., and Yang, D. L. (2017). Elevated precipitation modifies the relationship between plant diversity and soil bacterial diversity under nitrogen deposition in Stipa baicalensis steppe. *Appl. Soil. Ecol.* 119, 345–353. doi: 10.1016/j.apsoil.2017.06.005

Zhang, H. F., Wang, L. L., Liu, H. M., Zhao, J. N., Li, G., and Yang, D. L. (2018). Nitrogen deposition combined with elevated precipitation is conducive to maintaining the stability of the soil fungal diversity on the *Stipa baicalensis* steppe. *Soil Biol. Biochem.* 117, 135–138. doi: 10.1016/j.soilbio.2017.11.004

Zhang, K. P., Shi, Y., Jing, X., He, J. S., Sun, R. B., and Chu, H. Y. (2016). Effects of short-term warming and altered precipitation on soil microbial communities in alpine grassland of the tibetan plateau. *Front. Microbiol.* 7:1032. doi: 10.3389/fmicb.2016.01032

Zhang, Y., Dong, S. K., Gao, Q. Z., Liu, S. L., Zhou, H. K., and Wang, X. X. (2016). Climate change and human activities altered the diversity and composition of soil microbial community in alpine grasslands of the qinghai-tibetan plateau. *Sci. Total Environ.* 562, 353–363. doi: 10.1016/j.scitotenv.2016.03.221

Zheng, D., and Zhao, D. S. (2017). Characteristics of natural environment of the Tibetan plateau. *Sci. Technol. Rev.* 35, 13–22.

Zhou, Z. H., Wang, C. K., and Luo, Y. Q. (2020). Meta-analysis of the impacts of global change factors on soil microbial diversity and functionality. *Nat. Commun.* 11:3072. doi: 10.1038/s41467-020-16881-7

Zong, N., Shi, P. L., Song, M. H., Zhang, X. Z., Jiang, J., and Chai, X. (2016). Nitrogen critical loads for an alpine meadow ecosystem on the tibetan plateau. *Environ. Manag.* 57, 531–542. doi: 10.1007/s00267-015-0626-6

Conflict of Interest: The authors declare that the research was conducted in the absence of any commercial or financial relationships that could be construed as a potential conflict of interest.

Copyright © 2020 Xiao, Li, Yang, Peng, Yang and Zhou. This is an open-access article distributed under the terms of the Creative Commons Attribution License (CC BY). The use, distribution or reproduction in other forums is permitted, provided the original author(s) and the copyright owner(s) are credited and that the original publication in this journal is cited, in accordance with accepted academic practice. No use, distribution or reproduction is permitted which does not comply with these terms.

frontiers in Microbiology

ORIGINAL RESEARCH
published: 29 October 2020
doi: 10.3389/fmicb.2020.572596

The Enigmatic Thelebolaceae (Thelebolales, Leotiomycetes): One New Genus *Solomyces* and Five New Species

Zhiyuan Zhang[1], Chunbo Dong[1], Wanhao Chen[2], Quanrong Mou[1], Xiaoxiao Lu[1], Yanfeng Han[1,3], Jianzhong Huang[4] and Zongqi Liang[1]*

[1] Institute of Fungus Resources, Department of Ecology, College of Life Sciences, Guizhou University, Guiyang, China, [2] Department of Microbiology, Guiyang College of Traditional Chinese Medicine, Guiyang, China, [3] Key Laboratory of Plant Resource Conservation and Germplasm Innovation in Mountainous Region (Ministry of Education), Guizhou University, Guiyang, China, [4] Engineering Research Center of Industrial Microbiology, Ministry of Education, Fujian Normal University, Fuzhou, China

The family Thelebolaceae belongs to the order Thelebolales, class Leotiomycetes, and contains 22 genera. In this study, we introduce a new genus *Solomyces* gen. nov. in the family Thelebolaceae, which is supported by morphological observation and multilocus-based [internal transcribed spacers (ITS) + *LSU* and ITS + *LSU*+ *MCM7*+ *EF1A*+ *RPB2*] phylogenetic analysis. Maximum-likelihood and Bayesian phylogenetic inference analyses indicated that *Solomyces* is a distinct genus within this family. The new genus is compared against related Thelebolaceae genera, and its description and illustration are provided. This genus comprises one new species and one unnamed species (including two strains). We also report the addition of four new species – *Pseudogymnoascus shaanxiensis*, *Pseudogymnoascus guizhouensis*, *Pseudogymnoascus sinensis*, and *Geomyces obovatus* – in the family Thelebolaceae and present their morphological and phylogenetic characterizations.

Keywords: taxonomy, phylogeny, Thelebolales, new genus, new species

OPEN ACCESS

Edited by:
Gustavo Henrique Goldman, University of São Paulo, Brazil

Reviewed by:
Hiran A. Ariyawansa, National Taiwan University, Taiwan
Donald Henry Pfister, Harvard University, United States

****Correspondence:***
Yanfeng Han
swallow1128@126.com

Specialty section:
This article was submitted to Fungi and Their Interactions, a section of the journal Frontiers in Microbiology

Received: *15 June 2020*
Accepted: *29 September 2020*
Published: *29 October 2020*

Citation:
Zhang Z, Dong C, Chen W, Mou Q, Lu X, Han Y, Huang J and Liang Z (2020) The Enigmatic Thelebolaceae (Thelebolales, Leotiomycetes): One New Genus Solomyces and Five New Species. Front. Microbiol. 11:572596. doi: 10.3389/fmicb.2020.572596

INTRODUCTION

The class Leotiomycetes (Pezizomycotina) was erected by Eriksson and Winka (1997) to accommodate inoperculate discomycetes. Fungi in the class Leotiomycetes are ecologically diverse and include mycorrhizas, root and leaf endophytes, plant pathogens, aquatic and aeroaquatic hyphomycetes, mammalian pathogens, and saprobes (Johnston et al., 2019). Leotiomycetes currently comprises 19 orders and order-level clades, 54 families, and 13 family level clades (Ekanayaka et al., 2019; Karunarathna et al., 2020). Previously, however, this class included a wide range of taxa based on traditional morphological taxonomy (Korf, 1973; Spooner, 1987), and the current classification of Leotiomycetes is still largely based on morphologically defined taxa, especially at higher taxonomic levels (Johnston et al., 2019). Nevertheless, sexual or asexual morphs of many Leotiomycetes taxa are not recorded, and a few links between sexual and asexual morphs in Leotiomycetes have been confirmed (Sutton and Hennebert, 1995; Sati and Pathak, 2016; Ekanayaka et al., 2017; Johnston et al., 2019). Thelebolales, an order in the class Leotiomycetes, consists of Thelebolaceae and the *Alatospora–Miniancora* clade, in which some

genera (e.g., *Caccobius*, *Coprobolus*, and *Leptokalpion*) are erected based on their sexual, but not asexual, morphology (Wijayawardene et al., 2017).

Haeckel (1894) introduced the order Thelebolales; however, the taxonomy of this order has long been contentious. Some researchers believed that the order contained only one family (De Hoog et al., 2005), whereas others suggested that at least two families were involved (Ekanayaka et al., 2019; Johnston et al., 2019; Batista et al., 2020). The family Thelebolaceae is important in the order Thelebolales because of several species that can produce antifreeze proteins, ice-binding proteins, and some secondary metabolites with potential application values that offer valuable resources for biotechnological exploitation (Batista et al., 2020); the family was introduced by Eckblad (1968) and typified by the genus *Thelebolus* with *Thelebolus stercoreus* as the type species. Members of this family are characterized by absent, apothecial, or cleistothecial ascomata (Van Brummelen, 1985; Stchigel et al., 2001; De Menezes et al., 2017; Ekanayaka et al., 2019). During an extensive diversity survey of *Geomyces* and allied genera in China, we gathered a collection of fungal isolations. In this study, we introduced their morphological, cultural, and phylogenetic characterization and propose one new genus and five new species.

MATERIALS AND METHODS

Isolates and Morphology

Soil samples were obtained from Dali City, Yunnan Province; Guiyang City, Guizhou Province; Xi'an and Hanzhong City, Shaanxi Province; and Yichang City, Hubei Province, China. Samples were treated according to the method described by Zhang et al. (2019). Fungi were isolated using a modified baiting technique with chicken feathers as the substrate (Vanbreuseghem, 1952). The feathers were washed, thoroughly rinsed with distilled water, dried, cut into 2-cm fragments, and autoclaved. Plates containing soil material and sterile feathers were incubated at room temperature for 1 month. Fungi were isolated and purified using a conventional dilution technique described by Zhang et al. (2019), as follows: 2 g of soil sample was suspended in 9 ml of distilled water, and the prepared suspension was vortexed, diluted to 1:10,000, and cultured on Sabouraud's dextrose agar (SDA; 10 g of peptone, 40 g of dextrose, 20 g of agar, 1 L of ddH_2O) supplemented with chloramphenicol and cycloheximide. The plates were incubated at 25°C until fungal colony growth was observed. The axenic strains were then transferred to potato dextrose agar (PDA; Shanghai Bio-way Technology Co., Ltd., China) plates for purification. Dried holotypes were deposited in the Mycological Herbarium of the Institute of Microbiology, Chinese Academy of Sciences, Beijing, China (HMAS), or the Institute of Fungus Resources, Guizhou University (GZUIFR, formally the Herbarium of Guizhou Agricultural College; code, GZAC). Ex-type strains and other strains were deposited in the China General Microbiological Culture Collection Center (CGMCC) or the GZUIFR.

The pure strains were incubated on PDA at 25°C for 14 days in the dark to determine the macroscopic characteristics, diameters, and colony colors (surface and reverse). The characterization and measurement of fungal microscopic characteristics were performed in 25% lactic acid. Images were obtained using an optical microscope (OM, DM4 B, Leica, Germany) with differential interference contrast (DIC). The taxonomic descriptions and names of the new taxa were introduced into MycoBank[1] and Faces of Fungi[2].

DNA Extraction, PCR Amplification, and Sequencing

Total DNA was extracted using the BioTeke Fungus Genomic DNA Extraction kit (DP2032, BioTeke, Beijing, China) following the manufacturer's instructions. Total DNA was used for the amplification and sequencing of five fragments: ribosomal internal transcribed spacers (ITS; primers ITS1/ITS4) (White et al., 1990), the 28S LSU rRNA gene (primers LROR/LR7) (Vilgalys and Hester, 1990; Vilgalys and Sun, 1999), translation elongation factor 1 alpha (*EF1A*; primers 983F/2218R) (Rehner and Buckley, 2005), RNA polymerase II subunit 2 (*RPB2*; primers fRPB2-7cF/RPB2-3053b) (Liu et al., 1999; Reeb et al., 2004), and minichromosomal maintenance protein 7 (*MCM7*; primers MCM7-709/MCM7-1348) (Schoch et al., 2009). The PCR products were sequenced with the abovementioned primers at a commercial sequencing service provider (Shanghai Sangon Biological Engineering Technology & Services Co., Shanghai, China) in an ABI 3730xl DNA Analyzer, using the Sanger method. The consensus sequences were obtained using the SeqMan software v. 7 (DNASTAR Lasergene, Madison, WI, United States). Sequences generated in this study were deposited in GenBank (**Table 1**).

Phylogenetic Analyses

Sequence data were selected from data previously published by Crous et al. (2019), Ekanayaka et al. (2019), Johnston et al. (2019), and Minnis and Lindner (2013) and then downloaded from GenBank for molecular phylogenetic analyses (**Table 1**). Multiple sequence alignments for ITS, *LSU*, *MCM7*, *RPB2*, and *EF1A* were carried out using MAFFT v7.037b (Katoh and Standley, 2013). Sequence editing was performed with MEGA6 (Tamura et al., 2013). The concatenated ITS and *LSU*, and ITS, *LSU*, *MCM7*, *RPB2*, and *EF1A* sequences were assembled by SequenceMatrix v.1.7.8 (Vaidya et al., 2011). Gene concordance was assessed with the "hompart" command in PAUP4.0b10 (Swofford, 2002).

Sequence alignment and maximum-likelihood (ML) and Bayesian inference (BI) phylogenetic analyses were performed according to the methodology described by Zhang et al. (2019). Maximum-likelihood (ML) analyses were constructed with IQ-TREE v. 1.6.11 (Nguyen et al., 2015). The best-fit model of substitution for each locus was estimated using IQ-TREE's ModelFinder function (Kalyaanamoorthy et al., 2017) under the Bayesian information criterion (BIC). Bootstrap analysis was performed using the ultrafast bootstrap approximation (Minh et al., 2013) with 1,000 replicates, and bootstrap support (BS) ≥90% was considered as statistically significant. For

[1] www.Mycobank.org

[2] www.facesoffungi.org

TABLE 1 | List of strains used in the phylogenetic analysis.

Species	Strain	GenBank Accession				
		ITS	LSU	MCM7	RPB2	EF1A
Alatospora acuminata	CBS 104.88	MH862121	MH873811	NA	NA	NA
Alatospora constricta	CCM F-11302	KC834040	KC834017	NA	NA	NA
Alatospora pulchella	CCM F-502	KC834039	KC834019	NA	NA	NA
Antarctomyces pellizariae	UFMGCB 12416	KX576510	NA	NA	NA	NA
Antarctomyces psychrotrophicus	CBS 100573	MH874317	NA	NA	NA	NA
Cleistothelebolus nipigonensis	CBS 778.70	MH859938	MH871738	NA	NA	NA
Crinula caliciiformis	AFTOL-ID 272	KT225524	AY544680	NA	NA	NA
Epiglia gloeocapsae	CBS 126301	MH863968	MH875423	NA	NA	NA
	CBS 126302	MH863969	MH875424	NA	NA	NA
Geomyces auratus	CBS 108.14	KF039895	KF017864	KF017690	KF017746	KF017805
Geomyces obovatus	CGMCC 3.18491	MT509362	MT509376	MT534202	MT534216	MT534227
	CGMCC 3.18492	MT509363	MT509377	MT534203	MT534217	MT534228
Gorgomyces honrubiae	CCM F-12003	KC834057	KC834028	NA	NA	NA
	CCM F-12696	KC834058	NA	NA	NA	NA
Gymnostellatospora alpina	CBS 620.81	MH861383	MH873132	NA	NA	NA
	UAMH 9430	DQ117459	NA	NA	NA	NA
Holwaya mucida	NBRC 112552	LC425042	LC429385	NA	NA	NA
Leuconeurospora pulcherrima	CBS 343.76	KF049206	FJ176884	NA	FJ238367	FJ238409
Leuconeurospora polypaeciloides	UAMH 11459	KC884266	NA	NA	NA	NA
Leuconeurospora sp.	01NH01	JX270336	KF017814	KF017645	KF017699	KF017754
Leuconeurospora sp.	01NH04	JX270339	KF017815	KF017646	KF017700	KF017755
Leuconeurospora sp.	02NH04	JX270349	KF017817	KF017648	KF017702	KF017757
Leuconeurospora sp.	15PA04	JX270479	KF017841	KF017669	KF017725	KF017781
Miniancora allisoniensis	CCM F-30487	KC834064	NA	NA	NA	NA
Patinella hyalophaea	H.B. 9739	KT876978	KT876978	NA	NA	NA
Pseudeurotium ovale	CBS 531.71	MH860256	MH872019	NA	NA	NA
	CBS 460.69	MH859352	MH871109	NA	NA	NA
Pseudeurotium zonatum	CBS 329.36	AY129286	DQ470988	NA	DQ470940	DQ471112
	CBS 391.61	MH858096	MH869666	NA	NA	NA
Pseudogymnoascus appendiculatus	02NH11	JX270356	KF017819	KF017650	KF017704	KF017759
	07MA02	JX270402	KF017827	KF017658	KF017712	KF017767
Pseudogymnoascus bhattii	CBS 760.71	MH860337	MH872092	NA	NA	NA
	CBS 761.71	MH860338	MH872093	NA	NA	NA
	CBS 762.71	MH860339	MH872094	NA	NA	NA
Pseudogymnoascus destructans	20631-21	EU884921	KF017865	KF017691	KF017747	KF017806
Pseudogymnoascus guizhouensis	GZUIFR 376.1	MT509369	MT509383	MT534209	MT534223	MT534234
	GZUIFR 376.2	MT509370	MT509384	MT534210	MT534224	MT534235
	GZUIFR 376.3	MT509371	MT509385	MT534211	MT534225	MT534236
	GZUIFR 376.4	MT509372	MT509386	MT534212	MT534226	MT534237
Pseudogymnoascus lindneri	02NH05	JX270350	KF017818	KF017649	KF017703	KF017758
	LHU 158	MN542212	NA	NA	MN541384	MN541383
Pseudogymnoascus shaanxiensis	GZUIFR HZ5.7	MT509366	MT509380	MT534206	MT534220	MT534231
	GZUIFR CY1.8	MT509367	MT509381	MT534207	MT534221	MT534232
	GZUIFR 173.1	MT509368	MT509382	MT534208	MT534222	MT534233
	14PA06	JX270469	KF017839	KF017668	KF017723	KF017779
	RMF C 101	KF039896	KF017869	KF017695	KF017750	KF017810
Pseudogymnoascus roseus	05NY06	JX270385	KF017824	KF017655	KF017709	KF017764
	05NY08	JX270387	KF017825	KF017656	KF017710	KF017765
	05NY09	JX270388	KF017826	KF017657	KF017711	KF017766
	WSF 3629	KF039897	KF017870	KF017696	KF017751	KF017811

(Continued)

TABLE 1 | Continued

Species	Strain	GenBank Accession				
		ITS	LSU	MCM7	RPB2	EF1A
Pseudogymnoascus sinensis	CGMCC 3.18493	MT509364	MT509378	MT534204	MT534218	MT534229
	CGMCC 3.18494	MT509365	MT509379	MT534205	MT534219	MT534230
Pseudogymnoascus turneri	Ps5	MN542214	NA	NA	MN541382	MN541381
	LHU 121	MN542213	NA	NA	MN541380	MN541379
Pseudogymnoascus verrucosus	04NY16	JX270377	KF017822	KF017653	KF017707	KF017762
	24MN13	JX270621	KF017861	KF017687	KF017743	KF017802
	01NH08	JX270343	KF017816	KF017647	KF017701	KF017756
Pseudogymnoascus sp.	10NY09	JX270433	KF017830	KF017660	KF017715	KF017770
Pseudogymnoascus sp.	MN-Mycosel-7	KF039899	KF017872	KF017698	KF017753	KF017813
Pseudogymnoascus sp.	10NY10	JX270434	KF017831	NA	KF017716	KF017771
Pseudogymnoascus sp.	18VA08	JX270528	KF017848	KF017676	KF017731	KF017789
Pseudogymnoascus sp.	21IN01	JX270568	KF017854	KF017680	KF017737	KF017795
Pseudogymnoascus sp.	11MA05	JX270440	KF017833	KF017662	KF017718	KF017773
Pseudogymnoascus sp.	11MA07	JX270442	KF017834	KF017663	KF017719	KF017774
Pseudogymnoascus sp.	A07MA10	KF039893	KF017828	NA	KF017713	KF017768
Pseudogymnoascus sp.	24MN14	JX270622	KF017862	KF017688	KF017744	KF017803
Pseudogymnoascus sp.	18VA12	JX270532	KF017849	NA	KF017732	KF017790
Pseudogymnoascus sp.	18VA13	JX270533	KF017850	NA	KF017733	KF017791
Pseudogymnoascus sp.	12NJ13	JX270459	KF017838	KF017667	KF017722	KF017778
Pseudogymnoascus sp.	17WV06	JX270513	NA	KF017673	KF017729	KF017785
Ramgea ozimecii	CNF 2/9997	KY368752	KY368753	NA	NA	NA
Solomyces sinensis	CGMCC 3.18498	MT509373	MT509387	MT534213	NA	MT534238
	CGMCC 3.18499	MT509374	MT509388	MT534214	NA	MT534239
	CGMCC 3.18500	MT509375	MT509389	MT534215	NA	MT534240
Solomyces sp.	15PA02	JX270477	KF017840	NA	KF017724	KF017780
	17WV02	JX270509	KF017845	NA	KF017730	KF017786
Thelebolus balaustiformis	MUT 2357	NR_159056	NG_067559	NA	NA	NA
Thelebolus globosus	CBS 113940	MH862951	NG_067263	NA	NA	NA
Thelebolus spongiae	MUT 2359	MG813185	MG816493	NA	NA	NA

CBS, Westerdijk Fungal Biodiversity Institute, Utrecht, Netherlands; CGMCC, China General Microbiological Culture Collection Center, Beijing, China; GZUIFR, Guizhou University, Institute of Fungus Resources; CCM, Czech Collection of Microorganisms, Brno, Czechia; NBRC (IFO), Institute for Fermentation, Osaka, Japan; UAMH, UAMH Centre for Global Microfungal Biodiversity, Toronto, ON, Canada; MUT, Mycotheca Universitatis Taurinensis, Turin, Italy; NA, not available. DNA sequences for the new isolates were in blue.

Bayesian inference (BI), a Markov chain Monte Carlo (MCMC) algorithm was used to generate phylogenetic trees with Bayesian probabilities using MrBayes v.3.2 (Ronquist et al., 2012) for the combined sequence datasets. The selection of the best-fit nucleotide substitution model for each locus was calculated by the Akaike information criterion (AIC) with ModelTest v.3.7 (Posada and Crandall, 1998). After the BI analyses, both runs were examined with Tracer v.1.5 (Drummond and Rambaut, 2007) to determine burn-in and check for convergence.

Two multilocus phylogenies were analyzed to evaluate the various generic placements and establish the phylogenetic relationships in Thelebolaceae. The genus placement was evaluated based on a concatenated ITS and *LSU* dataset. This phylogeny was constructed to assess if *Solomyces* is a well-delimited genus. The second multilocus phylogeny was based on a concatenated alignment of ITS, *LSU*, *MCM7*, *RPB2*, and *EF1A* sequences and included 49 isolates of *Geomyces* and its allied genera. This analysis was performed to evaluate the generic boundaries and species groupings within the genera *Solomyces*, *Geomyces*, and *Pseudogymnoascus*. All the trees were displayed in FigTree 1.4.2[3] and edited in Microsoft Paint. DNA alignments have been deposited at TreeBASE.

RESULTS

Phylogenetic Analyses

The first concatenated matrix contains 1,220 nucleotides, i.e., 445 from the ITS and 775 from the *LSU*. The second concatenated alignment contained 2,808 nucleotides (ITS: 434, *LSU*: 806, *MCM7*: 503, *RPB2*: 437, and *EF1A*: 628). The best-fit evolutionary model for each locus in the two datasets is listed in **Table 2**. The tree topology of the Bayesian inference agrees with that of the ML tree (**Figures 1**, **2**). The phylogenies indicated that each genus clusters into a monophyletic clade (**Figure 1**). In

[3]http://tree.bio.ed.ac.uk/software/figtree

TABLE 2 | The best-fit evolutionary model in the phylogenetic analyses.

Dataset/phylogenetic analysis		Model				
		ITS	LSU	MCM7	RPB2	EF1A
First dataset	ML analysis	TIM2e + I + G4	K2P + R2			
	BI analysis	GTR + I + G	GTR + I + G			
Second dataset	ML analysis	TIM2e + R3	TPM2u + F + I	TNe + I + G4	TNe + I + G4	TIM2e + R3
	BI analysis	SYM + I + G	GTR + I	HKY + I + G	K80 + I + G	SYM + I + G

ML, maximum likelihood; BI, Bayesian inference.

the phylogenetic tree, the new genus *Solomyces* forms a well-supported (1 BYPP/100 MLBS) clade separated from other genera in Thelebolaceae (**Figure 1**). *Solomyces sinensis* represents a separate subclade and is located within the new genus near another unnamed species (includes two strains, 15PA02 and 17WV02, from Hibernacular soil). Furthermore, all the new species of *Pseudogymnoascus* and *Geomyces* are placed in a distinct branch.

Taxonomy

In this section, *Solomyces* Zhi.Y. Zhang, Y.F. Han and Z.Q. Liang, gen. nov. and five new species – *S. sinensis* Zhi.Y. Zhang, Y.F. Han and Z.Q. Liang, sp. nov.; *Geomyces obovatus* Zhi.Y. Zhang, Y.F. Han and Z.Q. Liang, sp. nov.; *Pseudogymnoascus guizhouensis* Zhi.Y. Zhang, Y.F. Han and Z.Q. Liang, sp. nov.; *Pseudogymnoascus shaanxiensis* Zhi.Y. Zhang, Y.F. Han and Z.Q. Liang, sp. nov.; and *Pseudogymnoascus sinensis* Zhi.Y. Zhang, Y.F. Han and Z.Q. Liang, sp. nov. – are described and illustrated. We also propose a new combination, *Gymnostellatospora bhattii* (Samson) Zhi.Y. Zhang, Y.F. Han and Z.Q. Liang, comb. nov. based on phylogenetic analyses.

Geomyces obovatus Zhi.Y. Zhang, Y.F. Han and Z.Q. Liang, sp. nov.

MycoBank number: MB 835718, Facesoffungi number: FoF 08691 (**Figure 3**).

Etymology: Referring to the obovoid conidia.

Holotype: permanently preserved in a metabolically inactive state, GZAC 20.8.

Description based on GZAC 20.8. Asexual: Colonies on PDA, reaching 28–30 mm in diameter after 14 days at 25°C, slightly felty to floccose, margin identified, khaki at center, and white at edge; reverse hazel. Aerial mycelium abundant, smooth and thin walled, septate, 0.5- to 2-μm wide. Racquet hyphae absent. Conidia abundant, normally terminal and intercalary conidia in a series of 1–4, rarely solitary on short stalk, smooth or echinulate, 3.0–5.0 × 2.5–4.0 μm (*av.* = 3.5 × 2.5 μm, *n* = 50). Terminal conidia obovoid, rarely subglobose; intercalary conidia alternate and pyriform, barrel or irregularly shaped.

Sexual morph: not observed.

Geographical distribution: China.

Material examined: China, Guizhou, Guiyang, Qianlingshan Park, 26°60′N, 106°69′E, from soil beside a road, September 2016, Zhi. Y. Zhang (GZAC 20.8 – holotype; CGMCC 3.18491 = GZUIFR QL20.8.1 – ex-type living cultures; ibid., CGMCC 3.18492 = GZUIFR QL20.8.2). The living cultures were kept in sterile 30% glycerol and deposited in a −80°C freezer.

Notes: The *Geomyces* was introduced by Traaen (1914), and several species have subsequently been described. Currently, the genus contains seven species (Traaen, 1914; Dal Vesco, 1957; Sigler and Carmichael, 1976; Hocking and Pitt, 1988; Li and Cui, 1989; Luo et al., 2016; Chen et al., 2017): *Geomyces auratus*, *Geomyces asperulatus*, *Geomyces vinaceus*, *Geomyces pulvereus*, *Geomyces laevis*, *Geomyces guiyangensis*, and *Geomyces fujianensis*. *G. asperulatus* and *G. vinaceus* likely belong to *Pseudogymnoascus* (Minnis and Lindner, 2013); *G. pulvereus* and *G. laevis* do not have any available sequence data; *G. pulvereus* lacks intercalary conidia (Hocking and Pitt, 1988), and *G. laevis* has oblong-elliptical or barrel-shaped intercalary conidia (Li and Cui, 1989). Only ITS sequences are available for *G. guiyangensis* and *G. fujianensis*, and the ITS data for CGMCC 3.18491 (the type strain of *G. obovatus*) show similarity to those of *G. guiyangensis* (strain G014512) (465/509; 91%, with 4 gaps) and *G. fujianensis* (strain G242) (464/526; 88%, with 11 gaps); however, the latter two species have no intercalary conidia (Luo et al., 2016; Chen et al., 2017). The proposed new species, *G. obovatus*, is morphologically and phylogenetically related to *G. auratus*, but they can be distinguished by their ITS (512/524; 97%, with three gaps), *LSU* (931/938; 99%, no gaps), *MCM7* (592/619; 95%, no gaps), *RPB2* (696/717; 97%, no gaps), and *EF1A* (843/855; 98%, with one gap) sequence data.

Gymnostellatospora bhattii (Samson) Zhi.Y. Zhang, Y.F. Han and Z.Q. Liang, comb. nov.

Basionym: *Pseudogymnoascus bhattii* Samson, *Acta Botanica Neerlandica* 21: 519. 1972.

Notes: This species was erected by Samson (1972) based on morphological characteristics. However, our phylogenetic analysis based on Thelebolaceae ITS and *LSU* data indicated that this species was closely related to *Gymnostellatospora* and separated from *Pseudogymnoascus*. Based on morphological characteristics, it was difficult to distinguish the closely related species, and even the genera, through traditional taxonomy, and modern phylogenetic methods were a very important adjunct. We therefore transferred *P. bhattii* to *Gymnostellatospora* and named the species *G. bhattii*.

Pseudogymnoascus guizhouensis Zhi.Y. Zhang, Y.F. Han and Z.Q. Liang, sp. nov.

MycoBank number: MB 835716, Facesoffungi number: FoF 08692 (**Figure 4**).

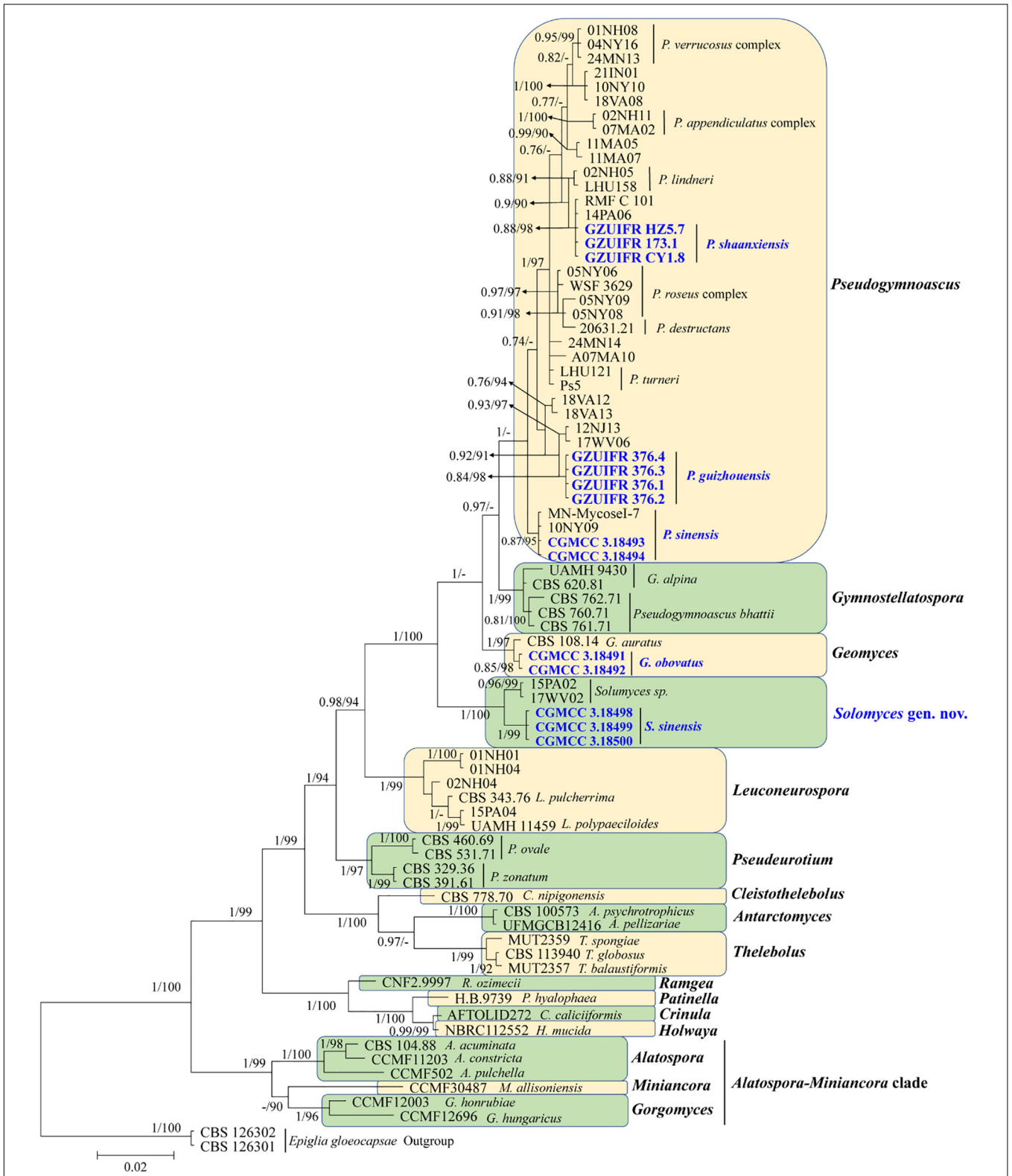


FIGURE 1 | Phylogenetic relationships among the genera in Thelebolales based on Bayesian inference and maximum-likelihood analyses of the concatenated internal transcribed spacers (ITS) and *LSU* dataset. Posterior probabilities ≥0.7 and maximum-likelihood bootstrap values ≥90% are shown above the internal branches. The new isolates are presented in bold and blue.

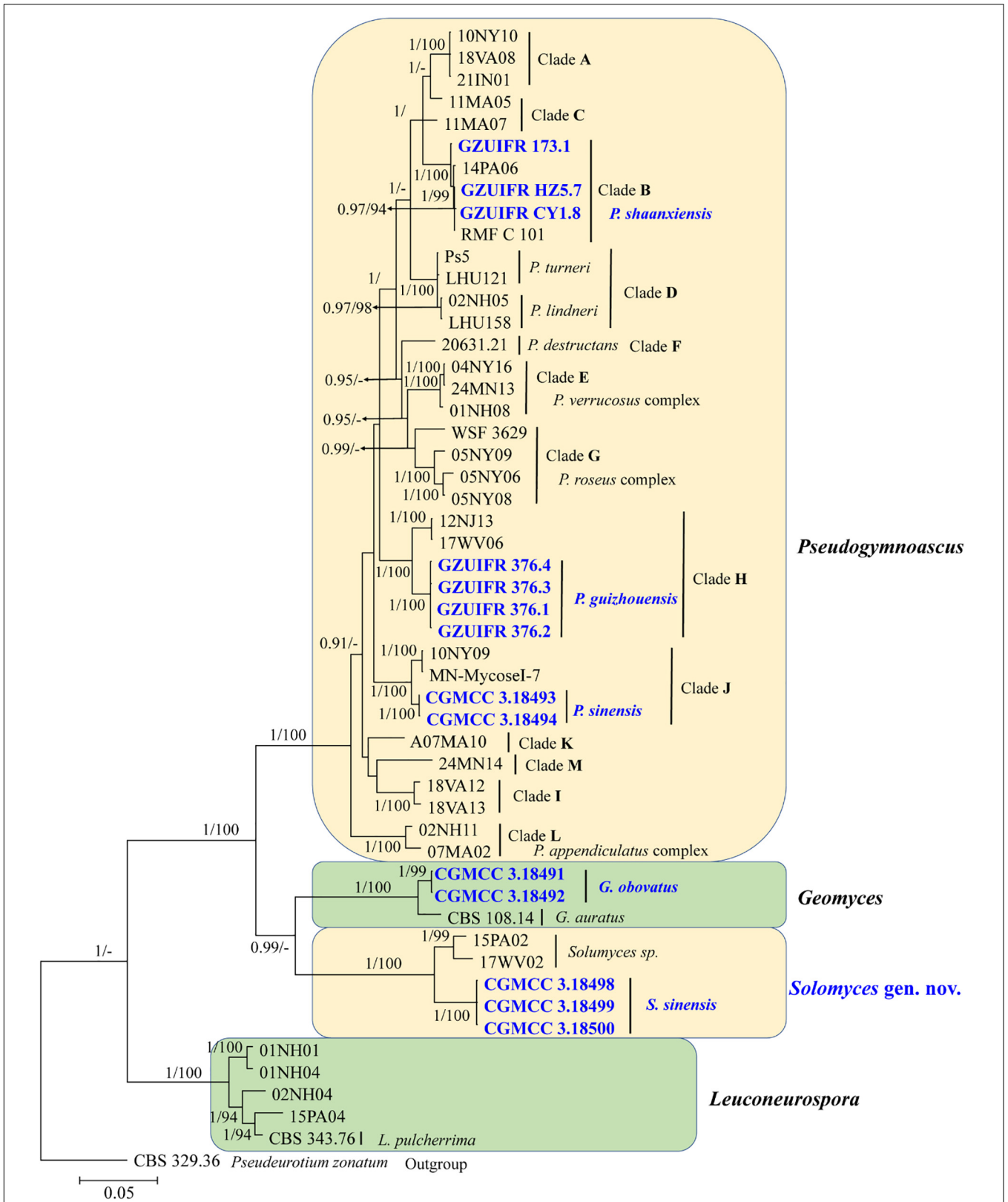


FIGURE 2 | The consensus tree from the Bayesian inference and *Geomyces* and its allied genera based on the ITS, *LSU*, *MCM7*, *RPB2*, and *EF1A* concatenated dataset. Posterior probabilities ≥0.7 and maximum-likelihood bootstrap values ≥90% are shown above the internal branches. The new isolates are presented in bold and blue.

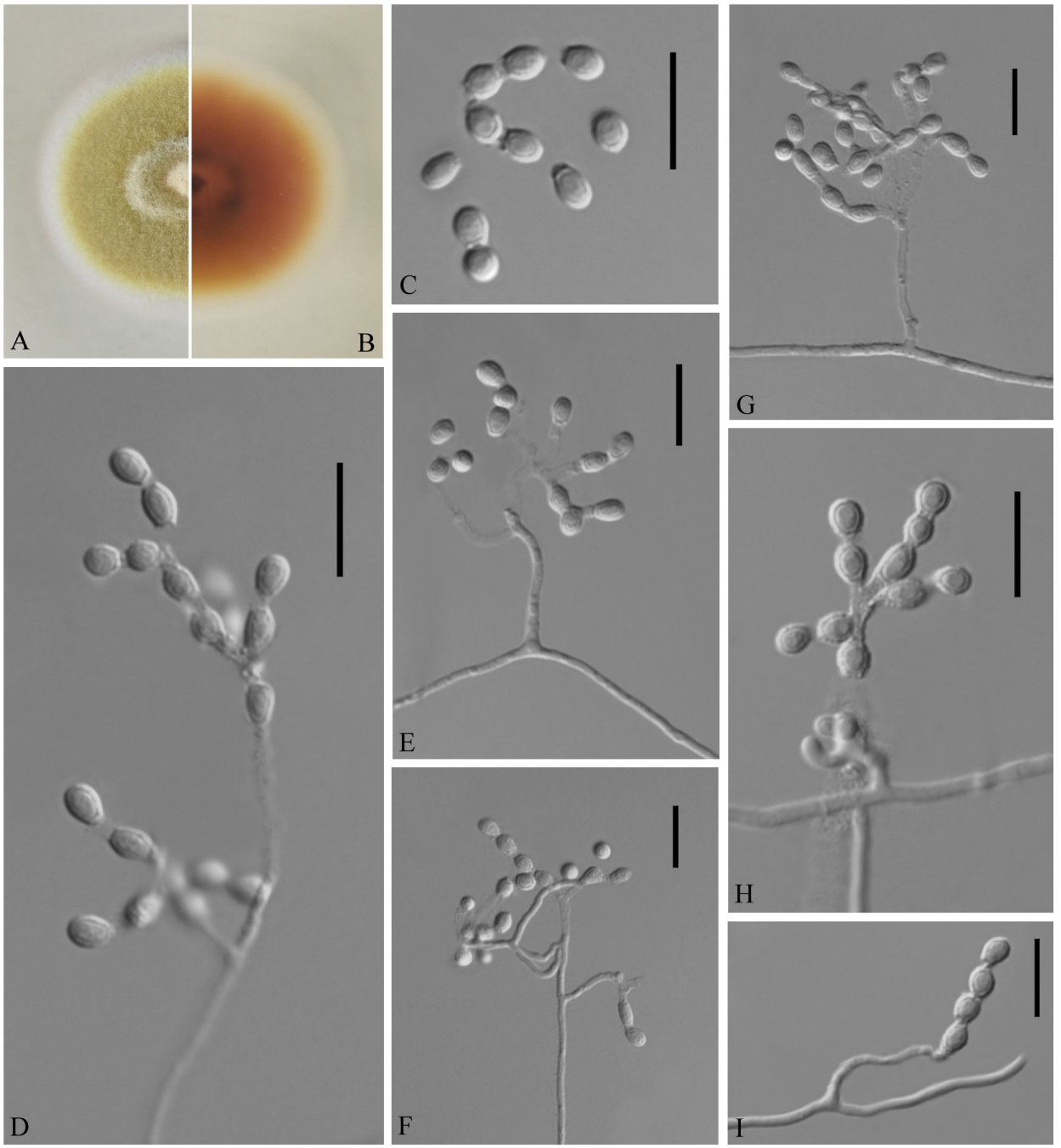


FIGURE 3 | *Geomyces obovatus* [from ex-holotype China General Microbiological Culture Collection Center (CGMCC) 3.18491]. **(A,B)** The front and reverse of a *G. obovatus* colony on potato dextrose agar (PDA) after 14 days at 25°C. **(C–I)** Conidiophores and conidia. Scale bars = 10 μm.

Etymology: Refers to the region from which the fungus was isolated.

Holotype: permanently preserved in a metabolically inactive state, GZAC 376.

Description based on GZAC 376. Asexual: Colonies on PDA, reaching 20–23 mm in diameter after 14 days at 25°C, elevate, powdery, floccose, margin identified, locally indented, pale purple at center and white at the edge, producing a clear exudate; reverse brown. Aerial mycelium abundant, smooth and thin walled, septate, 1.5- to 3.0-μm wide. Racquet hyphae absent. Conidia normally borne on verticillate branches, terminal, intergrading with intercalary conidia, sometimes borne laterally and solitary on hyphae, smooth walled or echinulate, obovoid, pyriform, subglobose or clavate, 3.0–5.5 × 3.0–3.5 μm (*av.* = 4.0 × 3.0 μm,

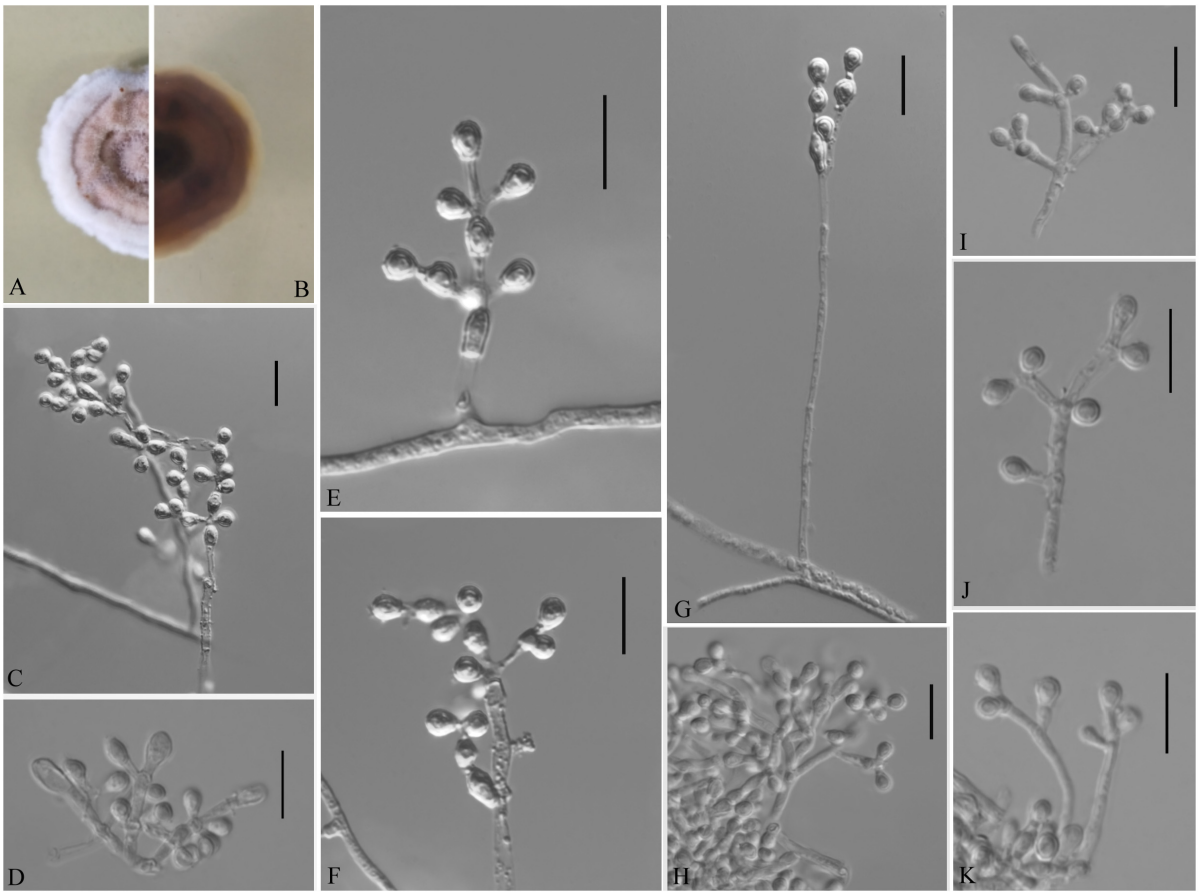


FIGURE 4 | *Pseudogymnoascus guizhouensis* [from ex-holotype Institute of Fungus Resources, Guizhou University (GZUIFR) 376.1]. **(A,B)** The front and reverse of a *P. guizhouensis* colony on PDA after 14 days at 25°C. **(C–K)** Conidiophores and conidia. Scale bars = 10 μm.

n = 50). Intercalary conidia are borne on the outer branches of the hyphae or verticillate hyphae, alternate, in series of 1–2, smooth walled or echinulate, cuneiform, barrel shaped, 3.5–6.0 × 3.0–3.5 μm (*av*. = 4.0 × 3.0 μm, *n* = 50).

Sexual morph: not observed.

Geographical distribution: China.

Material examined: China, Guizhou, Guiyang, Guizhou University, 26°45′N, 106°67′E, from epiphytic soil of *Cinnamomum camphora*, June 2019, Zhi. Y. Zhang (GZAC 376 – holotype; GZUIFR 376.1 – ex-type living culture; ibid., GZUIFR 376.2; ibid., GZUIFR 376.3; ibid., GZUIFR 376.4). The living cultures were kept in sterile 30% glycerol and deposited in a −80°C freezer.

Notes: Morphologically, *Pseudogymnoascus guizhouensis* is similar to *Pseudogymnoascus linderi*, *Pseudogymnoascus turneri* (both isolated from sediment), and *Pseudogymnoascus destructans* (isolated from a wing of a small brown bat, *Myotis lucifugus*), based on the obovoid and subglobose conidia. However, *P. guizhouensis* differs from *P. linderi* and *P. turneri* as it has cuneiform, barrel-shaped intercalary conidia (the intercalary conidia of *P. linderi* and *P. turneri* are globose to truncate) (Crous et al., 2019). *P. guizhouensis* can be distinguished from *P. destructans* by the size of conidia and intercalary conidia (4.0 × 3.0 μm vs. 5.0–12.0 × 2.0–3.5 μm, respectively) (Gargas et al., 2009). Phylogenetically, our isolates GZUIFR 376.1, GZUIFR 376.2, GZUIFR 376.3, and GZUIFR 376.4 cluster together very well and form a single clade separated from other *Pseudogymnoascus* species (**Figures 1**, **2**).

Pseudogymnoascus shaanxiensis Zhi.Y. Zhang, Y.F. Han and Z.Q. Liang, sp. nov.

MycoBank number: MB 835715, Facesoffungi number: FoF 08689 (**Figure 5**).

Etymology: Refers to Shaanxi, the province where the isolate was collected.

Holotype: permanently preserved in a metabolically inactive state, HMAS 255395.

Description based on HMAS 255395. Asexual: Colonies on PDA, reaching 21–23 mm in diameter after 14 days at 25°C, velvety to floccose, margins regular, white, producing a diffusible faint yellow pigment and clear exudates; reverse brown. Hyphae hyaline, smooth-walled, septate, 1.5- to 2.5-μm wide.

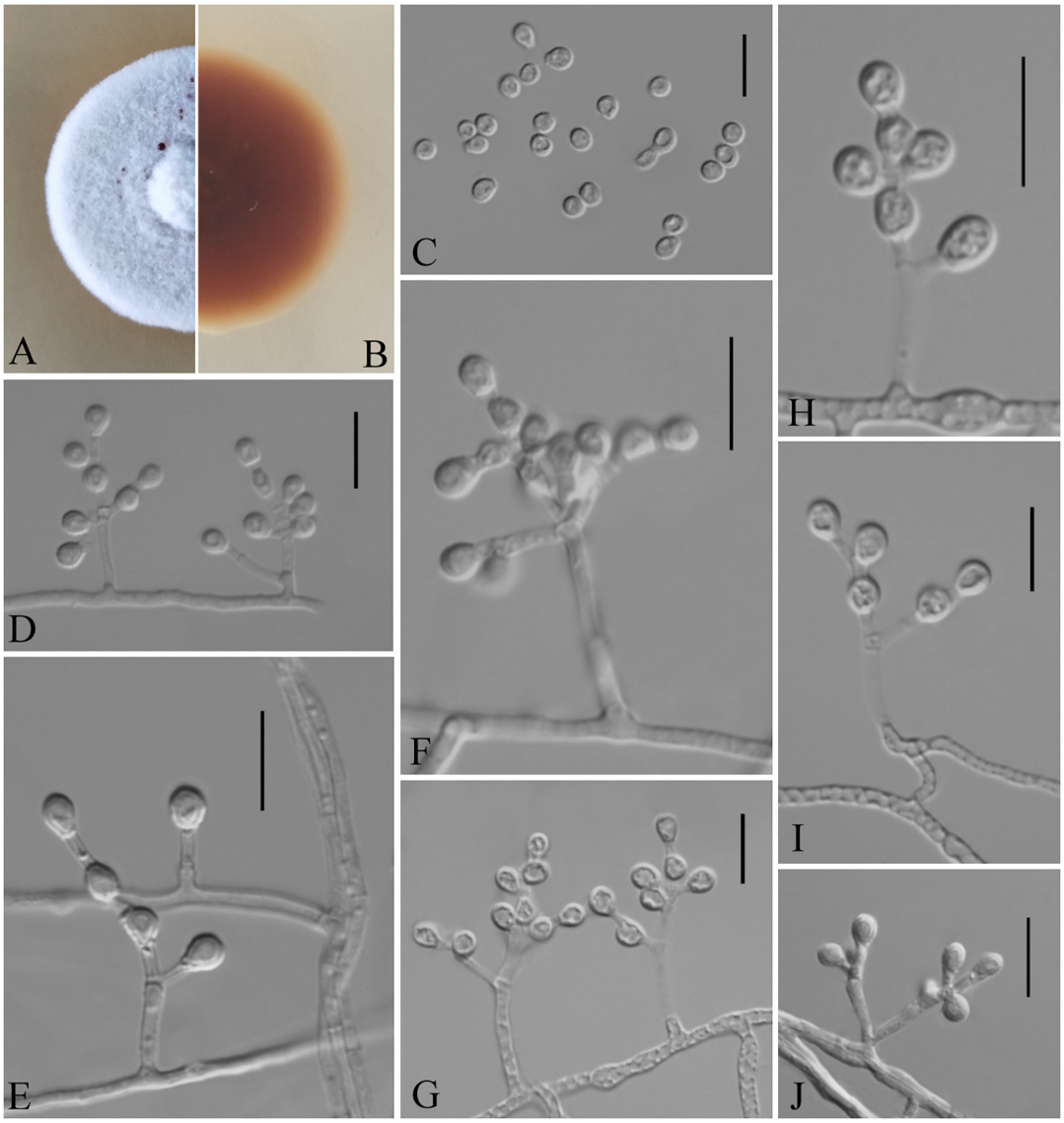


FIGURE 5 | *Pseudogymnoascus shaanxiensis* (from ex-holotype GZUIFR 173.1). **(A,B)** The front and reverse of a *P. shaanxiensis* colony on PDA after 14 days at 25°C. **(C)** Conidia. **(D–J)** Conidiophores and conidia. Scale bars = 10 μm.

Racquet hyphae absent. Conidia abundant, pyriform, sometimes subglobose, smooth 3.5–5.0 × 2.5–3.0 μm (*av.* = 4.0 × 3.0 μm, *n* = 50). Intercalary conidia subglobose, pyriform, or irregularly shaped, smooth, 3.5–4.0 × 3.0–4.0 μm (*av.* = 3.5 × 3.0 μm, *n* = 50). Terminal and lateral conidia on hyphae, short stalk or side branch, solitary, always forming verticillate and opposite branches with an acute angle to the axis near the apex.

Sexual morph: not observed.

Geographical distribution: China and America.

Material examined: China, Shaanxi, Xi'an, Xincheng district, 34°27′N, 108°95′E, from epiphytic soil of *Broussonetia papyrifera*, September 2018, Zhi. Y. Zhang (HMAS 255395 – holotype; GZUIFR 173.1 – ex-type living culture); Hanzhong, Shaanxi province, from epiphytic soil of *Trachycarpus fortunei*, September 2018, Zhi. Y. Zhang (GZUIFR HZ5.7); Yichang, Hubei province, from soil beside a park, September 2018, Zhi. Y. Zhang (GZUIFR CY 1.8). The living cultures were kept in sterile 30% glycerol and deposited in a −80°C freezer.

Notes: Morphologically, *P. shaanxiensis* resembles *Pseudogymnoascus appendiculatus* and *Pseudogymnoascus verrucosus* because of the pyriform conidia. However, *P. shaanxiensis* differs from *P. appendiculatus* and *P. verrucosus* based on its subglobose, pyriform intercalary conidia (the intercalary conidia of *P. appendiculatus* and *P. verrucosus*

are subglobose to elongate) (Rice and Currah, 2006). Phylogenetically, our isolates GZUIFR 173.1, GZUIFR HZ5.7, and GZUIFR CY 1.8 cluster with 14PA06 and RMF C 101 in a distinct subclade and are separated from other clades (**Figures 1**, **2**). Furthermore, since 2013 (Minnis and Lindner, 2013), isolates 14PA06 and RMF C 101 have remained an undescribed species owing to the lack of morphological characteristics. Therefore, we introduce *P. shaanxiensis* sp. nov. in this study.

Pseudogymnoascus sinensis Zhi.Y. Zhang, Y.F. Han and Z.Q. Liang, sp. nov.

MycoBank number: MB 835717, Facesoffungi number: FoF 08690 (**Figure 6**).

Etymology: In reference to China, the country where the type specimen was obtained.

Holotype: permanently preserved in a metabolically inactive state, HMAS 255394.

Description based on HMAS 255394. Asexual: Colonies on PDA, reaching 20–21 mm in diameter after 14 days at 25°C, powdery, floccose, margin identified, light pink at the center and pewter at the edge; reverse brown. Aerial mycelium abundant, smooth and thin walled, septate, 1- to 2-μm wide. Racquet hyphae absent. Conidia abundant, terminal and lateral conidia on hyphae, short stalk or side branches, sometimes forming verticillate and opposite branches with an acute angle to the axis near the apex, solitary, obovoid, 3.0–5.0 × 2.5–3.0 μm (*av.* = 4.0 × 2.5 μm, *n* = 50). Intercalary conidia are borne on the outer branches of the hyphae or verticillate hyphae, smooth walled, drum, obovoid, pyriform, or irregularly shaped, 3.0–4.5 × 2.5–5.0 μm (*av.* = 3 × 3 μm, *n* = 50).

Sexual morph: not observed.

Geographical distribution: China.

Material examined: China, Guizhou, Guiyang, the Affiliated Hospital of Guizhou Medical University, 26°59′N, 106°71′E, from soil beside a road, September 2016, Zhi. Y. Zhang (HMAS 255394 – holotype; CGMCC 3.18493 = GZUIFR K278.1 – ex-type living cultures; ibid., CGMCC 3.18494 = GZUIFR K278.2). The living cultures were kept in sterile 30% glycerol and deposited in a −80°C freezer.

Notes: Morphologically, *P. sinensis* is similar to *P. linderi* and *P. turner*, based on its obovoid conidia. However, *P. sinensis* differs from *P. linderi* and *P. turneri* as it has drum, obovoid, pyriform, or irregularly shaped intercalary conidia (the intercalary conidia of *P. linderi* and *P. turneri* are globose to truncate) (Crous et al., 2019). Phylogenetically, our isolates CGMCC 3.18493 and CGMCC 3.18494 cluster together very well and form a single clade separated from other *Pseudogymnoascus* species (**Figure 1**).

Solomyces Zhi.Y. Zhang, Y.F. Han and Z.Q. Liang, gen. nov.

MycoBank number: MB 835713; Facesoffungi number: FoF 08688.

Etymology: *Solo-* (from *Solum*), in reference to its isolation from soil.

Saprobic on soil. Asexual morph: *Conidia*: terminal and lateral conidia borne on hyphae, short protrusions, or side branches. Conidia solitary, sometimes 2 in chains, pyriform, sometimes subglobose. Intercalary conidia abundant, olivary, subglobose to globose. Sexual morph: Unknown.

Geographical distribution: China and America.

Type species: *Solomyces sinensis* Zhi.Y. Zhang, Y.F. Han and Z.Q. Liang.

Notes: *Solomyces* is introduced to accommodate *Solomyces sinensis* and another unnamed species (containing two strains, 15PA02 and 17WV02, from Hibernacular soil in Pennsylvania and West Virginia, respectively; Minnis and Lindner, 2013). The morphology of *Solomyces* species is similar to that of *Geomyces* and the asexual morphs of *Pseudogymnoascus*. However, *Geomyces* differ in having terminal and lateral conidia borne on hyphae, short protrusions or side branches; intercalary conidia barrel shaped, and conidiophores abundant, always forming verticillate and opposite branches with an acute angle to the axis near the apex (Van Oorschot, 1980; Chen et al., 2017). As can be seen in **Figures 1**, **2**, strains of these genera appear in distinct clades in a phylogeny based on multiple strains, thereby justifying the erection of the new genus *Solomyces*.

Solomyces sinensis Zhi.Y. Zhang, Y.F. Han and Z.Q. Liang, sp. nov.

MycoBank number: MB 835714, Facesoffungi number: FoF 08687 (**Figure 7**).

Etymology: In reference to China, the country where the type specimen was obtained.

Holotype: permanently preserved in a metabolically inactive state, HMAS 255397.

Description based on HMAS 255394. Asexual: Colonies on PDA, reaching 16–17 mm in diameter after 14 days at 25°C, elevate at the center, velvety to floccose, margins regular, pewter at the center and white at the edge, producing a diffusible faint yellow pigment and clear exudates; reverse brown. Aerial mycelium abundant, smooth and thin walled, septate, 1- to 2-μm wide. Terminal and lateral conidia borne on hyphae, short protrusions, or side branches. Conidia solitary, sometimes two in chains, pyriform, sometimes subglobose, smooth or rarely rough walled, ecru, 4.0–6.0 × 3.0–5.5 μm (*av.* = 5.5 × 4.0, *n* = 50). Intercalary conidia abundant, olivary, subglobose to globose, 4.0–7.0 × 3.0–5.5 μm (*av.* = 5.0 × 4.0, *n* = 50).

Sexual morph: not observed.

Geographical distribution: China.

Material examined: China, Guizhou, Guiyang, the Affiliated Hospital of Guizhou Medical University, 26°59′N, 106°71′E, from soil beside a road, September 2016, Zhi. Y. Zhang (HMAS 255397 – holotype; CGMCC 3.18498 = GZUIFR K277.1 – ex-type living cultures; ibid., CGMCC 3.18499 = GZUIFR K277.2; ibid., CGMCC 3.18500 = GZUIFR K277.3). The living cultures were kept in sterile 30% glycerol and deposited in a −80°C freezer.

Notes: *Solomyces sinensis* was isolated from soil in Guizhou Province, China. We did not compare morphological characteristics between *S. sinensis* and another two strains within *Solomyces* owing to the lack of morphological description of these two strains (Minnis and Lindner, 2013). However, *S.*

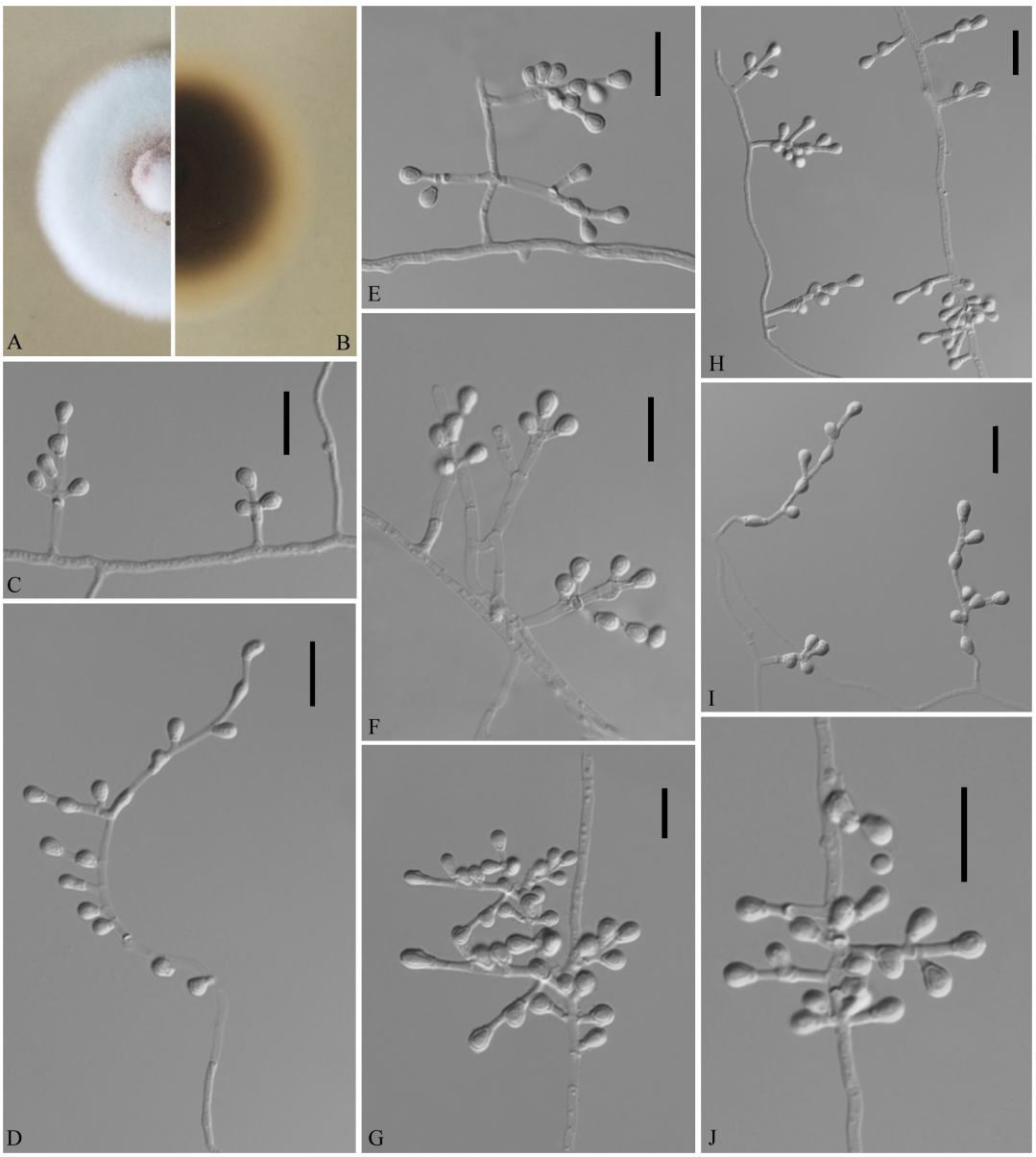


FIGURE 6 | *Pseudogymnoascus sinensis* (from ex-holotype CGMCC 3.18493). **(A,B)** The front and reverse of a *P. sinensis* colony on PDA after 14 days at 25°C. **(C–J)** Conidiophores and conidia. Scale bars = 10 μm.

sinensis is phylogenetically distinct from these strains with high statistical support (1.00 BYPP, 100% MLBS) (**Figures 1**, **2**).

DISCUSSION

In this study, *Solomyces* gen. nov. is introduced with an asexual morph. Five new species are also described. All the new taxa belong in the order Thelebolales, the members of which are ubiquitous in the environment. Several taxa belonging to this order have been isolated from tropical to arctic regions. They are often coprophilous and frequently isolated from freshwater and saline lakes (De Hoog et al., 2005). They have also been recorded from soils, epiphytic soils in tree holes (Chen et al., 2017), mine sediments (Crous et al., 2019), and sponges (Bovio et al., 2018). Thelebolales have been recorded as saprobic on dead plant material, rarely as plant-parasitic, and also as animal pathogens, e.g., the well-known white-nose disease of bats (Lorch et al., 2011). In addition, several members of Thelebolales are keratinophilic; i.e., they can invade and degrade keratin material (Saxena et al., 2005). All the proposed new taxa in our study were isolated using the baiting technique, a method specifically

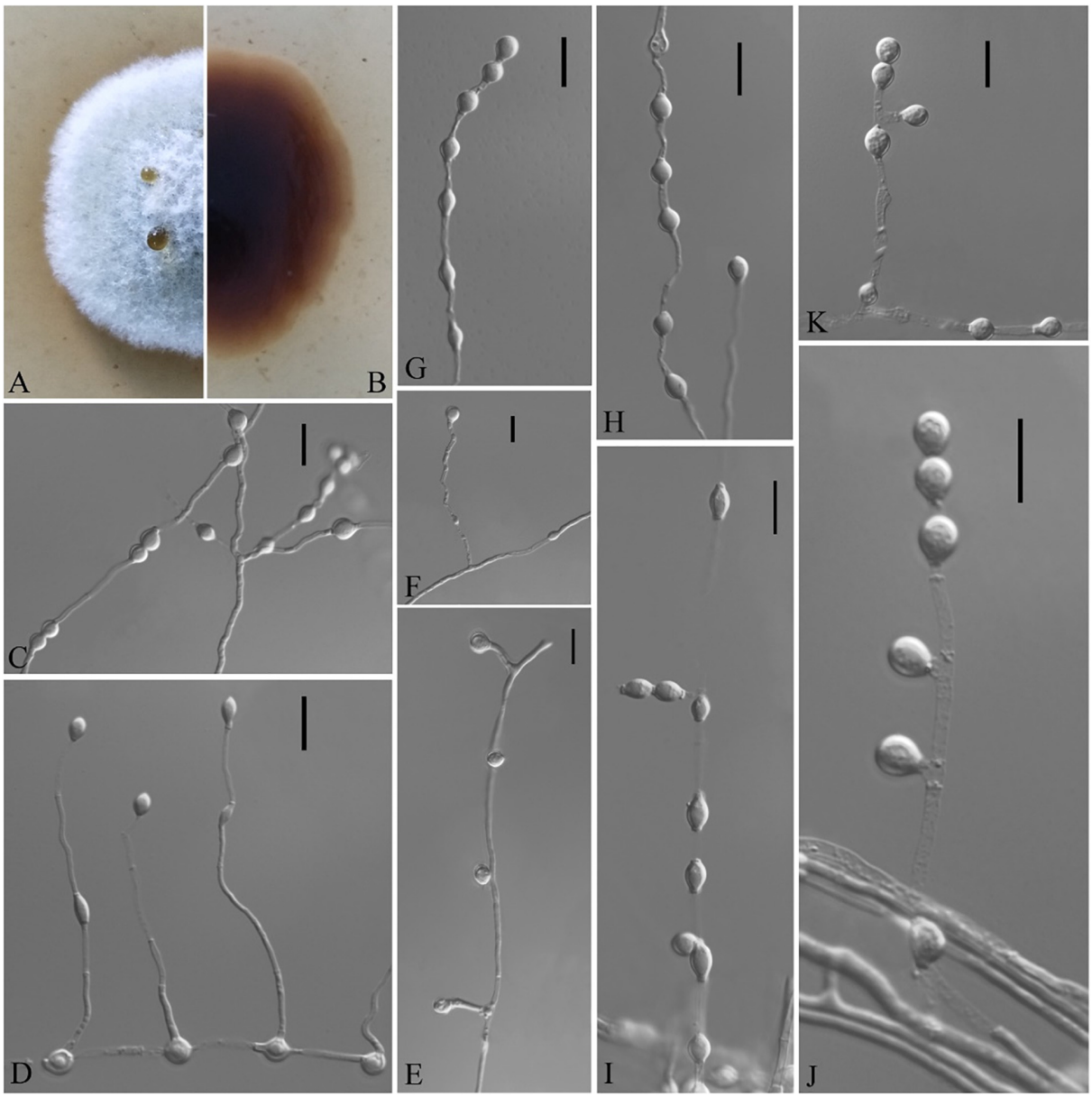


FIGURE 7 | *Solomyces sinensis* (from ex-holotype CGMCC 3.18498). **(A,B)** The front and reverse of a *S. sinensis* colony on PDA after 14 days at 25°C. **(C–K)** Conidiophores and conidia. Scale bars = 10 μm.

designed for the isolation of keratinophilic fungi. Consequently, additional studies are needed to assess whether our new taxa can also degrade keratin material.

Recent studies demonstrated that the Thelebolales comprise at least two families or groups (Ekanayaka et al., 2019; Johnston et al., 2019; Batista et al., 2020). Some studies have proposed that the Thelebolales consists of Pseudeurotiaceae and Thelebolaceae based on three distinct pieces of evidence (568 ITS sequences, 15 genes concatenated from 279 species, and a phylogenomic approach from 51 complete genomes) and on a phylogenomic approach, respectively (Johnston et al., 2019; Batista et al., 2020). The Thelebolaceae, represented by the *Thelebolus* and *Antarctomyces*, share a common ancestor with the family Pseudeurotiaceae, represented by the genus *Pseudogymnoascus* (Johnston et al., 2019; Batista et al., 2020). However, a different study indicated that Pseudeurotiaceae was nested within Thelebolaceae based on phylogenetic analysis and synonymized Pseudeurotiaceae under Thelebolaceae (Ekanayaka et al., 2019). The same authors discovered that several genera, previously classified as Leotiaceae and Leotiomycetes genera *incertae sedis*, clustered within Thelebolales as a sister clade to the Thelebolaceae and defined them as the *Alatospora–Miniancora* clade (Ekanayaka et al., 2019). The studies by Ekanayaka et al. contained more genus taxa in Thelebolales;

therefore, we continued the phylogenetic analysis in Thelebolales based on this study.

Recent reports have indicated that the Thelebolales contained 22 genera. However, because no ITS and *LSU* sequence data were available for *Ascophanus*, *Ascozonus*, *Caccobius*, *Coprobolus*, *Leptokalpion*, *Neelakesa*, and *Pseudascozonus* (Ekanayaka et al., 2019), we could not compare the phylogenetic relationships between these genera and *Solomyces*. In our phylogenetic analysis, our three isolates (CGMCC 3.18498, CGMCC 3.18499, and CGMCC 3.18500; *Solomyces sinensis*) and two isolates of Minnis and Lindner (2013) (15PA02 and 17WV02, from Hibernacular soil in Pennsylvania and West Virginia, respectively) formed an independent clade with strong statistical support (BYPP 1/MLBS 100%) and were close to *Geomyces*. Morphologically, the asexual stage of *Ascophanus*, *Ascozonus*, *Caccobius*, *Coprobolus*, *Leptokalpion*, *Neelakesa*, and *Pseudascozonus* is not recorded in the literature (Wijayawardene et al., 2017). Therefore, no morphological comparison can be done between these genera and *Solomyces*. However, *Solomyces* differs from Geomyces by terminal and lateral conidia borne on hyphae, short protrusions or side branches, olivary, subglobose to globose intercalary conidia, and absence of the forming verticillate and opposite branches with an acute angle to the axis near the apex of conidiophores (Sigler and Carmichael, 1976).

Based on morphological characteristics, it was difficult to distinguish closely related species, and even genera, using traditional taxonomy, and modern phylogenetic methods were a very important adjunct. Although Crous et al. (2019) described the new species, *P. linderi* and *P. turneri*, based on the similarity of morphological characteristics between these two new species and *P. bhattii*, they did not compare the phylogenetic relationship. Our phylogenetic analysis indicated that *P. bhattii* (type strain CBS 760.71) was nested within *Gymnostellatospora* (**Figure 1**), and we, therefore, transferred *P. bhattii* to the *Gymnostellatospora* and named it *G. bhattii*.

DATA AVAILABILITY STATEMENT

The sequences generated in this study can be found in GenBank. The accession numbers of the sequences deposited in GenBank are ITS: MT509362–MT509372, *LSU*: MT509376–MT509386, *MCM7*: MT534202–MT534212, *RPB2*: MT534216–MT534226, and *EF1A*: MT534227–MT534237.

AUTHOR CONTRIBUTIONS

YH and JH were responsible for conceptualization and funding acquisition. ZZ, CD, WC, QM, and XL were responsible for data acquisition. ZZ, CD, and WC did the formal analysis. ZZ wrote the first draft. YH and ZL wrote, reviewed, and edited the manuscript. All authors have read and agreed to the published version of the manuscript.

FUNDING

This work was supported by the Key-Area Research and Development Program of Guangdong Province (2018B020205003), the Program of High-level innovative scientific talents of Guizhou Province [(2020)6005], the Ministry of Science and Technology of China (2013FY110400), the National Natural Science Foundation of China (31460010 and 1860002), the Construction Program of Biology First-Class Discipline in Guizhou [GNYL(2017)009], and the Graduate Innovation Fund Project of Guizhou Province [YJSCXJH(2019)026].

REFERENCES

Batista, T. M., Hilário, H. O., de Brito, G. A. M., Moreira, R. G., Furtado, C., de Menezes, G. C. A., et al. (2020). Whole-genome sequencing of the endemic Antarctic fungus *Antarctomyces pellizariae* reveals an ice-binding protein, a scarce set of secondary metabolites gene clusters and provides insights on Thelebolales phylogeny. *Genomics* 112, 2915–2921. doi: 10.1016/j.ygeno.2020.05.004

Bovio, E., Garzoli, L., Poli, A., Prigione, V., Firsova, D., McCormack, G. P., et al. (2018). The culturable mycobiota associated with three Atlantic sponges, including two new species: *Thelebolus balaustiformis* and *T. spongiae*. *Fungal Syst. Evol.* 1, 141–167. doi: 10.3114/fuse.2018.01.07

Chen, W. H., Zeng, G. P., Luo, Y., Liang, Z. Q., and Han, Y. F. (2017). Morphological traits and molecular analysis for *Geomyces fujianensis* sp. nov. from China. *Mycosphere* 8, 38–43. doi: 10.5943/mycosphere/8/1/5

Crous, P. W., Wingfiled, M. J., Lombard, L., Roets, F., Swart, W. J., Alvarado, P., et al. (2019). Fungal planet description sheets: 951–1041. *Persoonia* 43, 223–425. doi: 10.3767/persoonia.2019.43.06

Dal Vesco, G. (1957). *Geomyces vinaceus*" n. sp. forma conidica di "*Pseudogymnoascus vinaceus*. *Raillo. Allionia* 3, 1–15.

De Hoog, G. S., Göttlich, E., Platas, G., Genilloud, O., Leotta, G., and van Brummelen, J. (2005). Evolution, taxonomy and ecology of the genus *Thelebolus* in Antarctica. *Stud. Mycol.* 51, 33–76.

De Menezes, G. C., Godinho, V. M., Porto, B. A., Gonçalves, V. N., and Rosa, L. H. (2017). *Antarctomyces pellizariae* sp. nov., a new, endemic, blue, snow resident psychrophilic ascomycete fungus from Antarctica. *Extremophiles* 21, 259–269. doi: 10.1007/s00792-016-0895-x

Drummond, A., and Rambaut, A. (2007). BEAST: bayesian evolutionary analysis by sampling trees. *BMC Evol. Biol.* 7:214. doi: 10.1186/1471-2148-7-214

Eckblad, F. E. (1968). The genera of the operculate discomycetes. A re-evaluation of their taxonomy, phylogeny and nomenclature. *Norw. J. Bot.* 15, 1–191.

Ekanayaka, A., Hyde, K. D., Gentekaki, E., McKenzie, E. H. C., Zhao, Q., Bulgakov, T. S., et al. (2019). Preliminary classification of Leotiomycetes. *Mycosphere* 10, 310–489. doi: 10.5943/mycosphere/10/1/7

Ekanayaka, A. H., Ariyawansa, H. A., Hyde, K. D., Jones, E. B. G., Daranagama, D. A., Phillips, A. J. L., et al. (2017). Discomycetes: the apothecial representatives of the phylum Ascomycota. *Fungal Divers.* 87, 237–298. doi: 10.1007/s13225-017-0389-x

Eriksson, O. E., and Winka, K. (1997). Supraordinal taxa of Ascomycota. *Myconet.* 1, 1–16.

Gargas, A., Trest, M. T., Christensen, M., Volk, T. J., and Blehert, D. S. (2009) Geomyces destructans sp. nov. associated with bat white-nose syndrome. *Mycotaxon* 108, 147–154. doi: 10.5248/108.147

Haeckel, E. (1894). *Systematische Phylogenie. Entwurf eines Natürlichen Systems der Organismen auf Grund ihrer Stammesgeschichte. Theil1, Systematische Phylogenie der Protisten und Pflanzen*. (Berlin: G. Reimer), 1–400.

Hocking, A. D., and Pitt, J. I. (1988). Two new species of xerophilic fungi and a further record of *Eurotium halophilicum*. *Mycologia* 80, 82–88. doi: 10.2307/3807497

Johnston, P. R., Quijada, L., Smith, C. A., Baral, H.-O., Hosoya, T., Baschien, C., et al. (2019). A multigene phylogeny toward a new phylogenetic classification of Leotiomycetes. *IMA Fungus* 10:1. doi: 10.1186/s43008-019-0002-x

Kalyaanamoorthy, S., Minh, B. Q., Wong, T. K., von Haeseler, A., and Jermiin, L. S. (2017). ModelFinder: fast model selection for accurate phylogenetic estimates. *Nat. Methods* 14, 587–589. doi: 10.1038/nmeth.4285

Karunarathna, A., Peršoh, D., Ekanayaka, A. H., Jayawardena, R. S., Thilini Chethana, K. W., Goonasekara, I. D., et al. (2020). *Patellariopsidaceae* Fam. Nov. With Sexual-Asexual Connection and a New Host Record for Cheirospora botryospora (Vibrisseaceae, Ascomycota). *Front. Microbiol.* 11:906. doi: 10.3389/fmicb.2020.00906

Katoh, K., and Standley, D. M. (2013). MAFFT multiple sequence alignment software version 7: improvements in performance and usability. *Mol. Biol. Evol.* 30, 772–780. doi: 10.1093/molbev/mst010

Korf, R. P. (1973). "Discomycetes and Tuberales," in *The Fungi: An Advanced Treatise*, Vol. IVA, eds G. C. Ainsworth, F. K. Sparrow, and A. S. Sussman (New York, NY: Academic Press).

Li, Z. Q., and Cui, C. Q. (1989). Study on the Psychrophilic/Psychrotrophic microorganisms. III. Geomyces laevis, a new species of Geomyces. *Mycosystema* 8, 47–50.

Liu, Y. J., Whelen, S., and Hall, B. D. (1999). Phylogenetic relationships among Ascomycetes: evidence from an RNA polymerase II subunit. *Mol. Biol. Evol.* 16, 1799–1808. doi: 10.1093/oxfordjournals.molbev.a026092

Lorch, J. M., Meteyer, C. U., Behr, M. J., Boyles, J. G., Cryan, P. M., Hicks, A. C., et al. (2011). Experimental infection of bats with Geomyces destructans causes white-nose syndrome. *Nature* 480, 376–378. doi: 10.1038/nature10590

Luo, Y., Chen, W. H., Wang, Y., Han, Y. F., and Liang, Z. Q. (2016). A new *Geomyces* species producing melanin in the medium. *Mycosystema* 35, 123–130. doi: 10.13346/j.mycosystema.140246

Minh, Q., Nguyen, M., and von Haeseler, A. A. (2013). Ultrafast approximation for phylogenetic bootstrap. *Mol. Biol. Evol.* 30, 1188–1195. doi: 10.1093/molbev/mst024

Minnis, A. M., and Lindner, D. L. (2013). Phylogenetic evaluation of *Geomyces* and allies reveals no close relatives of *Pseudogymnoascus destructans*, comb. nov., in bat hibernacula of eastern North America. *Fungal Biol.* 117, 638–649. doi: 10.1016/j.funbio.2013.07.001

Nguyen, L. T., Schmidt, H. A., von Haeseler, A., and Minh, B. Q. (2015). IQ-TREE: a fast and effective stochastic algorithm for estimating maximum-likelihood phylogenies. *Mol. Biol. Evol.* 32, 268–274. doi: 10.1093/molbev/msu300

Posada, D., and Crandall, K. A. (1998). Modeltest: testing the model of DNA substitution. *Bioinformatics* 14, 817–818. doi: 10.1093/bioinformatics/14.9.817

Reeb, V., Lutzoni, F., and Roux, C. (2004). Contribution of RPB2 to multilocus phylogenetic studies of the euascomycetes (Pezizomycotina, Fungi) with special emphasis on the lichen-forming Acarosporaceae and evolution of polyspory. *Mol. Phylogenet. Evol.* 32, 1036–1060. doi: 10.1016/j.ympev.2004.04.012

Rehner, S. A., and Buckley, E. (2005). A *Beauveria* phylogeny inferred from nuclear ITS and EF1-alpha sequences: evidence for cryptic diversification and links to *Cordyceps teleomorphs*. *Mycologia* 97, 84–98. doi: 10.3852/mycologia.97.1.84

Rice, A. V., and Currah, R. S. (2006). Two new species of *Pseudogymnoascus* with *Geomyces* anamorphs and their phylogenetic relationship with *Gymnostellatospora*. *Mycologia* 98, 307–318. doi: 10.3852/mycologia.98.2.307

Ronquist, F., Teslenko, M., van der Mark, P., Ayres, D. L., Darling, A., Höhna, S., et al. (2012). MrBayes 3.2: efficient Bayesian phylogenetic inference and model choice across a large model space. *Syst. Biol.* 61, 539–542. doi: 10.1093/sysbio/sys029

Samson, R. A. (1972). Notes on *Pseudogymnoascus*, *Gymnoascus* and related genera. *Acta Bot. Neerlandic.* 21, 517–527. doi: 10.1111/j.1438-8677.1972.tb00804.x

Sati, S. C., and Pathak, R. (2016). Anamorph (asexual stage) Teleomorph (sexual stage) Connections in Aquatic hyphomycetes. *Int. J. Plant Reprod. Biol.* 8, 128–135.

Saxena, P., Kumar, A., and Shrivastava, J. N. (2005). Keratinophilic fungi: a microbial way to manage poultry waste feathers. *Indian J. Microbiol.* 45, 151–154.

Schoch, C. L., Sung, G. H., López-Giráldez, F., Townsend, J. P., Miadlikowska, J., Hofstetter, V., et al. (2009). The Ascomycota Tree of Life: a phylum-wide phylogeny clarifies the origin and evolution of fundamental reproductive and ecological traits. *Syst Biol.* 58, 224–239. doi: 10.1093/sysbio/syp020

Sigler, L., and Carmichael, J. W. (1976). Taxonomy of *Malbranchea* and some other hyphomycetes with arthroconidia. *Mycotaxon* 4, 349–488.

Spooner, B. M. (1987). Helotiales of Australasia: geoglossaceae, Orbiliaceae, Scelrotiniaceae, Hyaloscyphaceae. *Bibl. Mycol.* 116, 1–711.

Stchigel, A. M., Josep, C. A., Mac Cormack, W., and Guarro, J. (2001). *Antarctomyces psychrotrophicus* gen. et sp. nov., a new ascomycete from Antarctica. Mycol. Res. 105, 377–382. doi: 10.1017/s0953756201003379

Sutton, B. C., and Hennebert, G. L. (1995). "Interconnections amongst anamorphs and their possible contribution to ascomycetes systematics," in *Ascomycete Systematics: Problems and Perspectives in the Nineties*, ed. D. L. Hawksworth (New York, NY: Plenum), 77–100.

Swofford, D. L. (2002). *PAUP* 4.0b10: Phylogenetic Analysis Using Parsimony (*and other methods)*. Sunderland, MA: Sinauer.

Tamura, K., Stecher, G., Peterson, D., Filipski, A., and Kumar, S. (2013). MEGA6: molecular evolutionary genetics analysis version 6.0. *Mol. Biol. Evol.* 30, 2725–2729. doi: 10.1093/molbev/mst197

Traaen, A. E. (1914). Untersuchungen über bodenpilze aus Norwegen. *Nytt Mag. Naturvidensk.* 52, 19–121.

Vaidya, G., Lohman, D. J., and Meier, R. (2011). SequenceMatrix: concatenation software for the fast assembly of multi-gene datasets with character set and codon information. *Cladistics* 27, 171–180. doi: 10.1111/j.1096-0031.2010.00329.x

Van Brummelen, J. (1985). *Pseudoascozonus*, a new genus of Pezizales. *Proc. Indian Acad. Sci.* 94, 363–367.

Van Oorschot, C. A. (1980). A revision of chrysosporium and allied genera (No. 20). *Stud. Mycol.* 20, 1–89.

Vanbreuseghem, R. (1952). Technique biologique pour l'isolement des dermatophytes du sol. *Ann. Soc. Belg. Med. Trop.* 32, 175–178.

Vilgalys, R., and Hester, M. (1990). Rapid genetic identification and mapping of enzymatically amplified ribosomal DNA from several *Cryptococcus* species. *J. Bacteriol.* 172, 4238–4246. doi: 10.1128/jb.172.8.4238-4246.1990

Vilgalys, R., and Sun, B. L. (1999). Ancient and recent patterns of geographic speciation in the oyster mushroom *Pleurotus* revealed by phylogenetic analysis of ribosomal DNA sequences. *Proc. Natl. Acad. Sci. U.S.A.* 91, 4599–4603. doi: 10.1073/pnas.91.10.4599

White, T. J., Bruns, T., Lee, S., and Taylor, J. (1990). "Amplification and direct sequencing of fungal ribosomal RNA genes for phylogenetics," in *PCR Protocols*, eds M. A. Innis, D. H. Gelfand, J. J. Sninsky, and T. J. White (San Diego, CA: Academic Press), 315–322. doi: 10.1016/B978-0-12-372180-8.50042-1

Wijayawardene, N. N., Hyde, K. D., Rajeshkumar, K. C., Hawksworth, D. L., Madrid, H., Kirk, P. M., et al. (2017). Notes for genera: Ascomycota. *Fungal Divers.* 86, 1–594. doi: 10.1007/s13225-017-0386-0

Zhang, Z. Y., Chen, W. H., Zou, X., Han, Y. F., Huang, J. Z., and Deshmukh, S. K. (2019). Phylogeny and taxonomy of two new *Plectosphaerella* (Plectosphaerellaceae, Glomerellales) species from China. *MycoKeys* 57, 47–60. doi: 10.3897/mycokeys.57.36628

Conflict of Interest: The authors declare that the research was conducted in the absence of any commercial or financial relationships that could be construed as a potential conflict of interest.

Copyright © 2020 Zhang, Dong, Chen, Mou, Lu, Han, Huang and Liang. This is an open-access article distributed under the terms of the Creative Commons Attribution License (CC BY). The use, distribution or reproduction in other forums is permitted, provided the original author(s) and the copyright owner(s) are credited and that the original publication in this journal is cited, in accordance with accepted academic practice. No use, distribution or reproduction is permitted which does not comply with these terms.

frontiers in Microbiology

ORIGINAL RESEARCH
published: 23 November 2020
doi: 10.3389/fmicb.2020.595427

Diversity and Geographic Distribution of Ligninolytic Fungi Associated With *Castanopsis sieboldii* Leaf Litter in Japan

Takashi Osono[1], Shunsuke Matsuoka[2] and Dai Hirose[3]*

[1] Faculty of Science and Engineering, Doshisha University, Kyoto, Japan, [2] Graduate School of Simulation Studies, University of Hyogo, Kobe, Japan, [3] School of Pharmacy, Nihon University, Funabashi, Japan

The diversity and geographic pattern of ligninolytic fungi were investigated within the distribution range of an evergreen tree, *Castanopsis sieboldii* (Fagaceae), in Japan. Fungal isolates obtained from 18 sites in subtropical and temperate regions in Japan were classified into 50 operational taxonomic units in Ascomycota and Basidiomycota according to the base sequence of the rDNA internal transcribed spacer region. Ordination by nonmetric multidimensional scaling showed the separation of fungal compositions between the study sites which was significantly related to the latitude, longitude, and mean annual temperature (MAT) of the study sites. We applied variation partitioning to separate the magnitude of the climatic, spatial, and leaf property factors and found the roles of MAT and spatial factors in structuring fungal assemblages, suggesting the importance of both niche processes and such non-niche processes as priority effect and dispersal limitation. The bleached area on leaf litter was greater at sites with higher MAT and precipitation located at lower latitudes and at sites where some major ligninolytic fungi occurred at greater relative frequencies, indicating that not only the climatic conditions but also the biogeographic patterns of distribution of ligninolytic fungi influence the decomposition of lignin in leaf litter.

Keywords: biogeography, bleaching, fungal community, spatial structure, decomposition

OPEN ACCESS

Edited by:
Dhanushka Nadeeshan Wanasinghe, Kunming Institute of Botany, China

Reviewed by:
Yong Zheng, Fujian Normal University, China
Kasun Thambugala, University of Sri Jayewardenepura, Sri Lanka

****Correspondence:***
Takashi Osono
tosono@mail.doshisha.ac.jp

Specialty section:
This article was submitted to Fungi and Their Interactions, a section of the journal Frontiers in Microbiology

Received: *16 August 2020*
Accepted: *26 October 2020*
Published: *23 November 2020*

Citation:
Osono T, Matsuoka S and Hirose D (2020) Diversity and Geographic Distribution of Ligninolytic Fungi Associated With Castanopsis sieboldii Leaf Litter in Japan. Front. Microbiol. 11:595427. doi: 10.3389/fmicb.2020.595427

INTRODUCTION

Fungi play central roles in the decomposition of lignin and other recalcitrant compounds, such as cutin and tannin, in leaf litter of forest trees (van der Wal et al., 2013; Baldrian, 2017). Fungi that selectively remove lignin cause extensive whitening (denoted here as bleaching) of litter materials and stimulate the turnover of carbon and nutrients in soil (Osono, 2020). Previous studies have demonstrated that fungi on leaf litter, including ligninolytic ones associated with the bleaching, show biogeographical patterns and respond sensitively to environmental change along climatic and elevational gradients at population and community levels (van Maanen et al., 2000; Gourbière et al., 2001; Tokumasu, 2001; Hagiwara et al., 2015; Matsukura et al., 2017). Such biogeographic patterns of fungal

diversity and composition have been reported to be influenced by climatic, edaphic, and vegetation factors, of which the climate is of particular importance (Peay et al., 2016; Bahram et al., 2018; Větrovský et al., 2019). In addition to the climate, recent studies have demonstrated the importance of spatial factors, such as priority effect and dispersal limitation, in producing the biogeographic patterns of fungal community composition across a range of spatial and temporal scales (Tedersoo et al., 2014; Peay et al., 2016), which contrasts to early predictions that fungi are probably long-distance dispersers and that their propagules are everywhere (Wit and Bouvier, 2006).

Considering the magnitude of ongoing global environmental change, it is crucial to explore how climate, vegetation, spatial, and other factors interact to affect the patterns of diversity and biogeography of fungi associated with leaf litter decomposition. However, factors affecting the biogeography of bleaching fungi on leaf litter have rarely been explored. In Asian forests of different climatic regions, Osono (2011) demonstrated that the diversity and species composition of fungal assemblages on leaf litter were closely related to the climatic gradient. In that study, however, the host tree species examined for fungi were different between the climatic regions, making it difficult to separate the effect on the fungal assemblages of climatic conditions from that of host tree species. Studies are thus needed on geographical patterns of bleaching fungi on leaf litter of single host tree species that are distributed along climatic gradients. We hypothesize that the taxonomic richness and composition of bleaching fungi associated with leaf litter of a single host tree species showed a geographic pattern and were related to climatic conditions, such as mean annual temperature (MAT), as well as spatial factors.

The purposes of the present study were to examine (i) the taxonomic richness and composition of ligninolytic fungi associated with the bleaching of leaf litter and (ii) the magnitude of relative importance of climate, leaf quality, and spatial factors affecting the composition of fungal assemblages within the distributional range of a single host tree species *Castanopsis sieboldii* (Makino) Hatus. ex T.Yamaz. et Mashiba (Fagaceae) in Japan. We chose *C. sieboldii* as the focal host species because this species is widely distributed across different climate regions of the Japanese archipelago (Aoki et al., 2014). Eighteen study sites in subtropical and temperate regions that cover almost the entire range of natural distribution of *C. sieboldii* in Japan were selected for the present study. This tree species is a dominant, canopy, and climax species in Japanese *Castanopsis*-type evergreen broad-leaved forests. These *Castanopsis*-type forests have features characteristic of the biodiversity and endemism of the subtropical and warm-temperate zones in Japan. The focal tree species is evergreen broad-leaved and relatively shade-tolerant. Bleached portions are obviously and easily found on the surface of these forests' leaf litter (Osono et al., 2008; **Figure 1**), making this leaf litter a suitable material for the study of the biogeographic pattern of ligninolytic fungi associated with the bleaching. Finally, bleached leaf area was measured at the study site so as to examine the roles of climatic factors, leaf property, and fungal occurrence on the geographic patterns of emergence of fungal bleaching on leaf litter.

MATERIALS AND METHODS

Study Sites and Sampling

Samples were collected at 18 study sites in subtropical and temperate regions in Japan (24.307 to 37.966°N, 123.847 to 140.120°E, 45 to 440 m a.s.l.; **Table 1** and **Figure 1**). The study sites were located in mature evergreen broad-leaved forests dominated by *C. sieboldii*, and cover almost the entire range of natural distribution of *C. sieboldii* in Japan, from Iriomote Island of the Ryukyu Islands, adjacent to the present southern boundary of Japan, to Sado Island, adjacent to its northern range. We selected the study sites based on following criteria although details in histories of the individual site are unknown: (i) forest canopy is closed and forest contains at least 20 individuals of *C. sieboldii* with diameter at breast height (DBH) >20 cm and (ii) there is no sign of large-scale natural and anthropogenic disturbance. Latitudes and longitudes of the sites are strongly correlated (Pearson's $r = 0.820$, $n = 18$, and $P < 0.001$), as the Japanese Archipelago is elongated from northeast to southwest.

Sampling was conducted once at each site in the summer (from July to September) from 2007 to 2013. At each site, we randomly set 10 quadrats (15 × 15 cm) at least 3 m from each other. A total of 20 leaves of *C. sieboldii* with evident bleaching and of which more than half of the original leaf area remained were collected from the surface of the forest floor within the quadrats, two leaves per quadrat. These leaves were placed in paper bags and preserved at 4°C for no longer than 3 days before the isolation of fungi.

Additional leaves of *C. sieboldii* with more than half of their original leaf area remaining were collected from the surface of the forest floor within the quadrat and were used to measure the bleached leaf area and total leaf area to calculate the relative bleached area according to the method described in Hagiwara et al. (2015). The bleached area is expressed as a percentage of the total leaf area, and the mean value of the bleached area was calculated for each study site (**Table 1**). Leaf disks (5.5 mm in diameter) were then excised from the bleached area and used for measurements of leaf mass per area (LMA) and content of acid unhydrolyzable residues (AUR) according to the methods described in Osono et al. (2008). The AUR fraction contains a mixture of organic compounds in various proportions, including condensed tannins, phenolic and carboxylic compounds, alkyl compounds such as cutin, and true lignin (Preston et al., 1997).

Fungal Isolation

Single leaf disks were excised from the bleached portion of individual leaves, using a sterile 5.5-mm-diameter cork borer, produced 20 leaf disks of bleached portions from each study site. Fungi were isolated from the disks using the surface disinfection method described by Osono et al. (2008). The surface-disinfected materials were plated on 9-cm Petri dishes containing lignocellulose agar (LCA) modified as described by Miura and Kudo (1970), two disks per plate. The plates were incubated at 20°C in darkness and observed for 4 weeks after the plating. Any fungal hyphae or spores that appeared on the plates were transferred to fresh LCA plates, incubated, and observed micromorphologically.

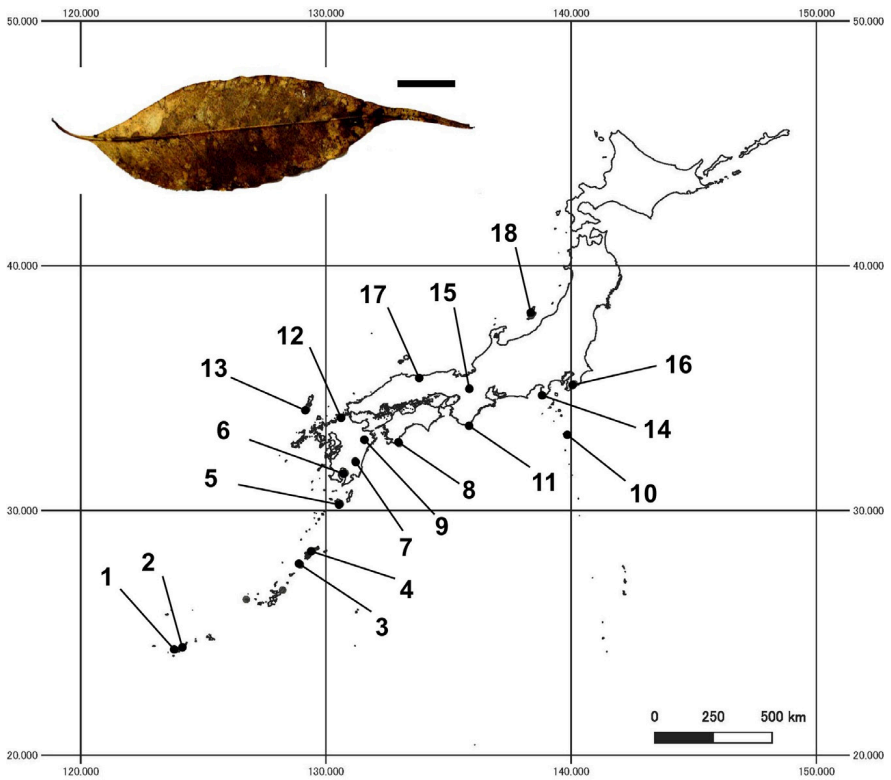


FIGURE 1 | Locations of 18 study sites in Japan, and a photo of a bleached leaf litter (bar = 1 cm). Site numbers are as in **Table 1**.

Isolates were tested for their potential activity to bleach leaf litter under a pure culture condition. Newly shed leaves of *C. sieboldii* without obvious fungal or faunal attack were oven-dried at 40°C for 1 week. The leaves were cut into pieces (approximately 2 cm × 2 cm) and autoclaved at 120°C for 20 min. The sterilized leaf pieces were placed on the surface of Petri dishes (6 cm diameter), one piece per plate, containing 20 ml of 1% malt extract agar [malt extract 2% and agar 2% (w/v)] previously inoculated with fungal isolates and incubated at 20°C for 12 weeks in the dark. After incubation, the leaf pieces were examined under a binocular microscope with magnification of 40× for the occurrence of bleaching on the leaf surface. Fungal isolates that caused bleaching were regarded as ligninolytic fungi. We judged 185 fungal isolates from 360 leaf disks (18 study sites × 20 leaves) to be ligninolytic fungi (**Supplementary Table 1**) and used them for molecular analysis as described below. Three control plates with sterilized leaves but no fungal inoculation were also incubated under the same conditions. No microbial colonies or bleaching developed on the control plates, indicating the effectiveness of the sterilization method used.

Determination of OTUs

The DNA sequences of the 185 samples of fungal isolates were analyzed. DNA extractions and PCR and sequencing reactions followed similar methods to those described by Hirose et al. (2016). The rDNA internal transcribed spacer (ITS) region was amplified using primers ITS1f (Gardes and Bruns, 1993)/LR3 (Vilgalys and Hester, 1990). The ITS sequences determined were compared with the rDNA sequences available in the GenBank database by means of BLAST+ (Camacho et al., 2009) and assigned taxonomically. The sequences determined in the present study were deposited in the DNA Data Bank of Japan (DDBJ; LC505073-LC505341; **Supplementary Table 1**).

The procedures used for bioinformatics analyses followed those described in Matsuoka et al. (2016). First, the whole rDNA ITS (i.e., ITS1-5.8S-ITS2) region of each sequence was extracted using ITSx version 1.0.11 (Bengtsson-Palme et al., 2013). The rDNA ITS sequences were then assembled using Claident pipeline v0.1.2013.08.10 (software available online: https://www.claident.org/). All sequences were assembled across the samples preliminarily at a threshold similarity from 90 to 99% at a 1% interval, and we adopted the threshold similarity of 96% in the present study because the number of operational taxonomic units (OTUs) increased abruptly at 97% sequence similarity. The resulting consensus sequences at 96% sequence similarity represented molecular OTUs. Record was kept of one fungal isolate in the present study even when more than two isolates belonging to the same OTU were obtained from single leaf disk. For each of the OTUs, taxonomic identification was conducted based on the query-centric auto-k-nearest-neighbor (QCauto) method (Tanabe and Toju, 2013) with the reference database from International Nucleotide Sequence Database Collaboration (INSDC) and subsequent taxonomic assignment with the lowest common ancestor (LCA) algorithm (Huson et al., 2007) as implemented in Claident. A benchmark analysis has shown that the combination of the QCauto and LCA algorithms is less

TABLE 1 | Location, climates, sampling month, bleached area on leaf litter (% total leaf area), leaf properties, and the number of fungal isolates for 18 study sites.

Site No.	Site name	Latitude (°N)	Longitude (°E)	Elevation (m)	MAT (°C)	MAP (mm)	Maximum snow depth (cm)	Sampling month	Bleached area	LMA (mg/cm^2)	AUR content (mg/g)	Number of isolates
1	Iriomote Is., Okinawa	24.307	123.847	176	23.2	2738.9	0	Sept 07	36.7 (4.9)	8.0 (0.7)	289	13
2	Ishigaki Is., Okinawa	24.419	124.167	72	23.0	2352.1	0	Sept 07	36.3 (4.5)	8.5 (0.5)	290	14
3	Tokunoshima Is., Kagoshima	27.774	128.964	286	19.7	2386.8	0	Sept 08	24.0 (3.1)	8.5 (0.3)	269	9
4	Amami-Oshima Is., Kagoshima	28.338	129.446	326	19.1	2897.1	0	Sept 08	31.8 (2.2)	8.3 (0.2)	284	6
5	Yakushima Is., Kagoshima	30.257	130.585	195	19.1	3589.8	0	Aug 09	26.3 (5.3)	9.2 (0.2)	306	7
6	Mt. Takakuma, Kagoshima	31.525	130.787	440	14.8	3014.8	0	Sept 08	12.7 (2.3)	8.0 (0.3)	312	10
7	Aya, Miyazaki	32.027	131.194	241	15.4	2838.8	0	Sept 09	18.0 (1.4)	10.2 (0.7)	301	5
8	Cape Ashizuri, Kochi	32.740	132.999	271	16.9	2458.8	0	Jul 10	19.6 (2.7)	8.3 (0.3)	304	21
9	Bungo-Ohno, Oita	32.894	131.540	289	14.3	2350.9	0	Sept 09	23.6 (2.6)	7.7 (0.3)	303	2
10	Hachijo Is., Tokyo	33.108	139.841	333	16.8	3014.6	0	Aug 12	22.5 (3.3)	7.8 (0.2)	318	23
11	Kii-Oshima, Wakayama	33.466	135.833	94	17.0	2547.1	0	Aug 11	14.5 (3.3)	8.2 (0.3)	288	15
12	Shiroyama, Fukuoka	33.815	130.590	113	15.5	1691.7	0	Sept 09	15.0 (1.6)	8.6 (0.4)	280	10
13	Tsushima Is., Nagasaki	34.142	129.218	347	14.0	2122.7	0	Sept 09	14.0 (3.0)	9.6 (0.5)	278	13
14	Izu Peninsula, Shizuoka	34.691	138.839	135	14.9	2042.9	2	Aug 11	21.1 (1.8)	8.2 (0.4)	265	13
15	Otsu, Shiga	35.004	135.857	130	14.3	1496.2	0	Jul 10	5.9 (1.5)	7.5 (0.7)	294	4
16	Kiyosumi, Chiba	35.176	140.120	195	13.5	2075.7	5	Aug 11	8.2 (2.2)	9.8 (0.6)	284	10
17	Kurayoshi, Tottori	35.425	133.824	45	14.2	1921.9	25	Sept 12	10.8 (1.5)	9.3 (0.5)	259	7
18	Sado Is., Niigata	37.966	138.368	73	12.9	1838.9	21	Sept 13	11.5 (1.2)	8.1 (0.3)	285	3

Values are means with standard errors in parentheses (n = 10). MAT, mean annual temperature; MAP, mean annual precipitation; LMA, leaf mass per area; AUR, acid unhydrolyzable residue. The site numbers are arranged in the order of latitude.

susceptible to erroneous sequences in database and returns the accurate taxonomic identification results among the existing methods of automated DNA metabarcoding (Tanabe and Toju, 2013). The results of Claident are given in **Supplementary Table 2**. Those OTUs with more than one isolates were regarded as major OTUs. Additional Blast search was conducted for taxonomic identification of the major OTUs.

Data Analyses

We prepared a datasheet of fungal assemblages indicating the number of isolates in each fungal OTU occurred for each site and calculated relative frequency of each OTU at each site as a percentage of the number of isolates with respect to the total number of isolates (i.e., 185). Data of air temperature, precipitation, and maximum snow depth were obtained from the nearest station of the Automatic Metrological Data Acquisition System (Japan Meteorological Agency) to each study site. We used nonmetric multidimensional scaling (NMDS) with the Bray-Curtis distance metric to analyze the variation of composition of fungal assemblages. The NMDS analysis was carried out with the metaNDS function with default settings of the vegan package of R software (Oksanen et al., 2019). The envfit command of the vegan package was then used to examine correlation of NMDS structure with the sampling month (July, August, and September), latitude, longitude, elevation, MAT, mean annual precipitation (MAP), maximum snow depth, LMA, and AUR content, by permutation tests (9999 permutations). One-way permutational multivariate analysis of variance (PERMANOVA) was conducted to explore whether the dissimilarity of OTU composition was related to the sampling month, geographical coordinates, climatic variables, and leaf properties.

We conducted the variation partitioning with distance-based redundancy analysis (db-RDA) to quantify the contribution of the environmental, spatial, and leaf property variables to the fungal assemblages (Peres-Neto et al., 2006). The detailed procedures are described in Matsuoka et al. (2016). First, data of fungal assemblages for 18 study sites were converted into the Bray-Curtis dissimilarity matrix. Then, we constructed environmental, spatial, and leaf property models. In the environmental model, forward selection procedure with 999 permutations with an alpha criterion = 0.05 (Blanchet et al., 2008) was performed for four environmental variables (mean annual temperature, annual precipitation, maximum snow depth, and elevation). In the spatial model, spatial variables extracted based on Moran's Eigenvector Maps (MEM; Borcard et al., 2004) using the dbmem command in the R adespatial package. The forward selection procedure was then performed for the MEM vectors to select spatial variables that significantly influenced community dissimilarities. In the leaf property model, forward selection procedure with 999 permutations with an alpha criterion = 0.05 was performed for two variables (LMA and AUR). Based on these three models, adjusted R^2 values for the environmental fraction, the spatial fraction, the leaf property fraction, and their shared fraction (Peres-Neto et al., 2006) were calculated using the capscale command in the vegan package.

We used generalized linear models (GLMs) to examine singly the effects of sampling month, geographical coordinates, climatic variables, leaf properties, and relative frequencies of major fungal OTUs on the bleached leaf area. An automatic stepwise model selection with Akaike information criterion (AIC) was performed to find the most parsimonious model, using the minimum AIC as the best-fit estimator. The error structure of the GLM was Gaussian. The glm function in the R software was used to perform the analysis.

RESULTS

Taxonomic Composition

A total of 185 fungal isolates possessing ligninolytic activity were obtained from 360 leaf disks from bleached portions of leaf litter collected at 18 sites (**Supplementary Table 1**), two to 23 isolates per site (**Table 1**). These fungi were classified into 50 OTUs, with 25 OTUs belonging each to Ascomycota (116 isolates) and to Basidiomycota (69 isolates; **Supplementary Table 2**). Of the 50 OTUs, 18 OTUs consisted of more than one isolate and regarded as major OTUs (**Table 2**), while the other 32 OTUs were singletons. The most frequent OTU was *Nemania diffusa* OTU_01, accounting for 25% (46) of the 185 isolates, followed by *Nemania bipapillata* OTU_02, *Gymnopus* sp. OTU_03, and *Nodulisporium* sp. OTU_04 (**Table 2**). All 25 OTUs in the Ascomycota belonged to Xylariaceae (Sordariomycetes) in such genera as *Xylaria, Hypoxylon, Nemania, Astrocystis, Biscogniauxia*, and *Nodulisporium* (**Supplementary Table 2**). The 25 OTUs in the Basidiomycota belonged to Agaricales or Russulales (Agaricomycetes); OTUs in Agaricales were assigned to *Mycena* in Tricholomataceae and *Gymnopus, Marasmius, Marasmiellus*, and *Crinipellis* in Marasmiaceae, and OTUs in Russulales belonged to Lachnocladiaceae (**Supplementary Table 2**). Six OTUs in the Ascomycota were assigned successfully to species by Claident, whereas no OTUs in the Basidiomycota were identified to species (**Supplementary Table 2**).

Geographic Pattern

Nemania diffusa OTU_01 occurred 13 of the 18 sites, followed by *Gymnopus* sp. OTU_03 (8 sites), Agaricomycetes sp. OTU_06 (7 sites), and *Xylaria arbuscula* OTU_05 (6 sites; **Table 2**). The NMDS ordination showed the separation of fungal OTU compositions between the study sites (**Figure 2**; stress value = 0.154). The ordination was significantly correlated with the latitude (R^2 = 0.610, P = 0.0008), longitude (R^2 = 0.473, P = 0.0067), and MAT (R^2 = 0.556, P = 0.002; **Figure 2**), but was not significantly ($P > 0.05$) correlated with the sampling month, elevation, MAP, maximum snow depth, LMA, or AUR content ("envfit" function). In the PERMANOVA, the fungal OTU composition was significantly affected by latitude (F-value = 1.52, R^2 = 0.087, and P = 0.039) and longitude (F-value = 1.73, R^2 = 0.099, and P = 0.011). In the variation partitioning (**Figure 3**), MAT was selected as an environmental variable, and two MEM vectors (MEM1 and MEM2) were selected as spatial variables. Values of MEM1 were significantly correlated with the longitude (Pearson's r = 0.688, n = 18, and

TABLE 2 | Taxon, number of isolates and sites of 18 major fungal OTUs.

OTU	Taxon	Phylum	Number of isolates	Number of sites
OTU_01	*Nemania diffusa*	Ascomycota	46	13
OTU_02	*Nemania bipapillata*	Ascomycota	20	3
OTU_03	*Gymnopus* sp.	Basidiomycota	20	8
OTU_04	*Nodulisporium* sp.	Ascomycota	11	5
OTU_06	Agaricomycetes sp.	Basidiomycota	10	7
OTU_05	*Xylaria arbuscula*	Ascomycota	9	6
OTU_07	*Xylaria cubensis*	Ascomycota	6	4
OTU_08	Agaricomycetes sp.	Basidiomycota	5	3
OTU_09	*Gymnopus* sp.	Basidiomycota	5	4
OTU_10	Agaricales sp.	Basidiomycota	4	4
OTU_12	Russulales sp.	Basidiomycota	3	2
OTU_14	*Xylaria cubensis*	Ascomycota	2	1
OTU_15	*Gymnopus* sp.	Basidiomycota	2	1
OTU_16	*Crinipellis* sp.	Basidiomycota	2	2
OTU_18	Lachnocladiaceae sp.	Basidiomycota	2	2
OTU_19	*Hypoxylon monticulosum*	Ascomycota	2	1
OTU_20	*Xylaria* sp.	Ascomycota	2	1
OTU_21	Xylariaceae sp.	Ascomycota	2	1

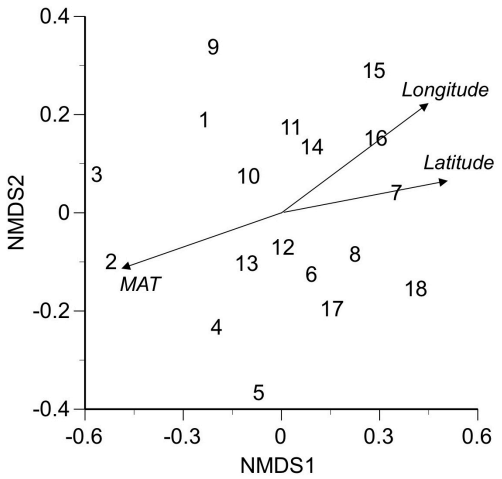


FIGURE 2 | Multivariate ordination of fungal assemblages in bleached portions of leaf litter at 18 sites, using nonmetric multidimensional scaling (NMDS, stress value = 0.154). Site numbers and abbreviation are as in **Table 1**. Three variables (latitude, longitude, MAT; italicized) with significant effects are indicated by arrows.

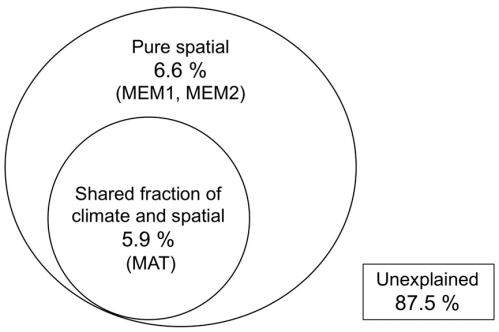


FIGURE 3 | Venn diagram showing pure and shared effects of spatial distance and climate on fungal assemblage composition as derived from variation partitioning analysis. Selected variables are in parentheses. No variables were selected in the leaf property model, i.e. the proportion of explained variation was zero.

$P = 0.0016$), and values of MEM2 were significantly correlated with the latitude (Pearson's $r = -0.823$, $n = 18$, and $P = 0.000027$) and longitude (Pearson's $r = -0.598$, $n = 18$, and $P < 0.0088$). The percentage explained by the environmental, spatial, and leaf property fractions was 5.9, 12.5, and 0%, respectively, and the shared fraction between environmental and spatial variables explained 5.9% of the variation in fungal assemblages, indicating the fraction explained by MAT was spatially structured. In total, therefore, 12.5% of the variation in fungal assemblages was explained, and the remaining 87.5% was unexplained.

Factors Relating to the Bleached Leaf Area

The bleached area accounted for 5.9% to 36.7% of the total leaf area at 18 sites (**Table 1**). The bleached area was significantly and negatively correlated with latitude and longitude and significantly and positively correlated with MAT, MAP, and the relative frequencies of *Gymnopus* sp. OTU_03, *Xylaria cubensis* OTU_07, *Gymnopus* sp. OTU_15, and Lachnocladiaceae sp. OTU_18 (**Table 3**). In contrast, the bleached area was not significantly ($P > 0.05$) correlated with the sampling month, elevation, maximum snow depth, LMA, AUR content, or the relative frequencies of other major OTUs. Stepwise model selection showed that MAT was the only predictor variable for the bleached leaf area (AIC = 108.73).

TABLE 3 | Results of generalized linear models (GLMs) for relationships between the bleached area and the geographic and climatic factors, leaf properties, and the relative frequency of major fungal OTUs.

	Coefficient	Deviance	*P*
Latitude	−2.12	1062	***
Longitude	−1.23	608	***
MAT	2.59	1083	***
MAP	0.01	391	*
OTU_03 (*Gymnopus* sp., Basidiomycota)	4.04	370	*
OTU_07 (*Xylaria cubensis*, Ascomycota)	11.20	293	*
OTU_15 (*Gymnopus* sp., Basidiomycota)	16.38	296	*
OTU_18 (Lachnocladiaceae sp., Basidiomycota)	30.15	472	**

*Results of simple regression of GLMs are shown; ***P < 0.001, **P < 0.01, and *P < 0.05. Those parameters with significant relationship at 5% level are indicated; the relationships with sampling month, elevation, LMA, AUR content, and the relative frequency of other major OTUs were not significant at 5% level and hence were not indicated. Abbreviations are as in* ***Table 1****.*

DISCUSSION

The taxa of ligninolytic fungi associated with *C. sieboldii* leaf litter in Japan have been reported as common ones in temperate and subtropical forests. Fungi in Xylariaceae were reported to be common components of fungal assemblages on leaf litter and frequently isolated from bleached portions of leaf litter (Osono, 2020). *Crinipellis, Gymnopus, Marasmiellus, Marasmius*, and *Mycena* in Basidiomycota are reported to be associated with the decomposition of lignin in leaf litter (Miyamoto et al., 2000; Valášková et al., 2007). The fungal isolates obtained from bleached portions of *C. sieboldii* leaf litter exhibited potential bleaching activity (**Table 2**), indicating that they are responsible for the bleaching in the field. In fact, these basidiomycetous taxa have repeatedly been shown to be capable of selective removal of lignin and other recalcitrant compounds from leaf litter (Osono, 2020). In contrast, fungi in Xylariaceae have been demonstrated to have a degree of ligninolytic activity but generally cause selective decomposition of components other than lignin, in accord with previous findings that xylariaceous fungi prefer cellulose to lignin (Nilsson and Daniel, 1989; Pointing et al., 2003).

The composition of fungal assemblages showed a geographical pattern across 18 sites that was correlated with the latitudinal and longitudinal gradient of MAT, as shown by NMDS (**Figure 2**), PERMANOVA, and variation partitioning (**Figure 3**). In the variation partitioning, the MAT had a spatial structure, as these strongly correlated for the 18 study sites (Pearson's $r = 0.945$, $P < 0.001$); hence, the effect of the latitude and MAT cannot be separated. Still, we detected significant effect of pure spatial fraction on fungal assemblages that was not shared by climatic variables (**Figure 3**), suggesting roles of unmeasured environmental variables that are spatially structured (Borcard and Legendre, 1994) or non-niche processes (Peay et al., 2016). In fact, some major OTUs were locally abundant and restricted to a few neighbor sites. For example, 12 (60%) of 20 isolates of *N. diffusa* OTU_02 were obtained from Site 10 (Hachijo Is.), and seven (64%) of 11 isolates of *Nodulisporium* sp. OTU_04 were from Site 1 (Iriomote Is.). The occurrence of locally-abundant OTUs implies a possible role of such non-niche processes as priority effect and dispersal limitation (Peay et al., 2010). In summary, the present study demonstrates the roles of climatic and spatial factors shaping the geographical pattern of ligninolytic fungi associated with the decomposition of leaf litter of single tree species.

The present study showed a clear gradient of the bleached area on the leaf surfaces of *C. sieboldii* which was greater at sites with higher MAT and precipitation located at lower latitudes and longitudes and at sites where *Gymnopus* spp., *Xylaria cubensis*, and Lachnocladiaceae sp. occurred at greater relative frequencies (**Table 3**). Previous studies have demonstrated that ligninolytic activity of fungi enhanced at higher temperatures (Osono, 2020) and at higher moisture condition (Fukasawa et al., 2013). Moreover, *Gymnopus* spp. and Lachnocladiaceae are shown to have potential capabilities to cause selective delignification in leaf litter (Osono et al., 2008). A few isolates of *X. cubensis* are reported to decompose lignin and other recalcitrant components actively (Osono, 2020), despite the general notion that xylariaceous fungi prefer cellulose to lignin, as discussed above. The result of the present study is consistent with the finding of a decomposition study showing that the decomposition of lignin and recalcitrant compounds is faster at warmer climates in an Asian climatic gradient (Osono, 2017). The present study suggests that not only the geographic location and climatic conditions but also the biogeographic patterns of distribution of ligninolytic fungi influence the decomposition of lignin in leaf litter.

The present study elucidated the biogeographic pattern of ligninolytic fungi associated with the bleaching of leaf litter of single tree species and the importance of climatic and spatial factors affecting the assembly of fungal assemblages. However, the explanatory power of climatic and spatial factors in the variation partitioning was low, and much of the variation in fungal assemblages remain unexplained. This suggests the importance of factors yet to be measured but affect the biogeography of bleaching fungi. Several factors may be invoked to explain such unexplained variation, such as tree species richness and composition and edaphic factors including nutrient levels (Zhang et al., 2018). Further studies are needed by incorporating more environmental variables to determine the main drivers of community assembly of ligninolytic fungi and to disentangle the relative importance of climatic, spatial, and other factors on their diversity and composition. We should note a further limitation of the present study that we used direct-observation and culture-dependent methods, which merits in confirming the potential bleaching activity for individual fungal isolates but could result in under-estimation of fungal richness due to selective retrieval of fungal isolates. Culture-independent methods such as DNA metabarcoding will be promising for comprehensive evaluation of the diversity and biogeography of ligninolytic fungi associated with the bleaching of leaf litter.

DATA AVAILABILITY STATEMENT

The datasets presented in this study can be found in online repositories. The names of the repository/repositories

and accession number(s) can be found in the article/ **Supplementary Material**.

AUTHOR CONTRIBUTIONS

TO designed this study. TO, SM, and DH collected samples and data in the field. TO and DH analyzed the samples collected. TO and SM analyzed data. TO wrote the manuscript text and prepared figures and tables. All authors reviewed the manuscript.

FUNDING

This study was partially supported by the Ministry of Education, Culture, Sports, Science, and Technology of Japan (MEXT; No. 18K05731) and Ichimura Foundation for New Technology to TO.

ACKNOWLEDGMENTS

We thank the staff at Arbocultural Research Institute and The University of Tokyo Chiba Forest, Graduate School of Agricultural and Life Sciences, The University of Tokyo, and at Kii-Oshima Research Station, Field Science Education and Research Center, Kyoto University for help with fieldwork; and Dr. Elizabeth Nakajima for critical reading of the manuscript.

SUPPLEMENTARY MATERIAL

The Supplementary Material for this article can be found online at: https://www.frontiersin.org/articles/10.3389/fmicb.2020.595427/full#supplementary-material

REFERENCES

Aoki, K., Ueno, S., Kamijo, T., Setoguchi, H., Murakami, N., Kato, M., et al. (2014). Genetic differentiation and genetic diversity of *Castanopsis* (*Fagaceae*), the dominant tree species in Japanese broadleaved evergreen forests, revealed by analysis of EST-associated microsatellites. *PLoS One* 9:e87429. doi: 10.1371/journal.pone.0087429

Bahram, M., Hildebrand, F., Forslund, S. K., Anderson, J. L., Soudzilovskaia, N. A., Bodegom, P. M., et al. (2018). Structure and function of the global topsoil microbiome. *Nature* 560, 233–237. doi: 10.1038/s41586-018-0386-6

Baldrian, P. (2017). Forest microbiome: diversity, complexity and dynamics. *FEMS Microbiol. Rev.* 41, 109–130.

Bengtsson-Palme, J., Ryberg, M., Hartmann, M., Branco, S., Wang, Z., Godhe, A., et al. (2013). Improved software detection and extraction of ITS1 and ITS2 from ribosomal ITS sequences of fungi and other eukaryotes for analysis of environmental sequencing data. *Methods Ecol. Evol.* 4, 914–919.

Blanchet, F. G., Legendre, P., and Borcard, D. (2008). Forward selection of explanatory variables. *Ecology* 89, 2623–2632. doi: 10.1890/07-0986.1

Borcard, D., and Legendre, P. (1994). Environmental control and spatial structure in ecological communities: an example using oribatid mites (*Acari*, *Oribatei*). *Environ. Ecol. Stat.* 1, 37–61. doi: 10.1007/bf00714196

Borcard, D., Legendre, P., Avois-Jacquet, C., and Tuomisto, H. (2004). Dissecting the spatial structure of ecological data at multiple scales. *Ecology* 85, 1826–1832. doi: 10.1890/03-3111

Camacho, C., Coulouris, G., Avagyan, V., Ma, N., Papadopoulos, J., Bealer, K., et al. (2009). BLAST+: architecture and applications. *BMC Bioinformatics* 10:421. doi: 10.1186/1471-2105-10-421

Fukasawa, Y., Osono, T., and Takeda, H. (2013). Effects of environmental moisture on twig litter decomposition by fungal colonizers. *J. Integr. Field Sci.* 10, 1–6. doi: 10.1007/s13225-010-0083-8

Gardes, M., and Bruns, T. D. (1993). ITS primers with enhanced specificity for basidiomycetes: application to the identification of mycorrhizae and rusts. *Mol. Ecol.* 21, 113–118. doi: 10.1111/j.1365-294x.1993.tb00005.x

Gourbière, F., van Maanen, A., and Debouzie, D. (2001). Associations between three fungi on pine needles and their variation along a climatic gradient. *Mycol. Res.* 105, 1101–1109. doi: 10.1016/s0953-7562(08)61973-5

Hagiwara, Y., Matsuoka, S., Hobara, S., Mori, A. S., Hirose, D., and Osono, T. (2015). Bleaching of leaf litter and associated fungi in subboreal and subalpine forests. *Can. J. Microbiol.* 61, 735–743. doi: 10.1139/cjm-2015-0111

Hirose, D., Hobara, S., Matsuoka, S., Kato, K., Tanabe, Y., Uchida, M., et al. (2016). Diversity and community assembly of moss-associated fungi in ice-free coastal outcrops of continental Antarctica. *Fungal Ecol.* 24, 94–101. doi: 10.1016/j.funeco.2016.09.005

Huson, D. H., Auch, A. F., Qi, J., and Schuster, S. C. (2007). MEGAN analysis of metagenomics data. *Genome Res.* 17, 377–386.

Matsukura, K., Hirose, D., Kagami, M., Osono, T., and Yamaoka, Y. (2017). Geographical distribution of rhytismataceaous fungi on *Camellia japonica* leaf litter in Japan. *Fungal Ecol.* 26, 37–44. doi: 10.1016/j.funeco.2016.11.006

Matsuoka, S., Kawaguchi, E., and Osono, T. (2016). Temporal distance decay of similarity of ectomycorrhizal fungal community composition in a subtropical evergreen forest in Japan. *FEMS Microbiol. Ecol.* 92:fiw061. doi: 10.1093/femsec/fiw061

Miura, K., and Kudo, M. (1970). An agar-medium for aquatic hyphomycetes. *Trans. Mycol. Soc. Jpa.* 11, 116–118.

Miyamoto, T., Igarashi, T., and Takahashi, K. (2000). Lignin-degrading ability of litter-decomposing basidiomycetes from Picea forests of Hokkaido. *Mycoscience* 45, 24–29.

Nilsson, T., and Daniel, G. (1989). Chemistry and microscopy of wood decay by some higher ascomycetes. *Holzforschung* 43, 11–18. doi: 10.1515/hfsg.1989.43.1.11

Oksanen, J., Blanchet, F. G., Friendly, M., Kindt, R., Legendre, P., McGlinn, D., et al. (2019). *Package 'vegan' Version 2.5-6*. Avaliable at: http://cran.r-project.org/web/packages/vegan/index.html (accessed August 8, 2020).

Osono, T. (2011). Diversity and functioning of fungi associated with leaf litter decomposition in Asian forests of different climatic regions. *Fungal Ecol.* 4, 375–385. doi: 10.1016/j.funeco.2011.02.004

Osono, T. (2017). Leaf litter decomposition of 12 tree species in a subtropical forest in Japan. *Ecol. Res.* 32, 413–422. doi: 10.1007/s11284-017-1449-0

Osono, T. (2020). Functional diversity of ligninolytic fungi associated with leaf litter decomposition. *Ecol. Res.* 35, 30–43. doi: 10.1111/1440-1703.12063

Osono, T., Ishii, Y., and Hirose, D. (2008). Fungal colonization and decomposition of *Castanopsis sieboldii* leaf litter in a subtropical forest. *Ecol. Res.* 23, 909–917. doi: 10.1007/s11284-007-0455-z

Peay, K. G., Garbelotto, M., and Bruns, T. D. (2010). Evidence of dispersal limitation in soil microorganisms: isolation reduces species richness on mycorrhizal tree islands. *Ecology* 91, 3631–3640. doi: 10.1890/09-2237.1

Peay, K. G., Kennedy, P. G., and Talbot, J. M. (2016). Dimensions of biodiversity in the Earth mycobiome. *Nat. Rev. Microbiol.* 14, 434–447. doi: 10.1038/nrmicro.2016.59

Peres-Neto, P. R., Legendre, P., Dray, S., and Borcard, D. (2006). Variation partitioning of species data matrices: estimation and comparison of fractions. *Ecology* 87, 2614–2625. doi: 10.1890/0012-9658(2006)87[2614:vposdm]2.0.co;2

Pointing, S. B., Parungao, M. M., and Hyde, K. D. (2003). Production of wood-decay enzymes, mass loss and lignin solubilization in woody by tropical Xylariaceae. *Mycol. Res.* 107, 231–235. doi: 10.1017/s0953756203007329

Preston, C. M., Trofymow, J. A., Sayer, B. G., and Niu, J. (1997). 13C nuclear magnetic resonance spectroscopy with cross-polarization and magic-angle spinning investigation of the proximate-analysis fractions used to assess litter quality in decomposition studies. *Can. J. Bot.* 75, 1601–1613. doi: 10.1139/b97-872

Tanabe, A. S., and Toju, H. (2013). Two new computational methods for universal DNA barcoding: a benchmark using barcode sequences of bacteria, archaea,

animals, fungi, and land plants. *PLoS One* 8:e76910. doi: 10.1371/journal.pone.0076910

Tedersoo, L., Bahram, M., Põlme, S., Kõljalg, U., Yorou, N. S., Wijesundera, R., et al. (2014). Global diversity and geography of soil fungi. *Science* 346:1256688.

Tokumasu, S. (2001). Geographical distribution of *Sporidesmium goidanichii* in pine forests of Japan. *Mycoscience* 42, 575–589. doi: 10.1007/bf02460957

Valášková, V., Šnajdr, J., Bittner, B., Cajthaml, T., Merhautová, V., Hofrichter, M., et al. (2007). Production of lignocellulose-degrading enzymes and degradation of leaf litter by saprotrophic basidiomycetes isolated from a *Quercus petraea* forest. *Soil Biol. Biochem.* 39, 2651–2660. doi: 10.1016/j.soilbio.2007.05.023

van der Wal, A., Geydan, T. D., Kuype, T. W., and de Boer, W. (2013). A thready affair: linking fungal diversity and community dynamics to terrestrial decomposition processes. *FEMS Microbiol. Rev.* 37, 477–494. doi: 10.1111/1574-6976.12001

van Maanen, A., Debouzie, D., and Gourbière, F. (2000). Distribution of three fungi colonizing fallen *Pinus sylvestris* needles along altitudinal transects. *Mycol. Res.* 104, 1133–1138. doi: 10.1017/s0953756299002282

Větrovský, T., Kohout, P., Kopecký, M., Machac, A., Man, M., Bahnmann, B. D., et al. (2019). A meta-analysis of global fungal distribution reveals climate-driven patterns. *Nat. Commun.* 10:5142.

Vilgalys, R., and Hester, M. (1990). Rapid genetic identification and mapping of enzymatically amplified ribosomal DNA from several *Cryptococcus* species. *J. Bacteriol.* 172, 4238–4246. doi: 10.1128/jb.172.8.4238-4246.1990

Wit, D. R., and Bouvier, T. (2006). 'Everything is everywhere, but, the environment selects'; what did baas becking and beijerinck really say? *Environ. Microbiol.* 8, 755–758. doi: 10.1111/j.1462-2920.2006.01017.x

Zhang, N., Li, Y., Wubet, T., Bruelheide, H., Liang, Y., Purahong, W., et al. (2018). Tree species richness and fungi in freshly fallen leaf litter: unique patterns of fungal species composition and their implications for enzymatic decomposition. *Soil Biol. Biochem.* 127, 120–126. doi: 10.1016/j.soilbio.2018.09.023

Conflict of Interest: The authors declare that the research was conducted in the absence of any commercial or financial relationships that could be construed as a potential conflict of interest.

Copyright © 2020 Osono, Matsuoka and Hirose. This is an open-access article distributed under the terms of the Creative Commons Attribution License (CC BY). The use, distribution or reproduction in other forums is permitted, provided the original author(s) and the copyright owner(s) are credited and that the original publication in this journal is cited, in accordance with accepted academic practice. No use, distribution or reproduction is permitted which does not comply with these terms.

frontiers in Microbiology

ORIGINAL RESEARCH
published: 24 November 2020
doi: 10.3389/fmicb.2020.581592

Crop-Zone Weed Mycobiomes of the South-Western Australian Grain Belt

Pippa J. Michael[1], Darcy Jones[1], Nicole White[2], James K. Hane[1], Michael Bunce[2] and Mark Gibberd[1]*

[1] Centre for Crop and Disease Management, School of Molecular and Life Sciences, Curtin University, Perth, WA, Australia,
[2] TRENDLab, School of Molecular and Life Sciences, Curtin University, Perth, WA, Australia

In the absence of a primary crop host, secondary plant hosts may act as a reservoir for fungal plant pathogens of agricultural crops. Secondary hosts may potentially harbor heteroecious biotrophs (e.g., the stripe rust fungus *Puccinia striiformis*) or other pathogens with broad host ranges. Agricultural grain production tends toward monoculture or a limited number of crop hosts over large regions, and local weeds are a major source of potential secondary hosts. In this study, the fungal phyllospheres of 12 weed species common in the agricultural regions of Western Australia (WA) were compared through high-throughput DNA sequencing. Amplicons of D2 and ITS were sequenced on an Illumina MiSeq system using previously published primers and BLAST outputs analyzed using MEGAN. A heatmap of cumulative presence–absence for fungal taxa was generated, and variance patterns were investigated using principal components analysis (PCA) and canonical correspondence analysis (CCA). We observed the presence of several major international crop pathogens, including basidiomycete rusts of the *Puccinia* spp., and ascomycete phytopathogens of the *Leptosphaeria* and *Pyrenophora* genera. Unrelated to crop production, several endemic pathogen species including those infecting Eucalyptus trees were also observed, which was consistent with local native flora. We also observed that differences in latitude or climate zones appeared to influence the geographic distributions of plant pathogenic species more than the presence of compatible host species, with the exception of Brassicaceae host family. There was an increased proportion of necrotrophic Ascomycete species in warmer and drier regions of central WA, compared to an increased proportion of biotrophic Basidiomycete species in cooler and wetter regions in southern WA.

Keywords: mycobiome, phyllosphere, fungi, plant pathogen, weeds

OPEN ACCESS

Edited by:
Dhanushka Nadeeshan Wanasinghe, Kunming Institute of Botany, China

Reviewed by:
Sajeewa S. N. Maharachchikumbura, University of Electronic Science and Technology of China, China
Mathabatha Evodia Setati, Stellenbosch University, South Africa

****Correspondence:***
James K. Hane
james.hane@curtin.edu.au

Specialty section:
This article was submitted to Fungi and Their Interactions, a section of the journal Frontiers in Microbiology

Received: *09 July 2020*
Accepted: *28 October 2020*
Published: *24 November 2020*

Citation:
Michael PJ, Jones D, White N, Hane JK, Bunce M and Gibberd M (2020) Crop-Zone Weed Mycobiomes of the South-Western Australian Grain Belt. Front. Microbiol. 11:581592. doi: 10.3389/fmicb.2020.581592

INTRODUCTION

In the absence of a primary crop host, secondary plant hosts may act as a reservoir for fungal plant pathogens that cause economically significant crop diseases. In a crop monoculture environment, readily available secondary hosts are commonly weed species (Narayanasamy, 2011), which may serve as important sources of inoculum for agricultural crops that are sown or planted in the following season. Outbreaks of crop diseases caused by fungi are typically monitored based on observations of disease symptoms or fungal spore counts, making early preventative control

measures (i.e., fungicide application) difficult or impossible to implement (Lindahl and Kuske, 2013). Epidemiological studies have highlighted the need for eradication of potential sources of inoculum (i.e., weeds) between growing seasons so as to restrict the incidence and spread of disease to newly planted crops (Narayanasamy, 2011). These studies have focused on a small number of pathogen species infecting major crops; however, little is known of the larger pool of fungal species that co-inhabit the plant phyllosphere (leaf surface and interior). Pathogens constitute a relatively minor proportion of a fungal community—or mycobiome (Sapkota et al., 2015; Donovan et al., 2018). Limited information on the composition of plant mycobiomes is available, with the majority of mycobiome surveys focusing on soil and human body environments (Donovan et al., 2018). Plant pathogens are not commonly featured, despite occasional reports in non-plant mycobiomes (Weyrich et al., 2017; Donovan et al., 2018). A study by Sapkota et al. (2015) found most fungal species to be common to all host cereal crops, with the exception of a few crop-specific pathogens, indicating that the majority of fungi in leaves are not host-specific and that host-specific pathogens live in a "sea" of non-specific fungi. How plant-associated mycobiomes react to inter-species interactions, environmental conditions, host genotype, and agronomic practices is largely unexplored.

Over 99,000 fungal species are documented; however, total diversity is estimated to be between 2.2 and 3.8 million species (Hawksworth and Lücking, 2017). Traditional culture-dependent studies have revealed an immense diversity of fungal communities colonizing the plant phyllosphere, although more recent metagenomic studies indicate that this may be underestimated (Peršoh, 2015). Phyllosphere mycobiomes are highly variable among leaves within an individual plant, with factors such as leaf position, canopy height, and leaf age shown to influence leaf-to-leaf variability (Kinkel, 1997). An overlap between fungi found in the phyllosphere and the air spora has also been reported (Levetin and Dorsey, 2006). A study on beech tree (*Fagus sylvatica*) looking at variability at four different spatial scales (tree, branch, group of leaves, and individual leaf) found the majority of variation occurred at the smallest spatial scale (i.e., between individual leaves), with intra-host variability of phyllosphere fungal populations distinctly greater than inter-host variability (Cordier et al., 2012). However, within a single tree canopy, mycobiome profiles become more similar with decreasing distance, suggesting that these differences may be minimized for a single sapling when it is small and has only a few leaves. When analyzing differences between individual trees, dissimilarity between mycobiomes was linked with genetic rather than geographic distance between trees (Cordier et al., 2012). Several studies have also found that genetic makeup of the plant host at both the species and cultivar/ecotype level was the major factor influencing fungal diversity on plant leaves (Joshee et al., 2009; Bálint et al., 2013; Hunter et al., 2015; Sapkota et al., 2015), with spatial and seasonal factors also having significant but lesser impacts. While Sapkota et al. (2015) found crop genotype was the principal factor in explaining mycobiome diversity in cereal phyllospheres, within each of the individual crops studied (wheat, winter, and spring barley), location also played an important role. Blixt et al. (2010) found that variation of community composition was greater between fields of diseased wheat (*Triticum aestivum*) than within fields as did Zimmerman and Vitousek (2012) who found that among-site diversity of a single tree species (*Metrosideros polymorpha*) contributed more than within-site diversity to the overall fungal community richness. In addition to spatial, temporal, and genetic factors, phyllosphere mycobiomes are also influenced by management factors, with fungicide use shown to have an impact on the composition of cereal leaf mycobiomes (Karlsson et al., 2014; Sapkota et al., 2015).

In this study, we identified the plant pathogens present in the phyllosphere mycobiomes of commonly found weed species adjacent to cropping fields. We also report differences in weed mycobiome composition in response to host species and spatial/climatic factors. This information on weed host-specific or region-specific association with pathogen species may become an increasingly important factor in developing new methods for crop disease management in the future.

MATERIALS AND METHODS

Field Sampling

Leaves from 12 common agricultural weed species (**Table 1**) were sampled from 15 locations across the Western Australian grain belt (**Figure 1**) over a 5-day period during autumn, 2016. All sites were located on road verges adjacent to cropping paddocks and selected for maximum number of weed species present. Environmental and spatial data were recorded for each site (**Table 2**), with climatic data from 1950 to 2020. The optimal number of individual plants required per site to be representative of the fungal biota present needed to be determined. Therefore, 10 leaves of two weed species (*Lolium rigidum* and *Raphanus raphanistrum*) were sampled from one site (Yoting) and the preliminary metagenome sequencing results were used to benchmark the appropriate number of leaves for sequencing (**Supplementary Figure 1**). Thus, for each weed species sampled at each site, one uppermost leaf from 10 individual plants were stored at 4°C during transport to the lab (24–48 h), then at −20°C. Each set of 10 leaves was randomly sub-sampled using a 5-mm disc punch and combined in a 5-ml sample vial until full prior to DNA sequencing.

DNA Extraction and Quantification

DNA was extracted using a QIAmp Plant Mini Kit (Qiagen, Venlo) with a modified protocol including (1) 600 μl of API digestion buffer; (2) overnight sample digestion at 65°C; and (3) the following day, addition of 195 μl of P3 to digests prior to putting on ice. A total volume of 400 μl was placed in a QIAcube, after which the remaining QIAmp Plant Mini Kit protocol was followed. Genomic DNA (gDNA) extracts were eluted in 100 μl of AE buffer and stored at −20°C, and then quantified and assessed for quality via real-time quantitative polymerase chain reaction (qPCR) at three dilutions (1:1, 1:10, and 1:100). Primer pairs were designed to amplify a highly conserved region of the 26S gene between the D1/D2 domains (Q1_F 5′ GTTGTTTGGGAATGCAGCTC 3′ and QB3_R 5′

TABLE 1 | Sampling incidence of 12 common weed species from 15 locations within the Western Australian grain belt.

Species	Family	Group	Common name	No. locations sampled
Arctotheca calendula L.	Asteraceae	Dicotyledon	Capeweed	14
Avena fatua L.	Poaceae	Monocotyledon	Wild oats	13
Bromus spp.	Poaceae	Monocotyledon	Brome grass	4
Echium plantagineum L.	Boraginaceae	Dicotyledon	Patterson's curse	2
Emex australis Steinh.	Polygonaceae	Dicotyledon	Doublegee	3
Erodium spp.	Geraniaceae	Dicotyledon	Erodium	4
Hordeum spp.	Poaceae	Monocotyledon	Barley grass	1
Hypochaeris radicata L.	Asteraceae	Dicotyledon	Flatweed	8
Lolium rigidum Gaud	Poaceae	Monocotyledon	Annual ryegrass	14
Oxalis pes-caprae L.	Oxalidaceae	Dicotyledon	Soursob	1
Raphanus raphanistrum L.	Brassicaceae	Dicotyledon	Wild radish	12
Vulpia spp.	Poaceae	Monocotyledon	Silvergrass	2

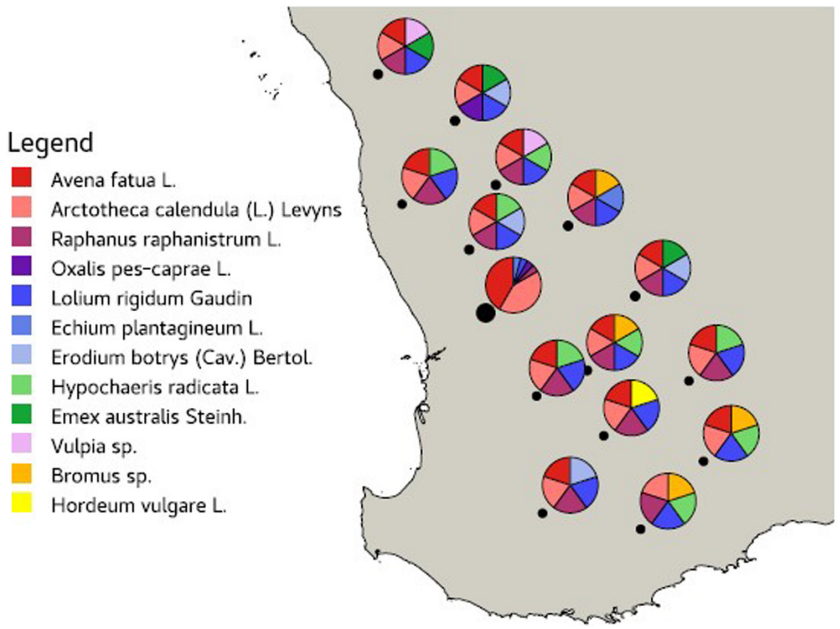


FIGURE 1 | Map of the Western Australian grain belt showing the 15 sampling locations (black dot) and the weed species sampled at each site.

AGTGCTTTTCATCTTTCCCTCAC 3′). qPCR was performed in 25-μl reactions containing 1 × PCR Gold Buffer, 2.5 mM $MgCl_2$, 0.4 mg/ml BSA, 0.25 mM of each dNTP, 0.4 μM of forward and reverse primer, 0.25 μl of AmpliTaq Gold, 0.6 μl of SYBR Green, and 2 μl of gDNA. The qPCR cycling conditions included an initial heat denaturation at 95°C for 5 min, 40 cycles of 95°C for 30 s, 52°C for 30 s, and 72°C for 45 s, and then a final extension at 72°C for 10 min. From the qPCR results, an optimal DNA concentration was selected for DNA sequencing, which was free of inhibition and yielded DNA of sufficient quality, as reported to facilitate reproducible quantitative data by (Murray et al., 2011).

High-Throughput DNA Sequencing

The D2 and ITS2 amplicons were sequenced on an Illumina MiSeq system utilizing previously published primers that were modified with a unique 8-bp Multiplex Identifier tag (MID-tag) and MiSeq adaptors for paired-end sequencing. For the D2 domain primers, U1_F (Putignani et al., 2008) and NL4_R (Kurtzman and Robnett, 1998) were utilized, and for the ITS2 region, fITS7_F (Ihrmark et al., 2012) and ITS4_R (White et al., 1990) were used. Independent MID-tagged qPCR setup for samples and controls were prepared in a physically separate ultra-clean laboratory and were carried out using each primer set in 25-μl reactions containing 1 × PCR Gold Buffer, 2.5 mM $MgCl_2$, 0.4 mg/ml BSA, 0.25 mM of each dNTP, 0.4 μM of forward and reverse MID-tag primer, 0.25 μl of AmpliTaq Gold, 0.6 μl of SYBR Green, and 2 μl of gDNA. The cycling conditions for qPCR using the U1_F/NL4_R (52°C annealing) and fITS7_F/ITS4_R (54°C annealing) primer sets were as follows: initial heat denaturation at 95°C for 5 min, followed by 40

TABLE 2 | Spatial and climatic details (averaged over 1950–2020) for each location.

Location	Latitude (°S)	Longitude (°E)	Annual rainfall (mm)	Annual mean temp (°C)	Annual min temp (°C)	Annual max temp (°C)	No. weeds sampled
Badgingarra	−30.2111	115.4599	521	19.2	12.3	25.6	5
Borden	−34.0256	118.2634	377	15.8	9.8	21.7	5
Buntine	−29.9852	116.5618	319	19.4	12.2	26.5	6
Harrismith	−32.9292	117.8300	356	16.5	9.6	22.8	5
Hyden	−32.2848	118.8303	342	17.1	9.9	24.5	5
Kalannie	−30.4651	117.4111	307	19.2	12.0	26.0	6
Kojonup	−33.8383	117.1103	505	15.5	9.1	21.6	5
Morawa	−29.0817	115.9865	308	20.0	12.8	27.6	6
Mullewa	−28.6862	115.1780	352	19.6	13.0	26.6	6
Newdegate	−33.2284	119.0020	357	16.0	9.5	22.9	5
Nungarin	−31.2907	118.1990	296	18.2	11.4	25.3	6
Pingelly	−32.4618	117.0406	427	16.7	9.9	23.7	5
Toodyay	−31.4870	116.4431	485	18.1	11.2	24.9	3
Walebing	−30.7444	116.2491	432	18.3	11.6	25.1	6
Yoting	−32.1621	117.6333	325	17.4	10.2	24.2	4

Data sourced from https://www.longpaddock.qld.gov.au/silo/.

cycles of 95°C for 30 s; 52°C or 54°C for 30 s (annealing step); and 72°C for 45 s followed by final extension at 72°C for 10 min. Multiplex Identifier-tagged PCR amplicons were generated in duplicate for each sample and pooled together to minimize the effects of PCR stochasticity. The pooled amplicons were quantified on a LabChip (with high-sensitivity chip) and then combined to produce a final library of equimolar ratio per sample. The final library was then purified on a PippinPrep with a size selection gate of 300–600 base pair capture following the manufacturer's protocol (PerkinElmer). The purified library was diluted with purified water and re-run on the LabChip to determine the volume required (2 nM) for Illumina MiSeq paired-end sequencing. For each MID-tagged qPCR assay, extraction and PCR controls were included, and if found to contain amplifiable DNA, these reactions were incorporated into the pooled MID-tagged DNA sequencing library. Illumina MiSeq sequencing was performed using a MiSeq Reagent Kit v2 (500 cycles) 250-bp paired-end protocol as per the manufacturer's instruction. Paired-end reads were stitched using Illumina's MiSeq Reporter software.

DNA Sequence Quality Filtering and Analyses

Stitched sequences were separated from unstitched, which had low overall phred scores and were discarded. MID-tags and gene-specific primers were trimmed from the sequences allowing for no mismatch in length or base composition using QIIME1 (extract_barcodes.py) and de-multiplexed using QIIME2 (Caporaso et al., 2010). De-multiplexed reads were then trimmed and filtered using v1.9 ($\leq$6 undetermined bases, quality cutoffs: $5' = 25$ and $3' = 22$) (Martin, 2011). Reads were then error-corrected using deblur (Amir et al., 2017) within QIIME2 (Caporaso et al., 2010), using a custom database of ITS [combining UNITE (Kõljalg et al., 2013), ITS2 (Ankenbrand et al., 2015), and NCBI bioproject: PRJNA177353] and LSU [combining RDP (Cole et al., 2013) and NCBI bioproject: PRJNA51803] sequences, but discarding those below 258 bp for ITS and 240 bp for D2 sequences. Similar sequences to these clustered consensus sequences in the NCBI nt and GSS databases were also found using BLAST + v2.2.6 (blastn). The BLAST databases were filtered before searching to exclude sequences with NCBI taxonomic IDs in the subtree below "12908" (unknown and environmental samples) or containing the keyword "Uncultured" in the sequence name.

Data Analysis

BLAST outputs were analyzed using MEGAN v6.11.2 (Huson et al., 2016) (Weighted LCA, Min Score: 50, Max Expected: 1e-5, Min Percent Identity: 70, Top Percent: 10.0, Min Support Percent: 0.05, Min Support: 1, Percent to cover: 50). Taxonomic lineages for OTUs were found and manipulated using custom scripts[1] based on the NCBI taxonomy database. OTUs with taxonomic assignments were associated with the samples and summarized to generate presence–absence profiles. Presence–absence profiles of fungal taxa were generated for each sample using a cumulative approach, whereby the presence of a low-level taxon also automatically assigned presence to its higher-level taxa. Patterns of variance were investigated using principal components analysis (PCA) using the scikit-learn python package (Pedregosa et al., 2011) as well as by performing canonical correspondence analysis (CCA) using the R package "vegan" (Oksanen et al., 2019). Species richness was also measured using the Shannon–Weaver and Simpson diversity indices in the R package "vegan." To infer the specific identities of OTUs, OTU sequences were searched with BLAST against the custom database developed for this study (see above). BLAST matches were filtered to contain

[1]https://github.com/darcyabjones/acc-to-tax

alignments with greater than 95% identical matches, and covering at least 90% of the OTU sequence.

RESULTS AND DISCUSSION

Crop-Zone Weeds Are Host to a Wide Range of Plant-Associated Fungi

Overall, 2391 and 1819 OTUs were detected from the sequenced ITS and D2 loci, respectively (**Supplementary Table 1**). As an indicator of the specificity of identification, 1231 ITS and 1086 D2 OTUs were directly assigned to NCBI taxonomy identifiers at genus level or lower via BLASTN to Genbank (nt and GSS), while 7 and 15 could not be assigned to any taxonomic identifiers (**Supplementary Table 2**). Most OTUs were assigned to taxa at or below the fungal classes Dothideomycetes, Tremellomycetes, and Sordariomycetes (**Supplementary Table 3**). Species richness was highest in weeds within the Brassicaceae and Polygonacae, followed by other host families that were not dissimilar. Among the fungal species taxa detected in weed samples, the heteroecious rusts of the *Puccinia* spp. (Zhao et al., 2016) (*Puccinia graminis*, *Puccinia bassiae*, *Puccinia coronata*, and *Puccinia malvacearum*) were prominently represented across multiple West Australian weed hosts (**Supplementary Table 3**). These reports of common Australian weeds as alternate hosts for the *Puccinia* rusts are analogous to a growing collection of reports across Europe, the United States, and Asia (Roelfs, 1982; Jin et al., 2010; Wang and Chen, 2013; Zhao et al., 2016). In this study, *P. graminis* was observed on *Bromus*; *P. bassiae* on *Echium* and *Avena*; *P. coronata* on *Bromus* and *Lolium*; and *P. malvacearum* on *Bromus*, *Lolium*, *Avena*, *Echium*, and *Raphanus*. Additional species of agricultural relevance that were identified tended to infect multiple hosts, including the following: *Leptosphaeria maculans*, *Leptosphaeria biglobosa*, *Drechslera campanulata* (syn. *Pyrenophora semeniperda*; ring spot of oat), and *Drechslera nobleae* (syn. *Pyrenophora phaeocomes*, pathogen of rye and pastures). Species endemic to Australia, including several species associated with native eucalypts (*Cladoriella eucalypti, Fusculina eucalypti, Plectosphaera eucalypti, Phacidiella eucalypti, Phaeococcomyces eucalypti*, and *Saccharata eucalyptorum*) (**Supplementary Table 2**), were detected, which were consistent with the local environment but unrelated to crop production. Several genera that contain well-known crop pathogen species were also detected, however, their species-level identities were inconclusive. These included *Cladosporium*, *Zymoseptoria*, *Phaeosphaeria*, *Bipolaris*, *Pyrenophora*, *Venturia*, *Colletotrichum*, *Fusarium*, *Taphrina*, and *Ustilago*. We looked for (using covariance analysis of presence–absence variation) consistent association of two or more species across samples, as well as the inverse mutual exclusion of species (**Supplementary Table 4**), but unlike similar previous studies (Sapkota et al., 2017), we did not observe strong evidence of species complexes or potential bio-control agents across these samples. While culture-independent methods, which are based on the extraction and analysis of nucleic acids, can provide a comprehensive overview of microbial communities, they have drawbacks such as the detection of DNA from dead cells (Müller and Ruppel,

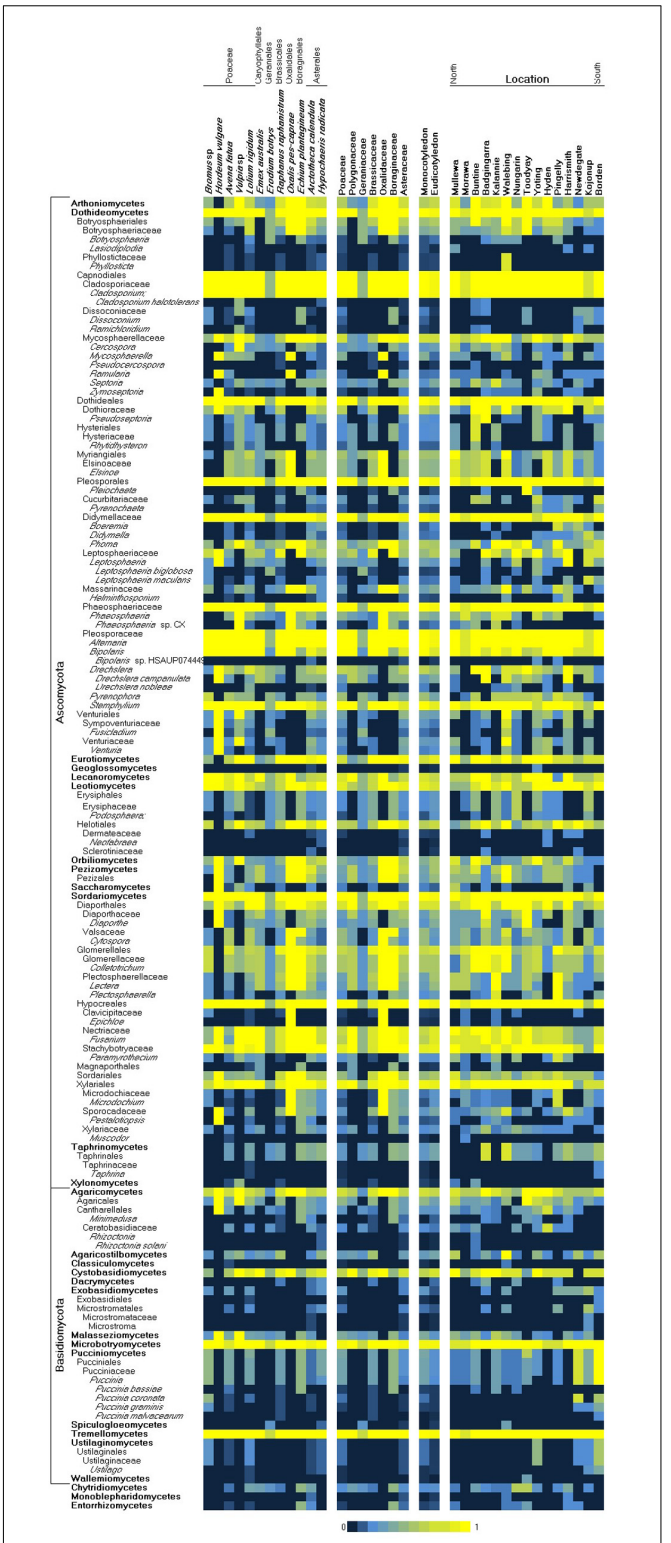


FIGURE 2 | Heatmap of the observed presence of common fungal pathogen genera/species by weed host species and collection location (left/North to right/South). A presence score from 0 to 1 (shown in blue–yellow) indicates the proportion of observed presence of a taxon across all samples of a common species or location, where 0 indicates total absence and 1 indicates ubiquity.

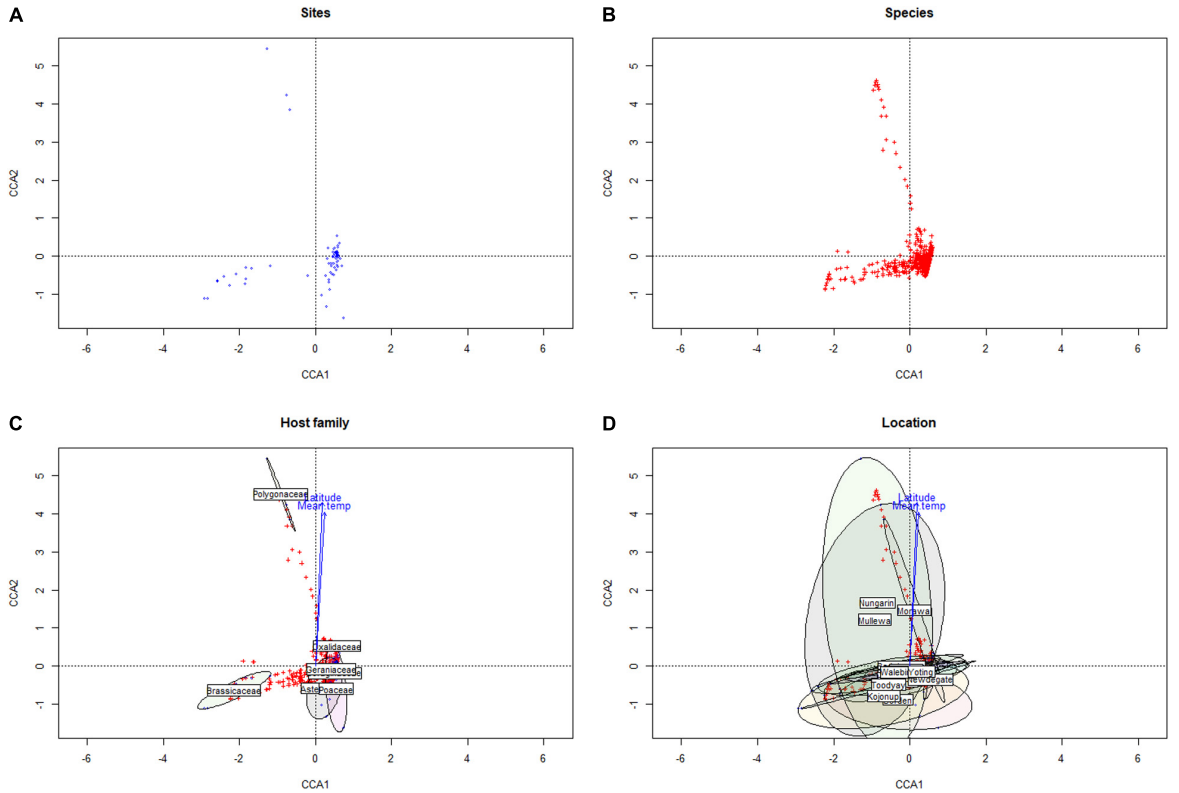


FIGURE 3 | Canonical correspondence analysis of sampled sites **(A)** and microbial taxa **(B)** versus climate conditions and geographic locations, with groupings presented by taxonomic family **(C)** and by location **(D)**.

2014) and dependence on well-annotated databases (Blackwell, 2011; Aylward et al., 2017). It has been reported that up to 20% of fungal sequences in major databases such as GenBank may be misidentified (Bridge et al., 2003; Nilsson et al., 2008). However, the internal transcribed spacer regions (ITS1 and ITS2) have been demonstrated to be taxonomic markers for fungi due to their length and discriminative sequence variation (Lindahl and Kuske, 2013). Nevertheless, an issue we encountered with the taxonomic mapping of OTUs was that mappings to the species level were not consistently achieved. Species level (or lower taxa) would be required in order to reliably assign a crop disease to an OTU and infer its potential host range. Species-level mapping was dependent on multiple factors including representation bias across different taxa in sequence databases, variable map-ability of reads across different taxa, and potential for some species to be present but undetectable. In this study, OTU alignments more often supported the genus-level over species-level mappings; hence, this limited our ability to infer fully the disease risks posed by crop-zone weeds. We have presented a taxonomic summary of genera likely to contain plant-pathogenic species in **Figure 2**, although in most cases, the presence of pathogenic species was inconclusive, as endophytic species may have also been detected.

Regional Biases

Within the Western Australian regions sampled, there appeared to be an overall trend for a relatively increased presence of Ascomycota in northern sample sites and a corresponding relative increase in Basidiomycota (particularly biotrophic rusts of the *Puccinia* spp.) in southern sites (**Figure 2**). Multivariate clustering of samples tended to form groups based on geographic locations rather than by the weed host (**Supplementary File 1**), suggesting that location and/or climate zone was a major factor influencing the weed phyllosphere. This was also supported by CCA (**Figure 3** and **Supplementary File 2**), which indicated that the phyllosphere composition was influenced by the continuous variables, latitude and mean temperature. Species distributions in the CCA corroborated the initial observation of a necrotrophic bias in hotter and dryer northern regions and a corresponding biotrophic bias in cooler and wetter southern regions (**Figure 3** and **Supplementary File 2**). CCA also indicated clustering of hosts of the Polygonaceae family with a strong association with northern latitudes and increased temperatures, which was due to the three *Emex* (syn. doublegee) samples having been exclusively obtained from sites in the northern wheatbelt (Mullewa, Morawa, and Nungarin). However, a host cluster by Brassicaceae (composed of 13 *R. raphanistrum* samples) along CCA1 could not be explained by latitude or temperature vectors and suggests that unique host-specific pathogens may be present on this weed species. The other host families were represented at all sites and did not exhibit any clustering by CCA.

This approximate north-to-south division may reflect that the northern regions in this study are warmer and drier, which may

suppress saprophytic and/or pathogen-suppressive microbial activity that would break down the stubble containing pathogen inoculum—a common problem with cereal necrotrophs (typically of the Ascomycota). Conversely, the southernmost regions of WA are cooler and have increased rainfall, which likely increases the spread and survivability of heteromecic/obligate biotrophic pathogens (typically of the Basidiomycota). Although crop pathogen species were in the relative minority within the phyllosphere, this appears to be consistent to other studies linking climate zones to the distribution of fungal pathogens (Bebber et al., 2014; Fisher et al., 2018).

CONCLUSION

This survey of the weed phyllospheres local to cereal crop-growing regions of Western Australia demonstrates the utility of this approach for the monitoring of plant pathogenic species and could be adapted for the purpose of monitoring for pathogen reservoirs and emerging crop disease risks. We report the presence of several important crop pathogen species within the phyllospheres of local weed hosts and observe that host range and climate zone are both important factors in determining their geographic distributions.

DATA AVAILABILITY STATEMENT

Sequence data was deposited in NCBI BioProject: https://www.ncbi.nlm.nih.gov/bioproject/672330.

AUTHOR CONTRIBUTIONS

PM, JH, and MG contributed to the conception and design of the study. PM conducted the field sampling. NW contributed to DNA extraction and sequencing. DJ and JH contributed to DNA sequence quality filtering and data analysis. PM, JH, DJ, and NW contributed to the manuscript. All authors contributed to the article and approved the submitted version.

FUNDING

This study was conducted within the Centre for Crop and Disease Management, a cooperative research center funded by the Grains and Research Development Corporation (GRDC) and Curtin University.

ACKNOWLEDGMENTS

This work was supported by resources provided by the Pawsey Supercomputing Centre with funding from the Australian and Western Australian Governments.

SUPPLEMENTARY MATERIAL

The Supplementary Material for this article can be found online at: https://www.frontiersin.org/articles/10.3389/fmicb.2020.581592/full#supplementary-material

Supplementary Figure 1 | Fungal species accumulation curves across 10 samples of *Lolium rigidum* and *Raphanus raphanistrum* leaves sampled from Yoting.

Supplementary Table 1 | OTU frequencies for ITS and D2 regions versus host taxonomy and sample locations.

Supplementary Table 2 | Assignment of taxa to OTUs via BLAST.

Supplementary Table 3 | Combined ITS and D2 relative frequencies of microbial taxa versus host taxonomy and sample locations. Each microbial taxon detected by either an ITS or D2 OTU sequence is expressed in terms of a number ranging from 0 to 1, where 1 indicates universal occurrence across host taxa or sample locations, and 0 indicates no occurrences.

Supplementary Table 4 | Co-variance tests for association of taxon pairs across samples. Taxon pairs with high or low co-variance may indicate biologically relevant associations or mutually exclusions across samples in this study.

Supplementary File 1 | Multivariate analyses of microbial taxa testing for relationships versus host species or sample locations.

Supplementary File 2 | Canonical correspondence analyses of microbial taxa testing for relationships between host taxa, pathogen taxa, sample location and climate.

REFERENCES

Amir, A., Mcdonald, D., Navas-Molina, J. A., Kopylova, E., Morton, J. T., Xu, Z. Z., et al. (2017). Deblur rapidly resolves single-nucleotide community sequence patterns. *mSystems* 2:e0191-16. doi: 10.1128/mSystems.00191-16

Ankenbrand, M. J., Keller, A., Wolf, M., Schultz, J., and Förster, F. (2015). ITS2 database V: twice as much. *Mol. Biol. Evol.* 32, 3030–3032. doi: 10.1093/molbev/msv174

Aylward, J., Steenkamp, E. T., Dreyer, L. L., Roets, F., Wingfield, B. D., and Wingfield, M. J. (2017). A plant pathology perspective of fungal genome sequencing. *IMA Fungus* 8, 1–15. doi: 10.5598/imafungus.2017.08.01.01

Bálint, M., Tiffin, P., Hallström, B., O'hara, R. B., Olson, M. S., Fankhauser, J. D., et al. (2013). Host genotype shapes the foliar fungal microbiome of balsam poplar (*Populus balsamifera*). *PLoS One* 8:e53987. doi: 10.1371/journal.pone.0053987

Bebber, D. P., Holmes, T., and Gurr, S. J. (2014). The global spread of crop pests and pathogens. *Glob. Ecol. Biogeogr.* 23, 1398–1407. doi: 10.1111/geb.12214

Blackwell, M. (2011). The fungi: 1, 2, 3. 5.1 million species? *Am. J. Bot.* 98, 426–438. doi: 10.3732/ajb.1000298

Blixt, E., Olson, Å, Lindahl, B., Djurle, A., and Yuen, J. (2010). Spatiotemporal variation in the fungal community associated with wheat leaves showing symptoms similar to stagonospora nodorum blotch. *Eur. J. Plant Pathol.* 126, 373–386. doi: 10.1007/s10658-009-9542-z

Bridge, P. D., Roberts, P. J., Spooner, B. M., and Panchal, G. (2003). On the unreliability of published DNA sequences. *New Phytol.* 160, 43–48. doi: 10.1046/j.1469-8137.2003.00861.x

Caporaso, J. G., Kuczynski, J., Stombaugh, J., Bittinger, K., Bushman, F. D., Costello, E. K., et al. (2010). QIIME allows analysis of high-throughput community sequencing data. *Nat. Methods* 7, 335–336. doi: 10.1038/nmeth.f.303

Cole, J. R., Wang, Q., Fish, J. A., Chai, B., Mcgarrell, D. M., Sun, Y., et al. (2013). Ribosomal database project: data and tools for high throughput rRNA analysis. *Nucleic Acids Res.* 42, D633–D642. doi: 10.1093/nar/gkt1244

Cordier, T., Robin, C., Capdevielle, X., Desprez-Loustau, M.-L., and Vacher, C. (2012). Spatial variability of phyllosphere fungal assemblages: genetic distance

predominates over geographic distance in a European beech stand (*Fagus sylvatica*). *Fungal Ecol.* 5, 509–520. doi: 10.1016/j.funeco.2011.12.004

Donovan, P. D., Gonzalez, G., Higgins, D. G., Butler, G., and Ito, K. (2018). Identification of fungi in shotgun metagenomics datasets. *PLoS One* 13:e0192898. doi: 10.1371/journal.pone.0192898

Fisher, M. C., Hawkins, N. J., Sanglard, D., and Gurr, S. J. (2018). Worldwide emergence of resistance to antifungal drugs challenges human health and food security. *Science* 360, 739–742. doi: 10.1126/science.aap7999

Hawksworth, D. L., and Lücking, R. (2017). Fungal diversity revisited: 2.2 to 3.8 million species. *Microbiol. Spectr.* 5, 1–2. doi: 10.1128/microbiolspec.FUNK-0052-2016

Hunter, P. J., Pink, D. A., and Bending, G. D. (2015). Cultivar-level genotype differences influence diversity and composition of lettuce (*Lactuca* sp.) phyllosphere fungal communities. *Fungal Ecol.* 17, 183–186. doi: 10.1016/j.funeco.2015.05.007

Huson, D. H., Beier, S., Flade, I., Górska, A., El-Hadidi, M., Mitra, S., et al. (2016). MEGAN community edition - interactive exploration and analysis of large-scale microbiome sequencing data. *PLoS Comput. Biol.* 12:e1004957. doi: 10.1371/journal.pcbi.1004957

Ihrmark, K., Bödeker, I., Cruz-Martinez, K., Friberg, H., Kubartova, A., Schenck, J., et al. (2012). New primers to amplify the fungal ITS2 region-evaluation by 454-sequencing of artificial and natural communities. *FEMS Microbiol. Ecol.* 82, 666–677. doi: 10.1111/j.1574-6941.2012.01437.x

Jin, Y., Szabo, L. J., and Carson, M. (2010). Century-old mystery of *Puccinia striiformis* life history solved with the identification of *Berberis* as an alternate host. *Phytopathology* 100, 432–435. doi: 10.1094/Phyto-100-5-0432

Joshee, S., Paulus, B. C., Park, D., and Johnston, P. R. (2009). Diversity and distribution of fungal foliar endophytes in New Zealand podocarpaceae. *Mycol. Res.* 113, 1003–1015. doi: 10.1016/j.mycres.2009.06.004

Karlsson, I., Friberg, H., Steinberg, C., and Persson, P. (2014). Fungicide effects on fungal community composition in the wheat phyllosphere. *PLoS One* 9:e111786. doi: 10.1371/journal.pone.0111786

Kinkel, L. L. (1997). Microbial population dynamics on leaves. *Annu. Rev. Phytopathol.* 35, 327–347. doi: 10.1146/annurev.phyto.35.1.327

Kõljalg, U., Nilsson, R. H., Abarenkov, K., Tedersoo, L., Taylor, A. F., Bahram, M., et al. (2013). Towards a unified paradigm for sequence-based identification of fungi. *Mol. Ecol.* 22, 5271–5277. doi: 10.1111/mec.12481

Kurtzman, C. P., and Robnett, C. J. (1998). Identification and phylogeny of ascomycetous yeasts from analysis of nuclear large subunit (26S) ribosomal DNA partial sequences. *Antonie Van Leeuwenh.* 73, 331–371. doi: 10.1023/A:1001761008817

Levetin, E., and Dorsey, K. (2006). Contribution of leaf surface fungi to the air spora. *Aerobiologia* 22, 3–12. doi: 10.1007/s10453-005-9012-9

Lindahl, B. D., and Kuske, C. R. (2013). "Metagenomics for study of fungal ecology," in *The Ecological Genomics of Fungi*, ed. F. Martin (Hoboken, NJ: Wiley-Blackwell), 279–303. doi: 10.1002/9781118735893

Martin, M. (2011). Cutadapt removes adapter sequences from high-throughput sequencing reads. *EMBnet J.* 17, 10–12. doi: 10.14806/ej.17.1.200

Müller, T., and Ruppel, S. (2014). Progress in cultivation-independent phyllosphere microbiology. *FEMS Microbiol. Ecol.* 87, 2–17. doi: 10.1111/1574-6941.12198

Murray, D. C., Bunce, M., Cannell, B. L., Oliver, R., Houston, J., White, N. E., et al. (2011). DNA-based faecal dietary analysis: a comparison of qPCR and high throughput sequencing approaches. *PLoS One* 6:e25776. doi: 10.1371/journal.pone.0025776

Narayanasamy, P. (2011). "Detection of fungal pathogens in the environment," in *Microbial Plant Pathogens Detection and Disease Diagnosis*, ed. P. Narayanasamy (Cham: Springer), 201–244. doi: 10.1007/978-90-481-9735-4

Nilsson, R. H., Kristiansson, E., Ryberg, M., Hallenberg, N., and Larsson, K.-H. (2008). Intraspecific ITS variability in the kingdom Fungi as expressed in the international sequence databases and its implications for molecular species identification. *Evol. Bioinform.* 4, 193–201. doi: 10.4137/EBO.S653

Oksanen, J., Blanchet, F. G., Friendly, M., Kindt, R., Legendre, P., McGlinn, D., et al. (2019). *vegan: Community Ecology Package. R Package Version 2.5-6*. Available online at: https://CRAN.R-project.org/package=vegan (accessed September 11, 2020).

Pedregosa, F., Varoquaux, G., Gramfort, A., Michel, V., Thirion, B., Grisel, O., et al. (2011). Scikit-learn: machine learning in python. *J. Mach. Learn. Res.* 12, 2825–2830.

Peršoh, D. (2015). Plant-associated fungal communities in the light of meta'omics. *Fungal Divers.* 75, 1–25. doi: 10.1007/s13225-015-0334-9

Putignani, L., Paglia, M. G., Bordi, E., Nebuloso, E., Pucillo, L. P., and Visca, P. (2008). Identification of clinically relevant yeast species by DNA sequence analysis of the D2 variable region of the 25-28S rRNA gene. *Mycoses* 51, 209–227. doi: 10.1111/j.1439-0507.2007.01472.x

Roelfs, A. P. (1982). Effects of barberry eradication on stem rust in the United States. *Plant Dis.* 66, 177–181. doi: 10.1094/Pd-66-177

Sapkota, R., Jørgensen, L. N., and Nicolaisen, M. (2017). Spatiotemporal variation and networks in the mycobiome of the wheat canopy. *Front. Plant Sci.* 8:1357. doi: 10.3389/fpls.2017.01357

Sapkota, R., Knorr, K., Jørgensen, L. N., O'hanlon, K. A., and Nicolaisen, M. (2015). Host genotype is an important determinant of the cereal phyllosphere mycobiome. *New Phytol.* 207, 1134–1144. doi: 10.1111/nph.13418

Wang, M. N., and Chen, X. (2013). First report of Oregon grape (*Mahonia aquifolium*) as an alternate host for the wheat stripe rust pathogen (*Puccinia striiformis* f. sp. *tritici*) under artificial inoculation. *Plant Dis.* 97, 839–839. doi: 10.1094/Pdis-09-12-0864-Pdn

Weyrich, L. S., Duchene, S., Soubrier, J., Arriola, L., Llamas, B., Breen, J., et al. (2017). Neanderthal behaviour, diet, and disease inferred from ancient DNA in dental calculus. *Nature* 544, 357–361. doi: 10.1038/nature21674

White, T. J., Bruns, T., Lee, S., and Taylor, J. (1990). "Amplification and direct sequencing of fungal ribosomal RNA genes for phylogenetics," in *PCR Protocols: a Guide to Methods and Applications*, eds M. Innis, D. Gelfand, J. Sninsky, and T. J. White (Michigan: Academic Press), 315–322. doi: 10.1016/b978-0-12-372180-8.50042-1

Zhao, J., Wang, M., Chen, X., and Kang, Z. (2016). Role of alternate hosts in epidemiology and pathogen variation of cereal rusts. *Annu. Rev. Phytopathol.* 54, 207–228. doi: 10.1146/annurev-phyto-080615-095851

Zimmerman, N. B., and Vitousek, P. M. (2012). Fungal endophyte communities reflect environmental structuring across a Hawaiian landscape. *Proc. Natl. Acad. Sci. U.S.A.* 109, 13022–13027. doi: 10.1073/pnas.1209872109

Conflict of Interest: The authors declare that the research was conducted in the absence of any commercial or financial relationships that could be construed as a potential conflict of interest.

Copyright © 2020 Michael, Jones, White, Hane, Bunce and Gibberd. This is an open-access article distributed under the terms of the Creative Commons Attribution License (CC BY). The use, distribution or reproduction in other forums is permitted, provided the original author(s) and the copyright owner(s) are credited and that the original publication in this journal is cited, in accordance with accepted academic practice. No use, distribution or reproduction is permitted which does not comply with these terms.

frontiers in Microbiology

ORIGINAL RESEARCH
published: 09 December 2020
doi: 10.3389/fmicb.2020.598321

Species Diversity With Comprehensive Annotations of Wood-Inhabiting Poroid and Corticioid Fungi in Uzbekistan

Yusufjon Gafforov[1,2,3,4,5,6,7], Alexander Ordynets[3], Ewald Langer[3], Manzura Yarasheva[2], Adriana de Mello Gugliotta[5], Dmitry Schigel[8,9], Lorenzo Pecoraro[10], Yu Zhou[11], Lei Cai[2] and Li-Wei Zhou[2,4]**

[1] Laboratory of Mycology, Institute of Botany, Academy of Sciences of the Republic of Uzbekistan, Tashkent, Uzbekistan, [2] State Key Laboratory of Mycology, Institute of Microbiology, Chinese Academy of Sciences, Beijing, China, [3] Department of Ecology, University of Kassel, Kassel, Germany, [4] Institute of Applied Ecology, Chinese Academy of Sciences, Shenyang, China, [5] Núcleo de Pesquisa em Micologia, Instituto de Botânica, São Paulo, Brazil, [6] Department of Ecology and Botany, Andijan State University, Andijan, Uzbekistan, [7] Tashkent State Agrarian University, Tashkent, Uzbekistan, [8] Faculty of Biological and Environmental Sciences, University of Helsinki, Helsinki, Finland, [9] Global Biodiversity Information Facility (GBIF), Secretariat, Universitetsparken, Copenhagen, Denmark, [10] School of Pharmaceutical Science and Technology, Health Sciences Platform, Tianjin University, Tianjin, China, [11] Graduate School of Geography, Clark University, Worcester, MA, United States

OPEN ACCESS

Edited by:
Peter Edward Mortimer, Kunming Institute of Botany, Chinese Academy of Sciences, China

Reviewed by:
Masoomeh Ghobad-Nejhad, Iranian Research Organization for Science and Technology, Iran
Belle Damodara Shenoy, CSIR-National Institute of Oceanography, India

***Correspondence:**
Yusufjon Gafforov
yugafforov@yahoo.com
Li-Wei Zhou
liwei_zhou1982@im.ac.cn

Specialty section:
This article was submitted to Fungi and Their Interactions, a section of the journal Frontiers in Microbiology

Received: 24 August 2020
Accepted: 09 November 2020
Published: 09 December 2020

Citation:
Gafforov Y, Ordynets A, Langer E, Yarasheva M, de Mello Gugliotta A, Schigel D, Pecoraro L, Zhou Y, Cai L and Zhou L-W (2020) Species Diversity With Comprehensive Annotations of Wood-Inhabiting Poroid and Corticioid Fungi in Uzbekistan. Front. Microbiol. 11:598321. doi: 10.3389/fmicb.2020.598321

Uzbekistan, located in Central Asia, harbors high diversity of woody plants. Diversity of wood-inhabiting fungi in the country, however, remained poorly known. This study summarizes the wood-inhabiting basidiomycte fungi (poroid and corticoid fungi plus similar taxa such as *Merismodes*, *Phellodon*, and *Sarcodon*) (Agaricomycetes, Basidiomycota) that have been found in Uzbekistan from 1950 to 2020. This work is based on 790 fungal occurrence records: 185 from recently collected specimens, 101 from herbarium specimens made by earlier collectors, and 504 from literature-based records. All data were deposited as a species occurrence record dataset in the Global Biodiversity Information Facility and also summarized in the form of an annotated checklist in this paper. All 286 available specimens were morphologically examined. For 138 specimens, the 114 ITS and 85 LSU nrDNA sequences were newly sequenced and used for phylogenetic analysis. In total, we confirm the presence of 153 species of wood-inhabiting poroid and corticioid fungi in Uzbekistan, of which 31 species are reported for the first time in Uzbekistan, including 19 that are also new to Central Asia. These 153 fungal species inhabit 100 host species from 42 genera of 23 families. Polyporales and Hymenochaetales are the most recorded fungal orders and are most widely distributed around the study area. This study provides the first comprehensively updated and annotated the checklist of wood-inhabiting poroid and corticioid fungi in Uzbekistan. Such study should be expanded to other countries to further clarify species diversity of wood-inhabiting fungi around Central Asia.

Keywords: Basidiomycota, Central Asia, distribution, substrate preferences, taxonomic diversity, GIS mapping

INTRODUCTION

Central Asia is a biological crossroads at the most westerly part of the Himalayan range and supports both Palearctic species and others representative of more southerly subtropical latitudes. The peculiarity of fauna and flora is due to its mixed characters: Indo-Himalayan, Mongolian, Eurasian, and Mediterranean species are present (Anonymous, 2001). Uzbekistan in the heart of Central Asia has a diversity of habitats that are globally and regionally important in ecological functions. The varying landscapes of high mountain ranges, wide steppes, deserts, and riparian wetlands in Uzbekistan result in a high diversity of habitats. The mountain areas occupy 15% of the territory of Uzbekistan. Biodiversity of Uzbekistan includes more than 27,000 species, including over 15,000 animal species; plants, algae, and fungi total about 11,000 species (Anonymous, 1998). The flora of Uzbekistan includes 4500 species of vascular plants, of which about 400 species are endemic, rare, and relict. Many of the animals and higher plants are included in the Red List of the International Union for Conservation of Nature (IUCN) and the Red Book of the Republic of Uzbekistan.

In contrast to the great number of publications dealing with the flora, limited studies document the fungi in Uzbekistan and Central Asia in general (Gafforov, 2017; Gafforov et al., 2017). Current surveys in areas of high plant endemism, such as tropical and subtropical regions, are actually showing an even higher ratio of fungal to plant diversity and uncovering an extraordinary number of endemic fungi (e.g., Crous et al., 2006; Mueller and Schmit, 2007; Schmit and Mueller, 2007; Aime and Brearley, 2012; Hawksworth, 2012). Mountains of the Central Asia Biodiversity Hotspot consist of two major mountain systems, the Pamir and the Tien Shan. Both belong to the most diverse regions in the world with respect to fauna and flora and are regarded as areas of occurrence of many endemic, relict, and endangered species. Therefore, diverse and regionally limited fungi are expected to exist in the region. However, while knowledge of fungal diversity is developing rapidly in some areas of the world, data on the fungi in Central Asia are severely limited (Gafforov et al., 2017; Antonelli et al., 2020; Cheek et al., 2020): the current knowledge of Uzbekistan fungal biodiversity status and even a rough estimate of the number of fungal species in countries of Central Asia is unavailable. This knowledge gap has significantly impeded understanding the role of the region in biogeographic history of Asia and prevented conservation efforts in the region.

Fungi are essential components of ecosystems and are both directly and indirectly important for human cultures. Various fungal species are key symbionts of trees enabling the survival of the latter in the arid areas (Varma, 1995; Stutz et al., 2000). Fungal names used in other regional floras have often been applied to fungi in Uzbekistan. However, the Uzbek fungi often represent new, unrelated species as was shown for Uzbekistan ascomycetous microfungi (Solieva and Gafforov, 2001, 2002; Gafforov and Hoshino, 2015; Gafforov, 2002, 2010, 2015, 2016a,b; Gafforov and Rakhimov, 2017; Gafforov et al., 2019; Wanasinghe et al., 2017, 2018a,b; Samarakoon et al., 2018; Pem et al., 2018, 2019a,b; Hyde et al., 2019, 2020; Yuan et al., 2020). Basidiomycetous fungi have received even less attention than ascomycetous microfungi (Gafforov, 2014; Gafforov et al., 2014, 2017).

Among the basidiomycetous macrofungi, especially those with poroid fertile surface of fruiting bodies (poroid fungi) and corticioid fertile surface (corticioid fungi) play several essential roles in forest ecosystems (Swift, 1982). Most of these fungi are saprobes causing brown or white wood rot, whereas some of them form ectomycorrhizae with woody plants. Therefore, they play an important function in nutrient cycling and soil formation (Soudzilovskaia et al., 2019). Some of them are also known to be serious pathogenic disease agents of ecologically and economically important coniferous and deciduous woody plants. Regardless of the relationship, wood-inhabiting basidiomycetous fungi are often treated as a single research object by both taxonomists and ecologists.

The first mycological investigations on wood-inhabiting fungi in Uzbekistan were started by Sinadskiy and Bondartseva in 1950, who reported 21 polypore species (Sinadskiy and Bodartseva, 1956, 1960; Kleyner, 1958; Panfilova and Gaponenko, 1963; Gaponenko, 1965; Sinadskiy, 1968). The first study specifically in state reserves of Uzbekistan listed 71 polypore species (Baltaeva, 1992, 1993). In the study of macrofungi of Fergana valley (Andijan, Fergana and Namangan Provinces), Tashkent Province, 25 species of poroid and corticioid fungi were reported (Khalikova, 1989; Iminova, 2009). However, the fungal species recorded in these studies were identified solely by morphological characters and no specimen was preserved, which makes the reassessment of taxonomic affiliation of these records impossible.

Recent developments in DNA sequencing have revolutionized identification and systematics of fungi. This has rapidly advanced the mycological communities' ability to document fungal biodiversity, distribution, ecological preferences, and biogeographic history (e.g., Hattori et al., 2012; Ovaskainen et al., 2013; Tsykun et al., 2013; Tedersoo et al., 2014). DNA barcodes can facilitate taxonomic research by increasing the ability to matching individuals regardless of the fruiting body, identifying specimens with morphological diagnostic characters either subtle, difficult to visualize, or absent, as well as reassessing intraspecific polymorphisms. With the aid of DNA sequences, research on the wood-inhabiting basidiomycetous fungi during the last decade has yielded some species previously unknown in Uzbekistan, as well as some species new to science (Gafforov, 2014; Gafforov et al., 2014, 2017; Yuan et al., 2017, 2020; Kan et al., 2017). Moreover, the first fungal checklist of the corticioid genus *Hyphodontia* from Central Asia was published (Gafforov et al., 2017). However, despite these steps forward, comprehensive information of the wood-inhabiting poroid and corticioid fungi is still unavailable in Uzbekistan.

On the basis of our own collections, literatures, and herbarium data reassessments, the present study aimed to recognize species diversity of wood-inhabiting poroid and corticioid fungi (plus similar taxa such as *Merismodes*, *Phellodon* and *Sarcodon*) in Uzbekistan from morphological and, where possible, phylogenetic perspectives, and also to provide comprehensive

annotations for these species including host, substratum, distribution, and occurring frequency.

MATERIALS AND METHODS

Vegetation and Climate of the Study Area

The Uzbekistan territory falls in the flora of Central Asian botanical region within the larger temperate Asia floral geographic region according to the World Geographical Scheme for Recording Plant Distributions' system (Brummitt, 2001). The main ecological forest types in Uzbekistan are mountain, desert, and flood-plain forests (**Figure 1**). The majority of Uzbekistan forests are xerophytic open woodlands of deciduous trees and shrubs, constituting about 7.3% of the territory (Botman, 2009). These forests play an important role in the protection and prevention from environmental degradation, particularly land degradation and natural disasters, and also in the conservation of biodiversity and preservation of water quality.

Uzbekistan has a continental climate with hot and dry summers and cold winters. Summer temperature often surpasses 40°C (104°F), and winter average temperature is about −2°C (28°F) but may fall as low as −40°C (−40°F). Most parts of the country are arid with average annual rainfall amounting to between 100 and 200 mm (3.9 and 7.9 in) and occurring mostly in winter and spring. Between July and September, little precipitation falls, essentially stopping the growth of vegetation during that period (Klein Tank et al., 2006; Lioubimtseva and Henebry, 2009).

Specimen Assembly

A total of 286 specimens of wood-inhabiting poroid and corticoid were examined. This includes 101 specimens from Mycological Herbarium of Estonian University of Life Sciences, Tartu, Estonia (TAAM); 3 specimens from Tashkent Mycological Herbarium, Institute of Botany of the Academy of Sciences of Uzbekistan, Tashkent (TASM); and 185 specimens from our own field surveys, which are deposited in TASM. Our own specimens were recently collected from Tashkent Botanical Garden (Tashkent city), Tashkent Province (Ugam-Chatkal State Nature National Park in Western Tien Shan Mountain), Jizzakh Province (Zaamin National Nature Park, Zaamin State Reserve in Turkestan range and Nurata State Reserve in Nurata range of Pamir-Alay), Surxondaryo Province (Baysun and Husar ranges in Pamir-Alay Mountains), and Fergana Valley (Namangan Province) (**Figure 2**). In addition, we reviewed 504 records of Uzbekistan fungi published between 1950 and 2020.



FIGURE 1 | Forest types in study area. **(A)** Mountain juniper forests. **(B)** Wild fruit tree forests in mountain. **(C)** Desert saxaul (*Haloxylon* spp.) forests. **(D)** Tugai Forests (Photo: Yusufjon Gafforov).

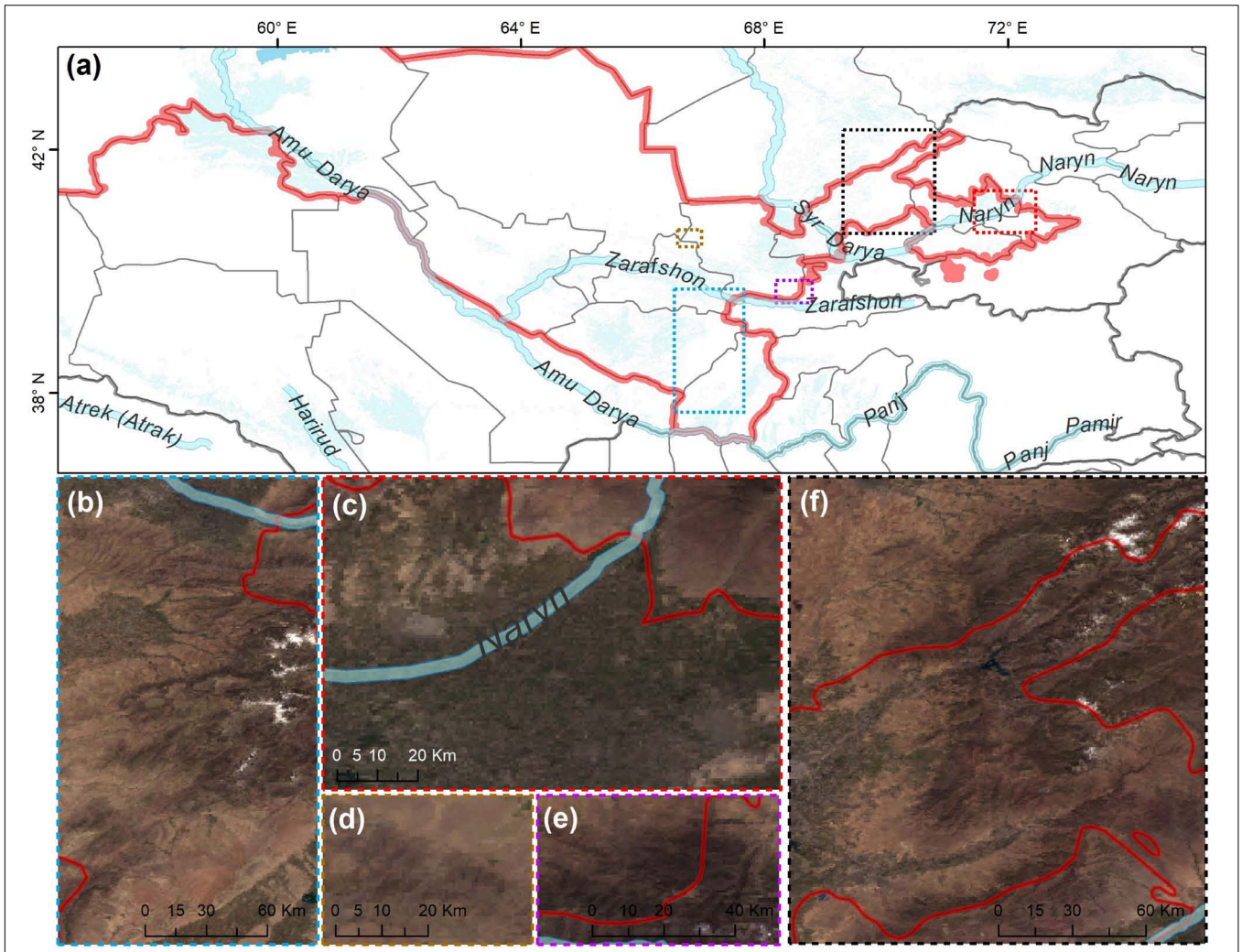


FIGURE 2 | Map of **(a)** Uzbekistan labeled with five principal collecting areas shown in panels **(b–f)**. The background map in panels **(b–f)** is the combination of bands 1, 4, 3 displays and R, G, B surface reflectance image using 500-m MODIS data (MODS09A1) acquired in July 2019 over Uzbekistan (by Yu Zhou).

Morphological Study

Morphological characters were described based on fresh and dried fruiting bodies. Microscopic characters of fruiting bodies were observed on dried specimens at a magnification up to 1000 × with a Leica DM 1000 (Tokyo, Japan) microscopes in 5% aqueous KOH plus 1% phloxine, Melzer's reagent for amyloid or dextrinoid reactions, cotton blue in lactic acid for cyanophily, and 1% aqueous cresyl blue for metachromatism (Hawksworth et al., 1995). Macromorphological characters of fruiting bodies and hymenophores were observed under a Leica M165 FC stereomicroscope. Scientific names, both of the fungi and the host plants, were checked for potential synonyms in the databases Index Fungorum (2020) and ThePlantList (2013), respectively. Species whose taxonomic placement is not established are listed under *incertae sedis*.

DNA Extraction, Amplification, and Sequencing

Genomic DNA was extracted from the dried basidiocarps of herbarium materials using DNeasy Plant Mini Kit (Qiagen, Valencia, CA, United States), QIAamp DNA Micro Kit (Qiagen), and the Extract-N-Amp Plant PCR Kit (Sigma-Aldrich, St. Louis, MO, United States), following protocols from the manufacturers, and was diluted as a template for subsequent amplification. PCR amplification targeted the internal transcribed spacer (ITS) region of the ribosomal RNA gene (rRNA), the universal DNA barcode for identification of fungi (Schoch et al., 2012), and the nuclear large ribosomal subunit (nLSU) region. Amplification was carried out using the fungal-specific primer sets ITS1F/ITS4b (Gardes and Bruns, 1996) and ITS1/ITS4 (White et al., 1990) for the ITS region and LR0R and LR5 for the nLSU region (Vilgalys and Hester, 1990;

Rehner and Samuels, 1994). Purified PCR products were sequenced using DNA ABI 3730 XL automated sequencers (Applied Biosystems) by Macrogen Inc. (Seoul, Korea), by Eurofins Genomics (Ebersberg, Germany), and by the Beijing Genomics Institute (Beijing, China). All newly generated sequences of poroid and corticoid species from Uzbekistan were submitted to GenBank (**Table 1**).

Phylogenetic Analyses

After a preliminary BLAST search, 40 sequences related to those from Uzbekistan specimens were downloaded from GenBank to assist species identification (**Table 1**). The datasets of ITS and nLSU regions were separately aligned using MAFFT 7.110 (Katoh and Standley, 2013) under the G-INI-i option (Katoh et al., 2005) and then the two alignments were concatenated. The concatenated alignment, deposited in TreeBASE[1] (accession number S26575), was subjected to an estimation of the best-fit evolutionary model using jModelTest (Guindon and Gascuel, 2003; Posada, 2008) with calculation under Akaike information criterion. Following this model, maximum likelihood (ML) and Bayesian inference (BI) methods were employed for phylogenetic analyses. The ML method was conducted using raxmlGUI 1.2 (Stamatakis, 2006; Silvestro and Michalak, 2012) with calculation of bootstrap (BS) replicates under the auto FC option (Pattengale et al., 2010). The BI method was conducted using MrBayes 3.2 (Ronquist et al., 2012). Two independent runs were employed. Each run had four chains and started from random trees. Trees were sampled every 1000th generation, of which the first 25% were removed and the other 75% were used for constructing a 50% majority consensus tree and calculating Bayesian posterior probabilities (BPPs). Tracer 1.5[2] was used to determine chain convergence. iTOL was used to visualize the tree to a circular form (Letunic and Bork, 2019).

GBIF Occurrence Dataset and Checklist Preparation

The occurrence data of wood-inhabiting poroid and corticioid fungi was extracted from 504 records in 19 publications as well as 185 records of our own recent collections in field surveys and 101 herbarium specimens from TAAM and TASM. All but collection data from TAAM (which are already displayed in GBIF) were formatted according to the Darwin Core Standard[3] and published as an occurrence dataset (Gafforov and Ordynets, 2020, [4]alternative identifier[5]). When compiling the annotated species checklist for this paper, for the sake of conciseness, all occurrence records were linked to 50 localities that are listed in the study.

GIS Data Processing

A point distribution map of fungal orders was produced using the ArcGIS 10.7 desktop software (ArcGISDesktop,2020). A GPS navigation device and Google Earth software[6] (2020) were used for geo-referencing all available occurrence data of wood-inhabiting poroid and corticioid fungi in the study sites. A WGS84 geographic coordinate system was used as a reference datum. The land cover data were adapted from the 500-m Moderate Resolution Imaging Spectroradiometer (MODIS) land cover product (MCD12Q1; Friedl et al., 2002) which has 17 IGBP classes, including water, evergreen needleleaf forests (ENF), evergreen broadleaf forests (EBF), deciduous needleleaf forests (DNF), deciduous broadleaf forests (DBF), mixed forests (MF), closed shrublands (CSH), open shrublands (OSH), woody savannas (WSA), savannas (SAV), grasslands (GRA), permanent wetlands, cropland (CRO), urban and built-up, cropland and natural vegetation mosaics (CNM), snow and ice, and barren. Considering the spatial distribution of irrigated and cultivated croplands, we further integrated these two classes from Klein et al. (2012). Data for roads, rivers, lake centerlines, and country boundaries were downloaded from the Natural Earth database (Natural Earth, 2020).

RESULTS

Phylogenetic Placement of Collections of Poroid and Corticoid Fungi From Uzbekistan

In addition to morphological characters, DNA sequences were used to identify certain specimens. A total of 114 ITS and 85 LSU sequences from 138 specimens representing 40 species were newly generated for this study, and submitted to GenBank (**Table 1**). The alignment used for phylogenetic analysis included 178 collections (**Table 1**). The best-fit evolutionary model for this alignment was estimated as GTR + I + G. In the ML method, the BS search stopped after 250 replicates. In the BI method, all chains were converged after 6 million generations, where the average standard deviation of split frequencies is 0.006815, the estimated sample sizes of all parameters are above 700, and the potential scale reduction factor approaches 1.0. Both phylogenetic methods generated congruent topologies in main lineages, and thus only the topology from the ML method is visualized in a circle form with BS and BPP at the nodes (**Figure 3**). From a phylogenetic perspective, 36 species were recovered and four potential new lineages representing members of *Hyphoderma*, *Neoantrodiella*, *Phlebia*, and *Vuilleminia* were identified from the newly sequenced specimens.

Species Diversity of Wood-Inhabiting Poroid and Corticoid Fungi in Uzbekistan

Taking literature information and morphological and phylogenetic evidence into consideration, we report 153 species of wood-inhabiting poroid and corticoid fungi including 149 described species and four single-specimen undescribed lineages belonging to 10 orders (Agaricales, Atheliales, Cantharellales, Corticiales, Gloeophyllales, Hymenochaetales, Russulales,

[1]http://www.treebase.org

[2]http://tree.bio.ed.ac.uk/software/tracer/

[3]https://dwc.tdwg.org

[4]https://doi.org/10.15468/vsru5z

[5]https://gbif.univer.kharkov.ua/resource?r=aphyllo_uz

[6]google.com/earth/versions/

TABLE 1 | Newly generated sequences and specimens used for the phylogenetic analyses.

Species	Specimens voucher	Host/geographic origin	GenBank accession no.		References
			ITS	LSU	
Athelia arachnoidea	CBS 105.18	Unknown/DE	MH854664	MH866181	Vu et al., 2019
	YG-G23	Fallen angiosperm/UZ	MT526279		This study
	YG/PS154	*Crataegus* sp./UZ		MT524543	This study
	YG1111	*Lonicera* sp./UZ		MT524544	This study
Aurantiporus fissilis	BRNM 699803	*Populus tremula*/CZ	HQ728292	HQ729002	Tomšovskyì, 2012
	YG/bot3	*Juglans regia*/UZ	MT526280	MT524545	This study
Bjerkandera adusta	CBS 371.52	Unknown/JP	MH857085	MH868620	Vu et al., 2019
	YG/bot23a	Unknown wood/UZ	MT526285	MT524549	This study
	YG-G41	Dead stump of *Prunus armeniaca*/UZ	MT526286		This study
	YG-O1	Fallen trunk of *Populus* sp./UZ	MT526284	MT524548	This study
	YG/PS172	*Juglans regia*/UZ	MT526281	MT524546	This study
	YG/PS183	Dried trunk of angiosperm/UZ	MT526283	MT524547	This study
	YG012	*Juglans regia*/UZ	MT526282		This study
Byssomerulius corium	CBS 836.72	Unknown/NL	MH860620		Vu et al., 2019
	YG-G21	Angiosperm fallen branch/UZ	MT526287	MT524550	This study
	YG-X3	Dried branch of *Prunus vulgaris*/UZ	MT526288	MT524551	This study
Cerrena unicolor	FD 299	Dead standing hardwood/US	KP135304	KP135209	Floudas and Hibbett, 2015
	YG-G28	Dried fallen stem of angiosperm/UZ	MT526292		This study
	YG/PS79	*Acer tataricum* subsp. *semenovii*/UZ	MT526291	MT524554	This study
	YG003	*Crataegus pseudoheterophylla* subsp. *turkestanica*/UZ	MT526289	MT524552	This study
	YG18	*Acer tataricum* subsp. *semenovii*/UZ	MT526290	MT524553	This study
Ceriporiopsis gilvescens	YG046	Dried angiosperm wood/UZ		MT524555	This study
	YG049	Rotten trunk of wood/UZ	MT526293		This study
	Yuan 2752	Unknown/CN	KF845953	KF845946	Zhao and Cui, 2014
Flavidoporia pulverulenta	BR3450	*Picea abies*/FR	JQ700280	JQ700280	Spirin et al., 2013
	YG/PS167	*Salix* sp./UZ	MT526295	MT524557	This study
	YG1110	*Salix alba*/UZ	MT526294	MT524556	This study
Fomes fomentarius	Cui 5769	Unknown/CN	KX885072	KX832056	Direct submission
	YG/bot2	*Populus* sp./UZ	MT526299	MT524558	This study
	YG/bot4	Decaying trunk of angiosperm/UZ	MT526300		This study
	YG/Un2	*Juglans regia*/UZ	MT526302		This study
	YG/PS174	*Juglans regia*/UZ	MT526301	MT524559	This study
	YG014	*Juglans regia*/UZ	MT526298		This study
	YG-60	Unknown wood/UZ	MT526296		This study
	YG-70	Unknown wood/UZ	MT526297		This study
Ganoderma adspersum	FGA1	*Pterocarya fraxinifolia*/IT	AM269771	AM269829	Guglielmo et al., 2007
	YG/bot24	*Acer saccharum*/UZ	MT526303	MT524560	This study
Ganoderma resinaceum	MFLU 19-2153	*Albizia mollis*/CN	MN398315	MN398328	Direct submission
	YG-X4	*Salix* sp./UZ	MT526304	MT524561	This study
Gloeophyllum abietinum	Dai 3595	*Pinus* sp./CN	JX524620	KC782732	He et al., 2014
	TAAM127397	Trunk of *Juniperus* sp./UZ	MT526305		This study
Hyphoderma setigerum	FP150263	Unknown/JM	GQ409528	KX065980	Direct submission
Hyphoderma sp.	YG/PS133	*Betula* sp./UZ	MT526306		This study
Hyphodontia zhixiangii	LWZ 20160909-4	*Juniperus* sp./UZ	NR154098		Kan et al., 2017
	YG1098	Unknown angiosperm branch/UZ	MT526308		This study
	YG1104	Fallen angiosperm branches/UZ	MT526307	MT524562	This study

(Continued)

TABLE 1 | Continued

Species	Specimens voucher	Host/geographic origin	GenBank accession no.		References
Inonotus hispidus	S45	*Vitis vinifera*/ES	EU282482	EU282484	González et al., 2009
	YG/AG1	*Morus alba*/UZ		MT524564	This study
	YG/bot1	Dried trunk angiosperm/UZ		MT524565	This study
	YG/PS148	*Malus sieversii*/UZ	MT526310	MT524567	This study
	YG/PS156	*Pinus* sp./UZ	MT526309	MT524563	This study
	YG/PS157	*Pinus* sp./UZ		MT524566	This study
Lentinus tigrinus	CBS 249.39	Unknown/Yugoslavia	MH856001	MH867501	Vu et al., 2019
	YG-J7	Dried strum of angiosperm/UZ	MT526312	MT524569	This study
	YG/PS162	*Malus domestica*/UZ	MT526311	MT524568	This study
	TAAM094847	*Acer* tree trunk/UZ	MT526313		This study
	TAAM094857	*Prunus armeniaca*/UZ	MT526314		This study
Lenzites warnieri	CIRM-BRFM 972	Unknown/FR	GU731567		Direct submission
	TAAM126870	*Populus nigra*/UZ	MT526315		This study
Lyomyces erastii	RM21	Unknown shrub/UZ	MT526316		This study
	162SAMHYP	*Sambucus racemosa*/FI	JX857801		Direct submission
Neoantrodiella sp.	TAAM104307	*Juniperus polycarpos* var. *seravschanica*/UZ	MT526317		This study
Neoantrodiella gypsea	Yuan 5589	Unknown/CN	KT203292	KT203313	Ariyawansa et al., 2015
Peniophora cinerea	He 3725	Unknown/CN	MK588769	MK588809	Direct submission
	YG058	*Juglans regia*/UZ	MT526318		This study
Peniophora incarnata	CBS 430.72	Unknown/NL	MH860518	MH872230	Vu et al., 2019
	YG/PS84	Fallen stem of deciduous wood/UZ	MT526319	MT524570	This study
Peniophorella praetermissa	GEL2182	*Betula* sp./NO	AY854081	AY700185	Direct submission
	YG-G16	*Juglans regia*/UZ	MT526320	MT524571	This study
	YG-G37	Fallen unknown angiosperm/UZ	MT526321		This study
	YG-G40	Fallen unknown angiosperm/UZ	MT526322		This study
Phellinus betulinus	DVB-Betula	*Betula nigra*/US	KU139151	KU139246	Brazee, 2015
	TAAM104436	*Betula tianschanica*/UZ	MT526323		This study
Phellinus pomaceus	CBS 171.32	Unknown/GB	AY558652	MH866714	Jeong et al., 2005; Vu et al., 2019
	TAAM126269	*Celtis australis* subsp. *caucasica*/UZ	MT526324	MT524572	This study
	TASM582	*Lonicera* sp./UZ	MT526326		This study
	YG/PS3X	*Cerasus tianshanica*/UZ	MT526328	MT524576	This study
	YG009	*Prunus dulcis*/UZ	MT526325	MT524574	This study
	YG/PS82	*Prunus* sp./UZ	MT526333		This study
	YG/S1	*Salix* sp./UZ		MT524573	This study
	YG51-ph	*Prunus* sp./UZ	MT526331		This study
	YG028	*Cerasus tianshanica*/UZ	MT526327	MT524575	This study
	YG052	*Prunus cerasifera*/UZ	MT526329		This study
	YG28	*Prunus mahaleb*/UZ	MT526330	MT524577	This study
	YG337	*Prunus cerasifera*/UZ	MT526332		This study
	YG1102	*Prunus* sp./UZ	MT526334		This study
Phlebia bresadolae	MG291	*Acer monspessulanum*/IR	KU213584		Ghobad-Nejhad and Langer, 2016
Phlebia cf. bresadolae	RLG10795s	Unknown/US	KY948785	KY948857	Justo et al., 2017
	YG/PS89	Unknown woody plants branch/UZ	MT526336	MT524578	This study
	YG/PS189	Fallen branch of angiosperm/UZ	MT526335		This study
Phlebia sp.	YG64	*Crataegus pseudoheterophylla* subsp. *turkestanica*/UZ	MT526337		This study
	YG326	Dead hardwood/UZ	MT526338	MT524579	This study
Phlebia rufa	MR 4280	Hardwood/US	KP135373	KX065989	Floudas and Hibbett, 2015; direct submission
	YG77	*Robinia pseudoacacia*/UZ	MT526339	MT524580	This study

(Continued)

TABLE 1 | Continued

Species	Specimens voucher	Host/geographic origin	GenBank accession no.		References
Phlebiella christiansenii	KHL 11689	Unknown/FI	EU118659	EU118659	Larsson, 2007
	YG-G22	*Gleditsia triacanthos*/UZ	MT526340		This study
	YG-G26	Fallen angiosperm/UZ	MT526341		This study
	YG-G36	Dried stump of deciduous/UZ	MT526342		This study
Phylloporia yuchengii	YG-J5	*Populus* sp./UZ	MT526344	MT524584	This study
	YG-J10	*Morus alba*/UZ		MT524585	This study
	YG-J11	*Morus alba*/UZ		MT524586	This study
	YG033	Dead angiosperm trunk and stem/UZ		NG060132	Gafforov et al., 2014
	YG043	*Juglans regia*/UZ	MT526343	MT524581	This study
	YG343	*Prunus* sp./UZ		MT524582	This study
	YG1093	*Crataegus pseudoheterophylla* subsp. *turkestanica*/UZ		MT524583	This study
	YG1011	*Crataegus* sp./UZ		MT524587	This study
Pilatoporus ibericus	O 10811	*Pinus* sp./IT	KR605772	KR605711	Han et al., 2016
	YG-G24	Trunk of angiosperm/UZ	MT526345	MT524588	This study
Radulomyces confluens	K(M) 181613	Unknown/GB	MK953390	MK953401	Leal-Dutra et al., 2020
	YGcor-80	Strum of angiosperm/UZ	MT526346		This study
	YG-G43	Dead stump/UZ		MT524589	This study
Rigidoporus ginkgonis	Cui 5125	Rotten wood of Ginkgo/CN	KY131877	KY131933	Wu et al., 2017
	YG-G2	Strum of deciduous/UZ		MT524590	This study
	YG-G3	Strum of deciduous/UZ		MT524591	This study
	YG-G35	Decay branch of angiosperm/UZ	MT526347	MT524592	This study
Sanghuangporus lonicerinus	Dai 17095	*Lonicera* sp./UZ	MF772787	MF772806	Zhu et al., 2019
	TAAM0104264	*Lonicera* sp./UZ	MT526352	MT524597	This study
	TAAM127578	Dry trunk of deciduous trunk/UZ	MT526353	MT524598	This study
	YG/PS92	*Lonicera* sp./UZ	MT526348		This study
	YG/PS129	*Lonicera* sp./UZ	MT526349	MT524594	This study
	YG/Un1	*Acer tataricum* subsp. *semenovii*/UZ	MT526350	MT524595	This study
	YG018	*Lonicera nummulariifolia*/UZ		MT524593	This study
	YG1112	*Lonicera* sp./UZ	MT526351	MT524596	This study
Schizophyllum commune	CBS 124811	Unknown	MH863418	MH874930	Vu et al., 2019
	YG-J2	*Populus* sp./UZ	MT526354	MT524599	This study
	YG/PS169	*Juglans regia*/UZ	MT526355	MT524600	This study
Stereum hirsutum	CBS 930.70	Unknown/UZ	MH860009	MH871796	Vu et al., 2019
	TAAM104393	Deciduous tree trunk/UZ	MT526367		This study
	TAAM126291	*Populus alba*/UZ	MT526368	MT524610	This study
	YG-G12	*Fraxinus excelsior*/UZ		MT524601	This study
	YG-G15	*Quercus* sp./UZ	MT526362	MT524605	This study
	YG/PS135	*Juglans regia*/UZ	MT526363	MT524606	This study
	YG/PS176	*Juglans regia*/UZ	MT526364	MT524607	This study
	YG51	*Acer* sp./UZ	MT526356	MT524602	This study
	YG030	*Acer tataricum* subsp. *semenovii*/UZ	MT526357		This study
	YG048	Unknown dried wood/UZ	MT526358		This study
	YG056	Unknown decay wood/UZ	MT526359	MT524603	This study
	YG057	*Acer tataricum* subsp. *semenovii*/UZ	MT526360		This study
	YG320	*Salix alba*/UZ	MT526361	MT524604	This study
	YG1091	Unknown woody branch/UZ	MT526365	MT524608	This study
	YG1092	Fallen trunk of angiosperm wood/UZ	MT526366		This study
	YG3.04.13	Dead fallen trunk of angiosperm/UZ		MT524609	This study

(Continued)

TABLE 1 | Continued

Species	Specimens voucher	Host/geographic origin	GenBank accession no.		References
Subantrodia uzbekistanica	Dai 17105	*Juniperus polycarpos* var. *seravschanica*/UZ	KX958183	KX958187	Yuan et al., 2017
	YG1100	Unknown woody branches/UZ	MT526370		This study
	YG1107	*Juniperus polycarpos* var. *seravschanica*/UZ	MT526371		This study
Trametes hirsuta	CBS 282.73	Unknown/DE	MH860685	MH872390	Vu et al., 2019
	RM44	Died angiosperm strum/UZ	MT526381		This study
	TAAM104394	*Juglans regia*/UZ	MT526369		This study
	YG/Ch40	Stem of angiosperm tree/UZ	MT526382	MT524614	This study
	YG/PS128	Unidentified angiosperm stem/UZ	MT526378	MT524612	This study
	YG/PS138	*Prunus* sp./UZ	MT526379		This study
	YG/PS168	*Juglans regia*/UZ	MT526380	MT524612	This study
	YG004	*Prunus armeniaca*/UZ	MT526372		This study
	YG007	*Prunus vulgaris*/UZ	MT526373		This study
	YG037	*Juglans regia*/UZ	MT526374		This study
	YG055	Unknown decay wood/UZ	MT526375		This study
	YG073	Dried unknown woody trunk/UZ	MT526376		This study
	YG314	*Prunus* sp./UZ	MT526377	MT524611	This study
Trametes trogii	Dai 11246	Unknown/CN	KC867380	KC867451	Li et al., 2016
	TAAM189940	unidentified wood/UZ	MT526387	MT524621	This study
	YG/bot23b	Fallen deciduous branch/UZ	MT534628		This study
	YG-G14	Unknown woody branches/UZ	MT534629	MT534627	This study
	YG-G17	Unknown strum of angiosperm/UZ	MT526383	MT524615	This study
	YG-G18	Unknown strum of angiosperm/UZ	MT526384	MT524616	This study
	YG-G19	Unknown strum of angiosperm/UZ		MT524617	This study
	YG-GX1	*Populus* sp./UZ	MT526388		This study
	YG/PS2X	Dried on *Salix* sp./UZ		MT524622	This study
	YG-J4	*Populus nigra*/UZ	MT526385	MT524619	This study
	YG-J6	*Populus nigra*/UZ	MT526386	MT524620	This study
	YG-JX4	*Populus* sp./UZ		MT524623	This study
	YG-N7	*Populus alba*/UZ		MT524618	This study
Trametes versicolor	Cui 9310	Unknown/CN	KC848266	KC848351	Direct submission
	YG-J3	*Prunus* sp./UZ	MT526389	MT524624	This study
	YG/PS170	*Juglans regia*/UZ		MT524625	This study
Trametes villosa	CBS 334.49	Unknown/AR	MH856545	MH868069	Vu et al., 2019
	YG/AG11	Dried stem of angiosperm/UZ	MT526390		This study
Vuilleminia comedens	CBS 428.72	Unknown/NL	MH860516	MH872229	Vu et al., 2019
Vuilleminia sp.	TAAM104410	*Lonicera* sp./UZ		MT524626	This study

Polyporales, Thelephorales and Trechisporales), 26 families, and 97 genera in Uzbekistan (**Table 2** and **Figure 4**). Data on own specimens and extracted from literature records are accessible as an occurrence dataset (Gafforov and Ordynets, 2020,[4] alternative identifier[5]). Among the 153 species, 31 are reported for the first time in Uzbekistan, including 19 also new to Central Asia. The orders represented by the most specimens are Polyporales (7 families, 59 genera, and 88 species) and Hymenochaetales (4; 20; 41). Together they contain 129 species or 84.3% of the total wood-inhabiting poroid and corticoid biota of Uzbekistan (**Table 2**). The most species-rich families are Polyporaceae (40 species in 25 genera), Hymenochaetaceae (25; 13), Fomitopsidaceae (21; 16), and Meruliaceae (15; 12) and contain 66 genera and 101 species that constitute 66% of the total poroid and corticoid species number. The genus with the highest number of recorded species are *Trametes* (9 species); *Inonotus* (5); *Ganoderma*, *Lentinus*, *Phellinus*, *Rigidoporus*, and *Stereum* (4 each); and *Antrodia*, *Cerioporus*, *Gloeophyllum*, *Fomitiporia*, *Hyphodontia*, *Lyomyces*, *Phlebia*, *Phylloporia*, *Postia*, and *Trichaptum* (3 each) that contain

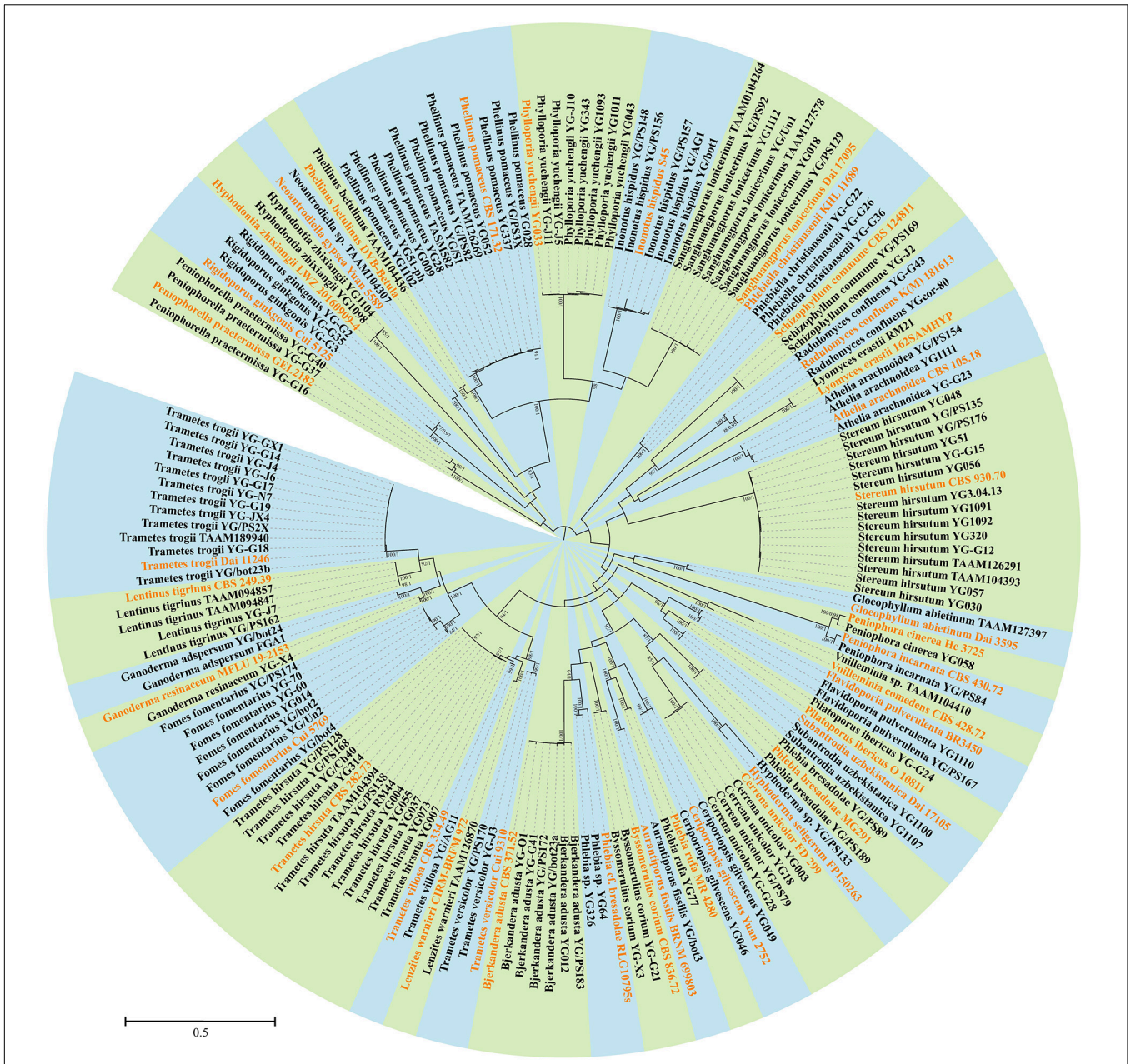

Phylloporia yuchengii YG433
Phylloporia yuchengii YG1111
Phylloporia yuchengii YG1112
Phylloporia yuchengii YG-J10
Phylloporia yuchengii YG343
Phylloporia yuchengii YG1093
Phylloporia yuchengii YG1011
Phylloporia yuchengii YG043
Inonotus hispidus YG/PS148
Inonotus hispidus YG/PS156
Inonotus hispidus SAS
Inonotus hispidus YG/PS157
Inonotus hispidus YG/AG1
Sanghuangporus lonicerinus YG/bot1
Sanghuangporus lonicerinus YG/PS92
Sanghuangporus lonicerinus YG/Un1
Sanghuangporus lonicerinus TAAM127578
Sanghuangporus lonicerinus YG018
Sanghuangporus lonicerinus YG/PS129
Sanghuangporus lonicerinus Dai 17005
Sanghuangporus lonicerinus KHL 11589
Phellinidium christianseniI YG-G22
Phellinidium christianseniI YG-G26
Phellinidium christianseniI YG-G36
Phellinidium christianseniI YG/PS169
Schizophyllum commune CBS 124811
Schizophyllum commune YG-J2
Schizophyllum commune YG-G43
Schizophyllum commune KMJ 181613
Radulomyces confluens YGcor-80
Radulomyces confluens KMJ 181613
Radulomyces RM21
Radulomyces erastii YG/PS154
Lyomyces erastii 162SAMHYP
Lyomyces erastii YG1111
Athelia arachnoidea CBS 105.18
Athelia arachnoidea YG-G23
Athelia arachnoidea YG048
Stereum hirsutum YG/PS135
Stereum hirsutum YG/PS176
Stereum hirsutum YG51
Stereum hirsutum YG-G15
Stereum hirsutum YG056
Stereum hirsutum CBS 930.70
Stereum hirsutum YG3.04.13
Stereum hirsutum YG1091
Stereum hirsutum YG1092
Stereum hirsutum YG320
Stereum hirsutum YG-G12
Stereum hirsutum TAAM126291
Stereum hirsutum TAAM104393
Stereum hirsutum YG057
Stereum hirsutum YG030
Gloeophyllum abietinum TAAM127397
Gloeophyllum abietinum Dai 3595
Peniophora cinerea He 3725
Peniophora cinerea YG058
Peniophora incarnata CBS 430.72
Peniophora incarnata YG/PS84
Vuilleminia comedens CBS 428.72
Vuilleminia sp. TAAM104410
Flavidoporia pulverulenta BR3450
Flavidoporia pulverulenta YG1110
Flavidoporia pulverulenta YG/PS167
Pilatoporus ibericus YG-G24
Pilatoporus ibericus O 10811
Subantrodia uzbekistanica Dai 17105
Subantrodia uzbekistanica YG1100
Subantrodia uzbekistanica YG1107
Phlebia bresadolae MG291
Phlebia bresadolae YG/PS89
Phlebia bresadolae YG/PS133
Hyphoderma sp. YG/PS129
Cerrena unicolor MG291
Cerrena unicolor YG003
Cerrena unicolor YG18
Cerrena unicolor YG/PS79
Cerrena unicolor YG-G28
Cerrena unicolor YG049
Ceriporiopsis gilvescens Yuan 2752
Ceriporiopsis gilvescens YG046
Phlebia rufa FR 4280
Phlebia rufa YG77
Aurantiporus fissilis BRNM 699803
Aurantiporus fissilis YG/bot3
Aurantiporus coriunt CBS 836.72
Bysomerulius corium YG-X3
Bysomerulius corium YG-G21
Phlebia cf. brevisbilar RLG10795s
Phlebia sp. YG64
Phlebia sp. YG326
Bjerkandera adusta YG/PS183
Bjerkandera adusta YG023
Bjerkandera adusta YG/bot23a
Bjerkandera adusta YG-G41
Bjerkandera adusta YG/PS172
Bjerkandera adusta YG-G37
Bjerkandera adusta CBS 371.92
Trametes versicolor YG-J3
Trametes versicolor YG/PS170
Trametes versicolor YG/PS178
Trametes versicolor CuI 5310
Trametes villosa CBS 334.49
Lenzites warnieri CIRM-BRFM 972
Lenzites warnieri TAAM126870
Trametes villosa YG/AG11
Trametes hirsuta YG073
Trametes hirsuta YG007
Trametes hirsuta YG037
Trametes hirsuta YG065
Trametes hirsuta YG/PS138
Trametes hirsuta YG/bot4
Trametes hirsuta TAAM104394
Trametes hirsuta YG/PS168
Trametes hirsuta YG/Ch40
Trametes hirsuta YG314
Trametes hirsuta YG/PS178
Trametes hirsuta CBS 238.75
Fomes fomentarius CuI 5760
Fomes fomentarius YG/bot4
Fomes fomentarius YG/PS168
Fomes fomentarius YG/PS174
Fomes fomentarius YG-70
Fomes fomentarius YG-60
Fomes fomentarius YG014
Fomes fomentarius YG/bot2
Fomes fomentarius YG/bot1
Ganoderma resinaceum MFLU 19-2153
Ganoderma resinaceum YG-X4
Ganoderma resinaceum YG/PS174
Ganoderma adspersum YG-A1
Ganoderma adspersum YG/bot24
Lentinus tigrinus YG/PS162
Lentinus tigrinus YG-J7
Lentinus tigrinus TAAM094847
Lentinus tigrinus TAAM094857
Lentinus tigrinus CBS 249.39
Trametes trogii Dai 11246
Trametes trogii YG/bot23b
Trametes trogii TAAM189940
Trametes trogii YG-G18
Trametes trogii YG/PS2X
Trametes trogii YG-JX4
Trametes trogii YG-G19
Trametes trogii YG-N7
Trametes trogii YG-G17
Trametes trogii YG-J6
Trametes trogii YG-J4
Trametes trogii YG-G14
Trametes trogii YG-GX1
Penidiella columbiana YG/PS2
Phellinus pomaceus YG/PS3X
Phellinus pomaceus YG337
Phellinus pomaceus YG028
Phellinus pomaceus YG/PS1
Phellinus pomaceus YG/PS2
Phellinus pomaceus YG/PS4
Phellinus pomaceus YG/PS5
Phellinus pomaceus YG/PS6
Phellinus pomaceus YG/PS7
Phellinus pomaceus YG/PS8
Phellinus pomaceus YG/PS9
Phellinus pomaceus YG/PS10
Phellinus pomaceus YG/PS11
Phellinus pomaceus YG/PS12
Phellinus pomaceus YG/PS13
Phellinus pomaceus YG/PS14
Phellinus pomaceus YG/PS15
Phellinus pomaceus YG/PS16
Phellinus pomaceus

TABLE 2 | Number of wood-inhabiting poroid and corticioid species in the most representative orders, families, and genera in the study area and proportion accounting for total species number.

ORDERS					FAMILIES				GENERA		
Order	**Family**	**Genera**	**Spp.**	**%**	**Family**	**Genera**	**spp.**	**%**	**Genera**	**spp.**	**%**
Polyporales	7	59	88	57.5	Polyporaceae	25	40	26.1	*Trametes*	9	5.87
Hymenochaetales	4	20	41	26.8	Hymenochaetaceae	13	25	16.3	*Inonotus*	5	3.25
Russulales	4	4	8	5.23	Fomitopsidaceae	16	21	13.7	*Antrodia*	4	2.61
Agaricales	4	4	4	2.63	Meruliaceae	12	15	9.9	*Ganoderma*	4	2.61
Thelephorales	2	3	3	1.97	Schizoporaceae	3	7	4.6	*Lentinus*	4	2.61
Gloeophyllales	1	1	3	1.97	Phanerochaetaceae	4	5	3.26	*Phellinus*	4	2.61
Corticiales	1	2	2	1.3	Ganodermataceae	1	4	2.61	*Stereum*	4	2.61
Atheliales es	1	1	1	0.65	Oxyporaceae	1	4	2.61	*Cerioporus*	3	2.61
Cantharellal	1	1	1	0.65	Stereaceae	1	4	2.61	*Hyphodontia*	3	2.61
Trechisporales	1	1	1	0.65	Gloeophyllaceae	1	3	1.98	*Phylloporia*	3	2.61
Subtotal	26	96	152	99.35	Subtotal	77	128	83.67	Subtotal	43	28.11
with uncertain (1)	0	1	1	0.65	Other families (16)	20	25	16.33	Other genera (87)	110	71.89
Total	**26**	**97**	**153**	**100%**	**26**	**97**	**153**	**100%**	**97**	**153**	**100%**

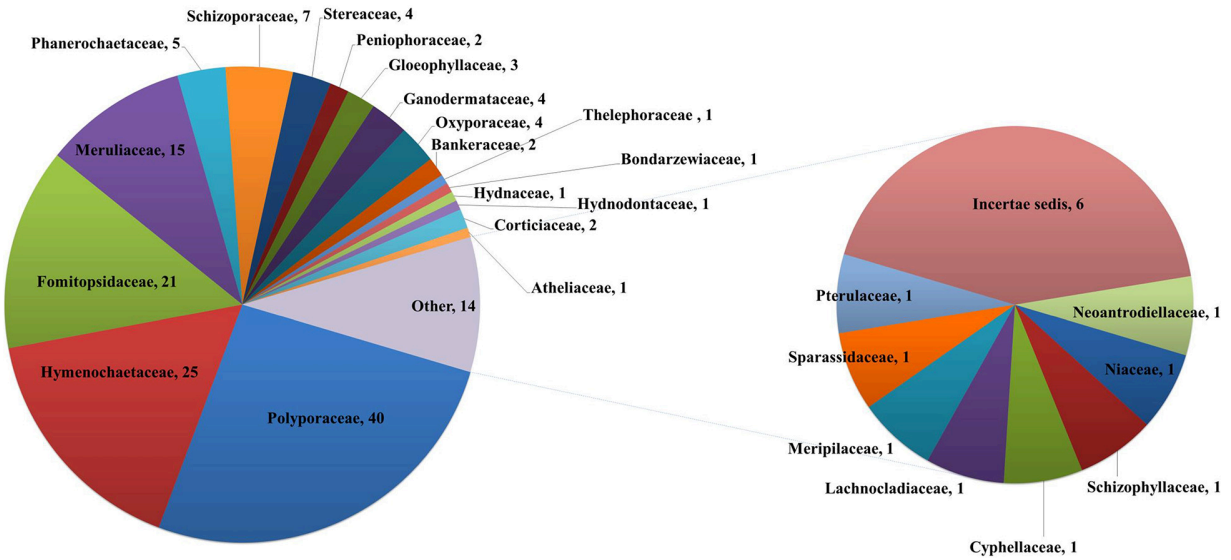


FIGURE 4 | Taxonomic composition of wood-inhabiting poroid and corticoid fungi at a family level.

numbers in brackets. Abbreviations used in these localities are as follows: Andijan Province—AP; Fergana Province—FP; Jizzakh Province; Karakalpakstan—K; Namangan Province—NMP; Navoi Province—NP; Qashqadaryo Province—QR; Samarkand Province—SP; Surkhandaryo Province—SRP; Syrdarya Province —SDR; Tashkent Province—TP; Tashkent botanical garden—TBG.

All territories of Uzbekistan except Kyzyl-kum desert (1); AP, Andijan District, Kutarma village (2); AP, Garden and Parks (3); AP, Shaxrixon district, Holdovonbek village (4); BP (5); FP (6); JP, Nurata State Reserve, Nurata Range, Pamir-Alay Mountain System (7); JP, Zaamin District, Zaamin National Park, Zaamin State Reserve in the South and South-east of the Turkestan Range (8); K, Lower-Amudarya Biosphere Reserve (9); Kyzyl-kum Desert (10); NMP, Chortoq District, Chortoq dam olishmaskani, Chortoq foothills (11); NMP, Haqiloobod District, Haquloobod village (12); NMP, Mingbuloq District, Qorasuv garden (13); NMP, National Parks and Gardens (14); NMP, Pop District, Chodaksay basin, Kurama Mountain Range of Western Tien Shan (15); NMP, Turaqurgon District, Kuymazor village, Pop and Chust foothills (16); NP, Sarmysh valley (17); NP. Tamdy District, Boymurot village, desert (18); QP, Hissar State Reserve in North-western of Hissar Range, Pamir-Alay Mountain System (19); QP, Yakkaobod village, Yakkabog forestry (20); SP, Zarafshan State Reserve, Zarafshan river valley, Pamir Mountains (21); SRP, Baysun District, Baysun village, Omonkhona, Baysun Mountain, South-western spurs of the Hissar Range in the Western part of the Pamir-Alay System (22); SRP, Baysun District, Darband village, Baysun Mountain, South-western spurs of the Hissar Range in the Western part of the



FIGURE 5 | Basidiocarps in situ. **(A)** *Radulomyces confluens*; **(B)** *Schizophyllum commune*; **(C)** *Bjerkandera adusta*; **(D)** *Phlebia rufa*; **(E)** *Laetiporus sulphureus*; **(F)** *Cerioporus squamosus*; **(G)** *Cerrena unicolor*; **(H)** *Fomes fomentarius* (Photo: Yusufjon Gafforov).

Pamir-Alay System (23); SRP, Baysun District, Machay village, Baysun Mountain, South-western spurs of the Hissar Range in the Western part of the Pamir-Alay System (24); SRP, Hissar Range of Pamir-Alay Mountains (25); SRP, Surkhan State Reserve (26); SDR (27); TBG (28); Tashkent, olimlar shaxarchasi (29); TP, Angren, Yangibod village, South-eastern slope of Chatkal Mountain Range of Western Tien Shan (30); TP, Bekabad District, NW of Bekabad, Dalverzin village (31); TP, Bustonliq District, Beldersay, Greater Chimgan, Chatkal Mountain Range of Western Tien Shan (32); TP, Bustonliq District, Burchmulla village, Kulabsay, Western Tien Shan Mountains (33); TP, Bustonliq District, Gazalkent, spurs of the Western Tien Shan (34); TP, Bustonliq District, Kayinarsay and Sarvasay, Western Tien Shan (35); TP, Bustonliq District, Kuksu River, Pskem Mountain Range of Western Tien Shan (36); TP, Bustonliq District, Onaulgansoy, Pskem river, Pskem Mountain Range of Western Tien Shan (37); TP, Bustonliq District, Oqtosh village, Ugam Mountain Range of Western Tien Shan (38);



FIGURE 6 | Basidiocarps *in situ* of **(A)** *Lentinus tigrinus*; **(B)** *Pyrofomes demidoffii*; **(C)** *Trametes hirsuta*; **(D)** *Trametes trogii*; **(E)** *Ganoderma adspersum*; **(F)** *Ganoderma applanatum*; **(G)** *Inonotus hispidus*; **(H)** *Phellinus igniarius* (Photo: Yusufjon Gafforov).

TP, Bustonliq District, Xojikent village, Ugam Mountain Range of Western Tien Shan (39); TP, Bustonliq District, Xumson village, Xumsonsoy, Ugam Mountain Range of the Western Tien Shan (40); TP, Bustonliq District, Yubileyniy village, Chimyonsoy, Chimgan, Chatkal Mountain Range of Western Tien Shan (41); TP, Bustonliq District, Yusufhona village, Mazarsay, Charvak Reservoir, Western Tien Shan Mountains (42); TP, Karankulsay, Kungurbuka Mountain, Ugam Range of Western Tien Shan (43); TP, Oxangoron District, Oxangoron basin river (44); TP, Parkent District, Chatkal Biosphere Reserve, Chatkal Mountain Range of Western Tien Shan (45); TP, Parkent District, Kumyshkan village, Chatkal Mountain Range

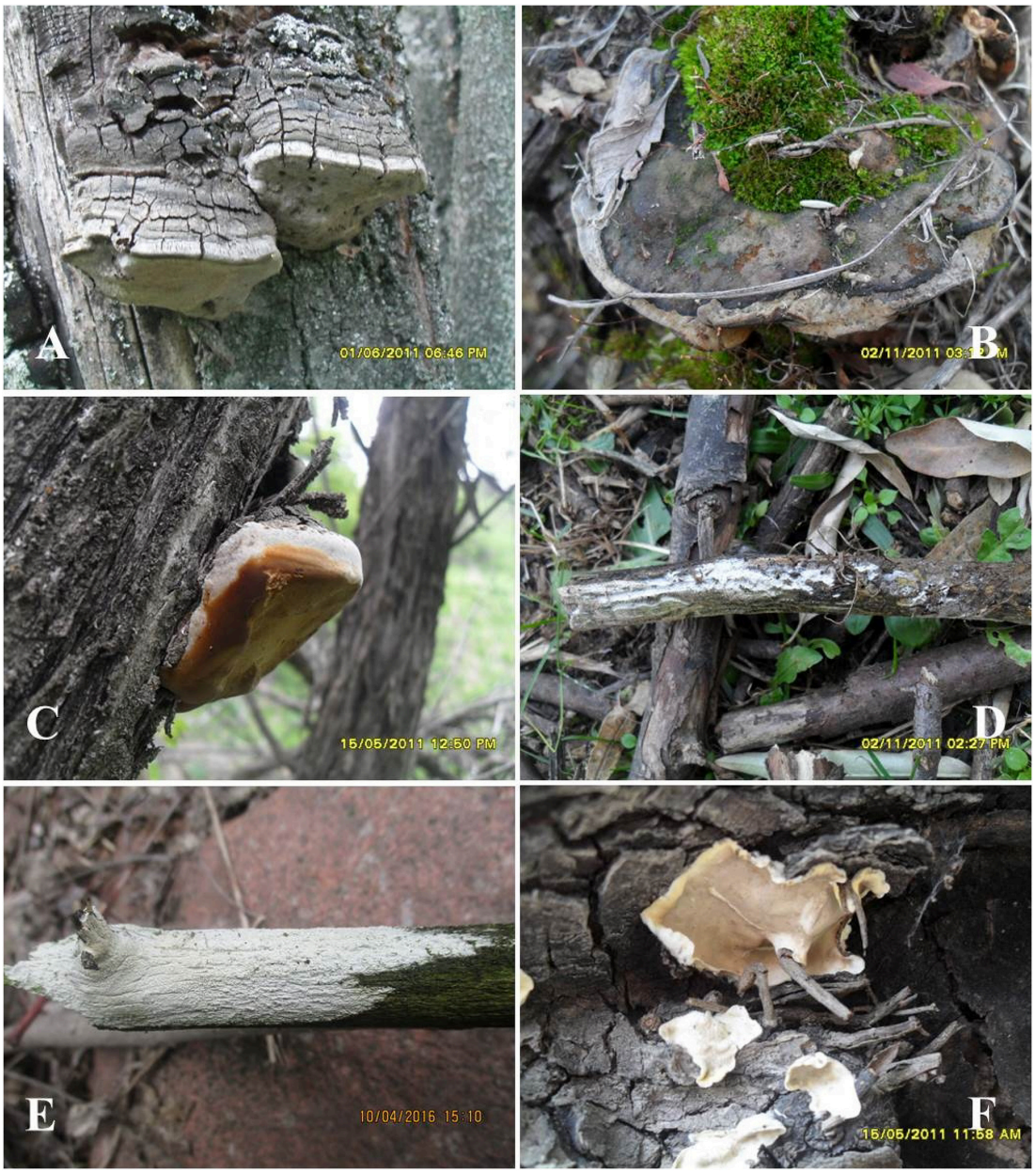


FIGURE 7 | Basidiocarps *in situ* of **(A)** *Phellinus pomaceus*; **(B)** *Phylloporia yuchengii*; **(C)** *Sanghuangporus lonicerinus*; **(D)** *Lyomyces erastii*; **(E)** *Lyomyces sambuci*; **(F)** *Stereum hirsutum* (Photo: Yusufjon Gafforov).

of Western Tien Shan Mountains (46); TP, Parkent District, Nivich and Qiziljar villages, Bashkyzylsay, Chatkal Biosphere Reserve, Chatkal Mountain Range of Western Tien Shan (47); TP, Tuyatashsoy, Western Tien Shan Mountains (48); TP, Ugam-Chatkal State Nature National Park, Western Tien Shan Mountains (49); TP, Yangikurgan village, Kurigansay river, Western Tien Shan Mountains (50).

AGARICALES Underw.

Cyphellaceae Lotsy

#***Chondrostereum purpureum*** (Pers.) Pouzar, Česká Mykol. 13(1): 17 (1959)

Specimen examined: (24): on *Acer pentapomicum* Stewart ex Brandis, 17 May 2016, YG-B01.

Pterulaceae Corner

#●***Radulomyces confluens*** (Fr.) M.P. Christ., Dansk bot. Ark. 19 (no. 2): 230 (1960)

Specimens examined: (39): on fallen rotten trunk, 2 Nov. 2011, YG006; (39): on trunks of angiosperm woody plant, 20 Nov. 2013, YGcor-80; (28): on dead stump, 2 Sept. 2013, YG-G43.

Niaceae Jülich

Merismodes anomala* (Pers.) Singer, Agaric. mod. Tax., Edn 3 (Vaduz): 665 (1975)

Specimen examined: (49): on dead branch of *Prunus* sp., 30 Apr. 1988, A. Kollom, TAAM127589.

Note: In TAAM, this specimen was originally labeled as *Cyphellopsis anomala* (Pers.) Donk.

Schizophyllaceae Quél.

●***Schizophyllum commune*** Fr., Observ. mycol. (Havniae) 1: 103 (1815)

Specimens examined: (40): on *Morus alba* L., 26 May 2011, YG047; (37): on dead trunk of *Juglans regia* L., 20 Sept. 2014, YG/PS169; (45): on a dry branch of *Celtis australis* subsp. *caucasica* (Willd.) C.C. Towns., 30 Apr. 1980, A. Kollom, TAAM127588; (20): on *Populus* sp., Sept. 2012, YG-J2.

Literature: Khalikova (1989), (49): on *Salix pentandra* L. and *Prunus armeniaca* L.; Iminova (2009), (4): on *Salix pentandra* L., *Ìàlus domestica*, *Prunus armeniaca*, Jun. 2000, Jul. 2004.

ATHELIALES Jülich

Atheliaceae Jülich

#●***Athelia arachnoidea*** (Berk.) Jülich, Willdenowia, Beih. 7: 53 (1972)

Specimens examined: (38): on fallen angiosperm branch, 3 Sept. 2013, YG-G23; (38): YG-G44; (37): on living branches of *Crataegus* sp., 18 Jun. 2014, YG/PS154; (8): on dried branches of *Lonicera paradoxa* Pojark., 26 May 2018, YG1111.

CANTHARELLALES Gäum.

Hydnaceae Chevall.

#***Sistotrema coroniferum*** (Höhn. and Litsch.) Donk, Fungus, Wageningen 26: 4 (1956)

Specimen examined: (37): on branches of *Betula* tree, 19 Jun. 2014, YG/PS95.

CORTICIALES K.H. Larss.

Corticiaceae Herter

#***Corticium roseum*** Pers., Neues Mag. Bot. 1: 111 (1794)

Specimen examined: (35): on stumps of *Juglans regia*, 31 Aug. 1963, A. Raitviir, TAAM043491.

¤●***Vuilleminia*** sp. Parmasto, Eesti NSV Tead. Akad. Toim., Biol. seer 16(4): 391 (1967)

Specimen examined: (36): on bark and at base of a trunk of *Lonicera* sp., E. Parmasto, 25 Apr. 1982, TAAM104410.

GLOEOPHYLLALES Thorn

Gloeophyllaceae Jülich

●***Gloeophyllum abietinum*** (Bull.) P. Karst., Bidr. Känn. Finl. Nat. Folk 37: 80 (1882)

Specimens examined: (49): on trunk of *Juniperus* sp., 23 Apr. 1982, A. Kollom, TAAM127397.

Literature: Baltaeva (1992, 1993), [(45): on *Pinus* sp., 10 May 1987; (8): on *Pinus* sp., 17 Jun. 1988; (7): on dried stem of *Pinus* sp., 28 Jul. 1988; (21): on stem of *Picea* sp., 21 Oct. 1988; (19): on *Juniperus* sp., 29 Jul. 1989].

Note: Although the species is easily recognizable in the field, to our surprise, we failed to find it.

Gloeophyllum odoratum (Wulfen) Imazeki, Bull. Tokyo Sci. Mus. 6: 75 (1943)

Literature: Baltaeva (1992), [(19): on wet trunk of *Biota* sp., 5 Sept. 1990].

Gloeophyllum trabeum (Pers.) Murrill, N. Amer. Fl. (New York) 9(2): 129 (1908)

Literature: Baltaeva (1992, 1993), [(45): on stump and trunk of *Quercus* sp., 1 Jun. 1987; (8): on strum of unknown woody plants, 1 Jun. 1987; (7): on trunk of deciduous tree, 4 Oct. 1988; (21): on fallen stem of angiosperm, 22 Jun. 1988; (19): on dried stem of *Quercus* sp., 19 Mar. 1988; (9): on *Quercus* sp., 7 May 1988].

POLYPORALES Gäum.

Meruliaceae Rea

Abortiporus biennis (Bull.) Singer, Mycologia 36(1): 68 (1944)

Literature: Baltaeva (1992), [(45): on dead attached branches of living *Quercus* sp., 12 Sept. 1990].

●***Aurantiporus fissilis*** (Berk. and M.A. Curtis) H. Jahn ex Ryvarden, Polyp. N. Eur. (Oslo) 2: 222 (1978).

≡ *Tyromyces fissilis* (Berk. and M.A. Curtis) Donk.

Specimen examined: (28): on living stem of *Juglans regia*, 9 Jun. 2014, YG/bot3.

Literature: Kravtzev (1950), (as *Tyromyces fissilis*, (19): on stem of *Malus* sp.); Baltaeva (1992, 1993), (as *Tyromyces fissilis*, (1): on various deciduous wood).

●***Bjerkandera adusta*** (Willd.) P. Karst., Meddn Soc. Fauna Flora fenn. 5: 38 (1879)

Specimens examined: (40): on dead stump of *Juglans regia*, 26 May 2011, YG012; (37): on dried *Juglans regia* log, 20 Jun. 2014, YG/PS172; (37): on dried trunk of angiosperm wood, 20 Jun. 2014, YG/PS183; (29): on dead stump of *Prunus armeniaca*, 2 Apr. 2013, YG-G41; (28): on unknown wood, 3 Sept. 2013, YG/bot23a; (47): on trunk of *Populus alba* L., 4 May 1988, I. Parmasto, TAAM126292; (19): on fallen trunk of *Populus* sp., 15 Jun. 2013, YG-O1.

Literature: Panfilova and Gaponenko (1963), [(44): on dried log of *Salix* sp.], Khalikova (1989), [(34): on decaying *Prunus armeniaca* log], Baltaeva (1992, 1993), [(49): on trunk of *Salix* sp., 13 Aug. 1986; (45): on dried stem and trunk of *Populus* sp., 25 Jul. 1986; (19): on decaying *Quercus* log, 6 May 1986; (6): on *Tilia* sp., 29 May 1989; (19): on stump of *Ulmus* sp., 28 Jun. 1988].

Note: This species is very common and occurs on dead and senescent deciduous wood. We mostly found it on *Juglans*, *Populus*, and *Prunus* species in Uzbekistan.

Bjerkandera fumosa (Pers.) P. Karst., Meddn Soc. Fauna Flora fenn. 5: 38 (1879)

Literature: Baymuratova (1963), [(27): on trunk of *Quercus* sp., 1962]; Khalikova (1989), [(28): on *Quercus* sp., Jun. 1983; (49): on dried trunk of *Populus* sp., Jul. 1984]; Baltaeva (1992, 1993), [(49): on *Populus* sp., 19 May 1985; (45): on stem of *Populus* sp., 6 Jun. 1986; (1): on trunk of hardwood].

Gelatoporia dichroa (Fr.) Ginns, Index Fungorum 156: 1 (2014)

≡ *Gloeoporus dichrous* (Fr.) Bres.

Literature: Panfilova and Gaponenko (1963), (as *Gloeoporus dichrous*, (49): dried stem of *Morus alba*, 1962); Baltaeva (1992, 1993), (as *Gloeoporus dichrous*, (45): on decaying *Picea* sp., 4 Jul. 1988; (8): on dried stem of *Pinus* sp., 6 Aug. 1987; (19): on *Pinus* sp., 18 Jul. 1989; (26): on *Pinus* sp., 10 Aug. 1989).

¤●***Hyphoderma* sp.**

Specimen examined: (37): on decaying branch of *Betula* sp., 19 Jun. 2014, YG/PS133.

Irpex lacteus (Fr.) Fr., Elench. fung. (Greifswald) 1: 142 (1828)

Literature: Kleyner (1958), [(25): on branch of *Pyrus* sp., 1957]; Baltaeva (1992, 1993), [(19): on stump of *Populus* sp., 19 Aug. 1985, (19): on *Ulmus* sp., 12 Aug. 1989; (8): on branch of *Alnus* sp., 9 Sept. 1986; (7): on *Quercus* sp., 4 Aug. 1987; (45): on dried stem of *Salix* sp., 16 Oct. 1988].

Irpiciporus litschaueri (Lohwag) Zmitr., Folia Cryptogamica Petropolitana (Sankt-Peterburg) 6: 105 (2018).

≡ *Spongipellis litschaueri* Lohwag

Literature: Baltaeva (1992, 1993), (as *Spongipellis litschaueri*, 7: on stem of *Malus* sp., 7 Aug. 198; (7): on trunk of *Quercus* sp., 14 Aug. 1986; (8): on *Fraxinus* sp., 29 Jul. 1988; (9): on *Quercus* sp., 19 Aug. 1987; (45): on stems of *Ulmus* sp., 4 Sept. 1987; (21): on angiosperm fallen wood, 27 Sept. 1987; (26): on dead *Fraxinus* branch, 3 Sept. 1989).

****Mycoacia aurea*** (Fr.) J. Erikss. and Ryvarden, Cortic. N. Eur. (Oslo) 4: 877 (1976).

≡ *Phlebia aurea* (Fr.) Nakasone

Specimen examined: (28): on a fallen rotten deciduous trunk, 20 Apr. 1982, E. Parmasto, TAAM104260.

Note: In TAAM, this specimen was originally labeled as *Phlebia aurea*.

•***Phlebia bresadolae*** Parmasto, Eesti NSV Tead. Akad. Toim., Biol. seer 16(4): 390 (1967)

Specimens examined: (37): on fallen branch of angiosperm, 18 Jun. 2014, YG/PS189; (37): on unknown woody plants branch, 19 Jun. 2014, YG/PS89.

¤•***Phlebia* sp.** (P. Karst.) Ryvarden, Rept. Kevo subarct. Res. Stn 8: 151 (1971)

Specimens examined: (39): on dead hardwood, 2 Nov. 2011, YG326; (40): on living *Crataegus pseudoheterophylla* subsp. *turkestanica*, 26 May 2011, YG64.

*•***Phlebia rufa*** (Pers.) M.P. Christ., Dansk bot. Ark. 19(no. 2): 164 (1960)

Specimen examined: (40): on living stems of *Robinia pseudoacacia* L., 26 May 2011, YG77.

Resiniporus resinascens (Romell) Zmitr., Folia Cryptogamica Petropolitana (Sankt-Peterburg) 6: 98 (2018)

≡ *Ceriporiopsis resinascens* (Romell) Domański

Literature: Baltaeva (1992, 1993), (as *Ceriporiopsis resinascens* (Romell) Domański, (45): on fallen branch of *Betula* sp., 7 May 1987; (19): on fallen log of *Populus* sp., 30 May 1987).

Sarcodontia spumea (Sowerby) Spirin, Mycena 1(1): 64–71 (2001)

≡ *Spongipellis spumeus* (Sowerby) Pat.

Literature: Baltaeva (1992, 1993), (as *Spongipellis spumeus* (Sowerby) Pat., (45): on fallen stem of *Ulmus* sp., 4 Sept. 1987; (21): on trunk of *Ulmus* sp., 27 Sept. 1987; (7): on stem of *Malus* sp., 7 Aug. 1986, (7): on *Quercus* sp., 19 Aug. 1989; (8): on *Fraxinus* sp., 29 Jul. 1988; (19): on dried trunk of *Fraxinus* sp., 3 Sept. 1989; (9): on dried strum of *Quercus* sp., 14 Aug. 1986).

****Steccherinum ciliolatum*** (Berk. and M.A. Curtis) Gilb. and Budington, J. Ariz. Acad. Sci. 6(2): 97 (1970).

Literature: Gafforov et al. (2017), [(45): on dead trunk of *Prunus spinosissima* (Bunge) Franch., 29 Apr. 1988, A. Kollom, TAAM127581].

Fomitopsidaceae Jülich

Amyloporia sinuosa (Fr.) Rajchenb., Gorjón and Pildain, Aust. Syst. Bot. 24(2): 117 (2011)

≡ *Antrodia sinuosa* (Fr.) P. Karst.

Literature: Baltaeva (1992), (as *Antrodia sinuosa* (Fr.) P. Karst., (21): on wet trunk of *Pinus* sp., 15 Aug. 1990).

Antrodia albida (Fr.) Donk, Persoonia 4(3): 339 (1966)

Literature: Kravtzev (1950), [(27): on *Quercus* sp.]; Baltaeva (1992, 1993), [(49): on bark of *Quercus* fallen branches, 5 Apr. 1987; (45): on fallen *Betula* trunk, 18 May 1986; (26): on stumps of *Populus* sp., 25 Jun. 1988; (8): on wet woody plant, 5 Apr. 1987].

Antrodia heteromorpha (Fr.) Donk, Persoonia 4(3): 339 (1966)

Literature: Baltaeva (1992), [(21): on rotten *Pinus* fallen trunk, 17 Aug. 1990].

Antrodia xantha (Fr.) Ryvarden, Norw. Jl Bot. (20): 8 (1973)

Specimens examined: (33): on trunk of *Juniperus polycarpos* var. *seravschanica*, 22 Apr. 1982, E. Parmasto, TAAM104400; (50): on rotten trunk of *Juniperus semiglobosa* Regel, 24 Apr. 1982, E. Parmasto, TAAM104301; (33): on fallen rotten trunk of *Juniperus semiglobosa*, 24 Apr. 1982, E. Parmasto, TAAM104289.

Literature: Baltaeva (1992, 1993), [(45): on *Pinus* sp., 19 Aug. 1988; (19): on *Juniperus polycarpos* var. *seravschanica*, 15 Aug. 1988; (21): on *Pinus* sp., 3 Jul. 1989; (7): on stumps of *Picea* sp., 13 Jul. 1989; (7): on *Juniperus* sp., 15 Jul. 1989; (49): on *Pinus* sp., 20 Jul. 1989].

Note: This species appears to be common in the study area. However, we did not find fresh specimens during our field trips.

#***Brunneoporus juniperinus*** (Murrill) Zmitr., Folia Cryptogamica Petropolitana (Sankt-Peterburg) 6: 86 (2018).

Specimen examined: (36): on base of tree of *Juniperus semiglobosa*, 25 Apr. 1982, M. Khalikova, TAAM104433.

Note: In TAAM, this specimen was originally labeled as *Antrodia juniperina* (Murrill) Niemelä and Ryvarden.

Climacocystis borealis (Fr.) Kotl. and Pouzar, Česká Mykol. 12(2): 103 (1958)

Literature: Baltaeva (1992, 1993), [(45): on old decaying trunks of *Pinus* sp., 24 Jul. 1988; (26): on fallen trunk of *Picea* sp., 26 Aug. 1989].

Daedalea quercina (L.) Pers., Syn. meth. fung. (Göttingen) 2: 500 (1801)

Literature: Baltaeva (1992), [(21): on stem of *Juglans regia*, 15 Aug. 1990].

*•***Flavidoporia pulverulenta*** (B. Rivoire) Audet, Mushrooms nomenclatural novelties 4: [1] (2017)

Specimens examined: (37): on trunk of *Salix* sp., 19 Jun. 2014, YG/PS167; (37): on rotten of branch of *Salix alba* L., 11 Sept. 2016, YG1110.

Fomitopsis betulina (Bull.) B.K. Cui, M.L. Han and Y.C. Dai, in Han, Chen, Shen, Song, Vlasák, Dai and Cui, Fungal Diversity 80: 359 (2016)

≡ *Piptoporus betulinus* (Bull.) P. Karst.

Literature: Panfilova and Gaponenko (1963); Khalikova (1989), (as *Piptoporus betulinus* (Bull.) P. Karst., (49): on stem of *Betula* sp.); Baltaeva (1992, 1993), (as *Piptoporus betulinus*, (45): on trunk of *Betula* sp., 14 Jul. 1987; (19): on wet *Betula* stems, 5 Aug. 1987; (26): on *Betula* sp., 30 Jun. 1988; (8): on dried

stems of *Betula* sp., 24 Aug. 1989); Iminova (2009), (as *Piptoporus betulinus*, (3): on *Betula tianschanica*, Jul.–Nov. 2003–2005).

Fomitopsis pinicola (Sw.) P. Karst., Meddn Soc. Fauna Flora fenn. 6: 9 (1881)

Specimen examined: (48): on *Juniperus polycarpos* var. *seravschanica*, J.K. Rotkevich, Jul. 1956, TASM002.

Literature: Baltaeva (1992, 1993), [(45): on living trunk of *Pinus* sp., 25 Jul. 1986; (7): on living trunk of *Pinus* sp., 11 Jun. 1987; (8): on living stem of *Picea* sp.; (21): on living *Pinus* tree, 3 Aug. 1987; (19): on fallen stem of conifer tree, 19 Jul. 1988].

Laetiporus sulphureus (Bull.) Murrill, Annls mycol. 18(1/3): 51 (1920)

Specimens examined: (28): on stem of *Salix* sp., 2 Sept. 2011, YG031; (28): on dried strum angiosperm wood, 3 Oct. 2011, YG041; (24): on *Acer tataricum* subsp. *semenovii* (Regel and Herder) A.E. Murray, 20 Aug. 2016, YG-B10.

Literature: Panfilova and Gaponenko (1963); Khalikova (1989), [(49): on living stem of *Prunus mahaleb* L. and *Juglans regia*]; Baltaeva (1992, 1993), [(45): on trunk of *Robinia pseudoacacia* L., 16 Oct. 1986; (1): on trunks of *Acacia*, 30 Jul. 1989; (1): on trunk of *Quercus*, 12 Sept. 1989].

Neoantrodia serialis (Fr.) Audet, Mushrooms nomenclatural novelties 6: [2] (2017)

≡ *Antrodia serialis* (Fr.) Donk

Literature: Baltaeva (1992), (as *Antrodia serialis*, (19): on dried of *Pinus* trunk, 6 Apr. 1989).

Phaeodaedalea incerta (Curr.) Tura, Zmitr., Wasser and Spirin, Biodiversity of the Heterobasidiomycetes and non-gilled Hymenomycetes (former Aphyllophorales) of Israel: 401 (2011).

= *Gloeophyllum sprucei* (Berk.) Teixeira

Literature: Baltaeva (1992), (as *Gloeophyllum sprucei*, (19): on wet branches of *Pinus* sp., 25 Jul. 1990).

Phaeolus schweinitzii (Fr.) Pat., Essai Tax. Hyménomyc. (Lons-le-Saunier): 86 (1900)

Literature: Baltaeva (1992, 1993), [(49): on dried fallen stem of *Pinus* sp., 30 Jul. 1989; (45): on trunk of *Picea* sp., 29 Jul. 1989]; Iminova (2009), [(3): on *Platanus orientalis*, Jun.–Jul. 2005].

*•***Pilatoporus ibericus*** (Melo and Ryvarden) Kotl. and Pouzar, Cryptog. Mycol. 14(3): 217 (1993)

Specimens examined: (49): on trunk of angiosperm tree, 3 Sept. 2013, YG-G24.

Postia caesia (Schrad.) P. Karst., Revue mycol., Toulouse 3(no. 9): 19 (1881)

≡ *Oligoporus caesius* (Schrad.) Gilb. and Ryvarden

Literature: Baltaeva (1992, 1993), (as *Oligoporus caesius*, (45): on stump of *Picea* sp., 17 Oct. 1987, 6 Nov. 1987; (8): on trunk of *Pinus* sp., 28 Oct. 1987; (7): on *Pinus* fallen branch, 12 Nov. 1988).

Postia sericeomollis (Romell) Jülich, Persoonia 11(4): 423 (1982)

≡ *Oligoporus sericeomollis* (Romell) Bondartseva

= *Chaetoporellus litschaueri* (Pilát) Bondartsev

Literature: Baltaeva (1992, 1993), (as *Oligoporus sericeomollis*, *Chaetoporellus litschaueri*), [(45): on stump of *Pinus* sp., 18 Sept. 1986; (19): on *Pinus* sp., 21 Jun. 1989; (8): on trunk of *Picea* sp., 9 May 1987; (7): on fallen branch of *Picea* sp., 9 May 1987].

Postia stiptica (Pers.) Jülich, Persoonia 11(4): 424 (1982)

≡ *Oligoporus stipticus* (Pers.) Gilb. and Ryvarden

Literature: Baltaeva (1992, 1993), (as *Oligoporus stipticus*, (45): on stump of *Pinus* sp, 9 Oct. 1987; (19): on *Pinus* sp., 24 Oct. 1987; (21): on fallen trunk of *Picea* sp., 6 Nov. 1988).

Osteina obducta (Berk.) Donk, Schweiz. Z. Pilzk. 44: 86 (1966)

≡ *Oligoporus obductus* (Berk.) Gilb. and Ryvarden

Literature: Baltaeva (1992), (as *Oligoporus obductus*, (21): on root of *Pinus* sp., 15 Aug. 1990).

Rhodofomes roseus (Alb. and Schwein.) Vlasák, Ćeská Mykol. 44(4): 235 (1990)

≡ *Fomitopsis rosea* (Alb. and Schwein.) P. Karst

Specimens examined: (45): on conifer fallen trunk, 15 Jun. 1980, S.S. Ramazanova, N4 (TASM).

Literature: Baltaeva (1992, 1993), (as *Fomitopsis rosea*, (45): on dead standing *Picea* trunk, 7 Apr. 1987; (45): on *Picea* sp., 21 May 1988; (8): on trunk of *Picea* sp., 9 Jun. 1987; (7): on fallen branch of *Pinus* sp., 30 May 1988; (14): on *Pinus* sp., 5 May 1989).

*•***Subantrodia uzbekistanica*** (Yuan, Gafforov and F. Wu) Audet, Mushrooms nomenclatural novelties 9: [1] (2017).

≡ ***Antrodia uzbekistanica*** Yuan, Gafforov and F. Wu

Specimens examined: (8): on Juniper tree rotten wood, 8 Sept. 2016, YG1014; (8): on trunk of *Juniperus* sp., 4 Sept. 2017, YG1103; (8): on rotten stem of *Juniperus polycarpos* var. *seravschanica* (Kom.) Kitam., 10 Sept. 2017, YG1107; (8): on unknown woody branches, 9 Sept. 2016, YG1100.

Literature: Yuan et al. (2017), (same place: as *Antrodia uzbekistanica*).

Phanerochaetaceae Jülich

*•***Byssomerulius corium*** (Pers.) Parmasto, Eesti NSV Tead. Akad. Toim., Biol. seer 16(4): 383 (1967)

Specimens examined: (28): on angiosperm fallen branch, 2 Sept. 2013, YG-G21; (7): on dried branch of *Prunus vulgaris* L., 28 Aug. 2013, YG-X3.

*Ceriporia purpurea*** (Fr.) Donk, Proc. K. Ned. Akad. Wet., Ser. C, Biol. Med. Sci. 74(1): 28 (1971)

Specimen examined: (45): on a deciduous tree, 1 May 1988, A. Kollom, TAAM127605.

*•***Ceriporiopsis gilvescens*** (Bres.) Domański, Acta Soc. Bot. Pol. 32(4): 731 (1963)

≡ *Tyromyces gilvescens* (Bres.) Ryvarden

Specimens examined: (28): on dried angiosperm wood, 14 Oct. 2011, YG046; (36): on base of rotten trunk of wood, 8 Jun. 2011, YG049; (32): on *Juniperus pseudosabina* Fisch. et C.A. Mey., 26 May 2011, YG008.

Literature: Baltaeva (1992, 1993), (as *Tyromyces gilvescens*, (45): on fallen branch of *Populus* sp., 2 May 1987; (19): on *Quercus* trunk, 19 Aug., 1988; (26): on died fallen of *Populus* sp., 1 Sept. 1988; (9): on rotten trunk of *Populus* sp., 10 Jul. 1987; (21): on rotten trunk of *Malus* sp., 21 Jul. 1986; (6): on dead stump and trunk of deciduous wood, 13 Apr. 1986).

Ceriporiopsis mucida (Pers.) Gilb. and Ryvarden, Mycotaxon 22(2): 364 (1985)

Literature: Baltaeva (1992), [(5): on dried branch of *Populus* sp., 28 Aug. 1990].

#***Efibula tuberculata*** (P. Karst.) Zmitr. and Spirin, in Zmitrovich, Malysheva and Spirin, Mycena 6: 33 (2006)

Specimen examined: (18): on fallen trunk of *Haloxyllon* sp., 6 Apr. 1979, K. Kalamees, TAAM120642.

Note: In TAAM, this specimen was originally labeled as *Athelia* sp.

Polyporaceae Fr. ex Corda

Cerioporus mollis (Sommerf.) Zmitr. and Kovalenko, Int. J. Med. Mushrooms 18(1): 33 (2016)

≡ *Datronia mollis* (Sommerf.) Donk

Literature: Baltaeva (1992, 1993), (as *Datronia mollis*, (45): on wet dead trunk of *Populus* sp., 10 May 1985; (19): on *Populus* sp., 21 Apr. 1986; (26): on *Populus* sp., 17 Jun. 1987).

Cerioporus squamosus (Huds.) Quél., Enchir. fung. (Paris): 167 (1886)

≡ *Polyporus squamosus* (Huds.) Fr.

Specimens examined: (50): on trunk of *Juglans regia*, 24 Apr. 1982, A. Kollom, TAAM127413; (36): on dried trunk and stem of angiosperm woody plant, 6 Jun. 2011, YG026; (37): on rotten trunk of *Acer tataricum* subsp. *semenovii*, 2 Sept. 2017, YG20170902; (22): on dried stump of *Populus alba*, 13 May 2015, YG-B02; (23): on *Acer* sp., 17 May 2015, YG-B05.

Literature: Panfilova and Gaponenko (1963), Akhmedova, 1966 (as *Polyporus squamosus*, (49): on trunk of *Juglans regia*); Khalikova (1989), (as *Polyporus squamosus*, (49): on *Pistacia* sp.); Baltaeva (1992, 1993), (as *Polyporus squamosus*, (1): on stump collar of *Quercus,* sp., 1988, on fallen big branch of *Juglans regia*, 1989); Iminova (2009), (as *Polyporus squamosus*, (3): on various woody plants, May–Jun. 2000–2004).

Note: This species is widespread on angiosperm woody plants across study area.

Cerioporus varius (Pers.) Zmitr. and Kovalenko, Int. J. Med. Mushrooms 18(1): 33 (2016)

≡ *Polyporus varius* (Pers.) Fr.

Literature: Baltaeva (1992), (as *Polyporus varius*, (45): on deadwood stem of *Quercus* sp., 23 Jun. 1990; (19): on fallen stem of *Lonicera* sp., 10 Aug. 1990).

●***Cerrena unicolor*** (Bull.) Murrill, J. Mycol. 9(2): 91 (1903)

Specimens examined: (28): on dried fallen stem of angiosperm tree, 2 Sept. 2013, YG-G28; (32): on *Acer tataricum* subsp. *semenovii*, 15 May 2011, YG18; (32): on dried stem of *Acer tataricum* subsp. *semenovii*, 15 May 2011, YG027; (38): on *Crataegus pseudoheterophylla* subsp. *turkestanica*, 1 Jun. 2011, YG003; (41): on a trunk of *Juglans regia*, 22 Apr. 1982, E. Parmasto, TAAM104271; (41): on dry twig of *Acer* sp., 22 Apr. 1982, A. Kollom, TAAM127385; (50): on dead trunk of *Salix* sp., 24 Apr. 1982, A. Kollom, TAAM127405; (37): on *Acer tataricum* subsp. *semenovii*, 19 Sept. 2014, YG/PS79; (45): on dry branch of *Celtis australis* subsp. *caucasica*, 29 Apr. 1988, A. Kollom, TAAM127582; (45): on *Celtis australis* subsp. *caucasica*, 3 May 1988, A. Kollom, TAAM127632; (45): on dry trunk of *Celtis australis* subsp. *caucasica*, 1 May 1988, I. Parmasto, TAAM126263; (47): on trunk of *Prunus mahaleb*, 29 Apr. 1988, I. Parmasto, TAAM126248.

Literature: Akhmedova (1966), [(49): on *Populus* sp.]; Khalikova (1989), [(49): on trunk of *Populus* sp., Jul. 1988]; Baltaeva (1992, 1993), [(1): on stump of *Quercus* sp., *Populus* sp., *Salix* sp., Jul.–Aug. 1988–1989].

Note: This species is widespread and causes damage to *Acer tataricum* subsp. *semenovii* trees in Tien Shan Mountain.

Coriolopsis gallica (Fr.) Ryvarden, Norw. Jl Bot. 19: 230 (1973)

≡ *Funalia gallica* (Fr.) Bondartsev and Singer

Literature: Panfilova and Gaponenko (1963), (as *Funalia gallica*, (49): on *Quercus* sp.); Khalikova (1989), (as *Funalia gallica*, (28): on stumps and dried trunks of *Fraxinus americana* L., Jun. 1986, Sept. 1986, Dendropark, May, 1987); Baltaeva (1992, 1993), [(45): on dried stem and branches of *Quercus* sp., 6 Jun. 1985, (45): on *Quercus* sp., 3 Jun. 1988, (45): on *Salix* sp., 17 Jul. 1987, (47): on *Populus* sp., 27 Jul. 1987; (8): on *Fraxinus* sp., 4 Jul. 1989; (7): on *Fraxinus* sp., 1 Aug. 1989; (19): on stem of *Fraxinus* sp., 20 Jul. 1986; (21): on trunk of *Populus* sp., 27 Jul. 1987; (6): on *Quercus* sp., 3 Jun. 1988; (9): on *Populus tremula* L., 1 Aug. 1989]; Iminova (2009), (as *Funalia gallica*, (3): on fallen trunks of *Platanus orientalis* L., May 2005, Sept. 2005).

Daedaleopsis confragosa (Bolton) J. Schröt., in Cohn, Krypt.-Fl. Schlesien (Breslau) 3.1(25–32): 492 (1888) [1889]

Literature: Baltaeva (1992), [(45): on decaying stem of *Betula* sp., 11 Aug. 1990; (6): on *Betula* sp., 12 Sept. 1991; on fallen tree of *Betula* sp., 6 Aug. 1990, on *Betula* sp., 19 Jul. 1988].

Dichomitus squalens (P. Karst.) D.A. Reid, Revta Biol., Lisb. 5(1–2): 150 (1965) [1964–5]

Literature: Baltaeva (1992, 1993), [(45): on the bark of *Pinus* sp., 9 May 1987; (21): on *Biota* sp., 21 Jun. 1989; (21): on *Pinus* sp., 14 May 1988; (7): on *Pinus* sp., 9 Jun. 1989; (8): on *Picea* sp., 20 Jun. 1988; (19): on living stem of old *Biota* sp., 19 Jul. 1988].

Diplomitoporus flavescens (Bres.) Domański, Acta Soc. Bot. Pol. (39): 191 (1970)

≡ *Antrodia flavescens* (Bres.) Ryvarden

Literature: Khalikova (1989), (as *Antrodia flavescens*, (49): on fallen logs of *Picea* sp., 22 Apr. 1980); Baltaeva (1992), (as *Diplomitoporus flavescens*), Baltaeva, 1993 (as *Antrodia flavescens*, (7): on *Picea* stump, 20 Jul. 1987; (26): on *Juniper* fallen stems, 17 Jun. 1987; (21): on *Pinus* trunk, 21 Jun. 1989).

Fibroporia vaillantii (DC.) Parmasto, Consp. System. Corticiac. (Tartu): 177 (1968)

≡ *Antrodia vaillantii* (DC.) Ryvarden

Literature: Baltaeva (1992, 1993), (as *Antrodia vaillantii*, (45): on trunk of *Picea* sp., 18 Aug. 1989).

●***Fomes fomentarius*** (L.) Fr., Summa veg. Scand., Sectio Post. (Stockholm): 321 (1849)

Specimens examined: (28): on living stem of *Populus* sp., 3 Sept. 2013, YG/bot2; (28): on decaying trunk of identified angiosperm, 4 Sept. 2013, YG/bot4; (40): on living trunk of *Juglans regia*, 26 May 2011, YG014; (28): on unknown wood, 7 Nov. 2014, YG-60, *ibit*., on unknown trunk decaying wood, YG-70; (38): on *Juglans regia*, 13 Sept. 2012, YG/Un2; (37): on dried *Juglans regia* trunk, 14 Sept. 2014, YG/PS174; (23): on living stem of *Juglans regia*, 13 Aug. 2015, YG-B03; (22): on dried stem of *Salix alba*, 17 Aug. 2016, YG-B04.

Literature: Panfilova and Gaponenko (1963); Akhmedova (1966); Khalikova (1989), [(49): on stem and trunk decaying and living *Juglans regia*]; Baltaeva (1992), [(1): on dead and living deciduous trees on *Malus* sp., *Quercus* sp., *Populus* sp.]; Iminova

(2009), [(3): on living stem of *Salix wilhelmsiana* M. Bieb., Sept. 2000; (4): on died trunk of *Salix alba*, Oct. 2001].

Note: This species is widespread on living trees in the study area.

Hapalopilus rutilans (Pers.) Murrill, Bull. Torrey bot. Club 31(8): 416 (1904)

= *Hapalopilus nidulans* (Fr.) P. Karst.

Literature: Baltaeva (1992, 1993), (as *Hapalopilus nidulans*, (49): on dead branch of *Betula* sp., 1 Jul. 1989, (49): on fallen stem of *Populus* sp., 14 Jul. 1989; (19): on fallen strums of *Populus* sp., 29 Jul. 1989).

Lentinus arcularius (Batsch) Zmitr., Int. J. Med. Mushrooms 12(1): 88 (2010)

≡ *Polyporus arcularius* (Batsch) Fr.

Literature: Khalikova (1989), (as *Polyporus arcularius*, (45): on dead branch of *Juglans regia*, May, 1982, Nov. 1983; (41): on *Salix interior* Rowlee, Apr.–May 1983); Iminova (2009), (as *Polyporus arcularius*; (11): dried trunk of *Juglans regia*, Apr. 2000, Nov. 2004).

Lentinus brumalis (Pers.) Zmitr., Int. J. Med. Mushrooms 12(1): 88 (2010)

≡ *Polyporus brumalis* (Pers.) Fr.

Literature: Schwartzman (1964), (as *Polyporus brumalis*, (49): on *Celtis australis* subsp. *Caucasica*); Baltaeva (1993), (as *Polyporus brumalis*, (21): on stem of branch of *Salix* sp., 21 Jul. 1987; (3): on *Salix* sp., 15 Aug. 1987; (45): on *Betula* sp., 10 May 1987; (19): on *Betula* sp., 20 Jul. 1988; (8): on *Populus* sp., 6 Sept. 1988; (7): on small branches of *Salix* sp., 24 Aug. 1987; (27): 20 Jul. 1988; (10): on dried stem of *Populus* sp., 24 Aug. 1989).

Lentinus substrictus (Bolton) Zmitr. and Kovalenko, Int. J. Med. Mushrooms 18(1): 35 (2016)

= *Polyporus ciliatus* Fr.

Literature: Baltaeva (1992), (as *Polyporus ciliatus*, (45): on branches of *Salix* sp., 15 Aug. 1987; (8): on *Salix* sp., 21 Aug. 1987; (7): on strum and branch of *Populus* sp., 6 Nov. 1988; (19): on *Betula* fallen trumps, 10 May 1987; (21): on *Betula* sp., 30 Aug. 1988; (3): on *Populus* sp., 24 Aug. 1989).

●***Lentinus tigrinus*** (Bull.) Fr., Syst. orb. veg. (Lundae) 1: 78 (1825)

≡ *Panus tigrinus* (Fr.) Sing.

Specimens examined: (28): on *Salix* sp., 24 Apr. 1989, K. Kalamees, TAAM144150; (28): on stump of *Lonicera* sp., 20 Apr. 1982, A. Kollom, TAAM104259; (40): on decaying *Juglans regia*, 26 May YG029; (33): on fallen trunk of angiosperm, 23 Apr. 1982, M. Khalikova, TAAM104290; (33): on trunk of *Juglans regia*, 23 Apr. 1982, E. Parmasto, TAAM104406; (33): on strum of *Salix* sp., 23 Apr. 1982, A. Kollom, TAAM127396; (41): on stump of unidentified wood, 23 Apr. 1982, A. Kollom, TAAM127381; (41): on trunk of angiosperm tree, 22 Apr. 1982, M. Khalikova, TAAM104275; (47): on *Salix* sp., 1 May 1988, A. Kollom, TAAM127603; (37): on trunk of *Malus domestica*, 18 Jun. 2014, YG/PS162; (17): on *Salix* sp., 7 May 1976, TAAM094856; (17): on stump of *Prunus armeniaca*, 7 May 1976, K. Kalamees and others, TAAM094857; (17): on *Acer* tree trunk, 7 May 1976, K. Kalamees and others, TAAM094847; (20): on dried trunks of angiosperm wood, 13 Jun. 2013, YG-J7.

Literature: Panfilova and Gaponenko (1963), [(44): on living trunk and stems of *Lonicera* sp., and on fallen dried trunk of *Acer* sp.]; Khalikova (1989), [(34): on dried stem of *Malus domestica*]; Iminova (2009), [(3): on *Salix wilhelmsiana*, on *Populus euphratica* Oliv., on living stem of *Populus talassica* Kom., Nov. 2005]; Iminova (2009), (as *Panus tigrinus*, (4): on *Salix linearifalia* Wolf.).

Note: This is a widespread species in the study area.

Lenzites betulinus (L.) Fr., Epicr. syst. mycol. (Upsaliae): 405 (1838) [1836–1838]

Literature: Baltaeva (1992, 1993), [(45): on fallen twigs of *Betula* sp., 17 Aug. 1987; (26): on *Populus* sp., 22 Jul. 1988; (10): on *Populus* sp., 10 Sept. 1988; (21): on *Salix* sp., 26 Sept. 1988, 18 Aug. 1989]

●***Lenzites warnieri*** Durieu and Mont., Annls Sci. Nat., Bot., sér. 4 14: 182 (1860)

Specimen examined: (49): on branch of *Populus nigra* L., 15 Jul. 1985, E. Krall, Z. Narbal, TAAM126870.

Literature: Baltaeva (1992, 1993), [(45): on wet branch of *Betula* sp., 17 Aug. 1987; (19): on *Populus* sp., 22 Jul. 1988; (7): died trunk of *Populus* sp. 10 Sept. 1988; (8): on *Salix* sp., 26 Sept. 1988; (26): on *Quercus* sp., 10 Aug. 1990; (18): on *Salix* sp., 18 Aug. 1988].

Neolentinus lepideus (Fr.) Redhead and Ginns, Trans. Mycol. Soc. Japan 26(3): 357 (1985)

≡ *Lentinus lepideus* (Fr.) Fr.

Literature: Khalikova (1989), (as *Lentinus lepideus*, (28): on softwood conifer stumps, Sept. 1980, 1982); Baltaeva (1992), (as *Lentinus lepideus*, (45): on *Populus* sp. 13 Sept. 1990); Iminova (2009), (as *Lentinus lepideus*, (2): on stem of *Populus talassica* Kom., Nov. 2005).

Perenniporia fraxinea (Bull.) Ryvarden, Grundr. Krauterk. 2: 307 (1978)

Literature: Baltaeva (1992), [(45): on stem of *Biota* sp., 13 Sept. 1990].

Picipes badius (Pers.) Zmitr. and Kovalenko, International Journal of Medicinal Mushrooms (Redding) 18(1): 35 (2016)

≡ *Polyporus badius* (Pers.) Schwein

Literature: Baltaeva (1992), (as *Polyporus badius*, (19): on stump of woody plant, 13 Jul. 1989).

Picipes melanopus (Pers.) Zmitr. and Kovalenko, International Journal of Medicinal Mushrooms (Redding) 18(1): 36 (2016)

≡ *Polyporus melanopus* (Pers.) Fr.

Literature: Baltaeva (1992), (as *Polyporus melanopus* (Pers.) Fr., (21): on *Prunus* sp., 2 Sept. 1990).

Podofomes trogii (Fr.) Pouzar, Česká Mykol. 25(1): 19 (1971)

≡ *Ischnoderma trogii* (Fr.) Teixeira

Literature: Khalikova (1989), (as *Ischnoderma trogii*, (49): on *Abies alba* Mill., Oct. 1982).

Polyporus lipsiensis (Batsch) E.H.L. Krause, Basidiomycetum Rostochiensium: 54 (1928)

≡ *Ganoderma lipsiense* (Batsch) G.F. Atk.

Literature: Iminova (2009), (as *Ganoderma lipsiense*, (6): on dried stem of angiosperm wood, Sept. 2002).

Pycnoporus cinnabarinus (Jacq.) P. Karst., Revue mycol., Toulouse 3 (no. 9): 18 (1881)

Literature: Baltaeva (1992), [(45): on strum of *Salix* sp., 13 Jun. 1990].

Pyrofomes demidoffii (Lév.) Kotl. and Pouzar, Reprium nov. Spec. Regni veg. 69: 140 (1964)

Specimen examined: (45): on living trunk of *Juniperus polycarpos* var. *seravschanica*, 29 Apr. 1988, I. Parmasto, TAAM126251.

Literature: Panfilova and Gaponenko (1963); Akhmedova (1966); Khalikova (1989), [(49): on living trunk of *Juniperus polycarpos* var. *seravschanica* and *Juniperus* sp.]; Baltaeva (1992, 1993), [(49): on trunk of living *Pinus* sp., 21 Jul. 1987; (45): on living Juniper trunk, 21 Jul. 1987; (8): on *Pinus* sp., 4 Jul. 1987; (7): on *Picea* sp., 25 Aug. 1989; (9): on *Pinus* sp., 14 Oct. 1987; (21): on *Pinus* sp., 14 Jul. 1987; (19): on *Picea* sp., 27 Jul. 1988].

Note: This species causes severe infections of living *Juniperus* trees in the study area.

Szczepkamyces campestris (Quél.) Zmitr., Folia Cryptogamica Petropolitana (Sankt-Peterburg) 6: 52 (2018)

Literature: Baltaeva (1992, 1993), [(45): on broken trunk of *Quercus* sp., 11 Mar. 1985; (3): on *Pyrus* sp., 6 Jul. 1988; (19): on stem and branch of *Aesculus* sp., 15 May 1986; (7): on dried trunk of *Populus* sp., 21 Aug. 1989].

Skeletocutis amorpha (Fr.) Kotl. and Pouzar, Česká Mykol. 12(2): 103 (1958)

Literature: Baltaeva (1992, 1993), [(45): on trunk of *Picea* sp., 15 Aug. 1987; (19): on *Picea* sp., 19 Aug. 1987; (19): on dried stem of *Abies alba*; (8): on trunk of *Pinus* sp., 8 Jul. 1988; (7): on *Abies alba*, 6 Aug. 1989; (21): on *Pinus* sp., 21 Aug. 1988].

Skeletocutis nivea (Jungh.) Jean Keller, Persoonia 10(3): 353 (1979)

≡ *Incrustoporia nivea* (Jungh.) Ryvarden

Literature: Baltaeva (1992), (as *Skeletocutis nivea*), Baltaeva (1993), (as *Incrustoporia nivea*, (49): on wet branches of *Salix* sp., 10 Jun. 1988; (45): on stem of *Fraxinus* sp., 24 Jun. 1989).

#***Tinctoporellus epimiltinus*** (Berk. and Broome) Ryvarden, Trans. Br. mycol. Soc. 73(1): 18 (1979)

Specimen examined: (47): on decayed branches of *Populus* sp., 19 May 1990, K. Kalamees, M. Vaasma, TAAM144614.

Note: In TAAM, this specimen was incorrectly labeled as *Phellinus* sp.

Trametes gibbosa (Pers.) Fr., Epicr. syst. mycol. (Upsaliae): 492 (1838) [1836–1838]

Literature: Baltaeva (1992, 1993), [(1): on wet trunk and stumps of deciduous woody plants: *Populus* sp., *P. tremula*, *Salix* sp., *Betula* sp., *Ulmus* sp.].

•***Trametes hirsuta*** (Wulfen) Lloyd, Mycol. Writ. 7(Letter 73): 1319 (1924)

Specimens examined: (28): on dried stem of living *Prunus vulgaris*, 3 Oct. 2011, YG312; (38): on dried unknown woody trunk, 1 Jun. 2011, YG073; (38): on unknown dried wood, 1 Jun. 2011, YG032; (38): on fallen trunk of angiosperm wood, 1 Jun. 2011, YG042; (38): on unknown decaying wood, 1 Jun. 2011, YG055; (40): on decaying *Juglans regia* log, 26 May 2011, YG002; (40): on trunk and branch of *Juglans regia*, 26 May 2011, YG037; (40): on *Prunus armeniaca*, 2 Nov. 2011, YG004; (40): on *Prunus vulgaris*, 2 Nov. 2011, YG007; (39): on living *Prunus* tree, 2 Nov. 2011, YG314; (37): on decaying, unidentified angiosperm stem, 19 Jun. 2014, YG/PS128; (37): on dead *Prunus* sp., 19 Jun. 2014, YG/PS138; (37): on dried stem of *Juglans regia*, 20 Jun. 2014, YG/PS168; (15): on died angiosperm strum, 9 Jul. 2017, RM44; (41): on stem of angiosperm tree, 14 Jul. 2014, YG/Ch40; (33): on fallen trunk of *Juglans regia*, 23 Apr. 1982, E. Parmasto, TAAM104394 in TAAM reported as *Antrodia* sp.

Literature: Panfilova and Gaponenko (1963), [(44): on *Prunus mahaleb*]; Khalikova (1989), [(49): on decaying branch of the *Quercus* tree]; Sinadskiy (1968), [(18): on fallen log of *Quercus*]; Baltaeva (1992, 1993), [(45): 1988, on stem of *Quercus* sp.; (21): on dried trunk of *Quercus* tree; (1): on various deciduous woody plant]; Iminova (2009), (as *Coriolus hirsutus* (Wulfen) Pat., (14): on fallen decaying branch of *Platanus orientalis* L. Jun. 2002; (14): on *Pinus brutia* var. *eldarica* (Medw.) Silba, May-Jun. 2002; 3: on dried trunk of *Prunus mahaleb*, Oct. 2003, *ibit*., (3): on dried on *Prunus mahaleb*, Nov. 2003).

Note: This is one of the most common and widespread species in Uzbekistan. This species is mostly found on *Prunus*, *Platanus*, *Pinus*, *Quercus*, and *Juglans* species in the study area.

Trametes ochracea (Pers.) Gilb. and Ryvarden, N. Amer. Polyp., Vol. 2 Megasporoporia - Wrightoporia (Oslo): 752 (1987)

= *Trametes zonatella* Ryvarden

Specimen examined: (47): on fallen stems of *Prunus* sp., 17 May 1990, K.Kalamees, M. Vaasma, TAAM144571.

Literature: Panfilova and Gaponenko (1963); Kravtzev (1950); Khalikova (1989), (as *Trametes zonatella*, (49): on fallen branch of woody plants, Apr. 1985, May 1985); Iminova (2009), [(6): on unknown wood trunk, May 2000, Jul. 2005]; Baltaeva (1992), (as *Trametes ochracea*), Baltaeva (1993), (as *Trametes zonatella*, (1): on died trunks and stumps of deciduous woody plants); Iminova (2009), (as *Coriolus zonatus* (Nees) Quél., (2): on stump of woody plants, May, 2000, Jul. 2005).

Trametes pubescens (Schumach.) Pilát, in Kavina and Pilát, Atlas Champ. l'Europe, III, Polyporaceae (Praha) 1: 268 (1939)

Literature: Baltaeva (1992), [(1): on died trunks, 1992].

Trametes suaveolens (L.) Fr., Epicr. syst. mycol. (Upsaliae): 491 (1838) [1836–1838]

Literature: Baltaeva (1992, 1993), [(49): on trunk of *Salix* sp., 5 Sept. 1987; (45): on *Salix* sp., 16 Apr. 1987; (8): on *Populus tremula*, 11 May 1988; (19): on *Populus tremula*, 9 Jul. 1988; (21): on *Populus tremula*, 21 Sept. 1988].

Trametes tephroleuca Berk. Hooker's J. Bot. Kew Gard. Misc. 6: 165 (1854)

Specimens examined: (33): on fallen trunk of *Juglans regia*, 23 Apr. 1982, E. Parmasto, TAAM104394a, *ibit*. TAAM104399; (33): on fallen trunk of *Juglans regia*, 23 Apr. 1982, K. Kalamees, TAAM104305; (41): on a trunk of *Juglans regia*, 22 Apr. 1982, E. Parmasto, TAAM104270a; (33): on a trunk of *Lonicera* sp., 22 Apr. 1982, E. Parmasto, TAAM104283; (45): on dry twig of *Prunus* sp., 29 Apr. 1988, I. Parmasto, TAAM126249; (45): on dead trunk of *Prunus mahaleb*, 2 May 1988, A. Kollom, TAAM127624; (45): on fallen twig of *Prunus mahaleb*, 3 May 1988, I. Parmasto, TAAM126285; (45): on a dry trunk of *Crataegus* sp., 29 Apr. 1988, A. Kollom, TAAM127579; (41): on dry branch of *Crataegus pseudoheterophylla* subsp. *turkestanica*, 22 Aprel 1988, A. Kollom, TAAM127382.

Literature: Khalikova (1989), [(33): on dried stem of *Malus sieversii*, 17 Apr. 1986]; Iminova (2009), (as *Coriolus tephroleucus* (Fr.) Bonk., (14): on *Prunus vulgaris* and *Juglans regia*, May 1999).

•***Trametes trogii*** Berk., in Trog, Mittheil. d. schweiz. Naturf. Ges. in Bern 2: 52 (1850)

≡ *Funalia trogii* (Berk.) Bondartsev and Singer

Specimens examined: (28): on fallen deciduous branch, 2 Sept. 2013, YG/bot23b; 11 Sept. 2014; (38): on *Acer tataricum* subsp. *semenovii*, 9 Sept. 2016, YG1017; (49): on dried decaying trunk of *Populus alba*, 17 Sept. 2014, YG-N6, *ibit*. on trunk of *Populus alba*, 17 Sept. 2014, YG-N7; (31): on unidentified wood, 17 Sept. 2009, O. Kurina, TAAM189940 (as *Funalia* sp. in TAAM); (37): on dried on *Salix* sp. trunk, 14 Sept. 2014, YG/PS2X; (20): on *Populus* sp., 14 Sept. 2014, YG-JX4; (20): on unknown stump of angiosperm, 13 Jun. 2013, YG-G17, *ibit*. 13 Jun. 2013, YG-G18, *ibit*. 13 Jun. 2013, YG-G19; (20): on *Populus nigra* L., 16 Jun. 2013, YG-J4; (20): on dried stem of living *Populus nigra*, 15 Jun. 2013, YG-J6; (20): on *Populus* sp., 16 Jun. 2013, YG-GX1; (8): on unknown woody branches, 13 Jun. 2016, YG-G14, *ibit*., 13 Jun. 2016, YG1090.

Literature: Panfilova and Gaponenko (1963); Khalikova (1989), (as *Funalia trogii*, (30): on *Populus* sp.; (49): on unknown wood plant); Baltaeva (1992, 1993), [(45): on stem of *Salix* sp. 12 Sept. 1990; (1): mainly on dead stump and trunk of woody plants: on *Salix* sp., 27 Oct. 1992; (1): on stump and trunk of *Fraxinus* sp., 12 Sept. 1991; on fallen of *Populus tremula*, 15 Nov. 1992].

Note: First report of this species on stumps and trunks of *Acer tataricum* subsp. *semenovii*, and *Populus nigra* in Uzbekistan.

•***Trametes versicolor*** (L.) Lloyd, Mycol. Notes (Cincinnati) 65: 1045 (1921) [1920]

≡ *Coriolus versicolor* (L.) Quél.

Specimens examined: (28): on trunk of *Betula* sp., 5 May 1988, I. Parmasto, TAAM126293; (28): on *Betula* trunk, 5 May 1988, A. Kollom, TAAM127635; (37): on dried stem of angiosperm wood, 19 Jun. 2014, YG/PS128-1; (37): on dried stem of angiosperm wood, 19 Jun. 2014, YG/PS170; (45): on trunk of *Prunus* sp., 22 Apr. 1982, A. Kollom, TAAM127389; (49): on a fallen deciduous trunk, 22 Apr. 1982, A. Kollom, TAAM127388; (35): on *Crataegus pseudoheterophylla* subsp. *turkestanica* (Pojark.) K.I.Chr., 31 Aug. 1963, A. Raitviir, TAAM043489; (50): on trunk of *Lonicera* sp., 24 Apr. 1982, A. Kollom, TAAM127403; (45): on dry trunk of *Celtis australis* subsp. *caucasica*, 3 May 1988, I. Parmasto, TAAM126287, (45): on dry twig of *Prunus mahaleb*, 2 May 1988, I. Parmasto, TAAM126284; (47): on fallen *Prunus* branch, 17 May 1990, K. Kalamees, M. Vaasma, TAAM144572; (47): 4 May 1988, I. Parmasto, TAAM126294; (20): on *Prunus* sp., 14 Jun. 2013, YG-J3.

Literature: Panfilova and Gaponenko (1963); Akhmedova (1966); Baltaeva (1992, 1993); Khalikova (1989), [(1): on *Prunus mahaleb*, *Malus* sp., *Quercus* sp., *Juglans regia*, *Populus* sp.]; Iminova (2009), (as *Coriolus versicolor*, (12): on dried and living stem of *Prunus vulgaris*, May 2003, Jun. 2004).

Note: This species was recorded for the first time in Uzbekistan, on *Betula* sp., *Celtis australis* subsp. *caucasica, Crataegus pseudoheterophylla* subsp. *turkestanica*, and *Lonicera* sp. in Uzbekistan.

*•***Trametes villosa*** (Sw.) Kreisel, Monografias, Ciencias, Univ. Habana, Ser. 4 16: 83 (1971)

Specimen examined: (29): on dried stem of angiosperm, 15 Jun. 2015, YG/AG11.

Trametopsis cervina (Schwein.) Tomšovský, Czech Mycol. 60(1): 7 (2008)

≡ *Trametes cervina* (Schwein.) Bres.

Literature: Baltaeva (1992, 1993), (as *Trametes cervina*, (19): on fallen branch of *Juglans regia*, 14 May 1987; (7): on *Juglans regia*, 5 Jul. 1987; (45): on dried stem of *Morus alba*, 15 May 1988; (21): on stem of *Juglans regia*, 5 Jul. 1987; (3): on *Malus domestica*, 27 Mar. 1988; (26): *Morus alba* trunk, 15 May 1988; (26): on dried *Morus nigra*, 4 Aug. 1988; (9): on rotten trunk of *Morus alba*, 6 Aug. 1989).

Note: We could not observe the species in the localities mentioned in Baltaeva (1992, 1993).

Tyromyces lacteus (Fr.) Murr, N. Amer. Fl. (New York) 9(1): 36 (1907)

Literature: Panfilova and Gaponenko (1963); Khalikova (1989), [(49): on died trunk of *Betula pendula* Roth].

Sparassidaceae Herter

Sparassis crispa (Wulfen) Fr., Syst. mycol. (Lundae) 1: 465 (1821)

Literature: Iminova (2009), [(3): on trunk of angiosperm trees, Aug. 2000, Sept. 2003, Oct. 2003].

Ganodermataceae Donk

•***Ganoderma adspersum*** (Schulzer) Donk, Proc. K. Ned. Akad. Wet., Ser. C, Biol. Med. Sci. 72(3): 273 (1969)

Specimens examined: (28): on died stump of *Acer saccharum* Marshall, 7 Jun. 2014, YG/bot24; (49): on strum of *Acer* sp., 12 Sept. 2011, YG/UG3; (49): on trunk of *Acer* sp., 12 Sept. 2014, YG/Gan1.

Literature: Gafforov (2014), [(28): on dead trunk of *Acer saccharum*, 14 Oct. 2011].

;*Note*: We found this species on decaying *Acer saccharum*, and this is the first report for *Ganoderma adspersum* on *Acer* from Central Asia. We collected *Ganoderma adspersum* only in Northeastern Uzbekistan. Outside of the study area, this species is mainly found in subatlantic or submediterranean regions and usually on trees such as *Tilia*, *Quercus*, *Fagus*, *Platanus*, and *Aesculus*.

Ganoderma applanatum (Pers.) Pat., Hyménomyc. Eur. (Paris): 143 (1887)

Specimen examined: (23): on *Juglans regia*, 18 Aug. 2016, YG-B06.

Literature: Panfilova and Gaponenko (1963); Khalikova (1989), [(49): on stump of *Juglans regia*]; Schwartzman (1964), [(49): on dried stem of angiosperm woody plants], Akhmedova (1966), [(49): on *Populus* sp.]; Baltaeva (1992), [(1): on deadwood stem and stumps of deciduous trees]; Baltaeva, 1993 [(45): on dead fallen trunk of *Populus* sp., 16 Jul. 1986]; Iminova (2009), [(14): on various angiosperm trunks, Sept. 2002].

Note: This species is widespread in the study area and causes root rot disease of walnut trees.

Ganoderma lucidum (Curtis) P. Karst., Revue mycol., Toulouse 3(no. 9): 17 (1881)

Literature: Panfilova and Gaponenko (1963); Schwartzman (1964); Khalikova (1989), [(49): on various deciduous wood]; Baltaeva (1992, 1993), [(49): on stump of deciduous wood, 13 Aug. 1989; (45): on living *Quercus* sp., 14 Aug. 1987; (19): on *Quercus* sp., 29 Jul. 1988; (19): on *Ulmus* sp., 2 Aug. 1988; (8): on stump of deciduous wood, 14 Aug. 1988; (6): on various deciduous woody plants, 9 Aug. 1989]; Iminova (2009), [(14): on trunks of angiosperm wood, 2000–2002].

#•***Ganoderma resinaceum*** Boud., in Patouillard, Bull. Soc. mycol. Fr. 5(2,3): 72 (1889)

Specimen examined: (8): on living stem of *Salix* sp., 7 Sept. 2016, YG-X4.

Meripilaceae Jülich

Grifola frondosa (Dicks.) Gray, Nat. Arr. Brit. Pl. (London) 1: 643 (1821)

≡ *Polyporus frondosus* (Dicks.) Fr.

Literature: Iminova (2009), (as *Polyporus frondosus*, (3): on living *Juglans regia*, Jun. 2002, Jul. 2003).

Family placement uncertain (incertae sedis)

*•***Phlebiella christiansenii*** (Parmasto) K.H. Larss. and Hjortstam, in Hjortstam and Larsson, Mycotaxon 29: 316 (1987)

Specimens examined: (28): on fallen woody plant branch, 2 Sept. 2013, YG-G4; (28): on *Gleditsia triacanthos* L., 2 Sept. 2013, YG-G22; (28): on stem of fallen angiosperm tree, 2 Sept. 2013, YG-G26; (28): on dried stump of deciduous tree, 3 Sept. 2013, YG-G36; (38): on stump of *Juglans regia*, 3 Sept. 2013, YG-G040.

HYMENOCHAETALES Oberw.

Hymenochaetaceae Imazeki and Toki

Fomitiporia hippophaeicola (H. Jahn) Fiasson and Niemelä, Karstenia 24(1): 25 (1984)

≡ *Phellinus hippophaeicola* H. Jahn

Literature: Baltaeva (1992, 1993), (as *Phellinus hippophaeicola*, (49): on *Elaeagnus rhamnoides* (L.) A. Nelson, 26 Apr. 1989; (45): on *Elaeagnus rhamnoides*, 3 Sept. 1989; (21): on *Elaeagnus rhamnoides*, 3 Oct. 1989).

Fomitiporia punctata (P. Karst.) Murrill, Lloydia 10: 254 (1947)

≡ *Phellinus punctatus* (P. Karst.) Pilát

Literature: Baltaeva (1992, 1993), (as *Phellinus punctatus*, (49): on *Ulmus* sp., 12 May 1988; (45): on *Crataegus* sp., 7 Aug. 1989; (45): on *Populus* sp., 21 Mar. 1987; (9): on *Populus* sp., 16 Apr. 1987; (21): on *Populus* sp., 9 Jul. 1987; (8): on *Ulmus* sp., 14 Aug. 1987; (8): on *Betula* sp., 21 Jul. 1989; (7): on *Ulmus* sp., 14 Aug. 1987; (19): on *Crataegus azarolus var. pontica* (K.Koch) K.I.Chr., 17 Apr. 1988).

Fomitiporia robusta (P. Karst.) Fiasson and Niemelä, Karstenia 24(1): 25 (1984)

≡ *Phellinus robustus* (P. Karst.) Bourdot and Galzin

Literature: Panfilova and Gaponenko (1963); Khalikova (1989), (as *Phellinus robustus*, (49): on strums of *Spiraea* sp.); Baltaeva (1992, 1993), (as *Phellinus robustus*, (45): on stump of *Pistacia* sp., 7 Apr. 198; (20): on *Castanea* sp., 4 Mar. 1988; (19): on *Quercus* sp., 14 Mar. 1987; (21): on stem of *Quercus* sp., 24 Apr. 1987; (49): on *Populus* sp., 19 Aug. 1988; (8): on *Castanea* sp., 19 May 1987; (7): on *Juglans regia*, 30 Apr. 1988); Iminova (2009), (as *Phellinus robustus*, (16): on stem of *Ìorus alba*, Apr. 2001).

Fulvifomes rimosus (Berk.) Fiasson and Niemelä, Karstenia 24(1): 26 (1984)

≡ *Phellinus rimosus* (Berk.) Pilát

Literature: Panfilova and Gaponenko (1963), (as *Phellinus rimosus*, (49): on trunk of *Pistacia vera*, 1963); Baltaeva (1992, 1993), (as *Phellinus rimosus*, (9): on *Quercus* trunk, 6 Jul. 1985; (21): on *Quercus*, 12 Jul. 1985; (19): on *Quercus* sp., 30 Jul. 1985; (45): on dried trunk of *Salix* sp., 25 Apr. 1986; (7): on *Salix* sp., 6 Jul. 1987; (8): on *Populus* sp., 19 Aug. 1989; (19): on *Populus* sp., 10 Apr. 1989).

Fuscoporia contigua (Pers.) G. Cunn., Bull. N.Z. Dept. Sci. Industr. Res., Pl. Dis. Div. 73: 4 (1948)

≡ *Phellinus contiguus* (Pers.) Pat.

Literature: Baltaeva (1992, 1993), (as *Phellinus contiguus*, (21): on stem of *Elaeagnus rhamnoides*, 19 Sept. 1986; (45): on fallen *Acacia* trunk, 27 Aug. 1987, 6 Sept. 1987; (19): on stem of *Alnus* sp., 23 Sept. 1987; (7): on *Alnus* sp., 16 Aug. 1988; (8): on dried stem of *Ulmus* sp., 19 Sept. 1988; (9): on *Ulmus* sp., 30 Aug. 1989).

Fuscoporia torulosa (Pers.) T. Wagner and M. Fisch., Mycol. Res. 105(7): 780 (2001)

≡ *Phellinus torulosus* (Pers.) Bourdot and Galzin

Literature: Khalikova (1989), (as *Phellinus torulosus* (Pers.) Bourdot and Galzin, (28): on living and died stems of *Quercus* sp., Jun.1986, Sept. 1987); Iminova (2009), (as *Phellinus torulosus*, (3): on *Betula tianschanica* Rupr., on *Salix babylonica* L., on *Pyrus communis* L., on *Morus nigra* L., Sept.–Oct. 1999–2003).

Inocutis tamaricis (Pat.) Fiasson and Niemelä, Karstenia 24(1): 25 (1984)

≡ *Inonotus tamaricis* (Pat.) Maire

Literature: Gaponenko (1965); Sinadskiy and Bodartseva (1956), (as *Inonotus tamaricis*, (10): on living stem of *Tamarix hispida* Willd.); Baltaeva (1992, 1993), (as *Inonotus tamaricis*, (9): on *Tamarix ramosissima* Ledeb., 27 Aug. 1989; (9): on *Tamarix* sp., 24 Sept. 1986; (26): on *Tamarix* sp., 6 May 1987; (21): on stem of living *Tamarix hispida*, 31 Sept. 1987; (10): on dried stem of *Tamarix hispida*, 18 Mar. 1988).

Inonotus andersonii (Ellis and Everh.) Černý, Česká Mykol. 17(1): 1 (1963)

Literature: Baltaeva (1992, 1993), [(45): on trunk of *Quercus* sp., 14 Aug. 1988, 2 Sept. 1989; (19): on stump of *Quercus* sp., 16 Sept. 1988].

Inonotus cuticularis (Bull.) P. Karst., Meddn Soc. Fauna Flora fenn. 5: 39 (1879)

Literature: Baltaeva (1992), [(19): on *Juglans regia*, 10 Jul. 1990].

•***Inonotus hispidus*** (Bull.) P. Karst., Meddn Soc. Fauna Flora fenn. 5: 39 (1879)

Specimens examined: (40): on stem of living *Juglans regia*, 26 May 2011, YG054; (38): on *Juglans regia*, 6 Jun. 2011, YG035; (38): on stem of *Juglans regia*, 11 Jun. 2014, YG/UG1; (37): on living *Pinus* sp., 19 Jun. 2014, YG/PS156; (37): on trunk of living *Pinus* sp., 19 Jun. 2014, YG/PS157; (37): on *Malus sieversii*, 14 Sept. 2014, YG/PS148; (39): on living *Juglans regia*, 9 Sept. 2016, YG1015; (22): on *Juglans regia*, 11 Aug. 2015, YG-B07; (28): on dried trunk angiosperm wood, 27 Sept. 2014, YG/bot1; (29): on living *Morus alba* stem, 17 Sept. 2015, YG/AG1; (23): on living stem of *Juglans regia*, 15 May 2016, YG-B08;

(41): on a wood of *Juglans regia*, 22 Apr. 1982, E. Parmasto, TAAM207844; (17): on a wood of *Morus alba*, 8 May 1976, K. Kalamees, TAAM080947.

Literature: Panfilova and Gaponenko (1963); Akhmedova (1966); Khalikova (1989); Baltaeva (1992, 1993); Iminova (2009), [(1): on living trunks of deciduous woody plants: *Malus domestica* Borkh., *M. sieversii* (Ledeb.) M.Roem., *Morus alba*, *Juglans regia*, *Prunus avium* (L.) L.].

Inonotus obliquus (Fr.) Pilát, Atlas Champ. l'Europe, III, Polyporaceae (Praha) 1: 572 (1942)

Specimens examined: (28): unknown angiosperm fallen trunk, 14 Oct. 2011, YG001.

Literature: Baltaeva (1992, 1993), [(45): on living *Betula* sp., 28 Aug. 1987; (19): on stump of *Fraxinus* sp., 21 May 1986; (7): on *Alnus* sp., 9 Jul. 1986; (8): on dried fallen trunk of *Salix* sp., 13 Jun. 1987; (9): on *Salix* sp., 20 Apr. 1988; (3): on *Salix* sp., 29 Jun. 1989].

Inonotus pseudohispidus Kravtzev, Bull. Acad. Sci. Kazakh SSR 98: 128 (1950)

Literature: Sinadskiy and Bodartseva (1956, 1960), (on living trunk of and *Populus pruinosa* Schrenk, *Populus euphratica* Oliv.); Baltaeva (1992, 1993), [(26): on *Populus* sp., 18 Jul. 1988; (9): trunk of *Populus* sp., 9 Aug. 1988; (21): on *Populus alba*, 20 Jul. 1989; (26): on *Populus* sp., 26 Aug. 1989].

Mensularia radiata (Sowerby) Lázaro Ibiza, Revta R. Acad. Cienc. exact. fis. nat. Madr. 14(11): 736 (1916)

≡ *Inonotus radiatus* (Sowerby) P. Karst.

Literature: Baltaeva (1992, 1993), (as *Inonotus radiatus*, (6): on dried branch of *Alnus* tree, 3 Jul. 1986; (7): on stump of angiosperm woody plants, 19 May 1987; (8): on dried trunk and braches of *Ulmus* sp., 17 Jun. 1989; (45): on died trunk of *Quercus* sp., 7 Jul. 1987; (19): on *Quercus* sp., 17 Jun. 1987; (21): on *Ulmus* sp., 20 Aug. 1989).

Phellinidium ferrugineofuscum (P. Karst.) Fiasson and Niemelä, Karstenia 24(1): 26 (1984)

≡ *Phellinus ferrugineofuscus* (P. Karst.) Bourdot and Galzin

Literature: Baltaeva (1992, 1993), (as *Phellinus ferrugineofuscus*, (45): on wood of *Pinus* sp., 15 Sept. 1988; (8): on *Pinus* sp., 24 Oct. 1988); (20): on stump of *Picea* sp., 6 Nov. 1987; (19): on *Picea* sp., 28 Oct. 1987).

Phellinopsis conchata (Pers.) Y.C. Dai, Fungal Diversity 45: 309 (2010)

≡ *Phellinus conchatus* (Pers.) Quél.

Literature: Baltaeva (1992, 1993), (as *Phellinus conchatus*, (45): on dried stump *Syringa* sp., 10 Sept. 1988; (7): on *Populus* sp., 5 Oct. 1988; (6): on *Alnus* sp., 29 Aug. 1989; (21): on *Ulmus* sp., 13 Nov. 1988; (26): on dried stem of *Populus* sp., 21 Oct. 1988; (19): on *Alnus* sp., 8 Sept. 1989; (21): on *Ulmus* sp., 13 Oct. 1988).

*•***Phellinus betulinus*** (Murrill) Parmasto, Folia cryptog. Estonica 43: 41 (2007)

Specimens examined: (50): on a trunk of *Betula tianschanica*, 24 Apr. 1982, E.Parmasto, TAAM104436; (50): on a dead branch of *Betula tianschanica*, 24 Apr. 1982, E.Parmasto, TAAM104285.

Phellinus igniarius (L.) Quél., Enchir. fungi. (Paris): 177 (1886)

Specimen examined: (50): on a trunk of *Salix* sp., 24 Apr. 1982, A.Kollom, TAAM127406.

Literature: Panfilova and Gaponenko (1963); Khalikova (1989), [(41): on live trunk of *Juglans regia*, 1 Jun. 1980, Sept. 1984]; Baltaeva (1992, 1993), [(45): on trunk of *Prunus vulgaris*, 10 Sept. 1988; (21): on trunk of *Prunus* sp., 9 Aug. 1988; (9): on trunk of *Acer* sp., 12 Apr. 1987; (14): on *Acer* sp., 19 Aug. 1987; (8): on *Salix* sp., 6 Apr. 1988; (7): on *Salix* sp., 16 Jul. 1989; (19): on dried trunk of *Salix* sp., 24 Jul. 1988]; Iminova (2009), [(3): on *Juglans regia*, Apr.-May 2000].

Note: This species causes white rot of broad-leaved trees from many genera and is most common on *Alnus*, *Betula*, and *Corylus* spp. (all Betulaceae) and *Salix* spp. (Salicaceae), also fairly common on *Acer* (Sapindaceae) and *Malus*, *Prunus*, and *Sorbus* spp. (all Rosaceae), more rarely on *Aesculus, Amelanchier, Carpinus, Carya, Castanea, Cratageus, Fraxinus, Hippophae, Hydrangea, Juglans, Laburnum, Morus, Populus, Pterocarya, Robinia, Pyrus, Syringa, Tilia*, and *Ulmus*. Since this species is defined both in a wide and in a narrow sense, the lists of hosts should be interpreted with care.

•***Phellinus pomaceus*** (Pers.) Maire, Mus. barcin. Scient. nat. Op., Ser. Bot. 15: 37 (1933)

= *Phellinus tuberculosus* Niemelä

Specimens examined: (33): on a living trunk of *Prunus* sp., 26 Apr. 1982, E. Parmasto, TAAM104413; (35): on *Prunus cerasifera* Ehrh., 31 Aug. 1963, A. Raitviir, TAAM043492; (33): on a fallen trunk of *Prunus* sp., 23 Apr. 1982, A. Kollom, TAAM127401; (41): on the base living fruit trees, 26 Apr. 1982, E. Parmasto, TAAM104434; (50): on a trunk of *Prunus mahaleb*, 24 Apr. 1982, A. Kollom, TAAM127411; (50): on a dry trunk of *Prunus erythrocarpa* (Nevski) Gilli, 24 Apr. 1982, A. Kollom, TAAM203618; (50): on a trunk of *Salix* sp., 24 Sept. 2014, YG/S1; (38): on *Prunus cerasifera*, 1 Jun. 2011, YG052; (38): on *Prunus* sp., 11 Sept. 2011, YG51-ph; (38): on dried *Prunus* tree, 12 Sept. 2014, YG/Ug01; (38): on living *Prunus* sp., 12 Sept. 2014, YG/Ug02; (39): on dried stem of *Prunus dulcis* (Mill.) D.A.Webb, 2 Nov. 2011, YG009; (39): on living stem of *Cerasus tianshanica* Pojark., 2 Nov. 2011, YG028, *ibit* on living stem of *Cerasus tianshanica* Pojark., 20 Sept. 2014, YG/PS3X; (39): on *Prunus cerasifera*, 2 Nov. 2011, YG337; (39): on living trunk of *Prunus cerasifera*, 2 Nov. 2011, YG338; (32): on *Prunus mahaleb*, 15 May 2011, YG28; (32): on dried trunk of *Prunus* sp., 13 Sept. 2014, YG/bil164; (37): on *Prunus* sp., 19 Sept. 2014, YG/PS82; (45): on a dry trunk of *Crataegus altaica* Ledeb., 2 May 1988, I. Parmasto, TAAM126247; (48): on *Lonicera* sp., Sept. 1982, N.I. Gaponenko, TASM582; (8): on dried stem of *Prunus* sp., 9 Sept. 2016, YG1102; (45): on dry branch of *Juglans regia*, 29 Apr. 1988, I. Parmasto, TAAM126253; (45): on dry trunk of *Celtis australis* subsp. *caucasica*, 1 May 1988, I. Parmasto, TAAM126269. In TAAM two specimens reported as *Phellinus* sp.

Literature: Panfilova and Gaponenko (1963); Khalikova (1989), (as *Phellinus tuberculosus*, (49): on trunks of Rosaceae family trees); Baltaeva (1992, 1993), (as *Phellinus tuberculosis*, (49): on *Prunus* spp., 10 May 1987; (45): on *Malus domestica*, 13 May 1987; (8): on *Malus* sp., 16 May 1989; (19): on *Prunus* sp., 26 May 1987); Iminova (2009), (as *Phellinus pomaceus*, (2): on *Prunus persica* (L.) Batsch, Apr. 2004); Iminova (2009), (as

Phellinus tuberculosis, (15): on living stem of *Cydonia oblonga* Mill., May 2003; (2): on trunk of living *Prunus domestica* L. and on *Malus domestica*, May–Aug. 2002).

Note: First report of this species is on *Celtis australis* subsp. *caucasica* and *Lonicera* sp. from Uzbekistan. Usually it is largely confined to trees belonging to the Rosaceae, chiefly on *Prunus* and rarely on *Malus*, *Pyrus*, and *Cydonia*, and causes white rot of the heartwood of living fruit trees. This species is widespread in the northern hemisphere and probably occurs wherever native species of *Prunus* from the stone fruit group and where peaches, cherries, and plums are cultivated as fruit trees. This species is also reported on *Acer*, *Alnus*, *Carpinus*, *Ceratonia*, *Cornus*, *Corylus*, *Crataegus*, *Fagus*, *Ficus*, *Juglans*, *Malus, Olea, Pyrus, Salix*, and *Ulmus*.

Phellinus tremulae (Bondartsev) Bondartsev and P.N. Borisov, Trut. Grib Evrop. Chasti SSSR Kavkaza [Bracket Fungi Europ. U.S.S.R. Caucasus] (Moscow-Leningrad): 358 (1953)

Literature: Baltaeva (1992, 1993), [(45): on trunk of *Populus tremula*, 20 Jul. 1985; (19): on *Populus tremula*, 16 Aug. 1985; (21): on *Populus tremula*, 10 Aug. 1986; (7): on *Populus* sp., 25 Aug. 1986; (26): on dried fallen of *Populus tremula*, 19 Aug. 1987; (6): on living of *Populus* sp., 8 Aug. 1988]; Khalikova (1989), [(49): on live trunk of *Populus* sp., 20 Jul. 1985].

Phylloporia ampelina (Bondartsev and Singer) Bondartseva, Mikol. Fitopatol. 17(4): 279 (1983)

≡ *Phellinus ampelinus* Bondartsev and Singer

Literature: Bondarceva and Parmasto (1986), (as *Phellinus ampelinus*, (49): on dead and live trunk of *Vitis vinifera* L.).

Phylloporia ephedrae* (Woron.) Parmasto, Proc. Indian Acad. Sci., Pl. Sci. 94(2–3): 377 (1985)

Specimens examined: (45): on stem of living *Ephedra equisetina* Bunge, 1 May 1988, I. Parmasto, TAAM126265; (45): on *Ephedra equisetina*, 2 May 1988, I. Parmasto, TAAM126279; (45): on stem of *Ephedra equisetina*, 1 May 1988, A. Kollom, TAAM127593.

Phylloporia yuchengii Gafforov, Tomšovský, Langer and L.W. Zhou, Cryptog. Mycol. 35(4): 318 (2015) [2014]

Specimens examined: (38): on trunk of *Juglans regia*, 1 Jun. 2011, YG043; (40): on *Prunus* sp., 11 Sept. 2011, YG343; (45): on a trunk of *Juglans regia*, 29 Apr. 1988, I. Parmasto, TAAM126260, in TAAM as *Phellinus* sp.; (7): on trunk of *Crataegus pseudoheterophylla* subsp. *turkestanica*, 11 Sept. 2015, YG1093; (39): on *Crataegus* sp., 9 Oct. 2016, YG1011; (8): on fallen unknown woody branches, 9 Sept. 2016, YG1101; (20): on trunk of *Populus* sp., 12 Jun. 2013, YG-J5; (20): on *Morus alba*, 13 Jun. 2013, YG-J10; (20): on *Morus alba*, 13 Jun. 2013, YG-J11.

Literature: Gafforov et al. (2014), [(38): on dead angiosperm trunk and stem, 1 Jun. 2011; (39): on dead angiosperm trunk, 2 Nov. 2011].

Note: This species was first described from northeastern Uzbekistan in 2014. Later, we collected this species in central and south Uzbekistan. It seems that this species is widespread in the study area. This species grows on *Crataegus*, *Juglans*, *Morus*, *Populus*, and *Prunus*, which represent four plant families.

Porodaedalea pini (Brot.) Murrill, Bull. Torrey bot. Club 32(7): 367 (1905)

≡ *Phellinus pini* (Brot.) Pilát

Literature: Baltaeva (1992, 1993), (as *Phellinus pini*, (1): on trunks and stumps of conifer tees); Khalikova (1989), (as *Phellinus pini*, (28): on live trunk of *Pinus pallasiana* D. Don, Oct. 1984); Iminova (2009), (as *Phellinus pini*, (13): on dried stem of angiosperm, May 2003).

•***Sanghuangporus lonicerinus*** (Bondartsev) Sheng H. Wu, L.W. Zhou and Y.C. Dai, in Zhou, Vlasák, Decock, Assefa, Stenlid, Abate, Wu and Dai, Fungal Diversity 77: 340 (2015)

≡ *Phellinus lonicerinus* (Bondartsev) Bondartsev and Singer

Specimens examined: (49): on dried stem of *Lonicera* sp., 8 Nov. 2016, YG1095; (36): on *Lonicera* sp., 8 Nov. 2016, YG1096; (32): on stem of living *Lonicera nummulariifolia* Jaub. and Spach, 15 May 2011, YG018; (41): on the base of a living trunk of *Lonicera* sp., 22 Apr. 1982, E. Parmasto, TAAM203688; (36): on a trunk of *Lonicera* sp., 25 Apr. 1982, E. Parmasto, TAAM104407; (36): on the base of a living trunk of *Lonicera* sp., 25 Apr. 1982, E. Parmasto, TAAM104439; (50): on at the base of *Lonicera* sp., 24 Apr. 1982, E. Parmasto, TAAM0104264; (50): on a dry trunk of *Lonicera* sp., 24 Apr. 1982, A. Kollom, TAAM127410; (39): on *Lonicera* sp., 9 Oct. 2016, YG1012; (50): on *Lonicera nummulariifolia*, 9 Oct. 2016, YG1013; (38): on *Lonicera* sp., 9 Sept. 2016, YG1016; (37): 19 Jun. 2014, on living stem of *Lonicera* sp., YG/PS92; (37): 20 Jun. 2014, dried stem of *Lonicera* sp., YG/PS129; (37): on *Acer* sp., 20 Jun. 2014; (30): on living stem of *Acer tataricum* subsp. *semenovii*, 5 May 2014, YG/Un1; (46): on a dry trunk of deciduous trunk, 29 Apr. 1988, A. Kollom, TAAM127578; (7): on *Lonicera* sp., 11 Sept. 2016, YG1094; (8): on *Lonicera* sp., 26 May 2018, YG1097; (8): on living stem of *Lonicera microphylla* Willd. ex Schult., 26 May 2018, YG1112.

Literature: Panfilova and Gaponenko (1963); Khalikova (1989); Iminova (2009), (*Phellinus lonicerinus*, (1): on *Lonicera* spp.).

Note: This species was thought to grow exclusively on *Lonicera*, but a new host *Acer tataricum* subsp. *semenovii* is recorded here from Uzbekistan.

Tropicoporus linteus (Berk. and M.A. Curtis) L.W. Zhou and Y.C. Dai, in Zhou, Vlasák, Decock, Assefa, Stenlid, Abate, Wu and Dai, Fungal Diversity 77: 344 (2015)

≡ *Phellinus linteus* (Berk. and M.A. Curtis) Teng

Specimen examined: (42): on dry branch of *Rosa fedtschenkoana* Regel, 21 Apr. 1982, E. Parmasto, TAAM104272 (as *Phellinus* sp. in TAAM).

Literature: Panfilova and Gaponenko (1963); Khalikova (1989), (as *Phellinus linteus*, (49): on dead and living trunk and stem of angiosperm woody plants); Baltaeva (1992, 1993), (as *Phellinus linteus*, (49): on *Salix* sp., 16 Aug. 1985, (45): on living trunk of *Lonicera* sp., 9 Apr. 1985; (21): on *Quercus* sp., 12 Sept. 1986; (7): on *Populus* sp., 5 May 1987; (8): on *Acer* sp., 4 Sept. 1989; (19): on *Ulmus* sp., 27 Aug. 1987); Iminova (2009), (as *Phellinus linteus*, (3): on *Salix wilhelmsiana*, Apr. 2000, May 2003).

Neoantrodiellaceae Y.C. Dai, B.K. Cui, Jia J. Chen and H.S. Yuan

¤•***Neoantrodiella*** sp.

Specimen examined: (33): on trunk of *Juniperus polycarpos* var. *seravschanica*, 22 Apr. 1982, E. Parmasto, TAAM104307.

Oxyporaceae Zmitr. and Malysheva

Rigidoporus corticola (Fr.) Pouzar, Folia geobot. phytotax. bohemoslov. 1(4): 368 (1966)

≡ *Oxyporus corticola* (Fr.) Ryvarden

Specimens examined: (49): on fallen trunk, 22 Sept. 2014, YG-P55, *ibit*., YG-P67; (49): on dried branch of angiosperm, 23 Sept. 2014, YG-P35.

Literature: Baltaeva (1992, 1993), (as *Oxyporus corticola*, (21): on stump of *Quercus* sp., 6 May, 1985; (21): on *Fraxinus* sp., 12 Aug. 1988; (45): on stem of *Fraxinus* sp., 6 May 1988; (20): on dried stem of living *Salix alba*, 29 Aug. 1989; (19): on dead trunk of *Populus* sp., 15 Apr. 1987; (9): on *Populus* sp., 30 Jul. 1987; (7): on *Populus tremula*, 19 Oct. 1987).

Rigidoporus latemarginatus (Durieu and Mont.) Pouzar, Folia geobot. phytotax. bohemoslov. 1(4): 368 (1966)

≡ *Oxyporus latemarginatus* (Durieu and Mont.) Donk

= *Chaetoporus ambiguus* (Bres.) Bondartsev and Singer

Literature: Baltaeva (1992), (as *Oxyporus latemarginatus*, (28): on stump of *Pyrus* sp., 16 Sept. 1990), Sinadskiy and Bodartseva, 1960 (as *Chaetoporus ambiguus*, (27): on *Elaeagnus rhamnoides*, Jun. 1960).

Rigidoporus populinus (Schumach.) Pouzar, Folia geobot. phytotax. bohemoslov. 1(4): 368 (1966)

≡ *Oxyporus populinus* (Schumach.) Donk

Literature: Panfilova and Gaponenko (1963), (as *Oxyporus populinus*, 49: on dead stem of *Acer tataricum* L.), Khalikova (1989), (as *Oxyporus populinus*, (49): on fallen branch and stem *Populus* sp., May 1987; on *Quercus* sp., Jun. 1988); Baltaeva (1992, 1993), (as *Oxyporus populinus*, (1): on dried stem of living *Sorbus* sp.).

●*****Rigidoporus ginkgonis*** (Y.C. Dai) F. Wu, Jia J. Chen and Y.C. Dai, in Wu, Chen, Ji, Vlasák and Dai, Mycologia 109(5): 761 (2017)

Specimens examined: (28): on fallen trunk and stump of deciduous woody plants, 2 Sept. 2013, YG-G2, *ibid*. on fallen trunk of deciduous woody plants, YG-G3; (28): on decaying branch of angiosperm, 3 Sept. 2013, YG-G35.

Schizoporaceae Jülich

Hyphodontia alutaria (Burt) J. Erikss., Symb. bot. upsal. 16(no. 1): 104 (1958)

Literature: Gafforov et al. (2017), [(28): on twigs and stem of *Pterocarya pterocarpa* Kunth ex I. Iljinsk, 2 Sept. 2013].

#***Hyphodontia arguta*** (Fr.) J. Erikss., Symb. bot. upsal. 16(no. 1): 104 (1958)

Specimen examined: (49): on fallen tree, 21 Oct. 2015, YG-X66.

●***Hyphodontia zhixiangii*** L.W. Zhou and Gafforov, Phytotaxa 299(2): 275 (2017)

Specimens examined: (8): on unknown angiosperm branch, 9 Sept. 2016, YG1098; (49): on fallen angiosperm branches, 7 Oct. 2016, YG1104.

Literature: Kan et al., 2017 [(8): on stem of *Juniperus* sp., 9 Sept. 2016].

Lyomyces crustosus (Pers.) P. Karst., Revue mycol., Toulouse 3(no. 9): 23 (1881)

Literature: Gafforov et al. (2017), [(38): on branch of living tree *Fraxinus pennsylvanica* Marshall, 3 Sept. 2013].

●***Lyomyces erastii*** (Saaren. and Kotir.) Hjortstam and Ryvarden, Syn. Fung. (Oslo) 26: 43 (2009)

Specimen examined: (15): on unknown shrub, 12 Jul. 2017, RM21.

Literature: Gafforov et al. (2017), [(39): on deciduous wood, 2 Nov. 2011].

Lyomyces sambuci (Pers.) P. Karst., Bidr. Känn. Finl. Nat. Folk 37: 153 (1882)

Literature: Gafforov et al. (2017), [(28): on dead wood of *Philadelphus* sp., 20 Apr. 1982; (39): on a dead branch of angiosperm, 2 Sept. 2013].

Xylodon paradoxus (Schrad.) Chevall., Fl. gén. env. Paris (Paris) 1: 274 (1826)

≡ *Schizopora paradoxa* (Schrad.) Donk

Literature: Baltaeva (1992, 1993), (as *Schizopora paradoxa*, (49): on trunks of *Quercus* sp., 20 Aug. 1989; (45): on trunk of *Quercus* sp., 7 Oct. 1988; (8): on *Quercus* sp., 19 Nov. 1989).

Taxa with uncertain position at the family level (incertae sedis)

Sidera lenis (P. Karst.) Miettinen, in Miettinen and Larsson, Mycol. Progr. 10(2): 136 (2011)

≡ *Diplomitoporus lenis* (P. Karst.) Gilb. and Ryvarden

≡ *Antrodia lenis* (P. Karst.) Ryvarden

Literature: Baltaeva (1992), (as *Diplomitoporus lenis*), Baltaeva, 1993 (as *Antrodia lenis*, (45): on trunk of *Pinus* sp., 8 Jul. 1988; (8): on *Pinus* sp., 6 Jul. 1989; (19): on wet of trunk of *Picea* sp., 27 Aug. 1989; (19): on *Picea* sp., 14 Jul. 1987); Khalikova (1989), (as *Antrodia lenis*, (49): on living *Juniperus* tree, 17 Jul. 1988).

Trichaptum abietinum (Pers.) Ryvarden, Norw. Jl Bot. 19: 237 (1972)

Literature: Baltaeva (1992, 1993), [(45): on wet trunk of *Pinus* sp., 12 Mar. 1988; (7): on stump of *Pinus* sp., 15 Aug. 1988; (19): on *Pinus* sp., 9 Jul. 1989].

Trichaptum biforme (Fr.) Ryvarden, Norw. Jl Bot. 19(3–4): 237 (1972)

= *Hirschioporus pergamenus* (Fr.) Bondartsev and Singer

Literature: Panfilova and Gaponenko (1963), (as *Hirschioporus pergamenus*, (49): on dried woody plants); Khalikova (1989), [(49): on dead trunk of angiosperms tree]; Baltaeva (1992, 1993), [(45): on fallen stem of *Populus* sp., 18 Jul. 1988; (26): on *Salix* sp., 18 Jul. 1988; 9: on dead trunk of *Populus* sp., 7 Sept. 1987; (21): on *Salix* sp., 15 Sept. 1987].

Trichaptum fuscoviolaceum (Ehrenb.) Ryvarden, Norw. Jl Bot. 19: 237 (1972)

Specimen examined: (49): on a fallen trunk of *Abies sibirica* Ledeb., 29 Aug. 1958, E. Parmasto, TAAM009360.

Literature: Baltaeva (1992), [(45): on stump of *Pinus* sp., 17 Aug. 1990].

Note: This species is reported for the first time on *Abies sibirica* from Uzbekistan.

RUSSULALES Kreisel ex P.M.Kirk, P.F.Cannon and J.C.David

Bondarzewiaceae Kotl. and Pouzar

Heterobasidion annosum (Fr.) Bref., Unters. Gesammtgeb. Mykol. (Liepzig) (8): 154 (1888)

Literature: Baltaeva (1992, 1993), [(49): on *Picea* sp., 10 Sept. 1988, 30 Jul. 1989; (45): on root of *Biota* sp., 15 Nov. 1987; (19): on stump of *Pinus* sp., 6 Sept. 1988; (7): on *Picea* sp., 10 Sept. 1988].

Lachnocladiaceae D.A. Reid

#***Vararia parmastoi*** Boidin and Lanq., Persoonia 12(3): 257 (1984)

Specimens examined: (50): on decayed trunk of *Juniperus semiglobosa*, 24 Apr. 1982, E. Parmasto, TAAM104302 (Paratype); (50): on dead roots of *Juniperus semiglobosa*, 24 Apr. 1982, E. Parmasto TAAM104303 (Isotype); (50): on a fallen rotten trunk of *Juniperus semiglobosa*, 24 Apr. 1982, E. Parmasto, TAAM104294; (36): on trunk of *Juniperus semiglobosa*, 25 Apr. 1982, E. Parmasto, TAAM104440.

Peniophoraceae Lotsy

Peniophora cinerea* (Pers.) Cooke, Grevillea 8(no. 45): 20 (1879)

Specimens examined: (39): on fallen trunks of angiosperm woody plant, 2 Nov. 2011, YG039; (39): on stem and dried branch of *Juglans regia*, 1 Jun. 2011, YG058.

Peniophora incarnata* (Pers.) P. Karst., Hedwigia 28: 27 (1889)

Specimen examined: (39): on fallen stem of deciduous wood, 16 Jun. 2014, YG/PS84.

Stereaceae Pilát

Stereum gausapatum* (Fr.) Fr., Hymenomyc. eur. (Upsaliae): 638 (1874)

Specimen examined: (49): on trunk of *Picea schrenkiana* Fisch. and C.A.Mey., 7 Sept. 2013, YG-Gxx.

Note: This species occurs on *Quercus*, *Castanea*, and *Carpinus* species in Europe, particularly in the Mediterranean area. Fruiting bodies develop on dead stems, rotten stumps, trunks, or more rarely on fallen branches and other debris of angiosperm woody plants. However, we found that species on the conifer tree, *Picea schrenkiana* from Western Tien Shan Mountains of Uzbekistan.

Stereum hirsutum (Willd.) Pers., Observ. mycol. (Lipsiae) 2: 90 (1800) [1799]

Specimens examined: (33): on deciduous tree trunk, 23 Apr. 1982, E. Parmasto, TAAM104393; (43): on unknown woody branch, 8 Sept. 2016, YG1091; (43): on fallen trunk of angiosperm wood, 8 Sept. 2016, YG1092; (40): on dried stem of *Juglans regia*, 26 May 2011, YG029; (46): on *Crataegus* sp., 13 May 1990, K. Kalamees and M. Vaasma, TAAM144492; (32): on *Acer tataricum* subsp. *semenovii*, 15 May 2011, YG030; (32): on *Acer* sp., 15 May 2011, YG51; (32): on unknown decaying wood, 15 May 2011 YG056; (32): on *Acer tataricum* subsp. *semenovii*, 15 May 2011, YG057; (32): on unknown dried wood, 7 Jun. 2011 YG048; (39): on stem of living *Salix iliensis* Regel, 2 Nov. 2011, YG034; (38): on *Juglans regia*, 1 Jun. 2011, YG109; (38): on dried stem of *Fraxinus excelsior* L., 3 Sept. 2013, YG-G12; (38): on *Quercus* sp., 3 Sept. 2013, YG-G15; (38): on dried stem of *Salix alba*, 3 Sept. 2013, YG320; (37): on living stem of *Juglans regia*, 19 Jun. 2014, YG/PS135; (37): on dried trunk of *Juglans regia*, 19 Jun. 2014, YG/PS176; (45): on a dry trunk of *Celtis australis* subsp. *caucasica*, 29 Apr. 1989, TAAM126246; (45): on *Crataegus pseudoheterophylla* subsp. *turkestanica*, 29 Apr. 1988, I. Parmasto, TAAM126255; (45): on trunk of *Quercus* sp., 29 Apr. 1988, A. Kollom, TAAM127585; (46): on trunk of *Populus alba*, 4 May 1988, I. Parmasto, TAAM126291 (as *Coriolopsis* sp.); (8): on fallen branch, 10 Sept. 2016, YG1099; (28): on dead fallen trunk of angiosperm, 3 Apr. 2013, YG3.04.13.

Literature: Panfilova and Gaponenko (1963), [(30): on *Populus* sp.]; Khalikova (1989), [(28): on dried branch of living *Quercus robur* L.]; Iminova (2009), [(14): on *Salix interior*, Apr. 2002; (3): on *Juglans regia*, May 2005].

Stereum rugosum* Pers., Neues Mag. Bot. 1: 110 (1794)

Specimen examined: (50): on a dead trunk of *Salix* sp., 24 Apr. 1982, TAAM127402

Note: This species is very common and widespread on moist various deciduous and coniferous forests dead trees in the northern hemisphere especially in Europe (Breitenbach and Kränzlin, 1986). It is rarely reported from East and South Asia (Dai, 2011). This is the first report of the species from the mountainous area of Central Asia.

Stereum subtomentosum* Pouzar, Ćeská Mykol. 18(3): 147 (1964)

Specimen examined: (28): on dead trunk of angiosperm, 24 Sept. 2014, YG-P37.

Note: This species is rare in the study area and generally reported in Betulaceae (*Alnus*, *Betula*, *Carpinus*) and Salicaceae (*Populus*, *Salix*) plant species from Europe. It is easily distinguished when fresh by the distinct yellowish exudate when cut. It is similar to *Stereum ostrea*, which, however, has a tropical or subtropical distribution and is distinguished by its oyster-like fruitbody and more brownish color.

THELEPHORALES Corner ex Oberw.

Bankeraceae Donk

Phellodon fuligineoalbus (J.C. Schmidt) R.E. Baird, in Baird, Wallace, Baker and Scruggs, Fungal Diversity 62: 63 (2013)

≡ *Bankera fuligineoalba* (J.C. Schmidt) Coker and Beers.

Literature: Schwartzman (1964), (as *Bankera fuligineoalba* (49): on *Salix caprea* L., and on *Betula pendula*).

Sarcodon imbricatus (L.) P. Karst., Revue mycol., Toulouse 3(no. 9): 20 (1881)

= *Sarcodon squamosus* (Schaeff.) Quél.

Literature: Schwartzman (1964), (as *Sarcodon squamosus* (49): on old stump of *Populus tremula*).

Thelephoraceae Chevall.

#***Pseudotomentella mucidula*** (P. Karst.) Svrćek, Ćeská Mykol. 12(2): 68 (1958)

Specimen examined: (47): on fallen trunk of *Pinus sibirica* Du Tour, 29 Aug. 1958, TAAM009363.

TRECHISPORALES K.H. Larss.

Hydnodontaceae Jülich

Fibuloporia desertorum (Kravtzev) Schwartzman, Flora Sporovykh Rastenii Kazakhstana [Cryptogamic Flora of Kazakhstan], 4, Auriculariales, Tremellales, Dacryomycetales, Exobasidiales, Aphyllophorales (Alma-Ata): 299 (1964)

≡ *Dextrinosporium desertorum* (Kravtzev) Bondartseva

Literature: Gaponenko (1965), (as *Dextrinosporium desertorum*, (10): on living *Haloxylon persicum*).

AGARICOMYCETES Doweld

order and family uncertain (incertae sedis)

TABLE 3 | Number of host family, genus, and species and number of wood-inhabiting poroid and corticioid species on host family in the study area.

Host family	No. of host genera	No. of host species	No. of fungal species
Salicaceae	2	16	72
Pinaceae	3	8	51
Rosaceae	9	27	48
Fagaceae	2	3	31
Juglandaceae	2	2	30
Betulaceae	2	4	25
Cupressaceae	2	5	16
Sapindaceae	2	6	16
Ulmaceae	1	1	11
Oleaceae	2	5	11
Moraceae	1	2	9
Caprifoliaceae	1	4	8
Cannabaceae	1	1	7
Leguminosae	3	3	6
Anacardiaceae	1	2	3
Platanaceae	1	1	3
Elaeagnaceae	1	1	3
Amaranthaceae	1	2	2
Tamaricaceae	1	3	1
Vitaceae	1	1	1
Ephedraceae	1	1	1
Hydrangeaceae	1	1	1
Malvaceae	1	1	1
Total: 23	42	100	n.a.

*•***Peniophorella praetermissa** (P. Karst.) K.H. Larss., Mycol. Res. 111(2): 192 (2007)

Specimens examined: (38): on living stem of *Juglans regia*, 3 Sept. 2013, YG-G16; (38): on fallen unknown angiosperm branches, 3 Sept. 2013, YG-G40; (28): on dried stump of deciduous tree, 3 Sept. 2013, YG-G37.

Substrate Preferences of Wood-Inhabiting Poroid and Corticioid Species in Uzbekistan

In this study, poroid and corticoid fungal species were found on 100 woody plant species belonging to 23 families and 42 genera. One hundred wood-inhabiting species (accounting for 65.3% of the total wood-inhabiting poroid and corticoid species of Uzbekistan) were recorded exclusively on deciduous wood, 33 species (21.6%) were found exclusively on coniferous wood, and 5 species were recorded as inhabiting both groups of woody plants (**Figure 8**). The hosts were not determined for the remaining 15 species. These wood-inhabiting fungi were most frequently found on hosts belonging to Salicaceae (72 fungal species), Pinaceae (51), Rosaceae (48), Fagaceae (31), Juglandaceae (30), Betulaceae (25), Cupressaceae (16), Sapindaceae (16), and Ulmaceae and Oleaceae (each 11). Collectively, these families host about 70% of fungal species present in the study area; other plant families host one to nine species (**Table 3**).

The highest number of wood-inhabiting poroid and corticoid species is reported in the following host genera: *Populus* (40 species, 26.4% of the total species number), *Quercus* (30, 19.6%), *Juglans*, *Pinus*, and *Salix* (each 29, 18.9%), *Betula* (20, 13.0%), *Picea* (19, 12.4%), *Prunus* (17, 11.15%), *Acer* (14, 9.2%), *Malus* (12, 7.8%), *Juniperus* and *Ulmus* (each 11, 7.1%), *Fraxinus* (10, 6.5%); other plant genera host one to nine fungal species (**Figure 9**).

Among the wood-inhabiting poroid and corticoid fungi, 25 species were associated with a wide range of plant hosts, such as *Phellinus pomaceus* (16 host species), *Stereum hirsutum* (14), *Trametes versicolor* (11), *Lentinus tigrinus* (10), *Cerrena unicolor* (9), *Bjerkandera adusta*, *Schizophyllum commune*, *Trametes hirsuta*, *T. tephroleuca*, and *T. trogii* (8 hosts each); *Coriolopsis gallica*, *Fomes fomentarius*, *Fomitiporia robusta*, *Tropicoporus linteus*, and *Laetiporus sulphureus* (7 each); *Irpex lacteus*, *Phylloporia yuchengii*, *Inonotus hispidus*, and *Cerioporus squamosus* (6 each); and *Fuscoporia torulosa*, *Trametes gibbosa*, *Antrodia xanthan*, *Phellinus igniarus*, *Lenzites warnieri*, and *Rigidoporus corticola* (5 each) (**Figure 10**). The other 128 wood-inhabiting poroid and corticoid fungi studied each grew on one to four host species. Regarding the host preference, some wood-inhabiting poroid and corticoid species are tolerant, such as *Phellinus pomaceus* recorded on 16 plant species of nine genera (*Prunus* sp., *P. mahaleb*, *P. cerasifera*, *P. erythrocarpa*, *P. dulcis*, *P. persica*, *P. domestica*, *Cerasus tianshanica*, *Cydonia oblonga*, *Celtis australis* subsp. *caucasica*, *Crataegus altaica*, *Juglans regia*, *Lonicera* sp., *Malus* sp., *M. domestica*, and *Salix* sp.), followed by *Stereum hirsutum* on 14 species of seven genera (*Juglans regia*, *Acer* sp., *A. tataricum* subsp. *semenovii*, *Salix iliensis*, *S. interior*, *S. alba*, *Fraxinus excelsior*, *Quercus* sp., *Q. robur*, *Celtis australis* subsp. *caucasica*, *Crataegus pseudoheterophylla* subsp. *turkestanica*, *Crataegus* sp., *Populus* sp., and *P. alba*), and *Trametes versicolor* on 11 species of nine genera (*Betula*, *Prunus*, *Crataegus*, *Lonicera*, *Quercus*, *Juglans*, *Populus*, *Malus*, and *Celtis*). Other wood-inhabiting species each colonized 1 to 10 plant species (**Figure 10**).

The Distribution Range and Niches of Wood-Inhabiting Poroid and Corticioid Fungi in Uzbekistan

By importing all known records of wood-inhabiting poroid and corticioid fungi in Uzbekistan into ArcGIS, a distribution GIS map of wood-inhabiting poroid and corticoid species in Uzbekistan was produced (**Figure 11**). The distribution of all records in the whole study area was first mapped (**Figure 11a**), and then five subareas where fungal records are relatively dense were presented (**Figures 11b–f**). Fungal species were most commonly collected in subarea **f** with 445 records in Western Tien Shan Mountains in Tashkent province, followed by subarea **b** with 142 records in Pamir-Alay Mountain in Samarkand, Qashqadaryo, and Surkhandaryo Provinces of Central and Southern Uzbekistan. Subareas **c**, **e**, and **d** have 58, 51, and 46 records, respectively, in Turkestan, Nurata, Kurama, and Fergana

ranges in Pamir Alay and Western Tien Shan Mountains in Navoi, Jizzakh, and Fergana valley of Uzbekistan (**Figures 11c–e**).

Polyporales is the most commonly collected fungal order with 451 records in urban and mountain areas of Uzbekistan. The next most abundant order is Hymenochaetales with 258 records mainly distributed in Tashkent Botanical Garden, Chatkal Biospheric, Nurata, Zarafshan, Surkhan, and Hissar State Reserves in North-eastren and southern Uzbekistan. The orders Russulales (42), Gleophyllales (13), and Agaricales (11) are distributed in coniferous and deciduous mixed forest trees in Ugam, Chatkal, Turkestan, Pskem, Nurata, and Hissar ranges in Pamiy-Alay and Westren Tien Shan Mountains. Other orders with fewer records include Atheliales (4), Thelephorales (4), Cantharellales (1), and Trechisporales (1). In addition, three records have uncertain taxonomic positions at the order level. The most frequently recorded species in Uzbekistan are *Phellinus pomaceus* (34 records); *Stereum hirsutum* (27); *Trametes hirsuta* (25); *T. trogii* (22); *Lentinus tigrinus* (21); *Sanghuangporus lonicerinus* and *Trametes versicolor* (20 each); *Cerrena unicolor*, *Fomes fomentarius*, and *Inonotus hispidus* (17 each); *Bjerkandera adusta* and *Phellinus igniarius* (14 each); *Coriolopsis gallica*, *Fomitopsis betulina*, and *Trametes tephroleuca* (13 each); *Fuscoporia contigua* (12); *Phylloporia yuchengii* and *Tropicoporus linteus* (each 11); *Antrodia xantha*, *Cerioporus squamosus*, *Fomitiporia robusta*, and *Rigidoporus corticola* (each 10); and *Ceriporiopsis gilvescens* (8).

DISCUSSION

In this study, we compiled for the first time the species diversity of wood-inhabiting poroid and corticioid fungi in Uzbekistan. Comprehensive information of these species is provided, including taxonomic diversity, substrate preference, and distribution of geographic and landscape position, on the basis of 790 fungal records collected from 1950 to 2020.

A total of 153 wood-inhabiting poroid and corticioid species, belonging to 10 orders, 26 families, and 97 genera, were confirmed to be present mainly based on literature references, morphological examinations, and also on phylogenetic analysis wherever possible. Of these 153 species, 19 are new for mycobiota to Central Asia and 31 are reported for the first time in Uzbekistan. In addition, four taxa that may be new to science were discovered and must be examined further. The fungal diversity reported here for Uzbekistan is much lower than that in other regions where the diversity of wood-inhabiting poroid and corticoid fungi is well explored. For example, 1210 wood-inhabiting poroid and corticioid species, including ecologically similar hydnoid fungi, are recorded in China (Dai, 2011, 2012). Also, the number of wood-inhabiting poroid fungi recorded is 492 and 394 in North America and Europe, respectively (Ryvarden and Melo, 2014; Zhou et al., 2016). The low species number in Uzbekistan is partly due to the relatively small area, but also due to the lack of systematic field surveys and thorough identification with the aid of molecular sequencing. Few scientists

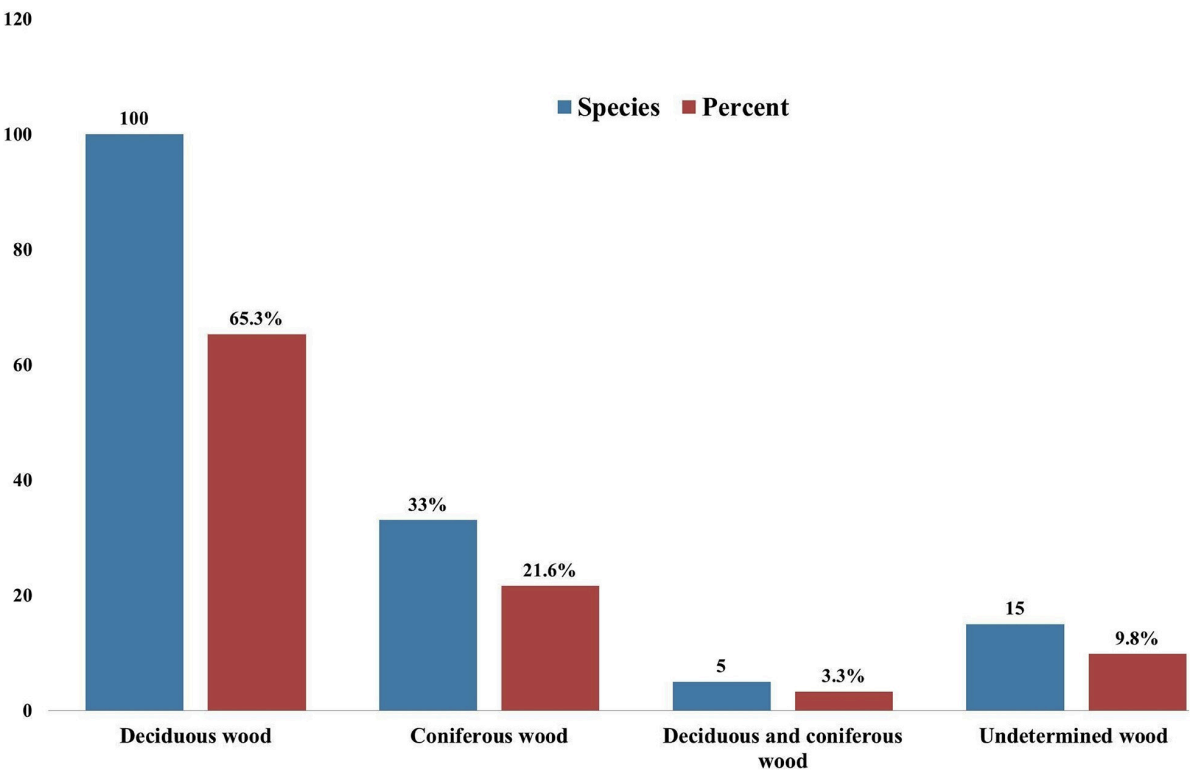


FIGURE 8 | Species richness and proportions of wood-inhabiting poroid and corticioid fungi on different wood types.

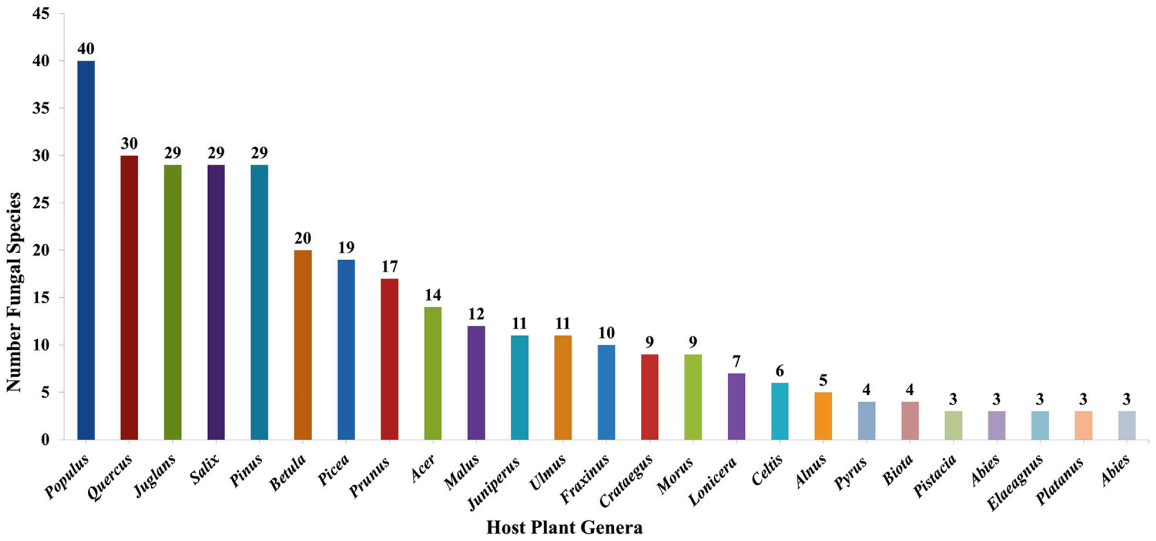


FIGURE 9 | Occurence numbers of wood-inhabiting poroid and corticioid fungi on most representative host genera.

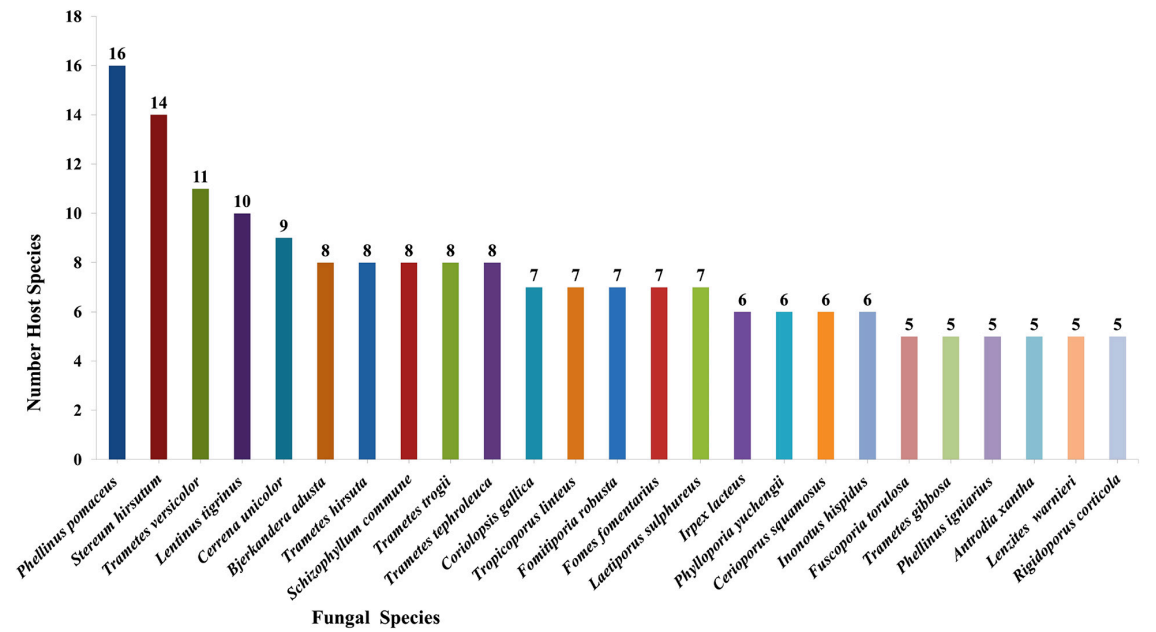


FIGURE 10 | Host species numbers of 25 wood-inhabiting poroid and corticioid species with the widest host range.

study the ecologically important fungi of Uzbekistan. Although this report is the most comprehensive study of diversity of wood-inhabiting poroid and corticiod fungi in Uzbekistan today, it must be considered provisional. In contrast, tens of taxonomists have jointly contributed records of hundreds of (mainly new) wood-inhabiting poroid and corticioid species in China since the publications of Dai (2011, 2012). Therefore, even if we have reported the most comprehensive diversity of wood-inhabiting poroid and corticioid fungi in Uzbekistan to date, the current knowledge has to be considered as a provisional species checklist to be complemented. It is known that higher diversity of plant species results in a higher diversity of associated fungal species (Küffer and Senn-Irlet, 2005; Yamashita et al., 2010; Hawksworth and Lücking, 2017). Uzbekistan, with its mountainous landscape, is characterized by a high diversity of trees and shrubs, perhaps 500–600 species (Eastwood et al., 2009). Therefore, maybe more taxa of wood-inhabiting poroid and corticioid species, including new and even endemic species, still await to be revealed from Uzbekistan (Hyde et al., 2020; Yuan et al., 2020).

Most of the reported wood-inhabiting poroid and corticioid fungi in Uzbekistan are wood decomposers,

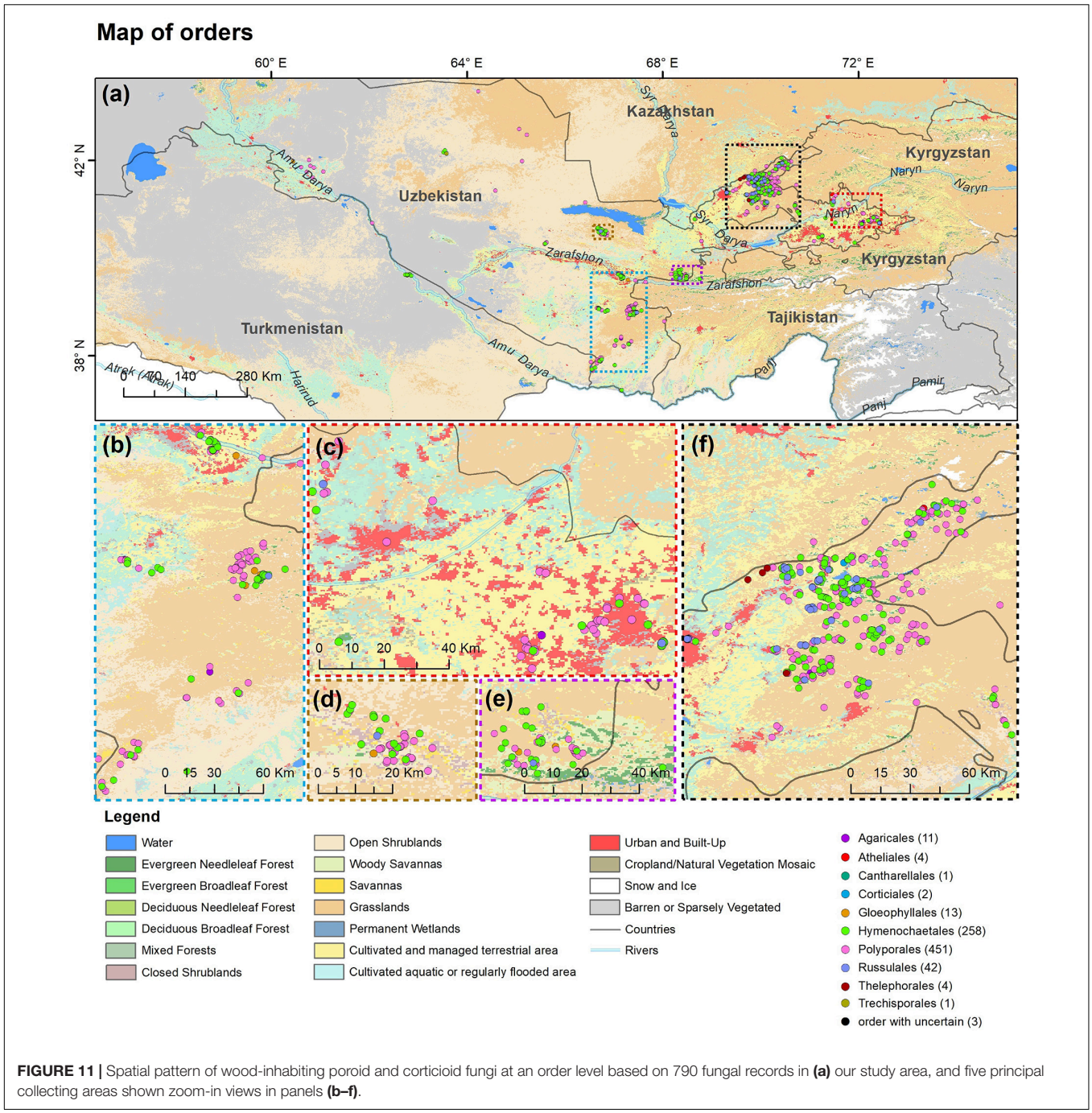


FIGURE 11 | Spatial pattern of wood-inhabiting poroid and corticioid fungi at an order level based on 790 fungal records in **(a)** our study area, and five principal collecting areas shown zoom-in views in panels **(b–f)**.

which release matter and energy to the ecological system. These saprophytic species possess powerful enzymes, which can effectively degrade lignocellulose (Riley et al., 2014). In the current Uzbekistan mycota, several species in *Trametes* are considered to have potential biotechnological applications (Kneževič et al., 2013; Wang and Chen, 2019; Yang et al., 2020).

Although the resource recycling functions are generally considered beneficial to trees, forests, and humans, some of the wood-inhabiting poroid and corticioid fungi studied inhabit living trees as forest pathogens. According to previous studies (Kleyner, 1958; Sinadskiy and Bodartseva, 1960; Panfilova and Gaponenko, 1963; Sinadskiy, 1968; Khalikova, 1989; Baltaeva, 1992; Gafforov, 2014; Gafforov et al., 2014) and our field observations, *Inonotus hispidus*, *Bjerkandera adusta*, *Cerrena unicolor*, *Lentinus tigrinus*, *Fomes fomentarius*, *Laetiporus sulphureus*, *Phylloporia yuchengii* and *Ganoderma applanatum*, *Aurantiporus fissilis*, and some species from the genera *Trametes* and *Phellinus* can cause root rot disease. In addition, moreover, *Cerrena unicolor* also produces a stem canker of living *Acer*

semenovii, *Juglans regia*, *Crataegus pseudoheterophylla* subsp. *Turkestanica*, and *Celtis australis* subsp. *caucasica*. Noteworthily, *Inonotus hispidus* is widespread in the walnut-fruit forests of Uzbekistan and damages up to 4% of the trees of *Juglans regia* and *Malus sieversii* trees in Baysun and Turkestan ranges of Pamir Alay Mountains (unpublished data Gafforov); *Phellinus igniarius* was observed both as a parasite and saprophyte of deciduous trees from the genera *Juglans*, *Salix*, and *Acer* in Ugam-Chatkal Natural State Park and Zaamin and Hissar State Reserve. The forest diseases caused by these wood-inhabiting poroid and corticioid fungi and the corresponding economic loss should be considered by relevant management departments.

In addition, some macrofungi including wood-inhabiting poroid and corticioid species are important edible and medicinal fungi (Wu et al., 2019; Zhou et al., 2020). Some poroid species known from Uzbekistan are recognized as valuable medicinal fungi, while *Grifola frondosa*, *Laetiporus sulphureus*, and *Sarcodon imbricatus* are important edible fungi. Cultivation of wood-inhabiting fungi is an important agricultural industry worldwide, especially in East Asia. Several medicinal and edible species, like *Ganoderma* spp. and *Auricularia* spp. in mainland China, *Taiwanofungus* in Taiwan, China, and *Sanghuangporus* spp. in South Korea, have huge economic value. In China, edible and medicinal fungi are the fifth largest crop industry (Dong et al., 2017). Industrial development of suitable endemic wood-inhabiting poroid and corticioid fungi will undoubtfully benefit the Uzbekistan economy. Uzbekistan materials must be directly studied for utilization of these fungal resources. For this purpose, strains of wood-inhabiting poroid and corticioid fungi firstly need to be isolated and preserved in public organizations.

The proportion of wood-inhabiting poroid and corticioid fungi found on different hosts differs in Uzbekistan from that in comparable temperate and warm temperate forest zones of China (Zhou et al., 2011). Compared with the proportions in temperate and warm temperate forest zone (Zhou et al., 2011), the proportion of wood-inhabiting poroid and corticioid species in Uzbekistan found on deciduous wood (72.46%) is similar, but the proportion on coniferous wood is much higher (23.91%) and that on both groups of wood is much lower (3.62%). The differences in the proportions on coniferous wood and both groups of wood compared to the Chinese case may be either the real status in Uzbekistan or a misleading failure to observe that some species recorded exclusively on coniferous wood do actually occur also on deciduous wood. Many more field surveys are needed to clarify this issue.

Among the 100 woody plant species belonging to 23 families and 42 genera recorded as hosts for wood-inhabiting poroid and corticioid species, Salicaceae, Pinaceae, and Rosaceae are the most favored, and *Populus*, *Quercus*, *Juglans*, and *Salix* are the most favored host genera.

To well understand the spatial patterns of wood-inhabiting poroid and corticioid fungi, their distributions associated with geography and landscapes were visualized using GIS maps (**Figure 11**). Wood-inhabiting poroid and corticioid species in Uzbekistan are distributed mostly in the regions of open shrublands and grasslands, and rarely in various kinds of forests. This distribution pattern is opposite to the natural habitats of such fungi as reported in previous studies. For example, Zhou and Dai (2012) reported that reserved forest with amounts of woody substrates for the growth of wood-inhabiting poroid fungi has significantly higher polypore diversity than unprotected forest. Moreover, normally, forests have higher species diversity of woody plants, which result in higher diversity of wood-inhabiting poroid fungi (Dai et al., 2015). This unusual phenomenon in Uzbekistan might be caused by a lower proportion of field surveys carried out in virginal forests due to difficult access. Therefore, more efforts should be made to reveal the diversity of wood-inhabiting poroid and corticioid fungi in the most primeval forests.

The two fungal orders with highest record diversity, viz., Polyporales and Hymenochaetales, are common in the whole studied area (**Figure 11a**). This reflects that geography and landscape factors do not have significant effects on the distribution of these two fungal orders. These two fungal orders have high species diversity (**Table 2**), resulting from a wide adaption to the environment. Species diversity of these two orders are also highest in other regions of the world (Dai, 2012; Ryvarden and Melo, 2014; Zhou et al., 2016). Russulales, the order with the third highest recorded diversity, also occurs in all five subareas, but mainly in the subarea **f**, viz., Western Tien Shan Mountains in Tashkent region (**Figure 11f**). Other orders and the species without a confirmed position at the order level are present only in small areas. Such species may be sensitive to environmental changes. So, to sustain species diversity of wood-inhabiting poroid and corticioid fungi, special attention should be paid to protecting their habitats. Using the GIS data, the potential future distribution of certain important (biotechnological, pathogenic, medicinal, and edible) wood-inhabiting poroid and corticioid species could be predicted. Similar studies have been performed on some wood-inhabiting poroid and corticioid species worldwide (Yuan et al., 2015; Elias et al., 2020). Generally, knowledge of species diversity and occurrence in an area is a baseline for benefiting from ecosystem services, monitoring environmental changes, and implementing conservation actions (Mueller and Schmit, 2007; Hibbett et al., 2007, 2011; Brock et al., 2009; Hyde et al., 2013; Osmundson et al., 2013; Truong et al., 2017). Therefore, the current GIS data are important for management and utilization of wood-inhabiting poroid and corticioid fungi in Uzbekistan.

In conclusion, this study provides the first comprehensive, thoroughly annotated checklist of species diversity of wood-inhabiting poroid and corticioid fungi in Uzbekistan. These species are ecologically and economically important as decomposers, pathogens, and sources of food and medicines. Beyond local scale, these data are also crucial as a supplement of the global knowledge of wood-inhabiting poroid and corticioid fungi and for elucidating the evolutionary history of wood-inhabiting poroid and corticioid fungi worldwide. More importantly, the current project exploring wood-inhabiting poroid and corticioid fungi in a less studied country may initiate similar explorations in other Central Asian countries and also other regions worldwide, which will largely fulfill the knowledge gap of wood-inhabiting poroid and corticioid fungi in certain rarely studied regions.

DATA AVAILABILITY STATEMENT

The datasets presented in this study can be found in online repositories. The names of the repository/repositories and accession number(s) can be found in the article/supplementary material.

AUTHOR CONTRIBUTIONS

YG and MY collected fungal specimens and performed DNA lab work. YG and AO were responsible for morphological identification and management of collection data. L-WZ and YG performed the molecular phylogenetic analyses. YZ mapped the fungal taxa. YG, AO, and L-WZ drafted the manuscript. EL, AG, DS, LP, and LC improved and revised it. All authors have read the final manuscript version and approved it. All authors contributed to the article and approved the submitted version.

FUNDING

This work was supported by the Ministry of Innovative Development of the Republic of Uzbekistan (Project Nos. P3-2014-0830174425 and P3-20170921183), CAS President's International Fellowship Initiative (PIFI) for Visiting Scientist (Grant No. 2018VBB0021), German Academic Exchange Service (DAAD) for a Visiting Fellowship (Grant Nos. A/13/03723 and 57314018), Erasmus Mundus Action 2 CASIA Postdoctoral Fellowship (Grant No. UZGT2-P3), and a TWAS-CNPq postdoctoral fellowship (Grant No. 190136/2013-8). L-WZ thanks the financial support from the Youth Innovation Promotion Association of the Chinese Academy of Sciences (No. 2017240).

ACKNOWLEDGMENTS

YG thanks Prof. Jan Stenlid (Swedish University of Agricultural Sciences, Sweden) for the use of his laboratory facilities, Dr. Indrek Sell (Estonia) for organizing a trip to TAAM herbarium in Tartu, Dr. Ivan Zmitrovich (Komarov Botanical Institute of the Russian Academy of Sciences, Russia) for helping with literature search, and Dr. Viacheslav Spirin (Finnish Museum of Natural History, University of Helsinki, Finland) for helping identify *Antrodia* species. The authors warmly thank TAAM curator Dr. Ilmy Parmasto and other staff members for issuing permission and technical help while studying herbarium specimens at the Estonian University of Life Sciences, Tartu, Estonia. They also thank Dr. Barbara Wilson (Corvallis, Oregon) for reviewing and for valuable comments on an earlier version of the manuscript. Dr. Oleh Prylutskyi (V.N. Karazin Kharkiv National University, Ukraine) and the GBIF helpdesk are acknowledged for the help with data publishing.

REFERENCES

Aime, M. C., and Brearley, F. Q. (2012). Tropical fungal diversity: closing the gap between species estimates and species discovery. *Biodivers. Conserv.* 21, 2177–2180. doi: 10.1007/s10531-012-0338-7

Akhmedova, F. G. (1966). *Mycoflora of South-Western Tien Shan Mountain*. Ph.D. dissertation, Institute of Botany, Uzbekistan Academy of Sciences, Tashkent.

Anonymous (1998). *UNDP/GEF: National Strategy and Action Plan*. Tashkent: Biodiversity of Conservation of Republic of Uzbekistan.

Anonymous (2001). *USAID Biodiversity Assessment for Uzbekistan*. Almaty: USAID Central Asian Republics Mission, 57.

Antonelli, A., Fry, C., Smith, R. J., Simmonds, M. S. J., Kersey, P. J., Pritchard, H. W., et al. (2020). *State of the World's Plants and Fungi 2020*. Kew: Royal Botanic Gardens. doi: 10.34885/172

ArcGIS Desktop (2020). Available online at: Desktop.arcgis.com/en

Ariyawansa, H. A., Hyde, K. D., Jayasiri, S. C., Buyck, B., Chethana, K. W. T., Dai, D. Q., et al. (2015). Fungal diversity notes 111–252—taxonomic and phylogenetic contributions to fungal taxa. *Fungal Divers.* 75, 27–274. doi: 10.1007/s13225-015-0355-4

Baltaeva, G. M. (1992). *Polypore Fungi (Polyporaceae s. lato) of Uzbekistan*. Ph.D. thesis. Komarov Botanical Institute, Russian Academy of Sciences, Saint Petersburg.

Baltaeva, G. M. (1993). Polypore fungi (Polyporaceae, Ganodermataceae, Hymenochaetaceae) of UzSSR. *Mikol. Fitopatol.* 32–36.

Baymuratova, G. T. (1963). *Mycoflora of Hungry Steppe*. Ph.D. thesis, Institute of Botany, Uzbekistan Academy of Sciences, Tashkent.

Bondarceva, M. A., and Parmasto, E. H. (1986). *Families Hymenochaetaceae, Lachnocladiaceae, Coniophoraceae, Schizophyllaceae (Order Aphyllophorales, Key to Fungi of the USSR), issue 1*. Moscow: Nauka Press.

Botman, E. (2009). Forest Rehabilitation in the Republic of Uzbekistan. *IUFRO World Ser.* 20, 253–299.

Brazee, N. J. (2015). Phylogenetic relationships among species of *Phellinus sensu stricto*, cause of white trunk rot of hardwoods, from northern North America. *Forests* 6, 4191–4211. doi: 10.3390/f6114191

Breitenbach, J., and Kränzlin, F. (1986). *Fungi of Switzerland, Vol. 2. Non Gilled Fungi - Heterobasidiomycetes, Aphyllophorales, Gasteromycetes. Mykologia*. Luzern: Lucerne Press.

Brock, P. M., Döring, H., and Bidartondo, M. I. (2009). How to know unknown fungi: the role of a herbarium. *New Phytol.* 181, 719–724. doi: 10.1111/j.1469-8137.2008.02703.x

Brummitt, R. K. (2001). *World Geographical Scheme for Recording Plant Distributions: Edition 2. International Working Group on Taxonomic Databases for Plant Sciences (TDWG)*. Pittsburgh: Carnegie Mellon University.

Cheek, M., Nic Lughadha, L., Kirk, P., Lindon, H., Carretero, J., Looney, B., et al. (2020). New discoveries: plants and Fungi. *Plants People Planet.* 2, 371–388. doi: 10.1002/ppp3.10148

Crous, P. W., Rong, I. H., Wood, A., Lee, S., Glen, H., Botha, W., et al. (2006). How many species of fungi are there at the tip of Africa? *Stud. Mycol.* 55, 13–33. doi: 10.3114/sim.55.1.13

Dai, Y. C. (2011). A revised checklist of corticioid and hydnoid fungi in China for 2010. *Mycoscience* 52, 69–79. doi: 10.1007/S10267-010-0068-1

Dai, Y. C. (2012). Polypore diversity in China with an annotated checklist of Chinese polypores. *Mycoscience* 53, 49–80. doi: 10.1007/s10267-011-0134-3

Dai, Y. C., Wei, Y. L., and Zhou, L. W. (2015). Polypore richness along an elevational gradient: a case study in Changbaishan Nature Reserve, Northeastern China. *Fungal Ecol.* 13, 226–228. doi: 10.1016/j.funeco.2014.07.002

Dong, C. H., Liu, Q. Z., and Zhang, J. J. (2017). Research progress on important edible and medicinal fungi in China over the last decade. *J. Microbiol.* 37, 1–9.

Eastwood, A., Lazkov, G., and Newton, F. (2009). *The Red List of Trees of Central Asia*. Cambridge: Fauna & Flora International Press.

Elias, S. G., Salvador-Montoya, C. A., Costa-Rezende, D. H., Guterres, D. C., Fernandes, M., and Drechsler-Santos, E. R. (2020). Studies on the biogeography of *Phellinotus piptadeniae* (Hymenochaetales, Basidiomycota): expanding the knowledge on its distribution and clarifying hosts relationships. *Fungal Ecol.* 45, 100912. doi: 10.1016/j.funeco.2020.100912

Floudas, D., and Hibbett, D. S. (2015). Revisiting the taxonomy of *Phanerochaete* (Polyporales, Basidiomycota) using a four gene dataset and extensive ITS sampling. *Fungal Biol.* 119, 679–719. doi: 10.1016/j.funbio.2015.04.003

Friedl, M. A., McIver, D. K., Hodges, J. C. F., Zhang, X. Y., Muchoney, D., Strahler, A. H., et al. (2002). Global land cover mapping from MODIS: algorithms and early results. *Remote Sens. Environ.* 83, 287–302. doi: 10.1016/S0034-4257(02)00078-0

Gafforov, Y. (2017). A preliminary checklist of Ascomycetous microfungi from Southern Uzbekistan. *Mycosphere* 8, 660–696. doi: 10.5943/mycosphere/8/4/12

Gafforov, Y., and Hoshino, T. (2015). Remarks on *Typhula* sp. in Uzbekistan. *Mycoscience* 56, 109–113. doi: 10.1016/j.myc.2014.04.003

Gafforov, Y., and Ordynets, A. (2020). *Aphyllophoroid fu$ngi of Uzbekistan. Institute of Botany of the Academy of Sciences of the Republic of Uzbekistan. Occurrence Dataset*. Available online at: GBIF.org (accessed August 13, 2020). doi: 10.15468/vsru5z

Gafforov, Y., Phookamsak, R., Jiang, H. B., Wanasinghed, D. N., and Juliev, M. (2019). *Ophiobolus hydei* sp. nov. (Phaeosphaeriaceae, Ascomycota) from Cirsium and Phlomoides in Uzbekistan. *Botany* 97, 671–680. doi: 10.1139/cjb-2019-0118

Gafforov, Y., and Rakhimov, D. (2017). *Diplodia* and *Dothiorella* species (Botryosphaeriaceae, Ascomycota) from Uzbekistan. *J. Bot. Res. Inst. Texas* 11, 455–467.

Gafforov, Y., Riebesehl, J., Ordynets, A., Langer, E., Yarasheva, M., Ghobad-Nejhad, M., et al. (2017). *Hyphodontia* (Hymenochaetales, Basidiomycota) and similar taxa from Central Asia. *Botany* 95, 1041–1056. doi: 10.1139/cjb-2017-0115

Gafforov, Y., Tomšovský, M., Langer, E., and Zhou, L. W. (2014). *Phylloporia yuchengii* sp. nov. (Hymenochaetales, Basidiomycota) from Western Tien Shan Mountains of Uzbekistan based on phylogeny and morphology. Cryptogamie Mycol. 35, 313–322. doi: 10.7872/crym.v35.iss4.2014.313

Gafforov, Y. S. (2002). Flora of Pycnidial fungi of Namangan region. *Uzbekistan Boil. J.* 2, 43–48.

Gafforov, Y. S. (2010). Ecological peculiarities and mycodiversity of parasite hyphalic fungi (Hyphales) of Fergana Valley and their spread on host plants. *Uzbekistan Boil. J.* 2, 46–51.

Gafforov, Y. S. (2014). Taxonomy and diversity of the genus *Ganoderma* Karst. (*Basidiomycota*) species in Uzbekistan. *Uzbekistan Biol. J. Spec. Issue* 22–25.

Gafforov, Y. S. (2015). *Species Diversity and Distribution of the Genus Ramularia Unger (Mycosphaerelaceae) in the Western Tien Shan. Plants and Animals of Ugam-Chatkal State National Natural Par*k. Tashkent: Chinor ERNk Press, 48–87.

Gafforov, Y. S. (2016a). Ascomycetous microfungi of Dendroflora of Boysun-botanical-geographic region. *Uzbekistan J. Ecol.* 12, 36–39.

Gafforov, Y. S. (2016b). *Coniothyrium*-like fungi (Ascomycota) from Western Tien Shan and South-Western Hissar mountains of Uzbekistan. *Uzbekistan Boil. J.* 4, 32–36.

Gaponenko, N. I. (1965). *Overview of Fungi in Bukhara Region*. Tashkent: FAN Press.

Gardes, M., and Bruns, T. D. (1996). "ITS-RFLP matching for the indetification of fungi," in *Methods in Molecular in Biology: Species Diagnostics Protocols: PCR and Other Nucleic Acid Methods*, ed. J. P. Clapp (Totowa, N.J: Humana Press. Inc), 177–186.

Ghobad-Nejhad, M., and Langer, E. (2016). First inventory of aphyllophoroid basidiomycetes of Zagros forests, W Iran. *Plant Biosyst.* 151, 844–854. doi: 10.1080/11263504.2016.1211199

González, V., Sánchez-Torres, P., Hinarejos, R., and Tuset, J. J. (2009). *Inonotus hispidus* fruiting bodies on grapevines with esca symptoms in Mediterranean areas of Spain. *J. Plant Pathol.* 91, 465–468. doi: 10.4454/jpp.v91i2.979

Guglielmo, F., Bergemann, S. E., Gonthier, P., Nicolotti, G., and Garbelotto, M. (2007). A multiplex PCR-based method for the detection and early identification of wood rotting fungi in standing trees. *J. Appl. Microbiol.* 103, 1490–1507. doi: 10.1111/j.1365-2672.2007.03378.x

Guindon, S., and Gascuel, O. (2003). A simple, fast and accurate algorithm to estimate large phylogenies by maximum likelihood. *Syst. Biol.* 52, 696–704. doi: 10.1080/10635150390235520

Han, M. L., Chen, Y. Y., Shen, L. L., Song, J., Vlasák, J., Dai, Y. C., et al. (2016). Taxonomy and phylogeny of the brown-rot fungi: *Fomitopsis* and its related genera. *Fungal Divers.* 80, 343–373. doi: 10.1007/s13225-016-0364-y

Hattori, T., Yamashita, S., and Susee, L. (2012). Diversity and conservation of wood-inhabiting polypores and other aphyllophoraceous fungi in Malaysia. *Biodivers. Conserv.* 21, 2375–2396. doi: 10.1007/s10531-012-0238-x

Hawksworth, D., and Lücking, R. (2017). "Fungal diversity revisited: 2.2 to 3.8 million species," in *The Fungal Kingdom*, Vol. 5, eds J. Heitman, B. Howlett, P. Crous, E. Stukenbrock, T. James, and N. Gow (Washington, DC: American Society of Microbiology), 79–95.

Hawksworth, D. L. (2012). Global species numbers of fungi: are tropical studies and molecular approaches contributing to a more robust estimate? *Biodivers. Conserv.* 21, 2425–2433. doi: 10.1007/s10531-012-0335-x

Hawksworth, D. L., Kirk, P. M., Sutton, B. C., and Pegler, D. N. (1995). *Ainsworth& Bisby's Dictionary of the Fungi*, 8th Edn. Wallingford: CABI Publishing.

He, S. H., Vlasák, J., and Dai, Y. C. (2014). *Hispidaedalea* gen. nov. and *Griseoporia taiwanense* sp. nov. (Gloeophyllales, Basidiomycota) based on morphological and molecular characters. Mycol. Prog. 13, 833–839. doi: 10.1007/s11557-014-0966-2

Hibbett, D., Abarenkov, K., Kõljalg, U., Öpik, M., Chai, B., Cole, J., et al. (2011). Sequence-based classification and identification of *Fungi*. *Mycologia* 108, 1049–1068. doi: 10.3852/16-130

Hibbett, D. S., Binder, M., Bischoff, J. F., Blackwell, M., Cannon, P. F., Eriksson, O. E., et al. (2007). A higher-level phylogenetic classification of the *Fungi*. *Mycol. Res.* 111, 509–547. doi: 10.1016/j.mycres.2007.03.004

Hyde, K. D., Jeewon, R., Chen, Y., Bhunjun, C. S., Calabon, M. S., Jiang, H. B., et al. (2020). The numbers of fungi: is the descriptive curve flattening? *Fungal Divers.* 103, 219–271. doi: 10.1007/s13225-020-00458-2

Hyde, K. D., Tennakoon, D. S., Jeewon, R., Bhat, J., Maharachchikumbura, S. S. N., Rossi, W., et al. (2019). Fungal diversity notes 1036–1150: taxonomic and phylogenetic contributions on genera and species of fungal taxa. *Fungal Divers.* 96, 1–242. doi: 10.1007/s13225-019-00429-2

Hyde, K. D., Udayanga, D., Manamgoda, D. S., Tedersoo, L., Larsson, E., Abarenkov, K., et al. (2013). Incorporating molecular data in fungal systematics: a guide for aspiring researchers. *Curr. Res. Environ. Appl. Mycol.* 3, 1–32. doi: 10.5943/cream/3/1/1

Iminova, M. M. (2009). *Macrofungi of Fergana Valley (within Uzbekistan)*. Ph.D. dissertation, Institute of Botany, Uzbekistan Academy of Sciences, Tashkent.

Index Fungorum. (2020). Available online at: http://indexfungorum.org/Names/Names.asp (accessed May 27, 2020).

Jeong, W. J., Lim, Y. W., Lee, J. S., and Jung, H. S. (2005). Phylogeny of *Phellinus* and related genera inferred from combined data of ITS and mitochondrial SSU rDNA sequences. *J. Microbiol. Biotechnol.* 15, 1028–1038.

Justo, A., Miettinen, O., Floudas, D., Ortiz-Santana, B., Sjökvist, E., Lindner, D., et al. (2017). A revised family-level classification of the Polyporales (Basidiomycota). *Fungal Biol.* 121, 798–824. doi: 10.1016/j.funbio.2017.05.010

Kan, Y. H., Gafforov, Y., Li, T., and Zhou, L. W. (2017). *Hyphodontia zhixiangii* sp. nov. (Schizoporaceae, Basidiomycota) from Uzbekistan. Phytotaxa 299, 273–279. doi: 10.11646/phytotaxa.299.2.12

Katoh, K., Kuma, K., Toh, H., and Miyata, T. (2005). MAFFT version 5: improvement in accuracy of multiple sequence alignment. *Nucleic. Acids. Res.* 33, 511–518. doi: 10.1093/nar/gki198

Katoh, K., and Standley, D. M. (2013). MAFFT multiple sequence alignment software version 7: improvements in performance and usability. *Mol. Biol. Evol.* 30, 772–780. doi: 10.1093/molbev/mst010

Khalikova, M. M. (1989). *Macrofungi of Tashkent Region*. Ph.D. thesis, Institute of Botany, Uzbekistan Academy of Sciences, Tashkent.

Klein, I., Gessner, U., and Kuenzer, C. (2012). Regional land cover mapping and change detection in Central Asia using MODIS time-series. *Appl. Geogr.* 35, 219–234. doi: 10.1016/j.apgeog.2012.06.016

Klein Tank, A. M. G., Peterson, T. C., Quadir, D. A., Dorji, S., Zou, X., Tang, H., et al. (2006). Changes in daily temperature and precipitation extremes in central and south Asia. *J. Geophys. Res.* 111:D16105. doi: 10.1029/2005JD006316

Kleyner, B. D. (1958). Polypore Fungi of Tashkent region. *Trudi Middle Asia* 3, 248–260.

Knežević, A., Milovanovič, I., Stajič, M., and Vukojevič, J. (2013). Potential of *Trametes* species to degrade lignin. *Int. Biodeter. Biodegr.* 85, 52–56. doi: 10.1016/j.ibiod.2013.06.017

Kravtzev, B. I. (1950). Fungal diseases of popular in Kazakhstan. *Bull. Acad. Sci. Kazakh SSR* 98:128.

Küffer, N., and Senn-Irlet, B. (2005). Influence of forest management on the species richness and composition of wood-inhabiting basidiomycetes in Swiss forests. *Biodivers. Conserv.* 14, 2419–2435. doi: 10.1007/s10531-004-0151-z

Larsson, K. H. (2007). Re-thinking the classification of corticioid fungi. *Mycol. Res.* 111, 1040–1063. doi: 10.1016/j.mycres.2007.08.001

Leal-Dutra, C. A., Griffith, G. W., Neves, M. A., Mclaughlin, D. J., Mclaughlin, E. G., Clasen, L. A., et al. (2020). Reclassification of Pterulaceae Corner (Basidiomycota- Agaricales) introducing the ant-associated genus *Myrmecopterula* gen. nov., *Phaeopterula* Henn. and the corticioid *Radulomycetaceae* fam. nov. *IMA Fungus* 11:2.

Letunic, I., and Bork, P. (2019). Interactive Tree Of Life (iTOL) v4: recent updates and new developments. *Nucleic Acids Res.* 47, 256–259. doi: 10.1093/nar/gkz239

Li, H. J., Si, J., Zhang, Y. Z., Sun, J., and He, S. H. (2016). Taxonomic and phylogenetic studies reveal a new species from *Funalia gallica* complex (Polyporales, Basidiomycota). *Mycol. Res.* 15, 1–8. doi: 10.1007/s11557-016-1167-y

Lioubimtseva, A. E., and Henebry, G. M. (2009). Climate and environmental change in arid Central Asia: impacts, vulnerability, and adaptations. *J. Arid Environ.* 73, 963–977. doi: 10.1016/j.jaridenv.2009.04.022

Mueller, G. M., and Schmit, J. P. (2007). Fungal biodiversity: what do we know? What can we predict? *Biodivers. Conserv.* 16, 1–5. doi: 10.1007/s10531-006-9117-7

Natural Earth (2020). Available online at: http://www.naturalearthdata.com/ (accessed June 8, 2011).

Osmundson, T. W., Robert, V. A., Schoch, C. L., Baker, L. J., Smith, A., Robich, G., et al. (2013). Filling gaps in biodiversity knowledge for macrofungi: contributions and assessment of an herbarium collection DNA barcode sequencing project. *PLoS One* 8:e62419. doi: 10.1371/journal.pone.0062419

Ovaskainen, O., Schigel, D., Ali-Kovero, H., Auvinen, P., Paulin, L., Norden, B., et al. (2013). Combining high-throughput sequencing with fruit body surveys reveals contrasting life-history strategies in fungi. *ISME J.* 7, 1696–1709. doi: 10.1038/ismej.2013.611

Panfilova, T. S., and Gaponenko, N. I. (1963). *Mycoflora of the Angren River Basin*. Tashkent: AN UzSSR Press.

Pattengale, N. D., Alipour, M., Bininda-Emonds, O. R. P., Moret, B. M. E., and Stamatakis, A. (2010). How many bootstrap replicates are necessary? *J. Comput. Biol.* 17, 337–354.

Pem, D., Gafforov, Y., Jeewon, R., Hongsanan, S., Promputtha, I., Doilom, M., et al. (2018). Multigene phylogeny coupled with morphological characterization reveal two new species of *Holmiella* and taxonomic insights within Patellariaceae. *Cryptogamie Mycol.* 39, 193–209. doi: 10.7872/crym/v39.iss2.2018.193

Pem, D., Jeewon, R., Gafforov, Y., Hongsanan, S., Phukhamsakda, C., Promputtha, I., et al. (2019a). *Melanocamarosporioides ugamica* gen. et sp. nov., a novel member of the family *Melanommataceae* from Uzbekistan. *Mycol. Prog.* 18, 471–481. doi: 10.1007/s11557-018-1448-8

Pem, D., Jeewon, J., Bulgakov, T., Gafforov, Y., Hongsanan, S., Phookamsak, R., et al. (2019b). Taxonomy and molecular phylogeny of *Thyrostroma ephedricola* sp. nov. (Dothidotthiaceae) and proposal for *Thyrostroma jaczewskii* comb. nov. *Phytotaxa* 416, 243–256. doi: 10.11646/phytotaxa.416.4.3

Posada, D. (2008). jModelTest: phylogenetic model averaging. *Mol. Biol. Evol.* 25, 1253–1256. doi: 10.1093/molbev/msn083

Rehner, S. A., and Samuels, G. J. (1994). Taxonomy and phylogeny of *Gliocladium* analysed from nuclear large subunit ribosomal DNA sequences. *Mycol. Res.* 98, 625–634. doi: 10.1016/S0953-7562(09)80409-7

Riley, R., Salamov, A. A., Brown, D. W., Nagy, L. G., Floudas, D., Held, B. W., et al. (2014). Extensive sampling of basidiomycete genomes demonstrates inadequacy of the white-rot/brown-rot paradigm for wood decay fungi. *Proc. Natl. Acad. Sci. U.S.A.* 111, 9923–9928. doi: 10.1073/pnas.1400592111

Ronquist, F., Teslenko, M., van der Mark, P., Ayres, D., Darling, A., Höhna, S., et al. (2012). MrBayes 3.2: efficient Bayesian phylogenetic inference and model choice across a large model space. *Syst. Biol.* 61, 539–542. doi: 10.1093/sysbio/sys029

Ryvarden, L., and Melo, I. (2014). Poroid fungi of Europe. *Synopsis Fung.* 31, 1–455.

Samarakoon, M. C., Gafforov, Y., Liu, N. G., Maharachchikumbura, S. S. N., Bhat, J. D., Liu, J. K., et al. (2018). Combined multi-gene backbone tree for the genus *Coniochaeta* with two new species from Uzbekistan. *Phytotaxa* 336, 043–058. doi: 10.11646/phytotaxa.336.1.3

Schmit, J. P., and Mueller, G. M. (2007). An estimate of the lower limit of global fungal diversity. *Biodivers. Conserv.* 16, 99–111. doi: 10.1007/s10531-006-9129-3

Schoch, C. L., Seifert, K. A., Huhndorf, S., Robert, V., Spouge, J. L., Levesque, C. A., et al. (2012). Nuclear ribosomal internal transcribed spacer (ITS) region as a universal DNA barcode marker for *Fungi. Proc. Natl. Acad. Sci. U.S.A.* 109, 6241–6246. doi: 10.1073/pnas.1117018109

Schwartzman, S. R. (1964). *Flora Sporowich Rastenii Kazachstana: Auriculariales, Tremellales, Dacryomycetales, Exobasidiales, Aphyllophorales*. Alma Ata: Nauka Press.

Silvestro, D., and Michalak, I. (2012). raxmlGUI: a graphical front-end for RAxML. *Org. Divers. Evol.* 12, 335–337. doi: 10.1007/s13127-011-0056-0

Sinadskiy, Y. B. (1968). To the question of pathogenic mycoflora of tree-shrub species of desert zones of Central Asia and Kazakhstan. *Mikol. Fitopotal.* 2, 148–149.

Sinadskiy, Y. B., and Bodartseva, M. A. (1956). Little-known polypore on *Populus* and *Tamarix* and their significance in the Karakalpak S.S.R. *Botanicheskii Zhur.* 41, 1177–1183.

Sinadskiy, Y. B., and Bodartseva, M. A. (1960). Diseases of tree and shrub species in the tugai forests of the Syr Darya. *Botanicheskii Zhur.* 45, 423–429.

Solieva, Y. S., and Gafforov, Y. S. (2001). New records for mycoflora of Uzbekistan. *J. Agrar Sci. Tashkent State Univ.* 3, 36–39.

Solieva, Y. S., and Gafforov, Y. S. (2002). New species and genera of micromycetes for flora of Uzbekistan. *Bull. Acad. Sci. Rep. Uzbekistan* 4, 42–45.

Soudzilovskaia, N. A., Bodegom, P. M., Terrer, C., Zelfde, M. V., McCallum, I., McCormack, M. L., et al. (2019). Global mycorrhizal plant distribution linked to terrestrial carbon stocks. *Nat. Commun.* 10:5077. doi: 10.1038/s41467-019-13019-2

Spirin, V., Miettinen, O., Pennanen, J., Kotiranta, H., and Niemelä, T. (2013). *Antrodia hyalina*, a new polypore from Russia, and *A. leucaena*, new to Europe. *Mycol. Prog.* 12, 53–61. doi: 10.1007/s11557-012-0815-0

Stamatakis, A. (2006). RAxML-VI-HPC: maximum likelihood-based phylogenetic analyses with thousands of taxa and mixed models. *Bioinformatics* 22, 2688–2690. doi: 10.1093/bioinformatics/btl446

Stutz, J. C., Copeman, R., Martin, C., and Morton, J. B. (2000). Patterns of species composition and distribution of arbuscular mycorrhizal fungi in arid regions of southwestern North America and Namibia, Africa. *Can. J. Bot.* 78, 237–245. doi: 10.1139/b99-183

Swift, M. J. (1982). "Basidiomycetes as components of forest ecosystems," in *Decomposer Basidiomycetes, their Biology and Ecology*, eds J. C. Frankland, J. N. Hedger, and M. J. Swift (Cambridge: Cambridge University Press).

Tedersoo, L., Bahram, M., Põlme, S., Kõljalg, U., Yorou, N. S., Wijesundera, R., et al. (2014). Global diversity and geography of soil fungi. *Science* 346:1256688. doi: 10.1126/science.1256688

ThePlantList (2013). *Version 1.1*. Available online at: http://www.theplantlist.org/ (accessed March 1, 2020).

Tomšovskyì, M. (2012). Delimitation of an almost forgotten species *Spongipellis litschaueri* (Polyporales, Basidiomycota) and its taxonomic position within the genus. *Mycol. Prog.* 11, 415–424. doi: 10.1007/s11557-011-0756-z

Truong, C., Mujic, A. B., Healy, R., Kuhar, F., Furci, G., Torres, D., et al. (2017). How to know the fungi: combining field inventories and DNA-barcoding to document fungal diversity. *New Phytol.* 3, 913–919. doi: 10.1111/nph.14509

Tsykun, T., Rigling, D., and Prospero, S. (2013). A new multilocus approach for reliable DNA-based identification of *Armillaria* species. *Mycologia* 105, 1059–1076. doi: 10.3852/12-209

Varma, A. (1995). "Ecophysiology and Application of Arbuscular Mycorrhizal Fungi in Arid Soils," in *Mycorrhiza*, eds A. Varma and B. Hock (Berlin: Springer Press). doi: 10.1007/978-3-662-08897-5_24

Vilgalys, R., and Hester, M. (1990). Rapid genetic identification and mapping of enzymatically amplified ribosomal DNA from several *Cryptococcus* species. *J. Bacteriol.* 172, 4239–4246. doi: 10.1128/jb.172.8.4238-4246.1990

Vu, D., Groenewald, M., de Vries, M., Gehrmann, T., Stielow, B., Eberhardt, U., et al. (2019). Large-scale generation and analysis of filamentous fungal DNA barcodes boosts coverage for kingdom fungi and reveals thresholds for fungal

species and higher taxon delimitation. *Stud. Mycol.* 92, 135–154. doi: 10.1016/j.simyco.2018.05.001

Wanasinghe, D. N., Hyde, K. D., Crous, P. W., Wijayawardene, N. N., Jeewon, R., Jones, E. B. G., et al. (2017). Phylogenetic revision of *Camarosporium* (Pleosporinae, Dothideomycetes) and allied genera. *Stud. Mycol.* 87, 207–256. doi: 10.1016/j.simyco.2017.08.001

Wanasinghe, D. N., Jeewon, R., Peršoh, D., Jones, E. B. G., Camporesi, E., Bulgakov, T. S., et al. (2018a). Taxonomic circumscription and phylogenetics of novel didymellaceous taxa with brown muriform spores. *Stud. Fungi* 3, 152–175. doi: 10.5943/sif/3/1/17

Wanasinghe, D. N., Phukhamsakda, C., Hyde, K. D., Jeewon, R., Lee, H. B., Jones, E. B. G., et al. (2018b). Fungal diversity notes 709–839: taxonomic and phylogenetic contributions to fungal taxa with an emphasis on fungi on Rosaceae. *Fungal Divers.* 89, 1–236. doi: 10.1007/s13225-018-0395-7

Wang, Y., and Chen, Z. H. (2019). Bioinformatics and enzymatics investigation of *Trametes laccase* for optical biosensing application. *J. Mater. Sci.* 54, 4970–4983. doi: 10.1007/s10853-018-03187-9

White, T. J., Bruns, T. D., Lee, S., and Taylor, J. (1990). "Amplification and direct sequencing of fungal ribosomal RNA genes for phylogenetics," in *PCR Protocols: A Guide to Methods and Applications*, eds M. A. Innis and D. H. Gelfand (London: Academic Press), 315–322.

Wu, F., Chen, J. J., Ji, X. H., Vlasák, J., and Dai, Y. C. (2017). Phylogeny and diversity of the morphologically similar polypore genera *Rigidoporus, Physisporinus, Oxyporus,* and *Leucophellinus*. *Mycologia* 109, 749–765. doi: 10.1080/00275514.2017.1405215

Wu, F., Zhou, L. W., Yang, Z. L., Bau, T., Li, T. H., and Dai, Y. C. (2019). Resource diversity of Chinese macrofungi: edible, medicinal and poisonous species. *Fungal Divers.* 98, 1–76. doi: 10.1007/s13225-019-00432-7

Yamashita, S., Hattori, T., and Abe, H. (2010). Host preference and species richness of wood-Inhabiting aphyllophoraceous fungi in a cool temperate area of Japan. *Mycologia* 102, 11–19. doi: 10.3852/09-008

Yang, X., Wu, Y., Zhang, Y., Yang, E., Qu, Y., Xu, H., et al. (2020). A thermo-active laccase isoenzyme from *Trametes trogii* and its potential for dye decolorization at high temperature. *Front. Microbiol.* 11:241. doi: 10.3389/fmicb.2020.00241

Yuan, H. S., Wei, Y. L., and Wang, X. G. (2015). Maxent modeling for predicting the potential distribution of Sanghuang, an important group of medicinal fungi in China. *Fungal Ecol.* 17, 140–145. doi: 10.1016/j.funeco.2015.06.001

Yuan, Y., Gafforov, Y., Chen, Y. Y., and Wu, F. (2017). A new species of *Antrodia* (Basidiomycota, Polyporales) from juniper forest of Uzbekistan. *Phytotaxa* 303, 47–55. doi: 10.11646/phytotaxa.303.1.3

Yuan, Y. S., Lu, X., Dai, Y. C., Hyde, K. H., Kan, Y. H., et al. (2020). Fungal diversity notes 1276–1391: taxonomic and phylogenetic contributions to fungal taxa. *Fungal Divers.* doi: 10.1007/s13225-020-00461-7

Zhao, C. L., and Cui, B. K. (2014). Phylogeny and taxonomy of *Ceriporiopsis* (Polyporales) with descriptions of two new species from southern China. *Phytotaxa* 164, 17–28. doi: 10.11646/phytotaxa.164.1.2

Zhou, L. W., and Dai, Y. C. (2012). Recognizing ecological patterns of wood-decaying polypores on gymnosperm and angiosperm trees in northeast China. *Fungal Ecol.* 5, 230–235. doi: 10.1016/j.funeco.2011.09.005

Zhou, L. W., Ghobad-Nejhad, M., Tian, X. M., Wang, Y. F., and Wu, F. (2020). Current status of 'Sanghuang' as a group of medicinal mushrooms and their perspective in industry development. *Food Rev. Int.* doi: 10.1080/87559129.2020.1740245

Zhou, L. W., Hao, Z. Q., Wang, Z., Wang, B., and Dai, Y. C. (2011). Comparison of ecological patterns of polypores in three forest zones in China. *Mycology* 2, 260–275. doi: 10.1080/21501203.2011.602726

Zhou, L. W., Nakasone, K. K., Burdsall, H. H., Ginns, J., Vlasák, J., and Miettinen, O. (2016). Polypore diversity in North America with an annotated checklist. *Mycol. Prog.* 15, 771–790. doi: 10.1007/s11557-016-1207-7

Zhu, L., Song, J., Zhou, J. L., Si, J., and Cui, B. K. (2019). Species diversity, phylogeny, divergence time, and biogeography of the genus *Sanghuangporus* (Basidiomycota). *Front. Microbiol.* 10:812. doi: 10.3389/fmicb.2019.00812

Conflict of Interest: The authors declare that the research was conducted in the absence of any commercial or financial relationships that could be construed as a potential conflict of interest.

Copyright © 2020 Gafforov, Ordynets, Langer, Yarasheva, de Mello Gugliotta, Schigel, Pecoraro, Zhou, Cai and Zhou. This is an open-access article distributed under the terms of the Creative Commons Attribution License (CC BY). The use, distribution or reproduction in other forums is permitted, provided the original author(s) and the copyright owner(s) are credited and that the original publication in this journal is cited, in accordance with accepted academic practice. No use, distribution or reproduction is permitted which does not comply with these terms.

frontiers in Microbiology

ORIGINAL RESEARCH
published: 14 December 2020
doi: 10.3389/fmicb.2020.602773

Bambusicolous *Arthrinium* Species in Guangdong Province, China

Indunil C. Senanayake[1,2], Jayarama D. Bhat[3,4], Ratchadawan Cheewangkoon[5] and Ning Xie[1]**

[1] Guangdong Provincial Key Laboratory for Plant Epigenetics, College of Life Science and Oceanography, Shenzhen University, Shenzhen, China, [2] Shenzhen Key Laboratory of Laser Engineering, College of Optoelectronic Engineering, Shenzhen University, Shenzhen, China, [3] Formerly, Department of Botany, Goa University, Taleigão, India, [4] No. 128/1J, Azad Co-Op Housing Society, Curca, India, [5] Department of Entomology and Plant Pathology, Faculty of Agriculture, Chiang Mai University, Chiang Mai, Thailand

A survey of bambusicolous fungi in Bijiashan Mountain Park, Shenzhen, Guangdong Province, China, revealed several *Arthrinium*-like taxa from dead sheaths, twigs, and clumps of *Bambusa* species. Phylogenetic relationships were investigated based on morphology and combined analyses of the internal transcribed spacer region (ITS), large subunit nuclear ribosomal DNA (LSU), beta tubulin (β-tubulin), and translation elongation factor 1-alpha (tef 1-α) gene sequences. Based on morphological characteristics and phylogenetic data, *Arthrinium acutiapicum* sp. nov. and *Arthrinium pseudorasikravindrae* sp. nov. are introduced herein with descriptions and illustrations. Additionally, two new locality records of *Arthrinium bambusae* and *Arthrinium guizhouense* are described and illustrated.

Keywords: Apiosporaceae, bamboo, fungal taxonomy, new locality records, novel species

OPEN ACCESS

Edited by:
Peter Edward Mortimer, Kunming Institute of Botany, Chinese Academy of Sciences, China

Reviewed by:
Dong-Qin Dai, Qujing Normal University, China
Saowaluck Tibpromma, Kunming Institute of Botany, Chinese Academy of Sciences, China

****Correspondence:***
Ratchadawan Cheewangkoon
ratcha.222@gmail.com
Ning Xie
Shainin@msn.cn

Specialty section:
This article was submitted to Evolutionary and Genomic Microbiology, a section of the journal Frontiers in Microbiology

Received: *11 September 2020*
Accepted: *02 November 2020*
Published: *14 December 2020*

Citation:
Senanayake IC, Bhat JD, Cheewangkoon R and Xie N (2020) Bambusicolous Arthrinium Species in Guangdong Province, China. Front. Microbiol. 11:602773. doi: 10.3389/fmicb.2020.602773

INTRODUCTION

Arthrinium Kunze is accommodated in Apiosporaceae, Xylariales, which is morphologically different from other xylariaceous genera by the presence of basauxic conidiophores and dark, aseptate, globose to lenticular conidia with a hyaline rim or germ slit (Minter, 1985; Petrini and Müller, 1986; Singh et al., 2012; Jiang et al., 2018; Pintos et al., 2019). Basauxic conidiophores simply mean elongation of conidiogenous cells from the basal growing point after formation of a single, terminal blastic conidium at its apex (Cole, 1986).

Arthrinium species are distributed worldwide in various hosts as endophytes, epiphytes, or saprobes, as well as plant pathogens on some commercial crops and ornamentals (Agut and Calvo, 2004; Ramos et al., 2010; Crous and Groenewald, 2013; Sharma et al., 2014; Senanayake et al., 2015; Wijayawardene et al., 2020). Also, species of *Arthrinium* (Schmidt and Kunze, 1817) inhabit a wide range of substrates, i.e., air, soil debris, lichens, marine algae (Agut and Calvo, 2004; Senanayake et al., 2015; Dai et al., 2016; Luo et al., 2019), and even human tissues (Sharma et al., 2014). The genus *Arthrinium* morphologically differs from other xylariaceous anamorphic genera by the presence of basauxic conidiogenous cells which arise from conidiophore mother cells (Schmidt and Kunze, 1817; Minter, 1985).

The commonly reported diseases by *Arthrinium* species are kernel blight of barley and brown culm streak of *Phyllostachys praecox* by *A. arundinis*, damping-off of wheat by *A. sacchari*, and culm rot of bamboos and *Phyllostachys viridis* by *A. phaeospermum* (Martínez-Cano et al., 1992; Mavragani et al., 2007; Chen et al., 2014; Li et al., 2016). Additionally, the causative agent of cutaneous infections of humans has been reported as *A. phaeospermum* (Rai, 1989; Zhao et al., 1990; De Hoog et al., 2000; Crous and Groenewald, 2013). Some *Arthrinium* species produce

bioactive compounds with pharmacological and medicinal properties (Hong et al., 2015), while some produce industrially important enzymes (Shrestha et al., 2015). Crous and Groenewald (2013) reviewed the genus *Arthrinium* based on morphology and multigene phylogeny. There are several subsequent studies providing additions to the genus (Singh et al., 2012; Sharma et al., 2014; Crous et al., 2015; Senanayake et al., 2015; Dai et al., 2016, 2017; Hyde et al., 2016; Réblová et al., 2016; Jiang et al., 2018, 2020; Wang et al., 2018; Pintos et al., 2019).

Several studies revealed bambusicolous *Arthrinium* species from Poaceae and Cyperaceae host plants in China (Dai et al., 2016, 2017; Jiang et al., 2018, 2020; Wang et al., 2018), and several *Arthrinium*-like taxa on dead leaves, clumps, and twigs of bamboo were collected from Shenzhen (China) during this study. The aims of this study are identifying these *Arthrinium*-like taxa based on morphology and phylogeny and describe and illustrate them. Phylogenetic relationships were investigated based on DNA sequence data of the internal transcribed spacer region (ITS), large subunit nuclear ribosomal DNA (LSU), beta tubulin (β-tubulin), and translation elongation factor 1-alpha (tef 1-α), and two new *Arthrinium* species from bamboo are introduced as *Arthrinium pseudorasikravindrae* and *A. acutiapicum* and two locality records, *Arthrinium bambusae* and *Arthrinium guizhouense*, are described and illustrated.

MATERIALS AND METHODS

Sample Collection and Fungal Isolation

Fresh specimens of *Arthrinium*-like taxa were collected from Bijiashan Mountain Park, Shenzhen, Guangdong Province, China, in September–October 2018, and the collection site has a tropical climate with abundant sunshine and rainfall all year round. The yearly average temperature is 22°C and vegetative type is tropical evergreen monsoon forests (Li et al., 2015). Specimens were brought to the laboratory in paper bags and they were examined under a stereomicroscope (Carl Zeiss Discovery V8), and blackish conidial mass and fruit bodies were observed. The fruit bodies were studied and photographed using a stereomicroscope fitted with a camera (ZEISS Axiocam 208). The micromorphological characters were studied and photographed using a compound microscope (Nikon Eclipse 80i) fitted with a digital camera (Canon 450D). All microscopic measurements such as the length of the conidiophores, conidiogenous cells, and conidia were made with Tarosoft image framework (v. 0.9.0.7).

Single conidial isolation was carried out following the method described by Senanayake et al. (2020a). Germinated conidia were aseptically transferred into fresh potato dextrose agar (PDA) plates, incubated at 20°C to obtain pure cultures, and later transferred to PDA slants and stored at 4°C for further study. Colony characteristics were recorded from cultures grown on PDA. Additionally, pure cultures were inoculated in 2% PDA together with sterilized bamboo leaves and incubated at 25°C for sporulation.

Fungarium materials are deposited in the Herbarium of Cryptogams, Kunming Institute of Botany, Academia Sinica (HKAS), and all the ex-type living cultures are deposited at the Culture Collection of Kunming Institute of Botany (KUMCC). Index Fungorum numbers[1] were obtained for the new strains.

DNA Extraction, PCR Amplification, and Sequencing

Fresh fungal mycelium grown on PDA for 2 weeks at 20°C in the dark was used for DNA extraction using fungal genomic DNA extraction kit (Biospin DNA Extraction Kit, Bioer Technology, Co. Ltd., Hangzhou, China) following the manufacturer's protocols. Polymerase chain reactions (PCR) and sequencing were carried out for the following loci: the complete ITS region with the primer pair of ITS1/ITS4 (White et al., 1990); the LSU ribosomal DNA, amplified and sequenced as a single fragment with primers LR0R/LR5 (Vilgalys and Hester, 1990); the tef 1-α gene with primers EF1-728F/EF2 (Carbone and Kohn, 1999; Rehner, 2001); and the β-tubulin gene with primers bt2a and bt2b (Glass and Donaldson, 1995).

The PCR amplification reactions were carried out with the following protocol. The total volume of the PCR reaction was 25 μl reaction volume containing 1 μl of DNA template, 1 μl of each forward and reverse primer, 12.5 μl of 2 × PCR Master Mix, and 9.5 μl of double-distilled sterilized water (ddH_2O). The reaction was conducted by running for 35 cycles following the condition of Senanayake et al. (2020b). The PCR products were observed on 1% agarose electrophoresis gel stained with ethidium bromide. Purification and sequencing of PCR products were carried out at Sunbiotech Company, Beijing, China. Sequence quality was checked and sequences were condensed with DNASTAR Lasergene v.7.1. Sequences derived in this study were deposited in GenBank and accession numbers were obtained (**Table 1**).

Sequence Alignments and Phylogenetic Analyses

BLASTn searches were made using the newly generated sequences to assist in taxon sampling for phylogenetic analyses. Jiang et al. (2018, 2020), Wang et al. (2018), and Pintos et al. (2019) were followed to obtain sequences from GenBank that are listed in **Table 1**. The concatenated ITS, LSU, β-tubulin, and tef 1-α sequence dataset comprised 101 strains of *Arthrinium*, while the outgroup taxon was *Pestalotiopsis chamaeropis* (CBS 237.38). DNA sequences of the ITS, LSU, β-tubulin, and tef 1-α were aligned using the online version of MAFFT v. 7.036[2] (Katoh et al., 2020) with default settings and manually adjusted using BioEdit 7.1.3 (Hall, 1999) to allow maximum alignment and minimum gaps. Further, single gene alignments were combined to obtain the final multiloci alignment that was containing 2,817 nucleotide characters, viz. 681 of ITS, 875 of LSU, 434 of β-tubulin, and 827 of tef 1-α. Both single and concatenated alignments were used for the analyses.

[1] http://www.indexfungorum.org

[2] http://mafft.cbrc.jp/alignment/server/large.html

TABLE 1 | Details of the isolates used in the phylogenetic analyses.

Species	Strains	Substrate	Location	GenBank Accession Number			
				ITS	LSU	β-Tubulin	tef 1-α
Arthrinium acutiapicum	**KUMCC 20-0209**	***Bambusa bambos***	**China**	**MT946342**	**MT946338**	**MT947365**	**MT947359**
A. acutiapicum	**KUMCC 20-0210**	***Bambusa bambos***	**China**	**MT946343**	**MT946339**	**MT947366**	**MT947360**
A. aquaticum	MFLU 18-1628	Submerged wood	China	MK828608	MK835806	N/A	N/A
A. arundinis	CBS 450.92	N/A	N/A	AB220259	N/A	AB220306	N/A
A. arundinis	CBS 114316	*Hordeum vulgare*	Iran	KF144884	KF144928	KF144974	KF145016
A. arundinis	AP11118A	*Bambusa* sp.	Spain	MK014868	MK014835	MK017974	MK017945
A. aureum	CBS 244.83	*Phragmites australis*		AB220251	KF144935	KF144981	KF145023
A. balearicum	CBS 145129	Poaceae sp.	Spain	MK014869	MK014836	MK017975	MK017946
A. bambusae	CGMCC 3.18335	Bamboo	China	KY494718	KY494794	KY705186	KY806204
A. bambusae	**KUMCC 20-0207**	***Bambusa dolichoclada***	**China**	**MT946346**	**MT946340**	**MT947370**	**MT947363**
A. bambusae	LC7107	Bamboo	China	KY494719	KY494795	KY705187	KY705117
A. camelliae-sinensis	CGMCC 3.18333	*Camellia sinensis*	China	KY494704	KY494780	KY705173	KY705103
A. camelliae-sinensis	LC8181	*Brassica campestris*	China	KY494761	KY494837	KY705229	KY705157
A. caricicola	CBS 145127	*Carex ericetorum*	Germany	MK014871	MK014838	MK017977	MK017948
A. chinense	CFCC 53036	*Fargesia qinlingensis*	China	MK819291	N/A	MK818547	MK818545
A. chinense	CFCC 53037	*Fargesia qinlingensis*	China	MK819292	N/A	MK818548	MK818546
A. curvatum	CBS 145131	*Carex* sp.	Germany	MK014872	MK014839	MK017978	MK017949
A. descalsii	CBS 145130	*Ampelodesmos mauritanicus*	Spain	MK014870	MK014837	MK017976	MK017947
A. dichotomanthi	CGMCC 3.18332	*Dichotomanthus tristaniaecarpa*	China	KY494697	KY494832	KY705167	KY705096
A. dichotomanthi	LC8175	*Dichotomanthus tristaniaecarpa*	China	KY494755	KY494831	KY705223	KY705151
A. esporlense	CBS 145136	*Phyllostachys aurea*	Spain	MK014878	MK014845	MK017983	MK017954
A. euphorbiae	IMI 285638b	*Bambusa* sp.	Bangladesh	AB220241	N/A	AB220288	NA
A. gaoyouense	CFCC 52301	*Phragmites australis*	China	MH197124	N/A	MH236789	MH236793
A. gaoyouense	CFCC 52302	*Phragmites australis*	China	MH197125	N/A	MH236790	MH236794
A. garethjonesii	JHB004	*Bambusa* sp.	China	KY356086	KY356091	N/A	N/A
A. garethjonesii	HKAS 96289	*Bambusa* sp.	China	NR_154736	NG_057131	N/A	N/A
A. guizhouense	LC5318	Air	China	KY494708	KY494784	KY705177	KY705107
A. guizhouense	**KUMCC 20-0206**	***Bambusa multiplex***	**China**	**MT946347**	**MT946341**	**MT947369**	**MT947364**
A. guizhouense	CGMCC 3.18334	Air	China	KY494709	KY494785	KY705178	KY705108
A. gutiae	CBS 135835	Gut of a grasshopper	India	KR011352	MH877577	KR011350	KR011351
A. hispanicum	IMI 326877	Maritime sand	Spain	AB220242	AB220336	AB220289	NA
A. hydei	KUMCC 16-0204	*Bambusa tuldoides*	China	KY356087	KY356092	N/A	NA
A. hydei	CBS 114990	Bamboo	China	KF144890	KF144936	KF144982	KF145024
A. hyphopodii	MFLUCC 15-0003	*Bambusa tuldoides*	China	KR069110	N/A	N/A	NA
A. hyphopodii	KUMCC 16-0201	Bamboo	China	KY356088	N/A	N/A	NA
A. hysterinum	ICPM6889	Bamboo	New Zealand	MK014874	MK014841	MK017980	MK017951
A. hysterinum	AP2410173	*Phyllostachys aurea*	Spain	MK014876	MK014843	N/A	N/A
A. ibericum	CBS 145137	*Arundo donax*	Portugal	MK014879	MK014846	MK017984	MK017955
A. italicum	CBS 145138	*Phragmites australis*	Spain	MK014880	MK014847	MK017985	MK017956
A. italicum	AP221017	*Phragmites australis*	Spain	MK014881	MK014848	MK017986	MK017957
A. japonicum	IFO 30500	*Carex despalata*	Japan	AB220262	AB220356	AB220309	N/A
A. japonicum	IFO 31098	*Carex despalata*	Japan	AB220264	AB220358	AB220311	N/A
A. jatrophae	MMI 00051	*Jatropha podagrica*	India	JQ246355	N/A	N/A	N/A
A. jiangxiense	CGMCC 3.18381	*Maesa* sp.	China	KY494693	N/A	KY705163	KY705092
A. jiangxiense	LC4578	*Camellia sinensis*	China	KY494694	KY494770	KY705164	KY705093
A. kogelbergense	CBS 113332	*Cannomois virgate*	South Africa	KF144891	KF144937	KF144983	KF145025
A. kogelbergense	CBS 113333	Restionaceae sp.	South Africa	KF144892	KF144938	KF144984	KF145026
A. locutum-pollinis	LC11683	*Brassica campestris*	China	MF939595	N/A	MF939622	MF939616
A. longistromum	MFLUCC 11-0479	Bamboo	Thailand	KU940142	KU863130	N/A	NA
A. longistromum	MFLUCC 11-0481	Bamboo	Thailand	KU940141	KU863129	N/A	NA
A. longistromum	MFLU 15-1184	*Bambusa* sp.	Thailand	NR_154716	N/A	N/A	NA
A. malaysianum	CBS 251.29	*Cinnamomum camphora*	N/A	KF144897	KF144943	KF144989	KF145031

(Continued)

TABLE 1 | Continued

Species	Strains	Substrate	Location	GenBank Accession Number			
				ITS	LSU	β-Tubulin	tef 1-α
A. malaysianum	CBS 102053	*Macaranga hullettii*	Malaysia	KF144896	KF144942	KF144988	KF145030
A. marii	CBS 497.90	Air	Spain	AB220252	KF144947	KF144993	KF145035
A. marii	CBS 114803	*Arundinaria hindsii*	China	KF144899	KF144945	KF144991	KF145033
A. mediterranei	IMI 326875	Air	Spain	AB220243	N/A	AB220290	NA
A. neosubglobosa	JHB006	Bamboo	China	KY356089	KY356094	N/A	NA
A. neosubglobosa	JHB007	Bamboo	China	KY356090	KY356095	N/A	NA
A. obovatum	CGMCC 3.18331	*Lithocarpus* sp.	China	KY494696	KY494834	KY705166	KY705095
A. obovatum	LC8177	*Lithocarpus* sp.	China	KY494757	KY494833	KY705225	KY705153
A. ovatum	CBS 115042	*Arundinaria hindsii*	China	KF144903	KF144950	KF144995	KF145037
A. paraphaeospermum	MFLUCC 13-0644	Bamboo	Thailand	KX822128	KX822124	N/A	NA
A. phaeospermum	CBS 114314	*Hordeum vulgare*	Iran	KF144904	KF144951	KF144996	KF145038
A. phaeospermum	CBS 114315	*Hordeum vulgare*	Iran	KF144905	KF144952	KF144997	KF145039
A. phragmitis	CPC 18900	*Phragmites australis*	Italy	KF144909	N/A	KF145001	KF145043
A. phragmitis	AP3218	*Phragmites australis*	Spain	MK014891	MK014858	MK017996	MK017967
A. phragmitis	AP2410172A	*Phragmites australis*	Spain	MK014890	MK014857	MK017995	MK017966
A. piptatheri	CBS 145149	*Piptatherum miliaceum*	Spain	MK014893	MK014860	N/A	MK017969
A. pseudoparenchymaticum	CGMCC 3.18336	Bamboo	China	KY494743	KY494830	KY705211	KY705139
A. pseudoparenchymaticum	LC8173	Bamboo	China	KY494753	KY494829	KY705221	KY705149
A. pseudorasikravindrae	**KUMCC 20-0208**	***Bambusa dolichoclada***	**China**	**MT946344**	**N/A**	**MT947367**	**MT947361**
A. pseudorasikravindrae	**KUMCC 20-0211**	***Bambusa dolichoclada***	**China**	**MT946345**	**N/A**	**MT947368**	**MT947362**
A. pseudosinense	CBS 135459	Bamboo	Netherlands	KF144910	KF144957	N/A	KF145044
A. pseudospegazzinii	CBS 102052	*Macaranga hullettii*	Malaysia	KF144911	KF144958	KF145002	KF145045
A. pterospermum	CBS 123185	*Machaerina sinclairii*	New Zealand	KF144912	KF144959	KF145003	NA
A. pterospermum	CBS 134000	*Machaerina sinclairii*	Australia	KF144913	KF144960	KF145004	KF145046
A. puccinioides	CBS 549.86	*Lepidosperma gladiatum*	Germany	AB220253	AB220347	AB220300	NA
A. qinlingense	CFCC 52303	*Fargesia qinlingensis*	China	MH197120	N/A	MH236791	MH236795
A. qinlingense	CFCC 52304	*Fargesia qinlingensis*	China	MH197121	N/A	MH236792	MH236796
A. rasikravindrae	NFCCI 2144	*Cissus* sp.	Netherlands	KF144914	N/A	N/A	NA
A. rasikravindrae	MFLUCC 11-0616	Bamboo	Thailand	KU940144	KU863132	N/A	NA
A. sacchari	CBS 212.30	*Phragmites australis*	UK	KF144916	KF144962	KF145005	KF145047
A. sacchari	CBS 301.49	Bamboo	Indonesia	KF144917	KF144963	KF145006	KF145048
A. saccharicola	CBS 191.73	Air	Netherlands	KF144920	KF144966	KF145009	KF145051
A. saccharicola	CBS 463.83	*Phragmites australis*	Netherlands	KF144921	KF144968	KF145010	KF145052
A. serenense	IMI 326869	N/A	Spain	AB220250	N/A	AB220297	NA
A. serenense	ATCC 76309	N/A	N/A	AB220240	N/A	AB220287	NA
A. sporophleum	CBS 145154	*Juncus* sp.	Spain	MK014898	MK014865	MK018001	MK017973
A. subglobosum	MFLUCC 11-0397	Bamboo	Thailand	KR069112	KR069113	N/A	NA
A. subroseum	LC7291	Bamboo	China	KY494751	KY494827	KY705219	KY705147
A. subroseum	CGMCC3.18337	Bamboo	China	KY494752	KY494828	KY705220	KY705148
A. thailandicum	MFLUCC 15-0199	Bamboo	Thailand	KU940146	KU863134	N/A	NA
A. thailandicum	MFLUCC 15-0202	Bamboo	Thailand	KU940145	KU863134	N/A	NA
A. tintinnabula	ICPM 6889	Bamboo	New Zealand	MK014874	MK014841	MK017980	MK017951
A. trachycarpum	CFCC 53038	*Trachycarpus fortune*	China	MK301098	N/A	MK303394	MK303396
A. trachycarpum	CFCC 53039	*Trachycarpus fortune*	China	MK301099	N/A	MK303395	MK303397
A. vietnamense	IMI 99670	*Citrus sinensis*	Vietnam	KX986096	KX986111	KY019466	NA
A. xenocordella	CBS 478.86	Soil	Zimbabwe	KF144925	KY494763	N/A	NA
A. xenocordella	CBS 595.66	Soil	Austria	KF144926	KF144971	KF145013	KF145055
A. yunnanum	MFLU 15-0002	*Phyllostachys nigra*	China	KU940147	KU863135	N/A	NA
A. yunnanum	CFCC 52312	Bamboo	China	MH191120	N/A	N/A	NA
Pestalotiopsis hamaeropis	CBS 237.38	N/A	Italy	MH855954	MH867450	KM199392	KM199474

Newly obtained sequences are indicated in black bold. ATCC, The American Type Culture Collection, Virginia, United States; CBS, Westerdijk Fungal Biodiversity Institute, Utrecht, The Netherlands; CFCC, China Forestry Culture Collection, Beijing, China; CGMCC, China General Microbiological Culture Collection, Beijing, China; CPC, Culture collection of Pedro Crous, housed at the Westerdijk Fungal Biodiversity Institute; HKAS, Herbarium of Cryptogams, Kunming, China; ICPM, International Collection of Microorganisms from Plants, Auckland, New Zealand; IFO, Institute for Fermentation, Osaka; IMI, Culture collection of CABI Europe UK Centre, UK; KUMCC, Culture Collection of Kunming Institute of Botany, Kunming, China; MFLU, Mae Fah Luang University Herbarium, Chiang Rai, Thailand; LC, Working collection of Lei Cai, housed at CAS, China; MFLUCC, Mae Fah Luang University Culture Collection, Chiang Rai, Thailand; NFCCI, National Fungal Culture Collection of India.

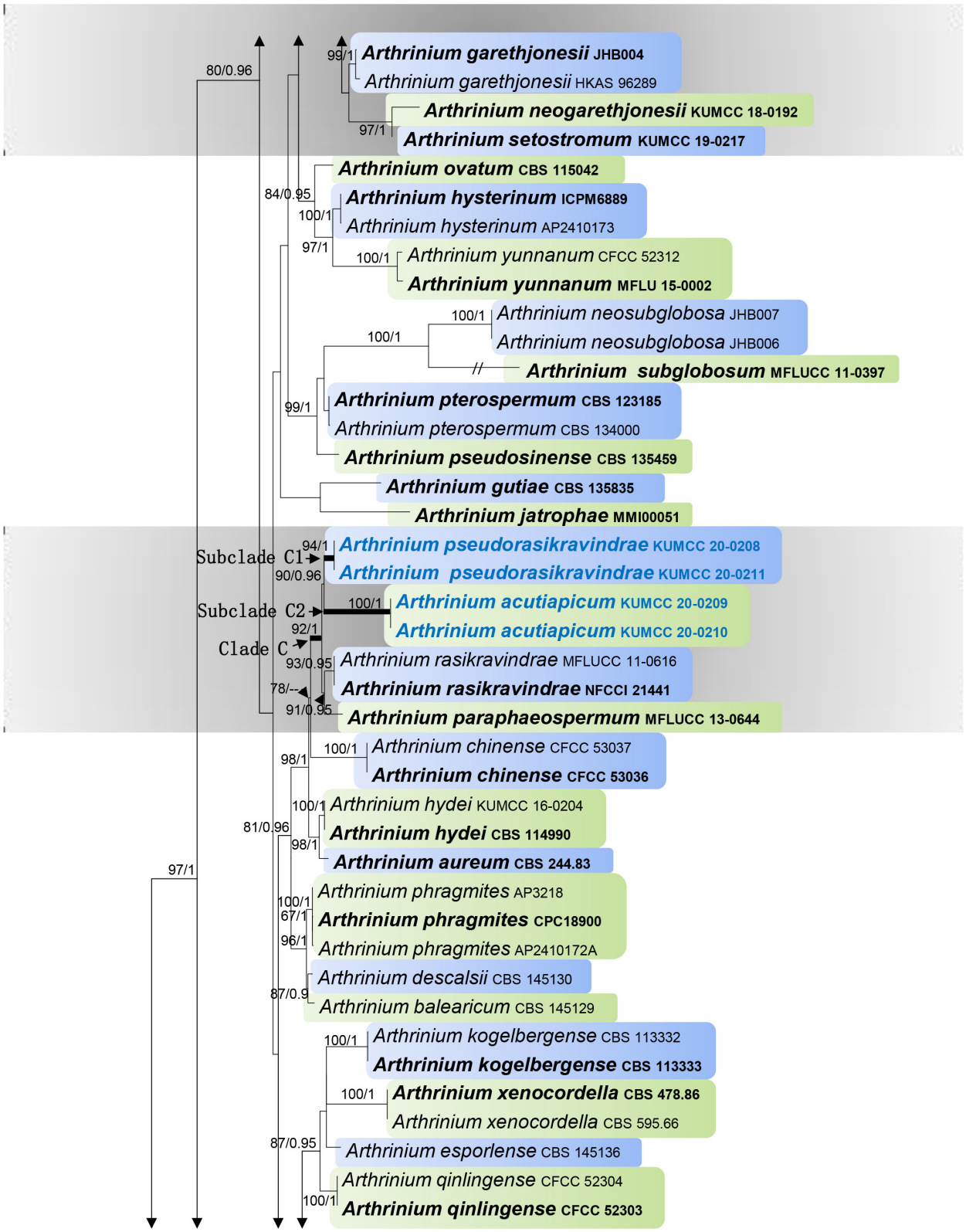


FIGURE 1 | Continued

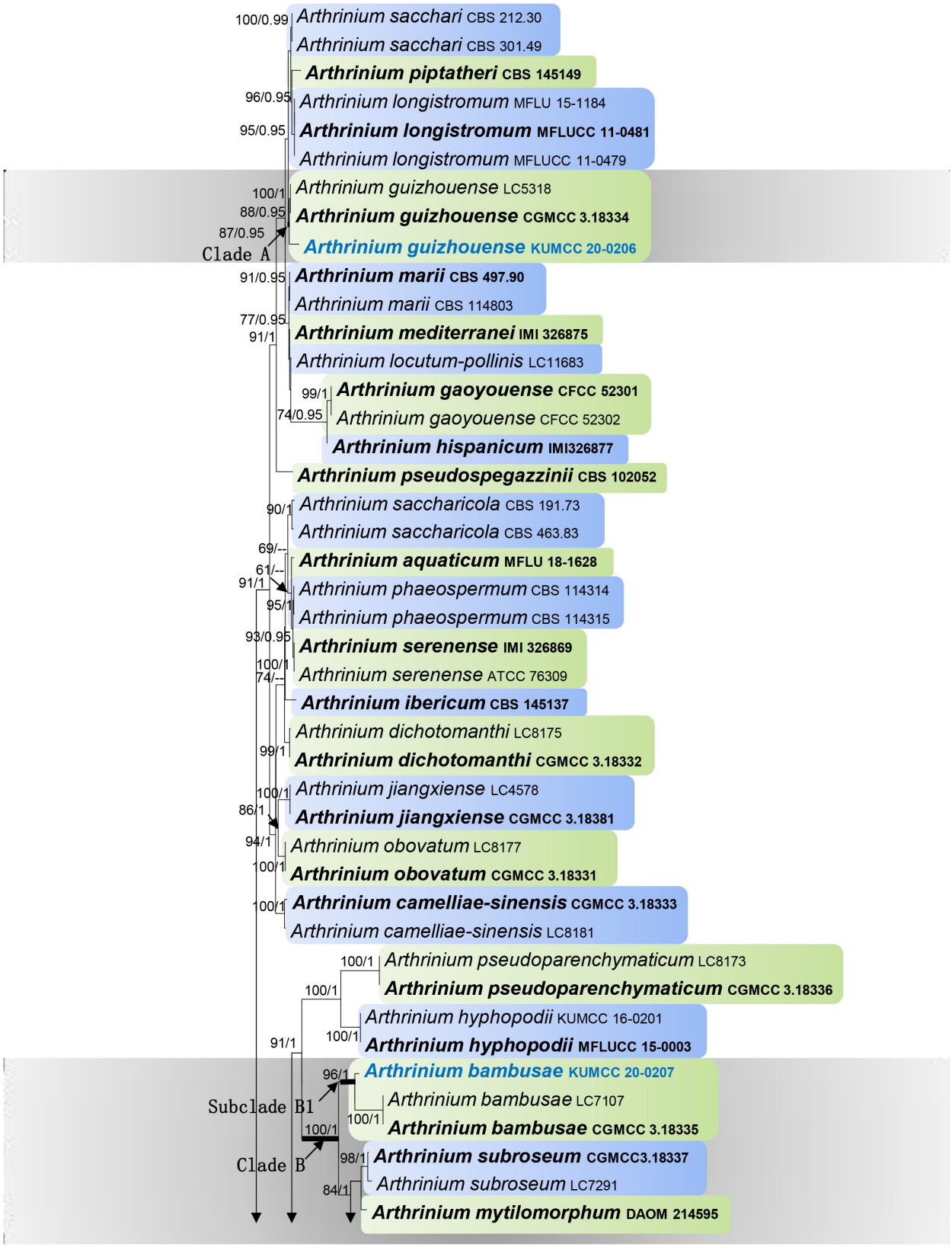


FIGURE 1 | Continued

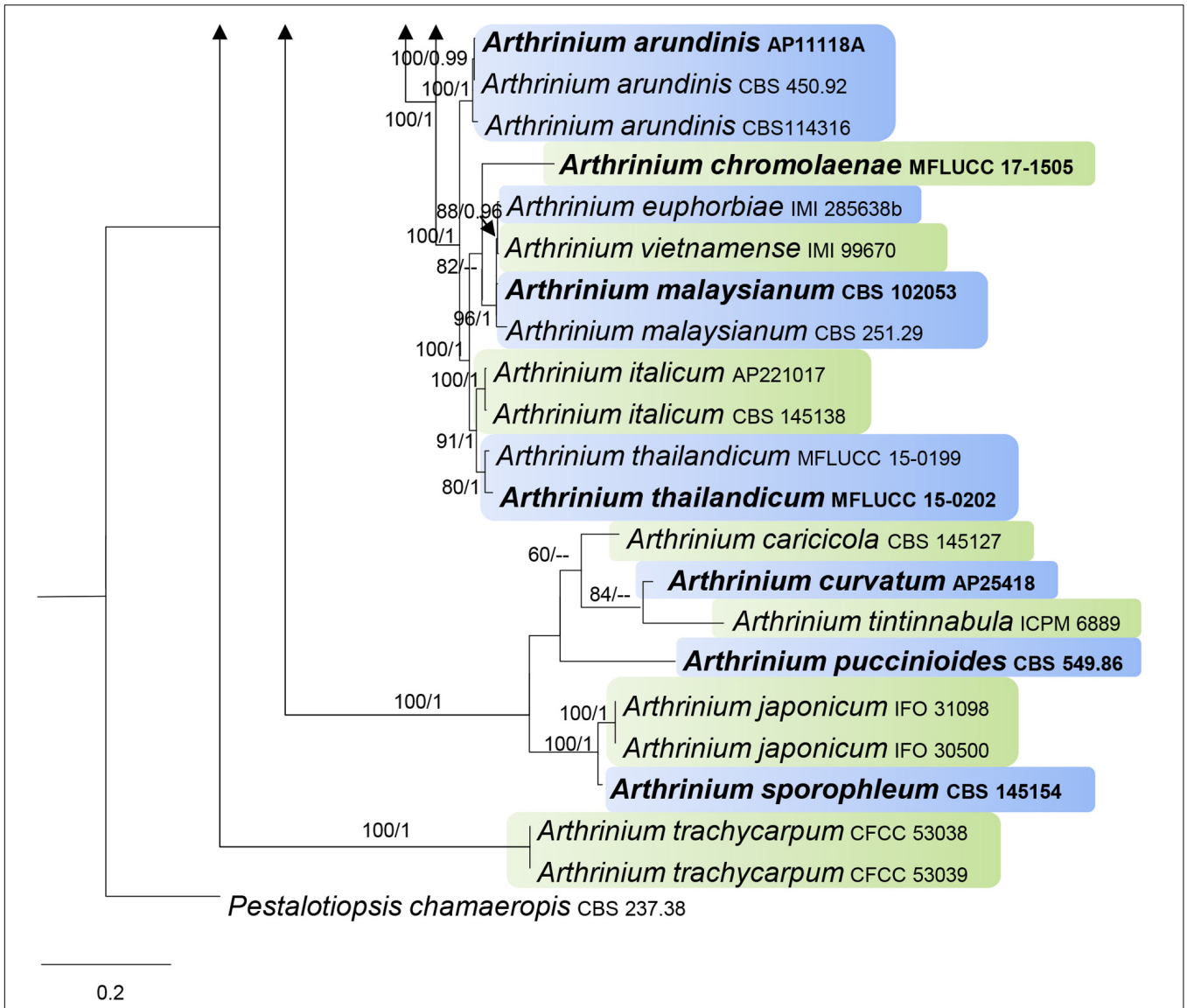


FIGURE 1 | Phylogram generated from maximum likelihood analysis based on combined internal transcribed spacer region (ITS), large subunit nuclear ribosomal DNA (LSU), β-tubulin, and tef 1-α sequence data. Bootstrap support values greater than 50% and Bayesian posterior probabilities greater than 0.90 are given at the nodes. The tree is rooted with *Pestalotiopsis chamaeropis* (CBS 237.38). Ex-type strains are in bold and the newly obtained sequences are indicated in blue bold.

Maximum likelihood analyses were performed by RAxML (Stamatakis and Alachiotis, 2010) implemented in raxmlGUIv.1.5 (Silvestro and Michalak, 2012) using the ML + rapid bootstrap setting and the GTR + I + G model of nucleotide substitution with 1,000 replicates. The matrix was partitioned for the different gene regions included in the combined multilocus analyses.

For the Bayesian inference (BI) analyses, the optimal substitution model for the combined dataset was determined to be GTR + I + G using the MrModeltest software v. 2.2 (Nylander, 2004). The BI analyses was computed with MrBayes v. 3.2.6 (Ronquist et al., 2012) with four simultaneous Markov chain Monte Carlo chains from random trees over 10 M generations (trees were sampled every 500th generation).

The distribution of log-likelihood scores was observed to check whether sampling is in stationary phase or not, and Tracer v1.5 was used to check if further runs were required to reach convergence or not (Rambaut and Drummond, 2007). The Bayesian analyses lasted until the average standard deviation of split frequencies has a value less than 0.01, and the consensus tree and posterior probabilities were calculated after discarding the first 20% of the sampled trees as burn-in. The phylogram was visualized in FigTree v. 1.4 (Rambaut, 2009). All the phylogenetic trees derived from this study were deposited in TreeBase[3] under accession number S27147.

[3]www.treebase.org

RESULTS

Phylogenetic Inferences

All individual trees generated under different criteria and from single gene datasets were essentially similar in topology and not significantly different from the tree generated from the concatenated dataset (not discussed herein). Additionally, this tree topology is similar to previous studies on *Arthrinium* (Dai et al., 2016; Jiang et al., 2018, 2020; Wang et al., 2018; Pintos et al., 2019).

Maximum likelihood analysis of *Arthrinium* species in this study with 1,000 bootstrap replicates yielded the best ML tree (**Figure 1**) with the likelihood value of –29,933.362493 and the following model parameters: estimated base frequencies—*A* = 0.239654, *C* = 0.250345, *G* = 0.255054, and *T* = 0.254948; substitution rates—AC = 1.275584, AG = 2.530572, AT = 1.397969, CG = 1.184045, CT = 4.063803, and GT = 1.0; proportion of invariable sites—*I* = 0.203121; gamma distribution shape parameter—α = 0.54383. The alignment contained a total of 1,756 distinct alignment patterns and 28.72% of undetermined characters. After discarding the first 20% of generations, 36,000 trees remained from which 50% consensus trees and posterior probabilities (PP) were calculated (**Figure 1**). Maximum likelihood bootstrap values ≥ 60% and BI ≥ 0.95 are given at each node. Tree topologies of the ML and Bayesian analyses were similar to each other and there are no significant differences.

There are 101 *Arthrinium* strains in this study together with a new isolate that is introduced here. All the ex-type strains of *Arthrinium* species were included if available, and other authentic strains were selected when sequences from ex-type strains are unavailable. Our new isolate KUMCC 20-0206 clustered with the type strain of *A. guizhouense* (CGMCC 3.18334) and another representative strain (LC5318) with 87% ML and 0.95 PP support. This clade (clade A) has a close phylogenetic affinity to *Arthrinium longistromum*, *A. piptatheri*, and *A. sacchari* with 95% ML and 0.95 PP support. Two strains of *A. bambusae* (CGMCC 3.18335 and LC7107) and the new isolate KUMCC 20-0207 were grouped in a separate clade with 96% ML and 1.00 PP support. This clade (subclade B1) shares a monophyletic relationship to *Arthrinium garethgonesii*, *A. mytilomotphum*, *A. neogarethjonesii*, *A. setostromun*, and *A. subroseum* with strong bootstrap supports (100% ML, 1.00 PP, clade B, **Figure 1**). Two new isolates, KUMCC 20-0208 and KUMCC 20-0211, were monophyletic in subclade C1 (**Figure 1**) with 90% ML and 0.96 PP support. Subclade C2 is also monophyletic with two novel strains, viz. KUMCC 20–0209 and KUMCC 20–0210, which are sisters to subclade C1 with 90% ML and 0.96 PP support (clade C, **Figure 1**). With these four new strains, clade C shares a close phylogenetic affiliation to *A. paraphaeospermum* and *A. rasikravindrae*.

Taxonomy

Arthrinium acutiapicum Senan. and Cheew. sp. nov. Figure 2

Index Fungorum number: IF557868

Etymology: Species epithet "acuti" refers to pointed and "apicum" refers to apex of conidiogenous cells.
Holotype: HKAS 107673

Saprobic on dead twigs of *Bambusa bambos* (L.) Voss. *Hyphae* 1.5–2.5 μm diam., hyaline, branched, septate, sparse. *Sexual morph*: undetermined. *Asexual morph*: *Conidiomata* 350–450 μm, pycnidial, immersed, aggregated, scattered, subglobose, ostiolate, black, coriaceous. *Conidiophores* reduced to conidiogenous cells. *Conidiogenous cells* 4–7 × 2–3 μm ($\bar{x}$ = 6.3 × 2.1 μm, *n* = 30), holoblastic, develop from conidiophore mother cells, erect, basauxic, cylindrical to ampulliform, apex pointed and hyaline, smooth and thick-walled, pale brown. *Conidia* 7.5–10 × 8.5–12 μm ($\bar{x}$ = 9.3 × 11.9 μm, *n* = 30), globose in surface view, subglobose to oval in side view, apex and base blunted, smooth-walled, brown to dark brown, with a dark equatorial slit.

Culture Characteristics

Colonies grew on PDA at 20°C in the dark attenuated 2 cm diam., within 7 days, flat, circular, entire margin, wooly, with abundant aerial mycelia, white in surface view and off-white to yellow in reverse. Sporulation occurred after 10 days on PDA incubated at 20°C in the dark without any host substrate. Conidia seem black mass and well spread on culture.

Specimen Examined

China, Guangdong Province, Shenzhen City, Futian District, northwest of Futian, Bijiashan Park, on dead twigs of *B. bambos* (L.) Voss (Poaceae), 23 September 2018, IS, SI 86 (HKAS 107673, holotype), ex-type culture, KUMCC 20-0210; *ibid* 15 October 2018, IS, SI 86-1 (HKAS 107674, paratype), ex-paratype culture KUMCC 20-0211.

Notes

Arthrinium acutiapicum forms a distinct subclade (subclade C2, **Figure 1**) with strong bootstrap support values (ML/PP = 90/0.96) in our phylogenetic analysis, which is a sister to the newly introduced species *A. pseudorasikravindrae*. Additionally, *A. acutiapicum* shows close phylogenetic affinities to *A. paraphaeospermum*, *A. pseudorasikravindrae*, and *A. rasikravindrae* in clade C (**Figure 1**) and *A. chinense*. Blast results of ITS, LSU, β-tubulin, and tef 1-α sequences of *A. acutiapicum* show high similarity to *A. hydei*, *A. paraphaeospermum*, and *A. rasikravindrae*. Morphologically, *A. acutiapicum* is distinct from *A. pseudorasikravindrae* by the reduction of conidiophores to conidiogenous cells, cylindrical to ampulliform, pale brown conidiogenous cells with pointed, hyaline apex and brown to dark brown, smooth-walled conidia with dark equatorial slit. Additionally, *A. acutiapicum* is distinct from *A. rasikravindrae* by the reduction of conidiophores to pale brown conidiogenous cells and dimorphous, acropleurogenously arising conidia.

Arthrinium bambusae M. Wang and L. Cai, in Wang et al. (2018) Figure 3

Index Fungorum number: IF 824906

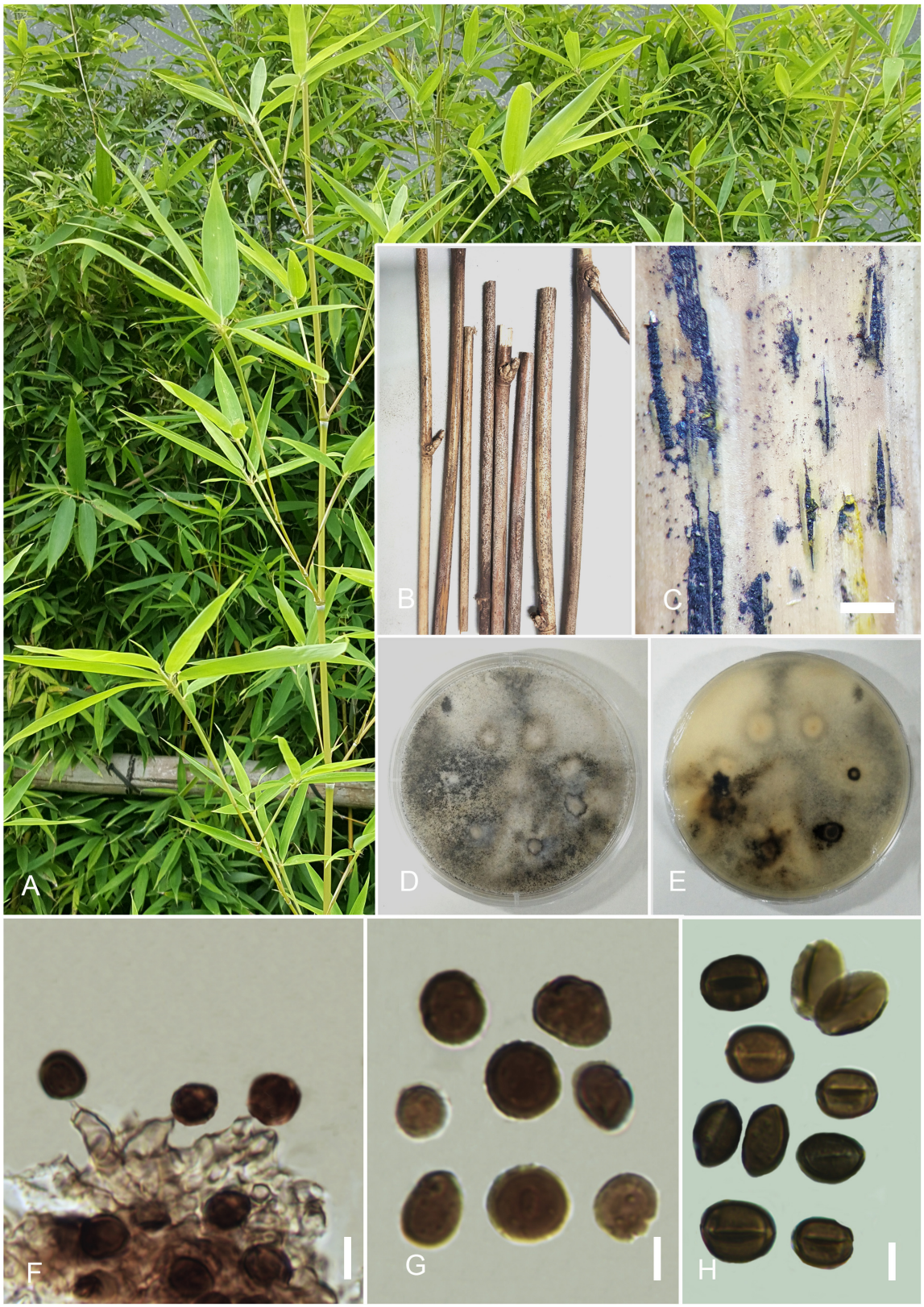


FIGURE 2 | *Arthrinium acutiapicum* (HKAS 107673). **(A)** Host. **(B)** Fungarium specimen. **(C)** Conidiomata on substrate. **(D)** Surface view of culture on potato dextrose agar (PDA). **(E)** Reverse view of culture on PDA. **(F)** Conidia and conidiogenous cells. **(G,H)** Conidia. Scale bars: **(C)** = 500 μm, **(F–H)** = 10 μm.

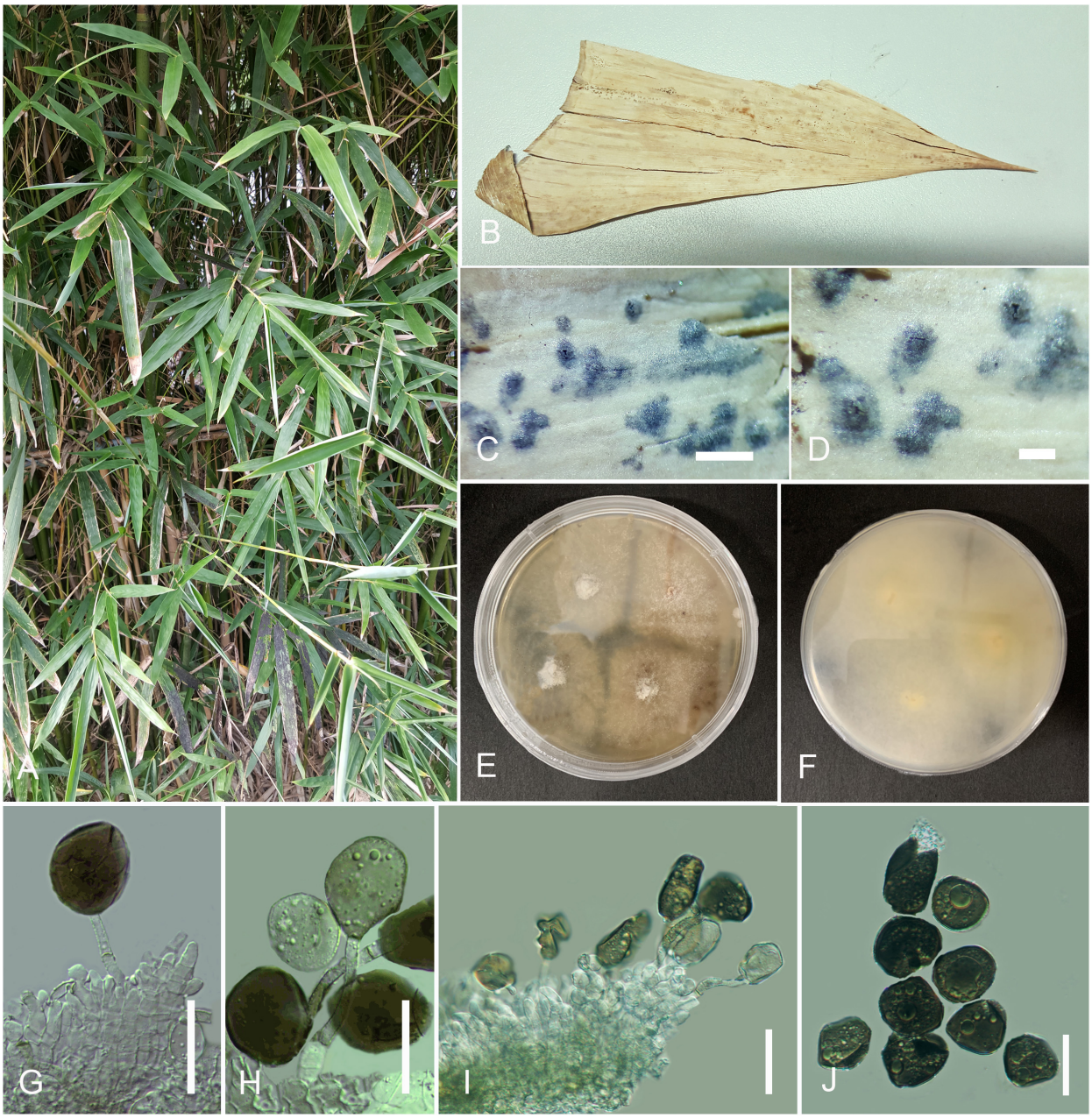


FIGURE 3 | *Arthrinium bambusae* (HKAS 107671). **(A)** Host. **(B)** Fungarium specimen. **(C,D)** Conidiomata on substrate. **(E,F)** Culture on potato dextrose agar (PDA; surface and reverse view). **(G–I)** Conidia and conidiogenous cells. **(J)** Conidia. Scale bars: **(C,D)** = 100 μm, **(G–J)** = 15 μm.

Saprobic on sheath of *Bambusa dolichoclada* Hayata. *Hyphae* 1–3 μm diam., hyaline, branched, septate, sparse. *Sexual morph*: undetermined. *Asexual morph*: appears as black, spotty patches on host surface. *Conidiomata* immersed, pycnidial, scattered, globose to slightly conical, ostiolate, black, coriaceous. *Conidiomatal wall* thin, comprising several layers of black, large cells of *textura angularis*. *Conidiophores* reduced to conidiogenous cells or rarely inconspicuous with cylindrical, thick-walled, hyaline. *Conidiogenous cells* 5–12 × 3–10 μm ($\bar{x}$ = 8.6 × 4 μm, n = 30), basauxic, holoblastic, develop from conidiophore mother cells, with periclinal thickening, doliiform to ampulliform or lageniform, erect, aggregated in clusters on hyphae, hyaline to pale brown, smooth. *Conidia* 10.5–17.5 × 8–15 μm ($\bar{x}$ = 15 × 12 μm, n = 30), subglobose to ellipsoid, guttulate, smooth to finely roughened, olivaceous to dark brown.

Culture Characteristics

Colonies grew on PDA at 20°C in the dark attenuated 2 cm diam., within 7 days, flat, spreading, margin circular, with abundant aerial mycelia, surface and reverse white to off-white.

Specimen Examined

China, Guangdong Province, Shenzhen City, Futian District, northwest of Futian, Bijiashan Park, on sheath of *B. dolichoclada* Hayata (Poaceae), 23 September 2018, IS, SI 80 (HKAS 107671), living culture, KUMCC 20-0207.

Notes

Arthrinium bambusae was introduced by Wang et al. (2018) from Guangdong Province, China, where our collection also was obtained. However, the exact locality is not mentioned in the original description there. The morphology of our collection was obtained from fungal structures on the host specimen, while Wang et al. (2018) had described the fungus from sporulated cultures. However, the morphology of our collection is similar to the holotype. Phylogenetically, *A. bambusae* clusters with *A. garethjonesii*, *A. neogarethjonesii*, *A. mytilomorphum*, *A. setostromum*, and *A. subroseum* with strong bootstrap value (ML/PP = 100/1), and the *A. bambusae* isolate (KUMCC 20-0207) clustered well with the ex-type culture (ML/PP = 96/1).

Arthrinium guizhouense M. Wang and L. Cai, in Wang et al. (2018) Figure 4

Index Fungorum number: IF824909

Saprobic on dead twigs of *Bambusa multiplex* (Lour.) Raeusch. ex Schult. f., appear as black mass coming out from ruptured bark. *Hyphae* hyaline, branched, septate, 1.5–6 μm diam. *Sexual morph*: undetermined. *Asexual morph*: *Conidiomata* 450–350 μm, picnidial, semi-immersed, aggregated, scattered, globose, ostiolate, black, coriaceous. *Conidiophores* reduced to conidiogenous cells. *Conidiogenous cells* 4–8 × 3–5 μm ($\bar{x}$ = 5.3 × 4 μm, *n* = 30), develop from conidiophore mother cells, erect, subglobose, basauxic, ampulliform or doliiform, hyaline to pale brown, smooth. *Conidia* 5–7 × 4–7 μm ($\bar{x}$ = 6.3 × 5.7 μm, *n* = 30), globose or subglobose, smooth to finely roughened, dark brown to black, with a longitudinal, hyaline, thin, germ slit.

Culture Characteristics

Colonies grew on PDA at 20°C in the dark attenuated 2 cm diam., within 5 days, flat, wooly, margin circular, with slight aerial mycelia, surface initially white, becoming grayish white and reverse yellowish white.

Specimen Examined

China, Guangdong Province, Shenzhen City, Futian District, northwest of Futian, Bijiashan Park, on twigs of *B. multiplex* (Lour.) Raeusch. ex Schult. f. (Poaceae), 23 September 2018, I.C. Senanayake, SI 84 (HKAS 107672), living culture, KUMCC 20-0206.

Notes

NCBI blast result for β-tubulin sequences of this isolate gives high sequence similarities to *A. guizhouense* (99.55%), *A. sacchari* (98.25%), *A. arundinis* (98.25%), and *A. marii* (95.62%) while *A. guizhouense* (93.41%) and *A. marii* (92.94%) for tef 1-α. Additionally, high blast similarities for ITS loci are *A. marii* (99.54%), *A. sacchari* (99.22%), *A. phaeospermum* (99.20%), *A. pseudospegazzinii* (98.13%), *A. longistromum* (98.72%), and *A. guizhouense* (99.83%) while *A. marii* (100%), *A. sacchari* (100%), *A. guizhouense* (100%), and *Apiospora montagnei* (100%) for LSU. In the phylogenetic analysis, this isolate (KUMCC 20-0206) clusters with the ex-holotype strain of *A. guizhouense* (CGMCC3.18334) with moderate support value (ML/PP = 87/0.95). Morphologically, this collection is closely similar to the holotype specimen of *A. guizhouense* having brown to black, smooth to finely roughened, globose or subglobose, conidia with pale brown, subglobose, ampulliform or doliiform conidiogenous cells. However, the holotype of *A. guizhouense* has been collected from the air in karst cave in Guizhou Province, China, and this collection was obtained from bamboo twigs in Guangdong Province. Hence, HKAS 107672 is identified as *A. guizhouense* based on morphology and phylogeny. This is the first record of *A. guizhouense* in Guangdong Province and on bamboo.

Arthrinium pseudorasikravindrae Senan., and Cheew. sp. nov. Figure 5

Index Fungorum number: IF 557870

Etymology: Species epithet the morphological similarity of this collection to *Arthrinium rasikravindrae.*

Holotype: HKAS 107669

Saprobic on sheaths of *B. dolichoclada* Hayata. *Mycelium* 1.5–3 μm in diam., consisting of smooth, hyaline, septate, branched, hyphae. *Sexual morph*: undetermined. Asexual morph: *Conidiophores* 10–15 × 3–7 μm ($\bar{x}$ = 12.3 × 5.2 μm, *n* = 30), basauxic, straight or flexuous, cylindrical, hyaline, thick, smooth-walled, aseptate. *Conidiogenous cells* 4–10 × 1.2–5 μm ($\bar{x}$ = 8.6 × 4.2 μm, *n* = 30), holoblastic, develop from conidiophore mother cells, ampulliform, cylindrical or doliiform, hyaline to olivaceous. *Conidia* 5–10 × 5.5–11 μm ($\bar{x}$ = 9.3 × 10.1 μm, *n* = 30), globose in face view, lenticular in side view, with a pale longitudinal slit, dark brown, thick-walled, finely roughened with one or two concentric pale rings.

Culture Characteristics

Colonies grew on PDA at 20°C in the dark attenuated 2 cm diam., within 5 days, flat, spreading, circular, margin filiform with abundant aerial mycelia, surface white to off-white and reverse pale yellow, sporulation occurs on 2% PDA incubated at 25°C after 2 weeks, black, conidial mass concentrated at colony margins. Sporulation occurred after 10 days on PDA incubated at 20°C in the dark without any host substrate. Conidia seem black mass and spread mostly in colony margins.

Specimen Examined

China, Guangdong Province, Shenzhen City, Futian District, northwest of Futian, Bijiashan Park, on sheath of *B. dolichoclada* Hayata (Poaceae), 23 September 2018, IS, SI 73 (HKAS 107669, holotype), ex-type culture, KUMCC 20-0208; *ibid* October 15, 2018, IS, SI 73-1 (HKAS 107670, paratype), ex-paratype culture KUMCC 20-0211.

Notes

Blast results of ITS, LSU, β-tubulin, and tef 1-α sequences of *A. pseudorasikravindrae* (KUMCC 20-0208, KUMCC 20-0211) show high similarity to *A. hydei*, *A. paraphaeospermum*, and *A. rasikravindrae.* In our phylogenetic analysis, *A. pseudorasikravindrae* forms a subclade (subclade C1, **Figure 1**)

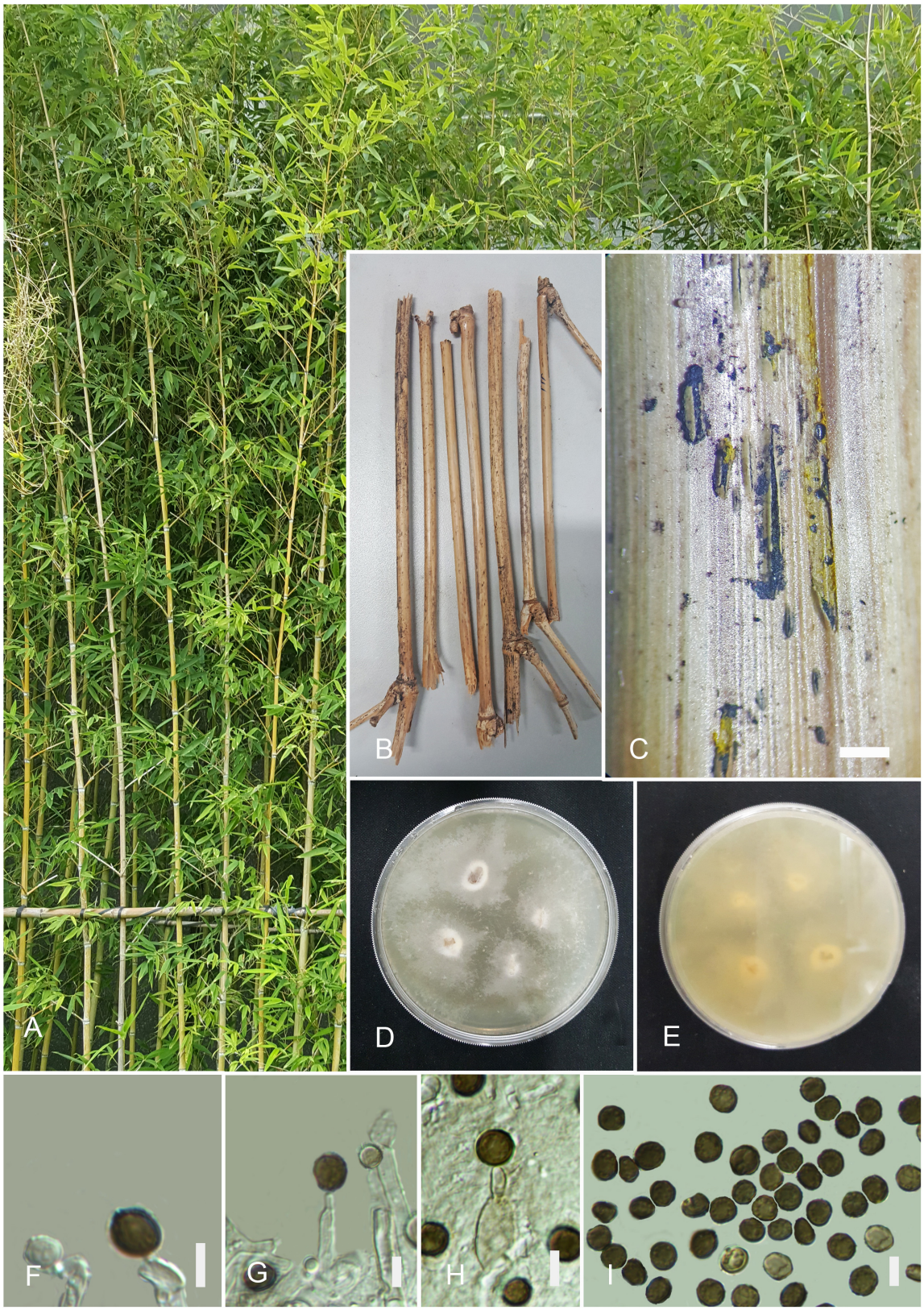


FIGURE 4 | *Arthrinium guizhouense* (HKAS 107672). **(A)** Host. **(B)** Fungarium specimen. **(C)** Conidiomata on substrate. **(D)** Surface view of culture on potato dextrose agar (PDA). **(E)** Reverse view of culture on PDA. **(F–H)** Conidia and conidiogenous cells. **(I)** Conidia. Scale bars: **(C)** = 1,000 μm, **(F–I)** = 5 μm.

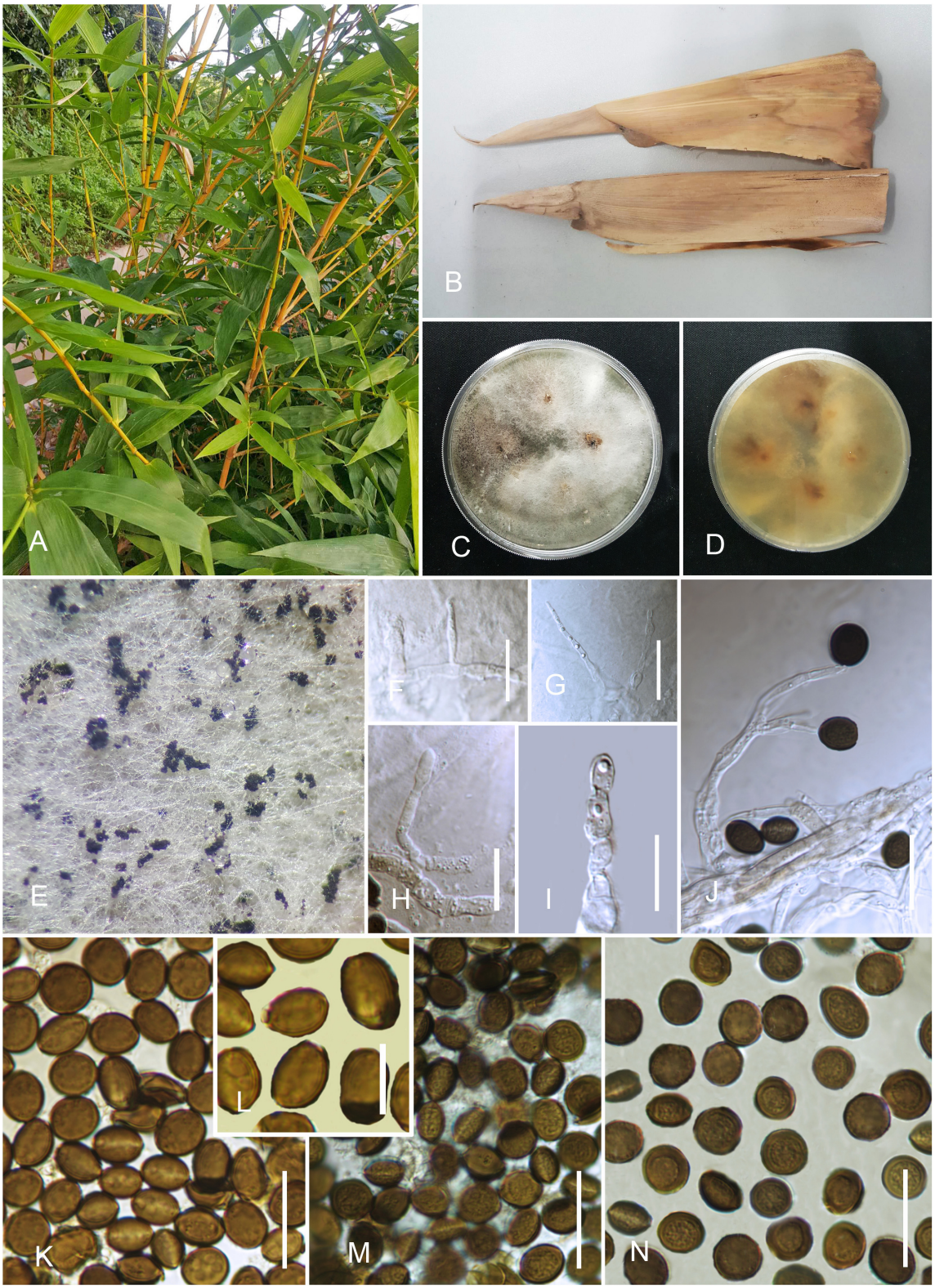


FIGURE 5 | *Arthrinium pseudorasikravindrae* (HKAS 107669). **(A)** Host. **(B)** Fungarium specimen. **(C)** Surface view of culture on potato dextrose agar (PDA). **(D)** Reverse view of culture on PDA. **(E)** Conidial mass on cultures. **(F–J)** Conidia, conidiogenous cells, and conidiophores. **(K–N)** Conidia (concentric pale rings are arrowed in **I**). Scale bars: **(F–N)** = 10 μm.

TABLE 2 | Morphological comparisons of species which are phylogenetically closely related to *Arthrinium acutiapicum* and *Arthrinium pseudorasikravindrae*.

Characters	*A. acutiapicum*	*A. chinense*	*A. paraphaeospermum*	*A. pseudorasikravindrae*	*A. rasikravindrae*
Host/substrate	*Bambusa bambos*/dead twigs	*Fargesia qinlingensis*/culms	*Bambusa* sp./culms	*Bambusa dolichoclada*/sheath	Soil, *Coffea arabica*/leaf, *Pinus thunbergii*/wood, marine submerged wood, *Oryza granulate*/leaf
Localities	China	China	Thailand	China	Norway, China, Japan
Life mode	Saprobic	Saprobic	Saprobic	Saprobic	Saprobic, endophytic
Conidiophore	Reduced to conidiogenous cells	Reduced to conidiogenous cells	Reduced to conidiogenous cells	10–15 × 3–7 μm, cylindrical, branched, aseptate thick-walled hyaline	5-90 × 1-1.5 μm, arising from swollen basal cells, unbranched, septate, thin-walled hyaline to subhyaline
Conidiogenous cell	4–7 × 2–3 μm, cylindrical to ampulliform with pointed apex, pale brown, apex hyaline	1.5–6.5 × 1–3.5 μm, aggregated in clusters on hyphae, doliiform to clavate or lageniform, hyaline to pale brown	25–30 × 4–6 μm, aggregated in clusters on hyphae, elongated, conical to ampulliform, hyaline	4–10 × 1.2–5 μm, phialidic with periclinal thickening, ampulliform, cylindrical or doliiform, hyaline to olivaceous	5–10 × 2–4 μm, phialidic with periclinal thickening, ampulliform, hyaline
Conidia	Monomorphous, 7.5–10 × 8.5–12 μm, globose in surface view, subglobose to oval in side view, brown to dark brown, smooth, apex and base blunted, dark equatorial slit	Monomorphous, 8.5–11 × 6.5–8 μm, subglobose to lenticular, brown to dark brown, smooth to finely roughened, a longitudinal germ slit	Dimorphous, globose 10–19 × 11–20 μm, ellipsoid to clavate 20–30 × 9–13 μm, brown, smooth to somewhat granular, with pale equatorial slit	Monomorphous, 5–10 × 5.5–11 μm, globose in surface view, lenticular in side view, dark brown, thick-walled, with a pale equatorial slit, finely roughened, one or two concentric pale rings	Dimorphous, lenticular 10-15 × 6-10.5 μm, elongate to clavate 15-25 × 7.5-10 μm, arising acropleurogenously, brown to olivaceous, smooth, two-walled, prominent truncate base and equatorial germ slit
References	This study	Jiang et al. (2020)	Hyde et al. (2016)	This study	Singh et al. (2012)

with strong bootstrap support values (ML/PP = 90/0.96), which is a sister to the newly introduced species *A. acutiapicum*. Additionally, *A. pseudorasikravindrae* shows close phylogenetic affinities to *A. chinense*, *A. paraphaeospermum*, and *A. rasikravindrae* (**Figure 1**).

Arthrinium pseudorasikravindrae is morphologically distinct from the above species (**Table 2**) by its thick-walled, finely roughened conidia with pale, equatorial slit and ampulliform, cylindrical or doliiform, basauxic conidiogenous cells. The morphology of *A. pseudorasikravindrae* is compared with other closely related species (**Table 2**). Therefore, considering morphological and molecular uniqueness, these isolates are introduced here as belonging to a new species, *A. pseudorasikravindrae*. HKAS 107669 and HKAS 107670 represent a distinct clade (clade A, **Figure 1**) which not known before in the phylogenetic analysis, and hence, these collections are introduced here as a new species based on their morphology and phylogeny.

DISCUSSION

Bamboo is an important group of flowering plants that helps to conserve and manage forest ecosystems and reduce soil erosion and it is also important for panda conservation and many more commercial applications such as making fishing rod, flute, paper, flooring material, etc. and as food for humans and livestock (Chapman and Peat, 1992). Members of bamboo belong to the family Poaceae comprising more than 115 genera with approximately 1,450 species (Gratani et al., 2008; Kelchner and Group, 2013), and bamboo occurs in all tropical, subtropical, and temperate regions as herbaceous or woody plants. Microfungi associate with bamboo in many ways and phytopathogenic or endophytic microfungi form diseases while saprobic microfungi help to decompose plant debris (Zhang and Wang, 1999; Hyde et al., 2002a,b).

The first monograph on bambusicolous fungi was published with 258 fungal species by Hino and Katumoto (1960), and 63 new species were introduced by Petrini et al. (1989). Eriksson and Yue (1998) provided a checklist of the ascomycetes on bamboo, while Zhang and Wang (1999) recorded 213 species described from bamboo in China. Kuai (1996) listed phytopathogenic bambusicolous fungi in China and Taiwan. Hyde et al. (2002a) reviewed bambusicolous fungi that grow on all bamboo substrates including the leaves, culms, branches, rhizomes, and roots and enlisted more than 1,100 species, which belong to 228 genera. Dai et al. (2018) have reviewed the taxonomy of bambusicolous fungi. This study is one of the articles in the series on bambusicolous microfungi in Guangdong Province. Herein, we collected *Arthrinium*-like taxa from bamboo plant samples from Shenzhen, Guangdong Province, China. Currently, there are 81 species in the *Arthrinium* (Species Fungorum, 2020) and only 61 have molecular data. More than 30% of holotypes of *Arthrinium* species have been collected in China (**Table 1**). Therefore, the aims of this paper were to study *Arthrinium*-like fungi in Guangdong Province and to introduce several putative new species by comparing them morphologically and genetically with existing taxa.

According to morphology and phylogeny, two novel *Arthrinium* species were obtained with two new locality records. Most phylogenetic studies on *Arthrinium* used ITS, β-tubulin, and tef 1-α; however, LSU has been added to the analyses

here. Negligible variations occur in tree topology in spite of adding LSU. *A. guizhouense* (HKAS 107672) is the first record in Guangdong Province and also from bamboo. The holotype of *A. guizhouense* was collected from the air in kart caves in Guizhou Province, China (Wang et al., 2018). This suggests that fungal conidioma in plant hosts release the conidia and conidia can survive in the air for a sufficiently long time. Our strain of *A. bambusae* is identical to the holotype which was collected from Guangdong Province on bamboo (Wang et al., 2018). Hence, this specimen can be used as an epitype if the holotype cannot be used for taxonomic purpose. The morphological differences between these two *Arthrinium* species are listed in **Table 2**. However, the life mode, host, and colony characters of these two species are not significantly different.

DATA AVAILABILITY STATEMENT

The datasets generated in this study can be found in online repositories. The names of the repository/repositories and accession number(s) can be found in the article/supplementary material.

AUTHOR CONTRIBUTIONS

IS designed the study, performed the morphological study and phylogenetic analyses, and wrote the manuscript. JB, NX, and RC reviewed and edited the manuscript. All authors approved the final manuscript.

FUNDING

This study was funded by Chiang Mai University postdoctoral research fund, Science and technology Project of Shenzhen City, Shenzhen Bureau of Science, Technology and Information (JCYJ20180305123659726), and National Natural Science Foundation of China (No. 31601014).

ACKNOWLEDGMENTS

We appreciate the kind support given by the laboratory staff of the College of Life Science and Oceanography, ShenzhenUniversity, Shenzhen, China, for the support in doing molecularwork. IS thanks Chiang Mai University and NX thanks the National Natural Science Foundation of China for funding this research. Our special thanks go to staff members of the Herbarium of Cryptogams, Kunming Institute of Botany, Academia Sinica (HKAS) and the Culture Collection of Kunming Institute of Botany (KUMCC) for depositing all the authentic cultures and fungarium specimens. IS thanks Dr. Shaun Pennycook for proposing Latin names of the new species.

REFERENCES

Agut, M., and Calvo, M. A. (2004). In vitro conidial germination in *Arthrinium aureum* and *Arthrinium phaeospermum*. *Mycopathologia* 157, 363–367. doi: 10.1023/B:MYCO.0000030432.08860.f3

Carbone, I., and Kohn, L. M. (1999). A method for designing primer sets for speciation studies in filamentous ascomycetes. *Mycologia* 91, 553–556. doi: 10.1080/00275514.1999.12061051

Chapman, G. P., and Peat, W. E. (1992). *An Introduction to Grasses (including Bamboos and Cereals)*. London: Redwood Press Ltd.

Chen, K., Wu, X. Q., Huang, M. X., and Han, Y. Y. (2014). First report of brown culm streak of *Phyllostachys praecox* caused by *Arthrinium arundinis* in Nanjing, China. *Plant Dis.* 98, 1274. doi: 10.1094/PDIS-02-14-0165-PDN

Cole, G. T. (1986). Models of cell differentiation in conidial fungi. *Microbiol. Rev.* 50, 95–132. doi: 10.1128/MMBR.50.2.95-132.1986

Crous, P. W., and Groenewald, J. Z. (2013). A phylogenetic re-evaluation of *Arthrinium*. *IMA Fungus* 4, 133–154. doi: 10.5598/imafungus.2013.04.01.13

Crous, P. W., Wingfield, M. J., Le Roux, J. J., Richardson, D. M., Strasberg, D., Shivas, R. G., et al. (2015). Fungal planet description sheets: 371-399. *Persoonia* 35, 264–327. doi: 10.3767/003158515X690269

Dai, D. Q., Jiang, H. B., Tang, L. Z., and Bhat, D. J. (2016). Two new species of *Arthrinium* (*Apiosporaceae*, *Xylariales*) associated with bamboo from Yunnan, China. *Mycosphere* 7, 1332–1345. doi: 10.5943/mycosphere/7/9/7

Dai, D. Q., Phookamsak, R., Wijayawardene, N. N., Li, W. J., Bhat, D. J., Xu, J. C., et al. (2017). Bambusicolous fungi. *Fungal Divers.* 82, 1–105. doi: 10.1007/s13225-016-0367-8

Dai, D. Q., Tang, L. Z., and Wang, H. B. (2018). "A review of bambusicolous ascomycetes," in *Bamboo: Current and Future Prospects*, ed. H. P. S. Abdul Khalil (IntechOpen), 210.

De Hoog, G. S., Guarro, J., Gene, J., and Figueras, M. J. (2000). *Atlas of Clinical Fungi*, 2nd Edn, Utrecht: Centraalbureau voor Schimmelcultures.

Eriksson, O., and Yue, J. Z. (1998). Bambusicolous pyrenomycetes, an annotated check-list. *Myconet* 1, 25–78.

Glass, N. L., and Donaldson, G. C. (1995). Development of primer sets designed for use with the PCR to amplify conserved genes from filamentous ascomycetes. *Appl. Environ. Microbiol.* 61, 1323–1330. doi: 10.1128/AEM.61.4.1323-1330.1995

Gratani, L., Crescente, M. F., Varone, L., Fabrini, G., and Digiulio, E. (2008). Growth pattern and photosynthetic activity of different bamboo species growing in the Botanical Garden of Rome. *Flora Morphol. Distrib. Funct. Ecol. Plants* 203, 77–84. doi: 10.1016/j.flora.2007.11.002

Hall, T. A. (1999). BioEdit: a user-friendly biological sequence alignment editor and analysis program for Windows 95/98/NT. *Nucleic Acids Symp. Ser.* 41, 95–98.

Hino, I., and Katumoto, K. (1960). *Icones Fungorum Bambusicolorum Japonicorum*. Kobe: The Fuji Bamboo Garden.

Hong, J. H., Jang, S., Heo, Y. M., and Min, M. (2015). Investigation of marine-derived fungal diversity and their exploitable biological activities. *Mar. Drugs* 13, 4137–4155. doi: 10.3390/md13074137

Hyde, K. D., Hongsanan, S., Jeewon, R., Bhat, D. J., McKenzie, E. H. C., Jones, E. B. G., et al. (2016). Fungal diversity notes 367-490: taxonomic and phylogenetic contributions to fungal taxa. *Fungal Divers.* 80, 1–270. doi: 10.1007/s13225-016-0373-x

Hyde, K. D., Zhou, D., and Dalisayl, T. (2002a). Bambusicolous fungi: a review. *Fungal Divers.* 9, 1–14.

Hyde, K. D., Zhou, D., McKenzie, E., Ho, W., and Dalisay, T. (2002b). Vertical distribution of saprobic fungi on bamboo culms. *Fungal Divers.* 11, 109–118.

Jiang, N., Li, J., and Tian, C. M. (2018). *Arthrinium* species associated with bamboo and reed plants in China. *Fungal Syst. Evol.* 2, 1–9. doi: 10.3114/fuse.2018.02.01

Jiang, N., Liang, Y. M., and Tian, C. M. (2020). A novel bambusicolous fungus from China, *Arthrinium chinense* (Xylariales). *Sydowia* 72, 77–83.

Katoh, K., Rozewicki, J., and Yamada, K. D. (2020). MAFFT online service: multiple sequence alignment, interactive sequence choice and visualization. *Brief. Bioinform.* 20, 1160–1166. doi: 10.1093/bib/bbx108

Kelchner, S. A., and Group, B. P. (2013). Higher level phylogenetic relationships within the bamboos (Poaceae: Bambusoideae) based on five plastid markers. *Mol. Phylogenet. Evol.* 67, 404–413. doi: 10.1016/j.ympev.2013.02.005

Kuai, S. Y. (1996). A checklist of pathogenic Bambusicolous fungi of mainland China and Taiwan. *J. For. Sci. Technol.* 4, 64–71.

Li, B. J., Liu, P. Q., Jiang, Y., Weng, Q. Y., and Chen, Q. H. (2016). First report of culm rot caused by *Arthrinium phaeospermum* on *Phyllostachys viridis* in China. *Plant Dis.* 100, 1013–1013. doi: 10.1094/PDIS-08-15-0901-PDN

Li, L., Chan, P. W., Wang, D., and Tan, M. (2015). Rapid urbanization effect on local climate: intercomparison of climate trends in Shenzhen and Hong Kong, 1968-2013. *Clim. Res.* 63, 145–155. doi: 10.3354/cr01293

Luo, Z.-L., Hyde, K. D., Liu, J.-K., Maharachchikumbura, S. S. N., Jeewon, R., Bao, D.-F., et al. (2019). Freshwater sordariomycetes. *Fungal Divers.* 99, 451–660. doi: 10.1007/s13225-019-00438-1

Martínez-Cano, C., Grey, W. E., and Sands, D. C. (1992). First report of *Arthrinium arundinis* causing kernel blight on barley. *Plant Dis.* 76:1077. doi: 10.1094/PD-76-1077B

Mavragani, D. C., Abdellatif, L., McConkey, B., Hamel, C., and Vujanovic, V. (2007). First report of damping-off of durum wheat caused by *Arthrinium sacchari* in the semi-arid Saskatchewan fields. *Plant Dis.* 91:469. doi: 10.1094/PDIS-91-4-0469A

Minter, D. W. (1985). A re-appraisal of the relationships between *Arthrinium* and other hyphomycetes. *Proc. Indian Acad. Sci.* 94, 281–308.

Nylander, J. A. A. (2004). *MrModeltest 2.0. Program Distributed by the Author*. Sweden: Evolutionary Biology Centre, Uppsala University.

Petrini, L. E., and Müller, E. (1986). Haupt-und nebenfruchtformen europäischer Hypoxylon-Arten (Xylariaceae, Sphaeriales) und verwandter Pilze. *Mycol. Helv.* 1, 501–627.

Petrini, O., Candoussau, F., and Petrini, L. (1989). Bambusicolous fungi collected in southwestern France 1982–1989. *Mycologia Helvetica* 3, 263–279.

Pintos, A., Alvarado, P., Planas, J., and Jarling, R. (2019). Six new species of *Arthrinium* from Europe and notes about *A. caricicola* and other species found in *Carex* spp. Hosts. *Mycokeys* 49, 15–48. doi: 10.3897/mycokeys.49.32115

Rai, M. K. (1989). Mycosis in man due to *Arthrinium phaeospermum* var. indicum. First case report of mycosis due to *Arthrinium phaeospermum* var. indicum in humans. *Mycoses* 32, 472–475. doi: 10.1111/j.1439-0507.1989.tb02285.x

Rambaut, A. (2009). *FigTree v1.4: Tree Figure Drawing Tool*. Available online at: http://tree.bio.ed.ac.uk/software/figtre?e/ (accessed July 25, 2020).

Rambaut, A., and Drummond, A. J. (2007). *Tracer v1, 4*. Available online at: http://beast.bio.ed.ac.uk/Tracer (accessed July 1, 2020).

Ramos, H. P., Braun, G. H., Pupo, M. T., and Said, S. (2010). Antimicrobial activity from endophytic fungi *Arthrinium* state of *Apiospora montagnei* Sacc. and *Papulaspora immersa*. *Braz. Arch. Biol. Technol.* 53, 629–632. doi: 10.1590/S1516-89132010000300017

Réblová, M., Miller, A. N., Rossman, A. Y., Seifert, K., Crous, P., Hawksworth, D., et al. (2016). Recommendations for competing sexual-asexually typified generic names in *Sordariomycetes* (except *Diaporthales, Hypocreales,* and *Magnaporthales*). *IMA Fungus* 7, 131–153. doi: 10.5598/imafungus.2016.07.01.08

Rehner, S. (2001). *Primers for Elongation Factor 1-α (EF1-α)*. Washington, DC: Insect Biocontrol Laboratory: USDA, ARS, PSI.

Ronquist, F., Teslenko, M., van der Mark, P., Ayres, D. L., Darling, A., Höhna, S., et al. (2012). MrBayes 3.2: efficient Bayesian phylogenetic inference and model choice across a large model space. *Syst Biol.* 61, 539–542. doi: 10.1093/sysbio/sys029

Schmidt, J. C., and Kunze, G. (1817). *Mykologische Hefte. 1*. Leipzig: Vossische Buchhandlung.

Senanayake, I. C., Jeewon, R., Hyde, K. D., Bhat, J. D., and Cheewangkoon, R. (2020a). Taxonomy and phylogeny of *Leptosillia cordylinea* sp. nov. from China. *Phytotaxa* 435, 213–226. doi: 10.11646/phytotaxa.435.3.1

Senanayake, I. C., Rathnayake, A. R., Marasinghe, D. S., Calabon, M. S., Gentekaki, E., Lee, H. B., et al. (2020b). Morphological approaches in studying fungi: collection, examination, isolation, sporulation and preservation. *Mycosphere* (in press).

Senanayake, I. C., Maharachchikumbura, S. S., Hyde, K. D., Bhat, J. D., Jones, E. G., Wendt, L., et al. (2015). Towards unraveling relationships in *Xylariomycetidae* (Sordariomycetes). *Fungal Divers.* 73, 73–144. doi: 10.1007/s13225-015-0340-y

Sharma, R., Kulkarni, G., Sonawane, M. S., and Shouche, Y. S. (2014). A new endophytic species of *Arthrinium* (*Apiosporaceae*) from *Jatropha podagrica*. *Mycoscience* 55, 118–123. doi: 10.1016/j.myc.2013.06.004

Shrestha, P., Ibáñez, A. B., Bauer, S., Glassman, S. I., Szaro, T. M., Bruns, T. D., et al. (2015). Fungi isolated from *Miscanthus* and sugarcane: biomass conversion, fungal enzymes, and hydrolysis of plant cell wall polymers. *Biotechnol. Biofuels* 8:1. doi: 10.1186/s13068-015-0221-3

Silvestro, D., and Michalak, I. (2012). raxmlGUI: a graphical front-end for RAxML. *Org. Divers. Evol.* 12, 335–337. doi: 10.1007/s13127-011-0056-0

Singh, S. M., Yadav, L. S., Singh, P. N., Hepat, R., Sharma, R., and Singh, S. K. (2012). *Arthrinium rasikravindrii* sp. nov. from Svalbard, Norway. *Mycotaxon* 122, 449–460. doi: 10.5248/122.449

Species Fungorum (2020). Available online at: http://www.speciesfungorum.org/Names/Names.asp (accessed July 10, 2020).

Stamatakis, A., and Alachiotis, N. (2010). Time and memory efficient likelihood-based tree searches on phylogenomic alignments with missing data. *J. Bioinform.* 26, 132–139. doi: 10.1093/bioinformatics/btq205

Vilgalys, R., and Hester, M. (1990). Rapid genetic identification and mapping of enzymatically amplified ribosomal DNA from several *Cryptococcus* species. *J. Bacteriol.* 172, 4238–4246. doi: 10.1128/JB.172.8.4238-4246.1990

Wang, M., Tan, X. M., Liu, F., and Cai, L. (2018). Eight new *Arthrinium* species from China. *Mycokeys* 34, 1–24. doi: 10.3897/mycokeys.34.24221

White, T. J., Bruns, T., Lee, S., and Taylor, J. (1990). Amplification and direct sequencing of fungal ribosomal RNA genes for phylogenetics. *PCR Protoc. Guide Methods Appl.* 18, 315–322. doi: 10.1016/B978-0-12-372180-8.50042-1

Wijayawardene, N. N., Hyde, K. D., Al-Ani, L. K. T., Tedersoo, L., Haelewaters, D., Fiuza, P. O., et al. (2020). Outline of Fungi and fungus-like taxa. *Mycosphere* 11, 1060–1456. doi: 10.5943/mycosphere/11/1/8

Zhang, L. Q., and Wang, X. G. (1999). Fungus resource of bamboos in China. *J. Bamboo Res.* 18, 66–72.

Zhao, Y. M., Deng, C. R., and Chen, X. (1990). *Arthrinium phaeospermum* causing dermatomycosis, a new record of China. *Acta Mycol.* 9, 232–235.

Conflict of Interest: The authors declare that the research was conducted in the absence of any commercial or financial relationships that could be construed as a potential conflict of interest.

Copyright © 2020 Senanayake, Bhat, Cheewangkoon and Xie. This is an open-access article distributed under the terms of the Creative Commons Attribution License (CC BY). The use, distribution or reproduction in other forums is permitted, provided the original author(s) and the copyright owner(s) are credited and that the original publication in this journal is cited, in accordance with accepted academic practice. No use, distribution or reproduction is permitted which does not comply with these terms.

frontiers in Microbiology

ORIGINAL RESEARCH
published: 07 January 2021
doi: 10.3389/fmicb.2020.596393

An Updated Global Species Diversity and Phylogeny in the Forest Pathogenic Genus *Heterobasidion* (Basidiomycota, Russulales)

*Yuan Yuan[1,2†], Jia-Jia Chen[3†], Kari Korhonen[4], Francis Martin[2,5] and Yu-Cheng Dai[2]**

[1] Institute of Microbiology, School of Ecology and Nature Conservation, Beijing Forestry University, Beijing, China, [2] Beijing Advanced Innovation Center for Tree Breeding by Molecular Design, Beijing Forestry University, Beijing, China, [3] Permanent Research Base of National Forestry and Grassland Administration, Jiangsu Vocational College of Agriculture and Forestry, Zhenjiang, China, [4] Natural Resources Institute Finland (Luke), Helsinki, Finland, [5] University of Lorraine, INRAE, Tree-Microbes Interaction Department, Champenoux, France

Heterobasidion species are amongst the most intensively studied polypores because several species are aggressive white rot pathogens of managed coniferous forests mainly in Europe and North America. In the present study, both morphological and multilocus phylogenetic analyses were carried out on *Heterobasidion* samples from Asia, Oceania, Europe and North America. Three new taxa were found, i.e., *H. armandii*, *H. subinsulare*, and *H. subparviporum* are from Asia and are described as new species. *H. ecrustosum* is treated as a synonym of *H. insulare*. So far, six taxa in the *H. annosum* species complex are recognized. *Heterobasidion abietinum*, *H. annosum*, and *H. parviporum* occur in Europe, *H. irregulare*, and *H. occidentale* in North America, and *H. subparviporum* in East Asia. The North American *H. irregulare* was introduced to Italy during the Second World War. Species in the *H. annosum* complex are pathogens of coniferous trees, except *H. subparviporum* that seems to be a saprotroph. Ten species are found in the *H. insulare* species complex, all of them are saprotrophs. The pathogenic species are distributed in Europe and North America; the Asian countries should consider the European and North American species as entry plant quarantine fungi. Parallelly, European countries should consider the American *H. occidentale* and *H. irregulare* as entry plant quarantine fungi although the latter species is already in Italy, while North America should treat *H. abietinum*, *H. annosum* s.s., and *H. parviporum* as entry plant quarantine fungi. Eight *Heterobasidion* species found in the Himalayas suggest that the ancestral *Heterobasidion* species may have occurred in Asia.

Keywords: taxonomy, phylogeny, new taxa, *Bondarzewiaceae*, pathogenic fungi

OPEN ACCESS

Edited by:
Peter Edward Mortimer, Kunming Institute of Botany, Chinese Academy of Sciences, China

Reviewed by:
Jan Stenlid, Swedish University of Agricultural Sciences, Sweden
Samantha Chandranath Karunarathna, Kunming Institute of Botany, China

***Correspondence:**
Yu-Cheng Dai
yuchengd@yahoo.com

† These authors have contributed equally to this work and share first authorship

Specialty section:
This article was submitted to Fungi and Their Interactions, a section of the journal Frontiers in Microbiology

Received: *19 August 2020*
Accepted: *30 November 2020*
Published: *07 January 2021*

Citation:
Yuan Y, Chen J-J, Korhonen K, Martin F and Dai Y-C (2021) An Updated Global Species Diversity and Phylogeny in the Forest Pathogenic Genus Heterobasidion (Basidiomycota, Russulales). Front. Microbiol. 11:596393. doi: 10.3389/fmicb.2020.596393

INTRODUCTION

The polypore genus *Heterobasidion* Bref., which belongs to the family *Bondarzewiaceae*, is one of the most intensively studied basidiomycetous genera because some species of *Heterobasidion* are aggressive pathogens of managed coniferous forests in Europe and North America (Woodward et al., 1998). Two morphological taxa, *H. annosum* (Fr.) Bref. and *H. insulare* (Murrill) Ryvarden, had generally been accepted in *Heterobasidion* (Murrill, 1908; Gilbertson and Ryvarden, 1986; Ryvarden and Gilbertson, 1993; Núñez and Ryvarden, 2001). However, mating studies have revealed that both *H. annosum* and *H. insulare* are in fact species complexes (Korhonen, 1978; Dai and Korhonen, 1999; Dai et al., 2002, 2003).

Three species, *Heterobasidion abietinum* Niemelä and Korhonen (Eur F-group), *H. annosum* (Fr.) Bref. sensu stricto (Eur P-group) and *H. parviporum* Niemelä and Korhonen (Eur S-group), have been recognized in Europe (Niemelä and Korhonen, 1998), and two species, *H. irregulare* Garbel. and Otrosina (NAm P-group) and *H. occidentale* Otrosina and Garbel. (NAm S-group), were described from North America (Otrosina and Garbelotto, 2010). Based on mating studies, the East Asian taxon in the *H. annosum* species complex was considered as *H. parviporum* (Dai and Korhonen, 1999, 2003; Dai et al., 2006; Dai, 2012; Chen et al., 2015). Similarly, investigations based on mating tests, morphological characteristics and molecular analyses revealed several species also within the Asian *H. insulare* complex: *H. linzhiense* Y. C. Dai and Korhonen (Dai et al., 2007), *H. australe* Y. C. Dai and Korhonen (2009), *H. ecrustosum* Tokuda, T. Hatt. and Y. C. Dai, *H. orientale* Tokuda, T. Hatt. and Y. C. Dai (Tokuda et al., 2009), *H. amyloideum* Y. C. Dai, Jia J. Chen and Korhonen, *H. tibeticum* Y. C. Dai, Jia J. Chen and Korhonen (Chen et al., 2014) and *H. amyloideopsis* Saba, C. L. Zhao, Khalid and Pfister (Zhao et al., 2017). In addition, *H. araucariae* P. K. Buchanan from Australia and adjacent regions (Buchanan, 1988) was confirmed to be a member of the *H. insulare* species complex (Chen et al., 2015).

Earlier phylogenetic analyses on the *H. annosum* complex used sequences of the internal transcribed spacer (ITS) and intergenic spacer (IGS) regions of the nuclear genes, and manganese peroxidase genes, and laccase genes (Maijala et al., 2003; Asiegbu et al., 2004). Later, several attempts were made to resolve the taxonomy of the *H. annosum* complex or *H. insulare* complex using multilocus phylogenetic approaches (Johannesson and Stenlid, 2003; Ota et al., 2006; Linzer et al., 2008; Chen et al., 2014). Recently, five species in the *H. annosum* species complex and eight species in *H. insulare* species complex were also recognized and confirmed by multilocus phylogenetic approaches, and divided into three groups based on five nuclear genes and two mitochondrial genes, i.e., ITS, the large nuclear ribosomal RNA subunit (nrLSU), the largest subunit of RNA polymerase II (RPB1), the second subunit of RNA polymerase II (RPB2), glyceraldehyde 3-phosphate dehydrogenase (GAPDH), mitochondrial ATP synthase subunit 6 (ATP6), and mitochondrial small subunit rDNA (mtSSU) (Chen et al., 2015).

Several hypotheses on the evolutionary scenarios of the *Heterobasidion* have been put forward (Otrosina et al., 1993; Ota et al., 2006; Linzer et al., 2008). Dalman et al. (2010) proposed that the *H. annosum* complex originated in Laurasia, *H. annosum* s.s./*H. irregulare* arose in Eurasia, and *H. parviporum*/*H. abietinum*/*H. occidentale*, which occurred in eastern Asia or western North America, emerged between 45 and 60 Ma in the Palaearctic; this conclusion was based on non-coding regions of elongation factor 1-α (EFA), glutathione-S-transferase (GST1), GAPDH, and transcription factor (TF). Recently, based on more species and samples of *Heterobasidion* and the fossil record, molecular dating suggested that ancestral *Heterobasidion* species originated in Eurasia occurred mainly during the Early Miocene (Chen et al., 2015; Zhao et al., 2017).

Based on a larger set of *Heterobasidion* samples from Asia, Oceania, Europe and North America, and using combined RPB1 and RPB2 sequence dataset, a further phylogenetic investigation on the genus is carried out. Four new taxa are detected, and three of them are described and illustrated in the present paper. Moreover, most relevant morphological characteristics of different species of *Heterobasidion* are compared.

MATERIALS AND METHODS

Morphological Studies

The studied specimens and cultures (**Table 1**) are deposited at the herbaria of Institute of Microbiology of the Beijing Forestry University (BJFC, Beijing, China), Natural Resources Institute Finland (Luke, Helsinki, Finland), U.S. Forest Service, Northern Research Station (CFMR, Madison, WI, United States), private herbarium of J. Vlasák (JV, České Budějovice, Czechia), and Landcare Research, New Zealand (PDD, Lincoln, New Zealand). Ecology and some macromorphological characters were based on field notes. Anatomy was studied, and measurements and drawings were made from slide preparations stained with Cotton Blue. Drawings were made with the aid of a drawing tube. In presenting the variation in the size of the spores, the 5% of the measurements at each end of the range are shown in parentheses. Basidiospore spine lengths are not included in the measurements. The following abbreviations are used: IKI = Melzer's reagent, IKI− = both non-amyloid and non-dextrinoid, IKI+ = amyloid, KOH = 5% potassium hydroxide, CB = Cotton Blue, CB+ = cyanophilous, L = mean spore length (arithmetic average of all spores), W = mean spore width (arithmetic average of all spores), Q = variation in the L/W ratios between the specimens studied, n = number of spores measured from given number of specimens. Color terms are from Petersen (1996).

DNA Extraction, PCR Amplification and Sequencing

The Rapid Plant Genome kit based on acetyl trimethylammonium bromide extraction (Aidlab Biotechnologies Co., Ltd., Beijing, China) was used to

TABLE 1 | Information on samples of *Heterobasidion* used in this study.

Species	Sample no.	Geographic origin	Host	GenBank accessions				
				ITS	nrLSU	RPB1	RPB2	GAPDH
Bondarzewia occidentalis	HHB 14803	Washington, United States	*Picea sitchensis*	DQ200923	DQ234539	DQ256049	AY218474	–
B. submesenterica	Cui 10724	Sichuan, China	*Abies ernestii*	KJ583205	KJ583219	KJ651627	KJ651720	KJ651752
Heterobasidion abietinum	00053/1	Trentino, Italy	*Picea abies*	KJ651451	KJ651509	KJ651630	KJ651723	KJ651754
H. abietinum	00055/6	Trentino, Italy	*Picea abies*	KJ651452	KJ651510	KJ651631	KJ651724	KJ651755
H. abietinum	00057/2	Trentino, Italy	*Abies alba*	KJ651453	KJ651511	KJ651632	KJ651725	KJ651756
H. amyloideum	**Cui 12656**	**Tibet, China**	***Pinus***	**MT146480**	**MT446029**	**MT157738**	**MT157761**	**MT157721**
H. amyloideum	**Cui 12274**	**Tibet, China**	***Abies***	**MT146481**	**MT446030**	**MT157739**	**MT157762**	**MT157722**
H. annosum	06071/1	Lazio, Italy	*Pinus pinea*	KJ651458	KJ651516	KF453497	KF453491	KJ651761
H. annosum	06125/2	Krasnoyarsk, Russia	*Pinus sylvestris*	KJ651459	KJ651517	KF453498	KF453492	KJ651762
H. annosum	06129/6	Krasnoyarsk, Russia	*Pinus sylvestris*	KJ583211	KJ583225	KF006499	KF033133	KJ651763
H. araucariae	65008	Queensland, Australia	*Araucaria cunninghamii*	KJ651462	KJ651520	KJ651636	KJ651729	KJ651766
H. araucariae	82001	Queensland, Australia	*Araucaria cunninghamii*	KJ651463	KJ651521	KJ651637	KJ651730	KJ651767
H. armandii	**Dai 17605**	**Yunnan, China**	***Pinus armandii***	**MT146482**	**MT446031**	**MT157740**	**MT157763**	–
H. armandii	**Dai 17606**	**Yunnan, China**	***Pinus armandii***	**MT146483**	**MT446032**	**MT157741**	**MT157764**	–
H. armandii	**Dai 17607**	**Yunnan, China**	***Pinus armandii***	**MT146484**	**MT446033**	**MT157742**	**MT157765**	–
H. australe	**Cui 12602**	**Yunnan, China**	***Pinus* sp.**	**MT146485**	**MT446034**	**MT157743**	**MT157766**	**MT157723**
H. australe	**Dai 13507**	**Yunnan, China**	***Pinus* sp.**	**MT146486**	**MT446035**	**MT157744**	**MT157767**	**MT157724**
H. australe	**Dai 13863**	**Yunnan, China**	***Pinus* sp.**	**MT146487**	**MT446036**	**MT157745**	**MT157768**	**MT157725**
H. insulare	**FPRI 429**	**Philippines**	***Pinus* sp.**	**MT146488**	**MT446037**	**MT157746**	**MT157769**	**MT157726**
H. insulare	**Dai 13933**	**Chongqing, China**	***Pinus massoniana***	**MT146489**	**MT446038**	**MT157747**	**MT157770**	**MT157727**
H. insulare	**Dai 15095**	**Jiangxi, China**	***Pinus massoniana***	**MT146490**	**MT446039**	**MT157748**	**MT157771**	**MT157728**
H. irregulare	57001/TI	North Carolina, United States	*Pinus strobus*	KJ651473	KJ651531	KJ651638	KJ651731	KJ651777
H. irregulare	88010/1	Vermont, United States	*Pinus* sp.	KJ651475	KJ651533	KJ651640	KJ651733	KJ651779
H. irregulare	01062	Ontario, Canada	*Pinus resinosa*	KJ651477	KJ651535	KJ651642	KJ651735	KJ651781
H. linzhiense	Cui 7216	Sichuan, China	*Abies* sp.	KJ651480	KJ651538	KF006524	KF033148	KJ651784
H. linzhiense	Cui 9645	Tibet, China	*Picea* sp.	KJ651481	KJ651539	KF033147	KF006523	KJ651785
H. linzhiense	Dai 5408	Tibet, China	*Picea* sp.	KJ651484	KJ651542	KF033154	KF006533	KJ651788

(Continued)

TABLE 1 | Continued

Species	Sample no.	Geographic origin	Host	GenBank accessions				
				ITS	nrLSU	RPB1	RPB2	GAPDH
H. occidentale	79034/TI	Alaska, United States	*Picea* sp.	KJ651485	KJ651543	KJ651645	KJ651738	KJ651789
H. occidentale	98004/TI	Oregon, United States	*Picea engelmannii*	KJ651488	KJ651546	KJ651648	KJ651741	KJ651792
H. occidentale	98005/TI	Oregon, United States	*Abies magnifica* var. *shastensis*	KJ651489	KJ651547	KJ651649	KJ651742	KJ651793
H. orientale	**Cui 11637**	**Heilongjiang, China**	**Unknown**	**MT146491**	**MT446040**	**MT157749**	**MT157772**	**MT157729**
H. orientale	**Cui 11815**	**Heilongjiang, China**	***Pinus* sp.**	**MT146492**	**MT446041**	**MT157750**	**MT157773**	**MT157730**
H. orientale	**Cui 12026**	**Heilongjiang, China**	***Picea* sp.**	**MT146493**	**MT446042**	**MT157751**	**MT157774**	**MT157731**
H. parviporum	04121/3	Artjärvi, Finland	*Picea abies*	KJ583212	KJ583226	KF453493	KF453499	KJ651800
H. parviporum	08021/7	Krasnoyarsk, Russia	*Picea abies*	KJ651498	KJ651556	KF453494	KF453500	KJ651803
H. parviporum	08123/TI	Irkutsk, Russia	*Picea abies*	KJ651500	KJ651558	KF453495	KF453501	KJ651805
H. sp.	Korhonen 05030	California, United States	*Pinus ponderosa*	MT146494	MT446043	MT157752	MT157775	–
H. sp.	Korhonen 05038	California, United States	*Pinus ponderosa*	MT146495	MT446044	MT157753	MT157776	–
H. sp.	Korhonen 05039	California, United States	*Pinus ponderosa*	MT146496	MT446045	MT157754	MT157777	–
H. subinsulare	**Dai 13842**	**Yunnan, China**	***Pinus* sp.**	**MT146497**	**MT446046**	**MT157755**	**MT157778**	**MT157732**
H. subinsulare	**Li 140804-30**	**Yunnan, China**	***Pinus* sp.**	**MT146498**	**MT446047**	**MT157756**	**MT157779**	**MT157733**
H. subparviporum	Cui 6961	Hubei, China	*Abies fargesii*	KJ651504	KJ651562	KJ651658	KJ651751	KJ651809
H. subparviporum	**Cui 9267**	**Tibet, China**	***Picea* sp.**	**MT146499**	**MT446048**	**MT157757**	**MT157780**	**MT157734**
H. subparviporum	**Dai 14803**	**Jilin, China**	***Picea* sp.**	**MT146500**	**MT446049**	**MT157758**	**MT157781**	**MT157735**
H. tibeticum	**Cui 12257**	**Tibet, China**	***Pinus* sp.**	**MT146501**	**MT446050**	**MT157759**	**MT157782**	**MT157736**
H. tibeticum	**Cui 12335**	**Tibet, China**	***Pinus* sp.**	**MT146502**	**MT446051**	**MT157760**	**MT157783**	**MT157737**

New sequences are shown in bold.

extract genomic DNA from dried fungal specimens and cultures, according to the manufacturer's instructions with some modifications (Chen et al., 2014). The PCR primers for all genes are listed in **Table 2**. The PCR procedure for nrLSU was as follows: initial denaturation at 94°C for 1 min, followed by 35 cycles at 94°C for 30 s, 50°C for 1 min, 72°C for 1.5 min, and a final extension at 72°C for 10 min. The following PCR protocol for GAPDH, and ITS was used: initial denaturation at 95°C for 3 min, followed by 35 cycles at 94°C for 40 s, (50°C for GAPDH, 54°C for ITS), 72°C for 1 min, and a final extension at 72°C for 10 min. The PCR procedure for *RPB1* and *RPB2* followed Justo and Hibbett (2011) with slight modifications: initial denaturation at 94°C for 2 min, followed by 10 cycles at 94°C for 40 s, 60°C for 40 s, 72°C for 2 min, then followed by 37 cycles at 94°C for 45 s, 55°C for 1.5 min and 72°C for 2 min, and a final extension at 72°C for 10 min. PCR products were purified with a Gel Extraction and PCR Purification Combo Kit (Spin-column) in Beijing Genomics Institute, Beijing, China. The purified products were then sequenced on an ABI-3730-XL DNA Analyzer (Applied Biosystems, Foster City, CA, United States) using the same primers as in the original PCR amplifications. All newly generated sequences were deposited at GenBank[1] and listed in **Table 1**.

[1]http://www.ncbi.nlm.nih.gov/

TABLE 2 | PCR primers used in this study.

Gene	Primer	Primer sequences (5′-3′)[a]	References
GAPDH	GAPDH-F	YGG TGT CTT CAC CAC CAC YGA SSA	Johannesson et al., 2000
	GAPDH-R	RTA NCC CCA YTC RTT RTC RTA CCA	Johannesson et al., 2000
ITS	ITS5	GGA AGT AAA AGT CGT AAC AAG G	White et al., 1990
	ITS4	TCC TCC GCT TAT TGA TAT GC	White et al., 1990
nrLSU	LROR	ACC CGC TGA ACT TAA GC	Vilgalys and Hester, 1990
	LR7	TAC TAC CAC CAA GAT CT	Vilgalys and Hester, 1990
RPB1	RPB1-Af	GAR TGY CCD GGD CAY TTY GG	Matheny et al., 2002
	RPB1-Cf	CCN GCD ATN TCR TTR TCC ATR TA	Matheny et al., 2002
RPB2	fRPB2-5F	GAY GAY MGW GAT CAY TTY GG	Liu et al., 1999; Matheny, 2005
	fRPB2-7cR	CCC ATR GCT TGY TTR CCC AT	Liu et al., 1999; Matheny, 2005

[a]*Degeneracr codes: S = G or C, W = A or T, R = A or G, Y = C or T, N = A or T or C or G, D = G or A or T, M = A or C.*

Phylogenetic Analysis

Bondarzewia occidentalis Jia J. Chen, B. K. Cui and Y. C. Dai and *B. submesenterica* Jia J. Chen, B. K. Cui and Y. C. Dai were used as outgroups (Chen et al., 2015). Sequences were aligned with BioEdit (Hall, 1999) and ClustalX (Thompson et al., 1997). Sequence alignments were deposited at TreeBase[2] (submission ID 25908).

Maximum parsimony (MP) analysis was applied to single-locus genealogies for ITS, nrLSU, RPB1, PPB2, and GAPDH, and combination datasets that contained the RPB1-RPB2 sequences. The tree construction procedure was performed in PAUP* version 4.0b10 (Swofford, 2002). All characters were equally weighted, and gaps were treated as missing data. Trees were inferred using the heuristic search option with TBR branch swapping and 1000 random sequence additions. Max-trees were set to 5000, branches of zero length were collapsed, and all parsimonious trees were saved. Clade robustness was assessed using a bootstrap analysis with 1000 replicates (Felsenstein, 1985). Descriptive tree statistics tree length (TL), consistency index (CI), retention index (RI), rescaled consistency index (RCI), and homoplasy index (HI), were calculated for each maximum parsimonious tree generated. Phylogenetic trees were visualized using Treeview (Page, 1996).

MrMODELTEST2.3 (Nylander, 2004) was used to determine the best-fit evolution model for the combined dataset for Bayesian inference (BI). The BI was calculated with MrBayes 3.1.2 (Ronquist and Huelsenbeck, 2003) with a general time reversible model of DNA substitution and an invgamma distribution rate variation across sites. Eight Markov chains were run from random starting tree for 1 M generations of RPB1 and RPB2 dataset, and sampled every 100 generations. The burn-in was set to discard the first 25% of the trees. A majority rule consensus tree of all remaining trees was calculated. Branches that received bootstrap values for MP and Bayesian posterior probabilities (BPP) greater than or equal to 75% (MP) and 0.95 (BPP) were considered as significantly supported.

To determine if the datasets were significantly conflicted, the partition homogeneity test option in PAUP 4.0b was used between the loci in all possible pairwise combinations using 1000 replicates and the heuristic general search option. This test randomly shuffles phylogenetically informative sites between two paired loci: if the datasets are compatible, shuffling sites between the loci should not produce summed tree lengths that are significantly greater than those produced by the observed data (Farris et al., 1994; Huelsenbeck et al., 1996).

[2]https://treebase.org/treebase-web/home.html

RESULTS

Molecular Phylogeny

All targeted DNA loci were successfully amplified and sequenced from our *Heterobasidion* samples and the outgroup species. Partition homogeneity test showed no conflicts for the RPB1 and RPB2 combined loci ($P = 0.019$, $P \geq 0.01$). Therefore, the amino acid sequences from RPB1 and RPB2 were combined into a single sequence set. The combined dataset included sequences from 46 specimens representing 18 species. The dataset had an aligned length of 2505 characters, of which 1796 characters were constant, 671 were variable and parsimony-uninformative, and 38 were parsimony-informative. The maximum parsimony analysis yielded four equally parsimonious tree (TL = 1033, CI = 0.789, HI = 0.925, RI = 0.730, RC = 0.211). The best model for the combined RPB1 + RPB2 estimated and applied in the Bayesian analysis: GTR + I + G, lset nst = 6, rates = invgamma; prset statefreqpr = dirichlet (1,1,1,1). The Bayesian analysis resulted in a topology similar to the MP analysis, with an average standard deviation of split frequencies = 0.006737, and only the MP tree was provided. Both bootstrap values (>50%) and BPPs (≥0.90) were shown at the nodes (**Figure 1**).

Three new species, *Heterobasidion armandii*, *H. subinsulare*, and *H. subparviporum* formed a well-supported phylogenetic lineages, respectively (100% MP, and 1 BPPs), and phylogenetically distinct from other known species of *Heterobasidion*.

According to the present phylogenetic analyses, *Heterobasidion* spp. consists of three lineages: (1) the lineage associated to pines, firs and spruces (*H. amyloideopsis*, *H. amyloideum*, *H. araucariae*, *H. armandii*, *H. australe*, *H. insulare*, *H. linzhiense*, *H. orientale*, *H. subinsulare*, and *H. tibeticum*); (2) lineage mainly associated to pines (*H. annosum*

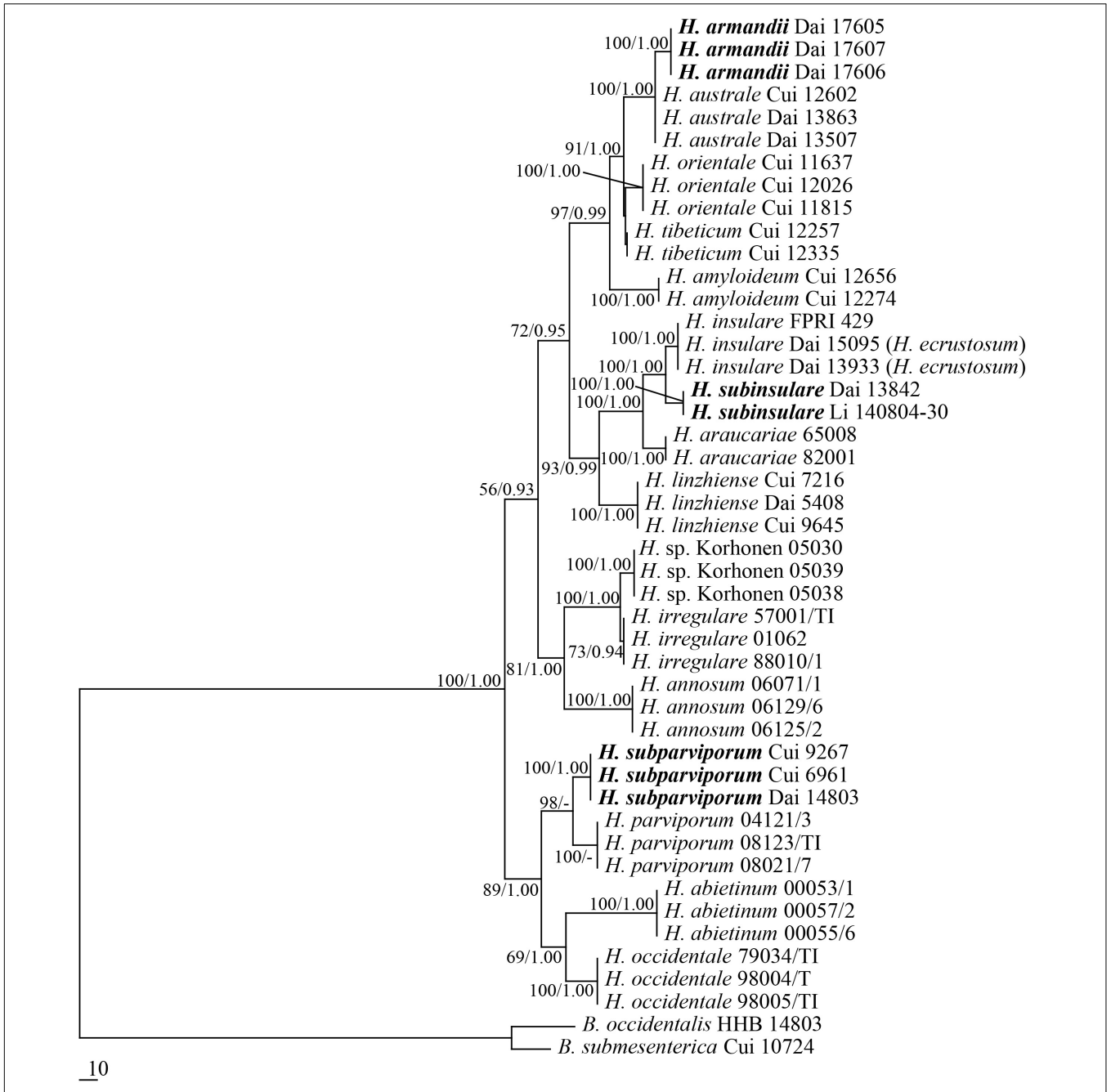


FIGURE 1 | Phylogeny of *Heterobasidion* and related species generated by Maximum Parsimony based on combined RPB1 + RPB2 sequences. Parsimony bootstrap values (before the slash markers) higher than 50% and Bayesian posterior probabilities (after the slash markers) more than 0.95 were indicated along branches.

s.s., *H.* sp. and *H. irregulare*); and (3) the lineage associated to firs and spruces (*H. abietinum*, *H. occidentale*, *H. parviporum*, and *H. subparviporum*).

Taxonomy

Heterobasidion armandii Y. C. Dai, Jia J. Chen and Yuan Yuan, sp. nov. Figures 2, 3

MycoBank MB 834572.

Type

China, Yunnan Province, Xiping County, Mopanshan Forest Park, alt.135 m, on stump of *Pinus armandii*, June 15, 2017, YC Dai 17605 (BJFC025137, holotype).

Diagnosis

Differs from other *Heterobasidion* species by its contextual skeletal hyphae are positive in Melzer's reagent, absence of



FIGURE 2 | Basidiocarps of *Heterobasidion armandii* (holotype, Dai 17605). Bar = 2 cm.

cystidia, presence of cystidioles, and subglobose to broadly ellipsoid basidiospores measuring 4.9−5.9 × 3.9−4.5 μm.

Etymology

Armandii (Lat.): referring to the species growing on *P. armandii*.

Description

Basidiocarps annual, pileate, usually imbricate, leathery and without odor or taste when fresh, corky when dry. *Pilei* semicircular to fan-shaped, projecting up to 3 cm, 7 cm wide, and 8 mm thick at base. *Pileal surface* white to cream when juvenile, becoming olivaceous buff with age, at least reddish brown to dark reddish brown at base, crustose, distinctly zonate; margin cream, blunt. *Pore surface* white when fresh, cream when dry, not glancing; *pores* mostly round to angular, (3−)4−5 per mm; dissepiments thin, entire to slightly lacerate. *Context* cream, woody hard when dry, azonate, up to 5 mm thick, with a thin black line under crust except for the margin. *Tubes* cream to buff, hard corky, up to 3 mm long. *Hyphal system* dimitic; generative hyphae without clamp connections; tramal skeletal hyphae dextrinoid, CB+, contextual skeletal hyphae weakly IKI+, CB+; hyphae unchanged in KOH (not dissolved). Contextual generative hyphae frequently present, colorless, thin- to slightly thick-walled, frequently simple septate, occasionally branched, 3–4 mm diam; contextual skeletal hyphae dominant, colorless, thick-walled with a wide to narrow lumen, rarely branched, flexuous, interwoven, 4–5.5 mm diam. Tramal generative hyphae infrequent, hyaline, thin-walled, frequently simple septate, occasionally branched, 2–3 mm diam; tramal skeletal hyphae dominant, hyaline, thick-walled with a wide to narrow lumen, rarely branched, flexuous, strongly interwoven without orientation, 3–4 mm diam. *Cystidia* absent. *Cystidioles* present, fusiform, occasionally with an apical simple septum. *Basidia* clavate to ampullaceal, with a simple basal septum and four sterigmata, 14−24 × 6−8 mm. *Basidioles* in shape similar to basidia, but distinctly shorter. *Basidiospores* subglobose to broadly ellipsoid, hyaline, fairly thick-walled, asperulate, mostly bearing a small guttule, IKI−, CB+, (4.8−)4.9−5.9(−6) × (3.8−)3.9−4.5(−4.8) mm, L = 5.12 mm, W = 4.11 mm, Q = 1.24–1.25 (n = 60/2).

Additional materials (paratypes) examined

China, Yunnan Province, Xiping County, Mopanshan National Park, alt.1450 m, on stump of *P. armandii*, June 15, 2017, Dai 17606 (BJFC025138), Dai 17607 (BJFC025139); August 16, 2019, Dai 20410 (BJFC032078). Luquan County, Jiaozishan Forest Park, alt.2650 m, on stump of *P. armandii*, November 4, 2018, Dai 19258 (BJFC027726), Dai 19259 (BJFC027727), Dai 19260 (BJFC027728) and Dai 19261 (BJFC027729).

Heterobasidion subinsulare Y. C. Dai, Jia J. Chen and Yuan Yuan, sp. nov. Figures 4, 5

MycoBank MB 834573.

Type

China, Yunnan Province, Tengchong County, Shuanghe Village, on stump of *Pinus* sp., August 5, 2014, YC Dai 13842 (BJFC017572, holotype).

Diagnosis

Differs from *Heterobasidion* species by big pores (1–3 per mm), a non-glancing pore surface, its contextual skeletal hyphae are negative in Melzer's reagent, presence of cystidia and cystidioles, and subglobose to broadly ellipsoid basidiospores measuring 5−5.7 × 3.8−5 μm.

Etymology

Subinsulare (Lat.): referring to the similarity to *H. insulare*.

Description

Basidiocarps annual, effused-reflexed to pileate, usually imbricate, leathery and without odor or taste when fresh, woody hard when dry. *Pilei* semicircular to fan-shaped, projecting up to 4 cm, 10 cm wide, and 4 cm thick at base. *Pileal surface* cream when dry, becoming buff to buff-yellow, crustose, azonate; margin buff-yellow to honey-yellow, blunt. *Pore surface* white when fresh, buff to clay-buff when dry, not glancing; pores angular to elongated, 1–3 per mm; dissepiments thin, entire to slightly lacerate. *Context* cream to buff-yellow, corky when dry, azonate, up to 0.5 cm thick. *Tubes* white to buff, hard corky, up to 3.5 cm long. *Hyphal system* dimitic; generative hyphae without clamp connections; skeletal hyphae CB+, dextrinoid near to the tube mouths, IKI− in other parts; hyphae unchanged in KOH (not dissolved). Contextual generative hyphae frequent, hyaline, thin- to slightly thick-walled, frequently simple septate and branched, 2–4 μm diam.; contextual skeletal hyphae dominant, hyaline, thick-walled with a wide lumen, rarely branched, flexuous, interwoven, 2.5–6 μm diam. Tramal generative hyphae frequent, hyaline, thin- to slightly thick-walled, occasionally simple septate, frequently branched, 2–3.5 μm diam; tramal skeletal hyphae dominant, hyaline, thick-walled with a wide lumen, rarely branched, flexuous, strongly interwoven without orientation, 2–5 μm diam. *Cystidia* present, thin-walled, clavate, moniliform or ventricose, 27−40 × 4−8 mm. *Cystidioles* present, thin-walled, fusiform, mostly with an apical simple septum, 22−25 × 4−8 μm. *Basidia* clavate to uniform, with a

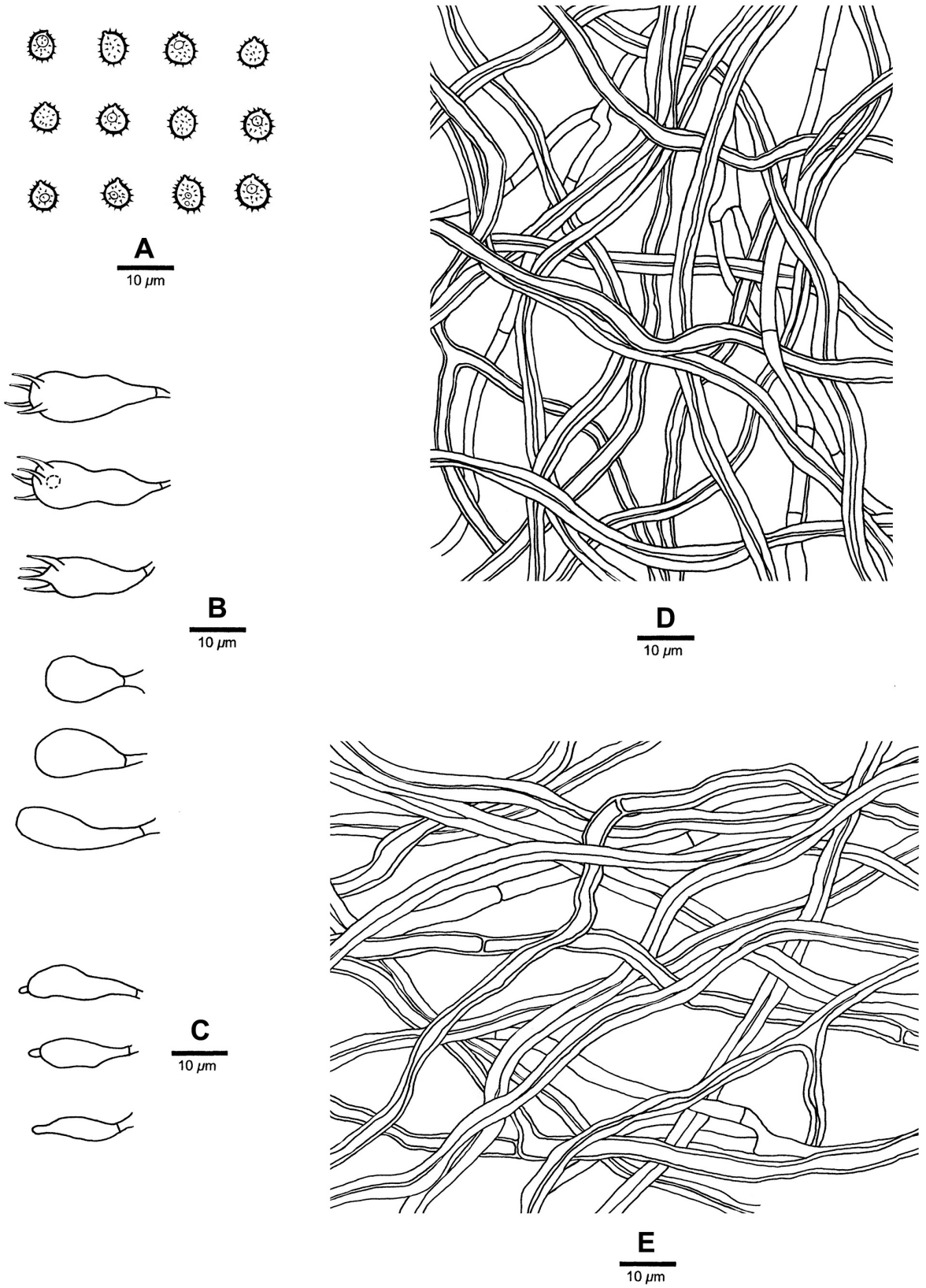


FIGURE 3 | Microscopic structures of *Heterobasidion armandii* (drawn from the holotype). **(A)** Basidiospores; **(B)** Basidia and basidioles; **(C)** Cystidioles; **(D)** Hyphae from trama; **(E)** Hyphae from context.

simple basal septum and four sterigmata, 18−28 × 4−6 μm. *Basidioles* in shape similar to basidia, but distinctly shorter. *Basidiospores* subglobose to broadly ellipsoid, hyaline, fairly thick-walled, asperulate, mostly bearing a small guttule, IKI−, CB+, (4.5−)5−5.7(−6) × (3.6−)3.8−5(−5.5) μm, L = 5.17 μm, W = 4.22 μm, Q = 1.22 (n = 30/1).

Additional material (paratype) examined

China, Yunnan Province, Tengchong County, on stump of *Pinus* sp., August 4, 2014, Li 140804-30 (BJFC018422).

Heterobasidion subparviporum Y. C. Dai, Jia J. Chen and Yuan Yuan, sp. nov. Figures 6, 7

MycoBank MB 834574.

Type

China, Hebei Province, Xinglong County, Wulingshan Nature Reserve, on fallen trunk of *Larix* sp., July 30, 2009, BK Cui 6961 (BJFC005448, holotype).

Diagnosis

Differs from *Heterobasidion* species by mostly round pores (3–5 per mm), amyloid contextual skeletal hyphae, absence of cystidia, presence of cystidioles, and subglobose to broadly ellipsoid basidiospores measuring 5−6.5 × 4−5.2 μm.

Etymology

Subparviporum (Lat.): referring to the similarity to *H. parviporum*.

Description

Basidiocarps perennial, pileate, usually imbricate, leathery and without odor or taste when fresh, hard corky when dry. *Pilei* semicircular to fan-shaped, projecting up to 6 cm, 9 cm wide, and 2.2 cm thick at base. *Pileal surface* buff to grayish brown or grayish dark, at least dark brown at base, crustose, distinctly zonate; margin cream to buff, dull, up to 2 mm. *Pore surface* white when fresh, cream to buff when dry, glancing; pores mostly round, occasionally irregular, 3–5 per mm; dissepiments thin, entire. *Context* buff to brown, corky when dry, azonate, up to 2 mm thick, with a thin black line under crust except for the margin. *Tubes* cream, hard corky, up to 20 mm long. *Hyphal system* dimitic; generative hyphae mostly simple septate; tramal skeletal hyphae dextrinoid, CB+; contextual skeletal hyphae IKI+, CB+, hyphae unchanged in KOH (not dissolved). Contextual generative hyphae infrequent, hyaline, thin-walled to slightly thick-walled, frequently simple septate and branched, 2–4 μm diam; contextual skeletal hyphae dominant, hyaline, thick-walled with a wide to narrow lumen, rarely branched, flexuous, interwoven, 2–4.5 μm diam. Tramal generative hyphae frequent, hyaline, thin-walled to slight thick-walled, frequently simple septate and branched, 1.7–3 μm diam; tramal skeletal hyphae dominant, hyaline, thick-walled with a narrow lumen, rarely branched, flexuous, strongly interwoven without orientation 1.5–3.5 μm diam. *Cystidia* absent. *Cystidioles* present, thin-walled, subulate, and ventricose, 13−26 × 4−6 μm, sometimes with a septum at the top. *Basidia* clavate to barrel-shaped, with a simple basal septum and four sterigmata, 18−24 × 4.5−8 μm. *Basidioles* in shape similar to basidia, but slightly smaller. *Basidiospores* subglobose to broadly ellipsoid, hyaline, fairly thick-walled, asperulate, IKI−, CB+, 5−6.5(−7) × (3.8−)4−5.2 μm, L = 5.65 μm, W = 4.35 μm, Q = 1.30–1.32 (n = 60/2).

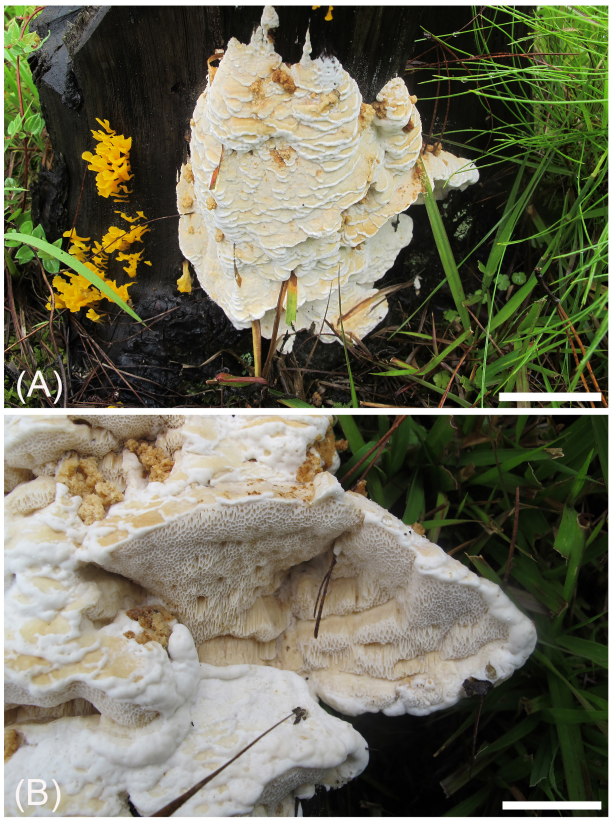


FIGURE 4 | Basidiocarps of *Heterobasidion subinsulare* (holotype, Dai 13842). Bars **(A)** = 5 cm, **(B)** = 1 cm.

Additional materials (paratypes) examined

China, Jilin Province, Antu County, Changbaishan Nature Reserve, on fallen trunk of *Picea* sp., September 13, 2014, Dai 14803 (BJFC017915); on living tree of *Abies* sp., September 21, 2019, Dai 20873 (BJFC032542). Xizang Autonomous Region (Tibet), Linzhi County, Lulang, on stump of *Picea* sp., September 16, 2010, Cui 9267 (BJFC008206).

Other materials examined

—*Heterobasidion abietinum*. Italy, on *Abies* sp., April 28, 2005, Dai 6557 (BJFC000943).

—*Heterobasidion amyloideum*. China, Xizang Auto. Reg. (Tibet), Linzhi County, Lulang, Sejila Mt., on fallen trunk of *Abies* sp., September 23, 2014, Cui 12274 (BJFC017155); Motuo County, on dead tree of *Abies* sp., September 21, 2014, Cui 12240 (BJFC017154); Milin County, Naligou, on fallen gymnosperm trunk, August 18, 2012, Li 1675 (isotype BJFC16026).

—*Heterobasidion annosum*. Belgium, on *Betula* sp., December 3, 2005, Dai 7445 (BJFC000949).

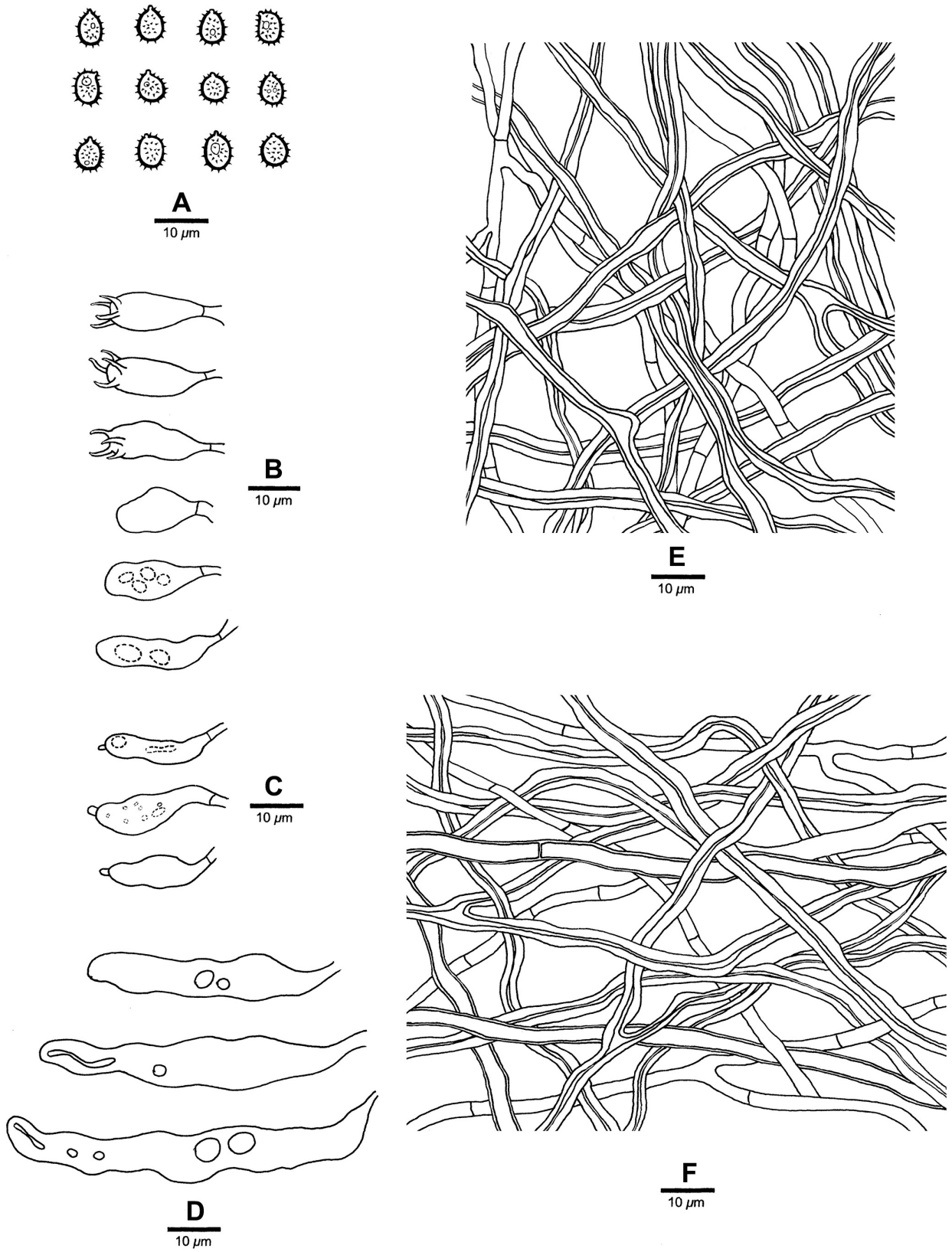


FIGURE 5 | Microscopic structures of *Heterobasidion subinsulare* (drawn from the holotype). **(A)** Basidiospores; **(B)** Basidia and basidioles; **(C)** Cystidioles; **(D)** Cystidia; **(E)** Hyphae from trama; **(F)** Hyphae from context.



FIGURE 6 | Basidiocarps of *Heterobasidion subparviporum* (paratype, Dai 14803). Bar = 4 cm.

—*Heterobasidion araucariae*. New Zealand, March 20, 1985, PDD 49003 (PDD).

—*Heterobasidion australe*. China, Zhejiang Province, Jinan County, Tianmushan Nat. Res., stump of *Pinus* sp., October 15, 2004, Dai 6330 (paratype BJFC000979); Yunnan Province, Nanhua County, Dazhongshan Nature Reserve, on fallen trunk of *Pinus* sp., September 11, 2015, Cui 12602 (BJFC028381); Huaning County, September 6, 2013, Dai 13507 (BJFC014968); Kunming, Wild duck Lake, July 28, 2014, Dai 13863 (BJFC017593).

—*Heterobasidion insulare*. Philippines, Luzon, Mountain Province, on *Pinus insularis*, 1962, FPRI 429 (CFMR). China, Chongqing, Geleshan Forest Park, stump of *Pinus* sp., July 23, 2014, Dai 13933 (BJFC017663); Jiangxi Province, Anyuan County, Sanbaishan Forest Park, root of *Pinus* sp., December 19, 2014, Dai 15095 (BJFC018207).

—*Heterobasidion irregulare*. United States, on *Pinus* sp., 2004, JV0405/3-J (JV).

—*Heterobasidion linzhiense*. China, Xizang Auto. Reg. (Tibet), Linzhi County, Lulang, fallen trunk of *Picea* sp., September 24, 2010, Cui 9645 (holotype, BJFC008582).

—*Heterobasidion occidentale*. United States, on *Abies* sp., August 2001, JV0108/87 (JV).

—*Heterobasidion orientale*. China, Heilongjiang Province, Yichun, Liangshui Nature Reserve, on fallen gymnosperm trunk, August 26, 2014, Cui 11637 (BJFC016831); on fallen trunk of *Pinus* sp., August 28, 2014, Cui 11815 (BJFC016890); on dead tree of *Picea*, August 31, 2014, Cui 12026 (BJFC016964).

—*Heterobasidion parviporum*. Estonia, on *Picea* sp., May 13, 1995, Dai 1930 (BJFC001016).

—*Heterobasidion* sp. United States, California, Lassen National Forest, on *Pinus ponderosa*, March 2005, Korhonen 05030, Korhonen 05038 and Korhonen 05039 (LUKE).

—*Heterobasidion tibeticum*. China, Xizang Auto. Reg. (Tibet), Bomi County, Tongmai, on fallen trunk of *Pinus* sp., September 22, 2014, Cui 12257 (BJFC017171); Linzhi County, September 24, 2014, Cui 12335 (BJFC017249); July 31, 2004, Dai 5468 (paratype, BJFC000958).

DISCUSSION

The current phylogeny considers that *Heterobasidion* species belong to three species complexes: the *H. annosum* F complex (previously treated as the *H. annosum* S group, Woodward et al., 1998), the *H. annosum* P complex and the *H. insulare* complex. The F complex of *H. annosum* includes four species which are mainly associated to true fir species (*Abies* Mill., *Picea abies* (L.) Karst. and *Tsuga* (Endl.) Carrière; Linzer et al., 2008; Dalman et al., 2010). *H. subparviporum* is mostly found on *Picea* in Asia, while *H. parviporum* is mostly associated to *Picea* in Europe and *H. abietinum* to *Abies* in Europe. *H. occidentale* is colonizing mostly *Tsuga* and *Abies* in western North America. The *H. annosum* P complex includes two taxa which mostly grow on pines: *H. annosum s.s.* in Eurasia, *H. irregulare* in North America (Linzer et al., 2008; Dalman et al., 2010). The *H. insulare* complex includes ten species which are associated to many species of Pinophyta (*Abies*, *Araucaria* Juss., *Keteleeria* Carr., *Larix* Mill., *Picea*, *Pinus* L., *Pseudolarix* Gordon, *Pseudotsuga* Carrière and *Tsuga*). *H. araucariae*, a species from Southern Hemisphere, is clustered into *H. insulare* complex, and is closely related to the species *H. insulare* and *H. subinsulare* (**Figure 1**).

Heterobasidion insulare (=*Trametes insularis* Murrill) was originally described from Philippines (Murrill, 1908) and its type specimen was collected from fallen log of *P. insularis* in the Benguet Province, Luzon, Philippines in 1905. In 1962, Mendoza obtained the isolate FPRI-429 from *P. insularis* in the Mountain Province, Luzon. The Benguet Province and Mountain Province are both located in the Cordillera Administrative Region of Luzon Island (**Figure 8**). FPRI-429 can thus be considered as the type locality of *H. insulare*. The present results confirmed that FPRI-429 and representatives of *H. ecrustosum* are nested in the same lineage; the latter taxon was described from central Japan to Okinawa, and from southern China (Tokuda et al., 2009). We did not find any distinct morphological difference between the *H. insulare* type and samples of *H. ecrustosum*. Hence, according to the current phylogeny and morphological studies, *H. ecrustosum* is treated as a synonym of *H. insulare*.

Heterobasidion armandii is closely related to *H. australe* (**Figure 1**) and the geographical distributions of the two species are overlapped in China. However, *H. australe* is characterized by a glancing pore surface, lacks cystidioles, and its contextual skeletal hyphae are negative in Melzer's reagent. Morphologically, *H. armandii* resembles *H. amyloideum* and *H. tibeticum* by similar pores (4–6 per mm in *H. amyloideum* and 3–6 per mm in *H. tibeticum*), basidiospores (4.9−5.8 × 3.9−4.5 μm in *H. amyloideum* and 4.5−6 × 3.6−5.3 μm in *H. tibeticum*) and amyloid contextual skeletal hyphae, but *H. amyloideum* and *H. tibeticum* differ from *H. armandii* by the presence of cystidia (Dai and Korhonen, 2009; Chen et al., 2014).

Heterobasidion subinsulare is closely related to *H. insulare* (**Figure 1**), but the latter lacks cystidia. *H. subinsulare* resembles *H. amyloideum* and *H. tibeticum* by having cystidia, but the latter two species have smaller pores (3–6 per mm) and amyloid contextual skeletal hyphae (Chen et al., 2014). *H. subinsulare*, *H. araucariae*, and *H. orientale* share similar pores, but *H. araucariae* can be distinguished from *H. subinsulare* by longer

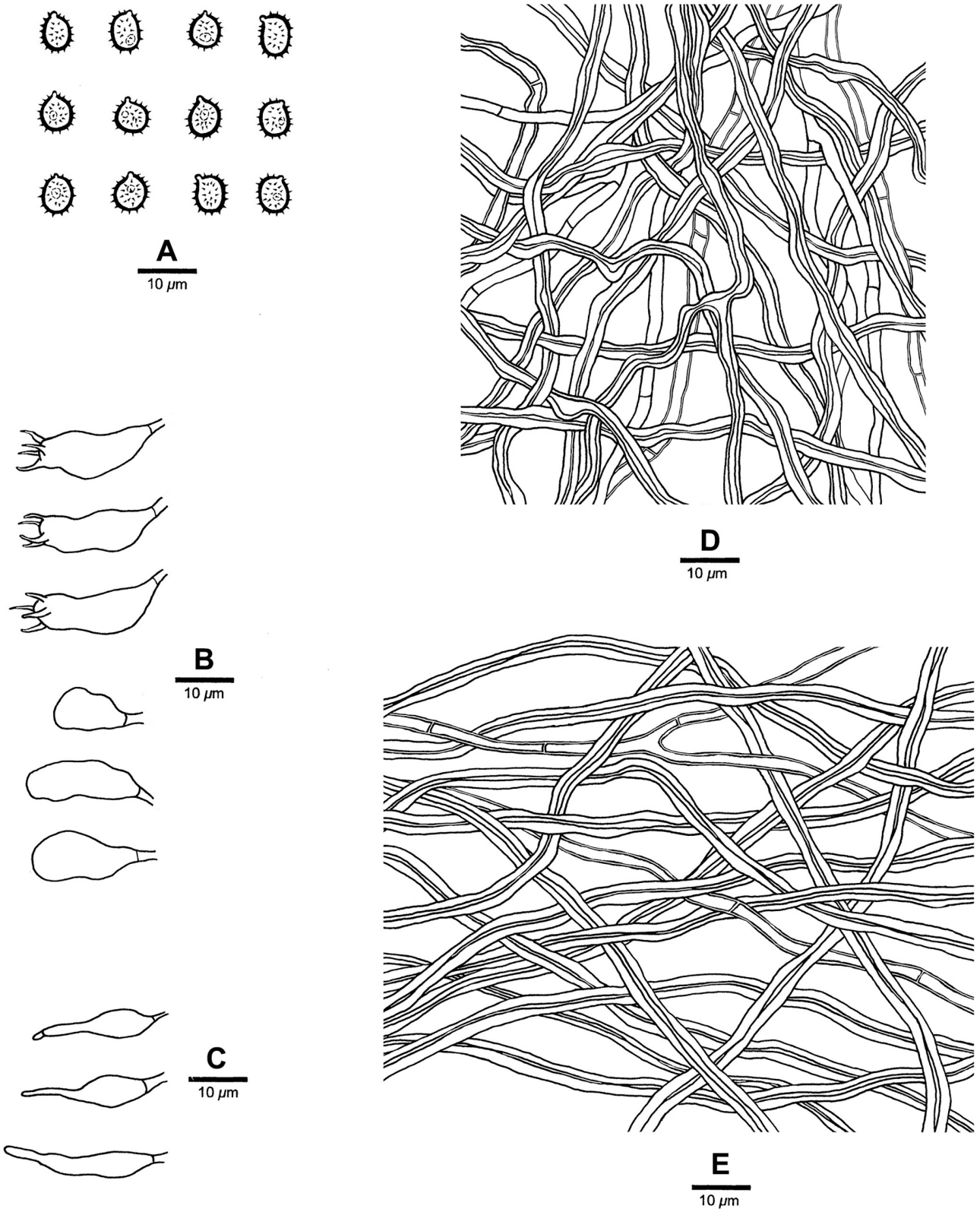


FIGURE 7 | Microscopic structures of *Heterobasidion subparviporum* (drawn from the holotype). **(A)** Basidiospores; **(B)** Basidia and basidioles; **(C)** Cystidioles; **(D)** Hyphae from trama; **(E)** Hyphae from context.

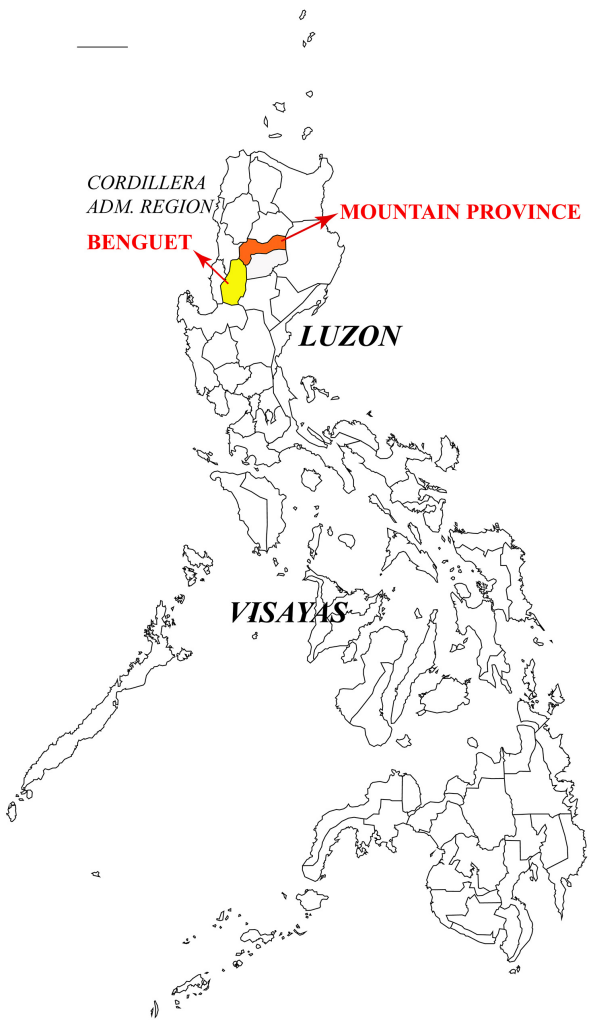


FIGURE 8 | Type locality of *Heterobasidion insulare* in Philippines.

basidiospores (5.8–6.5 μm vs. 5–5.7 μm) and lacking of cystidia, and *H. orientale* differs from *H. subinsulare* by the sharp pileal margin, dark reddish pileal surface and lacking of cystidia. In addition, *H. subinsulare* is distantly related to *H. amyloideum*, *H. tibeticum*, *H. araucariae*, and *H. orientale* in our current phylogeny (**Figure 1**).

Heterobasidion subparviporum is closely related to *H. parviporum* (**Figure 1**), and the latter was considered as same as the former according to the mating tests (Dai and Korhonen, 1999, 2003; Dai et al., 2006; Dai, 2012). Although both taxa are compatible in laboratory, they form two distinct lineages in our phylogeny (**Figure 1**). Morphologically, *H. subparviporum* differs from *H. parviporum* by longer cystidia (18–24 μm vs. 13–17 μm) and bigger basidiospores (5−6.5 × 4−5.2 μm vs. 4.2−5 × 3.8−4.2 μm). In addition, *H. parviporum* is a pathogen on *P. abies* in Europe, while *H. subparviporum* seems to be a saprophytic species according to our investigations. Based on the above data, we suggest that this Asian taxon is a new species *H. subparviporum*. The situation is similar with the European taxa *H. parviporum* and *H. abietinum*. These two taxa are partly sexually compatible (Capretti et al., 1990; Stenlid and Karlsson, 1991; Woodward et al., 1998), but they do not produce hybrids in nature. So they have been accepted at the species level (Niemelä and Korhonen, 1998; Otrosina and Garbelotto, 2010; Ryvarden and Melo, 2017).

Heterobasidion irregulare was proposed by Otrosina and Garbelotto (2010), and it was originally described as *Polyporus irregularis* Underwood on pine log from Auburn, Alabama, eastern United States (Underwood, 1897), although *P. irregularis* is an illegitimate name because there was earlier a fungus named *P. irregularis* Pers. (Persoon, 1825). The lectotype (NY730756) of *H. irregulare* was selected from the type material of *P. irregularis* Underwood, and the epitype (UC1935442) was selected from stump of *P. ponderosa* in the Modoc National Forest, California, western United States. However, three isolates Korhonen 05030, Korhonen 05038, and Korhonen 05039 associated to *P. ponderosa* from Lassen National Forest in California formed another lineage which is closely related to *H. irregulare* (**Figure 1**). Hence it is possible that another taxon exists in western North America. We did not have the basidiocarps of isolates Korhonen 05030, Korhonen 05038, and Korhonen 05039, and no information on their ecology. For the time being we treat this possible taxon as *H.* sp.

Heterobasidion amyloideopsis was described from Pakistan mostly based on phylogenetic analysis (Zhao et al., 2017). We studied its ITS (KT598384, KT598385), nrLSU (KT598386, KT598387), RPB1 (KT598390, KT598391), and RPB2 (KT598388, KT598389) sequences and found some of the sequences are uncorrect, and some of these sequences were deleted by NCBI. So the status of *H. amyloideopsis* is ambiguous.

A comparison of these three new species and their morphological and/or phylogenetically related species is also provided in **Supplementary Appendix 1**. The phylogenetic analyses on single loci (ITS, nrLSU, RPB1, RPB2, and GAPDH) were shown in **Supplementary Figures 1–5**).

CONCLUSION

To date, 15 species are recorded in the genus *Heterobasidion*, including three new species described in the present study.

Five species, *H. abietinum*, *H. annosum s.s.*, *H. irregulare*, *H. occidentale*, and *H. parviporum*, distributed in Europe and North America are forest pathogens. Ten Asian taxa are all saprotrophs, and the Asian countries ought to consider these five European and North American species as entry plant quarantine fungi. Parallelly, European countries should consider the American *H. occidentale* and *H. irregulare* as entry plant quarantine fungi (although the latter species is already in Italy), while North America should treat *H. abietinum*, *H. annosum* s.s. and *H. parviporum* as entry plant quarantine fungi. Eight *Heterobasidion* species found in the Himalayas suggest that the ancestral *Heterobasidion* species may have occurred in Asia, as was proposed also in the previous divergence and biogeographic studies on the genus.

DATA AVAILABILITY STATEMENT

The datasets presented in this study can be found in online repositories. The names of the repository/repositories and accession number(s) can be found in the article/ **Supplementary Material**.

AUTHOR CONTRIBUTIONS

YY, J-JC, and Y-CD designed the research and contributed to data analysis and interpretation. YY and J-JC performed the research. Y-CD and KK collected the materials. All authors wrote and revised the manuscript, contributed to the article, and approved the submitted version.

FUNDING

The research is supported by the Second Tibetan Plateau Scientific Expedition and Research Program (STEP, No. 2019QZKK0503).

ACKNOWLEDGMENTS

We thank Prof. Bao-Kai Cui (China) for allowing us to study his collections. We express our gratitude to Dr. Daniel L. Lindner (CFMR, United States) for loan of stock, to Dr. De-Wei Li (United States) for providing some literatures and improving this manuscript, and to Chang-Lin Zhao (China) for providing sequences.

SUPPLEMENTARY MATERIAL

The Supplementary Material for this article can be found online at: https://www.frontiersin.org/articles/10.3389/fmicb.2020.596393/full#supplementary-material

Supplementary Figure 1 | Phylogeny of ITS.

Supplementary Figure 2 | Phylogeny of nrLSU.

Supplementary Figure 3 | Phylogeny of RPB1.

Supplementary Figure 4 | Phylogeny of RPB2.

Supplementary Figure 5 | Phylogeny of GAPDH.

Supplementary Appendix 1 | A comparison of taxa in the *Heterobasidion*.

REFERENCES

Asiegbu, F. O., Abu, S., Stenlid, J., and Johansson, M. (2004). Sequence polymorphism and molecular characterization of laccase genes of the conifer pathogen *Heterobasidion annosum*. *Mycol. Res.* 108, 136–148. doi: 10.1017/S0953756203009183

Buchanan, P. K. (1988). A new species of *Heterobasidion* (Polyporaceae) from Australasia. *Mycotaxon* 32, 325–337.

Capretti, P., Korhonen, K., Mugnai, L., and Romagnoli, C. (1990). An intersterility group of *Heterobasidion annosum*, specialized to *Abies alba*. *Eur. J. Plant Pathol.* 20, 231–240. doi: 10.1111/j.1439-0329.1990.tb01134.x

Chen, J. J., Cui, B. K., Zhou, L. W., Korhonen, K., and Dai, Y. C. (2015). Phylogeny, divergence time estimation, and biogeography of the genus *Heterobasidion* (Basidiomycota, Russulales). *Fungal Divers.* 71, 185–200. doi: 10.1007/s13225-014-0317-2

Chen, J. J., Korhonen, K., Li, W., and Dai, Y. C. (2014). Two new species of the *Heterobasidion insulare* complex based on morphology and molecular data. *Mycoscience* 55, 289–298. doi: 10.1016/j.myc.2013.11.002

Dai, Y. C. (2012). Polypore diversity in China with an annotated checklist of Chinese polypores. *Mycoscience* 53, 49–80. doi: 10.1007/s10267-011-0134-3

Dai, Y. C., and Korhonen, K. (1999). *Heterobasidion annosum* group S identified in north-eastern China. *Eur. J. Plant Pathol.* 29, 273–279. doi: 10.1046/j.1439-0329.1999.00153.x

Dai, Y. C., and Korhonen, K. (2003). First report of *Heterobasidion parviporum* (S group of *H. annoum* sensu lato) on *Tsuga* spp. in Asia. *Plant Dis.* 87:1007. doi: 10.1094/PDIS.2003.87.8.1007B

Dai, Y. C., and Korhonen, K. (2009). *Heterobasidion australe*, a new polypore derived from the *Heterobasidion insulare* complex. *Mycoscience* 50, 353–356. doi: 10.1007/S10267-009-0491-3

Dai, Y. C., Vainio, E. J., Hantula, J., Niemelä, T., and Korhonen, K. (2002). Sexuality and intersterility within the *Heterobasidion insulare* complex. *Mycol. Res.* 106, 1435–1448. doi: 10.1017/S0953756202006950

Dai, Y. C., Vainio, E. J., Hantula, J., Niemelä, T., and Korhonen, K. (2003). Investigations on *Heterobasidion annosum* s.lat. in central and eastern Asia with the aid of mating tests and DNA fingerprinting. *For. Pathol.* 33, 269–286. doi: 10.1046/j.1439-0329.2003.00328.x

Dai, Y. C., Yu, C. J., and Wang, H. C. (2007). Polypores from eastern Xizang (Tibet), western China. *Ann. Bot. Fenn.* 44, 135–145.

Dai, Y. C., Yuan, H. S., Wei, Y. L., and Korhonen, K. (2006). New records of *Heterobasidion parviporum* in China. *For. Pathol.* 36, 287–293. doi: 10.1111/j.1439-0329.2006.00458.x

Dalman, K., Olson, A., and Stenlid, J. (2010). Evolutionary history of the conifer root rot fungus *Heterobasidion annosum* sensu lato. *Mol. Ecol.* 19, 4979–4993. doi: 10.1111/j.1365-294X.2010.04873.x

Farris, J. S., Källersjö, M., Kluge, A. G., and Bult, C. (1994). Testing significance of incongruence. *Cladistics* 10, 315–319. doi: 10.1111/j.1096-0031.1994.tb00181.x

Felsenstein, J. (1985). Confidence intervals on phylogenetics: an approach using bootstrap. *Evolution* 39, 783–791. doi: 10.1111/j.1558-5646.1985.tb00420.x

Gilbertson, R. L., and Ryvarden, L. (1986). *North American Polypores 1. Abortiporus - Lindtneria*. Oslo: Fungiflora, 1–433.

Hall, T. A. (1999). Bioedit: a user-friendly biological sequence alignment editor and analysis program for Windows 95/98/NT. *Nucleic Acids Symp. Ser.* 41, 95–98.

Huelsenbeck, J. P., Bull, J. J., and Cunningham, E. (1996). Combining data in phylogenetic analysis. *Trends Ecol. Evol.* 11, 152–158. doi: 10.1016/0169-5347(96)10006-9

Johannesson, H., Renvall, P., and Stenlid, J. (2000). Taxonomy of *Antrodiella* inferred from morphological and molecular data. *Mycol. Res.* 104, 92–99. doi: 10.1017/S0953756299008953

Johannesson, H., and Stenlid, J. (2003). Molecular markers reveal genetic isolation and phylogeography of the S and F intersterility group of the wood-decay fungus *Heterobasidion annosum*. *Mol. Phylogenet. Evol.* 29, 94–101. doi: 10.1016/S1055-7903(03)00087-3

Justo, A., and Hibbett, D. S. (2011). Phylogenetic classification of *Trametes* (Basidiomycota, Polyporales) based on a five-marker dataset. *Taxon* 60, 1567–1583. doi: 10.1002/tax.606003

Korhonen, K. (1978). Intersterility groups of *Heterobasidion annosum*. *Commun. Inst. For. Fenn.* 94:25.

Linzer, R. E., Otrosina, W. J., Gonthier, P., Bruhn, J., Laflamme, G., Bussières, G., et al. (2008). Inferences on the phylogeography of the fungal pathogen *Heterobasidion annosum*, including evidence of interspecific horizontal genetic transfer and of human-mediated, long range dispersal. *Mol. Phylogenet. Evol.* 46, 844–862. doi: 10.1016/j.ympev.2007.12.010

Liu, Y. J., Whelen, S., and Hall, B. D. (1999). Phylogenetic relationship among ascomycetes: evidence from an RNA polymerase II subunit. *Mol. Biol. Evol.* 16, 1799–1808. doi: 10.1093/oxfordjournals.molbev.a026092

Maijala, P., Harrington, T. C., and Raudaskoski, M. (2003). A peroxidase gene family and gene trees in *Heterobasidion* and related genera. *Mycologia* 95, 209–221. doi: 10.2307/3762032

Matheny, P. B. (2005). Improving phylogenetic inference of mushrooms with RPB1 and RPB2 nucleotide sequences (*Inocybe*; Agaricales). *Mol. Phylogenet. Evol.* 35, 1–20. doi: 10.1016/j.ympev.2004.11.014

Matheny, P. B., Liu, Y. J., Ammirati, J. F., and Hall, B. D. (2002). Using RPB1 sequences to improve phylogenetic inference among mushrooms (*Inocybe*, Agaricales). *Am. J. Bot.* 89, 688–698. doi: 10.3732/ajb.89.4.688

Murrill, W. A. (1908). Additional philippine polyporaceae. *Bull. Torrey Bot. Club* 35, 391–416. doi: 10.2307/2479285

Niemelä, T., and Korhonen, K. (1998). "Taxonomy of the genus *Heterobasidion*," in *Heterobasidion annosum: Biology, Ecology, Impact and Control*, eds S. Woodward, J. Stenlid, R. Karjalainen, and A. Hüttermann (Oxon: CAB International), 27–33. doi: 10.14492/hokmj/1381758488

Núñez, M., and Ryvarden, L. (2001). East Asian polypores 2. Polyporaceae s. lato. *Syn. Fung.* 14, 469–522.

Nylander, J. A. A. (2004). *MrModeltest 2.2. Program Distributed by the Author*. Uppsala: Uppsala University.

Ota, Y., Tokuda, S., Buchanan, P. K., and Hattori, T. (2006). Phylogenetic relationships of Japanese species of *Heterobasidion – H. annosum* sensu lato and an undetermined *Heterobasidion* sp. *Mycologia* 98, 717–725. doi: 10.3852/mycologia.98.5.717

Otrosina, W. J., Chase, T. E., Cobb, F. W., and Korhonen, K. (1993). Population structure of *Heterobasidion annosum* from North America and Europe. *Can. J. Bot.* 71, 1064–1071. doi: 10.1139/b93-123

Otrosina, W. J., and Garbelotto, M. (2010). *Heterobasidion occidentale* sp. nov. and *Heterobasidion irregulare* nom. nov.: a disposition of North American *Heterobasidion* biological species. *Fungal Biol.* 114, 16–25. doi: 10.1016/j.mycres.2009.09.001

Page, R. D. M. (1996). Treeview: application to display phylogenetic trees on personal computers. *Comput. Appl. Biosci.* 12, 357–358. doi: 10.1093/bioinformatics/12.4.357

Persoon, C. H. (1825). Mycologia Europaea 2. *Palmii: langen*, 1–214.

Petersen, J. H. (1996). *Farvekort. The Danish Mycological Society's Color-Chart*. Greve: Foreningen til Svampekundskabens Fremme.

Ronquist, F., and Huelsenbeck, J. P. (2003). MrBayes 3: bayesian phylogenetic inference under mixed models. *Bioinformatics* 19, 1572–1574. doi: 10.1093/bioinformatics/btg180

Ryvarden, L., and Gilbertson, R. (1993). European polypores 1. *Syn. Fung.* 7, 1–387.

Ryvarden, L., and Melo, I. (2017). Poroid fungi of Europe. 2th Edition. *Syn. Fung.* 37, 1–431.

Stenlid, J., and Karlsson, J. O. (1991). Partial intersterility in *Heterobasidion annosum*. *Mycol. Res.* 95, 1153–1159. doi: 10.1016/S0953-7562(09)80004-X

Swofford, D. L. (2002). *PAUP*: Phylogenetic analysis Using Parsimony (*and other Methods), version 4.0 Beta*. Sunderland, MA: Sinauer.

Thompson, J. D., Gibson, T. J., Plewniak, F., Jeanmougin, F., and Higgins, D. G. (1997). The CLUSTAL X windows interface: flexible strategies for multiple sequence alignment aided by quality analysis tools. *Nucleic Acids Res.* 25, 4876–4882. doi: 10.1093/nar/25.24.4876

Tokuda, S., Hattori, T., Dai, Y. C., Ota, Y., and Buchanan, P. K. (2009). Three species of *Heterobasidion* (Basidiomycota, Hericiales), *H. parviporum*, *H. orientale* sp. nov. and *H. ecrustosum* sp. nov. from East Asia. *Mycoscience* 50, 190–202. doi: 10.1007/S10267-008-0476-7

Underwood, L. M. (1897). Some new fungi, chiefly from Alabama. *Bull. Torrey Bot. Club* 24, 81–86. doi: 10.2307/2477799

Vilgalys, R., and Hester, M. (1990). Rapid genetic identification and mapping of enzymatically amplified ribosomal DNA from several *Cryptococcus* species. *J. Bacteriol.* 172, 4238–4246. doi: 10.1128/jb.172.8.4238-4246.1990

White, T. J., Bruns, T., Lee, S., and Taylor, J. W. (1990). "Amplification and direct sequencing of fungal ribosomal RNA genes for phylogenetics," in *PCR Protocols: A Guide to Methods and Applications*, eds M. A. Innis, D. H. Gelfand, J. J. Sninsky, and T. J. White (New York, NY: Academic Press), 315–322. doi: 10.1016/B978-0-12-372180-8.50042-1

Woodward, S., Stenlid, J., Karjalainen, R., and Hüttermann, A. (1998). "Preface," in *Heterobasidion annosum: Biology, Ecology, Impact and Control*, eds S. Woodward, J. Stenlid, R. Karjalainen, and A. Huttermann (Oxon: CAB International), xi–xii.

Zhao, C. L., Saba, M., Khalid, A. N., Song, J., and Pfister, D. H. (2017). *Heterobasidion amyloideopsis* sp. nov. (Basidiomycota, Russulales) evidenced by morphological characteristics and phylogenetic analysis. *Phytotaxa* 137, 199–210. doi: 10.11646/phytotaxa.317.3.4

Conflict of Interest: The authors declare that the research was conducted in the absence of any commercial or financial relationships that could be construed as a potential conflict of interest.

Copyright © 2021 Yuan, Chen, Korhonen, Martin and Dai. This is an open-access article distributed under the terms of the Creative Commons Attribution License (CC BY). The use, distribution or reproduction in other forums is permitted, provided the original author(s) and the copyright owner(s) are credited and that the original publication in this journal is cited, in accordance with accepted academic practice. No use, distribution or reproduction is permitted which does not comply with these terms.

frontiers in Microbiology

ORIGINAL RESEARCH
published: 08 January 2021
doi: 10.3389/fmicb.2020.608991

Three Novel Entomopathogenic Fungi From China and Thailand

De-Ping Wei[1,2,3], Dhanushka N. Wanasinghe[1,4,5], Jian-Chu Xu[1,4,5], Chaiwat To-anun[2], Peter E. Mortimer[1,5,6], Kevin D. Hyde[3,7,8,9], Abdallah M. Elgorban[10], Sumedha Madawala[11], Nakarin Suwannarach[12,13], Samantha C. Karunarathna[1,5,6,12,13], Saowaluck Tibpromma[1,5,6,12,13]* and Saisamorn Lumyong[12,13,14]**

[1] CAS Key Laboratory for Plant Diversity and Biogeography of East Asia, Kunming Institute of Botany, Chinese Academy of Sciences, Kunming, China, [2] Department of Entomology and Plant Pathology, Faculty of Agriculture, Chiang Mai University, Chiang Mai, Thailand, [3] Center of Excellence in Fungal Research, Mae Fah Luang University, Chiang Rai, Thailand, [4] World Agroforestry Centre, East and Central Asia, Kunming, China, [5] Centre for Mountain Futures, Kunming Institute of Botany, Kunming, China, [6] Yunnan Key Laboratory for Fungal Diversity and Green Development, Kunming Institute of Botany, Chinese Academy of Sciences, Kunming, China, [7] Mushroom Research Foundation, Chiang Mai, Thailand, [8] School of Science, Mae Fah Luang University, Chiang Rai, Thailand, [9] Innovative Institute of Plant Health, Zhongkai University of Agriculture and Engineering, Guangzhou, China, [10] Department of Botany and Microbiology, College of Sciences, King Saud University, Riyadh, Saudi Arabia, [11] Department of Botany, Faculty of Science, University of Peradeniya, Peradeniya, Sri Lanka, [12] Department of Biology, Faculty of Science, Chiang Mai University, Chiang Mai, Thailand, [13] Research Center of Microbial Diversity and Sustainable Utilization, Faculty of Science, Chiang Mai University, Chiang Mai, Thailand, [14] Academy of Science, The Royal Society of Thailand, Bangkok, Thailand

OPEN ACCESS

Edited by:
John R. Battista,
Louisiana State University,
United States

Reviewed by:
Nattawut Boonyuen,
National Center for Genetic Engineering and Biotechnology (BIOTEC), Thailand
Yusufjon Gafforov,
Institute of Botany, Academy of Sciences of the Republic of Uzbekistan, Uzbekistan

***Correspondence:**
Saisamorn Lumyong
scboi009@gmail.com
Saowaluck Tibpromma
saowaluckfai@gmail.com
Samantha C. Karunarathna
samantha@mail.kib.ac.cn;
samanthakarunarathna@gmail.com

Specialty section:
This article was submitted to Evolutionary and Genomic Microbiology, a section of the journal Frontiers in Microbiology

Received: 13 October 2020
Accepted: 30 November 2020
Published: 08 January 2021

Citation:
Wei D-P, Wanasinghe DN, Xu J-C, To-anun C, Mortimer PE, Hyde KD, Elgorban AM, Madawala S, Suwannarach N, Karunarathna SC, Tibpromma S and Lumyong S (2021) Three Novel Entomopathogenic Fungi From China and Thailand. Front. Microbiol. 11:608991. doi: 10.3389/fmicb.2020.608991

Entomopathogenic fungi are ubiquitous in tropical rainforests and feature a high level of diversity. This group of fungi not only has important ecological value but also medicinal value. Nevertheless, they are often ignored, and many unknown species have yet to be discovered and described. The present study aims to contribute to the taxonomical and phylogenetic understanding of the genus *Paraisaria* by describing three new species collected from Guizhou and Yunnan Provinces in China and Krabi Province in Thailand. The three novel species named *Paraisaria alba, P. arcta,* and *P. rosea* share similar morphologies as those in the genus *Paraisaria*, containing solitary, simple, fleshy stroma, completely immersed perithecia and cylindrical asci with thickened caps and filiform ascospores that often disarticulate at maturity. Phylogenetic analyses of combined LSU, SSU, TEF1-α, RPB1, RPB2, and ITS sequence data confirm their placement in the genus *Paraisaria.* In this study, the three entomopathogenic taxa are comprehensively described with color photographs and phylogenetic analyses. A synopsis table and a key to all treated species of *Paraisaria* are also included.

Keywords: Insect fungi, Ophiocordycipitaceae, *Paraisaria alba*, *Paraisaria arcta*, *Paraisaria rosea*, taxonomy, Yunnan Province

INTRODUCTION

Entomopathogenic fungi are a group of unicellular or multicellular, heterotrophic, eukaryotic microorganisms that can enter into a parasitic relationship with parasitized insects, killing or otherwise disabling their hosts (Samson et al., 1988). They reproduce via sexual or asexual spores, or both (Mora et al., 2017). It is of global importance to survey and describe insect pathogens (Hyde et al., 2019). Entomopathogenic fungi can act as natural enemies of agricultural pests and

play an important role in maintaining ecological balance (Fernández-Grandon et al., 2020; Sobczak et al., 2020). For example, fungal pathogens such as, *Coelomomyces, Culicinomyces,* and *Lagenidium* have the capacity to kill larva and adult mosquitoes, reducing their host population (Scholte et al., 2004). Some entomopathogenic fungi, e.g., *Beauveria bassiana, Beauveria brongniartii, Metarhizium anisopliae,* and *Verticillium lecanii*, have been developed as biocontrol agents usable against agricultural pests like aphids, locusts, grasshoppers and cockchafer in Africa and Europe (Roberts and Hajek, 1992; Shah and Pell, 2003). *Beauveria bassiana* and *B. brongniartii* were found to be especially safe bioinsecticides (Zimmermann, 2007). Additionally, some insect pathogens with pharmacological activities are frequently studied, such as *Cordyceps militaris* extract, which exhibits antitumor properties (Li et al., 2020). *Cordyceps* spp. have been utilized as therapeutic agents for metabolic-related disorders (Cao et al., 2020). *Cordyceps cicadae* has renoprotective effects on hypertensive renal injuries (Huang et al., 2020). Entomopathogenic fungi have important biotechnological applications (Hyde et al., 2019) and *Paraisaria* is no exception. Several studies have explored the importance of *Paraisaria* species, such as their antioxidative activity (Ma et al., 2012), nucleoside components (Suo et al., 2013), intracellular polysaccharide composition (Wang et al., 2019) and AGS gastric cancer cells anti-proliferation effects (Ye et al., 2015). Additionally, *P. heteropoda* reportedly produces anti-bacterial and anti-fungal compounds (Krasnoff et al., 2005). Experiments into optimal cultural conditions and nutritional sources were conducted by Sung et al. (2011). Applications of other species in this genus have been poorly studied.

Entomopathogenic fungi are phylogenetically diverse and taxonomically distributed in Ascomycota, Basidiomycota, Chytridiomycota, Entomophthoromycota, Microsporidia, Oomycota and Zygomycota (Vega et al., 2012; Araújo and Hughes, 2016; Mora et al., 2017). Different groups of entomopathogens usually develop respectively unique strategy to colonize their hosts (Mora et al., 2017). It is worth to mention that entomopathogenic taxa in Entomophthorales (Entomophthoromycota) enter into biotrophic relationships with their insect hosts, while those in Hypocreales (Ascomycota) can be hemibiotrophic at earlier stages and transform into saprophytism (Shah and Pell, 2003). The diversity, taxonomy and phylogeny of entomopathogenic fungi have been extensively studied recently (Aung et al., 2008; Mora et al., 2017; Hyde et al., 2018). Most insect pathogens are known from three families: Clavicipitaceae, Cordycipitaceae, and Ophiocordycipitaceae. They are found in the Hypocreales, Hypocreomycetidae, Sordariomycetes, Ascomycota (Sung et al., 2007a; Maharachchikumbura et al., 2016; Wijayawardene et al., 2018). The generic composition of Ophiocordycipitaceae underwent several changes over time (Sung et al., 2007a; Quandt et al., 2014; Maharachchikumbura et al., 2016; Shrestha et al., 2017; Wijayawardene et al., 2018), and currently ten genera are accepted (Hyde et al., 2020). New combinations of these genera were proposed for *Polycephalomyces* by Kepler et al. (2013), *Tolypocladium* by Quandt et al. (2014), *Perennicordyceps* by Matočec et al. (2014) and *Drechmeria*, *Harposporium*, *Ophiocordyceps,* and *Purpureocillium* by Spatafora et al. (2015). The genus *Paraisaria* was recently recovered in Ophiocordycipitaceae (Mongkolsamrit et al., 2019).

The genus *Paraisaria* was established by Samson and Brady (1983), with *P. dubia* as the type species, whose sexual morph was known as *Ophiocordyceps gracilis* (syn. *Cordyceps gracilis*). The sexual morph of this genus is characterized by solitary stromata with a stipe terminating in a globose or ellipsoid fertile head, completely immersed, ostiolate, gregarious perithecia, cylindrical asci and hyaline, filiform, multi-septate ascospores, which break into aseptate fragments when mature. Its asexual morphs are characterized by verticillate branched conidiophores, phialidic, flask-shaped, usually sympodially proliferating conidiogenous cells, which terminate in 1–4 necks, and aseptate, hyaline, smooth-walled conidia, which usually aggregate in slimy heads (Samson and Brady, 1983). Li et al. (2004) synonymized *Isaria gracilioides* under *P. gracilioides* and linked its sexual morph to *Ophiocordyceps gracilioides*. Evans et al. (2010) found the asexual morph of *P. myrmicarum* from a red ant host (*Myrmica rubra*) in a natural environment in the United Kingdom. Quandt et al. (2014) have dropped the genus *Paraisaria* and used its sexual genus *Ophiocordyceps* according to the 'one fungus one name' principle. Mongkolsamrit et al. (2019) resurrected *Paraisaria* on the basis of three new species, e.g., *P. orthopterorum*, *P. phuwiangensis,* and *P. yodhathaii* as well as eight new combinations, e.g. *P. amazonica* (Sanjuan et al., 2015), *P. blattarioides* (Sanjuan et al., 2015), *P. coenomyiae* (Ban et al., 2015), *P. gracilioides* (Kobayasi, 1941; Pérez-Villamares et al., 2017), *P. gracilis* (Samson and Brady, 1983; Pérez-Villamares et al., 2017), *P. heteropoda* (Sung et al., 2011; Mongkolsamrit et al., 2019), *P. paramyrmicarum* (= *P. myrmicarum*) (Evans et al., 2010) and *P. tettigonia* (Wen et al., 2016). So far, together with the three new species in this study, 14 species are accepted in *Paraisaria*.

This study is part of a larger survey of fungi in the Greater Mekong Subregion where we came across numerous new taxa (Hyde et al., 2018). In this study, three specimens of entomopathogenic fungi were collected from disturbed forests in China and Thailand, and the typical macro- and micro- morphological characteristics indicate that they are of the *Paraisaria* species. The multigene phylogenetic analysis of LSU, SSU, TEF1-α, RPB1, RPB2, and ITS confirmed their placement within *Paraisaria* as three distinct new species.

MATERIALS AND METHODS

Sample Collection, Isolation, and Morphological Studies

In this study, a total of four fungal specimens were collected. One specimen (HKAS 102484) was collected from Krabi Province in Thailand on an adult cricket. Two specimens (HKAS 102553 and HKAS 102552) on dead larvae of *Lepidoptera* sp. were collected from Guizhou Province of China. One specimen (HKAS 102546) was collected from Yunnan Province in China on *Coleoptera* sp. larva. Among them, the hosts of specimens

HKAS 102484, HKAS 102553 and HKAS 102552 were found completely immersed into soil with the stroma protruding from the ground in a forest. Specimen HKAS 102546 was found in a similar condition, but differed in that it was found under a karst stone formation. Macro-morphological characteristics of fresh collections were recorded with a camera (iPhone XS Max) in the field and then the specimens were transported to the laboratory in plastic boxes for subsequent studies. The culture of the specimen HKAS 102546 was created by transferring a small mass of mycelium inside the body of the host into potato dextrose agar (PDA, 1% w/v peptone) using a burned needle and incubated at room temperature (25°C). The pure culture was stored in twice-sterilized water, a 15% glycerinum solution and PDA medium, and deposited in the KUMCC culture collection of the Kunming Institute of Botany (KIB), Chinese Academy of Sciences (CAS). The fruiting bodies were dried with allochroic silica gel and deposited in KUN herbarium of KIB. Facesoffungi numbers were registered as outlined in Jayasiri et al. (2015).

The fresh fruiting bodies were examined and hand-sectioned under an Optec SZ660 stereo dissecting microscope. The key fungal structures viz. ascomata, perithecia, peridium, asci and ascospores were mounted in sterilized water or cotton blue solution slides and observed and photographed using a compound microscope (Nikon ECLIPSE Ni) with a digital camera (Canon EOS 600D) fitted on to the top of the microscope. These important fungal structures were measured with the Tarosoft (R) Image Frame Work program and the images used were processed with Adobe Photoshop CS3 Extended v. 10.0 (Adobe®, San Jose, CA, United States).

DNA Extraction, PCR Amplification, and Sequencing

The total DNA was extracted from stromal tissue of specimens HKAS 102552, HKAS 102553, HKAS 102484 and from fresh mycelium of KUMCC 20-0001 (ex-type culture of isolate HKAS 102546) using DNA extraction kit (Omega Fungus Genomic DNA Extraction Kit, China), following the protocol of the manufacturer. The obtained DNA was stored at −20°C in a refrigerator. The PCR amplification was performed in 25 μL volumes consisting 12.5 μL PCR mixture (2 × Taq PCR Master Mix, red dye) which contains Taq DNA polymerase, dNTPs, $MgCl_2$, a reaction buffer, a PCR reaction enhancer, an optimizer and stabilizer, 8.5 μL of twice-sterilized water, 1 μL of each primer and 2 μL of 30 μg/μl DNA template. The internal transcribed spacer (ITS1-5.8S-ITS2, ITS), large subunit ribosomal RNA (LSU rRNA), small subunit ribosomal RNA (SSU rRNA), translation elongation factor 1-alpha gene (TEF1-α) and RNA polymerase II largest subunit (RPB1) and RNA polymerase II second largest subunit (RPB2) were amplified with the primers and procedures mentioned in **Table 1**. The PCR products were sent to Tsingke company, Yunnan Province, China, for sequencing the above genes. The generated sequences were submitted to GenBank, and the accession numbers have been shown in **Table 2**.

TABLE 1 | Gene and primers used in the phylogenetic analyses.

Gene (reference)	Primer	Sequences	PCR condition
LSU (Vilgalys and Hester, 1990)	LROR	ACCCGCTGAACTTAAGC	(1) Initialization at for 3 min at 94°C. (2) 40 cycles of denaturation at 94°C for 45 s, annealing at 56°C for 50 s, and extension at 72°C for 1 min. (3) final elongation at 72°C for 10 min and (4) storage at 4°C.
	LR5	TCCTGAGGGAAACTTCG	
SSU (White et al., 1990)	NS1	GTAGTCATATGCTTGTCTC	
	NS4	CTTCCGTCAATTCCTTTAAG	
ITS (White et al., 1990)	ITS4	TCCTCCGCTTATTGATATGC	
	ITS5	GGAAGTAAAAGTCGTAACAAGG	
RPB1 (Castlebury et al., 2004)	CRPB1Af	CAYCCWGGYTTYATCAAGAA	(1) Initialization at 94°C for 2 min, (2) 10 cycles of denaturation at 94°C for 30 s, annealing at 64°C for 1 min, and extension at 72°C for 1 min, (3) followed by 35 cycles of denaturation at 94°C for 30 s, annealing at 54°C for 1 min, and extension at 72°C for 1 min and (4) final elongation at 72°C for 3 min. (5) storage at 4°C.
	CRPB1Cr	CCNGCDATNTCRTTRTCCATRTA	
TEF1-α (Rehner and Buckley, 2005)	983F	GCYCCYGGHCAYCGTGAYTTYAT	
	2218R	ATGACACCRACRGCRACRGTYTG	
RPB2 (Liu et al., 1999; Sung et al., 2007b)	RPB2-5F	GAYGAYMGWGATCAYTTYGG	(1) Initialization at 95°C for 3 min. (2) 40 cycles of denaturation at 95°C for 1 min, annealing at 52°C for 2 min, and extension at 72°C for 90 s. (3) final elongation at 72°C for 10 min and (4) storage at 4°C.
	RPB2-7cR	CCCATRGCTTGTYYRCCCAT	

TABLE 2 | GenBank accession numbers of the taxa used in the phylogenetic analyses.

Species	Specimen number	SSU	LSU	TEF1-α	RPB1	RPB2	ITS	References
Ophiocordyceps highlandensis	HKAS 83206	KM581282	–	–	KM581274	KM581278	–	Yang et al., 2015
Ophiocordyceps highlandensis	HKAS 83207	KM581284	–	–	KM581276	KM581280	–	Yang et al., 2015
Ophiocordyceps konnoana	EFCC 7295	EF468958	–	–	EF468862	EF468915	–	Araújo et al., 2018
Ophiocordyceps konnoana	EFCC 7315	EF468959	–	EF468753	EF468861	EF468916	–	Araújo et al., 2018
Ophiocordyceps melolonthae	OSC 110993	DQ522548	DQ518762	DQ522331	DQ522376	–	–	Sung et al., 2007a
Ophiocordyceps melolonthae	Ophgrc679	–	KC610768	KC610744	KF658666	–	–	Araújo et al., 2018
Ophiocordyceps nigrella	EFCC 9247	EF468963	EF468818	EF468758	EF468866	EF468920	–	Araújo et al., 2018
Ophiocordyceps ravenelii	OSC 110995	DQ522550	DQ518764	DQ522334	DQ522379	DQ522430	–	Araújo et al., 2018
Ophiocordyceps ravenelii	OSC 151914	KJ878932	–	KJ878978	KJ879012	KJ878950	–	Araújo et al., 2018
Ophiocordyceps superficialis	MICH 36253	EF468983	–	–	EF468883	–	–	Sung et al., 2007a
Ophiocordyceps variabilis	ARSEF 5365	DQ522555	DQ518769	DQ522340	DQ522386	DQ522437	–	Araújo et al., 2018
Ophiocordyceps variabilis	OSC 111003	EF468985	EF468839	EF468779	EF468885	EF468933	–	Araújo et al., 2018
Paraisaria alba	**HKAS 102484**	**MN943843**	**MN943839**	**MN929085**	**MN929078**	**MN929082**	**MN947219**	**This study**
Paraisaria amazonica	HUA 186143	KJ917562	KJ917571	KM411989	KP212902	KM411982	–	Ban et al., 2015
Paraisaria amazonica	HUA 186113	KJ917566	KJ917572	–	KP212903	KM411980	–	Ban et al., 2015
Paraisaria arcta	**HKAS 102553**	**MN943845**	**MN943841**	**MN929087**	**MN929080**	–	**MN947221**	**This study**
Paraisaria arcta	**HKAS 102552**	**MN943844**	**MN943840**	**MN929086**	**MN929079**	**MN929083**	**MN947220**	**This study**
Paraisaria blattarioides	HUA186093	KJ917559	KJ917570	KM411992	KP212910	–	–	Ban et al., 2015
Paraisaria blattarioides	HUA 186108	KJ917558	KJ917569	–	KP212912	KM411984	–	Ban et al., 2015
Paraisaria coenomyiae	NBRC 106964	AB968385	AB968413	AB968571	–	AB968533	AB968397	Ban et al., 2015
Paraisaria coenomyiae	NBRC 108993	AB968384	AB968412	AB968570	–	AB968532	AB968396	Ban et al., 2015
Paraisaria gracilioides	HUA 186095	KJ917556	–	KM411994	KP212914	–	–	Li et al., 2004
Paraisaria gracilioides	HUA 186092	KJ917555	KJ130992	–	KP212915	–	–	Mongkolsamrit et al., 2019
Paraisaria gracilis	EFCC 3101	EF468955	EF468810	EF468750	EF468858	EF468913	–	Araújo et al., 2018
Paraisaria gracilis	EFCC 8572	EF468956	EF468811	EF468751	EF468859	EF468912	–	Araújo et al., 2018
Paraisaria heteropoda	OSC 106404	AY489690	AY489722	AY489617	AY489651	–	–	Araújo et al., 2018
Paraisaria heteropoda	EFCC 10125	EF468957	EF468812	EF468752	EF468860	EF468914	JN049852	Araújo et al., 2018
Paraisaria orthopterorum	BBC 88305	–	MK332583	MK214080	MK214084	–	MH754742	Mongkolsamrit et al., 2019
Paraisaria orthopterorum	TBRC 9710	–	MK332582	MK214081	MK214085	–	MH754743	Mongkolsamrit et al., 2019
Paraisaria phuwiangensis	BBH 43491	–	MK192058	–	MH211351	–	MH188542	Mongkolsamrit et al., 2019
Paraisaria phuwiangensis	TBRC 9709	–	MK192057	MK214082	MK214086	–	MK192015	Mongkolsamrit et al., 2019

(Continued)

TABLE 2 | Continued

Species	Specimen number	SSU	LSU	TEF1-α	RPB1	RPB2	ITS	References
Paraisaria phuwiangensis	BBH 43492	–	MH201169	MH211355	MH211352	–	MH188541	Mongkolsamrit et al., 2019
Paraisaria rosea	**HKAS 102546**	**MN943846**	**MN943842**	**MN929088**	**MN929081**	**MN929084**	**MN947222**	**This study**
Paraisaria tettigonia	GZUH CS14062709	KT345955	–	KT375440	KT375441	–	KT345954	Wen et al., 2016
Paraisaria yodhathaii	BBH 43163	–	MK332584	MH211353	MH211349	–	MH188539	Mongkolsamrit et al., 2019
Paraisaria yodhathaii	TBRC 8502	–	MH201168	MH211354	MH211350	–	MH188540	Mongkolsamrit et al., 2019
Polycephalomyces formosus	ARSEF 1424	KF049615	KF049634	KF049689	KF049651	KF049671	KF049661	Xiao et al., 2018
Polycephalomyces nipponicus	BCC 2325	KF049622	KF049640	KF049696	KF049655	KF049677	KF049665	Xiao et al., 2018
Polycephalomyces ramosopulvinatus	EFCC 5566		KF049627	KF049682	KF049645	–	KF049658	Xiao et al., 2018
Polycephalomyces ramosus	MFLU 18-0162	MK863043	MK863050	–	–	–	MK863250	Xiao et al., 2018
Purpureocillium lilacinum	CBS 284.36	–	–	EF468792	EF468898	–	AY624189	Mongkolsamrit et al., 2019
Purpureocillium lilacinum	CBS 431.87	–	EF468844	EF468791	EF468897	–	AY624188	Mongkolsamrit et al., 2019
Purpureocillium takamizusanensis	NHJ 3497	EU369096	EU369033	EU369014	EU369053	EU369074	–	Sung et al., 2007a
Tolypocladium capitatum	NBRC 106327	JN941737	JN941404	–	JN992471	–	JN943317	Mongkolsamrit et al., 2019
Tolypocladium inflatum	CBS 567.84	–	MH873477	–	–	–	MH861779	Mongkolsamrit et al., 2019
Tolypocladium inflatum	CBS 127142	–	MH875875	–	–	–	MH864435	Mongkolsamrit et al., 2019
Tolypocladium japonicum	OSC 110991	DQ522547	DQ518761	DQ522330	DQ522375	DQ522428	JN049824	Mongkolsamrit et al., 2019
Tolypocladium ophioglossoides	NBRC 106331	JN941733	JN941408	–	JN992467	–	JN943320	Mongkolsamrit et al., 2019
Drechmeria gunnii	OSC 76404	AF339572	AF339522	AY489616	AY489650	DQ522426	JN049822	Mongkolsamrit et al., 2019
Drechmeria balanoides	CBS 250.82	AF339588	AF339539	DQ522342	DQ522388	DQ522442	MH861495	Mongkolsamrit et al., 2019
Harposporium anguillulae	ARSEF 5407	–	AY636080	–	–	–	–	Mongkolsamrit et al., 2019
Harposporium anguillulae	ARSEF 5593	–	AY636081	–	–	–	–	Mongkolsamrit et al., 2019
Harposporium helicoides	ARSEF 5354	AF339577	AF339527	–	–	–	–	Mongkolsamrit et al., 2019
Perennicordyceps prolifica	NBRC 100744	JN941709	JN941432	–	JN992443	–	–	Mongkolsamrit et al., 2019
Perennicordyceps prolifica	NBRC 101750	JN941708	JN941433	–	JN992442	–	JN943340	Ban et al., 2009
Perennicordyceps prolifica	NBRC 103838	JN941707	JN941434	–	JN992441	–	JN943339	Ban et al., 2009
Perennicordyceps cuboidea	NBRC 100941	–	AB378646	–	–	–	AB378666	Ban et al., 2009
Perennicordyceps cuboidea	NBRC 101742	–	AB378648	–	–	–	AB378667	Ban et al., 2009
Cordyceps militaris	OSC 93623	AY184977	AY184966	DQ522332	DQ522377	–	JN049825	Kepler et al., 2013
Cordyceps kyusyuensis	EFCC 5886	EF468960	EF468813	EF468754	EF468863	EF468917	–	Kepler et al., 2013

The new species generated in this study are in black bold.

Sequence Alignment and Phylogenetic Analyses

The generated sequences were assembled with Sequencing Project Management (SeqMan) (Clewley, 1995). The sequences for the combined alignment were selected based on the blast results of LSU, SSU, ITS, TEF, RPB1, and RPB2 as well as the recent references listed in **Table 2**. The individual gene alignment was aligned in MAFFT v. 7 web server[1] (Kuraku et al., 2013; Katoh et al., 2019). The alignments of each locus were improved by manually removing uninformative gaps and ambiguous regions using BioEdit v. 7.0.9.1 (Hall, 1999) and were concatenated in Sequence Matrix v. 1.7.8 (Vaidya et al., 2011). The final combined alignment was converted to a NEXUS file (.nex) with ClustalX2 v. 1.83 (Thompson et al., 1997) and was used for Bayesian inference (BI) analysis and Maximum parsimony analysis (MP). The optimum nucleotide substitution model of each gene was selected by MrModeltest v.2.3 (Nylaner, 2004) using the Akaike information criterion (AIC) method and was applied to Bayesian inference (BI) analysis that was performed using MrBayes on XSEDE (2.2.7a) (Ronquist and Huelsenbeck, 2003) on CIPRES Science Gateway[2]. The Bayesian posterior probability (BYPP) was estimated by the Markov Chain Monte Carlo (MCMC) technique. Six simultaneous Markov Chains were run for 2,000,000 generations with sampling every 1,000 generation. The first 25% of sampled trees were discarded during the burn-in period. Maximum likelihood analysis was carried out using RAxML-HPC2 on XSEDE (8.2.10) in CIPRES Science Gateway V. 3.3 (Miller et al., 2010), with default algorithm and bootstrap iterations were set to 1,000 and substitution model was set to GTRGAMMA + I. Maximum parsimony analysis was implemented in PAUP v. 4.0b10 (Swofford, 2002) through heuristic search with 1,000 random replicates of stepwise addition and tree-bisection-reconnection (TBR) of branch-swapping algorithm. Gaps were treated as missing data and max trees was set to 1,000. Branches collapsed when minimum branch length was zero. The consistency index (CI), retention index (RI), rescaled consistency index (RC) and homoplasy index (HI) were calculated for the maximum parsimony tree. For the delimitation of new species based on nucleotide comparison, we follow the suggestion of Jeewon and Hyde (2016).

The tree topologies were visualized in FigTree v1.4.0 (Rambaut, 2006) and edited in Microsoft power point (2016) and Adobe Photoshop CS3 Extended v. 10.0 (Adobe®, San Jose, CA, United States). The final alignment and trees were submitted to TreeBASE with submission number 25664[3].

RESULTS

Phylogenetic Analyses

Phylogenetic analyses were constructed with combined LSU, SSU, TEF1-α, RPB1, RPB2, and ITS sequences data of 58 representative taxa in Ophiocordycipitaceae. Trees were rooted to *Cordyceps militaris* (OSC 93623) and *C. kyusyuensis* (EFCC5886) in Cordycipitaceae. The alignment contains 5239 characters, including gaps (LSU: 918, SSU: 1027, TEF1-α: 906, RPB1: 664, RPB2: 1024, ITS: 700). Parsimony analysis of this dataset produced the 20 most parsimonious trees of 4833 steps in length, of which 3436 characters were constant, 380 variable characters parsimony-uninformative and 1423 characters parsimony-informative. The first parsimonious tree was represented as the best tree, with CI = 0.549, RI = 0.777, RC = 0.426 and HI = 0.451. The RAxML analysis of the combined dataset yielded a best scoring tree with a final ML optimization likelihood value of −30766.070218. The matrix had 2305 distinct alignment patterns, with 41.28% undetermined characters or gaps. Estimated base frequencies were as follows: A = 0.236752, C = 0.277080, G = 0.283017, T = 0.203151; substitution rates AC = 1.485223, AG = 3.851975, AT = 0.915108, CG = 1.456245, CT = 6.890167, GT = 1.000000; gamma distribution shape parameter α = 0.465094.

In the phylogenetic analyses (**Figure 1**), eight genera are included in Ophiocordycipitaceae labeled on the tree. With the exception of *Ophiocordyceps*, the other remaining genera are monophyletic and individually they received strong statistical support. The three novel entomopathogenic fungi grouped with the taxa in *Paraisaria* with significant statistical support (1.00 PP/100% ML/98% MP). *Paraisaria alba* (HKAS 102484) constitutes a sister phylogenetic affiliation to *P. yodhathaii* with 0.96 PP/98% MP statistical support. *Paraisaria rosea* (HKAS 102546) is closely related to *P. amazonica* and *P. blattarioides*, but this is statistically not supported in all three formats. Two strains of *P. arcta* grouped as an intermediate clade with close phylogenetic connection to *P. coenomyiae*, *P. gracilioides,* and *P. heteropoda*.

Taxonomy

Paraisaria alba D. P. Wei and K. D. Hyde, sp. nov. Figure 2

Etymology: *alba* refers to the white fertile head.

MycoBank number: MB 833999

Facesoffungi number: FoF 07239

Parasitic on an adult cricket (Orthoptera). **Sexual morph:** *Stroma* up to 26 mm in tall, single, unbranched, growing from the flank of the host. *Fertile head* 3.5 mm in diam., globose, white when fresh, yellow brown when dry. *Stipe* 22.5 × 1.2 mm, slightly flexuous, fleshy, white, glossy, not hollow. *Perithecia* 200–500 × 100–220 ($\bar{x}$ = 325 × 145, *n* = 20) μm, immersed, ovoid. *Asci* 160–250 × 2.5–5 ($\bar{x}$ = 200 × 3.5, *n* = 10) μm, unitunicate, hyaline, narrow cylindrical, attenuated toward the base, with thickened cap. *Peridium* 10–40 ($\bar{x}$ = 20, *n* = 30) μm in thick, comprising hyaline, thick-walled cell of *textura angularis*. *Apical cap* 4.6–7.4 × 3.2–4.9 ($\bar{x}$ = 6 × 3.8, *n* = 30) μm, with a narrow tunnel throughout the center. *Ascospores* filiform, equal to the asci in length, when mature, breaking into numerous secondary ascospores. *Secondary ascospores* 3–5 × 0.5–1.5 ($\bar{x}$ = 4 × 1, *n* = 30) μm, cylindrical, hyaline, smooth, one-celled, straight, with truncated ends.

[1]http://mafft.cbrc.jp/alignment/server

[2]https://www.phylo.org/portal2/home.action

[3]http://purl.org/phylo/treebase/phylows/study/TB2:S25664

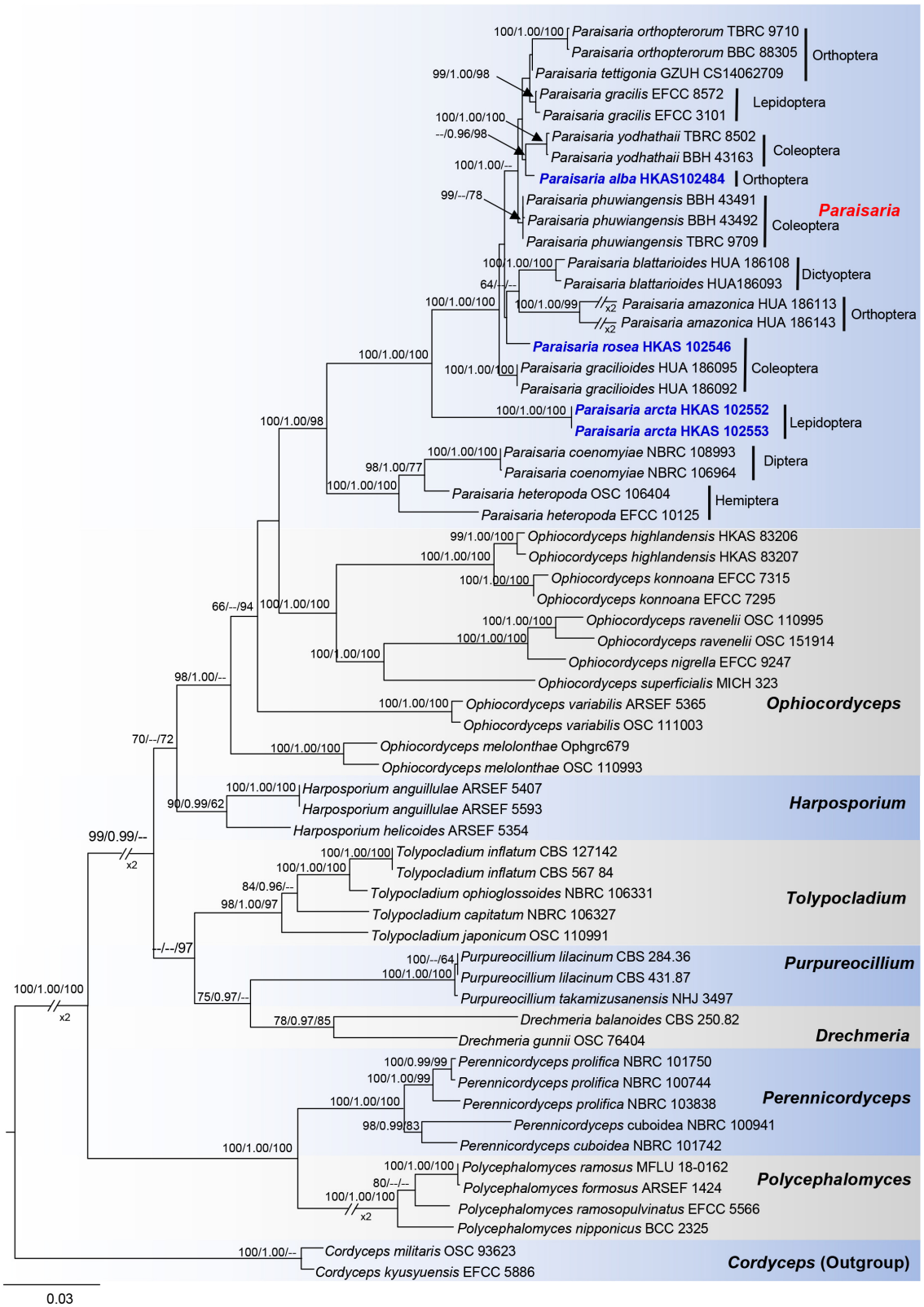


FIGURE 1 | Phylogram generated from maximum likelihood analysis based on combined LSU, SSU, TEF1-α, RPB1, RPB2, and ITS sequence data. Bootstrap values for BI equal to or higher than 95%, ML and MP equal to or greater than 60% are placed on the notes. The newly generated sequences are indicated in blue bold. The host order of *Paraisaria* species and the generic names are labeled in the right side.

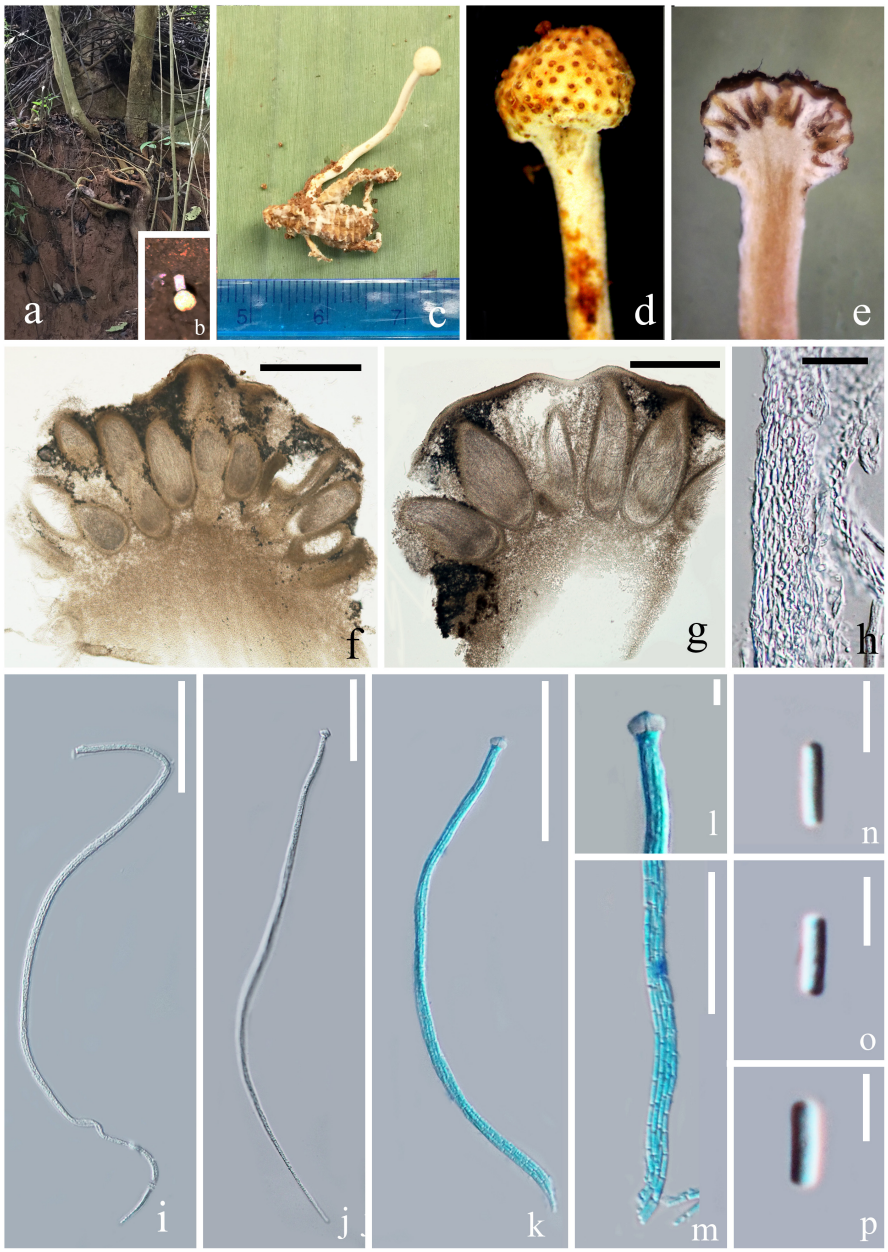


FIGURE 2 | *Paraisaria alba* (HKAS 102484, holotype). **(a)** Habitat. **(b)** Host imbedded into the soil with the stroma emerging from the ground. **(c)** Stroma arising from host. **(d)** Fertile head. **(e)** Longitudinal section through fertile head. **(f,g)** Perithecia. **(h)** Peridium. **(i–k)** Asci. **(l)** Ascus cap. **(m)** Part of the asci. **(n–p)** Secondary ascospores. Scale bars: **(f)** 500 μm, **(g)** 200 μm, **(h)** 20 μm, **(i–k)** 50 μm, **(m)** 30 μm, **(l,n–p)** 5 μm. (k–m mounted in cotton blue reagent.).

Material examined

Thailand, Krabi, Plai Phraya (N: 8°24′410″, E: 98°45′34″). On an adult cricket, 20 December 2018, *Deping Wei*, 211-1(HKAS 102484– holotype). We tried to culture *P. alba* by transferring a small piece of inner stroma tissue into a PDA medium using a sterilized needle, but growth was not observed.

Notes

The multigene phylogenetic analysis showed that *P. alba* groups with *P. yodhathaii* with fairly good statistical support (0.96 PP/98% MP, **Figure 1**). This relationship is, however, not supported by the ML analysis. *Paraisaria alba* differs from *P. yodhathaii* in having solitary stroma, a white fertile head, and smaller perithecia, asci and secondary ascospores, whereas *P. yodhathaii* has paired stromata, grayish yellow fertile head, larger perithecia and larger asci and secondary ascospores (**Table 3**). The comparison of the nucleotide sequences between *P. alba* and *P. yodhathaii* show 10 (including 6 gaps) out of 410 bp (2.4%), 6 out of 746 bp (0.8%), 5 out of 881 bp (0.56%) and 8 out of 534 bp differences (1.5%) in ITS, LSU, TEF1-α

TABLE 3 | Synopsis of *Paraisaria* species discussed in this study.

Species	Host	Distribution	Stroma (mm)	Fertile part (mm)	Perithecia (μm)	Asci (μm)	Part-ascospores (μm)	Asexual morphs
P. alba	Adult cricket (Orthoptera)	Thailand: Krabi Province	Solitary, 26 long	Globose, white, 3.5 in diam.	Ovoid, 200–500 × 100–220	160–250 × 2.5–5	3–5 × 0.5–1.5	Absent
P. amazonica[a,d,h]	Adult or imago of Acrididae (Orthoptera)	Colombia and Ecuador	Gregarious, 20–45 long	Subglobose to spherical, reddish brown, 2.5–5.5	Ovoid-ellipsoidal, 760–1100 × 220–400	325–450 × 5	9–17 × 0.5–2	Absent
P. arcta	Larva of Lepidoptera	China: Guizhou Province	Solitary, 16 long	Subglobose with constriction at center, white, 2 × 3	Ampulliform to ellipsoidal, 230–530 × 70–180	100–180 × 2–4	2.6– 4.2 × 0.5–1.3	Absent
P. blattarioides[c,h]	Adult of Blattaria (Dictyoptera)	Belize, Colombia and Ecuador	Gregarious, 14–20 long	Ovoid, subglobose, chestnut brown, 2–3 × 1.5–2.5	Ellipsoidal, 650–800 × 220–300	180–250(–300) × 4–5	6–16 × 1.5	Absent
P. coenomyiae[b]	Larva of *Coenomyia* (Diptera)	Japan	Solitary, 30–35 long	Ovoid, subglobose, chestnut brown, 8 × 10	Lanceolate, 700–750 × 200–220	500–750 × 7.8–8.0	8–15 × 1.8–2.5	Absent
P. gracilioides[b,e,h]	Larva of *Elateridae* (Coleoptera)	Bolivia, China, Colombia, Japan and Mexico	Usually solitary, 20–90 long	Spherical, pale rufous, 4–5.5	Ellipsoidal to naviform, 680–900 × 200–280	450–700 × 5–6.5	7–12 × 1–2	Present
P. gracilis[d,g,h]	Larva of *Hepialidae* (Lepidoptera)	Africa, America, Asia, Europe, and Oceania	Usually solitary, 40– 90 long	Globose to ellipsoidal, red ochreous to pale orange, 4–9 × 4–7	Elongate to oviform, (320–)560–840 × 200–360	(200–)400–528 × 5–8	5–9 × 1.5–2	Present
P. heteropoda[e]	Nymph of Cicadidae (*Hemiptera*)	Australia, Japan	Solitary, 120 long	Ovoid, cinnamon buff, 7–9 × 6–7	Ampulliform, 610–660 × 210	250–300 × 5.2–7	6–7.7 × 0.9–1	Present
P. myrmicarum	*Myrmica rubra* (Hymenoptera)	United Kingdom	–	–	–	–	–	Present
P. orthopterorum[f]	Nymph of Orthoptera	Thailand: Trat Province	Solitary, 10–45 long	Globose, gray orange, 2–4 × 3	Obclavate, 520–650 × 150–250	400 × 5	5–10 × 1–1.5	Present
P. phuwiangensis[f]	Larva of Elateridae (Coleoptera)	Thailand: Khon Kaen Province	Solitary, 30–50 long	Globose to subglobose, light brown, 4–8 × 4–7	Obpyriform, 800–1200 × 300–380	500 × 3–5	5–10 × 1–2	Present
P. rosea	Larva of Coleoptera	China: Yunnan Province	Solitary, 14.5 long	Subglobose, pale pink, 4.5 × 4	Ampulliform, 500–900 × 150–350	230–390 × 3.5–6	4–11 × 1.5–2.5	Present
P. tettigonia[f]	Adult of *Tettigonia* (Orthoptera)	China: Guizhou Province	Paired, 32.5–37.5 long	Globose, white, 2–2.5	Elongated to ampulliform, 520–680 × 205–275	530–615 × 6.5–9.3	6.7–9.4 × 1.5–2.3	Absent
P. yodhathaii[f]	Larva of *Elateridae* (Coleoptera)	Thailand: Khon Kaen Province	Gregarious, 20–35 long	Globose to subglobose, grayish yellow, 2–4 × 2–5	Obclavate, 650–800 × 160–250	480 × 5–6	5–10 × 1–2	Present

The new species generated in this study are in bold.[a]*Ban et al., 2009;* [b]*Ban et al., 2015;* [c]*Hennings, 1904;* [d]*Kobayasi, 1941;* [e]*Mains, 1940;* [f]*Mongkolsamrit et al., 2019;* [g]*Samson and Brady, 1983;* [h]*Sanjuan et al., 2015;* [i]*Wen et al., 2016.*

and RPB1 sequences, respectively. SSU and RPB2 sequences data of *P. yodhathaii* are not available in GenBank. Henceforth, we describe our collection as a new species in *Paraisaria* according to the guidelines of Jeewon and Hyde (2016).

Paraisaria arcta D. P. Wei and K. D. Hyde, sp. nov. Figure 3

Etymology: ***arcta*** refers to the constricted fertile head.

MycoBank number: MB 834000

Facesoffungi number: FoF 07240

Parasitic on larva of Lepidopteran larva. **Sexual morph:** *Stroma* 16 mm long, single, arising from the mouth of host larva. *Fertile head* 2 mm long, 3 mm wide, white, nearly globose, constricted at the center, with sticky and crystal-like substance on the surface. *Stipe* 14 mm long, 2 mm wide, straight, fleshy, white, glossy. *Perithecia* 230–530 × 70–180 ($\bar{x}$ = 387 × 113, n = 20) μm, completely immersed, ampulliform to ellipsoid. *Peridium* 14–20 ($\bar{x}$ = 17, n = 30) μm wide, composed of hyaline, thick-walled, smooth-walled cells of *textura angularis*. *Asci* 100–180 × 2–4 μm ($\bar{x}$ = 137 × 2.9, n = 15), unitunicate, hyaline, narrow cylindrical,

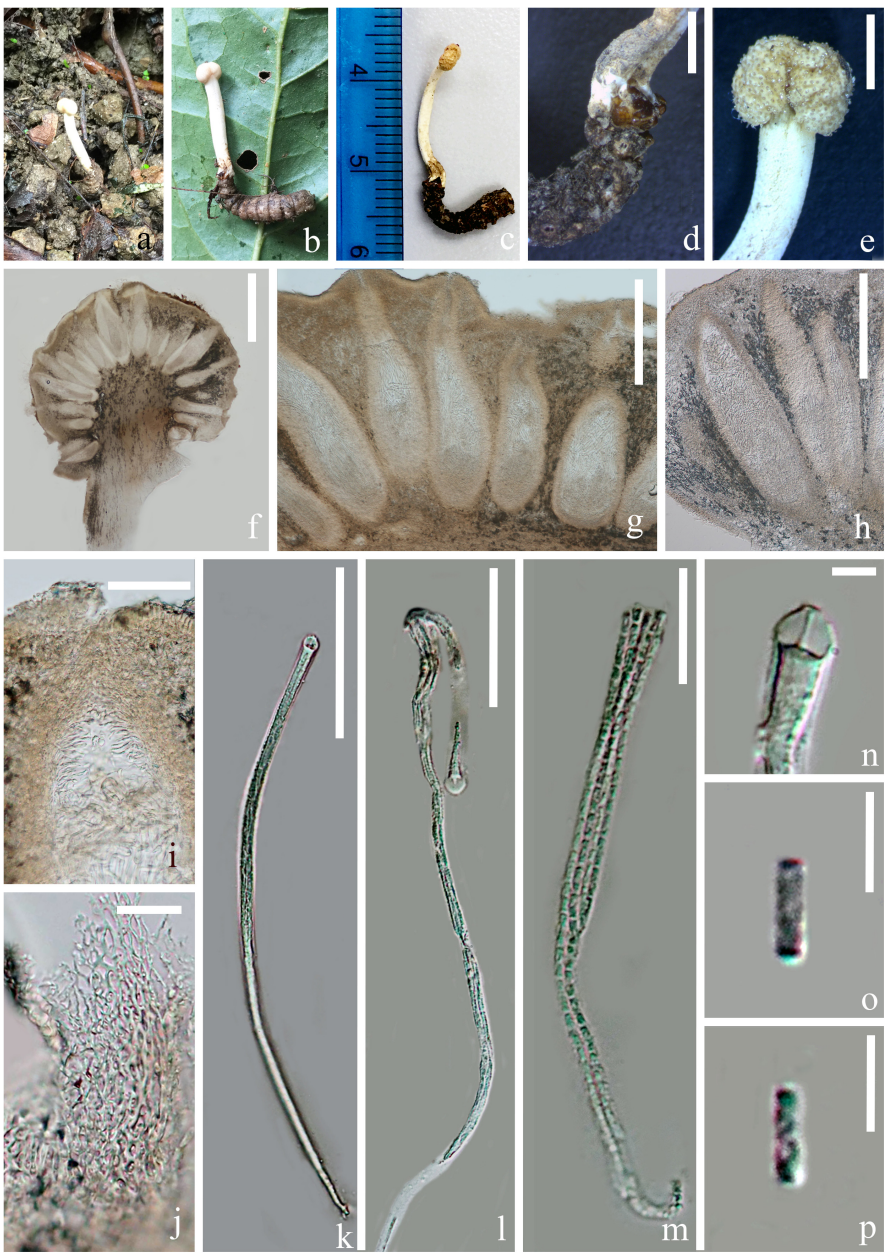


FIGURE 3 | *Paraisaria arcta* (HKAS 102553, holotype). **(a)** Substrate. **(b–d)** Stromata emerging from host mouth. **(e)** Fertile head. **(f–h)** Perithecia. **(i)** Ostiole. **(j)** Peridium. **(k,l)** Asci. **(m)** Parts of ascus. **(n)** Ascus cap. **(o,p)** Secondary ascospores. Scale bars: **(d,e)** 2000 μm, **(f)** 500 μm, **(g,h)** 200 μm, **(i,k)** 50 μm, **(j,m)** 15 μm, **(l)** 30 μm, (**n–p) 3** μm.

tapering toward the base, 8-spored, with thickened cap. *Apical cap* 3.5–4.5 × 2–3.6 μm thick ($\bar{x}$ = 4 × 2.8, *n* = 20), with a narrow tunnel throughout the center. *Ascospores* hyaline, narrow filiform, equal to the asci in length, when mature, breaking into numerous secondary ascospores. *Secondary ascospores* 2.6–4.2 × 0.5–1.3 μm ($\bar{x}$ = 3.3 × 0.9, *n* = 60), cylindrical, with truncated ends, hyaline, smooth, one-celled, straight.

Material examined

China, Guizhou Province, Qianxinan Buyei and Miao Autonomous Prefecture, Ceheng County, Gaofeng Villige (N: 24°57′33″, E: 105°50′1″), on dead larva of *Lepidoptera* sp., 6 August 2018, *Deping Wei,* GFC604 (HKAS 102553–holotype); GFC603 (HKAS 102552 – paratype). The culturing of *P. arcta* was tried by transferring a mass of mycelium found inside body of the larva host to a PDA medium using a sterilized needle. However, mycelium growth was not observed.

Notes

Paraisaria arcta resembles *P. alba* found in Krabi Province, Thailand and *P. tettigonia* discovered in Guizhou Province, China in having white fertile heads but differs from *P. alba* in its associated host and number of stromata are distinct from *P. tettigonia* (Wen et al., 2016). *Paraisaria arcta* can also be distinguished from the other species in *Paraisaria* by the color and shape of its fertile head. A conspicuous ravine throughout the center of the fertile head is present in *P. arcta*, which is lacking in the other species in this genus. The detailed comparisons are shown in **Table 3**. Multigene phylogenetic analysis showed *P. arcta* constitutes a distant clade from other species in *Paraisaria,* with strong statistical support (100% ML, 100% MP, 1.00 PP, **Figure 1**). Herein, we introduce this collection as a new species of *Paraisaria.*

Paraisaria rosea D. P. Wei and K. D. Hyde, sp. nov. Figures 4, 5

Etymology: *rosea* refers to its pink fertile head.

MycoBank number: MB834001

Facesoffungi number: FoF 07241

Parasitic on a larva of Coleoptera. Host buried in the soil, with the stroma erumpent from the ground. **Sexual morph:** *Stroma* up to 14.5 mm long, laterally emerging from the middle part of the larva body, simple, erect. *Fertile head* 4.5 × 4 mm, subglobose, pale pink at top and paler toward the base when fresh, pale yellow-brown when dry. *Stipe* 10 × 1.5 mm, white, straight, unbranched, glossy, cylindrical, inside not hollow. *Perithecia* 500–900 × 150–350 ($\bar{x}$ = 762 × 256, *n* = 30) μm, completely immersed, ampulliform, ostiolate. *Peridium* 9–15 ($\bar{x}$ = 12, *n* = 30) μm wide, composed of hyaline, thick-walled cells of *textura angularis* to *textura globulosa* to *textura prismatica*. *Asci* 230–390 × 3.5–6 ($\bar{x}$ = 280 × 5, *n* = 15) μm, hyaline, cylindrical, unitunicate, eight-spored, possessing a prominent apical cap. *Apical cap* 5–7 × 2–6 ($\bar{x}$ = 6 × 4, *n* = 20) μm, with a conspicuous tunnel throughout the center. *Ascospores* filiform, hyaline, breaking into secondary ascospores when mature. *Secondary ascospores* 4–11 × 1.5–2.5 ($\bar{x}$ = 7.5 × 2, *n* = 30) μm, hyaline, cylindrical with truncate ends, smooth-walled, aseptate. **Asexual morph:** Hyphomycetous. *Synnemata* producing from the center of culture after 16 months incubation in dark environment, composed of loose, septate hyphae, white, filamentous, aerial, straight, branched, fasciculate, bearing shining droplets and conidiophores. *Mycelium* 2.4–3.7 ($\bar{x}$ = 3, *n* = 10) μm in wide, septate, hyaline, smooth-walled. *Conidiophores* 33–48 ($\bar{x}$ = 41, *n* = 10) μm in height, irregularly differentiate from the synnemata, sparse, gregarious, branched. *Phialides* 5.8–11.5 × 3–5.5 ($\bar{x}$ = 8.6 × 4, *n* = 30) μm, ampulliform, 1-necked, hyaline, aseptate, enteroblastic, phialidic, monophialidic. *Conidia* 8–12 × 2–2.6 ($\bar{x}$ = 9.8 × 2.3, *n* = 50) μm, hyaline, cylindrical, smooth-walled, aseptate, with round ends.

Culture characteristics

Culture was made from mycelium inside body of the host larva, slowly growing on PDA, reaching 1.3 cm in diam after incubated at room temperature (25°C) for 50 days, convex, dense, with undulate edges, smooth surface become filamentous after forming aerial synnemata. The shooting conidia land on the surrounding culture and develop new colonies.

Material examined

China, Yunnan Province, Kunming, Western hill Park (N: 24°57′28″, E: 102°38′17″), on larva of *Coleoptera* sp. buried in soil, 27 July 2018, *Deping Wei*, XS2712 (HKAS 102546 – Holotype); (KUMCC 20-0001 – ex-type living culture).

Notes

Paraisaria rosea is closely related to *P. amazonica* and *P. blattarioides,* without any statistical support (**Figure 1**). However, *P. rosea* can be distinguished from these related species based on the number of stromata, the color of the fertile head and the size of asci and secondary ascospores (**Table 3**). The ITS sequence of *P. amazonica* and *P. blattarioides* are not available in GenBank database; the nucleotide differences in the TEF1-α, RPB1 and RPB2 region between *P. rosea* and the two above species are greater than 1.5% (**Table 4**). Thereby, we introduced *P. rosea* as a new species in this genus based on the distinctive morphology and molecular support.

DISCUSSION

The sexual morph of *Paraisaria* species phenotypically share an erect or slightly flexuous, cylindrical, colorless, fleshy stipe that terminates in a subglobose to globose fertile head and completely immersed perithecia. Asci are cylindrical with a thickened apical cap. Ascospores are hyaline, multi-septate and usually break into numerous cylindrical, truncated fragments at maturity. However, they can be distinguished according to their associated host, the number of stroma and the color of the fertile head. Species in this genus usually infect several stages of insects, such as larvae of Coleoptera, Diptera, and Lepidoptera; nymphs of Hemiptera and Orthoptera; or adults of Dictyoptera, Hymenoptera (ant) and Orthoptera (Evans et al., 2010; Sanjuan et al., 2015; Mongkolsamrit et al., 2019). According to the number of stromata, species of *Paraisaria* can be divided into three groups: solitary stroma, paired stromata and multiple stromata (see the key below). The shape of their fertile head features little variation,

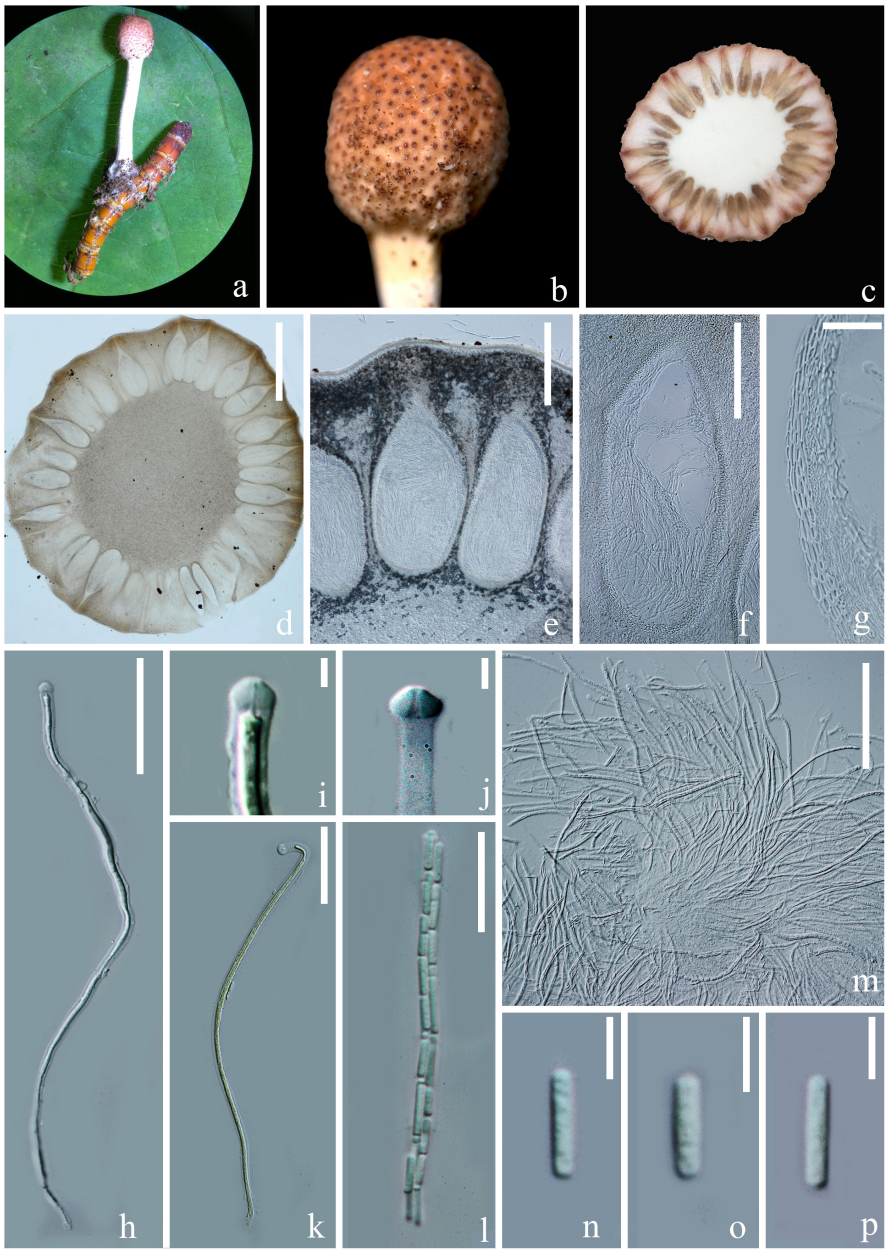


FIGURE 4 | Sexual morph of *Paraisaria rosea* (HKAS 102546, Holotype). **(a)** Stroma emerging from host. **(b)** Fertile head. **(c)** Transverse section of the fertile head. **(d–f)** Perithecia. **(g)** Peridium. **(h,k,m)** Asci. **(i,j)** Asci cap. **(l)** Part of ascus. **(n–p)** Secondary ascospores. Scale bars: **(d)** 1000 μm, **(e)** 300 μm, **(f)** 200 μm, **(g,m)** 30 μm, **(h,k)** 50 μm, **(l)** 20 μm, **(i,j, n–p)** 5 μm. (**k** mounted in Melzer's reagent).

though differing in color, ranging from white, pale pink, pale rufous, red ochreous to pale orange, chestnut, cinnamon buff, grayish, reddish brown to dark brown (see **Table 3**).

The asexual morphs of this genus are known in eight species, viz. *P. myrmicarum* (Evans et al., 2010), *P. gracilis* (Samson and Brady, 1983), *P. gracilioides* (Li et al., 2004), *P. rosea* (this study), *P. heteropoda*, *P. orthopterorum*, *P. phuwiangensis,* and *P. yodhathaii* (Mongkolsamrit et al., 2019). Their conidiophores are irregularly branched and generally develop from white, rope-like synnemata. Their phialides are flask-shaped, with a swollen base and narrow neck. Most species produce only one neck from the terminal phialides. Some species, e.g., *P. gracilis*, *P. gracilioides*, *P. myrmicarum* and *P. orthopterorum* produce 1–4 necks per phialides. Their conidia are cylindrical or ellipsoid or fusiform. Some species, e.g., *P. orthopterorum* and *P. yodhathaii* have both cylindrical and fusiform forms of conidia (Mongkolsamrit et al., 2019).

Sung et al. (2007a) have concluded that multi-gene phylogeny gave more deeper understanding of phylogenetic relationships of *Cordyceps* and Clavitipitaceae than that of single gene. Recently,

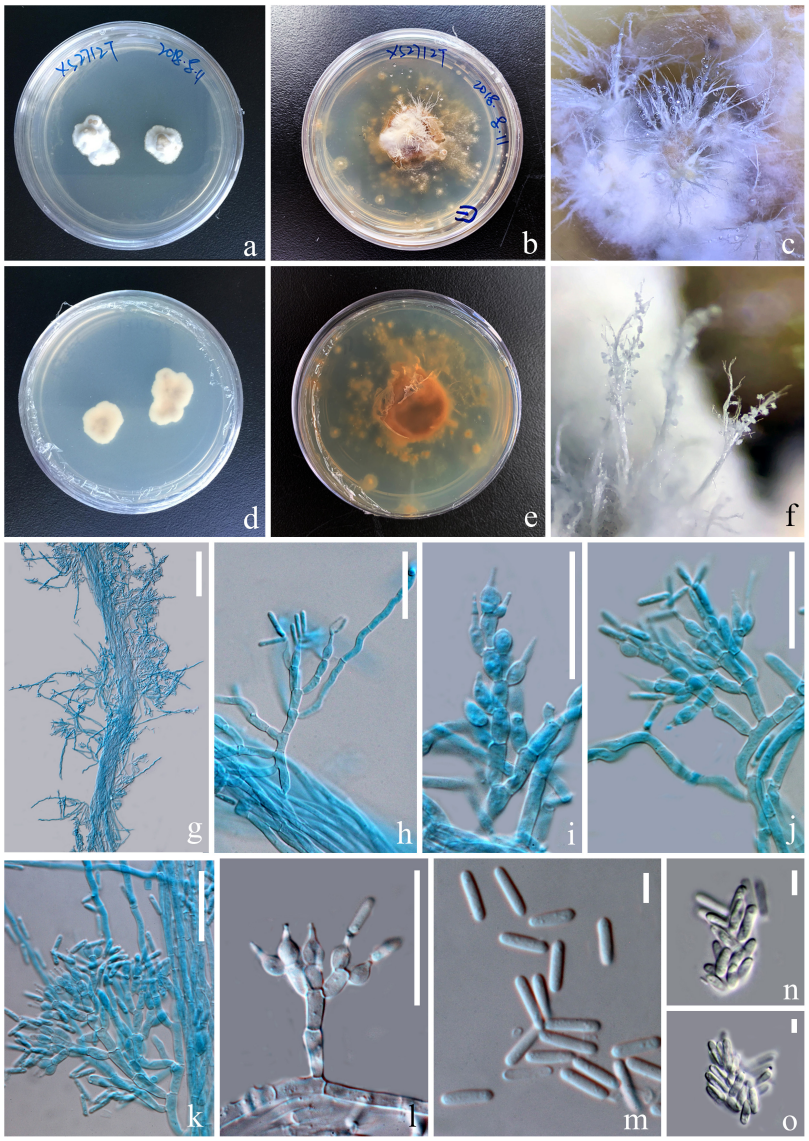


FIGURE 5 | Asexual morph of *Paraisaria rosea* (KUMCC 20-0001, ex-type). **(a,d)** Upper and lower views of cultures on PDA after 50 days. **(b,e)** Upper and lower views of cultures on PDA after 16 months incubation in dark environments. **(c,f)** Enlargement of aerial synnemata produced on culture. **(g)** Synnema bearing conidiophores. **(h–l)** Phialides. **(m)** Conidia. **(n,o)** Irregularly aggregated conidia. Scale bars: **(g)** 100 μm, **(h–l)** 30 μm, **(m–o)** 5 μm. (**h–k,m** mounted in cotton blue reagent.).

the combined LSU-TEF1-α-RPB1 datasets (Mongkolsamrit et al., 2019), combined SSU-LSU-TEF-RPB2 datasets (Ban et al., 2015), and combined SSU-LSU-TEF1-α-RPB1-RPB2 datasets (Quandt et al., 2014; Sanjuan et al., 2015) were allowed for intraspecific and intergeneric identification within Ophiocordycipitaceae. However, individual gene phylogenies are rarely utilized for identification of species in *Paraisaria*.

TABLE 4 | The comparison of nucleotide sequences between *Paraisaria rosea* and two close species.

Species	TEF1-α (bp)	RPB1 (bp)	RPB2 (bp)
Paraisaria amazonica	4.4% (38/862)	5.7% (37/642)	4.3% (31/711)
Paraisaria blattarioides	1.6% (14/862)	2.5% (16/629)	–

Key to the Accepted Species in *Paraisaria*

(1) Host belong to Hymenoptera.....*P. myrmicarum*
(1) Host not belong to Hymenoptera.....2
(2) Fertile part colorless.....3
(2) Fertile part pigmented.....4
(3) Fertile part constrict at the center.....***P. arcta***
(3) Fertile part is not constricted at the center.....5
(4) Stromata gregarious.....6

(4) Stromata solitary.....7
(5) Stromata branched.....*P. tettigonia*
(5) Stromata unbranched.....***P. alba***
(6) Stromata equal or shorter than 20 mm.....*P. blattarioides*
(6) Stromata longer than 20 mm.....8
(7) Attack nymph stage of host.....9
(7) Attack larva stage of host.....10
(8) Fertile part reddish brown.....*P. amazonica*
(8) Fertile part grayish yellow.....*P. yodhathaii*
(9) Stromata long, 120 mm.....*P. heteropoda*
(9) Stromata short, 10–45 mm.....*P. orthopterorum*
(10) Host belong to Coleoptera.....11
(10) Host belong to other order of insect.....12
(11) Stromata equal or shorter than 14.5 mm.....***P. rosea***
(11) Stromata longer than 14.5 mm.....13
(12) Pathogenic on larva of Diptera (*Coenomyia*). .....*P. coenomyiae*
(12) Pathogenic on larva of Lepidoptera (*Hepialidae*) .....*P. gracilis*
(13) Phialides solitary or in whorls of 2–3, with one neck.....*P. phuwiangensis*
(13) Phialides sympodially proliferating, with 1–4 necks.....*P. gracilioides*

DATA AVAILABILITY STATEMENT

The datasets presented in this study can be found in online repositories. The names of the repository/repositories and accession number(s) can be found below: https://www.ncbi.nlm.nih.gov/genbank/, MN943843, MN943839, MN929085, MN929078, MN929082, and MN947219; https://www.ncbi.nlm.nih.gov/genbank/, MN943845, MN943841, MN929087, MN929080, and MN947221; https://www.ncbi.nlm.nih.gov/genbank/, MN943844, MN943840, MN929086, MN929079, MN929083, and MN947220.

AUTHOR CONTRIBUTIONS

D-PW, DW, and SK: conceptualization. D-PW: data curation. D-PW and DW: formal analysis, methodology, and writing – original draft. SL, ST, and SK: funding acquisition. D-PW and DW: investigation. ST and SK: project administration. KH, J-CX, and PM: supervision. CT-a, AE, SM, ST, SK, KH, J-CX, PM, NS, and SL: writing – review and editing. All authors: contributed to the article and approved the submitted version.

FUNDING

We appreciate Thailand Research Fund (TRF) grant no. DBG6080013 entitled "The future of specialist fungi in a changing climate: baseline data for generalist and specialist fungi associated with ants, *Rhododendron* species and *Dracaena* species" for its financial support. We are grateful for the National Science Foundation of China (NSFC) project code 31750110478 for funding the sequencing cost. DW would like to thank CAS President's International Fellowship Initiative (PIFI) for funding his postdoctoral research (number 2019PC0008) and the 64th batch of China Postdoctoral Science Foundation (grant no. Y913083271). PM and DW thank the National Science Foundation of China for financial support under the following grants: 41761144055 and 41771063. SK thanks CAS President's International Fellowship Initiative (PIFI) young staff under the grant number: 2020FYC0002 and the National Science Foundation of China (NSFC) for funding this work under the project code 31851110759. ST would like to thank the International Postdoctoral Exchange Fellowship Program (number Y9180822S1), CAS President's International Fellowship Initiative (PIFI) (number 2020PC0009), China Postdoctoral Science Foundation and the Yunnan Human Resources, and Social Security Department Foundation for funding her postdoctoral research. The authors extend their appreciation to the researchers supporting project number (RSP-2021/56) King Saud University, Riyadh, Saudi Arabia. This work was partly supported by Chiang Mai University.

ACKNOWLEDGMENTS

We acknowledge Kunming Institute of Botany, Chinese Academy of Sciences for providing the laboratories and instruments for molecular work. We appreciate the Centre of Excellence in Fungal Research (Mae Fah Luang University) for providing funding for collecting trips and Dr. Shaun Pennycook is thanked for help in naming the new fungal species. Austin Smith at World Agroforestry (ICRAF), Kunming Institute of Botany, China, is thanked for English editing.

REFERENCES

Araújo, J. P., Evans, H. C., Kepler, R., and Hughes, D. P. (2018). Zombie-ant fungi across continents: 15 new species and new combinations within *Ophiocordyceps*. I. Myrmecophilous hirsutelloid species. *Stud. Mycol.* 90, 119–160. doi: 10.1016/j.simyco.2017.12.002

Araújo, J. P., and Hughes, D. P. (2016). Diversity of entomopathogenic fungi: which groups conquered the insect body? *Adv. Genet.* 94, 1–39. doi: 10.1016/bs.adgen.2016.01.001

Aung, O., Soytong, K., and Hyde, K. D. (2008). Diversity of entomopathogenic fungi in rainforests of Chiang Mai Province, Thailand. *Fungal Divers.* 30, 15–22.

Ban, S., Sakane, T., and Nakagiri, A. (2015). Three new species of *Ophiocordyceps* and overview of anamorph types in the genus and the family Ophiocordyceptaceae. *Mycol. Prog.* 14:1017. doi: 10.1007/s11557-014-1017-8

Ban, S., Sakane, T., Toyama, K., and Nakagir, A. (2009). Teleomorph–anamorph relationships and reclassification of *Cordyceps cuboidea* and its allied species. *Mycoscience* 50, 261–272. doi: 10.1007/S10267-008-0480-Y

Cao, C., Yang, S., and Zhou, Z. (2020). The potential application of *Cordyceps* in metabolic-related disorders. *Phytother. Res.* 34, 295–305. doi: 10.1002/ptr.6536

Castlebury, L. A., Rossman, A. Y., Gi-Ho, S., Hyten, A. S., and Spatafora, J. W. (2004). Multigene phylogeny reveals new lineage for *Stachybotrys chartarum*, the indoor air fungus. *Mycol. Res.* 108, 864–872. doi: 10.1017/S0953756204000607

Clewley, J. P. (1995). Macintosh sequence analysis software. *Mol. Biotechnol.* 3, 221–224. doi: 10.1007/bf02789332

Evans, H. C., Groden, E., and Bischoff, J. F. (2010). New fungal pathogens of the red ant, *Myrmica rubra*, from the UK and implications for ant invasions in the USA. *Fungal Biol.* 114, 451–466. doi: 10.1016/j.funbio.2010.03.007

Fernández-Grandon, G. M., Harte, S. J., Ewany, J., Bray, D., and Stevenson, P. C. (2020). Additive effect of botanical insecticide and entomopathogenic fungi on pest mortality and the behavioral response of its natural enemy. *Plants* 9:173. doi: 10.3390/plants9020173

Hall, T. (1999). BioEdit: a user-friendly biological sequence alignment editor and analysis program for windows 95/98/NT. *Nucleic Acids Symp. Ser.* 41, 95–98.

Hennings, P. (1904). Fungi amazonici II. a cl. Ernesto Ule collecti. *Hedwigia* 43, 246–249.

Huang, Y. S., Wang, X., Feng, Z., Cui, H., Zhu, Z., Xia, C., et al. (2020). *Cordyceps cicadae* prevents renal tubular epithelial cell apoptosis by regulating the SIRT1/p53 pathway in hypertensive renal injury. *Evidence-Based Complement. Altern. Med.* 1, 1–13. doi: 10.1155/2020/7202519

Hyde, K. D., Norphanphoun, C., Chen, J., Dissanayake, A. J., Doilom, M., Hongsanan, S., et al. (2018). Thailand's amazing diversity: up to 96% of fungi in northern Thailand may be novel. *Fungal Divers.* 93, 215–239. doi: 10.1007/s13225-018-0415-7

Hyde, K. D., Norphanphoun, C., Maharachchikumbura, S. S. N., Bhat, D. J., Jones, E. B. G., Bundhun, D., et al. (2020). Refined families of sodariomycetes. *Mycosphere* 11, 305–1059. doi: 10.5943/mycosphere/11/1/7

Hyde, K. D., Xu, J. C., Rapior, S., Jeewon, R., Lumyong, S., Niego, A. G. T., et al. (2019). The amazing potential of fungi: 50 ways we can exploit fungi industrially. *Fungal Divers.* 97, 1–136. doi: 10.1007/s13225-019-00430-9

Jayasiri, S. C., Hyde, K. D., Ariyawansa, H. A., Bhat, J., Buyck, B., Cai, L., et al. (2015). The faces of fungi database: fungal names linked with morphology, phylogeny and human impacts. *Fungal Divers.* 74, 3–18. doi: 10.1007/s13225-015-0351-8

Jeewon, R., and Hyde, K. D. (2016). Establishing species boundaries and new taxa among fungi: recommendations to resolve taxonomic ambiguities. *Mycosphere* 7, 1669–1677. doi: 10.5943/mycosphere/7/11/4

Katoh, K., Rozewicki, J., and Yamada, K. D. (2019). MAFFT online service: multiple sequence alignment, interactive sequence choice and visualization. *Brief. Bioinform.* 20, 1160–1166. doi: 10.1093/bib/bbx108

Kepler, R., Ban, S., Nakagir, A., Bischoff, J., Hywel-Jones, N., Owensby, C. A., et al. (2013). The phylogenetic placement of hypocrealean insect pathogens in the genus *Polycephalomyces*: an application of one fungus one name. *Fungal Biol.* 117, 611–622. doi: 10.1016/j.funbio.2013.06.002

Kobayasi, Y. (1941). The genus *Cordyceps* and its allies. *Sci. Rep. Tokyo Bunrika Daigaku Sec. B* 84, 53–260.

Krasnoff, S. B., Reátegui, R. F., Wagenaar, M. M., Gloer, J. B., and Gibson, D. M. (2005). Cicadapeptins I and II: new Aib-containing peptides from the entomopathogenic fungus *Cordyceps heteropoda*. *J. Nat. Prod.* 68, 50–55. doi: 10.1021/np0497189

Kuraku, S., Zmasek, C. M., Nishimura, O., and Katoh, K. (2013). aLeaves facilitates on-demand exploration of metazoan gene family trees on MAFFT sequence alignment server with enhanced interactivity. *Nucleic Acids Res.* 41, 22–28.

Li, C. R., Ming, L., Fan, M. Z., and Li, Z. Z. (2004). *Paraisaria gracilioides* comb. nov., the anamorph of *Cordyceps gracilioides*. *Mycosystema* 23, 165–166.

Li, L. Q., Song, A. X., Yin, J. Y., Siu, K. C., Wong, W. T., and Wu, J. Y. (2020). Anti-inflammation activity of exopolysaccharides produced by a medicinal fungus *Cordyceps sinensis* Cs-HK1 in cell and animal models. *Int. J. Biol. Macromol.* 149, 1042–1050. doi: 10.1016/j.ijbiomac.2020.02.022

Liu, Y., Whelen, S., and Hall, B. D. (1999). Phylogenetic relationships among ascomycetes: evidence from an RNA polymerase II subunit. *Mol. Biol. Evol.* 16, 1799–1808. doi: 10.1093/oxfordjournals.molbev.a026092

Ma, Y., Suo, F. Y., Wang, A. L., Lu, S., Ye, X., and Gong, J. (2012). Study on antioxidation activity of the broth of different originated *Ophiocordyceps gracilis* (Grev.) GH Sung, JM Sung, Hywel-Jones & Spatafora in vitro. *Chin. J. Biochem. Pharm.* 6:028.

Maharachchikumbura, S. S. N., Hyde, K. D., Jones, E. B. G., McKenzie, E. H. C., Bhat, J. D., Dayarathne, M. C., et al. (2016). Families of Sordariomycetes. *Fungal Divers.* 79, 1–317. doi: 10.1007/s13225-016-0369-6

Mains, E. B. (1940). *Cordyceps* species from British Honduras. *Mycologia* 32, 16–22. doi: 10.2307/3754313

Matočec, N., Kušan, I., and Ozimec, R. (2014). The genus *Polycephalomyces* (Hypocreales) in the frame of monitoring Veternica cave (Croatia) with a new segregate genus *Perennicordyceps*. *Ascomycete* 6, 125–133.

Miller, M. A., Pfeiffer, W., and Schwartz, T. (2010). "Creating the CIPRES science gateway for inference of large phylogenetic trees," in *Proceedings of the Gateway Computing Environments Workshop (GCE)*, New Orleans LA, 1–8.

Mongkolsamrit, S., Noisripoom, W., Arnamnart, N., Lamlertthon, S., Himaman, W., Jangsantear, P., et al. (2019). Resurrection of *Paraisaria* in the *Ophiocordycipitaceae* with three new species from Thailand. *Mycol. Prog.* 18, 1213–1230. doi: 10.1007/s11557-019-01518-x

Mora, M. A. E., Castilho, A. M. C., and Fraga, M. E. (2017). Classification and infection mechanism of entomopathogenic fungi. *Arq. Inst. Biol.* 84, 1–10. doi: 10.1590/1808-1657000552015

Nylaner, J. A. A. (2004). *MrModeltest v2. Program Distributed by the Author*. Uppsala: Uppsala University.

Pérez-Villamares, J., Burrola-Aguilar, C., Aguilar-Miguel, X., Sanjuan, T., and Jiménez-Sánchez, E. (2017). Nuevos registros de hongos entomopatógenos del género *Cordyceps s. l.* (Ascomycota: Hypocreales). del Estado de México. *Rev. Mex. Biodivers.* 88, 773–783. doi: 10.1016/j.rmb.2017.10.013

Quandt, C. A., Kepler, R. M., Gams, W., Araújo, J. P., Ban, S., Evans, H. C., et al. (2014). Phylogenetic-based nomenclatural proposals for *Ophiocordycipitaceae* (Hypocreales) with new combinations in *Tolypocladium*. *IMA Fungus* 5, 121–134. doi: 10.5598/imafungus.2014.05.01.12

Rambaut, A. (2006). *FigTree. Tree Figure Drawing Tool Version 1.3.1*. Edinburgh: University of Edinburgh.

Rehner, S. A., and Buckley, E. P. A. (2005). *Beauveria* phylogeny inferred from nuclear ITS and EF1-a sequences: evidence for cryptic diversification and links to *Cordyceps* teleomorphs. *Mycologia* 97, 84–98. doi: 10.3852/mycologia.97.1.84

Roberts, D. W., and Hajek, A. E. (1992). "Entomopathogenic fungi as bioinsecticides," in *Frontiers in Industrial Mycology*, ed. G. F. Leatham (Boston, MA: Springer), 144–159. doi: 10.1007/978-1-4684-7112-0_10

Ronquist, F., and Huelsenbeck, J. P. (2003). MrBayes 3: bayesian phylogenetic inference under mixed models. *Bioinformatics* 19, 1572–1574. doi: 10.1093/bioinformatics/btg180

Samson, R. A., and Brady, B. L. (1983). *Paraisaria*, a new genus for *Isaria dubia*, the anamorph of *Cordyceps gracilis*. *Trans. Br. Mycol. Soc.* 81, 285–290. doi: 10.1016/S0007-1536(83)80081-3

Samson, R. A., Evans, H. C., and Latgé, J. P. (eds). (1988). "Taxonomy of entomopathogenic fungi," in *Atlas of Entomopathogenic Fungi*, (Berlin: Springer), 5–16. doi: 10.1007/978-3-662-05890-9_2

Sanjuan, T. I., Franco-Molano, A. E., Kepler, R. M., Spatafora, J. W., Tabima, J., Vasco-Palacios, A. M., et al. (2015). Five new species of entomopathogenic fungi from the Amazon and evolution of Neotropical *Ophiocordyceps*. *Fungal Biol.* 119, 901–916. doi: 10.1016/j.funbio.2015.06.010

Scholte, E. J., Knols, B. G., Samson, R. A., and Takken, W. (2004). Entomopathogenic fungi for mosquito control: a review. *J. Insect Sci.* 4:19. doi: 10.1093/jis/4.1.19

Shah, P., and Pell, J. (2003). Entomopathogenic fungi as biological control agents. *Appl. Microbiol. Biotecnol.* 61, 413–423. doi: 10.4489/MYCO.2011.39.1.001

Shrestha, B., Sung, G. H., and Sung, J. M. (2017). Current nomenclatural changes in *Cordyceps* sensu lato and its multidisciplinary impacts. *Mycology* 8, 293–302. doi: 10.1080/21501203.2017.1386242

Sobczak, J. F., Arruda, I. D. P., Fonseca, E. O., Rabelo, P. J. Q., de Sousa Nóbrega, F. A., Pires, J. C., et al. (2020). Manipulation of wasp (Hymenoptera: Vespidae) behavior by the entomopathogenic fungus *Ophiocordyceps humbertii* in the Atlantic forest in Ceará, Brazil1. *Entomol. News* 129, 98–104. doi: 10.3157/021.129.0115

Spatafora, J. W., Quandt, C. A., Kepler, R. M., Sung, G. H., Shrestha, B., Hywel-Jones, N. L., et al. (2015). New 1F1N species combinations in *Ophiocordycipitaceae* (Hypocreales). *IMA Fungus* 6, 357–362. doi: 10.5598/imafungus.2015.06.02.07

Sung, G. H., Hyweljones, N. L., Sung, J. M., Luangsaard, J. J., Shrestha, B., and Spatafora, J. W. (2007a). Phylogenetic classification of *Cordyceps* and the clavicipitaceous fungi. *Stud. Mycol.* 57, 5–59. doi: 10.3114/sim.2007.57.01

Sung, G. H., Sung, J. M., Hywel-Jones, N. L., and Spatafora, J. W. (2007b). A multi-gene phylogeny of Clavicipitaceae (Ascomycota, Fungi): identification

of localized incongruence using a combinational bootstrap approach. *Mol. Phylogenet. Evol.* 44, 1204–1223. doi: 10.1016/j.ympev.2007.03.011

Sung, G. H., Shrestha, B., Han, S. K., and Sung, J. M. (2011). Cultural characteristics of *Ophiocordyceps heteropoda* collected from Korea. *Mycobiology* 39, 1–6. doi: 10.4489/myco.2011.39.1.001

Suo, F., Guo, R., Yu, H., Zeng, W., and Yang, J. (2013). Nucleoside/nucleotide components of *Ophiocordyceps gracilis* and *O. sinensis* strains from Xinjiang and Tibet. *Acta Edulis Fungi* 20, 55–60.

Swofford, D. L. (2002). *PAUP: Phylogenetic analysis using Parsimony, Version 4.0 b10*. Sunderland, MA: Sinauer Associates.

Thompson, J. D., Gibson, T. J., Plewniak, F., Jeanmougin, F., and Higgins, D. G. (1997). The CLUSTAL_X windows interface: flexible strategies for multiple sequence alignment aided by quality analysis tools. *Nucleic Acids Res.* 25, 4876–4882. doi: 10.1093/nar/25.24.4876

Vaidya, G., Lohman, D. J., and Meier, R. (2011). Sequence matrix: concatenation software for the fast assembly of multi-gene datasets with character set and codon information. *Cladistics* 27, 171–180. doi: 10.1111/j.1096-0031.2010.00329.x

Vega, F. E., Meyling, N. V., Luangsa-ard, J. J., and Blackwell, M. (2012). Fungal entomopathogens. *Insect Pathol.* 2, 171–220. doi: 10.1016/B978-0-12-384984-7.00006-3

Vilgalys, R., and Hester, M. (1990). Rapid genetic identification and mapping of enzymatically amplified ribosomal DNA from several *Cryptococcus* species. *J. Bacteriol.* 172, 4238–4246. doi: 10.1128/jb.172.8.4238-4246.1990

Wang, Y., Li, Z. L., Suo, F. Y., and Sun, D. P. (2019). Study of mycelial polysaccharide from *Paraisaria dubia* of *Ophiocordyceps gracilis* asexual. *China J. Chin. Mater.* 44, 1704–1709. doi: 10.19540/j.cnki.cjcmm.20190318.201

Wen, T. C., Xiao, Y. P., Zha, L. S., Hyde, K. D., and Kang, J. C. (2016). Multigene phylogeny and morphology reveal a new species, *Ophiocordyceps tettigonia*, from Guizhou Province, China. *Phytotaxa* 280, 141–151. doi: 10.11646/phytotaxa.280.2.4

White, T. J., Bruns, T., Lee, S., and Taylor, J. (1990). "Amplification and direct sequencing of fungal ribosomal RNA genes for phylogenetics," in *PCR Protocols. A Guide to Methods and Applications*, eds M. A. Innis, D. H. Gelfaud, J. J. Sninsky, and T. J. White (San Diego, CA: Academic Press), 315–322. doi: 10.1016/B978-0-12-372180-8.50042-1

Wijayawardene, N. N., Hyde, K. D., Lumbsch, H. T., Liu, J. K., Maharachchikumbura, S. S. N., Ekanayaka, A. H., et al. (2018). Outline of Ascomycota: 2017. *Fungal Divers.* 88, 167–263. doi: 10.1007/s13225-018-0394-8

Xiao, Y. P., Wen, T. C., Hongsanan, S., Jeewon, R., Luangsa-ard, J. J., Brooks, S., et al. (2018). Multigene phylogenetics of *Polycephalomyces* (*Ophiocordycipitaceae*, Hypocreales), with two new species from Thailand. *Sci. Rep.* 8:18087.

Yang, Z. L., Qin, J., Xia, C., Hu, Q., and Li, Q. Q. (2015). *Ophiocordyceps highlandensis*, a new species of a medicinal fungus from Yunnan, China. *Phytotaxa* 204, 287–295. doi: 10.11646/phytotaxa.204.4.5

Ye, X., Suo, F., Lu, S., and Wang, Z. (2015). Effect of *Ophiocordyceps gracilis* extract on the proliferation of AGS gastric cancer cells. *Acta Edulis Fungi* 22, 51–54.

Zimmermann, G. (2007). Review on safety of the entomopathogenic fungi *Beauveria bassiana* and *Beauveria brongniartii*. *Biocontrol Sci. Technol.* 17, 553–596. doi: 10.1080/09583150701309006

Conflict of Interest: The authors declare that the research was conducted in the absence of any commercial or financial relationships that could be construed as a potential conflict of interest.

Copyright © 2021 Wei, Wanasinghe, Xu, To-anun, Mortimer, Hyde, Elgorban, Madawala, Suwannarach, Karunarathna, Tibpromma and Lumyong. This is an open-access article distributed under the terms of the Creative Commons Attribution License (CC BY). The use, distribution or reproduction in other forums is permitted, provided the original author(s) and the copyright owner(s) are credited and that the original publication in this journal is cited, in accordance with accepted academic practice. No use, distribution or reproduction is permitted which does not comply with these terms.

frontiers in Microbiology

ORIGINAL RESEARCH
published: 04 February 2021
doi: 10.3389/fmicb.2021.631166

Species Diversity and Molecular Phylogeny of *Cyanosporus* (Polyporales, Basidiomycota)

*Shun Liu[1,2], Lu-Lu Shen[3], Yan Wang[1,2], Tai-Min Xu[1,2], Genevieve Gates[4] and Bao-Kai Cui[1,2]**

[1] Beijing Advanced Innovation Center for Tree Breeding by Molecular Design, Beijing Forestry University, Beijing, China, [2] School of Ecology and Nature Conservation, Institute of Microbiology, Beijing Forestry University, Beijing, China, [3] Yichang Academy of Agricultural Science, Yichang, China, [4] Tasmanian Institute of Agriculture, Hobart, TAS, Australia

OPEN ACCESS

Edited by:
Dhanushka Nadeeshan Wanasinghe, Key Laboratory for Plant Diversity and Biogeography of East Asia, Kunming Institute of Botany, China

Reviewed by:
Xin-Zhan Liu, Institute of Microbiology, Chinese Academy of Sciences, China
Hai-Sheng Yuan, Institute of Applied Ecology (CAS), China

***Correspondence:**
Bao-Kai Cui
cuibaokai@yahoo.com

Specialty section:
This article was submitted to Evolutionary and Genomic Microbiology, a section of the journal Frontiers in Microbiology

Received: *30 November 2020*
Accepted: *12 January 2021*
Published: *04 February 2021*

Citation:
Liu S, Shen L-L, Wang Y, Xu T-M, Gates G and Cui B-K (2021) Species Diversity and Molecular Phylogeny of Cyanosporus (Polyporales, Basidiomycota). Front. Microbiol. 12:631166. doi: 10.3389/fmicb.2021.631166

Cyanosporus is a cosmopolitan brown-rot fungal genus, recognizable by blue-tinted basidiocarps. Species in this genus were usually treated as belonging to the *Postia caesia* complex, however, recent phylogenetic analyses showed that this complex represents an independent genus. During further studies on *Cyanosporus*, five new species were discovered based on morphological features and molecular data. Phylogenetic analyses of *Cyanosporus* were conducted using the internal transcribed spacer (ITS) regions, the large subunit of nuclear ribosomal RNA gene (nLSU), the small subunit of nuclear ribosomal RNA gene (nSSU), the small subunit of mitochondrial rRNA gene (mtSSU), the largest subunit of RNA polymerase II (RPB1), the second largest subunit of RNA polymerase II (RPB2), and the translation elongation factor 1-α gene (TEF); illustrated descriptions of the new species are provided. In addition, fifteen species previously belonging to the *Postia caesia* complex are transferred to *Cyanosporus* and proposed as new combinations.

Keywords: brown-rot fungi, multi-loci phylogeny, new species, *Postia caesia* complex, species identification

INTRODUCTION

Boletus caesius Schrad. was described based on material from Germany (Schrader, 1794), and this name was subsequently sanctioned by Fries (1821), who considered *B. coeruleus* Schumach. a synonym of *Polyporus caesius* (Schrad.) Fr. In 1881 Karsten transferred *Boletus caesius* to *Postia* Fr. as *Postia caesia* (Schrad.) P. Karst. (Karsten, 1881). Murrill (1907) transferred this species to *Tyromyces* P. Karst. as *T. caesius* (Schrad.) Murrill and later McGinty (1909) proposed a new monotypic genus *Cyanosporus* McGinty for *Polyporus caesius*, based on its cyanophilous basidiospores, but *Cyanosporus caesius* was not widely used in subsequent studies (Donk, 1960; Jahn, 1963; Lowe, 1975), while *Tyromyces caesius* was commonly used. Later, *Postia caesia* was widely used (Papp, 2014). David (1974, 1980) described another two species: *P. luteocaesia* (A. David) Jülich and *P. subcaesia* (A. David) Jülich from Europe besides *Postia caesia* (Schrad.) P. Karst. Jahn (1979) noted that David's *P. subcaesia* included many forms and introduced *P. subcaesia* "f. minor," which was described as *P. alni* Niemelä & Vampola by Niemelä et al. (2001). Subsequently, Pieri and Rivoire (2005) introduced the fifth European species, *P. mediterraneocaesia*

M. Pieri & B. Rivoire in the *Postia caesia* complex. Papp (2014) provided a detailed nomenclatural review on the *Postia caesia* complex and proposed the subgenus *Postia* subg. *Cyanosporus* (McGinty) V. Papp for this complex which included five species viz., *P. alni*, *P. caesia*, *P. luteocaesia*, *P. mediterraneocaesia* and *P. subcaesia*. Miettinen et al. (2018) focused on the taxonomy of the *Postia caesia* complex based on morphological features and molecular evidence and increased the species number of the *Postia caesia* complex from 10 to 24. In their study, they only focused on the species concept of the *Postia caesia* complex, the taxonomic status of this complex among *Postia* and related genera are not mentioned.

Shen et al. (2019) carried out a comprehensive study on *Postia* and related genera and confirmed that the genus *Cyanosporus* is an independent genus rather than subgenus which containing 12 accepted species including seven new species of the *Postia caesia* complex. Furthermore, phylogenetic analyses showed that *Cyanosporus* belongs to the antrodia clade (Shen et al., 2019). Morphologically, *Cyanosporus* differs from other related genera by its bluish basidiocarps, usually narrow allantoid and thin- to slightly thick-walled basidiospores (McGinty, 1909; Shen et al., 2019). In the current study, the phylogenetic analysis of *Cyanosporus* was carried out based on the combined sequence dataset of ITS + nLSU + nSSU + mtSSU + RPB1 + RPB2 + TEF rRNA gene regions. Combining morphological characters and molecular evidence, thirty-one species belonging to the *Postia caesia* complex are now recognized in *Cyanosporus*, including five new species and fifteen new combinations.

MATERIALS AND METHODS

Taxa Sampling and Morphological Study

The examined specimens were deposited at the herbarium of the Institute of Microbiology, Beijing Forestry University (BJFC) with some duplicates at the Institute of Applied Ecology, Chinese Academy of Sciences (IFP). Morphological descriptions and abbreviations used in this study following Liu et al. (2019); Sun et al. (2020).

DNA Extraction and Molecular Analyses

The procedures for DNA extraction and polymerase chain reaction (PCR) used in this study were the same as described by Chen et al. (2017); Song and Cui (2017). The primer pairs ITS5 and ITS4 for ITS regions, LR0R and LR7 for nLSU regions, NS1 and NS4 for nSSU regions, MS1 and MS2 for mtSSU regions, RPB1-Af and RPB1-Cr for RPB1 gene, fRPB2-f5F and bRPB2-7.1R for RPB2 gene, EF1-983 F and EF1-1567R for TEF gene used in this study are the same as previous studies (White et al., 1990; Rehner, 2001; Matheny et al., 2002; Matheny, 2005).

The PCR cycling schedules for different DNA sequences of ITS, nLSU, nSSU, mtSSU, RPB1, RPB2, and TEF genes used in this study followed those used in Liu et al. (2019); Shen et al. (2019), Zhu et al. (2019); Sun et al. (2020) with some modifications. The PCR products were purified and sequenced at the Beijing Genomics Institute (BGI), China, with the same primers. All newly generated sequences were deposited in GenBank (**Table 1**). Additional sequences for phylogenetic analyses were downloaded from GenBank (**Table 1**). All sequences were aligned in MAFFT 7 (Katoh and Standley, 2013[1]) and manually adjusted in BioEdit (Hall, 1999). Alignments were spliced in Mesquite (Maddison and Maddison, 2017). The missing sequences were coded as "N," ambiguous nucleotides were coded as "N" following Chen et al. (2017). The final concatenated sequence alignment was deposited in TreeBase ([2]submission ID: 27274).

Phylogenetic analyses approaches used in this study followed Han et al. (2016); Cui et al. (2019). The congruences of the 7-gene (ITS, nLSU, nSSU, mtSSU, RPB1, RPB2, and TEF) were evaluated with the incongruence length difference (ILD) test (Farris et al., 1994) implemented in PAUP* 4.0b10 (Swofford, 2002), under heuristic search and 1000 homogeneity replicates. The sequences of *Antrodia serpens* (Fr.) Donk obtained from GenBank were used as outgroups for phylogenetic reconstruction. Maximum parsimony (MP) analysis was performed in PAUP* version 4.0b10 (Swofford, 2002). Maximum Likelihood (ML) analysis was performed in RAxmL v.7.2.8 with a GTR + G + I model (Stamatakis, 2006). Bayesian inference (BI) was calculated by MrBayes 3.1.2 (Ronquist and Huelsenbeck, 2003) with a general time reversible (GTR) model of DNA substitution and a gamma distribution rate variation across sites determined by MrModeltest 2.3 (Posada and Crandall, 1998; Nylander, 2004). Clade robustness was assessed using a bootstrap (BT) analysis with 1000 replicates (Felsenstein, 1985). Descriptive tree statistics tree length (TL), consistency index (CI), retention index (RI), rescaled consistency index (RC), and homoplasy index (HI) were calculated for each Most Parsimonious Tree (MPT) generated. The branch support was evaluated with a bootstrapping method of 1000 replicates (Hillis and Bull, 1993). Branches that received bootstrap supports for MP, ML greater than or equal to 75% and Bayesian posterior probabilities (BPP) greater than or equal to 0.95 were considered as significantly supported. The phylogenetic tree was visualized using FigTree v1.4.2[3].

RESULTS

Molecular Phylogeny

The ITS + TEF sequences dataset had an aligned length of 1166 characters, of which 646 characters were constant, 68 were variable and parsimony-uninformative, and 452 were parsimony-informative. MP analysis yielded 4 equally parsimonious trees (TL = 1983, CI = 0.417, RI = 0.726, RC = 0.303, HI = 0.583). The best model for the concatenate sequence dataset estimated and applied in the Bayesian inference was GTR + I + G with an equal frequency of nucleotides. ML analysis resulted in a similar topology as MP and Bayesian analyses, and only the ML topology is shown in **Figure 1**.

The combined three-gene (ITS + nLSU + TEF) sequences dataset had an aligned length of 2475 characters, of which 1752

[1]http://mafft.cbrc.jp/alignment/server/

[2]http://www.treebase.org

[3]http://tree.bio.ed.ac.uk/software/figtree/

TABLE 1 | A list of species, specimens, and GenBank accession number of sequences used for phylogenetic analyses in this study.

Species	Sample no.	Locality	GenBank accessions						
			ITS	nLSU	nSSU	mtSSU	RPB1	RPB2	TEF
Amaropostia stiptica	Cui 10043	China	KX900906	KX900976	KX901119	KX901046	KX901167	KX901219	/
A. stiptica	Cui 10981	China	KX900907	KX900977	KX901120	KX901047	KX901168	KX901220	
Amylocystis lapponica	HHB-13400-Sp	United States	KC585237	KC585059	/	/	/	/	/
A. lapponica	OKM-4418-Sp	United States	KC585238	KC585060	/	/	/	/	/
Antrodia serpens	Dai 7465	Luxemburg	KR605813	KR605752	KR605913	KR606013	/	KR610832	KR610742
A. serpens	Dai 14850	Poland	MG787582	MG787624	MG787731	MG787674	/	MG787798	MG787849
Cyanosporus alni	Petr Vampola 12.10.1995	Slovakia	MG137026	/	/	/	/	/	/
C. alni	Cui 7185	China	KX900879	KX900949	KX901092	KX901017	KX901155	KX901202	KX901254
C. alni	Dai 14845	Poland	KX900880	KX900950	KX901093	KX901018	KX901156	KX901203	KX901255
C. arbuti	Viacheslav Spirin 8327	United States	MG137039	/	/	/	/	/	MG137132
C. auricoma	Dai 20992	Belarus	**MW182169**	/	/	/	/	/	/
C. auricoma	Cui 13518	China	KX900887	KX900957	KX901100	KX901025	/	KX901209	/
C. auricoma	Cui 13519	China	KX900888	KX900958	KX901101	KX901026	/	/	/
C. auricoma	Tuomo Niemelä 8310	Finland	MG137040	/	/	/	/	/	/
C. auricoma	Viacheslav Spirin 4586	Russia	MG137042	/	/	/	/	/	/
C. bifaria	Viacheslav Spirin 6402	Russia	MG137043	/	/	/	/	/	MG137133
C. bifaria	Cui 17445	China	**MW182170**	**MW182223**	**MW182187**	**MW182206**	/	**MW191562**	**MW191528**
C. bifaria	Cui 17806	China	**MW182171**	**MW182224**	**MW182188**	**MW182207**	**MW191546**	/	**MW191529**
C. bubalinus	Cui 16976	China	**MW182172**	**MW182225**	**MW182189**	**MW182208**	**MW191547**	**MW191563**	**MW191530**
C. bubalinus	Cui 16985	China	**MW182173**	**MW182226**	**MW182190**	**MW182209**	**MW191548**	**MW191564**	**MW191531**
C. caesiosimulans	Viacheslav Spirin 4199	Russia	MG137061	/	/	/	/	/	MG137140
C. caesiosimulans	Otto Miettinen 16976	United States	MG137054	/	/	/	/	/	MG137137
C. caesius	Otto Miettinen 14156	Finland	MG137048	/	/	/	/	/	MG137134
C. caesius	Gerhard Schuster 51	Germany	MG137045	/	/	/	/	/	/
C. caesius aff AR	CIEFAP 350	Argentina	JX090110	JX090130	/	/	/	/	/
C. caesius aff AR	CIEFAP 174	Argentina	JX090109	JX090129	/	/	/	/	/
C. caesius aff GB	K 32713	United Kingdom	AY599576	/	/	/	/	/	/
C. caesius aff GB	K 32425	United Kingdom	AY599575	/	/	/	/	/	/
C. coeruleivirens	Dai 11834	China	KF699119	/	/	/	/	/	/
C. coeruleivirens	Otto Miettinen 12214	Indonesia	MG137063	/	/	/	/	/	/
C. coeruleivirens	Dai 19220	China	**MW182174**	**MW182227**	**MW182191**	**MW182210**	**MW191549**	/	**MW191532**
C. comata	Otto Miettinen 14755,1	United States	MG137066	/	/	/	/	/	/
C. comata	Cui 18388	China	**MW182175**	**MW182228**	**MW182192**	/	**MW191550**	/	**MW191533**
C. comata	Cui 18546	China	/	**MW182229**	**MW182193**	/	/	/	**MW191534**
C. cyanescens	Otto Miettinen 13602	Finland	MG137067	/	/	/	/	/	MG137142
C. cyanescens	Otto Miettinen 15919,2	Spain	MG137071	/	/	/	/	/	MG137144
C. fusiformis	Cui 10775	China	KX900868	KX900938	KX901081	KX901006	/	KX901191	KX901245
C. fusiformis	Dai 15036	China	KX900867	KX900937	KX901080	KX901005	/	KX901190	KX901244
C. glauca	Viacheslav Spirin 5317	Russia	MG137078	/	/	/	/	/	/

(Continued)

TABLE 1 | Continued

Species	Sample no.	Locality	GenBank accessions						
			ITS	nLSU	nSSU	mtSSU	RPB1	RPB2	TEF
C. glauca	Viacheslav Spirin 6580	Russia	MG137081	/	/	/	/	/	MG137145
C. gossypina	Bernard Rivoire 6658	France	/	/	/	/	/	/	MG137146
C. hirsutus	Cui 17050	China	**MW182176**	**MW182230**	**MW182194**	**MW182211**	**MW191551**	**MW191565**	**MW191535**
C. hirsutus	Cui 17053	China	**MW182177**	**MW182231**	**MW182195**	**MW182212**	**MW191552**	**MW191566**	**MW191536**
C. hirsutus	Cui 17055	China	**MW182178**	**MW182232**	**MW182196**	**MW182213**	**MW191553**	**MW191567**	**MW191537**
C. hirsutus	Cui 17083	China	**MW182179**	**MW182233**	**MW182197**	**MW182214**	**MW191554**	**MW191568**	**MW191538**
C. livens	Viacheslav Spirin 8728	United States	MG137090	/	/	/	/	/	MG137150
C. livens	Otto Miettinen 17177	United States	MG137082	/	/	/	/	/	MG137147
C. luteocaesia	Bernard Rivoire 2605	France	MG137091	/	/	/	/	/	/
C. magna	Cui 16983	China	**MW182180**	**MW182234**	**MW182198**	**MW182215**	**MW191555**	**MW191569**	**MW191539**
C. magna	Dai 10854	China	KF699117	/	/	/	/	/	/
C. magna	Otto Miettinen 10634	China	KC595944	KC595944	/	/	/	/	MG137151
C. mediterraneocaesius	LY BR 4274	France	KX900886	/	KX901099	KX901024	/	/	/
C. microporus	Cui 11014	China	KX900878	KX900948	KX901091	KX901016	/	KX901201	/
C. microporus	Dai 11717	China	KX900877	KX900947	KX901090	KX901015	/	KX901200	/
C. nothofagicola	Cui 16697	Australia	MW182181[a]	MW182235[a]	MW182199[a]	MW182216[a]	MW191556[a]	MW191570[a]	MW191540[a]
C. nothofagicola	Dai 18765	Australia	MW182182[a]	MW182236[a]	MW182200[a]	MW182217[a]	MW191557[a]	/	MW191541[a]
C. piceicola	Cui 10626	China	KX900862	KX900932	KX901075	KX901001	/	KX901185	/
C. piceicola	Cui 12158	China	KX900866	KX900936	KX901079	KX901004	KX901153	KX901189	KX901243
C. populi	Cui 17087a	China	**MW182183**	**MW182237**	**MW182201**	**MW182218**	**MW191558**	**MW191571**	**MW191542**
C. populi	Cui 17549	China	/	**MW182238**	**MW182202**	**MW182219**	**MW191559**	**MW191572**	**MW191543**
C. populi	Tuomo Niemelä 8379	Finland	MG137097	/	/	/	/	/	MG137154
C. populi	Otto Miettinen 17043	United States	MG137092	/	/	/	/	/	MG137153
C. simulans	Otto Miettinen 20422	Finland	MG137110	/	/	/	/	/	MG137160
C. simulans	Tuomo Niemelä 8846	Finland	MG137103	/	/	/	/	/	/
C. subcaesius	Josef Vlasák 0110/24	Czech Republic	MG137117	/	/	/	/	/	MG137164
C. subcaesius	Alix David 652	France	MG137116	/	/	/	/	/	/
C. subhirsutus	Cui 11330	China	KX900873	KX900943	KX901086	KX901011	/	KX901196	KX901250
C. subhirsutus	Dai 14892	China	KX900871	KX900941	KX901084	KX901009	/	KX901194	KX901248
C. submicroporus	Cui 16306	China	**MW182184**	**MW182239**	**MW182203**	**MW182220**	**MW191560**	**MW191573**	**MW191544**
C. submicroporus	Cui 17750	China	**MW182185**	**MW182240**	**MW182204**	**MW182221**	**MW191561**	/	**MW191545**
C. submicroporus	Cui 18156	China	**MW182186**	**MW182241**	**MW182205**	**MW182222**	/	**MW191574**	/
C. subviridis	Viacheslav Spirin 8774a	United States	MG137120	/	/	/	/	/	MG137166
C. subviridis	Reijo Penttilä 14376	Finland	/	/	/	/	/	/	MG137165
C. tenuis	Cui 10788	China	KX900885	KX900955	KX901098	KX901023	KX901161	KX901208	/
C. tenuis	Dai 12974	China	KX900884	KX900954	KX901097	KX901022	KX901160	KX901207	KX901258
C. tricolor	Cui 12233	China	KX900876	KX900946	KX901089	KX901014	/	KX901199	KX901253
C. tricolor	Cui 10790	China	KX900875	KX900945	KX901088	KX901013	/	KX901198	KX901252
C. ungulatus	Cui 10778	China	KX900870	KX900940	KX901083	KX901008	/	KX901193	KX901247
C. ungulatus	Dai 12897	China	KX900869	KX900939	KX901082	KX901007	KX901154	KX901192	KX901246

(Continued)

TABLE 1 | Continued

Species	Sample no.	Locality	GenBank accessions						
			ITS	nLSU	nSSU	mtSSU	RPB1	RPB2	TEF
C. yanae	Heikki Kotiranta 27606	Russia	MG137122	/	/	/	/	/	MG137168
C. yanae	Heikki Kotiranta 27454	Russia	MG137121	/	/	/	/	/	MG137167
Calcipostia guttulata	Cui 10028	China	KF727433	KJ684979	KX901139	KX901066	KX901182	KX901237	KX901277
C. guttulata	KHL 11739 (GB)	Finland	EU118650	EU118650	/	/	/	/	/
Cystidiopostia hibernica	Cui 2658	China	KX900905	KX900975	KX901118	KX901045	/	KX901218	/
C. hibernica	K(M)17352	Austria	AJ006665	/	/	/	/	/	/
Fuscopostia fragilis	Cui 10020	China	KX900912	KX900982	KX901126	KX901054	/	KX901226	KX901270
F. fragilis	JV 0610-8	Czech	JF950573	/	/	/	/	/	/
Oligoporus rennyi	KEW 57	Unknown	AY218416	AF287876	/	/	/	/	/
O. rennyi	MR 10497	Argentina	JX090117	/	/	/	/	/	/
Osteina obducta	Cui 9959	China	KX900923	KX900993	KX901143	KX901070	/	KX901239	/
O. obducta	Cui 10074	China	KX900924	KX900994	KX901144	KX901071	/	KX901240	/
Postia amurensis	Cui 1044	China	KX900902	KX900972	/	KX901043	/	/	/
P. amurensis	Dai 903	China	KX900901	KX900971	/	KX901042	/	/	/
P. hirsuta	Cui 11180	China	KJ684971	KJ684985	/	KX901039	/	/	/
P. hirsuta	Cui 11237	China	KJ684970	KJ684984	KX901113	KX901038	/	/	KX901266
P. lactea	Cui 9319	China	KX900894	KX900964	KX901106	KX901031	KX901165	KX901213	KX901262
P. lactea	Cui 11511	China	KX900893	KX900963	KX901105	KX901030	KX901164	KX901212	KX901261
Spongiporus leucospongia	JV 0709/123-J	United States	KX900918	KX900988	KX901137	KX901064	/	/	KX901275
S. leucospongia	OKM 4335	United States	KC585395	KC585228	/	/	/	/	/

New sequences for this study are indicated in bold.

characters were constant, 134 were variable and parsimony-uninformative, and 589 were parsimony-informative. MP analysis yielded 8 equally parsimonious trees (TL = 2222, CI = 0.473, RI = 0.770, RC = 0.365, HI = 0.527). The best model for the concatenate sequence dataset estimated and applied in the Bayesian inference was GTR + I + G with equal frequency of nucleotides. ML analysis resulted in a similar topology as MP and Bayesian analyses, and only the ML topology is shown in **Figure 2**.

The combined seven-gene (ITS + nLSU + nSSU + mtSSU + RPB1 + RPB2 + TEF) sequences dataset had an aligned length of 5855 characters, of which 4194 characters were constant, 300 were variable and parsimony-uninformative, and 1361 were parsimony-informative. MP analysis yielded 10 equally parsimonious trees (TL = 3951, CI = 0.585, RI = 0.806, RC = 0.471, HI = 0.415). The best model for the concatenate sequence dataset estimated and applied in the Bayesian inference was GTR + I + G with equal frequency of nucleotides. ML analysis resulted in a similar topology as MP and Bayesian analyses, and only the ML topology is shown in **Figure 3**.

The phylogenetic trees (**Figures 1**–**3**) inferred from ITS + TEF, ITS + nLSU + TEF and ITS + nLSU + nSSU + mtSSU + RPB1 + RPB2 + TEF gene sequences were obtained from 99 fungal samples representing 45 taxa of *Cyanosporus* and its related genera in the antrodia clade. Seventy-five samples representing thirty-one taxa of *Cyanosporus* clustered together and separated from species of *Postia* and other related genera.

Taxonomy

Cyanosporus bubalinus B.K. Cui & Shun Liu, **sp. nov.** (**Figures 4A–B**, **5**)

MycoBank: MB 838417

Differs from other *Cyanosporus* species by its tomentose, cream to buff pileal surface when fresh becoming cream to pinkish buff when dry and a white to cream pore surface when fresh becoming straw yellow to buff when dry, and round to angular small pores (5–8 per mm).

Type. — **CHINA**. Yunnan Province, Binchuan County, Jizu Mountain, on fallen branch of *Pinus*, 14 September 2018, *Cui 16985* (holotype, BJFC).

Etymology. — *Bubalinus* (Lat.): refers to the cream to buff pileal surface.

Basidiocarps. — Annual, pileate, solitary, soft and watery when fresh, becoming soft corky to fragile upon drying. *Pileus* shell-shaped, projecting up to 2.5 cm, 3.5 cm wide and 1.5 cm thick at base. *Pileal surface* white to cream when fresh, finely tomentose, becoming cream to pinkish buff upon drying; margin acute. *Pore surface* white to cream when fresh, becoming straw yellow to buff when dry; sterile margin narrow to almost lacking; *pores* round to angular, 5–8 per mm; *dissepiments* thin, entire to lacerate. *Context* white, corky, up to 1.2 cm thick. *Tubes* cream, fragile, up to 5 mm long.

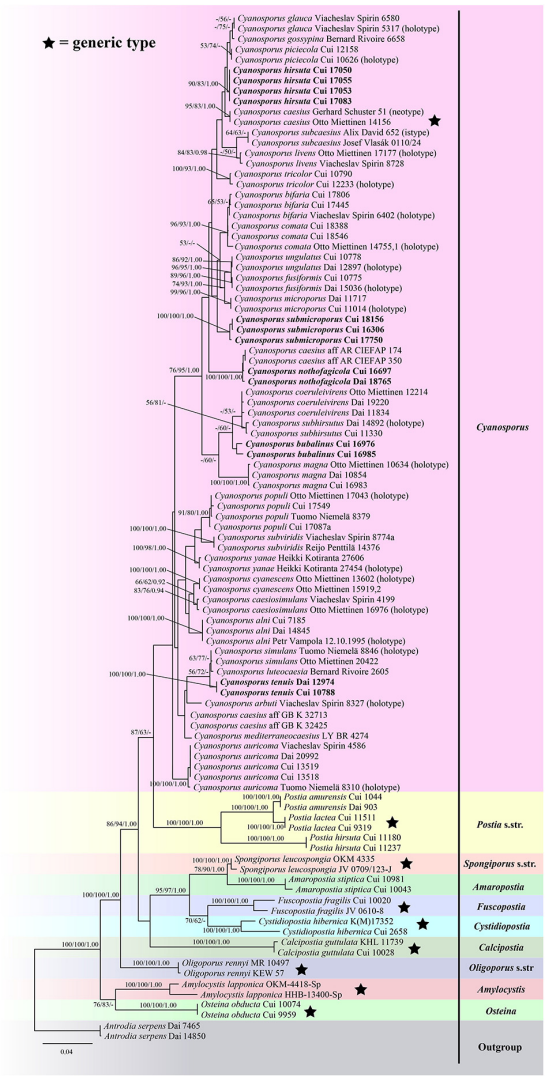


FIGURE 1 | Maximum likelihood tree illustrating the phylogeny of *Cyanosporus* and its related genera in the antrodia clade based on sequences dataset of ITS + TEF. Branches are labeled with maximum likelihood bootstrap higher than 50%, parsimony bootstrap proportions higher than 50% and Bayesian posterior probabilities more than 0.90 respectively. Bold names = New species.

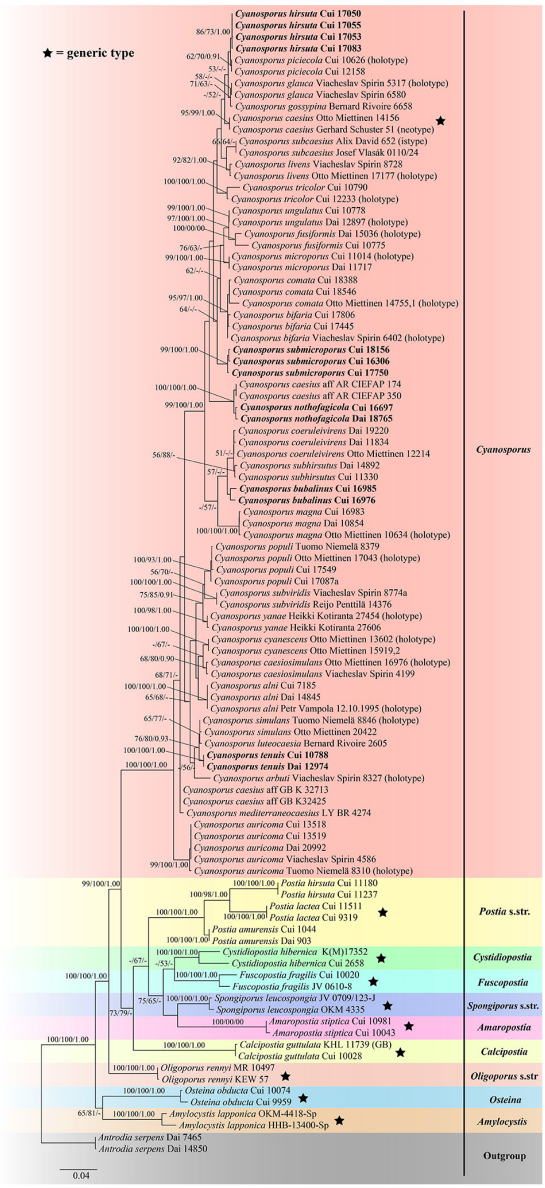


FIGURE 2 | Maximum likelihood tree illustrating the phylogeny of *Cyanosporus* and its related genera in the antrodia clade based on the combined sequences dataset of ITS + nLSU + TEF. Branches are labeled with maximum likelihood bootstrap higher than 50%, parsimony bootstrap proportions higher than 50% and Bayesian posterior probabilities more than 0.90 respectively. Bold names = New species.

Hyphal structure. — Hyphal system monomitic; generative hyphae with clamp connections, IKI–, CB–; tissues unchanged in KOH.

Context. — Generative hyphae hyaline, slightly thick-walled with a wide lumen, occasionally branched, loosely interwoven, 2.5–7.3 μm in diam.

Tubes. — Generative hyphae hyaline, thin- to slightly thick-walled, occasionally branched, interwoven, 2–4.2 μm in diam. *Cystidia* absent; *cystidioles* present, fusoid, thin-walled, 13.3–23.4 × 2.9–4.2 μm. *Basidia* clavate, bearing four sterigmata and a basal clamp connection, 11.6–19.8 × 4.3–5.6 μm; *basidioles* dominant, in shape similar to basidia, but smaller.

Basidiospores. — Cylindrical, slightly curved, hyaline, thin- to slightly thick-walled, smooth, occasionally with small oily drops, IKI–, CB–, (4.2–)4.3–4.8 × 1.2–1.7(–1.8) μm, L = 4.65 μm, W = 1.55 μm, Q = 2.98–3.09 (n = 60/2).

Notes. — In the phylogenetic trees (**Figures 1**–**3**), two specimens of *Cyanosporus bubalinus* formed a highly supported lineage (**Figures 1**–**3**), closely related to *C. coeruleivirens* (Corner) B.K. Cui, Shun Liu & Y.C. Dai, *C. magna* (Miettinen) B.K. Cui & Shun Liu and *C. subhirsutus* B.K. Cui, L.L. Shen &

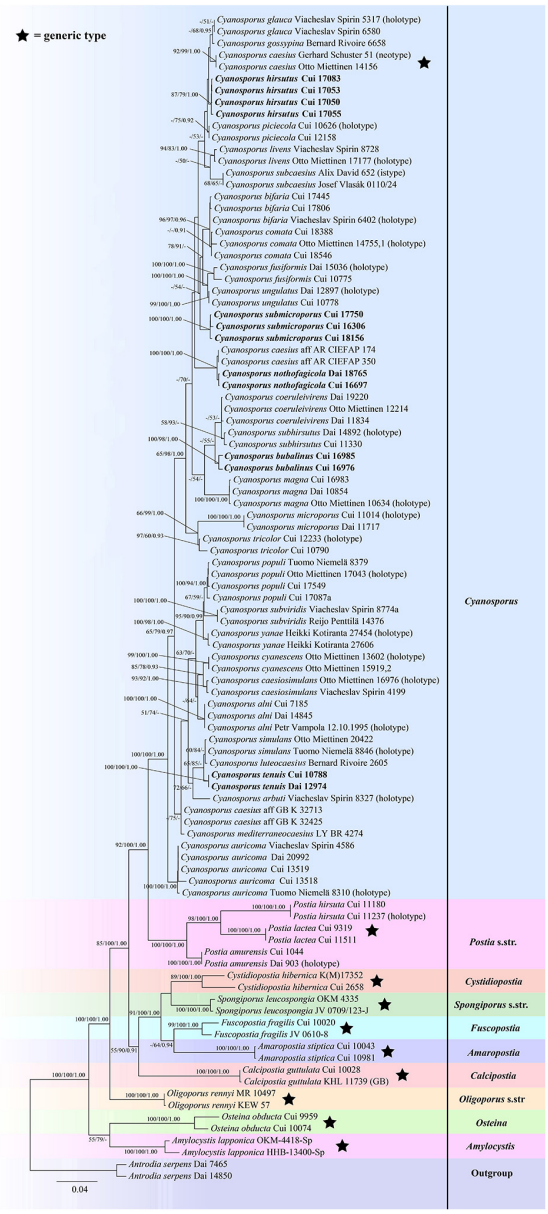


FIGURE 3 | Maximum likelihood tree illustrating the phylogeny of *Cyanosporus* and its related genera in the antrodia clade based on the combined sequences dataset of ITS + nLSU + nSSU + mtSSU + RPB1 + RPB2 + TEF. Branches are labeled with maximum likelihood bootstrap higher than 50%, parsimony bootstrap proportions higher than 50% and Bayesian posterior probabilities more than 0.90 respectively. Bold names = New species.

Y.C. Dai. Morphologically, *C. coeruleivirens* differs by having a white, cream to bluish-grayish pore surface, smaller basidia (8.8–13.5 × 3.3–4.3 μm) and smaller basidiospores (3.8–4.8 × 1–1.3 μm) (**Table 2**); *C. magna* differs from *C. bubalinus* in its larger pores (4–5 per mm), smaller basidia (10–12.5 × 3.2–4 μm) and smaller basidiospores (3.6–4.4 × 1.0–1.2 μm) (**Table 2**); *C. subhirsutus* differs by having a hirsute pileal surface when dry, larger pores (2–3 per mm), smaller basidia (10–12 × 4–6 μm) and smaller basidiospores (4–4.5 × 0.9–1.3 μm) (**Table 2**). *Cyanosporus microporus* B.K. Cui, L.L. Shen & Y.C. Dai and *C. piceicola* B.K. Cui, L.L. Shen & Y.C. Dai were also discovered from Yunnan Province. *Cyanosporus microporus* differs from the new species by its narrower basidiospores (4.5–4.9 × 1–1.2 μm, **Table 2**); *C. piceicola* differs by having a velutinate, cream to clay-buff pileal surface, with bluish gray zonation when fresh, larger and round pores (3–5 per mm) and narrower basidiospores (4–4.5 × 0.9–1.3 μm). *Cyanosporus bifaria* (Spirin) B.K. Cui & Shun Liu, *C. glauca* (Spirin & Miettinen) B.K. Cui & Shun Liu and *C. subviridis* (Ryvarden & Guzmán) B.K. Cui & Shun Liu are similar to *C. bubalinus* as they all have pileate basidiocarps and similar pores, however, they differ by narrower tramal hyphae (2.5–3.8 μm in *C. bifaria*, 2.6–3.3 μm in *C. glauca*, 2.5–3.2 μm in *C. subviridis*) and smaller basidia (9.8–14.8 × 3.4–4.5 μm in *C. bifaria*, 9.8–14.8 × 3.1–4.3 μm in *C. glauca*, 10–13 × 3.2–4.4 μm in *C. subviridis*) (**Table 2**); in addition, they are distantly related from *C. bubalinus* in phylogeny.

Additional specimen (paratype) examined: **CHINA**. Yunnan Province, Binchuan County, Jizu Mountain, on wood of *Pinus*, 14 September 2018, *Cui 16976* (BJFC).

Cyanosporus hirsutus B.K. Cui & Shun Liu, **sp. nov.** (**Figures 4C–D**, **6**)

MycoBank: MB 838418

Differs from other *Cyanosporus* species by its flabelliform to semicircular and distinctly hirsute pileus with ash gray to light grayish brown pileal surface, and cylindrical and slightly curved basidiospores (4.1–4.7 × 1.2–1.5 μm).

Type. — **CHINA**. Yunnan Province, Lijiang, Yulong Snow Mountain, on fallen trunk of *Picea*, 14 September 2018, *Cui 17083* (holotype, BJFC).

Etymology. — *Hirsutus* (Lat.): refers to the distinctly hirsute pileal surface.

Basidiocarps. — Annual, pileate, soft corky, without odor or taste when fresh, becoming corky to fragile upon drying. *Pileus* flabelliform to semicircular, projecting up to 5.2 cm, 9.5 cm wide and 1.5 cm thick at base. *Pileal surface* ash gray to light grayish brown with bluish gray zone when fresh, becoming grayish to grayish brown when dry, distinctly hirsute; margin acute. *Pore surface* cream when fresh, becoming straw yellow to olivaceous buff when dry; sterile margin narrow to almost lacking; *pores* angular, 5–7 per mm; *dissepiments* thin, entire. *Context* white, soft corky, up to 9 mm thick. *Tubes* cream, fragile, up to 7 mm long.

Hyphal structure. — Hyphal system monomitic; generative hyphae with clamp connections, IKI–, CB–; tissues unchanged in KOH.

Context. — Generative hyphae hyaline, thin- to slightly thick-walled with a wide lumen, occasionally branched, loosely interwoven, 2.7–8.2 μm in diam.

Tubes. — Generative hyphae hyaline, thin- to slightly thick-walled with a wide lumen, occasionally branched, interwoven, 2–5 μm in diam. *Cystidia* absent; *cystidioles* present, fusoid, thin-walled, 13.2–22.5 × 2.7–4.3 μm. *Basidia* clavate, bearing four sterigmata and a basal clamp connection, 13.6–15.5 × 3.4–4.7 μm; *basidioles* dominant, in a shape similar to basidia, but smaller.

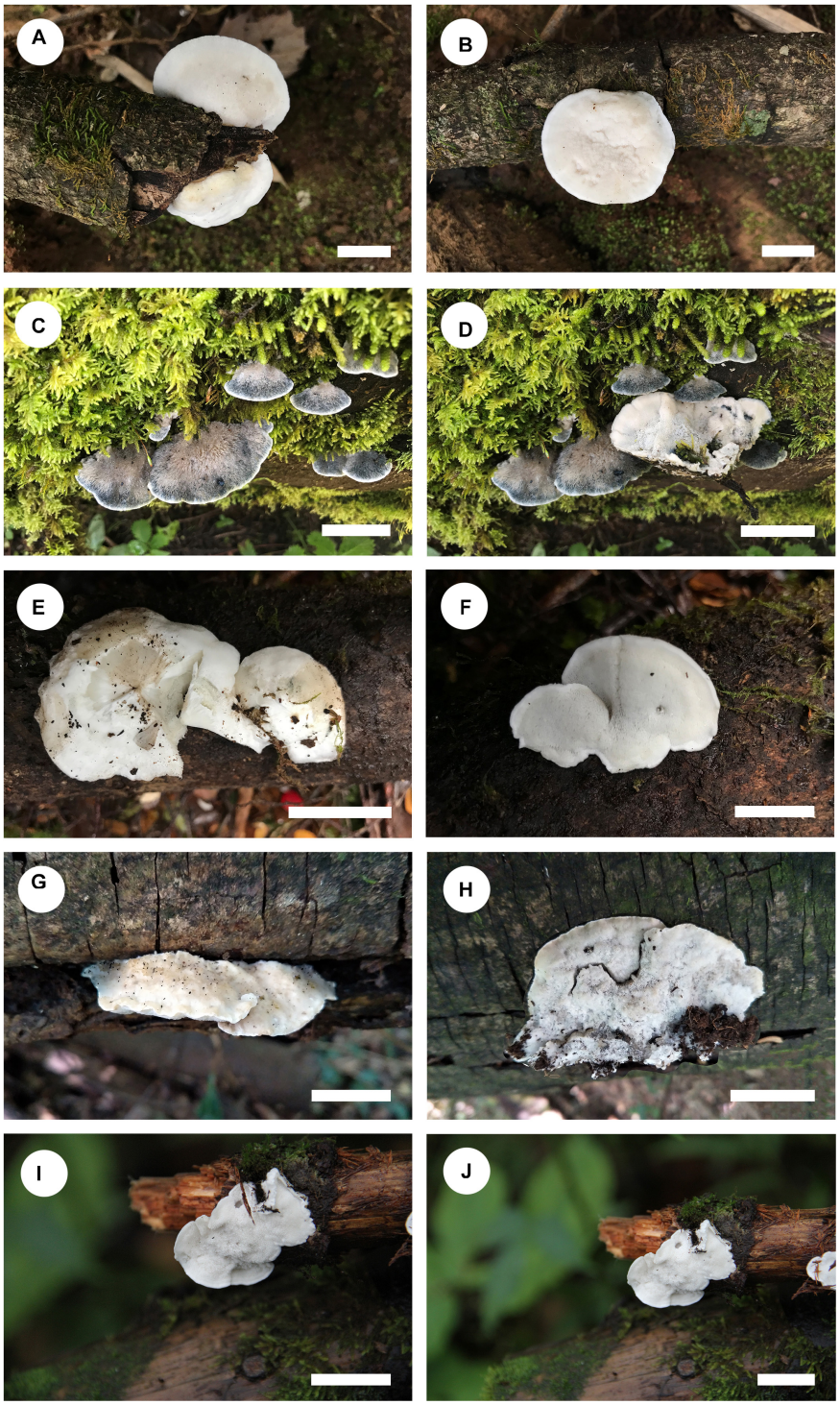


FIGURE 4 | Basidiocarps of *Cyanosporus* species. **(A,B)** *C. bubalinus*; **(C,D)** *C. hirsutus*; **(E,F)** *C. nothofagicola*; **(G,H)**. *C. submicroporus*; **(I,J)**. *C. tenuis* (scale bars: **A,B,I,J** = 1 cm; **C,D,E,F,G,H** = 2 cm).

Basidiospores. — Cylindrical, slightly curved, hyaline, thin- to slightly thick-walled, smooth, occasionally with small oily drops, IKI–, CB–, 4–4.7(–4.9) × (1–)1.2–1.5(–1.8) μm, L = 4.42 μm, W = 1.33 μm, Q = 3.18–3.52 (n = 90/3).

Notes. — Phylogenetically, *Cyanosporus hirsutus* grouped together with *C. caesius*, *C. glauca*, *C. gossypina* (Moug. & Lév.) B.K. Cui & Shun Liu, *C. mediterraneocaesius* (M. Pieri & B. Rivoire) B.K. Cui, L.L. Shen & Y.C. Dai and *C. piceicola*.

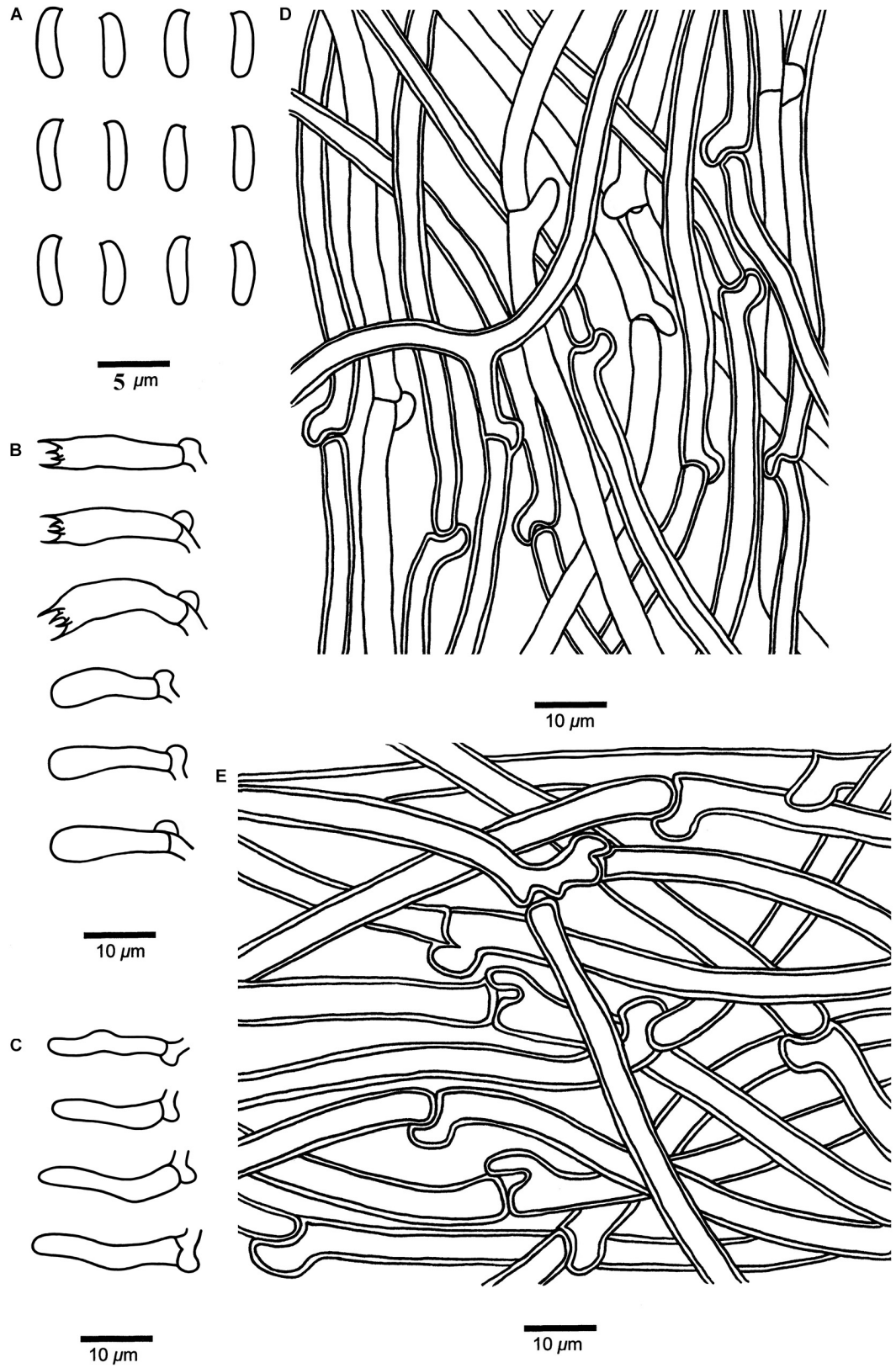


FIGURE 5 | Microscopic structures of *Cyanosporus bubalinus* (drawn from the holotype). **(A)** Basidiospores; **(B)** Basidia and basidioles; **(C)** Cystidioles; **(D)** Hyphae from trama; **(E)** Hyphae from context. Bars: **(A)** = 5 μm; **(B–E)** = 10 μm.

TABLE 2 | Comparisons of the main morphological characters of species in *Cyanosporus*.

Species	Distribution	Basidio-Carps	Pileal surface when dry	Pores per mm	Context hyphae (μm)	Tramal hyphae (μm)	Basidia (μm)	Basidiospores		Ref.
								L × W (μm)	Q = L/W	
C. alni	China (Guizhou, Hebei), Czech Republic, Denmark, Finland, Germany, Norway, Poland, Russia, Slovakia	Pileate/Effused-reflexed	Velutinate	4–6	3.9–5.5	2.9–3.6	10–14.8 × 3.3–4.2	4.3–6.1 × 1.1–1.3	4.22	Miettinen et al., 2018
C. arbuti	United States	Pileate/Effused-reflexed	Glabrous	6–8	3.2–4.6	2.4–3.1	11–17 × 3.3–4.2	4.1–5.1 × 1–1.2	4	Miettinen et al., 2018
C. auricoma	China (Inner Mongolia), Finland, Poland, Russia	Pileate/Effused-reflexed/Resupinate	Hirsute	4–6	4.2–5.2	3.1–4.0	14–20 × 3.8–5.3	4.4–5.6 × 1.5–1.8	3.06	Miettinen et al., 2018
C. bifaria	China (Jilin, Sichuan), Japan, Russia	Pileate	Velutinate	6–8	4–7	2.5–3.8	9.8–14.8 × 3.4–4.5	3.7–4.4 × 1–1.2	3.6	Miettinen et al., 2018
C. bubalinus	China (Yunnan)	Pileate	Tomentose	5–8	2.5–7.3	2–4.2	11.6–19.8 × 4.3–5.6	4.3–4.8 × 1.5–2	2.6–2.83	this study
C. caesius	Czech Republic, Denmark, Finland, France, Germany, Russia, Slovakia, Spain, United Kingdom	Pileate/Effused-reflexed	Hirsute	4–5	3.7–5.2	2.8–3.6	10–15 × 3.7–4.5	4.1–5.3 × 1.3–1.7	3.13	Miettinen et al., 2018
C. caesiosimulans	Finland, Russia, United States	Pileate/Effused-reflexed	Glabrous	5–7	3.4–5.2	2.9–3.8	10.5–15.5 × 3.2–5.2	4.2–5.5 × 1.1–1.4	3.93	Miettinen et al., 2018
C. coeruleivirens	China (Hunan, Jilin, Zhejiang), Indonesia, Russia	Pileate	Velutinate	6–8	3.6–6	2.4–3.4	8.8–13.5 × 3.3–4.3	3.8–4.8 × 1–1.3	3.64	Miettinen et al., 2018
C. comata	China (Sichuan, Xizang), United States	Pileate/Effused-reflexed	Velutinate	4–6	4.2–5.3	2.8–3.8	8.8–14.2 × 3.7–4.9	4.1–4.9 × 1.1–1.3	3.62	Miettinen et al., 2018
C. cyanescens	Estonia, Finland, France, Poland, Russia, Spain, Sweden	Pileate/Effused-reflexed	Glabrous	5–6	4.1–5.2	2.9–3.7	11.4–19.8 × 3.7–5.4	4.7–6.1 × 1.1–1.6	3.92	Miettinen et al., 2018
C. fusiformis	China (Guizhou, Sichuan)	Pileate/Effused-reflexed	Tomentose	4–5	3–5	2–4	12–15 × 4.5–6	4.5–5.2 × 0.8–1.1	5.21–5.45	Shen et al., 2019
C. glauca	China (Jilin), Russia	Pileate	Hirsute	5–8	3.4–5.1	2.6–3.3	9.8–14.8 × 3.1–4.3	4.1–5.4 × 1.1–1.5	3.64	Miettinen et al., 2018
C. gossypina	France	Pileate	Glabrous	4–6	3.6–4.8	2.3–3	8.7–16.8 × 3.8–5	4.1–5.1 × 1.2–1.7	3.11	Miettinen et al., 2018
C. hirsutus	China (Yunnan)	Pileate	Hirsute	5–7	2.7–8.2	2–5	13.6–15.5 × 3.4–4.7	4–4.7 × 1.2–1.5	3.18–3.52	this study
C. livens	Canada, United States	Pileate	Velutinate	4–6	3.7–5.3	2.9–4	9.3–14.3 × 4–5.3	4.1–5.7 × 1.1–1.5	3.74	Miettinen et al., 2018

(Continued)

TABLE 2 | Continued

Species	Distribution	Basidio-Carps	Pileal surface when dry	Pores per mm	Context hyphae (μm)	Tramal hyphae (μm)	Basidia (μm)	Basidiospores		Ref.
								L × W (μm)	Q = L/W	
C. luteocaesius	France	Pileate/Effused-reflexed	Tomentose	3–5	4.1–5.8	2.7–3.2	11.1–16.2 × 4–5.2	4.3–6.1 × 1.5–1.9	3.02	Miettinen et al., 2018
C. magna	China (Jilin, Hainan, Yunnan)	Pileate	Velutinate	4–5	4.2–6	2.2–3.3	10–12.5 × 3.2–4	3.6–4.4 × 1–1.2	3.51	Miettinen et al., 2018
C. mediterraneocaesius	France, Spain	Pileate/Effused-reflexed	Velutinate	5–6	3.1–4	2.3–3.2	12–18.5 × 3.5–4.6	4.2–5.8 × 1.3–1.7	3.26	Miettinen et al., 2018
C. microporus	China (Yunnan)	Pileate	Velutinate	6–8	3.5–6	2–4	11–13.5 × 4–5	4.5–4.9 × 1–1.2	4.47–4.52	Shen et al., 2019
C. nothofagicola	Australia	Pileate/Effused-reflexed	Tomentose	4–6	2.3–7.5	2–5	13.6–17.2 × 3.4–4.2	3.8–5 × 1–1.7	4.08–4.22	this study
C. piceicola	China (Sichuan, Xizang, Yunnan)	Pileate	Velutinate	3–5	5–7	2.5–4	13–16 × 4–5	4–4.5 × 0.9–1.3	3.75–3.97	Shen et al., 2019
C. populi	China (Jilin, Sichuan, Yunnan), Finland, Norway, Poland, Russia, United States	Pileate/Effused-reflexed	Glabrous	5–7	3.2–4.8	2.7–3.3	10–16 × 3.5–4.2	4.2–5.6 × 1–1.3	4.14	Miettinen et al., 2018
C. simulans	Canada, China, Estonia, Finland, France, Germany, Norway, Russia, United States	Pileate/Effused-reflexed/Resupinate	Glabrous	5–7	3.9–5	2.8–3.6	10–14.8 × 3.7–5.2	4.4–6.3 × 1.3–1.8	3.6	Miettinen et al., 2018
C. subcaesius	Czech Republic, Finland, France, Russia, United Kingdom	Pileate/Effused-reflexed	Glabrous	4–6	4.2–6.6	3.1–4.1	10.3–17.8 × 3.3–4.6	4–5.3 × 1–1.4	3.8	Miettinen et al., 2018
C. subhirsutus	China (Guizhou, Fujian, Yunnan)	Pileate	Hirsute	2–3	4–6	3–4.5	10–12 × 4–6	4–4.5 × 0.9–1.3	3.67–3.79	Shen et al., 2019
C. submicroporus	China (Sichuan, Yunnan)	Pileate	Velutinate	6–9	2.3–6.2	2–4.8	12.2–20.5 × 3.4–5.6	3.6–4.7 × 1–1.3	3.45–3.52	this study
C. subviridis	Finland, Mexico, United States	Pileate	Glabrous	6–8	4.8–5.8	2.5–3.2	10–13 × 3.2–4.4	3.8–4.5 × 1–1.3	3.58	Miettinen et al., 2018
C. tricolor	China (Sichuan, Xizang)	Pileate	Velutinate	4–5	3–5	2–3	12–15 × 4–5	4–4.8 × 0.8–1.2	4.55–4.87	Shen et al., 2019
C. tenuis	China (Sichuan)	Pileate/Effused-reflexed	Tomentose	5–7	2.6–7	2.2–4.8	18.2–27.6 × 3.7–6	4.7–6 × 1.3–2	2.89–2.93	This study
C. ungulatus	China (Sichuan)	Pileate	Glabrous	4–6	2.5–4.5	2–3	12–15 × 4–5	4.5–5 × 0.9–1.2	4.79–4.83	Shen et al., 2019
C. yanae	Russia	Pileate/Effused-reflexed	Glabrous	5–7	3–4	2.2–2.9	9–14 × 3.5–4.2	4.3–5.8 × 1.2–1.6	3.56	Miettinen et al., 2018

Morphologically, *C. hirsutus* is similar to *C. caesius* as both species share hairy and distinctly bluish basidiocarps, but *C. caesius* differs from *C. hirsutus* by its larger pores (4–5 per mm), and narrower hyphae of the context (3.7–5.2) (**Table 2**); *C. hirsutus* and *C. glauca* have similar-sized basidiospores, but *C. glauca* has a plumbeous to bluish gray or grayish brown pileal surface (Miettinen et al., 2018); *C. hirsutus* and *C. gossypina* have similar-sized pores and basidiospores, but *C. gossypina* has smaller basidiocarps with a cream to light gray pileal surface (Miettinen et al., 2018); *C. hirsutus* and *C. mediterraneocaesius* share similar-sized and similar-shaped pores, but *C. mediterraneocaesius* has larger basidiospores (4.2–5.8 × 1.3–1.7) (**Table 2**); *C. hirsutus* and *C. piceicola* both have a flabelliform pileus, with bluish gray zonate pileal surface, similar-sized pores and basidiospores, but *C. piceicola* has smaller basidiocarps (projecting up to 3 cm, 5.5 cm wide and 1.8 cm thick at base), thinner hyphae in the context (5–7 μm) and smaller basidia (13–16 × 4–5 μm) (Shen et al., 2019). *Cyanosporus microporus* and *C. subhirsutus* both have pileate basidiocarps with a blue tint to the pileal surface and slightly thick-walled basidiospores like *C. hirsutus*, but *C. microporus* differs in its smaller pores (6–8 per mm) and basidia (11–13.5 × 4–5 μm) (**Table 2**); *C. subhirsutus* differs in having larger pores (2–3 per mm) and smaller basidia (10–12 × 4–6 μm) (**Table 2**).

Additional specimens (paratypes) examined. **CHINA**. Yunnan Province, Lijiang, Yulong Snow Mountain, on fallen trunk of *Picea*, 14 September 2018, *Cui 17050*, *17053*, *17055*, *17070*, *17082* (BJFC).

Cyanosporus nothofagicola B.K. Cui, Shun Liu & Y.C. Dai, **sp. nov.** (**Figures 4E–F**, **7**)

MycoBank: MB 838419

Differs from other *Cyanosporus* species by its flabelliform to semicircular pileus with pale mouse gray to buff yellow pileal surface and cream to buff yellow pore surface when dry, cylindrical to allantoid basidiospores (3.8–5 × 1–1.7 μm), and growth on *Nothofagus*.

Type. — **AUSTRALIA**. Tasmania, Arve River Streamside Reserve, on fallen branch of *Nothofagus*, 15 May 2018, *Cui 16697* (holotype, BJFC).

Etymology. — (Lat.): refers to the frequent occurrence on *Nothofagus*.

Basidiocarps. — Annual, effused-reflexed to pileate, solitary, soft and watery, without odor or taste when fresh, becoming soft corky to fragile upon drying. *Pileus* flabelliform to semicircular, projecting up to 2.4 cm, 4.2 cm wide and 0.7 cm thick at base. *Pileal surface* buff to olivaceous buff when fresh, finely tomentose, becoming smooth, pale mouse gray to buff yellow when dry; margin acute. *Pore surface* white to cream when fresh, becoming cream to buff yellow when dry; sterile margin narrow to almost lacking; *pores* angular, 4–6 per mm; *dissepiments* thin, entire to lacerate. *Context* white, soft corky, up to 4 mm thick. *Tubes* cream, fragile, up to 3 mm long.

Hyphal structure. — Hyphal system monomitic; generative hyphae with clamp connections, IKI–, CB–; tissues unchanged in KOH.

Context. — Generative hyphae hyaline, thin- to slightly thick-walled with a wide lumen, occasionally branched, loosely interwoven, 2.3–7.5 μm in diam.

Tubes. — Generative hyphae hyaline, thin- to slightly thick-walled with a wide lumen, occasionally branched, interwoven, 2–5 μm in diam. *Cystidia* absent; *cystidioles* present, fusoid, thin-walled, 14.2–16.7 × 2.6–5.2 μm. *Basidia* clavate, bearing four sterigmata and a basal clamp connection, 13.6–17.2 × 3.4–4.2 μm; *basidioles* dominant, in shape similar to basidia, but smaller.

Basidiospores. — Cylindrical to allantoid, slightly curved, hyaline, thin- to slightly thick-walled, smooth, IKI–, CB–, 3.8–5 × (0.8–)1–1.7 μm, L = 4.62 μm, W = 1.15 μm, Q = 4.08–4.22 (n = 60/2).

Notes. — *Cyanosporus caesius* is also found in Tasmania, Australia. It has pileate or effused reflexed basidiocarps with a tomentose pileal surface and similar pores to *C. nothofagicola*, but it differs from the later by its plumbeous to bluish gray or grayish brown pileal surface (Miettinen et al., 2018).

Additional specimen (paratype) examined. **AUSTRALIA**. Tasmania, Arve River Streamside Reserve, on fallen trunk of *Nothofagus*, 15 May 2018, *Dai 18765* (BJFC).

Cyanosporus submicroporus B.K. Cui & Shun Liu, **sp. nov.** (**Figures 4G–H**, **8**)

MycoBank: MB 838420

Differs from other *Cyanosporus* species by its cream to pinkish buff pileal surface and white to smoke gray pore surface when fresh, buff to buff yellow pileal surface and buff to olivaceous buff pore surface when dry.

Type. — **CHINA**. Yunnan Province, Baoshan, Gaoligongshan Nature Reserve, on angiosperm wood, 8 November 2019, *Cui 18156* (holotype, BJFC).

Etymology. — *Submicroporus* (Lat.): refers to the new species resembling *Cyanosporus microporus* in morphology.

Basidiocarps. — Annual, pileate, soft and watery, without odor or taste when fresh, becoming corky to woody hard upon drying. *Pileus* flabelliform to semicircular, projecting up to 3.2 cm, 6.5 cm wide and 1.3 cm thick at base. *Pileal surface* cream to pinkish buff when fresh, velutinate, becoming rugose, buff to buff yellow when dry; margin acute. *Pore surface* white to smoke gray when fresh, becoming buff to olivaceous buff when dry; sterile margin narrow to almost lacking; *pores* round, 6–9 per mm; *dissepiments* thin, entire. *Context* cream to buff, corky, up to 5 mm thick. *Tubes* pale mouse gray to cream, fragile, up to 7 mm long.

Hyphal structure. — Hyphal system monomitic; generative hyphae with clamp connections, IKI–, CB–; tissues unchanged in KOH.

Context. — Generative hyphae hyaline, thin- to slightly thick-walled with a wide lumen, rarely branched, loosely interwoven, 2.3–6.2 μm in diam.

Tubes. — Generative hyphae hyaline, thin- to slightly thick-walled with a wide lumen, occasionally branched, interwoven, 2–4.8 μm in diam. *Cystidia* and *cystidioles* absent. *Basidia* clavate, bearing four sterigmata and a basal clamp connection, 12.2–20.5 × 3.4–5.6 μm; *basidioles* dominant, in shape similar to basidia, but smaller.

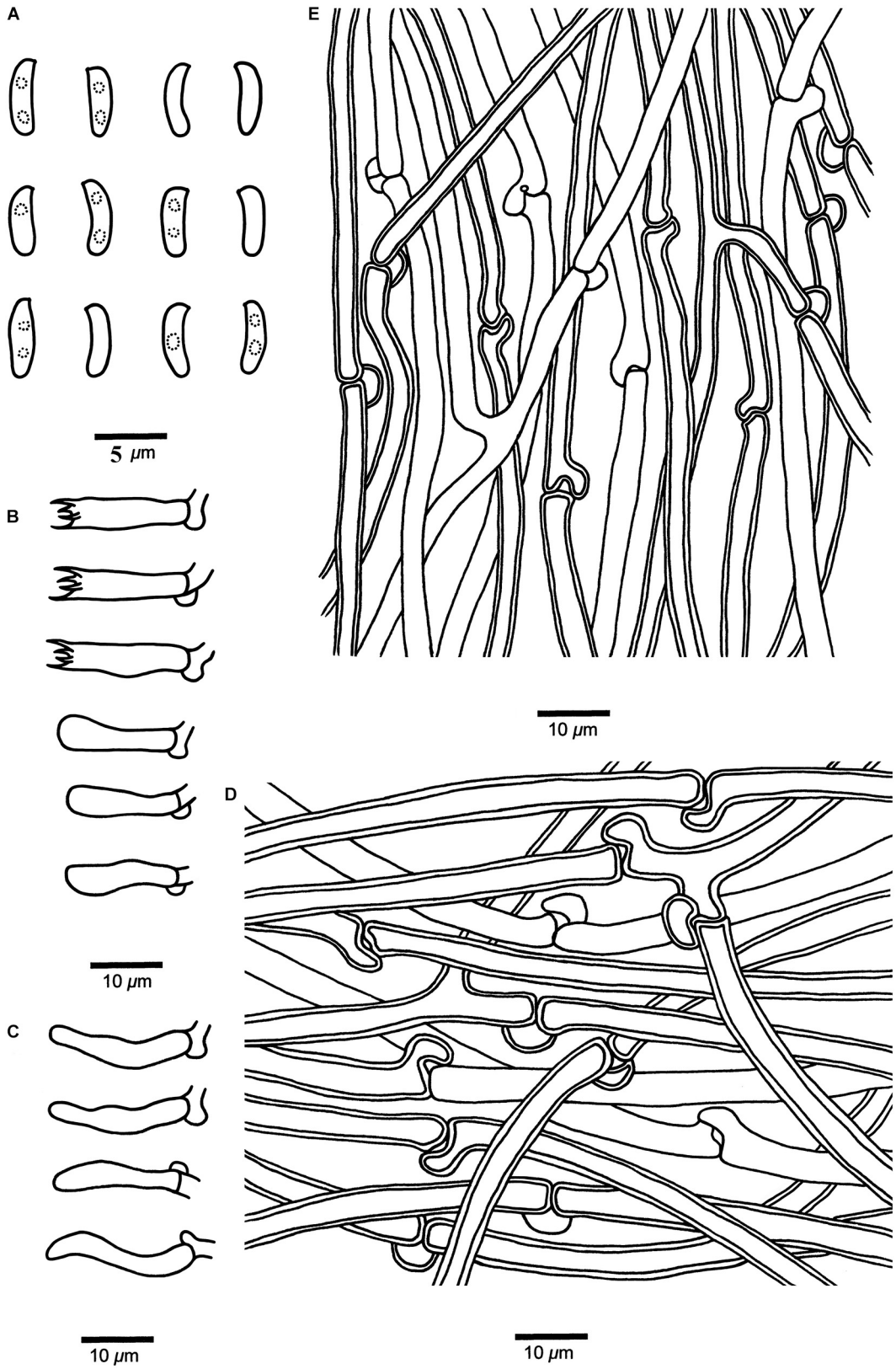


FIGURE 6 | Microscopic structures of *Cyanosporus hirsutus* (drawn from the holotype). **(A)** Basidiospores; **(B)** Basidia and basidioles; **(C)** Cystidioles; **(D)** Hyphae from trama; **(E)** Hyphae from context. Bars: **(A)** = 5 μm; **(B–E)** = 10 μm.

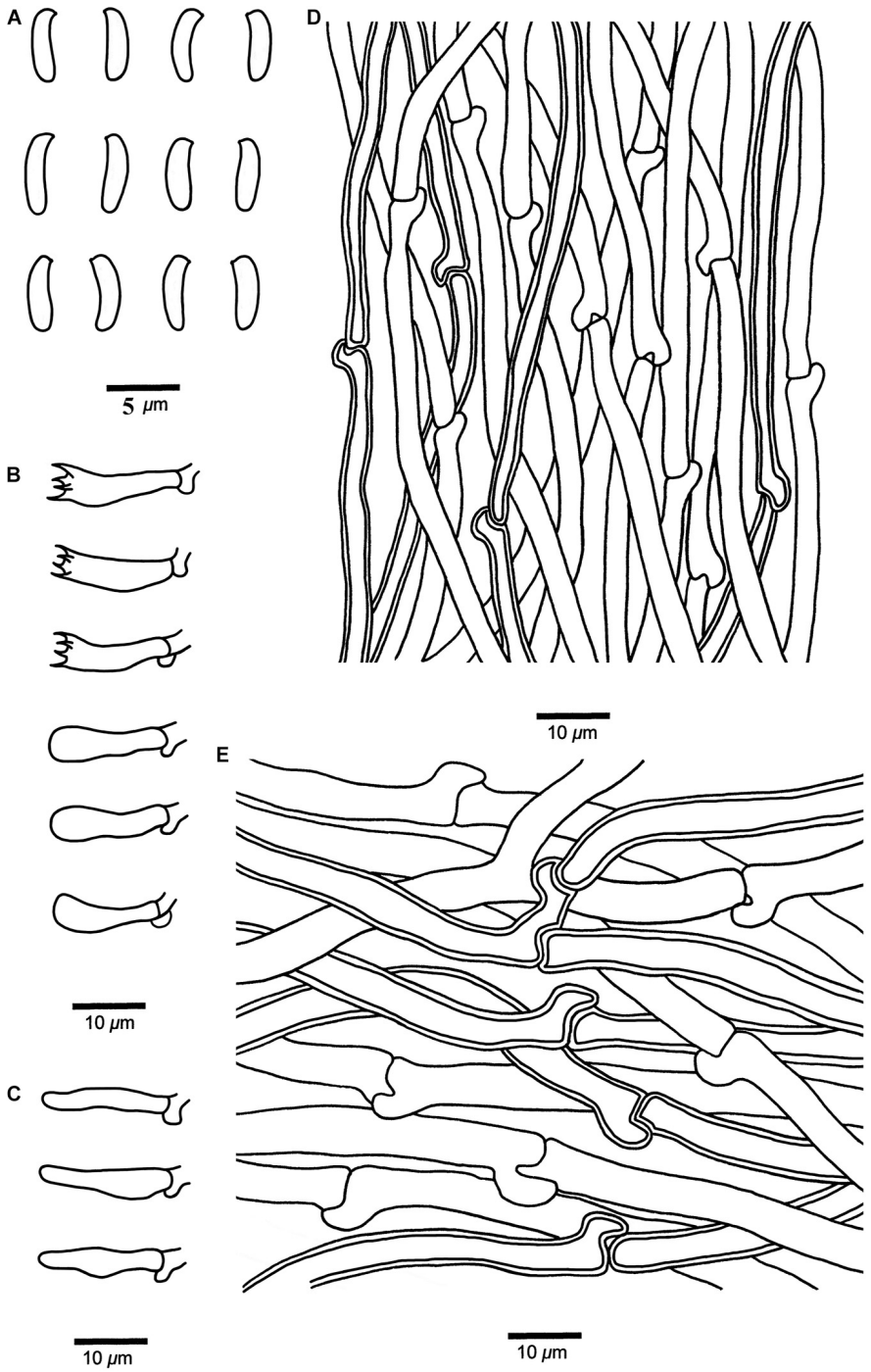


FIGURE 7 | Microscopic structures of *Cyanosporus nothofagicola* (drawn from the holotype). **(A)** Basidiospores; **(B)** Basidia and basidioles; **(C)** Cystidioles; **(D)** Hyphae from trama; **(E)** Hyphae from context. Bars: **(A)** = 5 μm; **(B–E)** = 10 μm.

Basidiospores. — Allantoid, slightly curved, hyaline, thin- to slightly thick-walled, smooth, occasionally with small oil drops, IKI–, weakly CB+, 3.6–4.7 × (0.9–)1–1.3 μm, L = 4.18 μm, W = 1.19 μm, Q = 3.45–3.52 (n = 90/3).

Notes. — In the phylogenetic tree the three specimens of *Cyanosporus submicroporus* formed a highly supported lineage (**Figures 1**-**3**), and are usually grouped together with *C. bifaria*, *C. comata* (Miettinen) B.K. Cui & Shun Liu, *C. fusiformis* B.K. Cui, L.L. Shen & Y.C. Dai and *C. ungulatus* B.K. Cui, L.L. Shen & Y.C. Dai. Morphologically, both *C. submicroporus* and *C. bifaria* have similar pores and basidiospores, but *C. bifaria* differs in having ochraceous hues, a strigose pileal surface, and

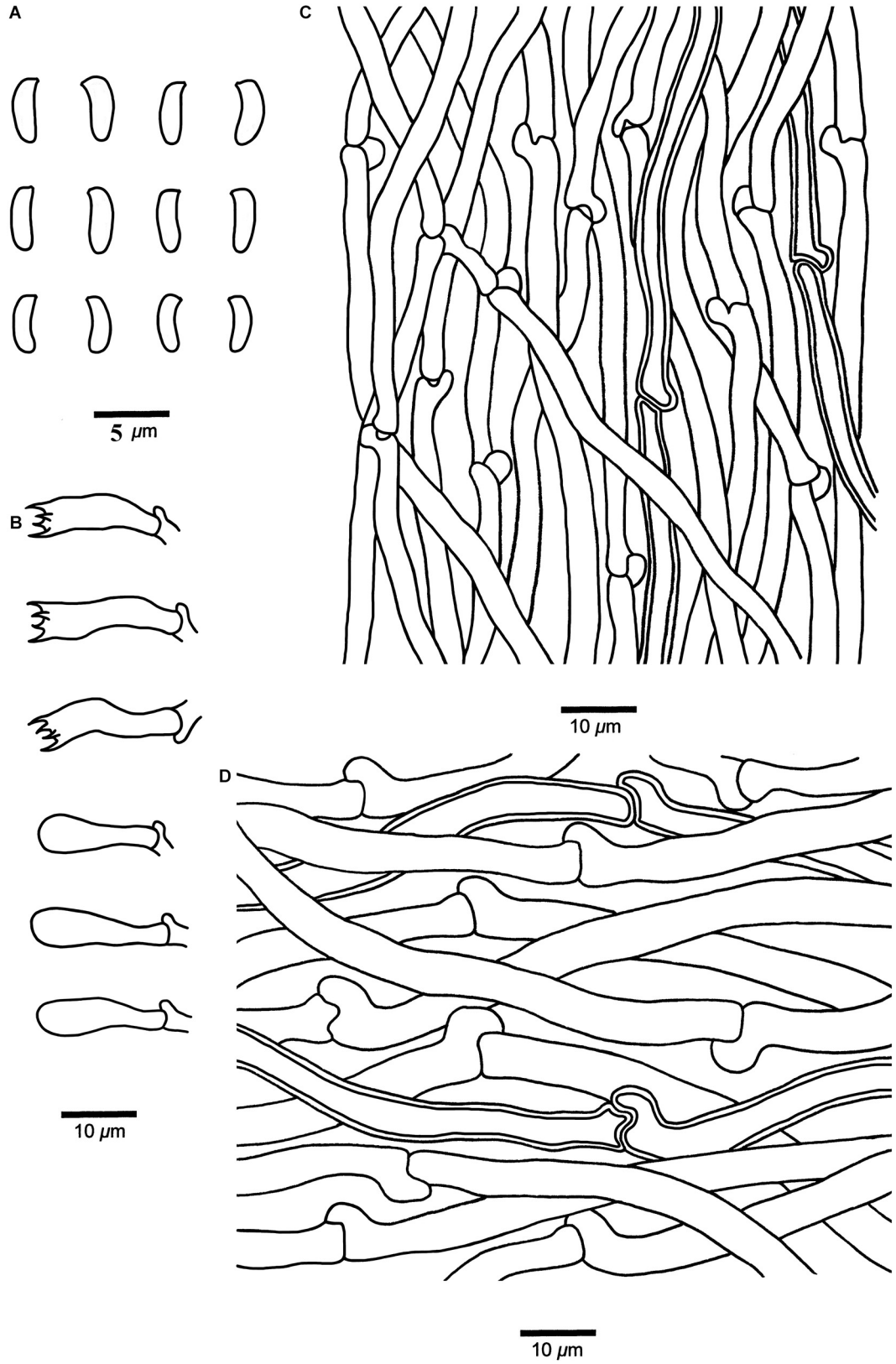


FIGURE 8 | Microscopic structures of *Cyanosporus submicroporus* (drawn from the holotype). **(A)** Basidiospores; **(B)** Basidia and basidioles; **(C)**. Hyphae from trama; **(D)** Hyphae from context. Bars: **(A)** = 5 μm; **(B–D)** = 10 μm.

smaller basidia (9.8–14.8 × 3.4–4.5 μm) (**Table 2**); *C. comata* has similar basidiospores to *C. submicroporus*, but differs in having conchate or effused-reflexed basidiocarps, and smaller basidia (8.8–14.2 × 3.7–4.9 μm) (**Table 2**); *C. fusiformis* and *C. ungulatus* differ in having larger pores (**Table 2**). *Cyanosporus submicroporus* is similar to *C. microporus* by having pileate basidiocarps with a velutinate pileal surface, and small and angular pores, but *C. microporus* differs in having thick-walled tramal generative hyphae, smaller basidia (11–13.5 × 4–5 μm) and longer basidiospores (4.5–4.9 × 1–1.2 μm) (**Table 2**).

Additional specimens (paratypes) examined. **CHINA**. Sichuan Province, Shimian County, on fallen angiosperm trunk, 14 September 2019, *Cui 17750* (BJFC); Yunnan Province, Chuxiong, Zixishan Nature Reserve, on fallen angiosperm trunk, 20 September 2017, *Cui 16306* (BJFC).

Cyanosporus tenuis B.K. Cui, Shun Liu & Y.C. Dai, **sp. nov.** (**Figures 4I–J**, **9**)

MycoBank: MB 838421

Differs from other *Cyanosporus* species by the thin basidiocarps, larger cystidioles (16.4–25.4 × 2.8–4.2 μm), and bigger basidiospores (4.7–6 × 1.3–2 μm).

Type. — **CHINA**. Sichuan Province, Luding County, Hailuogou Forest Park, on fallen trunk of *Picea*, 20 October 2012, *Cui 10788* (BJFC).

Etymology. — *Tenuis* (Lat.): refers to the thin basidiocarps.

Basidiocarps. — Annual, effused-reflexed to pileate, soft corky, without odor or taste when fresh, becoming corky to fragile upon drying. *Pileus* flabelliform, projecting up to 1.5 cm, 1.8 cm wide and 0.4 cm thick at base. *Pileal surface* buff to olivaceous buff when fresh, finely tomentose, becoming cream to olivaceous buff when dry; margin acute. *Pore surface* white to cream when fresh, becoming buff yellow to pinkish buff when dry; sterile margin narrow to almost lacking; pores angular, 5–7 per mm; dissepiments thin, entire to lacerate. *Context* cream, soft corky, up to 2 mm thick. *Tubes* pinkish buff, fragile, up to 2 mm long.

Hyphal structure. — Hyphal system monomitic; generative hyphae with clamp connections, IKI–, CB–; tissues unchanged in KOH.

Context. — Generative hyphae hyaline, thin- to slightly thick-walled with a wide lumen, occasionally branched, loosely interwoven, 2.6–7 μm in diam.

Tubes. — Generative hyphae hyaline, thin- to slightly thick-walled with a wide lumen, occasionally branched, interwoven, 2.2–4.8 μm in diam. *Cystidia* absent; *cystidioles* present, fusoid, thin-walled, 16.4–25.4 × 2.8–4.2 μm. *Basidia* clavate, bearing four sterigmata and a basal clamp connection, 18.2–27.6 × 3.7–6 μm; *basidioles* dominant, in a shape similar to basidia, but smaller.

Basidiospores. — Cylindrical, slightly curved, hyaline, thin- to slightly thick-walled, smooth, occasionally with small oil drops, IKI–, weakly CB+, (4.5–)4.7–6 × 1.3–2 μm, L = 5.44 μm, W = 1.76 μm, Q = 2.89–2.93 (n = 60/2).

Notes. — Phylogenetically, *Cyanosporus tenuis* grouped together with *C. arbuti* (Spirin) B.K. Cui & Shun Liu, *C. luteocaesius* (A. David) B.K. Cui, L.L. Shen & Y.C. Dai and *C. simulans* (P. Karst.) B.K. Cui & Shun Liu. Morphologically, *C. arbuti* differs in having narrower hyphae in the context and smaller basidiospores (4.1–5.1 × 1–1.2 μm) (**Table 2**); *C. luteocaesius* differs in larger pores (3–5 per mm; **Table 2**); *C. simulans* differs in smaller basidia (10–14.8 × 3.7–5.2 μm; **Table 2**). *Cyanosporus fusiformis*, *C. piceicola*, *C. tricolor* B.K. Cui, L.L. Shen & Y.C. Dai and *C. ungulatus* are also distributed in Sichuan Province, but *C. fusiformis* has a semicircular pileus, fusiform cystidioles presenting in the hymenium and narrow allantoid basidiospores (4.5–5.2 × 0.8–1.1 μm) (**Table 2**); *C. piceicola* has sub-rotund pileus, small angular pores, and slightly thick-walled and allantoid basidiospores (4–4.5 × 0.9–1.3 μm) (**Table 2**); *C. tricolor* has a white, blue, and pale mouse gray pileal surface when fresh (Shen et al., 2019); *C. ungulatus* has ungulate basidiocarps (Shen et al., 2019).

Additional specimen (paratype) examined. **CHINA**. Sichuan Province, Puge County, Luoji Mountain, on fallen trunk of *Picea*, 19 September 2012, *Dai 12974* (BJFC).

Cyanosporus arbuti (Spirin) B.K. Cui & Shun Liu, **comb. nov.**

MycoBank: MB 838422

Basionym: *Postia arbuti* Spirin, Fungal Systematics and Evolution 1: 113, 2018.

Notes. — *Postia arbuti* was described from the United States (Miettinen et al., 2018). It is characterized by conchate, pendant to effused-reflexed basidiocarps with almost glabrous to matt pileal surfaces. It usually grows on *Arbutus menziesii* and is widely distributed in temperate areas of North America (North-West). In our study, the phylogenetic analysis (**Figures 1–3**) strongly supports its placement in *Cyanosporus*. For a detailed description of *Postia arbuti*, see Miettinen et al. (2018).

Cyanosporus auricoma (Spirin & Niemelä) B.K. Cui & Shun Liu, **comb. nov.**

MycoBank: MB 838423

Basionym: *Postia auricoma* Spirin & Niemelä, Fungal Systematics and Evolution 1: 115, 2018.

= *Cyanosporus mongolicus* B.K. Cui, L.L. Shen & Y.C. Dai, Persoonia 42: 115, 2019.

Notes. — *Postia auricoma* was described by Miettinen et al. (2018) and *Cyanosporus mongolicus* was described by Shen et al. (2019). Phylogenetically, the two species formed a highly supported lineage (**Figures 1–3**) and as the morphological characters of *C. mongolicus* fit well with *Postia auricoma*, we treat *C. mongolicus* as a synonym of *P. auricoma*, and *P. auricoma* is transferred to *Cyanosporus* as a new combination.

Specimens examined: **CHINA**. Inner Mongolia, Ewenk, Honghuaerji Nature Reserve, on fallen trunk of *Pinus*, 19 October 2015, *Cui 13518*, *13519* (BJFC).

Cyanosporus bifaria (Spirin) B.K. Cui & Shun Liu, **comb. nov.**

MycoBank: MB 838424

Basionym: *Postia bifaria* Spirin, Fungal Systematics and Evolution 1: 115, 2018.

Notes. — *Postia bifaria* was described by Miettinen et al. (2018). The morphological characters of the two specimens from China fit well with *Postia bifaria* and phylogenetically they clustered together within the genus *Cyanosporus*. Based on morphological characters and phylogenetic analysis, we transferred *Postia bifaria* to *Cyanosporus* as a new combination. For a detailed description of *Postia bifaria*, see Miettinen et al. (2018).

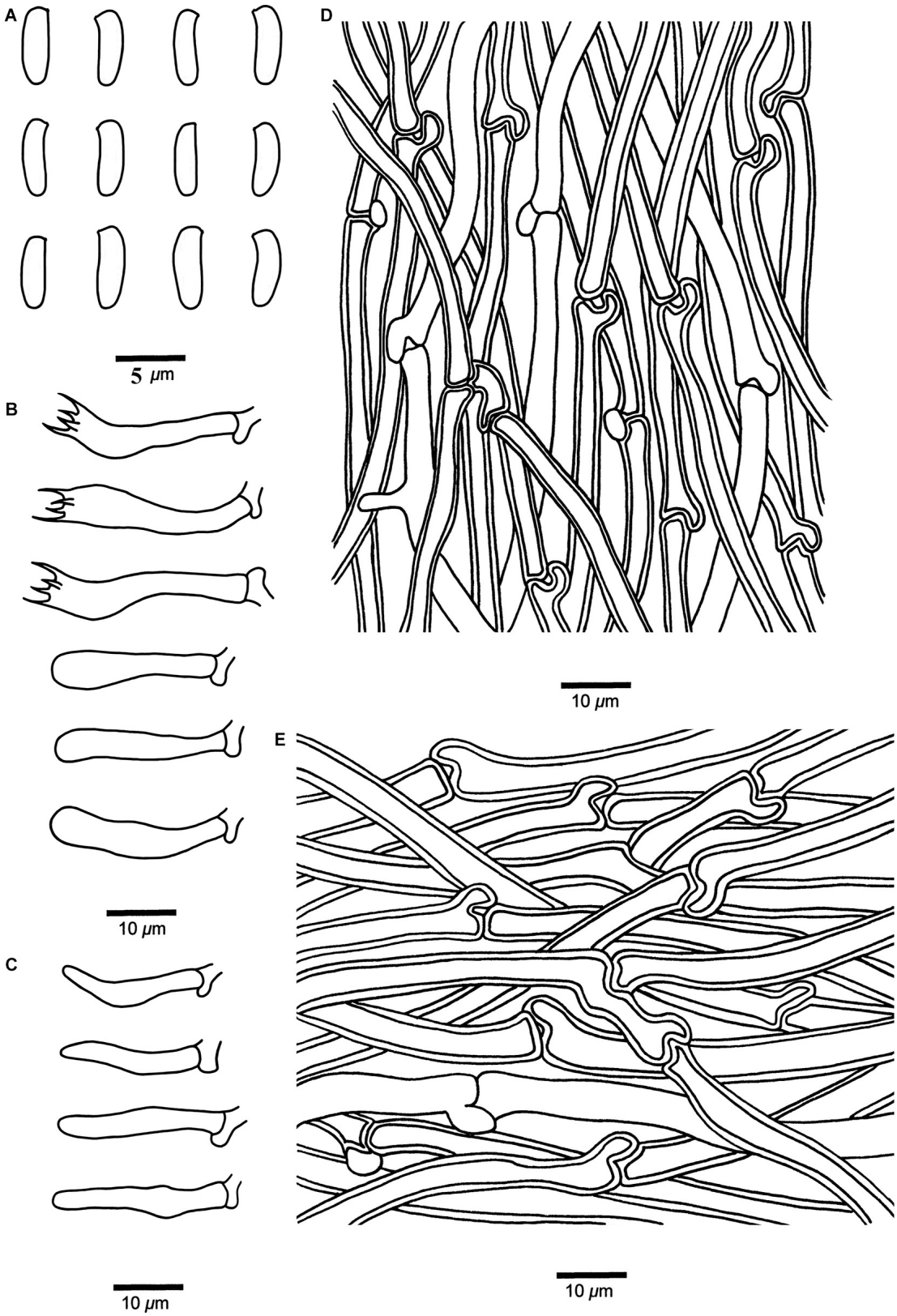


FIGURE 9 | Microscopic structures of *Cyanosporus tenuis* (drawn from the holotype). **(A)** Basidiospores; **(B)** Basidia and basidioles; **(C)** Cystidioles; **(D)** Hyphae from trama; **(E)** Hyphae from context. Bars: **(A)** = 5 μm; **(B–E)** = 10 μm.

Specimens examined: **CHINA**. Sichuan Province, Xiangcheng County, on fallen trunk of *Pinus*, 12 August 2019, *Cui 17445* (BJFC); Zhaojue County, on stump of *Pinus*, 16 September 2019, *Cui 17806* (BJFC).

Cyanosporus caesiosimulans (G.F. Atk.) B.K. Cui & Shun Liu, **comb. nov.**

MycoBank: MB 838425

Basionym: *Tyromyces caesiosimulans* G.F. Atk., Annales Mycologici 6: 61, 1908.

= *Postia caesiosimulans* (G.F. Atk.) Spirin & Miettinen, Fungal Systematics and Evolution 1: 117, 2018.

Notes. — *Tyromyces caesiosimulans* was introduced primarily based on its globose basidiospores (Atkinson, 1908). Miettinen et al. (2018) transferred it to the *Postia caesia* complex based on morphological and molecular evidence. In our study, the phylogenetic analysis strongly supports its placement in *Cyanosporus* (**Figures 1**–**3**). For a detailed description of *Postia caesiosimulans*, see Miettinen et al. (2018).

Cyanosporus coeruleivirens (Corner) B.K. Cui, Shun Liu & Y.C. Dai, **comb. nov.**

MycoBank: MB 838426

Basionym: *Tyromyces coeruleivirens* Corner, Beihefte zur Nova Hedwigia 96: 163, 1989.

= *Postia coeruleivirens* (Corner) V. Papp, Mycotaxon 129 (2): 411, 2015.

Notes. — *Tyromyces coeruleivirens* was described from Borneo (Corner, 1989). It has a greenish pileus, a monomitic hyphal system, and allantoid inamyloid basidiospores (Corner, 1989; Hattori, 2002), and was considered as a member of the *Postia caesia* group (Hattori, 2002). Papp (2014) transferred *Tyromyces coeruleivirens* to the *Postia caesia* complex as a new combination. In our study, *Postia coeruleivirens* is transferred to *Cyanosporus* as a new combination; phylogenetically it is closely related to *C. subhirsutus* (**Figures 1**–**3**). Morphologically, both *C. coeruleivirens* and *C. subhirsutus* have annual basidiocarps, a monomitic hyphal system and allantoid basidiospores, but *C. subhirsutus* differs in having a disc-shaped pileus, hirsute and zonate pileal surface and larger pores (2–3 per mm; Shen et al., 2019). For a detailed description of *Postia coeruleivirens*, see Miettinen et al. (2018).

Specimens examined: **CHINA**. Hunan Province, Changde, Hefu Forest Park, on fallen angiosperm trunk, 17 October 2018, *Dai 19220* (BJFC); Zhejiang Province, Hangzhou, Jiuxi Forest Park, on fallen angiosperm trunk, 17 October 2010, *Dai 11834* (BJFC).

Cyanosporus comata (Miettinen) B.K. Cui & Shun Liu, **comb. nov.**

MycoBank: MB 838427

Basionym: *Postia comata* Miettinen, Fungal Systematics and Evolution 1: 118, 2018.

Notes. — *Postia comata* was described from the United States (Miettinen et al., 2018). It is morphologically similar to *P. livens* Miettinen & Vlasák but differs in having mostly thick-walled tramal hyphae and slightly smaller basidiospores (Miettinen et al., 2018). Its closest relative is the East Asian *P. bifaria*, which has smaller pores (6–8 per mm) and basidiospores (3.7–4.4 × 1.0–1.2 μm), and thin-walled tramal hyphae that collapse (Miettinen et al., 2018). *Postia comata* is transferred to *Cyanosporus* as a new combination based on morphological characters and molecular phylogeny. For a detailed description of *Postia comata*, see Miettinen et al. (2018).

Specimens examined: **CHINA**. Sichuan Province, Jiuzhaigou County, Zhangzha, on stump of *Picea*, 19 September 2020, *Cui 18546* (BJFC); Xizang (Tibet), Mangkang County, on stump of *Abies*, 8 September 2020, *Cui 18388* (BJFC).

Cyanosporus cyanescens (Miettinen) B.K. Cui & Shun Liu, **comb. nov.**

MycoBank: MB 838428

Basionym: *Postia cyanescens* Miettinen, Fungal Systematics and Evolution 1: 119, 2018.

Notes. — *Postia cyanescens* was described by Miettinen et al. (2018). This species is characterized by thin, conchate to flabelliform basidiocarps with light bluish grayish tinted pore surfaces, and long and narrow basidiospores (4.7–6.1 × 1.1–1.6 μm). In our study, the phylogenetic analysis (**Figures 1**–**3**) strongly supports its placement in *Cyanosporus*, so we transferred *P. cyanescens* to *Cyanosporus* as a new combination. For a detailed description of *Postia cyanescens*, see Miettinen et al. (2018).

Cyanosporus glauca (Spirin & Miettinen) B.K. Cui & Shun Liu, **comb. nov.**

MycoBank: MB 838429

Basionym: *Postia glauca* Spirin & Miettinen, Fungal Systematics and Evolution 1: 120, 2018.

Notes. — *Postia glauca* was described by Miettinen et al. (2018), it is characterized by thin, small and conchate basidiocarps with plumbeous to bluish gray or grayish brown pileal surfaces, and cream to light bluish grayish pore surfaces. In our study, the phylogenetic analysis (**Figures 1**–**3**) supports its placement in *Cyanosporus*, so we transferred it to *Cyanosporus* as a new combination. For a detailed description of *Postia glauca*, see Miettinen et al. (2018).

Cyanosporus gossypina (Moug. & Lév.) B.K. Cui & Shun Liu, **comb. nov.**

MycoBank: MB 838430

Basionym: *Polyporus gossypinus* Moug. & Lév., Annales des Sciences Naturelles Botanique 9: 124, 1848.

= *Postia gossypina* (Moug. & Lév.) Spirin & B. Rivoire, Fungal Systematics and Evolution 1: 120, 2018.

Notes. — *Postia gossypina* was proposed by Miettinen et al. (2018). Based on morphological characters and phylogenetic analysis, we transferred *P. gossypina* to *Cyanosporus* as a new combination. For a detailed description of *Postia gossypina*, see Miettinen et al. (2018).

Cyanosporus livens (Miettinen & Vlasák) B.K. Cui & Shun Liu, **comb. nov.**

MycoBank: MB 838431

Basionym: *Postia livens* Miettinen & Vlasák, Fungal Systematics and Evolution 1: 120, 2018.

Notes. — *Postia livens* was described from North America. It is the most common representative of the *P. caesia* complex in North America, and it can be easily identified by its plumbeous to bluish gray to ochraceous pileal surface often with bluish tints (Miettinen et al., 2018). In our study, it grouped with other species of the *P. caesia* complex in *Cyanosporus* (**Figures 1**–**3**),

so, we transferred it into *Cyanosporus* as a new combination. For a detailed description of *Postia livens*, see Miettinen et al. (2018).

Cyanosporus magna (Miettinen) B.K. Cui & Shun Liu, **comb. nov.**

MycoBank: MB 838432

Basionym: *Postia magna* Miettinen, Fungal Systematics and Evolution 1: 121, 2018.

Notes. — *Postia magna* was described from China (Miettinen et al., 2018). Although we did not find the type specimen, we have examined two specimens from China, and its morphological characters fit well with this species. The phylogenetic analysis (**Figures 1–3**) also strongly supports its placement in *Cyanosporus*. So, we transferred *Postia magna* to *Cyanosporus* as a new combination. For a detailed description of *Postia magna*, see Miettinen et al. (2018).

Specimens examined: **CHINA**. Hainan Province, Ledong County, Jianfengling Nature Reserve, on fallen angiosperm trunk, 12 May 2009, Cui 10854 (BJFC); Jilin Province, Fusong County, Lushuihe Forest Park, on fallen angiosperm branch, 11 August 2011, *Cui 10094* (BJFC); Yunnan Province, Binchuan County, Jizu Mountain, on fallen angiosperm branch, 14 September 2018, *Cui 16983* (BJFC).

Cyanosporus populi (Miettinen) B.K. Cui & Shun Liu, **comb. nov.**

MycoBank: MB 838433

Basionym: *Postia populi* Miettinen, Fungal Systematics and Evolution 1: 122, 2018.

Notes. — *Postia populi* was described by Miettinen et al. (2018). Based on morphological characters and phylogenetic analyses, we transferred *P. populi* to *Cyanosporus* as a new combination. For a detailed description of *Postia populi*, see Miettinen et al. (2018).

Specimens examined: **CHINA**. Sichuan Province, Muli County, on fallen trunk of *Pinus*, 16 August 2019, *Cui 17549* (BJFC); Yunnan Province, Lijiang, Yulong Snow Mountain, on fallen trunk of *Picea*, 16 September 2018, *Cui 17087a* (BJFC).

Cyanosporus simulans (P. Karst.) B.K. Cui & Shun Liu, **comb. nov.**

MycoBank: MB 838434

Basionym: *Bjerkandera simulans* P. Karst., Revue Mycologique Toulouse 10: 73, 1888.

= *Postia simulans* (P. Karst.) Spirin & B. Rivoire, Fungal Systematics and Evolution 1: 123, 2018.

Notes. — This species was described by Karsten (1888) as *Bjerkandera simulans*. Recently, *Bjerkandera simulans* was treated as an independent species in the *Postia caesia* complex by Miettinen et al. (2018). In our study, the phylogenetic analysis (**Figures 1–3**) supports its placement in *Cyanosporus*. For a detailed description of *Postia simulans*, see Miettinen et al. (2018).

Cyanosporus subviridis (Ryvarden & Guzmán) B.K. Cui & Shun Liu, **comb. nov.**

MycoBank: MB 838435

Basionym: *Tyromyces subviridis* Ryvarden & Guzmán, Mycotaxon 78: 252, 2001.

= *Postia subviridis* (Ryvarden & Guzmán) Spirin, Fungal Systematics and Evolution 1: 125, 2018.

Notes. — *Tyromyces subviridis* was described from a highland conifer forest in Mexico (Guzmán and Ryvarden, 2001). Miettinen et al. (2018) studied the type specimen, and transferred it to the *Postia caesia* complex. In our study, the phylogenetic analysis (**Figures 1–3**) supports its placement in *Cyanosporus*. For a detailed description of *Postia subviridis*, see Miettinen et al. (2018).

Cyanosporus yanae (Miettinen & Kotiranta) B.K. Cui & Shun Liu, **comb. nov.**

MycoBank: MB 838436

Basionym: *Postia yanae* Miettinen & Kotir., Fungal Systematics and Evolution 1: 125, 2018.

Notes. — *Postia yanae* was described by Miettinen et al. (2018). It is characterized by effused-reflexed or resupinate basidiocarps with detached or adnate margins, and white, with light to strong bluish grayish tinted pore surfaces. In our study, the phylogenetic analysis (**Figures 1–3**) supports its placement in *Cyanosporus*. For a detailed description of *Postia yanae*, see Miettinen et al. (2018).

Other Specimens of *Cyanosporus* Examined

Cyanosporus alni (Niemelä & Vampola) B.K. Cui, L.L. Shen & Y.C. Dai. **CHINA**. Guizhou Province, Suiyang County, Kuankuoshui Nature Reserve, on fallen angiosperm trunk, 26 June 2014, *Dai 15060* (BJFC); Hebei Province, Xinglong County, Wulingshan Nature Reserve, on fallen angiosperm trunk, 29 August 2009, Cui 7185 (BJFC). **CZECH REPUBLIC**. Ceske Budejovice, on fallen trunk of *Fagus*, 22 November 2011, *Dai 12709* (BJFC). **FINLAND**. Uusimaa, Vantaa, Tamisto Nature Reserve, on fallen trunk of *Populus*, 4 November 2011, *Dai 12641* (BJFC). **POLAND**. Brynica, Mcrow, on fallen trunk of *Fagus*, 3 October 2014, *Dai 14845* (BJFC).

Cyanosporus caesius. **FINLAND**. Uusimaa, Vantaa, Tamisto Nature Reserve, on fallen trunk of *Picea*, 3 November 2011, *Dai 12605* (BJFC). **SPAIN**. Cadiz Province, Sierra Grazalema Natural Park, on fallen trunk of Abies, 22 November 2005, Dai 7438 (BJFC).

Cyanosporus fusiformis. **CHINA**. Guizhou Province, Suiyang County, Kuankuoshui Nature Reserve, on dead angiosperm tree, 26 November 2014, *Dai 15036* (BJFC, holotype); Sichuan Province, Luding County, Hailuogou Forest Park, on dead tree of *Rhododendron*, 20 October 2012, *Cui 10775* (BJFC, paratype).

Cyanosporus microporus. **CHINA**. Yunnan Province, Pu'er, Taiyanghe National Forest Park, on fallen angiosperm trunk, 8 July 2013, *Cui 11014* (BJFC, holotype); Chuxiong, Zixishan Nature Reserve, on dead angiosperm tree, 28 August 2010, *Dai 11717* (BJFC, paratype).

Cyanosporus piceicola. **CHINA**. Sichuan Province, Jiuzhaigou County, Jiuzhaigou Nature Reserve, on stump of *Picea*, 11 October 2012, *Cui 10626* (BJFC, holotype), on fallen trunk of *Picea*, 11 October 2012, *Cui 10617* (BJFC, paratype); Xizang (Tibet), Linzhi, Sejila Mountain, on fallen trunk of *Picea*, 18 September 2014, *Cui 12158* (BJFC, paratype); Milin County, Nanyigou Forest Park, on fallen trunk of *Picea*, 16 September 2014, *Cui 12088* (BJFC, paratype); Yunnan Province, Weixi

County, Laojunshan Nature Reserve, on fallen trunk of *Picea*, 21 September 2011, *Cui 10446* (BJFC, paratype).

Cyanosporus subhirsutus. **CHINA**. Fujian Province, Yongjing County, Huboliao Nature Reserve, on fallen angiosperm branch, 26 October 2013, *Cui 11330* (BJFC, paratype); Guizhou Province, Jiangkou County, Fanjingshan Nature Reserve, on fallen trunk of *Pterocarya*, 21 November 2014, *Dai 14892* (BJFC, holotype); Yunnan Province, Pu'er, Taiyanghe National Forest Park, on fallen angiosperm trunk, 8 July 2013, *Cui 11019* (BJFC, paratype).

Cyanosporus subcaesius. **FINLAND**. Helsinki, Arabia, on angiosperm stump, 23 November 1996, Dai 2345 (IFP); Vantaa, on fallen trunk of *Prunus*, 4 October 1997, Dai 2725 (IFP).

Cyanosporus tricolor. **CHINA**. Sichuan Province, Luding County, Hailuogou Forest Park, on fallen trunk of *Abies*, 20 October 2012, *Cui 10790* (BJFC, paratype), on fallen trunk of *Picea*, 20 October 2012, *Cui 10780* (BJFC, paratype); Xizang (Tibet), Motuo County, on fallen branch of *Abies*, 20 September 2014, *Cui 12233* (BJFC, holotype).

Cyanosporus ungulatus. **CHINA**. Sichuan Province, Mianning County, Lingshansi Park, on fallen branch of *Castanopsis*, 17 September 2012, *Dai 12897* (BJFC, holotype); Luding County, Hailuogou Forest Park, on fallen trunk of *Abies*, 20 October 2012, *Cui 10778* (BJFC, paratype).

DISCUSSION

The genus *Cyanosporus*, usually with blue-tinted basidiocarps, is easy to recognize, but identification to species level is difficult as morphological features are quite similar among the species. The main morphological characters of the species in *Cyanosporus* are provided in **Table 2**.

In our current phylogenetic analyses, the genus *Cyanosporus* is supported as an independent genus; 31 species grouped together and formed a highly supported lineage (100% BS, 100% MP, 1.00 BPP; **Figures 1–3**), and were distant from other genera of *Postia* sensu lato. The current study also confirmed that *Cyanosporus* belongs to the antrodia clade phylogenetically and clusters with other brown-rot fungal genera, such as *Amaropostia* B.K. Cui, L.L. Shen & Y.C. Dai, *Amylocystis* Bondartsev & Singer ex Singer, *Calcipostia* B.K. Cui, L.L. Shen & Y.C. Dai, *Cystidiopostia* B.K. Cui, L.L. Shen & Y.C. Dai, *Fuscopostia* B.K. Cui, L.L. Shen & Y.C. Dai, *Oligoporus* Bref., *Osteina* Donk, *Postia* Fr. and *Spongiporus* Murrill, which is similar to previous studies (Ortiz-Santana et al., 2013; Ryvarden and Melo, 2014; Han et al., 2016; Shen et al., 2019).

The nomenclatural and taxonomic history of the *Postia caesia* complex was critically reviewed by Papp (2014), the generic name of the *P. caesia* complex have been changed many times, Papp proposed *Cyanosporus* as a subgenus of *Postia* to contain the *P. caesia* complex. Miettinen et al. (2018) revised the species concept of the *Postia caesia* complex based on morphology and two gene markers (ITS and TEF) and discussed that TEF sequences are more reliable for molecular identification of the *P. caesia* complex than ITS sequences. They also indicated that host tree is important for species identification of the *P. caesia* complex; their study raised the species number of the *Postia caesia* complex from 10 to 24, but their study did not focus on the taxonomic status for the *P. caesia* complex of *Postia* sensu lato.

Previously, species identification of the *Postia caesia* complex was only based on morphological characters and host trees in China. Samples grown on angiosperm woods were usually identified as *Postia alni* Niemelä & Vampola and those on gymnosperm woods as *Postia caesia*; only two species were recorded from China before Dai (2012). Shen et al. (2019) carried out a comprehensive phylogenetic and taxonomic study of *Postia* and related genera based on morphological characters and the combined seven-gene (ITS + nLSU + nSSU + mtSSU + RPB1 + RPB2 + TEF) sequences, *Cyanosporus* was confirmed as an independent genus of *Postia* sensu lato and 12 species belonging to the *P. caesia* complex were recognized in *Cyanosporus*, which was distant from *Postia* s. s.

In the current study, the novel species were supported by phylogenetic analyses based on ITS + TEF sequences, ITS + nLSU + TEF sequences and ITS + nLSU + nSSU + mtSSU + RPB1 + RPB2 + TEF sequences, respectively, but for the ITS sequences, several species have very similar base pairs and could not be separated by ITS sequences. The suitable DNA barcoding gene is the TEF gene for species identification of *Cyanosporus*, this result is consistent with a previous study by Miettinen et al. (2018). Our study expanded the number of *Cyanosporus* species to 31 around the world including 19 species from China. Our study indicated that more cryptic species could be discovered by combined evidence of morphological characters, molecular data, host trees and distribution areas in species complexes. However, several species of the *Postia caesia* complex, such as, *P. africana* (Ryvarden) V. Papp, *P. amyloidea* (Corner) V. Papp, *P. atrostrigosa* (Cooke) Rajchenb. and *P. caesioflava* (Pat.) V. Papp, are not included in the current phylogenetic analysis due to the lack of DNA sequences. Although the morphological characters of these species fit well with *Cyanosporus*, we did not transfer them to *Cyanosporus* in the current study. A fully resolved phylogeny for *Cyanosporus* and its related genera requires evolutionary information from more samples and more conserved gene markers.

In addition, some species with yellow basidiocarps, such as *C. auricoma*, *C. caesioflava*, and *C. luteocaesius*, and some species with white to cream colored basidiocarps, such as *C. bubalinus* and *C. nothofagicola*, are grouped together within *Cyanosporus*; this expanded the concept of the genus to include taxa without blue-tinted basidiocarps. More novel species might be discovered from different regions in future studies.

DATA AVAILABILITY STATEMENT

The datasets presented in this study can be found in online repositories. The names of the repository/repositories and accession number(s) can be found below: http://purl.org/phylo/treebase, 27274.

AUTHOR CONTRIBUTIONS

B-KC and SL designed the experiments. SL, L-LS, GG, and B-KC prepared the samples. SL, YW, and T-MX conducted the molecular experiments and analyzed the data. SL, GG, and B-KC drafted the manuscript. All the authors approved the manuscript.

FUNDING

This research was supported by the Biodiversity Survey and Assessment Project of the Ministry of Ecology and Environment, China (No. 2019HJ2096001006), the National Natural Science Foundation of China (Nos. U2003211 and 31750001), and the Beijing Forestry University Outstanding Young Talent Cultivation Project (No. 2019JQ03016).

ACKNOWLEDGMENTS

We express our gratitude to Drs. Tom May (Royal Botanical Gardens Victoria, Australia), Xiao-Lan He (Sichuan Academy of Agricultural Sciences, China), and Yu-Cheng Dai (Beijing Forestry University, China) for help during field collections.

REFERENCES

Atkinson, G. F. (1908). Notes on some new species of fungi from the United States. *Ann. Mycol.* 6, 54–62.

Chen, Y. Y., Wu, F., Wang, M., and Cui, B. K. (2017). Species diversity and molecular systematics of Fibroporia (*Polyporales*, *Basidiomycota*) and its related genera. *Mycol. Prog.* 16, 521–533. doi: 10.1007/s11557-017-1285-1

Corner, E. J. H. (1989). Ad polyporaceas V. *Beih. Nova Hedwigia* 96, 1–218.

Cui, B. K., Li, H. J., Ji, X., Zhou, J. L., Song, J., Si, J., et al. (2019). Species diversity, taxonomy and phylogeny of *Polyporaceae* (*Basidiomycota*) in China. *Fungal Divers.* 97, 137–392. doi: 10.1007/s13225-019-00427-4

Dai, Y. C. (2012). Polypore diversity in China with an annotated checklist of Chinese polypores. *Mycoscience* 53, 49–80. doi: 10.1007/s10267-011-0134-3

David, A. (1974). Une nouvelle espèce de *Polyporaceae*: *Tyromyces* subcaesius. *B. Mens. Soc. Linn. Lyon* 43, 119–126.

David, A. (1980). Étude du genre *Tyromyces* sensu lato: répartition dans les genres Leptoporus, Spongiporus et *Tyromyces* sensu stricto. *B. Mens. Soc. Linn. Lyon* 49, 6–56. doi: 10.3406/linly.1980.10404

Donk, M. A. (1960). The generic names proposed for *Polyporaceae*. *Persoonia* 1, 173–302.

Farris, J. S., Källersjö, M., Kluge, A. G., Kluge, A. G., and Bult, C. (1994). Testing significance of incongruence. *Cladistics* 10, 315–319. doi: 10.1006/clad.1994.1021

Felsenstein, J. (1985). Confidence intervals on phylogenies: an approach using the bootstrap. *Evolution* 39, 783–791. doi: 10.2307/2408678

Fries, E. M. (1821). *Systema Mycologicum*, Vol. 1. Lund: Officina Berlingiana.

Guzmán, G., and Ryvarden, L. (2001). Studies in neotropical polypores 12. New and noteworthy polypores from Mexico. *Mycotaxon* 78, 245–256.

Hall, T. A. (1999). Bioedit: a user-friendly biological sequence alignment editor and analysis program for Windows 95/98/NT. *Nucleic Acids Symp. Ser.* 41, 95–98. doi: 10.1021/bk-1999-0734.ch008

Han, M. L., Chen, Y. Y., Shen, L. L., Song, J., Vlasák, J., Dai, Y. C., et al. (2016). Taxonomy and phylogeny of the brown-rot fungi: fomitopsis and its related genera. *Fungal Divers.* 80, 343–373. doi: 10.1007/s13225-016-0364-y

Hattori, T. (2002). Type studies of the polypores described by E.J.H. Corner from Asia and West Pacific Areas. IV. Species described in *Tyromyces* (1). *Mycoscience* 43, 307–315. doi: 10.1007/s102670200045

Hillis, D. M., and Bull, J. J. (1993). An empirical test of bootstrapping as a method for assessing confidence in phylogenetic analysis. *Syst. Biodivers.* 42, 182–192. doi: 10.1093/sysbio/42.2.182

Jahn, H. (1963). Mitteleuropäische Porlinge (*Polyporaceae* s. lato) und ihr Vorkommen in Westfalen. *Westfälische Pilzbriefe* 4, 1–143. doi: 10.1007/978-3-642-90915-3_1

Jahn, H. (1979). *Pilze die an Holz Wachsen*. Herford: Busse.

Karsten, P. A. (1881). Enumeratio boletinearum et polyporearum fennicarum, systemate novo dispositarum. *Rev. Mycol. Toulouse* 3, 16–19.

Karsten, P. A. (1888). Diagnoses fungorum nonnullorum novorum, in Fennia detectorum. *Rev. Mycol. Toulouse* 10, 73–75.

Katoh, K., and Standley, D. M. (2013). MAFFT Multiple sequence alignment software version 7: improvements in performance and usability. *Mol. Biol. Evol.* 30, 772–780. doi: 10.1093/molbev/mst010

Liu, S., Song, C. G., and Cui, B. K. (2019). Morphological characters and molecular data reveal three new species of Fomitopsis (*Basidiomycota*). *Mycol. Prog.* 18, 1317–1327. doi: 10.1007/s11557-019-01527-w

Lowe, J. L. (1975). *Polyporaceae* of North America. The genus *Tyromyces*. *Mycotaxon* 2, 1–82. doi: 10.1007/978-3-319-23534-9_1

Maddison, W. P., and Maddison, D. R. (2017). *Mesquite: A Modular System for Evolutionary Analysis, Version 3.2*. Avaliable at: http://mesquiteproject.org. (accessed October 2020).

Matheny, P. B. (2005). Improving phylogenetic inference of mushrooms with RPB1 and RPB2 nucleotide sequences (*Inocybe*, *Agaricales*). *Mol. Phylogenet. Evol.* 35, 1–20. doi: 10.1016/j.ympev.2004.11.014

Matheny, P. B., Liu, Y. J., Ammirati, J. F., and Hall, B. D. (2002). Using RPB1 sequences to improve phylogenetic inference among mushrooms (*Inocybe*. *Agaricales*). *Am. J. Bot.* 89, 688–698. doi: 10.3732/ajb.89.4.688

McGinty, N. J. (1909). A new genus, Cyanosporus. *Mycol. Notes* 33:436.

Miettinen, O., Vlasák, J., Rivoire, B., and Spirin, V. (2018). Postia caesia complex (*Polyporales*, *Basidiomycota*) in temperate Northern Hemisphere. *Fungal Syst. Evol.* 1, 101–129. doi: 10.3114/fuse.2018.01.05

Niemelä, T., Penttil, R., Kinnunen, J., Miettinen, O., and Turunen, O. (2001). Novelties and records of poroid Basidiomycetes in Finland and adjacent Russia. *Karstenia* 41, 1–21. doi: 10.29203/ka.2001.373

Nylander, J. A. A. (2004). *MrModeltest v2. Program Distributed by the Author*. Uppsala: Uppsala University.

Ortiz-Santana, B., Lindner, D. L., Miettinen, O., Justo, A., and Hibbett, D. S. (2013). A phylogenetic overview of the antrodia clade (*Basidiomycota*. *Polyporales*). *Mycologia* 105, 1391–1411. doi: 10.3852/13-051

Papp, V. (2014). Nomenclatural novelties in the Postia caesia complex. *Mycotaxon* 129, 407–413. doi: 10.5248/129.407

Pieri, M., and Rivoire, B. (2005). Postia mediterraneocaesia, une nouvelle espèce de polypore découverte dans le sud de l'Europe. *Bull. Semestriel Féd. Assoc. Mycol. Méditerranéennes* 28, 33–38.

Posada, D., and Crandall, K. A. (1998). Modeltest: testing the model of DNA substitution. *Bioinformatics* 14, 817–818. doi: 10.1093/bioinformatics/14.9.817

Rehner, S. (2001). *Primers for Elongation Factor 1-a (EF1-a)*. Avaliable at: https://www.docin.com/p-1613748809.html (accessed October 2020).

Ronquist, F., and Huelsenbeck, J. P. (2003). MrBayes 3: Bayesian phylogenetic inference under mixed models. *Bioinformatics* 19, 1572–1574. doi: 10.1093/bioinformatics/btg180

Ryvarden, L., and Melo, I. (2014). Poroid fungi of Europe. *Synop. Fungorum.* 31, 1–455.

Schrader, H. A. (1794). *Spicilegium Florae Germanicae*. Hannover: C. Ritscher.

Shen, L. L., Wang, M., Zhou, J. L., Xing, J. H., Cui, B. K., and Dai, Y. C. (2019). Taxonomy and phylogeny of Postia. Multi-gene phylogeny and taxonomy of the brown-rot fungi: postia (*Polyporales*, *Basidiomycota*) and related genera. *Persoonia* 42, 101–126. doi: 10.3767/persoonia.2019.42.05

Song, J., and Cui, B. K. (2017). Phylogeny, divergence time and historical biogeography of Laetiporus (*Basidiomycota*, *Polyporales*). *BMC Evol. Biol.* 17:102. doi: 10.1186/s12862-017-0948-5

Stamatakis, A. (2006). RAxML-VI-HPC: maximum likelihood-based phylogenetic analysis with thousands of taxa and mixed models. *Bioinformatics* 22, 2688–2690. doi: 10.1093/bioinformatics/btl446

Sun, Y. F., Costa-Rezende, D. H., Xing, J. H., Zhou, J. L., Zhang, B., Gibertoni, T. B., et al. (2020). Multi-gene phylogeny and taxonomy of Amauroderma s.l*at. (Ganodermataceae). Persoonia* 44, 206–239. doi: 10.3767/persoonia.2020.44.08

Swofford, D. L. (2002). *PAUP*. Phylogenetic Analysis Using Parsimony (*and other methods). Version 4.0b10.* Sunderland, MA: Sinauer Associates, doi: 10.1111/j.0014-3820.2002.tb00191.x

White, T. J., Bruns, T. D., Lee, S., and Taylor, J. (1990). Amplification and direct sequencing of fungal ribosomal RNA genes for phylogenetics. *PCR Protoc. Guide Methods Appl.* 18, 315–322. doi: 10.1016/B978-0-12-372180-8.50042-1

Zhu, L., Song, J., Zhou, J. L., Si, J., and Cui, B. K. (2019). Species diversity, phylogeny, divergence time and biogeography of the genus Sanghuangporus (*Basidiomycota*). *Front. Microbiol.* 10:812. doi: 10.3389/fmicb.2019.00812

Conflict of Interest: The authors declare that the research was conducted in the absence of any commercial or financial relationships that could be construed as a potential conflict of interest.

Copyright © 2021 Liu, Shen, Wang, Xu, Gates and Cui. This is an open-access article distributed under the terms of the Creative Commons Attribution License (CC BY). The use, distribution or reproduction in other forums is permitted, provided the original author(s) and the copyright owner(s) are credited and that the original publication in this journal is cited, in accordance with accepted academic practice. No use, distribution or reproduction is permitted which does not comply with these terms.

NOMENCLATURE

AR: Argentina; BI: Bayesian inference; BJFC: Herbarium of the Institute of Microbiology, Beijing Forestry University; BGI: Beijing Genomics Institute; BPP: Bayesian posterior probabilities; BT: Bootstrap; CB: Cotton Blue; CB +: cyanophilous; CB–: acyanophilous; GB: Great Britain; GTR + I + G: General time reversible + proportion invariant + gamma; CTAB: Cetyl trimethylammonium bromide; IFP: Herbarium of the Institute of Applied Ecology, Chinese Academy of Sciences; IKI: Melzer's reagent, IKI–: neither amyloid nor dextrinoid; ILD: Incongruence length difference test; ITS: Internal transcribed spacer; KOH: 5% potassium hydroxide; L: mean spore length (arithmetic average of all spores); ML: Maximum likelihood; MP: Maximum parsimony; MPT: Most Parsimonious Tree; mtSSU: Mitochondrial small subunit rRNA; n (a/b): number of spores (a) measured from given number (b) of specimens; nLSU: Nuclear large subunit rDNA; nSSU: Nuclear small subunit rRNA; Q: variation in the L/W ratios between the specimens studied; RPB1: DNA-directed RNA polymerase II subunit 1; RPB2: DNA-directed RNA polymerase II subunit 2; TL: Tree length; W: mean spore width (arithmetic average of all spores); CI: Consistency Index; RI: Retention Index; RC: Rescaled Consistency Index; HI: Homoplasy Index; TEF: Translation elongation factor 1-α.

frontiers in Microbiology

ORIGINAL RESEARCH
published: 10 February 2021
doi: 10.3389/fmicb.2021.622460

Global Phylogeny and Taxonomy of the Wood-Decaying Fungal Genus *Phlebiopsis* (Polyporales, Basidiomycota)

Ya-Nan Zhao[1], Shuang-Hui He[1], Karen K. Nakasone[2], K. L. Wasantha Kumara[3], Che-Chih Chen[4,5], Shi-Liang Liu[6], Hai-Xia Ma[7] and Man-Rong Huang[8]*

[1] Institute of Microbiology, School of Ecology and Nature Conservation, Beijing Forestry University, Beijing, China, [2] Center for Forest Mycology Research, Northern Research Station, U.S. Forest Service, Madison, WI, United States, [3] Department of Agricultural Biology, Faculty of Agriculture, University of Ruhuna, Kamburupitiya, Sri Lanka, [4] Department of Plant Pathology, National Chung Hsing University, Taichung, Taiwan, [5] Department of Biology, National Museum of Natural Science, Taichung, Taiwan, [6] State Key Laboratory of Mycology, Institute of Microbiology, Chinese Academy of Sciences, Beijing, China, [7] Institute of Tropical Bioscience and Biotechnology, Chinese Academy of Tropical Agricultural Sciences, Hainan, China, [8] Beijing Museum of Natural History, Beijing, China

OPEN ACCESS

Edited by:
Dhanushka Nadeeshan Wanasinghe, Chinese Academy of Sciences, China

Reviewed by:
Samantha Chandranath Karunarathna, Chinese Academy of Sciences, China
Asha Janadaree Dissanayake, University of Electronic Science and Technology of China, China

***Correspondence:**
Shuang-Hui He
shuanghuihe@yahoo.com

Specialty section:
This article was submitted to Evolutionary and Genomic Microbiology, a section of the journal Frontiers in Microbiology

Received: *10 November 2020*
Accepted: *22 January 2021*
Published: *10 February 2021*

Citation:
Zhao Y-N, He S-H, Nakasone KK, Wasantha Kumara KL, Chen C-C, Liu S-L, Ma H-X and Huang M-R (2021) Global Phylogeny and Taxonomy of the Wood-Decaying Fungal Genus Phlebiopsis (Polyporales, Basidiomycota). Front. Microbiol. 12:622460. doi: 10.3389/fmicb.2021.622460

An in-depth study of the phylogeny and taxonomy of the corticioid genus *Phlebiopsis* (Phanerochaetaceae) was conducted. Phylogenetic analyses of the ITS1-5.8S-ITS2 and nrLSU sequences demonstrated that *Phlebiopsis* is a strongly supported clade which is distinct from its sister clades of *Phaeophlebiopsis*, *Hapalopilus*, and *Rhizochaete*. Two genera, *Australohydnum* and *Hjortstamia*, are reduced to synonyms under *Phlebiopsis* as generic type species *A. griseofuscescens* and *H. friesii*, respectively, are embedded in the *Phlebiopsis* clade. Twenty-four lineages are resolved in the ITS phylogenetic tree of *Phlebiopsis*, including six new taxa, viz. *P. albescens*, *P. brunnea*, *P. cylindrospora*, *P. magnicystidiata*, *P. membranacea* and *P. sinensis*, from Sri Lanka and China. Five new combinations, viz. *Phaeophlebiopsis mussooriensis*, *Phlebiopsis bambusicola*, *P. dregeana*, *P. griseofuscescens* and *P. novae-granatae*, are proposed. *Phlebiopsis crassa* is a morphological species complex with three distinct lineages. *Phlebiopsis lamprocystidiata* is determined to be a later synonym of *P. darjeelingensis*. The new taxa are described, illustrated, and compared and contrasted to morphologically similar species. An emended description of *Phlebiopsis* is provided along with an identification key to 27 accepted species.

Keywords: corticioid fungi, five new combinations, identification key, Phanerochaetaceae, phlebioid fungi, six new species, white rot

Abbreviations: ITS, internal transcribed spacer; nrLSU, nuclear ribosomal large subunit; BJFC, herbarium of Beijing Forestry University, Beijing, China; CFMR, Centre for Forest Mycology Research, U.S. Forest Service, Madison, WI, United States; TNM, National Museum of Natural Science, Taichung, Taiwan, China; KOH, 2% (w/v) potassium hydroxide; IKI, Melzer's reagent; CB, cotton blue; IKI–, neither amyloid nor dextrinoid; CB–, acyanophilous; L, mean spore length; W, mean spore width; Q, L/W ratio, n (a/b), number of spores (a) measured from number of specimens (b); CTAB, cetyltrimethylammonium bromide; DNA, deoxyribonucleic acid; PCR, polymerase chain reaction; MP, maximum parsimony; ML, maximum likelihood; BI, Bayesian inference; TBR, tree-bisection reconnection; BPP, Bayesian posterior probability.

INTRODUCTION

In 1978, *Phlebiopsis* Jülich was suggested for *Thelephora gigantea* Fr. that has effused, ceraceous basidiomata with a smooth to odontoid hymenophore, a monomitic hyphal system with colorless, partially agglutinated, simple-septate hyphae, lamprocystidia with thick, colorless walls, and basidiospores with colorless, thin, smooth walls that do not react in Melzer's reagent or cotton blue (Jülich, 1978; Bernicchia and Gorjón, 2010). Over the next 40 years, 12 species with similar morphology were described in or transferred to the genus by Hjortstam and Ryvarden (1980), Jülich and Stalpers (1980), Dhingra (1987), Hjortstam (1987), Gilbertson and Adaskaveg (1993), Douanla-Meli and Langer (2009), Wu et al. (2010), Priyanka et al. (2011), Kaur et al. (2015), and Zhao et al. (2018). Morphologically, *Phlebiopsis* is similar to *Scopuloides* (Massee) Höhn. & Litsch. and some species of *Phanerochaete* P. Karst based on the characteristics of lamprocystidia and simple-septate generative hyphae. It was traditionally placed in the *Phanerochaete sensu lato* group (Rattan, 1977; Burdsall, 1985). Although Burdsall (1985) considered *Phlebiopsis* and *Scopuloides* to be synonyms of *Phanerochaete*, most researchers at the time recognized the genera as distinct (Eriksson et al., 1978, 1981, 1984; Jülich and Stalpers, 1980; Wu, 1990).

The generic circumscription of *Phlebiopsis* was expanded when molecular studies showed that *Phanerochaete crassa* (Lév.) Burds. and *Phlebiopsis gigantea* (Fr.) Jülich were closely related (de Koker et al., 2003; Greslebin et al., 2004; Wu et al., 2010; Floudas and Hibbett, 2015). With the inclusion of *P. crassa*, *Phlebiopsis* now also includes species with effused-reflexed, coriaceous basidiomata, a dimitic hyphal system, and lamprocystidia or skeletocystidia with light brown walls. In addition, based on both phylogenetic and morphological evidence, Floudas and Hibbett (2015) created *Phaeophlebiopsis* Floudas & Hibbett to accommodate *Phlebiopsis peniophoroides* Gilb. & Adask. and similar species with ceraceous, beige-brown basidiomata and subicula, lamprocystidia with brown walls, and small basidiospores. The limits of the *Phlebiopsis* clade were extended by Miettinen et al. (2016) who transferred six species into *Phlebiopsis*. The results of their phylogenetic study showed that the type species of *Castanoporus* Ryvarden, *Merulius castaneus* Lloyd, was nested in a clade with *P. gigantea* and, therefore, a synonym of *Phlebiopsis*. Similarly, *Dentocorticium pilatii* (Parmasto) Duehm & Michel, *Lopharia papyrina* (Mont.) Boidin, *Phanerochaete brunneocystidiata* Sheng H. Wu, and *Phanerochaete laxa* Sheng H. Wu clustered in the *Phlebiopsis* clade, and were all transferred to the genus. Based on the morphological similarity of *Thelephora friesii* Lév., the type of *Hjortstamia* Boidin and Gilles, 2003 to *L. papyrina* and *P. crassa*, they also transferred *T. friesii* to *Phlebiopsis*, thereby reducing *Hjortstamia* to a synonym of *Phlebiopsis*. *Phlebiopsis pilatii* (Parmasto) Spirin & Miettinen is unique in the genus for it has a dimitic hyphal system of simple-septate generative and microbinding (squelettoligatives) hyphae and finely branched hyphidia but lacks lamprocystidia or skeletal cystidia (Larsen and Gilberston, 1977; Duhem and Michel, 2009).

With *Hjortstamia* and *Castanoporus* as synonyms, *Phlebiopsis* became a morphologically heterogeneous genus with effused, effused-reflexed or pileate basidiomata with a membranous, ceraceous, corneous or coriaceous texture, hymenophore smooth to tuberculate, odontoid, or poroid, hyphal system monomitic or dimitic with a loose to compact subiculum, and typically with lamprocystidia or skeletocystidia with colorless to brown walls. In phylogenetic analyses of Phanerochaetaceae, *Phlebiopsis* species are in a clade sister to *Rhizochaete* Gresl., Nakasone & Rajchenb., *Hapalopilus* P. Karst. and *Phaeophlebiopsis*, but distant from *Phanerochaete sensu stricto* and *Scopuloides* (Floudas and Hibbett, 2015; Miettinen et al., 2016).

Another genus of interest is *Australohydnum* Jülich for it is similar to *Phlebiopsis* by its warted, irpicoid to hydnoid hymenophore, a dimitic hyphal system with colorless, encrusted skeletocystidia, and thin-walled, smooth basidiospores (Jülich, 1978). The morphological similarities between *Australohydnum* and *Phanerochaete* sensu lato were observed by Hjortstam and Ryvarden (1990). In a limited study of *Irpex* sensu stricto, sequences of *A. dregeanum* (Berk.) Hjortstam & Ryvarden and *I. vellereus* Berk. & Broome (a possible synonym of *A. dregeanum*) clustered together in a clade sister to *Phanerochaete chrysosporium* Burds. and *Phanerochaete sordida* (P. Karst.) J. Erikss. & Ryvarden (Lim and Jung, 2003). However, the phylogenetic relationship of *Australohydnum* within the Phanerochaetaceae remained unknown (Miettinen et al., 2016).

Among the 24 names of *Phlebiopsis* recovered in Index Fungorum[1] (accessed on 21 January2020), four species were transferred to *Phaeophlebiopsis*. Of the remaining 20 species, 11 were described originally from Asia (Dhingra, 1987; Wu, 2000, 2004; Priyanka et al., 2011; Kaur et al., 2015; Zhao et al., 2018; Xu et al., 2020). More than 150 specimens of *Phlebiopsis* were collected by the corresponding author from China and Southeast Asia in recent years. Based on these specimens and sequences obtained from GenBank, the phylogenetic analyses and taxonomic study of *Phlebiopsis* and related taxa in the Phanerochaetaceae were undertaken. This study is a contribution to the understanding of the diversity and phylogenetic relationships of crust fungi in China.

MATERIALS AND METHODS

Specimen Collection

Field trips for specimen collection in many kinds of Nature Reserves and Forest Parks in China and other countries were carried out by the authors. *In situ* photos of the fungi were taken with a Canon camera EOS 70D (Canon Corporation, Japan). Fresh specimens were dried with a portable drier (manufactured in Finland). Dried specimens were labeled and then stored in a refrigerator of minus 40°C for 2 weeks to kill the insects and their eggs before they were ready for morphological and molecular studies.

[1]http://www.indexfungorum.org/

Morphological Studies

Voucher specimens are deposited at the herbaria of Beijing Forestry University, Beijing, China (BJFC), Centre for Forest Mycology Research, U.S. Forest Service, Madison, WI, United States (CFMR), National Museum of Natural Science, Taichung, Taiwan, China (TNM) and Beijing Museum of Natural History, Beijing, China (BJM). The Sri Lankan voucher specimens are deposited in the Faculty of Agriculture, University of Ruhuna, Kamburupitiya, Sri Lanka and the herbarium of Beijing Forestry University, Beijing, China (BJFC), and were studied under the material transfer agreement signed by the two universities. Freehand sections were made from dried basidiomata and mounted in 2% (w/v) potassium hydroxide (KOH), 1% (w/v) phloxine, Melzer's reagent (IKI) or cotton blue (CB). Microscopic examinations were carried out with a Nikon Eclipse 80i microscope (Nikon Corporation, Japan) at magnifications up to 1000×. Drawings were made with the aid of a drawing tube. The following abbreviations are used: IKI–, neither amyloid nor dextrinoid; CB–, acyanophilous; L, mean spore length; W, mean spore width; Q, L/W ratio; n (a/b), number of spores (a) measured from number of specimens (b). Color codes and names follow Kornerup and Wanscher (1978).

DNA Extraction and Sequencing

A CTAB plant genomic DNA extraction Kit DN14 (Aidlab Biotechnologies Co., Ltd., Beijing, China) was used to extract total genomic DNA from dried specimens then amplified by the polymerase chain reaction (PCR), according to the manufacturer's instructions. The ITS1-5.8S-ITS2 region was amplified with the primer pair ITS5/ITS4 (White et al., 1990) using the following protocol: initial denaturation at 95°C for 4 min, followed by 34 cycles at 94°C for 40 s, 58°C for 45 s and 72°C for 1 min, and final extension at 72°C for 10 min. The nrLSU D1-D2 region was amplified with the primer pair LR0R/LR7[2] employing the following procedure: initial denaturation at 94°C for 1 min, followed by 34 cycles at 94°C for 30 s, 50°C for 1 min and 72°C for 1.5 min, and final extension at 72°C for 10 min. DNA sequencing was performed at Beijing Genomics Institute, and the sequences were deposited in GenBank[3] (**Table 1**). BioEdit v.7.0.5.3 (Hall, 1999) and Geneious Basic v.11.1.15 (Kearse et al., 2012) were used to review the chromatograms and for contig assembly.

Phylogenetic Analyses

Two separate datasets, the concatenated ITS-nrLSU sequences of species in the Phanerochaetaceae and ITS only sequences of *Phlebiopsis*, were analyzed. *Ceraceomyces serpens* (Tode) Ginns and *Phlebia acerina* Peck were selected as an outgroup for the ITS-LSU dataset, whilst *Rhizochaete radicata* (Henn.) Gresl., Nakasone & Rajchenb. was used in the ITS dataset (Floudas and Hibbett, 2015). For the concatenated dataset, the sequences of ITS and nrLSU were aligned separately using MAFFT v.7[4] (Katoh et al., 2017) with the G-INS-I iterative refinement algorithm, and optimized manually in BioEdit v.7.0.5.3. The separate alignments were then concatenated using Mesquite v.3.5.1 (Maddison and Maddison, 2018). The datasets were deposited in TreeBase[5] (submission ID: 26529 for Phanerochaetaceae ITS-LSU, 26530 for *Phlebiopsis* ITS).

Maximum parsimony (MP), maximum likelihood (ML) analyses and Bayesian inference (BI) were carried out by using PAUP* v.4.0b10 (Swofford, 2002), RAxML v.8.2.10 (Stamatakis, 2014), and MrBayes 3.2.6 (Ronquist et al., 2012), respectively. In MP analysis, trees were generated using 100 replicates of random stepwise addition of sequence and tree-bisection reconnection (TBR) branch-swapping algorithm with all characters given equal weight. Branch supports for all parsimony analyses were estimated by performing 1000 bootstrap replicates with a heuristic search of 10 random-addition replicates for each bootstrap replicate. In ML analysis, statistical support values were obtained using rapid bootstrapping with 1000 replicates, with default settings used for other parameters. For BI, the best-fit substitution model was estimated with jModeltest v.2.17 (Darriba et al., 2012). Four Markov chains were run for five million and three million generations for the Phanerochaetaceae ITS-LSU and *Phlebiopsis* ITS datasets, respectively, until the split deviation frequency value was lower than 0.01. Trees were sampled every 100th generation. The first quarter of the trees, which represented the burn-in phase of the analyses, were discarded, and the remaining trees were used to calculate posterior probabilities (BPP) in the majority rule consensus tree.

RESULTS

Phylogenetic Analyses

Forty-three ITS and 37 nrLSU sequences were generated for this study. The concatenated ITS-LSU dataset contained 101 ITS and 107 nrLSU sequences from 107 samples representing 86 Phanerochaetaceae taxa and the outgroup, while the ITS dataset contained 71 samples representing 21 *Phlebiopsis s.s.* taxa, a sample of *Irpex vellereus* and the outgroup (**Table 1**). The concatenated dataset had an aligned length of 2339 characters, of which 554 were parsimony-informative. MP analysis yielded one equally parsimonious tree (TL = 3603, CI = 0.360, RI = 0.695, RC = 0.250, HI = 0.640). The ITS dataset had an aligned length of 726 characters, of which 178 were parsimony-informative. MP analysis yielded 92 equally parsimonious trees (TL = 658, CI = 0.579, RI = 0.870, RC = 0.504, HI = 0.421). jModelTest suggested GTR + I + G and HKY + G were the best-fit models of nucleotide evolution for the concatenated ITS-LSU and ITS datasets, respectively. The average standard deviation of split frequencies of BI was 0.009223 and 0.007710 at the end of the run. ML and BI analyses resulted in almost identical

[2]http://www.biology.duke.edu/fungi/mycolab/primers.htm

[3]https://www.ncbi.nlm.nih.gov/

[4]http://mafft.cbrc.jp/alignment/server/

[5]http://treebase.org/treebase-web/home.html

TABLE 1 | Species and sequences used in the phylogenetic analyses.

Taxa	Voucher	Locality	ITS	nrLSU	References
Bjerkandera adusta	HHB-12826-Sp	United States	KP134983	KP135198	Floudas and Hibbett (2015)
B. centroamericana	L-13104-sp	Costa Rica	KY948791	KY948855	Justo et al. (2017)
Crepatura ellipsospora	CLZhao 1265	China	MK343692	MK343696	Ma and Zhao (2019)
Donkia pulcherrima	GC 1707-11	China	LC378994	LC379152	Chen et al. (2018b)
Geliporus exilisporus	Dai 2172	China	KU598211	KU598216	Yuan et al. (2017)
Hapalopilus eupatorii	Dammrich 10744	Germany	KX752620	KX752620	Miettinen et al. (2016)
H. percoctus	Miettinen 2008	Botswana	KX752597	KX752597	Miettinen et al. (2016)
H. nidulans	JV0206/2	Sweden	KX752623	KX752623	Miettinen et al. (2016)
Hyphodermella corrugata	MA-Fungi 5527	Morocco	FN600372	JN939597	Telleria et al. (2010)
H. poroides	Dai 10848	China	KX008368	KX011853	Zhao et al. (2017)
H. rosae	FP-150552	United States	KP134978	KP135223	Floudas and Hibbett (2015)
Irpex vellereus	CBS 515.92	India	AF479670	—	Lim and Jung (2003)
Odontoefibula orientalis	GC 1703-76	China	LC379004	LC379156	Chen et al. (2018b)
Oxychaete cervinogilvus	Schigel-5216	Australia	KX752596	KX752596	Miettinen et al. (2016)
Phaeophlebiopsis caribbeana	HHB-6990	United States	KP135415	KP135243	Floudas and Hibbett (2015)
P. himalayensis	He 3854	China	MT386378	MT447410	Present study
P. peniophoroides	FP-150577	United States	KP135417	KP135273	Floudas and Hibbett (2015)
P. ravenelii	CBS 411.50	France	MH856691	MH868208	Vu et al. (2019)
P. ravenelii	FCUG 2216	France	—	GQ470674	Wu et al. (2010)
Phanerina mellea	Miettinen 11393	Indonesia	KX752602	KX752602	Miettinen et al. (2016)
Phanerochaete arizonica	RLG-10248-Sp	United States	KP135170	KP135239	Floudas and Hibbett (2015)
P. australis	HHB-7105-Sp	United States	KP135081	KP135240	Floudas and Hibbett (2015)
P. bambusicola	Wu 0707-2	China	MF399404	MF399395	Wu et al. (2018b)
P. brunnea	He 1873	China	KX212220	KX212224	Liu and He (2016)
P. burtii	HHB-4618-Sp	United States	KP135117	KP135241	Floudas and Hibbett (2015)
P. canobrunnea	CHWC 1506-66	China	LC412095	LC412104	Wu et al. (2018a)
P. carnosa	HHB-9195	United States	KP135129	KP135242	Floudas and Hibbett (2015)
P. chrysosporium	HHB-6251-Sp	United States	KP135094	KP135246	Floudas and Hibbett (2015)
P. citrinosanguinea	FP-105385-Sp	United States	KP135100	KP135234	Floudas and Hibbett (2015)
P. concrescens	Spirin 7322	Russia	KP994380	KP994382	Volobuev et al. (2015)
P. cumulodentata	LE 298935	Russia	KP994359	KP994386	Volobuev et al. (2015)
P. cystidiata	Wu 1708-326	China	LC412097	LC412100	Wu et al. (2018a)
P. ericina	HHB-2288	United States	KP135167	KP135247	Floudas and Hibbett (2015)
P. incarnata	WEI 16-075	China	MF399406	MF399397	Wu et al. (2018b)
P. inflata	Dai 10376	China	JX623929	JX644062	Jia et al. (2014)
P. laevis	HHB-15519	United States	KP135149	KP135249	Floudas and Hibbett (2015)
P. livescens	FD-106	United States	KP135070	KP135253	Floudas and Hibbett (2015)
P. magnoliae	HHB-9829-Sp	United States	KP135089	KP135237	Floudas and Hibbett (2015)
P. porostereoides	He 1902	China	KX212217	KX212221	Liu and He (2016)
P. pseudomagnoliae	PP-25	South Africa	KP135091	KP135250	Floudas and Hibbett (2015)
P. pseudosanguinea	FD-244	United States	KP135098	KP135251	Floudas and Hibbett (2015)
P. rhodella	FD-18	United States	KP135187	KP135258	Floudas and Hibbett (2015)
P. robusta	Wu 1109-69	China	MF399409	MF399400	Wu et al. (2018b)
P. sanguinea	HHB-7524	United States	KP135101	KP135244	Floudas and Hibbett (2015)
P. sanguineocarnosa	FD-359	United States	KP135122	KP135245	Floudas and Hibbett (2015)
P. sordida	FD-241	United States	KP135136	KP135252	Floudas and Hibbett (2015)
P. stereoides	He 2309	China	KX212219	KX212223	Liu and He (2016)
P. subceracea	FP-105974-R	United States	KP135162	KP135255	Floudas and Hibbett (2015)
P. taiwaniana	Wu 0112-13	China	MF399412	MF399403	Wu et al. (2018b)
P. velutina	Kotiranta 25567	Russia	KP994354	KP994387	Volobuev et al. (2015)
Phlebia firma	Edman K268	Sweden	EU118654	EU118654	Larsson (2007)
P. lilascens	FCUG 2005	—	AF141622	AF141622	—
Phlebiopsis albescens	**He 5805***	**Sri Lanka**	**MT452526**	**—**	**Present study**

(Continued)

TABLE 1 | Continued

Taxa	Voucher	Locality	ITS	nrLSU	References
P. amethystea	URM 93248	Brazil	MK993644	MK993638	Xavier de Lima et al. (2020)
P. amethystea	URM 84741	Brazil	MK993645	MK993639	Xavier de Lima et al. (2020)
P. brunnea	**He 5822***	**Sri Lanka**	**MT452527**	**MT447451**	**Present study**
P. brunneocystidiata	Chen 666	China	MT561707	GQ470640	Wu et al. (2010), present study
P. brunneocystidiata	Chen 1143	China	—	GQ470639	Wu et al. (2010)
P. castanea	Spirin-5295	Russia	KX752610	KX752610	Miettinen et al. (2016)
P. castanea	GC 1612-6	China	KY688208	—	Chen et al. (2018a)
P. castanea	CLZhao 3501	China	MK269230	—	—
P. castanea	He 2489	China	—	MT447406	Present study
P. crassa group A	He 5205	Vietnam	MT452523	MT447448	Present study
P. crassa group A	He 5763	Sri Lanka	MT452524	MT447449	Present study
P. crassa group A	He 5855	China	MT452525	MT447450	Present study
P. crassa group A	He 6304	China	MT561714	MT598029	Present study
P. crassa group A	Wu 0504-22	China	MT561715	GQ470634	Wu et al. (2010), present study
P. crassa group B	He 3349	China	MT561712	MT447407	Present study
P. crassa group B	He 5866	China	MT386376	MT447408	Present study
P. crassa group B	He 6266	China	MT561713	MT598035	Present study
P. crassa group B	CLZhao 724	China	MG231790	—	—
P. crassa group B	MAFF 420737	Japan	AB809163	AB809163	—
P. crassa group C	KKN-86-Sp	United States	KP135394	KP135215	Floudas and Hibbett (2015)
P. crassa group C	FP-102496-sp	United States	AY219341	—	de Koker et al. (2003)
P. crassa group C	HHB 8834	United States	KP135393	—	Floudas and Hibbett (2015)
P. crassa group C	ME 516	United States	KP135395	—	Floudas and Hibbett (2015)
P. cylindrospora	**He 5932**	**China**	**MT386403**	**MT447444**	**Present study**
P. cylindrospora	**He 5984***	**China**	**MT386404**	**MT447445**	**Present study**
P. cylindrospora	**He 6054**	**China**	**MT561716**	**MT598030**	**Present study**
P. cylindrospora	**He 6063**	**China**	**MT561717**	**MT598031**	**Present study**
P. darjeelingensis	He 3874	China	MT386382	MT447418	Present study
P. darjeelingensis	He 5910	China	MT386383	MT447419	Present study
P. darjeelingensis	He 5913	China	MT386384	MT447420	Present study
P. darjeelingensis	Chen 1018	China	MT561709	GQ470647	Wu et al. (2010), present study
P. cf. dregeana	SFC 980804-4	Korea	AF479669	—	Lim and Jung (2003)
P. cf. dregeana	UOC-DAMIA-D46	Sri Lanka	KP734203	—	—
P. cf. dregeana	FLAS-F-60030	United States	KY654737	—	—
P. flavidoalba	FD-263	United States	KP135402	KP135271	Floudas and Hibbett (2015)
P. flavidoalba	Miettinen 17896	United States	KX752607	KX752607	Miettinen et al. (2016)
P. flavidoalba	CFMR4167	United States	KX065957	**—**	**—**
P. flavidoalba	HHB-4617	United States	KP135401	**—**	Floudas and Hibbett (2015)
P. friesii	He 5722	Sri Lanka	MT452528	MT447413	Present study
P. friesii	He 5817	Sri Lanka	MT452529	MT447414	Present study
P. friesii	He 5820	Sri Lanka	MT452530	MT447415	Present study
P. gigantea	He 5290	China	MT386381	MT447416	Present study
P. gigantea	Miettinen 15354	Finland	KX752605	**—**	Miettinen et al. (2016)
P. gigantea	CBS 935.70	Germany	MH860011	MH871798	Vu et al. (2019)
P. gigantea	FP-70857-Sp	United States	KP135390	KP135272	Floudas and Hibbett (2015)
P. griseofuscescens	He 5734	Sri Lanka	MT561708	MT598032	Present study
P. griseofuscescens	Cui 12629	China	MT561718	—	Present study
P. griseofuscescens	CLZhao 3692	China	MT180946	MT180950	Xu et al. (2020)
P. griseofuscescens	CLZhao 3705	China	MT180947	MT180951	Xu et al. (2020)
P. laxa	Wu 9311-17	China	MT561710	GQ470649	Wu et al. (2010), present study
P. magnicystidiata	**He 5648***	**China**	**MT386377**	**MT447409**	**Present study**
P. magnicystidiata	**He 20140719_18**	**China**	**MT561719**	—	**Present study**
P. magnicystidiata	**Wu 890805-1**	**China**	**MT561711**	**GQ470667**	Wu et al. (2010)**, present study**

(Continued)

TABLE 1 | Continued

Taxa	Voucher	Locality	ITS	nrLSU	References
P. membranacea	**He 3842**	**China**	**MT386400**	**MT447440**	**Present study**
P. membranacea	**He 3849***	**China**	**MT386401**	**MT447441**	**Present study**
P. membranacea	**He 6062**	**China**	**MT386402**	**MT447442**	**Present study**
P. pilatii	He 5114	China	MT386385	MT447421	Present study
P. pilatii	He 5165	China	MT386386	MT447422	Present study
P. pilatii	Dai 17041	China	KY971603	KY971604	Wu et al. (2017)
P. pilatii	Spirin 5048	Russia	KX752590	KX752590	Miettinen et al. (2016)
P. sinensis	**He 4295**	**China**	**MT386395**	**MT447433**	**Present study**
P. sinensis	**He 4665**	**China**	**MT386396**	**MT447434**	**Present study**
P. sinensis	**He 4673***	**China**	**MT386397**	**MT447435**	**Present study**
P. sinensis	**He 5662**	**China**	**MT386398**	**MT447436**	**Present study**
P. sp.	FP-102937	United States	KP135391	KP135270	Floudas and Hibbett (2015)
P. sp.	ECS1971	United States	KP135392	—	Floudas and Hibbett (2015)
P. sp.	He 3827	China	—	MT447437	Present study
P. yunnanensis	He 2623	China	MT386387	MT447423	Present study
P. yunnanensis	He 3249	China	MT386375	MT447425	Present study
P. yunnanensis	CLZhao 3958	China	MH744140	MH744142	Zhao et al. (2018)
P. yunnanensis	CLZhao 3990	China	MH744141	MH744143	Zhao et al. (2018)
Pirex concentricus	OSC-41587	United States	KP134984	KP135275	Floudas and Hibbett (2015)
Porostereum fulvum	LY: 18496	France	MG649453	MG649455	—
P. spadiceum	CBS 474.48	France	MH856438	MH867984	Vu et al. (2019)
Rhizochaete americana	FP-102188	United States	KP135409	KP135277	Floudas and Hibbett (2015)
R. belizensis	FP-150712	Belize	KP135408	KP135280	Floudas and Hibbett (2015)
R. brunnea	MR 229	Argentina	AY219389	AY219389	Greslebin et al. (2004)
R. violascens	KHL 11169	Norway	EU118612	EU118612	Larsson (2007)
R. filamentosa	HHB-3169-Sp	United States	KP135410	KP135278	Floudas and Hibbett (2015)
R. flava	PR 1141	Puerto Rico	KY273030	KY273033	Nakasone et al. (2017)
R. fouqueriae	KKN-121-sp	United States	KY948786	KY948858	Justo et al. (2017)
R. radicata	FD-123	United States	KP135407	KP135279	Floudas and Hibbett (2015)
R. sulphurina	HHB-5604	United States	KY273031	GU187610	Binder et al. (2010)
R. sulphurosa	URM 87190	Brazil	KT003522	KT003519	Chikowski et al. (2015)
Riopa metamorphosa	Spirin 2395	Russia	KX752601	KX752601	Miettinen et al. (2016)
R. pudens	Cui 3238	China	JX623931	JX644060	Jia et al. (2014)
Terana caerulea	FP-104073	United States	KP134980	KP135276	Floudas and Hibbett (2015)
Outgroup					
Ceraceomyces serpens	HHB-15692-Sp	United States	KP135031	KP135200	Floudas and Hibbett (2015)
Phlebia acerina	FD-301	United States	KP135378	KP135260	Floudas and Hibbett (2015)

New species are set in bold with type specimens indicated with an asterisk (*).

tree topologies compared to the MP analysis. The MP trees are shown in **Figures 1**, **2** with the parsimony bootstrap values (≥50%, first), Bayesian posterior probabilities (≥0.95, second) and likelihood bootstrap values (≥50%, third) labeled along the branches.

In the Phanerochaetaceae ITS-LSU tree (**Figure 1**), *Phlebiopsis*, *Phaeophlebiopsis*, *Hapalopilus*, and *Rhizochaete* formed a strongly supported clade (98/1/100). Within this clade, the *Phlebiopsis* species clustered together with relatively strong support values (69/1/98), and species of *Phaeophlebiopsis*, *Hapalopilus* and *Rhizochaete* were in the sister subclades. In the *Phlebiopsis* ITS tree (**Figure 2**), 24 lineages were resolved including 21 taxa of *Phlebiopsis* and '*Irpex vellereus*.' Samples of *P. crassa* were distributed in three distinct lineages. The six new species, *P. albescens*, *P. brunnea*, *P. cylindrospora*, *P. magnicystidiata*, *P. membranacea* and *P. sinensis*, formed distinct lineages.

Taxonomy

Phlebiopsis albescens Y.N. Zhao & S.H. He, sp. nov.

MycoBank: MB836023

Type – Sri Lanka, Avissawella, Salgala Forest, on fallen angiosperm twig, 3 March 2019, He 5805 (BJFC 030672, holotype; isotype in BJM).

Etymology – Refers to the white basidiomata.

Fruiting body – Basidiomata annual, resupinate, widely effused, closely adnate, inseparable from substrate,

ceraceous to crustose, first as small patches, later confluent up to 15 cm long, 1 cm wide, up to 80 μm thick in section. Hymenophore smooth, white (6A1), orange white (6A2) to pale orange (6A3), unchanged in KOH, not cracking on drying; margin indistinct, concolorous with hymenophore. Context white.

Microscopic structures – Hyphal system monomitic; generative hyphae simple-septate. Subiculum indistinct to

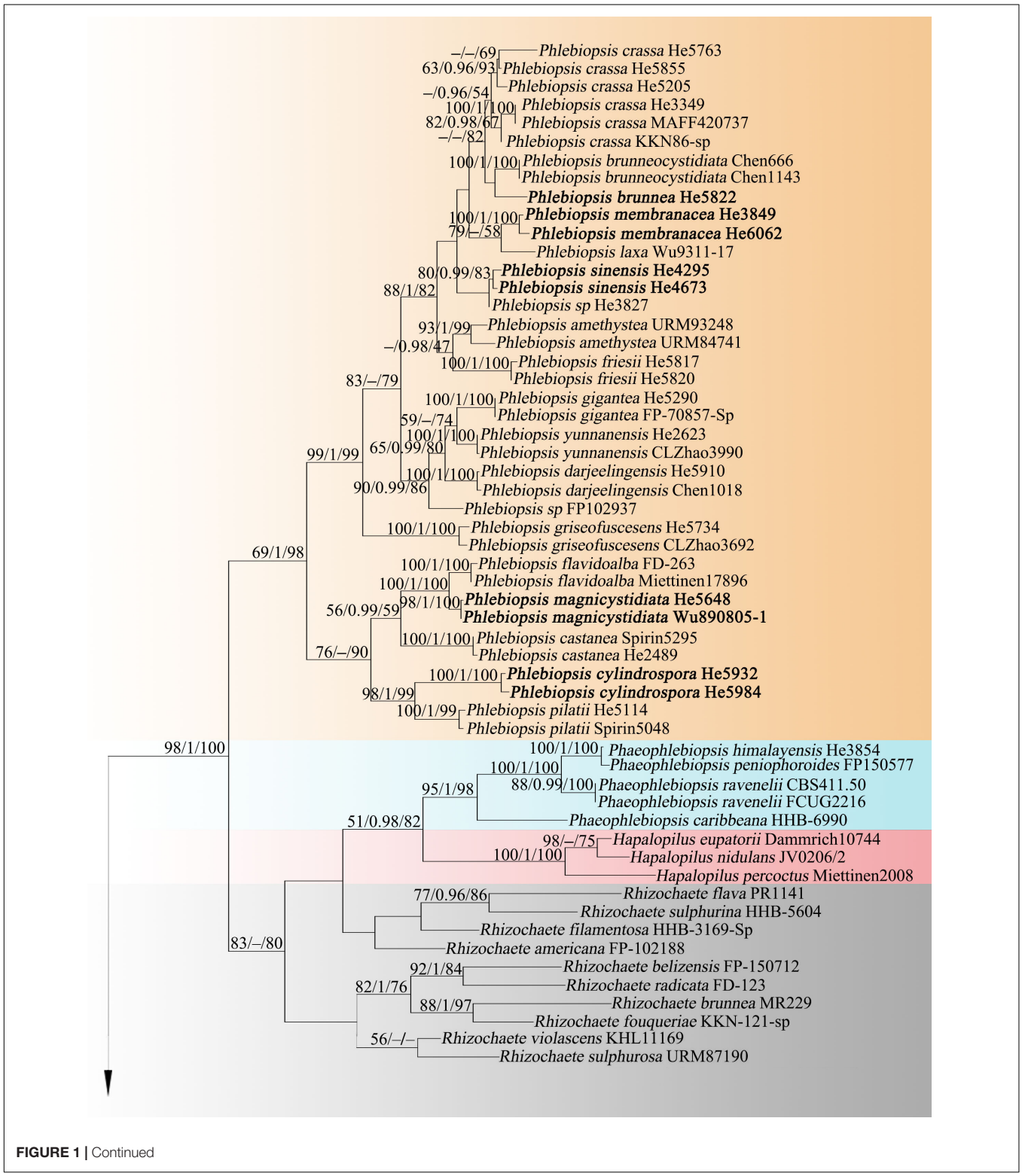


FIGURE 1 | Continued

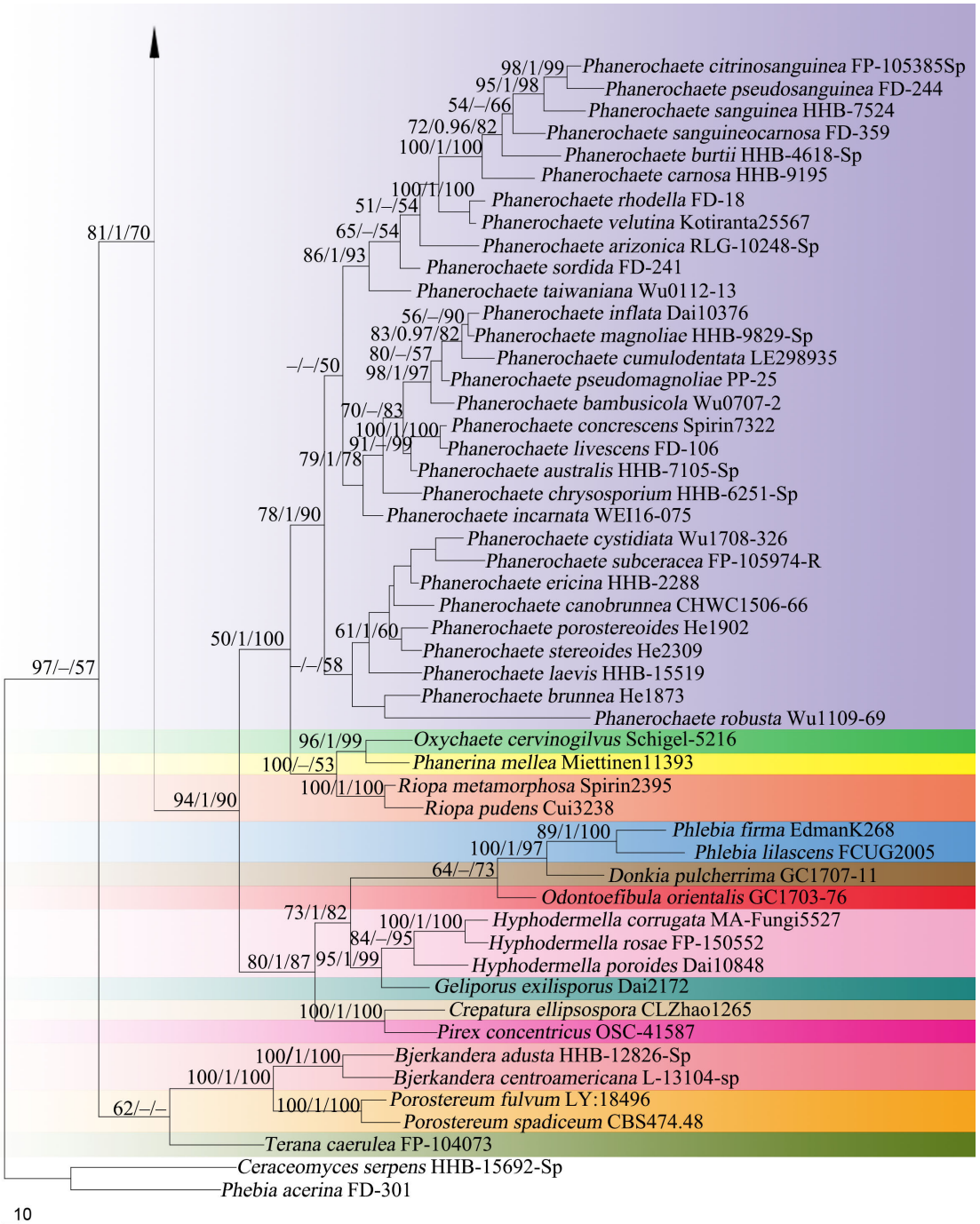


FIGURE 1 | Phylogenetic tree from maximum parsimony analysis from the concatenated ITS and nrLSU sequences of Phanerochaetaceae taxa. Branches are labeled with parsimony bootstrap values (≥50%, first), Bayesian posterior probabilities (≥0.95, second) and likelihood bootstrap values (≥50%, third). New species are set in bold.

absent. Subhymenium well developed; hyphae colorless, thin- to slightly thick-walled, tightly agglutinated, 2.5–4 μm in diam. Lamprocystidia abundant, conical, colorless to pale yellow, thick-walled, heavily encrusted with crystals along entire length, embedded or slightly projecting beyond hymenium, with one or two secondary septa, with a basal simple septum, 25–40 × 8–12 μm (without encrustations). Basidia clavate to cylindrical, colorless, thin-walled, with a basal simple septum and four sterigmata, 10–16 × 3–4.5 μm; basidioles numerous, similar to basidia but slightly smaller. Basidiospores oblong ellipsoid

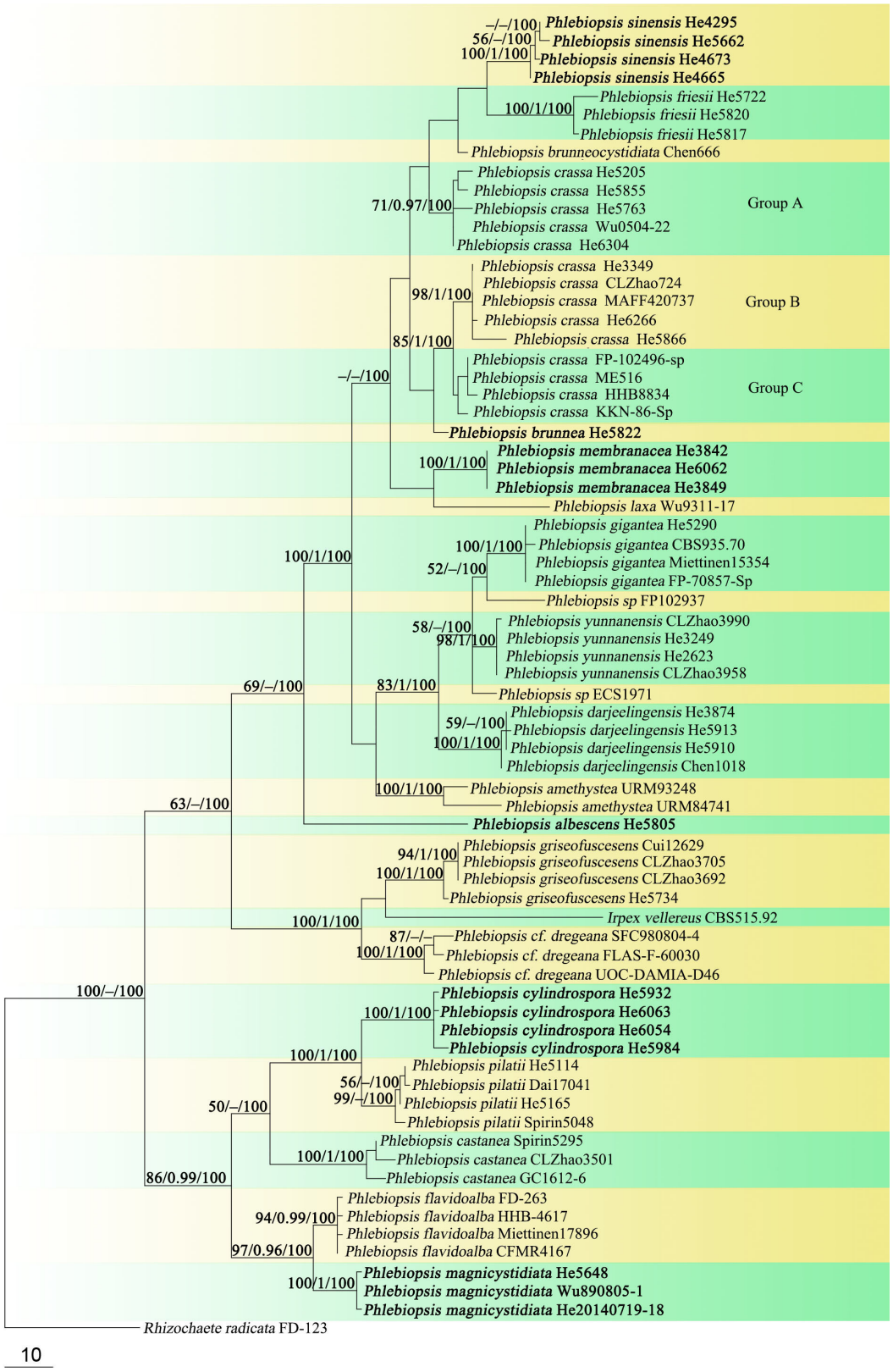


FIGURE 2 | Phylogenetic tree obtained from maximum parsimony analysis of ITS sequence data of *Phlebiopsis*. Branches are labeled with parsimony bootstrap values (≥50%, first), Bayesian posterior probabilities (≥0.95, second) and likelihood bootstrap values (≥50%, third). New species are set in bold.

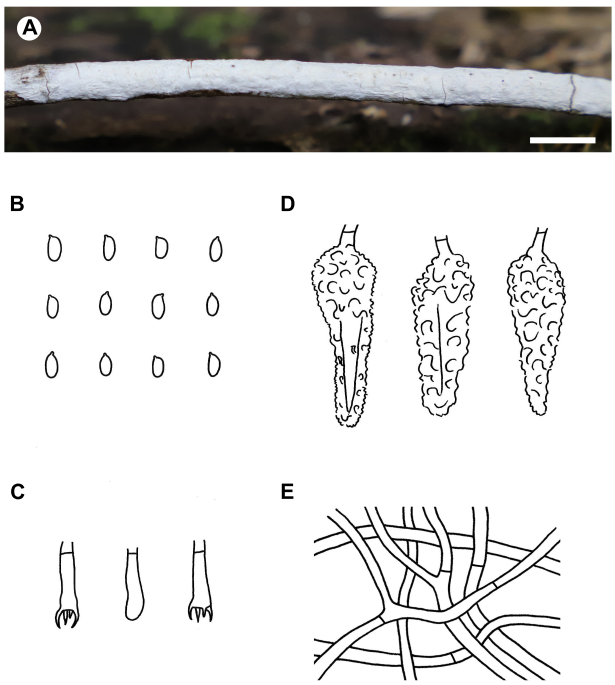


FIGURE 3 | *Phlebiopsis albescens* [from the holotype He 5805; scale bars: **A** = 1 cm, **B–E** = 10 μm]. **(A)** Basidiomata; **(B)** basidiospores; **(C)** basidia; **(D)** basidioles; **(E)** lamprocystidia.

to short cylindrical, colorless, thin-walled, smooth, IKI–, CB–, 3.5–5 × 2–2.2 (–2.5) μm, L = 4.4 μm, W = 2.1 μm, Q = 2.1 (n = 30/1).

Distribution – Sri Lanka.

Notes – *Phlebiopsis albescens* (**Figure 3**) is characterized by thin, white to pale orange basidiomata, an indistinct subiculum, short lamprocystidia (<40 μm long) and basidia (<16 μm long), and small basidiospores (<5 μm long). *Phlebiopsis punjabensis* G. Kaur, Avn.P. Singh & Dhingra, from India, also has thin, white basidomata and short lamprocystidia, 20–36 × 7–9.8 μm, but larger basidiospores, 5.3–8.5 × 2.5–4 μm (Kaur et al., 2015). Another species with short basidiospores, *P. yunnanensis* C.L. Zhao, from southern China, has thicker basidiomata, 100–500 μm thick, with a smooth to odontoid hymenophore, and ellipsoid basidiospores, 2.5–3.5 μm wide (Zhao et al., 2018). In the ITS phylogenetic tree (**Figure 2**), *P. albescens* formed its lineage and was not closely related to any other species for current sequences.

Phlebiopsis brunnea Y.N. Zhao & S.H. He, sp. nov.

MycoBank: MB836024

Type – Sri Lanka, Western Province, Mitirigala Nissarana Vanaya Forest Monastery, on fallen angiosperm branch, 4 March 2019, He 5822 (BJFC 030689, holotype; isotype in BJM).

Etymology – Refers to the brown context of basidiomata.

Fruiting body – Basidiomata annual, resupinate, widely effused, closely adnate, inseparable from substrate, coriaceous, developing as small patches then confluent, up to 20 cm long, 5 cm wide, up to 350 μm thick in section. Hymenophore smooth, brownish gray (6C2–6D2), brownish orange (6C3) to grayish brown (6D3), unchanged in KOH, not cracking on drying; margin thinning out, indistinct, concolorous or darker than hymenophore. Context pale brown.

Microscopic structures – Hyphal system pseudodimitic; generative hyphae simple-septate. Subiculum well-developed, a non-agglutinated, loosely interwoven tissue; skeletocystidia (skeletal hyphae) brown, distinctly thick-walled, slightly encrusted, up to 120 μm long, 14 μm wide; hyphae colorless to pale yellowish brown, thick-walled, smooth, moderately branched at right angles, frequently septate, 2–5 μm in diam. Subhymenium thin; skeletocystidia as in subiculum but shorter and more heavily encrusted; generative hyphae colorless, thin- to thick-walled, moderately branched, frequently septate, loosely interwoven, 2–4.5 μm in diam. Lamprocystidia subulate to fusiform, colorless, thin- to thick-walled, distal end encrusted with small crystals, projecting up to 30 μm beyond hymenium, with an obtuse or acute tip, with a basal simple septum, 35–65 × 7–12 μm. Basidia clavate to subcylindrical, colorless, thin-walled, with a basal simple septum and four sterigmata, 20–33 × 4.5–6 μm; basidioles numerous, similar to basidia but slightly smaller. Basidiospores oblong ellipsoid to subcylindrical, colorless, thin-walled, smooth, IKI–, CB–, 6.5–7.5 (–8) × 3–3.6 (–4) μm, L = 7.3 μm, W = 3.3 μm, Q = 2.2 (n = 30/1).

Distribution – Sri Lanka.

Notes – *Phlebiopsis brunnea* (**Figure 4**) is characterized by a coriaceous basidiomata with a smooth hymenophore and brown context, abundant, brown skeletocystidia in the subiculum and subhymenium, lamprocystidia, and oblong ellipsoid to subcylindrical basidiospores. *Hjortstamia bambusicola* (Berk. & Broome) Hjortstam & Ryvarden is similar with its grayish brown hymenophore and pseudodimitic hyphal system with brown skeletocystidia but with narrower basidiospores (2.5–3 μm wide) and grows on bamboo in Australia (Hjortstam and Ryvarden, 2005). *Phlebiopsis brunneocystidiata* (Sheng H. Wu) Miettinen has narrower lamprocystidia (5–8 μm wide) with brown walls and a host preference for Pandanaceae in Taiwan (Wu, 2004). Another similar species, *P. crassa* differs from *P. brunnea* by having effused-reflexed basidiomata with a more or less purple hymenophore and larger lamprocystidia, 50–120 × 8–20 μm (Burdsall, 1985; Hjortstam and Ryvarden, 1990). *Phlebiopsis brunnea* formed weakly supported sister lineages to *P. brunneocystidiata* or *P. crassa* group B and C in the ITS-LSU and ITS trees, respectively (**Figures 1**, **2**).

Phlebiopsis cylindrospora Y.N. Zhao & S.H. He, sp. nov.

MycoBank: MB836025

Type – China, Hainan Province, Lingshui County, Diaoluoshan Nature Reserve, on dead, small diameter bamboo, 2 July 2019, He 5984 (BJFC 030860, holotype; isotype in BJM).

Etymology – Refers to the cylindrical basidiospores.

Fruiting body – Basidiomata annual, resupinate, widely effused, closely adnate, inseparable from substrate, coriaceous, first as small patches, later confluent up to 20 cm long, 4 cm

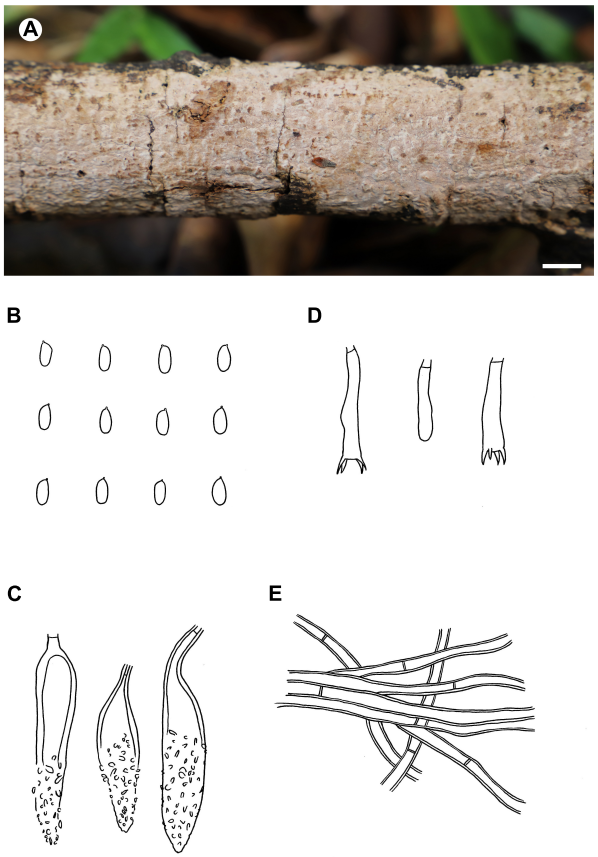


FIGURE 4 | *Phlebiopsis brunnea* (from the holotype He 5822; scale bars: **A** = 1 cm, **B–E** = 10 μm). **(A)** Basidiomata; **(B)** basidiospores; **(C)** lamprocystidia; **(D)** basidia and basidiole; **(E)** hyphae from subiculum.

wide, up to 150 μm thick in section. Hymenophore smooth, orange white (6A2), orange gray (6B2) to grayish orange (6B3), turning purple in KOH, not cracking on drying; margin thinning out, indistinct, slightly fimbriate, paler than or concolorous with hymenophore. Context gray.

Microscopic structures – Hyphal system monomitic; generative hyphae simple-septate. Subiculum distinct, a somewhat agglutinated, compact tissue, arranged more or less parallel to substrate; hyphae colorless, thick-walled, encrusted with yellow, resinous granules, infrequently branched, moderately septate, 2–4.5 μm in diam. Subhymenium indistinct; hyphae thin- to slightly thick-walled, heavily encrusted with yellow, resinous granules, frequently septate, more or less agglutinated, 2–4 μm in diam. Lamprocystidia numerous, subfusiform, colorless, thick-walled, apically encrusted with small crystals, embedded or slightly projecting beyond hymenium, 20–36 (–40) × 5–9 μm. Basidia clavate to subcylindrical, colorless, thin-walled, with a basal simple septum and four sterigmata, 12–16 × 4–5 μm; basidioles numerous, similar to basidia but slightly smaller. Basidiospores cylindrical, colorless, thin-walled, smooth, IKI–, CB–, (5–) 5.5–7.5 (–8) × 1.8–2.8 (–3) μm, L = 5.9 μm, W = 2.2 μm, Q = 2.4–3.1 (n = 90/3).

Additional specimens examined – China, Hainan Province, Qiongzhong County, Limushan Nature Reserve, on fallen angiosperm twig, 8 June 2016, He 3831 (BJFC 022333); on dead, small diameter bamboo, 8 June 2016, He 3882 (BJFC 022384, CFMR); Wuzhishan County, Wuzhishan Nature Reserve, on dead, small diameter bamboo, 10 June 2016, He 3926 (BJFC 022428); 30 June 2019, He 5922 (BJFC 030797), He 5932 (BJFC 030807), He 5936 (BJFC 030811) & He 5938 (BJFC 030813); Lingshui County, Diaoluoshan Nature Reserve, on dead, small diameter bamboo, 2 July 2019, He 5981 (BJFC 030857); 5 July 2019, He 6054 (BJFC 030930), He 6061 (BJFC 030937) & He 6063 (BJFC 030939); on fallen angiosperm branch, 5 July 2019, He 6038 (BJFC 030914). Thailand, Chiang Rai, Doi Pui, on rotten bamboo, 23 July 2016, He 4080 (BJFC 023521), He 4083 (BJFC 023524) & He 4094 (BJFC 023535, CFMR).

Distribution – China and Thailand.

Notes – *Phlebiopsis cylindrospora* (**Figure 5**) is characterized by pale-colored, smooth hymenophore that turns purple in KOH, a monomitic hyphal system with generative hyphae encrusted with yellow, resinous granules, small subfusiform lamprocystidia, cylindrical basidiospores, and habit on bamboo and woody angiosperms. It is similar to *P. punjabensis* that also has a pale-colored, smooth hymenophore and short lamprocystidia, but the latter species does not react with KOH and develops longer basidia (14–26 μm long), and slightly larger basidiospores (5.3–8.5 × 2.5–4 μm, Kaur et al., 2015). *Phlebiopsis albescens* differs from *P. cylindrospora* by its white hymenophore that

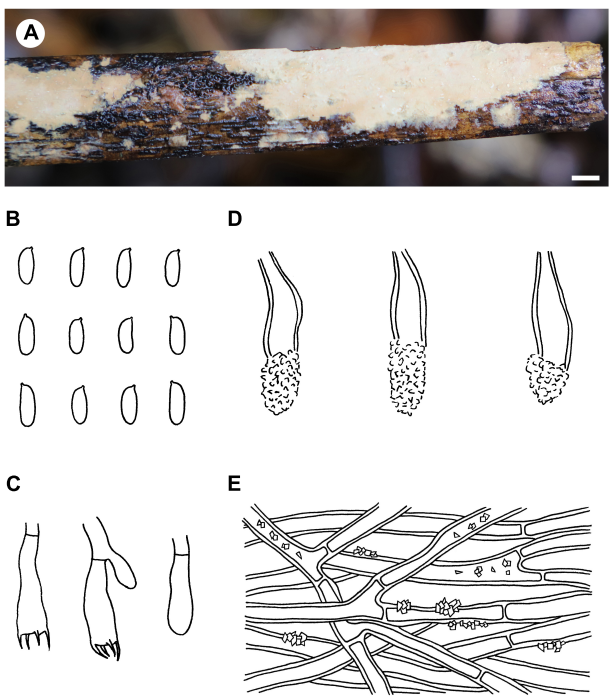


FIGURE 5 | *Phlebiopsis cylindrospora* (from the holotype He 5984; scale bars: **A** = 1 cm, **B–E** = 10 μm). **(A)** Basidiomata; **(B)** basidiospores; **(C)** basidia and basidiole; **(D)** lamprocystidia; **(E)** hyphae from subiculum.

is unchanged in KOH and distinctly smaller basidiospores (3.5–5 × 2–2.2 μm). The hymenophore in *P. friesii* (Lév.) Spirin & Miettinen turns purple in KOH also but is distinct from *P. cylindrospora* by having effused-reflexed basidiomata, a pseudodimitic hyphal system, and larger lamprocystidia, up to 80 × 20 μm (Hjortstam and Ryvarden, 1990). Although the phylogenetic trees (**Figures 1**, **2**) show that *P. cylindrospora* and *P. pilatii* are closely related, the latter species is distinct morphologically for it lacks lamprocystidia and develops finely branched dendrohyphidia and larger basidiospores, 8–10 × 4–4.5 μm (Parmasto, 1965; Larsen and Gilberston, 1977; Duhem and Michel, 2009).

Phlebiopsis magnicystidiata Y.N. Zhao & S.H. He, sp. nov.

MycoBank: MB836026

Type – China, Hunan Province, Guzhang County, Gaowangjie Nature Reserve, on dead angiosperm branch, 4 August 2018, He 5648 (BJFC 026710, holotype; isotype in BJM).

Etymology – Refers to the large lamprocystidia.

Fruiting body – Basidiomata annual, resupinate, widely effused, closely adnate, inseparable from substrate, ceraceous to coriaceous, up to 15 cm long, 5 cm wide, up to 400 μm thick in section. Hymenophore smooth to slightly odontoid with scattered tubercles, pruinose from projecting cystidia, grayish orange [6B(3–5)], brownish orange [6C(3–5)] to light brown [6D(4–6)], unchanged in KOH, sometimes sparsely and deeply cracked with age; margin thinning out, indistinct, concolorous with hymenophore. Context white.

Microscopic structures – Hyphal system monomitic; generative hyphae simple-septate. Subiculum indistinct to absent. Subhymenium thickening, well-developed; hyphae colorless, thin- to slightly thick-walled, frequently septate, slightly agglutinated, vertically arranged, 2–4.5 μm in diam. Lamprocystidia numerous, fusiform to subulate, colorless, thick-walled, heavily encrusted with crystals, embedded or projecting beyond hymenium up to 40 μm, with a basal simple septum, apex subacute, 40–80 × (7–) 9–13 (–15) μm (without encrustations). Basidia clavate, colorless, thin-walled, with a basal simple septum and four sterigmata, 20–30 × 5–6 μm; basidioles numerous, similar to basidia but slightly smaller. Basidiospores broadly ellipsoid to subglobose, colorless, thin-walled, smooth, IKI–, CB–, 4.5–6.5 (–6.8) × (3.5–) 3.8–4.8 μm, L = 5.6 μm, W = 4.3 μm, Q = 1.3–1.4 (n = 60/2).

Additional specimens examined – China, Yunnan Province, Mengla County, Wangtianshu Forest Park, on fallen angiosperm branch, 19 July 2014, He 20140719-18 (BJFC 019145); Taiwan Province, Taichung, Tunghai University, on dead branch of *Cassia siamea*, 5 August 1989, Wu 890805-1 (TNM F0022186).

Distribution – Hunan, Yunnan, and Taiwan Provinces in southern China.

Notes – *Phlebiopsis magnicystidiata* (**Figure 6**) is characterized by large lamprocystidia and broadly ellipsoid to subglobose basidiospores. It is morphologically similar to and phylogenetically closely related to *P. flavidoalba* (Cooke) Hjortstam (**Figures 1**, **2**) that has smooth hymenophore, slightly longer ellipsoid basidiospores (6–7.5 μm long) and a distribution

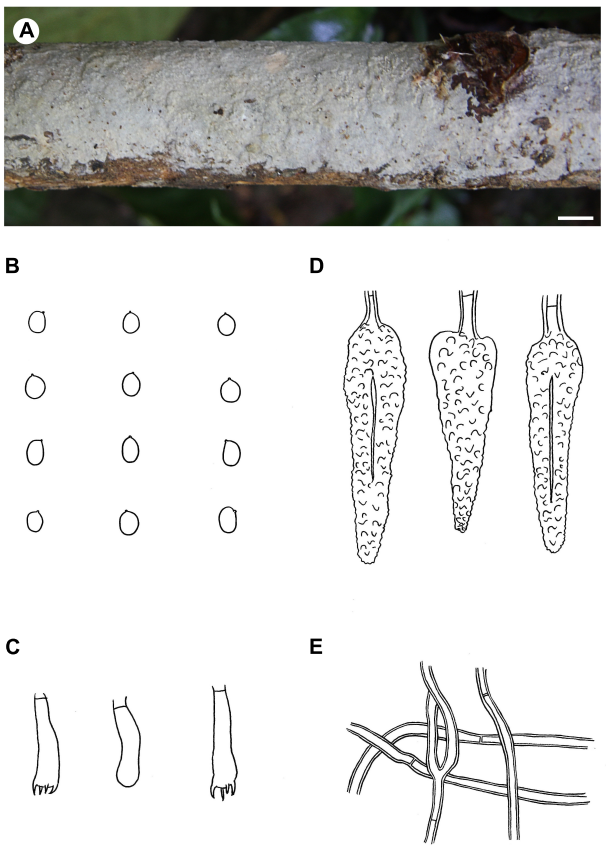


FIGURE 6 | *Phlebiopsis magnicystidiata* (**A** from He 20140719-18, **B–E** from the holotype He 5648; scale bars: **A** = 1 cm, **B–E** = 10 μm). **(A)** Basidiomata; **(B)** basidiospores; **(C)** basidia and basidiole; **(D)** lamprocystidia; **(E)** hyphae from subiculum.

in North and South America (Burdsall, 1985; Gilbertson and Blackwell, 1985). *Phlebiopsis gigantea* and *P. magnicystidiata* have similar lamprocystidia but the former differs in its well-developed subiculum, narrowly ellipsoid basidiospores, 5–7 × 2.5–3.5 μm, and often occurs on gymnospermous wood in the North Hemisphere (Eriksson et al., 1981; Bernicchia and Gorjón, 2010). Except for developing a distinct subiculum, *P. darjeelingensis* and *P. magnicystidiata* have similar sized lamprocystidia, basidia, and basidiospores (Dhingra, 1987). Reports of *P. flavidoalba* from India (Rattan, 1977) and Taiwan (Wu, 1990) need to be confirmed for they may be *P. magnicystidiata* instead.

Phlebiopsis membranacea Y.N. Zhao & S.H. He, sp. nov.

MycoBank: MB836027

Type – China, Hainan Province, Qiongzhong County, Limushan Nature Reserve, on dead, small diameter bamboo, 8 June 2016, He 3849 (BJFC 022351, holotype; isotype in BJM).

Etymology – Refers to the membranaceous basidiomata.

Fruiting body – Basidiomata annual, resupinate, widely effused, adnate, separable from substrate, membranaceous, up to 20 cm long, 5 cm wide, up to 250 μm thick in

section. Hymenophore smooth, orange white (6A2), orange gray (6B2), grayish orange [6B(3–5)] to brownish orange [6C(3–5)], unchanged in KOH, sometimes sparsely and finely cracked with age; margin thinning out, fimbriate, concolorous with hymenophore. Context gray.

Microscopic structures – Hyphal system pseudodimitic; generative hyphae simple-septate. Subiculum well-developed, a non-agglutinated, loosely interwoven tissue; skeletocystidia abundant, fusiform to clavate, brown, thick-walled, smooth, with an acute or obtuse apex, embedded, (30–) 40–70 × 8–15 μm; hyphae colorless, moderately to distinctly thick-walled, smooth, rigid, frequently branched at right angles, frequently septate, 3–5 μm in diam. Subhymenium thin; hyphae colorless, thin-walled, smooth, somewhat agglutinated, interwoven, 2–4.5 μm in diam. Hymenial cystidia scattered, similar to skeletocystidia in shape and size but with paler, thinner walls, and sparse encrustations at apex. Basidia clavate, colorless, thin-walled, with a basal simple septum and four sterigmata, 15–22 × 4–5 μm; basidioles numerous, similar to basidia but slightly smaller. Basidiospores oblong ellipsoid to subcylindrical, colorless, thin-walled, smooth, IKI–, CB–, 4.2–6.2 (–6.8) × 2–3 (–3.2) μm, L = 5.5 μm, W = 2.6 μm, Q = 1.9–2.3 (n = 90/3).

Additional specimens examined – China, Hainan Province, Qiongzhong County, Limushan Nature Reserve, on dead, small diameter bamboo, 8 June 2016, He 3842 (BJFC 022344); Lingshui County, Diaoluoshan Nature Reserve, on dead, small diameter bamboo, 5 July 2019, He 6062 (BJFC 030938).

Distribution – Hainan Province, southern tropical China.

Notes – *Phlebiopsis membranacea* (**Figure 7**) is characterized by membranaceous basidiomata with well-developed subicula, brown, smooth, thick-walled skeletocystidia, without lamprocystidia, and habit on bamboo in tropical China. Like *P. membranacea*, *Hjortstamia novae-granatae* (A.L. Welden) Hjortstam & Ryvarden, from Columbia, grows on bamboo but its brown, smooth skeletocystidia are tubular in shape and its basidiospores are larger, 5.5–7 × 3–4 μm (Hjortstam and Ryvarden, 1990). *Phlebiopsis laxa* (Sheng H. Wu) Miettinen like *P. membranacea* has membranaceous basidiomata and loosely arranged subicular hyphae but differs in having lamprocystidia and larger basidiospores, 8–10 × 4–5 μm (Wu, 2000). In the phylogenetic trees (**Figures 1**, **2**), *P. membranacea* is sister to *P. laxa*, though their relationship is not strongly supported.

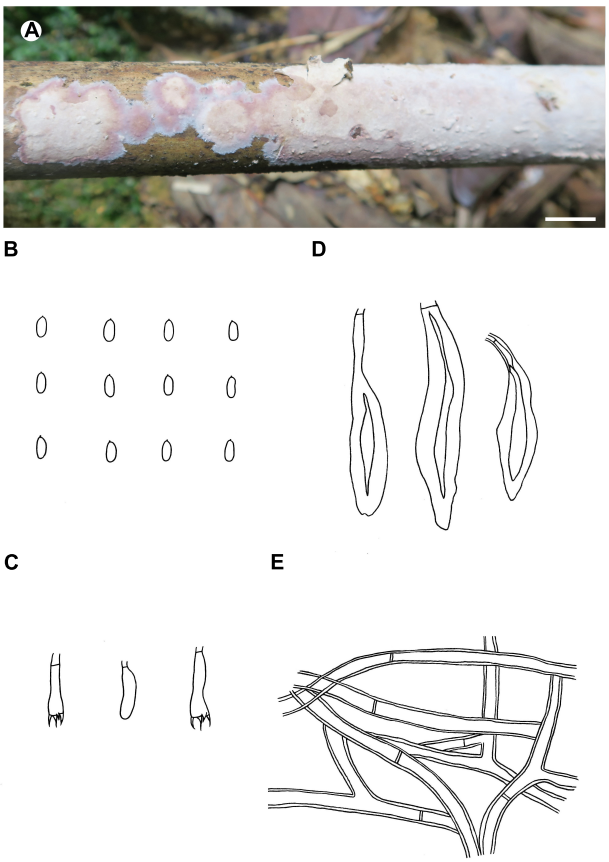


FIGURE 7 | *Phlebiopsis membranacea* (**A** from He 3842, **B–E** from the holotype He 3849; scale bars: **A** = 1 cm, **B–E** = 10 μm). **(A)** Basidiomata; **(B)** basidiospores; **(C)** basidia and basidiole; **(D)** hymenial cystidia; **(E)** hyphae from subiculum.

Phlebiopsis sinensis Y.N. Zhao & S.H. He, sp. nov.

MycoBank: MB836028

Type – China, Sichuan Province, Wanyuan County, Huaeshan Nature Reserve, on fallen angiosperm branch, 17 July 2013, He 4673 (BJFC 024192, holotype; isotype in BJM).

Etymology – Refers to the distribution in China.

Fruiting body – Basidiomata annual, resupinate to effused-reflexed with reflexed edges elevated and incurved with age, loosely adnate, easily detached from substrate, coriaceous, first as small patches, later confluent up to 15 cm long, 5 cm wide, up to 300 μm thick in section. Pileus projecting up to 1.5 mm; upper surface gray, slightly sulcate. Hymenophore smooth, brownish orange [6C(3–5)], grayish brown [6(D–F)3] to brown [6E(4–6)], unchanged in KOH, sometimes finely cracked with age; margin thinning out, distinct, white to gray, silky, slightly fimbriate, up to 1 mm wide. Context gray to yellowish brown.

Microscopic structures – Hyphal system pseudodimitic; generative hyphae simple-septate. Tomentum and cortex (a dark line between the tomentum and subiculum) present. Subiculum well-developed, a non-agglutinated tissue; skeletocystidia brown, thick-walled, encrusted at apex, embedded, intermediate forms between skeletocystidia and lamprocystidia observed; hyphae colorless to pale yellow, moderately to distinctly thick-walled, smooth, rarely branched, moderately septate, easily separated, more or less parallel to substrate, 3–6 μm in diam. Subhymenium indistinct. Lamprocystidia abundant, broadly fusiform to broadly subulate, usually with a long, curved stalk and resembling skeletocystidia, colorless to brown, thick-walled, heavily encrusted, 30–60 × 8–13 μm, projecting up to 30 μm. Basidia clavate, colorless, thin-walled, with a basal simple septum and four sterigmata, 20–30 × 4.5–5.5 μm; basidioles numerous, similar to basidia but slightly smaller. Basidiospores oblong ellipsoid to subcylindrical, colorless, thin-walled, smooth, IKI–,

CB–, (5–) 5.8–7.8 (–8) × (2.2–) 2.5–3.5 (–3.8) μm, L = 6.4 μm, W = 2.9 μm, Q = 2.1–2.4 (n = 90/3).

Additional specimens examined – China, Gansu Province, Pingliang County, Kongtongshan Nature Reserve, on construction wood, 3 August 2015, He 2416 (BJFC 020870, CFMR); Hubei Province, Wufeng County, Houhe Nature Reserve, on dead angiosperm branch, 16 August 2017, He 5081 (BJFC 024599); Hunan Province, Yongshun County, Xiaoxi Nature Reserve, on dead angiosperm branch, 6 August 2018, He 5662 (BJFC 026724); Inner Mongolia, Chifeng, Aohan County, Daheishan Nature Reserve, on fallen *Quercus mongolia* branch, 3 September 2015, Tiezhi Liu et al. (CFSZ 10714), on fallen *Pinus tabuliformis* branch, 19 September 2016, Tiezhi Liu et al. (CFSZ 12436); Jiangxi Province, Ji'an County, Jinggangshan Nature Reserve, on dead *Rhododendron* branch, 11 August 2016, He 4295 (BJFC 023737, CFMR); Liaoning Province, Zhuanghe County, Xianrendong Forest Park, on dead *Quercus* branch, 5 August 2017, He 4665 (BJFC 024184); Shaanxi Province, Foping County, Foping Nature Reserve, on fallen *Betula* branch, 11 September 2013, He 1907 (BJFC 016374); Sichuan Province, Baoxing County, Fengtongzhai Nature Reserve, on fallen angiosperm trunk, 18 September 2012, He 20120918-3 (BJFC 014609).

Distribution – Gansu, Hubei, Hunan, Jiangxi, Liaoning, Shaanxi and Sichuan Provinces and Inner Mongolia Autonomous Region of China.

Notes – *Phlebiopsis sinensis* (**Figure 8**) is characterized by effused to effused-reflexed, coriaceous basidiomata with well-developed subicula, brown skeletocystidia, lamprocystidia, and a temperate distribution. Submembranaceous-pellicular basidiomata, narrower cystidia (5–8 μm wide), and a tropical distribution distinguish *P. brunneocystidiata* from *P. sinensis* (Wu, 2004). Both *P. crassa* and *P. sinensis* develop effused-reflexed basidiomata, but the former species has a purple-tinted hymenophore, larger lamprocystidia, 50–120 × 8–20 μm, and a tropical distribution (Hjortstam and Ryvarden, 1990). Although the ITS tree (**Figure 2**) shows that *P. sinensis* and *P. friesii* are sister taxa, *P. friesii* is distinct morphologically with a hymenophore that turns purple in KOH and has a dimitic hyphal system with colorless to yellow skeletal hyphae (Hjortstam and Ryvarden, 1990).

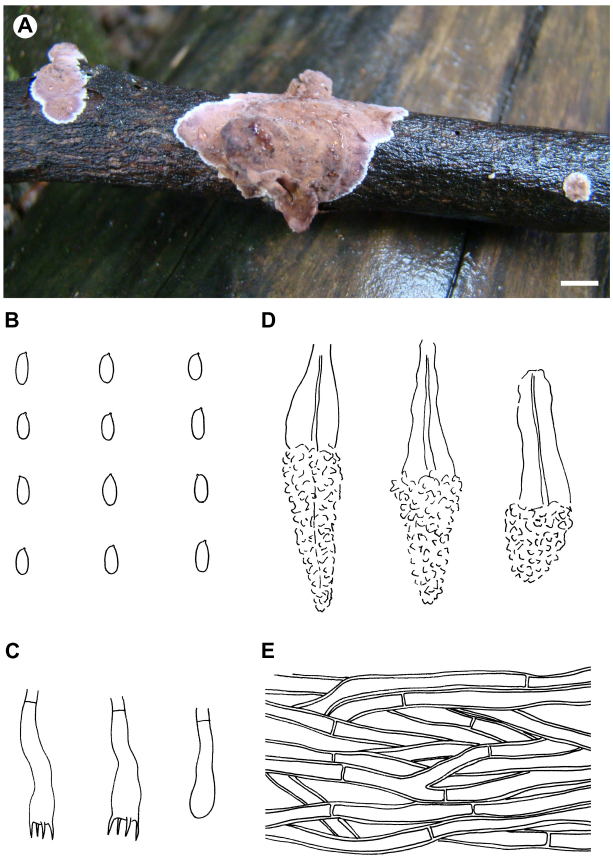


FIGURE 8 | *Phlebiopsis sinensis* (from He 4673; scale bars: **A** = 1 cm, **B–E** = 10 μm). **(A)** Basidiomata; **(B)** basidiospores; **(C)** basidia and basidiole; **(D)** lamprocystidia; **(E)** hyphae from subiculum.

Phaeophlebiopsis mussooriensis (Priyanka, Dhingra & N. Kaur) Nakasone & S.H. He, comb. nov.

MycoBank: MB836029

Synonym: *Phlebiopsis mussooriensis* Priyanka, Dhingra & N. Kaur, Mycotaxon 115: 255, 2011.

Notes – This species is characterized by a grayish yellow hymenophore, well-developed subiculum, thin-walled generative hyphae, lamprocystidia, and ellipsoid basidiospores (Priyanka et al., 2011). As mentioned in the protolog, *P. mussooriensis* is quite similar to *P. himalayensis*, now *Phaeophlebiopsis himalayensis* (Dhingra) Zmitr., differing primarily in basidiospore size and color change of hymenophore in KOH. Based on Priyanka et al.'s 2011 description, illustration, and comments, we propose the transfer of *P. mussooriensis* into *Phaeophlebiopsis*.

Phlebiopsis bambusicola (Berk. & Broome) Nakasone & S.H. He, comb. nov.

MycoBank: MB836030

Synonyms: *Corticium bambusicola* Berk. & Broome, Transactions of the Linnaean Society of London 2: 64, 1882. *Peniophora bambusicola* (Berk. & Broome) Sacc., Sylloge Fungorum 6: 647, 1888. *Hjortstamia bambusicola* (Berk. & Broome) Hjortstam & Ryvarden, Synopsis Fungorum 20: 37, 2005.

Notes – This Australian species is known only from the type and is characterized by a grayish brown hymenophore, a dimitic hyphal system, large, brown skeletocystidia, lamprocystidia, narrowly ellipsoid to allantoid basidiospores, and a habit on bamboo (Hjortstam and Ryvarden, 2005). Although similar to *P. crassa*, *P. bambusicola* has narrower basidiospores, 2.5–3 μm broad and is restricted by host preference and distribution.

Phlebiopsis dregeana (Berk.) Nakasone & S.H. He, comb. nov.

MycoBank: MB836031

Synonyms: *Corticium dregeanum* Berk., London Journal of Botany 5: 3, 1846. *Hymenochaete dregeana* (Berk.) Massee,

Botanical Journal of the Linnean Society 27: 114, 1890. *Terana dregeana* (Berk.) Kuntze, Revisio generum plantarum 2: 872, 1891. *Lopharia dregeana* (Berk.) P.H.B. Talbot, Bothalia 6: 57, 1951. *Irpex dregeanus* (Berk.) P.H.B. Talbot, Bothalia 6: 344, 1954. *Australohydnum dregeanum* (Berk.) Hjortstam & Ryvarden, Synopsis Fungorum 4: 61, 1990.

Notes – This is a poorly understood species that has been interpreted differently by various researchers. We take a narrow concept of *P. dreageana* based on studies of the type specimen and specimens restricted to Africa as described and illustrated by Massee (1891), Talbot (1951), Reid (1975), and Hjortstam and Ryvarden (1990). The ellipsoid basidiospores based on these studies are approximately 6.5–8 × 4–5 μm in size. Note that the cylindrical basidiospores illustrated by Reid (1975) are questionable for Hjortstam (1989) noted that basidia and spores were not observed in the type. Hjortstam and Ryvarden (1990) took a broad interpretation of *A. dreageanum* when they placed *Hydnum griseofuscescens* Reichardt from Australia and *Irpex vellereus* Berk. & Broome from Sri Lanka in synonymy; see below for further discussion of these two taxa. Although *A. dregeanum* has since been reported from India (De, 1998, as *Oxyporus vellereus*), South Korea (Lim, 2001; Lim and Jung, 2003), New Zealand (Buchanan and Ryvarden, 2000), Portugal (Melo and Hjortstam, 2002), Israel (Ţura et al., 2011), and Italy (Saitta et al., 2014), the basidiospore size, when given, is significantly smaller than the African collections.

Sequences from authentic specimens of the species are not available at present, but ITS sequences labeled "*Australohydnum dregeanum*" in GenBank, from United States, Korea and Sri Lanka, formed a strongly supported lineage within *Phlebiopsis* (**Figure 2**). The identity of the taxa in this lineage needs further study.

Phlebiopsis griseofuscescens (Reichardt) Nakasone & S.H. He, comb. nov.

MycoBank: MB836032

Synonyms: *Hydnum griseofuscescens* Reichardt, Verhandlungen der Zoologisch-Botanischen Gesellschaft Wien 16: 374, 1866. *Irpex griseofuscescens* (Reichardt) D.A. Reid, Kew Bulletin 17 (2): 273, 1963. *Australohydnum griseofuscescens* (Reichardt) Jülich, Persoonia 10 (1): 138, 1978. *Irpex vellereus* Berk. & Broome, Journal of the Linnean Society. Botany 14: 61, 1875. *Xylodon vellereus* (Berk. & Broome) Kuntze, Revisio generum plantarum 3 (2): 541, 1898. *Hirschioporus vellereus* (Berk. & Broome) Teng, Zhong Guo De Zhen Jun [Fungi of China]: 761, 1963. *Oxyporus vellereus* (Berk. & Broome) A. Roy & A.B. De, J. Mycopathol. Res.: 41, 1998. *Phlebiopsis lacerata* C.L. Zhao, Phytotaxa 440 (4): 274, 2020. *Hydnochaete philippinensis* Lloyd (as "*philippensis*"), Mycological Writings 7 (67): 1154, 1922. *Trichaptum venustum* (Berk.) G. Cunn., Bulletin of the New Zealand Department of Scientific and Industrial Research 164: 97, 1965.

Specimens examined – Sri Lanka, Western Province, Ingiriya, Dombagaskanda Forest Reserve, on fallen angiosperm branch, 27 February 2019, He 5734 (BJFC 030601). China, Sichuan Province, Miyi County, Haita Village, on fallen *Quercus* trunk, 13 September 2015, Cui 12629 (BJFC 028408) & Cui 12637 (BJFC 028416).

Notes – *Hydnum griseofuscescens* was described from Australia and is the type of *Australohydnum* (Jülich, 1978). It is characterized by resupinate to effused-reflexed basidiomata with a hydnoid, purplish brown hymenophore, a pseudodimitic hyphal system with simple-septate, colorless, generative hyphae, 4–9 μm broad, encrusted hymenial cystidia with colorless walls, and small ellipsoid basidiospores, 4–6 × 2.5–3 μm (Reid, 1956 as *Irpex vellerus*, Jülich, 1978). We follow Reid (1956, 1963) who determined that *H. griseofuscescens* and *I. vellereus,* described from Sri Lanka, were synonyms after studying the types of both species. Reid (1967) also reported that *T. venustum* sensu Cunningham (1965) is *H. griseofuscescens*. Based on morphological studies and sequence analyses, we determined that *P. lacerata* described from southern China (Xu et al., 2020) is conspecific with *P. griseofuscescens*.

Gilbertson and Adaskaveg (1993) described and illustrated *I. griseofuscescens* from Hawaii, but this species lacks encrusted hymenial cystidia and has small basidiospores, 4–4.5 × 2–2.5 μm. Similarly, De's (1998) description of *O. vellereus* from India appears to represent a different species with a monomitic hyphal system of colorless to pale brown hyphae and cylindrical basidiospores, 5.2–7 × 2–3 μm. One of the specimens cited, VBMN 80451, is also at CBS, CBS 515.92, and its ITS sequence is available from GenBank (AF479670) as "*Irpex vellereus*." This sequence was included in Lim and Jung (2003) and **Figure 2**, herein, where it is on a long branch, sister to *P. griseofuscescens*.

Phlebiopsis novae-granatae (A.L. Welden) Nakasone & S.H. He, comb. nov.

MycoBank: MB836033

Synonyms: *Lopharia novae-granatae* A.L. Welden [as '*nova-granata*'], Mycologia 67: 540, 1975. *Porostereum novae-granatum* (A.L. Welden) Hjortstam & Ryvarden [as '*nova-granatum*'], Synopsis Fungorum 4: 41, 1990. *Phanerochaete novae-granatae* (A.L. Welden) Sheng H. Wu [as '*nova-granata*'], Mycotaxon 88: 375, 2003. *Hjortstamia novae-granatae* (A.L. Welden) Hjortstam & Ryvarden [as '*nova-granata*'], Synopsis Fungorum 25: 19, 2008.

Notes – Reported from Colombia on bamboo, this species is characterized by a pale brown hymenophore and smooth skeletocystidia but lacking lamprocystidia (Welden, 1975; Hjortstam and Ryvarden, 1990). Because of its morphological similarity to *P. crassa*, the transfer of *P. novae-granatae* is proposed.

Phlebiopsis crassa Species Complex

Specimens examined – *Phlebiopsis crassa* group A: Vietnam, Ho Chi Minh City, the Botanical Garden Padua, on fallen angiosperm trunk, 13 October 2017, He 5205 (BJFC 024723). Sri Lanka, Central Province, Kandy, Peradeniya Botanic Garden, on fallen angiosperm branch, 2 March 2019, He 5763 (BJFC 030630). China, Guangdong Province, Renhua County, Danxiashan Nature Reserve, on fallen angiosperm trunk, 4 June 2019, He 5855 (BJFC 030730, **Figure 9A**); Yunnan Province, Qiubei County, Puzhehei Nature Reserve, 17 November 2019, He 6300 (BJFC, **Figure 9C**), He 6301

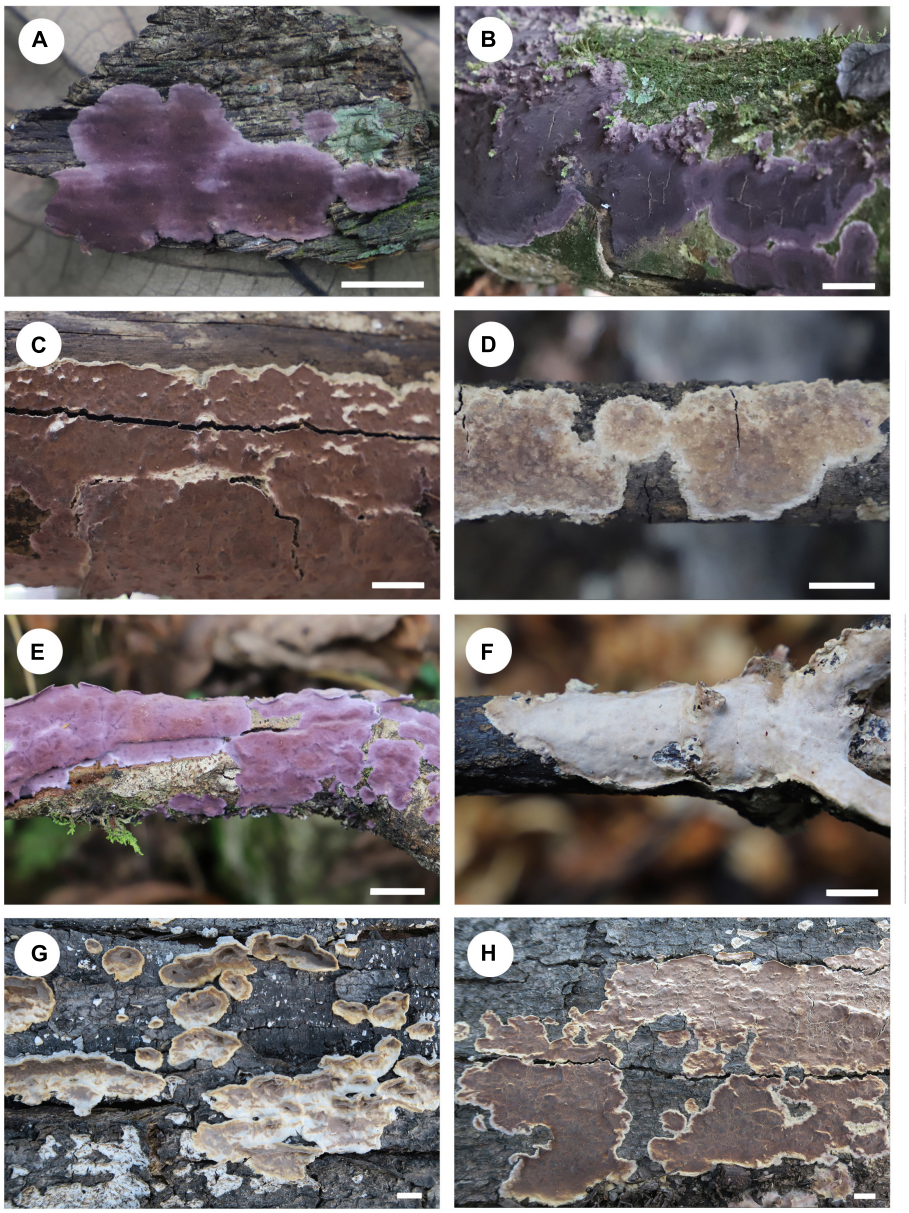


FIGURE 9 | Basidiomata of *Phlebiopsis crassa s.l.* (**A–D**: *P. crassa* group A, **E–H**: *P. crassa* group B; scale bars: **A–H** = 1 cm). **(A)** He 5855; **(B)** He 6303; **(C)** He 6300; **(D)** He 6301; **(E)** He 6266; **(F)** He 5866; **(G,H)** He 3349.

(BJFC, **Figure 9D**), He 6303 (BJFC, **Figure 9B**) & He 6304 (BJFC); Ximeng County, Mengsuolongtan Forest Park, on fallen angiosperm branch, 15 April 2005, Wu 0504-22 (TNM F0018719).

Phlebiopsis crassa group B: China, Guangdong Province, Renhua County, Danxiashan Nature Reserve, on fallen angiosperm branch, 4 June 2019, He 5866 (BJFC 030741, **Figure 9F**); Yunnan Province, Lushui County, Gaoligongshan Nature Reserve, on fallen angiosperm trunk, 29 November 2015, He 3349 (BJFC 021744, **Figures 9G,H**); Maguan County, Gulinqing Nature Reserve, on fallen angiosperm branch, 14 November 2019, He 6266 (BJFC, **Figure 9E**).

Phlebiopsis crassa group C: United States, Arizona, Pima County, Santa Rita Experimental Range, on *Fouquieria splendens*, 31 July 1976, K.K. Nakasone, KKN-86-sp (CFMR); Illinois, Coles County, Fox Ridge State Park, on hardwood, 24 September 1990, A.S. Methven, FP-1024996-sp (CFMR); Mississippi, Harrison County, Harrison Experimental Forest, on *Quercus* sp., 26 March 1976, H.H. Burdsall, Jr., HHB-8834-sp (CFMR).

Notes – Our phylogenetic analyses showed that samples of *P. crassa* group A from Vietnam, Sri Lanka and southern China

formed a distinct lineage and represent *P. crassa s.s.*, for the type was described from Vietnam (**Figures 1**, **2**). Collections from southern China and Japan, group B, and the United States, group C, clustered into two lineages in the ITS tree (**Figure 2**). All three lineages of *P. crassa* are morphologically similar, however. Unraveling this species complex is beyond the scope of this study, involving a number of presumed synonyms of *P. crassa*; see Lentz (1955) and Burdsall (1985).

Phlebiopsis darjeelingensis Dhingra, Nova Hedwigia 44: 222, 1987

Synonyms: *Phanerochaete lamprocystidiata* Sheng. H. Wu, Mycotaxon 90: 426, 2004. *Phlebiopsis lamprocystidiata* (Sheng H. Wu) Sheng H. Wu & Hallenb., Fungal Diversity 42: 116, 2010.

Notes – Because *P. darjeelingensis*, from India, and *P. lamprocystidiata*, from Taiwan, are nearly identical in morphology — basidiomata ceraceous when fresh then corneous when dried, well-developed subiculum of compactly packed, colorless hyphae, and cystidia and basidiospores of similar shape and size (Dhingra, 1987; Wu, 2004), we consider *P. lamprocystidiata* to be a later synonym of *P. darjeelingensis*. Zmitrovich (2018) transferred *Phlebiopsis lamprocystidiata* to *Phaeophlebiopsis* based on morphology, our phylogenetic analyses show that it belongs to *Phlebiopsis s.s.*, however.

DISCUSSION

The generic limits of *Phlebiopsis* has expanded over the last 40 years since its introduction in 1978 to include significant morphological range in basidiomata habit and texture and hymenophore configuration with the aid of molecular phylogenetic methods (Floudas and Hibbett, 2015; Miettinen et al., 2016; Zhao et al., 2018; Xavier de Lima et al., 2020; Xu et al., 2020). In this study, we emphasized sampling of *Phlebiopsis* taxa, and our overall results confirm those of Floudas and Hibbett (2015), Miettinen et al. (2016), and Chen et al. (2018b). In **Figures 1**, **2**, *Phlebiopsis*, including the types of *Australohydnum*, *P. griseofuscescens* and *Hjortstamia*, *P. friesii*, formed a well-supported clade in the Phanerochaetaceae and is closely related to *Phaeophlebiopsis*, *Hapalopilus* and *Rhizochaete*. The genera *Phlebiopsis* and *Australohydnum* were published simultaneously (Jülich, 1978) but the former is favored to avoid unnecessary name changes. So, we propose that *Australohydnum* is a synonym of *Phlebiopsis*. Twenty-four lineages were resolved in the ITS tree of *Phlebiopsis*, among which 18 are accepted species, including the *P. crassa* species complex and six new species described herein. Further study is required to identify the taxa named *P.* cf. *dregeana*, *Irpex vellerus*, *Phlebiopsis* sp. FP-102937 and *Phlebiopsis* sp. ECS-1971.

Among the 24 names of *Phlebiopsis* in Index Fungorum (accessed on 21 January 2021), we accept 17 taxa in *Phlebiopsis s.s.*, including 11 that are supported by molecular data. Five taxa, *P. himalayensis* Dhingra, *P. mussooriensis*, *P. peniophoroides* Gilb. & Adask., *P. ravenelii* (Cooke) Hjortstam, and *P. roumeguerei* (Bres.) Jülich & Stalpers were transferred to *Phaeophlebiopsis* based on morphology and sequence data. *Phlebiopsis lacerata* and *P. lamprocystidiata* are synonyms of *P. griseofuscescens* and *P. darjeelingensis*, respectively, as discussed above. Thus, 27 species of *Phlebiopsis* worldwide are accepted, including the six new species and four new combinations reported herein. An emended description of *Phlebiopsis* and an identification key to all species in the genus worldwide are presented below.

Phlebiopsis (Jülich) Nakasone & S.H. He, Emended

Synonyms: *Castanoporus* Ryvarden, 1991 Synopsis Fungorum 5: 121, 1991. *Hjortstamia* Boidin and Gilles, 2003 Bulletin de la Société Mycologique de France 118 (2): 99, 2003. *Australohydnum* Jülich, Persoonia 10 (1): 138, 1978.

Description: Basidiomata annual, resupinate, effused, effused-reflexed or pileate, ceraceous, membranaceous to coriaceous. Pilei, when present, tomentose, gray to brown. Hymenophore smooth, tuberculate, odontoid, hydnoid to poroid, white, gray, grayish brown, purplish brown or brown, turning purple in KOH in two species. Hyphal system monomitic or dimitic; generative hyphae simple-septate, colorless or rarely pale brown, in dimitic species with skeletal or, in one species, micro-binding hyphae. Subiculum absent to well-developed, colorless, brown, agglutinated or not, compact to loosely interwoven. Skeletocystidia absent or present, colorless or brown, distinctly thick-walled, smooth or encrusted. Hymenial cystidia or lamprocystidia typically present, colorless or light brown, thick-walled, usually encrusted. Dendrohyphidia present in one species, colorless, thin-walled, smooth, branched. Basidia clavate or subcylindrical, with four sterigmata and a basal simple septum. Basidiospores cylindrical, ellipsoid, broadly ellipsoid or subglobose, colorless, thin-walled, smooth, negative in Melzer's reagent, acyanophilous.

Type species: *Phlebiopsis gigantea* (Fr.) Jülich

Notes – The terminology relating to the cystidia observed in *Phlebiopsis* species is varied in the literature and thus confusing. There are up to three kinds of cystidia, but intermediate forms can develop to blur their distinctiveness. Lamprocystidia are found in most species of *Phlebiopsis* in the hymenium, often projecting, and may become embedded as the basidiomata thickens. They are typically conical or subfusiform with thick walls that are lightly to heavily encrusted in the upper half or apex. Skeletocystidia are found in dimitic or pseudodimitic species in which thick-walled hyphae in the subiculum curve toward the hymenium but remain embedded in the subiculum or subhymenium. The terminal ends may or may not be differentiated and usually lack encrustations. Hymenial cystidia are those structures that are similar to skeletocystidia but terminate in the hymenium and may be encrusted. In other cases, they are formed in the subhymenium and are smaller than lamprocystidia and not conical or heavily encrusted.

Key to 27 *Phlebiopsis* Species

1. Hymenophore poroid, irpicoid or hydnoid.....2
1. Hymenophore smooth, tuberculate or odontoid.....4
2. Basidiomata resupinate; hymenophore poroid to irpicoid; on gymnosperms..... *P. castanea*

2. Basidiomata effused-reflexed; hymenophore hydnoid; on angiosperms..... 3
3. Basidiospores 6.5–8 × 4–5 μm..... *P. dregeana*
3. Basidiospores 4.5–6 × 2.5–3 μm..... *P. griseofuscescens*
4. Dendrohyphidia present..... *P. pilatii*
4. Dendrohyphidia absent..... 5
5. Hyphal system pseudodimitic or dimitic..... 6
5. Hyphal system monomitic..... 13
6. Hymenophore turning purple in KOH..... *P. friesii*
6. Hymenophore unchanged in KOH..... 7
7. Basidiomata with well-developed pilei; skeletocystidia absent..... *P. papyrina*
7. Basidiomata resupinate to effused-reflexed; skeletocystidia present..... 8
8. Hymenophore without purple tints..... 9
8. Hymenophore with purple tint..... 12
9. Lamprocystidia none; basidiospores ≤ 6 μm long..... *P. membranacea*
9. Lamprocystidia present; basidiospores ≥ 6 μm long..... 10
10. Basidiomata resupinate to effused-reflexed; from temperate China..... *P. sinensis*
10. Basidiomata strictly resupinate; from tropical-subtropical Asia or Australia..... 11
11. Basidiospores 6–7 × 2.5–3 μm; on bamboo; from Australia..... *P. bambusicola*
11. Basidiospores 6.5–7.5 × 3–3.6 μm; on angiospermous wood; from Sri Lanka..... *P. brunnea*
12. Lamprocystidia brown to dark brown; South American species..... *P. amethystea*
12. Lamprocystidia colorless to pale brown; North American or Asian species..... *P. crassa s.l.*
13. Lamprocystidia none; skeletocystidia or hymenial cystidia present..... 14
13. Lamprocystidia present; skeletocystidia absent..... 15
14. Basidiospores 5.5–7 × 3–4 μm; on bamboo; from Colombia..... *P. novae-granatae*
14. Basidiospores 3.7–5.5 × 2.5–3.3 μm; on hardwood; from New Zealand..... *P. afibulata*
15. Basidiospores > 8 μm long, > 4 μm broad..... *P. laxa*
15. Basidiospores < 8 μm long, < 4 μm broad..... 16
16. Lamprocystidia small, generally < 40 μm long..... 17
16. Lamprocystidia large, generally > 40 μm long..... 20
17. Hymenophore purple in KOH..... *P. cylindrospora*
17. Hymenophore unchanged in KOH..... 18
18. Basidiospores broadly ellipsoid, 3.5–4.5 × 2.5–3.5 μm, $Q = 1.3$..... *P. yunnanensis*
18. Basidiospores narrowly ellipsoid to cylindrical..... 19
19. Basidiospores 3.5–5 × 2–2.2 μm..... *P. albescens*
19. Basidiospores 5.3–8.5 × 2.5–4 μm..... *P. punjabensis*
20. Lamprocystidia brown; on Pandanaceae; from Taiwan..... *P. brunneocystidiata*
20. Lamprocystidia colorless; on other plants; from various locations..... 21
21. Subiculum indistinct to absent..... 22
21. Subiculum distinct to well-developed..... 24
22. Basidia with two sterigmata..... *P. bicornis*
22. Basidia with four sterigmata..... 23
23. Basidiospores 5.5–7.5 × 3.5–4.5 μm; from North and South America..... *P. flavidoalba*
23. Basidiospores 4.5–6.5 × 3.8–4.8 μm; from Asia..... *P. magnicystidiata*
24. Basidiospores narrowly ellipsoid to ellipsoid, ≤ 3 μm broad..... 25
24. Basidiospores broadly ellipsoid, ≥4 μm broad..... 26
25. Hymenophore smooth, pale orange to rosy; lamprocystidia 40–50 × 6–7 μm; basidiospores < 2.5 μm wide; from Argentina..... *P. erubescens*
25. Hymenophore smooth to tuberculate, pale white to gray; lamprocystidia 60–90 × 10–20 μm; basidiospores ≥ 2.5 μm wide; from Northern Hemisphere..... *P. gigantea*
26. Lamprocystidia < 10 μm wide; from South America..... *P. galochroa*
26. Lamprocystidia > 10 μm wide; from Asia..... *P. darjeelingensis*

DATA AVAILABILITY STATEMENT

The datasets presented in this study can be found in online repositories. The names of the repository/repositories and accession number(s) can be found in the article/supplementary material.

AUTHOR CONTRIBUTIONS

S-HH designed the research, collected most of the specimens, and wrote the text. Y-NZ performed the phylogenetic analyses and did most of the measurement, descriptions and illustrations. KN loaned and examined type specimens of some related species, and revised language of the text. C-CC provided with some specimens and sequences. S-LL helped in field trips and species illustrations. KLWK and H-XM helped in field trips and collected some specimens. M-RH collected some specimens and helped in specimen preservation. All authors contributed to the article and approved the submitted version.

FUNDING

Financial support was provided by the National Natural Science Foundation of China (Grant Nos. 31870011 and 31750001).

ACKNOWLEDGMENTS

We would like to express our deep appreciation to Profs. Sheng-Hua Wu (National Museum of Natural Science, Taiwan, China), Tie-Zhi Liu (Chifeng University, Inner Mongolia, China), and Bao-Kai Cui (Beijing Forestry University, Beijing, China) for allowing us to study their specimens.

REFERENCES

Bernicchia, A., and Gorjón, S. P. (2010). *Fungi Europaei 12. Corticiaceae s.l.* Alassio: Edizioni Candusso.

Binder, M., Larsson, K. H., Matheny, P. B., and Hibbett, D. S. (2010). Amylocorticiales ord. nov. and Jaapiales ord. nov.: early-diverging clades of Agaricomycetidae dominated by corticioid forms. *Mycologia* 102, 865–880. doi: 10.3852/09-288

Boidin, J., and Gilles, G. (2003). À propos du genre *Lopharia* sensu lato (Basidiomycètes, Aphyllophorales). *Bull. Soc. Mycol. France* 118, 91–115.

Buchanan, P. K., and Ryvarden, L. (2000). An annotated checklist of polypore and polypore-like fungi recorded from New Zealand. *N. Zeal. J. Bot.* 38, 265–323. doi: 10.1080/0028825X.2000.9512683

Burdsall, H. H. Jr. (1985). *A Contribution to the Taxonomy of the Genus Phanerochaete. Mycologia Memoirs*. Lehre: J. Cramer. doi: 10.1080/0028825x.2000.9512683

Chen, C. C., Wu, S. H., and Chen, C. Y. (2018a). Four species of polyporoid fungi newly recorded from Taiwan. *Mycotaxon* 133, 45–54. doi: 10.5248/133.45

Chen, C. C., Wu, S. H., and Chen, C. Y. (2018b). *Hydnophanerochaete* and *Odontoefibula*, two new genera of phanerochaetoid fungi (Polyporales, Basidiomycota) from East Asia. *Mycokeys* 39, 75–96. doi: 10.3897/mycokeys.39.28010

Chikowski, R. S., Larsson, K. H., and Gibertoni, T. B. (2015). Three new combinations in *Rhizochaete* (Agaricomycetes, Fungi) and a new record to the Brazilian Amazonia. *Nova Hedwig.* 102, 185–196. doi: 10.1127/nova_hedwigia/2015/0298

Cunningham, G. H. (1965). Polyporaceae of New Zealand. *N. Zeal. Depart. Sci. Industr. Res. Bull.* 164:304.

Darriba, D., Taboada, G. L., Doallo, R., and Posada, D. (2012). jModelTest 2: more models, new heuristics and parallel computing. *Nat. Methods* 9:772. doi: 10.1038/nmeth.2109

De, A. B. (1998). Taxonomy of *Oxyporus vellereus* comb. nov. *J. Mycopathol. Res.* 36, 41–44.

de Koker, T., Nakasone, K. K., Haarhof, J., Burdsall, H. H. Jr., and Janse, B. J. H. (2003). Phylogenetic relationships of the genus *Phanerochaete* inferred from the internal transcribed spacer region. *Mycol. Res.* 107, 1032–1040. doi: 10.1017/S095375620300827X

Dhingra, G. S. (1987). The genus *Phlebiopsis* in the Eastern Himalayas. *Nova Hedwig.* 44, 221–227.

Douanla-Meli, C., and Langer, E. (2009). Fungi of Cameroon I. New corticioid species (Basidiomycetes). *Mycotaxon* 107, 95–103. doi: 10.5248/107.95

Duhem, B., and Michel, H. (2009). Une espèce nouvelle de *Corticium* s. st. Études dans les genre *Dendrocorticium* et *Dentocorticium* (Basidiomycotina). *Cryptogam. Mycol.* 30, 161–179.

Eriksson, J., Hjortstam, K., and Ryvarden, L. (1978). *The Corticiaceae of North Europe. Mycoaciella - Phanerochaete*, Vol. 5. Oslo, NO: Fungiflora.

Eriksson, J., Hjortstam, K., and Ryvarden, L. (1981). *The Corticiaceae of North Europe. Phlebia - Sarcodontia*, Vol. 6. Oslo, NO: Fungiflora.

Eriksson, J., Hjortstam, K., and Ryvarden, L. (1984). *The Corticiaceae of North Europe. Schizopora - Suillosporium*, Vol. 7. Oslo, NO: Fungiflora.

Floudas, D., and Hibbett, D. S. (2015). Revisiting the taxonomy of *Phanerochaete* (Polyporales, Basidiomycota) using a four gene dataset and extensive ITS sampling. *Fungal Biol.* 119, 679–719. doi: 10.1016/j.funbio.2015.04.003

Gilbertson, R. L., and Adaskaveg, J. E. (1993). Studies on wood-rotting basidiomycetes of Hawaii. *Mycotaxon* 49, 369–397.

Gilbertson, R. L., and Blackwell, M. (1985). Notes on the wood-rotting fungi on Junipers in the Gulf Coast region. *Mycotaxon* 24, 325–348.

Greslebin, A. G., Nakasone, K. K., and Rajchenberg, M. (2004). *Rhizochaete*, a new genus of phanerochaetoid fungi. *Mycologia* 96, 260–271. doi: 10.1080/15572536.2005.11832976

Hall, T. A. (1999). Bioedit: a user-friendly biological sequence alignment editor and analysis program for Windows 95/98/NT. *Nucleic Acids Symp. Ser.* 41, 95–98.

Hjortstam, K. (1987). A check-list to genera and species of corticioid fungi (Hymenomycetes). *Windahlia* 17, 55–85.

Hjortstam, K. (1989). Corticioid fungi described by M. J. Berkeley. *Kew Bull.* 44, 301–315. doi: 10.2307/4110803

Hjortstam, K., and Ryvarden, L. (1980). Studies in tropical Corticiaceae (Basidiomycetes) I. *Mycotaxon* 10, 269–287.

Hjortstam, K., and Ryvarden, L. (1990). *Lopharia* and *Porostereum* (Corticiacae). *Synopsis Fungorum* 4, 1–68. doi: 10.1007/978-3-319-23534-9_1

Hjortstam, K., and Ryvarden, L. (2005). New taxa and new combinations in tropical corticioid fungi, (Basidiomycotina, Aphyllophorales). *Synopsis Fungorum* 20, 33–41.

Jia, B. S., Zhou, L. W., Cui, B. K., Rivoire, B., and Dai, Y. C. (2014). Taxonomy and phylogeny of *Ceriporia* (Polyporales, Basidiomycota) with an emphasis of Chinese collections. *Mycol. Prog.* 13, 81–93. doi: 10.1007/s11557-013-0895-5

Jülich, W. (1978). Studies in resupinate Basidiomycetes - V. Some new genera and species. *Persoonia* 10, 137–140.

Jülich, W., and Stalpers, J. A. (1980). *The Resupinate Non-Poroid Aphyllophorales of the Temperate Northern Hemisphere. Verhandelingen der Koninklijke Nederlandse Akademie van Wetenschappen, Afd.* Amsterdam: Elsevier Science Ltd.

Justo, A., Miettinen, O., Floudas, D., Ortiz-Santana, B., Sjokvist, E., Lindner, D., et al. (2017). A revised family-level classification of the Polyporales (Basidiomycota). *Fungal Biol.* 121, 798–824. doi: 10.1016/j.funbio.2017.05.010

Katoh, K., Rozewicki, J., and Yamada, K. D. (2017). MAFFT online service: multiple sequence alignment, interactive sequence choice and visualization. *Brief. Bioinform.* 20, 1160–1166. doi: 10.1093/bib/bbx108

Kaur, G., Singh, A. P., and Dhingra, G. S. (2015). *Phlebiopsis punjabensis*, a new species from India. *Mycotaxon* 130, 907–909. doi: 10.5248/130.907

Kearse, M., Moir, R., Wilson, A., Stones-Havas, S., Cheung, M., Sturrock, S., et al. (2012). Geneious Basic: an integrated and extendable desktop software platform for the organization and analysis of sequence data. *Bioinformatics* 28, 1647–1649. doi: 10.1093/bioinformatics/bts199

Kornerup, A., and Wanscher, J. H. (1978). *Methuen Handbook of Colour*, 3rd Edn, London: E. Methuen and Co. Ltd.

Larsen, M. J., and Gilberston, R. L. (1977). Studies in *Laeticorticium* (Aphyllophorales, Corticiaceae) and related genera. *Norweg. J. Bot.* 24, 99–121.

Larsson, K. H. (2007). Re-thinking the classification of corticioid fungi. *Mycol. Res.* 111, 1040–1063. doi: 10.1016/j.mycres.2007.08.001

Lentz, P. L. (1955). *Stereum and Allied Genera of Fungi in the Upper Mississippi Valley*. Agriculture Monograph No. 24. Washington, DC: U.S. Department of Agriculture.

Lim, Y. W. (2001). *Systematic Study of Corticioid Fungi Based on Molecular Sequence Analyses*. Thesis, Seoul National University, Seoul.

Lim, Y. W., and Jung, H. S. (2003). *Irpex hydnoides*, sp. nov. is new to science, based on morphological, cultural and molecular characters. *Mycologia* 95, 694–699. doi: 10.1080/15572536.2004.11833073

Liu, S. L., and He, S. H. (2016). *Phanerochaete porostereoides*, a new species in the core clade with brown generative hyphae from China. *Mycosphere* 7, 648–655. doi: 10.5943/mycosphere/7/5/10

Ma, X., and Zhao, C. L. (2019). *Crepatura ellipsospora* gen. et sp. nov. in Phanerochaetaceae (Polyporales, Basidiomycota) bearing a tuberculate hymenial surface. *Mycol. Prog.* 18, 785–793. doi: 10.1007/s11557-019-01488-0

Maddison, W. P., and Maddison, D. R. (2018). *Mesquite: A Modular System for Evolutionary Analysis. Version 3.5.1*. Available online at: http://www.mesquiteproject.org (accessed April 15, 2020).

Massee, G. (1891). A monograph of the Thelephoraceae Part II. *J. Linnean Soc. Bot.* 27, 95–205. doi: 10.1111/j.1095-8339.1890.tb00801.x

Melo, I., and Hjortstam, K. (2002). *Australohydnum dregeanum* (Basidiomycetes, Stereaceae) in Europe. *Nova Hedwig.* 74, 527–532. doi: 10.1127/0029-5035/2002/0074-0527

Miettinen, O., Spirin, V., Vlasák, J., Rivoire, B., Stenroos, S., and Hibbett, D. S. (2016). Polypores and genus concepts in Phanerochaetaceae (Polyporales, Basidiomycota). *Mycokeys* 17, 1–46. doi: 10.3897/mycokeys.17.10153

Nakasone, K. K., Draeger, K. R., and Ortiz-Santana, B. (2017). A contribution to the taxonomy of *Rhizochaete* (Polyporales, Basidiomycota). *Cryptogam. Mycol.* 38, 81–99. doi: 10.7872/crym/v38.iss1.2017.81

Parmasto, E. (1965). Corticiaceae U.R.S.S. I. Descriptiones taxorum novarum. Combinationes novae. *Eesti NSV Teaduste Akadeemia Toimetised* 14, 220–233.

Priyanka, Dhingra, G. S., and Kaur, N. (2011). *Phlebiopsis mussooriensis* (Agaricomycetes), a new corticioid species from India. *Mycotaxon* 115, 255–258. doi: 10.5248/115.255

Rattan, S. S. (1977). *The Resupinate Aphyllophorales of the North Western Himalayas. Series Bibliotheca Mycologica*, Vol. 60. Vaduz, FL: Vaduz, 1–427.

Reid, D. A. (1956). New or interesting records of Australasian basidiomycetes. *Kew Bull.* 10, 631–648. doi: 10.2307/4113780

Reid, D. A. (1963). New or interesting records of Australasian Basidiomycetes: V. *Kew Bull.* 17, 267–308. doi: 10.2307/4118959

Reid, D. A. (1967). Review of polyporaceae of New Zealand by G. H. Cunningham. *Trans. Br. Mycol. Soc.* 50, 161–168. doi: 10.1016/S0007-1536(67)80076-7

Reid, D. A. (1975). *Type Studies of the Larger Basidiomycetes Described from Southern Africa (Contributions from the Bolus Herbarium)*. Cape Town: Bolus Herbarium, University of Cape Town.

Ronquist, F., Teslenko, M., van der Mark, P., Ayres, D. L., Darling, A., Hōhna, S., et al. (2012). MrBayes 3.2: efficient Bayesian phylogenetic inference and model choice across a large model space. *Syst. Biol.* 61, 539–542. doi: 10.1093/sysbio/sys029

Ryvarden, L. (1991). Genera of polypores, nomenclature and taxonomy. *Synopsis Fungorum* 5:115.

Saitta, A., Gargano, M. L., Compagno, R., and Venturella, G. (2014). *Australohydnum dregeanum* new to Italy. *Mycotaxon* 128, 179–183. doi: 10.5248/128.179

Stamatakis, A. (2014). RAxML Version 8: a tool for phylogenetic analysis and post-analysis of large phylogenies. *Bioinformatics* 30, 1312–1313. doi: 10.1093/bioinformatics/btu033

Swofford, D. L. (2002). *PAUP*: Phylogenetic Analysis Using Parsimony (*and Other Methods). Version 4.0b10*. Sunderland, MA: Sinauer Associates.

Talbot, P. H. B. (1951). Studies of some South African resupinate Hymenomycetes. *Bothalia* 6, 1–116. doi: 10.4102/abc.v6i1.1681

Telleria, M. T., Dueñas, M., Melo, I., and Martín, M. P. (2010). Morphological and molecular studies of *Hyphodermella* in the Western Mediterranean area. *Mycol. Prog.* 9, 585–596. doi: 10.1007/s11557-010-0666-5

Ţura, D., Zmitrovich, I. V., Wasser, S. P., Spirin, W. A., and Nevo, E. (2011). *Biodiversity of Cyanoprocaryotes, Algae and Fungi of Israel. Species diversity of Heterobasidiomycetes and Non-Gilled Hymenomycetes (former Aphyllophorales) in Israel*. Ruggell: A.R.A. Gantner Verlag K.-G.

Volobuev, S., Okun, M., Ordynets, A., and Spirin, V. (2015). The *Phanerochaete sordida* group (Polyporales, Basidiomycota) in temperate Eurasia, with a note on *Phanerochaete pallida*. *Mycol. Prog.* 14:80. doi: 10.1007/s11557-015-1097-0

Vu, D., Groenewald, M., de Vries, M., Gehrmann, T., Stielow, B., Eberhardt, U., et al. (2019). Large-scale generation and analysis of filamentous fungal DNA barcodes boosts coverage for kingdom fungi and reveals thresholds for fungal species and higher taxon delimitation. *Stud. Mycol.* 92, 1–20. doi: 10.1016/j.simyco.2018.05.001

Welden, A. L. (1975). Lopharia. *Mycologia* 67, 530–551. doi: 10.1080/00275514.1975.12019778

White, T. J., Bruns, T., Lee, S., and Taylor, J. (1990). "Amplification and direct sequencing of fungal ribosomal RNA genes for phylogenetics," in *PCR Protocols: A Guide to Methods and Applications*, eds M. A. Innis, D. H. Gelfand, J. J. Sninsky, and T. J. White (San Diego: Academic Press), 315–322. doi: 10.1016/B978-0-12-372180-8.50042-1

Wu, F., Fan, L. F., Liu, S. L., Zhou, X. J., and Yuan, H. S. (2017). Diversity of wood-decaying fungi from Shanxi Province, China. *Mycosystema* 36, 1487–1497.

Wu, S. H. (1990). The Corticiaceae (Basidiomycetes) subfamilies Phlebioideae, Phanerochaetoideae and Hyphodermoideae in Taiwan. *Acta Bot. Fenn.* 142, 1–123. doi: 10.1007/bf00213461

Wu, S. H. (2000). Six new species of *Phanerochaete* from Taiwan. *Bot. Bull. Acad. Sin.* 41, 165–174.

Wu, S. H. (2004). Two new species of *Phanerochaete* from Taiwan. *Mycotaxon* 90, 423–429.

Wu, S. H., Chen, C. C., and Wei, C. L. (2018a). Three new species of *Phanerochaete* (Polyporales, Basidiomycota). *Mycokeys* 41, 91–106. doi: 10.3897/mycokeys.41.29070

Wu, S. H., Chen, Y. P., Wei, C. L., Floudas, D., and Dai, Y. C. (2018b). Two new species of *Phanerochaete* (Basidiomycota) and redescription of *P. robusta*. *Mycol. Prog.* 17, 425–435. doi: 10.1007/s11557-017-1368-z

Wu, S. H., Nilsson, H. R., Chen, C. T., Yu, S. Y., and Hallenberg, N. (2010). The white-rotting genus *Phanerochaete* is polyphyletic and distributed throughout the phlebioid clade of the Polyporales (Basidiomycota). *Fungal Divers.* 42, 107–118. doi: 10.1007/s13225-010-0031-7

Xavier de Lima, V., Lira, C. S., Chikowski, R. S., Santos, C., Lima, N., and Gibertoni, T. B. (2020). Additions to neotropical stereoid fungi (Polyporales, Basidiomycota): one new species of *Lopharia* and one new combination in *Phlebiopsis*. *Mycol. Prog.* 19, 31–40. doi: 10.1007/s11557-019-01538-7

Xu, T. M., Zeng, Y. F., Cheng, Y. H., and Zhao, C. L. (2020). *Phlebiopsis lacerata* sp. nov (Polyporales, Basidiomycota) from southern China. *Phytotaxa* 440, 268–280. doi: 10.11646/phytotaxa.440.4.2

Yuan, Y., Chen, J. J., and He, S. H. (2017). *Geliporus exilisporus* gen. et. comb. nov., a xanthochroic polypore in Phanerochaetaceae from China. *Mycoscience* 58, 197–203. doi: 10.1016/j.myc.2017.01.006

Zhao, C. L., Liu, X. F., and Ma, X. (2018). *Phlebiopsis yunnanensis* sp. nov (Polyporales, Basidiomycota) evidenced by morphological characters and phylogenetic analysis. *Nova Hedwig.* 108, 265–279. doi: 10.1127/nova_hedwigia/2018/0508

Zhao, C. L., Ren, G. J., and Wu, F. (2017). A new species of *Hyphodermella* (Polyporales, Basidiomycota) with a poroid hymenophore. *Mycoscience* 58, 452–456. doi: 10.1016/j.myc.2017.06.007

Zmitrovich, I. V. (2018). Conspectus systematis Polyporacearum v. 1.0. *Folia Cryptogam. Petropolit.* 6, 1–145. doi: 10.1017/cbo9781139410656.004

Conflict of Interest: The authors declare that the research was conducted in the absence of any commercial or financial relationships that could be construed as a potential conflict of interest.

Copyright © 2021 Zhao, He, Nakasone, Wasantha Kumara, Chen, Liu, Ma and Huang. This is an open-access article distributed under the terms of the Creative Commons Attribution License (CC BY). The use, distribution or reproduction in other forums is permitted, provided the original author(s) and the copyright owner(s) are credited and that the original publication in this journal is cited, in accordance with accepted academic practice. No use, distribution or reproduction is permitted which does not comply with these terms.

frontiers in Microbiology

ORIGINAL RESEARCH
published: 19 February 2021
doi: 10.3389/fmicb.2021.627744

Parametarhizium (*Clavicipitaceae*) gen. nov. With Two New Species as a Potential Biocontrol Agent Isolated From Forest Litters in Northeast China

Siyu Gao[1†], Wei Meng[2†], Lixiang Zhang[1], Qun Yue[3], Xu Zheng[1] and Lijian Xu[1]*

[1] College of Advanced Agriculture and Ecological Environment, Heilongjiang University, Harbin, China, [2] College of Life Science, Northeast Forestry University, Harbin, China, [3] Biotechnology Research Institute, Chinese Academy of Agricultural Sciences, Beijing, China

A novel genus *Parametarhizium* with two new entomopathogenic species, *Parametarhizium changbaiense* and *Parametarhizium hingganense*, was introduced based on their morphological characteristics and a multigene phylogenetic analysis, which were isolated from the forest litters collected in Northeast China. To infer their phylogenetic relationships, a six-gene dataset consisting of DNA fragments of [nuclear small subunit rDNA (SSU) + LSU + TUB + TEF + RPB1 + RPB2] was used for phylogenetic analysis, including 105 related fungi. The new genus *Parametarhizium* formed a monophyletic clade basal to *Metarhizium* and its related genera (formerly *Metarhizium sensu lato*). *Parametarhizium* can be morphologically distinguished from related genera by the combination of the following characteristics: formation of white to yellow colonies on different media, candelabrum-like arrangement of cylindrical or obpyriform phialides, and small subglobose to ellipsoidal conidia. Both *P. hingganense* and *P. changbaiense* exhibited anti-insect activities against three farmland pests *Monolepta hieroglyphica*, *Callosobruchus chinensis*, and *Rhopalosiphum maidis*. This is the first report of entomopathogenic fungi exhibiting the anti-insect activity against *Mo. hieroglyphica*.

Keywords: 3 new taxa, taxonomy, phylogeny, biopesticide, *metarhizium*, entomopathogenic fungi

OPEN ACCESS

Edited by:
Peter Edward Mortimer, Chinese Academy of Sciences, China

Reviewed by:
Rajesh Jeewon, University of Mauritius, Mauritius
Nalin Nilusha Wijayawardene, Qujing Normal University, China

***Correspondence:**
Lijian Xu
xulijian@hlju.edu.cn;
xulijiancau@gmail.com

[†]These authors have contributed equally to this work

Specialty section:
This article was submitted to Evolutionary and Genomic Microbiology, a section of the journal Frontiers in Microbiology

Received: *11 November 2020*
Accepted: *15 January 2021*
Published: *19 February 2021*

Citation:
Gao S, Meng W, Zhang L, Yue Q, Zheng X and Xu L (2021) Parametarhizium (Clavicipitaceae) gen. nov. With Two New Species as a Potential Biocontrol Agent Isolated From Forest Litters in Northeast China. Front. Microbiol. 12:627744. doi: 10.3389/fmicb.2021.627744

INTRODUCTION

Fungi are diverse, with over 144,000 species (Willis, 2018), and about 2,000 new species are described every year (Hawksworth and Lücking, 2017). Fungi are a valuable natural resource and can be applied in agriculture and industry, such as biocontrol agents and antibiotic production (Aly et al., 2011; Filizola et al., 2019; Hyde et al., 2019). They can be used to control farmland pests as a

Abbreviations: BLAST, Basic Local Alignment Search Tool; BPP, Bayesian posterior probability; ITS, Internal transcribed spacer; LSU, Nuclear large subunit; rDNA; LT_{50}, Median lethal time; MEA, Malt extract agar; ML, Maximum likelihood; MLBS, Maximum likelihood bootstrap values; NCBI, National Center for Biotechnology Information; OA, Oatmeal agar; PDA, Potato dextrose agar; RPB1, RNA polymerase II largest subunit; RPB2, RNA polymerase II second largest subunit; SDAY, Sabouraud dextrose agar with yeast extract; SGSF125, *Parametarhizium changbaiense* SGSF125 isolate; SGSF355, *Parametarhizium hingganense* SGSF355 isolate; SSU, Nuclear small subunit rDNA; TEF, Translation elongation factor 1 alpha; TUB, Beta tubulin.

promising green alternative for chemical pesticides (Tulloch, 1976; Zimmermann, 2007; Brunner-Mendoza et al., 2018). However, only a few fungal genera are commercially developed as biocontrol agents such as *Metarhizium*, *Beauveria*, and *Trichoderma* (Zimmermann, 1993). Besides the species from the genera *Metarhizium*, *Beauveria*, and *Trichoderma*, the anti-insect activities of other fungi also deserve to be investigated extensively, especially newly discovered fungal species.

The family Clavicipitaceae (Ascomycota, Hypocreales) is a large group of fungi with 48 genera (including six new genera erected in 2020) and over 500 species[1] (Mongkolsamrit et al., 2020; Wijayawardene et al., 2020). Clavicipitaceae is morphologically characterized by cylindrical asci, thickened ascus apices, and filiform and multiseptate ascospores that tend to often disarticulate at maturity (Rogerson, 1970; Sung et al., 2007a). Fungi of Clavicipitaceae can grow in plants or invertebrates as symbionts or parasites, such as *Epichloë* spp. (symbionts of grasses), ergot fungi (*Claviceps* spp.) that parasitize ears of cereals, and *Metarhizium* spp. (parasites of insects) (Sung et al., 2007b; Schardl et al., 2013; Mongkolsamrit et al., 2020). *Metarhizium* is a ubiquitous genus of entomopathogenic fungi, being first discovered and erected in 1879 (Metchnikoff, 1879). Over the next 100 years, various new *Metarhizium* species were described based on their morphology characterized by dark spores and branched conidiophore with whorls of two to four phialides. Some *Metarhizium* species had been developed and become famous commercial biocontrol agents, such as *Metarhizium anisopliae*, *Metarhizium brunneum*, and *Metarhizium robertsii* (Meyling and Eilenberg, 2007; Zimmermann, 2007; Castrillo et al., 2011). With the increase in the fungal strain discovery of *Metarhizium* and its related genera, it is difficult to identify cryptic species by morphology alone (Bischoff et al., 2009; Luangsa-ard et al., 2017; Mongkolsamrit et al., 2020). Subsequently, multigene phylogenetic studies resulted in the delimitation of various lineages of *Metarhizium* into new species and genera (Bischoff et al., 2006, 2009; Kepler et al., 2014). Until 2014, according to the combination of phylogenetic and morphological studies, *Metarhizium* was expanded to over 30 species, which included members of the *Metarhizium flavoviride* and *M. anisopliae* complex as well as five additional *Metarhizium* spp. forming a more basal lineage within *Metarhizium* (Kepler et al., 2014). Since then, a dozen new species of *Metarhizium* were discovered including *Metarhizium baoshanense* (Chen et al., 2018), *Metarhizium argentinense* (Gutierrez et al., 2019), *Metarhizium purpureogenum* (Nishi et al., 2017), *Metarhizium bibionidarum* (Nishi et al., 2017), *Metarhizium chaiyaphumense* (Luangsa-ard et al., 2017), *Metarhizium kalasinense* (Luangsa-ard et al., 2017), *Metarhizium lepidopterorum* (Chen et al., 2019), *Metarhizium rongjiangense* (Chen et al., 2019), and *Metarhizium dendrolimatilis* (Chen et al., 2017). Recently, a more extensive multigene phylogenetic study of the Clavicipitaceae enabled the resolution of some of the basal lineages of *Metarhizium* (Mongkolsamrit et al., 2020). As a consequence, *Metarhizium* was redefined, leading to the erection of six new related genera, which are well-supported monophyletic groups based on the multigene phylogenetic analysis. Morphologically, the species of *Metarhizium* and related genera can be distinguished by the arrangement and shape of the phialides; the color, shape, and size of the conidia; and other characteristics (Mongkolsamrit et al., 2020). Although *Metarhizium* is one of the best-studied entomopathogenic fungi with some species being marketed as biocontrol agents, most of the newly described species related to *Metarhizium* in the last decade were rarely screened for their anti-insect activities.

Entomopathogenic fungi are mainly isolated from their hosts directly, which, however, are difficult to find in the field. Therefore, we started looking for alternative sources to find fungi with anti-insect activities. Forest litters naturally include fallen leaves, dead insects, feces, and diverse microorganisms such as fungi. Our previous studies showed that forest litter is a very promising substrate for the discovery of new fungal species in general as exemplified by the recently described *Myxotrichum albicans* (Liang et al., 2019). In this study, we identified and described a new genus related to *Metarhizium* represented by two new candelabrum-like species based on morphology and a multilocus phylogenetic reconstruction. In addition, their potential as biocontrol agents was evaluated by applying a spore-based anti-insect assay.

MATERIALS AND METHODS

Sample Collection

Forest litters were collected in the Changbai Mountains, Jilin province, China (42°24'N, 128°06'E), in October 2017 and Greater Hinggan mountains, Heilongjiang province, China (52°20'N, 124°42'E) in September 2018. The components of forest litters were mostly fallen leaves and a few twigs. The Changbai Mountains is a typical temperate-continental climate zone with an over 300-year-old broad-leaved Korean pine mixed forest. The dominant tree species are *Pinus koraiensis* Siebold et Zucc., *Tilia amurensis* Rupr., *Fraxinus mandshurica* Rupr., and *Quercus mongolica* Firsch. ex Turcz. The Greater Hinggan mountains are located within the cold temperate continental climate zone and consist of *Populus davidiana* Dode, *Betula platyphylla* Sukaczev, *Larix gmelinii* Rupr., and *Pinus sylvestris* L. as the dominant tree species.

Fungal Medium

The fungal medium comprised potato dextrose agar (PDA; 200 g potato, 20 g glucose, 20 g agar, and 1 L distilled water); 1/4 PDA (50 g potato, 5 g glucose, 20 g agar, and 1 L distilled water); Sabouraud dextrose agar with yeast extract (SDAY; 10 g yeast, 40 g glucose, 10 g peptone, 20 g agar, and 1 L distilled water); oatmeal agar (OA; 30 g oatmeal, 20 g agar, and 1 L distilled water); malt extract agar (MEA; 30 g malt, 20 g agar, and 1 L distilled water). Malt extract powder, agar powder, and yeast extract powder were manufactured by Aoboxing Biotech, Beijing, China. Glucose and peptone were manufactured by Kermel, Tianjin, China.

[1] http://www.outlineoffungi.org

Fungal Isolation

The forest litters were packed in sterile envelopes and stored at 4°C until used. Fungi were isolated according to Bills et al. (2004) and Liang et al. (2019). Briefly, a litter sample was pulverized and then subjected to a minisieve filtration. The particles in the range of 105–210 μm were transferred to 10 ml of sterile water. The 0.1 ml suspension of the particles was poured on 1/4 PDA and then cultured at 25°C for 2 weeks. During that time, newly emerging fungal colonies were directly transferred to new PDA plates. By this method, about 500 fungal isolates (data not shown) were obtained. The isolates SGSF125 and SGSF355 were suspected to be undescribed species based on their morphological traits and were used in this study. The specimens were deposited in the Herbarium of Microbiology and Phytopathology, Heilongjiang University (HMPHU 1243 and HMPHU 1244), and the living culture (preserved in a metabolically inactive state) was deposited in China General Microbiological Culture Collection Center (CGMCC 19143 and CGMCC 19144).

DNA Extraction and PCR

Fungal genomic DNA was extracted from 100 mg of fresh mycelia. DNA extraction followed a previously published protocol (Liang et al., 2019). The DNA nuclear small subunit rDNA (SSU), internal transcribed spacer (ITS), nuclear large subunit rDNA (LSU), beta tubulin (TUB), translation elongation factor 1 alpha (TEF), RNA polymerase II largest subunit (RPB1), and RNA polymerase II second largest subunit (RPB2) were amplified by PCR. PCR was conducted in 50 μl volumes consisting of 25 μl 2 × Es Taq Master Mix, 1 μl template, 2 μl forward primer, 2 μl reverse primer, 1 μl DNA template, and 20 μl ddH_2O. 2 × Es Master Mix was manufactured by CWBIO, Beijing, China. Primer sequence information is shown in **Supplementary Table S1**. Sequencing was performed using an ABI 3730 DNA analyzer and the BigDye Terminator mix v. 3.1 (Applied Biosystems, Foster City, California, Unites States). The sequences of the new species were submitted to GenBank (accession number is shown in **Supplementary Table S2**).

Physiological Assays

Each isolate was cultured in sterile 90 mm Petri dishes containing 20 ml of PDA and incubated at 20, 25, 30, and 35°C in complete darkness, for 2 weeks. The impact of different pH values (4, 5, 6, 7, 8, and 9) on fungal growth was also tested on PDA. The diameters of fungal colonies were measured every 2 days. After 14 days, 5 ml 0.05% Tween 80 was added to the PDA plates, and conidia were harvested with a sterile cotton swab and deposited into a sterile 10 ml-volume centrifuge tube. The conidial concentration was estimated using a hemocytometer.

Phylogenetic Analyses

A consensus sequence was obtained by aligning sequences from forward and reverse primers with MEGA v. 7.0 (Kumar et al., 2016) and then queried in the National Center for Biotechnology Information (NCBI) using the BLAST program[2]. The sequences from 105 fungi classified in *Metarhizium* and related genera in the Clavicipitaceae (Kepler et al., 2014; Mongkolsamrit et al., 2020) were obtained from GenBank (**Supplementary Table S2**) and aligned with MEGA v. 7.0 (ClustalW). Alignments were manually adjusted to allow maximum alignments and minimum gaps. The alignments were concatenated as a dataset for a multigene phylogenetic analysis (Kepler et al., 2014; Mongkolsamrit et al., 2020). The multigene phylogenetic analysis of the aligned sequences used RAxML as an optimality criterion, and statistical support was built on 1,000 bootstrap replicates (Edler et al., 2019). A general time-reversible (GTR) model with a gamma-distributed rate variation was used for the nucleotide partitions in the maximum-likelihood (ML) analysis. Markov chain Monte Carlo (MCMC) was used to estimate posterior probability by MrBayes v. 3.2.4 (Ronquist et al., 2012). Four simultaneous Markov chains were run for 3,000,000 generations (standard deviation of split frequencies less than 0.01), and trees were sampled every 1,000 generations. The first 2,000 trees representing the burn-in phase of the analysis were discarded, and the remaining trees were used to determine posterior probabilities in the majority rule consensus tree.

Collection of Insects

Adult insects of *Mo. hieroglyphica*, *Rhopalosiphum maidis*, and *Callosobruchus chinensis* were collected from the experimental fields of the Qiqihar Branch of Heilongjiang Academy of Agricultural Sciences from July and August in 2019. The insect adults were collected from fields, placed in a perforated plastic container, and then maintained at 25°C until use.

Anti-insect Assay

For pathogenicity assays, conidial suspensions were produced using the same method as in the physiological assays. The conidial concentration was adjusted to 1×10^8 conidia/ml using a hemocytometer. Adults of *C. chinensis* were immersed in conidial suspension for 5 s, and 20 adults were inoculated in each treatment (Noble et al., 2018). Adults of *Mo. hieroglyphica* were immersed in conidial suspension for 5 s, and 35 adults were inoculated in each treatment. The effect of fungal isolates on the mortality of *R. maidis* was evaluated by spraying (Hussain et al., 2015; Wu et al., 2020) 1 ml of each conidial suspension on 40 wingless adults per treatment. Tween 80 0.05% was applied as a control treatment. The treated insects were kept in 250 ml flasks with foods and maintained at 25 ± 1°C, 70 ± 5% RH in darkness for 10 days, and the survival of the insects was recorded daily. Cadavers were placed on wet filter paper disks in sterile 90 mm Petri dishes sealed with Parafilm and maintained in an incubator chamber at 25 ± 1°C and 70 ± 5% relative humidity (RH) to investigate mycosis. All the tests were performed in triplicate.

Statistical Analyses

All data were analyzed using SPSS for Windows Version 25.0 (SPSS Inc., Chicago, IL, United States). Data were shown as the mean ± standard error (SE) from three biological replicates. For multiple comparisons, Tukey's multiple comparison test was used for significance analysis, and *p*-values equal to 0.05 were

[2]http://www.ncbi.nlm.nih.gov/

considered significant. The significant differences were shown as different letters (such as a, b, and c) in tables and figures.

RESULTS

Colony Growth and Conidial Production at Different pH Values and Temperatures

There are two isolates, SGSF125 and SGSF355, isolated from the forest litters that are suspected as new species related to *Metarhizium* spp. according to their morphological traits. As suspected new species, the optimal pH and temperature of SGSF125 and SGSF355 were tested. The colony diameters and conidial productions of SGSF125 and SGSF355 on PDA at different temperatures, respectively, are shown in **Figure 1**. The optimal growth temperature of SGSF125 and SGSF355 was 25 and 30°C, respectively. At 25 and 30°C, SGSF355 had a higher growth rate and conidial production than SGSF125. SGSF355 had a wider optimal temperature range than SGSF125, and the conidial production of SGSF355 was similar at 25 and 30°C with no significant difference. The colony diameters of SGSF125 and SGSF355 were 13–18 mm on PDA on the 14th day.

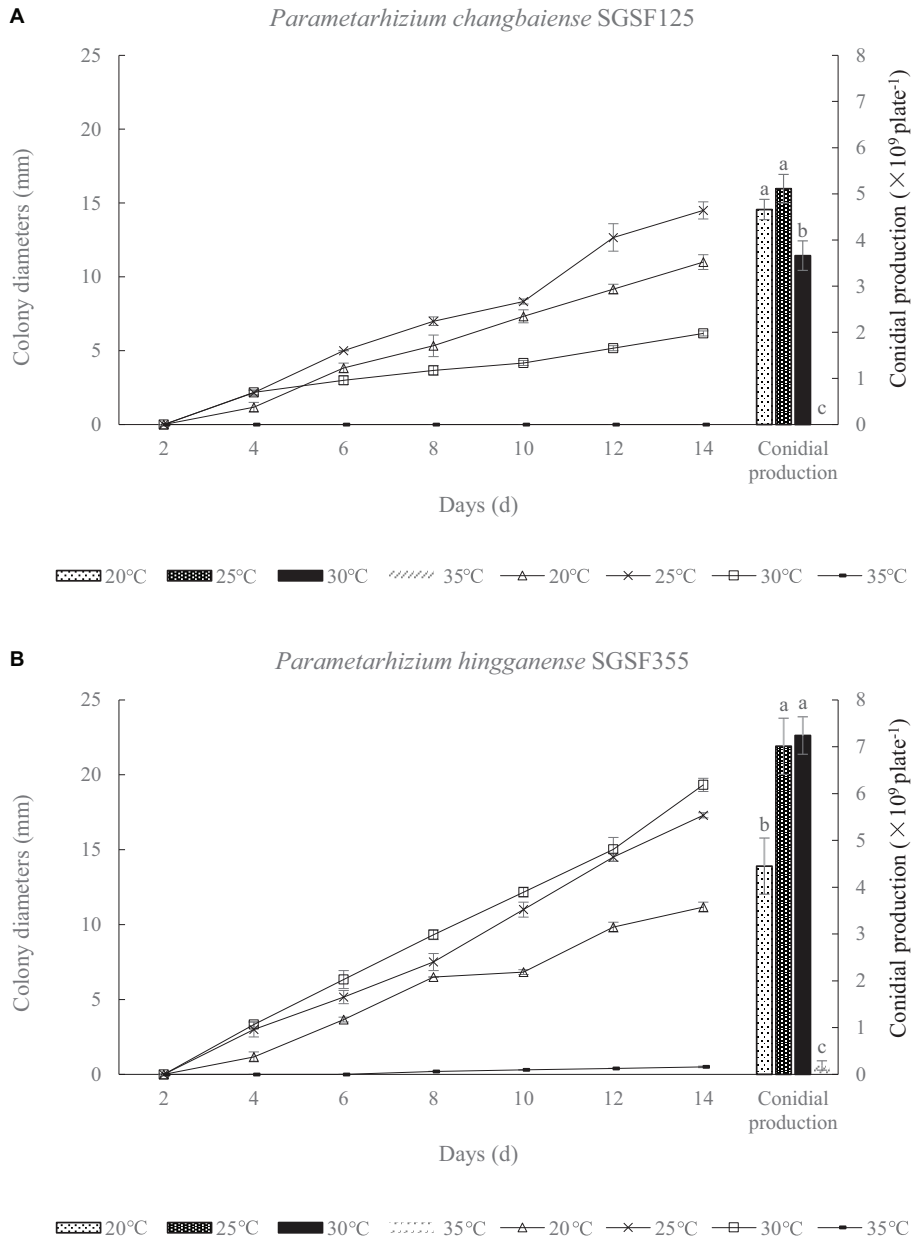


FIGURE 1 | Colony diameter and conidial production of *Parametarhizium chanbaiense* SGSF125 **(A)** and *Parametarhizium hingganense* SGSF355 **(B)** on potato dextrose agar (PDA). Different letters (a, b, and c) above bars indicate significant differences at the 0.05 level.

Meanwhile, colony diameters and conidial productions of the two isolates were measured at different pH values within a period of 2 weeks (**Table 1**). The optimal pH values of SGSF125 and SGSF355 were 5 (**Table 1**). At the same pH, the colony diameter and conidial production of SGSF355 were higher than SGSF125, except at pH 4 (**Table 1**).

Phylogenetic Analyses

The sequence similarity of seven molecular taxonomic markers SSU, ITS, LSU, TUB, TEF, RPB1, and RPB2 between the two new species was in the range of 93.0–99.7% (except for TUB, 86.5%), indicating their close relationship. In contrast, the similarity to *Metarhizium* species and taxa from other related genera was much lower in particular for the ITS (<89%), RPB sequences (<85%), and TUB (<81%) (**Figure 2** and **Supplementary Tables S3, S4**). All available sequences of the molecular taxonomic markers from the two new and closely related species (*Metarhizium* and the genera related to *Metarhizium*) were combined for a multigene phylogenetic analysis (**Supplementary Table S2**). The combined dataset concatenated a six-gene dataset consisting of DNA fragments of the SSU (735 bp), LSU (627 bp), TUB (253 bp), TEF (766 bp), RPB1 (492 bp), and RPB2 (778 bp). Sequences of the genus *Hypocrella* were used as an outgroup. ITS sequences were generated only for barcoding purposes and not included in the multigene analyses (Kepler et al., 2014; Mongkolsamrit et al., 2020). Modeltest 3.7 resulted in the selection of the GTR model with a proportion of invariable sites (I) and the gamma distribution shape parameter (G). This model was used in MrBayes 3.2.4 and RAxML GUI 2.0.0–beta.10. Bayesian analyses resulted in 2,000 "burn-in" trees. For the ML analysis in RAxML, the GTRGAMMA model was used for the nucleotide partitions. The phylogenetic analysis (**Figure 3**) based on a combined dataset comprising SSU, LSU, TUB, TEF, RPB1, and RPB2 showed that the new species formed a monophyletic clade whose bootstrap values (BSs) and Bayesian posterior probability (BPP) were 100% and 1, respectively. This monophyletic was basal to the clade (BS and BPP were 67% and 1, respectively) of *Metapochonia*, *Pochonia*, *Metarhizium*, and other related genera. To include as many genera in Clavicipitaceae as possible, a phylogenetic analysis only based on the LSU sequences from 34 genera in Clavicipitaceae was also carried out (**Supplementary Figure S1**). The new species also formed a monophyletic

TABLE 1 | Colony diameters and conidial productions of *Parametarhizium changbaiense* (SGSF125) and *Parametarhizium hingganense* (SGSF355).

Different pH treatment	Colony diameters		Conidial productions (per plate)	
	SGSF125	SGSF355	SGSF125	SGSF355
pH4	7.2 ± 0.17g	5.2 ± 0.02h	3.23×10^9f	2.69×10^9g
pH5	15.5 ± 0.03b	17.67 ± 0.02a	6.37×10^9c	7.82×10^9a
pH6	14.0 ± 0.03bc	16.17 ± 0.03a	6.34×10^9c	7.36×10^9b
pH7	13.2 ± 0.03cde	14.7 ± 0.02cdef	6.29×10^9cd	6.38×10^9c
pH8	11.7 ± 0.02def	13.3 ± 0.02cd	4.59×10^9e	5.97×10^9d
pH9	11.5 ± 0.00ef	11.3 ± 0.02f	4.56×10^9e	6.11×10^9cd

Different letters in colony diameters column (a, b, c, d, e, and f) or conidial productions column (a, b, c, d, e, f, and g) indicate significant differences at the 0.05 level.

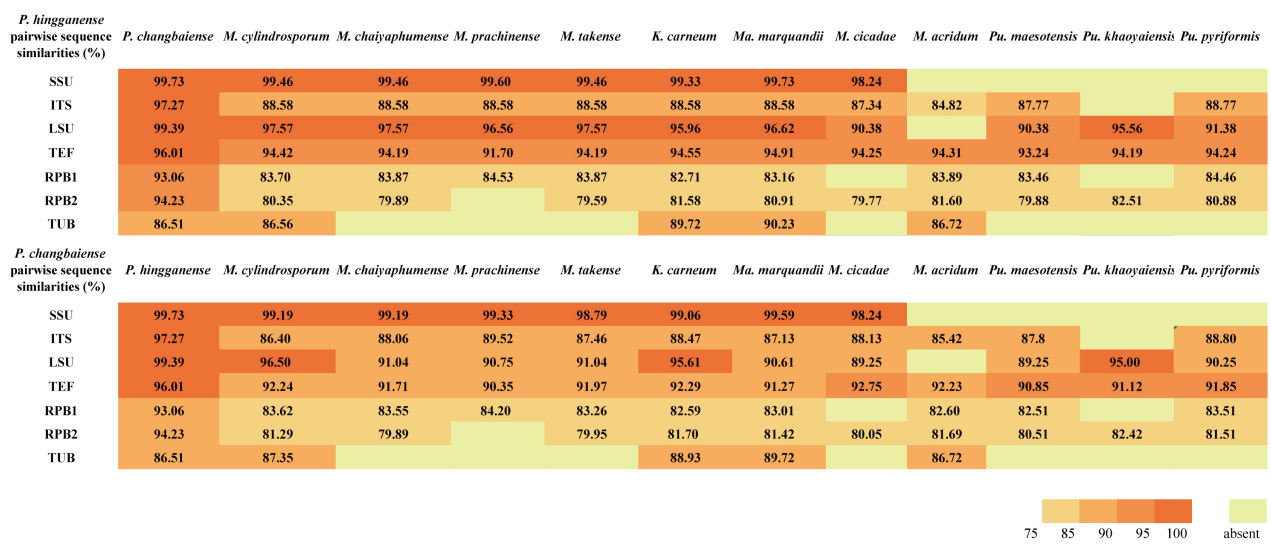


FIGURE 2 | Pairwise nucleotide sequence similarities (in %) for 7-locus from *Parametarhizium* spp. and morphologically similar species.

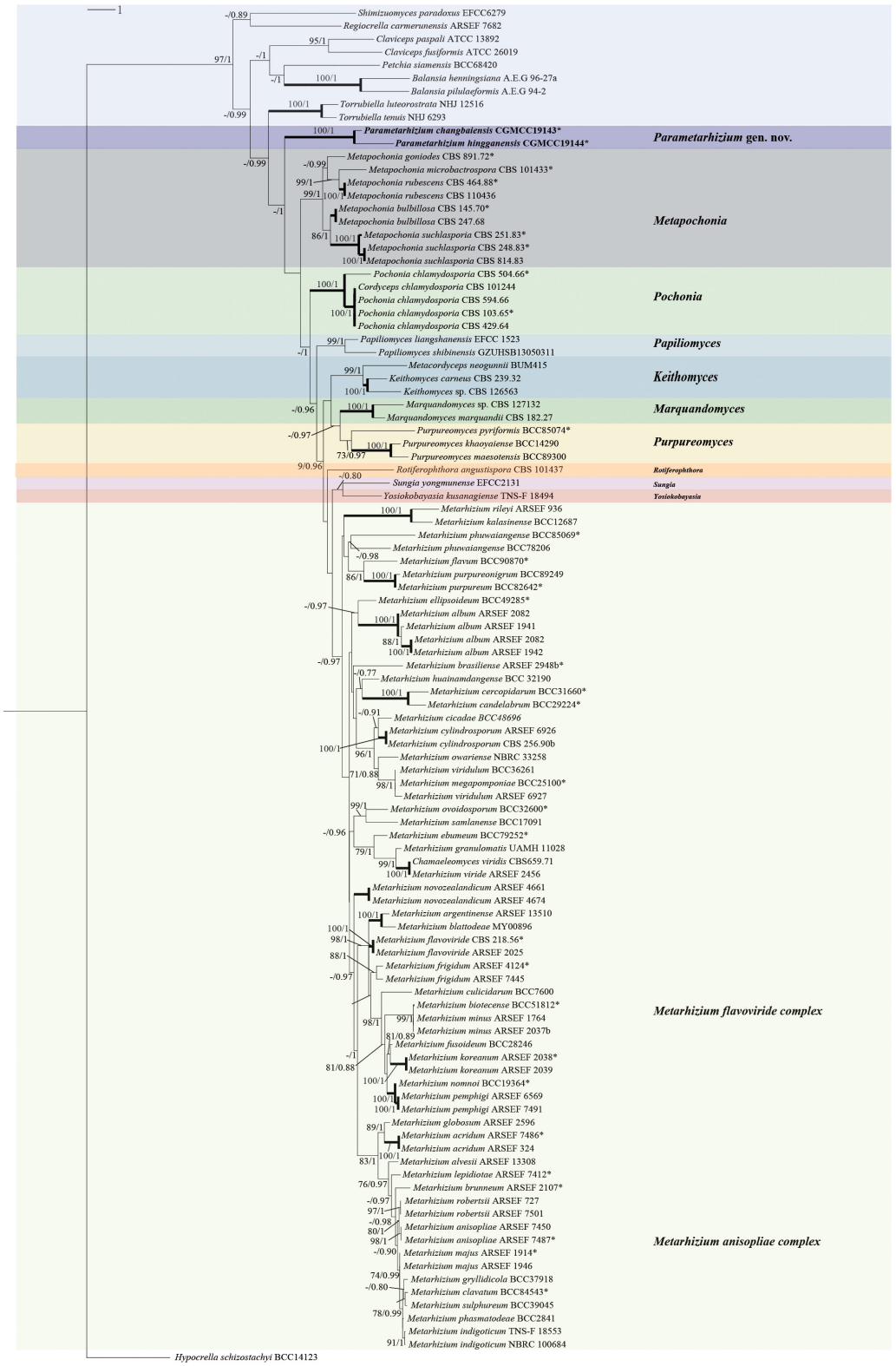


FIGURE 3 | Multigene phylogenetic analysis of *Parametarhizium* and related genera (*Clavicipitaceae*). Phylogenetic based on concatenated Nuclear small subunit rDNA (SSU), Nuclear large subunit rDNA (LSU), Beta tubulin (TUB), Translation elongation factor 1 alpha (TEF), RNA polymerase II largest subunit (RPB1), and RNA polymerase II second largest subunit (RPB2) using maximum likelihood as optimality criterion. ML bootstrap values/Bayesian posterior probability above 70% (MLBS)/0.7 (BPP) are shown on the nodes. *Ex-type material. Branches with 100% (MLBS) and 1.0 (BPP) support are highlighted by thickened lines.

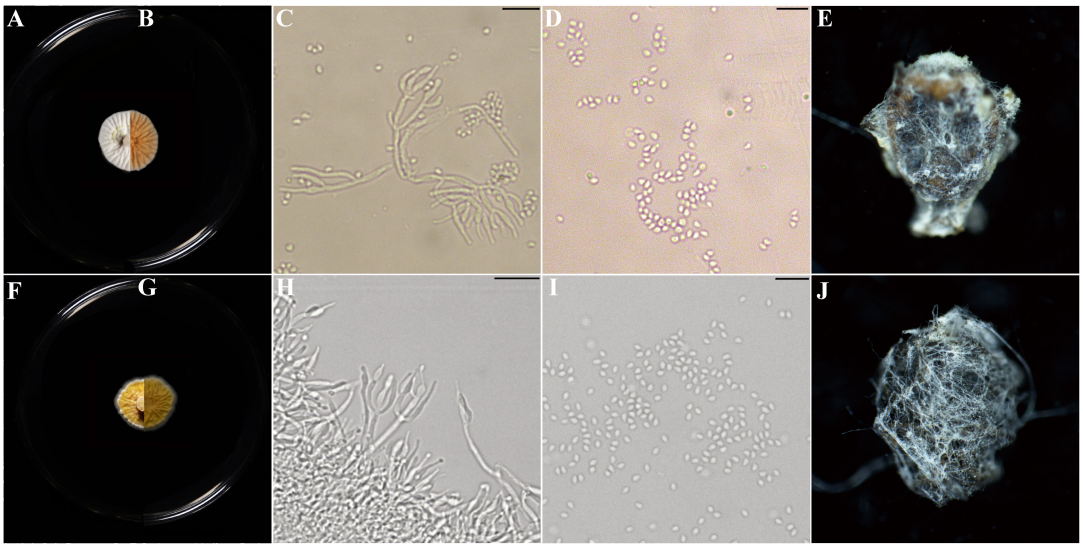


FIGURE 4 | Morphological characters of *Parametarhizium changbaiense* [from ex-holotype China General Microbiological Culture Collection Center (CGMCC) 19143] and *Parametarhizium hingganense* (from ex-holotype CGMCC 19144). **(A,B)** The front and reverse of a *P. changbaiense* colony on PDA after 14 days at 25°C. **(C,D)** The phialides and conidia of *P. changbaiense*. **(E)** *Rhopalosiphum maidis* infected by *P. changbaiense*. **(F,G)** The front and reverse of a *P. hingganense* colony on PDA after 14 days at 25°C. **(H,I)** The phialides and conidia of *P. hingganense*. **(J)** *R. maidis* infected by *P. hingganense*.

clade in the phylogenetic tree based on the LSU sequences. The isolated position of the new fungal isolates SGSF125 and SGSF355 in the multigene phylogenetic reconstruction together with their unique combination of morphological characteristics prompted us to erect a novel genus named *Parametarhizium*.

TAXONOMY

Parametarhizium S. Gao, W. Meng, Li Xiang Zhang, Q. Yue, L. J. Xu, gen. nov.

MycoBank no.: MB 837521

Etymology: based on its close morphological relationship to *Metarhizium*.

Type species: *Parametarhizium hingganense* S. Gao, W. Meng, Li Xiang Zhang, Q. Yue, L. J. Xu, sp. nov.

Diagnosis: Colonies white to yellow, velvety, exudate lemon yellow, sometimes radially sulcate, reverse pale yellow to brown. Conidiophores hyaline, arising from branches of aerial hyphae, with candelabrum-like arrangement of phialides. Phialides, 2–4 in whorls, cylindrical to obpyriform. Conidia subglobose to ellipsoidal, hyaline (1.1–) 1.2–2.2 (–2.8) × (1.0–) 1.6–1.7 (–2.6) μ m.

Description: Colonies on PDA, SDAY, MEA, OA, white to yellow, never green, radially sulcate, 25°C reaching 13–20 mm in 2 weeks, velvety; exudate lemon yellow; reverse pale yellow to brown. Hyphae hyaline, septate, smooth-walled, 0.8–2.5 μm wide. Conidiophores hyaline, smooth-walled (20–) 34–62 (–100) × (0.9–) 1.5–1.9 (–2.2) μm, arising from branches of aerial hyphae, with whorls of 2–4 phialides. Phialides candelabrum-like arrangement (2.7–) 5.6–17.5 (–26) × (1.2–) 1.4–2.3 (–2.5) μm, cylindrical to obpyriform. Conidia subglobose to ellipsoidal, hyaline to yellow (1.1–) 1.2–2.2 (–2.8) × (1.0–) 1.6–1.7 (–2.6) μ m (**Figure 4** and **Supplementary Figure S2**).

Notes: Compared with those of *Metarhizium*, the colonies of *Parametarhizium* are white to yellow (vs. green), and its subglobose-to-ellipsoidal conidia are smaller (<3.3 μm) than most of *Metarhizium* spp. *Parametarhizium* exhibits a candelabrum-like arrangement of phialides, while *Metapochonia* and *Pochonia* have *Verticillium*-like conidiophores, and other related genera show *Nomuraea*-like, *Paecilomyces*-like or *Lecanicillium*-like conidiophores.

Parametarhizium changbaiense S. Gao, W. Meng, Li Xiang Zhang, Q. Yue, L. J. Xu, sp. nov.

MycoBank no.: MB 837522

Etymology: referring to the location where the type material was collected.

Description: Colonies on PDA reaching 13–15 mm in 2 weeks, white, radially sulcate, velvety; reverse brown, radially sulcate. Colonies on SDAY reaching 15–17 mm, pale yellow, wrinkled, velvety, with undulate margin; reverse yellow. Colonies on MEA reaching 15–18 mm, white, flat; reverse brown. Colonies on OA reaching 18–19 mm, flat, initially white, turning lemon yellow due to the production of conidial masses, exudate lemon yellow; reverse pale yellow.

Hyphae hyaline, smooth-walled, 0.8–2.5 μm wide. Conidiophores arising from branches of aerial hyphae, bearing dense whorls of branches, terminating in branches with 2–4 phialides per branch, candelabrum–like arrangement of phialides. Phialides cylindrical (2.7–) 5.6–12.5 (–20) × (1.4–) 1.6–2.2 (–2.5) μm, with a short neck (0.9–) 1.2–5.5 (–7.6)

TABLE 2 | Morphological comparison of *Parametarhizium changbaiense* and *Parametarhizium hingganense* with similar species.

Species	Source	Phialides (μ m)	Conidia (μ m)	Colony color	References
Metarhizium acridum	Orthoptera	Cylindrical to slightly swollen, 7.0–7.5 × 2.1–2.9	Ovoid, 4.0–5.0 × 2.0–3.2	Dark yellow–green	Bischoff et al., 2009
Metarhizium cylindrosporum	Hemiptera (Cicada adult)	5–8 × 3–4.2	Microconidia ovoid, Subglobose, 3.3–6.7 × 3.3–4.2	Grayish–green	Tzean et al., 1993
Metarhizium chaiyaphumense	Hemiptera (Cicada nymph)	Clavate, 5–8 × 2–3	Microconidia ovoid, subglobose, 2–4 × 2–3	White–green	Luangsa-ard et al., 2017
Metarhizium cicadae	Hemiptera: Cicadidae	Cylindrical, 4–7 × 2–3.5	Microconidia ovoid, ellipsoid, 2–6 × 2.5–4	Dark–green	Mongkolsamrit et al., 2020
Metarhizium prachinense	Lepidoptera larva	Ovoid, obpyriform, 3–5 × 2	Subglobose, 3–5 × 1.5–2.5	White–green	Luangsa-ard et al., 2017
Metarhizium takense	Hemiptera (Cicada nymph)	Fusiomis, 5.0–8.0 × 2.0–3.0	Subglobose or ovoid, 3.0–5.0 × 2.0–3.0	Green	Luangsa-ard et al., 2017
Purpureomyces khaoyaiensis	Lepidoptera larva	*Lecanicillium*–like, 7–18 × 1–3	Ovoid, 2–3 × 1.5–3	White to cream	Mongkolsamrit et al., 2020
Purpureomyces maesotensis	Lepidoptera larva	*Lecanicillium*–like, 4–21 × 1.5–2	Ovoid, 3 × 1–2.5	White to lilac	Mongkolsamrit et al., 2020
Purpureomyces pyriformis	Lepidoptera larva	*Lecanicillium*–like, 8–22 × 1–2	Ovoid, 2–4 × 1.5–2	White to cream	Mongkolsamrit et al., 2020
Purpureomyces marquandii	Soil	Cylindrical, 8–15 × 1.5–2	Ellipsoidal, 2–3 × 1.5–2	Purple	Hywel-Jones, 1994
Keithomyces carneus	Soil	Cylindrical, 8–10 × 2.5–3.0	Globose, 3.5–5	White	Frisvad and Samson, 2004
Parametarhizium changbaiense	Forest litter	Cylindrical, 5.6–12.5 × 1.6–2.2	Subglobose, ellipsoid, 1.6–2.8 × 1.3–2.2	White to yellow	This study
Parametarhizium hingganense	Forest litter	Obpyriform, 7.0–17.5 × 1.4–2.3	Subglobose, ellipsoid, 1.1–3.3 × 1.0–2.6	Yellow	This study

× (0.6–) 0.7–1.1 (–1.3) μm. Conidia unicellular, subglobose to ellipsoidal, hyaline to yellow (1.6–) 2.2 (–2.8) × (1.3–) 1.7 (–2.2) μ m (**Figure 4** and **Supplementary Figure S2**).

Type: China, Jilin Province, Changbai Mountains, on litters of forest, October 2017, Li Zeyu and Liu Boyang (holotype HMPHU 1243, culture ex-type CGMCC 19143).

Gene sequences ex-holotype: MN589741 (ITS), MN589994 (LSU), MN590231 (SSU), MN908589 (TEF), MT921830 (TUB), MN917168 (RPB1a), MT921829 (RPB2a).

Sexual morph: not observed

Habitat: forest litters

Distribution: Changbai Mountains, Jilin province, China

Notes: *P. changbaiense* is compared with *P. hingganense*, *Keithomyces aciculare*, *M. flavoviride*, *Marquandomyces marquandii*, *Metarhizium frigidum*, and *Metarhizium suchlasporia*. The conidial size of *P. changbaiense* is smaller than those found in *M. flavoviride*, *M. frigidum*, and *K. aciculare*, and the color of their colonies is not white to yellow. *Ma. marquandii* differs from *P. changbaiense* by the *Paecilomyces*-like conidiophores and purplish colonies, while *M. suchlasporia* exhibits slender phialides. A detailed list of the diagnostic features and sequence similarities in comparison with related species can be found in **Table 2** and **Figure 2**.

Parametarhizium hingganense S. Gao, W. Meng, Li Xiang Zhang, Q. Yue, L. J. Xu, sp. nov.

MycoBank no.: MB 837523

Etymology: referring to the location where the type material was collected.

Description: Colonies on PDA reaching 17–18 mm in 2 weeks, yellow, radially sulcate, velvety, with undulate margin; exudate lemon yellow; reverse yellow, radially sulcate. Colonies on SDAY reaching 17–20 mm, pale yellow, wrinkled, velvety, with undulate margin; reverse brown, wrinkled. Colonies on MEA reaching 15–18 mm, lemon yellow, radially sulcate, velvety; reverse brown, radially sulcate. Colonies on OA reaching 18–19 mm, flat, initially cream, turning lemon yellow due to the production of conidial masses; reverse pale yellow.

Hyphae hyaline, septate, smooth-walled, 0.8–2.5 μm wide. Conidiophores arising from branches of aerial hyphae, bearing dense whorls of branches, terminating in branches with 2–4 phialides per branch, candelabrum-like arrangement of phialides. Phialides obpyriform (3.5–) 7.0–17.5 (–26) × (1.2–) 1.4–2.3 (–2.5) μm, with a long distinct neck, (1.6–) 2.5–7.1 (–8.5) × (0.5–) 0.6–1.1 (–1.2) μm. Conidia unicellular, subglobose to ellipsoidal, hyaline to yellow, (1.1–) 1.2 (–3.3) × (1.0–) 1.6 (–2.6) μ m (**Figure 4** and **Supplementary Figure S2**).

Type: China, Heilongjiang province, Greater Hinggan mountains, on litters of forest, September 2018, Li Zeyu and Liu Boyang (holotype HMPHU 1244, culture ex-type CGMCC 19144).

Gene sequences ex-holotype: MN055703 (ITS), MN061635 (LSU), MN055706 (SSU), MN065770 (TEF), MN061672 (TUB), MN917170 (RPB1a), MT939494 (RPB2a).

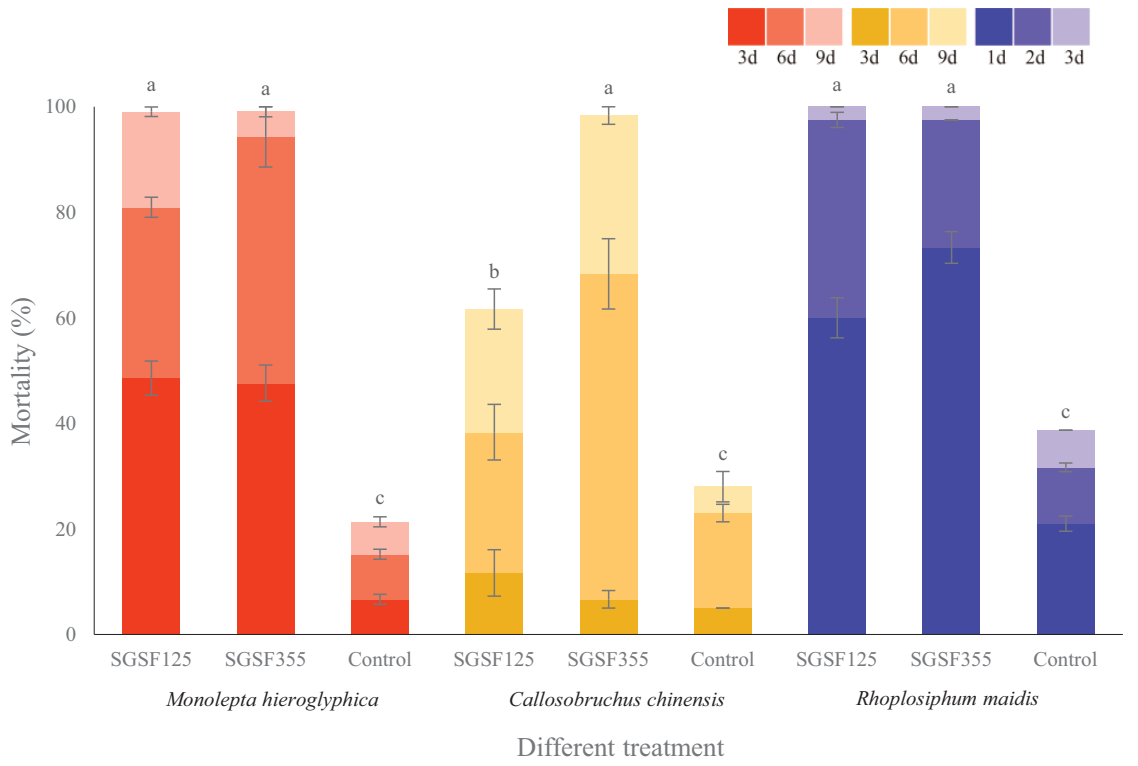


FIGURE 5 | Anti-insect activity screening of *Parametarhizium changbaiense* and *Parametarhizium hingganense* on the different day. Red columns are *Monolepta hieroglyphica*, yellow columns are *Callosobruchus chinensis,* and blue columns are *Rhopalosiphum maidis* Different letters (a, b, and c) above bars indicate significant differences at the 0.05 level.

Sexual morph: not observed

Habitat: forest litters

Distribution: Greater Hinggan mountains, Heilongjiang province, China.

Notes: *P. hingganense* is compared with *P. changbaiense*, *Keithomyces carneum*, *Ma. marquandii*, *Metarhizium globosum*, *Metarhizium minus*, and *Metarhizium blattodeae*. The phialides arrangement of *K. carneum* and *Ma. marquandii* is *Paecilomyces*-like, but *P. hingganense* possesses candelabrum-like conidiophores. The conidia of *M. blattodeae*, *M. globose*, and *M. minus* are bigger than those in *P. hingganense* and have different shapes. *P. changbaiense* and *P. hingganense* differ mainly in the shape of their phialides and colony characteristics. The phialides of *P. changbaiense* are cylindrical with a short neck, while those of *P. hingganense* are obpyriform with a long distinct neck. Colonies of *P. changbaiense* are white on PDA compared to the yellow colonies of *P. hingganense* (**Figure 4**). A detailed list of the diagnostic features and sequence similarities in comparison with related species can be found in **Table 2** and **Figure 2**.

Anti-insect Potentials of *P. changbaiense* and *P. hingganense*

Given the similarity to the core *Metarhizium*, the anti-insect abilities of *P. changbaiense* and *P. hingganense* were tested. *P. changbaiense* and *P. hingganense* were both pathogenic to *Mo. hieroglyphica*, *C. chinensis*, and *R. maidis* under laboratory conditions. The external white mycelia of *P. changbaiense* and *P. hingganense* on the cadavers of three tested insects firstly emerged from the abdomen and then gradually surrounded the insects. In contrast to green cadavers caused by most *Metarhizium* spp. such as *M. anisopliae* and *M. robertsii*, the color of cadavers caused by *P. changbaiense* and *P. hingganense* was white (**Figure 4** and **Supplementary Figure S3**). The mortality of *P. changbaiense* and *P. hingganense* to above their farmland insects was higher than 85%, and there was no significant difference between *P. changbaiense* and *P. hingganense* with the exception that *P. changbaiense* against *C. chinensis* was 61.67% (**Table 3**).

With respect to the cadaver rate, all of them were higher than 70%. The cadaver rate of *P. hingganense* to *C. chinensis* and *R. maidis* is significantly higher than that of *P. changbaiense* SGSF125. The median lethal time of *P. changbaiense* and *P. hingganense* strongly varied between the different insects but was significantly shorter than that of the control. Most of the *R. maidis* individuals died within a day after the treatment (4 days in the control), while *C. chinensis* individuals survived for around 6 days when treated with *P. hingganense* and 9 days when treated with *P. changbaiense* (11 days in the control). The effect on *Mo. hieroglyphica* was even more remarkable with a median lethal time of 3 days for both treatments compared to 11 days in the control (**Figure 5**). The results of the anti-insect assays

TABLE 3 | Mortality rates, LT_{50} (median lethal time) and cadaver rate of *Parametarhizium* spp. isolates.

Host species	Strain no.	Mortality (%)	Median lethal time (days)	Cadaver rate (%)
Monolepta hieroglyphica	*P. changbaiense*	99.05 ± 0.95a	3.13	95.56 ± 0.2a
	P. hingganense	99.05 ± 0.95a	2.92	98.89 ± 0.2a
	Control	32.38 ± 0.95c	11.17	0
Callosobruchus chinensis	*P. changbaiense*	61.67 ± 8.81b	9.41	73.33 ± 0.2c
	P. hingganense	98.33 ± 1.66a	6.37	85.00 ± 0.3b
	Control	40 ± 2.88c	10.67	0
Rhopalosiphum maidis	*P. changbaiense*	100 ± 0.00a	0.85	71.67 ± 0.2c
	P. hingganense	100 ± 0.00a	0.54	80.83 ± 0.2b
	Control	38.33 ± 2.2c	4.08	0

Different letters (a, b, and c) in the same column indicate significant differences at the 0.05 level.

implied that *P. changbaiense* and *P. hingganense* are non-host-specific entomopathogens and thus offer a biocontrol potential against farmland pests.

DISCUSSION

Although the discovery of new fungal taxa is on the rise, mycotaxonomy is still an ongoing challenge when introducing new fungal species. Jeewon and Hyde (2016) provided many recommendations for the appropriate use of phylogenetic and morphological data in species delineation, and in this study, we followed the guidelines to establish our new taxa. We proposed one new genus with two new species which are related to members of the *Metarhizium* complex (formerly *Metarhizium sensu lato*). According to the pairwise nucleotide sequence similarities for seven loci (**Figure 2**), the close relatives of *P. changbaiense* and *P. hingganense* are genus *Metarhizium* and its related genera (formerly *Metarhizium sensu lato*). Currently, the phylogenetic relationships of *Metarhizium* and its related genera are inferred based on DNA sequence analyses from multigenes (Mongkolsamrit et al., 2020). Since the related genera are not in the clade of the core *Metarhizium* forming monophyletic clades and their morphological traits are different from core *Metarhizium*, they have been renamed as other new genera, respectively, such as *Papiliomyces* and *Keithomyces* (Mongkolsamrit et al., 2020). The phylogeny shown in **Figure 3** was constructed from DNA sequence analyses of the SSU, LSU, TUB, TEF, RPB1, and RPB2 regions, which supported the current taxonomy of *Metarhizium* and its related genera erected in 2020. This phylogenetic analysis also strongly supported that *P. changbaiense* and *P. hingganense* form a monophyletic clade similar with the related genera erected in 2020 (Mongkolsamrit et al., 2020). Combined with morphological results, it is proposed that a new genus, *Parametarhizium*, is erected.

The morphological traits of *P. changbaiense* and *P. hingganense* are compared with their close species, including phialides arrangements, sizes and shapes of conidia, and colony colors (**Table 2**). The conidia of *Parametarhizium* are subglobose, and their size is smaller than that of *Metarhizium*, and the colony of *Parametarhizium* is yellow or white with the exudate compared with the green colony of *Metarhizium*. With respect to phialides arrangements, *Metarhizium* and its related genera have four kinds, candelabrum-like, *Verticillium*-like, *Paecilomyces*-like, and *Lecanicillium*-like. *Parametarhizium* is candelabrum-like. *Metapochonia* and *Pochonia* are *Verticillium*-like. *Keithomyces* and *Marquandomyces* are *Paecilomyces*-like. *Purpureomyces* and *Papiliomyces* are *Lecanicillium*-like. The conidiophores of *Sungia* erect with solitary, awl-shaped phialides. Furthermore, *Metapochonia*, *Pochonia*, *Sungia*, and *Marquandomyces* produce chlamydospores, but *Parametarhizium* on PDA, SDAY, MEA, and OA could not produce chlamydospores. In addition, the colony color of *Parametarhizium* is white to yellow, different from these close genera.

Since the conidia of *Parametarhizium* spp. are subglobose, the morphological traits of the related species producing subglobose conidia are compared and shown in **Table 2**. The conidia sizes of *Pu. khaoyaiensis*, *Pu. Maesotensis*, *Ma. marquandii* (Banihashemi, 2012) range within 2–3 × 2–3 μm and they are similar to *Parametarhizium*. However, the phialides arrangements of these four species are *Paecilomyces*-like which is different from *Parametarhizium*.

The anti-insect results implied the potentials of *P. hingganense* and *P. changbaiense* as new biocontrol agents against farmland pests. There are some reports about anti-insect activities against *C. chinensis* and *R. maidis* of the entomopathogenic fungi *B. bassiana*, *M. anisopliae,* and *Isaria fumosorosea* (Sajid et al., 2017; Khan et al., 2018). The mortality of *R. maidis* caused by *P. hingganense* and *P. changbaiense* is similar to *M. anisopliae* and higher than the others. To the best of our knowledge, no related studies about anti-insect activity of entomopathogenic fungi against *Mo. hieroglyphica* are published so far. Therefore, the two entomopathogens, *P. hingganense* and *P. changbaiense*, are the first fungal species reported to show anti-insect activity against *Mo. hieroglyphica.*

DATA AVAILABILITY STATEMENT

The datasets presented in this study can be found in online repositories. The names of the repository/repositories and accession number(s) can be found in the article/**Supplementary Material**.

AUTHOR CONTRIBUTIONS

SG isolated fungi, built up the phylogenetic tree, investigated anti-insect bioassay, and wrote the manuscript. WM designed the experiments, wrote the manuscript, and provided partial funding. LZ identified and provided insects. QY did the chemical analyses and revised the manuscript. XZ collected the insects. LX designed the experiments, identified the fungal isolates, wrote the manuscript, and provided partial funding. All authors discussed the results.

FUNDING

This work was funded by the National Natural Science Foundation of China (No. 31870528), the Natural Science Foundation of Heilongjiang Province (QC2015033), and Open Fund (No. 20200522-4) of Key Laboratory of Saline-alkali Vegetation Ecology Restoration, Ministry of Education (Northeast Forestry University).

ACKNOWLEDGMENTS

We appreciate Dr. Eric Kuhnert's help with the revision of manuscript and for his valuable suggestions.

SUPPLEMENTARY MATERIAL

The Supplementary Material for this article can be found online at: https://www.frontiersin.org/articles/10.3389/fmicb.2021.627744/full#supplementary-material

REFERENCES

Aly, A. H., Debbab, A., and Proksch, P. (2011). Fifty years of drug discovery from fungi. *Fungal Divers.* 50, 3–19. doi: 10.1007/s13225-011-0116-y

Banihashemi, Z. (2012). First report of *Paecilomyces marquandii* from Iran. *Rostaniha* 13, 207–210.

Bills, G. F., Christensen, M., Powell, M., and Thorn, G. (2004). "Saprobic soil fungi," in *Biodiversity of Fungi: Inventory and Monitoring Method*, eds G. M. Mueller, G. F. Bills, and M. S. Foster (Burlington, MA: Elsevier), 271–302.

Bischoff, J., Rehner, S., and Humber, R. (2006). *Metarhizium frigidum* sp. nov.: a cryptic species of *M. anisopliae* and a member of the *M. flavoviride* complex. *Mycologia* 98, 737–745. doi: 10.1080/15572536.2006.11832645

Bischoff, J., Rehner, S., and Humber, R. (2009). A multilocus phylogeny of the *Metarhizium anisopliae* lineage. *Mycologia* 101, 512–530. doi: 10.3852/07-202

Brunner-Mendoza, C., Reyes-Montes, M., Moonjely, S., Bidochka, M., and Toriello, C. (2018). A review on the genus *Metarhizium* as an entomopathogenic microbial biocontrol agent with emphasis on its use and utility in Mexico. *Biocontrol. Sci. Techn.* 29, 83–102. doi: 10.1080/09583157.2018.1531111

Castrillo, L., Griggs, M., Ranger, C., Reding, M., and Vandenberg, J. (2011). Virulence of commercial strains of *Beauveria bassiana* and *Metarhizium brunneum* (Ascomycota: Hypocreales) against adult *Xylosandrus germanus* (Coleoptera: Curculionidae) and impact on brood. *Biol. Control* 58, 121–126. doi: 10.1016/j.biocontrol.2011.04.010

Chen, W., Han, Y., Liang, J., and Liang, Z. (2019). Morphological and phylogenetic characterization of novel *Metarhizium* species in Guizhou, China. *Phytotaxa* 419, 189–196. doi: 10.11646/phytotaxa.419.2.5

Chen, W., Han, Y., Liang, J., Liang, Z., and Jin, D. (2017). *Metarhizium dendrolimatilis*, a novel *Metarhizium* species parasitic on *Dendrolimus* sp. larvae. *Mycosphere* 8, 31–37. doi: 10.5943/mycosphere/8/1/4

Chen, Z., Xu, L., Yang, X., Zhang, Y., and Yang, Y. (2018). *Metarhizium baoshanense* sp. nov., a New entomopathogen fungus from Southwestern China. *Pak. J. Zool.* 50, 1739–1746. doi: 10.17582/journal.pjz/2018.50.5.1739.1746

Edler, D., Klein, J., Antonelli, A., and Silvestro, D. (2019). raxmlGUI 2.0 beta: a graphical interface and toolkit for phylogenetic analyses using RAxML. *bioRxiv* [Preprint]. doi: 10.1101/800912

Filizola, P. R. B., Luna, M. A. C., de Souza, A. F., Coelho, I. L., Laranjeira, D., and Campos-Takaki, G. M. (2019). Biodiversity and phylogeny of novel *Trichoderma* isolates from mangrove sediments and potential of biocontrol against *Fusarium* strains. *Microb. Cell Fact.* 18:89. doi: 10.1186/s12934-019-1108-y

Frisvad, J., and Samson, R. (2004). Polyphasic taxonomy of *Penicillium* subgenus *Penicillium*. A guide to identif cation of food and airborne terverticillate Penicillia and their mycotoxins. *Stud. Mycol.* 2004, 1–173.

Gutierrez, A., Leclerque, A., Manfrino, R., Luz, C., Ferrari, W., Barneche, J., et al. (2019). Natural occurrence in Argentina of a new fungal pathogen of cockroaches, *Metarhizium argentinense* sp. nov. *Fungal. Biol. U.K.* 123, 364–372. doi: 10.1016/j.funbio.2019.02.005

Hawksworth, D., and Lücking, R. (2017). Fungal diversity revisited: 2.2 to 3.8 million species. *Microbiol. Spectr.* 5:FUNK-0052-2016. doi: 10.1128/microbiolspec

Hussain, A., Rizwan-ul-Haq, M., Al-Ayedh, H., Ahmed, S., and Al-Jabr, A. (2015). Effect of *Beauveria bassiana* infection on the feeding performance and antioxidant defence of red palm weevil, *Rhynchophorus ferrugineus*. *BioControl.* 60, 849–859. doi: 10.1007/s10526-015-9682-3

Hyde, K. D., Xu, J., Rapior, S., Jeewon, R., Lumyong, S., Niego, A. G. T., et al. (2019). The amazing potential of fungi: 50 ways we can exploit fungi industrially. *Fungal Divers.* 97, 1–136. doi: 10.1007/s13225-019-00430-9

Hywel-Jones, N. (1994). *Cordyceps khaoyaiensis* and *C. pseudomilitaris*, two new pathogens of lepidopteran larvae from Thailand. *Mycol. Res.* 98, 939–942. doi: 10.1016/S0953-7562(09)80267-0

Jeewon, R., and Hyde, K. (2016). Establishing species boundaries and new taxa among fungi: recommendations to resolve taxonomic ambiguities. *Mycosp.* 7, 1669–1677. doi: 10.5943/mycosphere/7/11/4

Kepler, R., Humber, R., Bischoff, J., and Rehner, S. (2014). Clarification of generic and species boundaries for *Metarhizium* and related fungi through multigene phylogenetics. *Mycologia* 106, 811–829. doi: 10.3852/13-319

Khan, B., Ahmad, K., Zafar, J., Shoukat, R., and Farooq, M. (2018). Efficacy of different entomopathogenic fungi on biological parameters of pulse beetle *Callosobruchus chinensis* L. (Coleoptera: Bruchidae). *J. Entomol. Zool. Stud.* 6, 1972–1976.

Kumar, S., Stecher, G., and Tamura, K. (2016). MEGA7: molecular evolutionary genetics analysis version 7.0 for bigger datasets. *Mol Biol Evol.* 33, 1870–1874. doi: 10.1093/molbev/msw054

Liang, J., Liu, B., Li, Z., Meng, W., Wang, Q., and Xu, L. (2019). *Myxotrichum albicans*, a new slowly-growing species isolated from forest litters in China. *Mycoscience* 60, 232–236. doi: 10.1016/j.myc.2019.03.002

Luangsa-ard, J. J., Mongkolsamrit, S., Thanakitpipattana, D., Khonsanit, A., Tasanathai, K., Noisripoom, W., et al. (2017). *Clavicipitaceous entomopathogens*: new species in *Metarhizium* and a new genus *Nigelia*. *Mycol. Prog.* 16, 369–391. doi: 10.1007/s11557-017-1277-1

Metchnikoff, E. (1879). *Maladies des Hannetons Duble. Zapiski Imperatorskogo Obshchestua Sel'skago Khozyaistra Yuzhnoi Rossii*. Odessa: Elsevier, 17–50.

Meyling, N., and Eilenberg, J. (2007). Ecology of the entomopathogenic fungi *Beauveria bassiana* and *Metarhizium anisopliae* in temperate agroecosystems: potential for conservation biological control. *Biol. Control.* 43, 145–155. doi: 10.1016/j.biocontrol.2007.07.007

Mongkolsamrit, S., Khonsanit, A., Thanakitpipattana, D., Tasanathai, K., Noisripoom, W., Lamlertthon, S., et al. (2020). Revisiting *Metarhizium* and the description of new species from Thailand. *Stud. Mycol.* 95, 171–251. doi: 10.1016/j.simyco.2020.04.001

Nishi, O., Shimizu, S., and Sato, H. (2017). *Metarhizium bibionidarum* and *M. purpureogenum*: new species from Japan. *Mycol. Prog.* 16, 987–998. doi: 10.1007/s11557-017-1333-x

Noble, R., Dobrovin-Pennington, A., Fitzgerald, J., Dew, K., Wilson, C., Ross, K., et al. (2018). Improving biocontrol of black vine weevil (*Otiorhynchus sulcatus*) with entomopathogenic fungi in growing media by incorporating spent mushroom compost. *BioControl.* 63, 697–706. doi: 10.1007/s10526-018-9877-5

Rogerson, C. T. (1970). The hypocrealean fungi (*Ascomycetes*, *Hypocreales*). *Mycologia* 62, 865–910. doi: 10.1080/00275514.1970.12019033

Ronquist, F., Teslenko, M., van der Mark, P., Ayres, D. L., Darling, A., Höhna, S., et al. (2012). MrBayes 3.2: efficient Bayesian phylogenetic inference and model choice across a large model space. *Syst. Biol.* 61, 539–542. doi: 10.1093/sysbio/sys029

Sajid, M., Bashir, N., Batool, Q., Munir, I., Ameen, M., and Munir, S. (2017). In-vitro evaluation of biopesticides (*Beauveria bassiana*, *Metarhizium anisopliae*, *Bacillus thuringiensis*) against mustard aphid *Lipaphis erysimi* kalt. (Hemiptera: Aphididae). *J. Entomol. Zool. Stud.* 5, 331–335.

Schardl, C. L., Young, C. A., Hesse, U., Amyotte, S. G., Andreeva, K., Calie, P. J., et al. (2013). Plant-symbiotic fungi as chemical engineers: multi-genome analysis of the clavicipitaceae reveals dynamics of alkaloid loci. *PLoS Genet.* 9:e1003323. doi: 10.1371/journal.pgen.1003323

Sung, G. H., Hywel-Jones, N. L., Sung, J. M., Luangsa-ard, J. J., Shrestha, B., and Spatafora, J. W. (2007a). Phylogenetic classification of *Cordyceps* and the clavicipitaceous fungi. *Stud. Mycol.* 57, 5–59. doi: 10.3114/sim.2007.57.01

Sung, G. H., Sung, J. M., Hywel-Jones, N. L., and Spatafora, J. W. (2007b). A multi-gene phylogeny of *Clavicipitaceae* (Ascomycota, Fungi): identification of localized incongruence using a combinational bootstrap approach. *Mol. Phylogenet. Evol.* 44, 1204–1223. doi: 10.1016/j.ympev.2007.03.011

Tulloch, M. (1976). The genus *Metarhizium*. *Trans. Br. Mycol. Soc.* 66, 407–411. doi: 10.1016/S0007-1536(76)80209-4

Tzean, S., Hsieh, L., Chen, J., and Wu, W. (1993). *Nomuraea cylindrospora* comb. Nov. *Mycologia* 85, 514–519. doi: 10.1080/00275514.1993.12026302

Wijayawardene, N. N., Hyde, K. D., Dai, D. Q., Tang, L. Z., Aptroot, A., Castañeda-Ruiz, R. F., et al. (2020). A dynamic portal for a community-driven, continuously updated classification of Fungi and fungus-like organisms: outlineoffungi.org. *Mycosphere* 11, 1514–1526. doi: 10.5943/mycosphere/11/1/11

Willis, K. J. (ed.) (2018). *State of the World's Fungi 2018. Report*. London: Royal Botanic Gardens.

Wu, S., Sarkar, S., Lv, J., Xu, X., and Lei, Z. (2020). Poor infectivity of *Beauveria bassiana* to eggs and immatures causes the failure of suppression on *Tetranychus urticae* population. *BioControl* 65, 81–90. doi: 10.1007/s10526-019-09970-0

Zimmermann, G. (1993). The entornopathogenic fungus *Metarhizium anisopliae* and its potential as a biocontrol agent. *Pestic. Sci.* 37, 375–379. doi: 10.1002/ps.2780370410

Zimmermann, G. (2007). Review on safety of the entomopathogenic fungus *Metarhizium anisopliae*. *Biocontrol Sci. Techn.* 17, 879–920. doi: 10.1080/09583150701593963

Conflict of Interest: The authors declare that the research was conducted in the absence of any commercial or financial relationships that could be construed as a potential conflict of interest.

Copyright © 2021 Gao, Meng, Zhang, Yue, Zheng and Xu. This is an open-access article distributed under the terms of the Creative Commons Attribution License (CC BY). The use, distribution or reproduction in other forums is permitted, provided the original author(s) and the copyright owner(s) are credited and that the original publication in this journal is cited, in accordance with accepted academic practice. No use, distribution or reproduction is permitted which does not comply with these terms.

frontiers in Microbiology

ORIGINAL RESEARCH
published: 09 March 2021
doi: 10.3389/fmicb.2021.647920

Inonotus rickii (Agaricomycetes, Hymenochaetaceae) in Brazilian Cerrado: Expanding Its Geographic Distribution and Host List

Lucas Leonardo-Silva[1], Ahmed M. Abdel-Azeem[2] and Solange Xavier-Santos[1]*

[1] Basic, Applied and Scientific Dissemination Micology Laboratory (FungiLab), Goiás State University, Anápolis, Brazil,
[2] Department of Botany and Microbiology, Faculty of Science, Suez Canal University, Ismailia, Egypt

Inonotus rickii (Pat.) Reid (Agaricomycetes: Hymenochaetaceae) is a poroid fungus characterized by the expressive production of chlamydospores, *in vivo* and *in vitro*, especially during its anamorphic stage. The species plays important ecological roles, standing out as a phytopathogen, affecting several species of ornamental and wild trees, mainly in tropical and subtropical regions. The infected trees develop canker and white rot of the wood, showing symptoms of reduced vegetative vigor and decline of leaves and branches which causes death in some cases. The first record of *I. rickii* for the Cerrado biome (Brazilian Savanna) and the first record as causal agent of canker in *Schinus molle* L. in Brazil is reported here. In addition, we present a checklist of its worldwide geographical distribution and known hosts, from an extensive bibliographic search in Google Scholar, SciELO, Scopus, and Web of Science databases. The species is widespread in tropical and subtropical zones; common in the American continent, especially in Central and South America and the Mediterranean region, and rare in temperate zones. We found specimens growing in both living and dead hosts, totalizing 70 species of hosts, distributed in 43 genera and 22 families. Of these, *Acer negundo* L. (10.5%), *Celtis australis* L. (6.5%), and *Platanus acerifolia* (Aiton) Willd. (4.8%), and the Fabaceae (30%), Fagaceae (10%), and Sapindaceae (8.6%) families were the most frequent. We present morphological descriptions and illustrations, as well as the growth characteristics in culture medium. Our study expands the known geographical distribution of *I. rickii*, including the Cerrado biome, as well as its structural, physiological characteristics, and its hosts.

Keywords: Brazilian Savanna, Canker, decay, phytopathogen, poroid fungi

OPEN ACCESS

Edited by:
Dhanushka Nadeeshan Wanasinghe, Key Laboratory for Plant Diversity and Biogeography of East Asia, Kunming Institute of Botany, Chinese Academy of Sciences, China

Reviewed by:
Zheng Wang, Yale University, United States
Yu Pei Tan, Department of Agriculture and Fisheries, Queensland Government, Australia

****Correspondence:***
Lucas Leonardo-Silva
lucasleonardo@outlook.com; lucasleo.bio@gmail.com

Specialty section:
This article was submitted to Evolutionary and Genomic Microbiology, a section of the journal Frontiers in Microbiology

Received: *30 December 2020*
Accepted: *15 February 2021*
Published: *09 March 2021*

Citation:
Leonardo-Silva L, Abdel-Azeem AM and Xavier-Santos S (2021) Inonotus rickii (Agaricomycetes, Hymenochaetaceae) in Brazilian Cerrado: Expanding Its Geographic Distribution and Host List. Front. Microbiol. 12:647920. doi: 10.3389/fmicb.2021.647920

INTRODUCTION

Inonotus rickii (Pat.) Reid is a poroid fungus that belongs to the family Hymenochaetaceae, class Agaricomycetes. It was described in South America in 1896 as *Ptychogaster cubensis* Pat., from a review of specimens from Cuba by Patouillard (1896). However, in 1908, the author observed that the species should be the anamorphic stage of a poroid fungus collected by Ricki in Brazil, recognized as *Xanthochrous rickii* Pat. (Patouillard, 1908); later the nomenclature was changed to *Polyporus rickii* (Pat.) Sacc. and Trotter (Saccardo and Trotter, 1912). In 1957, the species was recognized by Reid as *I. rickii* (Reid, 1957), currently accepted nomenclature, and its anamorphic stage as *P. cubensis*.

The relationship between the two life stages of the species has been confirmed by experimental studies carried by Davidson et al. (1942) and Stalpers (2000) and by molecular analysis of specimens collected from different geographical origins (Gottlieb et al., 2002; De Simone et al., 2011). *I. rickii* has a wide distribution in tropical, subtropical, and Mediterranean zones (Mazza et al., 2008; Ramos et al., 2008), where it is frequently found in trees in urban environments, mainly in its anamorphic stage (Mazza et al., 2008), which is considered a potential phytopathogen.

As a pathogen of woody plants, *I. rickii* infects branches and stems, causing canker and wood decay (Mazza et al., 2008; Annesi et al., 2010; De Simone et al., 2011). Adhesion and colonization of the substrate occurs due to the degradation of wood components, especially cellulose, hemicellulose and lignin, due to taxon enzymatic activity (Robles et al., 2014). When parasitizing the host, *I. rickii* can reach the heartwood, sapwood, and cambium, as well as provoke deep lesions resulting from the death of the bark tissues, characterizing the canker (Ramos et al., 2008; Annesi et al., 2010). Infected trees may show reduced vegetative growth, crown and branches decline and sparse foliage, which leads, in some cases, to death (Mazza et al., 2008; Ramos et al., 2008; Annesi et al., 2010).

The knowledge of this species-host began with reports describing the presence of a powdery mass of abundant ferruginous chlamydospores, which characterizes the anamorphic stage of the taxon in different plant hosts, but without mentioning its pathogenicity (Davidson et al., 1942). However, in the beginning of 2000, the diseases symptoms and pathological aspects became more evident in Europe. In Italy, the species was recorded in public gardens and wooded boulevards on *Acer negundo* L. and *Albizia julibrissin* Durazz. (Mazza et al., 2008; Annesi et al., 2010), and in Portugal, on *Celtis australis* L. (Ramos et al., 2008) causing serious damage or death of tree. Other reports in Chile (Sepúlveda et al., 2016), China (Cui et al., 2014), and Egypt (Shehata and Abdel-Wahab, 2013) also presented a similar situation regarding *Schinus molle* L., *Acacia richii*, A. Gray, *Citrus* spp. and *Vitis* spp. respectively. Based on the morphology of the basidiome and species of the host plants, the fungus called by different popular names e.g., "mapúa cheap," which means "mascarilla de la mapúa," in the Wayuu indigenous community of Colombia (Villalobos et al., 2017), or "Florcita de espinillo," "Florcita de molle," "Florcita de palo," "Hongo de espinillo," "Hongo de molle," and "Hongo de palo," in La Paz, Córboda, Argentina (Flamini et al., 2015).

In Brazil, information on *I. rickii* is mystery or fragmented and restricted to the holotype with unknown localities (Patouillard, 1908) and to occurrence records in the Caatinga biomes, on *Spondias* sp. (Umbuzeiro) (Drechsler-Santos et al., 2013; Maia et al., 2015); Atlantic Forest and Pampa without host identification (Campos-Santana and Loguercio-Leite, 2010; Maia et al., 2015). Here we report for the first time *I. rickii* in the Cerrado biome, which constitutes the first record of this species causing canker disease in *S. molle*. In addition, we present detailed morphological descriptions of both anamorphic and teleomorphic stages supported with illustrations, and updated checklist of its worldwide geographical distribution and known hosts up till now.

MATERIALS AND METHODS

Study Area

Samples were collected during the period from 2001 to 2020 in three conservation units of the Cerrado biome: the Estação Ecológica do Noroeste Paulista (EENP) (20°50′55″ S, 49°26′53″ W), located between the municipalities of São José do Rio Preto and Mirassol, São Paulo; the Floresta Nacional (FLONA) de Silvânia (16°38′30″ S, 48°39′02″ W), located in the municipality of Silvânia, Goiás; the Parque Estadual Altamiro de Moura Pacheco (PEAMP) (16°33′12″ S, 49°8′50″ W), inserted in the municipalities of Goianápolis, Goiânia and Nerópolis, Goiás, and urban areas (16°19′38″ S, 48°57′11″ W) in the municipality of Anápolis, Goiás, which are surrounded by several Cerrado fragments (**Figure 1**).

The Brazilian Cerrado is considered the richest savanna in the world and is the dominant biome in the Central Plateau of Brazil which covers part of the North, Northeast, South, and Southeast regions, representing approximately 25% of the country's territory. The Cerrado characterized by a rainy tropical climate, with high temperatures in summer and dry winter, this biome is known for its diverse landscapes represented by a vegetation mosaic, which includes forest, savanna, and grassland formations, where trees, shrubs, and undergrowth predominate, respectively (Klink and Machado, 2005; Ribeiro and Walter, 2008; WWF, 2015). Despite its great diversity, only 61% of the original Cerrado vegetation remains preserved (Sano et al., 2010). Sampling of our target species occurred in mesophilic forest (semideciduous dry forest) in which there is a predominance of tree species and canopy formation, occurring in interfluves and rich soil presented different levels of deciduous vegetation in the dry season (Ribeiro and Walter, 2008).

Morphological Characterization

Collected samples were dried at 40°C in oven and deposited in the Herbarium of the Universidade Estadual de Goiás (HUEG) and the Universidade Estadual Paulista (SJRP). Micro and macrophenotypic identification of basidiomata were carried out according to the relevant identification keys. For macroscopic characterization, the shape, consistency, color, dimension, and number of pores per mm of basidiomata were considered. For the description of the microscopic criteria, cross sections through the basidiomata in distilled water and 3% KOH were microscopically examined. Hyphal structure, hymenial setae, setal hyphae, basidia, basidiospores, and chlamydospores and their ornaments were examined according to Ryvarden (2004, 2005) and Ramos et al. (2008). Melzer reagent was used to test the amyloid reaction of the microstructures (Kirk et al., 2008). All microscopic criteria were observed by Olympus CX31 optical microscope (1000×) magnification, and the measurements were performed using the Piximètre software version 5.10 R 1541 (Henriot and Cheype, 2017). Abbreviations used for measurements of basidiospores and chlamydospores are: Q = quotient between length and width, Qm = medium value of Q and, N = number of measured structures. All

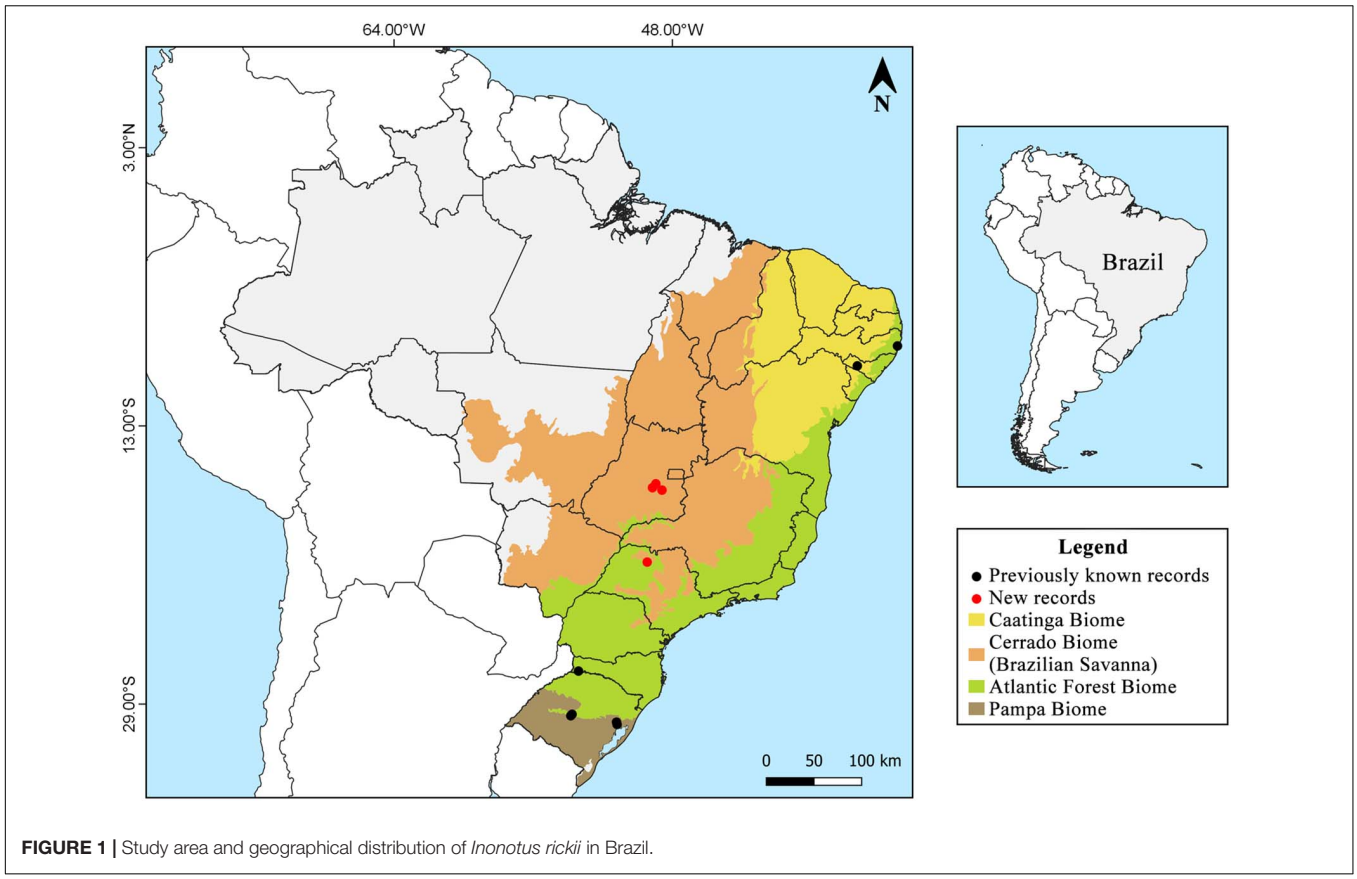


FIGURE 1 | Study area and geographical distribution of *Inonotus rickii* in Brazil.

photographs and measurements were made using 3% KOH as mounting medium. The color indication for all evaluated characters was based on Kornerup and Wanscher color cards (Kornerup and Wansher, 1978).

Fresh collected samples were plated out on potato dextrose agar (PDA) supplemented with 0.025 g/ml^{-1} of chloramphenicol as bactericidal and incubated in a BOD incubator at 25°C. Recovered colonies were characterized based on macro (shape, color, texture, and presence of exudates) and micromorphological criteria (hyphae, setal hyphae, and chlamydospores) according to relevant identification keys. The cultures were preserved according to Castellani (1963) and deposited in the collection of fungal cultures of the Laboratório de Micologia Básica, Aplicada e Divulgação Científica (FungiLab) of the Universidade Estadual de Goiás, Brazil.

Checklist of Geographical Distribution and Hosts

We collected the data from an extensive bibliographic search of Google Scholar[1], SciELO[2], Scopus[3], and Web of Science[4] by using different keywords: "*Inonotus rickii*" OR "*Polyporus rickii*" OR "*Ptychogaster cubensis*" OR "*Xanthochrous rickii*." Our data included all published articles, books, chapters, and abstracts available for access. For the worldwide geographical distribution of the species, we consider the specific location described by the authors and the geographic coordinates; when not available, they were obtained using the Latlong coordinate system (Latitude and Longitude Finder, 2020). The geographic distribution map was constructed using the Quantum GIS software (QGIS Development Team, 2020) and the climatic classification was determined between the North and South zones of both hemispheres as: tropical between 23°27′, subtropical 23°27′ and 46°54′, temperate 46°54′ and 66°33′, and polar 66°33′ and 90°, respectively (Peel et al., 2007; Eccles et al., 2019).

For the host checklist, we considered the absolute frequency the number of times the species was reported and relative frequency the quotient between the absolute frequency and the total of citations. The system of nomenclature, hierarchical classification and the name authority of the plant species followed The plant list (The Plant List, 2020).

[1] scholar.google.com.br
[2] www.scielo.org
[3] www.scopus.com
[4] www.webofknowledge.com

RESULTS

Taxonomic Treatment

Inonotus rickii (Pat.) D. A. Reid, Kew Bull. [12](2): 141 (1957). (**Figures 2**, **3**).

≡ *Xanthochrous rickii* Pat., Bull. Soc. Mycol. France 24(1): 6 (1908).



FIGURE 2 | *Inonotus rickii*. **(A)** Basidiome (HUEG 12067). **(B)** Anamorphic stage (HUEG 12062). **(C)** Chlamydospores attached to setal hyphae. **(D)** Generative hyphae, hyaline with simple septate (arrow). **(E)** Hymenial setae. **(F)** Setal hyphae and abundant chlamydospores. **(G)** Basidia hyaline, with projection of four sterigmatic structures and attached basidiospores. **(H)** Basidiospores. Bar = 1 cm **(A,B)**; 5 mm **(C)**; 5 μm **(D–H)**.

Description

Teleomorphic stage–basidiomata annual, 7.0–11 × 6.0–7.8 cm in size, solitary or aggregated in the form of semicircular shelves, sessile, pileate, and strongly attached to the substrate. Pileus applanate to ungulate, margin obtuse to undulate, soft and spongy consistency when fresh and firm and crumbly when dry. Pileal surface covered by a dense powdery layer formed by reddish brown chlamydospore (8D7). Pore surface also covered by chlamydospore, circular to angular pores, 2–4 pores per mm, thin and lacerated. Thick context and positive KOH reaction. Anamorphic stage–semicircular or cushion-shaped, soft and robust, velvety to the touch, reddish orange (8B8) when young and reddish brown (8E7) when mature, structured by a dense mass of chlamydospore attached to hyphae,

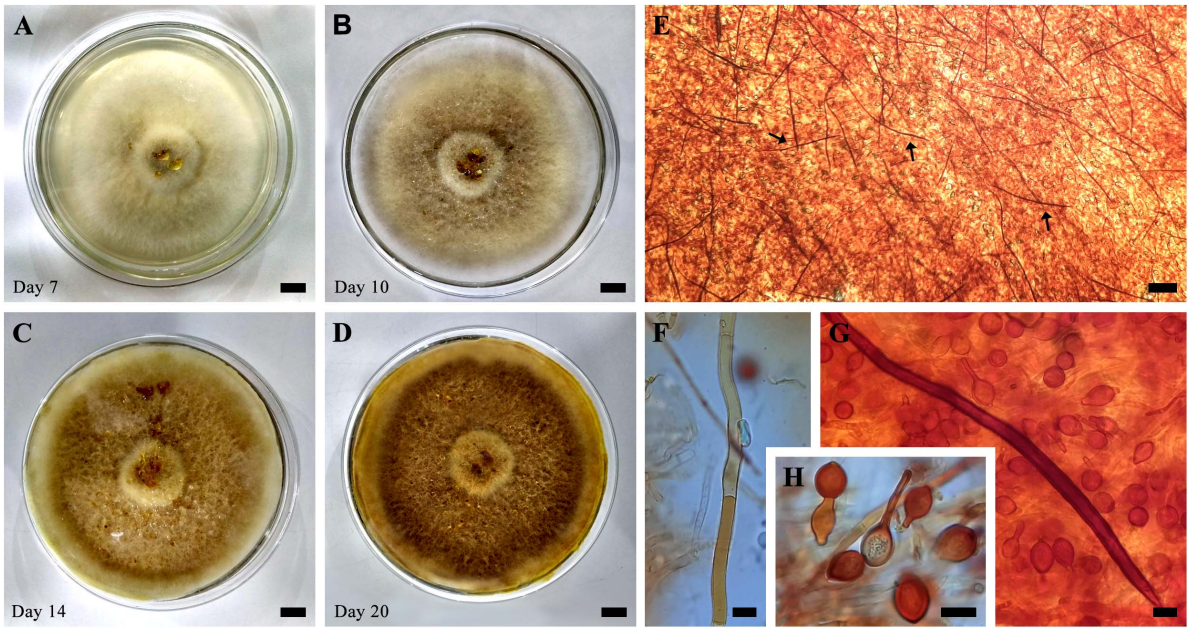


FIGURE 3 | (A–D) Evolution of growth in cultivation (SXS 37) in PDA at 25°C for 20 days. **(E)** Mycelial trama showing abundant setal hyphae (arrows). **(F)** Generative hyphae. **(G)** Setal hyphae and chlamydospores. **(H)** Chlamydospores. Bar = 1 cm **(A–D)**; 100 μm **(E)**; 10 μm **(F–H)**.

forming a structure similar to capillitium, which facilitates dispersion by anemophilia.

Hyphal system monomitic, with generative hyphae, hyaline, septate, ranging from brownish yellow (5C7) to brownish orange (6C8), thin-walled to thick-walled, occasionally branched, 3.0–6.6 μm in diam. Setal hyphae abundant in context, lanceolate, yellowish brown (5D5), thick-walled with a large lumen, with pointed apex, occasionally parallel to the hymenium, 8–20 μm in diam. and 110–200 μm long. Hymenial setae abundant, ventricular to subulate, dark brown (6F8), 14.3–63 × 5.0–18.4 μm, with thick-walled. Basidia hyaline, clavate to cylindric, 10 × 6.5 μm, with projection of four sterigmatic structures. Basidiospores abundant, subglobose to ellipsoid, (5.4) 5.9–8.7 (9.5) × (3.6) 4.3–6.2 (6.5) μm [Q = (1) 1.2–1.6 (2.1), Qm = 1.4, N = 50], golden yellow (5B7) to yellowish brown (5D5), dark brown (6F3), inamyloid, smooth with thick-walled. Chlamydospores abundant in the context, inamyloid, irregular, globose to subglobose, (7.4) 9.1–13.7 (15.5) × (6.9) 8.0–11.6 (13.9) μm [Q = 1.0–1.3 (1.9), Qm = 1.1, N = 50], orange (6A8) to reddish orange (7A8), dark brown (6F3), smooth with thick-walled.

In culture presents velutinous to cottony mycelium, occupying the entire length of the petri dish (90 × 15 mm) in 2 weeks of cultivation, yellowish white (2A2) when young, becoming grayish yellow (4B4) to dark yellow (4C8) when mature, production of exudates in the form of reddish orange droplets (8A8). Abundant production of chlamydospores of various shapes, occasionally attached to setal hyphae, also abundant and parallel in the hyphalic trama. The color and size characteristics of the cultures' microstructures are in accordance with those observed in the basidiomata.

Worldwide Geographical Distribution

Widespread in tropical and subtropical zones, considered then pantropical; common on the American continent, especially in Central and South America and the Mediterranean region, rare in temperate zones. There are records of the species in Argentina, Bahamas, Bermuda Islands, Brazil, Chile, China, Colombia, Costa Rica, Cuba, Egypt, France, Greece, Guadeloupe, Guinea, Haiti, India, Iran, Israel, Italy, Jamaica, Martinique, Mexico, Montenegro, Morocco, Myanmar, Pakistan, Paraguay, Peru, Philippines, Portugal, South Africa, Spain, Taiwan, United States, and Uruguay (**Figure 4**; Seaver and Waterston, 1946; Jaquenoud, 1985; Kotlaba and Pouzar, 1994; Chang and Fu, 1998; Stalpers, 2000; Gottlieb et al., 2002; Melo et al., 2002; Ryvarden, 2005; Martínez, 2006; Mata et al., 2007; Ghobad-Nejhad and Kotiranta, 2008; Annesi et al., 2010; Campos-Santana and Loguercio-Leite, 2010; Ţura et al., 2010; De Simone et al., 2011; Ouabbou et al., 2012; Shehata and Abdel-Wahab, 2013; Valenzuela et al., 2013; Cui et al., 2014; García et al., 2014a; Robles et al., 2015a; Sepúlveda et al., 2016; Villalobos et al., 2017; Maubet, 2020; Tchoumi et al., 2020). **Table 1** show detailed description of the species' worldwide geographic distribution, which contains the exact sampling location of each specimen described in the literature data found.

Geographical Distribution in Brazil

There are records in the Atlantic Forest areas in Pernambuco, Rio Grande do Sul and Santa Catarina, Caatinga areas in Alagoas and Bahia (record not shown in **Figure 1**, as the specific location was not found), Pampa areas in Rio Grande do Sul, and Cerrado areas (present study) in Goiás and São Paulo (**Figure 1**; Campos-Santana and Loguercio-Leite, 2010; Maia et al., 2015).

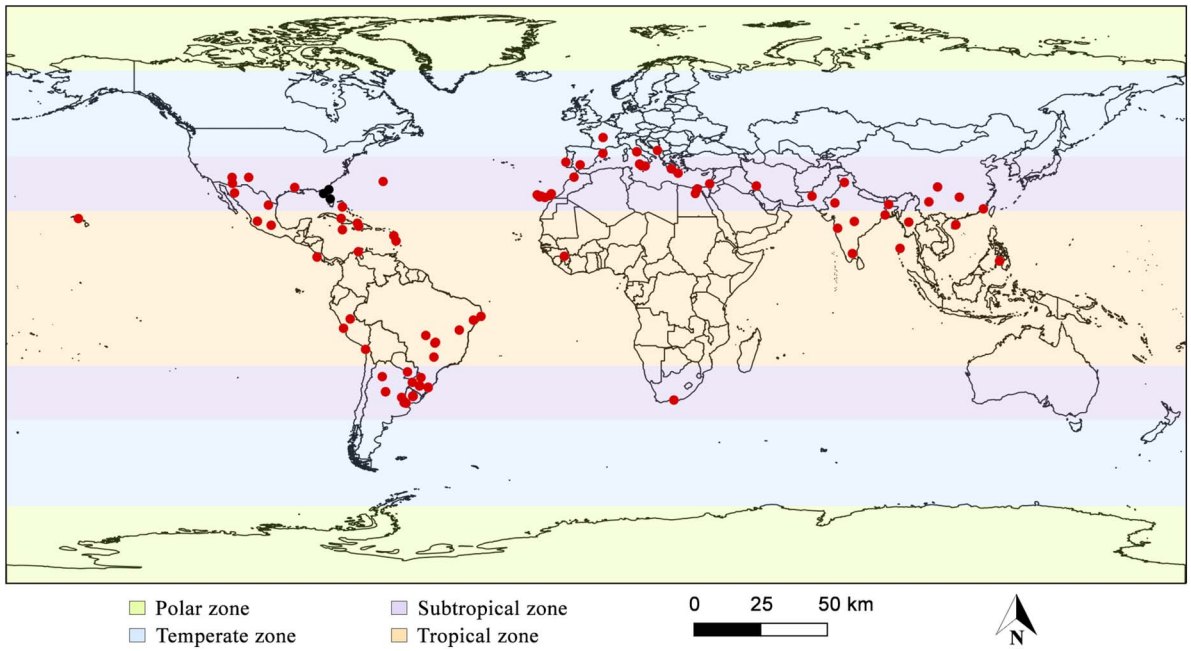


FIGURE 4 | Global geographical distribution of *Inonotus rickii*. Black dots highlight samples that may belong to another species, according to De Simone et al. (2011) and Cui et al. (2014).

Habitat and Substrate

We collect our specimens in the mesophilic forest in both stages of life, on dead wood and an unknown living host, and in urban areas in the anamorphic stage on living and dead *S. molle* trees. In the data set listed in the present review, we found 70 plant species distributed in 43 genera and 22 families (**Table 2**). Of these hosts, *A. negundo* (representing 10.5% of the total species), *C. australis* 6.5% and *Platanus acerifolia* 4.8%. On the family level Fabaceae came first by accounted 30% out of all host families followed by Fagaceae (10%) and Sapindaceae (8.6%). In the checklist, the host species referred as sp. or spp., were accounted for as a single species. **Table 2** presents a complete list of *I. rickii* hosts.

Material Examined

BRAZIL. São Paulo: São José do Rio Preto-Mirassol, Estação Ecológica do Noroeste Paulista, 13/XI/2001, *Xavier-Santos, S. (SJRP 28714)*, teleomorphic stage, found growing on fragment of dead wood, unknown host, isolated in culture with voucher number *SXS 37*; Goiás: Silvânia, Floresta Nacional de Silvânia, 26/VI/2009, Xavier-Santos, S. (*HUEG 13945*), anamorphic stage, growing on living tree, unknown host; Goianápolis-Goiânia-Nerópolis, Parque Estadual Altamiro de Moura Pacheco, 08/VIII/2014, *Xavier-Santos, S. (HUEG 12067)*, teleomorphic stage, found growing on living tree, unknown host; Anápolis, urban area, 20/III/2011, *Xavier-Santos, S. (HUEG 13944)*, anamorphic stage, growing on living tree, unknown host; Parque Ipiranga, 19/IX/2018, *Leonardo-Silva, L. (HUEG 12062)*, anamorphic stage, growing on a dead ornamental tree of *S. molle*, isolated in culture with voucher number *SXS 641*; ibid, 05/XII/2018, *Leonardo-Silva, L. (HUEG 11993)*, anamorphic stage, growing on living *S. molle*; ibid, 27/V/2019, *Leonardo-Silva, L. (HUEG 12063)*, anamorphic stage, growing on dead *S. molle*; ibid, 09/V/2020, *Leonardo-Silva, L. (HUEG 12994)*, anamorphic stage, growing on living *S. molle*; ibid, 09/V/2020, *Leonardo-Silva, L. (HUEG 12996)*, anamorphic stage, growing on dead *S. molle*; ibid, 09/V/2020, *Leonardo-Silva, L. (HUEG 12997)*, anamorphic stage, growing on living *S. mole*; ibid, 10/XI/2020, *Leonardo-Silva, L. (HUEG 13946)*, anamorphic stage, growing on dead *S. mole*.

Examined Reference Material

BRAZIL. Rio Grande do Sul: Santa Maria, 11/I/1993, *Gilberto Coelho (24–9) (ICN 097679)*; Alagoas: São José da Tapera, 17/VI/2008, *Drechsler-Santos (6) (URM 80418)*, on living tree, unknown host; ibid, 17/VI/2008, *Drechsler-Santos (21) (URM 80460)*, growing on living tree of *Spondias* sp. (Umbuzeiro); ibid, 17/VI/2008, *Drechsler-Santos (18) (URM 80582)*, an unknown living tree.

Comments

The morphological characteristics observed in collected samples coincide with those described by many authors (Gottlieb et al., 2002; Melo et al., 2002; Ryvarden, 2005). Measurements of setal hyphae recorded by Ryvarden (2005) and Campos-Santana and Loguercio-Leite (2010) were up to 250 μm or more long. Although these measurements are similar to our samples, we recorded smaller hyphal setae ranged between 110 and 200 μm in the examined materials and pure cultures. *I. rickii* is similar to *Inonotus patouillardii* (Rick) Imazeki in the field but differentiating itself by the abundant presence of chlamydospores. Our specimens were collected during both rainy

TABLE 1 | Referenced literature for the global geographical distribution of *Inonotus rickii*.

Country	Locality	References
Argentina	Acassuso, Buenos Aires Province	Gottlieb et al., 2002
	Argentina (location not specified)	Intini, 1988
	Buenos Aires City	Gottlieb et al., 2002; Mielnichuk and Lopez, 2007; Robles et al., 2011, 2012, 2015a,b
	Buenos Aires Province	Gottlieb et al., 2002
	Córdoba, Córdoba Province	Urcelay et al., 2012
	Gualeguay, Entre Ríos Province	Gottlieb et al., 2002
	La Plata, Buenos Aires Province	Gottlieb et al., 2002; Wright and Alberto, 2006; Murace et al., 2019
	Llavallol, Buenos Aires Province	Gottlieb et al., 2002
	Lomas de Zamora, Buenos Aires Province	Gottlieb et al., 2002
	Martínez, Buenos Aires Province	Gottlieb et al., 2002
	Rosario del Tala, Entre Ríos Province	Gottlieb et al., 2002
	Santo Tomé, Corrientes Province	Gottlieb et al., 2002
	Tucumán Province	Gottlieb et al., 2002
	Valle de Traslasierra, Córdoba Province	Flamini et al., 2015
	Yacanto, Córdoba Province	Gottlieb et al., 2002
Bahamas	Bahamas (location not specified)	Intini, 1988; Ryvarden, 2005
	Nassau	Davidson et al., 1942
Bermuda Islands	Bermuda Islands (location not specified)	Seaver and Waterston, 1946
Brazil	Anápolis, Goiás	Present study
	Bahia	Davidson et al., 1942; Stalpers, 2000
	Brazil (location not specified)	Davidson et al., 1942; Ryvarden, 1983; Intini, 1988
	Goiânia, Goiás	Present study
	Ipojuca, Pernambuco	Maia et al., 2015
	Mondaí, Santa Catarina	Campos-Santana and Loguercio-Leite, 2010
	Porto Alegre, Rio Grande do Sul	Campos-Santana and Loguercio-Leite, 2010
	Santa Maria, Rio Grande do Sul	Campos-Santana and Loguercio-Leite, 2010
	São José da Tapera, Alagoas	Drechsler-Santos et al., 2013
	São José do Rio Preto-Mirassol, São Paulo	Present study
Chile	Arica, Arica Province	Sepúlveda et al., 2016
China	Hainan Province	Cui et al., 2009; Dai et al., 2010; Yuan et al., 2015
	Jianyang, Sichuan Province	Zheng et al., 2011
	Panzhihua, Sichuan Province	Chen et al., 2014; Cui et al., 2014
Colombia	Uribia, Guajira	Villalobos et al., 2017
Costa Rica	Puntarenas, Cóbano	Mata et al., 2007
Cuba	Cuba (location not specified)	Murrill, 1919; Intini, 1988; Stalpers, 2000
Egypt	Beni Suef Province	Shehata and Abdel-Wahab, 2013
	Giza Province	Shehata and Abdel-Wahab, 2013
	Qalubyia Province	Shehata and Abdel-Wahab, 2013
France	France (location not specified)	Ryvarden, 2005
Greece	Crete, Iráklion	Kotlaba and Pouzar, 1994
	Monemvasia, Laconia	De Simone et al., 2011
Guadeloupe	Guadeloupe (location not specified)	Jaquenoud, 1985; Intini, 1988
Guinea	Guinea (location not specified)	Jaquenoud, 1985; Intini, 1988
Haiti	Haiti (location not specified)	Davidson et al., 1942; Intini, 1988
	Tortuga Island	Davidson et al., 1942
India	Andaman and Nicobar Islands, Manjari	Sharma and Mishra, 2015
	Calcutta, West Bengal	Davidson et al., 1942
	Dindigul, Tamil Nadu	Mowna Sundari et al., 2018
	India (location not specified)	Intini, 1988; Ryvarden, 2005
	Jodhpur, Rajasthan	Singh et al., 2013
	Pune, Maharashtra	Jagtap et al., 2018
	Western and Eastern Himalaya	Sharma and Mishra, 2015
Iran	Khuzestan Province	Ghobad-Nejhad and Kotiranta, 2008
Israel	Tel Aviv	Ţura et al., 2010
Italy	Catania, Sicily	Intini, 1988; Annesi et al., 2005, 2010; De Simone et al., 2011
	Palermo, Sicily	Jaquenoud, 1985; Venturella and Raimondo, 2004; Annesi et al., 2005, 2010; Venturella et al., 2006; De Simone et al., 2011
	Roma	Annesi et al., 2003, 2010, 2005; Mazza et al., 2008; De Simone et al., 2011
	Sicily	Ryvarden, 2005
Jamaica	Jamaica (location not specified)	Jaquenoud, 1985; Intini, 1988
Martinique	Fort-de-France	David and Rajchenberg, 1985; Jaquenoud, 1985; Intini, 1988
Mexico	Jalisco	Valenzuela et al., 2013
	Mexico City	Valenzuela et al., 2013
	Nuevo León	Valenzuela et al., 2013
	Sonora	Esqueda et al., 2010; Valenzuela et al., 2013
	Sonoran Desert, Nacapule Canyon	Raymundo et al., 2013
Montenegro	Budva	Kotlaba and Pouzar, 1994
Morocco	Forest of Mamora	Ouabbou et al., 2012
	Morocco (location not specified)	Intini, 1988

TABLE 1 | Continued

Country	Locality	References
	Lima	Davidson et al., 1942
Myanmar	Myanmar (location not specified)	Jaquenoud, 1985; Intini, 1988
Pakistan	Pakistan (location not specified)	Jaquenoud, 1985; Intini, 1988
Paraguay	San Lorenzo	Maubet, 2020
Peru	Peru (location not specified)	Intini, 1988; Ryvarden, 2005
Philippines	Mindanao	Gottlieb et al., 2002
Portugal	Lisboa	Melo et al., 2002; Ramos et al., 2008
South Africa	Knysna, Western Cape Province	Tchoumi et al., 2017, 2020
Spain	Barcelona	De Simone et al., 2011
	Canary Islands, Rosa del Taro	García et al., 2014a
	Córdoba	De Simone et al., 2011
	Gran Canaria, Canary Islands	Vergara et al., 2016
	La Gomera, Canary Islands	García et al., 2014b
	La Palma, Canary Islands	García et al., 2014b
	Lanzarote, Canary Islands	García et al., 2014b
	Seville	Intini, 2002a,b; Intini and Tello, 2003
	Spain (location not specified)	Intini, 2002b
	Tenerife, Canary Islands	García et al., 2014b
Taiwan	Kinmen County	Chang and Fu, 1998
United States	Arizona	Gilbertson et al., 1974; Ryvarden, 2004, 2005
	Florida	Davidson et al., 1942; Gilbertson and Ryvarden, 1986; Intini, 1988; Barnard, 1993; Ryvarden, 2004, 2005
	Hawaii (location not specified)	Intini, 1988
	Hawthorne, Florida*	De Simone et al., 2011
	Jacksonville, Florida*	De Simone et al., 2011
	Levy County, Florida*	De Simone et al., 2011
	Louisiana	Davidson et al., 1942; Gilbertson and Ryvarden, 1986; Intini, 1988; Ryvarden, 2004, 2005
	New Mexico	Sanogo and Lujan, 2018
	Oahu, Hawaii	Davidson et al., 1942
	Tucson, Arizona	Gilbertson and Ryvarden, 1986
Uruguay	Uruguay (location not specified)	Martínez, 2006

**Records of uncertain identification, according to De Simone et al. (2011) and Cui et al. (2014).*

and drought periods which reflected the resistance to the climatic variations of the Cerrado.

DISCUSSION

Our study expands and shed the light on the geographic distribution of the species with special reference to the Cerrado biome and updated list of plant hosts. *I. rickii* is easily described by the massive production of chlamydospores *in vitro* and *in vivo*,

TABLE 2 | Checklist of hosts of *Inonotus rickii* reported in the literature.

Family	Host species	AF	RF (%)
Adoxaceae	*Sambucus nigra* L. (Kotlaba and Pouzar, 1994; Annesi et al., 2003, 2005; De Simone et al., 2011)	4	3.2
Anacardiaceae	*Lithraea molleoides* (Vell.) Engl. (Flamini et al., 2015)	1	0.8
	Pistacia atlantica Desf. (Vergara et al., 2016)	1	0.8
	Schinus areira L. (Urcelay et al., 2012)	1	0.8
	Schinus molle L. (Intini, 1988, 2002b**; Annesi et al., 2003; Intini and Tello, 2003**; García et al., 2014a; Sepúlveda et al., 2016)	5	4.0
	Spondias sp. (Drechsler-Santos et al., 2013)	1	0.8
Altingiaceae	*Liquidambar styraciflua* L. (Nakasone, 1993)	1	0.8
Casuarinaceae	*Casuarina cunninghamiana* Miq. (Gottlieb et al., 2002)	1	0.8
	Casuarina equisetifolia L. (Valenzuela et al., 2013)	1	0.8
	Casuarina spp. (Gilbertson and Ryvarden, 1986; Wright and Alberto, 2006)	2	1.6
Cannabaceae	*Celtis australis* L. (Kotlaba and Pouzar, 1994; Gottlieb et al., 2002; Intini, 2002b**; Melo et al., 2002; Annesi et al., 2003, 2015; Intini and Tello, 2003**; Mazza et al., 2008; Ramos et al., 2008)	8	6.5
	Celtis iguanaea (Jacq.) Sarg. as *Celtis ehrenbergiana* (Klotzsch) Liebm. (Urcelay et al., 2012)	1	0.8
	Celtis spinosa Spreng. (Gottlieb et al., 2002)	1	0.8
	Celtis tala Gillies ex Planch. (Wright et al., 1988, unpublished; Gottlieb et al., 2002)	2	1.6
	Celtis sp. (Wright and Alberto, 2006)	1	0.8
Euphorbiaceae	*Hevea brasiliensis* (Willd. ex A. Juss.) Müll. Arg. (Cui et al., 2009; Dai et al., 2010)	2	1.6
Fabaceae	*Acacia caven* (Molina) Molina (Flamini et al., 2015)	1	0.8
	Acacia koa A. Gray (Davidson et al., 1942)	1	0.8
	Acacia melanoxylon R. Br. (Gottlieb et al., 2002)	1	0.8
	Acacia praecox Griseb. (Urcelay et al., 2012)	1	0.8
	Acacia richii A. Gray (Cui et al., 2014)	1	0.8
	Acacia visco Griseb. (Urcelay et al., 2012)	1	0.8
	Albizia julibrissin Durazz. (Annesi et al., 2007; Mazza et al., 2008)	2	1.6
	Albizia lebbeck (L.) Benth. (Ghobad-Nejhad and Kotiranta, 2008)	1	0.8
	Albizia sp. (Pieri and Rivoire, 1996)	1	0.8
	Cercidium sp. (Gilbertson and Ryvarden, 1986)	1	0.8
	Delonix regia (Hook.) Raf. (Tura et al., 2009; Ţura et al., 2010; Jagtap et al., 2018; Maubet, 2020)	4	3.2
	Gleditsia sinensis Lam. (Zheng et al., 2011)	1	0.8
	Haematoxylon brasiletto H. Karst (Villalobos et al., 2017)	1	0.8
	Parkinsonia aculeata L. (Gilbertson et al., 1974; Jaquenoud, 1985)	2	1.6

(Continued)

TABLE 2 | Continued

Family	Host species	AF	RF (%)
	Parkinsonia praecox (Ruiz and Pav.) Hawkins (Villalobos et al., 2017)	1	0.8
	Parkinsonia spp. (Jaquenoud, 1985, 1987; Gilbertson and Ryvarden, 1986; Ryvarden and Gilbertson, 1993; Annesi et al., 2003)	5	4.0
	Prosopis cineraria (L.) Druce (Singh et al., 2013)	1	0.8
	Prosopis juliflora (Sw.) DC. (Singh et al., 2013; Villalobos et al., 2017)	2	1.6
	Robinia pseudoacacia L. (Mazza et al., 2008; De Simone et al., 2011; Annesi et al., 2015)	3	2.4
	Styphnolobium japonicum (L.) Schott (Urcelay et al., 2012)	1	0.8
	Tamarindus indica L. (Davidson et al., 1942; David and Rajchenberg, 1985**; Jaquenoud, 1987**)	2	1.6
Fagaceae	*Quercus laevis* Walter as *Quercus catesbaei* Michx. (Davidson et al., 1942)	1	0.8
	Quercus cerris L. (Annesi et al., 2005; Fodor and Hâruta, 2016)	2	1.6
	Quercus laurifolia Michx. (Gilbertson and Ryvarden, 1986)	1	0.8
	Quercus nigra L. (Davidson et al., 1942)	1	0.8
	Quercus phellos L. (Davidson et al., 1942)	1	0.8
	Quercus sp. (Gilbertson and Ryvarden, 1986)	1	0.8
	Quercus geminata Small as *Quercus virginiana* var. *geminata* (Small) Sarg. (Davidson et al., 1942)	1	0.8
Icacinaceae	*Apodytes dimidiata* E. Mey. ex Arn. as *Apodytes dimidiata* subsp. *dimidiata* (Tchoumi et al., 2017)	1	0.8
Juglandaceae	*Carya illinoinensis* (Wangenh.) K. Koch (Sanogo and Lujan, 2018)	1	0.8
Malvaceae	*Chorisia* spp. (Urcelay et al., 2012)	1	0.8
	Brachychiton sp. (Murace et al., 2019)	1	0.8
Moraceae	*Ficus carica* L. (Michailides, 2003)	1	0.8
	Morus spp. (Urcelay et al., 2012)	1	0.8
Myricaceae	*Morella cerifera* (L.) Small as *Myrica cerifera* L. (Davidson et al., 1942; Seaver and Waterston, 1946; Gilbertson and Ryvarden, 1986; De Simone et al., 2011*)	4	3.2
	Myrica sp. (Gilbertson and Ryvarden, 1986)	1	0.8
Oleaceae	*Fraxinus* sp. (Valenzuela et al., 2013)	1	0.8
	Olea capensis subsp. *macrocarpa* (C. H. Wright) I. Verd. (Tchoumi et al., 2017**Tchoumi et al., 2020**)	1	0.8
Platanaceae	*Platanus acerifolia* (Aiton) Willd. (Mazza et al., 2008; Robles et al., 2011, 2012, 2015a,b; Annesi et al., 2015)	6	4.8
	Platanus × *hispanica* Mill. ex Münchh as *Platanus* × *hybrida* Brot. (Intini, 2002b; Intini and Tello, 2003)	1	0.8
	Platanus spp. (Gottlieb et al., 2002; Intini and Tello, 2003; Wright and Alberto, 2006)	3	2.4
Rhamnaceae	*Ziziphus spina-christi* (L.) Desf. (Ghobad-Nejhad and Kotiranta, 2008)	1	0.8
Rutaceae	*Citrus* spp. (Shehata and Abdel-Wahab, 2013)	1	0.8
Salicaceae	*Dovyalis caffra* (Hook.f. & Harv.) Sim as *Aberia caffra* Hook.f. & Harv. (Annesi et al., 2005)	1	0.8
Sapindaceae	*Acer negundo* L. (Pegler, 1967; Wright et al., 1988; unpublished; Gottlieb et al., 2002; Intini, 2002a**Intini, 2002b**; Annesi et al., 2003, 2010, 2005; Intini and Tello, 2003**; Venturella and Raimondo, 2004; Venturella et al., 2006; Wright and Alberto, 2006; Mazza et al., 2008; De Simone et al., 2011; Murace et al., 2019)	13	10.5
	Acer saccharinum L. (Gilbertson and Ryvarden, 1986)	1	0.8
	Acer sp. (Gottlieb et al., 2002)	1	0.8
	Koelreuteria paniculata Laxm. (Annesi et al., 2007; Mazza et al., 2008)	2	1.6
	Melicoccus bijugatus Jacq. (Pegler, 1967)	1	0.8
	Sapindus saponaria L. (Melo et al., 2002)	1	0.8
Ulmaceae	*Ulmus* sp. (Murace et al., 2019)	1	0.8
Verbenaceae	*Aloysia citriodora* Palau as *Lippia citriodora* (Palau) Kunth (Gottlieb et al., 2002)	1	0.8
	Lippia sp. (Wright and Alberto, 2006)	1	0.8
Vitaceae	*Vitis* spp. (Shehata and Abdel-Wahab, 2013)	1	0.8

Absolute frequency (AF) = number of times that species was cited (n = 125); relative frequency (RF) = percentage of citations of the species in relation to the total of host species found.
**Records of uncertain identification, according to De Simone et al. (2011) and Cui et al. (2014).*
***Articles that present the same data.*

mainly in the anamorphic stage, and the presence of setal hyphae in the context (Pegler, 1964; Melo et al., 2002; Ramos et al., 2008; Tura et al., 2009; Maubet, 2020). In all of our specimens we observe these characteristics. Furthermore, the taxonomic criteria observed in pure cultures are compatible with those described by Ramos et al. (2008) and Tura et al. (2009).

Inonotus rickii is considered one of the most nocive basidiomycete in urban trees (Ramos et al., 2008), parasitizing a large number of hosts, thus being able to form an effective biological corridor in the dissemination of the pathogen in this environment (Annesi et al., 2010). The infection of these trees has a great impact in some regions of the world, as ornamental trees when parasitized and with symptoms of the disease, lose their ornamental value and represent a great danger to other members of the population (Ramos et al., 2008).

In Europe, especially in Italy (Annesi et al., 2010) and Portugal (Ramos et al., 2008), it has been reported that canker caused in plant tissues has reduced the number of ornamental tree species in urban environments. In addition, in the Wayuu indigenous community in Colombia, it has been reported that the fungus has had an impact on local native vegetation, also parasitizing species of daily use, such as *Parkinsonia praecox*



FIGURE 5 | *Inonotus rickii* in its anamorphic stage on *Schinus molle*. **(A–C)** Fruiting projecting between the bark, bark and heartwood of dead tree. **(D)** Initial projection of the fruiting body on living tree. **(E)** Powdery, rust-colored coating on the wood, which was formed by the deposition of chlamydospores when removing fruiting; it is also possible to observe the lesions (arrows) caused by the infection along the trunk. Bar = 2 cm.

and *Haematoxylon brasiletto*, used for resin and paint extraction, respectively (Villalobos et al., 2017).

The most frequent host species of *I. rickii* are widely known as ornamental trees. However, some of the reported hosts are used as a food source (Barolo et al., 2014; Viveros Garciìa et al., 2018) or for extracting compounds for different applications (Sharma et al., 2018; Milena et al., 2019). This warns of the need to know the impact of *I. rickii* on species of local, regional and worldwide economics.

Our specimens were detected growing at the base of the stem and on main branches of living and dead trees, usually in the anamorphic stage. Only specimens SJRP 28714 and HUEG 12067 were sampled in their teleomorphic stage. Although the species produces reproductive structures in both stages of the life cycle, the teleomorphic phase occurs occasionally, with the anamorphic stage usually frequent (Mazza et al., 2008; Ramos et al., 2008).

The propagation of the species occurs mainly by the production and release of chlamydospores, which are more abundant in the anamorphic phase. At this stage, a structure sensitive to touch appears, which releases a large number of chlamydospores. On this occasion, in urban environments, dispersal is facilitated by tactile gardening activities in the maintenance of squares and parks, by anemophilia, by the contact of insects and other animals, including the flux of human traffic (Annesi et al., 2010). We observed that all specimens collected in an urban area (HUEG 11993, 12062, and 12063) were in the anamorphic stage and the dispersion of chlamydospores may have been facilitated by the activities mentioned before. Infection and development of the fungus occur when its spores (basidiospores or chlamydospores) are deposited on susceptible hosts, preferably due to the presence of dead wounds, scars, or fragments; these spores then germinate and promote the growth of the fungus within wood tissues (Phillips and Burdekin, 1989).

In the present study, we report for the first time occurrence of *I. rickii* on *S. molle* in Brazil. The fungus was found either as saprobic or as a pathogen, causing canker of the host plant. Belonging to the Anacardiaceae family, *S. molle* is an arboreal and perennial species, popularly known as pepper tree, pink pepper, American pepper, false pepper, aroeira salsa (Brazil) or aroeira mansa (Brazil). It is native to South America, but it was introduced and naturalized in several regions of the world, mainly as an ornamental in urban environments. Its great popularity as a cultivated plant is associated with its high tolerance to water and temperature availability, high growth rate and medicinal properties (Kramer, 1957; Goldstein and Coleman, 2004; Habte et al., 2020).

Anamorphic samples infected *S. molle* (HUEG 11993, 12062, and 12063) were developed over the trunk and main branches of the living and dead host. We observed that the individuals growing in the dead host (HUEG 12062 and 12063) occupied a large extension of the wood between the bark and bark, projecting over the crevices of the stem and reaching to the heart (**Figure 5**). On the other hand, samples that grew on a living host (HUEG 11993), initial canker development was observed, possibly due to the time of maturity of the fungus that was in the early stages of development (**Figure 5**). The presence of *I. rickii* in this plant has already been reported in Portugal (Melo et al., 2002), Chile, and Spain (Intini and Tello, 2003; Sepúlveda et al., 2016).

Parallel to studies of phytopathological interest, *I. rickii* has also been the subject of studies to prospect for secondary metabolites and lignocellulolytic enzymes involved in attacking the host and degrading the constituents of wood (Xavier-Santos et al., 2004; Tura et al., 2009; Chen et al., 2014), aiming, above all, at an option sustainable in the bioremediation of recalcitrant compounds. The species is also associated with cultural events in the Wayuu indigenous community, Colombia, in which women apply a layer of chlamydospores to their face, previously treated with sheep tallow to protect themselves from solar radiation (Villalobos et al., 2017). Moreover, taxonomic and phylogenetic aspects are still performed, specially to understand its anamorphic stage.

Although molecular studies carried on different samples confirmed the relationship between anamorphic and teleomorphic phases of *I. rickii*. A preliminary phylogenetic analysis of samples (anamorphic and teleomorphic) collected from different geographical origins showed came from Florida, United States, were separated from those came from Asia, South America and Europe (De Simone et al., 2011; Cui et al., 2014). An interesting aspect to consider that all species from the Florida were collected in the anamorphic stage and the teleomorphic stage has never been recorded in North America. These results suggest the existence of two possible distinct species and are reinforced by morphophysiological, ecological data and climatic conditions (De Simone et al., 2011; Cui et al., 2014). However, studies that analyze isolates from North America and other regions, as well as the holotype of both stages of life, are necessary to confirm the distinction.

CONCLUSION

Our study expands the knowledge of geographical distribution of *I. rickii*, including the Cerrado biome, as well as of its structural, physiological characteristics, and its hosts. Although common in tropical and subtropical regions, the specimens described here constitute the first documented records of the species for the Brazilian Cerrado and for the Midwest and Southeast regions, in addition to the first report on *S. molle* within Brazil. The checklist of hosts provided may assist in the development of practices for the control of the pathogen in urban areas with a high incidence of infections. Therefore, it should be mentioned here that, although the present study adds new data to information concerning *I. rickii*, this updated checklist must be considered as a provisional one always waiting for continuous supplementation.

DATA AVAILABILITY STATEMENT

The original contributions presented in the study are included in the article/supplementary material, further inquiries can be directed to the corresponding author/s.

AUTHOR CONTRIBUTIONS

LL-S and SX-S designed this study, collected and analyzed the samples, and wrote the manuscript text. LL-S prepared the figures and tables. AA-A reviewed and edited the manuscript. All authors have read and approved to the published version of the manuscript.

FUNDING

This study was financed in part by the Coordenação de Aperfeiçoamento de Pessoal de Nível Superior – Brasil (CAPES) – Finance Code 001 (Convênio n° 817164/2015 CAPES/PROAP).

ACKNOWLEDGMENTS

We are grateful to the Coordenação de Aperfeiçoamento de Pessoal de Nível Superior (CAPES), for the Ph.D. scholarship provided to the LL-S; to the administration of EENP, PEAMP, and Silvânia's FLONA for the support and authorization for collections in the area; to the To the ICN and URM herbaria, for lending material for comparative studies; to Hunter Lee Daniel, for reviewing the English language in the manuscript.

REFERENCES

Annesi, T., Bressanin, D., Coppola, R., Mazza, G., and Motta, E. (2007). Osservazioni su *Inonotus rickii* in alberate cittadine. *Micol. Ital.* 36, 39–43.

Annesi, T., Calienno, L., Picchio, R., De Simone, D., and Lo Monaco, A. (2015). Degradation of some technological features in the wood of ornamental species caused by *Inonotus rickii* (Pat.) Reid. *Drewno* 58, 5–18. doi: 10.12841/wood.1644-3985.136.01

Annesi, T., Coppola, R., D'Amico, L., and Motta, E. (2005). First report of *Aberia caffra* and *Quercus cerris* as hosts of *Inonotus rickii*. *Plant Dis.* 89:107. doi: 10.1094/PD-89-0107C

Annesi, T., Coppola, R., and Motta, E. (2003). Decay and canker caused by *Inonotus rickii* spreading on more urban tree species. *For. Pathol.* 33, 405–412. doi: 10.1046/j.1437-4781.2003.00340.x

Annesi, T., D'Amico, L., Bressanin, D., Motta, E., and Mazza, G. (2010). Characterization of Italian isolates of *Inonotus rickii*. *Phytopathol. Mediterr.* 49, 301–308. doi: 10.14601/Phytopathol_Mediterr-8402

Barnard, E. L. (1993). *Inonotus rickii* (Anamorph: *Ptychogaster cubensis*): a wood-decaying fungus of importance to Florida. *Plant Pathol. Circ.* 10–12.

Barolo, M. I., Ruiz Mostacero, N., and López, S. N. (2014). *Ficus carica* L. (Moraceae): an ancient source of food and health. *Food Chem.* 164, 119–127. doi: 10.1016/j.foodchem.2014.04.112

Campos-Santana, M., and Loguercio-Leite, C. (2010). Austro-American lignocellulolytic basidiomycetes (Agaricomycotina): new records. *Mycotaxon* 114, 377–392. doi: 10.5248/114.377

Castellani, A. (1963). Further researches on the long viability and growth of many pathogenic fungi and some bacteria in sterile distilled water. *Mycopathol. Mycol. Appl.* 20, 1–6. doi: 10.1007/BF02054872

Chang, T., and Fu, C.-S. (1998). Studies on eight species of polypores from Taiwan. *Fungal Sci.* 13, 75–83.

Chen, H.-P., Dong, W.-B., Feng, T., Yin, X., Li, Z.-H., Dong, Z.-J., et al. (2014). Four new sesquiterpenoids from fruiting bodies of the fungus *Inonotus rickii*. *J. Asian Nat. Prod. Res.* 16, 581–586. doi: 10.1080/10286020.2014.925451

Cui, B. K., Yu, C. J., and Li, H. J. (2009). Two species of *Inonotus* (Hymenochaetaceae) new to China. *For. Res.* 22, 784–787.

Cui, B. K., Zhao, C. L., Vlasák, J., and Dai, Y. C. (2014). A preliminary report on decay and canker of *Acacia richii* caused by *Inonotus rickii* in China. *For. Pathol.* 44, 82–84. doi: 10.1111/efp.12088

Dai, Y. C., D'Amico, L., Motta, E., and Annesi, T. (2010). First report of *Inonotus rickii* causing canker and decay on *Hevea brasiliensis* in China. *Plant Pathol.* 59, 806–806. doi: 10.1111/j.1365-3059.2009.02253.x

David, A., and Rajchenberg, M. (1985). Pore fungi from French Antilles and Guiana. *Mycotaxon* 22, 285–325.

Davidson, R. W., Campbell, W. A., and Weber, G. F. (1942). *Ptychogaster cubensis*, a wood-decaying fungus of southern oaks and waxmyrtle. *Mycol. Soc. Am.* 34, 142–153. doi: 10.1080/00275514.1942.12020885

De Simone, D., D'Amico, L., Bressanin, D., Motta, E., and Annesi, T. (2011). Molecular characterization of *Inonotus rickii*/*Ptychogaster cubensis* isolates from different geographic provenances. *Mycol. Prog.* 10, 301–306. doi: 10.1007/s11557-010-0702-5

Drechsler-Santos, E. R., Gibertoni, T. B., Calvacanti, M. A., de, Q., Ryvarden, L., and Góes-Neto, A. (2013). "Basidiomycota polypores - orelhas de pau," in *Guide to the Common Fungi of the Semiarid Region of Brazil*, eds M. A. Neves, I. Baseia, E. R. Drechsler-Santos, and A. Góes-Neto (Florianópolis: Tecc Editora).

Eccles, R., Zhang, H., and Hamilton, D. (2019). A review of the effects of climate change on riverine flooding in subtropical and tropical regions. *J. Water Clim. Chang.* 10, 687–707. doi: 10.2166/wcc.2019.175

Esqueda, M., Coronado, M., Gutierrez, A., Valenzuela, R., Chacón, S., Gilbertson, R. L., et al. (2010). "Hongos," in *Diversidad Biológica de Sonora*, eds F. E. M. Freaner and T. R. Van Devender (Mexico: BMC Public Health), 496.

Flamini, M., Robledo, G. L., and Suárez, M. E. (2015). Nombres y clasificaciones de los hongos según los campesinos de La Paz (Valle de Traslasierra, Córdoba, Argentina). *Bol. Soc. Argent. Bot.* 50, 265–289. doi: 10.31055/1851.2372.v50.n3.12518

Fodor, E., and Hâruta, O. (2016). *Quercus Robur*, *Q. Cerris* and *Q. Petraea* as hot spots of biodiversity. *J. Plant Dev.* 23, 187–210.

García, V. J. E., Inchaurtieta, E. B., Martín, L. C., López-Quintanilla, J. F., Rodríguez-Cabrera, C. C., and Vergara, J. I. V. (2014a). Dos nuevos hongos para la isla de Fuerteventura. *Majorensis* 10, 29–36.

García, V. J. E., Romero, D. B., Cabrera, C. C. R., and Godoy, S. J. (2014b). "Revisión y actualización de la biota fúngica de la isla de Fuerteventura," in *Proceedings of the XXI Coloquio de Histo- ria Canario-Americana (2014)*, (Casa de colon).

Ghobad-Nejhad, M., and Kotiranta, H. (2008). The genus *Inonotus* sensu lato in Iran, with keys to *Inocutis* and *Mensularia* worldwide. *Ann. Bot. Fenn.* 45, 465–476. doi: 10.5735/085.045.0605

Gilbertson, R. L., Martin, K. J., and Lindsey, J. P. (1974). *Annotated Check List and Host Index for Arizona Wood-Rotting Fungi*. Tucson, AZ: University of Arizona.

Gilbertson, R. L., and Ryvarden, L. (1986). *North American Polypores*. Oslo: Fungiflora.

Goldstein, D. J., and Coleman, R. C. (2004). *Schinus molle* L. (Anacardiaceae) Chicha production in the Central Andes. *Econ. Bot.* 58, 523–529. doi: 10.1663/0013-0001(2004)058[0523:SMLACP]2.0.CO;2

Gottlieb, A. M., Wright, J. E., and Moncalvo, J. M. (2002). *Inonotus* s. l. in Argentina – morphology, cultural characters and molecular analyses. *Mycol. Prog.* 1, 299–313. doi: 10.1007/s11557-006-0028-5

Habte, G., Nedi, T., and Assefa, S. (2020). Antimalarial activity of aqueous and 80% methanol crude seed extracts and solvent fractions of *Schinus molle* Linnaeus (Anacardiaceae) in *Plasmodium berghei* -Infected mice. *J. Trop. Med.* 2020:9473250. doi: 10.1155/2020/9473250

Henriot, A., and Cheype, J. L. (2017). *Pixiмètre, la Measure Des Dimensions Sur Images*. Available online at: http://www.piximetre.fr/ [Accessed November 13, 2020]

Intini, M. (1988). Contributo alla conoscenza dei funghi lignicoli italiani: *Inonotus rickii* (Pat.) Reid. *Micol. Ital.* 1, 49–53.

Intini, M. (2002a). First report of *Inonotus rickii* causing canker rot on boxelder in Europe. *Plant Dis.* 86, 922–922. doi: 10.1094/PDIS.2002.86.8.922C

Intini, M. (2002b). *Inonotus rickii* found in Spain. *Micol. Veg. Mediterr.* 17, 25–30.

Intini, M., and Tello, M. (2003). Comunicación, investigaciones sobre hongos xilófagos de arboles urbanos en Europa: primera cita de *Inonotus rickii* (Pat.) Reid en España. *Bol. Sanid. Veg. Plagas* 29, 277–279.

Jagtap, N., Ranadive, K., Jagtap, P., Chaudhari, N., Thopate, P., Jagtap, P., et al. (2018). Bioactive potentials of *Inonotus rickii* (Pat.) D. A. reid from Pune. *Ajanta* 7, 184–193.

Jaquenoud, M. (1985). *Inonotus rickii*, un polypore nouveau pour la flore européenne. *Mycol. Helv.* 1, 371–391.

Jaquenoud, M. (1987). Les cellules hymèniales d' *Inonotus rickii* trouvé en Europe. *Mycol. Helv.* 2, 209–215.

Kirk, P. M., Cannon, P. F., Minter, D. W., and Stalpers, J. A. (2008). *Dictionary of the Fungi*, 10th Edn. Wallingford: CABI.

Klink, C. A., and Machado, R. B. (2005). A conservação do Cerrado brasileiro. *Megadiversidade* 1, 147–155. doi: 10.1590/S0100-69912009000400001

Kornerup, A., and Wansher, J. H. (1978). *Handbook of Colour*, 3rd Edn. London: Eyre Methuen.

Kotlaba, F., and Pouzar, Z. (1994). Two new localities of *Inonotus rickii* in Europe. *Czech Mycol.* 47, 159–161. doi: 10.33585/cmy.47205

Kramer, F. L. (1957). The pepper tree, *Schinus molle* L. *Econ. Bot.* 11, 322–326. doi: 10.1007/BF02903811

Latitude and Longitude Finder (2020). Available online at: https://www.latlong.net/ [Accessed March 3, 2020].

Maia, L. C., De Carvalho Júnior, A. A., Cavalcanti, L. D. H., Gugliotta, A. D. M., Drechsler-Santos, E. R., Santiago, A. L. M. D. A., et al. (2015). Diversity of brazilian fungi. *Rodriguesia* 66, 1033–1045. doi: 10.1590/2175-7860201566407

Martínez, S. (2006). The genera *Inocutis* and *Inonotus* (Hymenochaetales) in Uruguay. *Mycotaxon* 96, 1–8.

Mata, M., Ruiz-Boyer, A., Carranza, J., and Ryvarden, L. (2007). Nuevos registros de hongos poliporoides (Basidiomycetes) para Costa Rica. *Bol. Soc. Micol. Madr.* 31, 123–130.

Maubet, Y. (2020). Hymenochaetaceae from Paraguay: revision of the family and new records. *Curr. Res. Environ. Appl. Mycol.* 10, 242–261. doi: 10.5943/cream/10/1/24

Mazza, G., Moriondo, M., Motta, E., and Annesi, T. (2008). Monitoraggio fitopatologico di *Inonotus rickii* nella città di Roma e applicazioni GPS-GIS. *Forest@* 5, 160–170. doi: 10.3832/efor0523-0050160

Melo, I., Ramos, P., and Caetano, M. F. F. (2002). First record of *Inonotus rickii* (Basidiomycetes, Hymenochaetaceae) in Portugal. *Port. Acta Biol.* 20, 265–269.

Michailides, T. J. (2003). "Diseases of Fig," in *Diseases of Tropical Fruit Crops*, ed. R. C. Ploetz (Wallingford: CABI), 527.

Mielnichuk, N., and Lopez, S. E. (2007). Interaction between *Epicoccum purpurascens* and xylophagous basidiomycetes on wood blocks. *For. Pathol.* 37, 236–242. doi: 10.1111/j.1439-0329.2007.00496.x

Milena, V., Tatjana, M., Gökhan, Z., Ivana, B., Aleksandra, C., Mohammad, M. F., et al. (2019). Advantages of contemporary extraction techniques for the extraction of bioactive constituents from black elderberry (*Sambucus nigra* L.) flowers. *Ind. Crops Prod.* 136, 93–101. doi: 10.1016/j.indcrop.2019.04.058

Mowna Sundari, T., Alwin Prem Anand, A., Jenifer, P., and Shenbagarathai, R. (2018). Bioprospection of Basidiomycetes and molecular phylogenetic analysis using internal transcribed spacer (ITS) and 5.8S rRNA gene sequence. *Sci. Rep.* 8:10720. doi: 10.1038/s41598-018-29046-w

Murace, M., Luna, M. L., Robledo, G., and Perelló, A. (2019). "Pudrición del leño en los árboles urbanos," in *Problemáticas Sanitarias del Arbolado. Enfermedades presentes en La Plata. Especial referencia a las de origen fúngico*, eds A. M. Aprea and M. A. Murace (Buenos Aires: Editorial de la Universidad de La Plata), 156.

Murrill, W. A. (1919). Cuban polypores and agarics. *Mycologia* 11, 22–32. doi: 10.1080/00275514.1919.12016771

Nakasone, K. K. (1993). "Diversity of lignicolous Basidiomycetes in coarse woody debris," in *Biodiversity and Coarse Woody Debris in Southern Forests*, eds J. W. McMim, D. A. J. Crossley, and G. A. Athens (Asheville, NC: USDA Forest Service Southern Research Station), 35–39.

Ouabbou, A., El-assfouri, A., Ouazzani-Touhami, A., Benkirane, R., and Douira, A. (2012). Bibliographic catalog of the forest of Mamora (Morocco) fungal flora. *J. Anim. Plant Sci.* 15, 2200–2242.

Patouillard, N. (1896). Champignons nouveaux ou peu connus. *Bull. Soc. Bot. Fr.* 12, 132–136.

Patouillard, N. (1908). Champignons nouveaux ou peu connus. *Bull. Soc. Bot. Fr.* 24, 1–12.

Peel, M. C., Finlayson, B. L., and McMahon, T. A. (2007). Updated world map of the Köppen-Geiger climate classification. *Hydrol. Earth Syst. Sci.* 11, 1633–1644. doi: 10.5194/hess-11-1633-2007

Pegler, D. N. (1964). A survey of the genus *Inonotus* (Polyporaceae). *Trans. Br. Mycol. Soc.* 47, 175–195. doi: 10.1016/S0007-1536(64)80051-6

Pegler, D. N. (1967). Notes on Indian Hymenochaetoïdeae. *Kew Bull.* 21, 39–49. doi: 10.2307/4108418

Phillips, D. H., and Burdekin, D. A. (1989). *Diseases of Forest and Ornamental Trees*. London: MACMILLAN.

Pieri, M., and Rivoire, B. (1996). À propos de quelques polypores (Aphyllophoromycetideae) rares ou critiques récoltes récemment. I. *Bull. Soc. Mycol. Fr.* 112, 163–187.

QGIS Development Team (2020). *QGIS Geographic Information System. Open Source Geospatial Foundation Project*. Available online at: https://qgis.org/en/site/ (accessed November 13, 2020).

Ramos, A. P., Caetano, M. F., and Melo, I. (2008). *Inonotus rickii* (Pat.) Reid: an important legnicolous Basidiomycete in urban trees. *Rev. Ciênc. Agrár.* 31, 159–167. doi: 10.19084/rca.15616

Raymundo, T., Valenzuela, R., Gutiérrez, A., Coronado, M. L., and Esqueda, M. (2013). Agaricomycetes xilófagos de la planicie central del desierto sonorense. *Rev. Mex. Biodivers.* 84, 417–424. doi: 10.7550/rmb.30828

Reid, D. A. (1957). New or interesting records of Australasian Basidiomycetes: III. *Kew Bull.* 12, 127–143. doi: 10.2307/4109115

Ribeiro, J. F., and Walter, B. M. T. (2008). "As principais fitofisionomias do bioma Cerrado," in *Cerrado: Ecologia e flora*, eds S. M. Sano, S. P. Almeida, and J. F. Ribeiro (Brasília, DF: Embrapa Informação Tecnológica), 152–212.

Robles, C. A., Carmarán, C. C., and Lopez, S. E. (2011). Screening of xylophagous fungi associated with *Platanus acerifolia* in urban landscapes: biodiversity and potential biodeterioration. *Landsc. Urban Plan.* 100, 129–135. doi: 10.1016/j.landurbplan.2010.12.003

Robles, C. A., Castro, M. A., and Castro, M. A. (2014). Wood decay by *Inonotus rickii* and *Bjerkandera adusta*: a micro- and ultra-structural approach. *IAWA J.* 35, 51–60. doi: 10.1163/22941932-00000047

Robles, C. A., Lopez, S. E., and Carmarán, C. C. (2015a). Basidiomicetes endofíticos de madera en *Platanus acerifolia* (Platanaceae) de Argentina: notas y estudios de cultivo. *Bol. Soc. Argent. Bot.* 50, 437–445. doi: 10.31055/1851.2372.v50.n4.12907

Robles, C. A., Lopez, S. E., McCargo, P. D., and Carmarán, C. C. (2015b). Relationships between fungal endophytes and wood-rot fungi in wood of *Platanus acerifolia* in urban environments. *Can. J. For. Res.* 45, 929–936. doi: 10.1139/cjfr-2014-0560

Robles, C., Carmarán, C., and Lopez, S. (2012). Molecular techniques based on ITS analysis: useful tools for the identification of wood-decay Basidiomycetes in urban trees? *Kurtziana* 37, 91–108.

Ryvarden, L. (1983). Type studies in the Polyporaceae 14. species described by N. Patouillard, either alone or with other mycologists. Harvard University, Cambridge, MA.

Ryvarden, L. (2004). *Neotropical Polypores Part 1*. Oslo: Fungiflora.

Ryvarden, L. (2005). *The Genus Inonotus a Synopsis*. Oslo: Fungiflora.

Ryvarden, L., and Gilbertson, R. L. (1993). *European Polypores*. Oslo: Fungiflora.

Saccardo, P. A., and Trotter, A. (1912). Sylloge fungorum omnium hucusque cognitorum. *Bull. Soc. Bot. Fr.* 21:270.

Sano, E. E., Rosa, R., Brito, J. L. S., and Ferreira, L. G. (2010). Land cover mapping of the tropical savanna region in Brazil. *Environ. Monit. Assess.* 166, 113–124. doi: 10.1007/s10661-009-0988-4

Sanogo, S., and Lujan, P. (2018). Rarity of a fungal pathogen and a parasitic flowering plant versus the commonness of a mycorrhizal fungus in *Pecan Orchards* in New Mexico. *Plant Heal. Prog.* 19, 207–211. doi: 10.1094/PHP-05-18-0024-S

Seaver, F. J., and Waterston, J. M. (1946). Contributions to the Mycoflora of Bermuda—IV. *Mycologia* 38, 180–201. doi: 10.1080/00275514.1946.12024051

Sepúlveda, G., Huanca, W., Cárdenas, S., Belmonte, E., Torres, T., and Latorre, B. A. (2016). First report of *Inonotus rickii* causing decay and death in *Schinus molle* in Chile. *Plant Dis.* 100:2320. doi: 10.1094/PDIS-01-16-0010-PDN

Sharma, J. R., and Mishra, D. (2015). A Synoptic mycoflora of wood-rotting fungi of Andaman. *Nelumbo* 57, 135–164. doi: 10.20324/nelumbo/v57/2015/87118

Sharma, S., Sharma, S., and Vig, A. P. (2018). Antigenotoxic potential of plant leaf extracts of *Parkinsonia aculeata* L. using Allium cepa assay. *Plant Physiol. Biochem.* 130, 314–323. doi: 10.1016/j.plaphy.2018.07.017

Shehata, A. S. F., and Abdel-Wahab, F. M. (2013). First record of *Ptychogaster cubensis* causing canker and decay on citrus and grape trees in Egypt. *Egypt. J. Phytopathol.* 41, 215–216. doi: 10.21608/ejp.2013.102006

Singh, S. K., Doshi, A., Pancholy, A., and Pathak, R. (2013). Biodiversity in wood-decay macro-fungi associated with declining arid zone trees of India as revealed by nuclear rDNA analysis. *Eur. J. Plant Pathol.* 136, 373–382. doi: 10.1007/s10658-013-0172-0

Stalpers, J. A. (2000). The genus *Ptychogaster*. *Karstenia* 40, 167–180. doi: 10.29203/ka.2000.368

Tchoumi, J. M. T., Coetzee, M. P. A., Rajchenberg, M., and Roux, J. (2020). Poroid Hymenochaetaceae associated with trees showing wood-rot symptoms in the garden route national park of South Africa. *Mycologia* 112, 722–741. doi: 10.1080/00275514.2020.1753160

Tchoumi, J. M. T., Coetzee, M. P. A., Vivas, M., Rajchenberg, M., and Roux, J. (2017). Wood-rotting basidiomycetes associated with declining native trees in timber-harvesting compartments of the garden route national park of South Africa. *Austral Ecol.* 42, 947–963. doi: 10.1111/aec.12524

The Plant List (2020). *A Working List of all Plant Species*. Available online at: http://www.theplantlist.org/ [Accessed November 13, 2020]

Tura, D., Zmitrovich, I. V., Wasser, S. P., and Nevo, E. (2009). Medicinal species from genera *Inonotus* and *Phellinus* (Aphyllophoromycetideae): cultural-morphological peculiarities, growth characteristics, and qualitative enzymatic activity tests. *Int. J. Med. Mushrooms* 11, 309–328. doi: 10.1615/IntJMedMushr.v11.i3.100

Ţura, D., Zmitrovich, I. V., Wasser, S. P., and Nevo, E. (2010). Checklist of hymenomycetes (Aphyllophorales s.l.) and heterobasidiomycetes in Israel. *Mycobiology* 38:256. doi: 10.4489/MYCO.2010.38.4.256

Urcelay, C., Robledo, G., Heredia, F., Morera, G., and Montaño, F. G. (2012). *Hongos de la Madera en el Arbolado Urbano de Córdoba*, 1st Edn. Córdoba: Instituto Multidisciplinario de Biología Vegetal.

Valenzuela, R., Raymundo, T., and Cifuentes, J. (2013). El género *Inonotus* s.l. (Hymenochaetales: Agaricomycetes) en México. *Rev. Mex. Biodivers.* 84, S70–S90. doi: 10.7550/rmb.31605

Venturella, G., Bernicchia, A., and Saitta, A. (2006). Three rare lignicolous fungi from Sicily (S Italy). *Acta Mycol.* 41, 95–98. doi: 10.5586/am.2006.013

Venturella, G., and Raimondo, F. M. (2004). I funghi cariogeni delle alberature di parchi, giardini e strade 1-18. *Quad. Bot. Amb. Appl.* 15, 181–201.

Vergara, J. I. V., Quintanilla, J. F. L., Inchaurtieta, E. B., Víboras, M. L., Pérez, J. D. R., and García, V. J. E. (2016). Contribución al conocimiento de los hongos del jardín botánico canario "viera y clavijo" (Gran Canaria, Islas Canarias). (II). *Bot. Macaronésica* 29, 15–24.

Villalobos, S., Mengual, M., and Henao-Mejía, L. G. (2017). Uso de los hongos, *Podaxis pistillaris*, *Inonotus rickii* y *Phellorinia herculeana* (Basidiomycetes), por la Etnia Wayuu en la Alta Guajira Colombiana. *Etnobiología* 15, 64–73.

Viveros Garciìa, J. C., Figueroa Rodriìguez, K. A., Gallardo Loìpez, F., Garciìa Peìrez, E., Ruiz Rosado, O., and Hernaìndez Rosas, F. (2018). Sistemas de manejo y comercializacioìn de tamarindo (*Tamarindus indica* L.) en tres

municipios de Veracruz. *Rev. Mex. Cienc. Agríc.* 3, 1217–1230. doi: 10.29312/remexca.v3i6.1373

Wright, J. E., and Alberto, E. (2006). *Guia de la Region Pampeana. II. Hongos Sin Laminillas*. Buenos Aires: LOLA.

WWF (2015). *The "Big Five" of the Cerrado*. Available online at: https://www.wwf.org.br/informacoes/english/?50242/The [Accessed November 13, 2020]

Xavier-Santos, S., Carvalho, C. C., Bonfá, M., Silva, R., Capelari, M., and Gomes, E. (2004). Screening for pectinolytic activity of wood-rotting Basidiomycetes and characterization of the enzymes. *Folia Microbiol.* 49, 46–52. doi: 10.1007/BF02931645

Yuan, Y., Bian, L., Wu, F., and Si, J. (2015). Floral composition and ecology of polypores in Hainan Province. *Chinese J. Ecol.* 34, 1689–1698.

Zheng, J. J., Lin, Q., Liu, W., and He, X. S. (2011). First discovery of *Inonotus rickii* on *Gleditsia sinensis*. *Mycosystema* 30, 128–132.

Conflict of Interest: The authors declare that the research was conducted in the absence of any commercial or financial relationships that could be construed as a potential conflict of interest.

Copyright © 2021 Leonardo-Silva, Abdel-Azeem and Xavier-Santos. This is an open-access article distributed under the terms of the Creative Commons Attribution License (CC BY). The use, distribution or reproduction in other forums is permitted, provided the original author(s) and the copyright owner(s) are credited and that the original publication in this journal is cited, in accordance with accepted academic practice. No use, distribution or reproduction is permitted which does not comply with these terms.

frontiers in Microbiology

ORIGINAL RESEARCH
published: 16 March 2021
doi: 10.3389/fmicb.2021.646821

Fungal Diversity and Community Assembly of Ectomycorrhizal Fungi Associated With Five Pine Species in Inner Mongolia, China

*Yong-Long Wang[1], Xuan Zhang[1], Ying Xu[1], Busayo Joshua Babalola[2], Si-Min Xiang[1], Yan-Ling Zhao[1] and Yong-Jun Fan[1,3]**

[1] Faculty of Biological Science and Technology, Baotou Teacher's College, Baotou, China, [2] State Key Laboratory of Mycology, Institute of Microbiology, Chinese Academy of Sciences, Beijing, China, [3] School of Life Science and Technology, Inner Mongolia University of Science and Technology, Baotou, China

Ectomycorrhizal (EM) fungi play vital roles in ensuring host plants' health, plant diversity, and the functionality of the ecosystem. However, EM fungal diversity, community composition, and underlying assembly processes in Inner Mongolia, China, where forests are typically semiarid and cold-temperate zones, attract less attention. In this study, we investigated EM fungal communities from 63 root samples of five common pine plants in Inner Mongolia across 1,900 km using Illumina Miseq sequencing of the fungal internal transcribed spacer 2 region. We evaluated the impact of host plant phylogeny, soil, climatic, and spatial variables on EM fungal diversity and community turnover. Deterministic vs. stochastic processes for EM fungal community assembly were quantified using β-nearest taxon index scores. In total, we identified 288 EM fungal operational taxonomic units (OTUs) belonging to 31 lineages, of which the most abundant lineages were *Tomentella–Thelephora*, *Wilcoxina*, *Tricholoma*, and *Suillus–Rhizopogon*. Variations in EM fungal OTU richness and community composition were significantly predicted by host phylogeny, soil (total nitrogen, phosphorus, nitrogen–phosphorus ratio, and magnesium), climate, and spatial distance, with the host plant being the most important factor. β-nearest taxon index demonstrated that both deterministic and stochastic processes jointly determined the community assembly of EM fungi, with the predominance of stochastic processes. At the Saihanwula site selected for preference analysis, all plant species (100%) presented significant preferences for EM fungi, 54% of abundant EM fungal OTUs showed significant preferences for host plants, and 26% of pairs of plant species and abundant fungal OTUs exhibited remarkably strong preferences. Overall, we inferred that the high diversity and distinctive community composition of EM fungi associated with natural pine species in Inner Mongolia and the stochastic processes prevailed in determining the community assembly of EM fungi. Our study shed light on the diversity and community assembly of EM fungi associated with common pine species in semiarid and cold temperate forests in Inner Mongolia, China, for the first time and provided a better understanding of the ecological processes underlying the community assembly of mutualistic fungi.

Keywords: ectomycorrhizal fungi, pine species, fungal diversity, community assembly, host phylogeny, plant-fungi preference, stochastic processes

OPEN ACCESS

Edited by:
Jadson Diogo Pereira Bezerra, Universidade Federal de Goiás, Brazil

Reviewed by:
Heng Gui, Kunming Institute of Botany (CAS), China
Dong Liu, Kunming Institute of Botany (CAS), China

****Correspondence:***
Yong-Jun Fan
fanyj1975@163.com

Specialty section:
This article was submitted to Evolutionary and Genomic Microbiology, a section of the journal Frontiers in Microbiology

Received: *28 December 2020*
Accepted: *19 February 2021*
Published: *16 March 2021*

Citation:
Wang Y-L, Zhang X, Xu Y, Babalola BJ, Xiang S-M, Zhao Y-L and Fan Y-J (2021) Fungal Diversity and Community Assembly of Ectomycorrhizal Fungi Associated With Five Pine Species in Inner Mongolia, China. Front. Microbiol. 12:646821. doi: 10.3389/fmicb.2021.646821

INTRODUCTION

The long-standing principle of community ecology is to examine the mechanisms underlying biodiversity conservation and community assembly (Chase, 2003; Nemergut et al., 2013; Zhou and Ning, 2017; Ladau and Eloe-Fadrosh, 2019). As an integral part of soil microorganisms, ectomycorrhizal (EM) fungi often establish mutual symbionts with many woody plants. For instance, they play vital roles in facilitating host plant fitness, forest biodiversity, and global nutrient cycling (Smith and Read, 2008; Tedersoo et al., 2020). Therefore, clarifying the underlying factors of EM fungi community assembly could vastly improve our predictability in the areas of sustainable forests, biochemical dynamics, and ecological processes under severe global changes.

Recent studies have emphasized that microbial communities are affected mainly by deterministic (niche theory) and stochastic processes (neutral theory) (Stegen et al., 2012; Nemergut et al., 2013; Bahram et al., 2018; Wang et al., 2020). The niche theory emphasizes that the species are under ecological selection pressure imposed by biotic and abiotic factors due to different habitats preference and fitness (Dumbrell et al., 2009; Stegen et al., 2012); neutral theory asserts the role of dispersal limitation, ecological drift, and diversification in predicting community assembly independent of ecological selection (Hubbell, 2001). It is widely accepted that deterministic and stochastic processes can jointly regulate microbial community assembly (e.g., Dumbrell et al., 2009; Wang et al., 2020), and the effect of the deterministic factors in describing the community assembly of EM fungi has been previously investigated. For example, host phylogeny was the most important determinant of the development of EM fungal communities associated with Betulaceae and Fagaceae species in Chinese forest ecosystems (Wu et al., 2018; Wang Y.L. et al., 2019) and Salicaceae species in Estonia (Tedersoo et al., 2013). Host plants can significantly affect EM fungal communities through host specificity/preference (Tedersoo et al., 2010a; van der Linde et al., 2018; Wang Y.L. et al., 2019) and modified rhizosphere microhabitats (Aponte et al., 2010). In comparison, some studies have shown that the host influence is absent or minor (Glassman et al., 2015, 2017; Miyamoto et al., 2015). A growing body of evidence indicates that phylogenetic analysis is a more effective technique than the use of plant identity to detect the host effect, as phylogenetic eigenvectors can represent different divisions at different taxonomic levels between host plants (Tedersoo et al., 2013). Similarly, abiotic environmental factors, including soil and climatic variables, have been reported as strong drivers of the EM fungal communities; for instance, climate difference and soil nutrients explained the largest variations of EM fungal community in two Japanese mountains (Miyamoto et al., 2015) and seven willow species in southeastern Minnesota, United States (Erlandson et al., 2016), respectively. In general, the effect of the deterministic process in defining the EM fungal community could be attributed to the selection of biotic and abiotic environmental variables on EM fungi through their fitness in response to the surrounding conditions (De Wit and Bouvier, 2006).

Stochastic processes such as dispersal limitation have been reported as an important driver of EM fungal community assembly (Glassman et al., 2015; Wu et al., 2018; Wang Y.L. et al., 2019). The reasons for dispersal limitation fall into two categories. On the one hand, fungal species differ in the characteristics associated with dispersal, such as spore size and yield, resulting in different dispersal abilities among fungal species (Peay et al., 2012; Kivlin et al., 2014; Peay and Bruns, 2014); on the other hand, the geographic distance could impede the movement of fungal individuals from one habitat to new suitable ones. Thus, these two factors contribute to the effect of dispersal limitation on the turnover of the EM fungal community. Several studies have shown that the geographic distance is a better indicator for the EM fungal community than other variables such as host plant, soil, and climatic parameters; for example, geographic distance explained the greatest variation in the EM fungal community associated with pine species across North America (Glassman et al., 2015).

The essential or best predictor variables responsible for the turnover of the EM fungal communities varied among studies. This inconsistency may have resulted from different spatial scales, forest types, and environmental variables. Previous studies have concentrated on EM fungal communities in subtropical, tropical, and temperate monsoon forest habitats where high biodiversity is present (Tedersoo et al., 2008, 2010a; Gao et al., 2015; Matsuoka et al., 2016). However, less attention has been given to EM fungi in semiarid and arid forests and cold temperate forests. Thus, EM fungal diversity and composition, the relative importance of host plant, soil, climate, and geographic distance on the EM fungal community, and the underlying ecological process driving EM fungal community assembly (stochastic and deterministic processes) in these forest ecosystems remain poorly understood.

The forests in Inner Mongolia, China, located in the semiarid and cold temperate zones, have relatively less precipitation and lower temperature when compared with subtropical, tropical, and warm forests. In the forests of Inner Mongolia, China, pine species are the most common woody plants, making a major ecological and economic contribution to the biodiversity of forests and humans, such as nuts and timber. However, pine-associated EM fungal diversity, community composition, and underlying assembly mechanisms in Inner Mongolia remain largely undefined. Here, we have identified the EM fungal community associated with pine species in Inner Mongolia, China, and we especially aimed to: (1) completely unveil EM fungal diversity and composition; (2) identify major factors influencing the diversity and composition of the EM fungi and evaluate the relative importance of deterministic and stochastic processes in shaping EM fungal community assembly; and (3) investigate the preference of the host and fungi in plant–EM fungal interactions. Thus, we assessed the EM fungal community of five common pine species in secondary forests in Inner Mongolia over approximately 1,900 km, using the Illumina Miseq sequencing of the internal transcribed fungal spacer 2 (ITS2). We also established the major drivers responsible for the shift in the EM fungal community by analyzing the impact of host plants, soil, climatic variables, and spatial distance, and we investigated the relative importance of deterministic and stochastic processes in shaping the EM fungal community assembly. We hypothesized that (1) host plant, abiotic variables (i.e., soil and climate), and

geographic distance all play significant roles in determining EM fungal community, but the host plant should be a stronger driver than other predictors; (2) significant partner preference should be present in pine–EM fungal associations; and (3) deterministic and stochastic processes concurrently control the community assembly of EM fungi.

MATERIALS AND METHODS

Sampling

We selected eight typical secondary forests, approximately 60 years old and with no history of disturbance, during the peak period of the growing season (**Supplementary Figure 1**). The selected forests were located in semiarid and cold temperate zones, with mean annual temperature (MAT) ranging from −4.75 to 5.97°C and mean annual precipitation (MAP) from 267 to 506 mm according to the climatic information extracted from the WorldClim dataset at 30-arc-second resolution (Hijmans et al., 2005). Pine species, with very few other EM hosts (Betulaceae and Salicaceae plants), were the dominant woody plants in each forest. At each site, 4–7 individuals were selected from each pine species. The fine roots were excavated by tracing the roots to the base of the trunk of every single plant. At each site, a sample of rhizosphere soil was collected from each individual and then combined as one composite sample. The individuals were at least 10 m apart to ensure the independence of the samples (Pickles et al., 2012). Root samples were transported to the laboratory in an icebox and kept at −20°C before processing. Soil samples were air-dried, sieved through 2 mm mesh, and then used for property analysis. A total of 63 root samples and eight soil samples were obtained in this study. Geographical coordinates and latitude were recorded using a high-sensitivity Global Positioning System instrument (M-241, Holux Technology Inc., Taiwan, China). Climatic conditions, including MAT and MAP of each site, were compiled from the WorldClim dataset at 30-arc-second resolution (Hijmans et al., 2005). Information on the geographic locations and climate is summarized in **Supplementary Table 1**.

Analysis of Soil Properties

Total nitrogen (N) was quantified by adopting the semi-micro-Kjeldahl process. Total phosphorus (P) was measured using iCAP 6300 inductively coupled plasma spectrometers (Thermo Science, Wilmington, United States). Total calcium (Ca) and magnesium (Mg) were measured in ICP Optima 8000 (Perkin-Elmer, Waltham, MA, United States). Information on soil properties can be found in **Supplementary Table 1**.

DNA Extraction, PCR, and MiSeq Sequencing

Before molecular analysis, the EM root tips were first detected and picked under a stereomicroscope. A total of 200 healthy EM root tips were randomly selected from each plant, resulting in 12,600 EM root tips from 63 samples used for DNA extraction. High throughput sequencing is becoming more popular in EM fungal community studies (e.g., Matsuoka et al., 2016; Van Geel et al., 2018; Wu et al., 2018; Wang Y.L. et al., 2019). Importantly, high throughput sequencing data can reflect the real dominant or rare taxa based on the relative sequencing abundance, whereas Sanger sequencing data present the frequency of EM root tips in samples. Thus, the method of high throughput sequencing based on the mixture of EM root tips was adopted in our study. The detailed process was as follows: the total genomic DNA of each sample was extracted using the modified cetyltrimethylammonium bromide method described in Gao et al. (2013). A two-step polymerase chain reaction (PCR) procedure has been adopted to amplify the fungal ITS2 region in the Veriti 96-well Thermal Cycler (Applied Biosystems, Foster City, United States). Briefly, the primers ITS1f (Gardes and Bruns, 1993) and ITS4 (White et al., 1990) were used to amplify the entire ITS region in 25 μl of reaction mixtures, including 1-U KOD-Plus-Neo DNA polymerase (Toyobo, Osaka, Japan), 2.5 μl of 10 × buffer, 2 mM of each deoxyribonucleotide triphosphate, 25 mM of magnesium sulfate, 10 μM of each primer, and approximately 5 ng of the DNA template. The PCR temperature profile included initial denaturation at 95°C for 5 min, 20 cycles at 94°C for 1 min, 58°C for 50 s, and 68°C for 30 s, and then final extension at 68°C for 10 min. The PCR products were diluted 30 times, and 1.5 μl solution was used as a template for the second PCR amplification. Primers fITS7 (Ihrmark et al., 2012) and ITS4 with unique barcode tags (12-base barcode sequence) were adopted to target the ITS2 region, and the PCR conditions were similar to the first amplification. Three replicates were used for each sample and then pooled to represent that sample. The pooled PCR products of each sample were purified using the Wizard SV Gel and the PCR Clean-Up System (Promega, Madison, United States). All purified PCR products were pooled with equimolar amounts and then sequenced to the Illumina MiSeq PE250 (Illumina, San Diego, CA, United States) platform at the Chengdu Institute of Biology Environmental Genome, Chinese Academy of Sciences, China.

Bioinformatic Analysis

Raw sequence data were filtered using the Quantitative Insights in Microbial Ecology platform (Caporaso et al., 2010) to exclude low-quality reads to those with uncertain bases >6, uneven to the primer or barcode sequence, duration <250 bp, or average quality score <20. The ITS2 region of the filtered sequences was extracted using the ITSx software (Bengtsson-Palme et al., 2013), and the possible chimera sequences were identified using the chimera.uchime command in Mothur 1.31.2 (Schloss et al., 2009) by referring to the entries in the unified DNA-based fungal species database (UNITE) (Kõljalg et al., 2013) and then discarded. After this step, the remaining sequences were clustered into operational taxonomic units (OTUs) at a 97% similarity threshold using the UPARSE pipeline (Edgar, 2013), during which singletons were also deleted. Using the simple local alignment search tool (BLAST) (Altschul et al., 1990), the representative sequence (most abundant) of each OTU was searched against the UNITE database (v. 8.2, release date: 02.04.2020). Fungal OTUs were first identified and assigned to taxonomic identity on the basis of the criteria proposed by

Tedersoo et al. (2014), then EM fungal OTUs were identified on the basis of Tedersoo and Smith (2013) and Tedersoo et al. (2014) if they better matched the known EM fungal taxa and lineages. To eliminate the effect of different sequencing depths across samples on the subsequent analysis, the EM fungal data were normalized to 1,055 (the smallest sample size) using the subsample command in Mothur. The representative sequences of each EM fungal OTU were deposited in the European Nucleotide Archive under study accession no. LR989273-LR989560. Information on EM fungi in the present study is shown in **Supplementary Table 2**.

Statistical Analysis

All statistical analyses were conducted in R 3.6.2 (R Development Core Team, 2019). The MaturaseK gene (matK) exists in chloroplasts, which is highly conserved in plant systematics, and is widely used in plant phylogeny analyses (Hilu and Liang, 1997; Cheng et al., 2000; Wang et al., 2000). Thus, the matK gene of the five pine species in the present study (**Supplementary Table 3**) was downloaded from the National Center for Biotechnology Information to create the host plant phylogenetic eigenvector used for the subsequent analysis, as other genes such as ITS were not fully accessible and the matK gene reflects the phylogeny of the pine species in this study. In MAFFT v. 7.215 (Katoh and Standley, 2013), the plant matK sequences were first aligned using the L-INS-i algorithm, and then a maximum likelihood phylogeny tree was created with 1,000 bootstrap replicates under the GTR model in MEGA ver 7.0 (Kumar et al., 2016; **Supplementary Figure 2**). After this, the phylogenetic distances between each plant species in the phylogenetic tree were calculated using the cophenetic.phylo command in the ape package (Paradis et al., 2004), and then the principal coordinate analysis (PCoA) was used to transform the pairwise distance matrix into phylogenetic eigenvectors using the cmdscale command in the vegan package (Oksanen et al., 2013). Similarly, the geographic distance between each site was first calculated on the basis of the geographic coordinates, and the resulting distance matrices were transformed into spatial eigenvectors of the principal coordinate of neighbor matrices (PCNM) using the pcnm command in the PCNM package (Dray et al., 2006), and only those with positive eigenvalues were retained for the subsequent analysis.

EM fungal OTU accumulation curves for each plant species were drawn using the specaccum command in the vegan package (Oksanen et al., 2013). The non-parametric Kruskal–Wallis test was used to determine the difference in EM fungal OTU richness between five plant species, as the data did not satisfy homogeneity of variance before and after logarithmic and square root transformation, and then the Conover test was used to conduct multiple comparisons between each plant species using the *post hoc*.kruskal.conover.test function in the PMCMR package (Pohlert, 2014). The Venn diagram was created to examine the shared and unique EM fungal OTUs among the five plant species using the online software E-venn[1].

[1]http://www.ehbio.com/test/venn/#/

Krona (v.2.6, Ondov et al., 2011) was adopted to visualize the taxonomic composition of EM fungi through the Krona pie chart. A Bray–Curtis dissimilarity matrix for fungal communities (Hellinger-transformed data) was calculated using the vegdist command in the vegan package (Oksanen et al., 2013). To measure the difference between the EM fungal communities of the plant species, the communities were ordinated by non-metric multidimensional scaling (NMDS) analysis through the use of the metaMDS command in the vegan package (Oksanen et al., 2013), and the confidence intervals of samples of each plant species were drawn from the NMDS ordination using the ordiellipse function. The significance of the difference between the five plant species in the fungal communities was assessed on the basis of the permutational multivariate variance analysis (PerMANOVA) by using the adonis command in the same package. Meanwhile, permutation analysis of multivariate dispersion (PERMDISP) (Anderson, 2001, 2006) was conducted to test whether groups differed in their dispersion by using the betadisper function in the vegan package (Oksanen et al., 2013). Reanalyses of NMDS, PerMANOVA, and PERMDISP were performed on the SHWL site data to confirm the host effect on EM fungal community. To further evaluate the variation of the relative abundances of dominant EM fungal lineages (>5% of total sequences) across different plant species, a non-parametric Kruskal–Wallis was used, as the data did not follow the normality and homogeneity of the variance, and the Conover test was used to conduct multiple comparisons as described earlier. To identify the key factors affecting the composition of the EM fungal community, the host phylogenetic, spatial, soil, and climatic variables were fit onto the ordination plot based on the environmental fitting test using the envfit command in the vegan package (Oksanen et al., 2013). Additionally, random forest modeling was adopted to identify the main drivers of the EM fungal OTU richness and community composition using the randomForest command in the randomForest package (Liaw and Wiener, 2002). The importance and significance of each predictor in response variables were evaluated using rfPermute and rp.importance commands in the rfPermute package (Archer, 2013), respectively. Mantel and partial mantel tests were conducted to determine the correlations between the EM fungal communities and the host phylogenetic and geographic distance using the mantel command in the vegan package (Oksanen et al., 2013). To assess the potential effect of dispersal limitation on the fungal community assembly, the Sloan neutral model was adopted by evaluating the relationship between the frequency of occurrence of OTUs and their relative abundance (logarithmic transformed) based on a parameter describing the migration rate "m" of the individual fungal OTUs (Sloan et al., 2006). The estimated "m" parameter indicates the probability that a random loss of an individual OTU from a local community would be replaced by dispersal from the metacommunity and, therefore, could be used as a dispersal limitation measure. The lower value of "m" suggests more limited dispersal in the turnover of the community.

Using phylogenetic information and associated randomization procedures to investigate underlying ecological

processes for microbial community assembly has become popular in recent years (Stegen et al., 2012, 2013; Wang et al., 2020). To evaluate phylogenetic community composition, the mean nearest taxon distance (MNTD) and the nearest taxon index (NTI) were calculated using the mntd and ses.mntd functions in the picant package (Kembel et al., 2010). The MNTD measures the mean nearest taxon distance between all pairs of OTUs in one sample, and the NTI measures the standard deviation of observed MNTD compared with randomized MNTD (Webb et al., 2002). When the NTI >2 in a single community or the mean NTI of all communities >0 significantly means taxa in the communities are more closely related than expected by chance, indicating phylogenetic clustering. When the NTI <-2 or mean NTI <0 significantly, this suggests phylogenetic over-dispersion and that species in the communities were distantly related. Additionally, if phylogenetic relatedness was not significantly different from null models, it indicates the predominance of stochastic processes. The significance was evaluated based on the one-sample *t*-test. To investigate the assembly process of the EM fungal community, phylogenetic turnover between communities was adopted in our study according to the framework proposed by Stegen et al. (2013) in which β-nearest taxon index (βNTI) was evaluated. Briefly, pairwise phylogenetic turnover among communities was quantified based on the MNTD metric (βMNTD) by using the comdistnt function in the picante package (Kembel et al., 2010) (abundance. weighted = TRUE). Then, the taxa labels of the phylogenetic tree were shuffled 999 times to generate null distributions of βMNTD among samples. The standard effect size of βMNTD (i.e., βNTI) was obtained based on the number of standard deviations that the observed βMNTD is from the mean of the null distribution. $|\beta NTI| > 2$ means that phylogenetic turnover is significantly greater (lower) compared with null distribution, implying the dominance of deterministic process, by contrast, when $|\beta NTI| < 2$, it suggests phylogenetic turnover is not significantly different from null expectation, indicating the important role of stochastic process in community assembly.

To evaluate the preference of the plant–fungal association and to eliminate the influence of the site on the analysis, the Saihanwula (SHWL) site, where the number of plant species was three, was selected for the preference analysis. Briefly, preference analysis evaluates the host and fungal preferences for their partners and two-dimensional preferences in pairs of plant species and fungal OTUs. The calculation of the relevant index was based on the presence/absence dataset by using original and randomized matrices. The detailed procedures have been described in Toju et al. (2016) and Wang Y.L. et al. (2019).

RESULTS

Ectomycorrhizal Fungal Database Summary

After quality filtering, a total of 969,290 non-chimeric ITS2 sequences were generated from 1,017,759 raw sequences, and

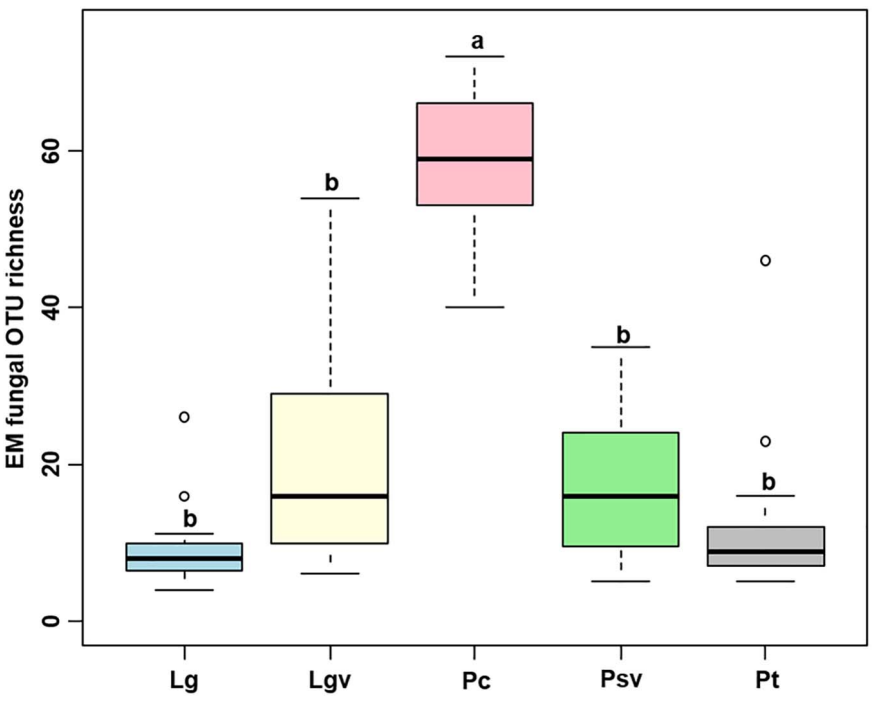


FIGURE 1 | Richness of ectomycorrhizal (EM) fungal operational taxonomic units (OTUs) in the five pine species. Bars without shared letters indicate significant differences in richness of fungal OTUs among the five plant species, according to Conover's test.

these high-quality sequences were clustered into 1,734 non-singleton OTUs (951,673), of which 349 (750,517) were identified as EM fungal. After the rarefication, a normalized dataset of 288 EM fungal OTUs was retained for further analysis. The 30 most abundant OTUs occupied 70% of the overall sequences, and 139 of 288 OTUs (48%) occurred in fewer than three samples (**Supplementary Figure 3**).

Ectomycorrhizal Fungal Diversity

The accumulation curves of each plant species did not show any signs of reaching an asymptote, suggesting that further sample collection may result in more unknown EM fungal OTUs (**Supplementary Figure 4**). The Kruskal–Wallis test showed that the EM fungal OTU richness was significantly different between plant species, and the multiple comparisons suggested that the fungal OTU richness of *Picea crassifolia* was significantly higher than that of the other four plant species (**Figure 1**). Random forest analysis indicated host phylogeny (PCoA1, 2, and 4), spatial distance (PCNM1, 2, and 3), MAP, soil N, N:P, and altitude significantly affected EM fungal OTU richness, whereas 62.62% of the richness variance was explained by the model (**Figure 2A**).

Ectomycorrhizal Fungal Community Composition and Assembly

Basidiomycota dominated 83% of total EM fungal reads, whereas Ascomycota only occupied 13% (**Supplementary Figure 5**). A total of 31 lineages were found in 63 root samples of five pine species in the current study, of which *Tomentella–Thelephora*, *Wilcoxina*, *Tricholoma*, *Suillus-Rhizopogon*, *Sebacina*, *Amphinema-Tylospora*, and *Inocybe* were the most abundant EM fungal lineages, accounting for 83.64% of total sequences (**Table 1**). The relative abundance of the seven abundant EM fungal lineages in each plant species is shown in **Figure 3**. The NMDS ordination showed that the EM fungal community was significantly different among the plant species (Adonis: $R^2 = 0.234$, $P = 0.001$, **Figure 4**), whereas the PERMDISP that indicated the dispersion among groups (plant

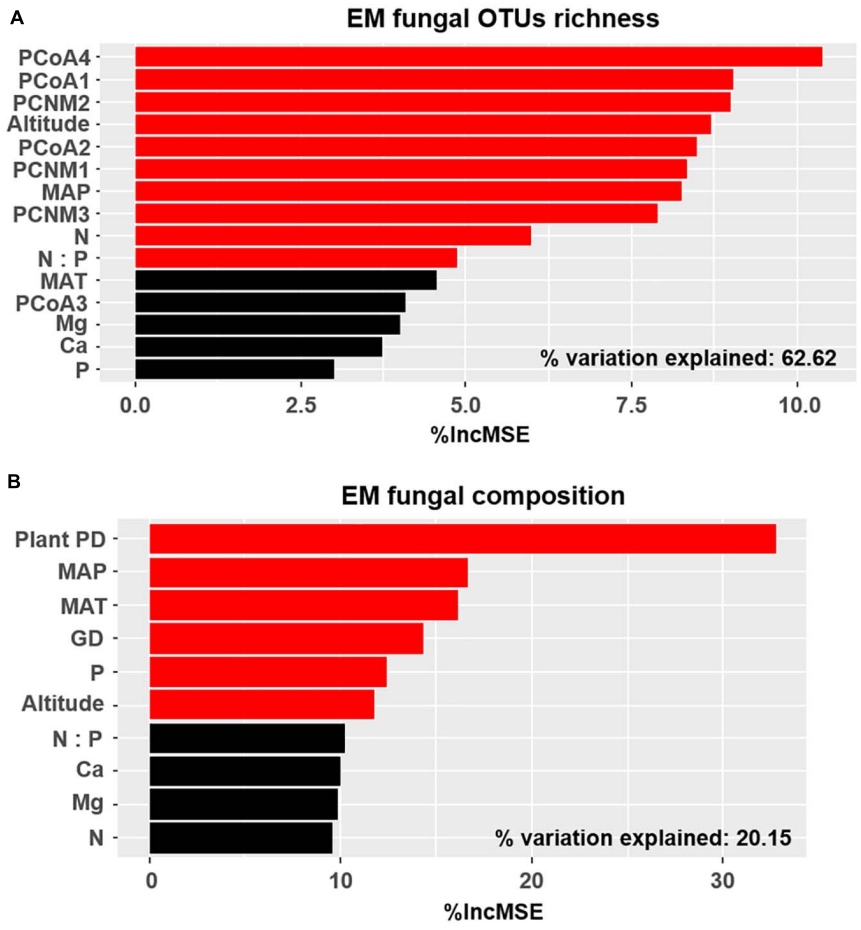


FIGURE 2 | Random forest model demonstrating relative importance of host plants, spatial, soil, and climatic variables for ectomycorrhizal (EM) fungal OTU richness **(A)** and community composition **(B)** %IncMSE, % of increase of mean square error; PCoA, principal coordinate analysis of host phylogeny; PCNM, principal coordinates of neighbor matrices; MAT, mean annual temperature; MAP, mean annual precipitation; P, soil total phosphorus; N, soil total nitrogen; Ca, soil total calcium; Mg, soil total magnesium; PD, phylogenetic distance; GD, geographic distance; Significant factors are shown in red ($P < 0.05$) and non-significant factors are shown in black ($P > 0.05$).

TABLE 1 | Relative abundance of each ectomycorrhizal (EM) fungal lineage in each plant species.

EM fungal lineage	Lg (%)	Lgv (%)	Pc (%)	Psv (%)	Pt (%)	Total (%)
/Tomentella–Thelephora	2.47	20.89	15.11	27.32	22.37	18.55
/Tricholoma	44.21	22.61	–	5.29	11.80	17.93
/Suillus–Rhizopogon	28.43	9.36	0.04	7.63	19.93	14.20
/Wilcoxina	7.46	3.75	14.30	24.07	12.07	11.36
/Sebacina	0.04	7.33	50.91	9.75	4.90	10.67
/Amphinema–Tylospora	0.02	4.32	5.62	6.57	10.83	5.86
/Inocybe	0.01	6.21	4.25	1.34	9.94	5.06
/Piloderma	13.04	6.90	–	0.32	–	4.19
/Tuber–Helvella	0.57	0.94	0.66	7.65	2.29	2.38
/Russula–Lactarius	–	5.53	–	2.87	0.40	2.10
/Geopora	0.49	0.57	0.16	1.73	4.62	1.81
/Cortinarius	0.01	4.63	0.83	–	0.01	1.35
/Clavulina	–	4.50	–	–	0.02	1.22
/Helotiales	0.40	0.09	5.74	0.03	0.07	0.76
/Hygrophorus	0.05	0.01	–	3.30	0.07	0.61
/Cenococcum	–	0.35	0.35	0.96	0.33	0.39
/Terfezia–Peziza depressa	1.37	0.01	–	0.51	0.06	0.35
/Pseudotomentella	1.40	0.16	–	0.01	–	0.29
/Serendipita	–	0.48	–	0.06	–	0.14
/Tomentellopsis	–	0.48	0.05	–	–	0.14
/Cantharellus	–	–	1.21	–	–	0.13
/Hebeloma–Alnicola	0.02	0.35	0.08	0.07	–	0.12
/Genea–Humaria	0.02	–	–	0.43	–	0.08
/Otidea	–	0.01	0.66	–	–	0.08
/Tarzetta	–	–	–	–	0.28	0.08
/Boletus	–	0.26	–	–	–	0.07
/Serendipita	–	0.21	–	0.01	–	0.06
/Meliniomyces	–	0.04	–	0.09	0.01	0.03
/Ramaria-Gautieria	–	0.03	–	–	–	<0.01
/Elaphomyces	–	–	0.01	–	–	<0.01
/Laccaria	–	–	–	–	0.01	<0.01

Lg, Larix gmelinii; Lgv, Larix gmelinii var. principis-rupprechtii; Pc, Picea crassifolia; Psv, Pinus sylvestris var. mongolica; Pt, Pinus tabuliformis.

species) differed significantly ($F = 9.42$, $P < 0.001$). Repeating the analysis of NMDS, PerMANOVA, and PERMDISP on the SHWL dataset indicated that the EM fungal communities were significantly among plant species ($R^2 = 0.37$, $P = 0.001$, **Supplementary Figure 6**), and the dataset did not vary significantly in dispersion by groups ($F = 2.57$, $P = 0.12$). The environmental fitting test indicated that host phylogeny (PCoA1 and 4), spatial distance (PCNM1 and 2), MAT, MAP, soil N, P, N:P, Mg, and altitude were significantly correlated with the EM fungal community (**Supplementary Figure 7**). Similarly, random forest analysis showed that plant phylogenetic distance, spatial distance, MAT, MAP, soil P, and altitude were the most significant determinants of dissimilarity in the EM fungal community, and the variation explained by the model was 20.15% (**Figure 2B**). Mantel and partial mantel analyses indicated that the EM fungal community was significantly correlated with host phylogenetic distance (Mantel $r = 0.335$, $P = 0.001$; partial Mantel $r = 0.228$, $P = 0.001$) and geographic distance (Mantel $r = 0.260$, $P = 0.001$; partial Mantel $r = 0.099$, $P = 0001$) (**Supplementary Figure 8**). The neutral model suggested dispersal limitation significantly affected the assembly of the EM fungal community ($R^2 = 0.258$, $m = 0.002$, **Figure 5**). The NTI values ranged from −1.58 to 1.47, and the mean NTI value across all samples was not significantly different from 0 ($P > 0.05$), indicating the phylogenetic relatedness in the communities was stochastic (**Figure 6A**). Most βNTI values fell within the range of −2 to 2, with βNTI >2 existing in only 5% of the cases, indicating that stochastic processes had a stronger effect on the community assembly of EM fungi than the deterministic processes in the present study (**Figure 6B**).

Plant–Fungus Preference

Preference analysis conducted at SHWL indicated that 13 out of 24 (54%) abundant EM fungal OTUs were significantly preferred to specific plant species, and all plant species (100%) showed a significant preference for some EM fungal OTUs; in addition, 19 out of 72 (26%) pairs of plant species and abundant fungal OTUs exhibited remarkably strong preferences (**Figure 7**).

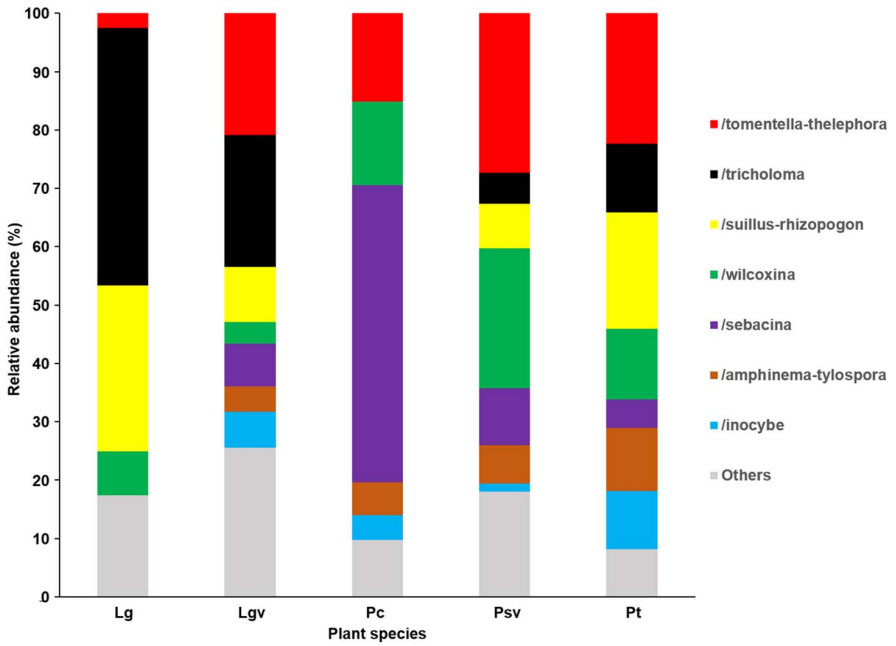


FIGURE 3 | Ectomycorrhizal fungal lineage and their relative abundance in five pine species. Here, we only showed abundant lineages (>5% of total sequences). Lg, *Larix gmelinii*; Lgv, *Larix gmelinii* var. principis-rupprechtii; Pc, *Picea crassifolia*; Psv, *Pinus sylvestris* var. mongolica; Pt, *Pinus tabuliformis*.

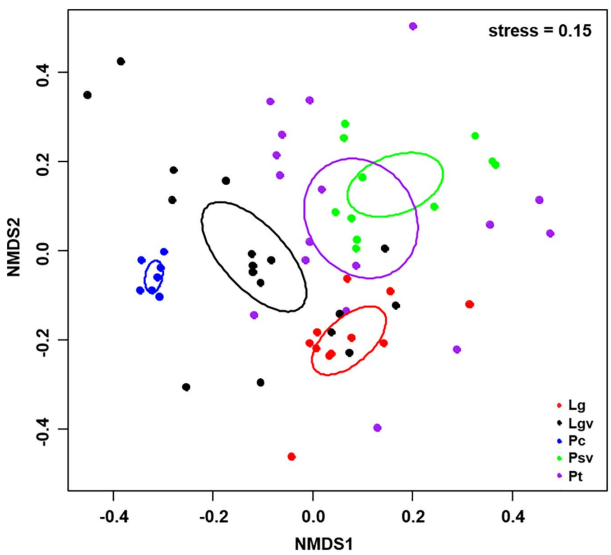


FIGURE 4 | Non-metric multidimensional scaling (NMDS) ordination of ectomycorrhizal fungal community composition based on Bray–Curtis distance (stress = 0.15). Ellipses delimit 95% confidence intervals around centroids for each pine species. Lg, *Larix gmelinii*; Lgv, *Larix gmelinii* var. principis-rupprechtii; Pc, *Picea crassifolia*; Psv, *Pinus sylvestris* var. mongolica; Pt, *Pinus tabuliformis*.

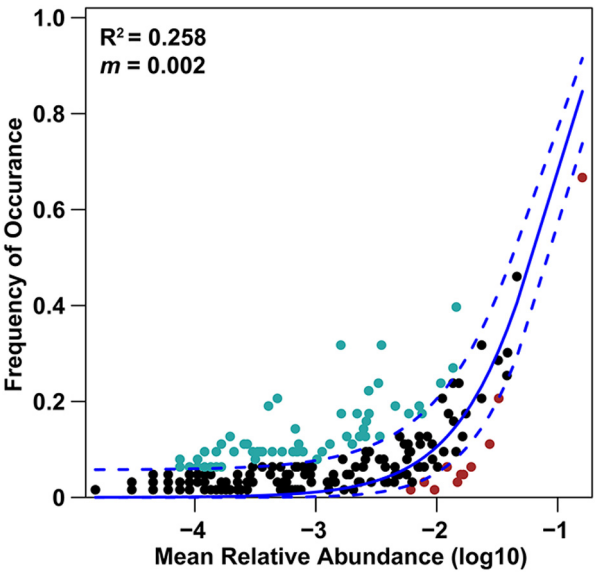


FIGURE 5 | Fit of neutral model for fungal OTUs. Solid blue line represents the predicted occurrence frequency, and dashed blue lines represent 95% confidence intervals around the model prediction; light blue and red dots indicate the OTUs that occur more and less frequently than given by the model; R^2 indicates the fit to the neutral model; m indicates immigration rate.

DISCUSSION

A total of 288 EM fungal OTUs belonging to 31 lineages were identified in this analysis, with a richness value of 17.49 ± 2.20 (mean ± SE) across all samples. The species rarefaction curve did not reach the plateau, implying our sample size was not adequate. Thus, more samples should be collected in our future study, which may introduce higher fungal diversity.

Here, we found that the richness of EM fungal OTUs was significantly affected by host phylogeny, spatial distance, MAP, soil N, N:P ratio, and altitude. This was consistent with the reports in many previous studies (Põlme et al., 2013; Tedersoo et al., 2013; Wu et al., 2018; Wang Y.L. et al., 2019). For example, host phylogenetic eigenvectors were the significant variables responsible for EM fungal OTU diversity in the studies involved in Betulaceae, Fagaceae, and Salicaceae plants (Tedersoo et al., 2013; Wu et al., 2018; Wang Y.L. et al., 2019). These studies combined with our study indicated that host plants play important roles in determining EM fungal diversity and further support the hypothesis that host taxonomic relatedness governs the "host effect" (Taylor, 2008; Tedersoo et al., 2013). The influence of MAP and soil nutrients on EM fungal richness is mainly because EM fungi should grow under suitable habitat conditions; indeed, previous studies have found that high precipitation and increased N supply could reduce EM fungal diversity (Cox et al., 2010; Tedersoo et al., 2013).

In our study, the dominant EM fungal lineages were *Tomentella–Thelephora*, *Tricholoma*, *Suillus–Rhizopogon*, *Wilcoxin*, *Sebacin*, *Amphinema–Tylospora*, and *Inocybe*, and lineages accounted for 83.64% of total sequences. The most abundant lineage was *Tomentella–Thelephora*, which was consistent with many previous studies involving various host plant groups investigated in different forest ecosystems (Tedersoo et al., 2013; Wang et al., 2017; Wu et al., 2018; Wang Y.L. et al., 2019) and in line with Tedersoo et al. (2010b) that indicated *Tomentella–Thelephora* was a globally distributed lineage. However, the dominance of lineages *Tricholoma*, *Suillus–Rhizopogon*, *Wilcoxin*, and *Amphinema–Tylospora* has rarely been recorded. For example, *Tricholoma* accounted for 17.93% of total sequences and occurred in 44 of 63 samples (69.84%), suggesting that this lineage was a widespread lineage associated with pine species in Inner Mongolia. Additionally, *Amphinema–Tylospora* has been reported as a Pinaceae-specific lineage in previous studies (Miyamoto et al., 2020; Vlk et al., 2020), and *Suillus* was found to be the dominant genus associated with *Larix gmelinii* (Miyamoto et al., 2020). Our findings indicate that pine species in Inner Mongolia may have a distinct EM fungal community. One explanation is climatic conditions; that is, the MAT and MAP in Inner Mongolia are lower compared with those in subtropical, tropical, and warm temperate areas; this may contribute to distinct EM fungal communities in Inner Mongolia, as MAT and MAP have been reported as strong drivers of EM fungal communities (Miyamoto et al., 2015). Soil development with different parent materials could give rise to the variations in soil physicochemical properties and thus may result in distinct microbial communities across different habitats (Alfaro et al., 2017; Sánchez-Marañón et al., 2017). Moreover, special species, such as *L. gmelinii* var. principis-rupprechtii, *Pinus sylvestris* var. mongolica, and *P. crassifolia* mainly distributed in Inner Mongolia, also could result in distinct EM fungal communities, which derived from host effect (Tedersoo et al., 2013).

The NMDS ordination combined with PerMANOVA suggested that host plants had a significant effect on the composition of the EM fungal community. Meanwhile, the environment fitting test and random forest analysis showed that host phylogeny, spatial distance, climatic variables, and some soil parameters significantly affected EM fungal community assembly, with host phylogeny being the strongest predictor. A similar finding has been reported in previous studies (Tedersoo et al., 2013; Wu et al., 2018; Wang Y.L. et al., 2019; Wang Z.H. et al., 2019), for example, studies involving Salicaceae, Betulaceae, and Fagaceae plant species all demonstrated that host plants were the most important determinant of EM fungal community assembly. In addition, 164 of 288 (56.94%) EM fungal OTUs existed in one plant species, Seventy-one OTUs (24.7%) appeared in two plant species, and only four OTUs were shared among the five pine species (**Supplementary Figure 9**). Meanwhile, the relative abundance of dominant lineages also showed a difference between host plants; for example, the relative abundance of *Tomentella–Thelephora* was significantly higher in *L. gmelinii* than in other hosts, and *Tricholoma* showed a significantly lower relative abundance in *P. crassifolia* than in other host plants (**Supplementary Figures 10A,B**). These results revealed that host plants had a significant impact on the EM fungal community. One explanation is the conservatism of the host phylogenetic niche (Losos, 2008); detailed, closely related plant species commonly showed more similarity than distantly related species in morphological and functional traits and appeared to share more similar fungal groups. A previous study indicated that host functional traits predicted 25 and 17% of the variation in root-associated pathogenetic and mycorrhizal fungal communities, whereas host effects were primarily due to host phylogeny (Wang Z.H. et al., 2019). Accordingly, our mantel tests showed that the dissimilarities of the EM fungal community increased significantly with the increase in plant phylogenetic distance (Mantel $r = 0.335$, $P = 0.001$), even after the control of variance in abiotic environmental factors and geographic distance (partial Mantel $r = 0.228$, $P = 0.001$), which further confirmed the important role of the host phylogenetic relationship in the community assembly of EM fungi. On the other hand, the preferences between plant and EM fungi generated over a long history of co-evolution could also contribute to the host effect on the fungal community, with all pine species and 54% of abundant EM fungal OTUs significantly preferring to certain partners, and 26% of plant–fungal pairs showing remarkably strong preferences in the SHWL dataset in the present study. Similar findings have been reported in previous studies involving EM fungi and Ericaceous fungi (Toju et al., 2016; Wu et al., 2018; Wang Y.L. et al., 2019).

Climate and soil parameters were found to affect EM fungal community in our study based on environmental fitting test and random forest analysis, and the effects of soil and climatic conditions on EM fungal communities have been intensively investigated in recent years (Miyamoto et al., 2015; Erlandson et al., 2016; Glassman et al., 2017). It has been well established that common fungal taxa grow

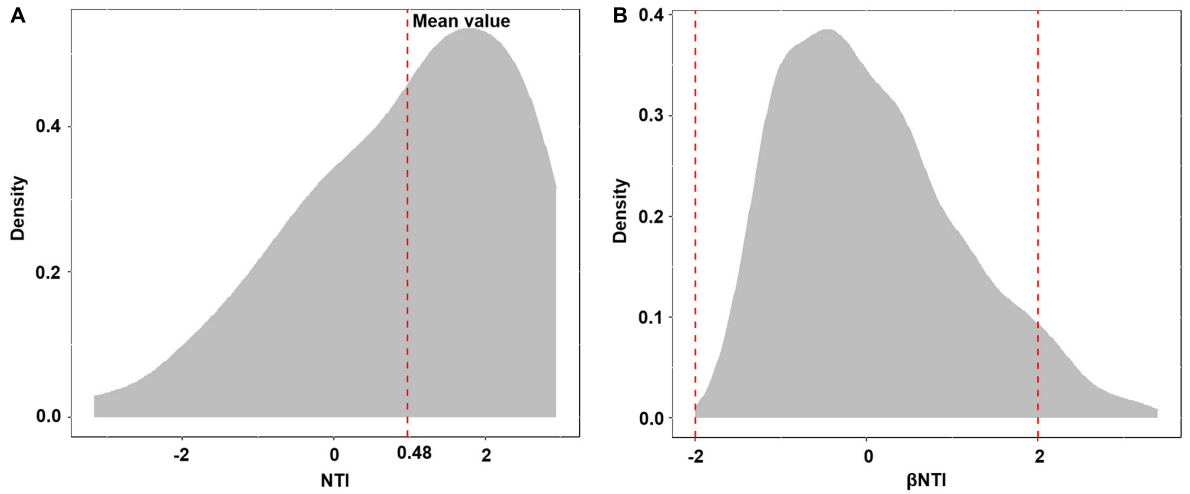


FIGURE 6 | Distribution of nearest taxon index (NTI) **(A)** and beta nearest taxon index (βNTI) **(B)**.

well in proper habitats in soil nutrients, water content, and temperature (Cox et al., 2010; Miyamoto et al., 2018; Guo et al., 2020). For example, the frequency of some fungal taxa decreased with an increase in temperature, whereas some exhibited an opposite trend (Miyamoto et al., 2018; Koizumi and Nara, 2019); similarly, the population of some fungal taxa increased by additional nutrient inputs, whereas some were inhibited (Corrales et al., 2017). These findings suggested that different fungal taxa commonly occupied distinct niche positions. Overall, the effect of host plants, soil, and climatic variables on the EM fungal community assembly indicated a significant deterministic process in this study.

Apart from host plant, soil, and climatic variables, spatial distance also significantly predicted EM fungal community. The dissimilarity of the EM fungal community significantly increased by raising the geographic distance revealed by mantel and partial mantel tests, thus indicating that dispersal limitation is an essential determinant of the community assembly of EM fungi. Indeed, the low *m*-value (0.002) of the neutral model analysis also suggested that EM fungi experienced serious dispersal limitation and the EM fungal community assembly was well described by the stochastic process. In recent years, dispersal limitation has been widely accepted as an important driver of community assembly of soil- and root-associated fungi (Beck et al., 2015; Glassman et al., 2015; Wang Y.L. et al., 2019). One explanation is a spatial distance, which could impede the dispersal of fungal propagules (e.g., fungal individuals, spore, hypha) (Peay et al., 2010). In addition, the fungi varied in their dispersal abilities, and the order in the fungi that arrived at the habitat could give rise to variations in the fungal community (Peay et al., 2012). The significant effect of dispersal limitation on the EM fungal community suggested significant stochastic processes in shaping the community assembly of EM fungi, which was confirmed by the βNTI analysis that demonstrated the predominance of stochastic processes.

Overall, both deterministic and stochastic processes jointly controlled the community assembly of EM fungi associated with the five common pine species in Inner Mongolia, China, with the predominance of stochastic process based on the βNTI analysis. Among the variables investigated in the present study, host phylogeny was a better predictor than soil, climatic, and geographic factors in shaping the EM fungal community. It should be noted that these variables explained only a small proportion of the variation in the fungal community (20.15%, **Figure 2B**). This can be explained by the relatively few factors used in the analysis in our study; for example, soil pH, moisture, and other nutrient elements (potassium, organic matters, and available N) were absent here, whereas they have been proven to affect the EM fungal community in previous studies (Roy et al., 2013; Erlandson et al., 2016; Glassman et al., 2017). Moreover, the stochastic process derived from ecological drift and diversification were suspected to explain the community variation, as the βNTI analysis indicated the predominance of stochastic process in community assembly, but this needs to be investigated in our future study.

In summary, to our knowledge, this is the first time the EM fungal community associated with pine species in the semiarid and cold temperate forests in Inner Mongolia, China has been investigated. We found a high diversity of EM fungi in the five pine species; that is, 288 EM fungal OTUs that belonged to 31 lineages were reported in the present study. Host plant, soil, and climatic variables coupled with spatial distance jointly established the EM fungal community assembly, with host phylogeny being the best predictor. In addition, deterministic and stochastic processes concurrently shaped the community assembly of EM fungi, but stochastic processes prevailed. Our study shed light on the fungal diversity and community assembly processes of EM fungi associated with common pine species in northern China.

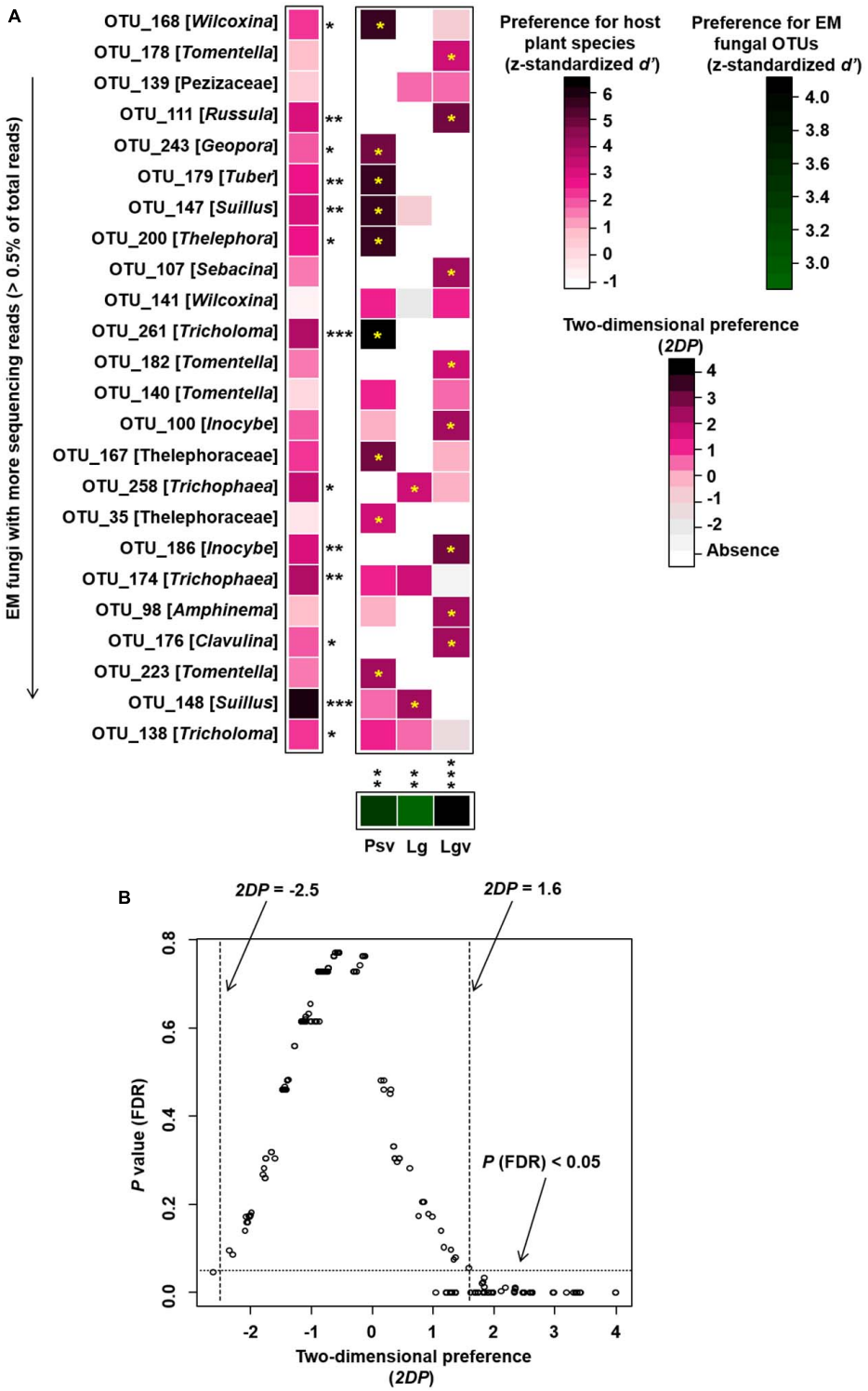


FIGURE 7 | Preferences observed in plant–fungus associations in Saihanwula. **(A)** standardized *d'* estimates of preferences for ectomycorrhizal (EM) fungal operational taxonomic units (OTUs) for indicated plant species (columns). Likewise, the standardized *d'* estimate of preferences for plant species is indicated for each of the observed fungal OTUs (row). A cell in the matrix indicates a two-dimensional preference (*2DP*) estimate, indicating the extent an association of a focal plant–fungus pair was observed more/less frequently than expected by chance. Cell with an asterisk inside represents significant preferences in plant–fungus pair. Because multiple species/OTUs were tested, the *P*-values are shown as false discovery rates (FDRs) in the plant/fungus analysis. **(B)** Relationship between *2DP* and FDR-adjusted *P*-values, *2DP* values larger than 1.6 represented strong preferences. Significance: $^{*}P < 0.05$, $^{**}P < 0.01$, $^{***}P < 0.001$. Psv, *Pinus sylvestris* var. mongolica; Lg, *Larix gmelinii*; Lgv, *Larix gmelinii* var. principis-rupprechtii.

DATA AVAILABILITY STATEMENT

The original contributions presented in the study are publicly available. This data can be found here: The representative sequences of each EM fungal OTU were deposited in the European Nucleotide Archive (ENA) under study accession no. LR989273-LR989560. Information on EM fungi in the present study is shown in **Supplementary Table 2**.

AUTHOR CONTRIBUTIONS

Y-LW and Y-JF conceived and designed the study. XZ and YX performed the experiments. Y-LW analyzed the data and drafted the manuscript. XZ, S-MX, YX, and Y-JF performed the field sampling work. BB gave some suggestions for English improvement. Y-JF revised and approved the final manuscript. All authors contributed to the article and approved the submitted version.

FUNDING

This study was supported financially by the Science and Technology Project of Inner Mongolia Autonomous Region (2019GG002), the Youth Science and Technology Talent Support Scheme of Colleges and Universities in Inner Mongolia Autonomous Region (NJYT-18-A21), and the Inner Mongolia Natural Science Foundation (2020MS03001).

ACKNOWLEDGMENTS

We thank Liang Zhang from the Genhe, GH, National Field Scientific Observation and Research Station of Forest Ecosystem in Greater Khingan Mountains, and Chang-Lin Xiang from SHWL for help during sampling. Additionally, we thank LetPub (www.letpub.com) for its linguistic assistance during the preparation of this manuscript.

SUPPLEMENTARY MATERIAL

The Supplementary Material for this article can be found online at: https://www.frontiersin.org/articles/10.3389/fmicb.2021.646821/full#supplementary-material

Supplementary Figure 1 | Sampling sites selected in the Inner Mongolia, China. GH, Genhe; SHWL, Saihanwula; HGL, Huangangliang; CF, Chifeng; HLH, Heilihe; WYD, Wangyedian; WLS, Wulashan; HLS, Helanshan.

Supplementary Figure 2 | Maximum likelihood phylogram showing phylogenetic placement of pine species based on matK genes, using *Betula platyphylla* as an outgroup. Scale bar represents 5% sequence divergence.

Supplementary Figure 3 | Ectomycorrhizal (EM) fungal operational taxonomic units (OTUs) ranked by relative abundance **(A)** and frequency **(B)**.

Supplementary Figure 4 | Species accumulation curves of ectomycorrhizal (EM) fungal operational taxonomic units (OTUs) in five pine species. Lg, *Larix gmelinii*; Lgv, *Larix gmelinii* var. principis-rupprechtii; Pc, *Picea crassifolia*; Psv, *Pinus sylvestris* var. mongolica; Pt, *Pinus tabuliformis*.

Supplementary Figure 5 | Krona chart of taxonomic affiliation of ectomycorrhizal (EM) fungi and their relative abundance. Inner circle represent higher taxonomic ranks and more detailed taxonomic ranks are presented in outer circles.

Supplementary Figure 6 | Non-metric multidimensional scaling (NMDS) ordination of ectomycorrhizal fungal community composition based on Bray-Curtis distance of Saihanwula dataset (stress = 0.07). Ellipses delimit 95% confidence intervals around centroids for each pine species. Lg, *Larix gmelinii*; Lgv, *Larix gmelinii* var. principis-rupprechtii; Psv, *Pinus sylvestris* var. mongolica.

Supplementary Figure 7 | Significant host, soil, climatic and spatial variables were fitted on the non-metric multidimensional scaling (NMDS) ordination of the EM fungal community composition.

Supplementary Figure 8 | Mantel tests describing the correlations between ectomycorrhizal (EM) fungal community dissimilarity and plant phylogenetic distance **(A)** and geographic distance **(B)**.

Supplementary Figure 9 | Venn diagram showing the shared and unique ectomycorrhizal fungal OTUs across the five pine species. Lg, *Larix gmelinii*; Lgv, *Larix gmelinii* var. principis-rupprechtii; Pc, *Picea crassifolia*; Psv, *Pinus sylvestris* var. mongolica; Pt, *Pinus tabuliformis*.

Supplementary Figure 10 | Multiple comparison of the relative abundance of abundant ectomycorrhizal fungal lineage (>5% of total sequences). **(A)** tomentella-thelephora, **(B)** tricholoma, **(C)** sebacina, and **(D)** inocybe. Bars without shared letters indicate significant differences according to Dunn's tests with Bonferroni adjustment at $P < 0.05$.

Supplementary Table 1 | Sampling sites, plant species and environmental variables in present study.

Supplementary Table 2 | Molecular identification of ectomycorrhizal fungi investigated in this study.

Supplementary Table 3 | Accession number of matK gene of the pine species and outgroup species in present study.

Supplementary Table 4 | Correlations of spatial, host, soil, and climatic variables with non-metric dimensional scale revealed by the environmental fitting test.

REFERENCES

Alfaro, F. D., Manzano, M., Marquet, P. A., and Gaxiola, A. (2017). Microbial communities in soil chronosequences with distinct parent material: the effect of soil pH and litter quality. *J. Ecol.* 105, 1709–1722. doi: 10.1111/1365-2745.12766

Altschul, S. F., Gish, W., Miller, W., Myers, E. W., and Lipman, D. J. (1990). Basic local alignment search tool. *J. Mol. Biol.* 215, 403–410. doi: 10.1016/S0022-2836(05)80360-2

Anderson, M. J. (2001). A new method for non-parametric multivariate analysis of variance. *Austral Ecol.* 26, 32–46. doi: 10.1111/j.1442-9993.2001.01070.pp.x

Anderson, M. J. (2006). Distance-based tests for homogeneity of multivariate dispersions. *Biometrics* 62, 245–253. doi: 10.1111/j.1541-0420.2005.00440.x

Aponte, C., García, L. V., Marañón, T., and Gardes, M. (2010). Indirect host effect on ectomycorrhizal fungi: leaf fall and litter quality explain changes in fungal communities on the roots of co-occurring Mediterranean oaks. *Soil Biol. Biochem.* 42, 788–796. doi: 10.1016/j.soilbio.2010.01.014

Archer, E. (2013). *rfPermute: Estimate Permutation P-Values for Random Forest Importance Metrics*. http://CRAN.Rproject.org/package=rfPermute

Bahram, M., Hildebrand, F., Forslund, S. K., Anderson, J. L., Soudzilovskaia, N. A., Bodegom, P. M., et al. (2018). Structure and function of the global topsoil microbiome. *Nature* 560, 233–237. doi: 10.1038/s41586-018-0386-6

Beck, S., Powell, J. R., Drigo, B., Cairney, J. W. G., and Anderson, I. C. (2015). The role of stochasticity differs in the assembly of soil- and root-associated fungal communities. *Soil Biol. Biochem.* 80, 18–25. doi: 10.1016/j.soilbio.2014.09.010

Bengtsson-Palme, J., Ryberg, M., Hartmann, M., Branco, S., Wang, Z., Godhe, A., et al. (2013). Improved software detection and extraction of ITS1 and ITS2 from ribosomal ITS sequences of fungi and other eukaryotes for analysis of environmental sequencing data. *Methods Ecol. Evol.* 4, 914–919. doi: 10.1111/2041-210X.12073

Caporaso, J. G., Kuczynski, J., Stombaugh, J., Bittinger, K., Bushman, F. D., Costello, E. K., et al. (2010). QIIME allows analysis of high-throughput community sequencing data. *Nat. Methods* 7, 335–336. doi: 10.1038/nmeth.f.303

Chase, J. M. (2003). Community assembly: when should history matter? *Oecologia* 136, 489–498. doi: 10.1007/s00442-003-1311-7

Cheng, Y., Nicolson, R. G., Tripp, K., and Chaw, S. M. (2000). Phylogeny of Taxaceae and Cephalotaxaceae genera inferred from chloroplast matK gene and nuclear rDNA ITS region. *Mol. Phylogenet. Evol.* 14, 353–365. doi: 10.1006/mpev.1999.0710

Corrales, A., Turner, B. L., Tedersoo, L., Anslan, S., and Dalling, J. W. (2017). Nitrogen addition alters ectomycorrhizal fungal communities and soil enzyme activities in a tropical montane forest. *Fungal Ecol.* 27, 14–23. doi: 10.1016/j.funeco.2017.02.004

Cox, F., Barsoum, N., Lilleskov, E. A., and Bidartondo, M. I. (2010). Nitrogen availability is a primary determinant of conifer mycorrhizas across complex environmental gradients. *Ecol. Lett.* 13, 1103–1113. doi: 10.1111/j.1461-0248.2010.01494.x

De Wit, R., and Bouvier, T. (2006). "Everything is everywhere, but, the environment selects"; what did Baas Becking and Beijerinck really say? *Environ. Microbiol.* 8, 755–758. doi: 10.1111/j.1462-2920.2006.01017.x

Dray, S., Legendre, P., and Peres-Neto, P. R. (2006). Spatial modelling: a comprehensive framework for principal coordinate analysis of neighbour matrices (PCNM). *Ecol. Model.* 196, 483–493. doi: 10.1016/j.ecolmodel.2006.02.015

Dumbrell, A. J., Nelson, M., Helgason, T., Dytham, C., and Fitter, A. H. (2009). Relative roles of niche and neutral processes in structuring a soil microbial community. *ISME J.* 4, 337–345. doi: 10.1038/ismej.2009.122

Edgar, R. C. (2013). UPARSE: highly accurate OTU sequences from microbial amplicon reads. *Nat. Methods* 10, 996–998. doi: 10.1038/nmeth.2604

Erlandson, S. R., Savage, J. A., Cavender-Bares, J. M., and Peay, K. G. (2016). Soil moisture and chemistry influence diversity of ectomycorrhizal fungal communities associating with willow along an hydrologic gradient. *FEMS Microbiol. Ecol.* 92:fiv148. doi: 10.1093/femsec/fiv148

Gao, C., Shi, N. N., Liu, Y. X., Peay, K. G., Zheng, Y., Ding, Q., et al. (2013). Host plant genus-level diversity is the best predictor of ectomycorrhizal fungal diversity in a Chinese subtropical forest. *Mol. Ecol.* 22, 3403–3414. doi: 10.1111/mec.12297

Gao, C., Zhang, Y., Shi, N. N., Zheng, Y., Chen, L., Wubet, T., et al. (2015). Community assembly of ectomycorrhizal fungi along a subtropical secondary forest succession. *N. Phytol.* 205, 771–785. doi: 10.1111/nph.13068

Gardes, M., and Bruns, T. D. (1993). ITS primers with enhanced specificity for basidiomycetes-application to the identification of mycorrhizae and rusts. *Mol. Ecol.* 2, 113–118. doi: 10.1111/j.1365-294X.1993.tb00005.x

Glassman, S. I., Peay, K. G., Talbot, J. M., Smith, D. P., Chung, J. A., Taylor, J. W., et al. (2015). A continental view of pine-associated ectomycorrhizal fungal spore banks: a quiescent functional guild with a strong biogeographic pattern. *N. Phytol.* 205, 1619–1631. doi: 10.1111/nph.13240

Glassman, S. I., Wang, I. J., and Bruns, T. D. (2017). Environmental filtering by pH and soil nutrients drives community assembly in fungi at fine spatial scales. *Mol. Ecol.* 26, 6960–6973. doi: 10.1111/mec.14414

Guo, J., Ling, N., Chen, Z., Xue, C., Li, L., Liu, L., et al. (2020). Soil fungal assemblage complexity is dependent on soil fertility and dominated by deterministic processes. *N. Phytol.* 226, 232–243. doi: 10.1111/nph.16345

Hijmans, R. J., Cameron, S. E., Parra, J. L., Jones, P. G., and Jarvis, A. (2005). Very high resolution interpolated climate surfaces for global land areas. *Int. J. Climatol.* 25, 1965–1978. doi: 10.1002/joc.1276

Hilu, K. W., and Liang, G. P. (1997). The matK gene: sequence variation and application in plant systematics. *Am. J. Bot.* 84, 830–839. doi: 10.2307/2445819

Hubbell, S. P. (2001). *The unified neutral theory of biodiversity and biogeography* (MPB-32). Princeton: Princeton University Press.

Ihrmark, K., Bödeker, I., Cruz-Martinez, K., Friberg, H., Kubartova, A., Schenck, J., et al. (2012). New primers to amplify the fungal ITS2 region–evaluation by 454-sequencing of artificial and natural communities. *FEMS Microbiol. Ecol.* 82, 666–677. doi: 10.1111/j.1574-6941.2012.01437.x

Katoh, K., and Standley, D. M. (2013). MAFFT Multiple Sequence Alignment Software Version 7: Improvements in Performance and Usability. *Mol. Biol. Evol.* 30, 772–780. doi: 10.1093/molbev/mst010

Kembel, S. W., Cowan, P. D., Helmus, M. R., Cornwell, W. K., Morlon, H., Ackerly, D. D., et al. (2010). Picante: R tools for integrating phylogenies and ecology. *Bioinformatics* 26, 1463–1464. doi: 10.1093/bioinformatics/btq166

Kivlin, S. N., Winston, G. C., Goulden, M. L., and Treseder, K. K. (2014). Environmental filtering affects soil fungal community composition more than dispersal limitation at regional scales. *Fungal Ecol.* 12, 14–25. doi: 10.1016/j.funeco.2014.04.004

Koizumi, T., and Nara, K. J. T. I. J. (2019). Ectomycorrhizal fungal communities in ice-age relict forests of Pinus pumila on nine mountains correspond to summer temperature. *ISME J.* 14, 189–201. doi: 10.1038/s41396-019-0524-7

Kõljalg, U., Nilsson, R. H., Abarenkov, K., Tedersoo, L., Taylor, A. F., Bahram, M., et al. (2013). Towards a unified paradigm for sequence-based identification of fungi. *Mol. Ecol.* 22, 5271–5277. doi: 10.1111/mec.12481

Kumar, S., Stecher, G., and Tamura, K. (2016). MEGA7: Molecular Evolutionary Genetics Analysis version 7.0 for bigger datasets. *Mol. Biol. Evol.* 33, 1870–1874. doi: 10.1093/molbev/msw054

Ladau, J., and Eloe-Fadrosh, E. A. (2019). Spatial, temporal, and phylogenetic scales of microbial ecology. *Trends Microbiol.* 27, 662–669. doi: 10.1016/j.tim.2019.03.003

Liaw, A., and Wiener, M. (2002). Classification and Regression by randomForest. *R News* 2, 18–22.

Losos, J. B. (2008). Phylogenetic niche conservatism, phylogenetic signal and the relationship between phylogenetic relatedness and ecological similarity among species. *Ecol. Lett.* 11, 995–1003. doi: 10.1111/j.1461-0248.2008.01229.x

Matsuoka, S., Mori, A. S., Kawaguchi, E., Hobara, S., and Osono, T. (2016). Disentangling the relative importance of host tree community, abiotic environment and spatial factors on ectomycorrhizal fungal assemblages along an elevation gradient. *FEMS Microbiol. Ecol.* 92:fiw044. doi: 10.1093/femsec/fiw044

Miyamoto, Y., Danilov, A. V., and Bryanin, S. V. J. M. (2020). The dominance of Suillus species in ectomycorrhizal fungal communities on *Larix gmelinii* in a post-fire forest in the Russian Far East. *Mycorrhiza* 2020, 1–12. doi: 10.1007/s00572-020-00995-3

Miyamoto, Y., Sakai, A., Hattori, M., and Nara, K. (2015). Strong effect of climate on ectomycorrhizal fungal composition: evidence from range overlap between two mountains. *ISME J.* 9, 1870–1879. doi: 10.1038/ismej.2015.8

Miyamoto, Y., Terashima, Y., and Nara, K. (2018). Temperature niche position and breadth of ectomycorrhizal fungi: Reduced diversity under warming predicted by a nested community structure. *Glob. Change Biol.* 24, 5724–5737. doi: 10.1111/gcb.14446

Nemergut, D. R., Schmidt, S. K., Fukami, T., O'Neill, S. P., Bilinski, T. M., Stanish, L. F., et al. (2013). Patterns and processes of microbial community assembly. *Microbiol. Mol. Biol. Rev.* 77, 342–356. doi: 10.1128/MMBR.00051-12

Oksanen, J., Kindt, R., Legendre, P., O'hara, B., Stevens, M. H. H., Oksanen, M. J., et al. (2013). *vegan: Community Ecology Package. R Package Version 2.0-10*. Available online at: http://CRAN.R-project.org/package=vegan [accessed date September 21, 2013]

Ondov, B. D., Bergman, N. H., and Phillippy, A. M. (2011). Interactive metagenomic visualization in a Web browser. *BMC Bioinformatics* 12:385. doi: 10.1186/1471-2105-12-385

Paradis, E., Claude, J., and Strimmer, K. (2004). APE: analyses of phylogenetics and evolution in R language. *Bioinformatics* 20, 289–290. doi: 10.1093/bioinformatics/btg412

Peay, K. G., and Bruns, T. D. (2014). Spore dispersal of basidiomycete fungi at the landscape scale is driven by stochastic and deterministic processes and generates variability in plant-fungal interactions. *N. Phytol.* 204, 180–191. doi: 10.1111/nph.12906

Peay, K. G., Garbelotto, M., and Bruns, T. D. (2010). Evidence of dispersal limitation in soil microorganisms: Isolation reduces species richness on mycorrhizal tree islands. *Ecology* 91, 3631–3640. doi: 10.1890/09-2237.1

Peay, K. G., Schubert, M. G., Nguyen, N. H., and Bruns, T. D. (2012). Measuring ectomycorrhizal fungal dispersal: macroecological patterns driven by microscopic propagules. *Mol. Ecol.* 21, 4122–4136. doi: 10.1111/j.1365-294X.2012.05666.x

Pickles, B. J., Genney, D. R., Anderson, I. C., and Alexander, I. J. (2012). Spatial analysis of ectomycorrhizal fungi reveals that root tip communities are structured by competitive interactions. *Mol. Ecol.* 21, 5110–5123. doi: 10.1111/j.1365-294X.2012.05739.x

Pohlert, T. (2014). *The pairwise multiple comparison of mean ranks package (PMCMR). R Package Version 4.2.* 2016. Available online at: http://CRAN.R-project.org/package=PMCMR [accessed January 25, 2017]

Põlme, S., Bahram, M., Yamanaka, T., Nara, K., Dai, Y. C., Grebenc, T., et al. (2013). Biogeography of ectomycorrhizal fungi associated with alders (*Alnus* spp.) in relation to biotic and abiotic variables at the global scale. *N. Phytol.* 198, 1239–1249. doi: 10.1111/nph.12170

R Development Core Team (2019). *R: A Language and Environment for Statistical Computing*. Vienna: R Foundation for Statistical Computing.

Roy, M., Rochet, J., Manzi, S., Jargeat, P., Gryta, H., and Moreau, P. A. (2013). What determines *Alnus*-associated ectomycorrhizal community diversity and specificity? A comparison of host and habitat effects at a regional scale. *New Phytol.* 198, 1228–1238. doi: 10.1111/nph.12212

Sánchez-Marañón, M., Miralles, I., Aguirre-Garrido, J. F., Anguita-Maeso, M., Millán, V., Ortega, R., et al. (2017). Changes in the soil bacterial community along a pedogenic gradient. *Sci. Rep.* 7:14593. doi: 10.1038/s41598-017-15133-x

Schloss, P. D., Westcott, S. L., Ryabin, T., Hall, J. R., Hartmann, M., Hollister, E. B., et al. (2009). Introducing mothur: open-source, platform-independent, community-supported software for describing and comparing microbial communities. *Appl. Environ. Microbiol.* 75, 7537–7541. doi: 10.1128/AEM.01541-09

Sloan, W. T., Lunn, M., Woodcock, S., Head, I. M., Nee, S., and Curtis, T. P. J. E. M. (2006). Quantifying the roles of immigration and chance in shaping prokaryote community structure. *Environ. Microbio* 8, 732–740. doi: 10.1111/j.1462-2920.2005.00956.x

Smith, S. E., and Read, D. J. (2008). *Mycorrhizal symbiosis*. London, UK: Academic Press.

Stegen, J. C., Lin, X., Konopka, A. E., and Fredrickson, J. K. (2012). Stochastic and deterministic assembly processes in subsurface microbial communities. *ISME J.* 6, 1653–1664. doi: 10.1038/ismej.2012.22

Stegen, J. C., Lin, X. J., Fredrickson, J. K., Chen, X., Kennedy, D. W., Murray, C. J., et al. (2013). Quantifying community assembly processes and identifying features that impose them. *ISME J.* 7, 2069–2079. doi: 10.1038/ismej.2013.93

Taylor, A. F. S. (2008). Recent advances in our understanding of fungal ecology. *Coolia* 51, 197–212.

Tedersoo, L., Bahram, M., Põlme, S., Kõljalg, U., Yorou, N. S., Wijesundera, R., et al. (2014). Global diversity and geography of soil fungi. *Science* 346:1256688. doi: 10.1126/science.1256688

Tedersoo, L., Bahram, M., and Zobel, M. (2020). How mycorrhizal associations drive plant population and community biology. *Science* 367:1223. doi: 10.1126/science.aba1223

Tedersoo, L., Jairus, T., Horton, B. M., Abarenkov, K., Suvi, T., Saar, I., et al. (2008). Strong host preference of ectomycorrhizal fungi in a Tasmanian wet sclerophyll forest as revealed by DNA barcoding and taxon-specific primers. *N. Phytol.* 180, 479–490. doi: 10.1111/j.1469-8137.2008.02561.x

Tedersoo, L., May, T. W., and Smith, M. E. (2010b). Ectomycorrhizal lifestyle in fungi: global diversity, distribution, and evolution of phylogenetic lineages. *Mycorrhiza* 20, 217–263. doi: 10.1007/s00572-009-0274-x

Tedersoo, L., Mett, M., Ishida, T. A., and Bahram, M. (2013). Phylogenetic relationships among host plants explain differences in fungal species richness and community composition in ectomycorrhizal symbiosis. *N. Phytol.* 199, 822–831. doi: 10.1111/nph.12328

Tedersoo, L., Sadam, A., Zambrano, M., Valencia, R., and Bahram, M. (2010a). Low diversity and high host preference of ectomycorrhizal fungi in Western Amazonia, a neotropical biodiversity hotspot. *ISME J.* 4, 465–471. doi: 10.1038/ismej.2009.131

Tedersoo, L., and Smith, M. E. (2013). Lineages of ectomycorrhizal fungi revisited: Foraging strategies and novel lineages revealed by sequences from belowground. *Fungal Biol. Rev.* 27, 83–99. doi: 10.1016/j.fbr.2013.09.001

Toju, H., Tanabe, A., and Ishii, H. (2016). Ericaceous plant–fungus network in a harsh alpine–subalpine environment. *Mol. Ecol.* 25, 3242–3257. doi: 10.1111/mec.13680

van der Linde, S., Suz, L. M., Orme, C. D. L., Cox, F., Andreae, H., Asi, E., et al. (2018). Environment and host as large-scale controls of ectomycorrhizal fungi. *Nature* 558, 243–258. doi: 10.1038/s41586-018-0189-9

Van Geel, M., Yu, K., Ceulemans, T., Peeters, G., van Acker, K., Geerts, W., et al. (2018). Variation in ectomycorrhizal fungal communities associated with Silver linden (Tilia tomentosa) within and across urban areas. *FEMS Microbiol. Ecol.* 94:fiy207. doi: 10.1093/femsec/fiy207

Vlk, L., Tedersoo, L., Antl, T., Větrovský, T., Abarenkov, K., Pergl, J., et al. (2020). Early successional ectomycorrhizal fungi are more likely to naturalize outside their native range than other ectomycorrhizal fungi. *N. Phytol.* 227, 1289–1293. doi: 10.1111/nph.16557

Wang, P., Li, S. P., Yang, X., Zhou, J. Z., Shu, W. S., Jiang, L., et al. (2020). Mechanisms of soil bacterial and fungal community assembly differ among and within islands. *Environ. Microbiol.* 22, 1559–1571. doi: 10.1111/1462-2920.14864

Wang, X., Liu, J., Long, D., Han, Q., and Huang, J. (2017). The ectomycorrhizal fungal communities associated with Quercus liaotungensis in different habitats across northern China. *Mycorrhiza* 27, 441–449. doi: 10.1007/s00572-017-0762-3

Wang, Y. L., Gao, C., Chen, L., Ji, N. N., Wu, B. W., Li, X. C., et al. (2019). Host plant phylogeny and geographic distance strongly structure Betulaceae-associated ectomycorrhizal fungal communities in Chinese secondary forest ecosystems. *FEMS Microbiol. Ecol.* 95:fiz037. doi: 10.1093/femsec/fiz037

Wang, Z. H., Jiang, Y., Deane, D. C., He, F. L., Shu, W. S., and Liu, Y. (2019). Effects of host phylogeny, habitat and spatial proximity on host-specificity and diversity of pathogenic and mycorrhizal fungi in a subtropical forest. *New Phytol.* 223, 462–474. doi: 10.1111/nph.15786

Wang, X. Q., Tank, D. C., and Sang, T. (2000). Phylogeny and divergence times in Pinaceae: evidence from three genomes. *Mol. Phylogenet. Evol.* 17, 773–781. doi: 10.1093/oxfordjournals.molbev.a026356

Webb, C. O., Ackerly, D. D., McPeek, M. A., and Donoghue, M. J. (2002). Phylogenies and community ecology. *Annu. Rev. Ecol. S.* 33, 475–505. doi: 10.1146/annurev.ecolsys.33.010802.150448

White, T. J., Bruns, T., Lee, S., and Taylor, J. W. (1990). "Amplification and directsequencing of fungal ribosomal RNA genes for phylogenetics," in *PCR Protocols:A Guide to Methods and Applications*, eds M. A. Innis, D. H. Gelfand, J. Sninsky, and T. J. White (San Diego, CA: Academic Press), 315–322.

Wu, B. W., Gao, C., Chen, L., Buscot, F., Goldmann, K., Purahong, W., et al. (2018). Host phylogeny is a major determinant of Fagaceae-associated ectomycorrhizal fungal community assembly at a regional scale. *Front. Microbiol.* 9:2409. doi: 10.3389/fmicb.2018.02409

Zhou, J., and Ning, D. (2017). Stochastic community assembly: does it matter in microbial ecology? *Microbiol. Mol. Biol. Rev.* 81, e00002–e17. doi: 10.1128/MMBR.00002-17

Conflict of Interest: The authors declare that the research was conducted in the absence of any commercial or financial relationships that could be construed as a potential conflict of interest.

Copyright © 2021 Wang, Zhang, Xu, Babalola, Xiang, Zhao and Fan. This is an open-access article distributed under the terms of the Creative Commons Attribution License (CC BY). The use, distribution or reproduction in other forums is permitted, provided the original author(s) and the copyright owner(s) are credited and that the original publication in this journal is cited, in accordance with accepted academic practice. No use, distribution or reproduction is permitted which does not comply with these terms.

frontiers in Microbiology

ORIGINAL RESEARCH
published: 17 March 2021
doi: 10.3389/fmicb.2021.650195

The Phylogenetic Relationship Revealed Three New Wood-Inhabiting Fungal Species From Genus *Trechispora*

Wei Zhao[1,2] *and Chang-Lin Zhao*[1,2]*

[1] *Key Laboratory for Forest Resources Conservation and Utilization in the Southwest Mountains of China, Ministry of Education, Southwest Forestry University, Kunming, China,* [2] *College of Biodiversity Conservation, Southwest Forestry University, Kunming, China*

OPEN ACCESS

Edited by:
Dhanushka Nadeeshan Wanasinghe, Key Laboratory for Plant Diversity and Biogeography of East Asia, Kunming Institute of Botany, Chinese Academy of Sciences, China

Reviewed by:
Baokai Cui, Beijing Forestry University, China
Yu-Cheng Dai, Beijing Forestry University, China

***Correspondence:**
Chang-Lin Zhao
Fungichanglinz@163.com

Specialty section:
This article was submitted to Evolutionary and Genomic Microbiology, a section of the journal Frontiers in Microbiology

Received: *08 January 2021*
Accepted: *01 February 2021*
Published: *17 March 2021*

Citation:
Zhao W and Zhao C-L (2021) The Phylogenetic Relationship Revealed Three New Wood-Inhabiting Fungal Species From Genus Trechispora. Front. Microbiol. 12:650195. doi: 10.3389/fmicb.2021.650195

Wood-inhabiting fungi play a significant role in wood degradation and the cycle of matter in the ecological system. In the present study, three new wood-inhabiting fungal species, *Trechispora bambusicola*, *Trechispora fimbriata*, and *Trechispora fissurata* spp. nov., are nested in *Trechispora*, which are proposed based on a combination of morphological features and molecular evidence. Sequences of internal transcribed spacer (ITS) and large subunit (nLSU) regions of the studied samples were generated, and the phylogenetic analyses were performed with maximum likelihood, maximum parsimony, and Bayesian inference methods. The phylogenetic analyses inferred from ITS showed that *T. bambusicola* was sister to *Trechispora stevensonii*, *T. fimbriata* grouped with *Trechispora nivea*, and *T. fissurata* grouped with *Trechispora echinospora*. The phylogenetic tree based on ITS + nLSU sequences demonstrated that *T. bambusicola* formed a single lineage and then grouped with *Trechispora rigida* and *T. stevensonii*. *T. fimbriata* was sister to *T. nivea*. *T. fissurata* grouped with *Trechispora thelephora*.

Keywords: Hydnodontaceae, phylogeny, taxonomy, wood-inhabiting fungi, Yunnan Province

INTRODUCTION

Trechispora P. Karst. (Hydnodontaceae, Trechisporales) was typified with *Trechispora onusta* P. Karst. (Karsten, 1890). It is characterized by the resupinate to effused basidiomata with smooth to hydnoid to poroid hymenophore, a monomitic or dimitic hyphal structure with clamped generative hyphae having typical ampullaceous septa, and short cylindric

Abbreviations: ITS, internal transcribed spacer; nLSU, large subunit; SWFC, herbarium of Southwest Forestry University, Kunming, China; KOH, 5% potassium hydroxide; CB, Cotton Blue; CB−, acyanophilous; IKI, Melzer's reagent; IKI−, both inamyloid and indextrinoid; L, mean spore length (arithmetic average for all spores); W, mean spore width (arithmetic average for all spores); Q, variation in the L/W ratios between The studied specimens, n (a/b), number of spores (a) measured from given number (b) of specimens, spore measurements do not include ornamentation; CTAB, cetyltrimethylammonium bromide; DNA, deoxyribonucleic acid; PCR, polymerase chain reaction; MP, maximum parsimony; ML, maximum likelihood; BI, Bayesian inference; TBR, tree-bisection reconnection.

basidia and smooth to verrucose or aculeate basidiospores (Karsten, 1890; Bernicchia and Gorjón, 2010). About 49 species are currently known in *Trechispora* worldwide (Liberta, 1966, 1973; Larsson, 1994, 1995, 1996; Ryvarden, 2002; Trichiès and Schultheis, 2002; Miettinen and Larsson, 2006; Ordynets et al., 2015; Xu et al., 2019) and Index Fungorum[1] and MycoBank[2].

Larsson (2007) addressed the classification of corticioid fungi and revealed that *Trechispora farinacea* (Pers.) Liberta grouped with *Trechispora hymenocystis* (Berk. and Broome) K.H. Larss., in which both species nested within the family Hydnodontaceae Jülich. Based on the large subunit nuclear ribosomal RNA gene (nLSU) datasets, Albee-Scott and Kropp (2010) supported to transfer *Hydnodon thelephorus* (Lév.) Banker to *Trechispora* as *Trechispora thelephora* (Lév.) Ryvarden. The order Trechisporales was studied employing the internal transcribed spacer (ITS) and nLSU regions, in which it suggested that *Porpomyces* Jülich, *Sistotremastrum* J. Erikss., *Subulicystidium* Parmasto, and *Trechispora* belonged to a highly supported clade and *Trechispora* belongs to Hydnodontaceae and was closely related to *Brevicellicium* K.H. Larss. and Hjortstam (Telleria et al., 2013). A phylogenetic study of *Trechispora* was addressed and demonstrated that *Trechispora cyatheae* Ordynets, Langer and K.H. Larss. and *Trechispora echinocristallina* Ordynets, Langer and K.H. Larss. clustered into *Trechispora* as new members, inferred from the combined data of the ITS and LSU datasets (Ordynets et al., 2015). The phylogeny of Trechisporales was inferred from a combined dataset of ITS-nLSU sequences and showed that *Porpomyces*, *Scytinopogon* Singer, and *Trechispora* grouped together and nested within family Hydnodontaceae (Liu et al., 2019). Phylogram generated from analysis of ITS sequence dataset of *Trechispora* showed that *Trechispora echinospora* Telleria was sister to the clade formed by *Trechispora araneosa* (Hohn. and Litsch.) K.H. Larss., *T. farinacea*, *T. hymenocystis*, and *Trechispora mollusca* (Pers.) Liberta with a low support (Phookamsak et al., 2019). The ITS + nLSU dataset comprised 22 species and revealed that *Trechispora yunnanensis* C.L. Zhao formed a monophyletic lineage within *Trechispora* and was closely related to *Trechispora byssinella* (Bourdot) Liberta and *Trechispora laevis* K.H. Larss. (Xu et al., 2019).

During the studies on wood-inhabiting fungi in southern China, three species of *Trechispora* could not be assigned to any described species. Obtaining sequences from the new taxa, the authors examine taxonomy and phylogeny of three new species within the genus *Trechispora*, based on the ITS and nLSU sequences.

MATERIALS AND METHODS

Morphology

The studied specimens are deposited at the herbarium of Southwest Forestry University (SWFC), Kunming, Yunnan Province, China. Macromorphological descriptions were based on field notes. Color terms follow Petersen (1996). Micromorphological data were obtained from the dried specimens and observed under a light microscope following Dai (2012). The following abbreviations were used: KOH = 5% potassium hydroxide, CB = Cotton Blue, CB− = acyanophilous, IKI = Melzer's reagent, IKI− = both inamyloid and indextrinoid, L = mean spore length (arithmetic average for all spores), W = mean spore width (arithmetic average for all spores), Q = variation in the L/W ratios between the studied specimens, n (a/b) = number of spores (a) measured from given number (b) of specimens, spore measurements do not include ornamentation.

Molecular Phylogeny

Cetyltrimethylammonium bromide (CTAB) rapid plant genome extraction kit-DN14 (Aidlab Biotechnologies Co., Ltd., Beijing, China) was used to obtain genomic deoxyribonucleic acid (DNA) from dried specimens, according to the manufacturer's instructions following Zhao and Wu (2017). ITS region was amplified with primer pair ITS5 and ITS4 (White et al., 1990). Nuclear LSU region was amplified with primer pair LR0R and LR7[3]. The polymerase chain reaction (PCR) procedures for ITS and nLSU following Zhao and Wu (2017). The PCR products were purified and directly sequenced at Kunming Tsingke Biological Technology Limited Company, Kunming, Yunnan Province, China. All newly generated sequences were deposited at GenBank (**Table 1**).

Sequencher 4.6 (GeneCodes, Ann Arbor, United States) was used to edit the DNA sequence. Sequences were aligned in MAFFT 7[4] using the "G-INS-I" strategy and manually adjusted in BioEdit (Hall, 1999). The sequence alignment was deposited in TreeBase (submission ID 25879). Sequences of *Fibrodontia alba* Yurchenko and Sheng H. Wu and *Fibrodontia gossypina* Parmasto retrieved from GenBank were used as an outgroup in the ITS + nLSU analyses by following Ordynets et al. (2015).

Maximum parsimony (MP) analyses were applied to the ITS + nLSU dataset sequences. Approaches to phylogenetic analysis followed Zhao and Wu (2017), and the tree construction procedure was performed in PAUP* version 4.0b10 (Swofford, 2002). All characters were equally weighted and gaps were treated as missing data. Trees were inferred using the heuristic search option with tree-bisection reconnection (TBR) branch swapping and 1000 random sequence additions. Max-trees were set to 5000, branches of zero length were collapsed, and all parsimonious trees were saved. Clade robustness was assessed using a bootstrap (BT) analysis with 1000 replicates (Felsenstein, 1985). Descriptive tree statistics tree length (TL), consistency index (CI), retention index (RI), rescaled consistency index (RC), and homoplasy index (HI) were calculated for each Maximum Parsimonious Tree generated. Datamatrix was also analyzed using maximum likelihood (ML) approach with RAxML-HPC2 through the Cipres Science Gateway with GTR + I + G molecular evolution model[5] (Miller et al., 2009). Branch support (BS) for ML analysis was determined by 1000 BT replicates.

[1]http://www.indexfungorum.org/Names/Names.asp

[2]https://www.mycobank.org/Biolomics.aspx?Table=Mycobank&Page=200&ViewMode=Basic

[3]http://lutzonilab.org/nuclear-ribosomal-dna/

[4]http://mafft.cbrc.jp/alignment/server/

[5]www.phylo.org

TABLE 1 | List of species, specimens, and GenBank accession numbers of sequences used in this study.

Species name	Sample no.	GenBank accession no.		References
		ITS	nLSU	
Fibrodontia alba	TNMF 24944	KC928274	KC928275	Yurchenko and Wu (2014)
Fibrodontia gossypina	GEL 5042	DQ249274	AY646100	Unpublished
Trechispora araneosa	KHL 8570	AF347084	AF347084	Larsson et al. (2004)
Trechispora bambusicola	CLZhao 3302	MW544021	MW520171	This study
Trechispora bambusicola	CLZhao 3305	MW544022	MW520172	This study
Trechispora bispora	CBS 142.63	MH858241	MH869842	Vu et al. (2019)
Trechispora byssinella	UC 2023068	KP814481	–	Unpublished
Trechispora cohaerens	TU 110332	UDB008249	–	Ordynets et al. (2015)
Trechispora cohaerens	TU 115568	UDB016421	–	Ordynets et al. (2015)
Trechispora confinis	KHL 11064	AF347081	AF347081	Larsson et al. (2004)
Trechispora cyatheae	FR-0219442	UDB024014	UDB024014	Ordynets et al. (2015)
Trechispora cyatheae	FR-0219443	UDB024015	UDB024015	Ordynets et al. (2015)
Trechispora echinocristallina	FR-0219445	UDB024018	UDB024018	Ordynets et al. (2015)
Trechispora echinocristallina	FR-0219448	UDB024022	UDB024022	Ordynets et al. (2015)
Trechispora echinospora	E11/37-03	JX392845	JX392846	Telleria et al. (2013)
Trechispora echinospora	E09/60-06	JX392847	JX392848	Telleria et al. (2013)
Trechispora echinospora	E11/37-05	–	JX392849	Telleria et al. (2013)
Trechispora farinacea	KHL 8451	AF347082	AF347082	Unpublished
Trechispora farinacea	KHL 8793	AF347089	AF347089	Larsson et al. (2004)
Trechispora fissurata	CLZhao 995	MW544026	MW520176	This study
Trechispora fissurata	CLZhao 4571	MW544027	MW520177	This study
Trechispora fimbriata	CLZhao 4154	MW544023	MW520173	This study
Trechispora fimbriata	CLZhao 7969	MW544024	MW520174	This study
Trechispora fimbriata	CLZhao 9006	MW544025	MW520175	This study
Trechispora hymenocystis	KHL 8795	AF347090	AF347090	Unpublished
Trechispora hymenocystis	TL 11112	UDB000778	UDB000778	Ordynets et al. (2015)
Trechispora incisa	EH 24/98	AF347085	–	Unpublished
Trechispora kavinioides	KGN 981002	AF347086	AF347086	Larsson et al. (2004)
Trechispora laevis	TU 115551	UDB016468	–	Ordynets et al. (2015)
Trechispora mollusca	DLL 2010-077	JQ673209	–	Ordynets et al. (2015)
Trechispora mollusca	DLL 2011-186	KJ140681	–	Ordynets et al. (2015)
Trechispora nivea	MA-Fungi 76238	JX392824	JX392825	Telleria et al. (2013)
Trechispora nivea	MA-Fungi 76257	JX392826	JX392827	Telleria et al. (2013)
Trechispora nivea	MA-Fungi 82480	JX392829	JX392830	Telleria et al. (2013)
Trechispora nivea	MA-Fungi 74044	JX392832	JX392833	Telleria et al. (2013)
Trechispora regularis	KHL 10881	AF347087	AF347087	Larsson et al. (2004)
Trechispora rigida	URM 85754	–	MH279999	Unpublished
Trechispora stevensonii	MA-Fungi 70669	JX392841	JX392842	Telleria et al. (2013)
Trechispora stevensonii	HJM 18087	–	MH290761	Unpublished
Trechispora stevensonii	KHL 14654	–	MH290762	Unpublished
Trechispora stevensonii	TU 115499	UDB016467	UDB016467	Ordynets et al. (2015)
Trechispora stellulata	UC 2022880	KP814437	–	Unpublished
Trechispora stellulata	UC 2023099	KP814451	–	Unpublished
Trechispora subsphaerospora	KHL 8511	AF347080	AF347080	Larsson et al. (2004)
Trechispora thelephora	URM 85757	–	MH280001	Unpublished
Trechispora thelephora	URM 85758	–	MH280002	Unpublished
Trechispora yunnanensis	CLZhao 210	MN654918	MN654921	Xu et al. (2019)
Trechispora yunnanensis	CLZhao 214	MN654919	MN654922	Xu et al. (2019)
Trechispora yunnanensis	CLZhao 215	MN654920	MN654923	Xu et al. (2019)

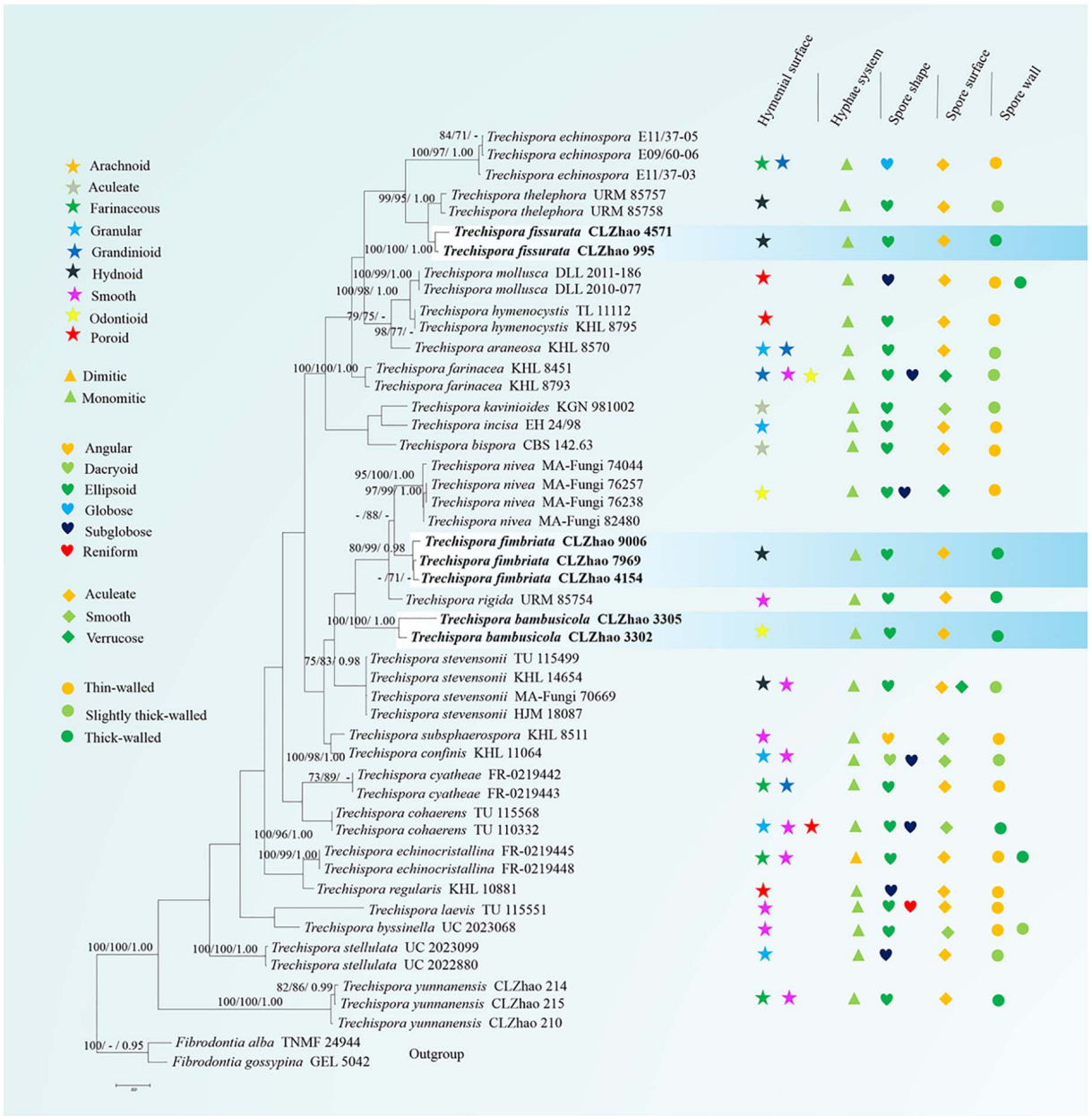


FIGURE 1 | Maximum Parsimony strict consensus tree illustrating the phylogeny of three new species and related species in *Trechispora* based on ITS sequences. Branches are labeled with maximum likelihood bootstrap values > 70%, parsimony bootstrap proportion values > 50%, and Bayesian posterior probabilities > 0.95, respectively.

MrModeltest 2.3 (Nylander, 2004) was used to determine the best-fit evolution model (GTR + I + G) for each data set for Bayesian inference (BI) of the phylogeny. BI was calculated with MrBayes 3.1.2 (Ronquist and Huelsenbeck, 2003). Four Markov chains were run for two runs from random starting trees for 1 million generations and trees were sampled every 100 generations; the first one-fourth of generations were discarded as burn-in. A majority rule consensus tree of all remaining trees was calculated. Branches were considered as significantly supported if they received ML BT values > 75%, MP BT values > 75%, or Bayesian posterior probabilities (PP) > 0.95.

RESULTS

Molecular Phylogeny

In the ITS dataset, the sequences from 43 fungal specimens representing 25 species were included. The dataset had an aligned length of 1034 characters, of which 521 characters

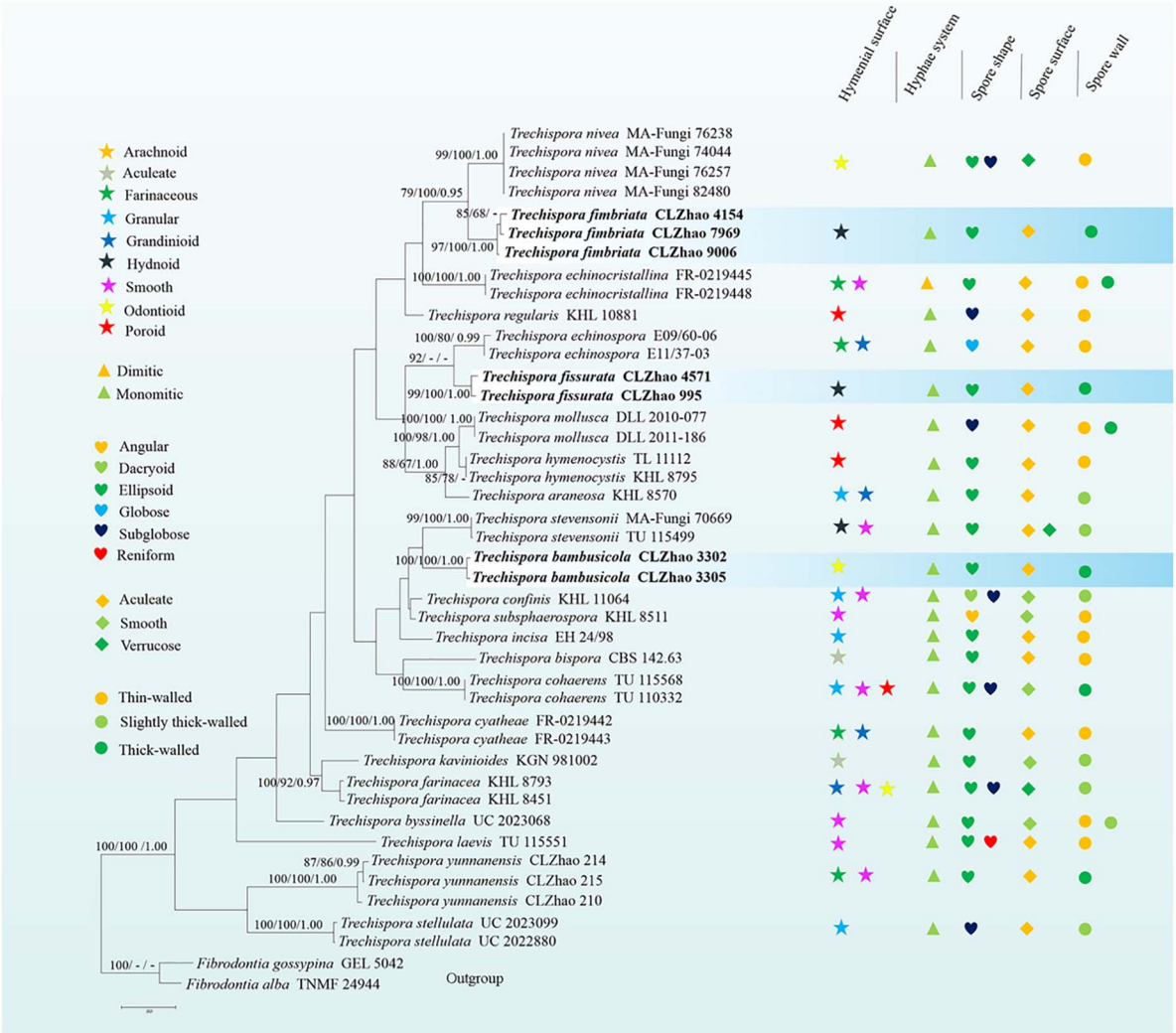


FIGURE 2 | Maximum Parsimony strict consensus tree illustrating the phylogeny of three new species and related species in *Trechispora* based on ITS + nLSU sequences. Branches are labeled with maximum likelihood bootstrap values > 70%, parsimony bootstrap proportion values > 50%, and Bayesian posterior probabilities > 0.95, respectively.

are constant, 86 are variable and parsimony-uninformative, and 427 are parsimony-informative. MP analysis yielded 26 equally parsimonious trees (TL = 2048, CI = 0.4561, HI = 0.5439, RI = 0.6174, RC = 0.2816). Best model for the ITS dataset estimated and applied in the Bayesian analysis: GTR + I + G, lset nst = 6, rates = invgamma; prset statefreqpr = dirichlet (1,1,1,1). Bayesian analysis and ML analysis resulted in a similar topology to MP analysis, with an average standard deviation of split frequencies = 0.009985 (BI).

The phylogeny (**Figure 1**) inferred from ITS sequences showed that *Trechispora bambusicola* was sister to *Trechispora stevensonii* (Berk. and Broome) K.H. Larss, and *Trechispora fimbriata* grouped with *Trechispora nivea*. *T. fissurata* grouped with *T. echinospora* Telleria, M. Dueñas, I. Melo, and M.P. Martín.

In the ITS + nLSU dataset, it included sequences from 49 fungal specimens representing 27 species. The dataset had an aligned length of 2256 characters, of which 1387 characters are constant, 188 are variable and parsimony-uninformative, and 681 are parsimony-informative. MP analysis yielded 100 equally parsimonious trees (TL = 2811, CI = 0.4963, HI = 0.5037, RI = 0.6409, RC = 0.3180). Best model for the ITS dataset estimated and applied in the Bayesian analysis: GTR + I + G, lset nst = 6, rates = invgamma; prset statefreqpr = dirichlet (1,1,1,1). Bayesian analysis and ML analysis resulted in a similar topology to MP analysis, with an average standard deviation of split frequencies = 0.009991 (BI).

The phylogenetic tree (**Figure 2**) inferred from ITS + nLSU sequences demonstrated 27 species of *Trechispora* and revealed that *T. bambusicola* formed a single lineage and then grouped with *Trechispora rigida* (Berk.) K.H. Larss. and *T. stevensonii*.

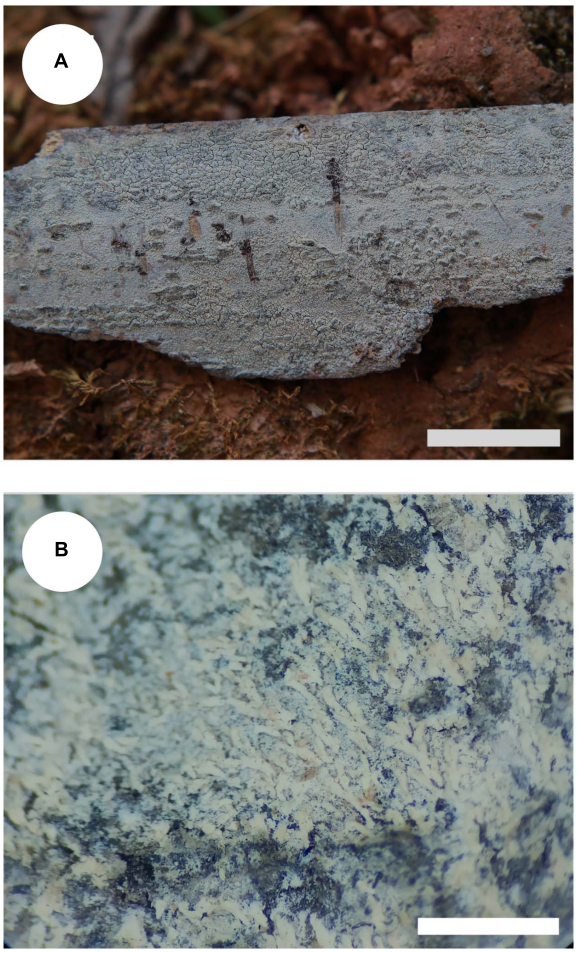


FIGURE 3 | Basidiomata of *Trechispora bambusicola* (holotype): Bars: **(A)** 2 cm; **(B)** 1 mm.

T. fimbriata was sister to *T. nivea*. *T. fissurata* grouped with *T. thelephora* (Lév.) Ryvarden.

Taxonomy

Trechispora bambusicola C.L. Zhao, sp. nov.

MycoBank no.: MB 838612 (**Figures 3**, **4**).

Holotype—China, Yunnan Province, Pu'er, Laiyanghe National Forest Park, on dead bamboo, 30 September 2017, CLZhao 3305 (SWFC).

Etymology—*Bambusicola* (Lat.): referring to occurrence on bamboo stump.

Basidiomata

Annual, adnate, soft, and fragile, without odor or taste when fresh, becoming granulose upon drying, up to 15 cm long and 5 cm wide, 50–300 μm thick. Hymenial surface odontioid, aculei cylindrical to conical, blunt, 0.3–0.5 mm long, white to cream when fresh, turn to cream to buff upon drying. Margin white to cream.

Hyphal structure

Monomitic, generative hyphae with clamp connections, hyaline, thick-walled, up to 0.7 μm, richly branched, 2–3 μm in diameter, IKI−, CB−; hyphae unchanged in KOH.

Hymenium

Cystidia and cystidioles absent; basidia shortly cylindrical to subclavate with median constriction, with 4-sterigmata and a basal clamp connection, 9–13 × 2.5–5 μm, basidioles dominant, in shape similar to basidia, but slightly smaller.

Basidiospores

Ellipsoid, hyaline, thick-walled, ornamented, sparse aculei, sharp, IKI−, CB−, (2.6−)2.9–3.5(−3.9) × 2–2.7 μm, L = 3.18 μm, W = 2.41 μm, Q = 1.26–1.38 (n = 60/2).

Type of rot

White rot.

Additional specimen examined

CHINA, Yunnan Province, Pu'er, Laiyanghe National Forestry Park, on dead bamboo, 30 September 2017, CLZhao 3302 (SWFC).

Trechispora fimbriata C.L. Zhao, sp. nov.

MycoBank no.: MB 838613 (**Figures 5**, **6**).

Holotype—China, Yunnan Province, Puer, Jingdong County, Wuliangshan National Nature Reserve, on the angiosperm trunk, October 5, 2017, CLZhao 4154 (SWFC).

Etymology—*Fimbriata* (Lat.): refers to the fimbriate margin of the basidiomata.

Basidiomata

Annual, adnate, without odor or taste when fresh, becoming fragile upon drying, up to 10 cm long and 3 cm wide, 100–200 μm thick. Hymenial surface hydnoid, with aculei, cylindrical, blunt, 0.4–0.7 mm long, white to pink when fresh, turn to pink to buff upon drying. Margin white to cream, thinning out, fimbriate.

Hyphal system

Monomitic, generative hyphae with clamp connections, hyaline, thick-walled, up to 0.6 μm, branched, 2–4 μm in diameter, IKI−, CB−; hyphae unchanged in KOH.

Hymenium

Cystidia and cystidioles absent; basidia shortly cylindrical with median constriction, with 4–6 sterigmata and a basal clamp connection, 7–11.5 × 3.5–5 μm, basidioles dominant, in shape similar to basidia, but slightly smaller.

Basidiospores

Ellipsoid, hyaline, thick-walled, ornamented, sparse aculei, sharp, IKI−, CB−, (2.5−)3–3.6(−3.8) × 2.4–3.2 μm, L = 3.25 μm, W = 2.63 μm, Q = 1.17–1.38 (n = 90/3).

Type of rot

White rot.

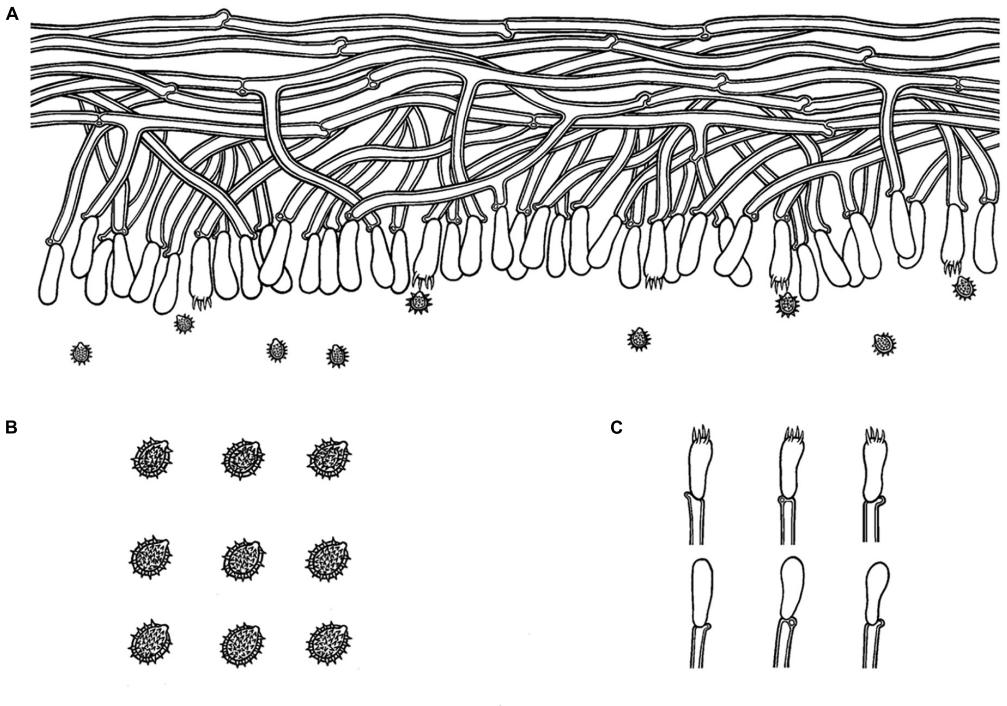


FIGURE 4 | Microscopic structures of *Trechispora bambusicola* (drawn from the holotype): **(A)** Section of hymenium. **(B)** Basidiospores. **(C)** Basidia and basidioles. Bars: **(A,C)** 10 μm; **(B)** 5 μm.

Additional specimens examined

China, Yunnan Province, Yuxi, Xinping County, Mopanshan National Forestry Park, on living tree of angiosperm, August 9, 2018, CLZhao 7969 (SWFC); on angiosperm trunk, October 15, 2018, CLZhao 9006 (SWFC).

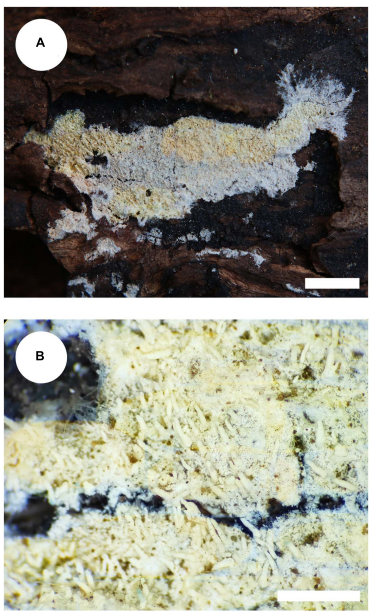


FIGURE 5 | Basidiomata of *Trechispora fimbriata* (holotype). Bars: **(A)** 5 mm; **(B)** 1 mm.

Trechispora fissurata C.L. Zhao, sp. nov.

MycoBank no.: MB 838614 (**Figures 7**, **8**).

Holotype—China, Yunnan Province, Puer, Jingdong County, Wuliangshan National Nature Reserve, on angiosperm trunk, October 6, 2017, CLZhao 4571 (SWFC).

Etymology—*Fissurata* (Lat.): refers to the cracking fissures on hymenial surface.

Basidiomata

Annual, adnate, without odor or taste when fresh, becoming cracking upon drying, up to 8 cm long and 4.5 cm wide, 400–800 μm thick. Hymenial surface hydnoid, with aculei, cylindrical to conical, sharp, 0.5–0.9 mm long, cream to straw yellow when fresh, turn to cream to yellow upon drying. Margin cream to yellow.

Hyphal system

Monomitic, generative hyphae with clamp connections, hyaline, thick-walled, up to 0.8 μm, branched, 2.5–5 μm in diameter, IKI−, CB−; hyphae unchanged in KOH.

Hymenium

Cystidia and cystidioles absent; basidia shortly clavate to tubular, with 4-sterigmata and a basal clamp connection, 8–10.5 × 2.5–4.5 μm, basidioles dominant, in shape similar to basidia, but slightly smaller.

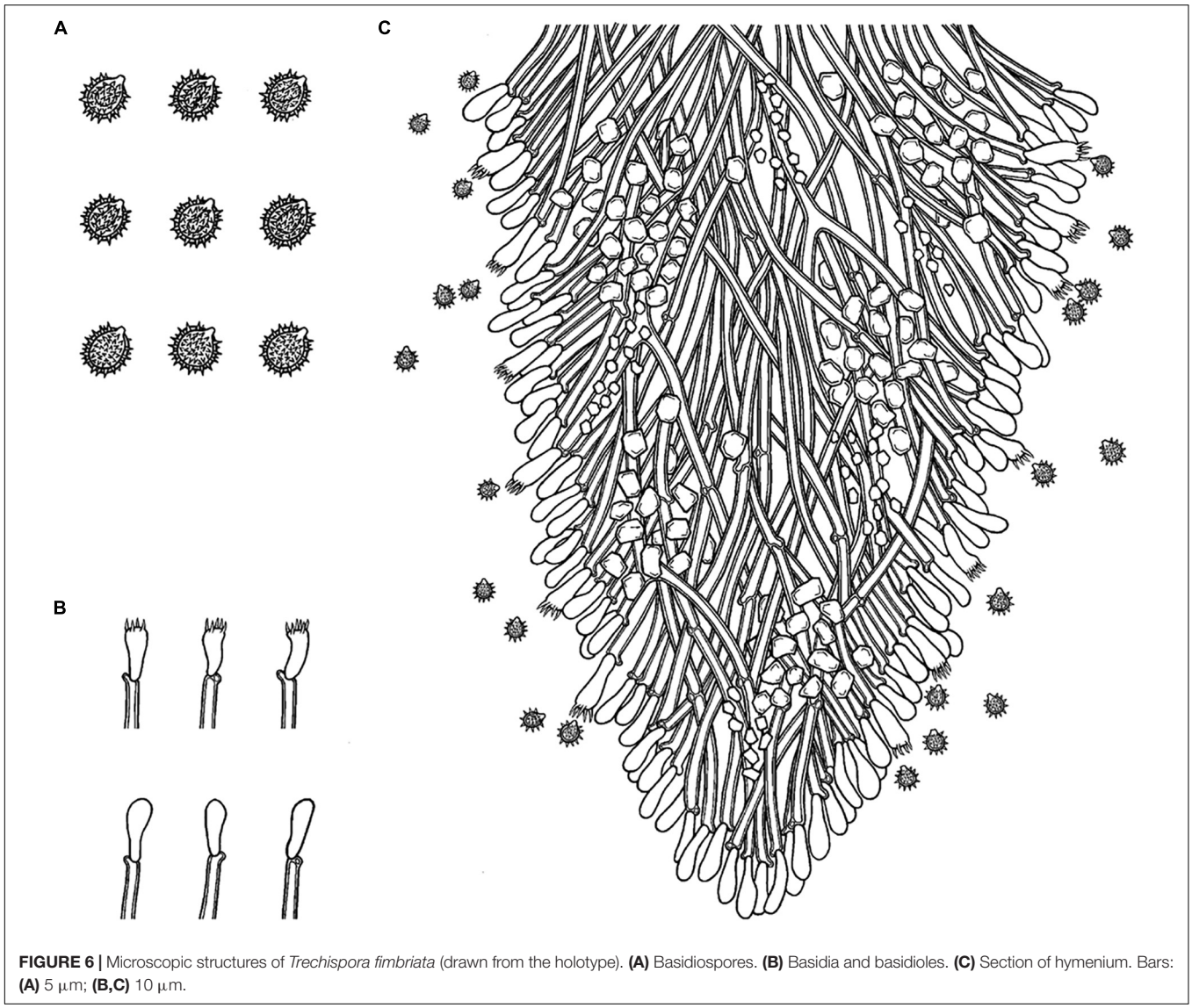


FIGURE 6 | Microscopic structures of *Trechispora fimbriata* (drawn from the holotype). **(A)** Basidiospores. **(B)** Basidia and basidioles. **(C)** Section of hymenium. Bars: **(A)** 5 μm; **(B,C)** 10 μm.

Basidiospores

Ellipsoid, hyaline, thick-walled, ornamented, dense aculei, sharp, IKI−, CB−, (3−)3.3–4(−4.3) × (2.5−)2.8–3.5(−3.9) μm, L = 3.67 μm, W = 3.19 μm, Q = 1.13–1.17 (n = 60/2).

Type of rot

White rot.

Additional specimen examined

CHINA, Yunnan Province, Yuxi, Xinping County, Mopanshan Forestry Park, on the fallen angiosperm branch, January 17, 2017, CLZhao 995 (SWFC).

DISCUSSION

Phylogenetically, Phookamsak et al. (2019) introduced the phylogram generated from BI analysis of ITS sequence dataset of *Trechispora* sequences and included most taxa in this genus, in which it implied the phylogenetic relationship among species of *Trechispora*. In the present study, based on the ITS sequences (**Figure 1**), *T. bambusicola* was sister to *T. stevensonii* (Berk. and Broome) K.H. Larss; *T. fimbriata* grouped with *T. nivea*; *T. fissurata* grouped with *T. echinospora* Telleria, M. Dueñas, I. Melo, and M.P. Martín. Further ITS + nLSU dataset (**Figure 2**) revealed that *T. bambusicola* formed a single lineage and then grouped with *T. rigida* and *T. stevensonii*; *T. fimbriata* was sister to *T. nivea*; *T. fissurata* grouped with *T. thelephora*. However, *T. rigida* differs in its dirty white to buff hymenophore (Larsson, 1996). *T. stevensonii* is separated from *T. bambusicola* by the smooth to hydnoid hymenophore and larger basidiospores (4–4.5 × 3–3.5 μm; Larsson, 1995). *T. nivea* differs from *T. fimbriata* by the white to light ochraceous hymenial surface (Persoon, 1794). *T. echinospora* differs from *T. fissurata* by the farinaceous to grandinioid hymenophore and larger, globose basidiospores (3.3–4 × 2.8–3.5 μm; Phookamsak et al., 2019) and *T. thelephora* differs in its pileate to stipitate

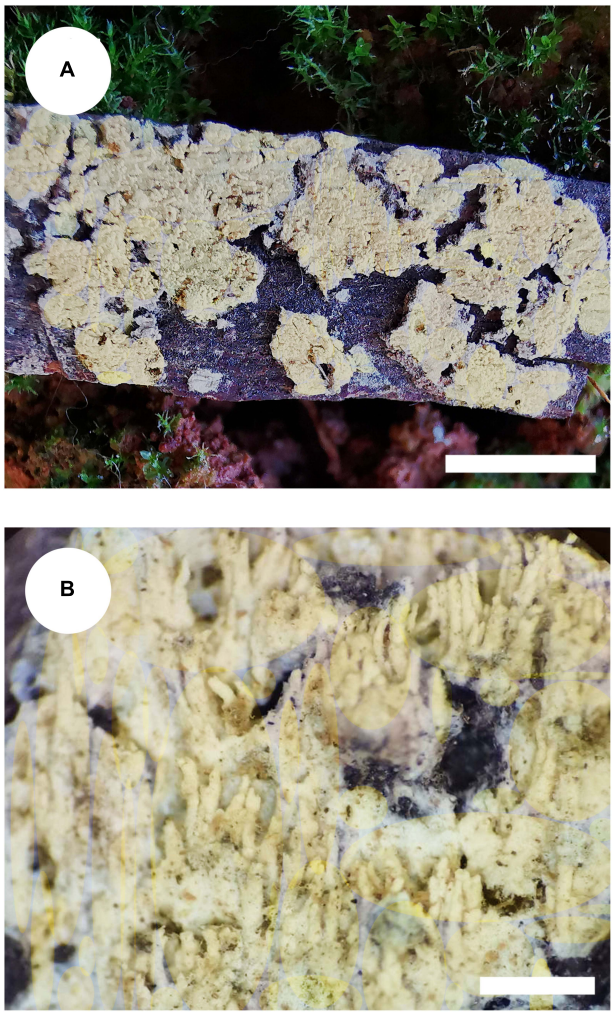


FIGURE 7 | Basidiomata of *Trechispora fissurata* (holotype). Bars: **(A)** 1 cm; **(B)** 1 mm.

with light yellow brown surface and larger (4–5 × 3.4–4.5 μm; Albee-Scott and Kropp, 2010).

In the present study, three new species, *T. bambusicola*, *T. fimbriata*, and *T. fissurata* spp. nov. are found from rotten wood. Morphologically, *T. bambusicola* is similar to *T. cyatheae* Ordynets, Langer and K.H. Larss. by sharing the characteristics of soft and fragile basidiomata. However, *T. cyatheae* differs from *T. bambusicola* by having farinaceous to grandinioid hymenophore and thin-walled generative hyphae (Ordynets et al., 2015).

Trechispora fimbriata has similar characteristics of having the fimbriate margin with *Trechispora canariensis* Ryvarden and Liberta, *Trechispora clancularis* (Park.-Rhodes) K.H. Larss., *Trechispora microspora* (P. Karst.) Liberta, *Trechispora stellulata* (Bourdot and Galzin) Liberta, and *Trechispora subhelvetica* (Parmasto) Liberta. However, *T. canariensis* differs in its arachnoid to pelliculose hymenophore and larger basidiospores (5–7 × 3–3.5 μm; Ryvarden and Liberta, 1978); *T. clancularis* differs in the poroid to irpicoid hymenophore and slightly cyanophilous basidiospores (Larsson, 1994); *T. stellulata* differs in the arachnoid to byssoid hymenophore with whitish hymenial surface (Liberta, 1966); and *T. subhelvetica* differs in the narrower basidiospores (3–4 × 2–2.5 μm; Parmasto, 1965).

Trechispora fissurata resembles several species with similar features of having the hydnoid hymenophore and a monomitic hyphal system: *T. nivea* (Pers.) K.H. Larss., *T. stevensonii* (Berk. and Broome) K.H. Larss., and *Trechispora verruculosa* (G. Cunn.) K.H. Larss., but *T. nivea* by the white to pale ochraceous hymenial surface and thin-walled generative hyphae encrusted with granular crystals (Bernicchia and Gorjón, 2010); *T. stevensonii* by the white to ochraceous hymenial surface and larger basidiospores (4–4.5 × 3–3.5 μm; Larsson, 1995); *T. verruculosa* by the slightly cyanophilous and larger basidiospores (4.5–5.5 × 3.5–4.5 μm; Larsson, 1996).

Currently, eight species of *Trechispora* have been reported from China (Dai, 2011; Xu et al., 2019), *Trechispora alnicola*, *Trechispora cohaerens*, *T. farinacea*, *T. microspora*, *T. nivea*, *Trechispora polygonospora* Ryvarden, *Trechispora subsphaerospora* (Litsch.) Liberta, and *T. yunnanensis*, and one species of *T. yunnanensis* was found in Yunnan Province of China and it differs from three new species by having a smooth to farinaceous hymenial surface and larger basidiospores (7–8.5 × 5–5.5 μm; Xu et al., 2019). Three new taxa do not closely group together in phylogenetic trees, and morphologically, *T. bambusicola* differs from *T. fimbriata* and *T. fissurata* by having granulose basidiomata with cream to buff hymenial surface and growth on dead bamboo. *T. fimbriata* differs in its fimbriate margin of the basidiomata with pink to buff hymenial surface.

In addition, the ectomycorrhizal fungi (EcM) play an important role in ecosystems based on their mutualistic association with many groups of plants (Heijden et al., 2015). Vanegas-León et al. (2019) discovered the Trechisporales basidiomes and root colonization from *T. thelephora* basidiome. In the present study, *T. fissurata* was sister to *T. thelephora* based on ITS + nLSU phylogenetic analysis (**Figure 2**), which implied that both species have close evolutionary relationship. However, *T. fissurata* grows on deeply decayed wood, and *T. thelephora* is a soil-inhabiting fungus. Therefore, future investigations in both inhabiting types are needed to determine whether the natural selection or other factors pushes the different direction on inhabiting soil/wood among *Trechispora*.

In the habitat and distribution, Hibbett et al. (2014) revealed that most species of *Trechispora* is considered as soil-inhabiting. Later, some species were found on deeply decayed wood fungi (Bernicchia and Gorjón, 2010; Dai, 2011). However, some species in *Trechispora* are a typical feature of ectomycorrhizal fungi as frequently forming basidiomes on soil (Dunham et al., 2007; Vanegas-León et al., 2019). In the neotropical and subtropical region, the ectomycorrhizal basidiomes are found; however, the researches on the new taxa related to wood-decaying fungi of *Trechispora* from China are poorly reported. Further studies may focus on the relationships between

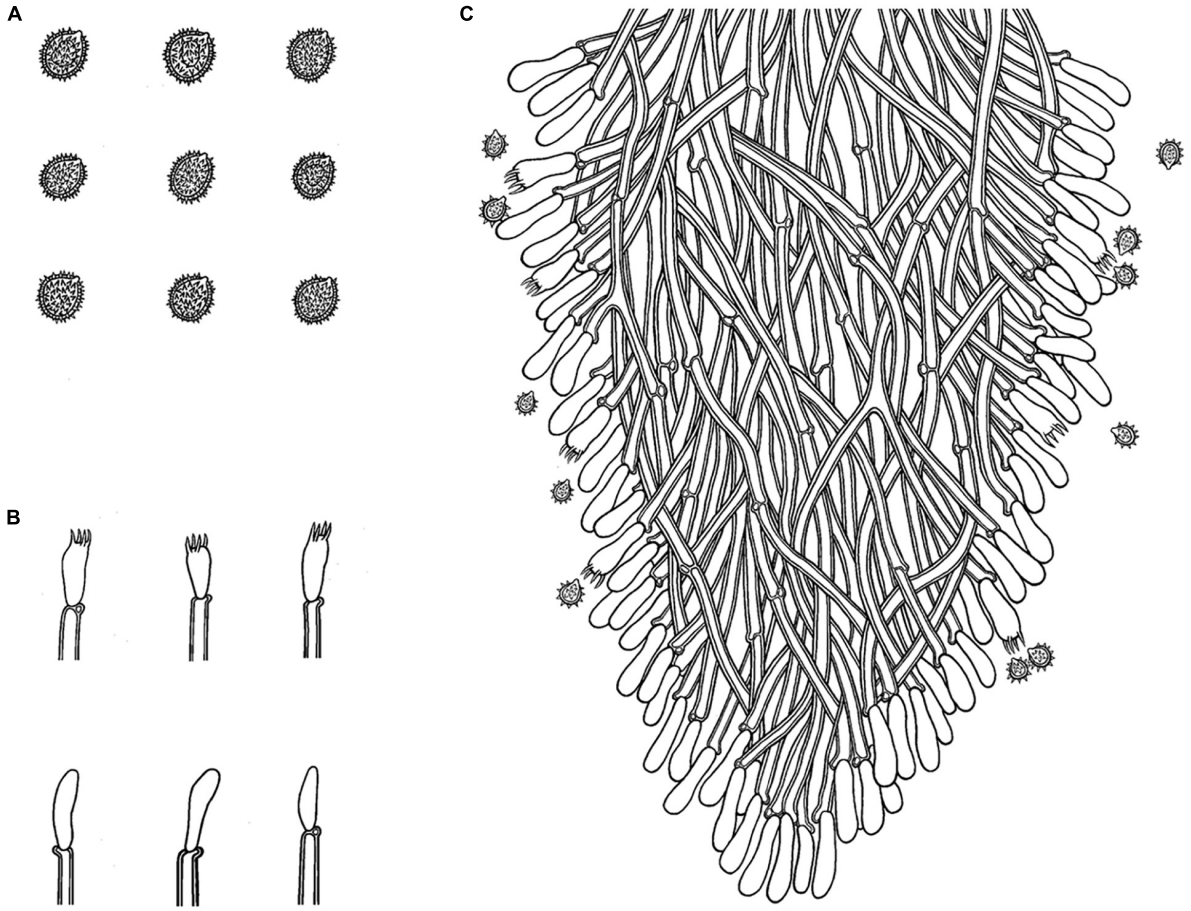


FIGURE 8 | Microscopic structures of *Trechispora fissurata* (drawn from the holotype). **(A)** Basidiospores. **(B)** Basidia and basidioles. **(C)** Section of hymenium. Bars: **(A)** 5 μm; **(B,C)** 10 μm.

the plants and species from *Trechispora* and try to better understand the evolutionary directions between soil-inhabiting and decayed wood fungi of *Trechispora*; many fungal studies on phylogeny and application were from these areas, which will be useful to push future researches for the genus *Trechispora* (Dai, 2011; Cui et al., 2019; Shen et al., 2019; Zhu et al., 2019; Richter et al., 2019; Angelini et al., 2020; Bao et al., 2020).

DISCLOSURE

All the experiments undertaken in this study comply with the current laws of the People's Republic of China.

DATA AVAILABILITY STATEMENT

The data presented in the study are deposited in the https://www.ncbi.nlm.nih.gov/GenBank and https://www.mycobank.org/page/Home/MycoBank repository accession number of GenBank (ITS MW544021-MW544027 and nLSU MW520171-MW520177) and MycoBank (MB 838612-MB 838614).

AUTHOR CONTRIBUTIONS

C-LZ collected the species. WZ performed the molecular phylogenetic analyses. Both authors were responsible for the morphological analysis and description of the collections, planned, organized, and evaluated critically the experimental parts, wrote the manuscript, contributed to the article, and approved the submitted version.

FUNDING

The research was supported by the Yunnan Fundamental Research Project (Grant No. 202001AS070043), the Key Laboratory of Forest Resources Conservation and Utilization in the Southwest Mountains of China Ministry of Education, Southwest Forestry University (KLESWFU-202003), and the High-level Talents Program of Yunnan Province (YNQR-QNRC-2018-111).

REFERENCES

Albee-Scott, S., and Kropp, B. R. (2010). A phylogenetic study of *Trechispora thelephora*. *Mycotaxon* 114, 395–399. doi: 10.5248/114.395

Angelini, C., Vizzini, A., Justo, A., Bizzi, A., and Kaya, E. (2020). First report of a neotropical agaric (*lepiota spiculata*, agaricales, basidiomycota) containing lethal α-amanitin at toxicologically relevant levels. *Front. Microbiol.* 11:1833. doi: 10.3389/fmicb.2020.01833

Bao, D. F., Mckenzie, E. H. C., Bhat, D. J., Hyde, K. D., and Su, H. Y. (2020). *Acrogenospora* (acrogenosporaceae, minutisphaerales) appears to be a very diverse genus. *Front. Microbiol.* 11:1606. doi: 10.3389/fmicb.2020.01606

Bernicchia, A., and Gorjón, S. P. (2010). *Fungi Europaei 12: Corticiaceae s.l.* Alassio: Edizioni Candusso.

Cui, B. K., Li, H. J., Ji, X., Zhou, J. L., Song, J., Si, J., et al. (2019). Species diversity, taxonomy and phylogeny of Polyporaceae (Basidiomycota) in China. *Fungal Divers.* 97, 137–392. doi: 10.1007/s13225-019-00427-4

Dai, Y. C. (2011). A revised checklist of corticioid and hydnoid fungi in China for 2010. *Mycoscience* 52, 69–79. doi: 10.1007/S10267-010-0068-1

Dai, Y. C. (2012). Polypore diversity in China with an annotated checklist of Chinese polypores. *Mycoscience* 53, 49–80. doi: 10.1007/s10267-011-0134-3

Dunham, S. M., Larsson, K. H., and Spatafora, J. W. (2007). Species richness and community composition of mat-forming ectomycorrhizal fungi in old- and second-growth Douglas-fir forests of the Hj Andrews Experimental Forest, Oregon, USA. *Mycorrhiza* 17, 633–645. doi: 10.1007/s00572-007-0141-6

Felsenstein, J. (1985). Confidence intervals on phylogenetics: an approach using bootstrap. *Evolution* 39, 783–791. doi: 10.1111/j.1558-5646.1985.tb00420.x

Hall, T. A. (1999). BioEdit: a user-friendly biological sequence alignment editor and analysis program for Windows 95/98/NT. *Nucleic Acids Symp. Ser.* 41, 95–98. doi: 10.1021/bk-1999-0734.ch008

Heijden, M. G., Martin, F. M., Selosse, M. A., and Sanders, I. R. (2015). Mycorrhizal ecology and evolution: the past, the present, and the future. *New Phytol.* 205, 1406–1423. doi: 10.1111/nph.13288

Hibbett, D. S., Bauer, R., Binder, M., Giachini, A. J., Hosaka, K., and Justo, A. (2014). "14 Agaricomycetes," in *Systematics and evolution*, eds D. J. McLaughlin, and J. W. Spatafora, (Berlin: Springer), 373–429.

Karsten, P. A. (1890). Fragmenta mycologica XXIX. *Dova Hedwig.* 29, 147–149.

Larsson, K. H. (1994). Poroid species in *Trechispora* and the use of calcium oxalate crystals for species identification. *Mycol. Res.* 98, 1153–1172. doi: 10.1016/S0953-7562(09)80200-1

Larsson, K. H. (1995). Taxonomy of *Trechispora farinacea* and proposed synonyms I. Species with a grandinioid or hydnoid hymenophore. *Symb. Bot. Ups.* 30, 101–118.

Larsson, K. H. (1996). New species and combinations in *Trechispora* (Corticiaceae, Basidiomycotina). *Nord. J. Bot.* 16, 83–98. doi: 10.1111/j.1756-1051.1996.tb00218.x

Larsson, K. H. (2007). Re-thinking the classification of corticioid fungi. *Mycol. Res.* 111, 1040–1063. doi: 10.1016/j.mycres.2007.08.001

Larsson, K. H., Larsson, E., and Koljalg, U. (2004). High phylogenetic diversity among corticioid homobasidiomycetes. *Mycol. Res.* 108, 983–1002. doi: 10.1017/S0953756204000851

Liberta, A. E. (1966). On *Trechispora*. *Taxon* 15, 317–319. doi: 10.2307/1216118

Liberta, A. E. (1973). The genus *Trechispora* (Basidiomycetes, Corticiaceae). *Canad. J. Bot.* 51, 1871–1892. doi: 10.1139/b73-240

Liu, S. L., Ma, H. X., He, S. H., and Dai, Y. C. (2019). Four new corticioid species in Trechisporales (Basidi omycota) from East Asia and notes on phylogeny of the order. *MycoKeys* 48, 97–113. doi: 10.3897/mycokeys.48.31956

Miettinen, O., and Larsson, K. H. (2006). *Trechispora elongata* species nova from North Europe. *Mycotaxon* 96, 193–198.

Miller, M. A., Holder, M. T., Vos, R., Midford, P. E., Liebowitz, T., Chan, L., et al. (2009). *The CIPRES Portals. – CIPRES*. Available online at: http://www.phylo.org/sub_sections/portal (accessed December 7, 2011).

Nylander, J. A. A. (2004). *MrModeltest v2. Program distributed by the author*. Uppsala: Evolutionary Biology Centre.

Ordynets, A., Larsson, K. H., and Langer, E. (2015). Two new *Trechispora* species from La Réunion Island. *Mycol. Progr.* 14:113. doi: 10.1007/s11557-015-1133-0

Parmasto, E. (1965). Corticiaceae U. R. S. S. I. Descriptiones taxorum. Combinationes noval [novarum]. *Izv. Akad. Nauk Èstonsk. SSR, Ser. Biol.* 14, 220–223.

Persoon, C. H. (1794). Neuer Versuch einer systematischen Eintheilung der Schwämme. *Neues Mag. Bot.* 1, 63–80.

Petersen, J. H. (1996). *Farvekort. The Danish Mycological Society's colour-chart*. Greve: Foreningen til Svampekundskabens Fremme.

Phookamsak, R., Hyde, K. D., Jeewon, R., Bhat, D. J., Jones, E. B. G., Maharachchikumbura, S., et al. (2019). Fungal diversity notes 929-1035: taxonomic and phylogenetic contributions on genera and species of fungi. *Fungal Divers.* 95, 1–273. doi: 10.1007/s13225-019-00421-w

Richter, C., Yurkov, A. M., Boekhout, T., and Stadler, M. (2019). Diversity of *Tilletiopsis*-Like Fungi in Exobasidiomycetes (Ustilaginomycotina) and Description of Six Novel Species. *Front. Microbiol.* 10:2544. doi: 10.3389/fmicb.2019.02544

Ronquist, F., and Huelsenbeck, J. P. (2003). MrBayes 3: B2017ayesian phylogenetic inference under mixed models. *Bioinformatics* 19, 1572–1574. doi: 10.1093/bioinformatics/btg180

Ryvarden, L. (2002). A note on the genus *Hydnodon* Banker. Some neotropical wood inhabiting fungi. *Syn. Fungorum* 15, 31–33.

Ryvarden, L., and Liberta, A. E. (1978). Contribution to the Aphyllophoralles of the Canary Islands 4. Two new species of *Trechispora* and *Xenmastella*. *Canad. J. Bot.* 56, 2617–2619. doi: 10.1139/b78-314

Shen, L. L., Wang, M., Zhou, J. L., Xing, J. H., Cui, B. K., and Dai, Y. C. (2019). Taxonomy and phylogeny of *Postia*. Multi-gene phylogeny and taxonomy of the brown-rot fungi: *Postia and its related genera*. *Persoonia* 42, 101–126. doi: 10.3767/persoonia.2019.42.05

Swofford, D. L. (2002). *PAUP*: Phylogenetic Analysis Using Parsimony (*and Other Methods). Version 4.0b10*. Sunderland, MA: Sinauer Associates.

Telleria, M. T., Melo, I., Dueñas, M., Larsson, K. H., and Paz Martin, M. P. (2013). Molecular analyses confirm *Brevicellicium* in Trechisporales. *IMA Fungus* 4, 21–28. doi: 10.5598/imafungus.2013.04.01.03

Trichiès, G., and Schultheis, B. (2002). *Trechispora* antipus sp. nov., une seconde espèce bisporique du genre *Trechispora* (Basidiomycota, Stereales). *Mycotaxon* 82, 453–458.

Vanegas-León, M. L., Sulzbacher, M. A., Rinaldi, A. C., Mélanie, Roy, and Neves, M. A. (2019). Are trechisporales ectomycorrhizal or non-mycorrhizal root endophytes? *Mycol. Progr.* 18, 1231–1240. doi: 10.1007/s11557-019-01519-w

Vu, D., Groenewald, M., de Vries, M., Gehrmann, T., Stielow, B., Eberhardt, U., et al. (2019). Large-scale generation and analysis of filamentous fungal DNA barcodes boosts coverage for kingdom fungi and reveals thresholds for fungal species and higher taxon delimitation. *Stud. Mycol.* 92, 135–154. doi: 10.1016/j.simyco.2018.05.001

White, T. J., Bruns, T., Lee, S., and Taylor, J. (1990). "Amplification and direct sequencing of fungal ribosomal RNA genes for phylogenetics," in *PCR Protocols: A Guide to Methods And Applications*, eds M. A. Innis, D. H. Gelfand, J. J. Sninsky, and T. J. White, (San Diego, CA: Academic Press), 315–322. doi: 10.1016/B978-0-12-372180-8.50042-1

Xu, T. M., Chen, Y. H., and Zhao, C. L. (2019). *Trechispora yunnanensis* sp. nov. from China. *Phytotaxa* 424, 253–261. doi: 10.11646/phytotaxa.424.4.5

Yurchenko, E., and Wu, S. H. (2014). *Fibrodontia alba* sp. nov. (Basidiomycota) from Taiwan. *Mycoscience* 55, 336–343. doi: 10.1016/j.myc.2013.12.004

Zhao, C. L., and Wu, Z. Q. (2017). *Ceriporiopsis kunmingensis* sp. nov. (Polyporales, Basidiomycota) evidenced by morphological characters and phylogenetic analysis. *Mycol. Progr.* 16, 93–100. doi: 10.1007/s11557-016-1259-8

Zhu, L., Song, J., Zhou, J. L., Si, J., and Cui, B. K. (2019). Species diversity, phylogeny, divergence time and biogeography of the genus *Sanghuangporus* (Basidiomycota). *Front. Microbiol.* 10:812. doi: 10.3389/fmicb.2019.00812

Conflict of Interest: The authors declare that the research was conducted in the absence of any commercial or financial relationships that could be construed as a potential conflict of interest.

Copyright © 2021 Zhao and Zhao. This is an open-access article distributed under the terms of the Creative Commons Attribution License (CC BY). The use, distribution or reproduction in other forums is permitted, provided the original author(s) and the copyright owner(s) are credited and that the original publication in this journal is cited, in accordance with accepted academic practice. No use, distribution or reproduction is permitted which does not comply with these terms.

frontiers in Microbiology

ORIGINAL RESEARCH
published: 22 March 2021
doi: 10.3389/fmicb.2021.643731

Seed Banks as Incidental Fungi Banks: Fungal Endophyte Diversity in Stored Seeds of Banana Wild Relatives

Rowena Hill[1,2], Theo Llewellyn[1,3], Elizabeth Downes[4], Joseph Oddy[5], Catriona MacIntosh[1,6], Simon Kallow[7,8], Bart Panis[9], John B. Dickie[7] and Ester Gaya[1]**

[1] Department of Comparative Plant and Fungal Biology, Royal Botanic Gardens, Kew, Richmond, United Kingdom, [2] School of Biological and Chemical Sciences, Faculty of Science and Engineering, Queen Mary University of London, London, United Kingdom, [3] Department of Life Sciences, Faculty of Natural Sciences, Imperial College London, London, United Kingdom, [4] Department for Environment, Food and Rural Affairs, London, United Kingdom, [5] Department of Plant Science, Rothamsted Research, Harpenden, United Kingdom, [6] School of Life Sciences, University of Glasgow, Glasgow, United Kingdom, [7] Collections Department, Royal Botanic Gardens, Kew, Millennium Seed Bank, Ardingly, United Kingdom, [8] Division of Crop Biotechnics, Department of Biosystems, Faculty of Bioscience Engineering, University of Leuven, Leuven, Belgium, [9] Bioversity International, Montpellier, France

OPEN ACCESS

Edited by:
Peter Edward Mortimer, Kunming Institute of Botany, Chinese Academy of Sciences, China

Reviewed by:
Jana M. U'Ren, The University of Arizona, United States
Asha Janadaree Dissanayake, University of Electronic Science and Technology of China, China

***Correspondence:**
Rowena Hill
R.Hill@kew.org
Ester Gaya
E.Gaya@kew.org

Specialty section:
This article was submitted to Evolutionary and Genomic Microbiology, a section of the journal Frontiers in Microbiology

Received: *18 December 2020*
Accepted: *19 February 2021*
Published: *22 March 2021*

Citation:
Hill R, Llewellyn T, Downes E, Oddy J, MacIntosh C, Kallow S, Panis B, Dickie JB and Gaya E (2021) Seed Banks as Incidental Fungi Banks: Fungal Endophyte Diversity in Stored Seeds of Banana Wild Relatives. Front. Microbiol. 12:643731. doi: 10.3389/fmicb.2021.643731

Seed banks were first established to conserve crop genetic diversity, but seed banking has more recently been extended to wild plants, particularly crop wild relatives (CWRs) (e.g., by the Millennium Seed Bank (MSB), Royal Botanic Gardens Kew). CWRs have been recognised as potential reservoirs of beneficial traits for our domesticated crops, and with mounting evidence of the importance of the microbiome to organismal health, it follows that the microbial communities of wild relatives could also be a valuable resource for crop resilience to environmental and pathogenic threats. Endophytic fungi reside asymptomatically inside all plant tissues and have been found to confer advantages to their plant host. Preserving the natural microbial diversity of plants could therefore represent an important secondary conservation role of seed banks. At the same time, species that are reported as endophytes may also be latent pathogens. We explored the potential of the MSB as an incidental fungal endophyte bank by assessing diversity of fungi inside stored seeds. Using banana CWRs in the genus *Musa* as a case-study, we sequenced an extended ITS-LSU fragment in order to delimit operational taxonomic units (OTUs) and used a similarity and phylogenetics approach for classification. Fungi were successfully detected inside just under one third of the seeds, with a few genera accounting for most of the OTUs–primarily *Lasiodiplodia*, *Fusarium*, and *Aspergillus*–while a large variety of rare OTUs from across the Ascomycota were isolated only once. *Fusarium* species were notably abundant–of significance in light of Fusarium wilt, a disease threatening global banana crops–and so were targeted for additional sequencing with the marker *EF1α* in order to delimit species and place them in a phylogeny of the genus. Endophyte community composition, diversity and abundance was significantly different across habitats, and we explored the relationship between

community differences and seed germination/viability. Our results show that there is a previously neglected invisible fungal dimension to seed banking that could well have implications for the seed collection and storage procedures, and that collections such as the MSB are indeed a novel source of potentially useful fungal strains.

Keywords: endophytic fungi, seed banking, seed mycobiome, banana, crop wild relatives, *Musa*, *Fusarium*

INTRODUCTION

Fungal endophytes (hereafter, endophytes) are fungi which live asymptomatically inside plant tissues (Petrini, 1991; Hardoim et al., 2015), and appear to be present in all land plants (Stone et al., 2000; Rodriguez et al., 2009; Rashmi et al., 2019). Certain endophytes are known to provide various benefits to the plant host, such as stress tolerance, growth promotion, and disease resistance (Redman et al., 2002; Waller et al., 2005; Bilal et al., 2018). As a result, endophytes have become of particular interest in agriculture due to their promise as pest and pathogen biocontrol agents, ideally replacing and/or reducing ecologically harmful chemical controls (Card et al., 2016; Bamisile et al., 2018; Vega, 2018) and aiding sustainable intensification of agriculture without increased use of chemical fertilisers (Le Cocq et al., 2016). Additionally, they can produce a suite of secondary metabolites as part of the plant-fungal interaction, providing a valuable opportunity for discovery of new therapeutically relevant bioactive compounds, such as antivirals and antibiotics (Gupta et al., 2020). Since endophytes are likely to comprise a considerable proportion of the more than 2 million estimated species of yet undiscovered fungi (Petrini, 1991; Arnold et al., 2000; Hawksworth and Lücking, 2017), capitalising on these potentially useful fungi requires continued efforts toward discovering endophyte diversity.

Collections are an important resource for biodiversity research, as they provide curated specimens spanning time and space (Funk, 2018; Pearce et al., 2020). Beyond prospecting for novel fungal diversity in dedicated mycological collections such as fungaria and culture collections (Dentinger et al., 2016; Andrew et al., 2018, 2019; Huang et al., 2018), we now recognise the potential for plant collections to be a source of fungal diversity too. Daru et al. (2018) showed that sequencing dried herbarium specimens can reveal novel endophyte diversity, with the caveat that it is extremely rare to recover viable endophytes in culture. Compared to herbaria, seed banks (preserved seed collections) are an alternative with the considerable advantage of being living collections, enabling isolation of live fungal strains in culture. This is particularly valuable as it facilitates the compilation of endophytic culture collections for further study, such as in inoculation experiments to identify strains that are beneficial to plant health (e.g., Waller et al., 2005; Bilal et al., 2018) or whole-genome-sequencing to investigate the genomic basis of the plant-endophyte interaction (e.g., Zuccaro et al., 2011; Niehaus et al., 2016; Knapp et al., 2018). Nevertheless, there is far less known about seed endophytes compared to those in leaves, the latter of which may be more abundant (Bayman et al., 1998; Ganley and Newcombe, 2006) although few studies have looked at both seed and foliar endophytes for the same host plant, and to our knowledge always in the wild.

Seed banks were initially conceived in the 20th century as a measure to conserve crop genetic diversity (Peres, 2016), the most famous example likely being the Svalbard Global Seed Vault (Westengen et al., 2013). The Millennium Seed Bank (MSB), managed by the Royal Botanic Gardens Kew, is the world's largest seed bank and part of a global partnership network for seed conservation (Liu et al., 2020). The MSB is notably directed to wild plant conservation, with one of its priorities being crop wild relatives (CWRs) (Liu et al., 2018). CWRs, the close relatives of our domesticated crop species, act as an additional pool of genetic diversity to breed improvements into our crops, such as increased productivity and resilience against disease and environmental stressors (Hajjar and Hodgkin, 2007; Brozynska et al., 2016). More recently, similar benefits have been equally demonstrated by inoculation of various crops with endophytes from CWRs (Murphy et al., 2018a,b, 2019). This potential role of CWR endophytes in both the health of wild plant populations and their crop counterparts brings in additional value to the MSB collections, making them not only important for plant conservation, but also plant microbiome conservation.

The role of endophytes in plant health is, however, more complicated than it first seems. Despite their ubiquity, the endophytic lifestyle remains somewhat of a mystery. While there are aforementioned examples of mutualistic endophytes found only to benefit the plant host, other fungi described as endophytes are found to be latent pathogens or decomposers (saprotrophs) (Slippers and Wingfield, 2007; Promputtha et al., 2010; Delaye et al., 2013; Nelson et al., 2020). This concept–that the term endophyte represents a range of functional roles within the plant host–has been referred to as the *endophytic continuum* (Schulz and Boyle, 2005). Of the 366 species classified as endophytes in the FUNGuild database as of December 2020: 140 (∼38%) are also classified as plant pathogens; 16 as saprotrophs (∼4%); and 17 (∼5%) as other various guilds (Nguyen et al., 2016). Indeed, in phylogenetic analysis, endophytes are commonly found to be closely related to pathogens and saprotrophs, as well as endolichenic fungi, their lichen-associated counterpart (Arnold et al., 2009; U'Ren et al., 2009, 2010). A habit switch from commensal to pathogenic has been observed in some endophytes due to unfavourable environmental conditions (Slippers and Wingfield, 2007; Ribeiro et al., 2020), and there is evidence that endophytes found only in living tissues don't significantly differ in cellulolytic activity (i.e., decomposing capacity) from those found only in dead leaves (U'Ren and Arnold, 2016).

Together, these evoke the obscure position of endophytes on the mutualistic-commensal-pathogenic spectrum and highlights our ignorance regarding their nutritional strategies.

Consequently, there is ambiguity as to which endophytes inhabiting stored seeds are beneficial–or even essential–to the plant host, and which are potentially harmful. This uncertainty has obvious implications in seed storage protocols, which most often focus on the harmful fungi. For example, in internationally recognised reports on best-practise gene banking, mention of fungi (and bacteria) is almost exclusively in the context of avoidance, with recommendations for the use of antifungals/antibiotics on collections (Food and Agriculture Organization, 2014; Center for Plant Conservation, 2018). These recommendations overlook an essential question: what is the impact of not preserving healthy endophyte communities when banking seeds? How do endophyte communities impact the success of recovered plant populations down the line? Such endophytic communities may be playing similar roles as the microbial associates of humans or animals, which we now know to be essential for normal, healthy functioning and imbalances of which cause disease (Dudek-Wicher et al., 2018). While great care is taken to optimise the phylogenetic and geographical diversity and longevity of MSB seed collections, consideration of the microbial communities associated with the seeds is notably absent (Liu et al., 2020). Considering that there are endophytes known to be implicated in germination and seedling success (Tamura et al., 2008; Hubbard et al., 2014; Li et al., 2017; Shearin et al., 2018; Leroy et al., 2019), this is a significant oversight.

To explore these issues and demonstrate the value of seed banks for endophyte discovery, we focused on a case study of CWRs of banana (and plantain, *Musa* spp. L.)–one of the most important crops in the world. Global production of banana is estimated to be 116 million tonnes annually, worth $31 billion (Food and Agriculture Organization, 2020b). *Musa* taxa are tall herbaceous monocarpic monocotyledons in the family Musaceae, order Zingiberales. They are native to tropical and subtropical Asia to western Pacific regions (Govaerts and Häkkinen, 2006) with approximately 80 taxa (hereon called "species") in the genus (Häkkinen and Väre, 2008; POWO, 2019). There are around 1,000 cultivars of edible bananas (Ruas et al., 2017; Food and Agriculture Organization, 2020a), most of which stem from two species: *Musa acuminata* Colla and *Musa balbisiana* Colla (Carreel et al., 2002; Langhe et al., 2009; Perrier et al., 2011; Rouard et al., 2018; Martin et al., 2020). In spite of this diversity, the vast majority of commercial banana plantations are clones of a single cultivar, Cavendish, which makes the crop highly susceptible to disease (Ordonez et al., 2015). In the 1970s, *Fusarium oxysporum* f. sp. *cubense* emerged to cause Fusarium Wilt of Cavendish bananas, and has since spread across the global tropics to most banana producing countries[1] (Dita et al., 2018). The predominant strain is commonly referred to as Foc TR4, and was recently proposed to belong to the novel species *Fusarium odoratissimum* (Maryani et al., 2019). Considering the global value of the banana crop, 85% of which is eaten locally as a major contribution to people's diets (Food and Agriculture Organization, 2020b), Foc TR4 represents a major threat to both economic and food security in banana producing countries. Stored banana CWR seeds are a precious conservation resource in light of the susceptible Cavendish banana cultivar, and so present a valuable case-study for investigating associated endophyte diversity.

While many endophytic species can be grown in culture, many more cannot, and so molecular tools are relied upon to detect much more of the true extent of endophytic diversity (e.g., Higgins et al., 2011; Parmar et al., 2018; U'Ren et al., 2019). Nonetheless, culturing is still a necessary tool, as it not only isolates strains for future study, but also provides an indication of which fungal strains are alive, which is particularly relevant when assessing post-storage endophytes. Here we used both a culture-dependent and culture-independent approach to maximise discovery of endophytic diversity from accessions belonging to six species of banana wild relatives in the genus *Musa*. By PCR-cloning individual seed DNA extractions for the culture-independent approach, we were able to assess the number of unique operational taxonomic units (OTUs)–a proxy for species–per seed. We made use of metadata and seed viability assessments from the MSB collections in order to explore the association of habitat, host *Musa* species, post-storage seed viability and germination rate with endophyte community composition, diversity and abundance.

MATERIALS AND METHODS

Seeds from 45 *Musa* accessions (with each accession containing 50 seeds collected from between one and five plant individuals belonging to the same *Musa* species in the sampling site) were obtained from the Millennium Seed Bank (MSB), all of which had been stored at −20°C. Seeds had been collected in 15 localities in Vietnam and Malaysia, with one accession collected from RBG Kew's living collections (see **Supplementary Table 1** for details). For each accession, seeds were randomly split into batches of 20 for fungal culturing, 10–20 for direct sequencing and 60 for seed viability assessment.

Seed Viability Assessment

Post-storage seed viability was assessed using two methods. Firstly, the tetrazolium chloride test (TTC) was carried out following the approach of Leist and Krämer (2011). Seeds were imbibed on agar for 3 days at 20°C. Then a proportion of the testa was removed using a scalpel on two lateral sides to expose the endosperm. Seeds were then soaked in 1% buffered 2,3,5-triphenyl tetrazolium chloride (pH6-8) for 2 days at 30°C in the dark. Staining patterns were recorded. Embryos that completely stained dark red, or that showed dark red staining at the embryonic axis (the opposite from the haustorium) were considered viable; light pink staining or white embryos were considered unviable. Fifty seeds per accession were tested.

The second viability test was embryo rescue (ER). In a laminar flow, seeds were sterilised by soaking them in 96% ethanol for 3 min, followed by 20% bleach (NaOCl containing 1 drop of detergent per 100 ml) for 20 min, then seeds were rinsed three times in sterilised water. Continuing in the laminar flow with sterile forceps and scalpel, embryos were extracted

[1] www.promusa.org

from seeds. This was done using an incision in the seed coat next to the micropyle and manipulating the seed in order to split the testa; the embryo was then gently removed. Embryos were subsequently transferred onto autoclaved half MS medium (Murashige and Skoog, 1962) in tubes using long forceps with the haustorium in contact with the medium and the embryonic axis upward. Tubes containing embryos were incubated in the dark at 27°C for 14 days after which they were put in a growth chamber in the light at 27°C for an additional 14 days. Six possible observations were recorded: shoot, callus, blackened colouration, no embryo, contamination, no change. Ten seeds per accession were tested.

Surface Sterilisation and Isolation of Fungal Cultures

Following the protocol of Arnold et al. (2007), seeds were surface sterilised by sequential immersion in 95% ethanol (10 s), 10% bleach (2 min), and 70% ethanol (2 min), then left to surface-dry under sterile conditions. For the culture-dependent approach 20 sterilised seeds per accession were plated on 2% malt extract agar (MEA), sealed with parafilm and incubated at room temperature. Emergent fungal growth was transferred to a new plate for pure culture isolation. Additionally, imprints of sterilised and unsterilised seeds were made on 2% MEA to confirm the efficacy of the sterilisation methodology, and to observe whether the same species found inside the seeds were also present externally on the unsterilised seed surface. Vouchers of culture isolates were cryopreserved and deposited at RBG Kew. Cryopreservation involved transferring ∼four 5 mm^2 squares of agar into each of two 2 ml tubes containing 1 ml of sterile 10% glycerol. Tubes were brought from room temperature to −80°C at the rate of 1°C per minute to prevent shock.

DNA Extraction and Sequencing

For the axenic cultures, DNA was extracted using the Extract-N-Amp Plant PCR Kit (Sigma-Aldrich, St. Louis, MO, United States) in 5 μl of extraction buffer and 5 μl of dilution buffer. For the culture-independent approach, 10–20 seeds were surface-sterilised as described above and individually transferred to sterile 2 ml collecting tubes, frozen at −80°C and pulverised using a Mixer Mill MM 400 (Retsch, Germany) with two sterilised stainless-steel beads per tube. The Qiagen DNeasy Plant Mini Kit (Qiagen, Redwood City, CA, United States) was used for direct extraction of the pulverised seeds according to the manufacturer's protocol, with DNA eluted in 100 μl of TE buffer.

Extract-N-Amp PCR ReadyMix was used for amplification of both culture and direct extractions. The total PCR reaction volume was 8 μl, consisting of 0.5 μl of extracted DNA, 4 μl Extract-N-Amp PCR ReadyMix, 3.42 μl of distilled water and 0.4 μl of each primer (100 μM). The primers used to amplify the ITS-partial LSU rDNA fragment were ITS1F (Gardes and Bruns, 1993) and LR3 (Vilgalys and Sun, 1994). Cycling conditions were as follows: 94°C for 3 min, 35 amplification cycles (94°C for 30 s, 53°C for 35 s, 72°C for 1 min, with the addition of 5 s to the extension phase per cycle), and 72°C for 4 min.

To account for the possibility of multiple species of fungal endophyte per seed, PCRs of direct extractions were cloned into the pCR™4-TOPO® *Escherichia coli* vector with the TOPO TA-Cloning Kit (Invitrogen, Carlsbad, CA, United States) according to the manufacturer's instructions. Up to 12 colonies were randomly picked and amplified in secondary PCR with the above cycle conditions and primers.

After examination with gel electrophoresis (1% agarose in TE buffer), all PCR products were purified using ExoSAP-IT (USB, Hudson, OH, United States) and both strands sequenced using the same primers as for amplification. Sequence reactions were carried out in 5 μl volumes–consisting of 1 μl 5× sequencing buffer, 2.05 μl ddH_20, 1 μl primer (1.25 μM), 0.5 μl purified PCR product and 0.45 μl BigDye Terminator v3.1 (Applied Biosystems, Foster City, CA, United States)–and run on an ABI 3730 DNA Analyzer (Applied Biosystems, Foster City, CA, United States). Sequences were manually edited with contiguous alignments using Geneious R7 v7.1.5 (Biomatters, New Zealand). Sequences from 642 endophytes (235 cultures, 280 direct sequences, and 127 clones) have been deposited in GenBank under accession numbers MW298868-MW299510.

OTU Delimitation and Taxonomic Identification

Sequences were clustered into OTUs using the *de novo* method USEARCH v10.0.240 as part of the UPARSE pipeline (Edgar, 2013). As USEARCH is sensitive to fragments of different length, ITSx (Bengtsson-Palme et al., 2013) was used prior to clustering to extract the 5.8S and ITS2 regions–shown to recover more fungal OTUs when used together (Heeger et al., 2019)–while LSU fragments were manually trimmed to the same length after alignment with MUSCLE v3.8.425 (Edgar, 2004) and visualisation in AliView v1.17 (Larsson, 2014). Dereplication was performed via removal of identical sequences using the fastx_uniques functions inbuilt to USEARCH. 5.8S-partial LSU OTUs were clustered using a 99% similarity threshold, guided by the optimal threshold for species discrimination using ITS/LSU identified by Vu et al. (2019). Singletons–OTUs comprising one sequence–were not discarded, as is common practise to reduce artefacts when using NGS datasets, because each sequence originated from Sanger sequencing of an individual seed extraction, and so was assumed to be "real."

Preliminary identification of OTUs was made via a local BLASTn v2.6.0 search (Camacho et al., 2009) against the UNITE v8.2 database, release 04.04.2020 (Abarenkov et al., 2020). Taxonomic identification of OTUs was inferred from the top UNITE hit, guided by Vu et al. (2019): ≥99% similarity for the same species; ≥98 similarity for the same genus; ≥96 similarity for the same family; ≥94 similarity for the same order; ≥92 similarity for the same class; and <92% similarity for the same phylum. Similarity-based identification was corroborated with a phylogenetic approach via the Tree-Based Alignment Selector (T-BAS) toolkit v2.2 (Miller et al., 2010; Carbone et al., 2019), a platform designed for preliminary placement and visualisation of unknown fungal sequences in curated multilocus phylogenies. Representative sequences for 181 OTUs were placed in the

6-loci *Pezizomycotina* v2.1 and the 6-loci Fungi reference trees (James et al., 2006; Carbone et al., 2017) with default settings and using the evolutionary placement algorithm (EPA) option from RAxML (Berger et al., 2011; Stamatakis, 2014). OTU taxon assignment was altered to reflect the lowest taxonomic level in agreement between both T-BAS and UNITE, with the UNITE species level identification used if T-BAS and UNITE agreed on genus and the UNITE percentage identity was ≥99%. All filtering of classification data was done using R v3.5.3 in RStudio v1.1.463 (RStudio Team, 2015; R Core Team, 2020), the script for which is available at https://github.com/Rowena-h/MusaEndophytes.

Sampling Effort and Community Analysis

For the purpose of these analyses, *Musa* subspecies and varieties were grouped under the same species. Sampling effort was assessed by producing species accumulation curves of the number of OTUs for the number of *Musa* accessions using the rarefaction method in the specaccum function from the R package vegan v2.5-6 (Oksanen et al., 2019). This was done including and excluding singleton OTUs for all *Musa* accessions (n = 45) as well as distinguishing between the three best sampled species–*M. acuminata* (n = 12), *M. balbisiana* (n = 16), and *Musa itinerans* (n = 14). The impact of detection method–culturing, direct sequencing or cloning–on species recovery was quantified with analysis of similarity (ANOSIM) (Clarke, 1993) using the vegan anosim function following confirmation that data dispersion was even using the vegan betadisper function.

The RBG, Kew accession and oil palm plantation accessions (1 locality in Malaysia) were excluded from the following analyses due to low sample size for the habitats and the former being a geographical outlier. Endophyte community composition was explored using non-metric multidimensional scaling (NMDS) implemented in the metaMDS function in vegan. OTU counts were filtered for the eight most common OTUs (abundance greater than 20) for the 33 accessions of *M. acuminata*, *M balbisiana*, and *M. itinerans* and six dimensions were selected for the NMDS using a scree plot (**Supplementary Figure 1**). Habitat information for *Musa* accessions was interpreted from the collection notes in the MSB's metadata records (**Supplementary Table 1**). To investigate the relationships between community composition and post-storage seed viability (i.e., what proportion of seeds from the accession contained a live embryo in the TTC testing) and post-storage germination rate (i.e., what proportion of embryos from the individual germinated in the ER testing), TTC and ER data for each *Musa* accession were fitted to the NMDS ordination using the vegan ordisurf function, which uses generalised additive models to fit a smooth response surface and is therefore appropriate for a non-linear relationship between the ordination and variable.

The impact of habitat and *Musa* species on the variation in community composition–both for the subset of common taxa visualised in the NMDS and for all OTUs including rare taxa–was tested with permutational multivariate analysis of variance (PERMANOVA) implemented in the vegan adonis and adonis2 functions using Bray-Curtis dissimilarity and 999 permutations. PERMANOVA with adonis considers variables sequentially, meaning that the test is performed on the first variable provided and the residual unexplained variance is left to be explained by the next variable, and so on. As variables can be correlated with each other, the order in which variables are added to the adonis formula impacts the results. In order to determine the unique impact of variables irrespective of order, i.e., marginal effect size (marginal R^2), we used the adonis2 function with the by = "margin" option, which reports the variance that is not explained by any of the other variables. The variables were then tested with adonis in order of decreasing marginal effect size to assess the total effect size (R^2). The vegan betadisper function was also used for permutational analysis of multivariate dispersions (PERMDISP) to assess whether data dispersion was uniform for each variable, as when sample sizes are unbalanced varying data dispersion can result in a significant PERMANOVA test even if group composition is not significantly different (Anderson and Walsh, 2013). The PERMDISP null hypothesis is that there is no difference in dispersion between groups, and so a significant p-value indicates that dispersion is not consistent.

In order to determine which of the habitats had significantly different community composition from the others, pairwise PERMANOVA was performed on both the subset of common taxa used in the NMDS as well as all OTUs including rare taxa. This was done using the pairwise.perm.manova function from the R package RVAideMemoire v0.9-78 (Hervé, 2020) with 999 permutations and multiple testing p-value correction using the Benjamini–Hochberg method (Benjamini and Hochberg, 1995). Difference in diversity–according to Shannon and Simpson diversity indices, both calculated with the vegan diversity function–and abundance of fungi per *Musa* accession for each habitat was assessed using the TukeyHSD function. All results were plotted in R with the ggplot2 v3.3.0 package (Wickham, 2016). Ellipses for each habitat in the NMDS plot were generated with the stat_ellipse function in ggplot2.

Fusarium Phylogenetic Analysis

Given the abundance of *Fusarium* in our dataset, a genus-specific phylogeny was reconstructed to elucidate the relationships of our *Fusarium* OTUs with already known species. While the UNITE identification described above recovered many 5.8S-partial LSU OTUs to apparent species level, it has been shown that the ITS locus is not sufficiently variable for species delimitation within this particular genus (Geiser et al., 2004). For this reason, all cultures and direct extractions belonging to the genus, as identified with UNITE and confirmed by T-BAS analyses, were selected for additional amplification of the translation elongation factor 1-α (*EF1α*) gene using the primers EF1 and EF2 (O'Donnell et al., 1998). Amplification and sequencing were performed as above, except for PCR cycle conditions, which were informed by da Silva et al. (2014). All new sequences were deposited in GenBank (MW319587-MW319636). OTUs based on *EF1α* sequences were also delimited as above.

Representative sequences for each OTU from this study (as provided by USEARCH) were aligned with already published *EF1α* data and, in addition to *EF1α*, RNA polymerase II largest (*RPB1*), and second largest subunit (*RPB2*) sequences were

also taken from the MycoBank website[2]. Taxon sampling was guided by O'Donnell et al. (2013), with the addition of taxa from the *Fusarium oxysporum* species complex (FOSC) (Maryani et al., 2019) and *Fusarium musae* (Van Hove et al., 2011) and *Neonectria coccinea* and *Cylindrocarpon cylindroides* were selected as the outgroup (**Supplementary Table 2**). Sequences for each gene were aligned using MUSCLE v3.8.425 (Edgar, 2004) and ambiguous regions were manually delimited and removed in AliView v1.17 (Larsson, 2014). Much of the variability in *EF1α* that makes it a valuable marker for *Fusarium* is located across three introns (Geiser et al., 2004), so introns were isolated from protein-coding regions and Gblocks v0.91b (Castresana, 2000) was used to select adequately aligned intron sites, with the "Allow gap positions" option to prevent loss of highly variable sites. To check for topological incongruence between genes, a maximum likelihood (ML) search was performed on individual alignments–partitioned by introns and codon position for protein-coding regions–using the GTRGAMMA substitution model with bootstrapping over 1000 replicates in RAxML v8.2.9 (Stamatakis, 2014). Conflicts between gene trees (defined as ≥70% bootstrap support (BS) for contradictory relationships) were manually identified for each of the three pairwise comparisons with help from the compat.py script (Kauff and Lutzoni, 2002, 2003) run in Python v3.7.9 using Biopython v1.78 (Cock et al., 2009). Taxa responsible for conflicts were removed. The three loci were concatenated using SequenceMatrix (Vaidya et al., 2011) and partitioned by gene, codon position and *EF1α* introns for the ML search, performed as above for individual gene trees–see https://github.com/Rowena-h/MusaEndophytes for the raw alignment and tree files. Species names were checked in Species Fungorum[3] and the species tree was plotted in R using ggtree v2.3.4 (Yu et al., 2017).

RESULTS

Most Endophyte-Colonised *Musa* Seeds Contained a Single OTU

ITS-partial LSU sequences of fungal endophytes were obtained from 533 *Musa* seeds, 31% of the total 1,710 seeds used in this study (+90 control seeds). One fungal isolate per seed was most commonly found, however up to 7 unique OTUs were detected via cloning in a small number of seeds (**Figure 1A**). Of the most sampled *Musa* species, *M. acuminata* had the lowest number of fungal isolates relative to total seeds while *M. itinerans* had the highest. No fungi were detected in *Musa gracilis*, however only one accession was sampled, which was also the case for *M. violascens* and *M. velutina*.

Lasiodiplodia, *Fusarium*, and *Aspergillus* Were the Most Common Genera

Not including duplicate clones, 642 sequences (GenBank accession numbers MW298868-MW299510) were clustered into 181 OTUs, of which 125 (69%) were singletons. Species accumulation curves including singleton OTUs were almost linear and with a high gradient, while the curves excluding singletons approached an asymptote, indicating that many rarer OTUs remain to be discovered but a considerable proportion of the most common OTUs were captured (**Figure 1B**).

Of the 181 OTUs, UNITE and T-BAS classified the vast majority to the Ascomycota (162, 90%), with a few belonging to the Basidiomycota (12, 7%) and the remaining as unclassified Fungi (7, 4%) (**Supplementary Data Sheet 1**). In almost equal proportion, most of the ascomycete OTUs fell in the classes Dothideomycetes, Eurotiomycetes, and Sordariomycetes (in order of abundance), in the respective orders of Botryosphaeriales, Eurotiales, and Hypocreales (**Figure 2**). The three most common genera were *Lasiodiplodia*, *Fusarium*, and *Aspergillus* (with 161, 123, and 117 occurrences, respectively), which together accounted for almost two thirds of the total number of sequenced endophytes. The most abundant OTUs were recovered from all sampling approaches–culture-dependent and culture independent (with additional cloning)–however each approach detected rare OTUs not found by the others (**Figure 3**). Data dispersion was even across methods (betadisper $p = 0.33$) and ANOSIM indicated that, while communities were significantly different according to different detection methods ($p = 0.001$), the strength of these differences between methods was relatively low ($R = 0.08$). 10 OTUs from inside the seeds were also isolated pre-sterilisation on the outside of seeds (**Supplementary Table 3**), but as all the surface sterilisation imprint controls showed no fungal growth, we were confident that these OTUs were not contaminants.

Endophyte Community Composition, Diversity and Abundance Changed With Habitat

There was a significant difference in endophyte communities across habitats when considering the most common OTUs (pooled from all detection methods) from *M. acuminata*, *M. balbisiana*, and *M. itinerans* accessions (adonis2 marginal $R^2 = 0.32$, $p = 0.001$; adonis $R^2 = 0.34$, $p = 0.001$) and also when including rare taxa, although with a smaller effect size (adonis2 marginal $R^2 = 0.18$, $p = 0.001$; adonis $R^2 = 0.21$, $p = 0.001$). *Musa* species was not found to be a significant factor for variance of taxa (**Table 1**). PERMDISP found data dispersion of common taxa to be similar across *Musa* species but not across habitats: dispersion was greatest in the habitat with the smallest sample size (roadside), suggesting a liberal PERMANOVA bias (**Supplementary Figure 2**) (Anderson and Walsh, 2013). However, PERMANOVA, PERMDISP, and NMDS together suggested that habitat was associated with both location and dispersion of the data. The NMDS visualisation showed that the ellipses for the jungle buffer, jungle edge and roadside habitats overlapped, but with data dispersion increasing with level of habitat disruption: from jungle buffer (least disrupted, most tightly clustered) to roadside (most disrupted, least tightly clustered) (**Figure 4A**). The pairwise PERMANOVA analysis confirmed that these three habitats were not significantly different to each other in community composition for the

[2]https://fusarium.mycobank.org/

[3]http://www.speciesfungorum.org/

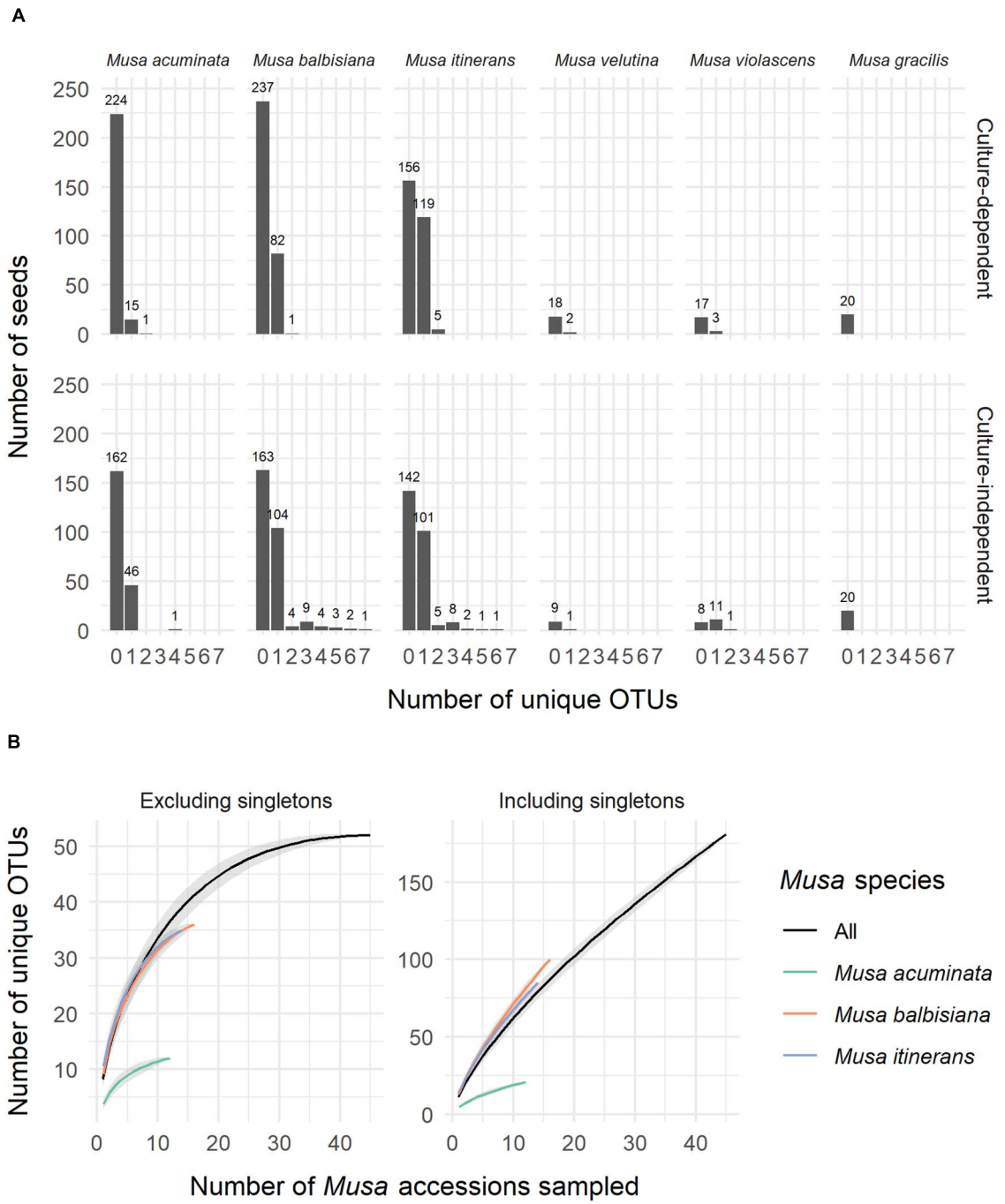


FIGURE 1 | (A) The number of unique OTUs per seed for each species of *Musa* from both the culture-dependent and independent approaches. **(B)** Species accumulation curves of OTUs by number of *Musa* accessions sampled, both excluding and including singletons and showing distinction between the three most sampled *Musa* species. Standard error is shaded grey around the lines.

common taxa visualised in the NMDS, while they were all significantly different from the ravine habitat (**Figure 4B**), which formed a separate cluster in the NMDS (**Figure 4A**). When including rare OTUs in the pairwise PERMANOVA, however, community composition was also significantly different between jungle buffer and roadside habitats (**Figure 4B**). Both diversity and abundance of endophytes per accession showed the same trend across habitats, with greatest diversity and abundance in the ravine habitat and least in the roadside habitat, with TukeyHSD identifying three statistically distinct groups for both Shannon diversity and abundance, although Simpson diversity was not statistically significant between habitats (**Figures 4C,D**). Oil palm

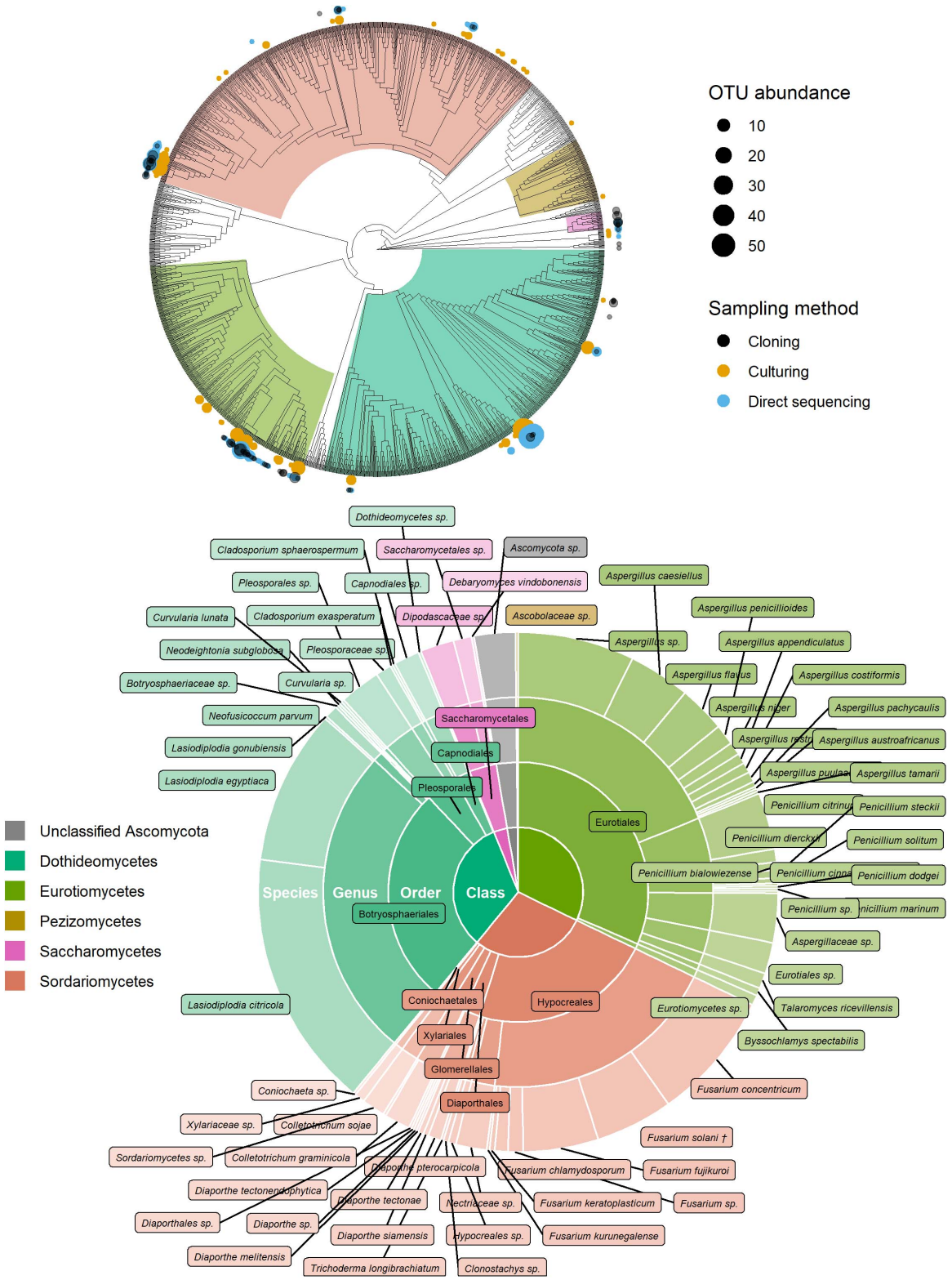


FIGURE 2 | Identification of ascomycete OTUs according to UNITE and phylogenetic placement in the T-BAS Pezizomycotina v2.1 tree. OTUs from this study are indicated on the T-BAS tree by circles on tips (top) with size proportional to number of times the OTU was detected and colour showing sampling method. Taxon classification as agreed by UNITE and T-BAS is summarised in a pie chart (bottom). (†) *Fusarium solani* = *Neocosmospora solani* (Sandoval-Denis et al., 2019).

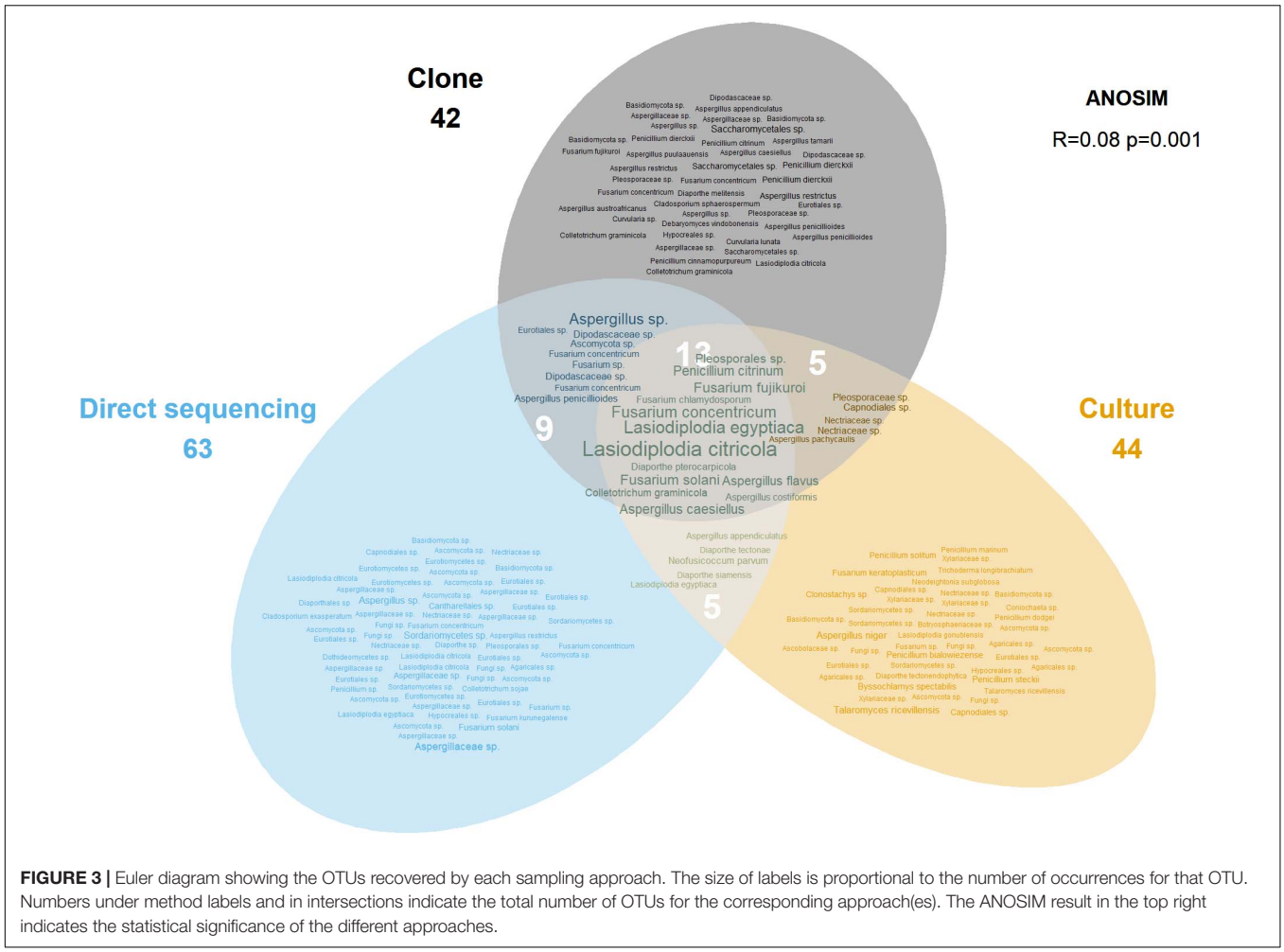


FIGURE 3 | Euler diagram showing the OTUs recovered by each sampling approach. The size of labels is proportional to the number of occurrences for that OTU. Numbers under method labels and in intersections indicate the total number of OTUs for the corresponding approach(es). The ANOSIM result in the top right indicates the statistical significance of the different approaches.

plantation accessions and the RBG, Kew accession were excluded from the main analyses due to low sample size (and as the latter was a geographical outlier), but endophyte abundance was comparatively low for both habitats (**Supplementary Figure 3**).

Fitting post-storage seed viability (TTC) to the NMDS ordination (ordisurf adjusted R^2 = 0.46, p = 7.46e-05) showed seed viability to have a non-linear relationship with the community structure, with accessions in the ravine habitat cluster and *Penicillium* and *Aspergillus* OTUs associated with lower viability measures and accessions in the jungle buffer habitat associated with higher viability measures (**Figure 4A**). Germination rate (ER) showed a similar relationship (ordisurf adjusted R^2 = 0.31, p = 0.006).

Fusarium Strains Were Phylogenetically Resolved to the *Fusarium fujikuroi*, "*Fusarium*" *solani*, and *Fusarium incarnatum-equiseti* Species Complexes

Additional *EF1α* sequencing and OTU clustering of the *Fusarium* taxa produced 10 *EF1α* OTUs. Phylogenetic analysis resolved these in the *incarnatum* clade of the *Fusarium incarnatum-equiseti* species complex (FIESC), in the *Fusarium solani* species complex (FSSC)–which has recently been reassigned to the genus *Neocosmospora* (Sandoval-Denis et al., 2019)–and in the *Fusarium fujikuroi* species complex (FFSC), with most OTUs placed within the latter (**Figure 5**). Disregarding the naming of taxa, our phylogeny was in general agreement with the most comprehensive phylogenies of the genus (O'Donnell et al., 2013, 2020), with the exception of not recovering geographically grouped clades (Asian, African, and American) in the FFSC,

TABLE 1 | Results of the statistical tests on Bray-Curtis dissimilarity matrices of both the subset of common OTUs visualised in the NMDS and all taxa including rare OTUs.

		PERMANOVA				PERMDISP
		adonis2		adonis		Betadisper
Dataset	Variable	Marginal R^2	p	R^2	p	p
Common taxa	Habitat	0.32	0.001	0.34	0.001	0.0310
	Musa species	0.07	0.055	0.07	0.055	0.0987
All taxa	Habitat	0.18	0.001	0.21	0.001	0.0059
	Musa species	0.08	0.101	0.08	0.101	1.25E-07

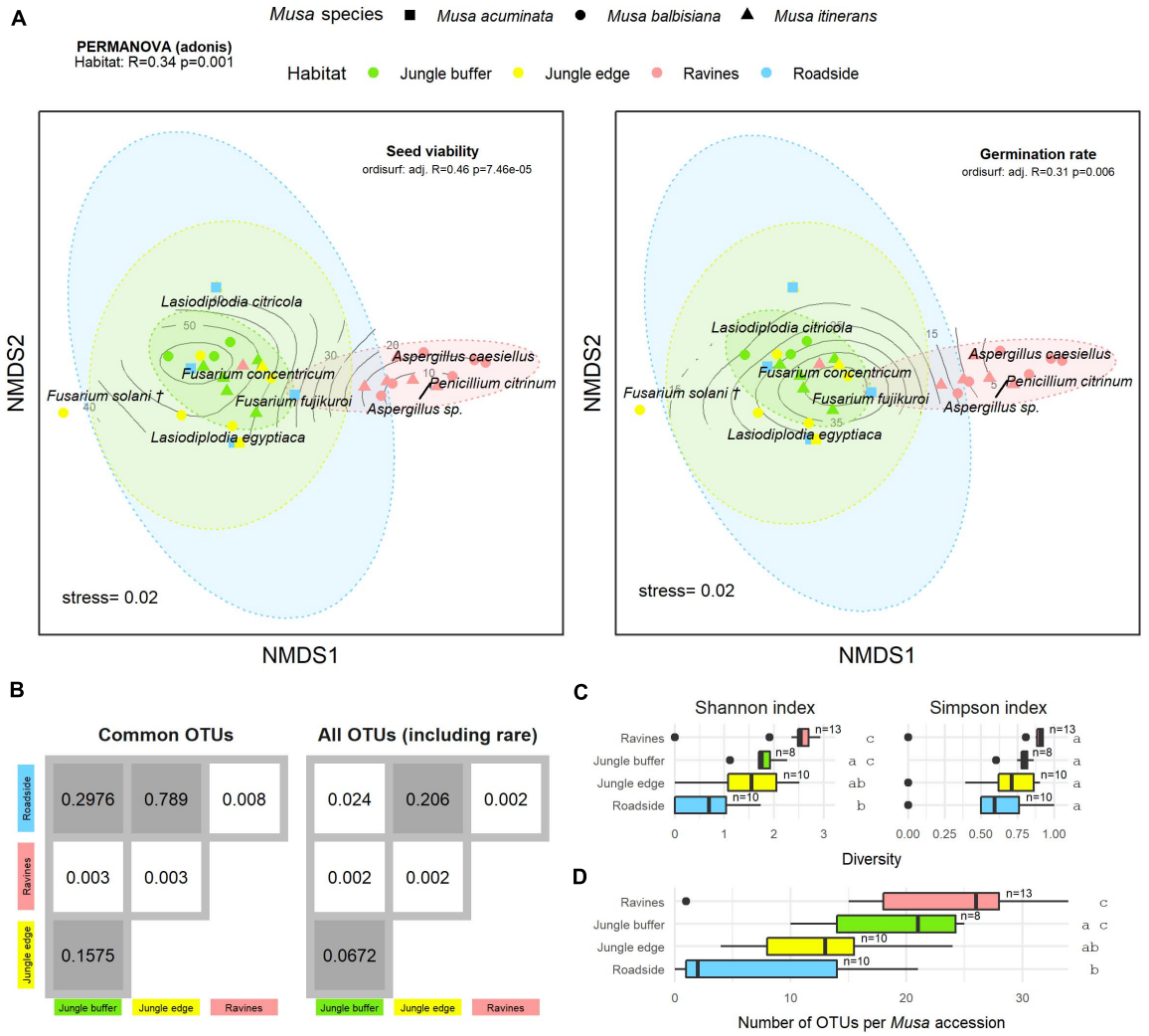


FIGURE 4 | (A) Non-metric multidimensional scaling (NMDS) plot of the most common OTUs, produced with metaMDS, fitted with post-storage seed viability (left) and germination rates (right). Contour lines indicate the fit of the seed viability and germination rate variables to the ordination using the ordisurf function, showing which points are associated with higher or lower seed viability. Each point represents one *Musa* accession, with shape showing host *Musa* species and colour showing habitat, while OTUs are shown in italic text. (†) *Fusarium solani* = *Neocosmospora solani* (Sandoval-Denis et al., 2019). Ellipses were generated with the stat_ellipse function in ggplot2. The PERMANOVA result in the top left indicates significant difference in endophyte community composition between habitats. **(B)** Matrix of pairwise PERMANOVA *p*-values showing whether endophyte community was significantly different between pairs of habitats, both for the subset of common OTUs visualised in the NMDS and including rare OTUs. Grey boxes indicate non-significant *p*-values (>0.5). Diversity according to Shannon and Simpson indices **(C)** and abundance of OTUs **(D)** per *Musa* accession in each habitat. Groups with significant difference of means as calculated by TukeyHSD are shown by letters on the right of the plots. Sample size (number of accessions) is shown to the right of boxes.

which was also one of the only species complexes that was not significantly supported. Across the whole phylogeny, 68% of all internodes were significantly supported. Extremely short branch and internode lengths indicated rapid divergence in the FFSC and FIESC clades, as well as in other species complexes such as FOSC and *Fusarium redolens* species complex.

DISCUSSION

In this study, we used both a culture-dependent and culture-independent approach to assess the diversity of endophytes in stored banana CWR seeds. In an example of the value of collections, we demonstrated the feasibility of endophyte discovery from seed banks, many strains of which can be isolated in culture for future study. By using cloning versus next-generation-sequencing methods for the culture-independent detection of seed endophytes, we were able to economically sequence individual seeds (rather than a pooled sample) to determine the endophyte capacity of the *Musa* seeds from the culture-independent approach, which could then be combined with the data on number of endophytes isolated in culture per seed. Of the seeds containing endophytes, the number of unique OTUs was biased toward one for both sampling

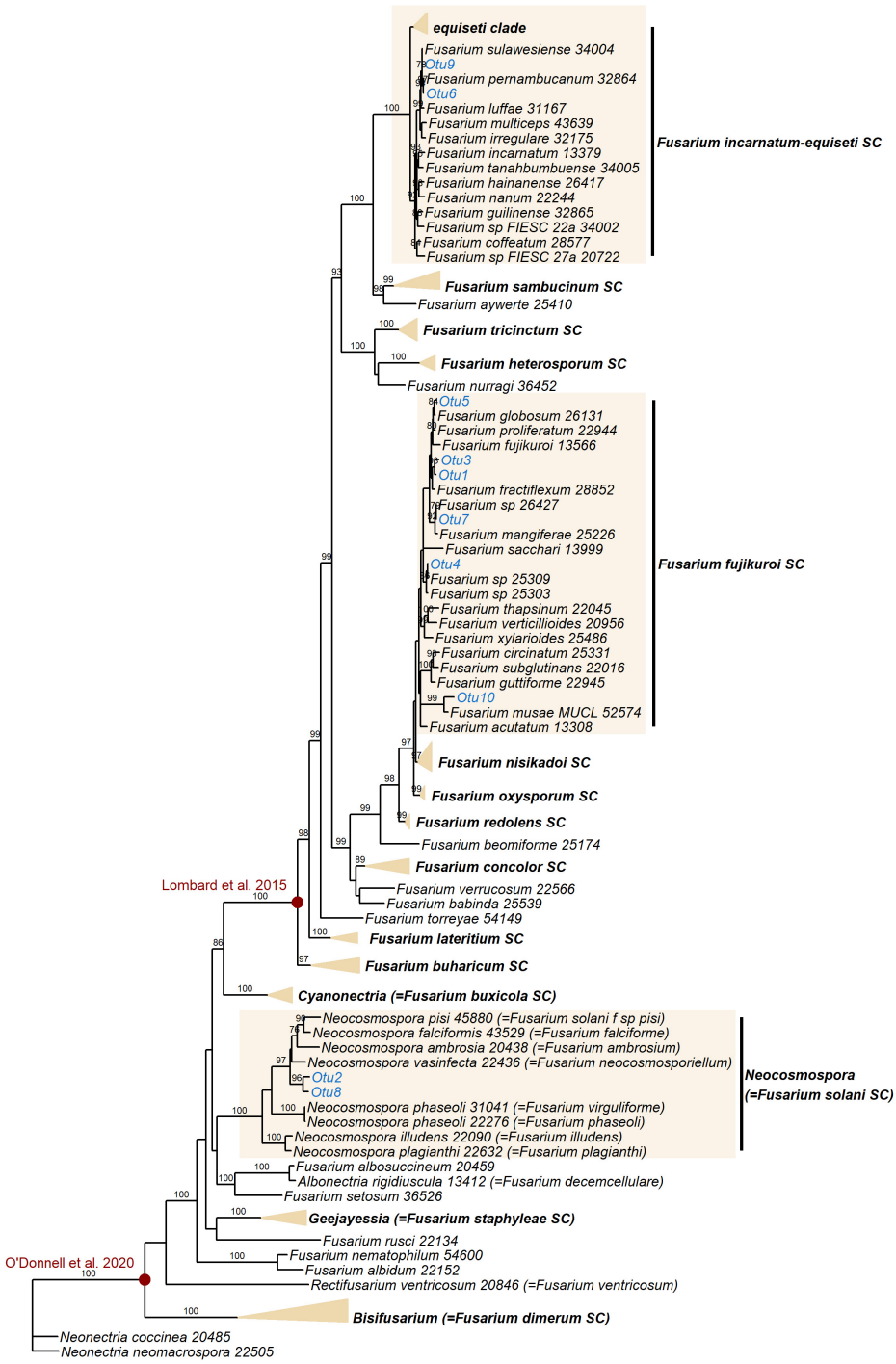


FIGURE 5 | Maximum likelihood RAxML tree reconstructing relationships of 130 taxa of *Fusarium* and closely related genera, including the *EF1α* OTUs delimited in this study (indicated in blue). Bootstrap support values ≥ 70% are shown on internodes. Genera and *Fusarium* species complexes (SC) which weren't represented by any OTUs in this study are collapsed where possible–the yellow triangles are vertically scaled for ease of visualisation, with horizontal length representing the longest branch in the species complex. Species complex and genus names are shown in bold. Red circles indicate generic limits of *Fusarium* proposed by Lombard et al. (2015) and O'Donnell et al. (2020).

approaches (**Figure 1A**), which suggests that there is some level of competitive exclusion in the limited physical space of the seed, as posited by Raghavendra et al. (2013). This is also in agreement with recent work on seeds from various alpine plants, which showed that, while bacterial endophytes appear to interact positively, fungi are usually mutually exclusive

(Wassermann et al., 2019). Similarly, during pathogenic invasion of radish seeds, it was found that a fungus altered the fungal endophyte community while a bacterium had no effect on either bacterial or fungal endophytes, although the authors noted that the different infection routes and thus microhabitats of the two pathogens could have contributed to the observed community differences (Rezki et al., 2016). Our seeds were all pre-dispersal (as all MSB seeds are), so there is also the possibility that the endophyte capacity was influenced by the lack of opportunity for seeds to acquire fungi from the soil, which is known to be a source of much seed endophyte diversity (e.g., U'Ren et al., 2009; Sarmiento et al., 2017). More insight into the dynamics of endophyte seed colonisation is needed, and would benefit from experimental inoculation combined with *in situ* visualisation of the physical space endophytes inhabit within the seed (e.g., Rath et al., 2014; Vági et al., 2014). Previous work on the specific localisation of seed endophytes has established that it varies depending on the species in question: some endophytic species are known to only be found in the seed coat (Oldrup et al., 2010) while others such as grass symbionts are found in the embryo and endosperm (Philipson and Christey, 1986; Zhang et al., 2017). Although in this study we did not establish the exact localisation of endophytes within the *Musa* seeds, the fact that we both cultured and directly sequenced many fungi from whole seeds whereas ER testing showed no or minimal "contamination" (i.e., any fungal growth from extracted embryos) suggests that most of the OTUs may have been located outside the embryo (**Supplementary Table 1**). However, as the ER testing only applies to culturable fungi and the embryo may contain endophytes that can only be detected through direct sequencing (**Figure 3**), with this data we cannot conclusively comment on the localisation of our taxa within the seeds. We also checked for OTUs present on the seed surface (**Supplementary Table 3**)–we were confident that these OTUs were also found as endophytes inside the seeds and not contaminations as we performed culture imprint controls to confirm the efficacy of the surface sterilisation method. Being both inside and outside the seed indicates that these strains were more likely generalists, horizontally transferred, for instance, from fruit to seed, rather than vertically transmitted endophytes, which would not be expected to be found outside the seed as well.

The genera found in the *Musa* seeds were largely similar to previous studies of *Musa* endophytes from roots and leaves (Sikora et al., 2008; Wang et al., 2014; Zakaria et al., 2016; Zakaria and Aziz, 2018), as well as other tropical tree endophytes, such as from cacao branches (Rubini et al., 2005) and rubber leaves (Vaz et al., 2018) and tropical orchid roots (Bayman and Otero, 2007). The most commonly found genera, *Lasiodiplodia*, *Fusarium*, and *Aspergillus*, are all ubiquitous in both endophytic and other contexts. The genus *Lasiodiplodia* is best known for the species *Lasiodiplodia theobromae*, a prevalent endophyte in the global tropics (Salvatore and Andolfi, 2020), but also an infamous pathogen of tropical fruit trees. For instance, *L. theobromae* has been found to cause crown rot in commercial banana (Sangeetha et al., 2012) and–among other *Lasiodiplodia* strains–stem and fruit rot in papaya (Netto et al., 2014) and dieback in mango (Rodríguez-Gálvez et al., 2017). Goos et al. (1961) similarly found *L. theobromae* (using the synonym *Botryodiplodia theobromae*) to be pervasive in seeds of *Musa* spp., although they did not report whether the colonised seeds or resulting plants had disease symptoms. They also found *L. theobromae* exclusively in the seed coat and micropylar plug versus the endosperm or embryo and echoed our above hypothesis that it is transferred from fruit to seed. This was also supported in *Musa ornata*, for which *Lasiodiplodia* colonisation was observed in all cases apart from those where embryos were removed from seeds under aseptic conditions (Burgos-Hernández et al., 2014). The two prevalent *Lasiodiplodia* OTUs in this study were classified as *Lasiodiplodia citricola* and *Lasiodiplodia egyptica*, both of which were first described from diseased plants: *Citrus* spp. showing "branch dieback, cankers and fruit rot" (Abdollahzadeh et al., 2010) and mango suffering dieback (Ismail et al., 2012), respectively. *L. egyptica* has also been implicated in stem-end rot of coconut (Rosado et al., 2016) and *L. citricola* in disease of English walnut (Chen et al., 2013). Although we could find no reports of these species as endophytes, their relatively recent description makes it likely that their full extent of occurrence has not been revealed. Sequencing phylogenetically informative loci for these endophytic *Lasiodiplodia* strains–e.g., *EF1α* and TUB2 (de Silva et al., 2019)–will be desirable in the future to confirm their identity with phylogenetic analysis.

Like *Lasiodiplodia*, multiple *Fusarium* strains are phytopathogenic (Aoki et al., 2014), and *Fusarium oxysporum* and *Fusarium graminearum* both feature in the top 10 most economically/scientifically important fungal plant pathogens (Dean et al., 2012). This is certainly relevant to commercial banana crops, which are under threat from Foc TR4, the causal agent of Fusarium Wilt (Dita et al., 2018). Fungi in the genus *Fusarium* are also known to be common endophytes in *Musa* species, however, having been previously isolated from either wild or commercial *Musa* in China, Thailand and Guatemala (zum Felde et al., 2003; Sikora et al., 2008; Wang et al., 2019). The species complexes represented in this study–FIESC, FFSC, and FSSC–are all known to comprise both phytopathogens and endophytes (Kavroulakis et al., 2007; Aoki et al., 2014; Niehaus et al., 2016; Bilal et al., 2018; Wang et al., 2019), and additionally both the FIESC and FSSC contain species that act as opportunistic human pathogens (Zhang et al., 2006; O'Donnell et al., 2009). Even within species, *Fusarium* strains can differ greatly in their proclivity to cause disease in their plant host–*in vitro* expression of secondary metabolites (including phytohormones and mycotoxins) in an orchid endophytic *Fusarium proliferatum* strain was shown to be distinct from expression in a pathogenic *F. proliferatum* strain (Niehaus et al., 2016). It has also been demonstrated that commercial banana roots can be protected from nematodes by endophytic FOSC strains (zum Felde et al., 2003; Mendoza and Sikora, 2009), the same species complex to which Foc TR4 belongs. We should highlight that the taxonomy of *Fusarium* is highly contested (Summerell, 2019). Recent dismantling and splitting of certain *Fusarium* species complexes into several distinct genera (Lombard et al., 2015), including reassigning species in the FSSC to the genus *Neocosmospora* (Sandoval-Denis et al., 2019), has received pushback, the main opposing argument being that

a broader generic concept benefits practitioners dealing with human and plant pathogens (O'Donnell et al., 2020). Different perspectives on the limits of the generic concept of *Fusarium* (illustrated in **Figure 5**) will no doubt continue to be debated.

Unlike the former two genera, *Aspergillus* is not known predominantly for plant-associated taxa, but rather for globally distributed air and soilborne saprotrophs, with some species infamously acting as opportunistic human pathogens (Bennett, 2010; Latgé and Chamilos, 2020). Nonetheless, *Aspergillus* species are also frequently found as endophytes, and an endophytic *Aspergillus fumigatus* strain isolated from *Oxalis corniculata* roots has been shown to promote growth in rice (Bilal et al., 2018). Intriguingly, the most prevalent OTU for the genus in this study was classified as *Aspergillus caesiellus*, which has been reported as a marine endophyte of seagrasses and sponges (Liu et al., 2010; Subrmaniyan et al., 2018). The second most prevalent OTU was *Aspergillus flavus*, a ubiquitous soil fungus known for contaminating stored grains with aflatoxins, and also an agent of aforementioned opportunistic diseases in animals and humans (Amaike and Keller, 2011). The range of plant-fungal interactions that are observed in these three genera emphasises the ongoing question we face for the endophytic lifestyle as a whole–how can we distinguish mutualistic or commensal endophytes from latent pathogens? Greater exploration of the genomic features and expression profiles of endophytes is required to tackle this issue, and seed banks provide an excellent resource for targeting economically, environmentally and scientifically important plant hosts from which to isolate strains for this purpose.

A relatively modest sampling effort was required to isolate the majority of common OTUs found across *Musa* species (**Figure 1B**), in agreement with other microfungi community studies (e.g., Paulus et al., 2006; Tisthammer et al., 2016; Vaz et al., 2018), but the vast majority of OTUs were singleton or low-abundance, a known phenomenon in microbial diversity (Lynch and Neufeld, 2015; Jia et al., 2018). A disproportionate number of rare taxa can obstruct community composition visualisation methods such as NMDS, and so low abundance taxa are often filtered out in order to visualise structural patterns (e.g., Miller et al., 2016; Huang et al., 2018; U'Ren et al., 2019). This is distinct from the practise of removing rare/singleton OTUs from high throughput sequencing datasets in case of sequencing artefacts (e.g., Brown et al., 2015). Poos and Jackson (2012) discussed two arguments for removal of rare taxa in multivariate analysis in the context of bioassessments: statistical impact ("rare species provide limited interpretative value and add noise") and biological impact ("rare taxa do not provide meaningful information beyond that captured by more common species"). For our comparison of endophyte communities between different host habitats, PERMANOVA analysis found the effect size of habitat on community variance to be greater when excluding rare taxa (**Table 1**), but when comparing the significance of individual habitats with pairwise PERMANOVA the inclusion of rare taxa revealed differences between habitats that were not found from the common taxa alone (**Figure 4B**). This challenges the "biological impact" argument above, however removal of rare taxa remains a practical compromise to enable visualisation of at least a subset of the community structure. A valid question is whether the rare taxa that were detected are conditionally rare (i.e., their abundance is based on abiotic conditions), or permanently rare. We would need repeated samples over time to clarify this, and although outside the scope of this study, seed bank collections are excellently positioned for addressing this in the future.

While the impact of "edge effect"–change in community structure at the boundary of habitats, whether natural or from e.g., encroaching human land use or bisecting roads–has been well documented for plant communities (Skole and Tucker, 1993; Harper et al., 2005; Kunert et al., 2015), it is far less studied in fungi (Crockatt, 2012; Ruete et al., 2016), and, to our knowledge, the concept has not been addressed in the context of endophytes. Our results comparing the jungle buffer, jungle edge and roadside habitats suggest that there may indeed be some level of edge effect manifested in the seed mycobiome of these *Musa* accessions, both in diversity and abundance (**Figures 4C,D**). While community composition did not differ between these three habitats for the most common taxa, when including rare taxa there was a significant difference between the jungle buffer and roadside habitats (**Figure 4B**). Seeing a community difference between these habitats when including rare and not just common taxa suggests that the rare endophytes may be more sensitive to edge effects, which would be consistent with the concept of biotic homogenisation as a result of ecosystem disruption (Mckinney and Lockwood, 1999; Parra-Sanchez and Banks-Leite, 2020). This is also supported by the fact that the Shannon index, which is sensitive to rare species, found a significant difference in diversity, while the Simpson index, which is sensitive to abundant species, did not (Morris et al., 2014). These results come with the caveat that the habitats as defined in this study are interpreted from the MSB seed collection data, which were not recorded with any particular study design in mind, and as such some entries are more complete than others and there can be subjectivity in how to infer habitat from the collection notes. While the extensive metadata attached to natural history collections can be incredibly powerful for studying patterns of biodiversity (Andrew et al., 2018, 2019; Funk, 2018; Pearce et al., 2020), the application of that data must be done with care.

Fitting post-storage seed viability (TTC) and germination rate (ER) data to the NMDS visualisation showed jungle habitat accessions to be associated with highest seed viability and ravine habitat accessions to be associated with lowest seed viability. As these assessments specifically measured post-storage viability/germination, we relied on the assumption that the same collection standards and procedures were always adhered to, as other factors have been shown to impact *Musa* seed viability such as maturity of the seed at collection and the speed of drying before cold storage (Kallow et al., 2020). Nonetheless, these results highlighted *Fusarium* and *Lasiodiplodia* strains, which would be particularly interesting to trial in experimental inoculation studies, to verify whether they impact the survivability of *Musa* seeds in storage, or indeed the germination rates of fresh seeds. Endophytic *Fusarium* strains have previously been found to promote germination and seedling growth of an Indonesian peatland grass (Tamura et al., 2008) and germination of orchid seeds (Bayman and Otero, 2007). In addition to the

aforementioned roles of *L. theobromae* in tropical fruit tree diseases, it has also been implicated in seed rot, for instance of slash pine (Cilliers et al., 1993), and to cause reduced germination rates in aridan and coconut seeds (Dugan et al., 2016). The role of seedborne *L. theobromae* on germination may be more nuanced, however, as it has been found to produce fatty acid esters, which can alternately inhibit and promote tobacco seed germination and seedling growth (Uranga et al., 2016). Considering the pathogenic role of numerous *Lasiodiplodia* species discussed above, it is interesting that this study saw *Lasiodiplodia* strains to be prevalent in *Musa* accessions with comparatively high post-storage seed viability. A previous study of *in vitro* germination of both stored and fresh *M. ornata* seeds found *Lasiodiplodia* to persistently infect seeds, with the implication that these seeds then decayed (Burgos-Hernández et al., 2014). Goos et al. (1961) reported a similar result for seeds of various *Musa* spp. in aseptic conditions, however they noted that germination was not significantly affected by *Lasiodiplodia* colonisation under "greenhouse conditions." This raises the question as to whether the pathogenic potential of *Lasiodiplodia* strains in *Musa* seeds is influenced by the abiotic conditions and/or co-occurrence of other fungi. Of course, without isolating specific strains and performing controlled pathogenicity tests, it is impossible to answer this, as different fungal strains can vary in their ability to cause disease regardless of secondary factors such as environment. It would also be interesting to look at the endosymbiotic or "endohyphal" bacteria associated with our strains, as these have been found, in rare cases, to be capable of effecting (pre-storage) seed germination and viability in a neotropical tree (Shaffer et al., 2018).

An interesting result was that the abundance of endophytes per *Musa* accession was greatest in the ravine habitat (**Figure 4B**), the same habitat that was adversely correlated with post-storage seed viability. Returning to the ambiguity of the endophytic lifestyle, this again raises the issue that it is not the mere presence of endophytes, but the identity of specific strains that may have implications for stored seeds. The difference in abundance and community composition in the ravine habitats could partially be explained by altitude, although unfortunately there was not sufficient altitude data for all accessions in the MSB records to test this. Previous studies on the effect of altitude on endophyte communities have suggested an inconsistent relationship (Granath et al., 2007; Hashizume et al., 2008; Zubek et al., 2009; Bonfim et al., 2016), no doubt partially due to the large number of confounding factors associated with changing altitude, such as variation in the host plant assemblages, as host availability is believed to be a main driver of endophyte community composition (U'Ren et al., 2019). Host availability may also have been a key factor as to why accessions in oil palm plantations and a botanical garden had low endophyte abundance (**Supplementary Figure 3**). Although the sample size for these habitats was too small to include them in the main analyses, these were the only managed habitats with, presumably, the least natural co-occurring plant assemblages.

There are a number of considerations for seed banking in the context of endophytes that are important to raise for future discussion and research. Firstly, our results show that habitat of the host plants from which seeds are collected could impact the associated endophyte communities, which may potentially have downstream consequences for seed survival. Collecting seeds from individuals in a range of habitats with different co-occurring plant species may be advisable to conserve endophytic diversity. As current seed bank protocol is to collect seeds pre-dispersal, before horizontal transmission of fungi from soil to seed, what, if any, impact does this have on subsequent viability of the seeds or health of the descendent plants? To our knowledge, only one study has made a direct comparison of endophytic communities in pre and post-dispersal seeds for the same plant individual, finding fewer endophytes in pre-dispersal seeds of a neotropical tree species, none of which were successfully isolated in culture (Gallery et al., 2007). Studies of buried seeds have shown that seeds acquire diverse endophytes through horizontal transmission from the soil (e.g., U'Ren et al., 2009; Sarmiento et al., 2017), but are also vulnerable to soilborne pathogens (Gallery et al., 2010). It could then be that the current protocol of storing pre-dispersal seeds is preferable, as it limits the acquisition of potential pathogens while still allowing the possibility for mutualistic endophytes to be vertically transmitted from the parent plant. The dynamics of endophyte transmission are likely to be highly variable between different plant groups, however, and more studies of seeds from different hosts, geographical areas and dispersal stages are needed to identify the optimal collection procedure for healthy microbiomes of stored seeds.

CONCLUSION

This study has demonstrated that seed banks provide huge potential for research into fungal endophyte communities. As well as being an untapped resource for new fungal diversity, the ability to isolate live strains from almost 40,000 global plant taxa curated by the MSB–a third of which are identified as having significant natural capital value (Liu et al., 2018)–provides far-reaching opportunities for future study of the role of endophytes in plant health. For this reason, although originally designed for conservation of plant genetic diversity, seed banks may have an equally important role in conserving the seed microbiome, and much more discussion and research is needed on how the seed collection and storage procedure can best accommodate this.

DATA AVAILABILITY STATEMENT

The datasets presented in this study can be found in online repositories. The names of the repository/repositories and accession number(s) can be found in the article/ **Supplementary Material**.

AUTHOR CONTRIBUTIONS

SK and JD provided the samples and contributed to the writing of the manuscript. RH, TL, ED, JO, and CM carried out the

molecular data collection. BP performed the embryo rescue testing. RH and EG designed and implemented the analysis of the results and wrote the manuscript. EG conceived the original idea and supervised the project. All authors contributed to the article and approved the submitted version.

FUNDING

This work was supported by the Charles Wolfson Charitable Trust and Pragnell Fund to EG; a sub-grant from the University of Queensland from the Bill & Melinda Gates Foundation project "BBTV mitigation: Community management in Nigeria, and screening wild banana progenitors for resistance" (OPP1130226) to SK; and the Royal Botanic Gardens Kew Pilot Study Fund awarded to RH, who is a Natural Environment Research Council funded Ph.D. student with the London NERC DTP (NERC Ref: NE/L002485/1). The Royal Botanic Gardens Kew is part funded by Grant in Aid from the UK Department for Environment, Food and Rural Affairs.

ACKNOWLEDGMENTS

We thank the Malaysian Agricultural Research and Development Institute and the Vietnamese Plant Resources Center for providing seeds to the MSB, in particular Binti Tahir, M. Anuar Rasyidi, M. N., Ahmad Syahman, M. D., Mohd Shukri, M. A., Suryanti, B., Dang Toan Vu, Tuong Dang Vu, Le Thi Loan, and Ngo Duc. We thank Toby Tydeman, Khushboo Gurung, Emily Kennedy, and Tom Bance for help in processing samples. We are grateful to Jana M. U'Ren for useful discussion and Bryn T. M. Dentinger for his generosity and inspiration at the outset of the study. Thanks also to the editor and the reviewers Jana M. U'Ren and Asha Janadaree Dissanayake for their valuable feedback.

SUPPLEMENTARY MATERIAL

The Supplementary Material for this article can be found online at: https://www.frontiersin.org/articles/10.3389/fmicb.2021.643731/full#supplementary-material

Supplementary Figure 1 | Scree plot up to 10 dimensions for the NMDS analysis (top) and stress plot for the chosen number of 6 dimensions (bottom).

Supplementary Figure 2 | Dispersion of data for each habitat for both the common taxa used in the NMDS and all taxa including rare OTUs, as assessed with betadisper. Sample size (number of accessions) is shown to the right of the plots. Sample size is less for the roadside habitat in the "All OTUs" category than in the diversity and abundance analyses (**Figures 4C,D**) because accessions with no OTUs detected are removed by betadisper.

Supplementary Figure 3 | Abundance of OTUs per *Musa* accession for each habitat including oil palm plantation and botanical garden. Groups with significant difference of means as calculated by TukeyHSD are shown by letters on the right of the plots. Sample size (number of accessions) is shown to the right of boxes.

Supplementary Table 1 | Millennium Seed Bank (MSB) serial numbers and metadata associated for the 45 wild *Musa* accessions used in this study.

Supplementary Table 2 | GenBank accession numbers for taxa used in the phylogenetic analysis. Accessions in bold were sequenced in this study.

Supplementary Table 3 | Summary of OTUs which were also found on the unsterilised seed surface.

Supplementary Data Sheet 1 | Classification of OTUs by UNITE and T-BAS and the inferred consensus.

REFERENCES

Abarenkov, K., Zirk, A., Piirmann, T., Pöhönen, R., Ivanov, F., Nilsson, R. H., et al. (2020). *UNITE General FASTA Release for Fungi. Version 04.02.2020*, UNITE community. doi: 10.15156/BIO/786368

Abdollahzadeh, J., Javadi, A., Goltapeh, E. M., Zare, R., and Phillips, A. J. L. (2010). Phylogeny and morphology of four new species of *Lasiodiplodia* from Iran. *Persoonia* 25, 1–10. doi: 10.3767/003158510X524150

Amaike, S., and Keller, N. P. (2011). *Aspergillus flavus*. *Annu. Rev. Phytopathol.* 49, 107–133. doi: 10.1146/annurev-phyto-072910-095221

Anderson, M. J., and Walsh, D. C. I. (2013). PERMANOVA, ANOSIM, and the Mantel test in the face of heterogeneous dispersions: what null hypothesis are you testing? *Ecol. Monogr.* 83, 557–574. doi: 10.1890/12-2010.1

Andrew, C., Büntgen, U., Egli, S., Senn-Irlet, B., Grytnes, J. A., Heilmann-Clausen, J., et al. (2019). Open-source data reveal how collections-based fungal diversity is sensitive to global change. *Appl. Plant Sci.* 7:e1227. doi: 10.1002/aps3.1227

Andrew, C., Diez, J., James, T. Y., and Kauserud, H. (2018). Fungarium specimens: a largely untapped source in global change biology and beyond. *Philos. Trans. R. Soc. B* 374:20170392. doi: 10.1098/rstb.2017.0392

Aoki, T., O'Donnell, K., and Geiser, D. M. (2014). Systematics of key phytopathogenic *Fusarium* species: current status and future challenges. *J. Gen. Plant Pathol.* 80, 189–201. doi: 10.1007/s10327-014-0509-3

Arnold, A. E., Henk, D. A., Eells, R. L., Lutzoni, F., and Vilgalys, R. (2007). Diversity and phylogenetic affinities of foliar fungal endophytes in loblolly pine inferred by culturing and environmental PCR. *Mycologia* 99, 185–206. doi: 10.3852/mycologia.99.2.185

Arnold, A. E., Maynard, Z., Gilbert, G. S., Coley, P. D., and Kursar, T. A. (2000). Are tropical fungal endophytes hyperdiverse? *Ecol. Lett.* 3, 267–274. doi: 10.1046/j.1461-0248.2000.00159.x

Arnold, A. E., Miadlikowska, J., Higgins, K. L., Sarvate, S. D., Gugger, P., Way, A., et al. (2009). A phylogenetic estimation of trophic transition networks for ascomycetous fungi: are lichens cradles of symbiotrophic fungal diversification? *Syst. Biol.* 58, 283–297. doi: 10.1093/sysbio/syp001

Bamisile, B. S., Dash, C. K., Akutse, K. S., Keppanan, R., and Wang, L. (2018). Fungal endophytes: beyond herbivore management. *Front. Microbiol.* 9:544. doi: 10.3389/fmicb.2018.00544

Bayman, P., Angulo-Sandoval, P., Báez-Ortiz, Z., and Lodge, D. J. (1998). Distribution and dispersal of *Xylaria* endophytes in two tree species in Puerto Rico. *Mycol. Res.* 102, 944–948. doi: 10.1017/S095375629700590X

Bayman, P., and Otero, J. T. (2007). "Microbial endophytes of orchid roots," in *Microbial Root Endophytes*, eds B. J. E. Schulz, C. J. C. Boyle, and T. N. Sieber (Berlin: Springer Berlin Heidelberg), 153–177. doi: 10.1007/3-540-33526-9_9

Bengtsson-Palme, J., Ryberg, M., Hartmann, M., Branco, S., Wang, Z., Godhe, A., et al. (2013). Improved software detection and extraction of ITS1 and ITS2 from ribosomal ITS sequences of fungi and other eukaryotes for analysis of environmental sequencing data. *Methods Ecol. Evol.* 4, 914–919. doi: 10.1111/2041-210X.12073

Benjamini, Y., and Hochberg, Y. (1995). Controlling the false discovery rate - a practical and powerful approach to multiple testing article. *J. R. Stat. Soc.* 57, 289–300. doi: 10.2307/2346101

Bennett, J. W. (2010). "An overview of the genus *Aspergillus*," in *Aspergillus: Molecular Biology and Genomics*, eds M. Machida and K. Gomi (Poole: Caister Academic Press).

Berger, S. A., Krompass, D., and Stamatakis, A. (2011). Performance, accuracy, and web server for evolutionary placement of short sequence reads under maximum likelihood. *Syst. Biol.* 60, 291–302. doi: 10.1093/sysbio/syr010

Bilal, L., Asaf, S., Hamayun, M., Gul, H., Iqbal, A., Ullah, I., et al. (2018). Plant growth promoting endophytic fungi *Aspergillus fumigatus* TS1 and *Fusarium proliferatum* BRL1 produce gibberellins and regulates plant endogenous hormones. *Symbiosis* 76, 117–127. doi: 10.1007/s13199-018-0545-4

Bonfim, J. A., Vasconcellos, R. L. F., Baldesin, L. F., Sieber, T. N., and Cardoso, E. J. B. N. (2016). Dark septate endophytic fungi of native plants along an altitudinal gradient in the Brazilian Atlantic forest. *Fungal Ecol.* 20, 202–210. doi: 10.1016/j.funeco.2016.01.008

Brown, S. P., Veach, A. M., Rigdon-Huss, A. R., Grond, K., Lickteig, S. K., Lothamer, K., et al. (2015). Scraping the bottom of the barrel: are rare high throughput sequences artifacts? *Fungal Ecol.* 13, 221–225. doi: 10.1016/j.funeco.2014.08.006

Brozynska, M., Furtado, A., and Henry, R. J. (2016). Genomics of crop wild relatives: expanding the gene pool for crop improvement. *Plant Biotechnol. J.* 14, 1070–1085. doi: 10.1111/pbi.12454

Burgos-Hernández, M., Castillo-Campos, G., Mata-Rosas, M., González, D., Vovides, A. P., and Murguía-González, J. (2014). Seed germination of the wild banana *Musa ornata* (Musaceae). *Seed Sci. Technol.* 42, 16–27. doi: 10.15258/sst.2014.42.1.02

Camacho, C., Coulouris, G., Avagyan, V., Ma, N., Papadopoulos, J., Bealer, K., et al. (2009). BLAST+: architecture and applications. *BMC Bioinformatics* 10:421. doi: 10.1186/1471-2105-10-421

Carbone, I., White, J. B., Miadlikowska, J., Arnold, A. E., Miller, M. A., Kauff, F., et al. (2017). T-BAS: tree-Based Alignment Selector toolkit for phylogenetic-based placement, alignment downloads and metadata visualization: an example with the Pezizomycotina tree of life. *Bioinformatics* 33, 1160–1168. doi: 10.1093/bioinformatics/btw808

Carbone, I., White, J. B., Miadlikowska, J., Arnold, A. E., Miller, M. A., Magain, N., et al. (2019). T-BAS Version 2.1: tree-based alignment selector toolkit for evolutionary placement of dna sequences and viewing alignments and specimen metadata on curated and custom trees. *Microbiol. Resour. Announc* 8, e328–19.

Card, S., Johnson, L., Teasdale, S., and Caradus, J. (2016). Deciphering endophyte behaviour: the link between endophyte biology and efficacious biological control agents. *FEMS Microbiol. Ecol.* 92:fiw114. doi: 10.1093/femsec/fiw114

Carreel, F., Gonzalez de Leon, D., Lagoda, P., Lanaud, C., Jenny, C., Horry, J. P., et al. (2002). Ascertaining maternal and paternal lineage within *Musa* by chloroplast and mitochondrial DNA RFLP analyses. *Genome* 45, 679–692. doi: 10.1139/g02-033

Castresana, J. (2000). Selection of conserved blocks from multiple alignments for their use in phylogenetic analysis. *Mol. Biol. Evol.* 17, 540–552. doi: 10.1093/oxfordjournals.molbev.a026334

Center for Plant Conservation (2018). *CPC Best Plant Conservation Practices to Support Species Survival in the Wild*. Kennett Square, PA: American Public Gardens Association.

Chen, S. F., Fichtner, E., Morgan, D. P., and Michailides, T. J. (2013). First report of *Lasiodiplodia citricola* and *Neoscytalidium dimidiatum* causing death of graft union of English walnut in California. *Plant Dis.* 97:993. doi: 10.1094/PDIS-10-12-1000-PDN

Cilliers, A. J., Swart, W. J., and Wingfield, M. J. (1993). A review of *Lasiodiplodia theobromae* with particular reference to its occurrence on coniferous seeds. *South African For. J.* 166, 47–52. doi: 10.1080/00382167.1993.9629398

Clarke, K. R. (1993). Non-parametric multivariate analyses of changes in community structure. *Aust. J. Ecol.* 18, 117–143. doi: 10.1111/j.1442-9993.1993.tb00438.x

Cock, P. J. A., Antao, T., Chang, J. T., Chapman, B. A., Cox, C. J., Dalke, A., et al. (2009). Biopython: freely available Python tools for computational molecular biology and bioinformatics. *Bioinformatics* 25, 1422–1423. doi: 10.1093/bioinformatics/btp163

Crockatt, M. E. (2012). Are there edge effects on forest fungi and if so do they matter? *Fungal Biol. Rev.* 26, 94–101. doi: 10.1016/j.fbr.2012.08.002

da Silva, F. P., Vechiato, M. H., and Harakava, R. (2014). EF-1α gene and IGS rDNA sequencing of *Fusarium oxysporum* f. sp. *vasinfectum* and *F. oxysporum* f. sp. *phaseoli* reveals polyphyletic origin of strains. *Trop. Plant Pathol.* 39, 64–73. doi: 10.1590/S1982-56762014000100008

Daru, B. H., Bowman, E. A., Pfister, D. H., and Arnold, A. E. (2018). A novel proof of concept for capturing the diversity of endophytic fungi preserved in herbarium specimens. *Philos. Trans. R. Soc. B* 374:20170395. doi: 10.1098/rstb.2017.0395

de Silva, N. I., Phillips, A. J. L., Liu, J. K., Lumyong, S., and Hyde, K. D. (2019). Phylogeny and morphology of *Lasiodiplodia* species associated with Magnolia forest plants. *Sci. Rep.* 9:14355. doi: 10.1038/s41598-019-50804-x

Dean, R., Van Kan, J. A. L., Pretorius, Z. A., Hammond-Kosack, K. E., Di Pietro, A., Spanu, P. D., et al. (2012). The Top 10 fungal pathogens in molecular plant pathology. *Mol. Plant Pathol.* 13, 414–430. doi: 10.1111/j.1364-3703.2012.2011.00783.x

Delaye, L., García-Guzmán, G., and Heil, M. (2013). Endophytes versus biotrophic and necrotrophic pathogens-are fungal lifestyles evolutionarily stable traits? *Fungal Divers.* 60, 125–135. doi: 10.1007/s13225-013-0240-y

Dentinger, B. T. M., Gaya, E., O'Brien, H., Suz, L. M., Lachlan, R., Díaz-Valderrama, J. R., et al. (2016). Tales from the crypt: genome mining from fungarium specimens improves resolution of the mushroom tree of life. *Biol. J. Linn. Soc.* 117, 11–32. doi: 10.1111/bij.12553

Dita, M., Barquero, M., Heck, D., Mizubuti, E. S. G., and Staver, C. P. (2018). Fusarium wilt of banana: current knowledge on epidemiology and research needs toward sustainable disease management. *Front. Plant Sci.* 9:1468. doi: 10.3389/fpls.2018.01468

Dudek-Wicher, R. K., Junka, A., and Bartoszewicz, M. (2018). The influence of antibiotics and dietary components on gut microbiota. *Gastroenterol. Rev.* 13, 85–92. doi: 10.5114/pg.2018.76005

Dugan, F. M., Lupien, S. L., Osuagwu, A. N., Uyoh, E. A., Okpako, E., and Kisha, T. (2016). New records of *Lasiodiplodia theobromae* in Seeds of *Tetrapleura tetraptera* from Nigeria and Fruit of *Cocos nucifera* From Mexico. *J. Phytopathol.* 164, 65–68. doi: 10.1111/jph.12384

Edgar, R. C. (2004). MUSCLE: multiple sequence alignment with high accuracy and high throughput. *Nucleic Acids Res.* 32, 1792–1797. doi: 10.1093/nar/gkh340

Edgar, R. C. (2013). UPARSE: highly accurate OTU sequences from microbial amplicon reads. *Nat. Methods* 10, 996–998. doi: 10.1038/nmeth.2604

Food and Agriculture Organization (2014). *Genebank Standards for Plant Genetic Resources for Food and Agriculture*. Rome: Food & Agriculture Org.

Food and Agriculture Organization (2020a). *Banana Market Review 2019*. Rome: Food & Agriculture Org.

Food and Agriculture Organization (2020b). *Banana Market Review Snapshot*. Rome: Food & Agriculture Org.

Funk, V. A. (2018). Collections-based science in the 21st Century. *J. Syst. Evol.* 56, 175–193. doi: 10.1111/jse.12315

Gallery, R. E., Dalling, J. W., and Arnold, A. E. (2007). Diversity, host affinity, and distribution of seed-infecting fungi: a case study with *Cecropia*. *Ecology* 88, 582–588. doi: 10.1890/05-1207

Gallery, R. E., Moore, D. J. P., and Dalling, J. W. (2010). Interspecific variation in susceptibility to fungal pathogens in seeds of 10 tree species in the neotropical genus *Cecropia*. *J. Ecol.* 98, 147–155. doi: 10.1111/j.1365-2745.2009.01589.x

Ganley, R. J., and Newcombe, G. (2006). Fungal endophytes in seeds and needles of *Pinus monticola*. *Mycol. Res.* 110, 318–327. doi: 10.1016/j.mycres.2005.10.005

Gardes, M., and Bruns, T. D. (1993). ITS primers with enhanced specificity for basidiomycetes - application to the identification of mycorrhizae and rusts. *Mol. Ecol.* 2, 113–118. doi: 10.1111/j.1365-294X.1993.tb00005.x

Geiser, D. M., Jiménez-Gasco, M. D. M., Kang, S., Makalowska, I., Veeraraghavan, N., Ward, T. J., et al. (2004). FUSARIUM-ID v. 1.0: a DNA sequence database for identifying *Fusarium*. *Eur. J. Plant Pathol.* 110, 473–479. doi: 10.1023/B:EJPP.0000032386.75915.a0

Goos, R. D., Cox, E. A., and Stotzky, G. (1961). *Botryodiplodia theobromae* and its association with *Musa* species. *Mycologia* 53, 262–277. doi: 10.2307/3756274

Govaerts, R., and Häkkinen, M. (2006). *World Checklist of Musaceae. Facilitated by the Royal Botanic Gardens, Kew*. Available online at: http://wcsp.science.kew.org/ (accessed December 17, 2020).

Granath, G., Vicari, M., Bazely, D. R., Ball, J. P., Puentes, A., and Rakocevic, T. (2007). Variation in the abundance of fungal endophytes in fescue grasses along altitudinal and grazing gradients. *Ecography (Cop.)* 30, 422–430. doi: 10.1111/j.2007.0906-7590.05027.x

Gupta, S., Chaturvedi, P., Kulkarni, M. G., and Van Staden, J. (2020). A critical review on exploiting the pharmaceutical potential of plant endophytic fungi. *Biotechnol. Adv.* 39:107462. doi: 10.1016/j.biotechadv.2019.107462

Hajjar, R., and Hodgkin, T. (2007). The use of wild relatives in crop improvement: a survey of developments over the last 20 years. *Euphytica* 156, 1–13. doi: 10.1007/s10681-007-9363-0

Häkkinen, M., and Väre, H. (2008). Typification and check-list of *Musa* L. names (Musaceae) with nomenclatural notes. *Adansonia* 30, 63–112.

Hardoim, P. R., van Overbeek, L. S., Berg, G., Pirttilä, A. M., Compant, S., Campisano, A., et al. (2015). The hidden world within plants: ecological and evolutionary considerations for defining functioning of microbial endophytes. *Microbiol. Mol. Biol. Rev.* 79, 293–320. doi: 10.1128/MMBR.00050-14

Harper, K. A., Macdonald, S. E., Burton, P. J., Chen, J., Brosofske, K. D., Saunders, S. C., et al. (2005). Edge influence on forest structure and composition in fragmented landscapes. *Conserv. Biol.* 19, 768–782. doi: 10.1111/j.1523-1739.2005.00045.x

Hashizume, Y., Sahashi, N., and Fukuda, K. (2008). The influence of altitude on endophytic mycobiota in *Quercus acuta* leaves collected in two areas 1000 km apart. *For. Pathol.* 38, 218–226. doi: 10.1111/j.1439-0329.2008.00547.x

Hawksworth, D., and Lücking, R. (2017). Fungal diversity revisited: 2.2 to 3.8 million species. *Microbiol. Spectr* 5:FUNK-0052-2016. doi: 10.1128/microbiolspec.FUNK-0052-2016

Heeger, F., Wurzbacher, C., Bourne, E. C., Mazzoni, C. J., and Monaghan, M. T. (2019). Combining the 5.8S and ITS2 to improve classification of fungi. *Methods Ecol. Evol.* 10, 1702–1711. doi: 10.1111/2041-210x.13266

Hervé, M. (2020). *RVAideMemoire: Testing and Plotting Procedures for Biostatistics*. Available online at: https://cran.r-project.org/package=RVAideMemoire (accessed December 16, 2020).

Higgins, K. L., Coley, P. D., Kursar, T. A., and Arnold, A. E. (2011). Culturing and direct PCR suggest prevalent host generalism among diverse fungal endophytes of tropical forest grasses. *Mycologia* 103, 247–260. doi: 10.3852/09-158

Huang, Y. L., Bowman, E. A., Massimo, N. C., Garber, N. P., U'Ren, J. M., Sandberg, D. C., et al. (2018). Using collections data to infer biogeographic, environmental, and host structure in communities of endophytic fungi. *Mycologia* 110, 47–62. doi: 10.1080/00275514.2018.1442078

Hubbard, M., Germida, J. J., and Vujanovic, V. (2014). Fungal endophytes enhance wheat heat and drought tolerance in terms of grain yield and second-generation seed viability. *J. Appl. Microbiol.* 116, 109–122. doi: 10.1111/jam.12311

Ismail, A. M., Cirvilleri, G., Polizzi, G., Crous, P. W., Groenewald, J. Z., and Lombard, L. (2012). *Lasiodiplodia* species associated with dieback disease of mango (*Mangifera indica*) in Egypt. *Australas. Plant Pathol.* 41, 649–660. doi: 10.1007/s13313-012-0163-1

James, T. Y., Kauff, F., Schoch, C. L., Matheny, P. B., Hofstetter, V., Cox, C. J., et al. (2006). Reconstructing the early evolution of Fungi using a six-gene phylogeny. *Nature* 443, 818–822. doi: 10.1038/nature05110

Jia, X., Dini-Andreote, F., and Falcão Salles, J. (2018). Community assembly processes of the microbial rare biosphere. *Trends Microbiol.* 26, 738–747. doi: 10.1016/j.tim.2018.02.011

Kallow, S., Longin, K., Sleziak, N. F., Janssens, S. B., Vandelook, F., Dickie, J., et al. (2020). Challenges for Ex Situ conservation of wild bananas: seeds collected in papua new guinea have variable levels of desiccation tolerance. *Plants* 9:1243. doi: 10.3390/plants9091243

Kauff, F., and Lutzoni, F. (2002). Phylogeny of the Gyalectales and Ostropales (Ascomycota, Fungi): Among and within order relationships based on nuclear ribosomal RNA small and large subunits. *Mol. Phylogenet. Evol.* 25, 138–156. doi: 10.1016/S1055-7903(02)00214-2

Kauff, F., and Lutzoni, F. (2003). *Compat.py - A Program to Detect Topological Conflict Between Supported Clades in Phylogenetic Trees*. Available online at: http://lutzonilab.org/downloadable-programs/ (accessed December 16, 2020).

Kavroulakis, N., Ntougias, S., Zervakis, G. I., Ehaliotis, C., Haralampidis, K., and Papadopoulou, K. K. (2007). Role of ethylene in the protection of tomato plants against soil-borne fungal pathogens conferred by an endophytic *Fusarium solani* strain. *J. Exp. Bot.* 58, 3853–3864. doi: 10.1093/jxb/erm230

Knapp, D. G., Németh, J. B., Barry, K., Hainaut, M., Henrissat, B., Johnson, J., et al. (2018). Comparative genomics provides insights into the lifestyle and reveals functional heterogeneity of dark septate endophytic fungi. *Sci. Rep.* 8:6321. doi: 10.1038/s41598-018-24686-4

Kunert, N., Aparecido, L. M. T., Higuchi, N., dos Santos, J., and Trumbore, S. (2015). Higher tree transpiration due to road-associated edge effects in a tropical moist lowland forest. *Agric. For. Meteorol.* 213, 183–192. doi: 10.1016/j.agrformet.2015.06.009

Langhe, E. D., Vrydaghs, L., De, P., Perrier, X., and Denham, T. (2009). Why Bananas Matter: an introduction to the history of banana domestication. *Ethnobot. Res. Appl.* 7, 165–177.

Larsson, A. (2014). AliView: a fast and lightweight alignment viewer and editor for large datasets. *Bioinformatics* 30:3276. doi: 10.1093/bioinformatics/btu531

Latgé, J.-P., and Chamilos, G. (2020). *Aspergillus fumigatus* and Aspergillosis in 2019. *Clin. Microbiol. Rev.* 33:e140–18. doi: 10.1128/CMR.00140-18

Le Cocq, K., Gurr, S. J., Hirsh, P. R., and Mauchline, T. H. (2016). Exploitation of endophytes for sustainable agricultural intensification. *Mol. Plant Pathol.* 18, 469–473. doi: 10.1111/mpp.12483

Leist, N., and Krämer, S. (2011). *ISTA Working Sheets on Tetrazolium Testing, Volume II, 1st Edition (2003)*. Bassersdorf: International Seed Testing Association.

Leroy, C., Maes, A. Q. M., Louisanna, E., and Séjalon-Delmas, N. (2019). How significant are endophytic fungi in bromeliad seeds and seedlings? Effects on germination, survival and performance of two epiphytic plant species. *Fungal Ecol.* 39, 296–306. doi: 10.1016/j.funeco.2019.01.004

Li, X. Z., Song, M. L., Yao, X., Chai, Q., Simpson, W. R., Li, C. J., et al. (2017). The effect of seed-borne fungi and *Epichloë* Endophyte on seed germination and biomass of *Elymus sibiricus*. *Front. Microbiol.* 8:2488. doi: 10.3389/fmicb.2017.02488

Liu, U., Breman, E., Cossu, T. A., and Kenney, S. (2018). The conservation value of germplasm stored at the Millennium Seed Bank, Royal Botanic Gardens, Kew, UK. *Biodivers. Conserv.* 27, 1347–1386. doi: 10.1007/s10531-018-1497-y

Liu, U., Cossu, T. A., Davies, R. M., Forest, F., Dickie, J. B., and Breman, E. (2020). Conserving orthodox seeds of globally threatened plants ex situ in the Millennium Seed Bank, Royal Botanic Gardens, Kew, UK: the status of seed collections. *Biodivers. Conserv.* 29, 2901–2949. doi: 10.1007/s10531-020-02005-6

Liu, W. C., Li, C. Q., Zhu, P., Yang, J. L., and Cheng, K. D. (2010). Phylogenetic diversity of culturable fungi associated with two marine sponges: *Haliclona simulans* and *Gelliodes carnosa*, collected from the Hainan Island coastal waters of the South China Sea. *Fungal Divers.* 42, 1–15. doi: 10.1007/s13225-010-0022-8

Lombard, L., van der Merwe, N. A., Groenewald, J. Z., and Crous, P. W. (2015). Generic concepts in Nectriaceae. *Stud. Mycol.* 80, 189–245. doi: 10.1016/j.simyco.2014.12.002

Lynch, M. D. J., and Neufeld, J. D. (2015). Ecology and exploration of the rare biosphere. *Nat. Rev. Microbiol.* 13, 217–229. doi: 10.1038/nrmicro3400

Martin, G., Cardi, C., Sarah, G., Ricci, S., Jenny, C., Fondi, E., et al. (2020). Genome ancestry mosaics reveal multiple and cryptic contributors to cultivated banana. *Plant J.* 102, 1008–1025. doi: 10.1111/tpj.14683

Maryani, N., Lombard, L., Poerba, Y. S., Subandiyah, S., Crous, P. W., and Kema, G. H. J. (2019). Phylogeny and genetic diversity of the banana Fusarium wilt pathogen *Fusarium oxysporum* f. sp. *cubense* in the Indonesian centre of origin. *Stud. Mycol.* 92, 155–194. doi: 10.1016/j.simyco.2018.06.003

Mckinney, M. L., and Lockwood, J. L. (1999). Biotic homogenization: a few winners replacing many losers in the next mass extinction. *Trends Ecol. Evol.* 14, 450–453.

Mendoza, A. R., and Sikora, R. A. (2009). Biological control of *Radopholus similis* in banana by combined application of the mutualistic endophyte *Fusarium oxysporum* strain 162, the egg pathogen *Paecilomyces lilacinus* strain 251 and the antagonistic bacteria *Bacillus firmus*. *BioControl* 54, 263–272. doi: 10.1007/s10526-008-9181-x

Miller, K. E., Hopkins, K., Inward, D. J. G., and Vogler, A. P. (2016). Metabarcoding of fungal communities associated with bark beetles. *Ecol. Evol.* 6, 1590–1600. doi: 10.1002/ece3.1925

Miller, M. A., Pfeiffer, W., and Schwartz, T. (2010). "Creating the CIPRES Science Gateway for inference of large phylogenetic trees," in *Proceedings of the Gateway Computing Environments Workshop (GCE)*, (New Orleans, LA), 1–8.

Morris, E. K., Caruso, T., Buscot, F., Fischer, M., Hancock, C., Maier, T. S., et al. (2014). Choosing and using diversity indices: insights for ecological applications from the German Biodiversity Exploratories. *Ecol. Evol.* 4, 3514–3524. doi: 10.1002/ece3.1155

Murashige, T., and Skoog, F. (1962). A revised medium for rapid growth and bio assays with tobacco tissue cultures. *Physiol. Plant.* 15, 473–497. doi: 10.1111/j.1399-3054.1962.tb08052.x

Murphy, B. R., Doohan, F. M., and Hodkinson, T. R. (2019). "Prospecting crop wild relatives for beneficial endophytes," in *Endophytes for a Growing World*, eds T. Hodkinson, F. Doohan, M. Saunders, and B. Murphy (Cambridge: Cambridge University Press), 390–410. doi: 10.1017/9781108607667.019

Murphy, B. R., Hodkinson, T. R., and Doohan, F. M. (2018a). Endophytic *Cladosporium* strains from a crop wild relative increase grain yield in Barley. *Biol. Environ. Proc. R. Irish Acad.* 118, 147–156. doi: 10.3318/bioe.2018.14

Murphy, B. R., Jadwiszczak, M. J., Soldi, E., and Hodkinson, T. R. (2018b). Endophytes from the crop wild relative *Hordeum secalinum* L. improve agronomic traits in unstressed and salt-stressed barley. *Cogent Food Agric.* 4:1549195. doi: 10.1080/23311932.2018.1549195

Nelson, A., Vandegrift, R., Carroll, G. C., and Roy, B. A. (2020). Double lives: transfer of fungal endophytes from leaves to woody substrates. *PeerJ* 8:e9341. doi: 10.7717/peerj.9341

Netto, M. S. B., Assunção, I. P., Lima, G. S. A., Marques, M. W., Lima, W. G., Monteiro, J. H. A., et al. (2014). Species of *Lasiodiplodia* associated with papaya stem-end rot in Brazil. *Fungal Divers.* 67, 127–141. doi: 10.1007/s13225-014-0279-4

Nguyen, N. H., Song, Z., Bates, S. T., Branco, S., Tedersoo, L., Menke, J., et al. (2016). FUNGuild: an open annotation tool for parsing fungal community datasets by ecological guild. *Fungal Ecol.* 20, 241–248. doi: 10.1016/j.funeco.2015.06.006

Niehaus, E. M., Münsterkötter, M., Proctor, R. H., Brown, D. W., Sharon, A., Idan, Y., et al. (2016). Comparative "Omics" of the *Fusarium fujikuroi* Species Complex Highlights Differences in Genetic Potential and Metabolite Synthesis. *Genome Biol. Evol.* 8, 3574–3599. doi: 10.1093/gbe/evw259

O'Donnell, K., Al-Hatmi, A. M. S., Aoki, T., Brankovics, B., Cano-Lira, J. F., Coleman, J. J., et al. (2020). No to *Neocosmospora*: phylogenomic and practical reasons for continued inclusion of the *Fusarium solani* species complex in the genus *Fusarium*. *mSphere* 5:e810–20. doi: 10.1128/msphere.00810-20

O'Donnell, K., Kistler, H. C., Cigelnik, E., and Ploetz, R. C. (1998). Multiple evolutionary origins of the fungus causing Panama disease of banana: concordant evidence from nuclear and mitochondrial gene genealogies. *Proc. Natl. Acad. Sci. U.S.A.* 95, 2044–2049. doi: 10.1073/pnas.95.5.2044

O'Donnell, K., Rooney, A. P., Proctor, R. H., Brown, D. W., McCormick, S. P., Ward, T. J., et al. (2013). Phylogenetic analyses of RPB1 and RPB2 support a middle Cretaceous origin for a clade comprising all agriculturally and medically important fusaria. *Fungal Genet. Biol.* 52, 20–31. doi: 10.1016/j.fgb.2012.12.004

O'Donnell, K., Sutton, D. A., Rinaldi, M. G., Gueidan, C., Crous, P. W., and Geiser, D. M. (2009). Novel multilocus sequence typing scheme reveals high genetic diversity of human pathogenic members of the *Fusarium incarnatum-F. equiseti* and *F. chlamydosporum* species complexes within the United States. *J. Clin. Microbiol.* 47, 3851–3861. doi: 10.1128/JCM.01616-09

Oksanen, J., Blanchet, F. G., Friendly, M., Kindt, R., Legendre, P., McGlinn, D., et al. (2019). *vegan: Community Ecology Package*. Available online at: https://cran.r-project.org/package=vegan (accessed October 13, 2020).

Oldrup, E., Mclain-Romero, J., Padilla, A., Moya, A., Gardner, D., and Creamer, R. (2010). Localization of endophytic *Undifilum* fungi in locoweed seed and influence of environmental parameters on a locoweed *in vitro* culture system. *Botany* 88, 512–521. doi: 10.1139/B10-026

Ordonez, N., Seidl, M. F., Waalwijk, C., Drenth, A., Kilian, A., Thomma, B. P. H. J., et al. (2015). Worse comes to worst: bananas and panama disease—when plant and pathogen clones meet. *PLoS Pathog.* 11:e1005197. doi: 10.1371/journal.ppat.1005197

Parmar, S., Li, Q., Wu, Y., Li, X., Yan, J., Sharma, V. K., et al. (2018). Endophytic fungal community of *Dysphania ambrosioides* from two heavy metal-contaminated sites: evaluated by culture-dependent and culture-independent approaches. *Microb. Biotechnol.* 11, 1170–1183. doi: 10.1111/1751-7915.13308

Parra-Sanchez, E., and Banks-Leite, C. (2020). The magnitude and extent of edge effects on vascular epiphytes across the Brazilian Atlantic Forest. *Sci. Rep.* 10:18847. doi: 10.1038/s41598-020-75970-1

Paulus, B. C., Kanowski, J., Gadek, P. A., and Hyde, K. D. (2006). Diversity and distribution of saprobic microfungi in leaf litter of an Australian tropical rainforest. *Mycol. Res.* 110, 1441–1454. doi: 10.1016/j.mycres.2006.09.002

Pearce, T. R., Antonelli, A., Brearley, F. Q., Couch, C., Campostrini Forzza, R., Gonçalves, S. C., et al. (2020). International collaboration between collections-based institutes for halting biodiversity loss and unlocking the useful properties of plants and fungi. *Plants People Planet* 2, 515–534. doi: 10.1002/ppp3.10149

Peres, S. (2016). Saving the gene pool for the future: seed banks as archives. *Stud. Hist. Philos. Biol. Biomed. Sci.* 55, 96–104. doi: 10.1016/j.shpsc.2015.09.002

Perrier, X., De Langhe, E., Donohue, M., Lentfer, C., Vrydaghs, L., Bakry, F., et al. (2011). Multidisciplinary perspectives on (*Musa* spp.) domestication. *Proc. Natl. Acad. Sci. U.S.A.* 108, 11311–11318. doi: 10.1073/pnas.1102001108

Petrini, O. (1991). "Fungal endophytes of tree leaves," in *Microbial Ecology of Leaves*, eds J. H. Andrew and S. S. Hirano (New York, NY: Springer), 179–197. doi: 10.1007/978-1-4612-3168-4_9

Philipson, M. N., and Christey, M. C. (1986). The relationship of host and endophyte during flowering, seed formation, and germination of *Lolium perenne*. *New Zeal. J. Bot.* 24, 125–134. doi: 10.1080/0028825X.1986.10409724

Poos, M. S., and Jackson, D. A. (2012). Addressing the removal of rare species in multivariate bioassessments: the impact of methodological choices. *Ecol. Indic.* 18, 82–90. doi: 10.1016/j.ecolind.2011.10.008

POWO (2019). *Plants of the World Online. Facilitated by the Royal Botanic Gardens, Kew*. Available online at: http://www.plantsoftheworldonline.org/ (accessed November 13, 2020).

Promputtha, I., Hyde, K. D., McKenzie, E. H. C., Peberdy, J. F., and Lumyong, S. (2010). Can leaf degrading enzymes provide evidence that endophytic fungi becoming saprobes? *Fungal Divers.* 41, 89–99. doi: 10.1007/s13225-010-0024-6

R Core Team (2020). *R: A Language and Environment for Statistical Computing*. Vienna: R Foundation for Statistical Computing.

Raghavendra, A. K. H., Newcombe, G., Shipunov, A., Baynes, M., and Tank, D. (2013). Exclusionary interactions among diverse fungi infecting developing seeds of Centaurea stoebe. *FEMS Microbiol. Ecol.* 84, 143–153. doi: 10.1111/1574-6941.12045

Rashmi, M., Kushveer, J. S., and Sarma, V. V. (2019). A worldwide list of endophytic fungi with notes on ecology and diversity. *Mycosphere* 10, 798–1079. doi: 10.5943/mycosphere/10/1/19

Rath, M., Grolig, F., Haueisen, J., and Imhof, S. (2014). Combining microtomy and confocal laser scanning microscopy for structural analyses of plant-fungus associations. *Mycorrhiza* 24, 293–300. doi: 10.1007/s00572-013-0530-y

Redman, R. S., Sheehan, K. B., Stout, R. G., Rodriguez, R. J., and Henson, J. M. (2002). Thermotolerance generated by plant/fungal symbiosis. *Science (80-.)* 298:1581. doi: 10.1126/science.1078055

Rezki, S., Campion, C., Iacomi-Vasilescu, B., Preveaux, A., Toualbia, Y., Bonneau, S., et al. (2016). Differences in stability of seed-associated microbial assemblages in response to invasion by phytopathogenic microorganisms. *PeerJ* 4:e1923. doi: 10.7717/peerj.1923

Ribeiro, T. H. C., Fernandes-Brum, C. N., de Souza, C. R., Dias, F. A. N., Almeida-Junior, O., de Regina, M., et al. (2020). Transcriptome analyses suggest that changes in fungal endophyte lifestyle could be involved in grapevine bud necrosis. *Sci. Rep.* 10:9514. doi: 10.1038/s41598-020-66500-0

Rodriguez, R. J., White, J. F. Jr., Arnold, A. E., and Redman, R. S. (2009). Fungal endophytes: diversity and functional roles. *New Phytol.* 182, 314–330. doi: 10.1111/j.1469-8137.2009.02773.x

Rodríguez-Gálvez, E., Guerrero, P., Barradas, C., Crous, P. W., and Alves, A. (2017). Phylogeny and pathogenicity of *Lasiodiplodia species* associated with dieback of mango in Peru. *Fungal Biol.* 121, 452–465. doi: 10.1016/j.funbio.2016.06.004

Rosado, A. W. C., Machado, A. R., Freire, F. D. C. O., and Pereira, O. L. (2016). Phylogeny, identification, and pathogenicity of *Lasiodiplodia* associated with postharvest stem-end rot of coconut in Brazil. *Plant Dis.* 100, 561–568. doi: 10.1094/PDIS-03-15-0242-RE

Rouard, M., Droc, G., Martin, G., Sardos, J., Hueber, Y., Guignon, V., et al. (2018). Three new genome assemblies support a rapid radiation in *Musa acuminata* (Wild Banana). *Genome Biol. Evol.* 10, 3129–3140. doi: 10.1093/gbe/evy227

RStudio Team (2015). *RStudio: Integrated Development for R*. Available online at: http://www.rstudio.com/ (accessed July 5, 2019).

Ruas, M., Guignon, V., Sempere, G., Sardos, J., Hueber, Y., Duvergey, H., et al. (2017). MGIS: managing banana (*Musa* spp.) genetic resources information

and high-throughput genotyping data. *Database* 2017:bax046. doi: 10.1093/database/bax046

Rubini, M. R., Silva-Ribeiro, R. T., Pomella, A. W. V., Maki, C. S., Araújo, W. L., Dos Santos, D. R., et al. (2005). Diversity of endophytic fungal community of cacao (*Theobroma cacao* L.) and biological control of *Crinipellis perniciosa*, causal agent of Witches' Broom Disease. *Int. J. Biol. Sci.* 1, 24–33. doi: 10.7150/ijbs.1.24

Ruete, A., Snäll, T., and Jönsson, M. (2016). Dynamic anthropogenic edge effects on the distribution and diversity of fungi in fragmented old-growth forests. *Ecol. Appl.* 26, 1475–1485. doi: 10.1890/15-1271

Salvatore, M. M., and Andolfi, A. (2020). The thin line between pathogenicity and endophytism: the case of *Lasiodiplodia theobromae*. *Agriculture* 10:488. doi: 10.3390/agriculture10100488

Sandoval-Denis, M., Lombard, L., and Crous, P. W. (2019). Back to the roots: a reappraisal of *Neocosmospora*. *Persoonia* 43, 90–185. doi: 10.3767/persoonia.2019.43.04

Sangeetha, G., Anandan, A., and Rani, S. U. (2012). Morphological and molecular characterisation of *Lasiodiplodia theobromae* from various banana cultivars causing crown rot disease in fruits. *Arch. Phytopathol. Plant Prot.* 45, 475–486. doi: 10.1080/03235408.2011.587986

Sarmiento, C., Zalamea, P.-C., Dalling, J. W., Davis, A. S., Stump, S. M., U'Ren, J. M., et al. (2017). Soilborne fungi have host affinity and host-specific effects on seed germination and survival in a lowland tropical forest. *Proc. Natl. Acad. Sci.* 114, 11458–11463. doi: 10.1073/pnas.1706324114

Schulz, B., and Boyle, C. (2005). The endophytic continuum. *Mycol. Res.* 109, 661–686. doi: 10.1017/S095375620500273X

Shaffer, J. P., Zalamea, P. C., Sarmiento, C., Gallery, R. E., Dalling, J. W., Davis, A. S., et al. (2018). Context-dependent and variable effects of endohyphal bacteria on interactions between fungi and seeds. *Fungal Ecol.* 36, 117–127. doi: 10.1016/j.funeco.2018.08.008

Shearin, Z. R. C., Filipek, M., Desai, R., Bickford, W. A., Kowalski, K. P., and Clay, K. (2018). Fungal endophytes from seeds of invasive, non-native *Phragmites australis* and their potential role in germination and seedling growth. *Plant Soil* 422, 183–194. doi: 10.1007/s11104-017-3241-x

Sikora, R. A., Pocasangre, L., Felde, A. Z., Niere, B., Vu, T. T., and Dababat, A. A. (2008). Mutualistic endophytic fungi and *in-planta* suppressiveness to plant parasitic nematodes. *Biol. Control* 46, 15–23. doi: 10.1016/j.biocontrol.2008.02.011

Skole, D., and Tucker, C. (1993). Tropical deforestation and habitat fragmentation in the amazon: satellite data from 1978 to 1988. *Science (80-.)* 260, 1905–1910. doi: 10.1126/science.260.5116.1905

Slippers, B., and Wingfield, M. J. (2007). Botryosphaeriaceae as endophytes and latent pathogens of woody plants: diversity, ecology and impact. *Fungal Biol. Rev.* 21, 90–106. doi: 10.1016/j.fbr.2007.06.002

Stamatakis, A. (2014). RAxML version 8: a tool for phylogenetic analysis and post-analysis of large phylogenies. *Bioinformatics* 30:1312. doi: 10.1093/bioinformatics/btu033

Stone, J. K., Bacon, C. W., and White, J. J. F. (2000). "An overview of endophytic microbes: endophytism defined," in *Microbial Endophytes*, eds C. W. Bacon and J. J. F. White (New York, NY: Marcel Dekker), 3–29. doi: 10.1163/_q3_SIM_00374

Subrmaniyan, R., Ponnambalam, S., and Thirunavukarassu, T. (2018). Inter species variations in cultivable endophytic fungal diversity among the tropical seagrasses. *Proc. Natl. Acad. Sci. India Sect. B - Biol. Sci.* 88, 849–857. doi: 10.1007/s40011-016-0817-9

Summerell, B. A. (2019). Resolving *Fusarium*: current status of the genus. *Annu. Rev. Phytopathol.* 57, 323–339. doi: 10.1146/annurev-phyto-082718-100204

Tamura, R., Hashidoko, Y., Ogita, N., Limin, S. H., and Tahara, S. (2008). Requirement for particular seed-borne fungi for seed germination and seedling growth of *Xyris complanata*, a pioneer monocot in topsoil-lost tropical peatland in Central Kalimantan, Indonesia. *Ecol. Res.* 23, 573–579. doi: 10.1007/s11284-007-0411-y

Tisthammer, K. H., Cobian, G. M., and Amend, A. S. (2016). Global biogeography of marine fungi is shaped by the environment. *Fungal Ecol.* 19, 39–46. doi: 10.1016/j.funeco.2015.09.003

Uranga, C. C., Beld, J., Mrse, A., Córdova-Guerrero, I., Burkart, M. D., and Hernández-Martínez, R. (2016). Fatty acid esters produced by *Lasiodiplodia theobromae* function as growth regulators in tobacco seedlings. *Biochem. Biophys. Res. Commun.* 472, 339–345. doi: 10.1016/j.bbrc.2016.02.104

U'Ren, J. M., and Arnold, A. E. (2016). Diversity, taxonomic composition, and functional aspects of fungal communities in living, senesced, and fallen leaves at five sites across North America. *PeerJ* 4:e2768. doi: 10.7717/peerj.2768

U'Ren, J. M., Dalling, J. W., Gallery, R. E., Maddison, D. R., Davis, E. C., Gibson, C. M., et al. (2009). Diversity and evolutionary origins of fungi associated with seeds of a neotropical pioneer tree: a case study for analysing fungal environmental samples. *Mycol. Res.* 113, 432–449. doi: 10.1016/j.mycres.2008.11.015

U'Ren, J. M., Lutzoni, F., Miadlikowska, J., and Arnold, A. E. (2010). Community analysis reveals close affinities between endophytic and endolichenic fungi in mosses and lichens. *Microb. Ecol.* 60, 340–353. doi: 10.1007/s00248-010-9698-2

U'Ren, J. M., Lutzoni, F., Miadlikowska, J., Zimmerman, N. B., Carbone, I., May, G., et al. (2019). Host availability drives distributions of fungal endophytes in the imperilled boreal realm. *Nat. Ecol. Evol.* 3, 1430–1437. doi: 10.1038/s41559-019-0975-2

Vági, P., Knapp, D. G., Kósa, A., Seress, D., Horváth, ÁN., and Kovács, G. M. (2014). Simultaneous specific in planta visualization of root-colonizing fungi using fluorescence in situ hybridization (FISH). *Mycorrhiza* 24, 259–266. doi: 10.1007/s00572-013-0533-8

Vaidya, G., Lohman, D. J., and Meier, R. (2011). SequenceMatrix: concatenation software for the fast assembly of multi-gene datasets with character set and codon information. *Cladistics* 27, 171–180. doi: 10.1111/j.1096-0031.2010.00329.x

Van Hove, F., Waalwijk, C., Logrieco, A., Munaut, F., and Moretti, A. (2011). *Gibberella musae* (*Fusarium musae*) sp. nov., a recently discovered species from banana is sister to *F. verticillioides*. *Mycologia* 103, 570–585. doi: 10.3852/10-038

Vaz, A. B. M., Fonseca, P. L. C., Badotti, F., Skaltsas, D., Tomé, L. M. R., Silva, A. C., et al. (2018). A multiscale study of fungal endophyte communities of the foliar endosphere of native rubber trees in Eastern Amazon. *Sci. Rep.* 8:16151. doi: 10.1038/s41598-018-34619-w

Vega, F. E. (2018). The use of fungal entomopathogens as endophytes in biological control: a review. *Mycologia* 110, 4–30. doi: 10.1080/00275514.2017.1418578

Vilgalys, R., and Sun, B. L. (1994). Ancient and recent patterns of geographic speciation in the oyster mushroom *Pleurotus* revealed by *phylogenetic* analysis of ribosomal DNA sequences. *Proc. Natl. Acad. Sci. U.S.A.* 91, 4599–4603.

Vu, D., Groenewald, M., de Vries, M., Gehrmann, T., Stielow, B., Eberhardt, U., et al. (2019). Large-scale generation and analysis of filamentous fungal DNA barcodes boosts coverage for kingdom fungi and reveals thresholds for fungal species and higher taxon delimitation. *Stud. Mycol.* 92, 135–154. doi: 10.1016/j.simyco.2018.05.001

Waller, F., Achatz, B., Baltruschat, H., Fodor, J., Becker, K., Fischer, M., et al. (2005). The endophytic fungus *Piriformospora indica* reprograms barley to salt-stress tolerance, disease resistance, and higher yield. *Proc. Natl. Acad. Sci. U.S.A.* 102, 13386–13391. doi: 10.1073/pnas.0504423102

Wang, M. M., Chen, Q., Diao, Y. Z., Duan, W. J., and Cai, L. (2019). *Fusarium incarnatum-equiseti* complex from China. *Persoonia* 43, 70–89. doi: 10.3767/persoonia.2019.43.03

Wang, X. J., Min, C. L., Ge, M., and Zuo, R. H. (2014). An endophytic sanguinarine-producing fungus from *Macleaya cordata*, *Fusarium proliferatum* BLH51. *Curr. Microbiol.* 68, 336–341. doi: 10.1007/s00284-013-0482-7

Wassermann, B., Cernava, T., Müller, H., Berg, C., and Berg, G. (2019). Seeds of native alpine plants host unique microbial communities embedded in cross-kingdom networks. *Microbiome* 7:108. doi: 10.1186/s40168-019-0723-5

Westengen, O. T., Jeppson, S., and Guarino, L. (2013). Global Ex-Situ crop diversity conservation and the svalbard global seed vault: assessing the current status. *PLoS One* 8:e64146. doi: 10.1371/journal.pone.0064146

Wickham, H. (2016). *ggplot2: Elegant Graphics for Data Analysis*. New York, NY: Springer International Publishing.

Yu, G., Smith, D. K., Zhu, H., Guan, Y., and Lam, T. T. Y. (2017). GGTREE: an R package for visualization and annotation of phylogenetic trees with their covariates and other associated data. *Methods Ecol. Evol.* 8, 28–36. doi: 10.1111/2041-210X.12628

Zakaria, L., and Aziz, W. N. W. (2018). Molecular identification of endophytic fungi from banana leaves (*Musa* spp.). *Trop. Life Sci. Res.* 29, 201–211. doi: 10.21315/tlsr2018.29.2.14

Zakaria, L., Izham, M., Jamil, M., and Anuar, I. S. M. (2016). Molecular characterisation of endophytic fungi from roots of wild banana (*Musa acuminata*). *Trop. Life Sci. Res.* 27, 153–162.

Zhang, N., O'Donnell, K., Sutton, D. A., Nalim, F. A., Summerbell, R. C., Padhye, A. A., et al. (2006). Members of the *Fusarium solani* species complex that cause infections in both humans and plants are common in the environment. *J. Clin. Microbiol.* 44, 2185–2190. doi: 10.1128/JCM.00120-06

Zhang, W., Card, S. D., Mace, W. J., Christensen, M. J., McGill, C. R., and Matthew, C. (2017). Defining the pathways of symbiotic *Epichloë* colonization in grass embryos with confocal microscopy. *Mycologia* 109, 153–161. doi: 10.1080/00275514.2016.1277469

Zubek, S., Błaszkowski, J., Delimat, A., and Turnau, K. (2009). Arbuscular mycorrhizal and dark septate endophyte colonization along altitudinal gradients in the tatra mountains. *Arctic Antarct. Alp. Res.* 41, 272–279. doi: 10.1657/1938-4246-41.2.272

Zuccaro, A., Lahrmann, U., Güldener, U., Langen, G., Pfiffi, S., Biedenkopf, D., et al. (2011). Endophytic life strategies decoded by genome and transcriptome analyses of the mutualistic root symbiont *Piriformospora indica*. *PLoS Pathog.* 7:e1002290. doi: 10.1371/journal.ppat.1002290

zum Felde, A., Pocasangre, L., and Sikora, R. A. (2003). "The potential use of microbial communities inside suppressive banana plants for banana root protection," in *Banana Root System: Towards A Better Understanding for its Productive Management*, eds D. W. Turner and F. E. Rosales (San José, Costa Rica: INIBAP), 169–177.

Conflict of Interest: The authors declare that the research was conducted in the absence of any commercial or financial relationships that could be construed as a potential conflict of interest.

Copyright © 2021 Hill, Llewellyn, Downes, Oddy, MacIntosh, Kallow, Panis, Dickie and Gaya. This is an open-access article distributed under the terms of the Creative Commons Attribution License (CC BY). The use, distribution or reproduction in other forums is permitted, provided the original author(s) and the copyright owner(s) are credited and that the original publication in this journal is cited, in accordance with accepted academic practice. No use, distribution or reproduction is permitted which does not comply with these terms.

frontiers in Microbiology

ORIGINAL RESEARCH
published: 23 March 2021
doi: 10.3389/fmicb.2021.654683

Morpho-Phylo Taxonomy of Novel Dothideomycetous Fungi Associated With Dead Woody Twigs in Yunnan Province, China

Peter E. Mortimer[1,2,3], Rajesh Jeewon[4], Jian-Chu Xu[1,3,5], Saisamorn Lumyong[2,6,7] and Dhanushka N. Wanasinghe[1,3]**

[1] CAS Key Laboratory for Plant Biodiversity and Biogeography of East Asia (KLPB), Kunming Institute of Botany, Chinese Academy of Sciences, Kunming, China, [2] Department of Biology, Faculty of Science, Chiang Mai University, Chiang Mai, Thailand, [3] Honghe Center for Mountain Futures, Kunming Institute of Botany, Yunnan, China, [4] Department of Health Sciences, Faculty of Medicine and Health Sciences, University of Mauritius, Reduit, Mauritius, [5] World Agroforestry Centre, East and Central Asia, Kunming, China, [6] Faculty of Science, Research Center of Microbial Diversity and Sustainable Utilization, Chiang Mai University, Chiang Mai, Thailand, [7] Academy of Science, The Royal Society of Thailand, Bangkok, Thailand

OPEN ACCESS

Edited by:
Baokai Cui,
Beijing Forestry University, China

Reviewed by:
ZongLong Luo,
Dali University, China
Jing Si,
Beijing Forestry University, China

***Correspondence:**
Saisamorn Lumyong
scboi009@gmail.com
Dhanushka N. Wanasinghe
dnadeeshan@gmail.com

Specialty section:
This article was submitted to Evolutionary and Genomic Microbiology, a section of the journal Frontiers in Microbiology

Received: *17 January 2021*
Accepted: *25 February 2021*
Published: *23 March 2021*

Citation:
Mortimer PE, Jeewon R, Xu J-C, Lumyong S and Wanasinghe DN (2021) Morpho-Phylo Taxonomy of Novel Dothideomycetous Fungi Associated With Dead Woody Twigs in Yunnan Province, China. Front. Microbiol. 12:654683. doi: 10.3389/fmicb.2021.654683

Within the field of mycology, macrofungi have been relatively well-studied when compared to microfungi. However, the diversity and distribution of microfungi inhabiting woody material have not received the same degree of research attention, especially in relatively unexplored regions, such as Yunnan Province, China. To help address this knowledge gap, we collected and examined fungal specimens from different plants at various locations across Yunnan Province. Our investigation led to the discovery of four species that are clearly distinct from extant ones. These taxonomic novelties were recognized based on morphological comparisons coupled with phylogenetic analyses of multiple gene sequences (non-translated loci and protein-coding regions). The monotypic genus *Neoheleiosa* gen. nov. (type: *N. lincangensis*) is introduced in Monoblastiaceae (Monoblastiales) for a woody-based saprobic ascomycete that possesses globose to subglobose or obpyriform ascomata with centric or eccentric, papillate ostioles, an ascomatal wall with thin-walled cells of textura globulosa, cylindric, pedicellate asci with an ocular chamber, and 1-septate, brown, guttulate, longitudinally striated, bicellular ascospores. *Neoheleiosa* has a close phylogenetic affinity to *Heleiosa*, nevertheless, it is morphologically dissimilar by its peridium cells and ornamented ascospores. *Acrocalymma hongheense* and *A. yuxiense* are described and illustrated as new species in Acrocalymmaceae. *Acrocalymma hongheense* is introduced with sexual and asexual (coelomycetous) features. The sexual morph is characterized by globose to subglobose, ostiolate ascomata, a peridium with textura angularis cells, cylindric-clavate asci with a furcate to truncate pedicel and an ocular chamber, hyaline, fusiform, 1-septate ascospores which are surrounded by a thick, distinct sheath, and the asexual morph is featured by pycnidial conidiomata, subcylindrical, hyaline, smooth, annelledic, conidiogenous cells, hyaline, guttulate, subcylindrical, aseptate conidia with mucoid ooze at the apex and with a rounded hilum at the base. *Acrocalymma yuxiense* is phylogenetically distinct from other extant species of *Acrocalymma* and

differs from other taxa in *Acrocalymma* in having conidia with three vertical eusepta. *Magnibotryascoma kunmingense* sp. nov. is accommodated in Teichosporaceae based on its coelomycetous asexual morph which is characterized by pycnidial, globose to subglobose, papillate conidiomata, enteroblastic, annelledic, discrete, cylindrical to oblong, hyaline conidiogenous cells arising from the inner layer of pycnidium wall, subglobose, oval, guttulate, pale brown and unicelled conidia.

Keywords: Ascomycota, coelomycetes, Honghe, Kunming, Pleosporales, Yuxi

INTRODUCTION

Dothideomycetes is the largest and most ecologically diverse class of Ascomycota (Hongsanan et al., 2020a), consisting of 28,729 species (Kirk, 2019). This class comprises saprobes, human and plant pathogens, endophytes, epiphytes, lichens, lichenicolous, nematode-trapping and rock-inhabiting members (Jeewon et al., 2017, 2018; Zhang J.F. et al., 2019; Hongsanan et al., 2020a). Hyde et al. (2013) provided the first comprehensive monograph of the families in Dothideomycetes. Since then, the taxonomies of Dothideomycetes have been updated with new taxa in several journal series, e.g., *Fungal Diversity notes*, *Fungal planet description sheets*, *Mycosphere notes*, *Fungal Biodiversity Profiles*, *Fungal Systematics and Evolution*, *New and Interesting Fungi*. Wijayawardene et al. (2014) provided an outline for the proposals of protection or suppression of generic names of Dothideomycetes. Consistent with the "one fungus-one name" concept, Rossman et al. (2015) provided recommendations for the nomenclature of pleomorphic genera in the class. Attributable to the continual changes of the taxa in this class, the taxonomy of Dothideomycetes is in a perpetual transitional state (Pem et al., 2019a), and as such, the outline of this class has been frequently revised (Wijayawardene et al., 2017, 2020). Recent publications by Hongsanan et al. (2020a,b) expanded the taxonomic concepts of families in the Dothideomycetidae, Pleosporomycetidae, and orders and families incertae sedis in Dothideomycetes. Hongsanan et al. (2020a,b) have accepted 38 orders and 210 families in Dothideomycetes. In order to provide a suitable platform to bring these data together, the website https://www.dothideomycetes.org was established by Pem et al. (2019a). Liu et al. (2017) proposed divergence time estimates as additional evidence for rearranging the internal classification of this class and this has been helpful to establish new families and species (Zhang S.N. et al., 2019, Bhunjun et al., 2021). The most recent order-level multi-gene phylogeny for Dothideomycetes is provided by Maharachchikumbura et al. (2021), which also introduced another two orders *viz*. Homortomycetales and Holmiellales, bringing the total number of orders to 40 in the class.

Monoblastiaceae is the only family in Monoblastiales comprising both lichenized and non-lichenized ascomycetes. Wijayawardene et al. (2020) accepted six genera in this family. Initiated by Hyde et al. (2020); Hongsanan et al. (2020b) synonymized Eriomycetaceae under Monoblastiaceae. Accordingly, this family currently includes 11 genera (Hongsanan et al., 2020b). The majority of these fungi grow on bark in tropical forests, but the family is also commonly found in leaf-inhabiting lichen communities (Aptroot and Sipman, 1993; Lücking, 2008). These foliicolous lichens can be useful in monitoring the environmental health of tropical forest ecosystems (Hongsanan et al., 2020b).

Alcorn and Irwin (1987) introduced *Acrocalymma* to accommodate *A. medicaginis*, which was previously identified as *Stagonospora meliloti*, known for causing root and foliar rot of *Medicago sativa* in Australia. In the phylogenetic analyses of Trakunyingcharoen et al. (2014), *Acrocalymma* species (*A. aquatica*, *A. cycadis*, *A. fici*, *A. medicaginis*, and *A. vagum*) represented an undefined lineage in Dothideomycetes for which the family name Acrocalymmaceae was introduced. They also showed that *Massarina walkeri* and *A. medicaginis* are congeneric and thus introduced a new combination, *A. walkeri*. Recently, Jayasiri et al. (2019) introduced another species, *Acrocalymma pterocarpi*, to this family. Dong et al. (2020) introduced the most recent species, *Acrocalymma bipolare*, a freshwater species recovered from submerged wood in the Nile River, Egypt.

Teichosporaceae was established by Barr (2002) based on morphological similarities of *Bertiella*, *Byssothecium*, *Chaetomastia*, *Immotthia*, *Loculohypoxylon*, *Moristroma*, *Sinodidymella*, and the type genus *Teichospora*. However, *Moristroma*, *Byssothecium* and *Bertiella* were excluded from the family by Lumbsch and Huhndorf (2010). Jaklitsch et al. (2016) revised Teichosporaceae and accepted only *Teichospora* in the family. The family Floricolaceae was also synonymized under Teichosporaceae by Jaklitsch et al. (2016), and every genus within this family became a synonym of *Teichospora*. however this current taxonomic rearrangement needs to be verified with wider sampling. In addition subsequent outlines did not follow the monotypic nature of Teichosporaceae (Wijayawardene et al., 2018). Currently, Teichosporaceae contains thirteen accepted genera (Hongsanan et al., 2020a).

The present research paper introduces two new species in Acrocalymmaceae, one new genus and a new species in Monoblastiaceae and one new species in Teichosporaceae from fifteen specimens collected from Honghe, Kunming, Lincang, Qujing, and Yuxi in Yunnan Province, China.

MATERIALS AND METHODS

Isolates and Specimens

Fungal materials were collected from various deciduous trees and dried woody litter in Yunnan Province, China during the

dry season. Collected samples were brought to the laboratory in Zip lock plastic bags. Samples were examined with an Olympus SZ61 Series microscope. Single ascospore isolation was carried out following the method described in Senanayake et al. (2020). Germinated spores were individually transferred to potato dextrose agar (PDA) plates and grown at 20°C in daylight. The living cultures were deposited at the Kunming Institute of Botany Culture Collection (KUMCC), Kunming, China, and duplicated at the China General Microbiological Culture Collection Center (CGMCC). Dry herbarium materials have been stored in the herbarium of Cryptogams Kunming Institute of Botany, Academia Sinica (KUN-HKAS). MycoBank numbers have been registered as outlined in MycoBank[1].

Morphological Observations

In hand sections of the ascomata/conidiomata, which were mounted in distilled water, the following characteristics were evaluated: ascomata/conidiomata diameter, height, color, and shape; width of peridium; and height and diameter of ostioles. Length and width (at the widest point) of asci, ascospores, conidiophores and conidia were also measured. Images were captured with a Canon EOS 600D digital camera fitted to a Nikon ECLIPSE Ni compound microscope. Measurements were made with the Tarosoft (R) Image Frame Work program, and images used for figures were processed with Adobe Photoshop CS5 Extended version 10.0 software (Adobe Systems, United States).

DNA Extraction, PCR Amplifications, and Sequencing

Genomic DNA was extracted from the axenic mycelium as described by Phookamsak et al. (2017). When the spores failed to germinate in culture, DNA was extracted directly from the fruiting bodies of the fungus as outlined by Wanasinghe et al. (2018b). DNA to be used as templates for Polymerase chain reaction (PCR) were stored at 4°C for use in regular work and duplicated at -20°C for long-term storage.

The primers and PCR protocols for each gene were conducted by following Thiyagaraja et al. (2020a) and Wanasinghe et al. (2020). PCR was carried out at a volume of 25 μl, which contained 12.5 μl of 2× Power Taq PCR MasterMix (Bioteke Co., China), 1 μl of each primer (10 μM), 1 μl genomic DNA and 9.5 μl deionized water. The amplified PCR fragments were sent to a commercial sequencing provider (BGI, Ltd., Shenzhen, China). The nucleotide sequence data acquired were deposited in GenBank (**Table 1**).

Molecular Phylogenetic Analyses

Sequencing and Sequence Alignment

Sequences generated from different primers were analyzed along with sequences retrieved from GenBank (**Tables 1**–**3**). Sequences with high similarity indices were determined from a BLAST search to find the closest matches with taxa in Pleosporales, and from recently published data (Thambugala et al., 2015; Jaklitsch et al., 2016; Jayasiri et al., 2019; Hongsanan et al., 2020b). The multiple alignments of all consensus sequences, as well as the reference sequences were automatically generated with MAFFT v. 7 (Kuraku et al., 2013; Katoh et al., 2019)[2], and improved manually when necessary using BioEdit v. 7.0.9.0 (Hall, 1999).

Phylogenetic Analyses

The single-locus datasets were examined for topological incongruences among loci for members of the analyses. The alignments were concatenated into a multi-locus alignment that was subjected to maximum-likelihood (ML) and Bayesian (BI) phylogenetic analyses.

The CIPRES Science Gateway platform (Miller et al., 2010) was used to perform RAxML and Bayesian analyses. ML analyses were made with RAxML-HPC2 on XSEDE v. 8.2.10 (Stamatakis, 2014) using GTR + GAMMA swap model with 1,000 bootstrap repetitions.

Evolutionary models for Bayesian analysis were selected independently for each locus using MrModeltest v. 2.3 (Nylander et al., 2008) under the Akaike Information Criterion (AIC) implemented in both PAUP v. 4.0b10 and GTR + I + G was selected as the best fit model for all three analyses. MrBayes analyses were performed setting GTR + I + G, 5 M generations, sampling every 1,000 generations, ending the run automatically when standard deviation of split frequencies dropped below 0.01 with a burn-in fraction of 0.25. ML bootstrap values equal or greater than 60% and BYPP greater than 0.95 are given above each node of every trees.

Phylograms were visualized with FigTree v1.4.0 program (Rambaut, 2014) and reorganized in Microsoft power point (2007) and Adobe Illustrator® CS5 (Version 15.0.0, Adobe®, San Jose, CA). The finalized alignments and trees were deposited in TreeBASE, submission ID: 27599[3].

RESULTS

Phylogenetic Analyses

Three analyses were performed in this study; the first is an updated phylogeny of the genera in Monoblastiaceae (**Figure 1**), whereas the remaining two datasets represent taxa in Acrocalymmaceae (**Figure 2**) and genera treated in Teichosporaceae (**Figure 3**), respectively.

Monoblastiaceae SSU, LSU, ITS, *tef*1, and mtSSU phylogeny (**Figure 1**): The alignment contained 25 isolates and the tree was rooted to *Elsinoe centrolobii* (CBS 222.50) and *E. phaseoli* (CBS 165.31). The final alignment contained a total of 4,062 characters used for the phylogenetic analyses, including alignment gaps. The RAxML analysis of the combined dataset yielded a best scoring tree with a final ML optimization likelihood value of −14276.596302. The matrix had 1,076 distinct alignment patterns, with 49.73% of undetermined characters or gaps. Parameters for the GTR + I + G model of the combined amplicons were as follows: Estimated base frequencies; *A* = 0.249541, *C* = 0.238483, *G* = 0.280978,

[1]http://www.MycoBank.org

[2]http://mafft.cbrc.jp/alignment/server/index.html

[3]http://purl.org/phylo/treebase/phylows/study/TB2:27599

TABLE 1 | Taxa used in the phylogenetic analysis of Monoblastiaceae and their corresponding GenBank numbers.

Species	Strain no.	GenBank accession no.				
		ITS	LSU	SSU	*tef*1	mtSSU
Acrocordia subglobosa	HTL940	NA	JN887392	JN887373	JN887417	GU327681
Anisomeridium cf. *willeyanum*	MPN549	NA	JN887393	NA	NA	JN887407
Anisomeridium phaeospermum	MPN539	NA	JN887394	JN887374	NA	NA
Anisomeridium sp.	MPN533	NA	JN887395	JN887375	JN887419	NA
Anisomeridium sp.	MPN540	NA	JN887397	JN887377	JN887420	JN887409
Anisomeridium sp.	MPN534	NA	JN887396	JN887376	NA	JN887408
Anisomeridium sp.	MPN542	NA	JN887398	JN887378	NA	JN887410
Anisomeridium ubianum	MPN94	NA	GU327709	JN887379	NA	GU327682
Elsinoe centrolobii	CBS 222.50	NR_148132	KX886969	NG_062717	DQ677934	NA
Elsinoe phaseoli	CBS 165.31	NR_148161	DQ678095	NG_062718	DQ677935	NA
Eriomyces heveae	MFLUCC 17-2232	NR_169673	MH109524	NA	NA	NA
Funbolia dimorpha	CPC 14170	JF951136	JF951156	JF951136	NA	NA
Funbolia dimorpha	CBS 126491	NA	NG_064276	NA	NA	NA
Heleiosa barbatula	JK 5548I	NA	GU479787	GU479753	NA	NA
Italiofungus phillyreae	CPC 35566	MT223804	MT223899	NA	NA	NA
Megalotremis verrucosa	Lucking 26316	NA	GU327718	JN887383	NA	GU327694
Myriangium hispanicum	CBS 247.33	KX887304	GU301854	GU296180	GU349055	NA
Neoheleiosa lincangensis	**HKAS 111911**	**MW424766**	**MW424781**	**MW424796**	**MW430102**	**MW422272**
Neoheleiosa lincangensis	**HKAS 111912**	**MW424765**	**MW424780**	**MW424795**	**MW430101**	**MW422273**
Neoheleiosa lincangensis	**HKAS 111913**	**MW424767**	**MW424782**	**MW424797**	**MW430103**	**MW422274**
Neoheleiosa lincangensis	**HKAS 111914**	**MW424764**	**MW424779**	**MW424794**	**MW430100**	**MW422275**
Phellinocrescentia guianensis	CBS 138913	NR_137935	NG_058119	NA	NA	NA
Pseudopassalora gouriqua	CBS 101954	NR_160207	NG_067272	NA	NA	NA
Pseudopassalora gouriqua	CPC 1811	NA	JN712565	NA	NA	NA
Trypetheliopsis kalbii	MPN243	NA	JN887406	JN887391	NA	GU327703

The newly generated sequences are indicated in bold. NA: Sequence data not available in GenBank.

TABLE 2 | Taxa used in the phylogenetic analysis of Acrocalymmaceae and their corresponding GenBank numbers.

Species	Strain no.	GenBank accession no.		
		SSU	LSU	ITS
Acrocalymma ampeli	MFLU 19-2734	MW079341	MW063211	MW063150
Acrocalymma ampeli	NCYU19-0008	MW079342	MW063212	MW063151
Acrocalymma aquaticum	MFLUCC 11-0208	JX276953	NG_042698	NR_121544
Acrocalymma fici	CBS 317.76	NA	NG_057056	NR_137953
Acrocalymma hongheense	**HKAS 111907**	**MW424792**	**MW424777**	**MW424763**
Acrocalymma hongheense	**HKAS 111908**	**MW424791**	**MW424776**	**MW424762**
Acrocalymma hongheense	**HKAS 111909**	**MW424790**	**MW424775**	**MW424761**
Acrocalymma medicaginis	MFLUCC 17-1439	MT214388	MT214433	MT214339
Acrocalymma medicaginis	MFLUCC 17-1423	MT214387	MT214432	MT214338
Acrocalymma medicaginis	CPC 24340	NA	KP170713	KP170620
Acrocalymma pterocarpi	MFLUCC 17-0926	MK347840	NG_066306	NA
Acrocalymma pterocarpi	NC13-171	NA	LC517881	LC517880
Acrocalymma vagum	CPC 24226	NA	NA	KP170636
Acrocalymma vagum	CPC 24225	NA	NA	KP170635
Acrocalymma walkeri	UTHSC DI16-195	NA	LN907338	NA
Acrocalymma yuxiense	**HKAS 111910**	**MW424793**	**MW424778**	**NA**
Ascocylindrica marina	MD6011	KT252905	KT252907	NA
Ascocylindrica marina	MF416	MK007124	MK007123	NA
Boeremia exigua	CBS 431.74	EU754084	EU754183	FJ427001

The newly generated sequences are indicated in bold. NA: Sequence data not available in GenBank.

TABLE 3 | Taxa used in the phylogenetic analysis of Teichosporaceae and their corresponding GenBank numbers.

Species	Strain no.	GenBank accession no.				
		ITS	LSU	SSU	*rpb2*	*tef1*
Asymmetrispora mariae	C134m	KU601580	KU601580	NA	NA	KU601614
Asymmetrispora mariae	C139	KU601582	KU601582	NA	NA	KU601615
Asymmetrispora mariae	C144	KU601583	KU601583	NA	NA	KU601613
Asymmetrispora mariae	C159	KU601584	KU601584	NA	NA	KU601612
Asymmetrispora mariae	CBS 124079	NA	JN851819	NA	NA	KR075166
Asymmetrispora tennesseensis	ANM 911	NA	GU385207	NA	NA	GU327769
Aurantiascoma minimum	ANM 60	NA	GU385182	NA	NA	NA
Aurantiascoma minimum	ANM 933	NA	GU385195	NA	NA	NA
Aurantiascoma minimum	GKM 169N	NA	GU385165	NA	NA	GU327768
Aurantiascoma minimum	SMH 2448	NA	GU385166	NA	NA	NA
Floricola clematidis	MFLUCC 17–2182	MT310638	MT214594	MT226706	NA	MT394651
Floricola striata	JK 5603K	NA	GU479785	GU479751	NA	NA
Floricola striata	JK 5678I	NA	GU301813	GU296149	GU371758	GU479852
Floricola viticola	IT-2178	KT305997	KT305993	KT305995	NA	NA
Magnibotryascoma acaciae	CPC 24801	KR611877	KR611898	NA	NA	NA
Magnibotryascoma kunmingense	**KUMCC 20-0254**	**MW424769**	**MW424784**	**MW424799**	**MW430112**	**MW430105**
Magnibotryascoma kunmingense	**KUMCC 20-0255**	**MW424770**	**MW424785**	**MW424800**	**MW430113**	**MW430106**
Magnibotryascoma kunmingense	**KUMCC 20-0256**	**MW424768**	**MW424783**	**MW424798**	**MW430111**	**MW430104**
Magnibotryascoma kunmingense	**KUMCC 20-0257**	**MW424771**	**MW424786**	**MW424801**	**MW430114**	**MW430107**
Magnibotryascoma kunmingense	**KUMCC 20-0259**	**MW424772**	**MW424787**	**MW424802**	**MW430115**	**MW430108**
Magnibotryascoma kunmingense	**KUMCC 20-0260**	**MW424773**	**MW424788**	**MW424803**	**MW430116**	**MW430109**
Magnibotryascoma kunmingense	**KUMCC 20-0261**	**MW424774**	**MW424789**	**MW424804**	**MW430117**	**MW430110**
Magnibotryascoma mali	MFLUCC 17-0933	MF173433	MF173429	MF173431	MF173437	MF173435
Magnibotryascoma melanommoides	MP5	KU601585	KU601585	NA	NA	KU601610
Magnibotryascoma rubriostiolatum	C158	KU601587	KU601587	NA	KU601596	KU601607
Magnibotryascoma rubriostiolatum	C158x	KU601588	KU601588	NA	KU601597	KU601608
Magnibotryascoma rubriostiolatum	TR5	KU601589	KU601589	NA	KU601598	KU601606
Magnibotryascoma rubriostiolatum	TR7	KU601590	KU601590	NA	KU601599	KU601609
Magnibotryascoma sp.	MFLUCC 12-0088	NA	KF531927	KF531928	NA	NA
Magnibotryascoma uniseriatum	ANM 909	NA	GU385206	NA	NA	NA
Misturatosphaeria aurantonotata	ATCC 42522	NA	U43479	U43461	AY485625	NA
Misturatosphaeria aurantonotata	GKM 1238	NA	GU385173	NA	NA	GU327761
Misturatosphaeria aurantonotata	GKM 1280	NA	GU385174	NA	NA	GU327762
Misturatosphaeria aurantonotata	SMH 4330	NA	GU385167	NA	NA	GU327770
Misturatosphaeria sp.	SMH 3747	NA	GU385196	NA	NA	NA
Paulkirkia arundinis	MFLUCC 12-0328	NA	KU848206	NA	NA	NA
Pseudoaurantiascoma kenyense	GKM 1195	NA	GU385194	NA	NA	GU327767
Pseudoaurantiascoma kenyense	GKM 234N	NA	GU385188	NA	NA	GU327765
Pseudoaurantiascoma kenyense	GKM L100Na	NA	GU385189	NA	NA	GU327766
Ramusculicola clematidis	MFLUCC 17-2146	MT310640	MT214596	MT226707	MT394707	MT394652
Ramusculicola thailandica	MFLUCC 10-0126	KP899138	KP888644	KP899130	NA	KR075170
Ramusculicola thailandica	MFLUCC 13-0284	KP899141	KP888647	KP899131	NA	KR075167
Teichospora auroafricana	CBS 119330	EU552115	EU552115	NA	NA	NA
Teichospora auroafricana	CBS 122674	MH863228	MH874755	NA	NA	NA
Teichospora claviformis	GKM 1210	NA	GU385212	NA	NA	GU327763
Teichospora grandicipis	CPC 1852	JN712456	JN712520	NA	NA	NA
Teichospora grandicipis	CPC 1853	JN712457	JN712521	NA	NA	NA
Teichospora kingiae	CPC 29104	KY173468	KY173557	NA	NA	NA
Teichospora mariae	C136	KU601581	KU601581	NA	KU601595	KU601611
Teichospora nephelii	CPC 27539	KY173469	KY173558	NA	NA	NA

(Continued)

TABLE 3 | Continued

Species	Strain no.	GenBank accession no.				
		ITS	LSU	SSU	*rpb2*	*tef1*
Teichospora proteae	CBS 122675	NA	EU552117	NA	NA	NA
Teichospora pusilla	C140	KU601586	KU601586	NA	NA	KU601605
Teichospora quercus	CBS 143396	MH107920	MH107966	NA	MH108010	MH108030
Teichospora trabicola	C134	KU601591	KU601591	NA	KU601600	KU601601
Teichospora trabicola	C141	KU601592	KU601592	NA	NA	KU601603
Teichospora trabicola	C160	KU601594	KU601594	NA	NA	KU601602
Torula chromolaenae	MFLUCC 17-1514	MT214383	MT214477	MT214428	MT235831	MT235792
Torula chromolaenae	MFLUCC 17-1504	MT214384	MT214478	MT214429	MT235832	MT235793

The newly generated sequences are indicated in bold. NA: Sequence data not available in GenBank.

T = 0.230998; substitution rates AC = 0.975103, AG = 2.399794, AT = 1.850660, CG = 1.423793, CT = 6.985604, GT = 1.000; proportion of invariable sites I = 0.411774; gamma distribution shape parameter α = 0.563137. The Bayesian analysis ran 125,000 generations before the average standard deviation for split frequencies reached below 0.01 (0.008726). The analysis generated 1,251 trees (saved every 100 generations) from which 939 were sampled after 25% of the trees were discarded as burn-in. The alignment contained a total of 1,077 unique site patterns.

Acrocalymmaceae SSU, LSU, and ITS phylogeny (**Figure 2**): The alignment contained 22 isolates and the tree was rooted to *Boeremia exigua* (CBS 431.74). The final alignment contained a total of 2,317 characters used for the phylogenetic analyses, including alignment gaps. The RAxML analysis of the combined dataset yielded a best scoring tree with a final ML optimization likelihood value of −5083.5038. The matrix had 265 distinct alignment patterns, with 31.12% of undetermined characters or gaps. Parameters for the GTR + I + G model of the combined amplicons were as follows: Estimated base frequencies; A = 0.250179, C = 0.212903, G = 0.27372, T = 0.263198; substitution rates AC = 2.467522, AG = 3.254238, AT = 3.774672, CG = 0.816185, CT = 11.170637, GT = 1.000; proportion of invariable sites I = 0.737361; gamma distribution shape parameter α = 0.95506. The Bayesian analysis ran 420,000 generations before the average standard deviation for split frequencies reached below 0.01 (0.009821). The analysis generated 4,201 trees (saved every 100 generations) from which 3,151 were sampled after 25% of the trees were discarded as burn-in. The alignment contained a total of 266 unique site patterns.

Teichosporaceae SSU, LSU, ITS, *tef*1, and *rpb*2 phylogeny (**Figure 3**): The alignment contained 58 isolates and the tree was rooted to *Torula chromolaenae* (MFLUCC 17-1504 and MFLUCC 17-1514). The final alignment contained a total of 4,474 characters used for the phylogenetic analyses, including alignment gaps. The RAxML analysis of the combined dataset yielded a best scoring tree with a final ML optimization likelihood value of −16749.008095. The matrix had 1,159 distinct alignment patterns, with 47.5% of undetermined characters or gaps. Parameters for the GTR + I + G model of the combined amplicons were as follows: Estimated base frequencies; A = 0.242588, C = 0.25624, G = 0.278572, T = 0.222599; substitution rates AC = 1.47144, AG = 3.993923, AT = 1.82804, CG = 1.343882, CT = 11.37556, GT = 1.000; proportion of invariable sites I = 0.495477; gamma distribution shape parameter α = 0.4815. The Bayesian analysis ran 390,000 generations before the average standard deviation for split frequencies reached below 0.01 (0.009894). The analysis generated 3,901 trees (saved every 100 generations) from which 2,926 were sampled after 25% of the trees were discarded as burn-in. The alignment contained a total of 1,162 unique site patterns.

The phylogenetic results obtained for each dataset are discussed where applicable in the descriptive notes below.

TAXONOMY

In the present study, one new genus and four new species were found. These taxa are subsequently described in the orders Monoblastiales and Pleosporales below.

Monoblastiaceae Walt. Watson, New Phytologist 28: 106 (1929)

Notes

Hongsanan et al. (2020b) accepted 11 genera viz. *Acrocordia*, *Anisomeridium*, *Caprettia*, *Eriomyces*, *Funbolia*, *Heleiosa*, *Megalotremis*, *Monoblastia*, *Phellinocrescentia*, *Pseudopassalora*, and *Trypetheliopsis* in Monoblastiaceae. Meanwhile, Crous et al. (2020) added *Italiofungus* to accommodate *Italiofungus phillyreae*, which was collected on leaves of *Phillyrea latifolia* from Italy. In this study, we add another genus, *Neoheleiosa* gen. nov. to Monoblastiaceae based on multi-gene phylogenetic evidences.

***Neoheleiosa* Mortimer gen. nov.**
MycoBank: MB838517
Etymology: The generic epithet reflects the similarity to *Heleiosa*.

Saprobic on dead wood. **Sexual morph:** *Ascomata*, solitary, scattered, immersed to erumpent, globose to subglobose or obpyriform, dark brown to black, coriaceous, ostiolate. *Ostiole* centric or eccentric, papillate, black, smooth, filled with hyaline cells when mature. *Peridium* comprising blackish to dark

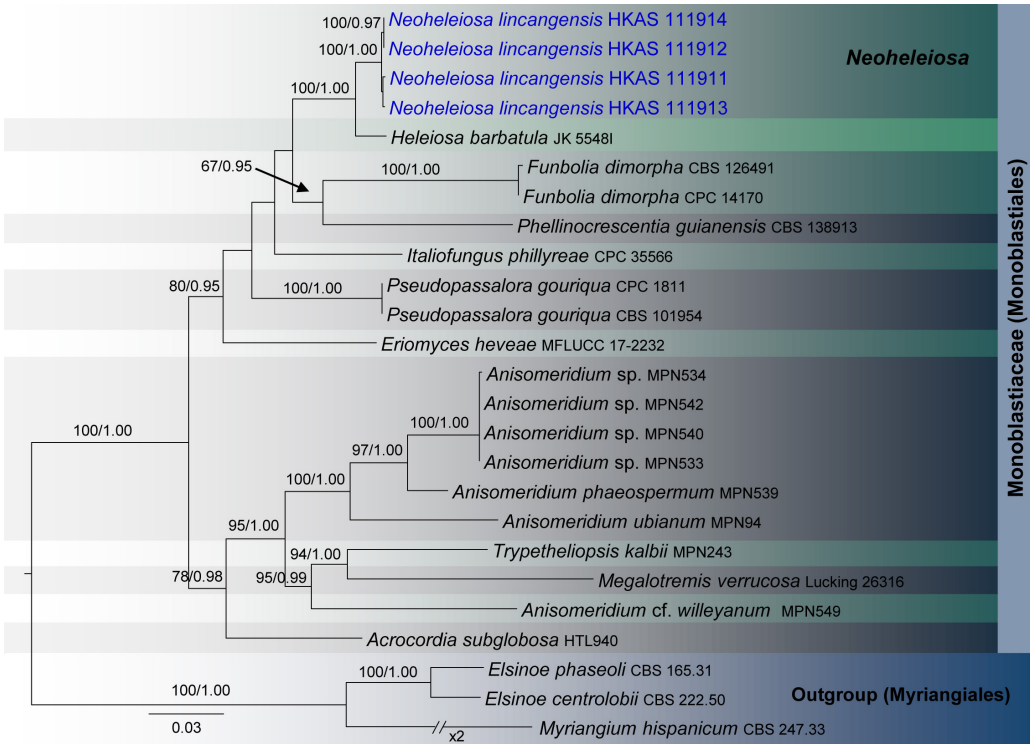


FIGURE 1 | RAxML tree based on a combined dataset of partial SSU, LSU, ITS, *tef*1, and mtSSU sequence analyses in Monoblastiaceae. Bootstrap support values for ML equal to or greater than 60%, Bayesian posterior probabilities (BYPP) equal to or greater than 0.95 are shown as ML/BI above the nodes. The new isolates are in blue. The scale bar represents the expected number of nucleotide substitutions per site.

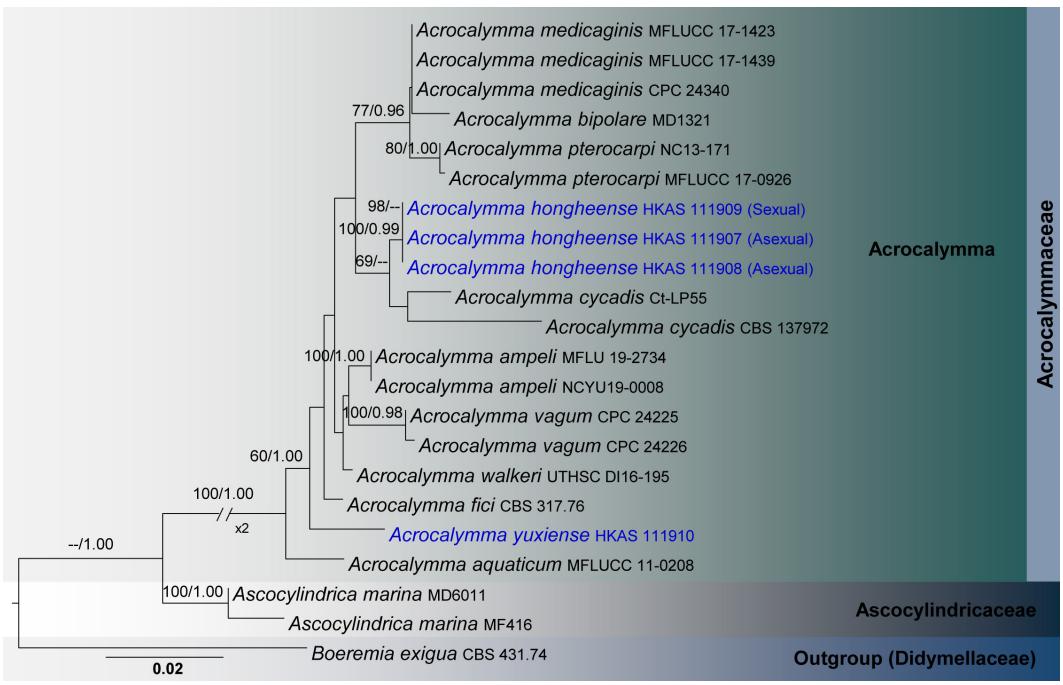


FIGURE 2 | RAxML tree based on a combined dataset of partial SSU, LSU and ITS sequence analyses in Acrocalymmaceae. Bootstrap support values for ML equal to or greater than 60%, Bayesian posterior probabilities (BYPP) equal to or greater than 0.95 are shown as ML/BI above the nodes. The new isolates are in blue. The scale bar represents the expected number of nucleotide substitutions per site.

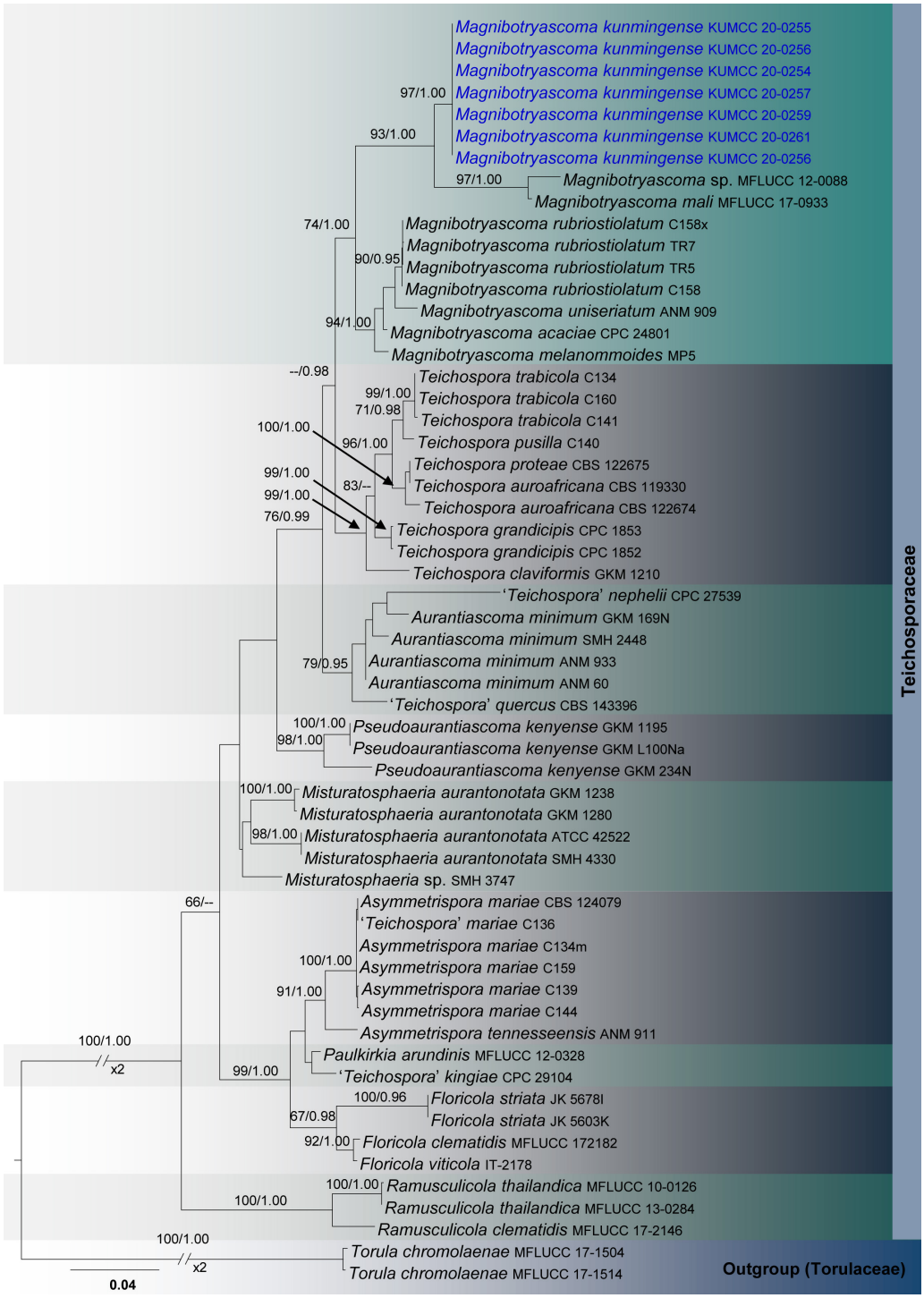


FIGURE 3 | RAxML tree based on a combined dataset of partial SSU, LSU, ITS, *tef*1, and *rpb2* sequence analyses in Teichosporaceae. Bootstrap support values for ML equal to or greater than 60%, Bayesian posterior probabilities (BYPP) equal to or greater than 0.95 are shown as ML/BI above the nodes. The new isolates are in blue. The scale bar represents the expected number of nucleotide substitutions per site.

brown, thin-walled cells of *textura globulosa*. *Hamathecium* comprising numerous, branched, septate, pseudoparaphyses. *Asci* 8-spored, bitunicate, fissitunicate, cylindric, pedicellate, rounded, and thick-walled at the apex, with an ocular chamber. *Ascospores* overlapping uniseriate, narrowly ovoid to clavate, 1-septate, initially hyaline, becoming dark brown at maturity,

with conically rounded ends, guttulate, thick walled, faintly longitudinally striated, lacking a mucilaginous sheath. **Asexual morph:** Undetermined.

Type species: *Neoheleiosa lincangensis*

***Neoheleiosa lincangensis* Mortimer sp. nov. Figure 4**.
MycoBank: MB838518
Etymology: The specific epithet reflects Lincang, from where the holotype was collected.
Holotype: HKAS 111914

Habitat terrestrial, s*aprobic* on dead twigs of *Pittosporum* sp. **Sexual morph:** *Ascomata*, 130–160 μm high, 200–250 μm diam. ($\bar{x}$ = 146 × 217 μm, *n* = 5), solitary, scattered, immersed to erumpent, globose to subglobose or obpyriform, dark brown to black, coriaceous, ostiolate. *Ostiole* 70–110 μm long, 30–50 μm diam. ($\bar{x}$ = 90 × 40 μm, *n* = 5), eccentric, papillate, black, smooth, filled with hyaline cells when mature. *Peridium* 8–12 μm thick at the base, 15–25 μm wide at sides, comprising blackish to dark brown, thin-walled cells of *textura globulosa*. *Hamathecium* 2–2.5 μm wide, comprising numerous, filamentous, branched, septate, pseudoparaphyses. *Asci* 115–135 × 10–12 μm ($\bar{x}$ = 124 × 10.6 μm, *n* = 30), 8-spored, bitunicate, fissitunicate, cylindrical, pedicel furcate, rounded and thick-walled at the apex, with an ocular chamber. *Ascospores* 16.5–17.5 × 7–9 μm ($\bar{x}$ = 17.1 × 8.2 μm, *n* = 30), overlapping uniseriate, narrowly ovoid to clavate, 1-septate, initially hyaline, becoming dark brown at maturity, with conically rounded ends, guttulate, thick walled, faintly longitudinally striated, lacking a mucilaginous sheath. **Asexual morph:** Undetermined.

Material Examined

China, Yunnan Province, Lincang, Yongde County, Bankaxiang, (N: 23.997479, E: 99.480670), on dead twigs of *Pittosporum* sp., 8 April 2019, D.N. Wanasinghe, DW0738-07 (HKAS 111914, holotype); *ibid*. DW0738-09 (HKAS 111911); DW0738-11 (HKAS 111912); DW0738-12 (HKAS 111913).

Notes

Four specimens with 1-septate, brown ascospores species were collected on dead twigs of *Pittosporum* from Bankaxiang in Yunnan Province. We made several attempts to obtain a culture via single spore isolations and direct isolation from fungal tissues (Senanayake et al., 2020). However, we were unable to get a pure culture, and DNA was extracted directly from the fruiting bodies. Sequence data of these four collections grouped in a strongly supported monophyletic clade in the concatenated SSU, LSU, ITS, *tef*1 and mtSSU sequence analyses (**Figure 1**). Morphologically all these collections were identical and there were no differences in their DNA sequence data. Thus, we recognize that all of these specimens belong to a single species, *Neoheleiosa lincangensis* sp. nov.

Acrocalymmaceae Crous and Trakun., IMA Fungus 5 (2): 404 (2014)

***Acrocalymma hongheense* Mortimer sp. nov. Figures 5**, **6**.
MycoBank: MB838519
Etymology: The specific epithet reflects Honghe, from where the holotype was collected.
Holotype: HKAS 111909

Habitat terrestrial, saprobic on dead woody litter. **Sexual morph:** *Ascomata* 180–220 μm high, 160–200 μm diam. ($\bar{x}$ = 196 × 184 μm, *n* = 5), dark brown, gregarious, immersed beneath host epidermis, visible as numerous, raised, dome-shaped areas on host surface, globose to subglobose, uni-loculate, glabrous with rough walls, coriaceous, ostiolate. *Ostioles* 50–80 μm long, 30–50 μm diam. ($\bar{x}$ = 70 × 40 μm, *n* = 5), centrally located, filled with hyaline cells. *Peridium* 25–40 μm wide, of unequal thickness, thick on sides toward the apex, composed of dark brown to black cells, arranged in *textura angularis*. *Hamathecium* composed of 1–2.5 μm wide, numerous, filamentous, branched, septate, pseudoparaphyses. *Asci* 100–140 × 15–22 μm ($\bar{x}$ = 118.9 × 18.5 μm, *n* = 30), 8-spored, bitunicate, cylindric-clavate, with a furcate to truncate pedicel, apically rounded with an ocular chamber. *Ascospores* 25–35 × 9.5–11 μm ($\bar{x}$ = 31.8 × 9.8 μm, *n* = 40), overlapping bi-seriate, hyaline, fusiform with acute ends, 1-septate, constricted at the septum, upper cell wider than lower cell, smooth-walled, surrounded by a thick, distinct sheath. **Asexual morph:** coelomycetous. *Conidiomata* 150–200 μm high, 180–220 μm diam. ($\bar{x}$ = 166 × 214 μm, *n* = 5), pycnidial, dark brown, immersed to semi-erumpent, globose, with a central ostiole. *Pycnidia wall* 10–20 μm wide, of unequal thickness, composed of dark brown to black cells, arranged in *textura angularis*. *Conidiophores* reduced to conidiogenous cells or with a single supporting cell. *Conidiogenous cells* 8–17 × 3.5–7 μm ($\bar{x}$ = 11.5 × 5.3 μm, *n* = 40), lining the inner cavity, subcylindrical, hyaline, smooth, annelledic, proliferating percurrently at apex, with prominent periclinal thickening at the apex. *Conidia* 20–35 × 7–9 μm ($\bar{x}$ = 27.3 × 7.5 μm, *n* = 40), hyaline, smooth, guttulate, solitary, subcylindrical, straight, obtusely rounded and with mucoid ooze at the apex, protuberant and with a rounded hilum at base, aseptate, guttulate, sometimes conidia becoming 1-septate.

Material Examined

China, Yunnan Province, Honghe Hani and Yi Autonomous Prefecture, Mengzi, (N: 23.185677, E: 103.413816), on woody litter, 16 March 2019, D.N. Wanasinghe, DW0375-004 (HKAS 111909, holotype); *ibid*. DW0375-005 (HKAS 111908); *ibid*. Yuxi, Yi and Dai Autonomous County, Yuanjiang Hani, (N: 23.740730, E: 103.413816), 24 May 2019, DW0636-014 (HKAS 111907).

Notes

During our investigation on the diversity of woody-based Dothideomycetes in Yunnan Province, three isolates (HKAS 111907, HKAS 111908, HKAS 111909) were recovered from decaying woody litter in Honghe and Yuxi counties. Two of them had asexual morphs while the third specimen had a sexual morph. Conidiomata, conidiophores and conidia of these asexual fungi morphologically resemble the remaining taxa in *Acrocalymma* (Alcorn and Irwin, 1987; Zhang et al., 2012; Crous et al., 2014;

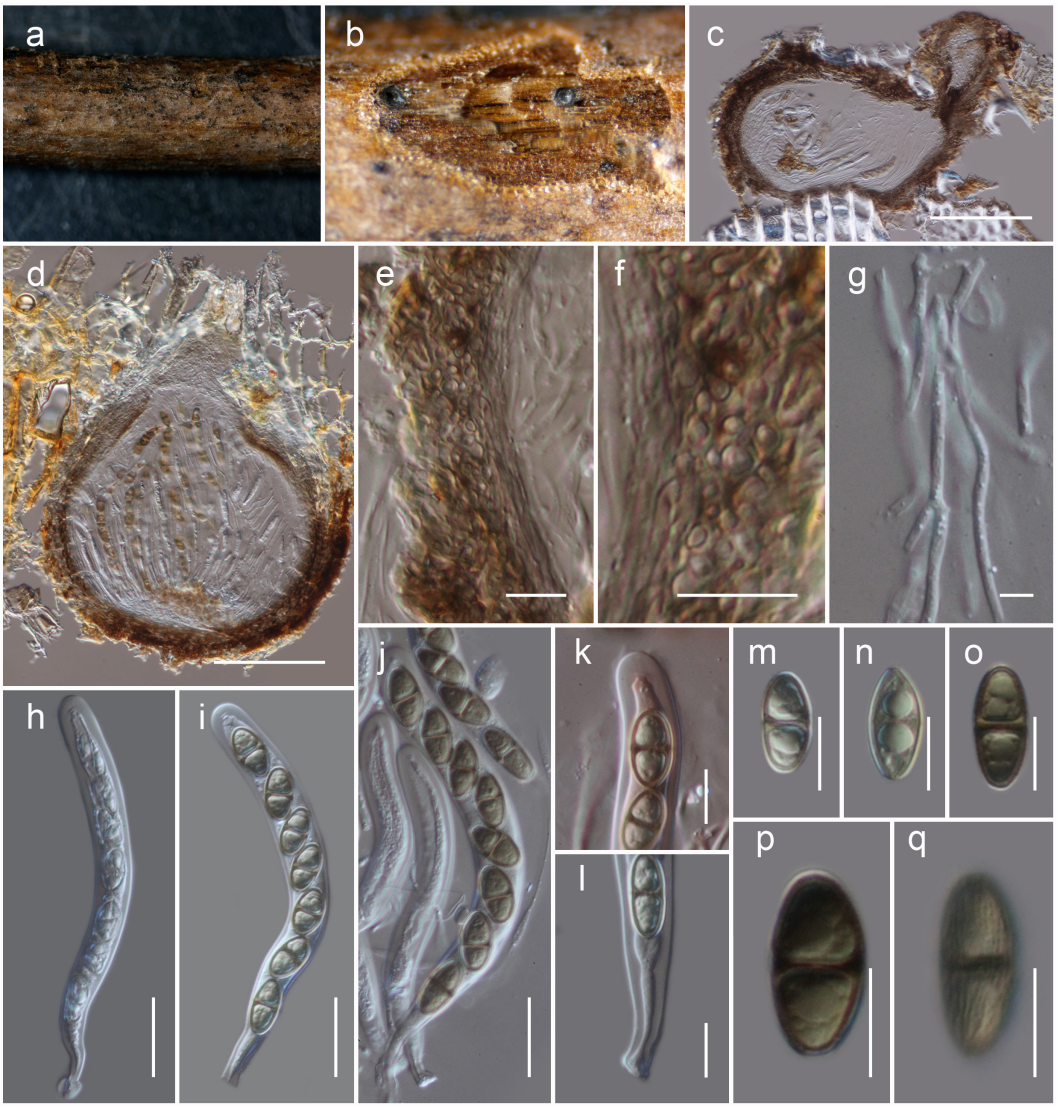


FIGURE 4 | *Neoheleiosa lincangensis* (HKAS 111914). **(a)** Ascomata observed on host substrate. **(b,d)** Horizontal sections of ascomata. **(c)** Vertical sections through an ascoma. **(e,f)** Cells of peridium. **(g)** Pseudoparaphyses. **(h–j)** Asci. **(k)** Ocular chamber. **(l)** Pedicel. **(m–q)** Ascospores (note: **q** longitudinally striated). Scale bars: **(c,d)** = 100 μm, **(e, f, k–q)** = 10 μm, **(g)** = 5 μm, **(h–j)** = 20 μm.

Trakunyingcharoen et al., 2014). The sexual morph was similar to *Acrocalymma pterocarpi*, which was the only known sexual morph in the genus, by its ascomata and asci features (Jayasiri et al., 2019). Phylogenetically, HKAS 111907, HKAS 111908, and HKAS 111909 are monophyletic with strong bootstrap supports (100% ML/0.99 BYPP, **Figure 2**). This clade has a sister relationship to *Acrocalymma cycadis* (CBS 137972 and Ct-LP55), but was not statistically supported. Within our new isolates, there were no nucleotide differences in ITS, LSU and SSU gene regions. Therefore, we recognize these three isolates belong to one species (Jeewon and Hyde, 2016), which we introduce as a new species herein.

Acrocalymma yuxiense **Mortimer sp. nov. Figure 7**.
MycoBank: MB838520

Etymology: The specific epithet reflects Yuxi, from where the holotype was collected.
Holotype: HKAS 111910

Habitat terrestrial, saprobic or weakly pathogenic on dried leaves of *Quercus* sp. **Sexual morph:** Undetermined. **Asexual morph:** coelomycetous, *Conidiomata* 130–170 μm high, 220–260 μm diam. ($\bar{x}$ = 155 × 242 μm, *n* = 5), pycnidial, dark brown, immersed to semi-erumpent, globose, with central ostiole. *Pycnidia wall* 10–30 μm wide, of unequal thickness, composed of dark brown to black cells, arranged in *textura angularis*. *Conidiophores* reduced to conidiogenous cells. *Conidiogenous cells* 4–8 × 2.5–4.5 μm ($\bar{x}$ = 6.3 × 3.4 μm, *n* = 20), lining the inner cavity, cylindrical to subcylindrical, hyaline, smooth, percurrently proliferating 1–2 times at apex, with

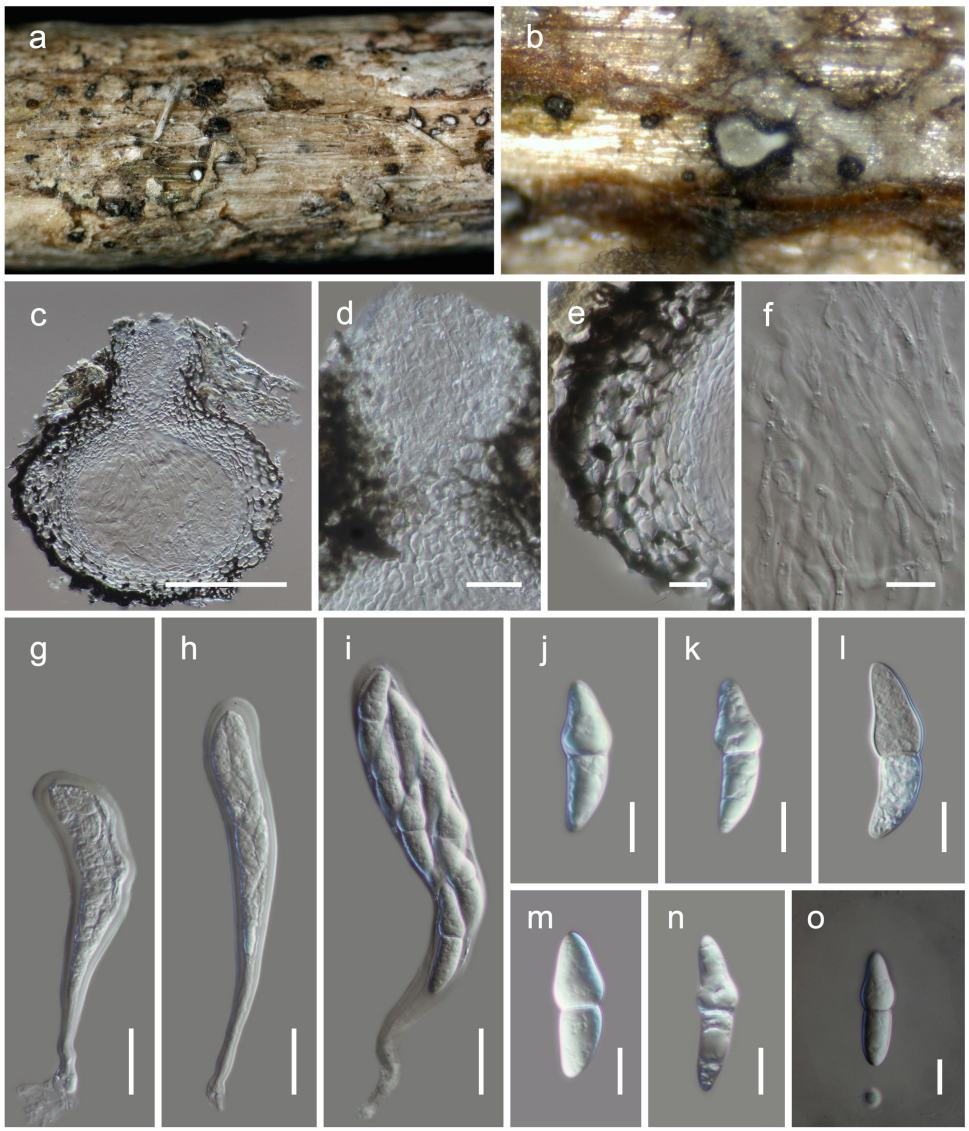


FIGURE 5 | Sexual morph of *Acrocalymma hongheense* (HKAS 111909). **(a)** Ascomata observed on host substrate. **(b)** Horizontal section of an ascoma. **(c)** Vertical sections through an ascoma. **(d)** Close up of ostiole. **(e)** Cells of peridium. **(f)** Pseudoparaphyses. **(g–i)** Asci. **(i–o)** Ascospores (note: **o** stained with Indian Ink). Scale bars: **(c)** = 50 μm, **(d,g–i)** = 20 μm, **(e,f,j–o)** = 10 μm.

prominent periclinal thickening at apex. *Conidia* 15–21 × 4–5 μm ($\bar{x}$ = 18.4 × 4.6 μm, n = 30), hyaline, smooth, guttulate, solitary, subcylindrical, straight, obtusely rounded at apex and base, 3-euseptate, guttulate, conidia sometimes 1-septate.

Material Examined

China, Yunnan Province, Yuxi (N: 24.210342, E: 102.540022), on dried leaves of *Quercus glauca*, 14 March 2019, D.N. Wanasinghe, DW0886-01 (HKAS 111910, holotype).

Notes

Acrocalymma yuxiense, collected from dried leaves of *Quercus glauca* in Yunnan, is in an independent lineage with weak support and is phylogenetically distinct from other extant species of *Acrocalymma* (**Figure 2**). This new species differs from other taxa in *Acrocalymma* in having conidia with 3 vertical eusepta while other species produce aseptate conidia.

Teichosporaceae M.E. Barr, Mycotaxon 82: 374 (2002)
***Magnibotryascoma kunmingense* Mortimer sp. nov. Figure 8**
MycoBank: MB838522
Etymology: The specific epithet reflects Kunming, from where the holotype was collected.
Holotype: HKAS 111919

Habitat terrestrial, saprobic on dead twigs. **Sexual morph:** Undetermined. **Asexual morph:** coelomycetous, *Conidiomata*

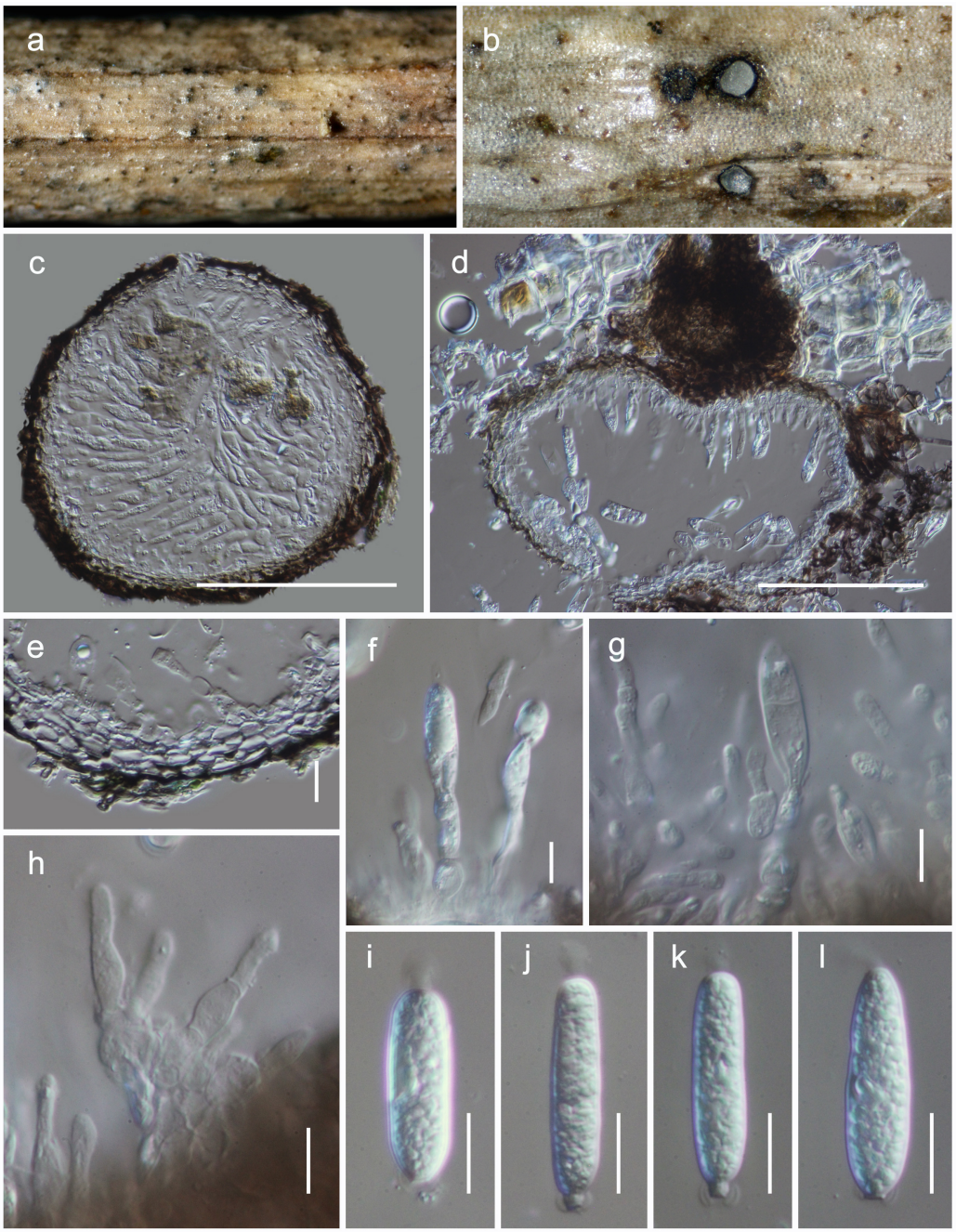


FIGURE 6 | Asexual morph of *Acrocalymma hongheense* (HKAS 111908). **(a)** Conidiomata observed on host substrate. **(b)** Horizontal section of a conidioma. **(c,d)** Vertical sections through conidiomata. **(e)** Cells of pycnidia wall. **(f–h)** Conidiogenous cells. **(i–l)** Conidia (note the mucoid mass oozing out from apex of all conidia). Scale bars: **(c,d)** = 100 μm, **(e–l)** = 10 μm.

150–180 μm high, 250–380 μm diam. ($\bar{x}$ = 161 × 323 μm, n = 5) pycnidial, solitary, aggregated, uniloculate, immersed, globose to subglobose, coriaceous, dark brown to brown, papillate, with a central ostiole. *Pycnidia wall* 20–30 μm wide, thick, 2-layered, with outer layer composed of light brown to brown cells of *textura angularis*, lined with a hyaline innermost layer bearing conidiogenous cells. *Conidiophores* reduced to conidiogenous cells. *Conidiogenous cells* 3–7 × 2–4.5 μm ($\bar{x}$ = 4.9 × 3.1 μm, n = 20), enteroblastic, annelledic, discrete, cylindrical to oblong, hyaline, arising from the inner layer of pycnidium wall. *Conidia* 3.8–5.1 × 2.5–3.4 μm ($\bar{x}$ = 4.4 × 3 μm, n = 30), subglobose, oval, guttulate, hyaline when immature, pale brown at maturity, aseptate, smooth-walled.

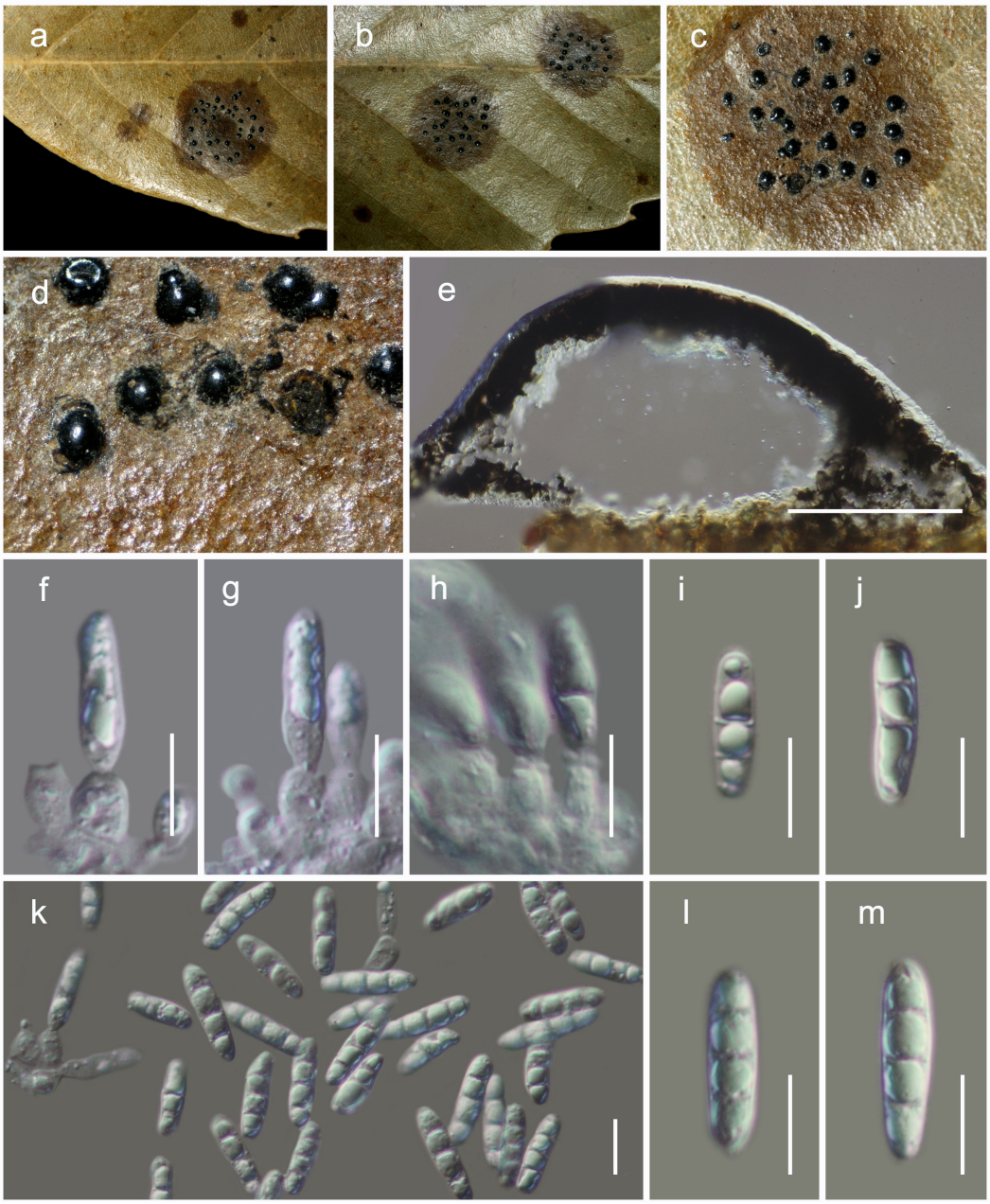


FIGURE 7 | *Acrocalymma yuxiense* (HKAS 111910). **(a)** Conidiomata observed on dried leaves of *Quercus* sp. **(e)** Vertical sections through a conidioma. **(f–h)** Conidiogenous cells. **(i–m)** Conidia. Scale bars: **(e)** = 100 μm, **(f–m)** = 10 μm.

Culture Characteristics

Colonies grew on PDA at 20°C in the dark reached 2 cm diam., within 14 days, dense, circular, slightly raised, surface smooth, entire margin, white in surface view and off-white to gray in reverse.

Material Examined

China, Yunnan Province, Kunming, Panlong District, (N: 25.139854, E: 102.737896), on dead twigs of *Machilus yunnanensis* Lecomte, 26 June 2020, D.N. Wanasinghe, DWKIB20-013B (HKAS 111919, holotype), ex-type culture (KUMCC 20-0254); *ibid*. *Acer cappadocicum* var. *sinicum* Rehd., DWKIB20-039 (HKAS 111916), culture (KUMCC 20-0255); *ibid*. DWKIB20-027 (HKAS 111921), culture (KUMCC 20-0256); *ibid*. DWKIB20-041 (HKAS 111915), culture (KUMCC 20-0257); *ibid*. Qujing, Luoping County, Changdixiang (N: 25.018503, E: 104.406763), DW1303-1 (HKAS 111917), culture (KUMCC 20-0261); *ibid*. Kunming, Xishan, (N: 25.043763, E: 102.482118), 18 July 2019, DW1287-9 (HKAS 111920), culture (KUMCC 20-0259); *ibid*. Kunming, Xishan, (N: 25.119848, E:

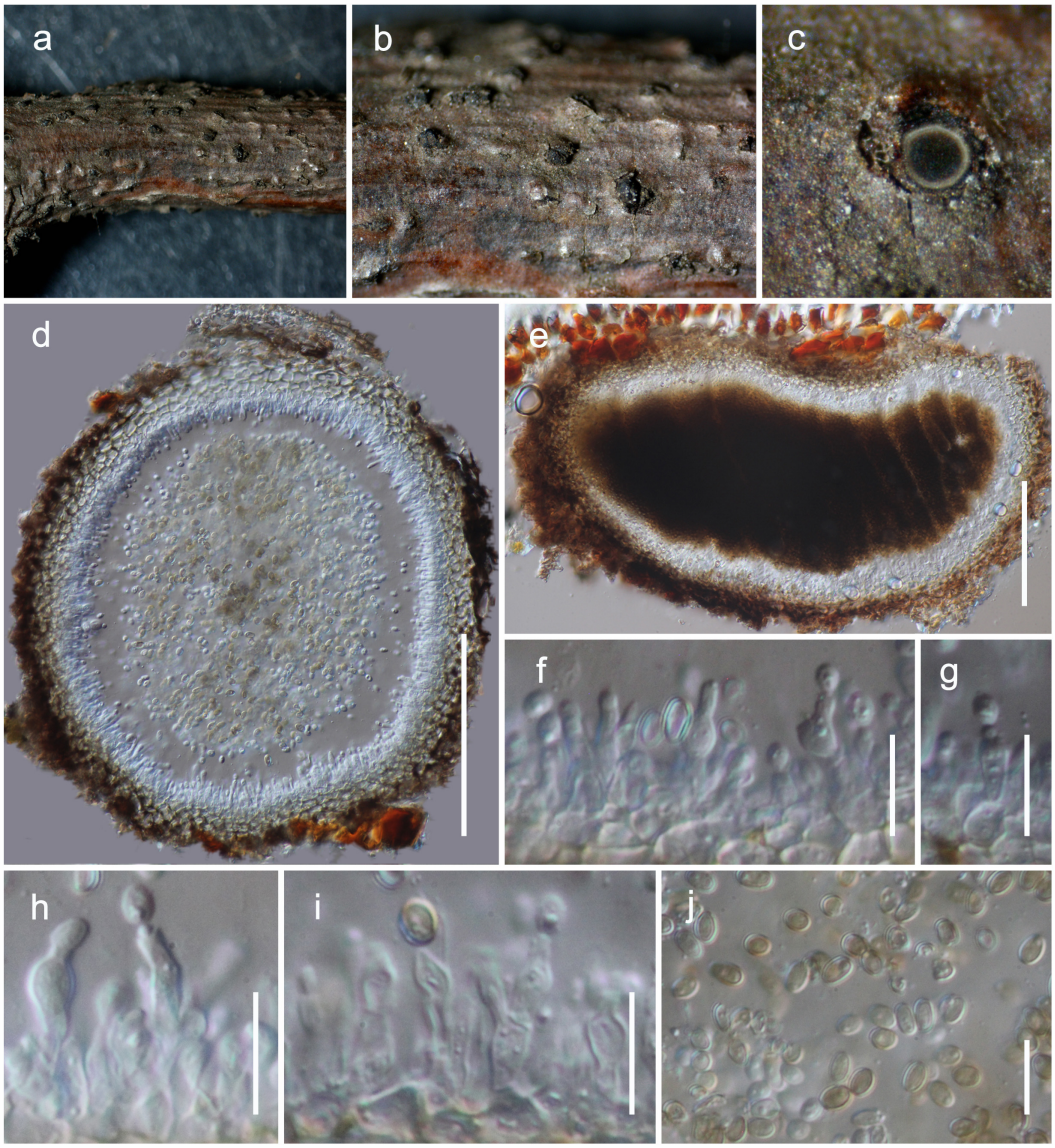


FIGURE 8 | *Magnibotryascoma kunmingense* (HKAS 111919). **(a,b)** Conidiomata observed on host **(c)** Horizontal section of a conidioma. **(e)** Vertical sections through a conidioma. **(f–i)** Conidiogenous cells. **(j)** Conidia. Scale bars: **(d,e)** = 100 μm, **(f–j)** = 10 μm.

102.546979), 19 July 2019, DW1344-5 (HKAS 111918), culture (KUMCC 20-0260).

Notes

Seven isolates of *Magnibotryascoma kunmingense* were obtained from *Acer cappadocicum* var. *sinicum*, *Machilus yunnanensis* and decaying woody litter in Kunming (Panlong and Xishan) and Qujing (Changdixiang). All these specimens were morphologically similar to *Magnibotryascoma mali* in terms of their conidial and conidiomatal characteristics. Phylogenetically, all strains of *Magnibotryascoma kunmingense* are monophyletic with 97% ML and 1.00 BI statistical support values (**Figure 3**). This clade constitutes a sister clade to *Magnibotryascoma* sp. (MFLUCC 12-0088) and *M. mali* (MFLUCC 17-0933).

DISCUSSION

The mountainous region of Yunnan Province, China is an important global biodiversity hotspot for studying the evolution of plants, animals, and fungi (Feng and Yang, 2018). The mountains of Southwest China; Eastern Himalaya-Nepal-India and Indo-Burma-India-Myanmar are included in the world's 35 biodiversity hotspots, and these three hotspot regions intersect in Yunnan Province (Myers et al., 2000; Mittermeier et al., 2005). As a result of the diverse landscape and climatic conditions within Yunnan Province, fungi in Yunnan Province have higher rates of endemism; however, they also share evolutionary connections with species from other regions of the world (Feng and Yang, 2018). Among them, wood-decaying Basidiomycota in tropical

China are well studied, and many new species have been documented (Dai et al., 2003, 2004, 2011; Cui et al., 2009; Wang et al., 2011; Yuan and Dai, 2012). This has facilitated better understanding of species diversity and the systematics of woody-based basidomycetous groups, such as Polyporales. However, woody-based microfungi such as Dothideomycetes are relatively neglected compared to the level of research conducted on Basidiomycetes (Wanasinghe et al., 2020). In the last few years, there has been increasing attention on woody-based microfungal occurrences, and more studies are reporting on the microfungal diversity, especially in Dothideomycetes, of Yunnan Province (Bao et al., 2018; Huang et al., 2018; Luo et al., 2018; Wanasinghe et al., 2018a, 2020, 2021; Rathnayaka et al., 2019; Qiao et al., 2020; Thiyagaraja et al., 2020b; Yasanthika et al., 2020).

In this study, we added taxonomic novelties in Acrocalymmaceae, Monoblastiaceae, and Teichosporaceae from Yunnan Province. To the best of our knowledge, these are the first accounts of the species in these three families from Yunnan Province. Within the broader region of China, there is one report of *Acrocalymma medicaginis* (Acrocalymmaceae) on *Trachycarpus fortunei* (Taylor and Hyde, 2003) and seven species from Teichosporaceae viz. *Magnibotryascoma mali* (on *Malus halliana*), *Sinodidymella verrucose* (on *Salsola gemmascens*), *Teichospora borealis* (on *Salix tianschanica*), *T. lonicerae* (on *Lonicera stenanthera*), *T. populi* (on *Populus* sp.), *T. solitaria* (on *Nitraria sibirica*), and *T. winteriana* (on *Hippophae rhamnoides*) currently documented (Yuan and Barr, 1995; Teng, 1996; Zhuang, 2005; Zhang et al., 2012; Hyde et al., 2017).

Neoheleiosa has a close phylogenetic affinity to *Heleiosa* with 100% ML and 1.00 BI support values (**Figure 1**). Kohlmeyer et al. (1996) introduced *Heleiosa* as a monotypic genus to accommodate *Heleiosa barbatula*, which is characterized by cylindrical asci with a short pedicel, 1-septate, ellipsoid ascospores with appendages. This fungus was found on senescent leaves of *Juncus* in salt marshes on the Atlantic coast of the United States (North Carolina, Virginia). Ascomata, asci and ascospore shapes of both genera were shown to be similar. However, the ascospores of *Neoheleiosa* do not have any appendages (**Figures 4m–q**), whereas *Heleiosa* have 10 or more short and curved hair-like subapical appendages at each end. Ascospores with a gelatinous sheath or appendages may help fungi to attach to plant substrates in aquatic or marine habitats (Shearer, 1993; Hyde and Goh, 2003; Jones, 2006; Devadatha et al., 2018; Hashimoto et al., 2018). The subapical appendages of *Heleiosa* ascospores could be an adaptation for its marine-based habitat and loss of appendaged ascospores in *Neoheleiosa* is potentially advantageous to adaptation to a non-aquatic habitat.

The surface ornamentation of spores, such as the presence of or absence of appendages, is often used in ascomycetous taxonomy to delineate species or genera (Jeewon et al., 2003; Liu et al., 2014; Phookamsak et al., 2014; Wijayawardene et al., 2016; Paz et al., 2017; Réblová et al., 2015, 2018; Pem et al., 2019b). Abbott and Currah (1997) and Villegas et al. (2005) reported spore ornamentation as a useful character in differentiating various genera within Helvellaceae and Gomphales. Jeewon et al. (2002) clearly demonstrated that species bearing appendages can form distinct phylogenetic lineages and discussed how this character can be a significant phylogenetic marker at the intergeneric level. Considering the similarities shown between our newly proposed genus and *Heleiosa*, we based our placement of these specimens in a new genus due to the lack of any appendages on the ascospores, a significant variation in morphology compared to the spores of *Heleiosa*. The ascospores of *Neoheleiosa* are ornamented with longitudinal streaks (**Figure 4q**), whereas *Heleiosa* have smooth-walled ascospores. Furthermore, the arrangement of peridium cells has been reported to be useful to demarcate different genera (Hyde et al., 2013; Tian et al., 2015; Ekanayaka et al., 2017; Paz et al., 2017; Senanayake et al., 2018). In our study, we observed that the peridium cells of *Heleiosa* are *textura angularis*, while *Neoheleiosa* have cells of *textura globulosa*. It could be possible that with wider collections in the future, species from these two genera will constitute distinct lineages that will further substantiate their generic placement, a scenario which has been reported in other studies (Huang et al., 2017; Wanasinghe et al., 2018b; Jaklitsch and Voglmayr, 2020).

Acrocalymmaceae includes a single genus with eight species viz. *Acrocalymma aquaticum*, *A. bipolare*, *A. cycadis*, *A. fici*, *A. medicaginis*, *A. pterocarpi*, *A. vagum* and *A. walker*. These are reported from terrestrial habitats, excluding *Acrocalymma aquatica* and *A. bipolare* (Zhang et al., 2012; Dong et al., 2020). The majority of these species are saprobic on various host substrates (Hongsanan et al., 2020a,b; Tennakoon et al., 2021). Only *Acrocalymma medicaginis* and *A. vagum* are reported as pathogens (Crous et al., 2014; Trakunyingcharoen et al., 2014). Moreover, *Acrocalymma medicaginis* is known as the causal agent of root and crown rot of *Medicago sativa* (Alcorn and Irwin, 1987). Even though there are only eight described species, more than 200 ITS sequences have been deposited from these species in GenBank. Endophytic strains of *Acrocalymma vagum* have the highest number of reported sequences, followed by *A. medicaginis*.

Thambugala et al. (2015) introduced *Magnabotrioscoma* to accommodate *M. uniseriata* (≡*Misturatosphaeria uniseriate*), which is morphologically distinct from the remaining genera in Floricolaceae. *Magnabotrioscoma* species have been reported as woody-based saprobes on *Clematis vitalba, Malus halliana, Ribes sanguineum*, *Robinia pseudoacacia*, *Salix* sp., and *Vaccinium myrtillus* from Belgium, China, Germany, Norway and the United Kingdom (Jaklitsch et al., 2016; Hyde et al., 2017; Phukhamsakda et al., 2020). In this study, we classified another species in this genus, *Magnibotryascoma kunmingensis*, growing on the decaying woody litter of *Acer cappadocicum* var. *sinicum* and *Machilus yunnanensis*. The sexual morph of the genus is characterized by erumpent to superficial ascomata lacking a subiculum and fusiform to elliptical and guttulate ascospores (Mugambi and Huhndorf, 2009; Thambugala et al., 2015;

Phukhamsakda et al., 2020), and the asexual morph has pycnidial conidiomata featuring aseptate and brown conidia (Crous et al., 2015; Jaklitsch et al., 2016). One interesting finding in this genus is the close connection between uncultured fungal strains (i.e., JF945459, KC978028, KX515906, LS994072) and endophytic strains (i.e., EF419935, EF419972, EF419996) with our new strains in BLAST search results. These strains are not linked to morphological details, and it is therefore difficult to provide further insights into their morpho-phylo relationships. This study reveals that there are potentially many new species awaiting discovery in this region (Hyde et al., 2018).

DATA AVAILABILITY STATEMENT

The datasets generated for this study can be found in the NCBI GenBank, MycoBank and TreeBASE.

AUTHOR CONTRIBUTIONS

PM, DW, and RJ designed the study. DW did the sample collection. PM and DW were involved in the phylogenetic analyses. SL and J-CX contributed for the research funds. All authors contributed to the writing, preparation, and submission of the manuscript.

FUNDING

The research was funded by the Key Research Project, Agroforestry Systems for Restoration and Bio-industry Technology Development (Grant No. 2017YFC0505101), Ministry of Sciences and Technology of China (Grant No. 2017YFC0505100). DW would like to thank the CAS President's International Fellowship Initiative (No. 2021FYB0005), the 64th batch of China Postdoctoral Science Foundation (Grant No. 2018M643549), and Postdoctoral Fund from the Human Resources and Social Security Bureau of Yunnan Province.

ACKNOWLEDGMENTS

Austin G. Smith at World Agroforestry (ICRAF), Kunming Institute of Botany, China, is thanked for English editing. Shaun Pennycook is thanked for nomenclatural advices. Lu Wen Hua and Li Qin Xian are thanked for their invaluable assistance. We express our sincere gratitude to D. J. Baht for his advices on fungal descriptions. PM thank Chiang Mai University for partial supported of this work. We acknowledge Kunming Institute of Botany, Chinese Academy of Sciences for providing the laboratories and instruments for molecular work. RJ thanks the University of Mauritius for support.

REFERENCES

Abbott, S. P., and Currah, R. S. (1997). The helvellaceae: systematic revision and occurrence in northern and northwestern North America. *Mycotaxon* 61, 1–125.

Alcorn, J. L., and Irwin, J. A. G. (1987). Acrocalymma medicaginis gen. et sp. nov. causing root and crown rot of *Medicago sativa* in Australia. *Trans. Brit. Mycol. Soc.* 88, 163–167. doi: 10.1016/s0007-1536(87)80211-5

Aptroot, A., and Sipman, H. J. M. (1993). Musaespora, a genus of pyrenocarpous lichens with campylidia, and other additions to the *Foliicolous lichen* flora of New Guinea. *Lichenologist* 25, 121–135. doi: 10.1017/s0024282993000192

Bao, D. F., Luo, Z. L., Jiu, J. K., Bhat, D. J., Sarunya, N., Li, W. L., et al. (2018). Lignicolous freshwater fungi in China III: three new species and a new record of Kirschsteiniothelia from northwestern yunnan province. *Mycosphere* 9, 755–768. doi: 10.5943/mycosphere/9/4/4

Barr, M. E. (2002). Teichosporaceae, another family in the *Pleosporales*. *Mycologia* 82, 373–389.

Bhunjun, C. S., Phukhamsakda, C., Jeewon, R., Promputtha, I., and Hyde, K. D. (2021). Integrating different lines of evidence to establish a novel ascomycete genus and family (Anastomitrabeculia, Anastomitrabeculiaceae) in *Pleosporales*. *J. Fungi* 7:94. doi: 10.3390/jof7020094

Crous, P. W., Schumacher, R. K., Wingfield, M. J., Lombard, L., Giraldo, A., Christensen, M., et al. (2015). Fungal systematics and evolution: FUSE 1. *Sydowia* 67, 81–118.

Crous, P. W., Shivas, R. G., Quaedvlieg, W., van der Bank, M., Zhang, Y., Summerell, B. A., et al. (2014). Fungal planet description sheets: 214–280. *Persoonia* 32, 184–306.

Crous, P. W., Wingfield, M. J., Schumacher, R. K., Akulov, A., Bulgakov, T. S., Carnegie, A. J., et al. (2020). New and interesting fungi. 3. *FUSE* 6, 157–231.

Cui, B. K., Dai, Y., and Bao, H. Y. (2009). Wood-inhabiting fungi in southern China 3. a new species of Phellinus (*Hymenochaetales*) from tropical China. *Mycotaxon* 110, 125–130. doi: 10.5248/110.125

Dai, Y. C., Cui, B. K., Yuan, H. S., He, S. H., Wei, Y. L., Qin, W. M., et al. (2011). Wood-inhabiting fungi in southern China 4. polypores from hainan province. *Ann. Bot. Fenn.* 48, 219–231. doi: 10.5735/085.048.0302

Dai, Y., Härkönen, M., and Niemelä, T. (2003). Wood-inhabiting fungi in southern China 1. polypores from hunan province. *Ann. Bot. Fenn.* 40, 381–393.

Dai, Y., Wei, Y., and Wang, Z. (2004). Wood-inhabiting fungi in southern China 2. polypores from sichuan province. *Ann. Bot. Fenn.* 41, 319–329.

Devadatha, B., Sarma, V. V., Jeewon, R., Wanasinghe, D. N., Hyde, K. D., and Jones, E. B. G. (2018). Thyridariella, a novel marine fungal genus from India: morphological characterization and phylogeny inferred from multigene DNA sequence analyses. *Mycol. Prog.* 17, 791–804. doi: 10.1007/s11557-018-1387-4

Dong, W., Wang, B., Hyde, K. D., McKenzie, E. H. C., Raja, H. A., Tanaka, K., et al. (2020). Freshwater *Dothideomycetes*. *Fungal Divers.* 105, 319–575.

Ekanayaka, A. H., Ariyawansa, H., Hyde, K., Jones, E., Daranagama, D., Phillips, A. J. L., et al. (2017). DISCOMYCETES: the apothecial representatives of the phylum ascomycota. *Fungal Divers.* 87, 237–298. doi: 10.1007/s13225-017-0389-x

Feng, B., and Yang, Z. (2018). Studies on diversity of higher fungi in Yunnan, southwestern China: a review. *Plant Divers.* 40, 165–171. doi: 10.1016/j.pld.2018.07.001

Hall, T. A. (1999). BioEdit: a user-friendly biological sequence alignment editor and analysis program for Windows 95/98/NT. *Nucl. Acid. Symp. Ser.* 41, 95–98.

Hashimoto, A., Hirayama, K., Takahashi, H., Matsumura, M., Okada, G., Chen, C. Y., et al. (2018). Resolving the *Lophiostoma bipolare* complex: generic delimitations within *Lophiostomataceae*. *Stud. Mycol.* 90, 161–189. doi: 10.1016/j.simyco.2018.03.001

Hongsanan, S., Hyde, K. D., Phookamsak, R., Wanasinghe, D. N., McKenzie, E. H. C., Sarma, V. V., et al. (2020a). Refined families of *Dothideomycetes*: dothideomycetidae and pleosporomycetidae. *Mycosphere* 11, 1553–2107. doi: 10.5943/mycosphere/11/1/13

Hongsanan, S., Hyde, K. D., Phookamsak, R., Wanasinghe, D. N., McKenzie, E. H. C., Sarma, V. V., et al. (2020b). Refined families of *Dothideomycetes*: orders and families incertae sedis. *Fungal Divers.* 105, 17–318.

Huang, S., Jeewon, R., Wanasinghe, D. N., Manawasinghe, I., Bulgakov, T. S., Hyde, K. D., et al. (2017). Phylogenetic taxonomy of Dematiopleospora fusiformis sp. nov. (*Phaeosphaeriaceae*) from Russia. *Phytotaxa* 316, 239–249. doi: 10.11646/phytotaxa.316.3.3

Huang, S., Maharachchikumbura, S. S. N., Jeewon, R., Bhat, D. J., Chomnunti, P., Hyde, K. D., et al. (2018). Morphological and molecular taxonomy of *Jahnula dianchia* sp. nov. (Jahnulales) from submerged wood in Dianchi Lake, Yunnan China. *Mycol. Prog.* 17, 547–555. doi: 10.1007/s11557-018-1390-9

Hyde, K. D., and Goh, T. K. (2003). "Adaptations for dispersal in filamentous freshwater fungi," in *Freshwater Mycology*, eds K. M. Tsui and K. D. Hyde (Hong Kong: Fungal Diversity Press), 231–258.

Hyde, K. D., Dong, Y., Phookamsak, R., Jeewon, R., Bhat, D. J., Jones, E. B. G., et al. (2020). Fungal diversity notes 1151–1276: taxonomic and phylogenetic contributions on genera and species of fungal taxa. *Fungal Divers.* 100, 5–277.

Hyde, K. D., Jones, E. B. G., Liu, J. K., Ariyawansa, H. A., Boehm, E., Boonmee, S., et al. (2013). Families of *Dothideomycetes*. *Fungal Divers.* 63, 1–313. doi: 10.1007/978-3-319-23534-9_1

Hyde, K. D., Norphanphoun, C., Abreu, V. P., Bazzicalupo, A., Chethana, T. K. W., Clericuzio, M., et al. (2017). Fungal diversity notes 603–708: taxonomic and phylogenetic notes on genera and species. *Fungal Divers.* 87, 1–235.

Hyde, K. D., Norphanphoun, C., Chen, J., Dissanayake, A. J., Doilom, M., Hongsanan, S., et al. (2018). Thailand's amazing diversity: up to 96% of fungi in northern Thailand may be novel. *Fungal Divers.* 93, 215–239. doi: 10.1007/s13225-018-0415-7

Jaklitsch, W. M., and Voglmayr, H. (2020). Fenestelloid clades of the cucurbitariaceae. *Persoonia* 44, 1–40. doi: 10.3767/persoonia.2020.44.01

Jaklitsch, W. M., Olariaga, I., and Voglmayr, H. (2016). Teichospora and the teichosporaceae. *Mycol. Prog.* 15, 1–20.

Jayasiri, S. C., Hyde, K. D., Jones, E. B. G., McKenzie, E. H. C., Jeewon, R., Phillips, A. J. L., et al. (2019). Diversity, morphology and molecular phylogeny of *Dothideomycetes* on decaying wild seed pods and fruits. *Mycosphere* 10, 1–186. doi: 10.5943/mycosphere/10/1/1

Jeewon, R., and Hyde, K. D. (2016). Establishing species boundaries and new taxa among fungi: recommendations to resolve taxonomic ambiguities. *Mycosphere* 7, 1669–1677. doi: 10.5943/mycosphere/7/11/4

Jeewon, R., Cai, L., Zhang, K., and Hyde, K. D. (2003). Dyrithiopsis lakefuxianensis gen et sp. nov. from Fuxian Lake, Yunnan, China and notes on the taxonomic confusion surrounding Dyrithium. *Mycologia* 95, 911–920. doi: 10.2307/3762019

Jeewon, R., Liew, E. C., and Hyde, K. D. (2002). Phylogenetic relationships of *Pestalotiopsis* and allied genera inferred from ribosomal DNA sequences and morphological characters. *Mol. Phylogenet. Evol.* 25, 378–392. doi: 10.1016/s1055-7903(02)00422-0

Jeewon, R., Wanasinghe, D. N., Rampadaruth, S., Puchooa, D., Zhou, L., Liu, A., et al. (2017). Nomenclatural and identification pitfalls of endophytic mycota based on DNA sequence analyses of ribosomal and protein genes phylogenetic markers: a taxonomic dead end? *Mycosphere* 8, 1802–1817. doi: 10.5943/mycosphere/8/10/7

Jeewon, R., Yeung, Q. S. Y., Wanasinghe, D. N., Rampadarath, S., Puchooa, D., and Wang, H. (2018). Hidden mycota of pine needles: molecular signatures from PCR-DGGE and Ribosomal DNA phylogenetic characterization of novel phylotypes. *Sci. Rep.* 8:18053.

Jones, E. B. G. (2006). Form and function of fungal spore appendages. *Mycoscience* 47, 167–183. doi: 10.1007/s10267-006-0295-7

Katoh, K., Rozewicki, J., and Yamada, K. D. (2019). MAFFT online service: multiple sequence alignment, interactive sequence choice and visualization. *Brief. Bioinformatics.* 20, 1160–1166. doi: 10.1093/bib/bbx108

Kirk, P. M. (2019). *Catalogue of Life*. Available online at: http://www.catalogueoflife.org (accessed January 16, 2021).

Kohlmeyer, J., Volkmann-Kohlmeyer, B., and Eriksson, O. E. (1996). Fungi on *Juncus roemerianus*. 8. New bitunicate ascomycetes. *Can. J. Bot.* 74, 1830–1840. doi: 10.1139/b96-220

Kuraku, S., Zmasek, C. M., Nishimura, O., and Katoh, K. (2013). aLeaves facilitates on-demand exploration of metazoan gene family trees on MAFFT sequence alignment server with enhanced interactivity. *Nucleic Acids Res.* 41, W22–W28.

Liu, J. K., Hyde, K. D., Jeewon, R., Phillips, A. J., Maharachchikumbura, S. S. N., Ryberg, M., et al. (2017). Ranking higher taxa using divergence times: a case study in *Dothideomycetes*. *Fungal Divers.* 84, 75–99. doi: 10.1007/s13225-017-0385-1

Liu, J. K., Phookamsak, R., Dai, D. Q., Tanaka, K., Jones, E. B. G., Xu, J. C., et al. (2014). Roussoellaceae, a new pleosporalean family to accommodate the genera *Neoroussoella gen*. nov., Roussoella and *Roussoellopsis*. *Phytotaxa* 181, 001–033.

Lücking, R. (2008). *Foliicolous Lichenized Fungi. Flora Neotropica*. New York: New York Botanical Garden Press 103, 1–867.

Lumbsch, H. T., and Huhndorf, S. M. (2010). Outline of Ascomycota 2009. *Myconet* 14, 1–64.

Luo, Z. L., Hyde, K. D., Liu, J. K., Bhat, D. J., Bao, D. F., Li, W. L., et al. (2018). Lignicolous freshwater fungi from China II: Novel Distoseptispora (*Distoseptisporaceae*) species from northwestern Yunnan Province and a suggested unified method for studying lignicolous freshwater fungi. *Mycosphere* 9, 444–461. doi: 10.5943/mycosphere/9/3/2

Maharachchikumbura, S. S. N., Wanasinghe, D. N., Cheewangkoon, R., and Al-Sadi, A. M. (2021). Uncovering the hidden taxonomic diversity of fungi in Oman. *Fungal Divers*. In press. doi: 10.1007/s13225-020-00467-1

Miller, M. A., Pfeiffer, W., and Schwartz, T. (2010). "Creating the CIPRES science gateway for inference of large phylogenetic trees," in *Proceedings of the Gateway Computing Environments Workshop (GCE) 14 Nov 2010*, (New Orleans, LA: Institute of Electrical and Electronics Engineers), 1–8.

Mittermeier, R. A., Gil, P. R., Hoffman, M., Brookscristina, P., and Goettsch Mittermeier, G. (2005). *Hotspots Revisited: Earth's Biologically Richest and Most Endangered Terrestrial Ecoregions*. Mexico: Cemex.

Mugambi, G. K., and Huhndorf, S. M. (2009). Molecular phylogenetics of *Pleosporales*: *Melanommataceae* and *Lophiostomataceae* re-circumscribed (*Pleosporomycetidae*, *Dothideomycetes*, Ascomycota). *Stud. Mycol.* 64, 103–121. doi: 10.3114/sim.2009.64.05

Myers, N., Mittermeier, R. A., Mittermeier, C. G., da Fonseca, G. A., and Kent, J. (2000). Biodiversity hotspots for conservation priorities. *Nature* 403, 853–858. doi: 10.1038/35002501

Nylander, J. A. A., Wilgenbusch, J. C., Warren, D. L., and Swofford, D. L. (2008). AWTY (are we there yet?): a system for graphical exploration of MCMC convergence in Bayesian phylogenetics. *Bioinformatics* 24, 581–583. doi: 10.1093/bioinformatics/btm388

Paz, A., Bellanger, J. M., Lavoise, C., Molia, A., ławrynowicz, M., Larsson, E., et al. (2017). The genus Elaphomyces (Ascomycota, Eurotiales): a ribosomal DNA-based phylogeny and revised systematics of European 'deer truffles'. *Persoonia* 38, 197–239. doi: 10.3767/003158517x697309

Pem, D., Hongsanan, S., Doilom, M., Tibpromma, S., Wanasinghe, D. N., Dong, W., et al. (2019a). https://www.dothideomycetes.org: an online taxonomic resource for the classification, identification, and nomenclature of *Dothideomycetes*. *Asian J. Mycol.* 2, 287–297. doi: 10.5943/ajom/2/1/19

Pem, D., Hyde, K. D., Doilom, M., Camporesi, E., Hongsanan, S., Rampadarath, S., et al. (2019b). Multigene phylogenetic analyses to establish new Valsaria species and taxonomic significance of spore ornamentation. *PLoS One* 14:e0217982. doi: 10.1371/journal.pone.0217982

Phookamsak, R., Liu, J. K., McKenzie, E., Manamgoda, D., Ariyawansa, H. A., Thambugala, K. M., et al. (2014). Revision of *Phaeosphaeriaceae*. *Fungal Divers.* 68, 159–238.

Phookamsak, R., Wanasinghe, D. N., Hongsanan, S., Phukhamsakda, C., Huang, S. K., Tennakoon, D. S., et al. (2017). Towards a natural classification of *Ophiobolus* and ophiobolus-like taxa; introducing three novel genera Ophiobolopsis, Paraophiobolus and Pseudoophiobolus in *Phaeosphaeriaceae* (*Pleosporales*). *Fungal Divers.* 87, 299–339. doi: 10.1007/s13225-017-0393-1

Phukhamsakda, C., McKenzie, E. H. C., Phillips, A. J. L., Jones, E. B. G., Bhat, D. J., Stadler, M. et al. (2020). Microfungi associated with *Clematis* (Ranunculaceae) with an integrated approach to delimiting species boundaries. *Fungal Divers*. 101, 1–204. doi: 10.1007/s13225-020-00448-4

Qiao, M., Hua, Z., Lv, R., and Yu, Z. (2020). Neodactylariales, Neodactylariaceae (*Dothideomycetes*, *Ascomycota*): new order and family, with a new species from China. *MycoKeys* 73, 69–85. doi: 10.3897/mycokeys.73.54054

Rambaut, A. (2014). *FigTree v1.4: Tree Figure Drawing Tool*. Available online at: http://treebio.ed.ac.uk/software/figtree/ (accessed January 9, 2021).

Rathnayaka, A. R., Dayarathne, M. C., Maharachchikumbura, S. S. N., Liu, J. K., Tennakoon, D. S., and Hyde, K. D. (2019). Introducing Seriascoma yunnanense sp. nov. (Occultibambusaceae, *Pleosporales*) based on evidence from morphology and phylogeny. *Asian J. Mycol.* 2, 245–253. doi: 10.5943/ajom/2/1/15

Réblová, M., Fournier, J., and Štěpánek, V. (2015). Pisorisporiales, a new order of aquatic and terrestrial fungi for Achroceratosphaeria and Pisorisporium gen. *nov. in the Sordariomycetes*. *Persoonia* 34, 40–49. doi: 10.3767/003158515x685544

Réblová, M., Miller, A. N., Réblová, K., and Štěpánek, V. (2018). Phylogenetic classification and generic delineation of Calyptosphaeria gen. nov., *Lentomitella*, Spadicoides and Torrentispora (Sordariomycetes). *Stud. Mycol.* 89, 1–62. doi: 10.1016/j.simyco.2017.11.004

Rossman, A., Crous, P. W., Hyde, K. D., Hawksworth, D. L., Aptroot, A., Bezerra, J. L., et al. (2015). Recommended names for pleomorphic genera in *Dothideomycetes*. *IMA Fungus* 6, 507–523.

Senanayake, I. C., Jeewon, R., Chomnunti, P., Wanasinghe, D. N., Norphanphoun, C., Karunarathna, A., et al. (2018). Taxonomic circumscription of Diaporthales based on multigene phylogeny and morphology. *Fungal Divers.* 93, 241–443. doi: 10.1007/s13225-018-0410-z

Senanayake, I. C., Rathnayaka, A. R., Marasinghe, D. S., Calabon, M. S., Gentekaki, E., Lee, H. B., et al. (2020). Morphological approaches in studying fungi: collection, examination, isolation, sporulation and preservation. *Mycosphere* 11, 2678–2754. doi: 10.5943/mycosphere/11/1/20

Shearer, C. A. (1993). The freshwater ascomycetes. *Nova Hedwigia* 56, 1–33.

Stamatakis, A. (2014). RAxML version 8: a tool for phylogenetic analysis and post-analysis of large phylogenies. *Bioinformatics* 30, 1312–1313. doi: 10.1093/bioinformatics/btu033

Taylor, J. E., and Hyde, K. D. (2003). *Microfungi of Tropical and Temperate Palms*. Hong Kong: Fungal Divers Press, 1–459.

Teng, S. C. (1996). *Fungi of China*. Ithaca, NY: Mycotaxon, Ltd, 1–586.

Tennakoon, D. S., Kuo, C. H., Maharachchikumbura, S. S. N., Thambugala, K. M., Gentekaki, E., Phillips, A. J. L., et al. (2021). *Taxonomic and Phylogenetic Contributions to Leaf Litter Inhabiting Microfungi Associated with Celtis Formosana, Ficus Ampelas, f. septica, Macaranga tanarius and Morus australis*. Hong Kong: Fungal Divers.

Thambugala, K. M., Hyde, K. D., Tanaka, K., Tian, Q., Wanasinghe, D. N., Ariyawansa, H. A., et al. (2015). Towards a natural classification and backbone tree for *Lophiostomataceae*, *Floricolaceae*, and *Amorosiaceae fam. nov*. *Fungal Divers.* 74, 199–266. doi: 10.1007/s13225-015-0348-3

Thiyagaraja, V., Lücking, R., Ertz, D., Wanasinghe, D. N., Karunarathna, S. C., Camporesi, E., et al. (2020a). Evolution of non-lichenized, saprotrophic species of Arthonia (*Ascomycota*, *Arthoniales*) and resurrection of Naevia, with notes on Mycoporum. *Fungal Divers.* 102, 205–224. doi: 10.1007/s13225-020-00451-9

Thiyagaraja, V., Wanasinghe, D. N., Worthy, F., and Karunarathna, S. C. (2020b). Addition to Melanommataceae: a new geographical record of *Alpinaria rhododendri* from Shangri La, China. *Asian J. Mycol.* 3, 335–344. doi: 10.5943/ajom/3/1/8

Tian, Q., Liu, J. K., Hyde, K. D., Wanasinghe, D. N., Boonmee, S., Jayasiri, S. C., et al. (2015). Phylogenetic relationships and morphological reappraisal of Melanommataceae (*Pleosporales*). *Fungal Divers.* 74, 267–324. doi: 10.1007/s13225-015-0350-9

Trakunyingcharoen, T., Lombard, L., Groenewald, J. Z., Cheewangkoon, R., To-anun, C., Alfenas, A. C., et al. (2014). Mycoparasitic species of Sphaerellopsis, and allied lichenicolous and other genera. *IMA Fungus* 5, 391–414. doi: 10.5598/imafungus.2014.05.02.05

Villegas, M., Cifuentes, J., and Estrada-Torres, A. (2005). Sporal characters in *Gomphales* and their significance for phylogenetics. *Fungal Divers.* 18, 157–175.

Wanasinghe, D. N., Jeewon, R., Gareth Jones, E. B., Boonmee, S., Kaewchai, S., Manawasinghe, I. S., et al. (2018a). Novel palmicolous taxa within *Pleosporales*: multigene phylogeny and taxonomic circumscription. *Mycol. Prog.* 17, 571–590. doi: 10.1007/s11557-018-1379-4

Wanasinghe, D. N., Mortimer, P. E., and Xu, J. (2021). Insight into the systematics of microfungi colonizing dead woody twigs of *Dodonaea viscosa* in Honghe (China). *J. Fungi* 7:180. doi: 10.3390/jof7030180

Wanasinghe, D. N., Phukhamsakda, C., Hyde, K. D., Jeewon, R., Lee, H. B., Jones, E. B. G., et al. (2018b). Fungal diversity notes 709–839: taxonomic and phylogenetic contributions to fungal taxa with an emphasis on fungi on Rosaceae. *Fungal Divers.* 89, 1–236. doi: 10.1007/s13225-018-0395-7

Wanasinghe, D. N., Wijayawardene, N. N., Xu, J., Cheewangkoon, R., and Mortimer, P. E. (2020). Taxonomic novelties in Magnolia-associated pleosporalean fungi in the Kunming Botanical Gardens (Yunnan, China). *PLoS One* 15:e0235855. doi: 10.1371/journal.pone.0235855

Wang, B., Cui, B. K., Li, H. J., Du, P., and Jia, B. S. (2011). Wood-rotting fungi in eastern China 5. polypore diversity in Jiangxi Province. *Ann. Bot. Fenn.* 48, 237–246. doi: 10.5735/085.048.0304

Wijayawardene, N. N., Crous, P. W., Kirk, P. M., Hawksworth, D. L., Boonmee, S., Braun, U., et al. (2014). Naming and outline of Dothideomycetes-2014 including proposals for the protection or suppression of generic names. *Fungal Divers.* 69, 1–55.

Wijayawardene, N. N., Hyde, K. D., Al-Ani, L. K. T., Tedersoo, L., Haelewaters, D., Rajeshkumar, K. C., et al. (2020). Outline of fungi and fungus-like taxa. *Mycosphere* 11, 1060–1456. doi: 10.5943/mycosphere/11/1/8

Wijayawardene, N. N., Hyde, K. D., Lumbsch, H. T., Liu, J. K., Maharachchikumbura, S. S. N., Ekanayaka, A. H., et al. (2018). Outline of ascomycota: 2017. *Fungal Divers.* 88, 167–263. doi: 10.1007/s13225-018-0394-8

Wijayawardene, N. N., Hyde, K. D., Rajeshkumar, K. C., Hawksworth, D. L., Madrid, H., Kirk, P. M., et al. (2017). Notes for genera: ascomycota. *Fungal Divers.* 86, 1–594.

Wijayawardene, N. N., Hyde, K. D., Wanasinghe, D. N., Papizadeh, M., Goonasekara, I. D., Camporesi, E., et al. (2016). Taxonomy and phylogeny of dematiaceous coelomycetes. *Fungal Divers.* 77, 1–316. doi: 10.1007/s13225-016-0360-2

Yasanthika, E., Dissanayake, L. S., Wanasinghe, D. N., Karunarathna, S. C., Mortimer, P. E., Samarakoon, B. C., et al. (2020). Lonicericola fuyuanensis (*Parabambusicolaceae*) a new terrestrial pleosporalean ascomycete from Yunnan province, China. *Phytotaxa* 446, 103–113. doi: 10.11646/phytotaxa.446.2.3

Yuan, H., and Dai, Y. (2012). Wood-inhabiting fungi in southern China. 6. polypores from guangxi autonomous region. *Ann. Bot. Fenn.* 49, 341–351. doi: 10.5735/085.049.0605

Yuan, Z. Q., and Barr, M. E. (1995). Some new taxa and new records of the genera Pleospora and Teichospora from Xinjiang. China. *Mycotaxon* 54, 111–116.

Zhang, J. F., Liu, J. K., Jeewon, R., Wanasinghe, D. N., and Liu, Z. Y. (2019). Fungi from Asian Karst formations III. molecular and morphological characterization reveal new taxa in *Phaeosphaeriaceae*. *Mycosphere* 10, 202–220. doi: 10.5943/mycosphere/10/1/3

Zhang, S.-N., Hyde, K. D., Jones, E. B. G., Jeewon, R., Cheewangkoon, R., and Liu, J.-K. (2019). Striatiguttulaceae, a new pleosporalean family to accommodate the genera *Longicorpus gen*. nov. and *Striatiguttula gen*. nov., from palms in mangrove ecosystem. *MycoKeys* 49, 99–129. doi: 10.3897/mycokeys.49.30886

Zhang, Y., Crous, P. W., Schoch, C. L., and Hyde, K. D. (2012). *Pleosporales*. *Fungal Divers.* 53, 1–221. doi: 10.1007/978-3-319-23534-9_1

Zhuang, W. Y. (2005). *Fungi of Northwestern China*. Ithaca, NY: Mycotaxon, Ltd, 1–430.

Conflict of Interest: The authors declare that the research was conducted in the absence of any commercial or financial relationships that could be construed as a potential conflict of interest.

Copyright © 2021 Mortimer, Jeewon, Xu, Lumyong and Wanasinghe. This is an open-access article distributed under the terms of the Creative Commons Attribution License (CC BY). The use, distribution or reproduction in other forums is permitted, provided the original author(s) and the copyright owner(s) are credited and that the original publication in this journal is cited, in accordance with accepted academic practice. No use, distribution or reproduction is permitted which does not comply with these terms.

frontiers in Microbiology

ORIGINAL RESEARCH
published: 26 March 2021
doi: 10.3389/fmicb.2021.644979

Taxonomy and Phylogeny of the *Fomitopsis pinicola* Complex With Descriptions of Six New Species From East Asia

*Shun Liu[1,2], Mei-Ling Han[3], Tai-Min Xu[1,2], Yan Wang[1,2], Dong-Mei Wu[4] and Bao-Kai Cui[1,2]**

[1] Beijing Advanced Innovation Center for Tree Breeding by Molecular Design, Beijing Forestry University, Beijing, China, [2] Institute of Microbiology, School of Ecology and Nature Conservation, Beijing Forestry University, Beijing, China, [3] College of Life Sciences, Langfang Normal University, Langfang, China, [4] Biotechnology Research Institute, Xinjiang Academy of Agricultural and Reclamation Sciences/Xinjiang Production and Construction Group Key Laboratory of Crop Germplasm Enhancement and Gene Resources Utilization, Shihezi, China

Fomitopsis pinicola is a common brown-rot fungal species found in northern hemisphere. It grows on many different gymnosperm and angiosperm trees. Recent studies show that it is a species complex; three species from North America and one species from Europe have been recognized in this complex. In the current study, six new species in the *Fomitopsis pinicola* complex were discovered from East Asia, based on morphological characters and phylogenetic analyses inferred from the sequence data of the internal transcribed spacer (ITS) regions, the second subunit of RNA polymerase II (RPB2), and the translation elongation factor 1-α gene (TEF). Detailed descriptions of the six new species are provided. Our results also indicates that species of the *F. pinicola* complex from East Asia usually have limited distribution areas and host specialization.

Keywords: brown-rot fungi, host specialization, multi-gene phylogeny, polypore, species complex

OPEN ACCESS

Edited by:
Peter Edward Mortimer, Kunming Institute of Botany, Chinese Academy of Sciences, China

Reviewed by:
Daniel L. Lindner, Center for Forest Mycology Research, Northern Research Station, Forest Service (USDA), United States
Chang-lin Zhao, Southwest Forestry University, China

***Correspondence:**
Bao-Kai Cui
cuibaokai@yahoo.com

Specialty section:
This article was submitted to Evolutionary and Genomic Microbiology, a section of the journal Frontiers in Microbiology

Received: *22 December 2020*
Accepted: *02 March 2021*
Published: *26 March 2021*

Citation:
Liu S, Han M-L, Xu T-M, Wang Y, Wu D-M and Cui B-K (2021) Taxonomy and Phylogeny of the Fomitopsis pinicola Complex With Descriptions of Six New Species From East Asia. Front. Microbiol. 12:644979. doi: 10.3389/fmicb.2021.644979

INTRODUCTION

Fomitopsis P. Karst. was established by Karsten and typified by *F. pinicola* (Sw.) P. Karst. (Karsten, 1881). It is characterized by a perennial or annual growth habit, is sessile to effused-reflexed, has tough to woody hard basidiocarps, has a white to tan or pinkish-colored pore surface with mostly small and regular pores, has a dimitic to trimitic hyphal system with clamped generative hyphae, and has a hyaline, thin-walled, smooth, and ellipsoid to subglobose basidiospores which are negative in Melzer's reagent; it causes a brown rot (Ryvarden and Johansen, 1980; Gilbertson and Ryvarden, 1986; Ryvarden and Gilbertson, 1993; Núñez and Ryvarden, 2001; Han et al., 2016).

Fomitopsis pinicola has been intensively studied because it has the function of dispelling wind-evil and dampness, and has anti-tumor (Dai et al., 2009; Sun et al., 2016), antifungal, antioxidant, immunomodulation, and neuroprotective activities (Guler et al., 2009; Bao et al., 2015;

Abbreviations: BI, Bayesian inference; BJFC, Herbarium of the Institute of Microbiology, Beijing Forestry University; BGI, Beijing Genomics Institute; BPP, Bayesian posterior probabilities; BT, Bootstrap; CB, Cotton Blue; CB–, acyanophilous; GTR + I + G, General time reversible + proportion invariant + gamma; IKI, Melzer's reagent; IKI–, neither amyloid nor dextrinoid; ILD, incongruence length difference test; ITS, internal transcribed spacer; KOH, 5% potassium hydroxide; L, mean spore length (arithmetic average of all spores); ML, maximum likelihood; MP, maximum parsimony; MPT, most parsimonious tree; n (a/b), number of spores (a) measured from given number (b) of specimens; Q, variation in the L/W ratios between the specimens studied; RPB2, DNA-directed RNA polymerase II subunit 2; TL, tree length; W, mean spore width (arithmetic average of all spores); CI, consistency index; RI, retention index; RC, rescaled consistency index; HI, homoplasy index; TEF, translation elongation factor 1-α.

Sun et al., 2016; Guo and Wolf, 2018). Högberg et al. (1999) showed that all European populations of *F. pinicola* belong to one intersterility group. Ryvarden and Stokland (2008) described *Fomitopsis ochracea* Ryvarden & Stokland from Alberta on *Populus tremuloides* that was distinguished from *F. pinicola* by substrate preference, basidiospore morphology, and match flame test to the lacquered pilei surface. Subsequently, this species was proven to belong to the *F. pinicola* complex (Haight et al., 2019). Haight et al. (2016) suggested that *F. pinicola* is a species complex comprised of at least four well-supported phylogenetic species, three in North America (*F. ochracea* and two previously undescribed species) and one in Europe (*F. pinicola*). Haight et al. (2019) described two new species: *F. mounceae* Haight & Nakasone and *F. schrenkii* Haight & Nakasone from North America in the *F. pinicola* complex. Until now, four species have been recognized in the *F. pinicola* complex; *F. mounceae*, *F. ochracea*, and *F. schrenkii* from North America and *F. pinicola* from Europe.

In some cases, fungi species boundaries based on morphology misrepresents the number of existing species (Leavitt et al., 2011). Due to geographic isolation, lack of migration, and genetic drift there may be variation among populations, although this genetic variation is not always obvious (Haight et al., 2016). Cryptic species of species complexes are proving to be extremely common in higher fungi, particularly those with wide geographic distributions or host ranges (Haight et al., 2016); they share similar morphological characteristics and phylogenetic relationships to known species. More cryptic species could be discovered by combining evidence of morphological characters, molecular data, host trees, and distribution areas in species complexes (Liu et al., 2021).

In recent years, taxonomic and phylogenetic studies of *Fomitopsis* have been carried out in China and several new species have been described (Li et al., 2013; Han et al., 2014, 2016; Han and Cui, 2015; Liu et al., 2019), but none have been focused on the *F. pinicola* complex. Samples collected from China were still identified as *F. pinicola* complex in these studies. With more and more specimens collected from different areas of China, Vietnam, and of East Asia, six new species of the *F. pinicola* complex have been discovered based on morphological characters and phylogenetic analysis of ITS + RPB2 + TEF gene regions.

MATERIALS AND METHODS

Taxa Sampling and Morphological Study

The examined specimens were deposited in the herbarium of the Institute of Microbiology, Beijing Forestry University (BJFC, Beijing, P. R. China). Morphological descriptions and abbreviations used in this study follow Han et al. (2016) and Liu et al. (2019).

DNA Extraction and Molecular Analyses

The procedures for DNA extraction and polymerase chain reaction (PCR) used in this study were the same as described by Chen et al. (2017) and Song and Cui (2017). The primer pairs ITS5 and ITS4 for ITS regions, fRPB2-f5F and bRPB2-7.1R for the RPB2 gene, and EF1-983 F and EF1-1567R for the TEF gene used in this study are the same as in previous studies (White et al., 1990; Rehner, 2001; Matheny, 2005).

The PCR cycling schedules for different DNA sequences of ITS, RPB2, and TEF genes used in this study followed those used in Zhu et al. (2019) and Sun et al. (2020) with some modifications. The PCR procedure for ITS was the initial denaturation at 95°C for 3 min, followed by 35 cycles of denaturation at 94°C for 40 s, annealing at 54°C for 45 s, and extension at 72°C for 1 min, and a final extension at 72°C for 10 min. The PCR procedure for RPB2 was the initial denaturation at 94°C for 2 min, followed by 37 cycles of denaturation at 94°C for 45 s, annealing at 56°C for 90 s, and extension at 72°C for 2 min, and a final extension at 72°C for 10 min. The PCR procedure for TEF was the initial denaturation at 95°C for 3 min, followed by 35 cycles of denaturation at 94°C for 40 s, annealing at 54–57°C for 45 s and extension at 72°C for 1 min, and a final extension at 72°C for 10 min. The PCR products were purified and sequenced at the Beijing Genomics Institute (BGI), China, with the same primers. All newly generated sequences were deposited in GenBank (**Table 1**). Additional sequences for phylogenetic analyses were downloaded from GenBank (**Table 1**). All sequences were aligned in MAFFT 7 (Katoh and Standley, 2013)[1] and manually adjusted in BioEdit (Hall, 1999). Alignments were spliced in Mesquite (Maddison and Maddison, 2017). The missing sequences were coded as "N," ambiguous nucleotides were coded as "N" followed Chen et al. (2017). The final concatenated sequence alignment was deposited in TreeBase[2] (submission ID: 27439).

Phylogenetic analyses approaches used in this study followed Han et al. (2016) and Cui et al. (2019). The congruences of the 3-gene (ITS, RPB2 and TEF) were evaluated with the incongruence length difference (ILD) test (Farris et al., 1994) implemented in PAUP* 4.0b10 (Swofford, 2002), under heuristic search and 1000 homogeneity replicates. The sequences of *Daedalea quercina* (L.) Pers obtained from GenBank were used as outgroups for the phylogeny of the *Fomitopsis pinicola* complex, and sequences of *Laetiporus zonatus* B.K. Cui & J. Song were used as outgroups for the phylogeny of the *Fomitopsis pinicola* complex and related taxa. A maximum parsimony (MP) analysis was performed in PAUP* version 4.0b10 (Swofford, 2002). A maximum likelihood (ML) analysis was performed in RAxmL v.7.2.8 with a GTR + G + I model (Stamatakis, 2006). Bayesian inference (BI) was calculated by MrBayes 3.1.2 (Ronquist and Huelsenbeck, 2003) with a general time reversible (GTR) model of DNA substitution and a gamma distribution rate variation across sites determined by MrModeltest 2.3 (Posada and Crandall, 1998; Nylander, 2004). Clade robustness was assessed using a bootstrap (BT) analysis with 1000 replicates (Felsenstein, 1985). The branch support was evaluated with a bootstrapping method of 1000 replicates (Hillis and Bull, 1993). Branches that received bootstrap supports for the MP and ML, greater than or equal to 75% and Bayesian posterior probabilities (BPP) greater than or equal to 0.95, were considered

[1]http://mafft.cbrc.jp/alignment/server/

[2]http://www.treebase.org

TABLE 1 | A list of species, specimens, and GenBank accession numbers of sequences used in this study.

Species name	Sample no.	Locality	GenBank accessions		
			ITS	RPB2	TEF
Antrodia tanakae	Cui 9743	China	KR605814	KR610833	KR610743
A. tanakae	Yuan 1106	China	KP715313	KR610835	KP715343
Daedalea quercina	Dai 12152	Czechia	KP171207	KR610809	KR610717
D. quercina	Dai 2260	Sweden	KR605792	KR610808	KR610718
Fomitopsis abieticola	Cui 10532	China	**MN148230**	**MN158174**	**MN161745**
F. abieticola	Cui 10521	China	**MN148231**	**—**	**MN161746**
F. betulina	Cui 10756	China	KR605797	KR610815	KR610725
F. betulina	Dai 11449	China	KR605798	KR610816	KR610726
F. cana	Cui 6239	China	JX435777	KR610761	KR610661
F. cana	Dai 9611	China	JX435776	KR610762	KR610660
F. durescens	Overholts 4215	United States	KF937293	—	—
F. durescens	O 10796	Venezuela	KF937292	KR610766	KR610669
F. hengduanensis	Cui 16259	China	**MN148232**	**MN158175**	**MN161747**
F. hengduanensis	Cui 17056	China	**MN148233**	**MN158176**	**MN161748**
F. kesiyae	Cui 16437	Vietnam	**MN148234**	**MN158177**	**MN161749**
F. kesiyae	Cui 16466	Vietnam	**MN148235**	**MN158178**	**MN161750**
F. massoniana	Cui 2848	China	**MN148236**	**—**	**MN161751**
F. massoniana	Cui 9058	China	**MN148237**	**—**	**MN161752**
F. massoniana	Cui 11288	China	**MN148238**	**MN158179**	**MN161753**
F. massoniana	Cui 11304	China	**MN148239**	**—**	**MN161754**
F. meliae	Dai 10035	China	KR605774	—	KR610683
F. meliae	Ryvarden 16893	Unknown	KR605776	KR610775	KR610681
F. mounceae	AFTOL ID 770	United States	AY786056	AY864874	AY705967
F. mounceae	DR 366	United States	KF169624	KF169693	KF178349
F. mounceae	JAG 08 19	United States	KF169626	KF169695	KF178351
F. mounceae	JEH 78	Canada	KF169629	KF169698	KF178354
F. mounceae	Tuomo Niemelä 2530	Canada	**MN148240**	**—**	**MN161755**
F. mounceae	Teuvo Ahti 60351	Canada	**MN148241**	**—**	**MN161756**
F. mounceae	OM 18782	United States	**MN148242**	**—**	**MN161757**
F. mounceae	Spirin 8367	United States	**MN148243**	**—**	**MN161758**
F. ochracea	HHB 19692	United States	KF169594	KF169663	KF178319
F. ochracea	HHB 19670	United States	KF169593	KF169662	KF178318
F. ochracea	JEH 38	United States	KF169603	KF169672	KF178328
F. ochracea	LT 18	United States	KF169616	KF169685	KF178341
F. ochracea	OM 18568	United States	**MN148244**	**—**	**MN161759**
F. ochracea	OM 18673	United States	**MN148245**	**—**	**MN161760**
F. ochracea	Spirin 8165	United States	**MN148246**	**—**	**MN161761**
F. pinicola	FCUG 2056	Sweden	KF169654	KF169723	KF178379
F. pinicola	HK 19330	Russia	KF169655	KF169724	KF178380
F. pinicola	LT 323	Estonia	KF169651	KF169720	KF178376
F. pinicola	LT 319	Estonia	KF169652	KF169721	KF178377
F. pinicola	AT Fp 1	Sweden	MK208852	MK236362	MK236359
F. pinicola	AT Fp 2	Sweden	MK208853	MK236363	MK236360
F. schrenkii	FP 105881 R	United States	KF169641	KF169710	KF178366
F. schrenkii	JEH 144	United States	KF169621	MK208857	MK236355
F. schrenkii	JEH 150	United States	KF169622	MK208858	MK236356
F. schrenkii	JV 1209/61 J	United States	**MN148247**	**MN158180**	**MN161762**
F. schrenkii	Inkeri Ahonen 58	United States	**MN148248**	**—**	**MN161763**
F. subpinicola	Cui 9836	China	**MN148249**	**MN158181**	**MN161764**
F. subpinicola	Cui 9819	China	**MN148250**	**—**	**MN161765**
F. subpinicola	Dai 11101	China	**MN148251**	**MN158182**	**MN161766**

Continued

TABLE 1 | Continued

Species name	Sample no.	Locality	GenBank accessions		
			ITS	RPB2	TEF
F. subpinicola	Dai 11206	China	**MN148252**	**MN158183**	**MN161767**
F. subpinicola	Dai 13480	China	**MN148253**	**MN158184**	**MN161768**
F. subpinicola	Yuan 4912	China	**MN148254**	**—**	**MN161769**
F. subtropica	Cui 10578	China	KR605787	KR610791	KR610698
F. subtropica	Cui 10140	China	JQ067651	KR610789	KR610699
F. tianshanensis	Wei 1568	China	**MN148255**	**—**	**MN161770**
F. tianshanensis	Wei 1473a	China	**MN148256**	**—**	**MN161771**
F. tianshanensis	Wei 1462a	China	**MN148257**	**—**	**MN161772**
F. tianshanensis	Cui 16821	China	**MN148258**	**—**	**MN161773**
F. tianshanensis	Cui 16823	China	**MN148259**	**—**	**MN161774**
F. tianshanensis	Cui 16825	China	**MN148260**	**—**	**MN161775**
F. tianshanensis	Cui 16828	China	**MN148261**	**—**	**MN161776**
F. tianshanensis	Cui 16830	China	**MN148262**	**—**	**MN161777**
Laetiporus zonatus	Dai 13633	China	KX354481	KX354676	KX354635
L. zonatus	Cui 10404	China	KF951283	KT894797	KX354639
Niveoporofomes spraguei	JV 0509/62	United States	KR605786	KR610788	KR610697
N. spraguei	4638	France	KR605784	KR610786	KR610696
Rhodofomes roseus	Cui 10520	China	KC507162	KR610783	KR610692
R. roseus	Cui 10633	China	KR605782	KR610784	KR610693
Rhodofomitopsis feei	LR 14115	Costa Rica	KF999923	—	—
R. feei	JV 0610/K9-Kout	Mexico	KF999922	—	KR610673
Rubellofomes cystidiatus	Cui 5481	China	KF937288	KR610765	KR610667
R. cystidiatus	Yuan 6304	China	KR605769	—	KR610668

New sequences are shown in bold.

as significantly supported (Shen et al., 2019; Sun et al., 2020). The phylogenetic tree was visualized using FigTree v1.4.2[3].

RESULTS

Molecular Phylogeny

The combined 3-gene (ITS, RPB2, TEF) dataset to infer the phylogeny of species in the *Fomitopsis pinicola* complex included sequences from 52 fungal samples representing 11 taxa. The dataset had an aligned length of 1750 characters including gaps (553 characters for ITS, 641 characters for RPB2, 556 characters for TEF), of which 1403 characters were constant, 32 were variable and parsimony-uninformative, and 315 were parsimony-informative. Maximum parsimony analysis yielded 12 equally parsimonious trees (TL = 470, CI = 0.785, RI = 0.872, RC = 0.684, HI = 0.215). The best model for the combined ITS + RPB2 + TEF sequences dataset estimated and applied in the Bayesian analysis was GTR + I + G with equal frequency of nucleotides. Bayesian analysis and ML analysis resulted in a similar topology as the MP analysis, and only the MP tree inferred from the combined three-gene dataset is shown in **Figure 1**.

The combined three-gene (ITS, RPB2, TEF) dataset infer the phylogeny of species in the *Fomitopsis pinicola* complex and the related group included sequences from 74 fungal samples representing 21 taxa. The dataset had an aligned length of 1848 characters including gaps (641 characters for ITS, 641 characters for RPB2, 566 characters for TEF), of which 1063 characters were constant, 41 were variable and parsimony-uninformative, and 744 were parsimony-informative. MP analysis yielded 10 equally parsimonious trees (TL = 2428, CI = 0.521, RI = 0.762, RC = 0.397, HI = 0.479). The best model for the concatenate sequence dataset estimated and applied in the Bayesian inference was GTR + I + G with an equal frequency of nucleotides. Bayesian analysis and ML analysis resulted in a similar topology as the MP analysis, and only the MP tree inferred from the combined three-gene sequences dataset is shown in **Figure 2**.

The phylogenetic trees (**Figures 1**, **2**) generated by Maximum parsimony, Maximum likelihood and Bayesian analyses showed that the six new species, *Fomitopsis abieticola*, *F. hengduanensis*, *F. kesiyae*, *F. massoniana*, *F. subpinicola,* and *F. tianshanensis* grouped together with *F. mounceae*, *F. ochracea*, *F. pinicola,* and *F. schrenkii*, thus, the species number of the *F. pinicola* complex increased to 10 around the world.

Taxonomy

Fomitopsis abieticola B.K. Cui, M.L. Han & Shun Liu, **sp. nov.** (**Figures 3A,B**, **4**).

MycoBank: MB 838908

Fomitopsis abieticola is characterized by its large pores (2–4 per mm), long cystidioles (17.5–50.2 × 4.3–9.5 μm),

[3]http://tree.bio.ed.ac.uk/software/figtree/

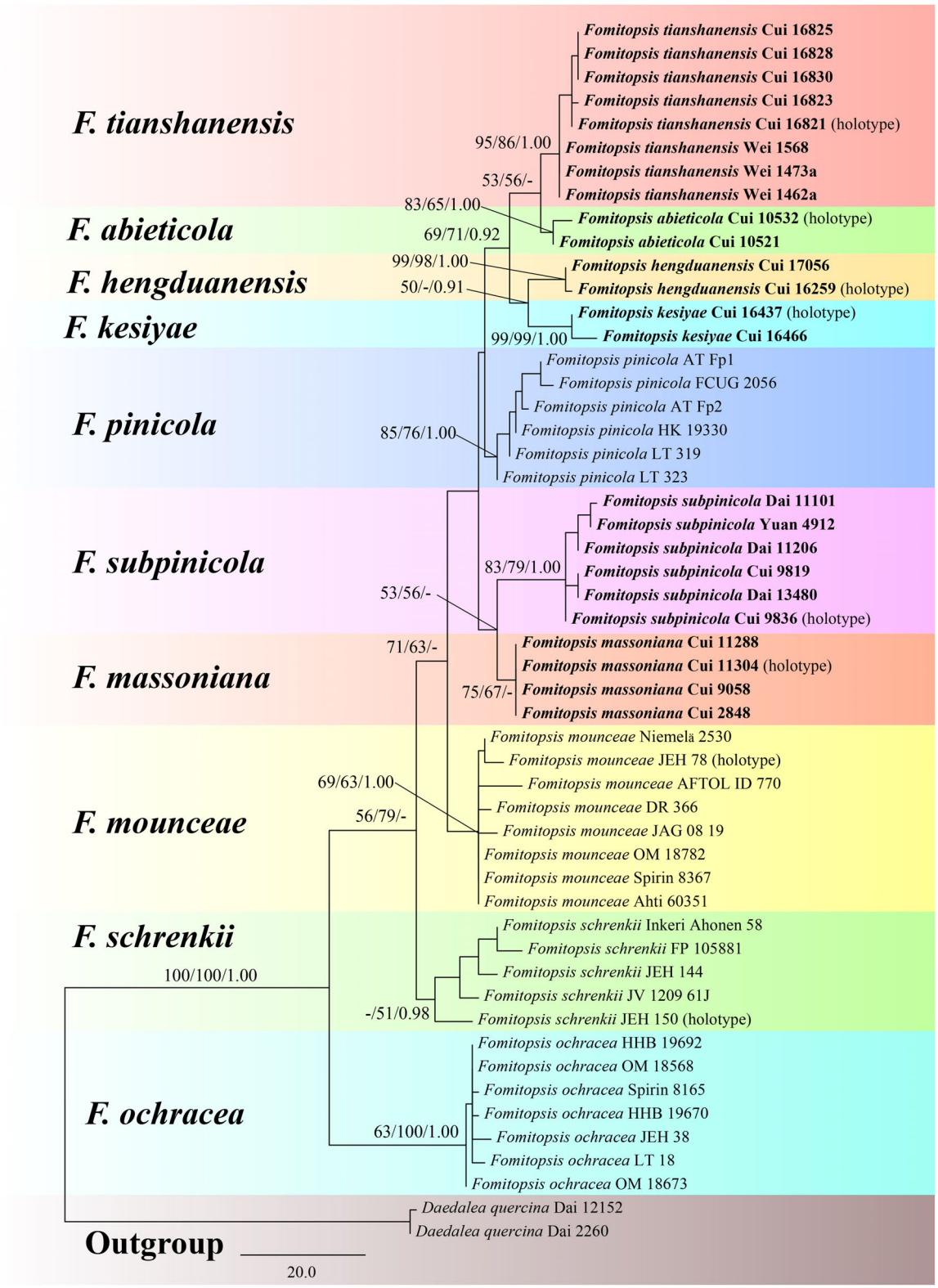


FIGURE 1 | Maximum parsimony tree illustrating the phylogeny of the *Fomitopsis pinicola* complex based on the combined sequences dataset of ITS + RPB2 + TEF. *Daedalea quercina* served as the outgroup. Branches are labeled with maximum likelihood bootstrap higher than 50%, maximum parsimony bootstrap proportions higher than 50% and Bayesian posterior probabilities more than 0.95. Bold names = New species.

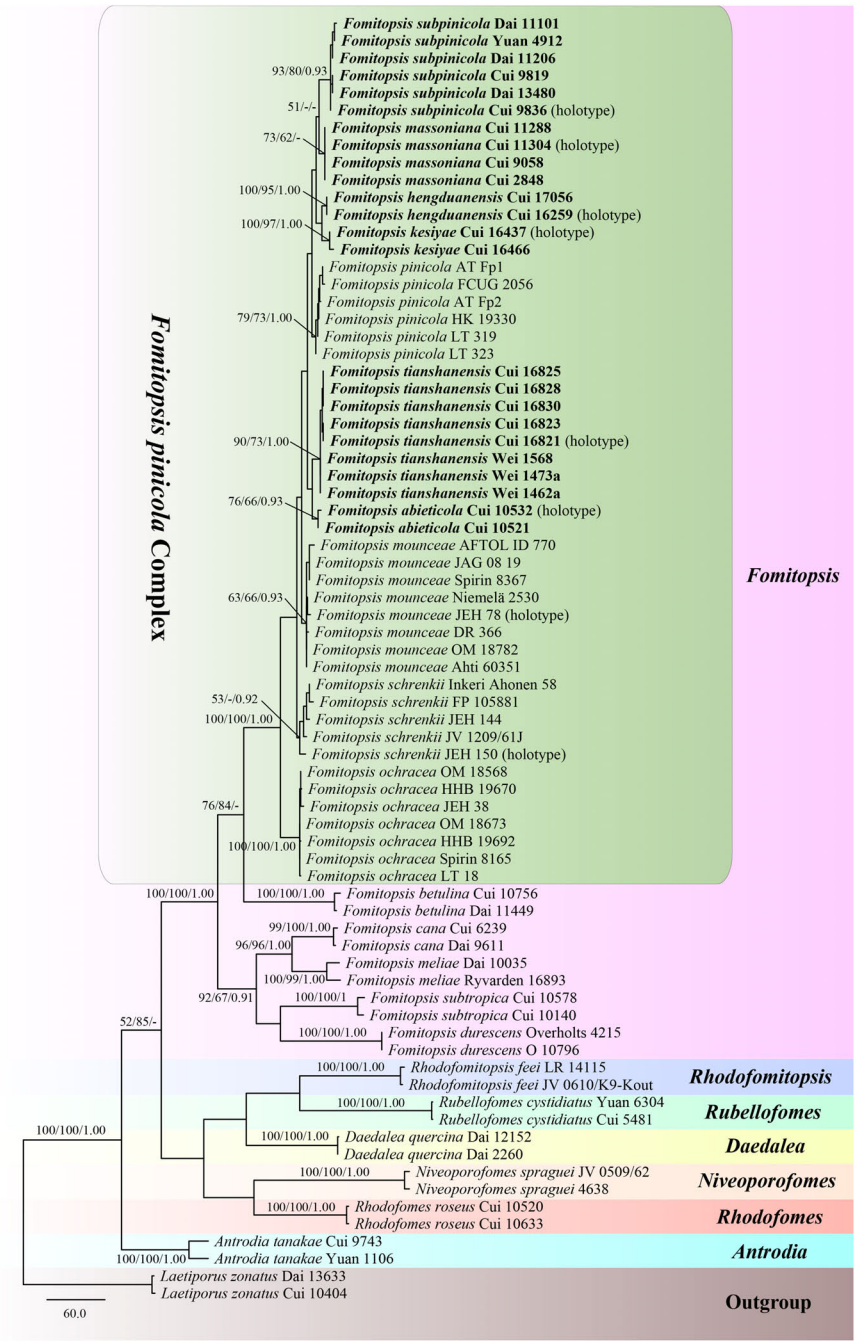


FIGURE 2 | Maximum parsimony tree illustrating the phylogeny of the *Fomitopsis pinicola* complex and related group based on the combined sequences dataset of ITS + RPB2 + TEF. *Laetiporus zonatus* served as the outgroup. Branches are labeled with maximum likelihood bootstrap higher than 50%, maximum parsimony bootstrap proportions higher than 50% and Bayesian posterior probabilities more than 0.95. Bold names = New species.

long basidia (20.8–40.5 × 5.5–11.5 μm) and big basidiospores (7–9 × 4–5 μm), and grows on *Abies*.

Type. — **CHINA**. Yunnan Province, Shangri-La County, Pudacuo National Park, on stump of *Abies*, 24 September 2011, *Cui 10532* (Holotype, BJFC 011427).

Etymology. —*Abieticola* (Lat.), refers to the host tree genus *Abies*.

Basidiocarps. —Annual to perennial, pileate, sessile, solitary, hard corky, without odor or taste when fresh, woody hard and light in weight upon drying. Pilei semicircular to ungulate, projecting up to 6.5 cm long, 8.5 cm wide, 2.5 cm thick at base. Pileal surface cream to pinkish buff when fresh, becoming honey-yellow to grayish brown when dry, glabrous, small nodules appear near the base, rough, azonate; margin cream, slightly

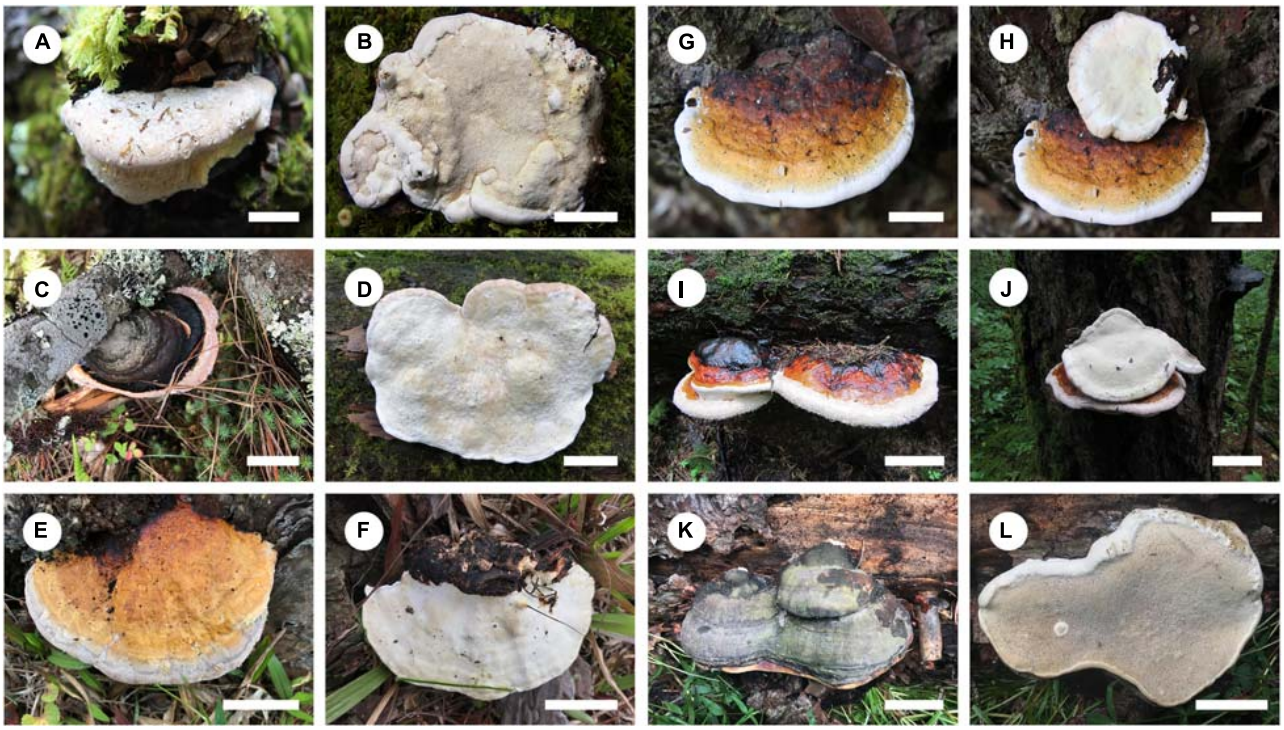


FIGURE 3 | Basidiocarps of the *Fomitopsis pinicola* complex species. **(A,B)** *F. abieticola*; **(C,D)** *F. hengduanensis*; **(E,F)** *F. kesiyae*; **(G,H)** *F. massoniana*; **(I,J)** *F. subpinicola*; **(K,L)** *F. tianshanensis*. Bars: **A,B,D,E,F** = 2 cm; **G,H** = 1 cm; **C,I,J** = 3 cm; **K,L** = 5 cm.

paler than pileal surface, obtuse. Pore surface cream to pinkish buff when fresh, becoming buff to curry-yellow when dry; sterile margin distinct, white to cream when fresh, becoming olivaceous buff to clay-buff when dry, up to 10 mm wide; pores round to angular, 2–4 per mm; dissepiments slightly thick to thick, entire. Context cream to straw-yellow, woody hard, up to 1.5 cm thick. Tubes concolorous with pore surface, woody hard, up to 1 cm long.

Hyphal structure. —Hyphal system dimitic; generative hyphae bearing clamp connections; skeletal hyphae IKI–, CB–; tissues unchanged in KOH.

Context. —Generative hyphae infrequent, hyaline, thin-walled, rarely branched, 2.5–5 μm in diam; skeletal hyphae dominant, yellowish brown to cinnamon brown, thick-walled with a narrow lumen to subsolid, rarely branched, straight, interwoven, 2.3–8.2 μm in diam.

Tubes. —Generative hyphae infrequent, hyaline, thin-walled, rarely branched, 1.9–3.2 μm in diam; skeletal hyphae dominant, hyaline, thick-walled with a wide lumen, occasionally branched, more or less straight, interwoven, 2.2–7.2 μm in diam. Cystidia absent, but fusoid cystidioles occasionally present, hyaline, thin-walled, 17.5–50.2 × 4.3–9.5 μm. Basidia clavate, bearing four sterigmata and a basal clamp connection, 20.8–40.5 × 5.5–11.5 μm; basidioles dominant, in shape similar to basidia, but smaller.

Spores. —Basidiospores oblong-ellipsoid to ellipsoid, hyaline, thin-walled, smooth, IKI–, CB–, 7–9(–9.2) × (3.2–)4–5 μm, L = 7.85 μm, W = 4.26 μm, Q = 1.83–1.89 (*n* = 60/2).

Type of rot. —Brown rot.

Additional specimen (paratype) examined: **CHINA**. Yunnan Province, Shangri-La County, Pudacuo National Park, on stump of *Abies*, 24 September 2011, *Cui 10521* (BJFC 011416).

Fomitopsis hengduanensis B.K. Cui & Shun Liu, **sp. nov.** (**Figures 3C,D**, **5**).

MycoBank: MB 838909

Fomitopsis hengduanensis is characterized by laccate pileus with pale dark gray to reddish brown surface at base and cream to flesh-pink toward the margin when fresh, oblong-ellipsoid to ellipsoid basidiospores (5.2–6 × 3.2–3.6 μm) and is distributed in high altitude areas of the Hengduan Mountains.

Type. —**CHINA**, Yunnan Province, Lanping County, Tongdian, Laojunshan of Hengduan Mountains, Luoguqing, on dead tree of *Picea*, 18 September 2017, *Cui 16259* (Holotype, BJFC 029558).

Etymology. —*Hengduanensis* (Lat.), refers to the species distributed in the area of Hengduan Mountains.

Basidiocarps. —Annual to perennial, pileate, sessile, solitary, hard corky, without odor or taste when fresh, woody hard and light in weight upon drying. Pilei applanate, semicircular to ungulate, projecting up to 7.5 cm long, 9 cm wide, 3 cm thick at base. Pileal surface laccate, colors varied but usually pale dark gray to reddish brown at base and cream to flesh-pink toward the margin when fresh, curry-yellow, mouse-gray to reddish brown at base and buff to clay-buff toward the margin when dry, glabrous, sulcate, concentrically zonate; margin acute to obtuse. Pore surface white to cream when fresh, becoming buff

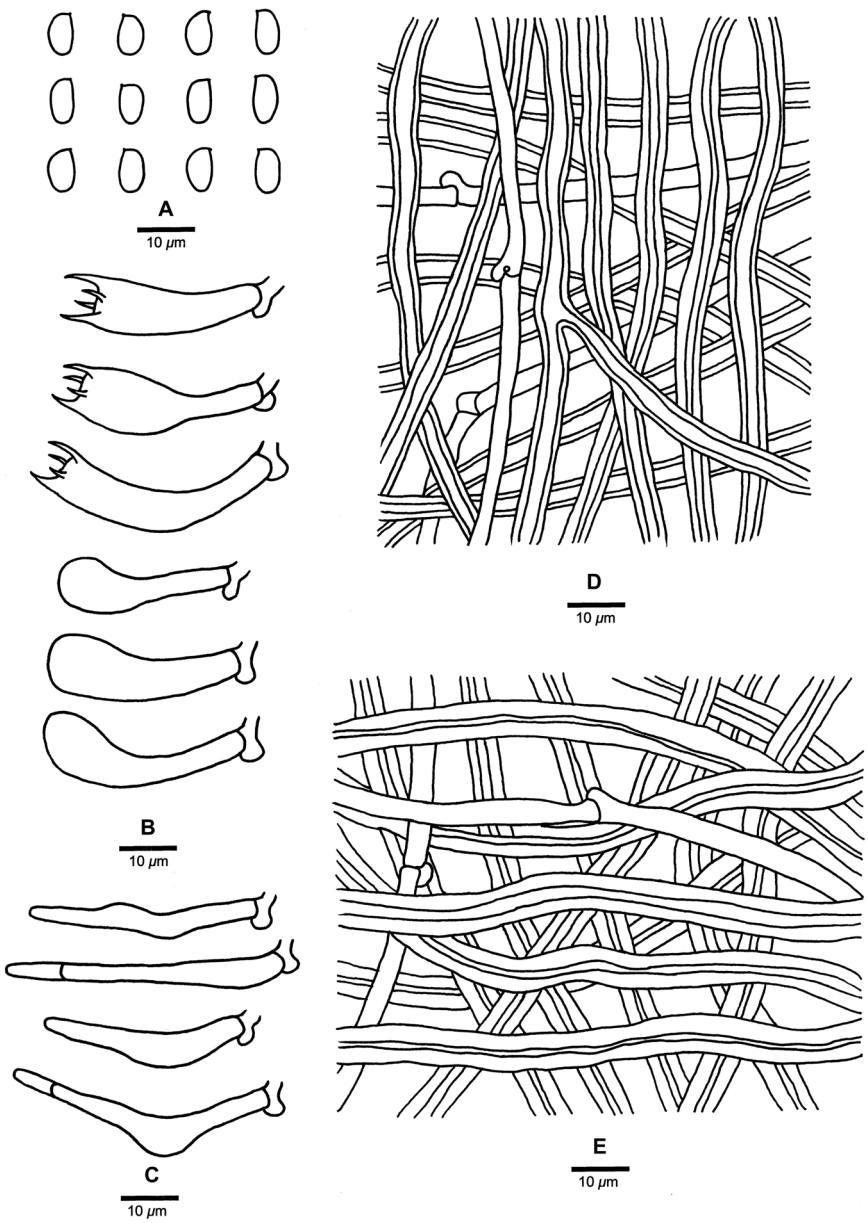


FIGURE 4 | Microscopic structures of *Fomitopsis abieticola* (drawn from the holotype). **(A)** Basidiospores; **(B)** Basidia and basidioles; **(C)** Cystidioles; **(D)** Hyphae from trama; **(E)** Hyphae from context. Bars: **A–E** = 10 μm.

to straw-yellow when dry; sterile margin distinct, cream, up to 4 mm wide; pores round to angular, 6–8 per mm; dissepiments thick, entire. Context cream to straw-yellow, woody hard, up to 1.4 cm thick. Tubes concolorous with pore surface, woody hard, up to 0.5 cm long.

Hyphal structure. —Hyphal system dimitic; generative hyphae bearing clamp connections; skeletal hyphae IKI–, CB–; tissues unchanged in KOH.

Context. —Generative hyphae infrequent, hyaline, thin- to slightly thick-walled, rarely branched, 1.9–4.3 μm in diam; skeletal hyphae dominant, hyaline to pale yellowish, thick-walled with a narrow lumen to subsolid, rarely branched, straight, interwoven, 2–8.5 μm in diam.

Tubes. —Generative hyphae infrequent, hyaline, thin-walled, rarely branched, 1.3–3.5 μm in diam; skeletal hyphae dominant, hyaline, thick-walled with a wide lumen, occasionally branched, more or less straight, interwoven, 1.7–7.5 μm in diam. Cystidia absent, but fusoid cystidioles occasionally present, hyaline, thin-walled, 13.2–36.5 × 2.5–5.4 μm. Basidia clavate, bearing four sterigmata and a basal clamp connection, 16.6–34.5 × 5.4–10.2 μm; basidioles dominant, in shape similar to basidia, but smaller.

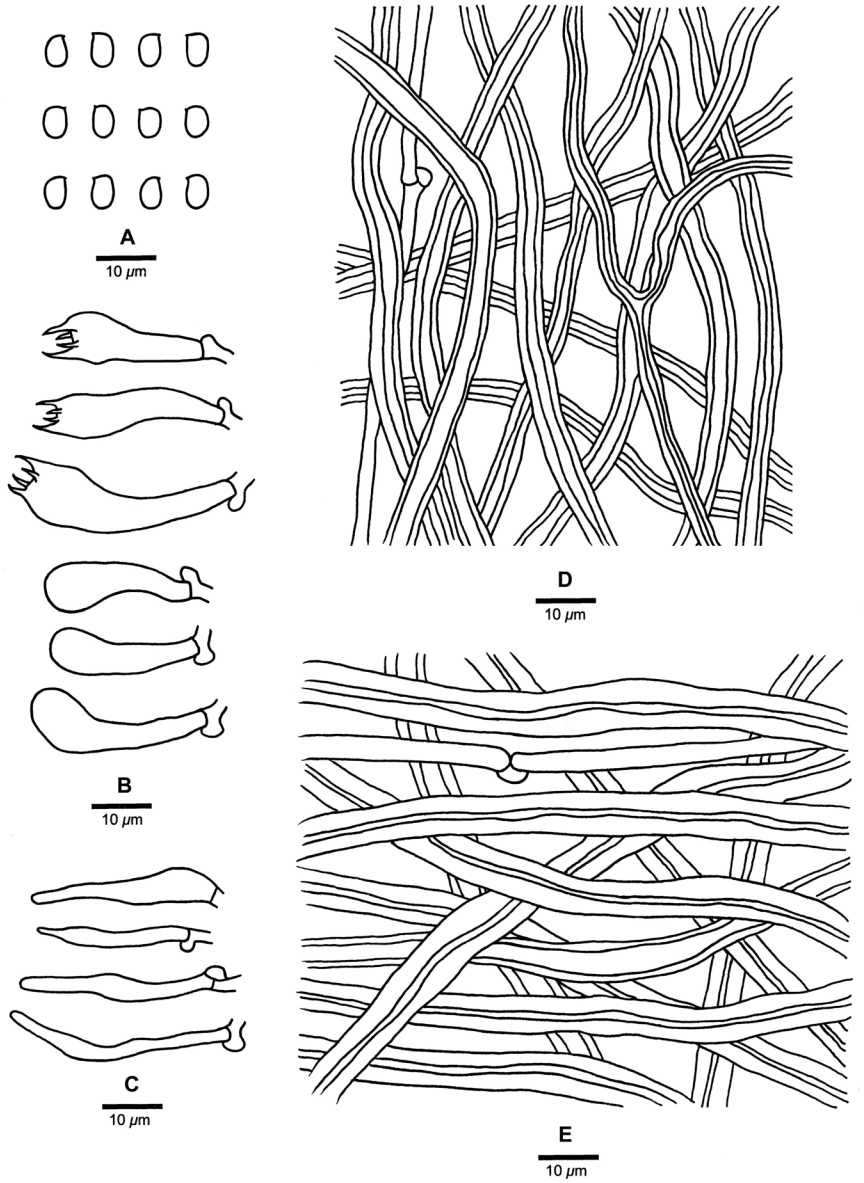


FIGURE 5 | Microscopic structures of *Fomitopsis hengduanensis* (drawn from the holotype). **(A)** Basidiospores; **(B)** Basidia and basidioles; **(C)** Cystidioles; **(D)** Hyphae from trama; **(E)** Hyphae from context. Bars: **A–E** = 10 μm.

Spores. —Basidiospores oblong-ellipsoid to ellipsoid, hyaline, thin-walled, smooth, IKI–, CB–, (5–)5.2–6(–6.2) × (3–)3.2–3.6(–4) μm, L = 5.44 μm, W = 3.41 μm, Q = 1.57–1.63 (*n* = 60/2).

Type of rot. —Brown rot.

Additional specimen (paratype) examined: **CHINA**. Yunnan Province, Lijiang, Yulong xueshan of Hengduan Mountains, on fallen trunk of *Picea*, 16 September 2018, *Cui 17056* (BJFC 030355).

Fomitopsis kesiyae B.K. Cui & Shun Liu, **sp. nov.** (**Figures 3E,F**, **6**).

MycoBank: MB 838910

Fomitopsis kesiyae is characterized by its buff yellow to orange-yellow buff pileal surface when fresh, reddish brown to yellowish brown when dry, and grows on *Pinus kesiya* and is distributed in tropical areas of Vietnam.

Type. — **VIETNAM**. Dam Dong Province, Da Lat, Bidoup Nui Ba National Park, on living tree of *Pinus kesiya*, 15 October 2017, *Cui 16437* (Holotype, BJFC 029736).

Etymology. — *Kesiyae* (Lat.), refers to the host tree species *Pinus kesiya*.

Basidiocarps. — Annual, pileate, sessile, hard corky, without odor or taste when fresh, woody hard and light in weight upon drying. Pilei applanate, semicircular to sectorial, projecting up to 4.7 cm long, 6.5 cm wide, 4 cm thick at base. Pileal surface laccate, buff yellow to orange-yellow buff when fresh, becoming

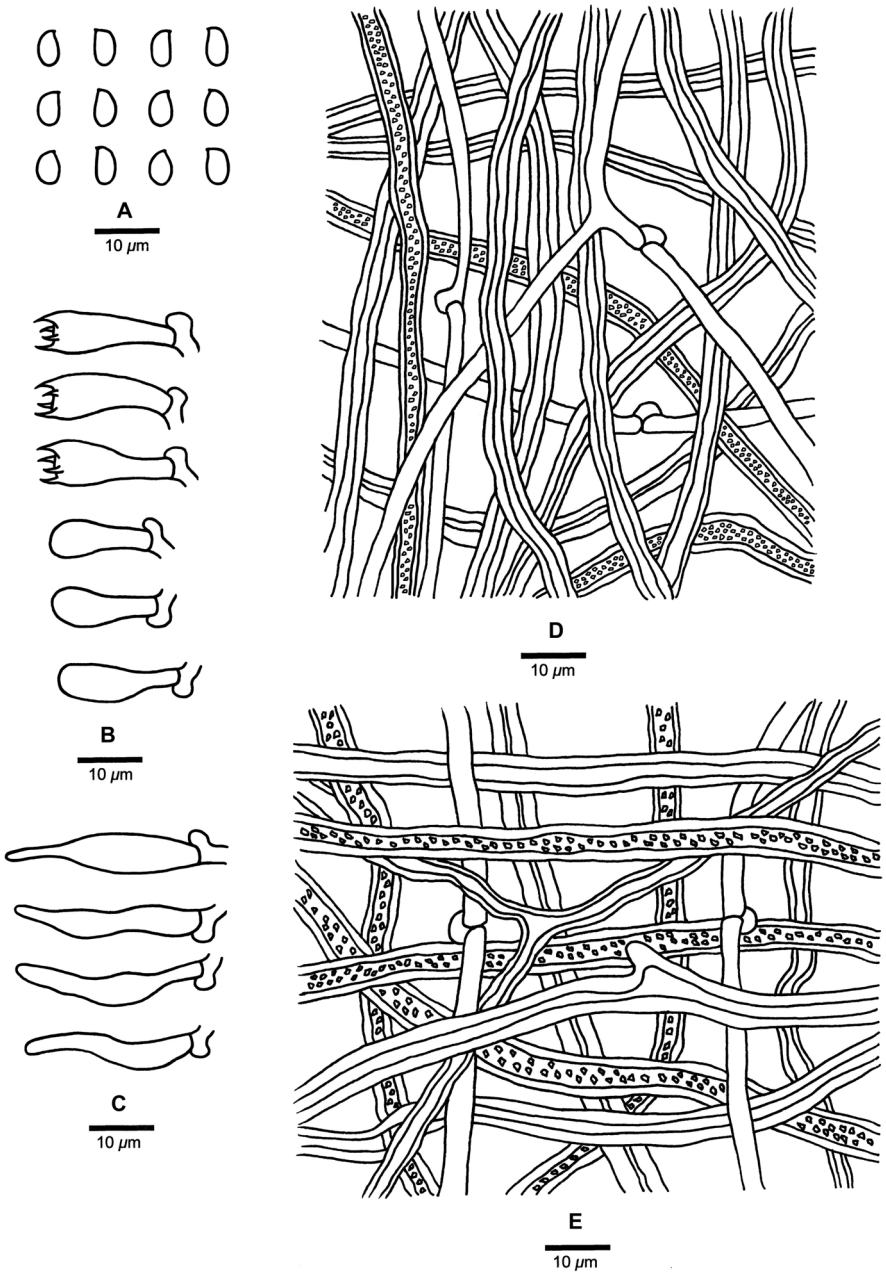


FIGURE 6 | Microscopic structures of *Fomitopsis kesiyae* (drawn from the holotype). **(A)** Basidiospores; **(B)** Basidia and basidioles; **(C)** Cystidioles; **(D)** Hyphae from trama; **(E)** Hyphae from context. Bars: **A–E** = 10 μm.

reddish brown to yellowish brown when dry, glabrous, sulcate, azonate; margin cream, distinctly paler than the pileal surface, obtuse. Pore surface white to cream when fresh, olivaceous buff to cinnamon-buff when dry; sterile margin distinct, buff to honey-yellow, up to 3 mm wide; pores round to angular, 6–8 per mm, dissepiments thick, entire. Context cream to straw-yellow, corky, up to 1.2 cm thick. Tubes concolorous with pore surface, hard corky, up to 1 cm long.

Hyphal structure. — Hyphal system dimitic; generative hyphae bearing clamp connections; skeletal hyphae IKI–, CB–; tissues unchanged in KOH. Small polyhedric or irregular crystals present among context and tubes.

Context. — Generative hyphae infrequent, hyaline, thin- to slightly thick-walled, rarely branched, 1.9–4.2 μm in diam; skeletal hyphae dominant, yellowish brown to cinnamon brown, thick-walled with a wide to narrow lumen, occasionally branched, straight to flexuous, interwoven, 2.2–9.2 μm in diam.

Tubes. — Generative hyphae infrequent, hyaline, thin-walled, occasionally branched, 1.9–3 μm in diam; skeletal hyphae dominant, hyaline to pale yellowish, thick-walled with a wide to

narrow lumen, rarely branched, more or less straight, interwoven, 1.7–6.2 μm in diam. Cystidia absent, but fusoid cystidioles occasionally present, hyaline, thin-walled, 11.5–30.4 × 2.6–6 μm. Basidia clavate, bearing four sterigmata and a basal clamp connection, 16–20.3 × 4.8–7.2 μm; basidioles dominant, in shape similar to basidia, but smaller.

Spores. — Basidiospores oblong-ellipsoid to ellipsoid, hyaline, thin-walled, smooth, IKI–, CB–, (4.5–)4.8–5.3(–6) × (2.8–)3–3.5(–4) μm, L = 5.04 μm, W = 3.11 μm, Q = 1.60–1.65 (*n* = 60/2).

Type of rot. — Brown rot.

Additional specimen (paratype) examined: **VIETNAM**. Dam Dong Province, Da Lat, Bidoup Nui Ba National Park, on fallen trunk of *Pinus kesiya*, 16 October 2017, *Cui 16466* (BJFC 029765).

Fomitopsis massoniana B.K. Cui, M.L. Han & Shun Liu, **sp. nov.** (**Figures 3G,H**, 7).

MycoBank: MB 838911

Fomitopsis massoniana is characterized by its effused-reflexed to pileate basidiocarps, applanate to triquetrous or irregular

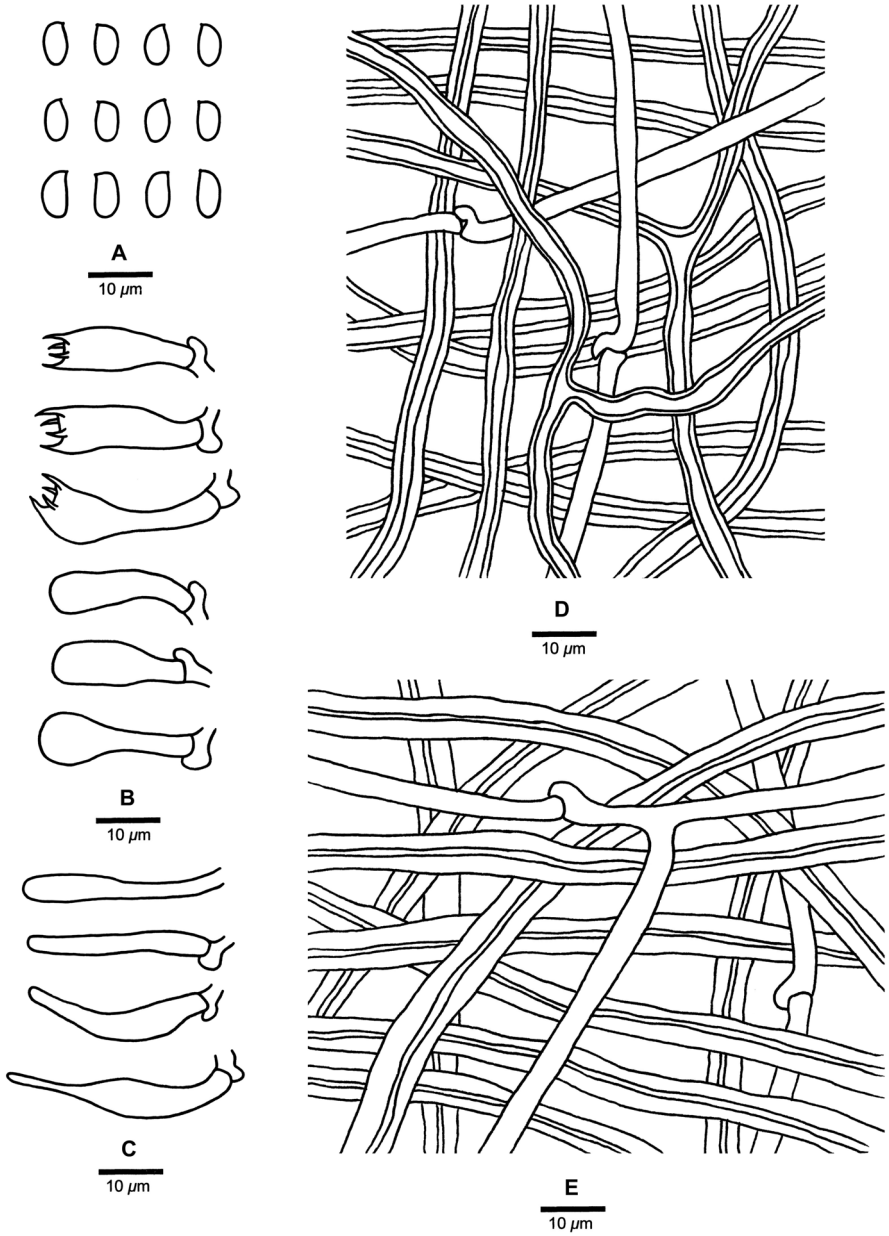


FIGURE 7 | Microscopic structures of *Fomitopsis massoniana* (drawn from the holotype). **(A)** Basidiospores; **(B)** Basidia and basidioles; **(C)** Cystidioles; **(D)** Hyphae from trama; **(E)** Hyphae from context. Bars: **A–E** = 10 μm.

pilei with buff-yellow to apricot-orange pileal surface when fresh, buff to grayish brown when dry, a white to cream pore surface when fresh, cream to buff when dry, and grows on *Pinus massoniana*.

Type. — **CHINA**. Fujian Province, Wuping County, Liangyeshan Nature Reserve, on dead tree of *Pinus massoniana*, 25 October 2013, *Cui 11304* (Holotype, BJFC 015420).

Etymology. — *Massoniana* (Lat.), refers to the host tree species *Pinus massoniana*.

Basidiocarps. — Annual, effused-reflexed to pileate, sessile, hard corky, without odor or taste when fresh, woody hard and light in weight upon drying. Pilei applanate to triquetrous or irregular, projecting up to 4 cm long, 4.2 cm wide, 1.5 cm thick at base. Pileal surface laccate, buff-yellow to apricot-orange when fresh, becoming buff to grayish brown when dry, glabrous, sulcate, azonate; margin white to cream, obtuse. Pore surface white to cream when fresh, turning cream to buff when dry; sterile margin distinct, cream, up to 4 mm wide; pores round, 5–7 per mm, dissepiments thick, entire. Context cream to straw-yellow, woody hard, up to 0.8 cm thick. Tubes concolorous with pore surface, woody hard, up to 0.4 cm long.

Hyphal structure. — Hyphal system dimitic; generative hyphae bearing clamp connections; skeletal hyphae IKI–, CB–; tissues unchanged in KOH.

Context. — Generative hyphae infrequent, hyaline, thin- to slightly thick-walled, occasionally branched, 2–4.5 μm in diam; skeletal hyphae dominant, hyaline, thick-walled with a narrow lumen to subsolid, rarely branched, straight, interwoven, 2.2–8.2 μm in diam.

Tubes. — Generative hyphae infrequent, hyaline, thin-walled, rarely branched, 1.8–4 μm in diam; skeletal hyphae dominant, hyaline, thick-walled with a narrow lumen to narrow lumen, occasionally branched, more or less straight, interwoven, 2–7.2 μm in diam. Cystidia absent, but fusoid cystidioles occasionally present, hyaline, thin-walled, 14.8–36 × 3.8–6 μm. Basidia clavate, bearing four sterigmata and a basal clamp connection, 17–26.5 × 5.5–7.9 μm; basidioles dominant, in shape similar to basidia, but smaller.

Spores. — Basidiospores oblong-ellipsoid, hyaline, thin-walled, smooth, IKI–, CB–, (5.8–)6.2–7.3(–7.6) × (3–)3.3–4 μm, L = 6.91 μm, W = 3.53 μm, Q = 1.93–1.99 (*n* = 90/3).

Type of rot. — Brown rot.

Additional specimens (paratypes) examined: **CHINA**. Fujian Province, Wuping County, Liangyeshan Nature Reserve, on dead tree of *Pinus massoniana*, 25 October 2013, *Cui 11288* (BJFC 015404); Wuyishan County, Longchuan Valley, on dead tree of *Pinus massoniana*, 16 October 2005, *Cui 2848* (BJFC 000719); Guangdong Province, Fengkai County, Heishiding Nature Reserve, on fallen trunk of *Pinus massoniana*, 2 July 2010, *Cui 9058* (BJFC 007996).

Fomitopsis subpinicola B.K. Cui, M.L. Han & Shun Liu, **sp. nov.** (**Figures 3I,J**, **8**).

MycoBank: MB 838912

Fomitopsis subpinicola is characterized by its apricot-orange, scarlet to fuscous pileal surface when fresh, reddish brown to dark brown when dry, occasionally septated skeletal hyphae and is distributed in Northeast China.

Type. — **CHINA**. Heilongjiang Province, Yichun, Fenglin Nature Reserve, on fallen trunk of *Pinus koraiensis*, 2 August 2011, *Cui 9836* (Holotype, BJFC 010729).

Etymology. — *Subpinicola* (Lat.), refers to the new species resembling *F. pinicola* in morphology.

Basidiocarps. — Annual, pileate, sessile, hard corky, without odor or taste when fresh, woody hard and light in weight upon drying. Pilei applanate, circular to sectorial, projecting up to 7.5 cm long, 8.5 cm wide, 4.5 cm thick at base. Pileal surface laccate, apricot-orange, scarlet to fuscous when fresh, becoming reddish brown to dark brown upon drying, glabrous, sulcate, azonate; margin white to cream, distinctly paler than the pileal surface, obtuse. Pore surface white to cream when fresh, turning buff yellow to buff when dry; sterile margin distinct, white to cream, up to 6 mm wide; pores round, 6–8 per mm, dissepiments thick, entire. Context cream to straw-yellow, woody hard, up to 1.2 cm thick. Tubes concolorous with pore surface, woody hard, up to 0.5 cm long.

Hyphal structure. — Hyphal system dimitic; generative hyphae bearing clamp connections; skeletal hyphae IKI–, CB–; tissues unchanged in KOH.

Context. — Generative hyphae infrequent, hyaline, thin- to slightly thick-walled, rarely branched, 2–3.2 μm in diam; skeletal hyphae dominant, yellowish brown to cinnamon brown, thick-walled with a narrow lumen to subsolid, occasionally branched, straight, interwoven, 2.2–6.8 μm in diam.

Tubes. — Generative hyphae infrequent, hyaline, thin-walled, rarely branched, 1.8–3 μm in diam; skeletal hyphae dominant, yellowish brown to cinnamon brown, thick-walled with a wide to narrow lumen, occasionally septate, without clamps, rarely branched, straight, interwoven, 1.9–6.2 μm in diam. Cystidia absent, but fusoid cystidioles occasionally present, hyaline, thin-walled, 14.5–34.6 × 3.2–7.2 μm. Basidia clavate, bearing four sterigmata and a basal clamp connection, 16–24.5 × 4.5–9 μm; basidioles dominant, in shape similar to basidia, but smaller.

Spores. — Basidiospores oblong-ellipsoid to ellipsoid, hyaline, thin-walled, smooth, IKI–, CB–, (4–)4.3–5.5(–5.9) × (2.5–)2.7–3.3(–3.5) μm, L = 4.94 μm, W = 2.97 μm, Q = 1.65–1.69 (*n* = 90/3).

Type of rot. — Brown rot.

Additional specimens (paratypes) examined: **CHINA**. Heilongjiang Province, Yichun, Fenglin Nature Reserve, on fallen trunk of *Pinus koraiensis*, 1 August 2011, *Cui 9819* (BJFC 010712); Tangyuan County, Daliangzihe Forest Park, on living tree of *Pinus koraiensis*, 26 August 2008, *Yuan 4912* (BJFC 015654); Inner Mongolia, Genhe, Greater Khingan Mountains Nature Reserve, on *Larix*, 28 August 2009, *Dai 11101* (BJFC 015660), *Dai 11206* (BJFC 015661); Jilin Province, Antu County, Changbaishan Nature Reserve, on fallen trunk of *Betula*, 7 September 2013, *Dai 13480* (BJFC 014941).

Fomitopsis tianshanensis B.K. Cui & Shun Liu, **sp. nov.** (**Figures 3K,L**, **9**).

MycoBank: MB 838913

Fomitopsis tianshanensis is characterized by its effused-reflexed to pileate basidiocarps with soft corky texture when fresh, large pores (1–3 per mm) and long tubes (up to 2.5 cm),

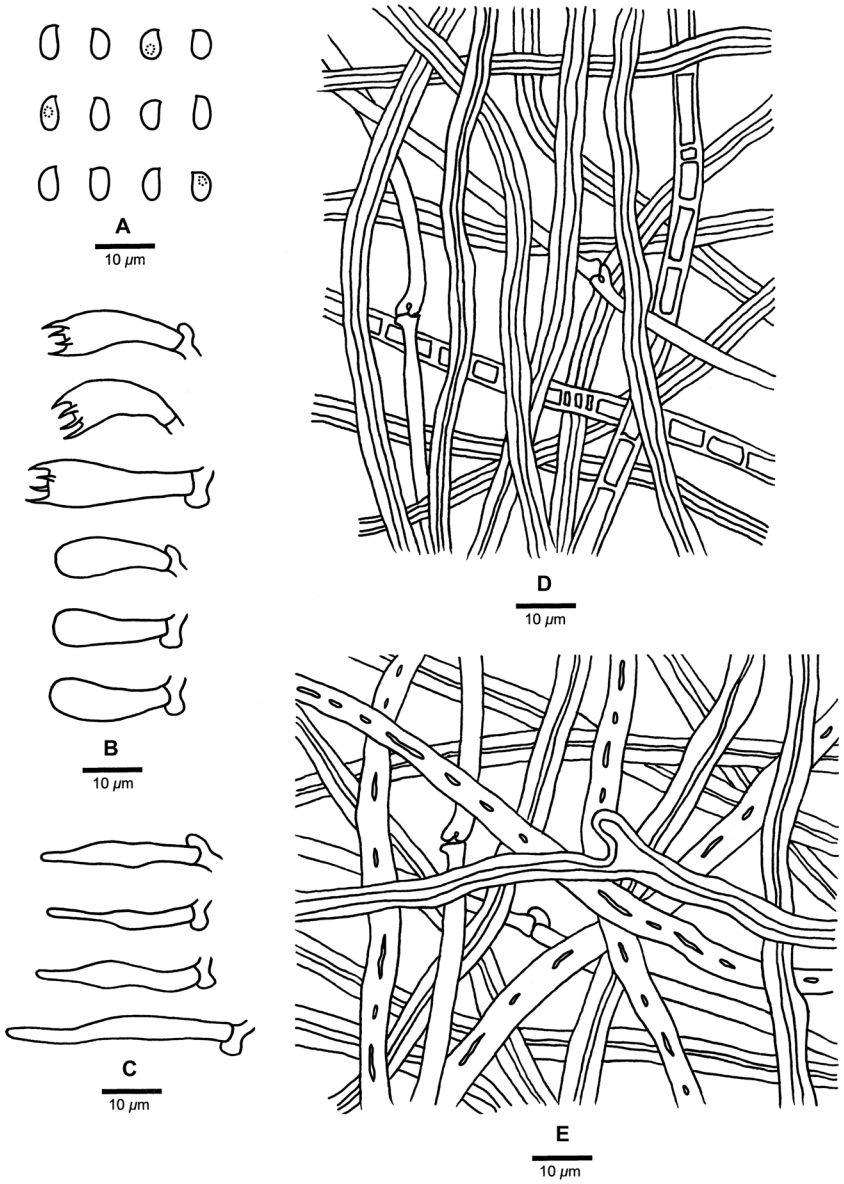


FIGURE 8 | Microscopic structures of *Fomitopsis subpinicola* (drawn from the holotype). **(A)** Basidiospores; **(B)** Basidia and basidioles; **(C)** Cystidioles; **(D)** Hyphae from trama; **(E)** Hyphae from context. Bars: **A–E** = 10 μm.

grows on *Picea* and is distributed in Tianshan Mountains Xinjiang, China.

Type. — **CHINA**. Xinjiang Autonomous Region, Fukang County, Tianshan Tianchi Nature Reserve, on fallen trunk of *Picea schrenkiana*, 4 July 2018, *Cui 16821* (Holotype, BJFC 030120).

Etymology. — *Tianshanensis* (Lat.), refers to the species located at the Tianshan regions.

Basidiocarps. — Annual to perennial, effused-reflexed to pileate, sessile, soft corky, without odor or taste when fresh, hard corky and light in weight upon drying. Pilei applanate, semicircular to ungulate, projecting up to 11 cm long, 20 cm wide, 7 cm thick at base. Pileal surface dark bluish gray to yellowish brown when fresh, becoming fawn to deep olive when dry, slightly velutinate, small nodules appear near the base, rough, azonate; margin cream to cinnamon, obtuse to acute. Pore surface cream to pinkish buff when fresh, becoming faint yellow to light pink when dry; sterile margin distinct, cream to buff, up to 3 mm wide; pores mostly round, occasionally angular, 1–3 per mm, dissepiments thick, entire. Context cream to buff, corky, up to 3.5 cm thick. Tubes concolorous with pore surface, hard corky, up to 2.5 cm long.

Hyphal structure. — Hyphal system dimitic; generative hyphae bearing clamp connections; skeletal hyphae IKI–, CB–; tissues unchanged in KOH.

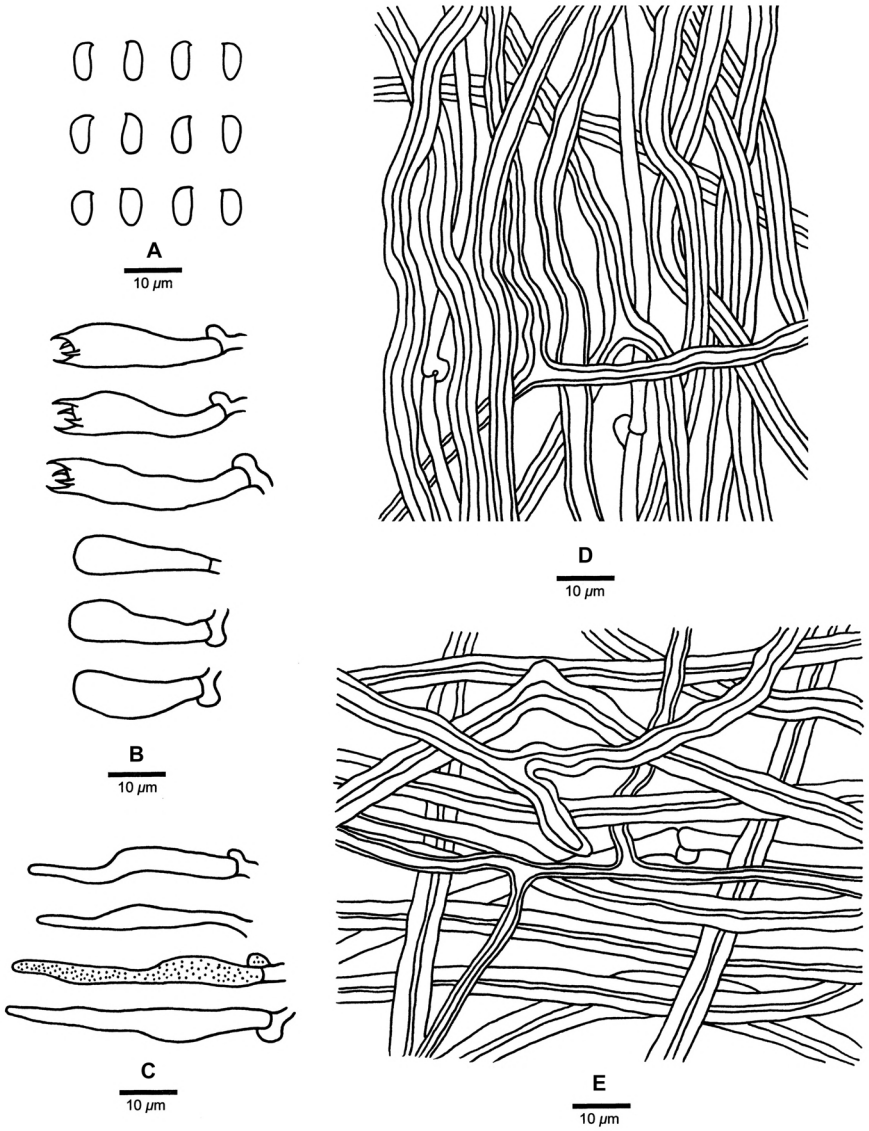


FIGURE 9 | Microscopic structures of *Fomitopsis tianshanensis* (drawn from the holotype). **(A)** Basidiospores; **(B)** Basidia and basidioles; **(C)** Cystidioles; **(D)** Hyphae from trama; **(E)** Hyphae from context. Bars: **A–E** = 10 μm.

Context. — Generative hyphae infrequent, hyaline, thin- to slightly thick-walled, rarely branched, 2–4 μm in diam; skeletal hyphae dominant, yellowish brown to cinnamon brown, thick-walled with a narrow lumen to subsolid, occasionally branched, straight to flexuous, interwoven, 2.2–7.2 μm in diam.

Tubes. — Generative hyphae infrequent, hyaline, thin-walled, rarely branched, 1.9–3.2 μm in diam; skeletal hyphae dominant, hyaline to pale yellowish, thick-walled with a wide lumen, occasionally branched, straight to flexuous, 2–6.9 μm in diam, interwoven. Cystidia absent, sometimes skeletal hyphae penetrated into the hymenium, but not forming typical catahymenium; cystidioles present, fusoid, hyaline, thin-walled, 15.5–44 × 3.3–6.5 μm. Basidia clavate, bearing four sterigmata and a basal clamp connection, 17–32.5 × 4.2–9.5 μm; basidioles dominant, in shape similar to basidia, but smaller.

Spores. — Basidiospores oblong-ellipsoid, sometimes tapering at apiculus, hyaline, thin-walled, smooth, IKI–, CB–, (6–)6.3–7(–7.2) × (3–)3.2–3.8(–4) μm, L = 6.62 μm, W = 3.52 μm, Q = 1.85–1.93 (*n* = 90/3).

Type of rot. — Brown rot.

Additional specimens (paratypes) examined: **CHINA**. Xinjiang Autonomous Region, Urumqi, Nanshan Park, on fallen trunk of *Picea schrenkiana*, 5 July 2018, *Cui 16823* (BJFC 030122), *Cui 16825* (BJFC 030124), *Cui 16828* (BJFC 030127); Shawan County, Lujiaowan Park, on stump of *Picea schrenkiana*, 6 July 2018, *Cui 16830* (BJFC 030129).

Other Specimens of the *Fomitopsis pinicola* Complex Examined

Fomitopsis mounceae. **CANADA**. 3 August 2000, *Teuvo Ahti 60351* (H); on *Picea glauca*, 25 July 1982, *Tuomo Niemelä 2530* (H). **UNITED STATES**. On *Betula*, 15 September 2014, *OM 18782* (H); on *Tsuga heterophylla*, 11 September 2014, *Spirin 8367* (H).

Fomitopsis ochracea. **UNITED STATES**. *OM 18568* (H), *OM 18673* (H); on *Picea*, *Spirin 8165* (H).

Fomitopsis schrenkii. **UNITED STATES**. 7 September 1992, *Inkeri Ahonen 58* (BJFC 013921); Turkey Creek, Chricahua Mountain, Arizona, on *Douglas fir*, September 2012, *Josef Vlasák 1209/61-J* (BJFC 015604).

Fomitopsis pinicola. **FINLAND**. Helsinki, Vantaa, Tamisto Nature Reserve, on fallen trunk of *Picea*, 16 August 2012, *Dai 12869* (BJFC 013149), *Dai 12870* (BJFC 013150). **ITALY**. Roma, Trentino Altoadie, Trento, Molveno, on *Picea*, 28 April 2005, *Dai 6553* (IFP). **POLAND**. On dead tree of *Pinus*, 3 October 2014, *Dai 14841* (BJFC 017955); Lesser Poland Voivodeship, Gorce National Park, on *Picea abies*, 9 July 1985, *Pekka Nuorteva* (H).

DISCUSSION

Based on the phylogenetic analyses, 10 species of the *Fomitopsis pinicola* complex grouped together (**Figures 1**, **2**), including six new species from East Asia: *F. abieticola*, *F. hengduanensis*, *F. kesiyae*, *F. massoniana*, *F. subpinicola*, and *F. tianshanensis*. The main morphological characters of species in the *F. pinicola* complex are provided in **Table 2**.

In the phylogenetic trees (**Figures 1**, **2**), *Fomitopsis abieticola* is closely related to *F. tianshanensis*. Morphologically, both *F. abieticola* and *F. tianshanensis* have an annual to perennial growth habit, cream to pinkish pore surface when fresh, and large pores, but *F. tianshanensis* differs in its soft corky basidiocarps when fresh, and usually grows on *Picea*. *Fomitopsis schrenkii* has similar pores (3–4 per mm), but it has smaller basidia (12–22 × 6–8 μm), and slightly wider basidiospores (5.7–6.7 × 3.7–4.2 μm). *Fomitopsis hengduanensis* was also discovered in the Yunnan Province, but *F. hengduanensis* differs with smaller pores (6–8 per mm) and smaller basidiospores (5.2–6 × 3.2–3.6 μm).

Phylogenetically, *Fomitopsis hengduanensis* grouped together with *F. kesiyae* (**Figures 1**, **2**). Morphologically, *F. hengduanensis* and *F. kesiyae* share a white to cream pore surface when fresh and have similar pores, but *F. kesiyae* differs in having a buff yellow to orange-yellow buff pileal surface when fresh, reddish brown to yellowish brown when dry, and grows on the *Pinus kesiya* tree. *Fomitopsis pinicola*, *F. schrenkii* and *F. mounceae* all have similar pilei, but they have larger pores (4–6 per mm in *F. pinicola*, 3–4 per mm in *F. schrenkii*, 3–5 per mm in *F. mounceae*; **Table 2**). *Fomitopsis subpinicola* has similar sized pores, but it has smaller basidia (16.1–24.5 × 4.5–9 μm) and basidiospores (4.3–5.5 × 2.7–3.3 μm) and is distributed in south northeast China.

Fomitopsis kesiyae was described from Vietnam on the tree of *Pinus kesiya*. Phylogenetically, two sampled specimens of *F. kesiyae* formed a high supported lineage (99% ML, 99% MP, 1.00 BPP) and are closely related to *F. hengduanensis* (**Figures 1**, **2**). However, *F. hengduanensis* differs in having larger basidia (16.6–34.5 × 5.4–10.2 μm) and basidiospores (5.2–6 × 3.2–3.6 μm). *Fomitopsis subpinicola* has similar sized pores (6–8 per mm) and basidiospores (4.3–5.5 × 2.7–3.3 μm), but it has an apricot-orange, scarlet to fuscous pileal surface when fresh, and is reddish brown to dark brown when dry. *Fomitopsis massoniana* has a similar colored pileal surface when fresh and similar sized pores (5–7 per mm), but it has larger basidiospores (6.2–7.3 × 3.3–4 μm) and grows on *Pinus massoniana* rather than *Pinus kesiya*.

Morphologically, *Fomitopsis massoniana* is similar to *F. kesiyae*; both species have an annual growth habit and a similar colored pileal surface when fresh. However, *F. kesiyae* differs in having smaller basidiospores (4.8–5.3 × 3–3.5 μm), is distributed in Vietnam, and grows on *Pinus kesiya*. *Fomitopsis hengduanensis* has similar sized pores (6–8 per mm), but compared to *F. massoniana*, *F. hengduanensis* has larger sized basidiocarps, a laccate pileal surface with pale dark gray to reddish brown at base and cream to flesh-pink toward the margin when fresh, and smaller sized basidiospores (5.2–6 × 3.2–3.6 μm). Phylogenetically, these two species are distinct from each other (**Figures 1**, **2**). *Fomitopsis massoniana* is closely related to *F. subpinicola*, they share a cream to buff pore surface and have similar sized pores, but *F. subpinicola* has smaller basidiospores (4.3–5.5 × 2.7–3.3 μm).

Fomitopsis subpinicola can be easily separated from *F. pinicola* by its apricot-orange, scarlet to fuscous pileal surface when fresh, reddish brown to dark brown when dry, smaller basidiospores (4.3–5.5 × 2.7–3.3 μm) and is located in the Northeast of China. Phylogenetically, *F. subpinicola* is closely related to *F. massoniana*. Morphologically, *F. subpinicola* is similar to *F. massonian*, which has an annual growth habit and white to cream pore surface when fresh. But *F. massoniana* differs by its effused-reflexed to pileate basidiocarps, lager basidiospores (6.2–7.3 × 3.3–4 μm) and grows on the *Pinus massoniana* tree. *Fomitopsis hengduanensis* and *F. kesiyae* have similar sized pores (6–8 per mm), but *F. hengduanensis* has larger sized basidia (16.6–34.5 × 5.4–10.2 μm), *F. kesiyae* has a buff yellow to orange-yellow buff pileal surface when fresh, reddish brown to yellowish brown when dry, and grows on the *Pinus kesiya* tree.

Phylogenetically, specimens of *Fomitopsis tianshanensis* formed a well-supported lineage (**Figures 1**, **2**) and are grouped with *F. abieticola*. But *F. abieticola* differs from *F. tianshanensis* in having large sized cystidioles (17.5–50.2 × 4.3–9.5 μm), basidia (20.8–40.5 × 5.5–11.5 μm), and basidiospores (7–9 × 4–5 μm). *Fomitopsis pinicola* also grows mainly on *Picea*, but it has smaller pores (4–6 per mm), a brownish orange to black pileal surface at base and buff-yellow to cinnamon toward the margin when fresh, and is distributed in Europe.

Previously, *Fomitopsis pinicola* was used as a broad species concept, specimens from Europe, North America, and East Asia were all identified as *F. pinicola* based on morphological characters (Gilbertson and Ryvarden, 1986; Ryvarden and Gilbertson, 1993; Núñez and Ryvarden, 2001; Dai, 2012; Ryvarden and Melo, 2014). Recent phylogenetic analyses indicated that *F. pinicola* is a species complex and represent

TABLE 2 | A comparison of species in the *Fomitopsis pinicola* complex.

Species	Distribution	Basidio-	Pileal surface	Host	Pores (per mm)	Cystidia (μm)	Basidiospores		References
		carps	when fresh				L × W (μm)	Q = L/W	
F. abieticola	Southwestern China	Annual to perennial; pileate	Cream to pinkish buff	*Abies*	2–4	17.5–50.2 × 4.3–9.5	7–9 × 4–5	1.83–1.89	This study
F. hengduanensis	High altitude areas of the Hengduan Mountains of southwestern China	Annual to perennial; pileate	Pale dark gray to reddish brown at base and cream to flesh-pink toward the margin	*Picea*, *Pinus*	6–8	13.2–36.5 × 2.5–5.4	5.2–6 × 3.2–3.6	1.57–1.63	This study
F. kesiyae	Tropical areas of Vietnam	Annual; pileate	Buff yellow to orange-yellow buff	*Pinus kesiya*	6–8	11.5–30.4 × 2.6–6	4.8–5.3 × 3–3.5	1.60–1.65	This study
F. massoniana	Southeastern China	Annual; effused-reflexed to pileate	Buff-yellow to apricot-orange	*Pinus massoniana*	5–7	14.8–36 × 3.8–6	6.2–7.3 × 3.3–4	1.85–1.9	This study
F. mounceae	Canada, northern United States	Perennial; pileate	Brownish orange to black at base and pale orange to grayish orange toward the margin	*Abies*, *Betula*, *Larix*, *Picea*, *Populus*, *Pseudotsuga*	3–5	16–35 × 3–6.5	5.8–6.6 × 3.4–4	1.7–1.9	Haight et al., 2019
F. ochracea	Canada, northern United States	Perennial; pileate	Brownish gray to grayish brown at base and orange White to pale orange toward the margin	*Abies*, *Picea*, *Populus*	4–5	20–40 × 4–6.5	5.1–5.9 × 3.6–4	1.3–1.4	Haight et al., 2019
F. pinicola	Europe	Perennial; pileate	Brownish orange to black at base and buff-yellow to cinnamon toward the margin	Mostly on *Picea* and *Pinus*, occasionally on other different gymnosperm or angiosperm wood	4–6	18–60 × 3–9	6–9 × 3–4.5	1.8–2.2	Ryvarden and Melo, 2014; Haight et al., 2016, 2019
F. schrenkii	Western and southwestern United States	Perennial; effused-reflexed to pileate	Grayish orange to olive brown at base and grayish orange to grayish yellow toward the margin	*Abies*, *Picea*, *Pinus*, *Pseudotsuga*	3–4	16–30 × 3–8	5.7–6.7 × 3.7–4.2	1.5–1.6	Haight et al., 2019
F. subpinicola	Northeastern China	Annual; pileate	Apricot-orange, scarlet to fuscous	Mostly on *Pinus koraiensis*, occasionally on *Larix*, *Betula*	6–8	14.5–34.6 × 3.2–7.2	4.3–5.5 × 2.7–3.3	1.65–1.69	This study
F. tianshanensis	Tianshan Mountains of northwestern China	Annual to perennial, effused-reflexed to pileate	Dark bluish gray to yellowish brown	*Picea*	1–3	15.5–44 × 3.3–6.5	6.3–7 × 3.2–3.8	1.9–1.96	This study

several different species. Haight et al. (2016) proposed four well-supported clades: one lineage *F. pinicola* sensu stricto from Europe and three lineages from North America. Subsequently, Haight et al. (2019) identified these three lineages as *F. mounceae*, *F. ochracea,* and *F. schrenkii* from North America, and *F. pinicola* is restricted to Eurasia and does not occur in North America. In the current study, samples previously identified as *F. pinicola* from China and Vietnam in East Asia represent six distinct species. Furthermore, our results indicated that species of the *F. pinicola* complex usually have limited distribution areas and host specialization. In East Asia, *F. abieticola* is distributed in southwestern China and grows on *Abies*; *F. hengduanensis* is distributed in high altitude areas of the Hengduan Mountains of southwestern China, and it mostly grows on *Picea*, occasionally on other gymnosperm wood; *F. kesiyae* is distributed in tropical areas of Vietnam and grows only on *Pinus kesiya*; *F. massoniana* is distributed in southeastern China and grows only on *Pinus massoniana*; *F. subpinicola* was found in northeastern China and grows mainly on *Pinus koraiensis*, occasionally on other gymnosperm or angiosperm wood; *F. tianshanensis* is distributed in Tianshan Mountains of northwestern China and only grows on *Picea schrenkiana*. In Europe, *F. pinicola* is widespread, and it mostly grows on *Picea* and *Pinus*, occasionally on other different gymnosperm or angiosperm wood (Ryvarden and Melo, 2014). In North America, *F. mounceae* and *F. ochracea* is distributed in Canada and the northern United States, and they grow on different gymnosperm or angiosperm wood (Ryvarden and Stokland, 2008; Haight et al., 2019); *F. schrenkii* is distributed in western and southwestern regions of the United States and mostly grows on different gymnosperm wood, rarely on angiosperm wood (Haight et al., 2019). Among the wood-rotting fungi, some other polypore genera also have limited distribution areas and host specializations, such as *Bondarzewia* Singer (Song et al., 2016), *Heterobasidion* Bref. (Chen et al., 2015; Yuan et al., 2020), *Laetiporus* Murrill (Song and Cui, 2017), and *Sanghuangporus* Sheng H. Wu, L.W. Zhou & Y.C. Dai (Zhu et al., 2019).

Key to Accepted Species of *Fomitopsis pinicola* Complex

1. Distribution in East Asia	2
1. Distribution in North America or Europe	7
2. Pores < 5 per mm	3
2. Pores 5–8 per mm	4
3. Basidiospores oblong-ellipsoid to ellipsoid, 7–9 × 4–5 μm	*F. abieticola*
3. Basidiospores oblong-ellipsoid, 6.3–7 × 3.2–3.8 μm	*F. tianshanensis*
4. Distribution in tropical areas	*F. kesiyae*
4. Distribution in temperate areas	5
5. Basidiocarps annual to perennial; pileal surface cream to flesh-pink toward the margin when fresh	*F. hengduanensis*
5. Basidiocarps annual; pileal surface white to cream toward the margin when fresh	6
6. Basidiospores oblong-ellipsoid, 6.2–7.3 × 3.3–4 μm	*F. massoniana*
6. Basidiospores oblong-ellipsoid to ellipsoid, 4.3–5.5 × 2.7–3.3 μm	*F. subpinicola*
7. Pilei never with reddish brown band	*F. ochracea*
7. Pilei with reddish brown band	8
8. Distribution in Europe; basidia < 20 μm long	*F. pinicola*
8. Distribution in North America; basidia > 20 μm long	9
9. Basidiospores ellipsoid to cylindrical, Q = 1.6–1.9	*F. mounceae*
9. Basidiospores ellipsoid to broadly cylindrical, Q = 1.5–1.6	*F. schrenkii*

DATA AVAILABILITY STATEMENT

The datasets presented in this study can be found in an online repository. The name of the repository and accession number can be found below: https://treebase.org/treebase-web/search/study/summary.html?id=27994&x-access-code=ab2495717aaf081f0557e6680c381710&agreement=ok, submission ID: 27994.

AUTHOR CONTRIBUTIONS

B-KC and SL designed the experiment. SL, M-LH, D-MW, and B-KC prepared the samples. SL, T-MX, and YW conducted the molecular experiments and analyzed the data. SL, D-MW, and B-KC drafted the manuscript. All the authors approved the manuscript.

FUNDING

This research was supported by the National Natural Science Foundation of China (Nos. U2003211, 31750001), the Scientific and Technological Tackling Plan for the Key Fields of Xinjiang Production and Construction Corps (No. 2021AB004) Beijing Forestry University Outstanding Young Talent Cultivation Project (No. 2019JQ03016), and the Biodiversity Survey and Assessment Project of the Ministry of Ecology and Environment, China (No. 2019HJ2096001006).

ACKNOWLEDGMENTS

We express our gratitude to Drs. Yu-Cheng Dai (China), Josef Vlasák (Czech Republic), and the curators of herbaria of H and IFP for loaning the specimens. Drs. De-Wei Li (United States), Jie Song (China), and Ms. Xing Ji (China) are thanked for companionship during field collections.

REFERENCES

Bao, H. Y., Sun, Q., Huang, W., Sun, X., Bau, T., and Li, Y. (2015). Immunological regulation of fermentation mycelia of *Fomitopsis pinicola* on mice. *Mycosystema* 34, 287–292.

Chen, J. J., Cui, B. K., Zhou, L. W., Korhonen, K., and Dai, Y. C. (2015). Phylogeny, divergence time estimation, and biogeography of the genus *Heterobasidion* (Basidiomycota, Russulales). *Fungal Divers.* 71, 185–200. doi: 10.1007/s13225-014-0317-2

Chen, Y. Y., Wu, F., Wang, M., and Cui, B. K. (2017). Species diversity and molecular systematics of *Fibroporia* (Polyporales. Basidiomycota) and its related genera. *Mycol. Prog.* 16, 521–533. doi: 10.1007/s11557-017-1285-1

Cui, B. K., Li, H. J., Ji, X., Zhou, J. L., Song, J., Si, J., et al. (2019). Species diversity, taxonomy and phylogeny of Polyporaceae (Basidiomycota) in China. *Fungal Divers.* 97, 137–392. doi: 10.1007/s13225-019-00427-4

Dai, Y. C. (2012). Polypore diversity in China with an annotated checklist of Chinese polypores. *Mycoscience* 53, 49–80. doi: 10.1007/s10267-011-0134-3

Dai, Y. C., Yang, Z. L., Cui, B. K., Yu, C. J., and Zhou, L. W. (2009). Species diversity and utilization of medicinal mushrooms and fungi in China (Review). *Int. J. Med. Mushrooms* 11, 287–302. doi: 10.1615/IntJMedMushr.v11.i3.80

Farris, J. S., Källersjö, M., Kluge, A. G., Kluge, A. G., and Bult, C. (1994). Testing significance of incongruence. *Cladistics* 10, 315–319. doi: 10.1006/clad.1994.1021

Felsenstein, J. (1985). Confidence intervals on phylogenies: an approach using the bootstrap. *Evolution* 39, 783–791. doi: 10.1111/j.1558-5646.1985.tb00420.x

Gilbertson, R. L., and Ryvarden, L. (1986). *North American polypores*, Vol. 1. Oslo: Fungiflora.

Guler, P., Akata, I., and Kutluer, F. (2009). Antifungal activities of *Fomitopsis pinicola* (Sw.: Fr.) Karst. and *Lactarius vellereus* (Pers.). *Fr. Afr. J. Biotechnol.* 8, 3811–3813. doi: 10.5897/AJB09.719

Guo, S. S., and Wolf, D. R. (2018). Study on neuroprotective effects of water extract of *Fomitopsis pinicola* on dopaminergic neurons in vitro. *Chin. J. Pharma.* 15, 582–586.

Haight, J. E., Laursen, G. A., Glaeser, J. A., and Taylor, D. L. (2016). Phylogeny of *Fomitopsis pinicola*: a species complex. *Mycologia* 108, 925–938. doi: 10.3852/14-225R1

Haight, J. E., Nakasone, K. K., Laursen, G. A., Redhead, S. A., Taylor, D. L., and Glaeser, J. A. (2019). *Fomitopsis mounceae* and *F. schrenkii*—two new species from North America in the *F. pinicola* complex. *Mycologia* 111, 339–357. doi: 10.1080/00275514.2018.1564449

Hall, T. A. (1999). Bioedit: a user-friendly biological sequence alignment editor and analysis program for Windows 95/98/NT. *Nucleic Acids Symp. Ser.* (Oxford) 41, 95–98. doi: 10.1021/bk-1999-0734.ch008

Han, M. L., and Cui, B. K. (2015). Morphological characters and molecular data reveal a new species of *Fomitopsis* (Polyporales) from southern China. *Mycoscience* 56, 168–176. doi: 10.1016/j.myc.2014.05.004

Han, M. L., Chen, Y. Y., Shen, L. L., Song, J., Vlasák, J., Dai, Y. C., et al. (2016). Taxonomy and phylogeny of the brown-rot fungi: *Fomitopsis* and its related genera. *Fungal Divers.* 80, 343–373. doi: 10.1007/s13225-016-0364-y

Han, M. L., Song, J., and Cui, B. K. (2014). Morphology and molecular phylogeny for two new species of *Fomitopsis* (Basidiomycota) from South China. *Mycol. Prog.* 13, 905–914. doi: 10.1007/s11557-014-0976-0

Hillis, D. M., and Bull, J. J. (1993). An empirical test of bootstrapping as a method for assessing confidence in phylogenetic analysis. *Syst. Biodivers.* 42, 182–192. doi: 10.1093/sysbio/42.2.182

Högberg, N., Holdenreider, O., and Stenlid, J. (1999). Population structure of the wood decay fungus *Fomitopsis pinicola*. *Heredity* 83, 354–360. doi: 10.1038/sj.hdy.6885970

Karsten, P. A. (1881). Symbolae ad mycologiam Fennicam. 8. *Acta Soc. Fauna Flora Fenn.* 6, 7–13.

Katoh, K., and Standley, D. M. (2013). MAFFT Multiple sequence alignment software version 7: improvements in performance and usability. *Mol. Biol. Evol.* 30, 772–780. doi: 10.1093/molbev/mst010

Leavitt, S. D., Fankhauser, J. D., Leavitt, D. H., Porter, L. D., Johnson, L. A., and Clair, L. L. S. (2011). Complex patterns of speciation in cosmopolitan "rock posy" lichens—discovering and delimiting cryptic fungal species in the lichen-forming *Rhizoplaca melanophthalma* species-complex (Lecanoraceae, Ascomycota). *Mol. Phylogenet. Evol.* 59, 587–602. doi: 10.1016/j.ympev.2011.03.020

Li, H. J., Han, M. L., and Cui, B. K. (2013). Two new *Fomitopsis* species from southern China based on morphological and molecular characters. *Mycol. Prog.* 12, 709–718. doi: 10.1007/s11557-012-0882-2

Liu, S., Shen, L. L., Wang, Y., Xu, T. M., Gates, G., and Cui, B. K. (2021). Species diversity and molecular phylogeny of *Cyanosporus* (Polyporales, Basidiomycota). *Front. Microbiol.* 12:631166. doi: 10.3389/fmicb.2021.631166

Liu, S., Song, C. G., and Cui, B. K. (2019). Morphological characters and molecular data reveal three new species of *Fomitopsis* (Basidiomycota). *Mycol. Prog.* 18, 1317–1327. doi: 10.1007/s11557-019-01527-w

Maddison, W. P., and Maddison, D. R. (2017). *Mesquite: a modular system for evolutionary analysis, Version 3.2*. http://mesquiteproject.org

Matheny, P. B. (2005). Improving phylogenetic inference of mushrooms with RPB1 and RPB2 nucleotide sequences (Inocybe. Agaricales). *Mol. Phylogenet. Evol.* 35, 1–20. doi: 10.1016/j.ympev.2004.11.014

Núñez, M., and Ryvarden, L. (2001). East Asian polypores 2. *Synop. Fungorum* 14, 170–522.

Nylander, J. A. A. (2004). *MrModeltest v2. Program distributed by the author*. Uppsala: Evolutionary Biology Centre, Uppsala University.

Posada, D., and Crandall, K. A. (1998). Modeltest: testing the model of DNA substitution. *Bioinformatics* 14, 817–818. doi: 10.1093/bioinformatics/14.9.817

Rehner, S. (2001). *Primers for Elongation Factor 1-a (EF1-a)*. Available online at: http://ocid.nacse.org/research/deephyphae/EF1primer.pdf (accessed on 20 May 2020).

Ronquist, F., and Huelsenbeck, J. P. (2003). MrBayes 3: Bayesian phylogenetic inference under mixed models. *Bioinformatics* 19, 1572–1574. doi: 10.1093/bioinformatics/btg180

Ryvarden, L., and Gilbertson, R. L. (1993). European polypores 1. *Abortiporus–Lindtneria*. *Synop. Fungorum* 6, 1–387.

Ryvarden, L., and Johansen, I. (1980). *A preliminary polypora flora of East Africa*. Oslo: Fungiflora.

Ryvarden, L., and Melo, I. (2014). Poroid fungi of Europe. *Synop. Fungorum* 31, 1–455.

Ryvarden, L., and Stokland, J. (2008). *Fomitopsis ochracea* nova species. *Synop. Fungorum* 25, 44–46.

Shen, L. L., Wang, M., Zhou, J. L., Xing, J. H., Cui, B. K., and Dai, Y. C. (2019). Taxonomy and phylogeny of *Postia*. Multi-gene phylogeny and taxonomy of the brown-rot fungi: *Postia* (Polyporales, Basidiomycota) and related genera. *Persoonia* 42, 101–126. doi: 10.3767/persoonia.2019.42.05

Song, J., and Cui, B. K. (2017). Phylogeny, divergence time and historical biogeography of *Laetiporus* (Basidiomycota, Polyporales. *BMC Evol. Biol.* 17:102. doi: 10.1186/s12862-017-0948-5

Song, J., Chen, J. J., Wang, M., Chen, Y. Y., and Cui, B. K. (2016). Phylogeny and biogeography of the remarkable genus *Bondarzewia* (Basidiomycota. Russulales). *Sci. Rep.* 6:34568. doi: 10.1038/srep34568

Stamatakis, A. (2006). RAxML-VI-HPC: maximum likelihood-based phylogenetic analysis with thousands of taxa and mixed models. *Bioinformatics* 22, 2688–2690. doi: 10.1093/bioinformatics/btl446

Sun, Q., Huang, W., Bao, H. Y., Bau, T., and Li, Y. (2016). Anti-tumor and antioxidation activities of solid fermentation products of *Fomitopsis pinicola*. *Mycosystema* 35, 965–974.

Sun, Y. F., Costa-Rezende, D. H., Xing, J. H., Zhou, J. L., Zhang, B., Gibertoni, T. B., et al. (2020). Multi-gene phylogeny and taxonomy of *Amauroderma* s.lat. (Ganodermataceae). *Persoonia* 44, 206–239. doi: 10.3767/persoonia.2020.44.08

Swofford, D. L. (2002). *PAUP*. Phylogenetic analysis using parsimony (*and other methods). Version 4.0b10*. Sunderland, MA: Sinauer Associates, doi: 10.1111/j.0014-3820.2002.tb00191.x

White, T. J., Bruns, T. D., Lee, S., and Taylor, J. (1990). *Amplification and direct sequencing of fungal ribosomal RNA genes for phylogenetics in PCR Protocols, a*

guide to methods and applications. Cambridge, MA: Academic Press. 315–322. doi: 10.1016/B978-0-12-372180-8.50042-1

Yuan, Y., Chen, J. J., Korhonen, K., Martin, F. M., and Dai, Y. C. (2020). An updated global species diversity and phylogeny in the forest pathogenic genus *Heterobasidion* (Basidiomycota. Russulales). *Front. Microbiol.* 11:596393. doi: 10.3389/fmicb.2020.596393

Zhu, L., Song, J., Zhou, J. L., Si, J., and Cui, B. K. (2019). Species diversity, phylogeny, divergence time and biogeography of the genus *Sanghuangporus* (Basidiomycota). *Front. Microbiol.* 10:812. doi: 10.3389/fmicb.2019.00812

Conflict of Interest: The authors declare that the research was conducted in the absence of any commercial or financial relationships that could be construed as a potential conflict of interest.

Copyright © 2021 Liu, Han, Xu, Wang, Wu and Cui. This is an open-access article distributed under the terms of the Creative Commons Attribution License (CC BY). The use, distribution or reproduction in other forums is permitted, provided the original author(s) and the copyright owner(s) are credited and that the original publication in this journal is cited, in accordance with accepted academic practice. No use, distribution or reproduction is permitted which does not comply with these terms.

frontiers in Microbiology

ORIGINAL RESEARCH
published: 07 April 2021
doi: 10.3389/fmicb.2021.661281

Additions to the Genus *Arthrinium* (Apiosporaceae) From Bamboos in China

Yao Feng[1,2], Jian-Kui (Jack) Liu[3], Chuan-Gen Lin[4], Ya-Ya Chen[2,5], Mei-Mei Xiang[6] and Zuo-Yi Liu[2]**

[1] College of Agriculture, Guizhou University, Guiyang, China, [2] Guizhou Key Laboratory of Agricultural Biotechnology, Guizhou Academy of Agricultural Sciences, Guiyang, China, [3] School of Life Sciences and Technology, University of Electronic Science and Technology, Chengdu, China, [4] Centre of Excellence in Fungal Research, Mae Fah Luang University, Chiang Rai, Thailand, [5] Institute of Crop Germplasm Resources, Guizhou Academy of Agricultural Sciences, Guiyang, China, [6] Innovative Institute for Plant Health, Zhongkai University of Agriculture and Engineering, Guangzhou, China

Arthrinium has a widespread distribution occurring in various substrates (e.g., air, soil debris, plants, lichens, marine algae and even human tissues). It is characterized by the basauxic conidiogenesis in the asexual morph, with apiospores in the sexual morph. In this study, seventeen isolates of *Arthrinium* were collected in China. Based on their morphology and phylogenetic characterization, four new species (*A. biseriale*, *A. cyclobalanopsidis*, *A. gelatinosum,* and *A. septatum*) are described and seven known species (*A. arundinis*, *A. garethjonesii*, *A. guizhouense*, *A. hydei*, *A. neosubglobosa*, *A. phyllostachium* and *A. psedoparenchymaticum*) are identified, of which the sexual morph of three species (*A. guizhouense*, *A. phyllostachium* and *A. psedoparenchymaticum*) and asexual morph of *A. garethjonesii* are reported for the first time. The detailed descriptions, illustrations and comparisons with related taxa of these new collections are provided. Phylogenetic analyses of combined ITS, LSU, TUB2, and TEF sequence data support their placements in the genus *Arthrinium* and justify the new species establishments and identifications of known species.

Keywords: 4 new taxa, asexual-sexual morphs, multi-genes, phylogeny, taxonomy

OPEN ACCESS

Edited by:
Peter Edward Mortimer, Kunming Institute of Botany, Chinese Academy of Sciences, China

Reviewed by:
Indunil Senanayake, Shenzhen University, China
ZongLong Luo, Dali University, China

****Correspondence:***
Jian-Kui (Jack) Liu
liujiankui@uestc.edu.cn
Zuo-Yi Liu
gzliuzuoyi@163.com

Specialty section:
This article was submitted to Evolutionary and Genomic Microbiology, a section of the journal Frontiers in Microbiology

Received: *30 January 2021*
Accepted: *10 March 2021*
Published: *07 April 2021*

Citation:
Feng Y, Liu J-K, Lin C-G, Chen Y-Y, Xiang M-M and Liu Z-Y (2021) Additions to the Genus Arthrinium (Apiosporaceae) From Bamboos in China. Front. Microbiol. 12:661281. doi: 10.3389/fmicb.2021.661281

INTRODUCTION

The genus *Arthrinium* Kunze belongs to the family Apiosporaceae, which was introduced by Hyde et al. (1998) and typified by the genus *Apiospora* (Ellis, 1971; Seifert et al., 2011; Hyde et al., 2020). *Arthrinium* is the largest genus within Apiosporaceae and it has a widespread distribution on variety of hosts, 77 species have been recorded by Species Fungrom (March, 2021). Classification of *Arthrinium* was primarily based on conidial shape, conidiophores, sterile cells, and the presence of setae. Some morphologically different taxa (genera) grouped with *Arthrinium* when use the molecular data (Crous and Groenewald, 2013). Thus, those characteristics could be not fully inferred about the phylogenetic relationships for *Arthrinium* (Crous and Groenewald, 2013; Wang et al., 2018; Pintos et al., 2019). Except for being reported as saprobes (Agut and Calvo, 2004; Crous and Groenewald, 2013; Dai et al., 2016, 2017; Jiang et al., 2018; Wang et al., 2018; Jiang et al., 2019, 2020; Luo et al., 2019; Pintos et al., 2019; Yan et al., 2019; Mapook et al., 2020; Senanayake et al., 2020a; Tang et al., 2020), the species of *Arthrinium* also includes phytopathogenic fungi, for instance, *A. arundinis* causing brown culm

streak of *Phyllostachys praecox, A. phaeospermum* causing culm rot on *Phyllostachys viridis* and cutaneous infections of humans (Rai, 1989; Zhao et al., 1990; Martínez-Cano et al., 1992; Mavragani et al., 2007; Crous and Groenewald, 2013; Li et al., 2016; Wang et al., 2018).

we are carrying out the survey of fungal diversity in Karst formations of the Asian region, and many new taxa are described in last few years (Li et al., 2016; Chen et al., 2017, 2020; Zhang et al., 2017, 2019; Feng et al., 2019; Liu et al., 2019; Dissanayake et al., 2020b). In this study, seventeen *Arthrinium*-like were collected in Guizhou and Guangdong province, China and can be recognized as eleven *Arthrinium* species based on morphological characters and phylogeny inferred from the multi-gene sequences data (ITS, LSU, TUB2, and TEF) analyses, which four new species (*A. biseriale*, *A. cyclobalanopsidis*, *A. gelatinosum,* and *A. septatum*) and seven known species (*A. arundinis*, *A. garethjonesii*, *A. guizhouense*, *A. hydei*, *A. neosubglobosa*, *A. phyllostachium* and *A. psedoparenchymaticum*) are introduced and identified, respectively. The aim of this study is to describe these new taxa with detailed descriptions and illustrations, and also provide their phylogenetic relationships within *Arthrinium* based on multi-gene analysis.

MATERIALS AND METHODS

Sample Collection, Morphological Studies and Isolation

Samples were collected from Guizhou and Guangdong Province in China. Fungal fruiting bodies were examined by using stereomicroscope (Motic SMZ 168). Free hand sections of fungal structures were mounted in water for microscopic studies and photomicrography. Images were taken by using a Nikon ECLIPSE Ni compound microscope fitted with a Canon EOS 70D digital camera. All measurements were taken by using Tarosoft Image Frame Work software (IFW) (Liu et al., 2010), and photo plates were processed with Adobe Photoshop CS6 software (Adobe Systems, United States).

The single spore isolation followed the method described in Senanayake et al. (2020b). Parts of morphological descriptions were based on sporulated cultures on WA (Water Agar) at room temperature (ca. 25°C). Type specimens were deposited in the herbarium of Cryptogams Kunming Institute of Botany Academia Sinica (HKAS), Kunming, China and Guizhou Academy of Agriculture sciences Herbarium (GZAAS). Pure cultures were deposited in China General Microbiological Culture Collection Center (CGMCC) and Guizhou Culture Collection (GZCC). Faces of Fungi[1] number is obtained as described in the paper by Jayasiri et al. (2015), and the new taxa are registered in Index Fungorum (2021).

DNA Extraction, PCR Amplification and Sequencing

Fungal mycelia were scraped from the pure culture which were growing on PDA (Potato Dextrose Agar) for one week at 25°C in dark. DNA was extracted by using Ezup Column Fungi Genomic DNA Purification Kit (Sangon Biotech, China) from fresh fungal mycelia, but some were extracted directly from fruiting bodies by using Forensic DNA Kit (Omega Bio-Tek, China). Four gene regions, large subunit rDNA (LSU), internal transcribed spacer (ITS), beta-tubulin (TUB2) and the translation elongation factor 1-alpha (TEF) gene were amplified by the primer pairs LR0R and LR5 (Vilgalys and Hester, 1990), ITS5 and ITS4, T1 (O'Donnell and Cigelnik, 1997) and Bt2b (Glass and Donaldson, 1995), EF1-728F and EF-2 (O'Donnell et al., 1998; Carbone and Kohn, 1999), respectively. Polymerase chain reaction (PCR) was carried out in 25 μL reaction volume containing 12.5 μL 2 × PCR Master Mix (Sangon Biotech, China), 9.5 μL ddH_2O, 1 μL of each primer and 1 μL DNA template. The annealing temperatures were adjusted to 56°C for ITS, LSU and TUB2, and 55°C for TEF. PCR products were sent to sequence at Sangon Biotech Co., Ltd., China. The PCR products were examined using 1.2% agarose electrophoresis gel stained with ethidium bromide. PCR products were purified and sequenced by Sangon Biotech (Shanghai) Co., Ltd., China. New generated nucleotide sequences were submitted in GenBank (**Table 1**).

Phylogenetic Analyses

Phylogenetic analyses were performed based on ITS, LSU, TUB2 and TEF sequence data. The related strains of Apiosporaceae (**Table 1**) used for analysis were referred to BLAST[2] results and relevant publications (Wang et al., 2018; Jiang et al., 2019, 2020; Pintos et al., 2019; Tang et al., 2020). Sequences were obtained from GenBank and aligned using MAFFT v. 7 (Katoh and Standley, 2013). Manual adjustment was also performed when it is necessary by using BioEdit v. 7.0 (Hall, 1999). The alignment of sequences data used in analyses is deposited in TreeBASE under the accession number S27728. The analyses of maximum parsimony (MP), maximum likelihood (ML) and Bayesian inference (BI) were carried out as detailed in Dissanayake et al. (2020a) and programs used including PAUP v.4.0b 10 (Hillis and Bull, 1993; Swofford, 2002), raxmlGUI v. 1.3 (Silvestro and Michalak, 2012), and MrBayes v3.1.2 (Rannala and Yang, 1996; Huelsenbeck and Ronquist, 2001; Zhaxybayeva and Gogarten, 2002; Nylander, 2004). Trees were visualized with FigTree v1.4.2 (Rambaut, 2012) and the layout was edited using Adobe Illustrator CS6.

RESULTS

Phylogeny

To determine the phylogenetic placement of the new collections in this study, the combined ITS, LSU, TUB2 and TEF data set comprised 119 taxa with *Seiridium phylicae* (CPC 19962 and CPC 19965) as the outgroup taxa. The concatenated alignment comprises 2,770 characters (ITS: 1–635; LSU: 636–1,454; TUB2: 1,455–2,300; TEF: 2,301–2,770) including gaps, of which 1,361 characters were constant, and 1,279 characters are parsimony informative and 130 are parsimony uninformative. Maximum

[1]http://www.facesoffungi.org/

[2]https://blast.ncbi.nlm.nih.gov/Blast.cgi

TABLE 1 | GenBank accession numbers of species included in the phylogenetic study.

Species	Strain no.	GenBank Accession Numbers			
		LSU	ITS	TEF	TUB2
Arthrinium acutiapicum	KUMCC 20–0209	MT946338	MT946342	MT947359	MT947365
A. acutiapicum	KUMCC 20–0210	MT946339	MT946343	MT947360	MT947366
A. aquaticum	MLFU 18–1628	MK835806	MK828608	N/A	N/A
A. arundinis	CBS 106.12	KF144927	KF144883	KF145015	KF144973
A. arundinis	CBS 114316	KF144928	KF144884	KF145016	KF144974
A. arundinis	**GZCC 20–0116**	**MW478899**	**MW481720**	**MW522952**	**MW522968**
A. aureum	CBS 244.83	KF144935	AB220251	KF145023	KF144981
A. balearicum	CBS 145129	MK014836	MK014869	MK017946	MK017975
A. bambusae	LC7107	N/A	KY494719	KY705117	KY705187
A. bambusae	LC7106	KY494794	KY494718	KY806204	KY705186
A. bambusicola	MFLUCC 20–0144	MW173087	MW173030	MW183262	N/A
A. biseriale	**CGMCC 3.20135**	**MW478885**	**MW481708**	**MW522938**	**MW522955**
A. biseriale	**GZCC 20–0099**	**MW478886**	**MW481709**	**MW522939**	**MW522956**
A. biseriale	**GZCC 20–0100**	**MW478887**	**MW481710**	**MW522940**	**MW522957**
A. camellia-sinensis	LC8181	KY494837	KY494761	KY705157	KY705229
A. camellia-sinensis	LC5007	KY494780	KY494704	KY705103	KY705173
A. caricicola	CBS 145127	MK014838	MK014871	MK017948	MK017977
A. chinense	CFCC53036	N/A	MK819291	MK818545	MK818547
A. chinense	CFCC53037	N/A	MK819292	MK818546	MK818548
A. chromolaenae	MFLUCC 17-1505	MT214436	MT214342	N/A	N/A
A. cyclobalanopsidis	**CGMCC 3.20136**	**MW478892**	**MW481713**	**MW522945**	**MW522962**
A. cyclobalanopsidis	**GZCC 20–0103**	**MW478893**	**MW481714**	**MW522946**	**MW522963**
A. descalsii	CBS 145130	MK014837	MK014870	MK017947	MK017976
A. dichotomanthi	LC8175	KY494831	KY494755	KY705151	kY705223
A. dichotomanthi	LC4950	KY494773	KY494697	KY705096	KY705167
A. esporlense	CBS 145136	MK014845	MK014878	MK017954	MK017983
A. euphorbiae	IMI 285638b	AB220335	AB220241	N/A	AB220288
A. gaoyouense	CFCC 52301	N/A	MH197124	MH236793	MH236789
A. gaoyouense	CFCC 52302	N/A	MH197125	MH236794	MH236790
A. garethjonesii	KUMCC16–0202	KY356091	KY356086	N/A	N/A
A. garethjonesii	**GZCC 20–0115**	**MW478894**	**MW481715**	**MW522947**	**N/A**
A. gelatinosum	**KHAS 11962**	**MW478888**	**MW481706**	**MW522941**	**MW522958**
A. gelatinosum	**GZAAS 20–0107**	**MW478889**	**MW481707**	**MW522942**	**MW522959**
A. guizhouense	LC5318	KY494784	KY494708	KY705107	KY705177
A. guizhouense	LC5322	KY494785	KY494709	KY705108	KY705178
A. guizhouense	**GZCC 20–0114**	**MW478895**	**MW481716**	**MW522948**	**MW522964**
A. gutiae	CBS 135835	KR149063	KR011352	KR011351	KR011350
A. hispanicum	IMI 326877	AB220336	AB220242	N/A	AB220289
A. hydei	CBS 114990	KF144936	KF144890	KF145024	KF144982
A. hydei	KUMCC 16–0204	KY356092	KY356087	N/A	N/A
A. hydei	**GZCC 20–0113**	**MW478900**	**MW481721**	**MW522953**	**N/A**
A. hyphopodii	KUMCC 16–0201	KY356093	KY356088	N/A	N/A
A. hyphopodii	MFLUCC15–0003	N/A	KR069110	N/A	N/A
A. hysterinum	CBS 145134	MK014843	MK014876	N/A	N/A
A. hysterinum	ICMP 6889	MK014841	MK014874	MK017951	MK017980
A. ibericum	CBS 145137	MK014846	MK014879	MK017955	MK017984
A. italicum	CBS 145138	MK014847	MK014880	MK017956	MK017985
A. japonicum	IFO 30500	AB220356	AB220262	N/A	AB220309
A. japonicum	IFO 31098	AB220358	AB220264	N/A	AB220311
A. jatrophae	MMI 00052	N/A	JQ246355	N/A	N/A
A. jatrophae	AMH–9557	N/A	JQ246355	N/A	N/A

(Continued)

TABLE 1 | Continued

Species	Strain no.	GenBank Accession Numbers			
		LSU	ITS	TEF	TUB2
A. jiangxiense	LC4577	KY494769	KY494693	KY705092	KY705163
A. jiangxiense	LC4578	KY494770	KY494694	KY705093	KY705164
A. kogelbergense	CBS 113332	KF144937	KF144891	KF145025	KF144983
A. kogelbergense	CBS 113333	KF144938	KF144892	KF145026	KF144984
A. locuta-pollinis	LC11683	N/A	MF939595	MF939616	MF939622
A. longistromum	MFLUCC 11–0481	KU863129	KU940141	N/A	N/A
A. longistromum	MFLUCC 11–0479	KU863130	KU940142	N/A	N/A
A. malaysianum	CBS 102053	KF144942	KF144896	KF145030	KF144988
A. malaysianum	CBS 251.29	KF144943	KF144897	KF145031	KF144989
A. marii	CBS 497.90	KF144947	AB220252	KF145035	KF144993
A. mediterranei	IMI 326875	AB220337	AB220243	N/A	AB220290
A. minus	CBS 145131	MK014839	MK014872	MK017949	MK017978
A. mytilomorphum	DAOM 214595	N/A	KY494685	N/A	N/A
A. garethjonesii	KUMCC 18–0192	MK070898	MK070897	N/A	N/A
A. neosubglobosa	KUMCC 16–0203	KY356095	KY356090	N/A	N/A
A. neosubglobosa	JHB006	KY356094	KY356089	N/A	N/A
A. neosubglobosa	**GZAAS 20–0099**	**MW478901**	**MW481705**	**MW522954**	**MW522969**
A. obovatum	LC8177	KY494833	KY494757	KY705153	KY705225
A. obovatum	LC4940	KY494772	KY494696	KY705095	KY705166
A. ovatum	CBS 115042	KF144950	KF144903	KF145037	KF144995
A. paraphaeospermum	MFLUCC 13–0644	KX822124	KX822128	N/A	N/A
A. phaeospermum	CBS 114314	KF144951	KF144904	KF145038	KF144996
A. phaeospermum	CBS 114315	KF144952	KF144905	KF145039	KF144997
A. phragmites	CPC 18900	KF144956	KF144909	KF145043	KF145001
A. phyllostachium	MFLUCC 18–1101	MH368077	MK351842	MK340918	MK291949
A. phyllostachium	**GZCC 20–0111**	**MW478896**	**MW481717**	**MW522949**	**MW522965**
A. phyllostachium	**GZCC 20–0112**	**MW478897**	**MW481718**	**MW522950**	**MW522966**
A. piptatheri	CBS 145149	MK014860	MK014893	MK017969	N/A
A. pseudoparenchymaticum	LC7234	KY494819	KY494743	KY705139	KY705211
A. pseudoparenchymaticum	LC8173	KY494829	KY494753	KY705149	KY705221
A. pseudoparenchymaticum	**GZCC 20–0117**	**MW478898**	**MW481719**	**MW522951**	**MW522967**
A. pseudorasikravindrae	KUMCC 20–0208	N/A	MT946344	MT947361	MT947367
A. pseudorasikravindrae	KUMCC 20–0211	N/A	MT946345	MT947362	MT947368
A. pseudosinense	CPC 21546	KF144957	KF144910	KF145044	N/A
A. pseudosinense	CBS 135459	N/A	KF144910	KF145044	N/A
A. pseudospegazzinii	CBS 102052	KF144958	KF144911	KF145045	KF145002
A. pterospermum	CBS 123185	KF144959	KF144912	N/A	KF145003
A. pterospermum	CPC 20193	KF144960	KF144913	KF145046	KF145004
A. puccinioides	CBS 145150	MK014861	MK014894	MK017970	MK017998
A. puccinioides	CBS 549.86	AB220347	AB220253	N/A	AB220300
A. qinlingense	CFCC 52303	N/A	MH197120	MH236795	MH236791
A. qinlingense	CFCC 52304	N/A	MH197121	MH236796	MH236792
A. rasikravindrae	CBS 145152	MK014863	MK014896	MK017971	MK017999
A. rasikravindrae	LC7115	KY494797	KY494721	KY705118	KY705189
A. rasikravindrae	NFCCI 2144	N/A	JF326454	N/A	N/A
A. sacchari	CBS 212.30	KF144963	KF144917	KF145048	KF145006
A. sacchari	CBS 301.49	KF144962	KF144916	KF145047	KF145005
A. saccharicola	CBS 191.73	KF144966	KF144920	KF145051	KF145009
A. saccharicola	CBS 463.83	KF144968	KF144921	KF145053	KF145011
A. septatum	**CGMCC 3.20134**	**MW478890**	**MW481711**	**MW522943**	**MW522960**
A. septatum	**GZCC 20–0109**	**MW478891**	**MW481712**	**MW522944**	**MW522961**

(Continued)

TABLE 1 | Continued

Species	Strain no.	GenBank Accession Numbers			
		LSU	ITS	TEF	TUB2
A. serenense	IMI 326869	AB220344	AB220250	N/A	AB220297
A. setostromum	KUMCC 19–0217	MN528011	MN528012	MN527357	N/A
A. sporophleum	CBS 145154	MK014865	MK014898	MK017973	MK018001
A. subglobosum	MFLUCC 11–0397	KR069113	KR069112	N/A	N/A
A. subroseum	LC7292	KY494828	KY494752	KY705148	KY705220
A. thailandicum	MFLUCC 15–0199	KX986111	KU940146	N/A	N/A
A. thailandicum	MFLUCC 15–0202	KU863133	KU940145	N/A	N/A
A. trachycarpum	CFCC 53038	N/A	MK301098	MK303396	MK303394
A. trachycarpum	CFCC 53039	N/A	MK301099	MK303397	MK303395
A. urticae	IMI 326344	AB220339	AB220245	N/A	N/A
A. vietnamese	IMI 99670	KX986111	KX986096	N/A	KY019466
A. xenocordella	CBS478.86	KF144970	KF144925	KF145055	KF145013
A. xenocordella	CBS 595.66	KF144971	KF144926	N/A	N/A
A. yunnanum	DDQ 00281	KU863136	KU940148	N/A	N/A
A. yunnanum	MFLU 15–0002	N/A	KU940147	N/A	N/A
Seiridium phylicae	CPC 19962	NG 042759	LT853092	LT853189	LT853239
Seiridium phylicae	CPC 19965	KC005809	LT853093	LT853190	LT853240

The newly generated sequence is shown in bold. AMH: Ajrekar Mycological herbarium, Pune, Maharashtra, India; CBS: Westerdijk Fungal Biodiversity Institute, Utrecht, Netherlands; CFCC: China Forestry Culture Collection Center, Beijing, China; CGMCC: China General Microbiological Culture Collection Center, Beijing, China; CPC: Culture collection of Pedro Crous, housed at the Westerdijk Fungal Biodiversity Institute; DAOM: Canadian Collection of Fungal Cultures, Ottawa, Canada; DDQ: D.Q. Dai; GZAAS: Guizhou Academy of Agricultural Sciences herbarium, China; GZCC: Guizhou Culture Collection, China; HKAS: Herbarium of Cryptogams Kunming Institute of Botany Academia Sinica; ICMP: International Collection of Microorganisms from Plants, New Zealand; IFO: Institute for Fermentation, Osaka, Japan; IMI: Culture collection of CABI Europe UK Centre, Egham, UK; JHB: H.B. Jiang; KUMCC: Culture collection of Kunming Institute of Botany, Yunnan, China; LC: Working collection of Lei Cai, housed at CAS, China; MFLUCC: Mae Fah Luang University Culture Collection, Chiang Rai, Thailand; NFCCI: National Fungal Culture Collection of India.

likelihood, maximum parsimony and Bayesian analyses were performed, respectively, and presented consistent topologies. The best scoring RAxML tree (**Figure 1**) is obtained with a final likelihood value of -27544.434044. Estimated base frequencies were as follows: A = 0.236829, C = 0.253015, G = 0.251523, T = 0.258634; substitution rates AC = 1.154254, AG = 2.738844, AT = 1.073582, CG = 0.896658, CT = 4.134885, GT = 1.000000; The gamma distribution shape parameter alpha is equal to 0.332641 and the Tree-Length equal to 3.795226.

Phylogenetic analyses showed that our newly collected seventeen taxa clustered into eleven clades and can be recognized as seven known species (*Arthrinium arundinis*, *A. garethjonesii*, *A. guizhouense*, *A. hydei*, *A. neosubglobosa*, *A. phyllostachium*, *A. psedoparenchymaticum*) and four new species (*A. biseriale*, *A. cyclobalanopsidis*, *A. gelatinosum*, *A. septatum*) (**Figure 1**).

Taxonomy

Arthrinium biseriale Y. Feng and Z.Y. Liu, sp. nov. Figure 2

Index Fungorum number: IF558136

Facesoffungi number: FoF 09569

Etymology: The epithet refers to the ascospores are arranged in two rows in the ascus.

Holotype: HKAS 111961

Saprobic on dead bamboo culms, forming black, lenticular spots on the host surface, with stromata breaking through raised cracks with black center, and merge with each other with age, forming an erumpent black mass visible at the naked eye. **Sexual morph:** *Stromata* scattered to gregarious, immersed to erumpent, later becoming superficial, dark brown to black, fusiform, forming a slit-like opening at the apex, multi-loculate, membranous, with a periphysate ostiole. *Ascomata* 122–153 μm high, 138–207 μm diam, arranged in rows, dark brown to black. *Peridium* 11–19 μm wide, composed of several layers of dark brown to hyaline cells of *textura angularis*. *Hamathecium* 3–4 μm wide, comprising dense, hyaline, septa paraphyses. *Asci* 84–116 μm × 18–25 μm ($\bar{x}$ = 97 μm × 21 μm, n = 20), 8-spored, unitunicate, clavate, apically rounded, with an indistinct pedicel. *Ascospores* 22–28 μm × 7–11 μm ($\bar{x}$ = 25 μm × 9 μm, n = 30), biseriate, fusiform, curved at the bottom, obtuse at both ends, slightly wider in the middle, hyaline, 1-septate, constricted at the septum, mostly curved at the lower cell, rarely straight, with a large upper cell and a small lower cell, smoothwalled. The lower cell has 1-guttulate, the upper cell has 1–3 big guttulate in the middle surrounded by multiple small guttulate with a shallow 4–7 μm thick gelatinous sheath in the early. Growing to a later stage, the guttulate filled the entire spore, and the gelatinous sheath dissolves easily. **Asexual morph:** On WA, *Hyphae* 2.5–6.0 μm diam, hyaline, branched, septate, some curled in a ring structure. *Conidiophores* 12.0–44.0 μm × 2.5–5.0 μm ($\bar{x}$ = 20.0 μm × 3.5 μm, n = 20), straight or flexuous, smooth, thin-walled, unbranched, hyaline to pale brown, cylindrical, cyathiform, having transverse septa, often reduced to conidiogenous cells. *Conidiogenous cells* 5.0–22.0 μm × 2.5–5.0 μm ($\bar{x}$ = 10.0 μm × 3.5 μm, n = 20), integrated, hyaline to pale brown, doliiform to ampulliform, or lageniform.

Conidia 7–9 μm long (n = 30), brown, smooth in surface view, and 7–11 μm long (n = 30), lenticular, with a paler equatorial slit in side view, globose to ellipsoid with many guttules.

Culture characters

Ascospores germinated on WA within 24 h and germ tubes produced from middle and lower end. Colonies fast

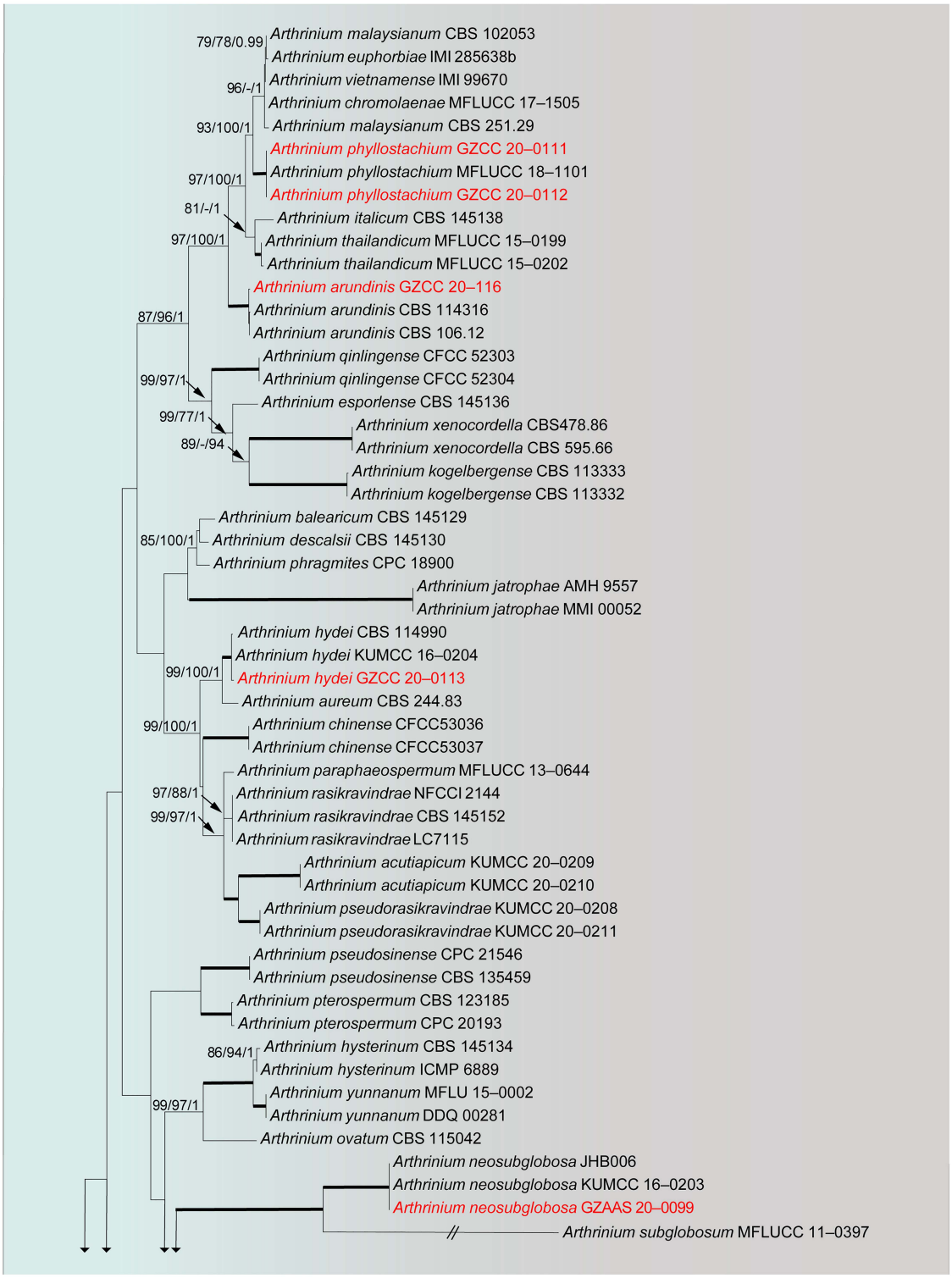


FIGURE 1 | Continued

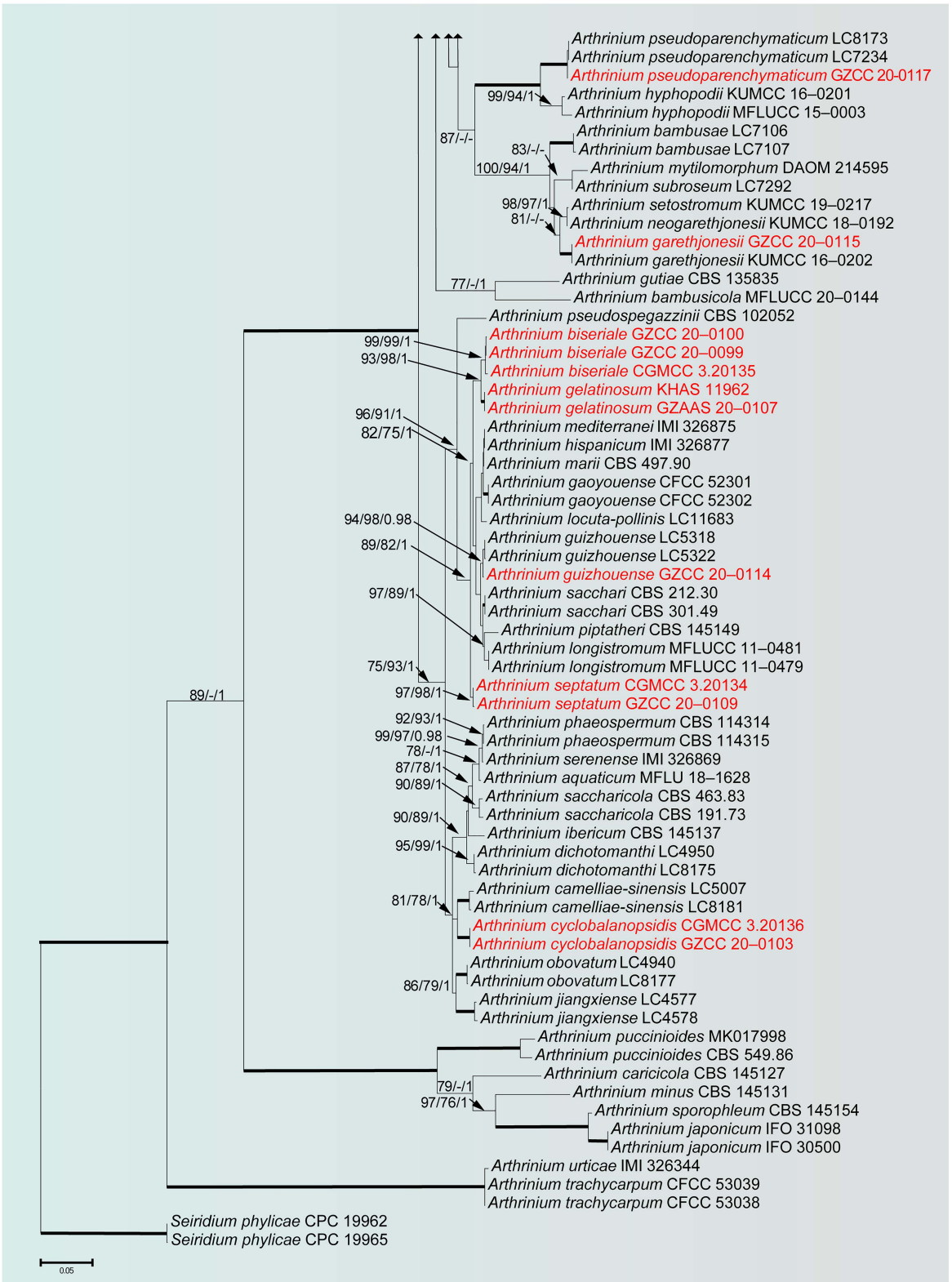


FIGURE 1 | RAxML tree of representatives based on a combined dataset of ITS, LSU, TUB2 and TEF sequences. Bootstrap support values for ML, MP (≥75%) and Bayesian (≥0.95) are given at the nodes (ML/MP/BI). Branches with ML, MP and BI equal 100, 100 and 1 are in bold. The tree is rooted with *Seiridium phylicae* (CPC 19962 and CPC 19965). New strains are shown in red.

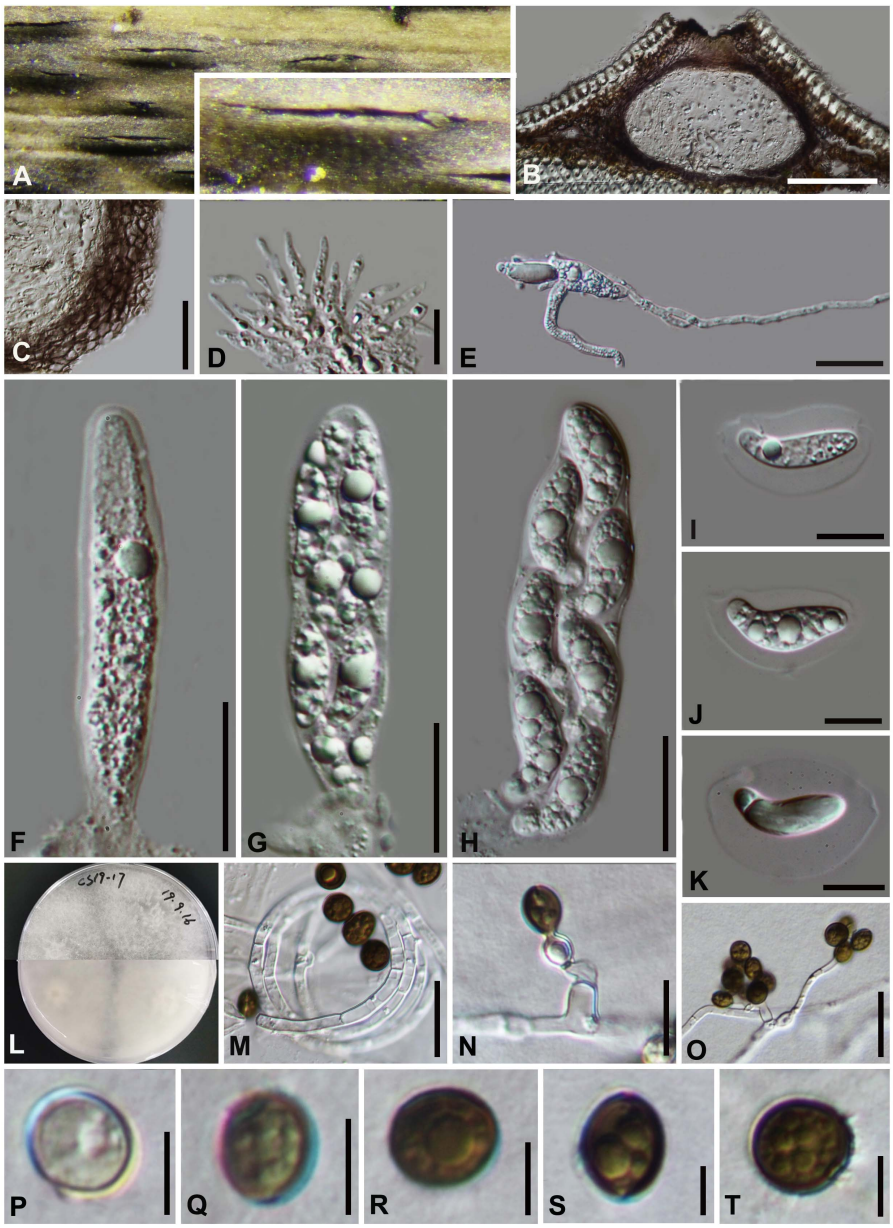


FIGURE 2 | ***Arthrinium biseriale*** (HKAS 111961**, holotype**). **(A)** Appearance of stromata on bamboo host. **(B)** Vertical section of stroma. **(C)** Peridium. **(D)** Paraphyses. **(E)** Germinating ascospore. **(F–H)** Asci. **(I–K)** Ascospore. **(L)** Culture. **(M)** Hyphae. (**N**,**O)** Conidiophore and conidiogenous cells. (**P–T)** Conidia. **Scale bars: (B)** = 50 μm. **(C)** = 20 μm. **(D)** = 10μm. **(E–H)** = 20 μm. **(I–K)** = 10 μm. **(M)** = 20 μm. **(N)** = 10 μm. **(O)** = 20 μm. **(P–T)** = 5 μm.

grown on PDA at 25°C, reached 7 cm in 7 days at 25°C. Colonies evenly tiled, with a large number of aerial hyphae, white, velvety, thin, gray-white on the reverse side and dirty white in the center.

Materials examined

China, Guizhou Province, Chishui City, Zhuhai National Forest Park, on dead culms of bamboo, 10 July 2019, Yao Feng, CS19-17 (HKAS 111961, holotype; GZAAS 20–0102, isotype), ex-type living cultures, CGMCC 3.20135 = GZCC 20–0101. *Ibid*., on dead base of the bamboo stem, 10 July 2019, Yao Feng, CS 19-25 (GZAAS 20–0101), living culture, GZCC 20–0100. *Ibid*., on dead branch of bamboo, 11 July 2019, Ya-Ya Chen, CS 013 (GZAAS 20–0100), living culture, GZCC 20–099.

Notes

Three strains representing *Arthrinium biseriale* clustered in a well-supported clade which are closely related to *A. gelatinosum*, but phylogenetically distinct and can be recognized as two different species (99% sequence similarity in ITS; 99% in TEF; 98% in TUB2). Morphologically, *Arthrinium biseriale* has smaller stromata (122–153 μm × 138–207 μm vs. 144–199

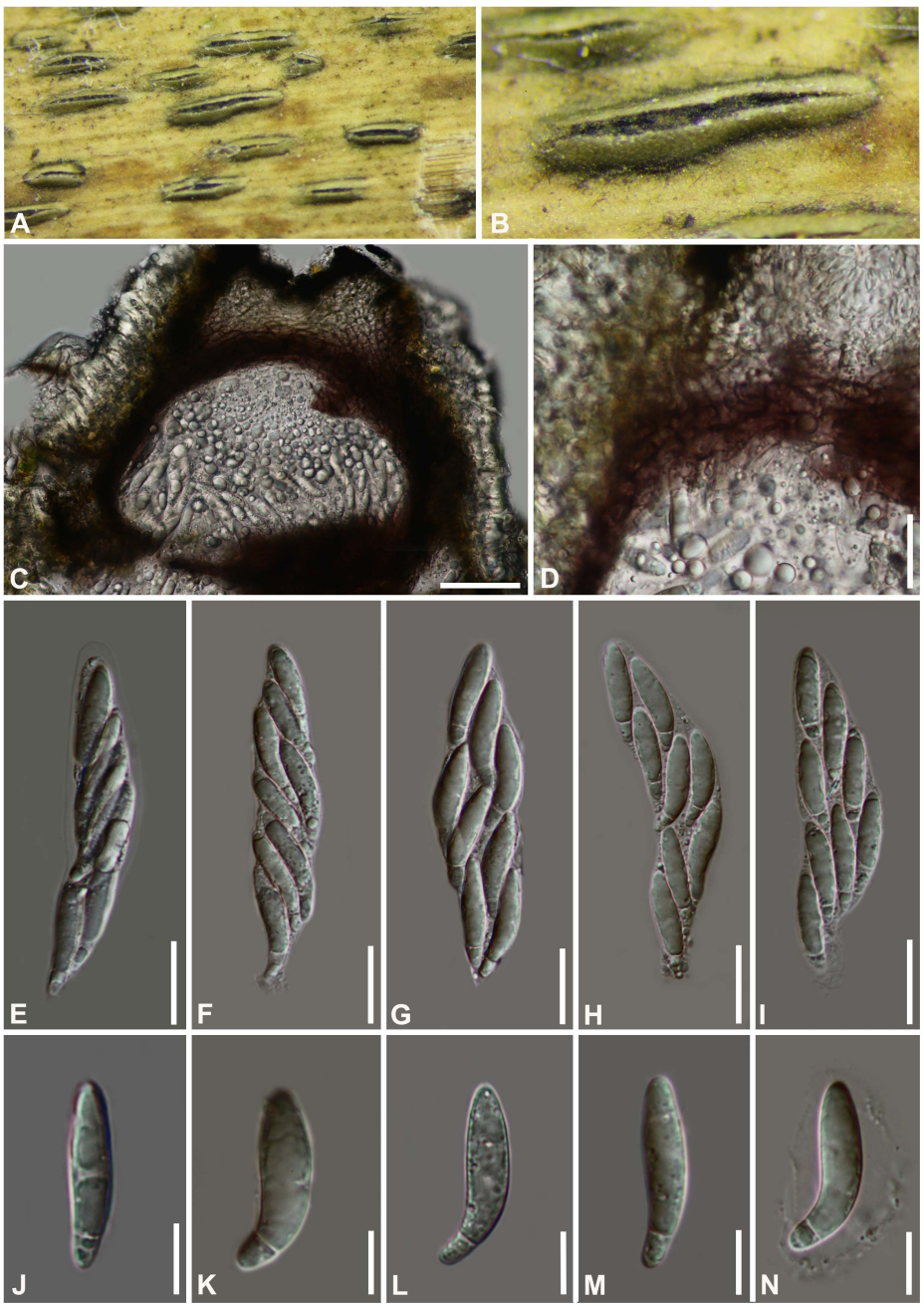


FIGURE 3 | ***Arthrinium gelatinosum*** **(**HKAS 111962, **holotype)**. **(A,B)** Appearance of stromata on bamboo host. **(C)** Vertical section of stroma. **(D)** Peridium. **(E–I)** Asci. **(J–N)** Ascospore. **Scale bars: (C)** = 50 μm. **(D–I)** = 20 μm. **(J–N)** = 10 μm.

μm × 184–214 μm) and the spores of *A. biseriale* are more curved than those of *A. gelatinosum*.

Arthrinium gelatinosum Y. Feng and Z.Y. Liu, sp. nov. Figure 3

Index Fungorum number: IF558137

Facesoffungi number: FoF 09570

Etymology: The epithet refers to the ascospore surrounded by gelatinous sheath.

Holotype: HKAS 111962

Saprobic on dead bamboo culms, forming black, lenticular spots on the host surface, with stromata breaking through raised cracks with black center. **Sexual morph:** *Stromata* solitary to gregarious, immersed to erumpent, fusiform, with long axis broken at the top by one cracks. *Ascomata* 144–199 μm high μm × 184–214 μm wide, uniseriate or irregularly arranged beneath stromata, pseudothecial, black, globose to subglobose with a flattened base. *Peridium* composed of 5 or 6 layers of

brown cells arranged in *textura angularis*, with a conspicuous perfusate ostiole. *Hamathecium paraphyses* hyphae-like. *Asci* 85–121 μm × 15–24 μm ($\bar{x}$ = 100 μm × 17 μm, *n* = 20), 8-spored, unitunicate, clavate, apically rounded, broadly cylindrical, with an indistinct pedicel. *Ascospores* (27−) 28-31 (−32) μm × 6–8 μm ($\bar{x}$ = 30 μm × 7 μm, *n* = 30), apiosporic, clavate to fusiform with narrowly rounded ends, composed of a large guttate and small guttate, hyaline, smooth-walled, surrounded by a gelatinous sheath. Growing to a later stage, the guttate filled the entire spore, and the gelatinous sheath dissolves easily. **Asexual morph:** undetermined.

Materials examined

China, Guizhou Province, Chishui City, Zhuhai National Forest Park, on dead culms of bamboo, 10 July 2019, Yao Feng, CS19-32 (HKAS 111962, holotype; GZAAS20–0108, isotype). *Ibid*., Chishui National Scenic Area, on dead branch of bamboo, 10 July 2019, Yao Feng, CS 19–29 (GZAAS 20–0107).

Notes

Two taxa representing *Arthrinium gelatinosum* cluster in a well-supported lineage (ML/MP/BI = 93/98/1, **Figure 1**), which is a sister to *A. biseriale*, and they are phylogenetically distinct species.

Arthrinium septatum Y. Feng and Jian K. Liu, sp. nov. Figure 4

Index Fungorum number: IF558138

Facesoffungi number: FoF 09571

Etymology: The epithet refers to the septate conidiophore.

Holotype: HKAS 111960

Saprobic on dead bamboo culms. **Sexual morph:** *Stromata* scattered to gregarious, immersed to erumpent, initially breaks through a black spot on the host, later visible as black, raised, lenticular or dome-shaped, and will grow into a linear shape at the later stage of growth. Ostiolate, with the long axis broken at the top revealing the ostioles of pseudothecia. *Ascomata* 88–195 μm high × 160–185 μm wide ($\bar{x}$ = 140 μm × 173 μm, *n* = 10), arranged in rows, brown to dark brown, subglobose with a flattened base. *Peridium* with several layers of cells arranged in *textura angularis*, with a conspicuous ostiole 50–90 μm in diameter, periphysate. *Hamathecium paraphyses* hyphae-like, septate, hyaline. *Asci* 75–104 μm × 17–26 μm ($\bar{x}$= 91 μm × 20 μm, *n* = 20), 8-spored, clavate, cylindrical, apically rounded, with distinct pedicel. *Ascospores* (24−) 25–30 (−32) μm × (6−) 8–10 (−11) μm ($\bar{x}$ = 29 μm × 9 μm, *n* = 30), biseriate, broad fusiform to cylindrical, with a large upper cell and a small lower cell, hyaline, 1-septate, constricted at septum, slightly curved, smooth-walled, with many guttules, with a large guttule at the center of large upper cell, with a distinct gelatinous sheath. **Asexual morph:** On PDA, *Hyphae* 2–4 μm in diameter, hyaline, branched, septate. *Conidiophores* 12.0–63.0 × 2–5 ($\bar{x}$ = 313 μm × 3 μm, *n* = 20), straight or flexuous, smooth, thin-walled, septate, hyaline to light brown, cylindrical, sometimes reduced to conidiogenous cells. *Conidiogenous cells* 4.0–18.0 × 1.5–4.0 ($\bar{x}$ = 10.0 μm × 2.5 μm, *n* = 20), solitary on hyphae, integrated, branched, ampuliform, cylindrical, hyaline to brown. *Conidia* 8–11 (−13) μm long (*n* = 30), brown, smooth, guttulate, globose to ellipsoid in surface view. and (8−) 9–13 (−14) μm long (*n* = 30), lenticular with a paler equatorial slit in side view. *Sterile cells* (13−) 14–21 (−27) μm × 5–7 (−9) μm elongated, mixed among conidia.

Culture characteristics

Ascospores germinated on WA within 24 h. Colonies on PDA reached 8 cm in 7 days at 25 °C, flat, aerial mycelium white. The hyphae in the center are cottony, dense, and there is a thin circle of hyphae at the edge. Reverse grayish white with a dirty white patch.

Materials examined

China, Guizhou Province, Chishui City, Zhuhai National Forest Park, on dead culms of bamboo, 10 July 2019, Yao Feng, CS19-8 (HKAS 111960, holotype; GZAAS 20–0109, isotype), ex-type living culture CGMCC 3.20134 = GZCC20–0108. *Ibid.*, on dead branch of bamboo, 11 July 2019, Ya-Ya Chen, CS 025 (GZAAS 20–0111), living culture GZCC 20–0109.

Notes

Two isolates, representing *Arthrinium septatum*, grouped in a well-supported clade and appear to be distinct from other *Arthrinium* species phylogenetically (**Figure 1**). *Arthrinium septatum* resembles to *A. biseriale* in having biseriate, broad fusiform to cylindrical ascospores and cylindrical, clavate asci. However, *Arthrinium septatum* differs from *A. biseriale* by having smaller stromata (160–185 μm diam vs. 138–207 μm diam) and asci (75–104 × 17–26 μm vs. 84–116 μm × 18–25 μm).

Arthrinium cyclobalanopsidis Y. Feng and Jian K. Liu, sp. nov. Figure 5

Index Fungorum number: IF558139

Facesoffungi number: FoF 09572

Etymology: The epithet "cyclobalanopsidis" refers to the host plant, *Cyclobalanopsidis glauca* (Thunb.) Oerst.

Holotype: HKAS 111963

Saprobic on *Cyclobalanopsidis glauca* (Thunb.). **Sexual morph:** Undetermined. **Asexual morph:** On PDA, *Hyphae* 2.5–5.5 μm in diameter, hyaline, septate, branched with chain structure. *Conidiophores* reduced to the conidiogenous cells. *Conidiogenous cells* 6.0–19.0 μm × 2.5–7.0 μm ($\bar{x}$ = 11.0 μm × 4.5 μm, *n* = 20), aggregated in clusters on hypha, pale brown, ampuliform or cylindrical. *Conidia* 8–12 μm long (*n* = 30), brown, smooth, globose to ellipsoid in surface view, and 10–14 μm long (*n* = 30), lenticular, with a paler equatorial slit in side view. *Sterile cells* elongated, rolled up, sometimes mixed among conidia.

Culture characteristics

Conidia germinated on WA within 12 h. Sporulated on PDA, Colonies flat, margin circular, fluffy, sparse, white, with dirty white patches in center, reverse white, with sparse aerial mycelium, reached 8 cm in 7 days at 25°C.

Material examined

China, Guizhou Province, Qianxinan Buyi and Miao Autonomous Prefecture, Ceheng County, on Leaf of *cyclobalanopsidis glauca* (Thunb.) Oerst., 13 May 2018, Yao Feng, G81 (HKAS 111963, holotype; GZAAS 20–0096, isotype),

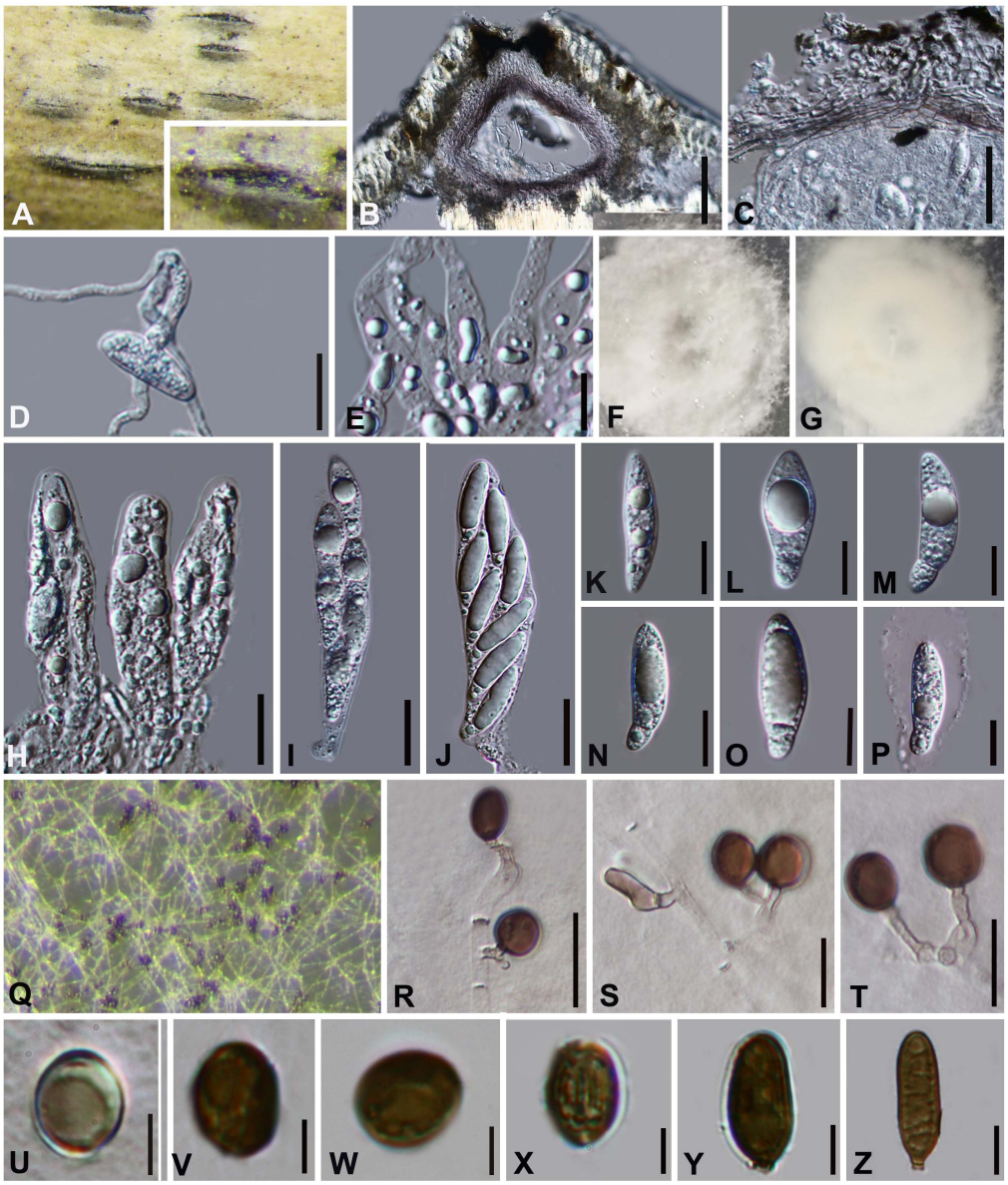


FIGURE 4 | ***Arthrinium septatum*** (HKAS 111960, **holotype**). **(A)** Appearance of stromata on bamboo host. **(B)** Vertical section of stroma. **(C)** Peridium. **(D)** Germinating ascospore. **(E)** Paraphyses. (**F**,**G**) Culture. **(H–J)** Asci. **(K–P)** Ascospore. **(Q)** Colony on PDA producing conidia masses. **(R–T)** Conidiophore and conidiogenous cells. **(U–X)** Conidia. **(Y,Z)** Sterile cell. **Scale bars: (B)** = 50 μm. **(C,D)** = 25 μm. **(E)** = 10 μm. **(H–J)** = 20 μm. **(K–P)** = 10 μm. **(R–T)** = 10 μm. **(U–Z)** = 5 μm.

ex-type living cultures, CGMCC 3.20136 = GZCC 20–0102. *Ibid.*, 20 Oct. 2019, Yao Feng, G82 (GZAAS 20–0097), living culture GZCC 20–0103.

Notes

Two isolates, representing *Arthrinium cyclobalanopsidis*, cluster together with *A. camelliae-sinensis* which was introduced by Wang et al. (2018) from *Camellia sinensis* (**Figure 1**). *Arthrinium cyclobalanopsidis* can be distinguished from *A. camelliae-sinensis* (567/572 in ITS; 390/414 in TEF; 715/748 in TUB2). Morphologically, *Arthrinium cyclobalanopsidis* resembles to *A. camelliae-sinensis* in having similar conidia (8–12 μm × 10–14 μm vs. 9.0–13.5 μm × 7.0–12.0 μm), but can be distinguished by its relatively longer conidiogenous cells (6.0–19.0 μm vs. 4.0–9.5 μm).

Arthrinium garethjonesii D.Q. Dai and H.B. Jiang, Mycosphere 7 (9): 1337 (2017). Figure 6

Saprobic on dead bamboo branch. **Sexual morph**: See Dai et al. (2016). **Asexual morph:** *Sporodochia* on host with hair-like setae, also grow in the gaps of the perithecia and scatter on the surface of the perithecia, black. *Conidiophores* reduced to conidiogenous

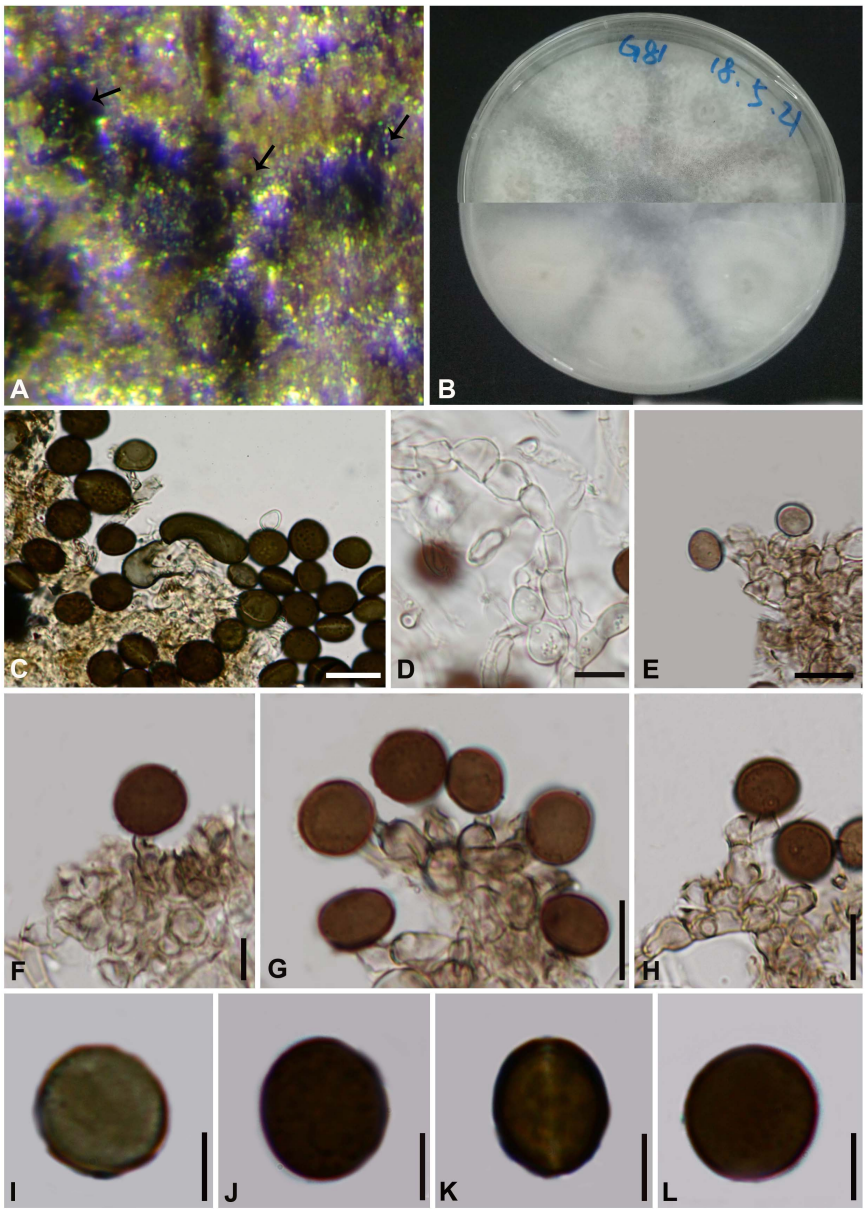


FIGURE 5 | ***Arthrinium cyclobalanopsidis*** **(**HKAS 111963, **holotype) (A)** Conidia masses on host. **(B)** Culture. **(C)** Sterile cell mixed among conidia. **(D)** Hyphae of chain structure. **(E–H)** Conidiogenous cells and conidia. **(I–L)** Conidia. **Scale bars: (C–H)** = 10 μm. **(I–L)** = 5 μm.

cells. *Conidiogenous cells* (5−) 6–19 (−20) μm × (2−) 3–5 (−7) μm ($\bar{x}$ = 11 μm × 4 μm, n = 20), aggregated in black sporodochia, hyaline to pale brown, smooth, ampulliform. *Conidia* (14–) 16–19 (–20) μm diam, brown, smooth, granular, globose to subglobose in surface view, and (16−) 17–22 (−23) μm diam, with pale equatorial slit in side view.

Culture characteristics

Conidia germinated on WA within 12 h, colonies fast growing on PDA, reached 8 cm in 7days at 25°C, fluffy, circular, dense, raised at center, white, reverse reddish. Hyphae 2–4 μm diam, hyaline to pale brown, branched, septate.

Material examined

China, Guizhou Province, Chishui City, Zhuhai National Forest Park, on dead branches of bamboo, 10 July 2019, Yao Feng, CS19-9 (GZAAS 20–0117); living culture GZCC 20–0115.

Notes

Arthrinium garethjonesii was originally described by Dai et al. (2016) based on the sexual morph from dead bamboo culms (HKAS 96289) collected from Yunnan Province, China. Our phylogenetic result (**Figure 1**) indicates that our collection is identical to *Arthrinium garethjonesii* and we report its asexual morph for the first time in this study.

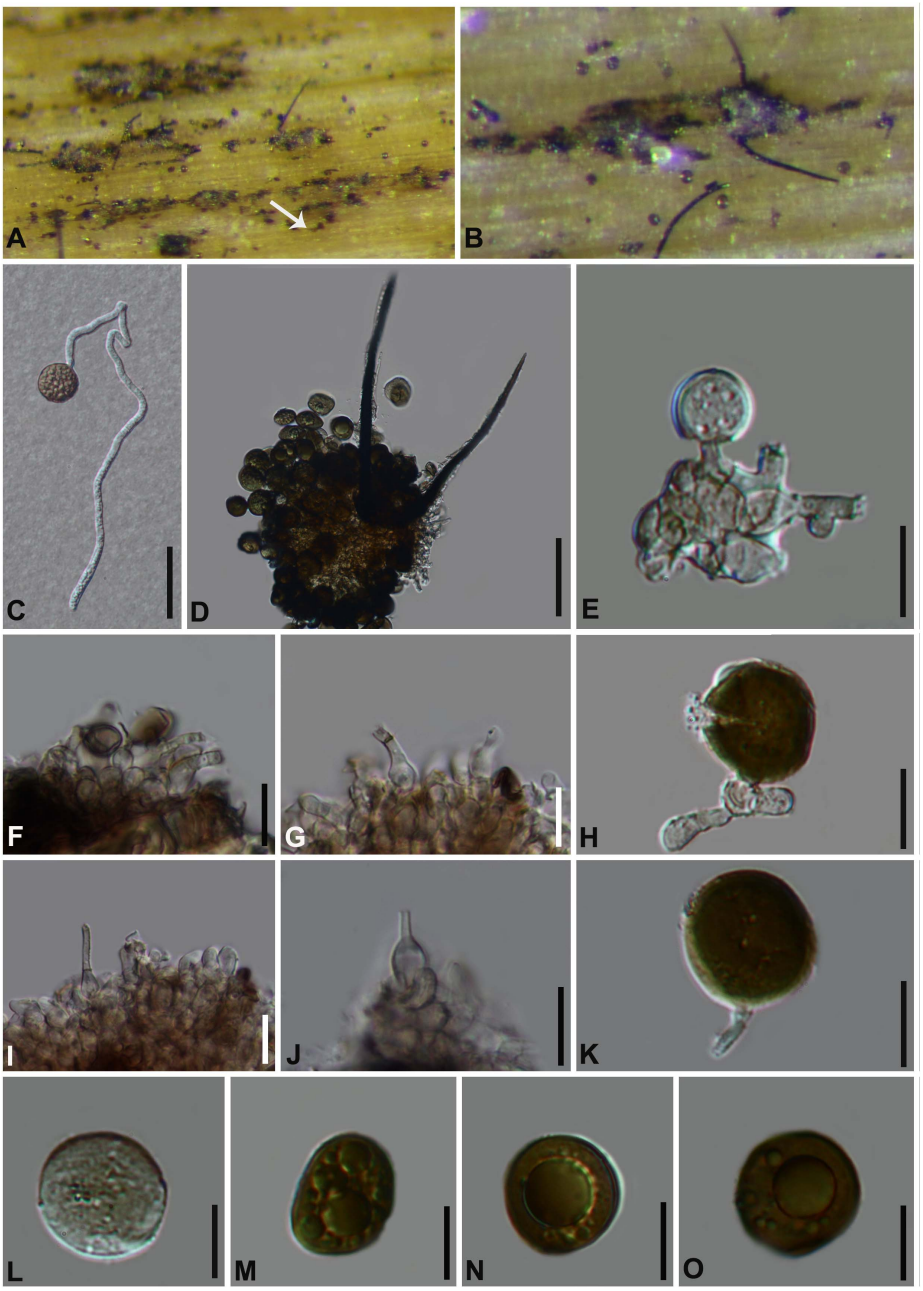


FIGURE 6 | ***Arthrinium garethjonesii*** (GZAAS 20–0117) **(A,B)** Appearance of sporodochia on bamboo host. **(C)** Germinating conidia. **(D)** Conidia with setae. **(E–K)** Conidiogenous cells and conidia. **(L–O)** Conidia. **Scale bars: (C)** = 30 μm. **(D)** = 50 μm. **(E)** = 20 μm. **(F,G)** = 10 μm. **(H)** = 5 μm. **(I,J)** = 10 μm. **(K–O)** = 5 μm.

Arthrinium guizhouense M. Wang and L. Cai, Mycokeys 34: 13 (2018). Figure 7

Saprobic on dead bamboo culms, forming black, lenticular spots on the host surface, stromata breaking through raised cracks with black center. **Sexual morph:** *Stromata* solitary to gregarious, immersed to erumpent, fusiform, with long axis broken at the top by one cracks. *Ascomata* 188–220 μm high × 170–200 μm wide, uniseriate or irregularly arranged beneath stromata, pseudothecial, black, globose to subglobose. *Peridium* composed of 5 or 6 layers of brown cells arranged in *textura angularis*, *Hamathecium paraphyses* 3–5 μm, hyaline, hyphae-like, septate. *Asci* (80−) 94–106 (−107) μm × (20−) 21–23 (−24) μm, 8-spored, clavate, apically rounded, broadly cylindrical, with an indistinct pedicel. *Ascospores* (24−) 25–32 (−33) μm × (6−) 7–9 (−10) μm ($\bar{x}$ = 31 μm × 8 μm, n = 30), apiosporic, clavate to fusiform



FIGURE 7 | ***Arthrinium guizhouense*** (GZAAS 20–0114). **(A)** Appearance of stromata on bamboo host. **(B)** Vertical section of stroma. **(C)** Peridium. **(D–F)** Asci. **(G)** Germinating ascospore. **(H,I)** Culture. **(J–O)** Ascospore. **(P)** Colony on WA producing conidia masses. **(Q,R)** Conidiogenous cells giving rise to conidia. **(S–V)** Conidia. **(W)** Sterile cell. **Scale bars: (B,C)** = 50 μm. **(D–F)** = 30 μm. **(G)** = 50 μm. **(J–O)** = 20 μm. **(Q,R) =** 10 μm. **(S–W) =** 5 μm.

with narrowly rounded ends, composed of a large upper cell and small lower cell, hyaline, smooth-walled, surrounded an inconspicuous gelatinous sheath. **Asexual morph:** *Hyphae* 2.5–7.5 μm diam, hyaline, branched, septate. *Conidiophores* reduced to conidiogenous cells. *Conidiogenous cells* 4–12 μm × 2–5 μm ($\bar{x}$ = 8 μm × 3 μm, n = 20), erect, aggregated in clusters on hyphae, pale brown, smooth, subglobose, ampulliform or doliiform. *Conidia* 5–8 μm long (n = 30), dark brown to black, smooth, globose or subglobose, and 6–8 μm long (n = 30), lenticular, with a paler equatorial slit in side view. *Sterile cells* elongated, rolled up, sometimes mixed among conidia.

Culture characteristics

On PDA, colonies very fast, reached 8 cm in 8 days at 25°C, velvety, circular, with regular edge, middle densely and raised white, dense at above the from margin, aerial mycelia, surface initially white, became grayish and reverse white.

Material examined

China, Guangdong Province, Guangzhou City, on decaying bamboo culms, 03 Sep. 2019, Yao Feng, GZ 23 (GZAAS 20–0114); living culture GZCC 20–0114.

Notes

Arthrinium guizhouense was introduced from air in a karst cave (asexual morph was provided from the culture) in Guizhou province, China by Wang et al. (2018). In this study, one collection was found as saprobe on bamboo in Guangzhou, China and it is identified as *A. guizhouense* based on the phylogeny and morphology evidences. In addition, our new collection provides the sexual morph which only the asexual morph was illustrated by Wang et al. (2018) and Senanayake et al. (2020a).

Arthrinium phyllostachium C.L. Yang, X.L. Xu and K.D. Hyde, Phytotaxa 406 (2): 102 (2019). Figure 8

Saprobic on dead bamboo culms, **Sexual morph:** *Stromata* scattered to gregarious, immersed to erumpent, later becoming superficial, dark brown to black, fusiform, forming a slit-like opening at the apex, with stromata breaking through raised cracks with black center. *Ascomata* 135–185 μm high, 157–215 μm diam, multi-loculate, with a periphysate ostiole, arranged in rows, clustered, gregarious, ampulliform, dark brown to black. *Peridium* 20–25 μm wide, composed of several layers of dark brown to brown cells of *textura angularis*. *Hamathecium* 3–5 μm wide, comprising dense, hyaline, septate paraphyses, hyphae-like. *Asci* 66–98 × 17–27 ($\bar{x}$ = 85 μm × 21 μm, n = 20), 8-spored, unitunicate, clavate, apedicellate, apically rounded. *Ascospores* 29–34 μm × 7–10 μm ($\bar{x}$ = 32 μm × 9 μm, n = 30), biseriate, elliptical, hyaline, 1-septate, constricted at the septum, mostly curved at the lower cell, rarely straight, with a large upper cell and a small lower cell, smooth-walled, with a shallow gelatinous sheath. **Asexual morph:** On WA, *Hyphae* 1.5–4.0 μm in diameter, hyaline, septate, branched. *Conidiophores* reduced to the conidiogenous cells. *Conidiogenous cells* (8—) 9–28 (—31.5) μm × (1.5—) 2–4 (—6) μm ($\bar{x}$ = 20 μm × 3 μm, n = 20), aggregated in clusters on hypha or solitary, erect, ampuliform or cylindrical, arising holoblastically from vegetative hyphae, monoblastic, or polyblastic, sympodial, terminal, cylindrical to clavate, ampulliform, hyaline, smooth, thin-walled. *Conidia* 5–8 μm long (n = 30), brown, smooth, globose to ellipsoid in surface view, and 7–9 μm long (n = 30), lenticular, with a paler equatorial slit in side view. *Sterile cells* light brown, elongated, and occasionally irregularly angled.

Culture characters

Ascospores germinated on WA within 24 h and germ tubes produced from Upper, middle and lower end. Colonies fast growed on PDA at 25°C, flat, spreading, the middle is white, smooth, the edge surface tapetum, gray-white, indistinct aerial hyphae, the reverse side is yellowish in the middle, and the edge is grayish white.

Materials examined

China, Guizhou Province, Chishui City, Zhuhai National Forest Park, on dead culms of bamboo, 10 July 2019, Yao Feng, CS 19-23 (GZAAS 20–0112), living culture GZCC 20–0111; *Ibid*., Chishui National Scenic Area, on dead culms of bamboo, 10 July 2019, Ya-Ya Chen, CS004 (GZAAS 20–0113), living culture GZCC 20–0112.

Notes

Arthrinium phyllostachium was introduced by Yang et al. (2019) based on the asexual morph and phylogeny analyses. It was collected from culms of *Phyllostachys heteroclada* (Poaceae) in China (Yang et al., 2019). The phylogenetic results showed that our new collections are identical to *A. phyllostachium*, Yang et al. (2019) only provided the asexual morph and the sexual morph is given in this study.

Arthrinium pseudoparenchymaticum M. Wang and L. Cai, Mycokeys 34 (1): 17 (2018), Figure 9

Saprobic on dead bamboo culms, forming black, lenticular spots on the host surface, with stromata breaking through raised cracks with black center. **Sexual morph:** *Ascomata* 187–242 μm high × 242–373 μm wide, uniseriate, or irregularly arranged beneath stromata, black, globose to subglobose with a flattened base. *Peridium* composed of 5–7 layers of brown cells arranged in *textura angularis*, with a conspicuous perfusate ostiole. *Hamathecium paraphyses* 4–8 μm, hyphae-like, septa hyaline. *Asci* (95—) 107–110 (—133) μm × 23–25 (—27) μm, 8-spored, broadly cylindrical, clavate or subglobose, apically rounded, with an indistinct pedicel. *Ascospores* (35–) 35–43 (–44) × (10–) 11–13 μm ($\bar{x}$ = 41 × 12, n = 30), apiosporic, clavate to fusiform with narrowly rounded ends, composed of a large upper cell and small lower cell, hyaline, smooth-walled, surrounded by a gelatinous sheath. **Asexual morph:** On WA, *Hyphae* 1.5–4 μm diam, hyaline to pale brown, branched, septate. *Conidiophore* extends from the vegetative hypha, up to 60 μm long. *Conidiogenous cells* 10.0–40.0 μm × 3.0–6.0 μm, scattered in clusters on hyphae, smooth, unbranched, hyaline to pale yellow, smooth, erect, subcylindrical. *Conidia* 17–27 μm × 17–21 μm ($\bar{x}$ = 23 μm × 19 μm, n = 30), pale to light brown, smooth, globose to subglobose, sometimes lobed or dentate, polygonal or irregular in surface view.

Culture characteristics

Ascospores germinating on WA within 24 h and germ tubes produced from upper. Colonies fast growing on PDA at 25°C, under 12 h light/12 h dark, cottony, circular, sparse, raised, with irregular edge, white in center.

Material examined

China, Guangdong Province, Guangzhou City, on decaying bamboo culms, 3 Sep. 2019, Yao Feng, GZ18 (GZAAS 20–0115), living culture GZCC20–0117.

Notes

Arthrinium pseudoparenchymaticum was introduced by Wang et al. (2018) based on the asexual morph characters and phylogeny analyses. It was originally collected from bamboo in China (Wang et al., 2018). In this study, a fresh specimen was collected and it

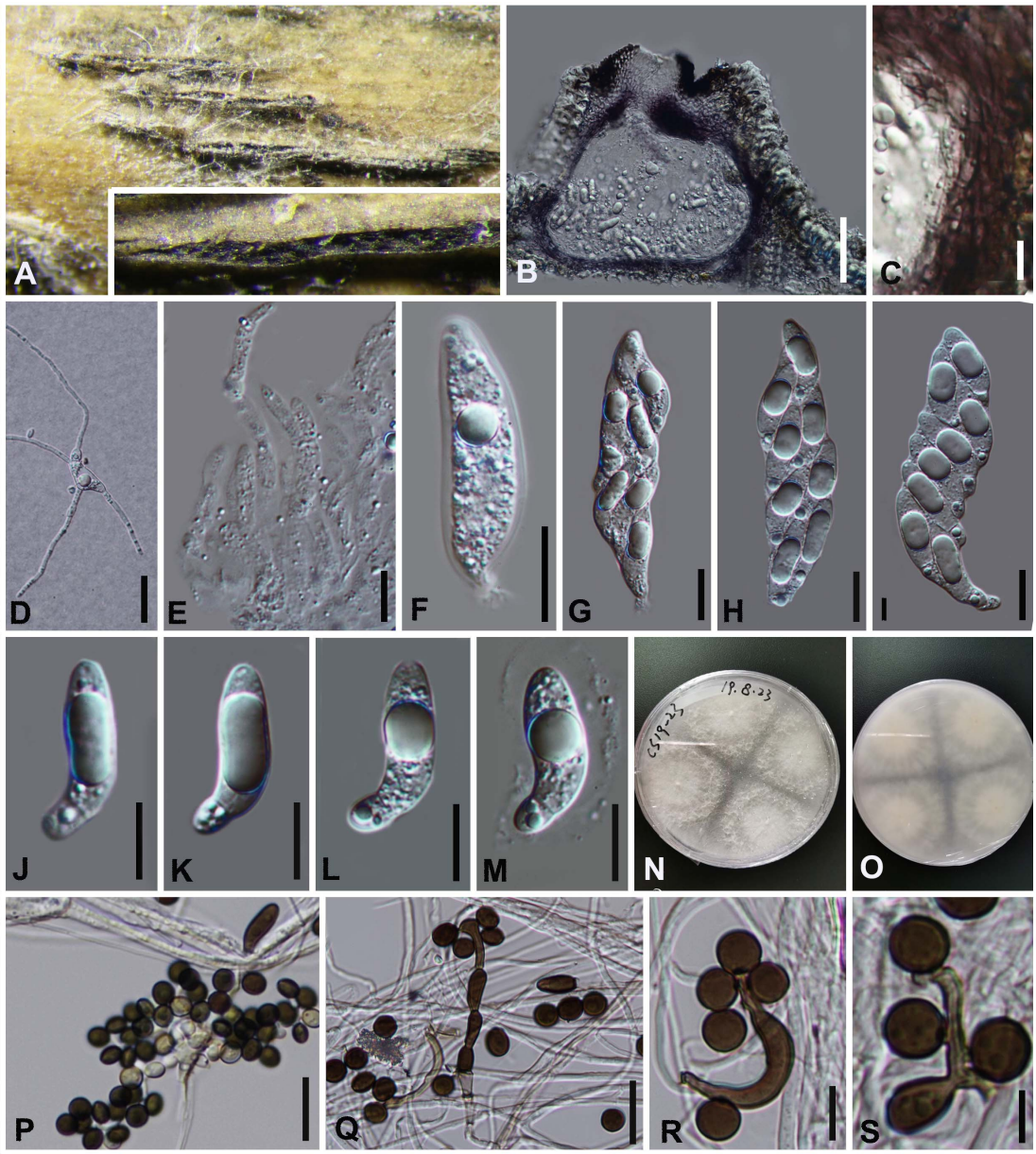


FIGURE 8 | ***Arthrinium phyllostachium*** (GZAAS 20–0112) **(A)** Appearance of stromata on bamboo host. **(B)** Vertical section of stroma. **(C)** Peridium. **(D)** Germinating ascospore. **(E)** Paraphyses. **(F–I)** Asci. (**J–M)** Ascospore. (**N**,**O)** Culture. **(P–S)** Conidiogenous cells and conidia. **Scale bars: (B)** = 50 μm. **(C)** = 10 μm. **(D)** = 20 μm. **(E)** = 20 μm. **(F–I)** = 30 μm. **(J–M)** = 10 μm. **(P,Q)** = 20 μm. **(R–S)** = 10 μm.

is identical to *A. pseudoparenchymaticum* (**Figure 1**), both sexual and asexual morphs were described and illustrated (**Figure 9**).

Arthrinium arundinis (Corda) Dyko and B. Sutton, Mycotaxon 8: 119 (1979). Figure 10.

Saprobic on dead bamboo culms. **Asexual morph:** On PDA, *Hyphae* 2–3 μm diam, consisting of smooth, hyaline, branched, septate. *Conidiophores* reduced to conidiogenous cells. *Conidiogenous cells* 3–8 μm × 2–5 μm, aggregated in clusters on hyphae, pale brown, smooth, ampulliform. *Conidia* (4–) 5–6 (–7) μm, brown, smooth, globose in surface view, and (4—) 5–7 (—8) μm diam, lenticular with pale equatorial slit in side view. *Sterile cells* at times intermingled among conidia. **Sexual morph:** Undetermined.

Culture characteristics

The colony is flat, cotton-like, thick and dense, with sparse aerial mycelia. The surface of PDA is white and the reverse side is grayish white.

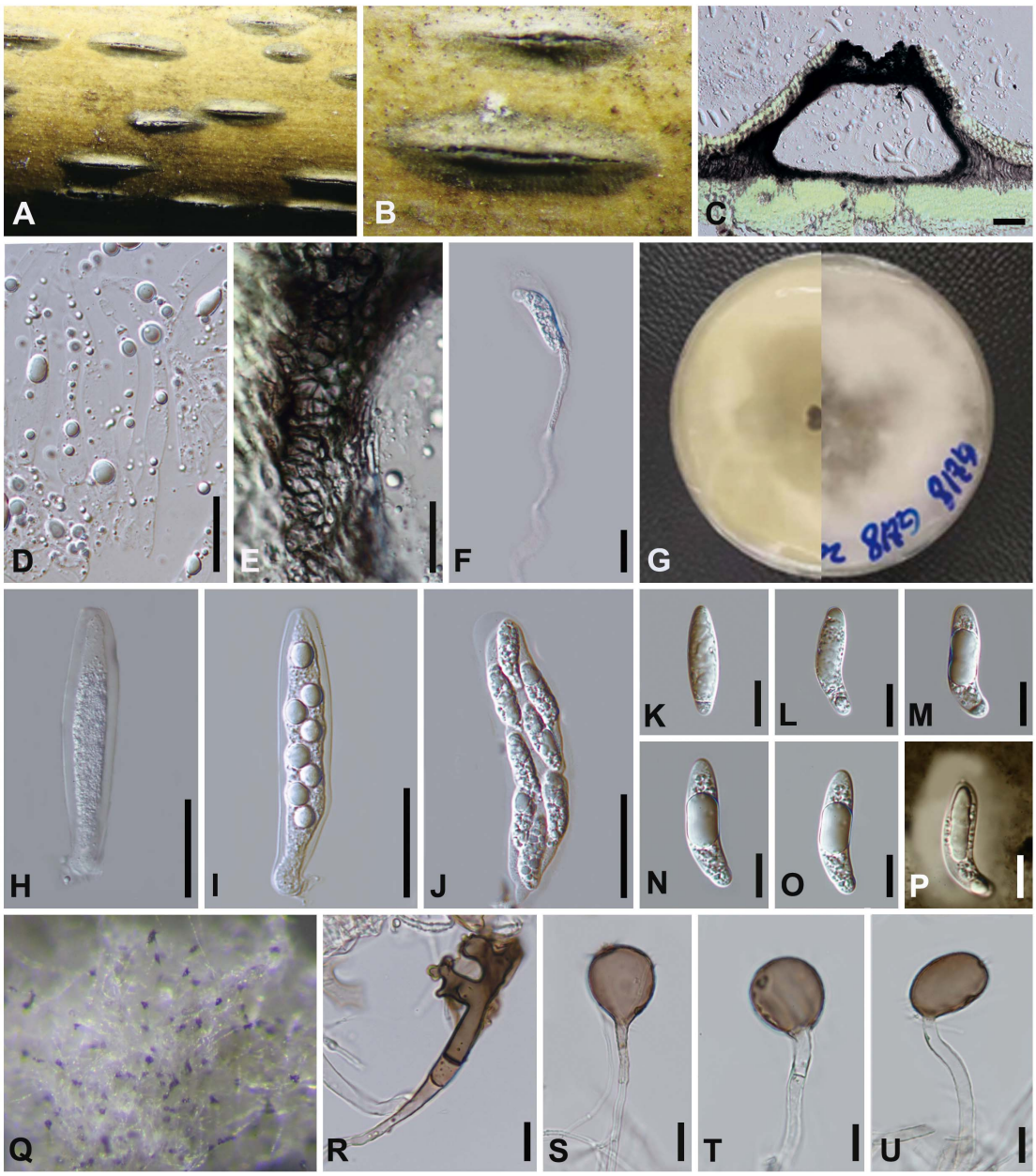


FIGURE 9 | ***Arthrinium pseudoparenchymaticum*** (GZAAS 20–0115) **(A,B)** Appearance of stromata on bamboo host. **(C)** Vertical section of stroma. **(D)** Paraphyses. **(E)** Peridium. **(F)** Germinating ascospore. **(G)** Culture. **(H–J)** Asci. **(K–O)** Ascospore. **(P)** Ascospore in Indian ink and present clear gelatinous sheath. **(Q)** Colony on WA producing conidia masses. **(R)** Dentate conidia. **(S–U)** Conidiogenous cells giving rise to conidia. **Scale bars: (C)** = 50 μm. **(D–F)** = 20 μm. **(H–J)** = 30 μm. **(K–P)** = 15 μm. **(R–U)** = 15 μm.

Materials examined

China, Guizhou Province, Chishui City, Zhuhai National Forest Park, on dead culms of bamboo, 10 July 2019, Yao Feng, CS 19-7 (GZAAS 20–0116), living culture GZCC 20–0116.

Notes

Our collection clusters together with the isolates of *Arthrinium arundinis* (**Figure 1**) and its morphology lines up with the type species. Therefore we identify it as *Arthrinium arundinis*.

Arthrinium hydei Crous, IMA Fungus 4 (1): 142 (2013). Figure 11

Saprobic on bamboo leaves. **Asexual morph:** *Colonies* on the host punctiform, pulvinate, blackish brown. *Conidiophores* pale brown, smooth, transversely septate, subcylindrical. *Conidiogenous cells* 5–15 × 3–6 μm, brown, smooth, subcylindrical to doliiform to lageniform. *Conidia* (13–) 14–19 (–20) μm diam in surface view, brown, roughened, globose, and 15–20 μm diam,

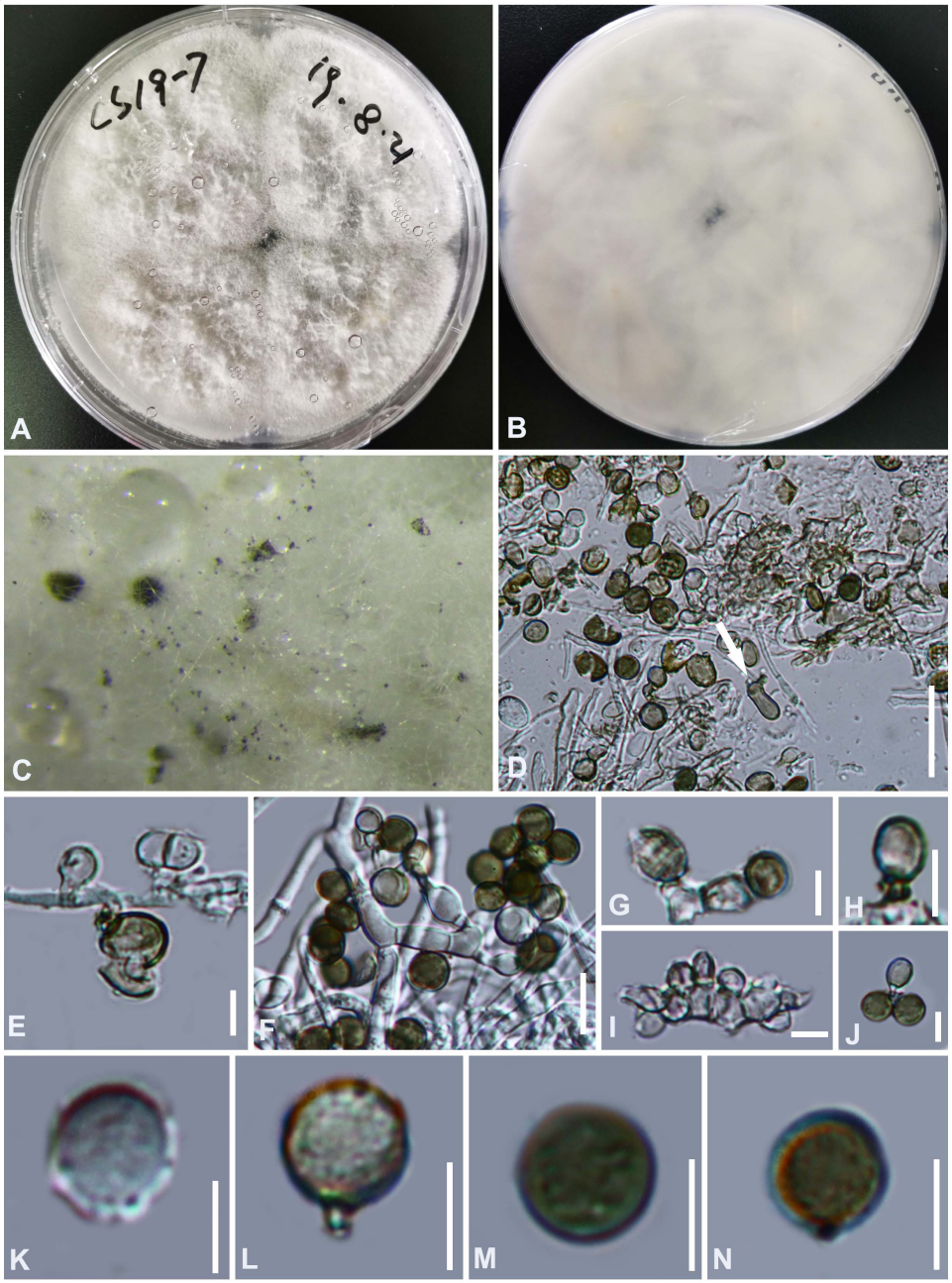


FIGURE 10 | ***Arthrinium arundinis*** (GZAAS 20–0116) **(A,B)** culture. **(C)** Colonies on culture. **(D)** Sterile cell mixed among conidia. **(E–J)** Conidiogenous cells and conidia. **(K–N)** Conidia. **Scale bars: (D)** = 50 μm. **(E)** = 5 μm. **(F)** = 10 μm. **(G–N)** = 5 μm.

lenticular with pale equatorial slit in side view. **Sexual morph:** Undetermined.

Culture characteristics

Colonies flat, spreading, with sparse aerial mycelium. On PDA surface and reverse pale luteous. Mycelium consisting of smooth, hyaline to pale brown, branched, septate, 2.0–4.5 μm diam hyphae.

Materials examined

China, Guizhou Province, Guiyang City, Baihua Lake, on bamboo leaves, 20 April 2018, Yao Feng, 67 (GZAAS 20–0098), living culture GZCC20–0113.

Notes

This collection is identified as *Arthrinium hydei* based on both morphological characters and molecular data. Crous and Groenewald (2013) originally described *A. hydei*

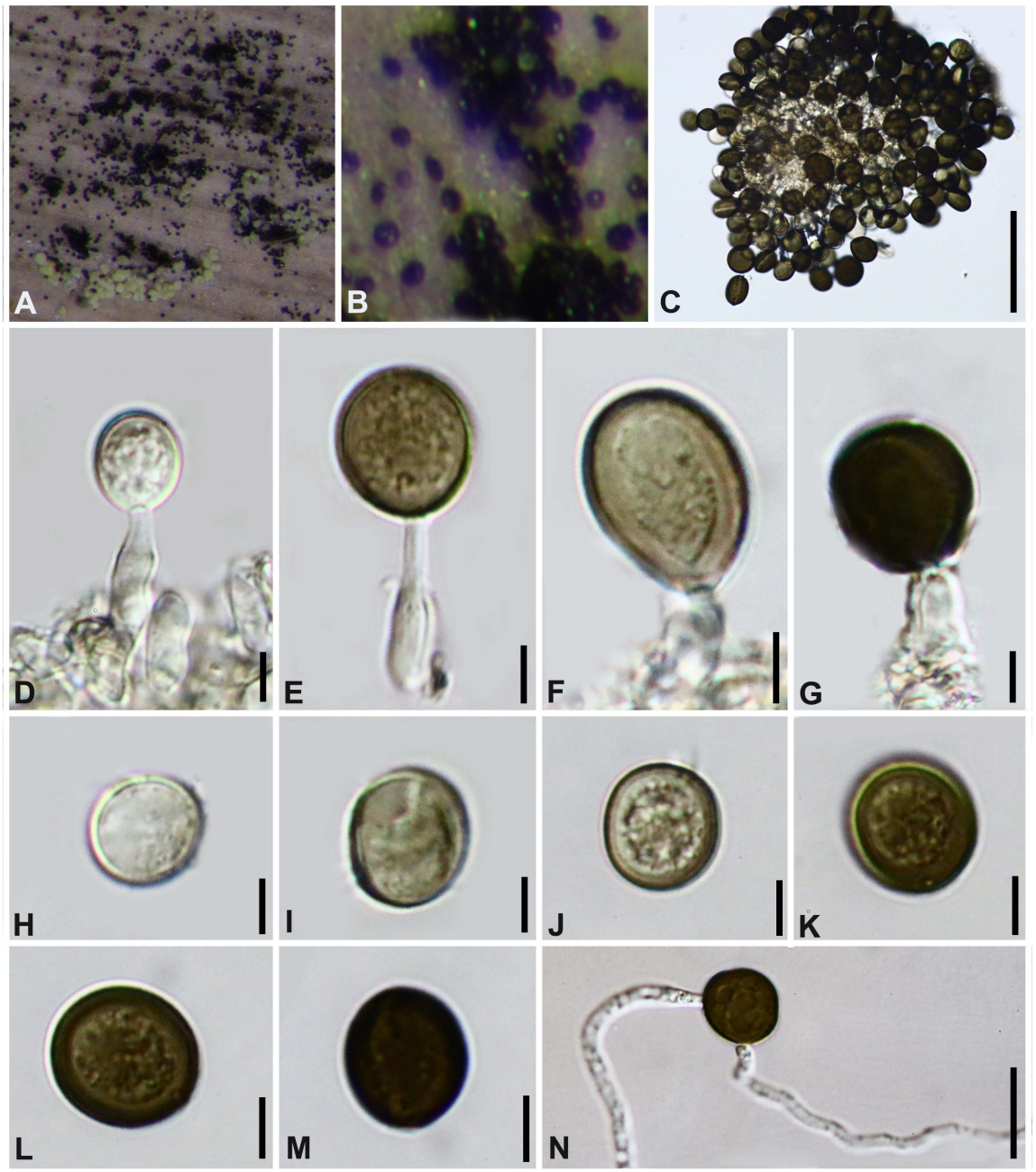


FIGURE 11 | ***Arthrinium hydei*** (GZAAS 20–0098) **(A,B)** Colonies on substrate. **(C–F)** Conidiogenous cells and conidia. **(G–M)** Conidia. **(N)** Germinating conidia. **Scale bars: (C)** = 50 μm. **(D–M)** = 5 μm. **(N)** = 25 μm.

based on the asexual morph from a culture (CBS 114990) which was isolated from bamboo culms in Hong Kong, China; we found this species in Guizhou from the substrate in nature with its asexual morph.

Arthrinium neosubglobosa D.Q. Dai and H.B. Jiang, Mycosphere 7 (9): 1337 (2017) Figure 12.

Saprobic on dead bamboo culms. **Sexual morph:** *Stromata* scattered to gregarious, superficial to raised, with a slit-like opening, dark brown to black, naviculate, with black papillate ostiole, multi-loculate. *Ascomata* 205–328 μm high, 168–345 μm, perithecial, arranged in a row, immersed in stromata, later becoming erumpent through host surface to superficial, obpyriform to ampulliform, dark brown, membranous. Ostiole raised from center of *Ascomata*, internally lined with periphyses. *Peridium* 4 layers, outer layer composed of dark brown, cells of *textura prismatica*, inner layer thin, with hyaline cells of *textura angularis*. *Hamathecium* 4.0–5.5 μm wide, comprising dense

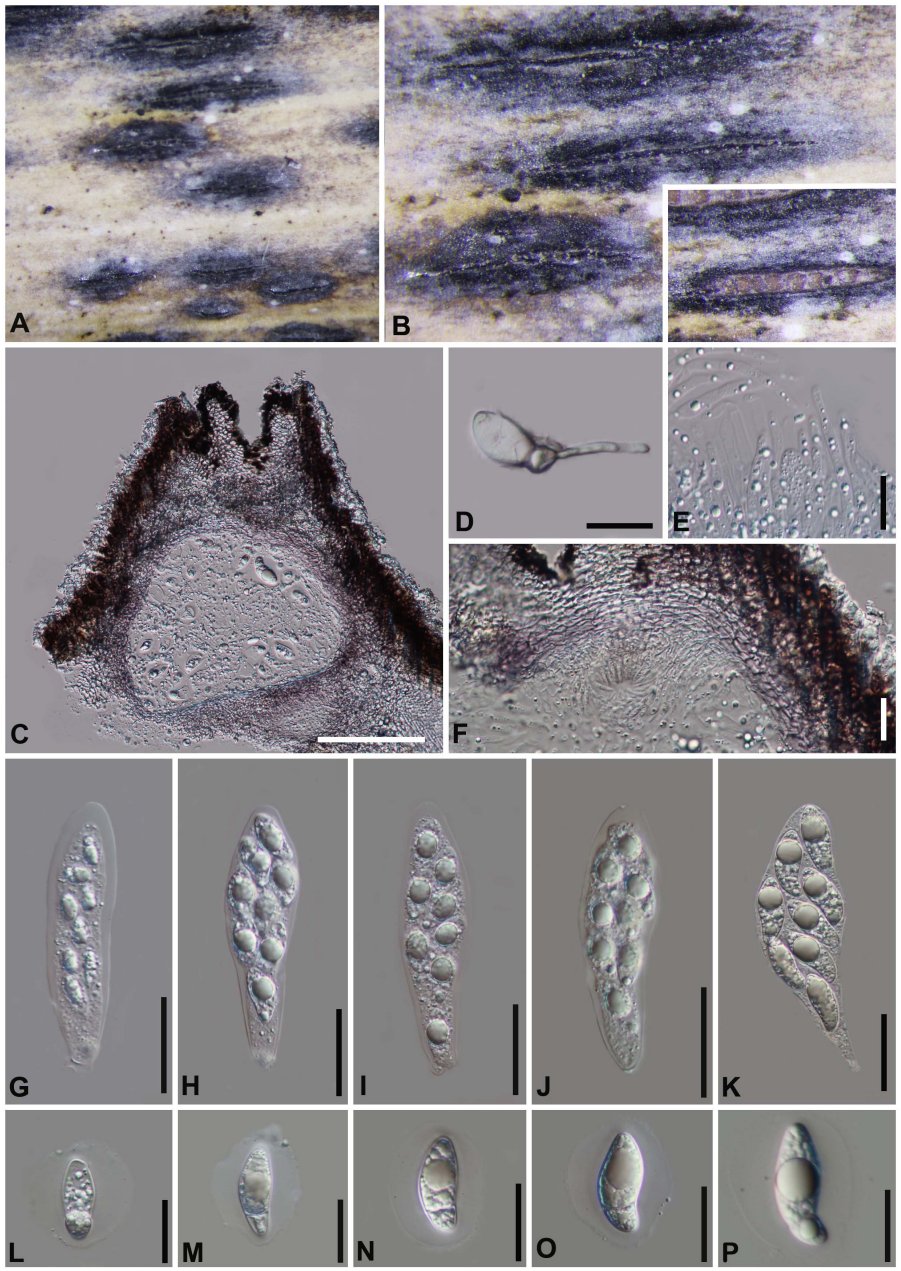


FIGURE 12 | ***Arthrinium neosubglobosa*** (GZAAS 20–0099). **(A,B)** Appearance of stromata on bamboo host. **(C)** Vertical section of stroma. **(D)** Germinating ascospore. **(E)** Paraphyses. **(F)** Peridium. **(G–K)** Asci. **(L–P)** Ascospore. **Scale bars: (C)** = 100 μm. **(D–F)** = 20 μm. **(G–K)** = 30 μm. **(L–P)** = 20 μm.

paraphyses, indistinctly aseptate, unbranched, not anastomosing, filamentous, clustered embedded in gelatinous matrix. *Asci* 80–119 μm × 20–37 μm ($\bar{x}$ = 97 μm × 28 μm, n = 20), 8-spored, unitunicate, clavate, with a short pedicel, apically rounded. *Ascospores* 25–36 μm × 11–15 μm ($\bar{x}$ = 29 μm × 13 μm, n = 30), 2-seriate, elliptical, hyaline, 1-septate, constricted at the septum, mostly curved at the lower cell, rarely straight, with a large upper cell and a small lower cell, smoothwalled, 1-guttulate, with a shallow 8–12 μm thick gelatinous sheath. **Asexual morph:** Undetermined.

Materials examined

China, Guizhou Province, Zunyi City, Daozhen County, on dead culms of bamboo, 15 August 2018, Yao Feng, DZ22 (GZAAS 20–0099).

Notes

Arthrinium neosubglobosa was introduced by Dai et al. (2016) based on the sexual morph characters and phylogeny analyses. The pure culture was attempted by single spore isolation and the DNA was extracted directly from the fruiting body, the

new collection is identified as *A. neosubglobosa* based on the phylogeny (**Figure 1**) and morphology evidences.

DISCUSSION

Arthrinium species have been reported from many hosts, includes hive-stored pollen lichens, marine algae, soil debris, gut of insects and nodules of human skin (Sharma et al., 2014; Crous et al., 2015, Senanayake et al., 2015; Wijayawardene et al., 2017, Zhao et al., 2018), it can be concluded that *Arthrinium* is ecologically diverse. Bamboo, as one of the most reported host, is a gramineous plant integrating economy and ornamental value (Gratani et al., 2008; Kelchner and Bamboo Phylogeny Group, 2013; Dai et al., 2016, 2017; Jiang et al., 2018, 2019, 2020; Wang et al., 2018; Yang et al., 2019), there is more than 115 genera with approximately 1,450 species. According to incomplete statistics, more than 1,100 species of fungi on bamboo were reported (Hyde et al., 2002a,b; Dai et al., 2016, 2017; Senanayake et al., 2020a; Tang et al., 2020; Wijesinghe et al., 2020). It is of great significance to excavate and identify the fungi on bamboo.

Several studies have shown (Crous and Groenewald, 2013; Dai et al., 2016, Dai et al., 2017; Wang et al., 2018; Yang et al., 2019) that it is difficult to identify the *Arthrinium* species solely rely on morphology and the multi-gene phylogenetic analyses are needed in the identification and classification of *Arthrinium*. The morphology of conidia is variable which can be depending on the period of incubation on different habitats, for example, *A. biseriale*, *A. gelatinosum* and *A. septatum*, are very similar in morphology, but molecular data distinguish them into different species; Our collection *A. pseudoparenchymaticum* differs from the type specimen (LC 8173) in the morphology of conidiophores, the size of conidiogenous cells is also different, while the molecular data supported them as the same species. These results are in agreement with the previous observations and publications (Crous and Groenewald, 2013; Dai et al., 2016, Dai et al., 2017; Wang et al., 2018, Yang et al., 2019). In addition, as a high diverse group, it is also difficult to distinguish species within *Arthrinium* by only using ITS and LSU gene regions, and the protein genes (TEF and TUB2) are not available for many species in the genus which bring potential problem once the new or existing taxa are introduced and identified, respectively. For example the absent of the protein genes (TEF and TUB2) of *Arthrinium garethjonesii* would bring the troubles in identification of *Arthrinium setostromum* as it is hard to confirm whether they are same species or not as they are identical in ITS and LSU gene regions, as well as the close phylogenetic relationship (**Figure 1**). It would be necessary to provide protein genes when new taxa are introduced in these well-study and diverse groups.

DATA AVAILABILITY STATEMENT

The data presented in the study can be found in the Genbank. The accession numbers of the sequences deposited in GenBank are ITS: MW481705—MW481721; LSU: MW478885–MW478901; TEF:MW522938–MW522954; and TUB: MW522955–MW522969.

AUTHOR CONTRIBUTIONS

YF and J-KL: conceptualization. YF and Y-YC: methodology. YF, C-GL, and J-KL: formal analysis. YF, Y-YC, M-MX, and J-KL: resources. YF: writing—original draft preparation. C-GL, Z-YL, and J-KL writing—review and editing. Z-YL and J-KL: supervision. All authors approved to publish the version of final manuscript.

FUNDING

This study was supported by the Joint Fund of the National Natural Science Foundation of China and the Karst Science Research Center of Guizhou province (Grant No. U1812401); the Research of Featured Microbial Resources and Diversity Investigation in Southwest Karst area (Project No. 2014FY120100); and the Guizhou Graduate Research Funding: Taxonomic and Phylogenetic studies of microfungi from Bamboo in Guizhou (Qian Jiao He YJSCXJH [2019] 022).

ACKNOWLEDGMENTS

We thank Ning-Guo Liu, Sheng-Nan Zhang, Jing Yang, Qiu-Jiu Shang, and Milan C. Samarakoon for their suggestions on phylogeny in this study.

REFERENCES

Agut, M., and Calvo, M. A. (2004). In vitro conidial germination in *Arthrinium aureum* and *Arthrinium phaeospermum*. *Mycopathologia* 157, 363–367. doi: 10.1023/B:MYCO.0000030432.08860.f3

Carbone, I., and Kohn, L. M. (1999). A method for designing primer sets for speciation studies in filamentous ascomycetes. *Mycologia* 91, 553–556. doi: 10.1080/00275514.1999.12061051

Chen, Y. Y., Dissanayake, A., Liu, Z. Y., and Liu, J. K. (2020). Additions to Karst Fungi 4: *Botryosphaeria* spp. associated with woody hosts in Guizhou province, China including *B. guttulata* sp. nov. *Phytotaxa* 454, 186–202. doi: 10.11646/phytotaxa.454.3.2

Chen, Y. Y., Maharachchikumbura, S. S. N., Liu, J. K., Hyde, K. D., Nanayakkara, R. R., Zhu, G. S., et al. (2017). Fungi from asian karst formations I. *Pestalotiopsis photinicola* sp.nov., causing leaf spots of *Photinia serrulata*. *Mycosphere* 8, 103–110. doi: 10.5943/mycosphere/8/1/9

Crous, P. W., and Groenewald, J. Z. (2013). A phylogenetic re-evaluation of *Arthrinium*. *IMA Fungus* 4, 133–154. doi: 10.5598/imafungus.2013.04.01.13

Crous, P. W., Wingfield, M. J., Le Roux, J. J., Richardson, D. M., Strasberg, D., Shivas, R. G., et al. (2015). Fungal planet description sheets: 371-399. *Persoonia* 35, 264–327. doi: 10.3767/003158515X690269

Dai, D. Q., Jiang, H. B., Tang, L. Z., and Bhat, D. J. (2016). Two new species of *Arthrinium* (Apiosporaceae, Xylariales) associated with bamboo from Yunnan, China. *Mycosphere* 7, 1332–1345. doi: 10.5943/mycosphere/7/9/7

Dai, D. Q., Phookamsak, R., Wijayawardene, N. N., Li, W. J., Bhat, D. J., Xu, J. C., et al. (2017). *Bambusicolous fungi*. *Fung. Divers.* 82, 1–105.

Dissanayake, A. J., Bhunjun, C. S., Maharachchikumbura, S. S. N., and Liu, J. K. (2020a). Applied aspects of methods to infer phylogenetic relationships amongst fungi. *Mycosphere* 11, 2652–2676. doi: 10.5943/mycosphere/11/1/18

Dissanayake, A. J., Chen, Y. Y., and Liu, J. K. (2020b). Unravelling diaporthe species associated with woody hosts from karst formations (Guizhou) in China. *J. Fungi* 6:251. doi: 10.3390/jof6040251

Ellis, M. B. (1971). *Dematiaceous Hyphomycetes*. Kew: Commonwealth Mycological Institute, 608.

Feng, Y., Zhang, S. N., and Liu, Z. Y. (2019). *Tremateia murispora* sp. nov. (Didymosphaeriaceae, Pleosporales) from Guizhou, China. *Phytotaxa* 416, 79–87. doi: 10.11646/phytotaxa.416.1.10

Glass, N. L., and Donaldson, G. C. (1995). Development ofprimer sets designed for use with the PCR to amplify conserved genes from filamentous ascomycetes. *Appl. Environ. Microbiol.* 61, 1323–1330. doi: 10.1128/aem.61.4.1323-1330.1995

Gratani, L., Crescente, M. F., Varone, L., Fabrini, G., and Digiulio, E. (2008). Growth pattern and photosynthetic activity of different bamboo species growing in the Botanical Garden of Rome. *Flora Morphol. Distrib. Funct. Ecol. Plants* 203, 77–84. doi: 10.1016/j.flora.2007.11.002

Hall, T. A. (1999). "BioEdit: a user-friendly biological sequence alignment editor and analysis program for Windows 95/98/NT," in *Nucleic Acids Symposium Series*. 95–98.

Hillis, D. M., and Bull, J. J. (1993). An empirical test of bootstrapping as a method for assessing confidence in phylogenetic analysis. *Syst. Biol.* 42, 182–192. doi: 10.1093/sysbio/42.2.182

Huelsenbeck, J. P., and Ronquist, F. (2001). MRBAYES: bayesian inference of phylogenetic trees. *Bioinformatics* 17, 754–755. doi: 10.1093/bioinformatics/17.8.754

Hyde, K. D., Fröhlich, J., and Taylor, J. E. (1998). Fungi from palms. XXXVI. Reflections on unitunicate ascomycetes with apiospores. *Sydowia* 50, 21–80.

Hyde, K. D., Norphanphoun, C., Maharachchikumbura, S. S. N., Bhat, D. J., Jones, E. B. G., Bundhun, D., et al. (2020). Refined families of Sordariomycetes. *Mycosphere* 11, 305–1059. doi: 10.5943/mycosphere/11/1/7

Hyde, K. D., Zhou, D., and Dalisayl, T. (2002a). Bambusicolous fungi: a review. *Fung. Divers.* 9, 1–14.

Hyde, K. D., Zhou, D., McKenzie, E., Ho, W., and Dalisay, T. (2002b). Vertical distribution of saprobic fungi on bamboo culms. *Fungal Divers.* 11, 109–118.

Jayasiri, C. S., Hyde, K. D., Ariyawansa, H. A., Bhat, J., Buyck, B., Cai, L., et al. (2015). The faces of fungi database: fungal names linked with morphology, phylogeny and human impacts. *Fungal Divers.* 74, 3–18. doi: 10.1007/s13225-015-0351-8

Jiang, H. B., Hyde, K. D., Doilom, M., Karunarathna, S. C., Xu, J. C., and Phookamsak, R. (2019). *Arthrinium setostromum* (Apiosporaceae, Xylariales), a novel species associated with dead bamboo from Yunnan, China. *Asia. J. Mycol.* 2, 254–268. doi: 10.5943/ajom/2/1/16

Jiang, N., Li, J., and Tian, C. M. (2018). *Arthrinium* species associated with bamboo and reed plants in China. *Fungal Syst. Evol.* 2, 1–9. doi: 10.3114/fuse.2018.02.01

Jiang, N., Liang, Y. M., and Tian, C. M. (2020). A novel bambusicolous fungus from China, *Arthrinium chinense* (Xylariales). *Sydowia* 72, 77–83. doi: 10.12905/0380

Katoh, K., and Standley, D. M. (2013). MAFFT multiple sequence alignment software version 7: improvements in performance and usability. *Mol. Biol. Evol.* 30, 772–780. doi: 10.1093/molbev/mst010

Kelchner, S. A., and Bamboo Phylogeny Group (2013). Higher level phylogenetic relationships within the bamboos (Poaceae: Bambusoideae) based on five plastid markers. *Mol. Phylogenet. Evol.* 67, 404–413. doi: 10.1016/j.ympev.2013.02.005

Li, B. J., Liu, P. Q., Jiang, Y., Weng, Q. Y., and Chen, Q. H. (2016). First report of culm rot caused by *Arthrinium phaeospermum* on *Phyllostachys viridis* in China. *Plant Dis.* 100, 1013–1013. doi: 10.1094/PDIS-08-15-0901-PDN

Liu, J. K., Chomnunti, P., Cai, L., Phookamsak, R., Chukeatirote, E., Jones, E. B. G., et al. (2010). Phylogeny and morphology of *Neodeightonia palmicola* sp. nov. from palms. *Sydowia* 62, 261–276.

Liu, N. G., Bhat, D. J., Hyde, K. D., and Liu, J. K. (2019). *Conioscypha tenebrosa* sp. nov. (Conioscyphaceae) from China and notes on *Conioscypha* species. *Phytotaxa* 413, 159–171. doi: 10.11646/phytotaxa.413.2.5

Luo, Z., Hyde, K. D., Liu, J. K., Maharachchikumbura, S. S. N., Jeewon, R., Bao, D. F., et al. (2019). Freshwater Sordariomycetes. *Fungal Divers.* 99, 451–660. doi: 10.1007/s13225-019-00438-1

Mapook, A., Hyde, K. D., McKenzie, E. H. C., Gareth, J. E. B., Bhat, D. J., Jeewon, R., et al. (2020). Taxonomic and phylogenetic contributions to fungi associated with the invasive weed *Chromolaena odorata* (Siam weed). *Fungal Divers.* 101, 1–175. doi: 10.1007/s13225-020-00444-8

Martínez-Cano, C., Grey, W. E., and Sands, D. C. (1992). First report of *Arthrinium arundinis* causing kernel blight on barley. *Plant Dis.* 76, 1077. doi: 10.1094/PD-76-1077B

Mavragani, D. C., Abdellatif, L., McConkey, B., Hamel, C., and Vujanovic, V. (2007). First report of damping-off of durum wheat caused by *Arthrinium sacchari* in the semi-arid Saskatchewan fields. *Plant Dis.* 91:469. doi: 10.1094/pdis-91-4-0469a

Nylander, J. A. A. (2004). *MrModeltest v2. Program Distributed by the Author*. Uppsala: Evolutionary Biology Centre, Uppsala University.

O'Donnell, K., and Cigelnik, E. (1997). Two divergent intragenomic rDNA ITS2 types within a monophyletic lineage of the fungus Fusarium are nonorthologous. *Mol. Phylogenet. Evol.* 7, 103–116. doi: 10.1006/mpev.1996.0376

O'Donnell, K., Kistler, H. C., Cigelnik, E., and Ploetz, R. C. (1998). Multiple evolutionary origins of the fungus causing Panama disease of banana: concordant evidence from nuclear and mitochondrial gene genealogies. *Proc. Natl. Acad. Sci. U.S.A.* 95, 2044–2049. doi: 10.1073/pnas.95.5.2044

Pintos, A., Alvarado, P., Planas, J., and Jarling, R. (2019). Six new species of *Arthrinium* from Europe and notes about *A. caricicola* and other species found in Carex spp. *Hosts. Mycokeys* 49, 15–48. doi: 10.3897/mycokeys.49.32115

Rai, M. K. (1989). Mycosis in man due to *Arthrinium phaeospermum* var. indicum. First case report. *Mycoses* 32, 472–475. doi: 10.1111/j.1439-0507.1989.tb02285.x

Rambaut, A. (2012). *). FigTree, Version 1.4. 2*. Edinburgh: University of Edinburgh.

Rannala, B., and Yang, Z. (1996). Probability distribution of molecular evolutionary trees: a new method of phylogenetic inference. *J. Mol. Evol.* 43, 304–311. doi: 10.1007/BF02338839

Seifert, K., Morgan-Jones, G., Gams, W., and Kendrick, B. (2011). *The Genera of Hyphomycetes.[CBS Biodiversity Series 9]*. Utrecht: CBS-KNAW Fungal Biodiversity Centre.

Senanayake, I. C., Bhat, J. D., Cheewangkoon, R., and Xie, N. (2020a). Bambusicolous *Arthrinium* species in guangdong province. *China. Front. Microbiol.* 11:602773. doi: 10.3389/fmicb.2020.602773

Senanayake, I. C., Maharachchikumbura, S. S., Hyde, K. D., Bhat, J. D., Jones, E. G., McKenzie, E. H., et al. (2015). Towards unraveling relationships in Xylariomycetidae (Sordariomycetes). *Fungal Divers.* 73, 73–144. doi: 10.1007/s13225-015-0340-y

Senanayake, I. C., Rathnayake, A. R., Marasinghe, D. S., Calabon, M. S., Gentekaki, E., Lee, H. B., et al. (2020b). Morphological approaches in studying fungi: collection, examination, isolation, sporulation and preservation. *Mycosphere* 11, 2678–2754. doi: 10.5943/mycosphere/11/1/20

Sharma, R., Kulkarni, G., Sonawane, M. S., and Shouche, Y. S. (2014). A new endophytic species of *Arthrinium* (Apiosporaceae) from Jatropha podagrica. *Mycoscience* 55, 118–123. doi: 10.1016/j.myc.2013.06.004

Silvestro, D., and Michalak, I. (2012). raxmlGUI: a graphical front-end for RAxML. *Org. Divers. Evol.* 12, 335–337. doi: 10.1007/s13127-011-0056-0

Swofford, D. L. (2002). *PAUP*: Phylogenetic Analysis Using Parsimony (*and Other Methods). Version 4*. Sunderland, MA: Sinauer Associates.

Tang, X., Goonasekara, I. D., Jayawardena, R. S., Jiang, H. B., Li, J. F., Hyde, K. D., et al. (2020). *Arthrinium bambusicola* (Fungi, Sordariomycetes), a new species from *Schizostachyum brachycladum* in northern Thailand. *Biodivers. Data J.* 8:e58755. doi: 10.3897/BDJ.8.e58755

Vilgalys, R., and Hester, M. (1990). Rapid genetic identification and mapping of enzymatically amplified ribosomal DNA from several *Cryptococcus* species. *J. Bacteriol.* 172, 4238–4246. doi: 10.1128/jb.172.8.4238-4246.1990

Wang, M., Tan, X. M., Liu, F., and Cai, L. (2018). Eight new *Arthrinium* species from China. *MycoKeys* 34, 1–24. doi: 10.3897/mycokeys.34.24221

Wijayawardene, N. N., Hyde, K. D., Rajeshkumar, K. C., Hawksworth, D. L., Madrid, H., Kirk, P. M., et al. (2017). Notes for genera: ascomycota. *Fungal Divers.* 86, 1–594. doi: 10.1007/s13225-017-0386-0

Wijesinghe, S. N., Wang, Y., Camporesi, E., Wanasinghe, D. N., Boonmee, S., and Hyde, K. D. (2020). A new genus of Bambusicolaceae (Pleosporales) on *Corylus avellana* (Fagales) from Italy. *Biodivers. Data J.* 8:e55957. doi: 10.3897/BDJ.8.e55957

Yan, H., Jiang, N., Liang, L. Y., Yang, Q., and Tian, C. M. (2019). *Arthrinium trachycarpum* sp. nov. from *Trachycarpus fortunei* in China. *Phytotaxa* 400, 203–210. doi: 10.11646/phytotaxa.400.3.7

Yang, C. L., Xu, X. L., Dong, W., Wanasinghe, D. N., Liu, Y. G., and Hyde, K. D. (2019). Introducing *Arthrinium phyllostachium* sp. nov. (Apiosporaceae, Xylariales) on *Phyllostachys heteroclada* from Sichuan Province, China. *Phytotaxa* 406, 091–110. doi: 10.1127/nova_hedwigia/2019/0526

Zhang, J. F., Liu, J. K., Hyde, K. D., Chen, Y. Y., Liu, Y. X., and Liu, Z. Y. (2017). Two new species of *Dyfrolomyces* (Dyfrolomycetaceae, Dothideomycetes) from karst landforms. *Phytotaxa* 313:267. doi: 10.11646/phytotaxa.313.3.4

Zhang, J. F., Liu, J. K., Jeewon, R., Wanasinghe, D. N., and Liu, Z. Y. (2019). Fungi from Asian Karst formations III. Molecular and morphological characterization reveal new taxa in Phaeosphaeriaceae. *Mycosphere* 10, 202–220. doi: 10.5943/mycosphere/10/1/3

Zhao, Y. M., Deng, C. R., and Chen, X. (1990). *Arthrinium phaeospermum* causing dermatomycosis, a new record of China. *Acta Mycol. Sin.* 9, 232–235.

Zhao, Y. Z., Zhang, Z. F., Cai, L., Peng, W. J., and Liu, F. (2018). Four new filamentous fungal species from newly-collected and hivestored bee pollen. *Mycosphere* 9, 1089–1116. doi: 10.5943/mycosphere/9/6/3

Zhaxybayeva, O., and Gogarten, J. P. (2002). Bootstrap, Bayesian probability and maximum likelihood mapping: exploring new tools for comparative genome analyses. *BMC Genom.* 3:4. doi: 10.1186/1471-2164-3-4

Conflict of Interest: The authors declare that the research was conducted in the absence of any commercial or financial relationships that could be construed as a potential conflict of interest.

Copyright © 2021 Feng, Liu, Lin, Chen, Xiang and Liu. This is an open-access article distributed under the terms of the Creative Commons Attribution License (CC BY). The use, distribution or reproduction in other forums is permitted, provided the original author(s) and the copyright owner(s) are credited and that the original publication in this journal is cited, in accordance with accepted academic practice. No use, distribution or reproduction is permitted which does not comply with these terms.

frontiers in Microbiology

ORIGINAL RESEARCH
published: 12 April 2021
doi: 10.3389/fmicb.2021.643505

An Unexpectedly High Number of New *Sutorius* (Boletaceae) Species From Northern and Northeastern Thailand

Santhiti Vadthanarat[1,2], Roy E. Halling[3], Mario Amalfi[4,5], Saisamorn Lumyong[1,2,6] and Olivier Raspé[7,8]**

[1] Department of Biology, Faculty of Science, Chiang Mai University, Chiang Mai, Thailand, [2] Research Center of Microbial Diversity and Sustainable Utilization, Faculty of Science, Chiang Mai University, Chiang Mai, Thailand, [3] Institute of Systematic Botany, New York Botanical Garden, Bronx, NY, United States, [4] Botanic Garden Meise, Meise, Belgium, [5] Fédération Wallonie-Bruxelles, Service Général de l'Enseignement Universitaire et de la Recherche Scientifique, Bruxelles, Belgium, [6] Academy of Science, The Royal Society of Thailand, Bangkok, Thailand, [7] School of Science, Mae Fah Luang University, Chiang Rai, Thailand, [8] Center of Excellence in Fungal Research, Mae Fah Luang University, Chiang Rai, Thailand

OPEN ACCESS

Edited by:
Peter Edward Mortimer,
Kunming Institute of Botany, Chinese Academy of Sciences, China

Reviewed by:
Samantha Chandranath Karunarathna,
Kunming Institute of Botany, Chinese Academy of Sciences, China
Zheng Wang,
Yale University, United States

***Correspondence:**
Saisamorn Lumyong
scboi009@gmail.com
Olivier Raspé
olivier.ras@mfu.ac.th

Specialty section:
This article was submitted to Evolutionary and Genomic Microbiology, a section of the journal Frontiers in Microbiology

Received: 18 December 2020
Accepted: 08 March 2021
Published: 12 April 2021

Citation:
Vadthanarat S, Halling RE, Amalfi M, Lumyong S and Raspé O (2021) An Unexpectedly High Number of New Sutorius (Boletaceae) Species From Northern and Northeastern Thailand. Front. Microbiol. 12:643505. doi: 10.3389/fmicb.2021.643505

Sutorius is a poroid genus in Boletaceae that typically has chocolate brown to reddish brown or purplish brown basidiomata with a finely scaly stipe and produces a reddish brown spore deposit. During the survey on diversity of boletes in Northern and Northeastern Thailand, several *Sutorius* collections were obtained. Combined evidence from morphology and phylogenetic analyses of a combined three-gene data set (*atp*6, *tef*1 and *rpb*2) of the *Sutorius* collections along with selected Boletaceae in the *Pulveroboletus* group indicated that Thai collections represent seven new *Sutorius* species. The analyses also indicated that *Tylopilus maculatoides* belongs in *Sutorius*. Therefore, the transfer of *T. maculatoides* to *Sutorius* is proposed. Full descriptions and illustrations of the seven new species and *S. maculatoides* are presented in this study. With the seven new species and the new combination, eight of the eleven described *Sutorius* species are known to occur in Northern and Northeastern Thailand, whereas only one species is known from each of two continents, the Americas and Australia.

Keywords: *Boletales*, eight new taxa, multigene phylogeny, mushrooms, *Pulveroboletus* group, taxonomy

INTRODUCTION

Sutorius Halling, Nuhn and N.A. Fechner was established in 2012 to accommodate two bolete species, *Boletus eximius* Peck [current name = *Sutorius eximius* (Peck) Halling, Nuhn and Osmundson] and *Leccinum australiense* Bougher and Thiers [current name = *Sutorius australiensis* (Bougher and Thiers) Halling and N.A. Fechner] (Halling et al., 2012). Typical characteristics of *Sutorius* are stipitate–pileate basidiomata with poroid hymenophore, chocolate to reddish brown or purplish brown basidiomata with finely scaly stipe, and a reddish brown spore deposit. The original publication of *Sutorius* also reported two *Sutorius* specimens originating from Chiang Mai Province, in Northern Thailand. One of them was morphologically identified as *S. eximius*, whereas another was phylogenetically recognized as a different species from *S. eximius* and *S. australiensis*. However, the latter was not described as a new species at that time (Halling et al., 2012). In 2016,

Wu et al., recombined several bolete species (e.g., *Boletus brunneissimus* W.F. Chiu; *B. hainanensis* T.H. Li and M. Zang; *B. luridiformis* Rostk.; *B. obscureumbrinus* Hongo; *B. tomentulosus* M. Zang W.P. Liu and M.R. Hu) into the genus *Sutorius* based on their phylogenetic inferences. They also described several new *Sutorius* species from China (e.g., *S. ferrugineus* G. Wu, F. Li and Zhu L. Yang; *S. ferrugineus* G. Wu, F. Li and Zhu L. Yang; *S. rubriporus* G. Wu and Zhu L. Yang). Later, Chai et al. (2019) restudied the phylogenetic relationships of several Boletaceae specimens from subtropical and tropical China, reinstated the genus *Neoboletus* Gelardi, Simonini and Vizzini and recombined all *Sutorius* species described in Wu et al. (2016) to be into this latter. Chai et al. (2019) also newly described a third species of *Sutorius*, *Sutorius subrufus* N.K. Zeng, H. Chai and S. Jiang from Southern China. Moreover, the phylogeny in that study suggested an additional five undescribed *Sutorius* species clustering in 10 independent linages (three described species included). That inference also indicated the exemplars identified as *S. eximius*, originating from several different countries (China, Costa Rica, Indonesia, and United States), were in a polytomic lineage (Chai et al., 2019). So far, the distribution of *Sutorius* has been recorded to occur in several regions including the Americas, Africa, Asia, and Australia (Singer, 1947; Smith and Thiers, 1971; Fulgenzi et al., 2007; Chandrasrikul et al., 2011; Halling et al., 2012; Chai et al., 2019). At present, only three species have been placed in the genus (Halling et al., 2012; Chai et al., 2019).

In Thailand, there were a few reports of *Sutorius* species, originally identified as *Tylopilus eximius* (Peck) Singer (current name = *S. eximius*) (Chantorn et al., 2007; Chandrasrikul et al., 2008; Vadthanarat, 2009; Vadthanarat et al., 2010). However, the identifications in those reports were based on morphological evidence only, and further phylogenetic studies are needed to confirm those identifications. One Asian species of Boletaceae, *Tylopilus maculatoides* E. Horak, also has similar morphological characters as *Sutorius*. That name was proposed for *Boletus maculatus* Corner non-Raddi based on morphological evidence (Horak, 2011). However, the species has not been included in a phylogenetic context until now (see below).

In this study, morphological and phylogenetic analyses of several *Sutorius* collections, including *T. maculatoides* collections, inferred seven new *Sutorius* species among the Thai collections. Moreover, the phylogram also showed that *T. maculatoides* clustered within the *Sutorius* clade with high support. Consequently, the new combination *Sutorius maculatoides* is proposed. Their phylogenetic affinities and reports of other *Sutorius* species from Thailand or elsewhere are critically discussed.

MATERIALS AND METHODS

Specimen Collection

Fresh basidiomata of *Sutorius* were collected in Chiang Mai Province in the North and Ubon Ratchathani Province, Northeastern Thailand, in 2012 to 2018. They were photographed in the field and then wrapped in aluminum foil for later description in the laboratory. The specimens were then dried after the morphological description in an electric drier at 45°C–50°C. Examined specimens were deposited at Department of National Parks, Wildlife and Plant Conservation, Bangkok, Thailand (BKF), Chiang Mai University, Chiang Mai, Thailand (CMUB), and Mae Fah Luang University, Chiang Rai, Thailand (MFLU) with duplicates in Botanic Garden Meise, Belgium (BR).

Morphological Studies

Macroscopic descriptions were made based on the detailed field notes and photographs of fresh basidiomata. Color codes are based on Kornerup and Wanscher (1978). Macrochemical reactions (color reactions) were observed using aqueous solutions of 10% KOH, 28–30% NH_4OH, and Melzer reagent. Microscopic structures were observed from dried specimens and rehydrated in 5% potassium hydroxide or 1% ammoniacal Congo red. For dimensions of microscopic features, a minimum of 50 basidiospores (20 for other structures) were randomly measured at 1,000 × using a calibrated ocular micrometer on an Olympus CX31 compound microscope. The notations "[*n*/*m*/*p*]" show the number of basidiospores "*n*" measured from the number of basidiomata "*m*" of the number of collections "*p*." Dimensions of microscopic structure are presented in the following (*a*–) *b*–*c*–*d* (–*e*), in which "*c*" contains an average, "*b*" is the 5th percentile, "*d*" is the 95th percentile, and extreme values "*a*" and "*e*" are shown in parentheses. *Q* is the length/width ratio. Sections of the pileipellis were cut radially, perpendicularly to the surface halfway between the disc and margin of pileus. Sections of stipitipellis or the squamules on the stipe were taken halfway along the stipe length (Li et al., 2011; Hosen et al., 2013; Li et al., 2014; Zhu et al., 2015). All microscopic features were drawn free hand using an Olympus Camera Lucida model U-DA.

DNA Extraction, Polymerase Chain Reaction Amplification, and DNA Sequencing

Genomic DNA was extracted from fresh tissue preserved in CTAB or approximately 10–15 mg of dried tissue using a CTAB isolation procedure adapted from Doyle and Doyle (1990). Parts of three protein-coding genes, *atp*6, *tef*1, and *rpb*2, were amplified by polymerase chain reaction (PCR) and sequenced. ITS-5.8 region of the nuclear ribosomal DNA was not sequenced because in Boletaceae, ITS commonly shows high levels of intraindividual polymorphisms for indels, thus mostly preventing straightforward phylogenetic analysis and moreover often making cloning necessary to obtain a sequence. The selected protein-coding genes have shown multiple times their usefulness for investigating phylogenetic relationships, at both infrageneric and suprageneric levels (e.g., Wu et al., 2016; Vadthanarat et al., 2019). For the amplification of *atp*6, ATP6-1M40F and ATP6-2M primers were used, with following the protocol and PCR program in Raspé et al. (2016). The primers EF1-983F and EF1-2218R (Rehner and Buckley, 2005) were used to amplify *tef*1 gene, and bRPB2-6F and bRPB2-7.1R primers (Matheny, 2005) were used to amplify *rpb*2 gene. PCR

products were purified by adding 1 U of exonuclease I and 0.5 U FastAP alkaline phosphatase (Thermo Scientific, St. Leon-Rot, Germany) and incubating at 37°C for 1 h, followed by inactivation at 80°C for 15 min. Sequencing was performed by Macrogen Inc. (Korea and the Netherlands) with PCR primers, except for *atp*6, for which universal primers M13F-pUC(-40) and M13F(-20) were used; for *tef*1, additional sequencing was performed with the two internal primers, EF1-1577F and EF1-1567R (Rehner and Buckley, 2005).

Alignment and Phylogeny Inference

The sequences were assembled in GENEIOUS Pro v. 6.0.6 (Biomatters). All nucleotide sequences, including nucleotide sequences obtained from GenBank, were aligned using MAFFT version 7 (Katoh and Standley, 2013) on the server accessed at http://mafft.cbrE.jp/alignment/server/.

Before combining the data partitions, topological incongruence between the datasets was assessed using maximum likelihood (ML) and Bayesian inference (BI) separately on each of the four character sets, *atp*6, *tef*1 exons, *rpb*2 exons, and the three introns of *tef*1 + the intron of *rpb*2. Paired trees were examined for conflicts involving only nodes with ML bootstrap (BS) > 75% and Bayesian posterior probabilities (PPs) > 0.95 (Mason-Gamer and Kellogg, 1996; Lutzoni et al., 2004; Reeb et al., 2004). A conflict was assumed to be significant if two different relationships for the same set of taxa (one being monophyletic and the other non-monophyletic) were observed in rival trees. For ML, phylogenetic inference was performed using RAxML (Stamatakis, 2006) on the CIPRES web portal (RAxML-HPC2 on XSEDE; Miller et al., 2009), using the GTRCAT model with 25 categories. Three *Butyriboletus* species were used as outgroup based on the phylogeny in Vadthanarat et al. (2019). Statistical support of clades was obtained with 1,000 rapid BS replicates. For BI, the best-fit model of substitution among those implementable in MrBayes was estimated separately for each character set using jModeltest (Darriba et al., 2012) on the CIPRES portal, based on the Bayesian information criterion. The selected models were HKY + I + G for *atp*6, SYM + I + G for *tef*1 exons, and K80 + I + G for *rpb*2 exons and intron partition. The Bayesian analysis was performed with MrBayes 3.2.6 software for Windows (Ronquist et al., 2012).

Then, phylogenetic inference of a combined, partitioned dataset was performed, using ML under the same model mentioned above. The phylogenetic tree was inferred from a single analysis with four character sets: *atp*6, *tef*1 exons, *rpb*2 exons and the three introns of *tef*1 + the intron of *rpb*2. The same combined dataset was also analyzed by BI, based on the best-fit model mentioned previously. The two runs of five chains were run for 1,000,000 generations and sampled every 200 generations. At the end of the run, the average deviation of split frequencies was 0.008306, and the potential scale reduction factor values of all parameters were close to 1. The burn-in phase (25%) was estimated by checking the stationarity in the plot generated by the sump command. A total of 7,396 stationary trees were used to reconstruct a 50% majority rule consensus tree and calculate the Bayesian PPs.

RESULTS

Phylogenetic Analyses

Fifty-four sequences from *Sutorius* collections corresponding to 11 phylogenetic species were newly generated and deposited in GenBank. The combined alignment of the three loci studied contained 190 sequences (32 for *atp*6, 80 for *tef*1, 78 for *rpb*2) from 80 specimens (**Table 1**) and was 2,681 characters long (gaps included) (TreeBase no. 27286).

The single-gene trees were very similar in topology (**Supplementary Figures 1–4**), except for one supported conflict. In the *tef*1 exons tree (**Supplementary Figure 2**), *Sutorius pachypus* formed a clade sister to *S. australiensis* with high support (BS = 75%, PP = 0.92). This is in conflict with the topology of the tree based on the introns character set (**Supplementary Figure 4**), in which *S. pachypus* formed a clade sister to *Sutorius rubinus* (BS = 87%, PP = 0.97). Partitioned analyses of a dataset combining *atp*6, *tef*1 exons, and *rpb*2 exons sequences were also performed (**Supplementary Figure 5**). Its tree topology showed no conflict to the single partitions of *atp*6, *tef*1 exons, and *rpb*2 exons trees. Consequently, the combination of four-partition analyses was used to infer the relationship between species in this study.

Maximum likelihood and BI trees of the combined three-gene dataset showed similar topologies without any supported conflict (Bootstrap support values, BS ≥ 70% and PP ≥ 0.90; **Figure 1**). The phylogram of RAxML bipartitions (**Figure 1**) indicated that all selected Boletaceae formed eight highly supported generic clades (BS = 100% and PP = 1 for *Sutorius*, *Pulveroboletus*, *Suillellus*, *Rubroboletus*, *Crocinoboletus*, and *Butyriboletus*; BS = 94% and PP = 1 for the *Neoboletus* clade). All *Sutorius* exemplars clustered together in a strongly supported clade, sister to *Neoboletus* (BS = 70% and PP = 0.90). In the *Sutorius* clade, 17 terminal, species-level clades were resolved with high support, including the three previously described species clades (clade 5 = *S. eximius*, clade 6 = *S. subrufus*, and clade 11 = *S. australiensis*); 7 clades of new, undescribed species originating from Thailand (clades 4, 7, 8, 9, 10, 12, and 17), with one clade (clade 13) containing *T. maculatoides* (WAT25793); and two Thai collections (OR0626 and OR0758). Also, six clades of unnamed species were inferred (clades 1 and 2 from China; clade 3 from Costa Rica; clades 14, 15, and 16 from Togo, Zimbabwe, and Burundi, respectively).

Taxonomy

Sutorius maculatoides (E. Horak) Vadthanarat, Raspé and Lumyong **comb. nov.**

MycoBank: MB838055

Figures 2, **3**

Basionym: *B. maculatus* Corner, *Boletus* in Malaysia: 160, 1972, non-Raddi, Mem. Mat. Fis. Soc. Ital. Sci. Modena, Pt. Mem. Fis. 13: 352. 1807.

Synonymy: *T. maculatoides* E. Horak, Malayan Forest Records 51: 98, 2011.

Description (based on Thai specimens): *Basidiomata* small- to medium-sized. *Pileus* (1.8) 2.4 to 4.6 cm in diameter, at

TABLE 1 | List of collections used for DNA analyses of the genus *Sutorius*, with origin, GenBank accession numbers, and reference(s).

Species	Voucher	Origin	*atp6*	*tef1*	*rpb2*	Reference(s)
Butyriboletus appendiculatus	VDKO0193b	Belgium	MG212537	MG212582	MG212624	Vadthanarat et al. (2018)
Butyriboletus cf. *roseoflavus*	OR0230	China	KT823974	KT824040	KT824007	Raspé et al. (2016)
Butyriboletus pseudoregius	VDKO0925	Belgium	MG212538	MG212583	MG212625	Vadthanarat et al. (2018)
Caloboletus firmus	BOS-372	Belize	—	MK721080	MK766288	Kuo and Ortiz-Santana (2020)
Caloboletus inedulis	MICH:KUO-07031403	United States	—	MK721081	MK766289	Kuo and Ortiz-Santana (2020)
Caloboletus radicans	VDKO1187	Belgium	MG212540	MG212584	MG212626	Vadthanarat et al. (2018)
Caloboletus yunnanensis	HKAS69214	China	—	KJ184568	KT990396	Zhao et al. (2014); Wu et al. (2016)
Crocinoboletus cf. *laetissimus*	OR0576	Thailand	KT823975	KT824041	KT824008	Raspé et al. (2016)
Crocinoboletus rufoaureus	HKAS53424	China	—	KF112206	KF112710	Wu et al. (2014)
Neoboletus brunneissimus	HKAS52660	China	—	KF112143	KF112650	Wu et al. (2014)
Neoboletus ferrugineus	HKAS77617	China	—	KT990788	KT990430	Wu et al. (2016)
Neoboletus ferrugineus	HKAS77718	China	—	KT990789	KT990431	Wu et al. (2016)
Neoboletus flavidus	HKAS58724	China	—	KU974137	KU974145	Wu et al. (2016)
Neoboletus flavidus	HKAS59443	China	—	KU974136	KU974144	Wu et al. (2016)
Neoboletus hainanensis	HKAS63515	China	—	KT990808	KT990449	Wu et al. (2016)
Neoboletus hainanensis	HKAS74880	China	—	KT990790	KT990432	Wu et al. (2016)
Neoboletus hainanensis	HKAS90209	China	—	KT990809	KT990450	Wu et al. (2016)
Neoboletus hainanensis	HKAS59469	China	—	KF112175	KF112669	Wu et al. (2016)
Neoboletus junquilleus	AF2922	France	MG212552	MG212596	MG212638	Vadthanarat et al. (2018)
Neoboletus magnificus	HKAS54096	China	—	KF112149	KF112654	Wu et al. (2014)
Neoboletus magnificus	HKAS74939	China	—	KF112148	KF112653	Wu et al. (2014)
Neoboletus obscureumbrinus	HKAS63498	China	—	KT990791	KT990433	Wu et al. (2016)
Neoboletus obscureumbrinus	HKAS77774	China	—	KT990792	KT990434	Wu et al. (2016)
Neoboletus obscureumbrinus	HKAS89027	China	—	KT990794	KT990436	Wu et al. (2016)
Neoboletus rubriporus	HKAS57512	China	—	KF112151	KF112656	Wu et al. (2014)
Neoboletus rubriporus	HKAS83026	China	—	KT990795	KT990437	Wu et al. (2016)
Neoboletus rubriporus	HKAS89174	China	—	KT990796	KT990438	Wu et al. (2016)
Neoboletus sanguineoides	HKAS57766	China	—	KT990799	KT990440	Wu et al. (2016)
Neoboletus sanguineoides	HKAS74733	China	—	KT990800	KT990441	Wu et al. (2016)
Neoboletus sanguineoides	HKAS55440	China	—	KF112145	KF112652	Wu et al. (2014)
Neoboletus sanguineus	HKAS80823	China	—	KT990802	KT990442	Wu et al. (2016)
Neoboletus sanguineus	HKAS68587	China	—	KF112150	KF112657	Wu et al. (2014)
Neoboletus sanguineus	HKAS90211	China	—	KT990804	KT990444	Wu et al. (2016)
Neoboletus sp.	HKAS76660	China	—	KF112180	KF112731	Wu et al. (2014)
Neoboletus sp.	OR0128	Thailand	MH614686	MH614734	MH614781	Vadthanarat et al. (2019)
Neoboletus sp.	HKAS76851	China	—	KF112144	KF112651	Wu et al. (2014)
Neoboletus tomentulosus	HKAS77656	China	—	KT990806	KT990446	Wu et al. (2016)
Neoboletus tomentulosus	HKAS53369	China	—	KF112154	KF112659	Wu et al. (2014)
Neoboletus tomentulosus	HKAS77614	China	—	KT990805	KT990445	Wu et al. (2016)
Neoboletus venenatus	HKAS63535	China	—	KT990807	KT990448	Wu et al. (2016)
Pulveroboletus aff. *ravenelii*	ADK4360	Togo	KT823957	KT824023	KT823990	Raspé et al. (2016)
Pulveroboletus aff. *ravenelii*	ADK4650	Togo	KT823959	KT824025	KT823992	Raspé et al. (2016)
Pulveroboletus aff. *ravenelii*	HKAS53351	China	—	KF112261	KF112712	Wu et al. (2014)
Pulveroboletus fragrans	OR0673	Thailand	KT823977	KT824043	KT824010	Raspé et al. (2016)
Pulveroboletus ravenelii	REH2565	United States	KU665635	KU665636	KU665637	Raspé et al. (2016)
Pulveroboletus sp.	HKAS57665	China	—	KF112264	KF112715	Wu et al. (2014)
Pulveroboletus sp.	HKAS74933	China	—	KF112262	KF112713	Wu et al. (2014)
Rubroboletus legaliae	VDKO0936	Belgium	KT823985	KT824051	KT824018	Raspé et al. (2016)
Rubroboletus rhodoxanthus	HKAS84879	China	—	KT990831	KT990468	Wu et al. (2016)
Rubroboletus satanas	VDKO0968	Belgium	KT823986	KT824052	KT824019	Raspé et al. (2016)
Suillellus luridus	VDKO0241b	Belgium	KT823981	KT824047	KT824014	Raspé et al. (2016)
Suillellus subamygdalinus	HKAS53641	China	—	KT990841	KT990478	Wu et al. (2016)
Sutorius aff. *eximius*	HKAS50420	China	—	KT990750	KT990387	Wu et al. (2016)

(Continued)

TABLE 1 | Continued

Species	Voucher	Origin	*atp6*	*tef1*	*rpb2*	Reference(s)
Sutorius aff. *eximius*	HKAS52672	China	—	KF112207	KF112802	Wu et al. (2014)
Sutorius aff. *eximius*	HKAS56291	China	—	KF112208	KF112803	Wu et al. (2014)
Sutorius aff. *eximius*	HKAS59657	China	—	KT990887	KT990505	Wu et al. (2016)
Sutorius aff. *eximius*	TWO-986	Costa Rica	—	MK721180	MK766383	Kuo and Ortiz-Santana (2020)
Sutorius australiensis	REH9441	Australia	MG212567	JQ327032*	MG212652	Vadthanarat et al. (2018); *Halling et al. (2012)
Sutorius australiensis	REH9485	Australia	—	MK721165	MK766367	Kuo and Ortiz-Santana (2020)
Sutorius australiensis	REH10021	Australia	—	MK721166	MK766368	Kuo and Ortiz-Santana (2020)
Sutorius eximius	REH9400	United States	MG212568	JQ327029*	MG212653	Vadthanarat et al. (2018); *Halling et al. (2012)
Sutorius eximius	REH10038	United States	—	MK721167	MK766369	Kuo and Ortiz-Santana (2020)
Sutorius maculatoides	OR0758	Thailand	**MN067462**	**MN067481**	**MN067498**	This study
Sutorius maculatoides	WAT25793	Malaysia	**MN067463**	**MN067482**	—	This study
Sutorius maculatoides	OR0626	Thailand	**MN067461**	**MN067480**	—	This study
Sutorius mucosus	OR0851 (type)	Thailand	**MN067464**	**MN067483**	**MN067499**	This study
Sutorius pachypus	OR0411 (type)	Thailand	**MN067465**	**MN067484**	**MN067500**	This study
Sutorius pachypus	SV0098	Thailand	**MN067466**	**MN067485**	**MN067501**	This study
Sutorius pachypus	TWO1171	Thailand	**MW194871**	—	—	This study
Sutorius pseudotylopilus	OR0378B (type)	Thailand	MH614692	MH614740	MH614787	Vadthanarat et al. (2019)
Sutorius pseudotylopilus	SV0401	Thailand	**MN067467**	**MN067486**	**MN067502**	This study
Sutorius pseudotylopilus	SV0415	Thailand	**MN067468**	**MN067487**	**MN067503**	This study
Sutorius rubinus	OR0379	Thailand	MH614693	MH614741	MH614788	Vadthanarat et al. (2019)
Sutorius rubinus	OR0403 (type)	Thailand	**MN067469**	**MN067488**	**MN067504**	This study
Sutorius rubinus	OR0409	Thailand	**MN067470**	**MN067489**	**MN067505**	This study
Sutorius rubinus	OR1255	Thailand	**MN067471**	**MN067490**	**MN067506**	This study
Sutorius sp.	ADK2396	Zimbabwe	**MN067477**	**MN067495**	**MN067511**	This study
Sutorius sp.	ADK4369	Togo	**MN067478**	**MN067496**	**MN067512**	This study
Sutorius sp.	JD669	Burundi	**MN067479**	**MN067497**	**MN067513**	This study
Sutorius subrufus	FHMU2101	China	—	MH879730	MH879747	Chai et al., 2019
Sutorius subrufus	FHMU2006	China	—	MH879729	MH879746	Chai et al., 2019
Sutorius ubonensis	SV0032 (type)	Thailand	**MN067472**	**MN067491**	**MN067507**	This study
Sutorius ubonensis	SV0203	Thailand	**MN067473**	**MN067492**	**MN067508**	This study
Sutorius ubonensis	SV0353	Thailand	**MN067474**	**MN067493**	**MN067509**	This study
Sutorius obscuripellis	OR0949 (type)	Thailand	**MN067475**	**MN067494**	**MN067510**	This study
Sutorius vellingae	ECV3603 (type)	Thailand	**MN067476**	JQ327033	—	This study; Halling et al. (2012)

Newly generated sequences are shown in bold font.

first hemispherical with straight margin becoming convex with deflexed margin; *surface* subrugulose, dull, minutely tomentose, at first dark lilac (10–11F3–6) becoming purplish to reddish brown to brown (8F6, 7E5) in age, gradually paler to the margin. *Pileus context* 4–5 mm thick halfway to the margin, firm, yellowish off-white (4A2), near the center grayish to purplish white (14–15C–E2) at first, then yellowish white (4A2) in age, with scattered small violet–brown (11F4–6) encrustations. *Stipe* central, terete to slightly compressed, cylindrical, slightly wider at the base, 2.4–4.5 × 0.6–1.2 cm; *surface* finely scabrous with groups of brown to dark brown (7–8F4–6) granulose squamules on purplish gray (15C2, 15D3) background; *basal tomentum* little developed, white. *Stipe context* solid, pale grayish orange (5B2), virgated with grayish purple (15–16C3), with scattered small violet–brown (11F4–6) encrustations. *Hymenophore* tubulose, subventricose to adnexed to broadly adnexed, depressed around stipe; *tubes* easily separable, at first grayish brown (7D3) then brownish orange (6C6) with age, 8–9 mm long halfway to the margin; *pores* 0.2–0.4(0.7) mm wide at midradius, regular roundish; at first lilac-gray (15–16E3 to 15C2) slightly paler near the margin, becoming pale reddish brown (9D–E4) with age. *Odor* fungoid. *Taste* mild. *Spore print* reddish brown (8E/F5).

Macrochemical reactions: KOH: pale greenish yellow on pileus, pileus context, stipe and stipe context; pale brownish orange on hymenophore. NH_4OH: pale greenish yellow on pileus, on pileus context bluish white (21A2) when young or negative in mature basidiomes; greenish yellow on stipe; greenish yellow then purplish on stipe context.

Basidiospores [165/3/3] (7.8–) 8.3–10.9–13.2 (–14.1) × (3–) 3.3–4–4.7 (–5.6) µm, *Q* = (2.02–) 2.24–2.69–3.18 (–3.41), narrowly ellipsoid to subcylindrical with slight suprahilar depression, thin-walled, smooth, brownish to yellowish hyaline in water, yellowish hyaline in KOH or NH_4OH, inamyloid. *Basidia* 4-spored (23–) 23–26–31 (–32) × (10–) 10–11–13 (–14) µm, with sterigmata up to 4 µm long, clavate, hyaline, inamyloid. *Cheilocystidia* (19–) 19–22–27 (–27) × (6–) 6–8–9 (–9) µm, frequent, fusiform, thin-walled, hyaline. *Pleurocystidia*

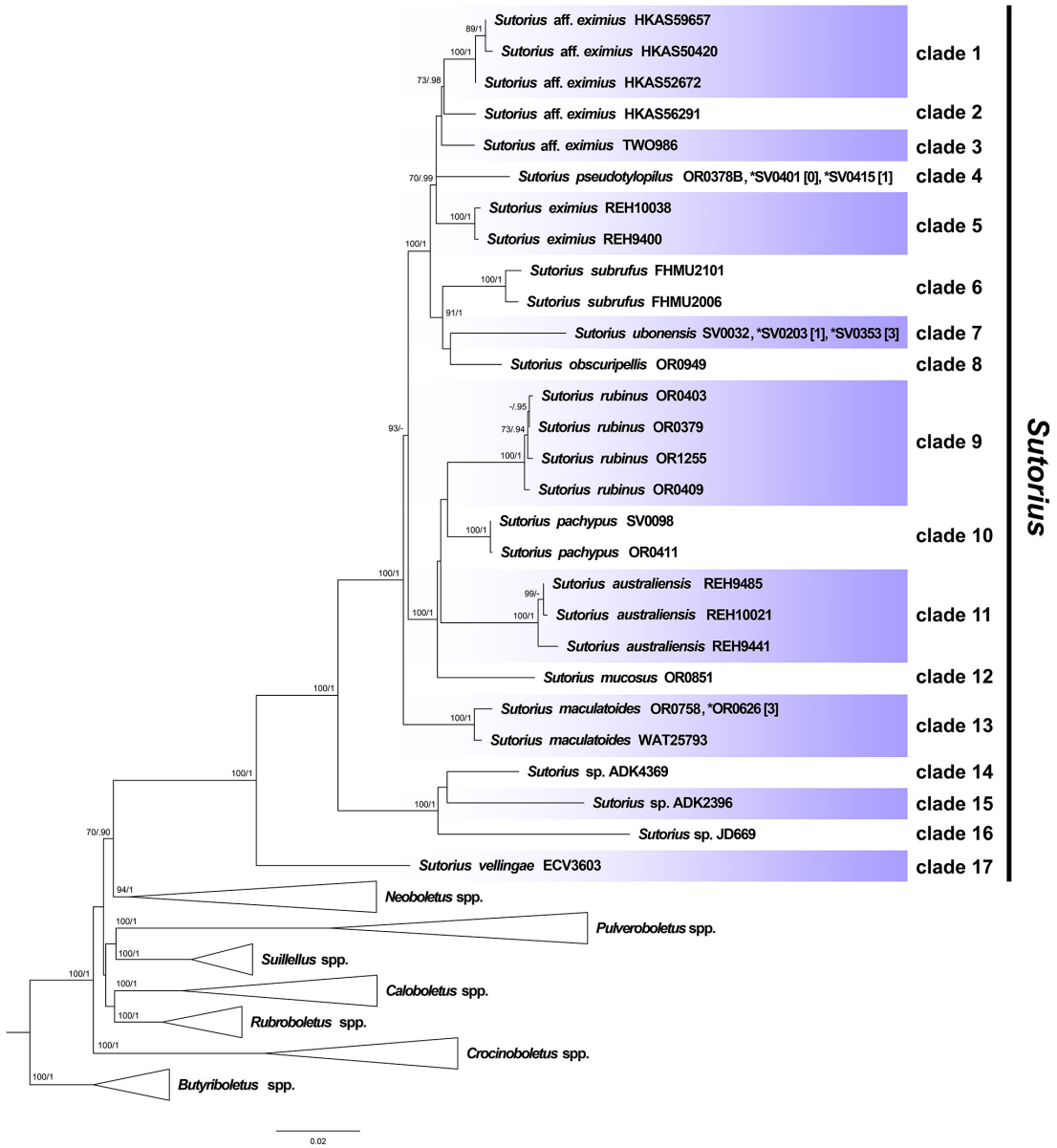


FIGURE 1 | Phylogenetic tree inferred from the three-gene dataset (*atp*6, *rpb*2 and *tef*1), of *Sutorius* species and selected Boletaceae in *Pulveroboletus* group, using Maximum Likelihood and Bayesian Inference methods (ML bipartition tree is presented). The three *Butyriboletus* species were used as outgroup. All generic clades, excluding *Sutorius*, that were highly supported were collapsed. Seventeen species-level clades within *Sutorius* are indicated with label. Bootstrap support values (BS $\geq$ 70%) and posterior probabilities (PP $\geq$ 0.90) are shown above the supported branches. The star (*) indicates additional collections with exactly identical sequences or sequences differing only by heteromorphisms in *tef*1 (with the number of heteromorphisms mentioned in square brackets [ ]).

(32–) 32–38–45 (–45) × (6–) 6–8–10 (–10) μm, infrequent, narrowly fusiform, thin-walled, hyaline. *Hymenophoral trama* divergent becoming boletoid in age, 21–52 μm wide, with regular mediostratum 9–22 μm wide. *Pileipellis* a sub-ixotrichoderm to intricate trichoderm, 135–212 μm thick, terminal cells (12–55 × 5–11 μm) fusiform with slightly tapering apex, pale yellowish brown in water, mostly hyaline to pale yellowish brown in KOH or NH_4OH, with scattered loose crystals. *Pileus context* made of strongly interwoven, hyaline, thin-walled hyphae, 8–13 μm wide, with scattered loose crystals. *Stipitipellis* a disrupted hymeniderm, 100–120 μm thick, composed of parallel hyphae, with terminal cell 11–33 × 7–10 μm of thin-walled, hyaline hyphae, giving rise to clusters of caulocystidia and basidiole-like cells, with scattered loose crystals. *Caulocystidia* (18–) 18–26–37 (–38) × (8–) 8–11–15 (–15) μm, frequent, fusiform to broadly fusiform with subacute apex, thin-walled, hyaline. *Stipe context* composed of parallel, 4- to 12-μm-wide hyphae, with scattered loose crystals. *Clamp connections* not seen in any tissue.

Microscopic description (based on WAT25793): *Basidiospores* (11.4–) 11.5–12.1–12.7 (–13.5) × (4.1–) 4.2–4.5–4.8 (–4.9) μm,

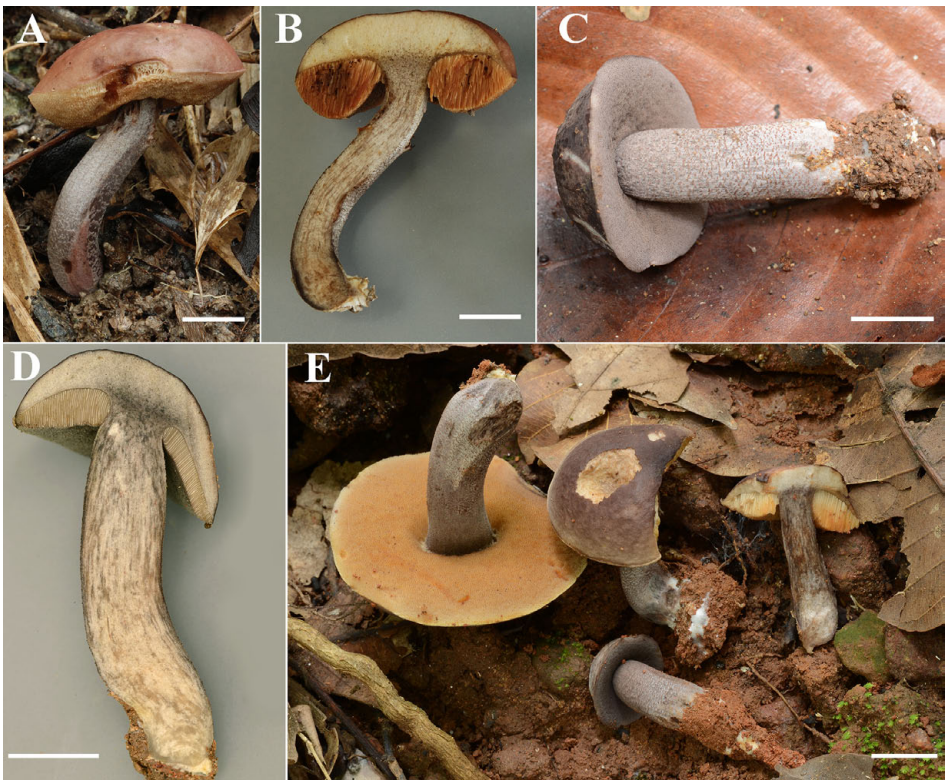


FIGURE 2 | (A–E) Fresh basidiomata of *Sutorius maculatoides* (**A,B**: OR0626; **C,D**: OR0754; **E**: OR758). Scale bars: **(A–E)** = 1 cm.

Q = (2.42–) 2.42–2.68–2.94 (–3.05), N = 72, narrowly ellipsoid to subcylindrical with slight suprahilar depression, thin-walled, smooth, brownish to yellowish hyaline in water, yellowish hyaline in KOH and NH_4OH, inamyloid. *Basidia* 4-spored (21–) 21–24–28 (–29) × (9–) 10–11–12 (–12) µm, with sterigmata up to 3 µm long, clavate, yellowish hyaline to yellowish-brown in KOH, inamyloid. *Cheilocystidia* (15–) 16–21–24 (–24) × (6–) 6–7–8 (–8) µm, frequent, fusiform, thin-walled hyaline. *Pleurocystidia* (31–) 31–36–43 (–43) × (5–) 5–6–7 (–7) µm, quite rare, narrowly fusiform, thin-walled, hyaline. *Pileipellis* a sub-ixotrichoderm to intricate trichoderm, 67- to 132-µm-thick, thin-walled hyphae, with fusiform terminal cells (11–53 × 6–11 µm) with slightly tapering apex. *Pileus context* made of moderately interwoven hyaline hyphae, 6–13 µm wide. *Stipitipellis* a disrupted hymeniderm, 65–85 µm thick, composed of parallel hyphae, with rounded terminal cell 14–40 × 5–10 µm of thin-walled, hyaline hyphae; at places the terminal cells grouped with caulocystidia into clusters, with scattered loose crystals. *Stipe context* composed of parallel 4- to 14-µm-wide hyaline, thin-walled hyphae. *Caulocystidia* (20–) 20–28–37 (–37) × (7–) 8–11–15 (–15) µm, frequent, fusiform to broadly fusiform with subacute apex, thin-walled, hyaline. *Clamp connections* not seen in any tissue.

Habitat: Solitary to gregarious on soil, in hill forest dominated by *Dipterocarpus obtusifolius*, *Dipterocarpus tuberculatus*, *Shorea obtusa*, and *Shorea siamensis*.

Distribution: Malaysia, Singapore, and Thailand.

Collections examined: **MALAYSIA:** Forest Research Institute Kepong, MNS foray along rovers' trail, 27 February 1994, Roy Watling, WAT25793 (E). **THAILAND:** Chiang Mai Province: Doi Suthep-Pui National Park, 18°48′47″N–98°56′11″E, elev. 540 m, May 18, 2015, Olivier Raspé, OR0626 (BKF, CMUB); –ibid., 18°47′37″N–98°55′41″E, elev. 770 m, May 24, 2015, Olivier Raspé and Santhiti Vadthanarat, OR0754 (BKF, CMUB); –ibid., 18°47′38″N–98°55′42″E, elev. 770 m, May 26, 2015, Olivier Raspé and Santhiti Vadthanarat, OR0758 (BKF, CMUB); Mae On District, Ban Huay Kaew community forest, 18°52′7.15″N–99°17′38.92″E. 750 m, July 17, 2017, Olivier Raspé, OR1414 (CMUB, BR).

Notes: Corner (1972) described *B. maculatus* from Malaysia. However, it was a later non-homotypic homonym of *B. maculatus* Raddi described in 1807. Consequently, Horak (2011) gave the new epithet *maculatoides*. He also transferred the species to *Tylopilus*. Here, we present phylogenetic evidence supporting placement in *Sutorius*. In our phylogenetic inference (**Figure 1**), all *S. maculatoides* collections clustered together in a well-supported terminal clade (clade 13), within the *Sutorius* clade. The macromorphological and micromorphological characters of *S. maculatoides* also support its position in *Sutorius*. Therefore, the new combination *S. maculatoides* is proposed for *T. maculatoides*. In our phylogeny, among the *S. maculatoides* specimens, the Thai collections (OR0626 and OR0758) were molecularly slightly divergent from the Malaysian specimen (WAT25793). Being the amount of divergence is lower than

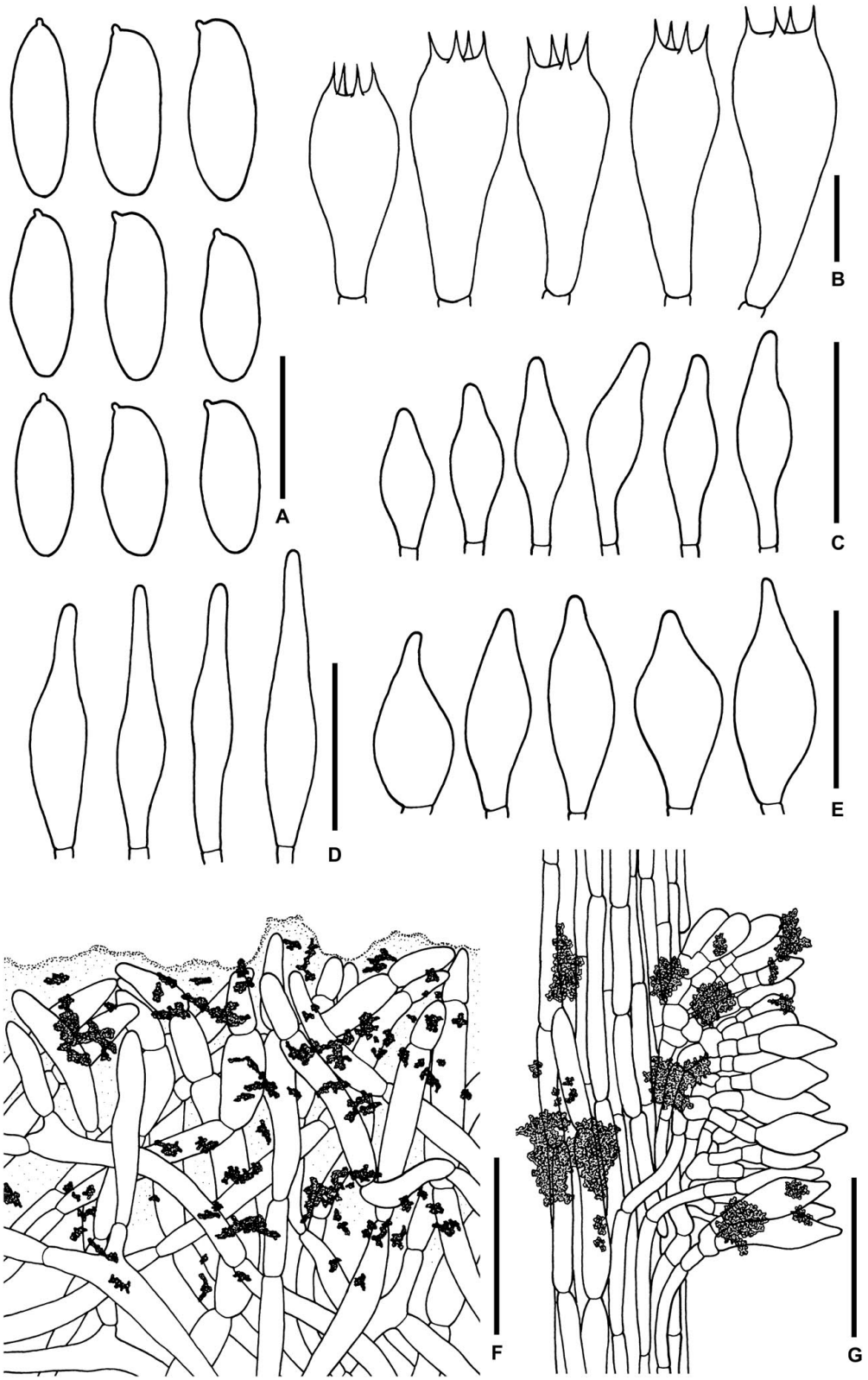


FIGURE 3 | Microscopic features of *Sutorius maculatoides*. **(A)** Basidiospores. **(B)** Basidia. **(C)** Cheilocystidia. **(D)** Pleurocystidia. **(E)** Caulocystidia. **(F)** Pileipellis. **(G)** Stipitipellis. All drawings were made from OR0758. Scale bars: **(A,B)** = 10 μm; **(C–E)** = 25 μm; **(F,G)** = 50 μm.

the one observed between sister species, we consider those differences in the range of intraspecific genetic variability and compatible with conspecific, geographically distant populations.

Sutorius maculatoides is characterized by the following characteristics: dark lilac pileus with lilac gray pores at first, with age becoming reddish brown and reddish pale brown, respectively; presence of cheilocystidia and infrequent pleurocystidia; pileipellis a sub-ixotrichoderm composed of moderately interwoven hyphae, with fusiform terminal cells that slightly taper at the apex.

In this study, *S. maculatoides* is redescribed based on specimens from Thailand (OR0626 and OR0758) and Malaysia (WAT25793), which were compared to the description of *T. maculatoides* E. Horak (Horak, 2011). Microcharacteristics of Watling's specimen were similar to Horak's description including size and shape of basidiospores, basidia, and pileipellis. However, the cheilocystidia in Watling's specimen (15–24 × 6–8 μm) are shorter than in Horak's description (35–45 × 6–11 μm), but Horak did not separately describe the length of cheilocystidia and pleurocystidia. He also did not mention the frequency of both types of cystidia. By comparison, microscopic characters between Watling's specimen and the Thai specimens were almost identical. However, the minimum value of the length of basidiospores in Watling's specimen (11.4–13.5 × 4.1–4.9 μm) is higher than for the Thai specimens (7.8–14.1 × 3–5.6 μm). The lower minimum value of length of basidiospores in Thai specimens could be explained by small quantitative differences between geographically distant populations or the less mature stage of some basidiomata from Thai collections. Moreover, according to our observations on *Sutorius*, this genus usually shows high within-species variation in spore size, which was also noted originally by Halling et al. (2012).

Sutorius mucosus Vadthanarat, Raspé and Lumyong **sp. nov.**

MycoBank: MB838057

Figures 4A–C, **5**

Typification: **THAILAND:** Chiang Mai Province: Mae Taeng District, Pha Deng village, 19°6′31″N–98°44′30″E, elev. 1,050 m, July 29, 2014, Olivier Raspé and Anan Thawthong, OR0851 (MFLU: holotype; BR: isotype).

Etymology: from Latin mucosus, means mucus, referring to a strongly gelatinized pileipellis.

Description: *Basidiomata* medium-sized. *Pileus* 9 cm in diameter, planoconvex with straight margin, margin slightly exceeding (1 mm); *surface* subrugulose, dull, waxy to subviscid, almost smooth to minutely tomentose under the lens, reddish brown (8E/F8). *Pileus context* 8–10 mm halfway to the margin, soft, dull yellowish white (4A2), with scattered small groups of reddish brown (9F5–7) encrustations, slightly reddening (5A2–3) when cut. *Stipe* central, terete, cylindrical, × 1.2 cm; *surface* subscabrous, with granulose squamules, purplish brown to dark brown (10–11F4–7), uplifted by pale brown (5B/C3–5) hyphae; *stipe context* solid, slightly turgid, beige (4B/C3). *Hymenophore* tubulose, ventricose; *tubes* easily separable, pale orange (5A2–3), 7–9 mm long halfway to the margin; *pores* 0.2–0.3(0.5) mm wide at midradius, roundish to angular near the stipe, pore topography irregular, brown to brownish gray (7B4–5 to 8D/E4). *Odor* and *taste* not observed. *Spore print* reddish brown (8E/F8).

Macrochemical reactions: KOH: yellowish on pileus context.

Basidiospores (10.4–) 10.8–13.8–15 (–15.4) × (4.3–) 4.6–5–5.5 (–5.6) μm, Q = (2.24–) 2.47–2.76–3.04 (–3.06), N = 55, narrowly ellipsoid to subcylindrical with slight suprahilar depression, thin-walled, smooth, brownish to yellowish hyaline in water, yellowish hyaline in KOH or NH_4OH, inamyloid. *Basidia* 4-spored (23–) 23–26–30 (–30) × (10–) 10–11–13 (–13) μm, with sterigmata up to 4 μm long, clavate, hyaline, inamyloid. *Cheilocystidia* and *Pleurocystidia* not seen. *H. trama* slightly divergent to boletoid 17–42 μm wide, with subregular mediostratum 7–12 μm wide. *Pileipellis* an ixotrichoderm, 75–125 μm thick, made of moderately interwoven, gelatinized, hyaline hyphae, with terminal cells 11–37 × 7–11 μm, fusiform to utriform with rounded to tapping apex, pale yellowish to brownish hyaline in water, mostly hyaline to yellowish hyaline in KOH or NH_4OH, with scattered loose crystals. *Pileus context* composed of strongly gelatinized hyaline hyphae 8–16 μm wide, at places with scattered loose crystals. *Stipitipellis* a disrupted hymeniderm 200–450 (600) μm thick composed of parallel hyphae, with terminal cell 15–29 × 6–9 μm of thin-walled, hyaline hyphae, giving rise to clusters of basidiole-like cells and caulocystidia, with scattered loose crystals. *Caulocystidia* (19–) 19–27–36 (–36) × (8–) 8–11–15 (–15) μm, not frequent, fusiform to broadly fusiform, thin-walled, hyaline. *Stipe context* composed of parallel, 8- to 12-μm-wide gelatinized hyphae, somewhere covered with some encrustations on the wall, with scattered loose crystals. *Clamp connections* not seen.

Habitat: Solitary on soil in evergreen hill forest dominated by *Castanopsis* spp., *Lithocarpus* spp. mixed with *D. obtusifolius*, *Dipterocarpus costatus*, *Sh. obtusa*, and *Sh. siamensis*.

Distribution: Chiang Mai Province, Northern Thailand.

Notes: *S. mucosus* description is based on a single collection (OR0851); however, the strongly gelatinized pileipellis is a strikingly unique character, which, together with the phylogenetic evidence, which resolved this specimen as an isolated branch, within the *Sutorius* lineage, supports our interpretation of OR0851 as a new, distinct species. Other important characters that allow differentiating *S. mucosus* are the fusiform to utriform pileipellis terminal cells with rounded to subacute apex and the lack of cheilocystidia and pleurocystidia.

Phylogenetically, *S. mucosus* is resolved as an isolated branch, within a clade comprising three other distinct *Sutorius* species, including *S. rubinus* (clade 9), *S. pachypus* (clade 10), and *S. australiensis* (clade 11). However, they are morphologically different, and none of them has a strong gelatinized pileipellis, which is the most striking diagnostic character of *S. mucosus*. The other differences are as follows: *S. pachypus* has, on average, a wider stipe (2.5–4 cm wide) and paler stipe surface, presence of cheilocystidia and pleurocystidia, and palisadodermal pileipellis composed of subcylindrical terminal cells with rounded to subacute apex. *S. australiensis* has a trichoderm pileipellis with elongated to cylindrical hyphae with obtuse apex terminal cells. *S. rubinus* also has a trichoderm pileipellis but with different shapes of terminal cells, which are fusiform to broadly

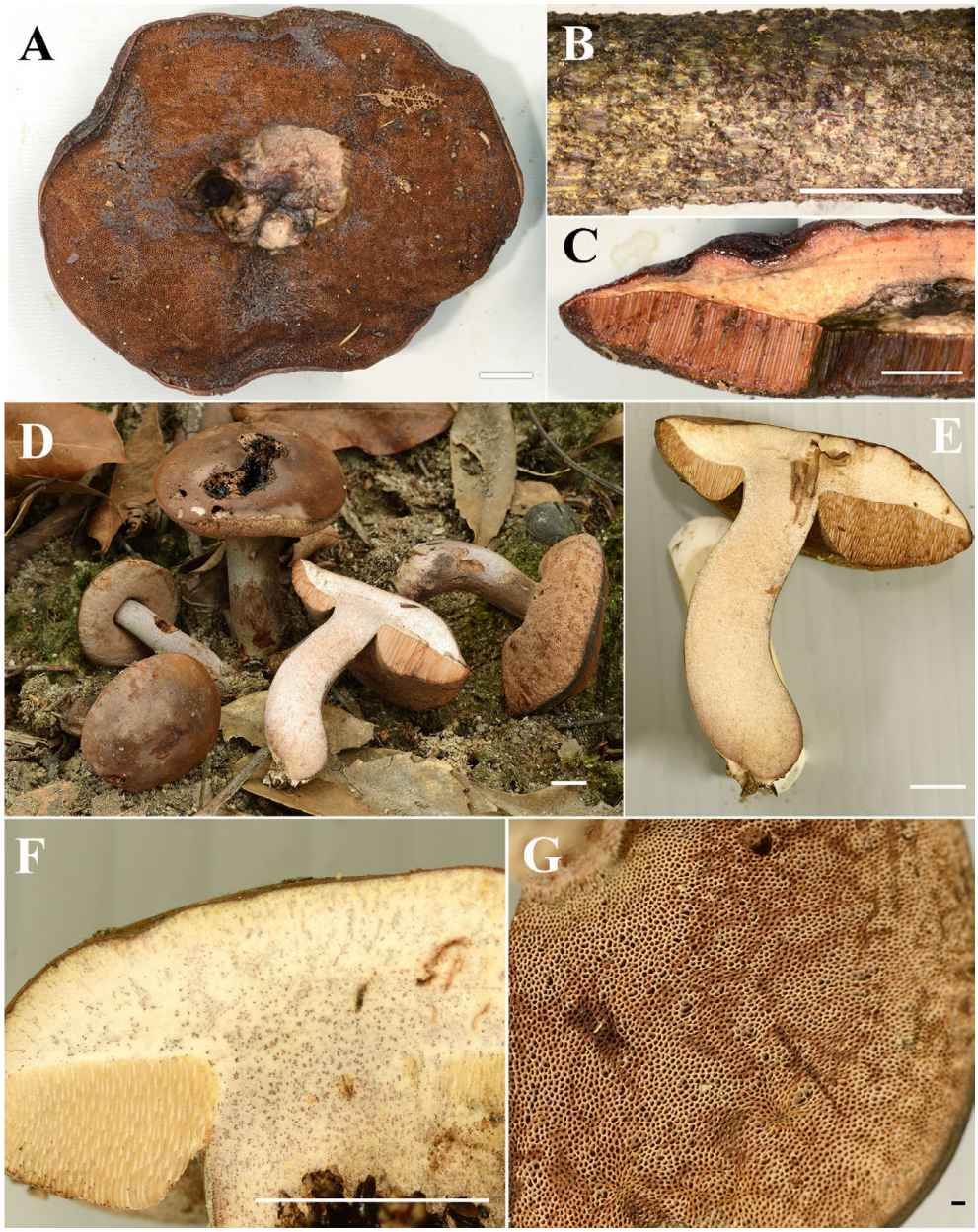


FIGURE 4 | (A–C) Fresh basidiomata of *Sutorius mucosus* specimen voucher OR0851 holotype (**A**: pores surface, **B**: stipe surface, **C**: slimy pileus and context with tubes). **(D–G)** Fresh basidiomata of *Sutorius obscuripellis* OR0949 holotype. Scale bars: **(A–F)** = 1 cm, **(G)** = 1 mm.

fusiform with acuminate to subacute or acute apex, and presence of cheilocystidia.

Sutorius obscuripellis Vadthanarat, Raspé and Lumyong **sp. nov.**

MycoBank: MB838059

Figures 4D–G, 6

Typification: **THAILAND:** Chiang Mai Province: Mae On District, Pok village, 18°53′11″N–99°22′11″E, elev. 710 m, July 29, 2015, Olivier Raspé, OR0949 (CMUB: holotype, BR: isotype).

Etymology: from Latin *obscurus* and *pellis*, referring to the dark pileipellis.

Description: *Basidiomata* small- to medium-sized. *Pileus* (3.5) 4.5–6 cm in diameter convex to planoconvex, with straight margin; *surface* even, minutely and densely matted tomentose, dull, violet–brown to dark brown (10F5–6 to 9E4), with patchy color variation, sometimes gradually paler to margin. *Pileus context* 6–9 mm thick halfway to the margin, yellowish white (4A2), more brownish near the pellis, slowly turning pale red–brown when cut, with scattered small groups of reddish brown to dark brown (9E4–5, 9F5–6) encrustations. *Stipe* clavate to cylindrical (3.5) 3.8–5.5 × 0.8–1.7 cm; *surface* dull, even to finely scabrous, violet-gray (18D2, 16E2) with

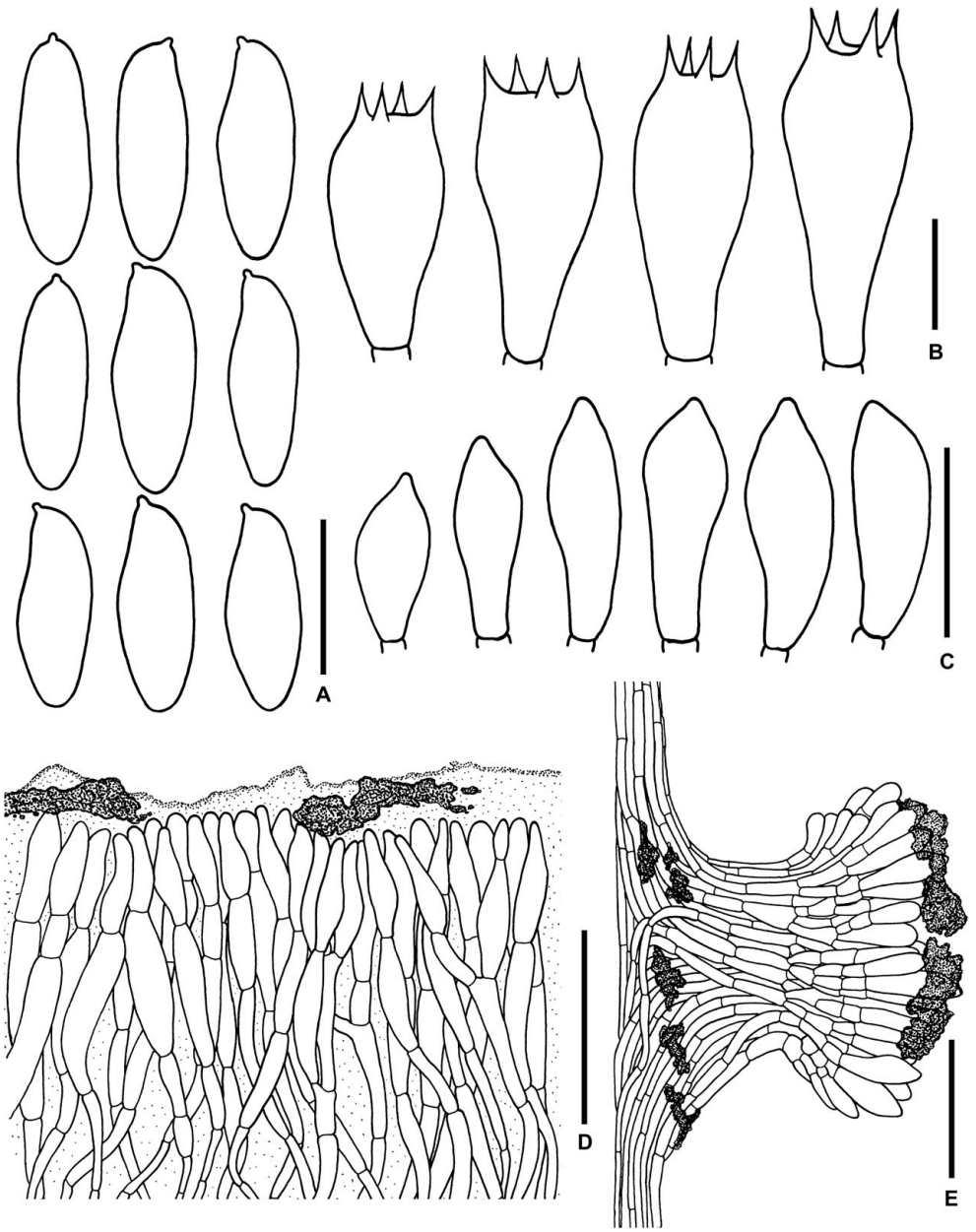


FIGURE 5 | Microscopic features of *Sutorius mucosus*. **(A)** Basidiospores, **(B)** Basidia, **(C)** Caulocystidia, **(D)** Pileipellis, **(E)** Stipitipellis. All drawings were made from OR0581. Scale bars: **(A,B)** = 10 μm; **(C)** = 25 μm; **(D,E)** = 50 μm.

violet–brown (10E43–5) granulose squamules; *basal tomentum* off-white to yellowish white. *Stipe context* solid, fleshy fibrous, light purplish brown (12B2), more purplish at the base, with scattered small groups of reddish brown to dark brown (9E4–5, 9F5–6) encrustations. *Hymenophore* tubulose, adnexed to adnate, depressed around stipe, ventricose; *tubes* orange–gray (6B2), 6–13 mm long, easily separable, turning red–brown on bruising; *pores* 0.2–0.5 mm wide at midradius, roundish, regularly arranged, with subregular pore surface, pale violet-gray (9–10B3), becoming paler with age, slightly reddish brown on bruising, with scattered small groups of reddish brown to dark brown encrustations, composite pores uncommon. *Odor* not recorded. *Taste* slightly bitter at first, then mild. *Spore print* not recorded.

Macrochemical reactions: KOH: dull yellow on pileus; yellow or pale yellow on pileus context, stipe, stipe context, and hymenophore. NH_4OH: yellowish with only slight violet aura on pileus; yellowish on stipe and pileus context; negative on hymenophore and stipe context.

Basidiospores (9.6–)9.8–10.8–12.2 (–13.5) × (3.6–) 3.8–4.2–4.6 (–5.1) μm, Q = (2.19–) 2.34–2.55–2.83 (–2.97), N = 72, narrowly ellipsoid to subcylindrical with slightly suprahilar

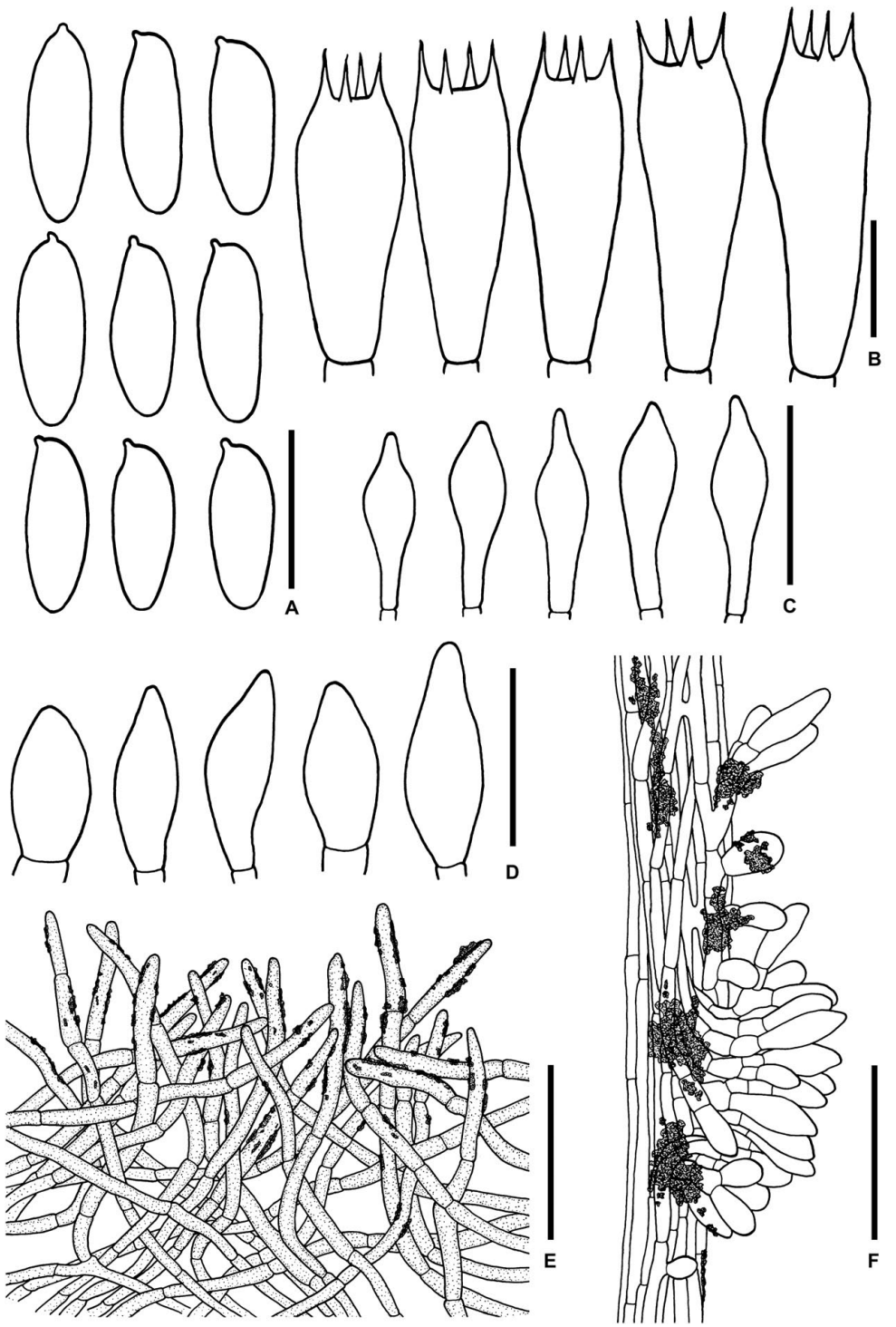


FIGURE 6 | Microscopic features of *Sutorius obscuripellis*. **(A)** Basidiospores. **(B)** Basidia. **(C)** Cheilocystidia. **(D)** Caulocystidia. **(E)** Pileipellis. **(F)** Stipitipellis. All drawings were made from OR0949. Scale bars: **(A,B)** = 10 μm; **(C,D)** = 25 μm; **(E,F)** = 50 μm.

depression, thin-walled, smooth, brownish to yellowish hyaline in water, yellowish hyaline in KOH and NH_4OH, inamyloid. *Basidia* 4-spored (23–) 23–26–30 (–30) × (8–) 8–10–11 (–11) μm, with sterigmata up to 5 μm long, clavate, hyaline, inamyloid. *Cheilocystidia* (18–) 19–24–30 (–31) × (6–) 6–7–9 (–9) μm, frequent, fusiform, thin-walled, hyaline. *Pleurocystidia* not seen. *H. trama* divergent to boletoid, 47–91 μm wide; with 12–48 μm wide of regular mediostratum. *Pileipellis* an intricate

trichoderm, 100–170 μm thick, made of loosely interwoven terminal cells 17–65 × 3–6 μm, with subacute to rounded apex, brown to dark in water especially the terminal cells, less brown in KOH or NH_4OH. *Pileus context* composed of moderately interwoven, 6- to 12 (15)-μm-wide hyphae, brownish to yellowish hyaline, with some scattered parietal encrustations and loose crystals. *Stipitipellis* a disrupted hymeniderm 100–125 μm thick, composed of parallel hyphae, anastomosing at places, with terminal cell 10–24 × 6–12 μm of thin-walled hyaline hyphae, giving rise to clusters of caulocystidia and basidiole-like cells, with scattered loose crystals. *Caulocystidia* (19–) 20–26–38 (–38) × (6–) 6–11–20 (–22) μm, broadly fusiform, thin-walled, hyaline. *Stipe context* composed of parallel 5- to 8 (12)-μm-wide hyphae, with scattered loose crystals. *Clamp connections* not seen in any tissue.

Habitat: On soil, gregarious to fasciculate in hill forest dominated by *Castanopsis* spp. *Lithocarpus* spp. mixed with some *Dipterocarpus* spp. and regularly subject to fire.

Distribution: Chiang Mai Province, Northern Thailand.

Notes: Based on a single collection (OR0949), *S. obscuripellis* is characterized by the following combination of characteristics: basidiomata small- to medium-sized; pale violet–gray pores color; lack of pleurocystidia; *Pileipellis* an intricate trichoderm composed of brown to dark hyphae with cylindrical terminal cells with subacute to rounded apex, showing scattered small parietal brownish yellow to reddish pale to dark brown encrustations. Phylogenetically, *S. obscuripellis* formed a clade (clade 8) sister to *Sutorius ubonensis* (clade 7) and *S. subrufus* (clade 6). However, the latter two species are morphologically different from *S. obscuripellis* as follows: *S. ubonensis* has larger basidiomata, darker pores, and basidiomata especially when young, pleurocystidia, and a slightly gelatinized tomentose pileipellis, and has so far only been found in dry dipterocarp forest in Ubon Ratchathani Province, in northeastern Thailand. *S. subrufus* has larger basidiomata, a stipe surface and context turning more reddish when injured, presence of pleurocystidia, and a trichoderm pileipellis composed of cylindrical hyphae and clavate or subclavate terminal cells with obtuse apex, colorless to yellowish in KOH (Chai et al., 2019), whereas *S. obscuripellis* has the pileipellis composed of brown to dark brown hyphae, colorless to brownish yellow to pale brown in KOH.

Sutorius pachypus Vadthanarat, Raspé and Lumyong **sp. nov.**

MycoBank: MB838060

Figures 7A–E, **8**

Typification: **THAILAND:** Chiang Mai Province: Mae Taeng District, Behind Wat Pah Deng, 19°06′38″N–98°44′32″E, elev. 1,055 m, June 7, 2012, Olivier Raspé and Komsit Wisitrassameewong, OR0411 (MFLU: holotype; BR: isotype).

Etymology: from Greek means "thick" referring to the wide stipe.

Description: *Basidiomata* medium-sized. *Pileus* 4.5–9 cm in diameter; at first hemispherical then convex to planoconvex with deflexed, slightly exceeding margin (1–2 mm); *surface* subrugulose, dull, minutely tomentose, at first dark reddish brown to dark brown (9F5–6) becoming pale reddish brown (8–9D/E4–7), gradually paler to the margin. *Pileus context* 1.5–1.7 cm halfway to the margin, pale grayish orange (6A2) to purplish gray (17C3, 17D4) at place, with scattered small groups of dark reddish brown (9F5–6) encrustations, unchanging or slightly reddening when cut. *Stipe* central, wide, cylindrical (5.5) 6–6.5 × 2.5–4 cm; *surface* even to finely scabrous, dry, reddish to grayish gray (10B–D2) darker at the base (10D/E3), with pale violet gray (10D2) to violet brown (10F3–4) granulose squamules; *basal tomentum* little developed, white. *Stipe context* solid, orange white (5A2), yellowish orange to purplish gray (6D5, 12D/E3) virgate, slightly reddening when cut (especially near the base). *Hymenophore* tubulose, adnexed, slightly depressed around stipe; *tubes* easily separable, pale orange (5A2), 10–12 mm long halfway to the margin; *pores* at first dark violet brown (11F4) becoming brown (8F5–6). *Spore print* not recorded.

Macrochemical reactions: KOH: yellowish brown on pileus and stipe; NH_4OH: yellowish brown with greenish to pinkish aura on pileus; orange with blue green aura on stipe.

Basidiospores from the type (immature) (5.8–) 6.6–7.5-8.4 (–8.8) × (2.9–) 3.2–3.7–4.2 (–4.4) μm, Q = (1.6–) 1.7–2.04–2.41 (–2.47), N = 55, oblong to ellipsoid with suprahilar depression, thin-walled, smooth, yellowish to brownish hyaline in water, yellowish hyaline in KOH or NH_4OH, inamyloid. From voucher TWO1171 (9–) 9.5–11–13.6 (–14) × (3.9–) 3.9–4.4–4.9 (–5.2) μm, N = 50 Q = (2.06–) 2.18–2.51–2.98 (–3.11), narrowly ellipsoid to subcylindrical with suprahilar depression, thin-walled, smooth, yellowish to brownish hyaline in water, yellowish hyaline in KOH or NH_4OH, inamyloid. *Basidia* 4-spored, rarely 2-spored (24–) 25–28–34 (–36) × (8–) 8–9–11 (–13) μm, with sterigmata up to 4.5 μm long, narrowly clavate to clavate, hyaline, inamyloid. *Cheilocystidia* (20–) 22–30–39 (–43) × (4–) 4–7–11 (–11) μm, frequent, narrowly fusiform to fusiform, thin-walled, hyaline. *Pleurocystidia* (29–) 29–34–40 (–40) × (5–) 5–6–7 (–7) μm, infrequent to rare, same shape as the cheilocystidia, thin-walled, hyaline. *H. trama* divergent 45–78 μm wide, with subregular mediostratum 18–26 μm wide. *Pileipellis* a palisadoderm when young becoming trichoderm, 97–128 μm thick, composed of thin-walled hyphae, with terminal cells 16–47 × 3–7.5 μm, cylindrical to subcylindrical with rounded to subacute apex somewhere, slightly yellowish to reddish pale brown in water, mostly hyaline to yellowish pale brown somewhere in KOH or NH_4OH. *Pileus context* made of strongly interwoven hyaline hyphae, 6–16.5 μm wide, with scattered loose crystals. *Stipitipellis* a disrupted hymeniderm, 80–110 μm thick, composed of parallel hyphae, with terminal cell 13–43 × 5–9.5 μm of thin-walled, hyaline hyphae, giving rise to clusters of caulocystidia, basidiole-like cells and scarce basidia, with scattered encrustations. *Caulocystidia* (24–) 25–35–51 (–55) × (7–) 8–10–14 (–14) μm, frequent in groups, fusiform, thin-walled, hyaline. *Stipe context* composed of parallel 4- to 13.5-μm-wide hyphae, with scattered encrustations. *Clamp connections* not seen in any tissue.

Habitat: Solitary to gregarious, on soil, in hill evergreen forest dominated by *Castanopsis* spp., *Lithocarpus* spp. mixed with *Sh. obtusa*, *Sh. siamensis*, *D. obtusifolius* and *D. costatus*.

Distribution: Chiang Mai Province, Northern Thailand.

Additional collections examined: **THAILAND:** Chiang Mai Province: Mae Taeng District, Behind Wat Pah Deng,

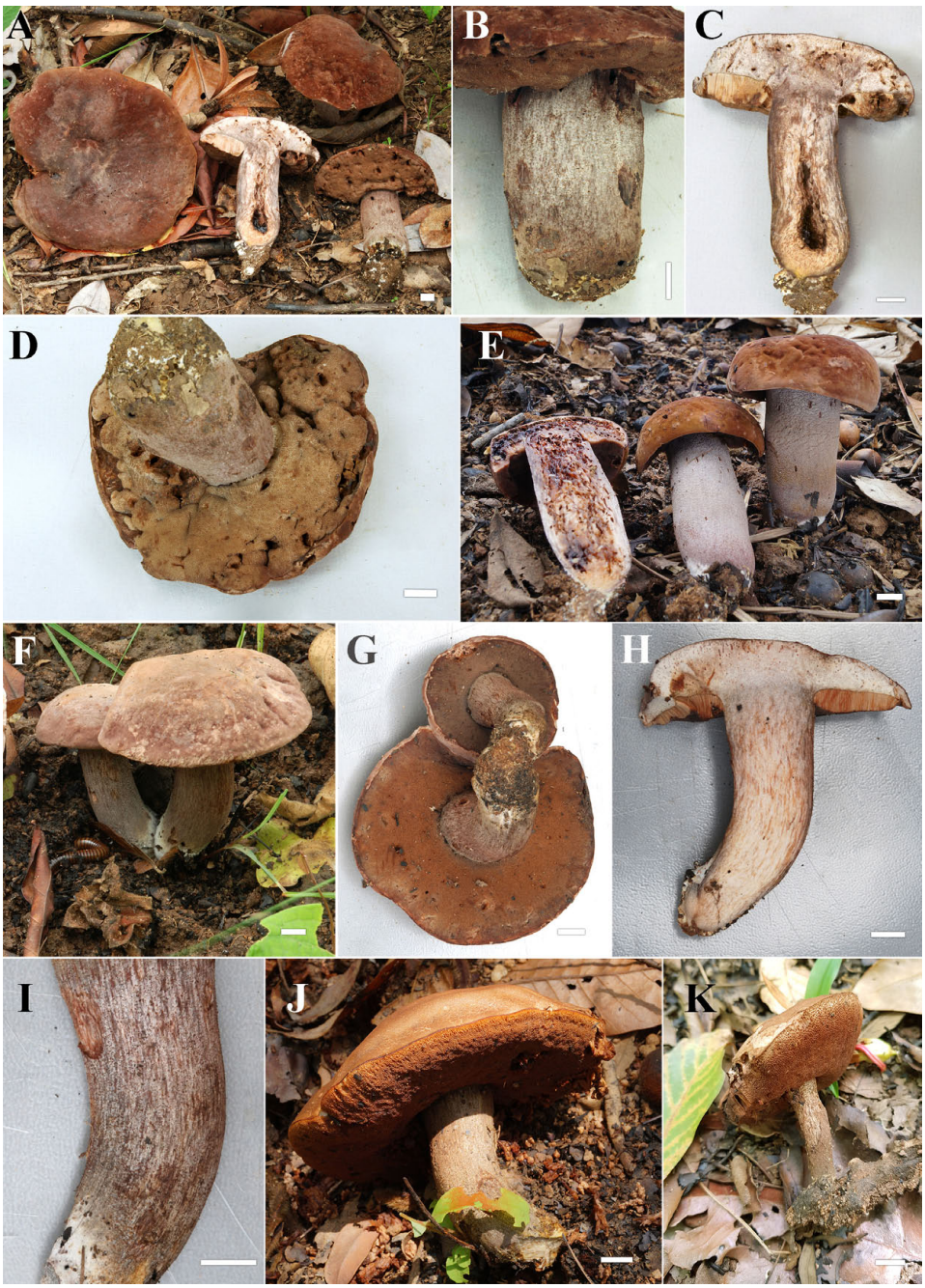


FIGURE 7 | (A–E) Fresh basidiomata of *Sutorius pachypus* (**A–D**: OR0411, **E**: SV0098). **(F–K)** Fresh basidiomata of *Sutorius pseudotylopilus* (**F–I**: OR0378B, **J**: SV0401, **K**: SV0415). Scale bars: **(A–K)** = 1 cm.

19°06′31″N–98°44′28″E, elev. 1,070 m, July 7, 2015, Santhiti Vadthanarat, SV0098 (CMUB, BR). –ibid., Baan Mae Sae, Highway 1095 at km 55, 19°14′32.6″N–98°38′29.4″E, elev. 990 m, June 10, 2006, Osmundson, TWO1171 (MFLU, NY).

Notes: *S. pachypus* is characterized by the following combination of characteristics: medium-sized basidiomata; wide cylindrical stipe with granulose squamules on the stipe surface that mostly are pale violet gray to violet brown at places; pileipellis is a palisadoderm to trichoderm, subcylindrical terminal cells with rounded to subacute apex; presence of cheilocystidia and pleurocystidia. The holotype (OR0411) has oblong to ellipsoid basidiospores because it is immature. However, a mature specimen (TWO1171) has the typical shape of basidiospores, which are narrowly ellipsoid to subcylindrical with suprahilar depression. The specimen (TWO1171) was originally morphologically identified as *S. eximius* (Halling et al., 2012),

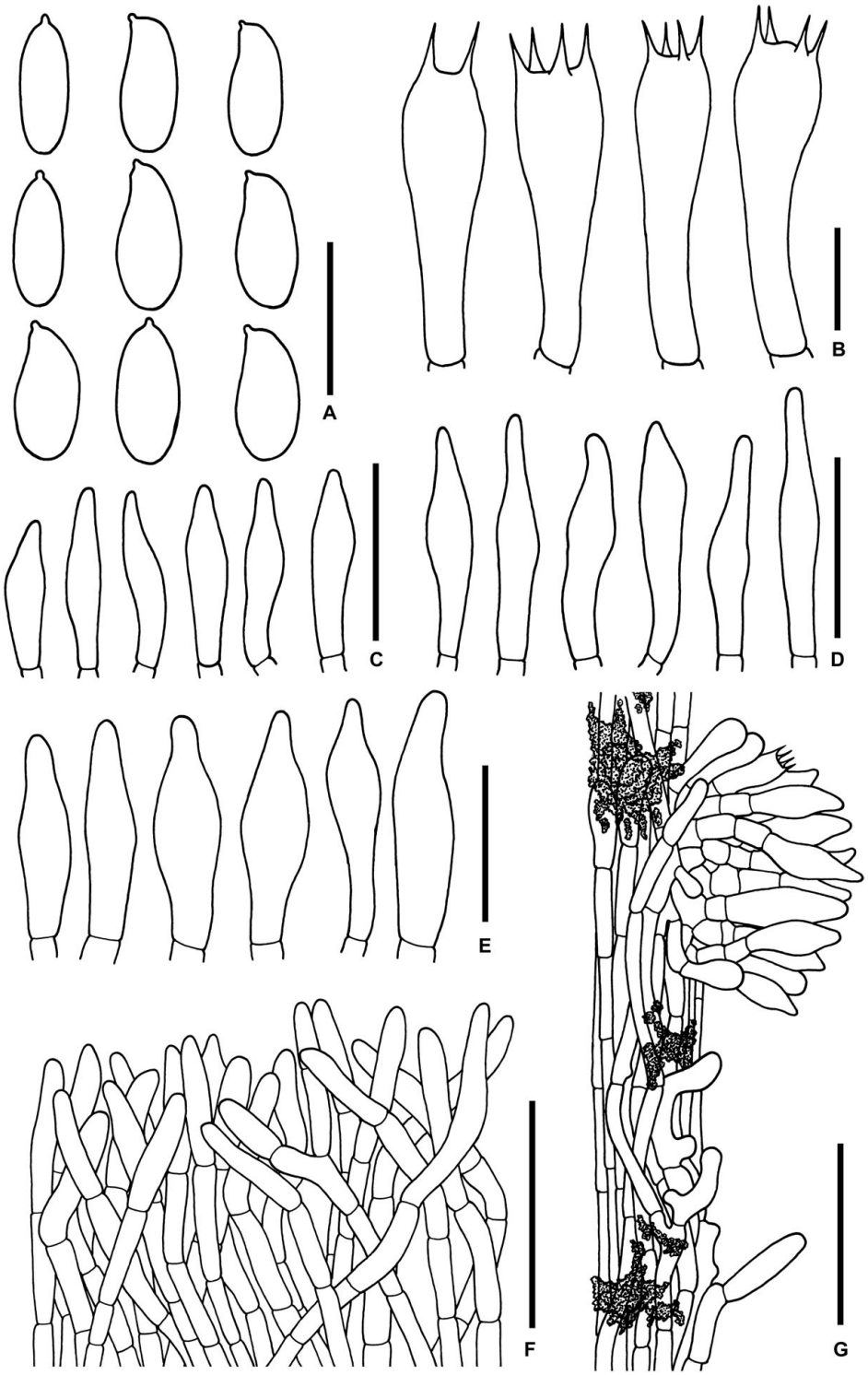


FIGURE 8 | Microscopic features of *Sutorius pachypus*. **(A)** Basidiospores. **(B)** Basidia. **(C)** Cheilocystidia. **(D)** Pleurocystidia. **(E)** Caulocystidia. **(F)** Pileipellis. **(G)** Stipitipellis. All drawings were made from OR0411. Scale bars: **(A,B)** = 10 μm; **(C–E)** = 25 μm; **(F,G)** = 50 μm.

but our more detailed examination and phylogenetic analyses indicate a new species, *S. pachypus*. Phylogenetically, *S. pachypus* formed a clade (clade 10) closely related to *S. rubinus* (clade 9), *S. australiensis* (clade 11), and *S. mucosus* (clade 12). However, all of those differ from *S. pachypus* mainly in having a narrower stipe with darker granulose squamules. The other differences are as

follows: *S. rubinus* has redder basidiomata, lacks pleurocystidia, and has a trichoderm pileipellis with fusiform to broadly fusiform terminal cells with acuminate apex. *S. australiensis* has darker violet–brown pores (when young), and it has been found so far only in Australia. *S. mucosus* lacks both cheilocystidia and pleurocystidia and has a waxy to subviscid pileus, an ixotrichoderm pileipellis with fusiform to utriform terminal cells with rounded to tapering apex.

Sutorius pseudotylopilus Vadthanarat, Raspé and Lumyong **sp. nov.**

MycoBank: MB838061

Figures 7F–K, **9**

Typification: **THAILAND**: Chiang Mai Province: Mae On District, Ban Huay Keaw community forest, 18°51′55″N–98°17′23″E, elev. 710 m, June 4, 2012, Olivier Raspé and Komsit Wisitrassameewong, OR0378B (MFLU: holotype; BR: isotype).

Etymology: From Greek *pseudo*–, false, and *Tylopilus* refers to the macromorphological similarity to the genus *Tylopilus*.

Description: *Basidiomata* medium-sized. *Pileus* 5.0–12 cm in diameter, at first convex with inflexed margin becoming planoconvex to depressed with straight margin, margin slightly exceeding (1–2 mm); *surface* even to subrugulose, dull, matted tomentose to cracked tomentose with age, patchy, grayish brown to reddish brown, brown (9–10E3–4, 7F5–6, 8F3–4). *Pileus context* 10–20 mm thick halfway to the margin, yellowish white to orange white (4A2 to 5A2), with scattered small groups of reddish brown (9F6–7) encrustations, slowly slightly reddening when cut. *Stipe* central, terete, cylindrical to slightly tapering downward, 7.5–9.5 × 1.5–2.5 cm; *surface* even, dull, dry, grayish brown to reddish brown (7–8 D/E 3–4), with grayish brown to dark brown (8–9F3–4) fine scabrous squamules; *basal tomentum* little developed, white to yellowish white. *Stipe context* solid, orange white (5A2) near the cap to yellowish white (4A2) to greenish white (3B3) at the base, grayish brown to reddish brown (7–8 D/E 3–4) virgate, with scattered brownish gray (8–10E2) or reddish brown (9D4, 9F4–5) encrustations, slowly slightly reddening when cut. *Hymenophore* tubulose, narrowly adnexed to adnate, subventricose to ventricose, sometimes slightly depressed around the stipe; *tubes* easily separable, brown to reddish brown (7–8E4–5), 7–15 mm long halfway to the margin, unchanged or slightly reddening when cut; *pores* 0.4–0.8 mm wide at midradius, mostly roundish, at first dark purple (11F3–4) becoming dark brow to brown (8–9F5–6 to 7F5–6) with age. *Odor* not observed *taste* slightly acid. *Spore print* not observed.

Macrochemical reactions: KOH: yellowish then brownish on the cap, stipe, and pileus context; yellowish or greenish on stipe context; yellowish on hymenium. NH_4OH: yellowish red on the pileus; yellowish to brownish on pileus context, stipe, stipe context, and hymenium.

Basidiospores [168/3/3] (9.3–) 10.2–11.9–14 (–15.5) × (3.4–) 3.9–4.3–5 (–5) μm, Q = (2.18–) 2.4–2.78–3.24 (–3.82). From the type (9.3–) 9.6–11.1–13.1 (–14.1) × (3.4–) 3.8–4.2–4.5 (–4.7) μm, Q = (2.18–) 2.25–2.66–3.44 (–3.82), N = 53, narrowly ellipsoid to subcylindrical with slight of suprahilar depression, thin-walled, smooth, brownish to yellowish hyaline in water, yellowish hyaline in KOH or NH_4OH, inamyloid. *Basidia* 4-spored, (19–) 20–24–28 (–28) × (9–) 9–10–11 (–11) μm, with sterigmata up to 4 μm long, clavate, hyaline, inamyloid. *Cheilocystidia* (21–) 21–24–33 (–33) × (4–) 4–6–7 (–7) μm, frequent, mostly cylindrical to fusiform with rounded to tapering apex, thin-walled, hyaline. *Pleurocystidia* not seen. *H. trama* divergent to boletoid 30–44 μm wide, with regular to subregular mediostratum 7.5–23 μm wide. *Pileipellis* an intricate to flattened trichoderm, 85–130 μm thick, made of loosely to moderately interwoven hyphae, thin-walled, mostly hyaline to yellowish pale brown in KOH or NH_4OH, with slightly curly cylindrical terminal cells 14–46 × 3.5–6 μm with rounded apex, with scattered loose crystals. *Pileus context* made of strongly interwoven hyaline hyphae, 5.5–8.5 μm wide, with scattered loose crystals. *Stipitipellis* a disrupted palisadoderm, 90–110 μm thick, with clusters of basidiole-like cells 9–25 × 4–9 μm of thin-walled, mostly hyaline to pale yellowish brown hyphae, subtended by short chains of 3–4 (sub) isodiametric cells, with scattered encrustations. *Caulocystidia* (18–) 18–25–30 (–30) × (7–) 7–10–12 (–12) μm, infrequent, fusiform to broadly fusiform, thin-walled, hyaline. *Stipe context* composed of parallel, 4- to 11-μm-wide hyphae, with scattered encrustations. *Clamp connections* not seen in any tissue.

Habitat: Solitary or fasciculate on soil, in dipterocarp forest dominated by *D. obtusifolius*, *D. tuberculatus*, *Sh. obtusa*, and *Sh. siamensis* and a few *Hopea* sp., as well as *Castanopsis* spp.

Distribution: Chiang Mai Province, Northern Thailand.

Notes: *Sutorius pseudotylopilus* is characterized by the following combination of characteristics: medium-sized basidiomata, purplish to reddish brown basidiomata when young; lack of pleurocystidia; pileipellis constituted by an intricate to flattened trichoderm with cylindrical, slightly curly terminal cells with rounded apex. Phylogenetically, the three *S. pseudotylopilus* specimens formed a clade (clade 4) sister to three undescribed *Sutorius* species: clade 1 contains three specimens from China (HKAS59657, HKAS52672, and HKAS56291); *Sutorius* clade 2 contains another specimen from China (HKAS56291), and *Sutorius* clade 3 contains one specimen (TWO986) from Costa Rica in Central America. The closest described species is *S. eximius* (American species) in clade 5. However, *S. eximius* morphologically differs from *S. pseudotylopilus* by the following characteristics: stipe context unchanging when injured; presence of pleurocystidia (Singer, 1947; Smith and Thiers, 1971; Halling et al., 2012). Moreover, based on our latest phylogenetics analyses with more *Sutorius* exemplars, we hypothesize that *S. eximius* is restricted to North America (clade 5).

Additional collections examined: **THAILAND:** Chiang Mai Province: Mae On District, Ban Huay Kaew community forest, 18°51′56″N–99°17′24″E, elev. 700 m, June 1, 2017, Santhiti Vadthanarat, SV0401 (CMUB, BR); –ibid., 18°51′55″N–99°17′24″E, elev. 700 m, May 14, 2018, Santhiti Vadthanarat, SV0415 (CMUB, BR).

Sutorius rubinus Vadthanarat, Raspé and Lumyong **sp. nov.**

MycoBank: MB838062

Figures 10A–F, **11**

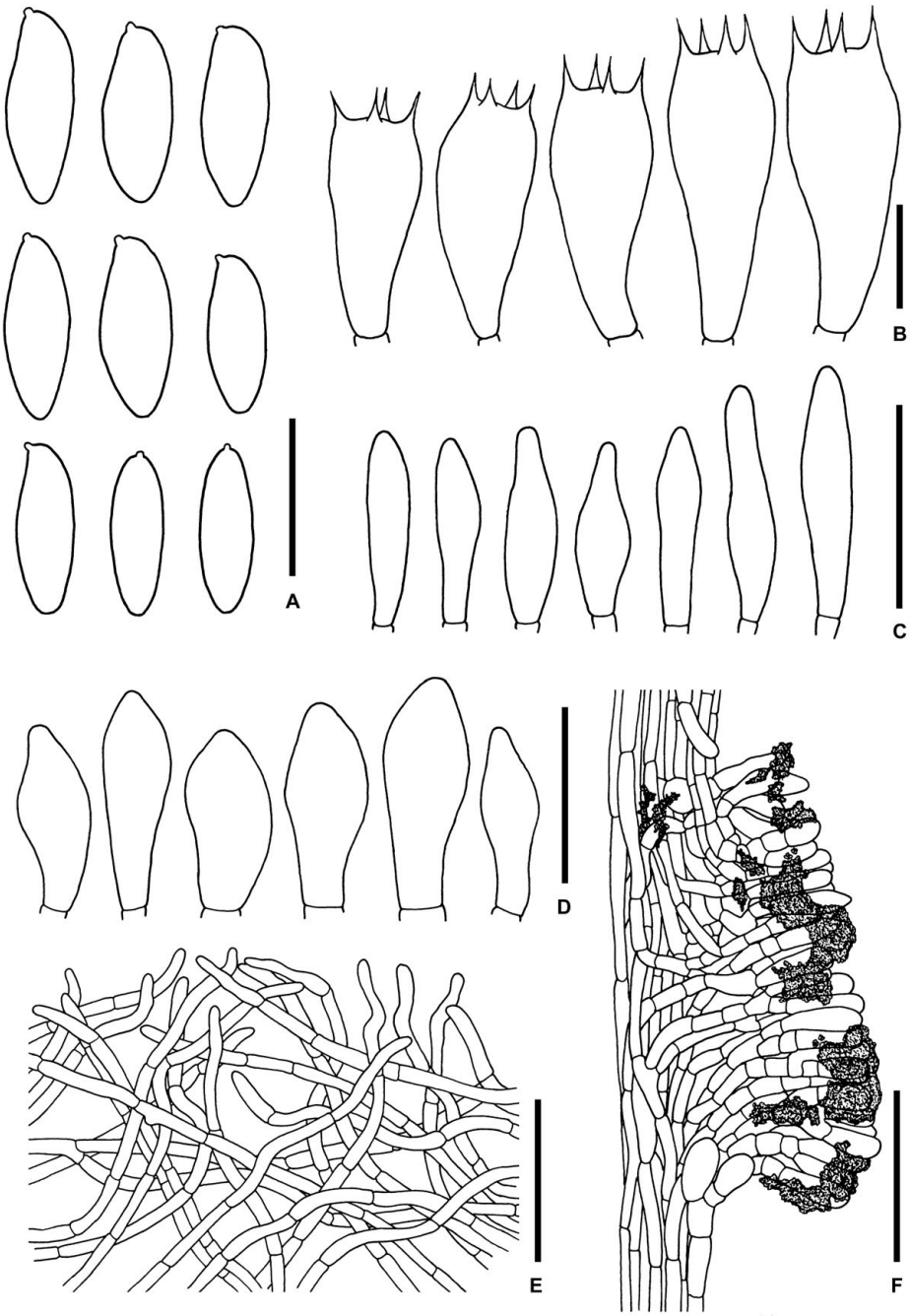


FIGURE 9 | Microscopic features of *Sutorius pseudotylopilus*. **(A)** Basidiospores. **(B)** Basidia. **(C)** Cheilocystidia. **(D)** Caulocystidia. **(E)** Pileipellis. **(F)** Stipitipellis. All drawings were made from OR0378B. Scale bars: **(A,B)** = 10 μm; **(C,D)** = 25 μm; **(E,F)** = 50 μm.

Typification: **THAILAND:** Chiang Mai Province: Mae Taeng District, Pha Deng village, 19°06′38″N–98°44′32″E, elev. 1,055 m, June 7, 2012, Olivier Raspé and Komsit Wisitrassameewong, OR0403 (MFLU: holotype; BR: isotype).

Etymology: From Latin rubinus, red, referring to basidiomata color.

Description: *Basidiomata* medium-sized. *Pileus* 4.5–7.5 cm in diameter, convex to planoconvex, with slightly deflexed, becoming straight margin, which is slightly exceeding (1–2 mm) especially when young; *surface* at first subrugulose to rugose becoming scabrous to subrugulose at center, tomentose, reddish dark brown (9F4–6) becoming reddish dark brown (8F5–8) to reddish brown (8D/E6–8) with age, gradually paler to the margin. *Pileus context* 5–10 mm thick halfway to the margin, orange white (5A2), with scattered small groups of reddish brown (8–9D4–5) encrustations. *Stipe* central, terete to slightly compressed,



FIGURE 10 | (A–F) Fresh basidiomata of *Sutorius rubinus* (**A**: OR0379, **B**: OR0403, **C–E**: OR0409, **F**: pores surface when young in OR1255). **(G–K)** Fresh basidiomata of *Sutorius ubonensis*. (**G**: SV0029, **H**: SV0032, **I**: SV0203, **J**: SV0313, **K**: SV0353 a collection from a local market in Ubon Ratchathani Province). **(L)** Fresh basidiomata of *Sutorius vellingae* specimen voucher ECV3603. Scale bar: **(A–L)** = 1 cm.

cylindrical to subclavate or tapering downwards, sometimes with subbulbous base, 5–6.5 × 0.8–2.2 cm; *surface* finely scabrous, reddish gray to grayish brown (8 D/E 2–3) densely covered with reddish brown to dark brown (8F4–5) granulose squamules; *basal tomentum* white to off-white. *Stipe context* solid, orange white to pinkish white (5A2 to 7A2), reddish to grayish brown to dark brown (8D–F3–5) virgate, with scattered small groups of reddish brown (8–9D4–5) encrustations, unchanged

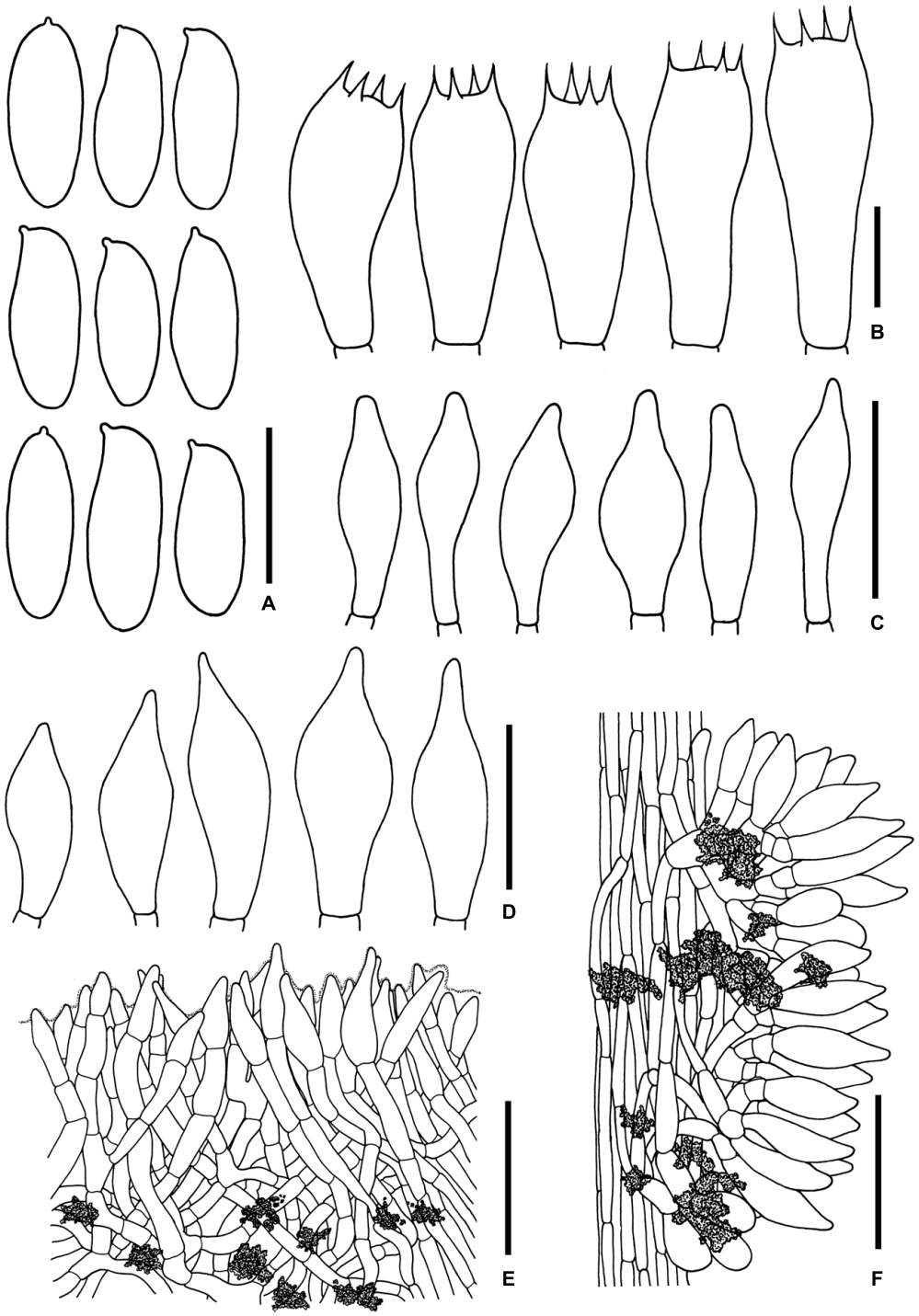


FIGURE 11 | Microscopic features of *Sutorius rubinus*. **(A)** Basidiospores. **(B)** Basidia. **(C)** Cheilocystidia. **(D)** Caulocystidia. **(E)** Pileipellis. **(F)** Stipitipellis. All drawings were made from OR0403. Scale bars: **(A,B)** = 10 μm; **(C,D)** = 25 μm; **(E,F)** = 50 μm.

or slightly reddening when cut. *Hymenophore* tubulose, adnexed to narrowly adnexed, ventricose, slightly depressed around the stipe; *tubes* dull yellowish white (3A3–4) when young becoming orange-brown (7E7) with age, easily separable, 6–11 mm long halfway to the margin; *pores* 0.3–0.5 mm wide at midradius, mostly roundish, at first grayish orange (5D3–4) becoming orange to pale orange (5A3–4 to 6B6–7) with age, with scattered small groups of reddish dark brown (8F3–4) encrustations. *Odor* and *taste* not observed. *Spore print* not observed.

Macrochemical reactions: KOH: dark brown to black on the stipe, reddish on the hymenophore, negative on the pileus, pileus context, and stipe context.

Basidiospores [168/3/3] (8.7–) 9.6–10.8–12.1 (–13.1) × (3.5–) 3.9–4.3–4.8 (–5.1) μm, *Q* = (2.03–) 2.2–2.5–2.82 (–2.96). Form the type (8.7–) 9.3–10.5–12.1 (–12.3) × (3.5–) 3.9–4.4–4.9 (–5.1) μm, *Q* = (2.03–) 2.06–2.4–2.73 (–2.81), *N* = 57, narrowly ellipsoid to subcylindrical with slightly suprahilar depression, thin-walled, smooth, yellowish hyaline in KOH or NH_4OH, inamyloid. *Basidia* 4-spored (23–) 23–27–31 (–31) × (10–) 10–11–13 (–13) μm, with sterigmata up to 4 μm long, clavate, hyaline, inamyloid. *Cheilocystidia* (20–) 20–26–32 (–32) × (5–) 5–7–8 (–8) μm, frequent, narrowly fusiform to fusiform with subacute apex, thin-walled, hyaline. *Pleurocystidia* not seen. *H. trama* divergent, 42–80 μm wide, with regular to subregular mediostratum 8–27 μm wide. *Pileipellis* an intricate trichoderm to slightly gelatinized intricate trichoderm, 60–110 μm thick, made of densely interwoven, thin-walled, smooth, hyaline hyphae 4–12 μm wide, with terminal cells 11–40 × 5–12 μm, fusiform to broadly fusiform with acuminate apex, slightly yellowish to reddish pale brown in water, mostly hyaline to yellowish pale brown in KOH or NH_4OH. *Pileus context* made of strongly interwoven hyphae, 6–18 μm wide, thin-walled, with scattered loose crystals. *Stipitipellis* a disrupted hymeniderm, 90–120 μm thick, composed of parallel hyphae, thin-walled, with terminal cells 19–30 × 11–14 μm, giving rise to clusters of caulocystidia and basidiole-like cells, with scattered encrustations. *Caulocystidia* (23–) 23–31–40 (–40) × (8–) 8–12–18 (–18) μm, frequent, fusiform with subacute apex, thin-walled, hyaline. *Stipe context* composed of parallel, 8- to 12-μm-wide hyphae, with scattered encrustations. *Clamp connections* not seen in any tissue.

Habitat: Solitary to gregarious, on soil, in evergreen hill forest dominated by *Castanopsis* spp., *Lithocarpus* spp. mixed with *D. tuberculatus*, *D. obtusifolius*, *Sh. obtusa*, and *Sh. siamensis*.

Distribution: Chiang Mai Province, Northern Thailand

Notes: *S. rubinus* is characterized by the following combination of characteristics: medium-sized basidiomata, dark reddish brown to reddish brown; lack of pleurocystidia; pileipellis a trichoderm with fusiform to broadly fusiform terminal cells with acuminate apex.

Phylogenetically, all *S. rubinus* specimens formed a clade (clade 9) close to three *Sutorius* species including *S. pachypus* (clade 10), *S. australiensis* (clade 11), and *S. mucosus* (clade 12). Nevertheless, they are morphologically different from *S. rubinus* as follows: *S. pachypus* has on average wider (2.5–4 cm wide) stipe and has pleurocystidia, and the pileipellis is a palisadoderm composed of subcylindrical with rounded to subacute apex. *S. australiensis* has dark violet brown pores when young, a trichoderm pileipellis composed of elongated to cylindrical elements with obtuse apex and is found only in Australia. *S. mucosus* has a waxy to subviscid pileus with an ixotrichoderm forming the pileipellis composed of gelatinized hyphae, with fusiform to utriform terminal cells with rounded to subacute apex.

Additional collections examined: **THAILAND:** Chiang Mai Province: Mae On District, Ban Huay Keaw community forest, 18°51′55″N–99°17′23″E, elev. 710 m, June 4, 2012, Jie Chen and Olivier Raspé, OR0379 (MFLU12-0231); Mae Taeng District, Pha Deng village, 19°06′38″N–98°44′32″E, elev. 1,055 m, June 7, 2012, Olivier Raspé and Komsit Wisitrassameewong, OR0409 (MFLU12-0261); ibid., June 24, 2016, Olivier Raspé, OR1255 (CMUB, BR).

Sutorius ubonensis Vadthanarat, Raspé and Lumyong **sp. nov.**

MycoBank: MB838066

Figures 10G–K, **12**

Typification: **THAILAND:** Ubon Ratchathani Province: Trakan Phuet Phon District, Ban Huay Fai community forest, 15°32'44"N–105°10'15"E, elev. 160 m, July 11, 2014, Santhiti Vadthanarat, SV0032 (CMUB: holotype; BR: isotype).

Etymology: ubonensis refers to Ubon Ratchathani Province where the species was found.

Description: *Basidiomata* medium-sized. *Pileus* (5.5) 8.0–10.5(12) cm in diameter, at first hemispherical to convex with straight to slightly inflexed margin, becoming convex to planoconvex to depressed with straight to slightly reflexed margin, margin slightly exceeding (1–2 mm), elastic; *surface* even to subrugulose, dull, subviscid when wet, minutely tomentose, at first violet to violet brown (10E4) to dark brown (9F5–6), later become reddish gray (10B2) to dull red or brownish gray (10C/D3) at the center, getting paler to brownish gray to (8C2) near the margin, sometimes patchy of reddish gray (8–9C/E3–4) purplish brown (10F4–5) or brown (6E6). *Pileus context* 10–18 mm thick halfway to the margin, yellowish white to orange white (4A2 to 5A2), with scattered small groups of reddish brown (9D4–6) encrustations, unchanged. *Stipe* central, terete to subcompressed, cylindrical to subclavate or tapering downwards (4.8) 5.2–8.5 × 1.8–3.2 cm; *surface* even to finely scabrous, slightly venose to rimose near the cap, dull to slightly shiny, dry, purplish gray to brownish gray (9–10C/E2), scattered of reddish brown to dark brown (9F4–5) granulose squamulose; *basal tomentum* off-white to yellowish white. *Stipe context* solid, slightly fibrous, yellowish white (4A2 to 5A2) to slightly purplish gray (15B/C2) near the stipitipellis, grayish brown to purplish brown (8–9E/F3–5) virgate, with scattered brownish gray (8–10E2) or reddish brown (9D4 to 9F4–5) encrustations, unchanged. *Hymenophore* tubulose, adnate, subventricose to ventricose; *tubes* easily separable, at first purplish to yellowish gray (8C2 to 6B3 to 5B3–4) becoming yellowish orange to brownish orange (5B3–4 to 6B3–4) with age, 8–13 mm long halfway to the margin; *pores* 0.3–0.8 mm wide at midradius, mostly roundish, slightly elongated near the stipe, subregular especially when young, dark brown to purplish dark brown (9F4–6 to 10F3–5) at first, become brown (7F5–6) to orange brown (6E4–5, 7E5–6) with age. *Odor* fungoid to slightly acidulate. *Taste* mild to slightly acid. *Spore print* brownish orange (7C3) to dark brown (7F6–7) in mass.

Macrochemical reactions: KOH: rapidly slightly greenish and then yellow on pileus and stipe; yellowish on pileus context, stipe context, and hymenium. NH_4OH: yellowish with greenish to purplish aura on the cap and stipe; yellowish on pileus context, stipe context, and hymenium.

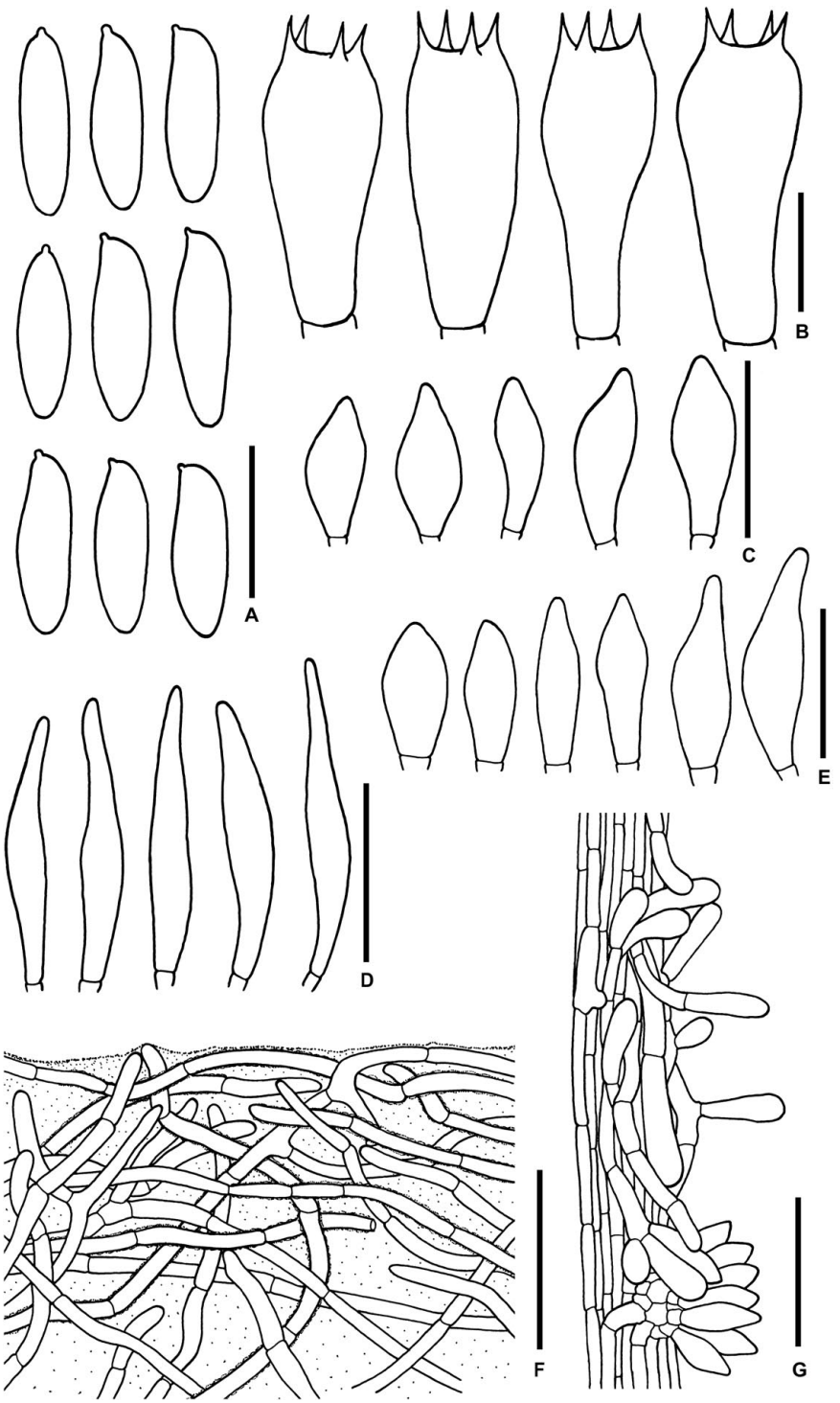


FIGURE 12 | Microscopic features of *Sutorius ubonensis*. **(A)** Basidiospores. **(B)** Basidia. **(C)** Cheilocystidia. **(D)** Pleurocystidia. **(E)** Caulocystidia. **(F)** Pileipellis. **(G)** Stipitipellis. Drawings **(A–D)** were made from SV0032, **(F,G)** were made from SV0029. Scale bars: **(A,B)** = 10 μm; **(C–E)** = 25 μm; **(F,G)** = 50 μm.

Basidiospores [172/3/2] (8.7–) 9.8–12–14.7 (–16.8) × (3.1–) 3.4–4–4.4 (–4.7) μm *Q* = (2.61–) 2.42–3.01–3.63 (–3.93). From the type (10.1–) 11.1–13.4–16.6 (–16.8) × (3.6–) 3.7–4.1–4.6 (–4.7) μm, *Q* = (2.68–) 2.74–*3.27*–3.81 (–3.93), *N* = 57, narrowly ellipsoid to subcylindrical with slightly suprahilar depression, thin-walled, smooth, brownish to yellowish hyaline in water, yellowish hyaline in KOH or NH_4OH, inamyloid. *Basidia* 4-spored (19–) 19–22–25 (–25) × (9–) 9–10–11 (–11) μm,

with sterigmata up to 4 μm long clavate, hyaline, inamyloid. *Cheilocystidia* (19–) 19–23–28 (–28) × (6–) 6–8–10 (–10) μm, frequent, fusiform, thin-walled, hyaline. *Pleurocystidia* (34–) 35–40–47 (–47) × (5–) 5–6–7 (–7) μm, frequent, narrowly fusiform, thin-walled, hyaline. *H. trama* divergent to boletoid, 57–78 μm wide, with 18–42 μm wide of regular mediostratum. *Pileipellis* a tomentum to slightly gelatinized tomentum, 89–118 μm thick, composed of moderately interwoven, hyaline, thin-walled hyphae, with terminal cells 19–57 × 5–8.5 μm, cylindrical with rounded apex, some hyphae were covered with mucus on the wall, at places with scattered of loose crystals. *Pileus context* made of strongly interwoven hyphae, 8.5–13 μm wide, at places with scattered of loose crystals. *Stipitipellis* hyphae vertically oriented (80–95 μm thick), pointing out of terminal cell 10–35 × 4–12.5 μm of thin-walled with rounded apex, hyaline hyphae, giving rise to clusters of *caulocystidia*, which (23–) 23–27–35 (–35) × (7–) 7–10–13 (–13) μm, frequent in group, fusiform, thin-walled, hyaline, with somewhere scattered of loose crystals especially near the surface. *Stipe context* composed of parallel, 4.5- to 8-μm-wide hyphae, with scattered small loose crystals. *Clamp connections* not seen in any tissue.

Habitat: Solitary to gregarious, sometimes fasciculate, on soil in dipterocarp forest dominated by *D. obtusifolius*, *D. tuberculatus*, *Dipterocarpus intricatus*, *Sh. obtusa*, and *Sh. siamensis*.

Distribution: Ubon Ratchathani Province, Northeastern Thailand.

Notes: *S. ubonensis* is characterized by the combination of following characteristics: medium sized basidiomata, purplish gray when young becoming purplish to reddish brown with age; unchanged context; pileipellis a tomentum to slightly gelatinized tomentum, with cylindrical terminal elements with rounded apex; found in dipterocarp forest in Northeastern Thailand. Morphologically, *S. ubonensis* is superficially similar to *S. eximius* in macro-characters especially when young. Both species are also similar in some microscopic characters including the presence and shape of cheilocystidia, pleurocystidia, and caulocystidia, as well as the shape of elements on pileipellis. However, they are different in pileipellis structure, with *S. eximius* having a trichoderm, whereas *S. ubonensis* has a tomentum to slightly gelatinized tomentum. The two species also occur on different continents, with *S. ubonensis* being found in Ubon Ratchathani Province, Northeastern Thailand, Southeast Asia, whereas *S. eximius* is found in North America (Singer, 1947; Smith and Thiers, 1971; Halling et al., 2012).

Phylogenetically, *S. ubonensis* (clade 7) was clusters in a poorly supported, long-branch, sister to *S. obscuripellis* (clade 8) from Chiang Mai Province, Thailand, and *S. subrufus* (clade 6) from China. However, these two species differ from *S. ubonensis* as follows: *S. obscuripellis* has smaller basidiomata and is also paler, especially when young; lacks pleurocystidia; and has a trichoderm pileipellis composed of slightly dark to dark hyphae, with cylindrical terminal cells with subacute to rounded apex. So far, S. *obscuripellis* has been found only in Chiang Mai Province. *S. subrufus* also has paler basidiomata; paler pores, especially when young, which are pale brown to brown to pale reddish brown; stipe surface and context turn reddish when injured; a trichoderm pileipellis, composed of rather vertically arranged, with clavate or subclavate terminal cells, with obtuse apex; found in the forests dominated by Fagaceae trees, including *Lithocarpus* spp. (Chai et al., 2019). So far, *S. ubonensis* is the only *Sutorius* species found in Ubon Ratchathani Province, Northeastern Thailand. It occurs in dry dipterocarp forest at the lowest elevation (about 150–175 m) compared to the other *Sutorius* species.

Additional collections examined: **THAILAND:** Ubon Ratchathani Province: Trakan Phuet Phon District, Ban Huay Fai community forest, 15°32′43.58″N–105°10′16″E, elev. 160 m, July 11, 2014, Santhiti Vadthanarat, SV0029 (CMUB, BR); –ibid., 15°32′42”N–105°10′16″E, elev. 175 m, July 24, 2016, Santhiti Vadthanarat, SV0313 (CMUB, BR); –ibid., 15°32′42”N–105°10′16″E, elev. 160 m, July 15, 2017, Santhiti Vadthanarat, SV0405 (CMUB, BR); –ibid., 15°32′43”N–105°10′17″E, elev. 160 m, July 15, 2017, Santhiti Vadthanarat, SV0407 (CMUB, BR); –ibid., 15°32′43”N–105°10′15″E, elev. 175 m, July 15, 2017, Santhiti Vadthanarat, SV0410 (CMUB, BR); Sri Suk Village, Khok Tam Lae community forest, 15°35′46″N–105°06′35″E, elev. 150 m, August 6, 2015, Santhiti Vadthanarat, SV0203 (CMUB, BR); Trakan Phuet Phon market, September 22, 2016, Santhiti Vadthanarat, SV0353 (CMUB, BR).

Sutorius vellingae Vadthanarat, Raspé and Lumyong **sp. nov.**

MycoBank: MB838065

Figures 10L, **13**

Typification: **THAILAND:** Chiang Mai Province: Mae Taeng District, Baan Mae Sae, Highway 1095 at km 55, 19°14′32.6″N–98°38′29.4″E, elev. 990 m, July 4, 2007, Else C. Vellinga, ECV3603 (MFLU: holotype, NY isotype).

Etymology: Named after Else C. Vellinga, who collected the type specimen.

Description: *Basidiomata* medium-sized. *Pileus* 7 × 5.1 cm, convex, margin slightly exceeding (1 mm); *surface* even to subrugulose, dark brown (8F6–7) with some purple (10F7) shining through at places; *pileus context* 12–13 mm thick halfway to the margin, yellowish white (2A2), with scattered small groups of reddish brown (9E/D7–8) encrustations. *Stipe* central, curved, cylindrical to slightly compressed, 6.8 × 1.6 cm; *surface* even to finely scabrous, with some veins on the upper part, dull to slightly shiny, reddish gray to grayish brown (9C2–3), scattered with reddish brown (10F8) granulose squamules to purplish dark brown (9–10F4–6) granulose squamules near the base; *basal tomentum* little developed, yellowish white; *stipe context* solid, marmorate to virgate, yellowish white (2–3A2) and brownish red (10E6–7) to violet brown (10F6–7), with scattered small groups of reddish brown (9E/D7–8) encrustations. *Hymenophore* tubulose, adnate; *tubes* pinkish white (9A2), 7 mm long halfway to the margin; *pores* fine, subregular, violet brown (10F8). *Odor* fungoid. *Taste* not distinctive. *Spore print* not observed.

Basidiospores (9–) 9.5–10.4–11.1 (–11.5) × (3.6–) 3.8–4.2–4.6 (–4.8) μm, *Q* = (2.22–) 2.22–2.52–2.82 (–2.93), *N* = 65, narrowly ellipsoid to subcylindrical with slight suprahilar depression, thin-walled, smooth, brownish to yellowish hyaline in water, yellowish hyaline in KOH or NH_4OH, inamyloid. *Basidia* 4-spored (19–) 19–24–28 (–28) × (10–) 10–11–12 (–12) μm, with sterigmata

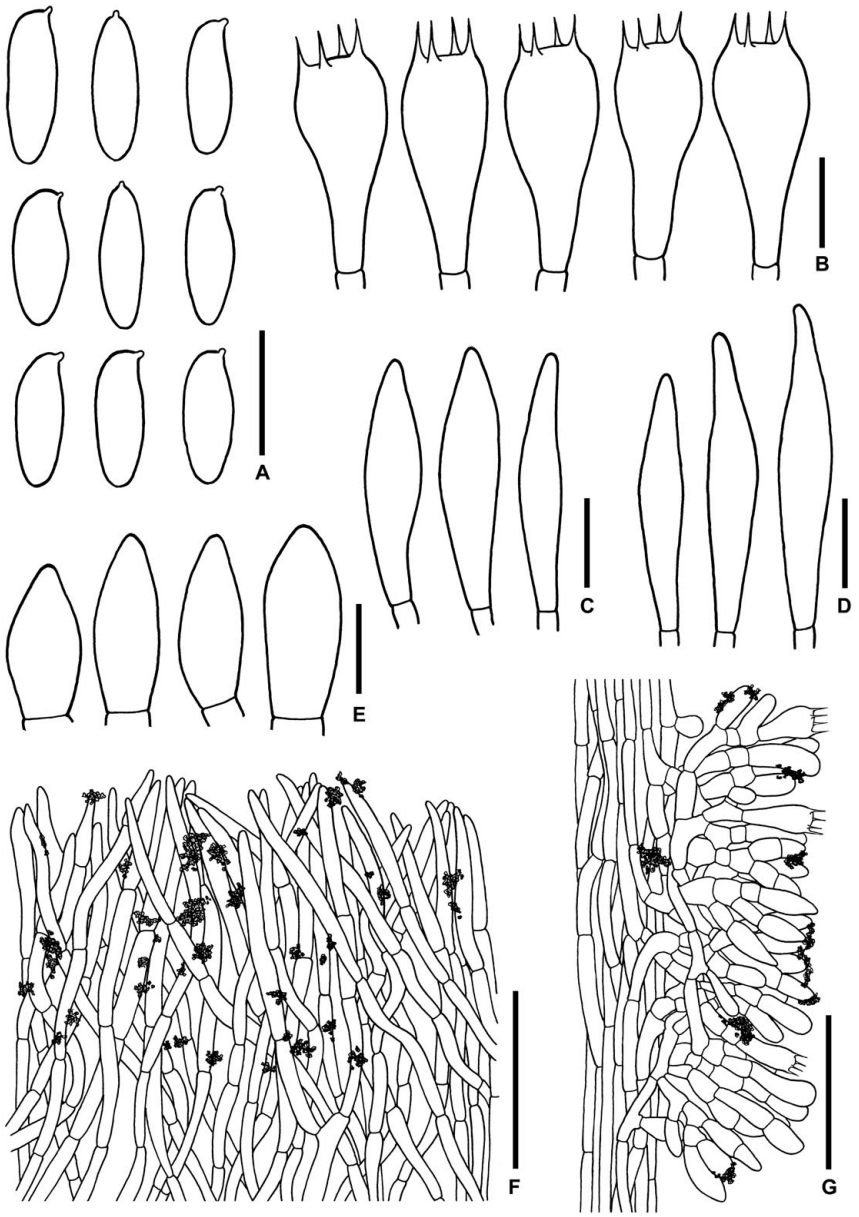


FIGURE 13 | Microscopic features of *Sutorius vellingae*. **(A)** Basidiospores. **(B)** Basidia. **(C)** Cheilocystidia. **(D)** Pleurocystidia. **(E)** Caulocystidia. **(F)** Pileipellis. **(G)** Stipitipellis. All drawings were made from ECV3603. Scale bars: **(A–E)** = 10 μm; **(F,G)** = 50 μm.

up to 4.5 μm long clavate, hyaline, inamyloid. *Cheilocystidia* 28–29 × 5–8 μm, rare, narrowly fusiform to fusiform, thin-walled, hyaline. *Pleurocystidia* 29–35 × 6–7 μm, rare, narrowly fusiform to fusiform, thin-walled, hyaline. *H. trama* divergent, 36–77 μm wide, with 10–31 μm wide of subregular mediostratum. *Pileipellis* a trichoderm, 110–140 μm thick, thin-walled hyphae, composed of cylindrical terminal cells 23–61 × 4–7 μm, with subacute to acute apex, slightly yellowish hyaline in water, slightly greenish to yellowish hyaline in KOH or NH_4OH, with scattered yellowish-brown parietal encrustations. *Pileus context* made of moderately interwoven hyaline hyphae, 4–10 μm wide, with scattered reddish brown loose crystals in water or NH_4OH. *Stipitipellis* a disrupted hymeniderm, 130–175 μm thick, composed of parallel hyaline hyphae anastomosing at places and terminal cells 13–19 × 7–8 μm, thin-walled, giving rise to clusters of basidiole-like cells and caulocystidia, with scattered loose crystals. *Caulocystidia* (17–) 17–21–30 (–30) × (7–) 7–9–11 (–11) μm, frequent in groups, fusiform to broadly fusiform, thin-walled, hyaline. *Stipe context* composed of parallel 4.5- to 9-μm-wide hyphae, with scattered loose crystals. *Clamp connections* not seen in any tissue.

Habitat: Solitary under *Castanopsis* and *Lithocarpus* trees.

Distribution: Chiang Mai Province, Northern Thailand.

Notes: The *Sutorius* specimen voucher ECV3603 was first recognized as a taxon discrete from *S. eximius* and *S. australiensis*

in the original publication of *Sutorius*, based on phylogenetic analysis of a combined *LSU* + *tef*1 dataset (Halling et al., 2012). However, it was not described as a new species at that time because of the solitary nature of the collection. In this study, that same specimen was further studied and is hypothesized to be a new species, *S. vellingae*. Based on that single collection, *S. vellingae* is characterized by the combination of following characteristics: marked violet brown pore color; pileipellis trichoderm composed of cylindrical terminal cells with subacute to acute apex; rare, narrowly fusiform to fusiform cheilocystidia and pleurocystidia; and its very distinct, isolated phylogenetic position within *Sutorius*.

Key to *Sutorius* Species Worldwide

1 Distribution in the Americas or Australia..... **2**
1′ Distribution in Asia..... **3**
2 Found in the Americas..... ***S. eximius***
2′ Found in Australia..... ***S. australiensis***
3 Pileipellis a palisadoderm or trichoderm to intricate trichoderm..... **4**
3′ Pileipellis a tomentum to slightly gelatinized tomentum composed of cylindrical terminal elements; basidiomata medium sized; at first pileus and pores purple to purplish brown to dark brown becoming purplish to reddish brown..... ***S. ubonensis***
4 Pileipellis composed of wide cylindrical hyphae, with terminal cells fusiform to broadly fusiform or utriform (5–12 μm wide)..... **5**
4′ Pileipellis composed of cylindrical hyphae, with narrow cylindrical to cylindrical terminal cells (3–7 μm wide)..... **7**
5 Pileipellis strongly gelatinized, composed of slimy hyphae, with terminal cells fusiform to utriform with rounded to subacute apex..... ***S. mucosus***
5′ Pileipellis not to slightly gelatinized, composed of hyphae with terminal cells fusiform to broadly fusiform with acuminate or tapering apex..... **6**
6 Basidiomata reddish dark brown to reddish brown; pores grayish orange at first; pileipellis with fusiform to broadly fusiform terminal cells, with acuminate apex..... ***S. rubinus***
6′ Basidiomata dark lilac to purplish to reddish brown, pores lilac gray at first; pileipellis with fusiform terminal cells, with tapering apex..... ***S. maculatoides***
7 Pileipellis an intricate trichoderm..... **8**
7′ Pileipellis a palisadoderm or trichoderm composed of almost vertically arranged hyphae..... **9**
8 Basidiomata small- to medium-sized, pileus 3.5–6 cm in diam.; pileipellis composed of cylindrical hyphae, terminal cells cylindrical with subacute to rounded apex, with scattered small parietal encrustations, brown in KOH..... ***S. obscuripellis***
8′ Basidiomata medium-sized, pileus 5–9.5 cm in diam.; pileipellis composed of cylindrical hyphae with terminal cells cylindrical and slightly curly, mostly hyaline to yellowish pale brown in KOH ..... ***S. pseudotylopilus***
9 Terminal cells of the pileipellis cylindrical with obtuse to rounded apex; pleurocystidia frequent..... **10**
9′ Terminal cells of the pileipellis are cylindrical with tapering to acute apex; pleurocystidia rare..... ***S. vellingae***
10 Basidiomata with wide cylindrical stipe 5.5–6.5 × 2.5–4 cm; stipe surface unchanging when injured ..... ***S. pachypus***
10′ Basidiomata with subcylindrical stipe 6–10 × 1–2.2 cm; stipe surface usually reddening when injured ..... ***S. subrufus***

DISCUSSION

Sutorius species are morphologically roughly similar to each other by their chocolate to reddish brown or purplish brown basidiomata, with granulose squamules scattered or transversely scissurate scales on the stipe surface. For this reason, macromorphological features are often not enough for species identification. Observation of microscopic characters is needed. The dimensions and *Q*-value of the basidiospores are the characters commonly used to differentiate species in the Boletaceae. In *Sutorius*, however, the dimensions and *Q*-value of the basidiospores seem to be poor characters for species delineation, because spore size and *Q*-value, especially the length of the basidiospores, can vary greatly within the same species and sometimes within the same individual. For example, in this study, the basidiospore length of *S. ubonensis* varied from 10.1 to 16.8 μm in the same basidioma, and from 8.7 to 16.8 μm between different collections. Therefore, in this study, the dimensions and *Q*-value of basidiospores were not used to differentiate species. On the basis of this study and previously published data, the appropriate set of characters for species identification of *Sutorius* is the combination of macromorphological features including basidiomata size, color, and stipe surface, and microscopic characters such as the arrangement and shape of terminal cells of the pileipellis, and the presence/absence or frequency of hymenophoral cystidia. Those characters mentioned above show little intraspecific variability and allow a clear-cut species delimitation. Some of the new species, namely, *S. mucosus*, *S. obscuripellis*, and *S. vellingae*, were described based on a single collection or basidiomata. However, all morphological and phylogenetic evidence was reliable and compelling enough to describe those species as new. During our survey in the North of Thailand, starting in 2012, we could not get more collections of those species, which suggests that those species are uncommon or rare. More collections of those species would be useful to better describe and understand the intraspecific genetic and morphological variability.

In the literature, *Sutorius eximius* has also been reported from Thailand (as *T. eximius*) (Chantorn et al., 2007; Chandrasrikul et al., 2008; Vadthanarat, 2009; Vadthanarat et al., 2010). Those reports were based on morphological characters only. Our phylogenetic analyses on Thai collections showed that they belong to eight different species, but none of them belongs in *S. eximius*. The phylogenetically closest species to *S. eximius* (voucher REH9400, from United States) was *S. pseudotylopilus*, but it differs morphologically and ecologically from *S. eximius* (see in *S. pseudotylopilus* notes). Morphologically, the most similar species is *S. ubonensis*, which was previously reported as *T. eximius* from Ubon Ratchathani Province (Vadthanarat, 2009;

Vadthanarat et al., 2010). Another report of *T. eximius* was from Nam Nao national park, Northeastern Thailand (Chantorn et al., 2007). We could not obtain the specimen for this study, but it can reasonably be assumed that, again, it belongs to a different species, other than *S. eximius*.

In Northeastern Thailand, *S. ubonensis* is one of the wild edible boletes that is collected and consumed by local people. It is called "Hed Pheung Khao Kam" or "Hed Pheung E-Dam," which means purple or blackish bolete. The price of *S. ubonensis* is usually about 200–300 THB/kg. Local people usually cook it by steaming or boiling over a long time period. They also believe that if it is not properly cooked, it might be poisonous.

In this study, a total of seven new *Sutorius* species and one new combination are proposed from Thailand and Southeast Asia. Before this study, only three *Sutorius* species were described worldwide, with one species from each of three continents, the Americas, Australia, and Asia (Halling et al., 2012; Chai et al., 2019). At present, 11 *Sutorius* species are known including the eight additional species in this study. In addition to those 11 species, our phylogeny (**Figure 1**) resolved six more terminal clades, which are phylogenetically distinct from all the described species. Among the six species, three are from Africa (Togo, Zimbabwe, and Burundi; clades 14, 15, and 16), two are from Asia (China; clades 1 and 2), and another was from Central America (Costa Rica; clade 3). Moreover, in previous studies, some undescribed *Sutorius* species were also phylogenetically evidenced from China, Zambia, and Indonesia, but have not yet been described (Halling et al., 2012; Chai et al., 2019). In South America, several *Sutorius* collections from Guyana were also morphologically identified and reported as *T. eximius* (Fulgenzi et al., 2007). Unfortunately, those latter collections were not added in our phylogeny because there were no sequences available in GenBank compatible with our phylogenetic study, and we have not been able to obtain the specimens. They might correspond as allies to some of the newly described species in this study. It is noteworthy that, so far, there is not any *Sutorius* collection known from Europe (Fulgenzi et al., 2007; Halling et al., 2012; Chai et al., 2019). Phylogenetically, the African specimens clustered together in a well-supported subclade within *Sutorius,* sister to another highly supported subclade comprising American, Australian, and Asian specimens with the exception of *S. vellingae* (ECV3603). *S. vellingae* (ECV3603) was not in the same clade with the other Asian species, but formed an isolated terminal clade, sister to all other *Sutorius* species. The pattern of two well-supported clades of African specimens sister to the others was also observed in the genus *Pulveroboletus* (Badou et al., 2018).

This study has refined the original concept of *Sutorius* and its members proposed by Halling et al. (2012) and Chai et al. (2019). An unexpectedly large number of *Sutorius* species were found and described in this study from Northern and Northeastern Thailand. Over a 7-year period (2012–2018), 26 *Sutorius* collections were obtained, of which 17 were obtained from northern Thailand (seven sites in three districts). These collections belonged to six novel and one known species. The other nine collections were from northeastern Thailand (collected from three sites in one district) and belonged to a single new species, different from those found in northern Thailand. Such a high diversity in a relatively small area, compared the single species known from the Americas and the single species known from Australia, was unexpected. It might be explained, however, by the location of the studied area in the Indo-Burma biodiversity hotspot. This hotspot is characterized by a wide variation in land form, climate, and latitude, which has led to the development of diverse natural habitats that support a high biodiversity (van Dijk et al., 2004). Moreover, the complex geological history associated with the Pleistocene climate oscillations has been suggested to produce the many localized centers of endemism observed in the hotspot (van Dijk et al., 2004). Northern Thailand, in particular, has a wide range of elevations, from around 300 m a.s.l. to 2,565 m a.s.l. at Doi Inthanon, the highest mountain in Thailand. This results in a diversity of forest types, many of which are dominated by ectomycorrhizal trees belonging to the Dipterocarpaceae, Fagaceae, Betulaceae, or Pinaceae. The center of diversity of *Sutorius* thus appears to be located in the studied area or possibly more broadly in the Greater Maekong Subregion. This region has been shown to shelter a high diversity of fungi, many of which only recently described or still unknown to science (e.g., Hyde et al., 2018; Thongbai et al., 2018). More studies on *Sutorius* are, however, needed in order to better document the distribution of this genus and clearly understand its biogeographic structure.

DATA AVAILABILITY STATEMENT

The datasets presented in this study can be found in online repositories. The names of the repository/repositories and accession number(s) can be found in the article/**Supplementary Material**.

AUTHOR CONTRIBUTIONS

OR, SV, and SL conceived and designed the study. SV, OR, and MA analyzed the data. SV, OR, and RH collected the specimens. SV and OR performed the experiments and wrote the manuscript. All authors reviewed and edited the manuscript.

FUNDING

This research work was partially supported by the Chiang Mai University and the Center of Excellence on Biodiversity (BSC), Office of Higher Education Commission, Thailand (BDC-PG3-161005).

ACKNOWLEDGMENTS

OR is grateful to the National Fund for Scientific Research, Belgium (FNRS) for travel grants. The authors are grateful

for the permit number 0907.4/4769 granted by the Department of National Parks, Wildlife and Plant Conservation, Ministry of Natural Resources and Environment for collecting in Doi Suthep-Pui National Park. The publication of this work was financially supported by Mae Fah Luang University.

SUPPLEMENTARY MATERIAL

The Supplementary Material for this article can be found online at: https://www.frontiersin.org/articles/10.3389/fmicb.2021.643505/full#supplementary-material

REFERENCES

Badou, A. S., De Kesel, A., Raspé, O., Ryberg, M. K., Guelly, A. K., and Yorou, N. S. (2018). Two new African siblings of *Pulveroboletus ravenelii* (Boletaceae). *MycoKeys* 43, 115–130. doi: 10.3897/mycokeys.43.30776

Chai, H., Liang, Z. Q., Xue, R., Jiang, S., Luo, S. H., Wang, Y., et al. (2019). New and noteworthy boletes from subtropical and tropical China. *MycoKeys* 46, 55–96. doi: 10.3897/mycokeys.46.31470

Chandrasrikul, A., Suwanarit, P., Sangwanit, U., Lumyong, S., Payapanon, A., Sanoamuang, N., et al. (2011). *Checklist of Mushrooms (Basidiomycetes) in Thailand*. Bangkok: Natural Resources and Environmental Policy and Planning, 432.

Chandrasrikul, A., Suwanarit, P., Sangwanit, U., Morinaga, T., Nishizawa, Y., and Murakami, Y. (2008). *Diversity of Mushrooms and Macrofungi in Thailand*. Bangkok: Kasersart University Press, 514.

Chantorn, K., Pachinburavan, A., and Sanoamuang, N. (2007). Nine new records of boletes (*Boletales*, *Hymenomycetes*) from Nam Nao and Phu Rua national Parks, Thailand. *KKU Res. J.* 12, 257–264.

Darriba, D., Taboada, G. L., Doallo, R., and Posada, D. (2012). jModelTest2: more models, new heuristics and parallel computing. *Nat. Methods* 9:772. doi: 10.1038/nmeth.2109

Doyle, J. J., and Doyle, J. L. (1990). Isolation of plant DNA from fresh tissue. *Focus* 12, 13–15.

Fulgenzi, T. D., Henkel, T. W., and Halling, R. E. (2007). *Tylopilus orsonianus* sp. nov. and *Tylopilus eximius* from Guyana. *Mycologia* 99, 622–627. doi: 10.1080/15572536.2007.11832556

Halling, R. E., Nuhn, M., Fechner, N. A., Osmundson, T. W., Soytong, K., Arora, D., et al. (2012). *Sutorius*: a new genus for *Boletus eximius*. *Mycologia* 104, 951–961.

Horak, E. (2011). *Revision of Malaysian Species of Boletales s.l. (Basidiomycota) Described by Corner EJH (1972, 1974)*. Malaysia: Forest Research Institute and Ministry of Natural Resources and Environment, 283.

Hosen, M. I., Feng, B., Wu, G., Zhu, X. T., Li, Y. C., and Yang, Z. L. (2013). *Borofutus*, a new genus of *Boletaceae* from tropical Asia: phylogeny, morphology and taxonomy. *Fungal Divers.* 58, 215–226. doi: 10.1007/s13225-012-0211-8

Hyde, K. D., Norphanphoun, C., Chen, J., Dissanayake, A. J., Doilom, M., Hongsanan, S., et al. (2018). Thailand's amazing diversity: up to 96% of fungi in northern Thailand may be novel. *Fungal Divers.* 93, 215–239. doi: 10.1007/s13225-018-0415-7

Katoh, K., and Standley, D. M. (2013). MAFFT Multiple sequence alignment software version 7: improvements in performance and usability. *Mol. Biol. Evol.* 30, 772–780. doi: 10.1093/molbev/mst010

Kornerup, A., and Wanscher, J. H. (1978). *) Methuen Handbook of Colour*, 3rd Edn. London: Eyre Methuen Ltd.

Kuo, M., and Ortiz-Santana, B. (2020). Revision of leccinoid fungi, with emphasis on North American taxa, based on molecular and morphological data. *Mycologia* 112, 197–211. doi: 10.1080/00275514.2019.1685351

Li, Y. C., Feng, B., and Yang, Z. L. (2011). *Zangia*, a new genus of Boletaceae supported by molecular and morphological evidence. *Fungal Divers.* 49, 125–143. doi: 10.1007/s13225-011-0096-y

Li, Y. C., Ortiz-Santana, B., Zeng, N. K., and Feng, B. (2014). Molecular phylogeny and taxonomy of the genus *Veloporphyrellus*. *Mycologia* 106, 291–306. doi: 10.3852/106.2.291

Lutzoni, F., Kauff, F., Cox, C. J., McLaughlin, D., Celio, G., Dentinger, B., et al. (2004). Assembling the fungal tree of life: progress, classification, and evolution of subcellular traits. *Am. J. Bot.* 91, 1446–1480.

Mason-Gamer, R. J., and Kellogg, E. A. (1996). Testing for phylogenetic conflict among molecular data sets in the tribe *Triticeae* (Gramineae). *Syst. Biol.* 45, 524–545. doi: 10.1093/sysbio/45.4.524

Matheny, P. B. (2005). Improving phylogenetic inference of mushrooms with RPB1 and RPB2 nucleotide sequences (*Inocybe*; Agaricales). *Mol. Phylogenet. Evol.* 35, 1–20. doi: 10.1016/j.ympev.2004.11.014

Miller, M. A., Holder, M. T., Vos, R., Midford, P. E., Liebowitz, T., Chan, L., et al. (2009). *The CIPRES portals. CIPRES*. Available online at: http://www.phylo.org/portal2/home (accessed November 8, 2020).

Raspé, O., Vadthanarat, S., De Kesel, A., Degreef, J., Hyde, K. D., and Lumyong, S. (2016). *Pulveroboletus fragrans*, a new Boletaceae species from Northern Thailand, with a remarkable aromatic odor. *Mycol. Prog.* 15:38.

Reeb, V., Lutzoni, F., and Roux, C. (2004). Contribution of *RPB2* to multilocus phylogenetic studies of the euascomycetes (*Pezizomycotina*, Fungi) with special emphasis on the lichen-forming Acarosporaceae and evolution of polyspory. *Mol. Phylogenet. Evol.* 32, 1036–1060. doi: 10.1016/j.ympev.2004.04.012

Rehner, S. A., and Buckley, E. (2005). A *Beauveria* phylogeny inferred from nuclear ITS and EF1-α sequences: evidence for cryptic diversification and links to *Cordyceps* teleomorphs. *Mycologia* 97, 84–98. doi: 10.1080/15572536.2006.11832842

Ronquist, F., Teslenko, M., van der Mark, P., Ayres, D., Darling, A., Höhna, S., et al. (2012). MrBayes 3.2: efficient bayesian phylogenetic inference and model choice across a large model space. *Syst. Biol.* 61, 539–542. doi: 10.1093/sysbio/sys029

Singer, R. (1947). The boletoideae of florida with notes on extralimital species III. *Am. Midl. Nat.* 37, 1–135. doi: 10.2307/2421647

Smith, A. H., and Thiers, H. D. (1971). *The Boletes of Michigan*. Ann Arbor: University of Michigan Press.

Stamatakis, A. (2006). RAxML-vi-hpc: maximum likelihood-based phylogenetic analyses with thousands of taxa and mixed models. *Bioinformatics* 22, 2688–2690. doi: 10.1093/bioinformatics/btl446

Thongbai, B., Hyde, K. D., Lumyong, S., and Raspé, O. (2018). High undescribed diversity of *Amanita* section *Vaginatae* in northern Thailand. *Mycosphere* 9, 462–494. doi: 10.5943/mycosphere/9/3/3

Vadthanarat, S. (2009). *Some Ecological and Biological Characters of Brownish Purple Bolete, Tylopilus eximius Peck*. Bachelor's thesis, Ubon Ratchathani University, Thailand

Vadthanarat, S., Lumyong, S., and Raspé, O. (2019). *Cacaoporus*, a new Boletaceae genus, with two new species from Thailand. *MycoKeys* 54, 1–29. doi: 10.3897/mycokeys.54.35018

Vadthanarat, S., Raspé, O., and Lumyong, S. (2018). Phylogenetic affinities of the sequestrate genus *Rhodactina* (*Boletaceae*), with a new species, *R. rostratispora* from Thailand. *MycoKeys* 29, 63–80. doi: 10.3897/mycokeys.29.22572

Vadthanarat, S., Tanpong, S., and Pukahuta, C. (2010). "Inventory survey of wild mushrooms in community forests in Trakarn Phuetphon, Ubon Ratchathani," in *The Proceedings of the 4th Ubon Ratchathani University Research Conference*, (Thailand: Ubon Ratchathani).

van Dijk, P. P., Tordoff, A. W., Fellowes, J., Lau, M., and Jinshuang, M. (2004). "Indo-Burma," in *Hotspots Revisited. Earth's Biologically Richest and Most Endangered Terrestrial Ecoregions*, eds R. A. Mittermeier, P. G. Gil, and M. Hoffman (Chicago: University of Chicago Press), 323–330.

Wu, G., Feng, B., Xu, J., Zhu, X. T., Li, Y. C., Zeng, N. K., et al. (2014). Molecular phylogenetic analyses redefine seven major clades and reveal 22 new generic clades in the fungal family *Boletaceae*. *Fungal Divers.* 69, 93–115. doi: 10.1007/s13225-014-0283-8

Wu, G., Li, Y. C., Zhu, X. T., Zhao, K., Han, L. H., Cui, Y. Y., et al. (2016). One hundred noteworthy boletes from China. *Fungal Divers.* 81, 25–188. doi: 10.1007/s13225-016-0375-8

Zhao, K., Wu, G., Feng, B., and Yang, Z. L. (2014). Molecular phylogeny of *Caloboletus* (Boletaceae) and a new species in East Asia. *Mycol. Prog.* 13, 1127–1136.

Zhu, X. T., Wu, G., Zhao, K., Halling, R. E., and Yang, Z. L. (2015). *Hourangia*, a new genus of *Boletaceae* to accommodate *Xerocomus cheoi* and its allied species. *Mycol. Prog.* 14:37.

Conflict of Interest: The authors declare that the research was conducted in the absence of any commercial or financial relationships that could be construed as a potential conflict of interest.

Copyright © 2021 Vadthanarat, Halling, Amalfi, Lumyong and Raspé. This is an open-access article distributed under the terms of the Creative Commons Attribution License (CC BY). The use, distribution or reproduction in other forums is permitted, provided the original author(s) and the copyright owner(s) are credited and that the original publication in this journal is cited, in accordance with accepted academic practice. No use, distribution or reproduction is permitted which does not comply with these terms.

frontiers in Microbiology

ORIGINAL RESEARCH
published: 23 April 2021
doi: 10.3389/fmicb.2021.655910

New Glomeromycotan Taxa, *Dominikia glomerocarpica* sp. nov. and *Epigeocarpum crypticum* gen. nov. et sp. nov. From Brazil, and *Silvaspora* gen. nov. From New Caledonia

*Janusz Błaszkowski[1], Khadija Jobim[2], Piotr Niezgoda[1], Edward Meller[3], Ryszard Malinowski[3], Paweł Milczarski[4], Szymon Zubek[5], Franco Magurno[6], Leonardo Casieri[7], Wojciech Bierza[6], Tomasz Błaszkowski[8], Thomas Crossay[9] and Bruno Tomio Goto[2]**

[1] Laboratory of Plant Protection, Department of Shaping of Environment, West Pomeranian University of Technology in Szczecin, Szczecin, Poland, [2] Departamento de Botânica e Zoologia, Universidade Federal do Rio Grande do Norte, Natal, Brazil, [3] Laboratory of Soil Science and Environmental Chemistry, Department of Shaping of Environment, West Pomeranian University of Technology in Szczecin, Szczecin, Poland, [4] Department of Genetics, Plant Breeding and Biotechnology, West Pomeranian University of Technology in Szczecin, Szczecin, Poland, [5] Faculty of Biology, Institute of Botany, Jagiellonian University, Kraków, Poland, [6] Institute of Biology, Biotechnology and Environmental Protection, Faculty of Natural Sciences, University of Silesia in Katowice, Katowice, Poland, [7] Mycorrhizal Applications LLC at Bio-Research & Development Growth Park, St. Louis, MO, United States, [8] Department of General and Oncological Surgery, Pomeranian Medical University in Szczecin, Szczecin, Poland, [9] Institut des Sciences Exactes et Appliquées (EA 7484), Université de la Nouvelle Calédonie, Nouméa, New Caledonia

Examination of fungal specimens collected in the Atlantic rain forest ecosystems of Northeast Brazil revealed many potentially new epigeous and semihypogeous glomerocarp-producing species of the phylum Glomeromycota. Among them were two fungi that formed unorganized epigeous glomerocarps with glomoid spores of almost identical morphology. The sole structure that distinguished the two fungi was the laminate layer 2 of their three-layered spore wall, which in spores of the second fungus crushed in PVLG-based mountants contracted and, consequently, transferred into a crown-like structure. Surprisingly, phylogenetic analyses of sequences of the 18S-ITS-28S nuc rDNA and the *rpb1* gene indicated that these glomerocarps represent two strongly divergent undescribed species in the family Glomeraceae. The analyses placed the first in the genus *Dominikia*, and the second in a sister clade to the monospecific generic clade *Kamienskia* with *Kamienskia bistrata*. The first species was described here as *Dominikia glomerocarpica* sp. nov. Because *D. glomerocarpica* is the first glomerocarp-forming species in *Dominikia*, the generic description of this genus was emended. The very large phylogenetic distance and the fundamental morphological differences between the second species and *K. bistrata* suggested us to introduce a new genus, here named as *Epigeocarpum* gen. nov., and name the new species *Epigeocarpum crypticum* sp. nov. In addition, our analyses also focused

OPEN ACCESS

Edited by:
Dhanushka Nadeeshan Wanasinghe, Kunming Institute of Botany, Chinese Academy of Sciences, China

Reviewed by:
Kasun Thambugala, University of Sri Jayewardenepura, Sri Lanka
Rungtiwa Phookamsak, Kunming Institute of Botany, Chinese Academy of Sciences, China

***Correspondence:**
Bruno Tomio Goto
brunogoto@hotmail.com

Specialty section:
This article was submitted to Evolutionary and Genomic Microbiology, a section of the journal Frontiers in Microbiology

Received: *19 January 2021*
Accepted: *09 March 2021*
Published: *23 April 2021*

Citation:
Błaszkowski J, Jobim K, Niezgoda P, Meller E, Malinowski R, Milczarski P, Zubek S, Magurno F, Casieri L, Bierza W, Błaszkowski T, Crossay T and Goto BT (2021) New Glomeromycotan Taxa, Dominikia glomerocarpica sp. nov. and Epigeocarpum crypticum gen. nov. et sp. nov. From Brazil, and Silvaspora gen. nov. From New Caledonia. Front. Microbiol. 12:655910. doi: 10.3389/fmicb.2021.655910

on an arbuscular mycorrhizal fungus originally described as *Rhizophagus neocaledonicus*, later transferred to the genus *Rhizoglomus*. The analyses indicated that this species does not belong to any of these two genera but represents a new clade at the rank of genus in the Glomeraceae, here described as *Silvaspora* gen. nov.

Keywords: arbuscular mycorrhizal fungi, cryptic species, morphology, molecular phylogeny, 18S-ITS-28S nuc rDNA, *rpb1*

INTRODUCTION

In the phylum Glomeromycota, the largest group is represented by species producing glomoid spores, which arise blastically at tips of cylindrical or funnel-shaped sporogenous hyphae, as spores of *Glomus macrocarpum* (see **Supplementary Table 1** for species authors), the type species of *Glomus* and the Glomeromycota (Clements and Shear, 1931; Schüßler and Walker, 2010; Oehl et al., 2011). Of the 330 known species of the Glomeromycota, approximately 60 were originally described to form glomoid spores in epigeous or hypogeous unorganized glomerocarps, i.e., fruit bodies with randomly distributed spores inside them (Gerdemann and Trappe, 1974; Morton, 1988; Jobim et al., 2019). Importantly, of the glomerocarpic species, only seven (*Diversispora epigaea*, *Funneliformis mosseae*, *Glomus arborense*, *G. macrocarpum*, *Glomus pallidum*, *Glomus tenerum*, and *Glomus warcupii*) were managed to grow in culture, and only eight (*D. epigaea*, *Diversispora sporocarpia*, *G. macrocarpum*, *Redeckera megalocarpa*, *Redeckera fulva*, *Redeckera pulvinata*, *Sclerocarpum amazonicum*, and *Sclerocystis sinuosa*) were provided with molecular data (Jobim et al., 2019), which essentially makes this group of fungi ascribed to the Glomeromycota difficult to characterize and classify.

Among many unorganized glomerocarps, previously found from our studies in the Brazilian Northeast, there were two whose glomoid spores first seemed to be identical in morphology to each another but differed from glomoid spores of described species of the Glomeromycota. Further studies of the phenotypic features of the spores revealed very small differences and, consequently, suggested that the glomerocarps represent two semicryptic undescribed species. BLAST searchers using initial molecular data about these fungi confirmed this hypothesis and showed that these species are probably related to the genera *Dominikia* and *Kamienskia* in the family Glomeraceae.

"Crypticity" in fungal taxonomy is an aspect known for several phyla (Matute and Sepúlveda, 2019). Also, molecular analyses of some morphological species of the Glomeromycota suggest that they contain cryptic phylogenetic species, in which differences in morphology do not occur, are very small and inconclusive, or are invisible using traditional research methods and tools. Examples of such species are *Rhizoglomus irregulare* and *Septoglomus constrictum* (Stockinger et al., 2014; Błaszkowski, pers. observ.).

The disclosure of cryptic species strongly depends on the molecular markers used in phylogenetic identification. Currently, of the many markers that have been used in phylogenetic studies of the Glomeromycota (Błaszkowski et al., 2018a,b, 2019a,b; Jobim et al., 2019; Magurno et al., 2019), those comprising the partial small subunit (18S), internal transcribed spacer (ITS1-5.8S-ITS2 = ITS), and partial large subunit (28S) nuc rDNA segment (= 18S-ITS-28S), as well as the largest subunit of RNA polymerase II (*rpb1*) gene, have the highest resolution power and characterize the highest proportion of described species within the Glomeromycota (Krüger et al., 2012; Stockinger et al., 2014; Al-Yahya'ei et al., 2017). The first marker allowed to separate, for example, *Rhizoglomus dunense* from *Rhizoglomus clarum*, whose morphologies are almost identical, but sequence divergence is very high (13.3%; Al-Yahya'ei et al., 2017). The sequence resolution of the *rpb1* gene is higher and indicating that *R. irregulare* likely contains at least one cryptic species (Stockinger et al., 2014) and strongly confirming the uniqueness of *R. dunense* with a dissimilarity of 8.1% from *R. clarum*. According to literature data and our analyses, 18S-ITS-28S and *rpb1* sequences show interspecies differences when they differ by ≥3% and approximately 1%, respectively (Krüger et al., 2012; Stockinger et al., 2014; Błaszkowski et al., 2019b; Corazon-Guivin et al., 2019b). The large proportion of species provided with molecular data contained in the two markers allows both to compare a relatively large number of species and to better define the phylogenetic divergences between species belonging to different higher taxonomic ranks. Moreover, it is widely recognized that the concatenation of sequences of the ribosomal RNA-coding genes with sequences of protein-coding genes significantly increases phylogenetic resolving power for revealing relationships between analyzed taxa (Miadlikowska et al., 2014).

The genera *Dominikia* and *Kamienskia* were erected in the phylum Glomeromycota mainly due to phylogenetic analyses of 18S-ITS-28S sequences of six species originally described in the genus *Glomus* and the newly described *Dominikia disticha* (Błaszkowski et al., 2015a). The type species of these new genera became *Dominikia minuta* and *Kamienskia bistrata*. The main characters shared by the two fungi were hyaline or pale-colored, small spores (10- to 65-μm diameter when globose) formed in hypogeous clusters, which were produced in pot trap cultures, but were not found in the field-collected rhizosphere samples used to inoculate the cultures. Therefore, it was suggested that species of *Dominikia* and *Kamienskia* sporulate rarely or seasonally and were not found in the field soils because their delicate spores quickly break down before soil sampling (Błaszkowski et al., 2015a).

Later, new species of *Dominikia* and *Kamienskia* were described, whose spores were either (i) similar in color and size (*Dominikia lithuanica*, *Dominikia litorea*, *Kamienskia divaricata*), (ii) darker-colored (*Dominikia aurea*, *Dominikia bernensis*, *Dominikia compressa*, *Dominikia duoreactiva*,

Dominikia emiratia), (iii) larger (*D. compressa*, *D. duoreactiva*, *D. emiratia*), and (iv) formed mainly singly (*Dominikia difficilevidera*) (Oehl et al., 2014, 2015; Błaszkowski et al., 2015b, 2016, 2018c; Al-Yahya'ei et al., 2017) compared to the spores of the species listed above.

Recently, *Kamienskia perpusilla* and *K. divaricata* were transferred to a newly erected genus, *Microkamienskia* with a newly described species, *Microkamienskia peruviana* (Corazon-Guivin et al., 2019a), and *D. litorea* and *D. emiratia* became members of the new genera *Microdominikia* and *Orientoglomus*, respectively (Corazon-Guivin et al., 2019b). In addition, Corazon-Guivin et al. (2019b) described a new, monospecific genus, *Nanoglomus*, with *Nanoglomus plukenetiae*, sp. nov., with very similar morphology to *K. perpusilla*, but phylogenetically closely related to species of clades previously treated as *Dominikia*. All the taxa were erected mainly based on phylogenetic analyses of 18S-ITS-28S sequences and divergences of the sequences from other most closely related species, although Corazon-Guivin et al. (2019b) also showed morphological differences in the spore wall and subtending hypha between these taxa.

All described species of *Dominikia* and *Kamienskia* and their closest molecular relatives possess morphological characters distinguishing them from each other. However, none of these species has a morphological synapomorphy that would clearly demonstrate a generic separateness.

Recently, a new AMF, namely, *Rhizophagus neocaledonicus*, was described, which in the field lived in symbiosis with metallophytes in ultramafic soil in New Caledonia (Crossay et al., 2018). It was soon reassigned to the genus *Rhizoglomus*, as *Rhizoglomus neocaledonicum* (Turrini et al., 2018), because the generic name *Rhizophagus* should not be assigned to any species in the Glomeromycota (Sieverding et al., 2014). The assignment of this species into the genus *Rhizoglomus* (treated as *Rhizophagus*) was made based on a maximum likelihood phylogenetic analysis of 18S-ITS-28S sequences, even though the *Rhizoglomus* clade with the basally positioned *R. neocaledonicum* obtained only 49% bootstrap support. Moreover, the genetic divergence of *R. neocaledonicum* from the six *Rhizoglomus* species considered in the analysis was in the order of values separating clades of the Glomeromycota at the rank of genus. The sister species to the *Rhizoglomus* clade was a member of the genus *Sclerocystis*, *S. sinuosa* (Crossay et al., 2018). Molecular phylogenetic analyses performed by Turrini et al. (2018) confirmed the basal position and strong genetic divergence of *R. neocaledonicum* in the *Rhizoglomus* clade. However, they did not include *S. sinuosa* in their analyses. Further phylogenetic analyses of 18S-ITS-28S sequences of all *Rhizoglomus* species with available DNA barcodes and representatives of the other genera of the Glomeraceae accommodated *R. neocaledonicum* between the recently described monospecific genus *Halonatospora*, represented by *Halonatospora pansihalos*, and *S. sinuosa*, of which the latter was located basally to the other species of *Rhizoglomus* (Błaszkowski et al., 2018b, 2019b). Thus, the information presented above suggested that the New Caledonian fungus does not belong to *Rhizoglomus* but represents a new clade at the rank of genus in the Glomeraceae.

Therefore, the aims of this study were (i) to document that the two Brazilian fungi are new species of the Glomeromycota, (ii) to determine the molecular phylogenetic position of these fungi among their generic relatives of known phylogenies, and (iii) to describe in detail the morphology of these fungi. Moreover, we tested the hypothesis that *R. neocaledonicum* is a member of an undescribed genus in the Glomeraceae using already available and newly collected morphological and molecular data about this species.

MATERIALS AND METHODS

Origin of Study Material

The glomerocarps of the two fungi were sampled by K. Jobim at Parque das Trilhas, belonging to the Serra de Baturité Environmental Protection Area (Baturité EPA; 4°16′36.8″ S, 38°56′20.4″ W; 865 m above sea level) in the Guaramiranga municipality. The area covers 32,690 hectares located in the Northeast portion of the State of Ceará, 90 km from Fortaleza (Governo do Ceará, 2018) and is part of the Atlantic Forest. It houses a rich biodiversity with a high degree of endemism and includes a high percentage of preserved remnants of the Atlantic Forest that constitute a refuge for species originating from humid habitats, such as the Atlantic and Amazon forests (Figueiredo and Barbosa, 1990; Girão, 2006). In this region, annual mean temperatures are 19–22°C, and the average annual sum of rainfalls is 1,500 mm (Governo do Ceará, 2018). The high rainfalls, the altitude range between 100 and 1,000 m above sea level, and the exposure to humid air masses render the Baturité EPA one of the most humid areas in the State of Ceará (Governo do Ceará, 2018). The glomerocarps of these species, tentatively named "Species 1" and "Species 2," were found in July 2018 and April 2018, respectively.

Collection of Glomerocarps, Establishment, and Growth of Single-Species Cultures

The glomerocarps of the two fungi were found employing the methodology used by Jobim et al. (2019) for collecting glomerocarpic species. Single-species pot cultures for each of the collected fungi were established by inoculating sterile growth substrate with fragments of the glomerocarps, of which each fragment contained at least 100 spores. The plant host used in the pot cultures was *Plantago lanceolata* L. The composition of the growth substrate, the methods of culture establishment, inoculation, and growing conditions were as those described by Błaszkowski et al. (2012).

Extraction of Spores and Staining of Mycorrhizal Structures

The spore conglomerations used for the establishment of single-species cultures were extracted from the glomerocarps by means of a preparation needle under a dissecting microscope. Attempts at extracting spores from the single-species cultures of the two fungi were performed by a method characterized

by Błaszkowski et al. (2015b). Roots of *P. lanceolata* from the single-species cultures were stained following the protocol of Błaszkowski (2012).

Microscopy and Nomenclature

Morphological features of spores and phenotypic and histochemical characters of spore wall layers of the two fungi were characterized based on at least 100 spores of each species mounted in water, lactic acid, polyvinyl alcohol/lactic acid/glycerol (PVLG, Omar et al., 1979), and a mixture of PVLG and Melzer's reagent (1:1, vol/vol). The preparation of spores for study and photography were as those described previously (Błaszkowski, 2012; Błaszkowski et al., 2012). Types of spore wall layers are those defined by Walker (1983) and Błaszkowski (2012). Color names were from Kornerup and Wanscher (1983). Nomenclature of fungi and the authors of fungal names are from the Index Fungorum website, http://www.indexfungorum.org/AuthorsOfFungalNames.htm; see **Supplementary Table 1**. The terms "glomerospores" and "glomerocarps" were used for spores and fruit bodies produced by AMF, as proposed by Goto and Maia (2006) and Jobim et al. (2019).

Voucher specimens of the proposed new species [spores permanently mounted in PVLG and a mixture of PVLG and Melzer's reagent (1:1, vol/vol) on slides] were deposited at UFRN hebarium (Brazil; holotypes on slides and dry glomerocarps in vials) and in the Laboratory of Plant Protection, Department of Shaping of Environment (LPPDSE; isotypes on slides and dry glomerocarps in vials), West Pomeranian University of Technology in Szczecin, Poland.

DNA Extraction, Polymerase Chain Reaction, Cloning, and DNA Sequencing

Genomic DNA of the two potentially new species was extracted separately from fragments of glomerocarps containing approximately 20 spores. Details on spores preparation prior to polymerase chain reaction (PCR), PCR conditions, and primers used to obtain 18S-ITS-28S amplicons were as described in Krüger et al. (2009), Błaszkowski et al. (2014), and Symanczik et al. (2014), respectively.

The *rpb1* sequences of *Rhizoglomus dalpeae* were obtained by amplification with primers designed by Stockinger et al. (2014) following the recommended conditions. We used the same DNA, from which 18S-ITS-28S sequences had been obtained (Błaszkowski et al., 2019b). The first PCR with DNA of this species was performed with the primers RPB1-DR160mix (a, b, c, d) and RPB1-HS2680GPr, whereas the second PCR with RPB1-HS189GPf and RPB1-DR1210r.

The *rpb1* sequences of "Species 1" and "Species 2" were amplified with a nested approach. The primer set consisted of two forward primers, RPB1-3F and RPB1-4F, on the third and fourth exon, respectively, and two reverse primers, RPB1-5R and RPB1-5RN, on the fifth exon of the gene (**Table 1**). The *rpb1* sequences of *R. neocaledonicum* and *Rhizoglomus silesianum* were amplified using the primer RPB1-4F1, designed on the fourth exon to match all the *rpb1* sequences available for the Glomeraceae (with a maximum tolerance of one mismatch), in combination with RPB1-5R. The three forward primers were used at a final concentration = 200 nM, whereas the concentration of reverse primers was higher (**Table 1**) to compensate the gap in the Tm predicted using Oligo/Analyzer[1]. DreamTaq DNA Polymerase (Thermo Fisher) was used for the amplifications in 20 μL final volume according to the manufacturer's specifications, adding $MgCl_2$ 3 mM and bovine serum albumin 0.5 μg μL^{-1} as final concentrations only in the PCR on raw DNA. The thermal cycling was as follows: 5 min initial denaturation (95°C), 40 cycles (30 cycles in the nested PCR) of 30-s denaturation (95°C), 30-s annealing, elongation at 72°C (**Table 1**), and 5-min (72°C) final elongation.

Cloning and sequencing of the PCR products were as those described by Błaszkowski et al. (2015a). The sequences were deposited in GenBank (MW507148–57, MW541060–67).

Sequence Alignment and Phylogenetic Analyses

Comparative analyses of 18S-ITS-28S and *rpb1* sequences of the two fungi, using BLAST, confirmed our initial hypotheses that the fungi of our study are undescribed species of the Glomeromycota (see section "Introduction"). In particular, these analyses indicated that "Species 1" belongs to *Dominikia*, and the closest relative of "Species 2" is *K. bistrata*. Three sequence alignments were created in order (*i*) to determine the position of the new *Dominikia* sp. among its generic relatives, (*ii*) to assess the robustness of the relationship of the second new species with *K. bistrata*, and (*iii*) to test the hypothesis expressed previously (Błaszkowski et al., 2019b) and here that *R. neocaledonicum* should represent a new genus. The first alignment consisted

[1]https://eu.idtdna.com

TABLE 1 | Primers characteristics and PCR conditions used for the amplification of the *rpb1* sequences.

Primer	Nucleotide sequence (5′–3′)	Position on the sequence	In combination with	Expected amplicon length	Ta°C	t elong.
RPB1-3F	GTC TTC GTG CAG TTT GGG A	727–745	RPB1-5R [1 μM]	≈1,410 bp	55	1 min 30 s
RPB1-4F	CTA GGC CTG ATT GGA TGA T	1,204–1,222	RPB1-5RN [500 nM]	≈870 bp	54	1 min
RPB1-4F1	GCT CGT CCT GAT TGG ATG A	1,203–1,221	RPB1-5R [1 μM]	≈935 bp	55	1 min
RPB1-5R	ACG ATT TGT TTT GGT ACC AT	2,119–2,138				
RPB1-5RN	TTC ATC TCA TCA CCA TCA A	2,048–2,066				

The position of primers is given based on sequence of Rhizoglomus intraradices HG316020.1. The final concentration of the reverse primers is provided for each combination, as well as the expected product size, the temperature of annealing (Ta), and the time of elongation (t elong).

of sequences of the 18S-ITS-28S nuc rDNA region or part thereof, which characterized all sequenced species of *Dominikia*, *Kamienskia*, and *Rhizoglomus*, as well as representative species of all other genera of the Glomeraceae *sensu* Schüßler and Walker (2010), Oehl et al. (2011), Błaszkowski et al. (2015a, 2018a,b), Corazon-Guivin et al. (2019a,b,c), Jobim et al. (2019), and Wijayawardene et al. (2020), except for the genus *Simiglomus* (a total of 15 genera; **Figure 1**). The alignment contained 139 sequences of 48 species of the Glomeraceae (including our two new species), of which the *Rhizoglomus natalense* KJ210824 and KJ210826 sequences represented the 28S locus only. To increase the phylogenetic signal from *S. sinuosa*, the 18S-ITS-28S sequence, not available in the GenBank database, was obtained by assembling the overlapping sequences AJ133706 (18S), AJ437106 (18S-ITS-28S), and FJ461846 (28S) generated from the same isolate MD126. The second alignment consisted of *rpb1* sequences from all species of the 18S-ITS-28S alignment that have been provided with *rpb1* sequences (**Figure 2**). This alignment included 75 sequences of 29 species in 14 genera of the Glomeraceae (including our two new species). The third alignment contained concatenated 18S-ITS-28S and *rpb1* sequences in the same number and species composition as in the *rpb1* alignment (**Figure 3**). In all three alignments, the outgroup was represented by seven sequences of four species of the family Entrophosporaceae. Data about the origin of the sequences used are presented in **Supplementary Table 2**.

Identity values of the 18S-ITS-28S and *rpb1* sequences of the two new species were calculated separately for each species using BioEdit (Hall, 1999). With the same program, we calculated the sequence divergence of these new species and *R. neocaledonicum* from sequences of their closest relatives (**Figures 1**, **2**). All comparisons were performed on sequences of the same length.

Indels were coded as binary characters by means of FastGap 1.2 (Borchsenius, 2009), with the possibility to code missing data to be recognized by the phylogenetic inference programs. The coded binary character sets were added to the respective nucleotide alignments, as described in Błaszkowski et al. (2014). The 18S-ITS-28S, *rpb1*, and 18S-ITS-28S + *rpb1* alignments were aligned separately with MAFFT 7 using the auto option[2].

In order to reconstruct the phylogenetic positions of the two new species among sequenced species of the Glomeraceae, as well as to confirm our hypothesis on the phylogeny of *R. neocaledonicum*, Bayesian inference (BI) and maximum likelihood (ML) phylogenetic analyses of the alignments were performed via CIPRES Science Gateway 3.1 (Miller et al., 2010). GTR + G was predicted as best substitution model for the DNA partitions in the BI analysis by using jModelTest2 (Darriba et al., 2012). For the indel partition, F81 model was chosen as suggested in the MrBayes manual. Four Markov chains were run over 1 million generations in MrBayes 3.2 (Ronquist et al., 2012), sampling every 1,000 generations, with a burn-in at 3,000 sampled trees. The ML phylogenetic tree inference, using a maximum likelihood/1,000 rapid bootstrapping run, was computed with RAxML 8.2.12 (Stamatakis, 2014) using the GTRGAMMA algorithm. To improve the accuracy of phylogenetic reconstruction (Lanfear et al., 2012; Nagy et al., 2012), in both BI and ML analyses, the 18S-ITS-28S alignment was divided into four partitions: 18S, ITS, 28S, and the binary (indel) character set. Two partitions (gene and indel set) were used for the *rpb1* alignment. The same partitioning scheme was used in the 18S-ITS-28S + *rpb1* alignment with concatenated sequences, resulting in six partitions totally. We assumed that clades were supported when BI posterior probability and ML bootstrap support values were ≥0.95 and ≥70%, respectively. The phylogenetic trees obtained in the analyses were visualized and rooted in Archaeopteryx.js[3].

RESULTS

General Data and Phylogeny

Data about the numbers of base pairs as well as variable and parsimony informative sites of the 18S-ITS-28S, *rpb1*, and 18S-ITS-28S + *rpb1* alignments are presented in **Table 2**. The identity values of the 18S-ITS-28S sequences of "Species 1" and "Species 2" (five sequences each) were 98.6 and 99.4%, respectively, and the identity values of the *rpb1* sequences of these species (two sequences each) were 99.1%. The identities of the three 18S-ITS-28S and two *rpb1* sequences of *Rhizoglomus neocaledonicum* were 99.5 and 99.7%, respectively.

In the 18S-ITS-28S and 18S-ITS-28S + *rpb1* trees, the topologies of the family Glomeraceae clade, reconstructed from BI and ML analyses, were identical (**Figures 1**, **3**). Additionally, for all trees (**Figures 1–3**), the branches of the outgroup Entrophosporaceae clade received full or strong BI and ML support. Instead, the topologies of the *rpb1* Glomeraceae clade slightly differed depending on the algorithm used in the analyses. The differences regarded only the positions of the monospecific genera *Microdominikia* and *Orientoglomus* (**Figure 2**). In the *rpb1* BI tree, *Microdominikia litorea* was a basal clade to the clades with *Orientoglomus emiratium* and *Dominikia* spp. Instead, in the *rpb1* ML tree, the relationships between *Orientoglomus*, *Microdominikia*, and *Dominikia* clades were not supported (**Figure 2**).

In all trees, 18S-ITS-28S, *rpb1*, 18S-ITS-28S + *rpb1*, "Species 1" (=*Dominikia glomerocarpica*) clustered in a sister clade to the clade with *D. aurea*, and "Species 2" (= *Epigeocarpum crypticum*) populated a sister clade to the clade with *K. bistrata* (**Figures 1–3**). Both BI and ML analyses of all three alignments supported the tie between "Species 1" and *D. aurea* (BI = 0.99–1.0; ML = 74–97%; **Figures 1–3**). Instead, the node connecting "Species 2" with *K. bistrata* obtained moderate or strong supports in BI and ML analyses of the 18S-ITS-28S (0.99/88) and 18S-ITS-28S + *rpb1* (1/96) alignments (**Figures 1**, **3**), but neither BI nor ML analysis of the *rpb1* alignment supported (0.68/52) the tie between these species (**Figure 2**).

In the 18S-ITS-28S and 18S-ITS-28S + *rpb1* trees, the clades with "Species 1" and "Species 2" obtained full supports in both analyses, and in the *rpb1* tree, the supports for both species were

[2]http://maft.cbre.jp/alignment/server/

[3]https://sites.google.com/site/cmzmasek/home/software/archaeopteryx-js

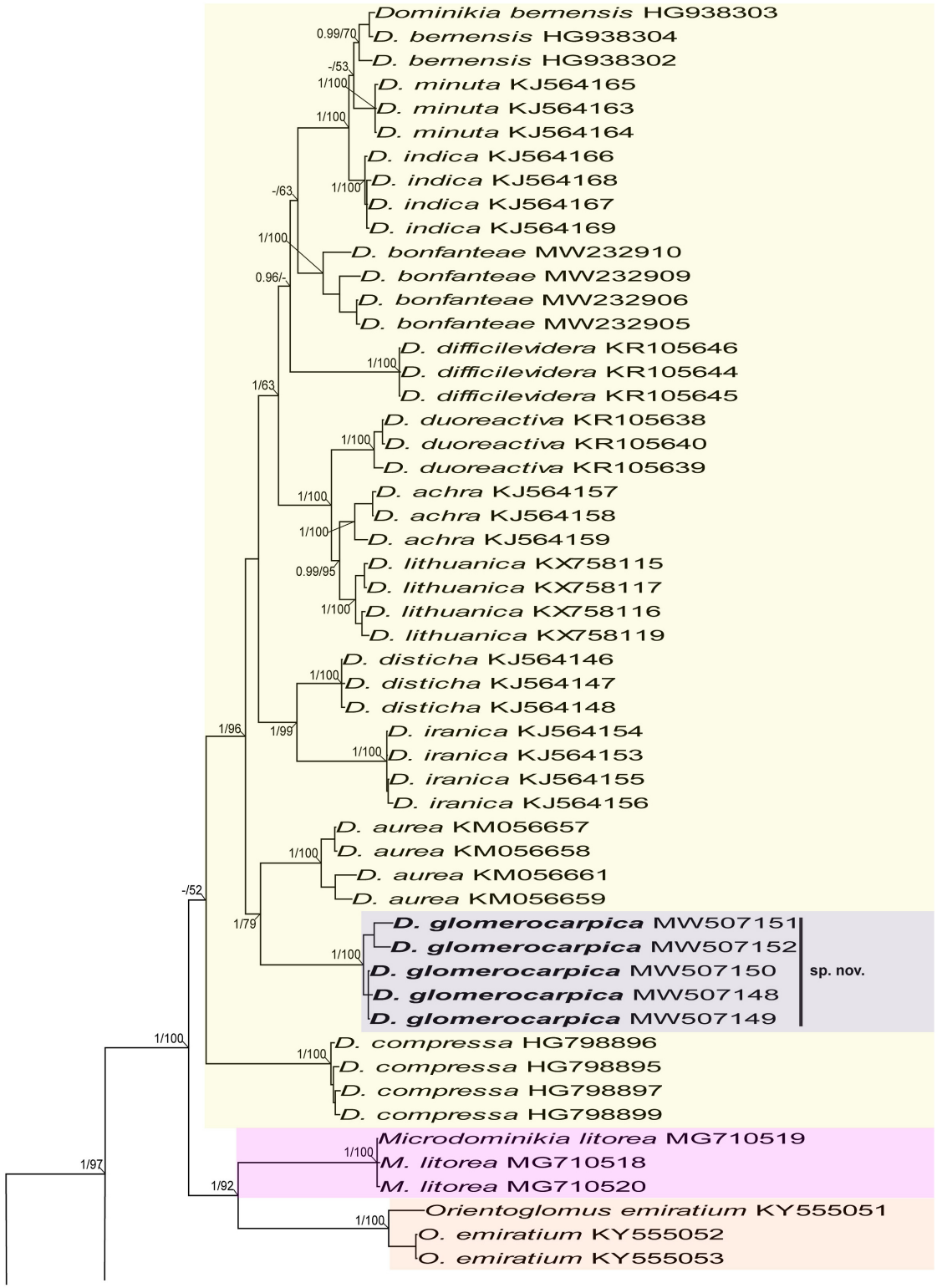


FIGURE 1 | Continued

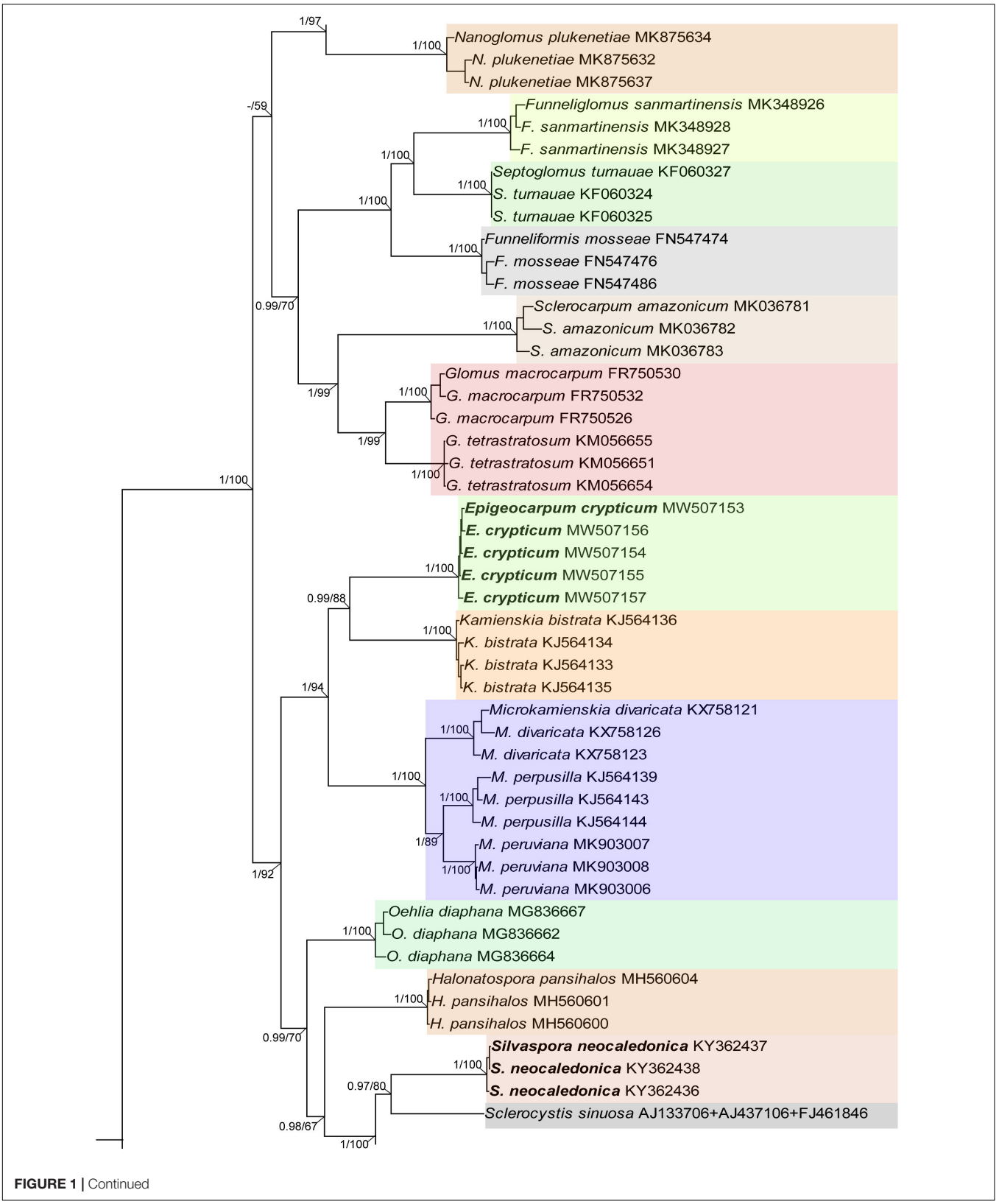


FIGURE 1 | Continued

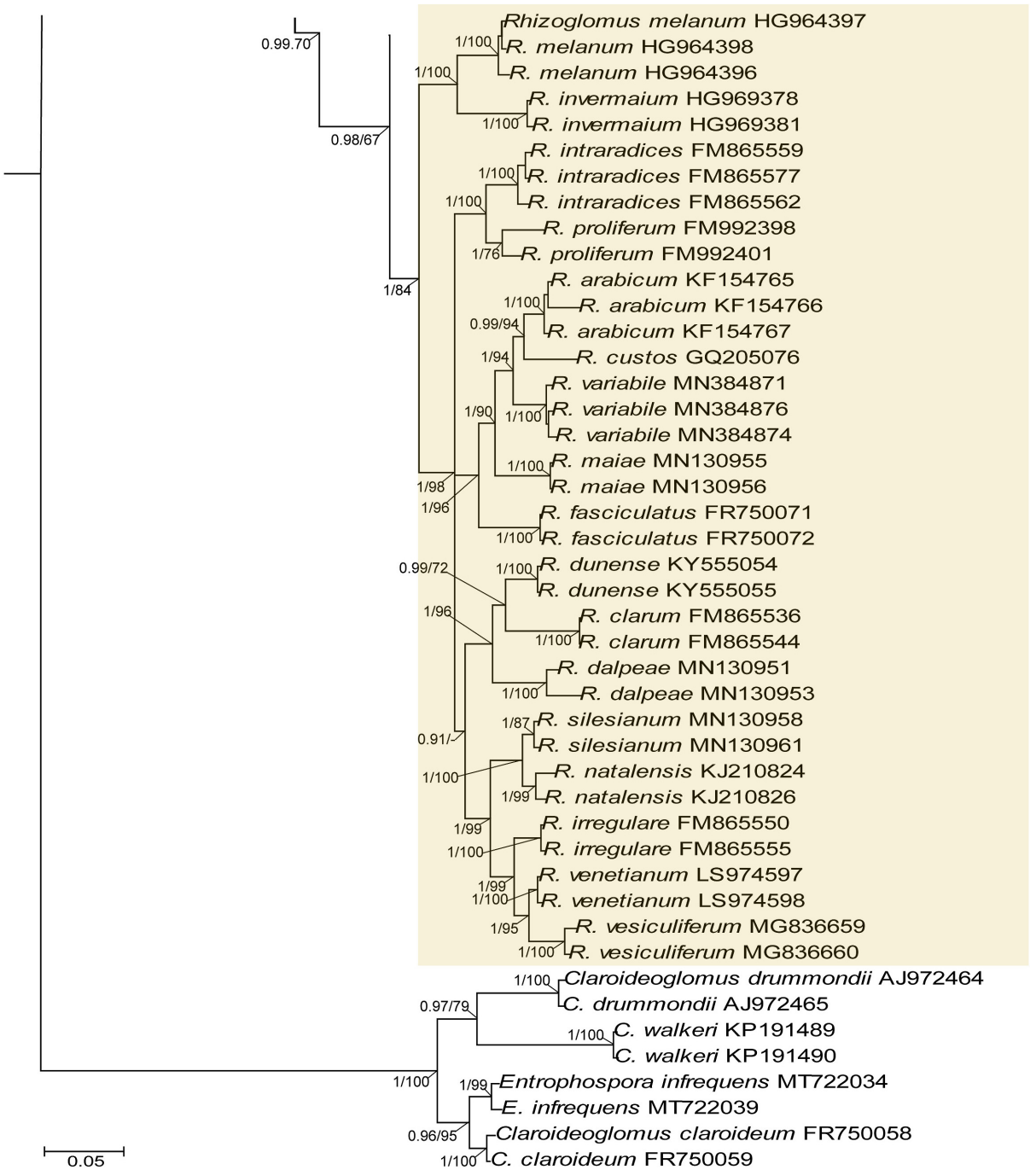


FIGURE 1 | A 50% majority rule consensus phylogram inferred from a Bayesian inference analysis of 18S-ITS-28S nuc rDNA sequences of *Dominikia glomerocarpica* and *Epigeocarpum crypticum*, as well as 50 other species of AMF, including *Claroideoglomus claroideum*, *Claroideoglomus drummondii*, *Claroideoglomus walkerii*, and *Entrophospora infrequens* as outgroup. The Bayesian posterior probabilities ≥0.90 and ML bootstrap values ≥50% are shown near the branches, respectively. Bar indicates 0.05 expected change per site per branch.

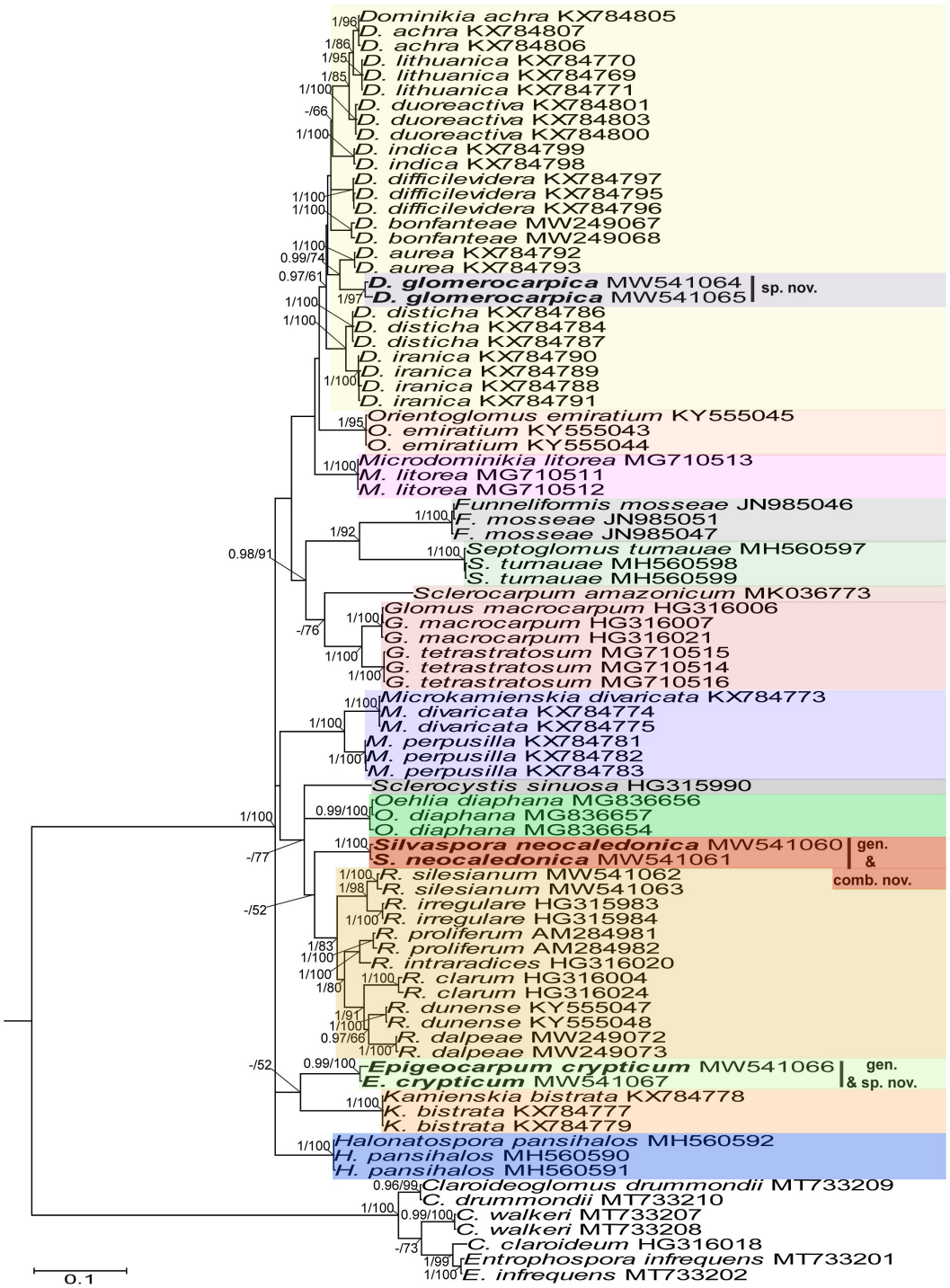


FIGURE 2 | A 50% majority rule consensus phylogram inferred from a Bayesian inference analysis of *rpb1* sequences of *D. glomerocarpica* and *E. crypticum*, as well as 34 other species of AMF, including *C. claroideum*, *C. drummondii*, *C. walkerii*, and *E. infrequens* as outgroup. The Bayesian posterior probabilities ≥0.90 and ML bootstrap values ≥50% are shown near the branches, respectively. Bar indicates 0.1 expected change per site per branch.

full or high (BI = 1.0, ML = 97% for "Species 1" and BI = 0.99, ML = 100% for "Species 2"; **Figures 1**, **3**).

The *R. neocaledonicum* (=*Silvaspora neocaledonica*) clade in the 18S-ITS-28S, *rpb1*, and 18S-ITS-28S + *rpb1* trees obtained full supports in both BI and ML analyses (**Figures 1–3**). In the 18S-ITS-28S and 18S-ITS-28S + *rpb1* trees, *R. neocaledonicum* was placed in a sister clade to *S. sinuosa* (**Figures 1**, **3**). The node linking the two species was moderately supported in both BI and

TABLE 2 | Characteristics of the sequence alignments analyzed.

Name of alignment	Number of sequences	Number of species	Number of base pairs	Number of variable sites	Number of parsimony informative sites
18S-ITS-28S	147	52	2,492	1,094	978
rpb1	86	36	2,841	1,390	1,195
18S-ITS-28S + *rpb1*	86	36	4,074	2,350	2,067

ML analyses of the 18S-ITS-28S alignment (BI = 0.97, ML = 80%), whereas only the BI analysis of the 18S-ITS-28S + *rpb1* alignment moderately (BI = 0.97) supported this association (**Figures 1**, **3**). The closest neighbors of the *R. neocaledonicum*–*S. sinuosa* clade were the generic clades *Halonatospora* and *Rhizoglomus*, respectively. In the *rpb1* tree, *R. neocaledonicum* sequences clustered basally with weak support (BI = 0.77, ML = 52) to the *Rhizoglomus* spp. clade (**Figure 2**).

The molecular distances between "Species 1" and *D. aurea*, calculated based on comparisons of their 18S-ITS-28S and *rpb1* sequences, were 8.5–10.2% and 4.3–4.8%, respectively. The divergences of the 18S-ITS-28S and *rpb1* sequences of "Species 2" and *K. bistrata* were 14.5–15.6% and 11.0–11.6%, respectively. The 18S-ITS-28S and *rpb1* sequences of *R. neocaledonicum* and *S. sinuosa* differed by 22.7–22.9% and 11.4%, respectively. The 18S-ITS-28S and *rpb1* sequences of *R. neocaledonicum* and *Rhizoglomus* spp. differed by 12.5–18.5% and 10.8–13.0%, respectively.

Considering the results of the phylogenetic analyses and comparisons of sequences of the two species found in northeast Brazil and the AMF originally described as *Rhizophagus neocaledonicus* discussed above, as well as the morphological distinctiveness of these species from their closest phylogenetically relatives, below we characterize the two species from Brazil as *D. glomerocarpica* sp. nov. and *E. crypticum* gen. nov. et sp. nov. In addition, we emend the morphological description of and transfer *Rhizophagus neocaledonicum* to a new genus, *Silvaspora* gen. nov., with *S. neocaledonica* comb. nov. Because *D. glomerocarpica* is the first glomerocarp-forming species in *Dominikia*, the definition of this genus was emended.

Taxonomy

Erection of New Genera

Epigeocarpum Błaszk., B.T. Goto, Jobim, Niezgoda & Marguno, gen. nov.

MycoBank No. MB838879.

Etymology: Latin, *Epigeocarpum*, *Epigeo* (=soil surface) and *carpum* (=fruit body), referring to the habitat, in which the type species of the new genus formed glomerocarps (=sporocarps).

Type species: *E. crypticum* Jobim, Błaszk., Niezgoda, Magurno & B.T. Goto

Diagnosis: Differs from *K. bistrata*, the phylogenetically closely related species of the monospecific genus *Kamienskia*, in (*i*) producing compact, epigeous, yellow-colored glomerocarps with a peridium and hyaline to light yellow, glomoid spores having a three-layered spore wall, of which the laminate layer 2 is relatively thick compared to the small spores size, contracts and, consequently, transfers into a crown-like structure in spores crushed in PVLG-based mountants and stains in Melzer's reagent; (*ii*) the possession of a septum separating the spore subtending hyphal lumen from the spore interior; and (*iii*) the nucleotide composition of sequences of the 18S-ITS-28S nuc rDNA region and the *rpb1* gene.

Genus description: Producing glomoid glomerocarps in a compact epigeous unorganized glomerocarp. Spores hyaline to light yellow (4A4), usually globose to subglobose, 34–46 μm diameter, with a spore wall consisting of three permanent, smooth layers. Spore wall layer (swl) 2 laminate, usually transferring into a crown-like structure due to contracting in spores crushed in PVLG and PVLG + Melzer's reagent. Only swl 2 stains in Melzer's reagent. Subtending hypha funnel-shaped with a wall continuous with swl 1 and 2 and an open pore at the spore base; the channel connecting the lumen of the subtending hypha with the interior of spores closed by a septum continuous with swl 3; the septum usually positioned at half the thickness of swl 2; the subtending hyphal lumen gradually narrowing in maturing spores due to thickening of subtending hyphal wall layer 2.

Silvaspora Błaszk., Niezgoda, B.T. Goto, Crossay & Magurno, gen. nov.

MycoBank number MB838881.

Type species: *S. neocaledonica* (D. Redecker, Crossay & Cilia) Błaszk., Niezgoda, B.T. Goto, Crossay & Magurno, comb. nov. MycoBank MB838882.

Specimens examined: 3,768–3,772 (LPPDSE).

Etymology: *Silvaspora*, in honor of Dr. Gladstone Alves da Silva, Departamento de Micologia, CCB, Universidade Federal de Pernambuco, Brazil, in recognition of his important contribution to taxonomy and ecology of arbuscular mycorrhizal fungi.

Diagnosis: Differs from other genera in the Glomeraceae mainly in the nucleotide composition of sequences of the 18S-ITS-28S nuc rDNA region and the *rpb1* gene.

Genus description: Forming colored glomoid glomerospores with a spore wall consisting of three layers, of which only layer 1, forming the spore surface, is impermanent and hyaline to brightly colored. Subtending hypha colored similarly to the spore wall, cylindrical, slightly funnel-shaped, or constricted at the spore base, with a pore occluded due to thickening subtending hyphal wall layer 2 continuous with the laminate spore wall layer 2, rarely slightly open. Forming mycorrhiza with arbuscules, vesicles, and hyphae staining dark in trypan blue.

Emendation of the Genus *Dominikia* Błaszk., Chwat & Kovács Emend. Błaszk., Niezgoda, Magurno, Jobim & B.T. Goto

Genus description: Fungi forming glomoid-like spores in soil or epigeous glomerocarps (=sporocarps). Hypogeous spores usually produced in unorganized (with random distribution), loose to



FIGURE 3 | A 50% majority rule consensus phylogram inferred from a Bayesian inference analysis of 18S-ITS-28S + *rpb1* sequences of *D. glomerocarpica* and *E. crypticum*, as well as 34 other species of AMF, including *C. claroideum*, *C. drummondii*, *C. walkerii*, and *E. infrequens* as outgroup. The Bayesian posterior probabilities ≥0.90 and ML bootstrap values ≥50% are shown near the branches, respectively. Bar indicates 0.1 expected change per site per branch.

compact clusters, rarely singly, sometimes inside roots. Epigeous sporocarps compact with hundreds to thousands of randomly distributed glomerospores. Spores hyaline to yellow brown, small, 17–87 μm diameter when globose. Spore wall with two to three layers. Layer 1, forming the spore surface, mucilaginous, short-lived, or unit (not divided into sublayers), semipermanent to permanent, only slightly or not deteriorating with age. Layer 2 unit or laminate, permanent. Layer 3 flexible to semiflexible,

permanent. Layers 1 and 3 staining or not staining in Melzer's reagent. Spore subtending hypha cylindrical to funnel-shaped with a pore open or occluded by a septum (i) continuous with the innermost lamina(e) of the laminate spore wall layer 2 or 3, (ii) connecting the inner surfaces of the innermost subtending hyphal wall layer, (iii) continuous with the flexible to semiflexible innermost spore wall layer, and (iv) sometimes as in (iii) and still by another underlying septum connecting the inner surfaces of the innermost subtending hyphal wall layer. Forming vesicular–arbuscular or only arbuscular mycorrhiza staining dark in Trypan blue.

Type species: *Dominikia minuta* (Błaszk., Tadych & Madej) Błaszk., Chwat & Kovács Mycotaxon 76, 189. 2000.

Other accepted species. Dominikia achra (Błaszk., D. Redecker, Koegel, Schützek, Oehl & Kovács) Błaszk., Chwat & Kovács.

Basionym. *Glomus achrum* Błaszk., D. Redecker, Koegel, Schützek, Oehl & Kovács, Botany 87, 262. 2009.

Dominikia aurea (Oehl & Sieverd.) Blaszk. Chwat, G.A. Silva & Oehl.

Basionym. *Glomus aureum* Oehl & Sieverd. J. Appl. Bot., Angew. Bot. 77, 111. 2003.

Dominikia bernensis Oehl, Palenz., Sánchez-castro & G.A. Silva.

Dominikia bonfanteae Magurno, Niezgoda, B.T. Goto & Błaszk.

Dominikia compressa (Sieverd. Oehl, Palenz., Sánchez-Castro & G.A. Silva) Oehl, Palenz., Sánchez-Castro & G.A. Silva.

Basionym. *Glomus compressum* Sieverd., Oehl, Palenz., Sánchez-Castro & G.A. Silva, Nova Hedwigia 99, 433. 2014.

Dominikia difficilevidera Błaszk., Góralska & Chwat.

Dominikia disticha Błaszk., Chwat & Kovács.

Dominikia duoreactiva Błaszk., Góralska & Chwat.

Dominikia indica (Błaszk., Wubet & Harikumar) Błaszk., G.A. Silva & Oehl.

Basionym. *Glomus indicum* Błaszk., Wubet & Harikumar, Botany 88, 134. 2010.

Dominikia iranica (Błaszk., Kovács & Balázs) Błaszk., Chwat & Kovács.

Basionym. *Glomus iranicum* Błaszk., Kovács & Balázs, Mycologia 102, 1457. 2010.

Dominikia lithuanica Błaszk., Chwat & Góralska.

Description of New Species and a New Combination

Dominikia glomerocarpica Jobim, Błaszk., Niezgoda, Magurno & B.T. Goto, sp. nov. **Figures 4A–H**.

MycoBank No. MB838883.

Etymology: Latin, *glomerocarpica*, referring to the glomerocarps (=sporocarps) produced by the species.

Specimens examined: Brazil, Parque das Trilhas, belonging to the Serra de Baturité Environmental Protection Area (4°16′36.8″ S, 38°56′20.4″ W; 865 m above sea level) in the Guarapiranga municipality, Ceará State, a glomerocarp found by K. Jobim in July 2018. Holotype. A fragment of a glomerocarp and a slide with spores no. UFRN-Fungos 3282, isotypes: a vial with a fragment of a glomerocarp no. 3802 and slides with spores no. 3773–3782 (LPPDSE).

Diagnosis: Differs from *D. aurea*, the sister phylogenetic relative, in (i) the habitat of production and the features of the structure forming the spore conglomeration; (ii) spore color, the composition of the spore wall and the phenotypic and biochemical properties of the spore wall layers; (iii) the characters of the septum separating the spore subtending hyphal lumen from the spore interior; and (iv) the nucleotide composition of sequences of the 18S-ITS-28S nuc rDNA region and the *rpb1* gene.

Description: Glomerospores formed in a compact epigeous glomerocarp. *Glomerocarp* yellowish gray (4B2) to grayish yellow (4B3); approximately 3.30 × 3.38 mm (**Figure 4A**). *Peridium* thin, hyaline to pale gray (1B1), only partially covering glomerospores' conglomerations. *Gleba* yellowish white (4A2) to grayish yellow (4B3), with hyaline; straight or branched hyphae; (1.6−)3.2(−4.8) μm wide, with a wall 0.8–1.1 μm thick; staining pinkish white (7A2) to pastel red (9A6) in Melzer's reagent; glomerocarp hosting hundreds of glomerospores (=spores; **Figures 4B–H**). *Spores* arise blastically at tips of sporogenous hyphae (**Figures 4C,D,F–H**). Spores hyaline to light yellow (4A5); globose to subglobose; (30−)39(−46) μm diameter; rarely ovoid; 34–39 μm × 40–46 μm; with one subtending hypha (**Figures 4B–H**). *Spore wall* composed of three permanent, smooth layers (**Figures 4C,E–H**). Layer 1, forming the spore surface, uniform (not containing visible sublayers), semiflexible, hyaline, (0.8−)1.2(−1.5) μm thick, tightly adherent to the upper surface of layer 2 (**Figures 4C,E–H**). Layer 2 laminate, semiflexible, hyaline to light yellow (4A5), (1.8−)8.2(−10.5) μm thick; consisting of very thin, <0.5 μm thick, laminae, tightly adherent to each other, not separating even in vigorously crushed spores; not contracting in spores crushed in PVLG-based mountants (**Figures 4C,E–H**). Layer 3 flexible, hyaline, approximately 1.0 μm thick, usually slightly contracting and separating from the lower surface of layer 2 in intact spores and spores crushed in PVLG, except for its funnel-shaped part associated with the inner surfaces of the laminate layer 2 forming the channel that connect the spore interior with the lumen of the subtending hypha (**Figures 4C,E–H**). In Melzer's reagent, only spore wall layer 2 stains pastel red (9B7) to brownish violet (11D8; **Figure 4H**). *Subtending hypha* hyaline to light yellow (4A5); straight or recurved, funnel-shaped; (4.0−)5.8(−8.5) μm wide at the spore base (**Figures 4C–H**); not braking in crushed spores. *Wall of subtending hypha* hyaline to light yellow (4A5); (2.0−)2.5(−3.2) μm thick at the spore base; consisting of two layers continuous with spore wall layers 1 and 2 (**Figure 4H**). *Pore* (0.6−)0.9(−1.4) μm wide and open at the spore base; the channel connecting the lumen of the subtending hypha with the interior of spores closed by a septum continuous with spore wall layer (swl) 3; the septum usually positioned at half the thickness of swl 2; the subtending hyphal lumen gradually narrowing in maturing spores due to thickening of subtending hyphal wall layer 2 (**Figures 4C,E–G**). Spore content of hyaline oily substance. *Germination* unknown.

Mycorrhizal associations: no molecular analyses were performed on roots of the plant species that grew in the place where the glomerocarp of *D. glomerocarpica* was found.

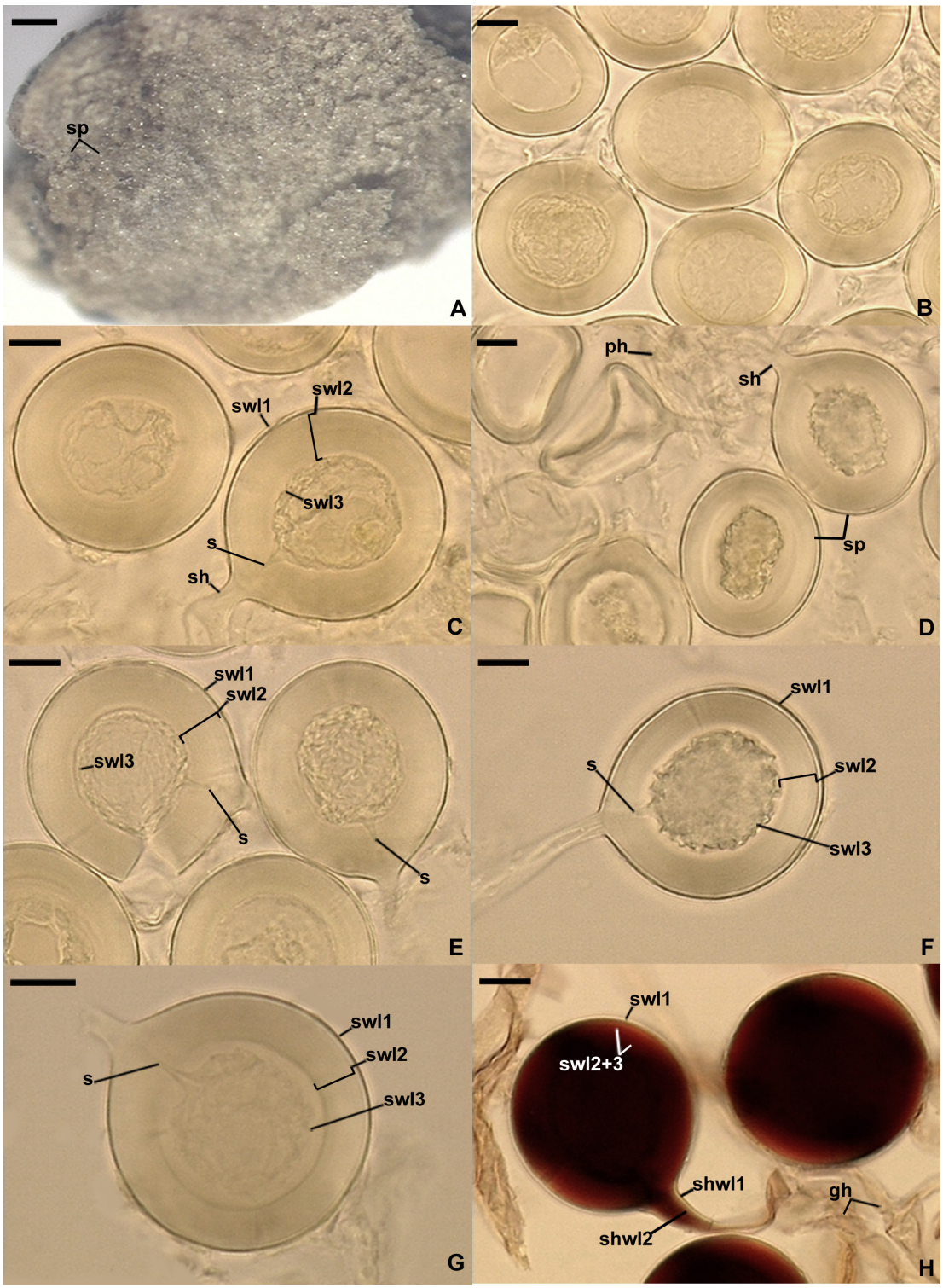


FIGURE 4 | *Dominikia glomerocarpica*. **(A)** Glomerocarp (=sporocarp) with glomerospores (=spores; sp). **(B)** Intact spores. **(C–G)** Intact and crushed spores with a three-layered spore wall (swl1–3) and a subtending hypha (sh); note that swl2 did not change in shape in crushed spores, and swl3 usually slightly contracted and separated from the lower surface of the laminate swl2 in intact and crushed spores and formed a septum (s) located at approximately half the length of the channel connecting the subtending hyphal lumen with the spore interior; peridial hyphae (ph) are visible in **(D)**. **(H)** Intact spores with swl1–3, subtending hyphal wall layers (shwl) 1 and 2, and glebal hyphae (gh) mounted in PVLG + Melzer's reagent. **(A)** Dry specimen. **(B–G)** Spores in PVLG. **(H)** Spores in PVLG + Melzer's reagent. **(A)** Light microscopy. **(B–H)** Differential interference microscopy. Scale bars: **(A)** = 200 μm, **(B–H)** = 10 μm.

Attempts to grow *D. glomerocarpica* in single-species cultures with *P. lanceolata* as host plant failed.

Distribution and habitat: the Parque das Trilhas, being part of the Serra de Baturité Environmental Protection Area in Brazil, is so far the sole known site of occurrence of *D. glomerocarpica*. The geographic location and climate of this site were characterized in Section "Materials and Methods."

BLAST searches indicated that *D. glomerocarpica* has not been found in other environments around the word before. The highest identities of 18S-ITS-28S and *rpb1* sequences of this species compared with sequences of the two loci deposited in GenBank were only 93.78 and 95.84%, respectively.

Epigeocarpum crypticum Jobim, Błaszk., Niezgoda, Magurno & B.T. Goto, sp. nov. **Figures 5A–H**.

MycoBank No. MB838880.

Etymology: Latin, *crypticum*, referring to the very small and hidden morphological differences compared to the very large differences in the DNA nucleoid composition between *E. crypticum* and its closest molecular relative, *K. bistrata*.

Specimens examined: Brazil, Parque das Trilhas, belonging to the Serra de Baturité Environmental Protection Area (4°16′36.8″ S, 38°56′20.4″ W; 865 m above sea level) in the Guarapiranga municipality, Ceará State, a glomerocarp found by K. Jobim in April 2018. Holotype: A fragment of a glomerocarp and a slide with spores no. UFRN-Fungos 3283, isotypes: a vial with a fragment of a glomerocarp no. 3803 and slides with spores no. 3783–3801 (LPPDSE).

Diagnosis: As that regarding the genus *Epigeocarpum* (see above).

Description: Glomerospores formed in a compact epigeous glomerocarp. *Glomerocarp* yellowish white (4A2) to grayish yellow (4B3); 1.65 mm × 1.69 mm (**Figure 5A**). *Peridium* thin, yellowish white (3A2) to pale yellow (3A3), only partially covering glomerospores' conglomerations (**Figure 5A**). *Gleba* yellowish white (4A2) to light yellow (4A5), with hyaline; straight or branched hyphae; (2.2−)5.1(−7.5) μm wide, with a wall 0.6–1.8 μm thick; staining reddish white (7A2) to grayish red (8B6) in Melzer's reagent; glomerocarp hosting hundreds of glomerospores (=spores; **Figures 5A–H**). *Spores* arise blastically at tips of sporogenous hyphae. Spores hyaline to light yellow (4A4); globose to subglobose; (34−)40(−46) μm diameter; rarely ovoid; 34–44 μm × 40–51 μm; with one subtending hypha (**Figures 5B–H**). *Spore wall* composed of three permanent, smooth layers (**Figures 5B–H**). Layer 1, forming the spore surface, uniform (not containing visible sublayers), semiflexible, hyaline, (0.8−)1.5(−2.0) μm thick, tightly adherent to layer 2 in spores immersed in water, but frequently slightly separated from the upper surface of layer 2, even in intact spores, due to contracting of layer 2 in PVLG-based mountants (**Figures 5B–H**). Layer 2 laminate, semiflexible, hyaline to light yellow (4A4), (2.0−)8.0(−12.5) μm thick; consisting of very thin, <0.5 μm thick, laminae, tightly adherent to each other, not separating even in vigorously crushed spores; usually transforming into a crown-like structure due to contracting in spores crushed in PVLG and PVLG + Melzer's reagent (**Figures 5C–H**). Layer 3 flexible, hyaline, approximately 1.0 μm thick, usually slightly contracting and separating from the lower surface of layer 2 in intact spores and spores crushed in PVLG, except for its funnel-shaped part associated with the inner surfaces of the laminate layer 2 forming the channel that connect the spore interior with the lumen of the subtending hypha (**Figures 5C–E,G,H**). In Melzer's reagent, only spore wall layer 2 stains reddish white (7A2) to brownish violet (11D8; **Figures 5F,H**). *Subtending hypha* hyaline to light yellow (4A4); straight or recurved, funnel-shaped; (4.4−)6.6(−9.0) μm wide at the spore base (**Figures 5C,D,F–H**); not braking in crushed spores. *Wall of subtending hypha* hyaline to light yellow (4A4); (2.0−)2.8(−3.3) μm thick at the spore base; consisting of two layers continuous with spore wall layers 1 and 2 (**Figures 5C,F,G,H**). *Pore* (0.6−)1.1(−1.6) μm wide and open at the spore base; the channel connecting the lumen of the subtending hypha with the interior of spores closed by a septum continuous with spore wall layer (swl) 3; the septum usually positioned at half the thickness of swl 2; the subtending hyphal lumen gradually narrowing in maturing spores due to thickening of subtending hyphal wall layer 2 (**Figure 5G**). Spore content of hyaline oily substance. *Germination* unknown.

Mycorrhizal associations: No molecular analyses were performed on roots of the plant species that grew in the place where the glomerocarp of *E. crypticum* was found. Attempts to grow *E. crypticum* in single-species cultures with *P. lanceolata* as host plant failed.

Distribution and habitat: The physical presence of *E. crypticum* was so far found only in Parque das Trilhas. The geographic location of the park and other characteristics of the habitat, in which the glomerocarp of *E. crypticum* was discovered, are described in *Distribution and habitat* regarding *D. glomerocarpica* (see above).

BLAST's searches suggested that *E. crypticum* was also associated with roots of native plants growing in a petroleum-polluted soil of the Amazon region of Ecuador. The identity of the 28S MH504057 sequence compared to the 18S-ITS-28S sequences of *E. crypticum* was 98.5%. The identity of *E. crypticum rpb1* sequences compared to those listed by BLAST was only ≤92.7%.

Silvaspora neocaledonica (D. Redecker, Crossay & Cilia) Błaszk., Niezgoda, B.T. Goto, Crossay & Magurno, comb. nov. **Figures 6A–D**.

MycoBank number MB838882.

Basionym: *Rhizophagus neocaledonicus* D. Redecker, Crossay & Cilia, Mycol. Prog. 17, 739. 2018.

Synonym: *Rhizophagus neocaledonicum* (D. Redecker, Crossay & Cilia) Oehl, Turrini & Giovann. Mycol. Prog. 17, 1218. 2018.

Description: Glomerospores formed singly and in loose clusters of 2–3 in soil, roots, and in root organ culture. *Spores* dark chestnut to coffee brown [orange (6C7) to brown (6E8)]; usually globose to subglobose; (61–)75(−90) μm diameter; sometimes oblong to irregular; 68–82 μm × 95–113 μm; with one subtending hypha (**Figures 6A–C**). *Spore wall* composed of three layers (**Figures 6A,B**). Layer 1, forming the spore surface, evanescent, short-lived, hyaline to yellowish white (4A2), 1.0–2.5 μm thick, usually highly deteriorated or completely sloughed off in mature spores. Layer 2 laminate, permanent, dark brown [orange (6C7) to brown (6E8)], (4.2–)6.1(−8.8) μm thick. Layer 3 uniform (without visible sublayers), bright brown [golden yellow

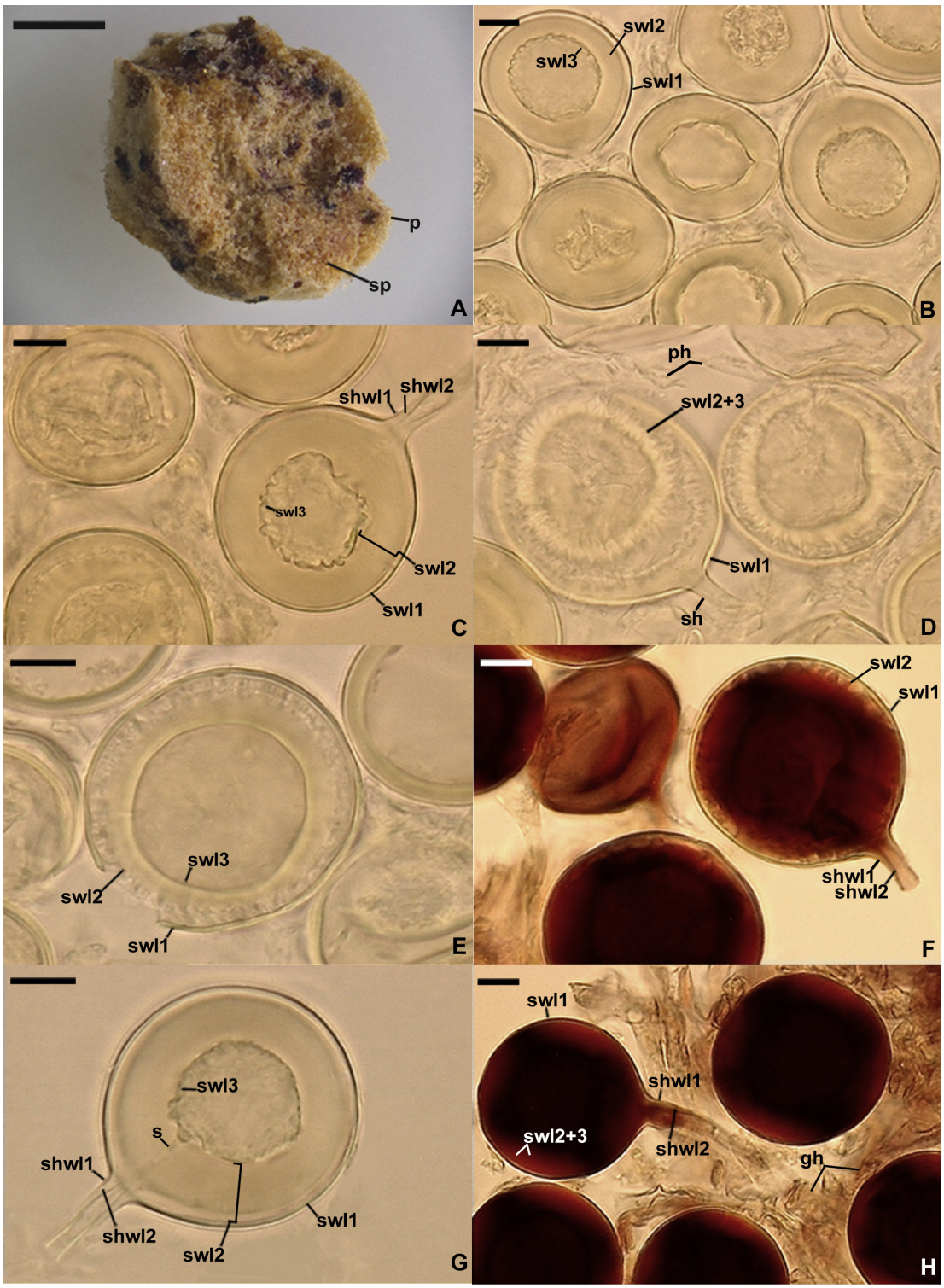


FIGURE 5 | *Epigeocarpum crypticum*. **(A)** Glomerocarp (=sporocarp) with glomerospores (=spores; sp). **(B)** Spores on which no pressure was applied; note that spore wall layer (swl) 2 slightly contracted and separated from the lower surface of swl1, and swl3 only slightly separated from the lower surface of swl2. **(C–G)** Spore wall layers (swl) 1–3 and subtending hyphal wall layers (shwl) 1 and 2 of spores on which pressure was applied; note that the laminate swl2 transferred into a crown-like structure, and swl3 usually slightly contracted and separated from the lower surface of swl2 and formed a septum (s) located at approximately half the length of the channel connecting the subtending hyphal lumen with the spore interior; peridial hyphae (ph) are visible in **(D)**. **(H)** Intact spores with swl1–3, shwl1 and 2, and glebal hyphae (gh) mounted in PVLG + Melzer's reagent. **(A)** Dry specimen. **(B–E,G)** Spores in PVLG. **(F,H)** Spores in PVLG + Melzer's reagent. **(A)** Light microscopy. **(B–H)** Differential interference microscopy. Scale bars: **(A)** = 200 μm, **(B–H)** = 10 μm.

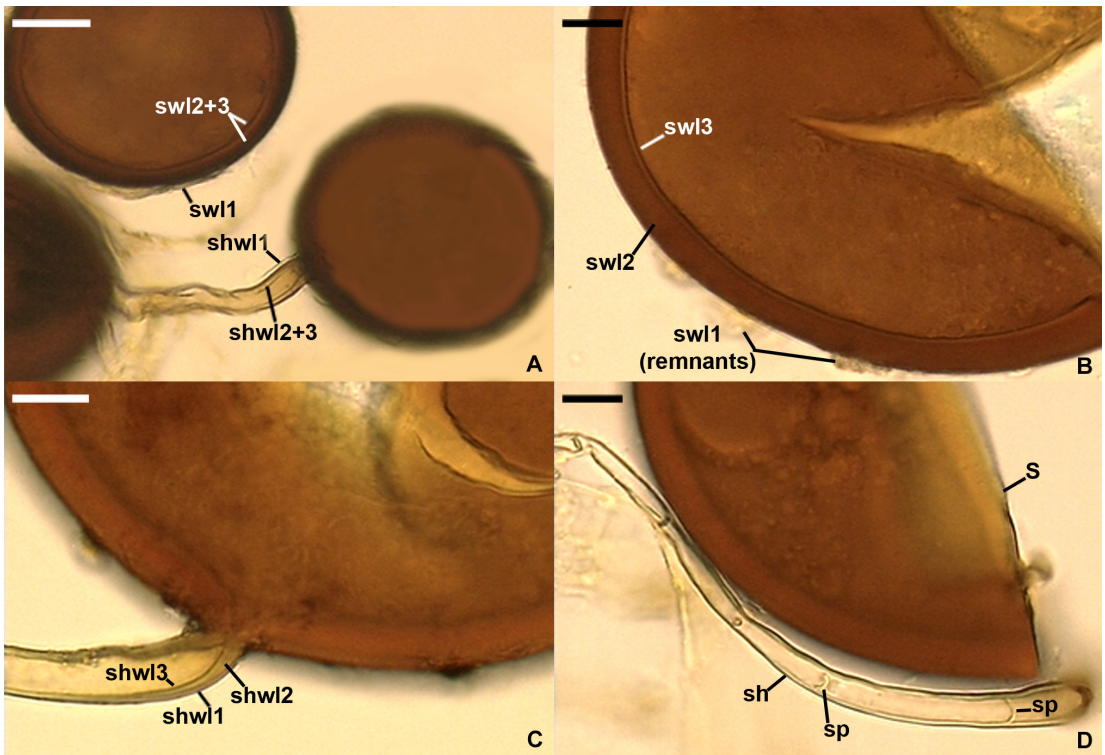


FIGURE 6 | *Silvaspora neocaledonica*. **(A)** Spores with a spore wall (sw) consisting of three layers (swl1–3). **(B)** Spore wall layers (swl) 1–3; swl1 is almost completely sloughed off. **(C)** Subtending hyphal wall layers (shwl) 1–3. **(D)** Spore (s) and subtending hypha (sh) with two septa (sp) indicated. **(A,B,D)** Spores in PVLG. **(C)** Spores in PVLG + Melzer's reagent. **(A–D)** Differential interference microscopy. Scale bars: **(A)** = 20 μm, **(B–D)** = 10 μm.

(5B7) to orange (6B7)], 0.8–1.2 μm thick, usually tightly adherent to the lower surface of layer 2, even in vigorously crushed spores, difficult to detect and characterize due to the similarity in appearance to and almost inseparability from the innermost laminae of the laminate layer 2. None of spore wall layers 1–3 stains in Melzer's reagent. *Subtending hypha* pale orange (5A3) to light orange (5A4); cylindrical, slightly funnel-shaped, or slightly constricted at the spore base; (6.2−)8.3(−11.6) μm wide at the spore base (**Figures 6A,C,D**). *Wall of subtending hypha* pale orange (5A3) to light orange (5A4); (1.6−)2.8(−5.4) μm thick at the spore base; consisting of three layers continuous with spore wall layers 1–3; subtending hyphal wall (shwl) layer 3 usually is difficult to see because it is thin, similarly colored, and tightly adherent to shwl2 (**Figures 6A,C**). *Pore* usually occluded due to thickening of spore wall layer 2 and subtending hyphal wall layer 2 (**Figures 6C,D**), rarely slightly open at the spore base; the subtending hyphal lumen occasionally with some transverse septa widely distributed along the subtending hypha (**Figure 6D**). *Germination* through subtending hypha. *Mycorrhiza* with arbuscules, vesicles, and hyphae staining lightly to dark in trypan blue.

Notes: The description presented above was prepared based on the original description of this species and examination of its spores provided by T. Crossay. We added color names of spores and spore wall layers determined from Kornerup and Wanscher (1983) to compare them with the color of the subtending hypha, whose pigmentation was not characterized in the original description of *S. neocaledonica*. Also, we changed some measurement values when they differed from the range of measurements given by Crossay et al. (2018) and replaced the name of spore wall layer 1, originally determined as mucilaginous, into evanescent. A mucilaginous spore wall layer *sensu* Stürmer and Morton (1997) stains in Melzer's reagent, whereas spore wall layer 1 of *S. neocaledonica* does not react in this reagent. Finally, we significantly extended the characterization of the subtending hypha compared to that originally published.

Specimens examined: 3768–3772 (LPPDSE).

Distribution and habitat: To date, this species is known only from the type locality: Noumea, in the rhizosphere soil of *Alphitonia neocaledonica* (Schltr.) Guillaumin growing in an ultramafic *maquis* in the New Caledonia (Crossay et al., 2018). BLAST searches of 18S-ITS-28S and *rpb1* sequences indicated that *S. neocaledonica* has not been recorded in other regions of the world.

DISCUSSION

As we expected based on exploratory morphological and molecular phylogenetic analyses, our extended phylogenetic analyses of sequence alignments containing representatives of

all genera of the Glomeraceae, using 18S-ITS-28S and *rpb1* data, unambiguously and strongly confirmed our hypothesis that the two glomerocarps found in Northeast Brazil are two new species of the Glomeromycota (**Figures 1–3**). Surprisingly, these morphologically almost identical fungi represent strongly phylogenetically divergent taxa in the Glomeraceae, one belonging to *Dominikia* and the second neighboring the monospecific genus *Kamienskia* (**Figures 1–3**). The divergences of 18S-ITS-28S and *rpb1* sequences between the new species, *D. glomerocarpica* and *E. crypticum*, were 18.5–19.0% and 11.0–11.8%, respectively.

Another interesting finding in our analyses was that the sister species of *D. glomerocarpica* was *D. aurea* (**Figures 1–3**), which presents significant morphological differences. *D. glomerocarpica* is distinguished morphologically by (i) the formation of a compact, epigeous glomerocarp with a peridium; (ii) the production of small, colorless to light yellow (4A4), glomoid spores; (iii) the possession of a spore wall consisting of three permanent, smooth layers, of which the colorless to light yellow (4A4) laminate layer 2 is distinctly thick compared to the spore size and stains dark in Melzer's reagent; and (*iv*) the formation of an invaginated septum continuous with spore wall layer 3, which is usually located at half the length of the channel connecting the lumen of the spore subtending hypha with the spore interior (**Figures 4A–H**).

D. aurea was originally described to produce hypogeous, peridium-free, 450–1,200 μm × 510–1,600 μm diameter, glomerocarps (called sporocarps), consisting of tightly packed spores. However, the microphotographs presented in the article of Oehl et al. (2003) and our specimens testify that *D. aurea* spores arise mainly in compact, hypogeous clusters (Błaszkowski, 2012) rather than in typical unorganized glomerocarps, as the much larger, epigeous glomerocarp with a peridium formed by *D. glomerocarpica*. Also, we often extracted loose clusters with few spores and single spores of *D. aurea*. Moreover, *D. aurea* spores are much darker colored and never are colorless at maturity, have a 1.2- to 2.4-fold thinner and only two-layered spore wall, of which layer 1 is impermanent, usually completely sloughed off in mature spores, and stains in Melzer's reagent. Finally, the pore of the spore subtending hypha is closed by a curved septum, which is continuous with the innermost laminae of the laminate spore wall layer 2 and is located at or up to 5 μm below the spore base (Oehl et al., 2003; Błaszkowski, 2012). The clear distinctiveness of *D. aurea* and *D. glomerocarpica* also proved the large molecular divergences between their 18S-ITS-28S and *rpb1* sequences, which were 8.5–10.2% and 4.3–4.8%, respectively.

Another surprising finding of our efforts to establish the taxonomic status of the Brazilian fungi was the placement of the previously named "Species 2" in a sister clade to the monospecific, generic clade represented by *K. bistrata* (**Figures 1–3**). However, the two species differ fundamentally in morphology and are separated from one another by a very large molecular distance (11.0–15.5%). Therefore, we erected a new genus for "Species 2," named *Epigeocarpum*, typified by *E. crypticum*, despite the fact that the morphological characters distinguishing and clearly separating this species from *K. bistrata* are shared by other members of the Glomeraceae, as discussed below.

The distinctive morphological features of *E. crypticum* are (i) the production of small, colorless or light yellow (4A5), glomoid spores in a compact, epigeous glomerocarp with a peridium; (ii) a spore wall composed of three permanent, smooth layers, of which the much thicker laminate layer 2 stains dark in Melzer's reagent and, most importantly, contracts and transfers into a crown-like structure in spores crushed in PVLG and PVLG + Melzer's reagent; and (iii) the formation of a septum by spore wall layer 3 of characters and location similar to those of the septum of *D. glomerocarpica* spores (**Figures 5A–H**).

K. bistrata does not produce epigeous glomerocarps with a peridium, but its spores are grouped in loose to compact hypogeous clusters (Błaszkowski et al., 2009a; Błaszkowski, 2012). Most importantly, the spore wall of *K. bistrata* is 2.2- to 4.4-fold thinner than the *E. crypticum*'*s*, consists of only two colorless layers, of which the uniform layer 1 is thicker than the laminate layer 2, none of these layers stains in Melzer's reagent, and the channel connecting the lumen of the spore subtending hypha with the spore interior is not closed by any septum.

As mentioned above, one of the distinctive features of the two here newly described species is the location of the septum separating the lumen of the spore subtending hypha from the spore interior (**Figures 4C,F,G**, **5G**). The septum usually occurs at half the thickness of the laminate spore wall layer 2 as similarly described for *Rhizoglomus maiae* (Błaszkowski et al., 2019b), whereas for all other glomoid spore-producing species, the septum is formed at or slightly below the spore base. Moreover, *R. maiae* also produces compact, epigeous clusters with spores, whose spore wall structure and phenotypic properties of its components are like those of *D. glomerocarpica* and *E. crypticum*, except for the contractility of spore wall layer 2 of *E. crypticum* (**Figures 5D–F**). Thus, the location of the septum in these three species, belonging to three far related genera of the Glomeraceae, clearly proves that this feature is phylogenetically uninformative.

The formation of the septum much above the spore base in *D. glomerocarpica*, *E. crypticum*, and *R. maiae* probably is associated with the spore wall ontogeny and particularly with the differentiation of the distinctively thick laminate spore wall layer 2 by these fungi. As ontogenetic studies of spores of *Claroideoglomus claroideum* revealed, the innermost spore wall layer 4, forming an invaginated septum at or slightly below the spore base, arises after the full differentiation of the laminate spore wall layer 3 (Stürmer and Morton, 1997). Most likely, a similar sequence of events occurs during the development of the spore wall of *D. glomerocarpica*, *E. crypticum*, and *R. maiae*. However, the laminate spore wall layer 3 of *C. claroideum* is a relatively thin component of the entire spore wall, and consequently, the full differentiation of this layer is faster than that of the much thicker laminate spore wall layer 2 of the three main species discussed above. Therefore, the formation of the invagination of spore wall layer 4 of *C. claroideum*, shaped by the available space (the channel connecting the spore subtending hyphal lumen with the spore interior) in which the development of this layer is initiated, starts relatively earlier and closer to the spore base.

Another structure distinguishing *E. crypticum* is the contracting laminate spore wall layer 2, which takes the shape of a crown in spores crushed in PVLG-based mountants (**Figures 5D–F**). A spore wall layer of similar properties was also found in *Microkamienskia perpusilla*, originally described as *Glomus perpusillum* (Błaszkowski et al., 2009b), although the contracting spore wall layer 2 of *M. perpusilla* is a unit structure (not divided into visible sublayers) and does not transform into a crown following crushing of spores in PVLG-based mountants. Therefore, it seems that the contractility of spore wall layer 2 of *E. crypticum* is also not a generic synapomorphy of the new genus *Epigeocarpum*.

In summary, the sole characters convincingly rendering the genus *Epigeocarpum* unique are those residing in its DNA. Importantly, the genetic differences between the 18S-ITS-28S (14.5–15.6%) and *rpb1* (11.0–11.6%) sequences of *E. crypticum* and *K. bistrata* are similar to those between sequences of directly neighboring species of most of the genera present in the tree depicted in **Figures 1**, **2**. Several examples of pairwise comparisons are displayed in **Supplementary Table 3**. Of the described species producing unorganized glomerocarps with glomoid spores, whose molecular phylogeny is uncertain or unknown, *D. glomerocarpica* and *E. crypticum* most closely resemble *Glomus microcarpum* and *Glomus nanolumen*; the spores of these species are similar in color and size. The main differences readily separating the four species reside in their spore wall structure, the phenotypic and histochemical features of the spore wall components, and the characters of the pore connecting the subtending hyphal lumen with the spore interior.

Glomus microcarpum was originally characterized as having one, thick spore wall, which was also found by Gerdemann and Trappe (1974) and Berch and Fortin (1984). Instead, Błaszkowski (2012) defined and illustrated this species as producing spores with a spore wall consisting of two layers: a short-lived, quickly sloughing off, or semipermanent, slowly decomposing, thin layer 1, forming the spore surface, and a permanent, thick, laminate layer 2, staining dark red in Melzer's reagent. Similar specimens identified as *G. microcarpum* with a spore wall as that characterized by Błaszkowski (2012) were presented by Oehl et al. (2011) and repeatedly found in Northeast Brazil (unpublished data). Of the Glomeromycota species grown in culture, only *Sieverdingia tortuosa* produced spores with a one-layered spore wall (Błaszkowski et al., 2019a), and in most of glomoid and glomoid-like spore-producing species, their laminate spore wall layer is covered with a relatively thin, usually short-lived, rarely permanent layer (Oehl et al., 2011; Błaszkowski, 2012). In field-collected spores, this outer spore wall layer is usually strongly or completely sloughed off, and therefore, it is difficult to detect or no longer present. On top of our knowledge, *G. microcarpum* has not yet been grown in culture, which makes impossible to examine spores at different developmental stages. However, regardless of the number of layers existing in the spore wall of the true *G. microcarpum*, the structure of the spore wall and the phenotypic properties of its components in *D. glomerocarpica* and *E. crypticum* (**Figures 4B–H**, **5B–H**) differ clearly from those characterized above for *G. microcarpum*. The sequence identity, obtained by BLAST, of 18S-ITS-28S sequences of *E. crypticum* compared to 38 18S-ITS-28S sequences of *G. microcarpum* deposited in GenBank is only 87.5–92.02%. Unfortunately, no data were published about the morphology of the "donor" of the sequences ascribed to *G. microcarpum*. Thus, there is an urgent need for unambiguous morphological and molecular characterization of *G. microcarpum*, one of the first two described species currently classified in the phylum Glomeromycota and until 2010 regarded as the type species of *Glomus* (e.g., Gerdemann and Trappe, 1974).

Regarding *G. nanolumen*, its glomerocarps do not contain a peridium, and most importantly, their spores have a two-layered spore wall only, of which the laminate layer 2 is not uniform in thickness but differs two to three times in its different regions, and none of these layers stains in Melzer's reagent (Koske and Gemma, 1989; Błaszkowski, 2012). Moreover, the subtending hypha of *G. nanolumen* is 1.6- to 2.5-fold wider at the spore base, and the channel connecting the subtending hyphal lumen with the spore interior is open.

Three evidences unambiguously justified the erection of the new monospecific genus *Silvaspora* in the Glomeraceae for the New Caledonian fungus, originally described as *R. neocaledonicus* (Crossay et al., 2018) and here renamed *S. neocaledonica*. First, our phylogenetic analyses of the 18S-ITS-28S and 18S-ITS-28S + *rpb1* alignments, containing sequences of all sequenced *Rhizoglomus* species, placed the New Caledonian fungus in a clade at the rank of genus, and importantly, the clade was located in the sister relation to the genus *Sclerocystis*, which was outside the *Rhizoglomus* clade (**Figures 1**, **3**). Thus, assigning the New Caledonian fungus to *Rhizoglomus* would make this genus polyphyletic. Moreover, although the analyses of *rpb1* sequences clustered the New Caledonian fungus with *Rhizoglomus* spp., this grouping did not obtain either BI or ML support (**Figure 2**). Second, the divergences of 18S-ITS-28S and *rpb1* sequences of the New Caledonian fungus from those of *S. sinuosa* were 22.7–22.9% and 11.4%, respectively. Thus, these divergence values were similar to the sequence divergences of other neighboring genera in the Glomeraceae (see above). Third, the mode of formation and morphology of spores of *S. sinuosa* differ fundamentally from those of *S. neocaledonica* (Gerdemann and Bakshi, 1976; Błaszkowski, 2012; Crossay et al., 2018; pers. observ.). All *Sclerocystis* species *sensu* Schüßler and Walker (2010) produce organized glomerocarps, in which glomoid-like spores arise radially from a central sterile plexus of mycelium, and the spores have a one-layered spore wall. Instead, *S. neocaledonica* produces spores singly or in clusters of 2 to 3, and their spore wall consists of three layers (**Figures 6A–D**; Crossay et al., 2018; pers. observ.).

We did not include into our phylogenetic analyses the monospecific genus *Simiglomus* with *Simiglomus hoi* because it was erected based on two sequences of the 18S gene (Oehl et al., 2011), which in our alignments is represented only by approximately 240 base pairs, and the origination of these sequences is uncertain, as stated by Redecker et al. (2013). Thus, further studies are needed to clarify the status of *Simiglomus* in the Glomeraceae.

The known glomerocarpic species probably constitute a small part of those existing in nature, mainly due to the difficulty in finding and characterizing these fungi. Collecting glomerocarps by raking and searching the upper soil layer and buried plant fragments is much more time-consuming and tiring than the

wet-sieving and decanting method (Gerdemann and Nicolson, 1963) commonly used to find specimens of the Glomeromycota. Interestingly, Gerdemann and Trappe (1974) stated that finding glomerocarps is also related to the acquisition of a so-called hypogeous instinct. Attempts to grow glomerocarpic fungi in culture rarely succeeded, and therefore their characterization, defined only on the basis of field-collected specimens, may lack accurateness. Besides, the morphological and molecular characterization of these fungi may be impossible due to the degradation of their physical structures and DNA (pers. observ.). Importantly, the few described glomerocarpic species with known molecular phylogeny belong to various taxonomic groups in the Glomeromycota, and frequently they miss genus-specific morphological characters. Moreover, molecular phylogenetic analyses have shown that glomerocarpic-like fruit bodies with glomoid-like spores are also produced by fungal taxa not belonging to the Glomeromycota (Yamamoto et al., 2020). Also, the trophic status of glomerocarpic and glomerocarpic-like species is unclear, particularly that of epigeocarpic species. In order to know the real representativeness of glomerocarpic species in the Glomeromycota and determine their trophic and taxonomic status, the collection of specimens of this group of fungi and the study of their ecology and phylogeny should be significantly intensified.

DATA AVAILABILITY STATEMENT

The datasets generated for this study can be found in online repositories. The names of the repository/repositories and accession number(s) are as follows: GenBank MW507148-MW507157, MW541060-MW541067, and MW249072-MW249073.

AUTHOR CONTRIBUTIONS

BG, FM, JB, PN, and SZ were responsible for conceptualization and funding acquisition. BG, FM, JB, and PN were responsible for data acquisition. FM, JB, PN, TB, and WB performed analyses. JB and FM wrote the first draft. BG, EM, FM, JB, KJ, LC, PN, RM, PM, SZ, TC, and WB wrote, reviewed, and edited the manuscript. All authors have read and agreed to the published version of the manuscript.

FUNDING

Part of this work was supported by Polish National Centre of Science, grant no. 2020/37/N/NZ9/00509, as well as by Conselho Nacional de Desenvolvimento Científico e Tecnológico (CNPq) that provided research grants to BG and financial support in the projects "Sporocarpic species of arbuscular mycorrhizal fungi (Glomeromycota): taxonomy, systematic and evolution" (proc. 408011-2016-5) and "Glomerocarpic species of arbuscular mycorrhizal fungi in areas of extreme biological relevance (proc. 311945/2019-8)." We also thank Universidade Federal do Rio Grande do Norte for covering the costs of JB's stay as visiting professor (Internationalization incentive program PPg/UFRN/2017) and the visit of BG as a collaborating researcher in West Pomeranian University of Technology in Szczecin from December 2019 to January 2020. Thanks are due to Coordenação de Aperfeiçoamento de Pessoal de Nível Superior (CAPES) for providing Ph.D. scholarships to KJ. The research was funded, in part, by the Institute of Botany at the Jagiellonian University, project no. N18/DBS/000002.

SUPPLEMENTARY MATERIAL

The Supplementary Material for this article can be found online at: https://www.frontiersin.org/articles/10.3389/fmicb.2021.655910/full#supplementary-material

REFERENCES

Al-Yahya'ei, M. N., Mullath, S. K., AlDhaheri, L. A., Kozłowska, A., and Błaszkowski, J. (2017). *Dominikia emiratia* and *Rhizoglomus dunense*, two new species in the glomeromycota. *Botany* 95, 629–639. doi: 10.1139/cjb-2016-0294

Berch, S. M., and Fortin, J. A. (1984). A lectotype for *Glomus microcarpum* (endogonaceae, zygomycetes). *Mycologia* 76, 190–193. doi: 10.1080/00275514.1984.12023827

Błaszkowski, J. (2012). *Glomeromycota. W. Szafer Institute of Botany*. Kraków: Polish Academy of Sciences.

Błaszkowski, J., Chwat, G., and Góralska, A. (2016). *Dominikia lithuanica* and *Kamienskia divaricata*: new species in the glomeromycota. *Botany* 94, 1075–1085. doi: 10.1139/cjb-2016-0167

Błaszkowski, J., Chwat, G., Góralska, A., Ryszka, P., and Kovács, G. M. (2015a). Two new genera, *Dominikia* and *Kamienskia*, and *D. disticha* sp. nov. in glomeromycota. *Nova Hedwigia* 100, 225–238. doi: 10.1127/nova_hedwigia/2014/0216

Błaszkowski, J., Chwat, G., Symanczik, S., and Góralska, A. (2015b). *Dominikia duoreactiva* and *D. difficilevidera*, two new species in the glomeromycota. *Botany* 93, 389–396. doi: 10.1139/cjb-2015-0016

Błaszkowski, J., Chwat, G., Góralska, A., Ryszka, P., and Orfanoudakis, M. (2014). *Septoglomus jasnowskae* and *Septoglomus turnauae*, two new species of arbuscular mycorrhizal fungi (glomeromycota). *Mycol. Prog.* 13, 999–1009. doi: 10.1007/sl1557-014-0985-z

Błaszkowski, J., Kovács, G. M., Gáspár, B. K., Balázs, T. K., Buscot, F., and Ryszka, P. (2012). The arbuscular mycorrhizal *Paraglomus majewskii* sp. nov. represents a new distinct basal lineage in para*Glomeraceae* (glomeromycota). *Mycologia* 104, 148–156. doi: 10.3852/10-430

Błaszkowski, J., Niezgoda, N., de Paiva, J. N., da Silva, K. J. G., Theodoro, R. C., Jobim, K., et al. (2019a). *Sieverdingia* gen. nov., *S. tortuosa* comb. nov., and *Diversispora peloponnesiaca* sp. nov. in the diversisporaceae (glomeromycota). *Mycol. Prog.* 18, 1363–1382. doi: 10.1007/s11557-019-01534-x

Błaszkowski, J., Niezgoda, N., Piątek, M., Magurno, F., Malicka, M., Zubek, S., et al. (2019b). *Rhizoglomus dalpeae, R. maiae*, and *R. silesianum*, new species. *Mycologia* 111, 965–980. doi: 10.1080/00275514.2019.1654637

Błaszkowski, J., Niezgoda, P., Goto, B. T., and Dalpé, Y. (2018a). A new genus, *Oehlia* with *Oehlia diaphana* comb. nov. and an emended description of *Rhizoglomus vesiculiferum* comb. nov. in the glomeromycotina. *Nova Hedwigia* 107, 501–518. doi: 10.1127/nova_hedwigia/2018/0488

Błaszkowski, J., Niezgoda, P., Goto, B. T., and Kozłowska, A. (2018b). *Halonatospora* gen. nov. with *H. pansihalos* comb. nov. and *Glomus bareae* sp. nov. (glomeromycota; *Glomeraceae*). *Botany* 96, 737–748. doi: 10.1139/cjb-2018-0107

Błaszkowski, J., Ryszka, P., and Kozłowska, A. (2018c). Dominikia litorea, a new species in the glomeromycotina, and biogeographic distribution of *Dominikia*. *Phytotaxa* 338, 241–254. doi: 10.11646/phytotaxa.338.3.2

Błaszkowski, J., Ryszka, P., Oehl, F., Koegel, S., Wiemken, A., Kovács, G. M., et al. (2009a). *Glomus achrum and G. bistratum,* two new species of arbuscular mycorrhizal fungi (*Glomeromycota*) found in maritime sand dunes. *Botany* 87, 260–271. doi: 10.1139/B08-138

Błaszkowski, J., Kovács, G. M., and Balázs, T. (2009b). *Glomus perpusillum,* a new arbuscular mycorrhizal fungus. *Mycologia* 101, 245–253. doi: 10.1111/j.1469-8137.2009.02874.x

Borchsenius, F. (2009). *FastGap 1.2. Department of Biosciences*. Denmark: Aarhus University.

Clements, F. E., and Shear, C. L. (1931). *Genera of fungi*. New York, USA: Hafner Publishing Co.

Corazon-Guivin, M. A., Cerna-Mendoza, A., Guerrero-Abad, J. C., Vallejos-Tapullima, A., Carballar-Hernández, S., da Silva, G. A., et al. (2019a). *Microkamienskia* gen. nov. and *Microkamienskia peruviana*, a new arbuscular mycorrhizal fungus from western amazonia. *Nova Hedwigia* 109, 355–368. doi: 10.1127/nova_hedwigia/2019/0551

Corazon-Guivin, M. A., Cerna-Mendoza, A., Guerrero-Abad, J. C., Vallejos-Tapullima, A., Carballar-Hernández, S., da Silva, G. A., et al. (2019b). *Nanoglomus plukenetiae*, a new fungus from peru, and a key to small-spored *Glomeraceae* species, including three new genera in the "*Dominikia* complex/clades". *Mycol. Prog.* 18, 1395–1409. doi: 10.1007/s11557-019-01522-1

Corazon-Guivin, M. A., Mendoza, A. C., Guerrero-Abad, J. C., Vallejos-Tapullima, A., Carballar-Hernández, S., da Silva, G. A., et al. (2019c). *Funneliglomus* gen. nov., and *Funneliglomus sanmartinensis*, a new arbuscular mycorrhizal fungus from the amazonia region in peru. *Sydowia* 71, 17–24. doi: 10.12905/0380.sydowia71-2019-0017

Crossay, T., Cilia, A., Cavaloc, Y., Amir, H., and Redecker, D. (2018). Four new species of arbuscular mycorrhizal fungi (*Glomeromycota*) associated with endemic plants from ultramafic soils of new caledonia. *Mycol. Prog.* 17, 729–744. doi: 10.1007/s11557-018-1386-5

Darriba, D., Taboada, G., Doallo, R., and Posada, D. (2012). jModelTest 2: more models, new heuristics and parallel computing. *Nat. Methods* 9:772. doi: 10.1038/nmeth.2109

Figueiredo, M. A., and Barbosa, M. A. (1990). *A vegetação e flora na serra de Baturité*. Mossoró-RN: Coleção Mossoroense, 747.

Gerdemann, J. W., and Bakshi, B. K. (1976). Endogonaceae of india: two new species. *Trans. Brit. Mycol. Soc.* 66, 340–343. doi: 10.1016/S0007-1536(76)80068-X

Gerdemann, J. W., and Nicolson, T. H. (1963). Spores of mycorrhizal *Endogone* species extracted from soil by wet-sieving and decanting. *Trans. Brit. Mycol. Soc.* 46, 235–244. doi: 10.1016/S0007-1536(63)80079-0

Gerdemann, J. W., and Trappe, J. M. (1974). The *Endogonaceae* in the pacific northwest. *Mycol. Mem.* 5, 1–76.

Girão, J. B. C. (2006). "História da Área de Proteção Ambiental da Serra de Baturité," in *Desenvolvimento sustentável: desafios e discussões*, ed. D. R. C. Pinheiro (Fortaleza: ABC Editora), 367–384.

Goto, B. T., and Maia, L. C. (2006). Glomerospores: a new denomination for the spore of *Glomeromycota*, a group molecularly distinct from the zygomycota. *Mycotaxon* 96, 129–132.

Governo do Ceará. (2018). *Apa da Serra de Baturité. Disponível em*. Available Online at: http://www.funceme.br

Hall, T. A. (1999). BioEdit: a user-friendly biological sequence alignment editor and analysis program for Windows 95/98/NT. *Nucleic Acids Symp. Ser.* 41, 95–98.

Jobim, K., Błaszkowski, J., Niezgoda, P., Kozłowska, A., Zubek, S., Mleczko, P., et al. (2019). New sporocarpic taxa in the phylum Glomeromycota: *Sclerocarpum amazonicum* gen. et sp. nov. in the family *Glomeraceae* (glomerales) and *Diversispora sporocarpia* sp. nov. in the *Diversisporaceae* (diversisporales). *Mycol. Prog.* 18, 369–384. doi: 10.1007/sl1557-018-01462-2

Kornerup, A., and Wanscher, J. H. (1983). *Methuen handbook of colour*, 3rd Edn. London: Eyre Methuen.

Koske, R. E., and Gemma, J. N. (1989). *Glomus nanolumen* (*Endogonaceae*), a new species from hawaii. *Mycologia* 81, 935–938. doi: 10.1080/00275514.1989.12025685

Krüger, M., Krüger, C., Walker, C., Stockinger, H., and Schüßler, A. (2012). Phylogenetic reference data for systematics and phylotaxonomy of arbuscular mycorrhizal fungi from phylum to species-level. *New Phytol.* 193, 970–984. doi: 10.1111/j.1469-8137.2011.03962.x

Krüger, M., Stockinger, H., Krüger, C., and Schüßler, A. (2009). DNA-based level detection of glomeromycota: one PCR primer set for all arbuscular mycorrhizal fungi. *New Phytol.* 183, 212–223. doi: 10.1111/j.1469-8137.2009.02835.x

Lanfear, R., Calcott, B., Ho, S. Y. W., and Guindon, S. (2012). Partition finder: combined selection of partitioning schemes and substitution models for phylogenetic analyses. *Mol. Biol. Evol.* 29, 1695–1701. doi: 10.1093/molbev/mss020

Magurno, F., Malicka, M., Posta, K., Wozniak, G., Lumini, E., and Piotrowska-Seget, Z. (2019). Glomalin gene as molecular marker for functional diversity of arbuscular mycorrhizal fungi in soil. *Biol. Fert. Soils* 55, 411–417. doi: 10.1007/s00374-019-01354-x

Matute, D. R., and Sepúlveda, V. E. (2019). Fungal species boundaries in the genomics era. *Fungal Genet. Biol.* 131:103249. doi: 10.1016/j.fgb.2019.103249

Miadlikowska, J., Kauff, F., Högnabba, F., Oliver, J. C., Molnár, K., Fraker, E., et al. (2014). A multigene phylogenetic synthesis for the class *Lecanoromycetes* (ascomycota): 1307 fungi representing 1139 infrageneric taxa, 317 genera and 66 families. *Mol. Phylogenet. Evol.* 79, 132–168. doi: 10.1016/j.ympev.2014.04.003

Miller, M. A., Pfeiffer, W., and Schwartz, T. (2010). *Creating the CIPRES science gateway for inference of large phylogenetic trees. In: Proceedings of the Gateway Computing Environments Workshop; 14 Nov 2010*. New Orleans, LA: IEEE, 1–8.

Morton, J. B. (1988). Taxonomy of VA mycorrhizal fungi: classification, nomenclature, and identification. *Mycotaxon* 32, 267–324.

Nagy, L. G., Kocsube, S., Csana, Z., Kovacs, G. M., Petkovits, T., Lgyi, C. V., et al. (2012). Re-mind the gap! insertion – deletion data reveal neglected phylogenetic potential of the nuclear ribosomal internal transcribed spacer (ITS) of fungi. *PLoS One* 7:e49794. doi: 10.1371/journal.pone.0049794

Oehl, F., da Silva, G. A., Goto, B. T., and Sieverding, E. (2011). Glomeromycota: three new genera and glomoid species reorganized. *Mycotaxon* 116, 75–120. doi: 10.5248/116.75

Oehl, F., Sánchez-Castro, I., Ferreira de Sousa, N. M. F., Silva, G., and Palenzuela, J. (2015). Dominikia bernensis, a new arbuscular mycorrhizal fungus from a swiss no-till farming site, and *D. aurea, D. compressa* and *D. indica*, three new combinations in *Dominikia*. *Nova Hedwigia* 101, 65–76. doi: 10.1127/nova_hedwigia/2014/0235

Oehl, F., Sánchez-Castro, I., Palenzuela, J., Silva, G., and Sieverding, E. (2014). *Glomus compressum*, a new arbuscular mycorrhizal fungus from different agro-ecosystems in central europe. *Nova Hedwigia* 99, 429–439. doi: 10.1127/0029-5035/2014/0200

Oehl, F., Wiemken, A., and Sieverding, E. (2003). *Glomus aureum*, a new sporocarpic arbuscular mycorrhizal fungal species from European grasslands. *J. Appl. Bot.* 77, 111–115.

Omar, M. B., Bollan, L., and Heather, W. A. (1979). A permanent mounting medium for fungi. *Bull. Br. Mycol. Soc.* 13, 31–32. doi: 10.1016/S0007-1528(70)80038-3

Redecker, D., Schüßler, A., Stockinger, H., Stürmer, S. L., Morton, J. B., and Walker, C. (2013). An evidence-based consensus for the classification of arbuscular mycorrhizal fungi (Glomeromycota). *Mycorrhiza* 23, 515–531. doi: 10.1007/s00572-013-0486-y

Ronquist, F., Teslenko, M., Mark, P. V. D., Ayres, D. L., Darling, A., Hohna, S., et al. (2012). MrBayes 3.2: efficient Bayesian phylogenetic inference and model choice across a large model space. *Syst. Biol.* 61, 539–542. doi: 10.1093/sysbio/sys029

Schüßler, A., and Walker, C. (2010). *The Glomeromycota. A species list with new families and new genera*. Gloucester: Royal Botanic Garden Edinburgh.

Sieverding, E., da Silva, G. A., Berndt, R., and Oehl, F. (2014). Rhizoglomus, a new genus of the *Glomeraceae*. *Mycotaxon* 129, 373–386. doi: 10.5248/129.373

Stamatakis, A. (2014). RAxML version 8: a tool for phylogenetic analysis and post-analysis of large phylogenies. *Bioinformatics* 30, 1312–1313. doi: 10.1093/bioinformatics/btu033

Stockinger, H., Peyret-Guzzon, M., Koegel, S., Bouffaud, M.-L., and Redecker, D. (2014). The largest subunit of RNA polymerase II as a new marker gene to study assemblages of arbuscular mycorrhizal fungi in the field. *PLoS One* 9:e107783. doi: 10.1371/journal.pone.0107783

Stürmer, S. L., and Morton, J. B. (1997). Developmental patterns defining morphological characters in spores of four species in *Glomus*. *Mycologia* 89, 72–81. doi: 10.2307/3761174

Symanczik, S., Błaszkowski, J., Chwat, G., Boller, T., Wiemken, A., and Al-Yahya'ei, M. N. (2014). Three new species of arbuscular mycorrhizal fungi discovered at one location in a desert of oman: *Diversispora omaniana*, *Septoglomus nakheelum* and *Rhizophagus arabicus*. *Mycologia* 106, 243–259. doi: 10.3852/106.2.243

Turrini, A., Saran, M., Giovannetti, M., and Oehl, F. (2018). *Rhizoglomus venetianum*, a new arbuscular mycorrhizal fungal species from a heavy metal-contaminated site, downtown venice in italy. *Mycol. Prog.* 17, 1213–1224. doi: 10.1007/s11557-018-1437-y

Walker, C. (1983). Taxonomic concepts in the *Endogonaceae*: spore wall characteristics in species descriptions. *Mycotaxon* 18, 443–455.

Wijayawardene, N. N., Hyde, K. D., Al-Ani, L. K. T., Tedersoo, L., Haelewaters, D., Rajeshkumar, K. C., et al. (2020). Outline of fungi and fungus-like taxa. *Mycosphere* 11, 1060–1456. doi: 10.5943/mycosphere/11/1/8

Yamamoto, K., Degawa, Y., and Yamada, A. (2020). Taxonomic study of *Endogonaceae* in the japanese islands: new species of *Endogone*, *Jimgerdemannia*, and *Vinositunica*, gen. nov. *Mycologia* 112, 309–328. doi: 10.1080/00275514.2019.1689092

Conflict of Interest: The authors declare that the research was conducted in the absence of any commercial or financial relationships that could be construed as a potential conflict of interest.

Copyright © 2021 Błaszkowski, Jobim, Niezgoda, Meller, Malinowski, Milczarski, Zubek, Magurno, Casieri, Bierza, Błaszkowski, Crossay and Goto. This is an open-access article distributed under the terms of the Creative Commons Attribution License (CC BY). The use, distribution or reproduction in other forums is permitted, provided the original author(s) and the copyright owner(s) are credited and that the original publication in this journal is cited, in accordance with accepted academic practice. No use, distribution or reproduction is permitted which does not comply with these terms.

frontiers in Microbiology

ORIGINAL RESEARCH
published: 06 May 2021
doi: 10.3389/fmicb.2021.654380

Biogeography and Ecology of Magnaporthales: A Case Study

*Jia-Wei Feng, Wei-Ting Liu, Jia-Jie Chen and Chu-Long Zhang**

Ministry of Agriculture Key Laboratory of Molecular Biology of Crop Pathogens and Insects, Institute of Biotechnology, Zhejiang University, Hangzhou, China

The order Magnaporthales belongs to Sordariomycetes, Ascomycota. Magnaporthales includes five families, namely Ceratosphaeriaceae, Pseudohalonectriaceae, Ophioceraceae, Pyriculariaceae, and Magnaporthaceae. Most Magnaporthales members are found in Poaceae plants and other monocotyledonous herbaceous plants ubiquitously as plant pathogens or endophytic fungi, and some members are found in decaying wood or dead grass as saprophytic fungi. Therefore, studying the biogeography and ecology of Magnaporthales is of great significance. Here, we described the biodiversity of endophytic Magnaporthales fungi from Poaceae at three latitudes in China and conducted a meta-analysis of the geography and ecology of Magnaporthales worldwide. We found that Magnaporthales is a dominant order in the endophytic fungi of Poaceae. More than half of the endophytic Magnaporthales fungi have a taxonomically uncertain placement. Notably, few endophytic fungi are grouped in the clusters with known saprophytic or pathogenic Magnaporthales fungi, indicating that they may have saprophytic and parasitic differentiation in nutritional modes and lifestyles. The meta-analysis revealed that most species of Magnaporthales have characteristic geographical, host, and tissue specificity. The geographical distribution of the three most studied genera, namely *Gaeumannomyces*, *Magnaporthiopsis*, and *Pyricularia*, in Magnaporthales may depend on the distribution of their hosts. Therefore, studies on the endophytic fungal Magnaporthales from monocotyledonous plants, including Poaceae, in middle and low latitudes will deepen our understanding of the biogeography and ecology of Magnaporthales.

Keywords: biodiversity, endophytic fungi, meta-analysis, Poaceae, specificity

OPEN ACCESS

Edited by:
Dhanushka Nadeeshan Wanasinghe, Kunming Institute of Botany, Chinese Academy of Sciences, China

Reviewed by:
Sajeewa S. N. Maharachchikumbura, University of Electronic Science and Technology of China, China
Indunil Senanayake, Shenzhen University, China

****Correspondence:***
Chu-Long Zhang
clzhang@zju.edu.cn

Specialty section:
This article was submitted to Evolutionary and Genomic Microbiology, a section of the journal Frontiers in Microbiology

Received: *16 January 2021*
Accepted: *19 March 2021*
Published: *06 May 2021*

Citation:
Feng J-W, Liu W-T, Chen J-J and Zhang C-L (2021) Biogeography and Ecology of Magnaporthales: A Case Study. Front. Microbiol. 12:654380. doi: 10.3389/fmicb.2021.654380

INTRODUCTION

Magnaporthales belongs to Sordariomycetes, Ascomycota. Thongkantha et al. (2009) first introduced the new order Magnaporthales to accommodate Magnaporthaceae, based on the results of morphology and phylogenetic analysis of the large subunit of ribosomal DNA (LSU) and the small subunit of ribosomal DNA (SSU). Klaubauf et al. (2014) separated *Pyricularia* and its related genera and *Ophioceras* and its related genera from Magnaporthaceae and introduced two separate families, Pyriculariaceae and Ophioceraceae, respectively, to accommodate them, according to morphological observation and two-loci phylogenetic analysis of LSU and the large subunit of RNA polymerase II (*RPB1*). Based on the phylogenetic analysis of representative species and genera of Magnaporthales, Luo et al. (2015a) identified three families in Magnaporthales,

including Magnaporthaceae, Pyriculariaceae, and Ophioceraceae, and clarified their nutrition and infection modes. Based on four-loci phylogenetic analysis of LSU, SSU, translation elongation factor 1 (*TEF1*), and the second largest subunit of RNA polymerase (*RPB2*), Maharachchikumbura et al. (2016) accepted three families in Magnaporthales, Magnaporthaceae, Ophioceraceae, and Pyriculariaceae, and placed *Pseudohalonectria* in the genera incertae sedis of Magnaporthale. According to the molecular clock analysis of LSU, SSU, *TEF1*, and *RPB2*, Hyde et al. (2017) suggested that Distoseptisporaceae, with divergence times of 121 million years ago (MYA), should be placed within Magnaporthales. Hongsanan et al. (2017) introduced a new family Pseudohalonectriaceae to accommodate *Pseudohalonectria*, based on the molecular clock analysis of LSU, SSU, *TEF1*, and *RPB2*. Zhang et al. (2018) renewed a time-frame for the evolution of Magnaporthales by analyzing the phylogenomics of representative species and genera of Magnaporthales. Magnaporthales originated 31 MYA, and its pathogenic branch originated 21 MYA. According to a multi-loci phylogenetic analysis of LSU, *RPB2*, and *TEF1*, Luo et al. (2019) introduced a new family Ceratosphaeriaceae in Magnaporthales to accommodate *Ceratosphaeria*, and raised Distoseptisporaceae to a new order Distoseptisporales.

Species of Ceratosphaeriaceae, Pseudohalonectriaceae, and Ophioceraceae are saprophytic fungi growing on decaying wood or dead grass. Ceratosphaeriaceae species grow on decaying wood or dead twigs in terrestrial habitats (Luo et al., 2019). Pseudohalonectriaceae species are saprophytic fungi in submerged rotten wood or twigs (Hongsanan et al., 2017; Luo et al., 2019). Ophioceraceae species are isolated from submerged rotten wood or dead herbs (Shearer et al., 1999).

Pyriculariaceae mainly infect shoots of Poaceae or other monocotyledonous plants, including rice, maize, wheat, bluegrass, and *Digitaria*. Members of the family produce an appressorium, and all are pathogenic fungi (Zhang et al., 2016). The rice blast fungus, *Pyricularia oryzae*, is a model fungus to study the interaction between plants and fungi (Valent, 1990). *P. oryzae* was found to infect not only the shoots of rice plants but also roots of rice (Sesma and Osbourn, 2004; Marcel et al., 2010).

Magnaporthaceae species are reported in all plant tissues, including leaf, stem, and root. Their nutritional modes and lifestyles are complex, and most of them are necrotrophic or hemibiotrophic parasites with a host preference, infecting both Poaceae and Cyperaceae. *Buergenerula, Gaeumannomyces*, *Magnaporthiopsis*, *Nakataea*, *Pseudophialophora*, and *Slopeiomyces* are pathogenic fungi. Among them, the take-all fungus of cereals, i.e., *Gaeumannomyces graminis* (Hernández-Restrepo et al., 2016) and summer patch fungus of turf grass, i.e., *Magnaporthiopsis poae* (Luo and Zhang, 2013) are the two most important pathogens. *Bussabanomyces*, *Falciphora*, and *Pseudophialophora* are endophytic fungi (Yuan et al., 2010; Klaubauf et al., 2014; Luo et al., 2015b, 2017). *Kohlmeyeriopsis* was derived from the dead stem of *Juncus effusus* with unknown nutritional modes and lifestyles (Klaubauf et al., 2014). Notably, *Aquafiliformis* are saprophytic fungi on decaying wood and exist in aquatic habits (Luo et al., 2019). *Plagiosphaera* are saprophytes on dead stem and exist in terrestrial habitats (Song et al., 2019). Species of *Muraeriata* are isolated from bark or wood and exist in terrestrial habitats (Huhndorf et al., 2008).

Healthy plants contain abundant endophytic fungi and many unknown species of endophytic fungi; therefore, more unknown biological functions of endophytic fungi need to be explored (Arnold and Lutzoni, 2007; Rodriguez et al., 2009). Poaceae is the most economically important family among seed plants. It includes the main food crops of humans, such as *Oryza sativa*, *Triticum aestivum*, *Zea mays*, and *Sorghum bicolor* (Kellogg, 2015). The survival and reproduction of Poaceae are positively affected by endophytic fungi. In the past, much attention was paid to clavicipitaceous endophytic fungi, namely *Neotyphodium*/*Epichloë*, which are widely distributed in gramineous plants, primarily in the temperate zone, and play an important role in the resistance of gramineous plants to biotic and abiotic stresses (Clay and Schardl, 2002). However, studies on endophytic Magnaporthales fungi are limited, therefore, studies on the endophytic Magnaporthales fungi associated with Poaceae are of great significance. We studied endophytic fungi from healthy plants of Poaceae growing at three provinces, namely Yunnan, Zhejiang, and Inner Mongolia of China, in the tropical, subtropical, and mid-temperate zones, respectively. A total of 220 strains from 1,821 isolates of endophytic fungi belonged to Magnaporthales, with the relative frequency of 12.1% (Liu et al., 2021). The aims of the present study were: (1) to determine the phylogenetic relationships of endophytic Magnaporthales fungi from Poaceae in three geographic origins using a five-loci sequence, including the internal transcribed spacer of ribosomal DNA (ITS), LSU, DNA replication licensing factor (*MCM7*), *RPB1*, and *TEF1* as well as to analyze the relationship between endophytic Magnaporthales fungi and their host tissues and sites; and (2) to conduct a meta-analysis of the global geographic distribution of the genera of Magnaporthales and the species of *Gaeumanomyces*, *Magnaporthiopsis*, and *Pyricularia*, as well as to analyze the relationships between various species of Magnaporthales and their hosts and tissues.

MATERIALS AND METHODS

Collections and Isolations

Between 2017 and 2018, healthy plant samples of the Poaceae family were obtained from those growing at three provinces, namely Yunnan, Zhejiang, and Inner Mongolia of China, in tropical, subtropical, and mid-temperate zones, respectively. Fungal endophytes were isolated as described elsewhere (Yuan et al., 2010). Briefly, the roots and shoots were scissored to ∼5-cm long fragments, and then tissue fragments were then surface disinfected sequentially with 75% alcohol for 3 min and with 1% (available chlorine) sodium hypochlorite for 10 min. The surface disinfected tissue fragments were scissored to ∼0.5-cm long pieces and then placed on malt extract agar media supplemented with 50 μg/mL ampicillin and streptomycin sulfate. The hyphal tips growing on the edge of the tissue pieces were transferred to a new PDA plate from which the fungal cultures were obtained.

Fungal DNA Extraction, Polymerase Chain Reaction (PCR) Amplification, and Sequencing

Genomic DNA was extracted from cultures grown on PDA by using a modified protocol suggested by a previous study (Cubero et al., 1999). Five loci, including ITS, LSU, *MCM7*, *RPB1*, and *TEF1,* were amplified and sequenced with the primers ITS 1 and ITS4 (White et al., 1990); LS1 and LR5 (Rehner and Samuels, 1995); MCM7-709 and MCM7-1348 (Schmitt et al., 2009); EF1-728F and EF1-986R (Carbone and Kohn, 1999); and RPB1-Ac and RPB1-Cr (Matheny et al., 2002; Castlebury et al., 2004). The PCR protocols were followed as suggested by a previous study (Zhang et al., 2011).

Sequence Alignment, and Phylogenetic Analysis

Sequences were initially aligned with MAFFT (Katoh and Standley, 2013) using *Cryphonectria parasitica* EP155 as the outgroup, followed by curing with BMGE (Dereeper et al., 2010). The cured sequence alignments were then concatenated with the SequenceMatrix (Vaidya et al., 2011). Finally, a multi-loci phylogenetic tree with ITS, LSU, *MCM7*, *RPB1*, and *TEF1* was constructed with the iqtree v. 1.6.12 (Minh et al., 2020) by using the maximum likelihood (ML) method. A network of diverse endophytic Magnaporthales fungal species from gramineous plants in different locations and from different tissues were analyzed by using the Cytoscape version 3.6.1.

Meta-Analysis

Meta-analyses for all known species of Magnaporthales were performed. First, according to sequences of the representative species or genera of Magnaporthales, records with sequence information with Per. ident value $\geq$ 94.3%, a threshold of filamentous fungi based on the genus level (Vu et al., 2019), were retrieved from GenBank. Then, sequences containing information of accession number, host, and country were screened by using the R version 4.0.2, and the ITS phylogenetic tree were constructed to determine its classification status to the genus. Network diagrams were used to show the relationship among various species of Magnaporthales, and its host and tissue were analyzed as above. Geographical distribution of genera of Magnaporthales and species of *Gaeumanomyces*, *Magnaporthiopsis*, and *Pyricularia* were analyzed in R version 4.0.2.

RESULTS

Biodiversity of Endophytic Magnaporthales Fungi From Poaceae

The retrieved representative sequences used in the study are listed in **Supplementary Table 1**. The sequences obtained in this study were deposited in the GenBank (accession numbers: MW482542-MW482856, MW478904-MW479096, MW478040-MW478116, MW056504-MW056512, MW055655-MW055657, and MW055631-MW055654). We performed multiple sequence alignments of ITS, LSU, *MCM7*, *RPB1*, and *TEF1* of endophytic fungi of Magnaporthales with those of the representative species of Magnaporthales, and constructed a multi-loci phylogenetic tree with ITS, LSU, *MCM7*, *RPB1*, and *TEF1* (**Figure 1**) using the maximum likelihood (ML) method. Multi-loci phylogenetic analysis provided a strongly supported clade for families, genera, and species of Magnaporthales.

The multi-loci phylogenetic tree (**Figure 1**) showed five main clusters corresponding to Pseudohalonectriaceae, Ceratosphaeriaceae, Ophioceraceae, Pyriculariaceae, and Magnaporthaceae. Of the 220 endophytic Magnaporthales strains, six were grouped in a clade containing *Ophioceras* species within the Ophioceraceae cluster, four were grouped in two subclades within the Pyriculariaceae cluster, indicating that they belong to two taxonomically uncertain genera of Pyriculariaceae; and 209 were grouped within the Magnaporthaceae cluster, of which 83 were grouped within eight known genera, namely *Gaeumannomyces*, *Magnaporthiopsis*, *Falciphora*, *Nakataea*, *Omnidemptus*, *Bifusisporella*, *Pseudophialophora*, and *Aquafiliformis*, whereas 126 were grouped in nine subclades, indicating that they belong to nine taxonomically uncertain genera of Magnaporthaceae. More than half of Magnaporthaceous strains we isolated are taxonomically uncertain. Therefore, studies on cryptic Magnaporthaceous endophytic fungi will help understand the biodiversity, biogeography, and ecology of Magnaporthales.

Pseudohalonectriaceae, Ceratosphaeriaceae, and Ophioceraceae are saprophytic fungi. Notably, six endophytic fungal strains in this study belong to *Ophioceras* of Ophioceraceae, thus we speculated that these endophytes could be viaphytes that undergo an interim stage in healthy plant tissues (Nelson et al., 2020). The genera of *Aquafiliformis*, *Muraeriata*, and *Plagiosphaera* reported on decayed wood or dead stems of herbs in aquatic or terrestrial habitats, three endophytic fungal strains in this study belong to *Aquafiliformis* and the genera of *Aquafiliformis*, *Muraeriata*, and *Plagiosphaera* form a separate cluster from Magnaporthaceae. Therefore, we speculated that this branch may be in transition between saprophytic and parasitic. The results may be helpful for us to study the evolution of saprophytic and parasitic fungi in Magnaporthales. Species in Pyriculariaceae are pathogenic fungi. Four endophytic fungal strains in this study, isolated from shoots of healthy plants, belong to two taxonomically uncertain genera of Pyriculariaceae. We speculate that these strains may be pathogenic to plants under the condition of latent infection.

We analyzed the relationship between host tissue and site (**Figures 2**, **3**) and found that *Omnidemptus affinis* and unidentified *Omnidemptus* clade 1 and 3 were collected both in Zhejiang and Yunnan, whereas others were only collected in Zhejiang, Yunnan, or Inner Mongolia. Thus, most Magnaporthales species have characteristics of geographical specificity. Only one species was collected in Inner Mongolia, and most species came from Yunnan and Zhejiang. Moreover, the diversity of species collected in Yunnan was significantly higher than that in Zhejiang and Inner Mongolia (**Figure 2**). The number of species isolated from shoots of Poaceae is more than that from roots (**Figure 3**). Unidentified *Omnidemptus*

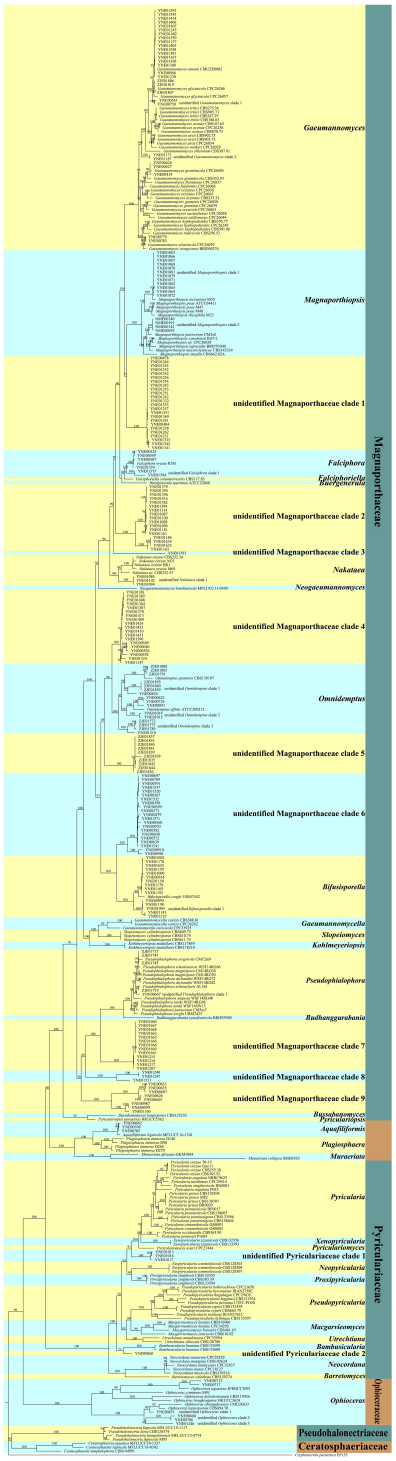


FIGURE 1 | Multi-loci phylogenetic tree based on ITS, LSU, *MCM7*, *RPB1*, and *TEF1* using maximum likelihood (ML).

clade 3, unidentified Magnaporthaceae clade 1, and unidentified *Bifusisporella* clade 1 were collected both from the roots and shoots, but the other species were only collected from roots or shoots, indicating that most species have tissue specificity and only a few have extensive colonization in plants.

Meta-Analysis

By using R, we drew a map of the global geographic distribution of genera of Magnaporthales. A total of 1,378 strains with abundant information were collected by layer screening. Finally, by analyzing the information, we selected 1,378 strains with abundant information of Magnaporthales.

Data analysis revealed that fungi of Magnaporthales can be collected from the shoot and root, and displayed great diversity in the shoot and root. Most species are collected only from the root or shoot, whereas *Gaeumannomyces graminicola* and *P. oryzae* can be collected from both shoots and roots, which shows that most species have characteristics of tissue specificity (**Figure 4**). Notably, some endophytic fungal records belong to *Ophioceras* (**Figure 4**), which was consistent with our investigation (**Figure 3**). The host range of Magnaporthales is wide, including Poaceae, Cyperaceae, Ericaceae, Juncaceae, Musaceae, Rubiaceae, Commelinaceae, Fabaceae, Myrtaceae, Urticaceae, and Zingiberaceae (**Figure 5**). The main hosts of Magnaporthales are Poaceae, and the second hosts are Cyperaceae. We speculate that is because Poaceae has been studied more. We found that most species, except unidentified *Pseudophialophora* clade 1 and *Ophioceras leptosporum,* had host specificity. Unidentified *Pseudophialophora* clade 1 uses Poaceae and Cyperaceae as hosts. *Ophioceras leptosporum* uses Myrtaceae and Rubiaceae as hosts.

According to the meta-analysis, strains of Magnaporthales are mainly distributed in middle and low latitudes, with almost none in high latitudes, and the diversity of endophytes in middle latitudes is higher than that in low latitudes. We found that *Gaeumannomyces*, *Magnaporthiopsis*, and *Pyricularia* have a wide distribution range and abundant species (**Figure 6**), so we mapped the global geographic information map of *Gaeumannomyces*, *Magnaporthiopsis,* and *Pyricularia* to show the distribution of different species in each genus (**Figures 7–9**). *Gaeumannomyces* and *Magnaporthiopsis* are mainly distributed in temperate regions, whereas *Pyricularia* in tropical and temperate regions. The three genera have characteristics of host specificity (**Figure 5**), indicating that their geographical distribution depends on their host distribution.

DISCUSSION

The study of Magnaporthales dates back to the 19th century, when *Nakataea oryzae* (= *Magnaporthe salvinii*) and *Pyricularia grisea* (= *Magnaporthe grisea*) were found to infect rice and *Digitaria* (Thongkantha et al., 2009). Currently, five families, namely Ceratosphaeriaceae, Pseudohalonectriaceae, Ophioceraceae, Pyriculariaceae, and Magnaporthaceae, are accommodated in Magnaporthales with 1, 1, 1, 11, and 22 accepted genera, respectively (Hyde et al., 2020; Wijayawardene et al., 2020). In this study, endophytic Magnaporthales fungi were identified by collecting Poaceae at different latitudes and their taxonomic status was analyzed by phylogenetic

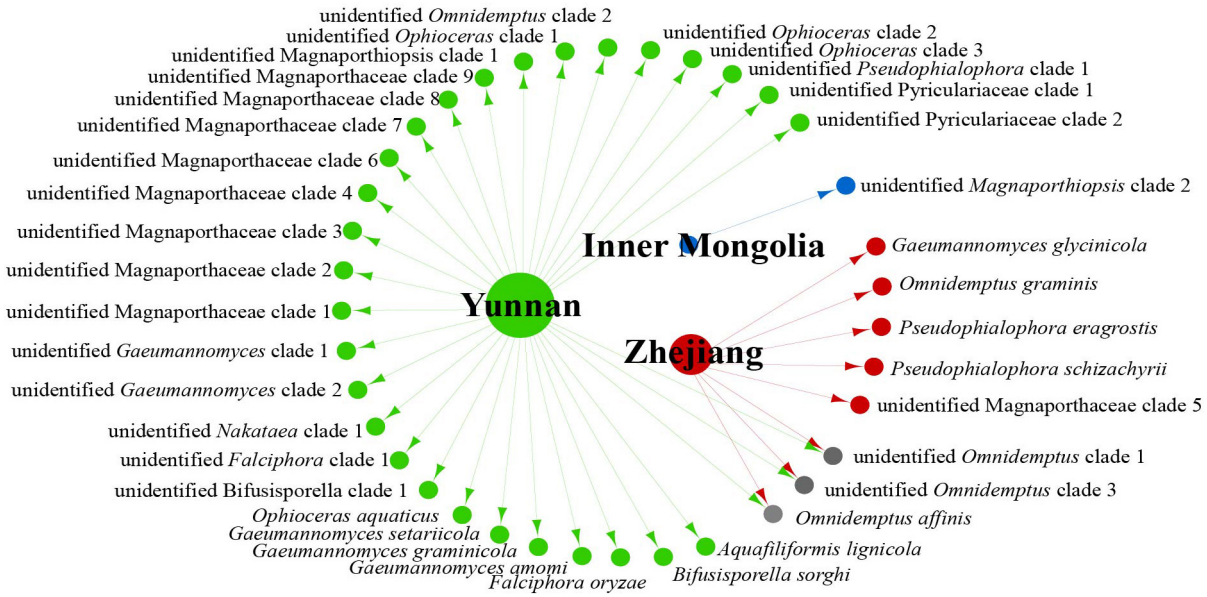


FIGURE 2 | Network of endophytic fungal Magnaporthales species diversity from gramineous plants in Yunnan, Zhejiang, and Inner Mongolia.

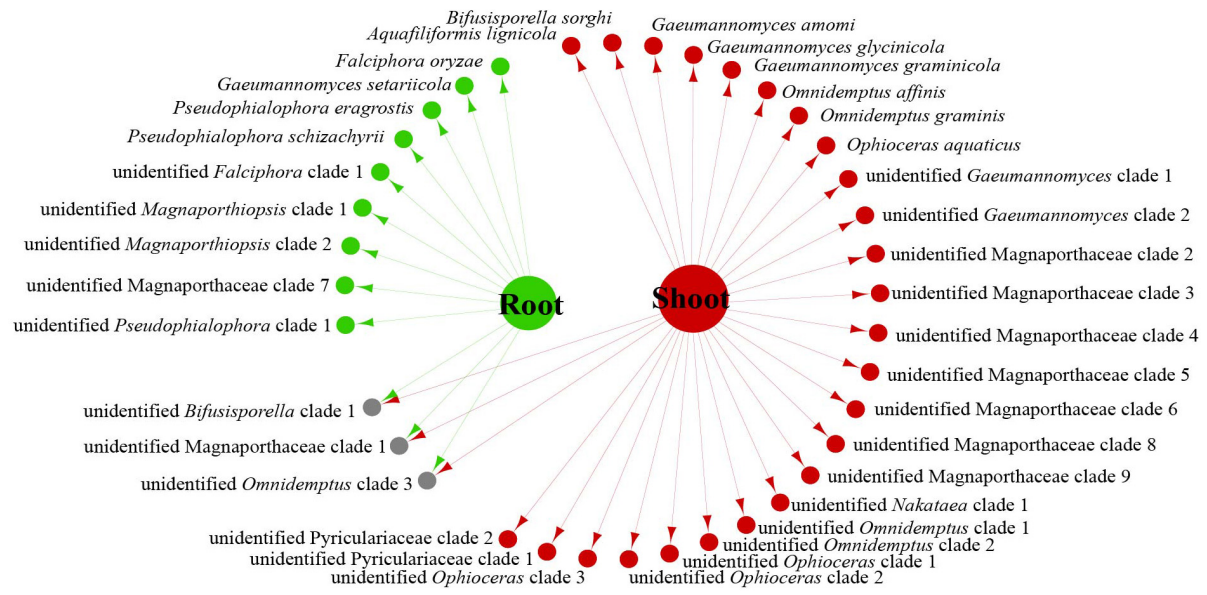


FIGURE 3 | Network of endophytic fungal Magnaporthales species diversity from shoots and roots of gramineous plants in Yunnan, Zhejiang, and Inner Mongolia.

analysis. These results indicated that 220 endophytic Magnaporthales strains we isolated were grouped in 20 subclades. Of them, two subclades in Pyriculariaceae and nine subclades in Magnaporthaceae represented presumably novel taxa (genera). As most of the Magnaporthales strains isolated are taxonomically uncertain, further taxonomical analysis is required.

The relationships among the hosts, tissues, and latitudes using a network diagram sum up the information on the biogeographic distribution, host range, and tissues. Meta-analysis indicated that most of the Magnaporthales species possess characteristics of geographical, host, and tissue specificities. However, there were exceptions relative to endophytic fungi in this study. For example, *Gaeumannomyces* was the most studied genus in Magnaporthaceae. *G. amomi* was described as an endophyte from the leaves and pseudostem of herbaceous plants *Amomum siamense* (Zingiberaceae) and *Alpinia malaccensis* (Zingiberaceae) in Thailand (Bussaban et al., 2001); *G. glycinicola* was isolated from the pods of herbaceous plant *Glycine max* (Fabaceae) in Indiana, United States, as a pathogen

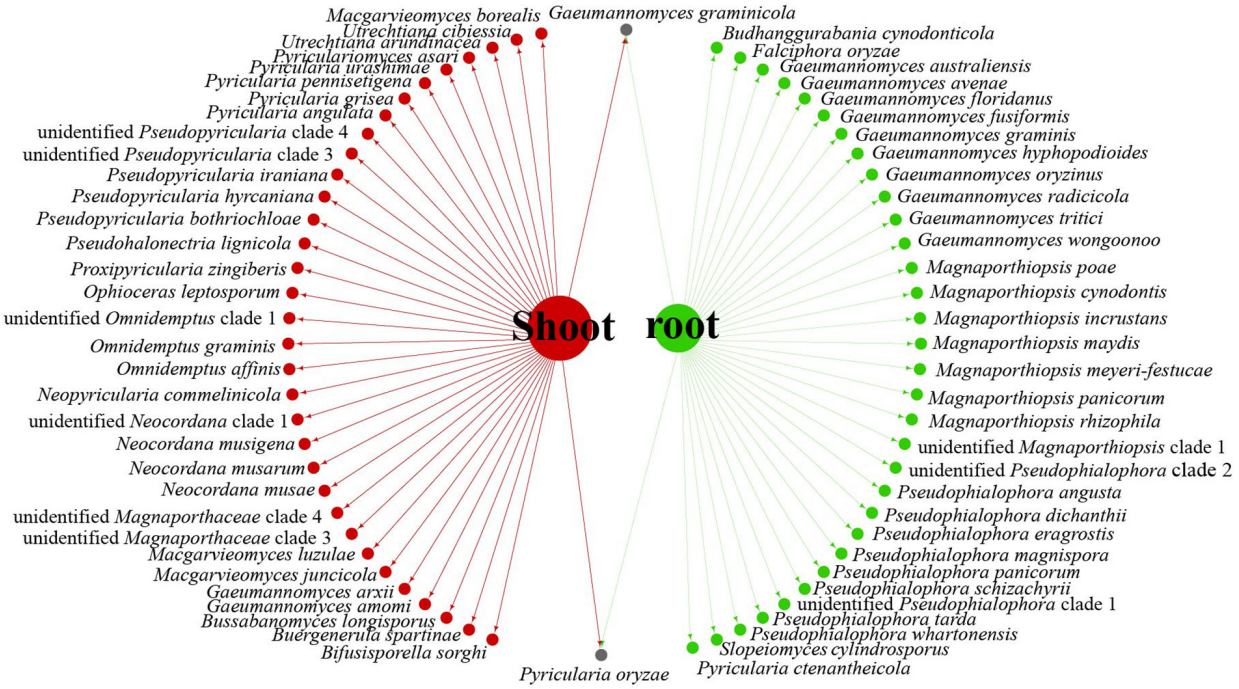


FIGURE 4 | Network of parasitic fungal Magnaporthales species from shoots and roots using meta-analysis.

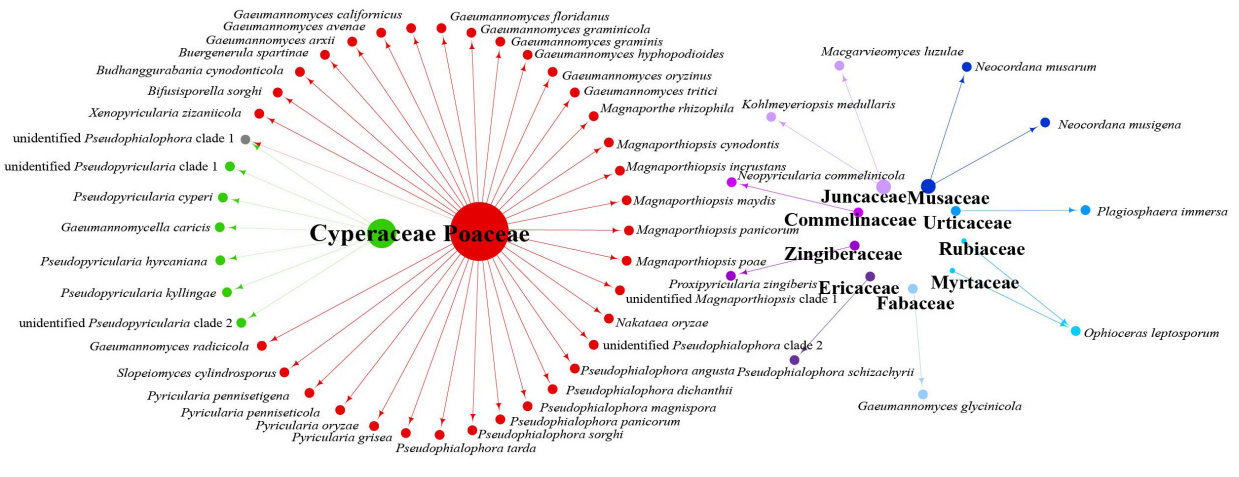


FIGURE 5 | Network of parasitic fungal Magnaporthales species from different host families using meta-analysis.

(Hernández-Restrepo et al., 2016); *G. graminicola* was isolated from the stem base of the grass hosts *Ctenanthe* (Marantaceae) in Netherlands and from *Stenotaphrum secundatum* (Poaceae) and *Eremochloa ophiuroides* (Poaceae) in the United States (Hernández-Restrepo et al., 2016); and *Gaeumannomyces setariicola* was isolated from the host *Setaria italica* (Poaceae) in South Africa (Hernández-Restrepo et al., 2016). In this study, except for two unidentified *Gaeumannomyces* clades (presumably novel species), 17, 3, and another 3 strains belonging to *G. amomi*, *G. glycinicola*, and *G. graminicola*, respectively, were recovered from the shoots of Poaceae plants, and two strains belonging to *G. setariicola* were recovered from the roots of Poaceae plants. These observations indicated that *Gaeumannomyces* species are possibly distributed in herbaceous plant hosts with broader geographical distribution, but exhibit tissue (root and shoot) specificity. For example, in case of *Falciphora* and *Pseudophialophora*, *Falciphora oryzae* (= *Harpophora oryzae*) was first isolated from the roots of wild rice as fungal endophytes (Yuan et al., 2010), four strains belonging to *F. oryzae* and two strains belonging to an unidentified *Falciphora* clades (presumably novel species) were isolated from the roots of three different species of Poaceae (including wild rice) in

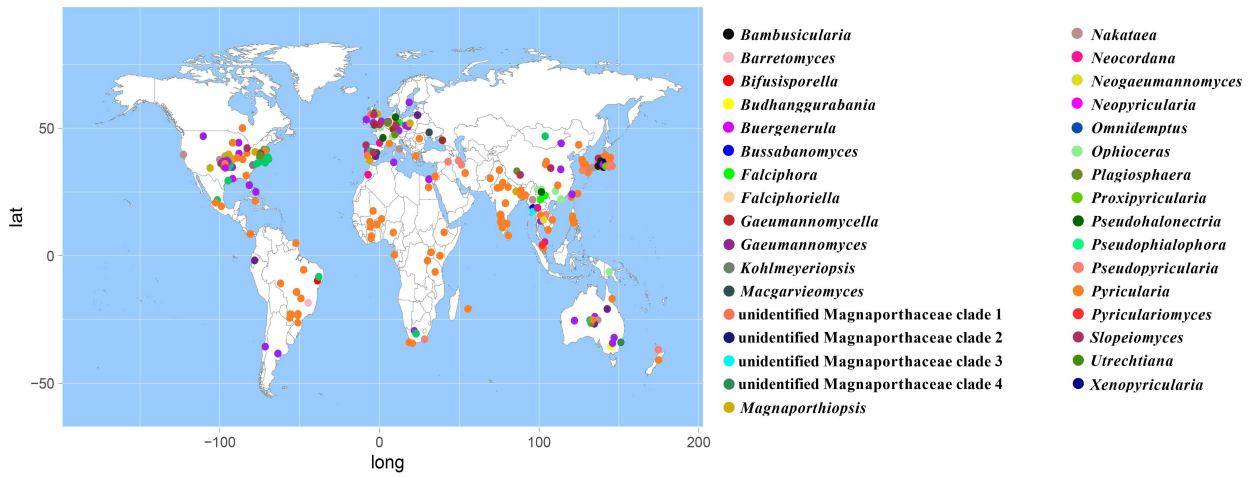


FIGURE 6 | Geographical distribution of Magnaporthales genera using meta-analysis.

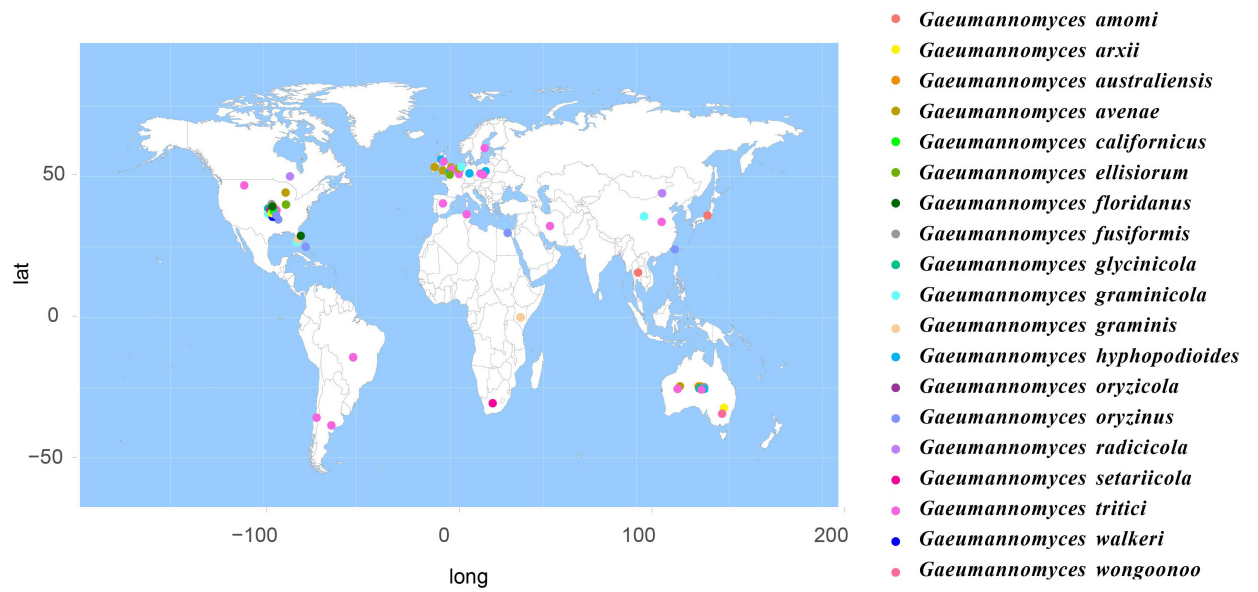


FIGURE 7 | Geographical distribution of *Gaeumanomyces* using meta-analysis.

the Yunnan province in this study. This result indicated that *Falciphora* may be locally distributed in the plant roots of Yunnan province, but in different Poaceae hosts as fungal endophytes. *Pseudophialophora* species were uncovered from the roots of Poaceae grass in the New Jersey Pine Barrens of United States as fungal endophytes (Luo et al., 2014, 2015b). Five strains belonging to *Pseudophialophora eragrostis*, *Pseudophialophora schizachyrii*, and an unidentified *Pseudophialophora* clade 1 (presumably novel species) were recovered from the roots of Poaceae grass in the Zhejiang and Yunnan provinces (**Figures 2**, **3**), and an unidentified *Pseudophialophora* clade 1 was also recovered from the root of Cyperaceae host plant by meta-analysis (**Figure 4**). It indicated that *Pseudophialophora* species may be specifically colonized in the plant roots and not only in Poaceae plants but also in other monocotyledonous herbaceous plants with global distribution. Therefore, further extensive sampling of the shoots and roots of herbaceous plants, including Poaceae, Cyperaceae, Ericaceae, Juncaceae, Musaceae, Rubiaceae, Commelinaceae, Fabaceae, Myrtaceae, Urticaceae, and Zingiberaceae, in the middle and low latitudes would help better understand the biogeography, ecology, nutritional modes, lifestyles, and evolution of Magnporthales fungi as well as lay a foundation for further study about the interaction between Magnaporthales and plants.

The evolution of fungal pathogenicity was preliminarily revealed by comparative genomic analysis. Saprophytic fungi first evolved into biotrophic pathogenic fungi, and the biotrophic pathogenic fungi evolved into necrotrophic pathogenic fungi

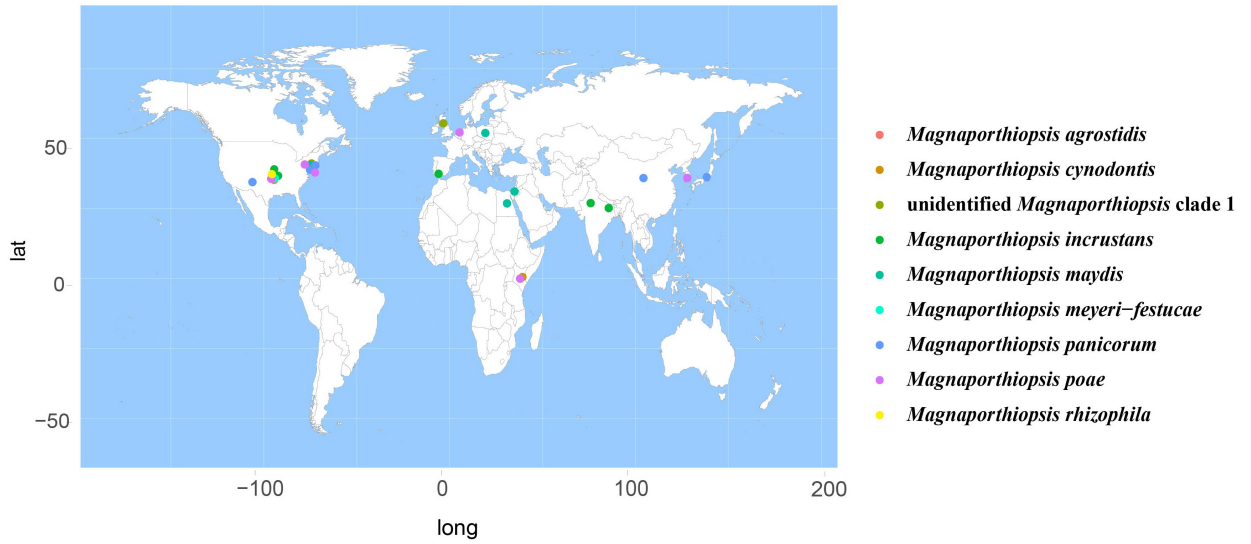


FIGURE 8 | Geographical distribution of *Magnaporthiopsis* using meta-analysis.

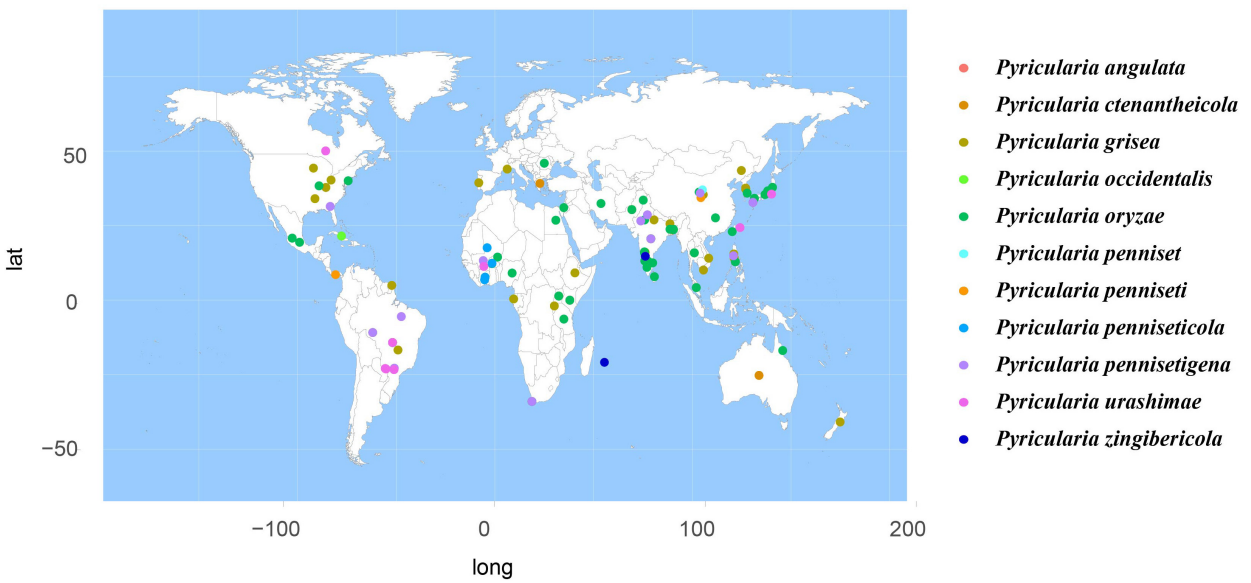


FIGURE 9 | Geographical distribution of *Pyricularia* using meta-analysis.

and specific biotrophic pathogenic fungi (Spanu, 2012). Magnaporthales exhibit saprophytic and parasitic (pathogenic fungi, endophytic fungi) differentiation in the nutritional modes and lifestyles (Luo et al., 2015a). Differentiation in the nutrition and lifestyles for families of Magnaporthales reflect the evolution of the order Magnaporthales from its ancestors to saprophytic and parasitic fungi (Zhang et al., 2018). Moreover, Magnaporthales exhibit differentiation with root and shoot infections in the infection patterns (Luo et al., 2015a). Pyriculariaceae mainly infects the shoot of Poaceae or other monocotyledonous plants, whereas Magnaporthaceae can infects all portions of Poaceae or other monocotyledonous plants. In our previous study (Xu et al., 2014, 2015), we noted that the endophytic fungi *F. oryzae* (= *H. oryzae*) of Magnaporthaceae originated from pathogenic fungi by comparing the genomic and transcriptomic data. The mechanism of evolution involved changes in the gene composition and expression regulation involved in plant disease resistance responses, autotrophic metabolism, signal transduction, and substance transport. These changes lead to the differentiation of endophytic and pathogenic fungi. Zhang et al. constructed the maximum credibility tree by genome wide analysis, which support that Magnaporthales originated 31 MYA and diverged to different nutritional fungi about 24 MYA, to Poaceae and other monocotyledonous plants

about 21 MYA, and to saprophytic fungi on decayed wood in aquatic and terrestrial habitats about 20 MYA and speculated that horizontal gene transfer, secretome and avirulence effector genes, and transposable elements were involved in the differentiation of host or environmental adaptation (Zhang et al., 2018). However, the evolution of saprophytic fungi that live in aquatic or terrestrial habits and parasitic fungi (pathogenic fungi or endophytic fungi) that infect Poaceae or other monocotyledonous plants remain unclear. Thus, the evolution of endophytic and pathogenic fungi also need further analyses. Endophytic fungal species in the clade of *Ophioceras* of Ophioceraceae, the subclade in Magnaporthaceae consisting of *Aquafiliformis*, *Muraeriata,* and *Plagiosphaera* and unknown endophytic fungi in Pyriculariaceae obtained in this study provide the opportunity to study differences in the evolution of saprophytic and parasitic fungi, and pathogenic and endophytic fungi, and to explore the lifestyles and nutritional modes of their common ancestor. In particular, whether there is a gene flow between saprophytic and parasitic fungi, and pathogenic and endophytic fungi, and if this gene migration is unidirectional or bidirectional? These problems are worthy of further exploration.

DATA AVAILABILITY STATEMENT

The datasets presented in this study can be found in online repositories. The names of the repository/repositories and accession number(s) can be found in the article/ **Supplementary Material**.

AUTHOR CONTRIBUTIONS

J-WF performed phylogenetic analysis and meta-analysis, DNA extraction and sequencing, and phylogenetic analysis. W-TL coordinated DNA extraction and sequencing. J-JC coordinated fungal isolation, DNA extraction and sequencing. C-LZ initiated the project, supervised all steps of the experimental work and wrote the manuscript. All authors contributed to the article and approved the submitted version.

FUNDING

This work was supported by the National Natural Science Foundation of China (Grant No. 31870010).

SUPPLEMENTARY MATERIAL

The Supplementary Material for this article can be found online at: https://www.frontiersin.org/articles/10.3389/fmicb.2021.654380/full#supplementary-material

REFERENCES

Arnold, A. E., and Lutzoni, F. (2007). Diversity and host range of foliar fungal endophytes: are tropical leaves biodiversity hotspots? *Ecology* 88, 541–549. doi: 10.1890/05-1459

Bussaban, B., Lumyong, S., Lumyong, P., Hyde, K. D., and McKenzie, E. (2001). Two new species of endophytes (ascomycetes) from Zingiberaceae sporulating in culture. *Nova Hed.* 73, 487–493. doi: 10.1127/nova.hedwigia/73/2001/487

Carbone, I., and Kohn, L. M. (1999). A method for designing primer sets for speciation studies in filamentous ascomycetes. *Mycologia* 91, 553–556. doi: 10.2307/3761358

Castlebury, L. A., Rossman, A. Y., Sung, G. H., Hyten, A. S., and Spatafora, J. W. (2004). Multigene phylogeny reveals new lineage for *Stachybotrys chartarum*, the indoor air fungus. *Mycol. Res.* 108, 864–872. doi: 10.1017/S0953756204000607

Clay, K., and Schardl, C. (2002). Evolutionary origins and ecological consequences of endophyte symbiosis with grasses. *Am. Nat.* 160S, S99–S127. doi: 10.1086/342161

Cubero, O. F., Crespo, A., Fatehi, J., and Bridge, P. D. (1999). DNA extraction and PCR amplification method suitable for fresh, herbarium-stored, lichenized, and other fungi. *Plant Syst. Evol.* 216, 243–249. doi: 10.1007/BF01084401

Dereeper, A., Audic, S., Claverie, J., and Blanc, G. (2010). BLAST-EXPLORER helps you building datasets for phylogenetic analysis. *BMC Evol. Biol.* 10:8. doi: 10.1186/1471-2148-10-8

Hernández-Restrepo, M., Groenewald, J. Z., Elliott, M. L., Canning, G., McMillan, V. E., and Crous, P. W. (2016). Take-all or nothing. *Stud. Mycol.* 83, 19–48. doi: 10.1016/j.simyco.2016.06.002

Hongsanan, S., Maharachchikumbura, S. S. N., Hyde, K. D., Samarakoon, M. C., Jeewon, R., Zhao, Q., et al. (2017). An updated phylogeny of *Sordariomycetes* based on phylogenetic and molecular clock evidence. *Fungal Divers.* 84, 25–41. doi: 10.1007/s13225-017-0384-2

Huhndorf, S. M., Greif, M., Mugambi, G. K., and Miller, A. N. (2008). Two new genera in the *Magnaporthaceae*, a new addition to *Ceratosphaeria* and two new species of Lentomitella. *Mycologia* 100, 940–955. doi: 10.3852/08-037

Hyde, K. D., Maharachchikumbura, S. S. N., Hongsanan, S., Samarakoon, M. C., Lücking, R., Pem, D., et al. (2017). The ranking of fungi: a tribute to David L. Hawksworth on his 70th birthday. *Fungal Divers.* 84, 1–23. doi: 10.1007/s13225-017-0383-3

Hyde, K. D., Norphanphoun, C., Maharachchikumbura, S. S. N., Bhat, D. J., and Jones, E. B. G. (2020). Refined families of *Sordariomycetes*. *Mycosphere* 11, 305–1059. doi: 10.5943/mycosphere/11/1/7

Katoh, K., and Standley, D. M. (2013). MAFFT multiple sequence alignment software version 7: improvements in performance and usability. *Mol. Biol. Evol.* 30, 772–780. doi: 10.1093/molbev/mst010

Kellogg, E. A. (2015). *Flowering Plants. Monocots: Poaceae*. Cham: Springer International Publishing AG.

Klaubauf, S., Tharreau, D., Fournier, E., Groenewald, J. Z., Crous, P. W., de Vries, R. P., et al. (2014). Resolving the polyphyletic nature of *Pyricularia* (*Pyriculariaceae*). *Stud. Mycol.* 79, 85–120. doi: 10.1016/j.simyco.2014.09.004

Liu, W. T., Chen, J. J., Feng, J. W., Xia, C. Y., Shao, Y. X., Zhu, Y. X., et al. (2021). Diversity of endophytic fungi associated with plants of Poaceae from Yunnan, Zhejiang and Inner Mongolia. *Mycosystema* 40, 1–11. doi: 10.13346/j.mycosystema.200240

Luo, J., Qiu, H., Cai, G., Wagner, N. E., Bhattacharya, D., and Zhang, N. (2015a). Phylogenomic analysis uncovers the evolutionary history of nutrition and infection mode in rice blast fungus and other Magnaporthales. *Sci. Rep.* 5:9448. doi: 10.1038/srep09448

Luo, J., Walsh, E., Blystone, D., and Zhang, N. (2015b). Five new *Pseudophialophora* species from grass roots in the oligotrophic pine barrens ecosystem. *Fungal Biol.* 119, 1205–1215. doi: 10.1016/j.funbio.2015.08.016

Luo, J., Walsh, E., and Zhang, N. (2014). Four new species in *Magnaporthaceae* from grass roots in New Jersey Pine Barrens. *Mycologia* 106, 580–588. doi: 10.3852/13-306

Luo, J., Walsh, E., and Zhang, N. (2017). Toward monophyletic generic concepts in Magnaporthales: species with *Harpophora* asexual states. *Mycologia* 107, 641–646. doi: 10.3852/14-302

Luo, J., and Zhang, N. (2013). Magnaporthiopsis, a new genus in Magnaporthaceae (*Ascomycota*). *Mycologia* 105, 1019–1029. doi: 10.3852/12-359

Luo, Z., Hyde, K. D., Liu, J. J., Maharachchikumbura, S. S. N., Jeewon, R., Bao, D.-F., et al. (2019). Freshwater sordariomycetes. *Fungal Divers.* 99, 451–660. doi: 10.1007/s13225-019-00438-1

Maharachchikumbura, S. S. N., Hyde, K. D., Jones, E. B. G., McKenzie, E. H. C., Bhat, J. D., Dayarathne, M. C., et al. (2016). Families of sordariomycetes. *Fungal Divers.* 79, 1–317. doi: 10.1007/s13225-016-0369-6

Marcel, S., Sawers, R., Oakeley, E., Angliker, H., and Paszkowski, U. (2010). Tissue-adapted invasion strategies of the rice blast fungus magnaporthe oryzae. *Plant Cell* 22, 3177–3187. doi: 10.1105/tpc.110.078048

Matheny, P. B., Liu, Y., Ammirati, J. F., and Hall, B. D. (2002). Using RPB1 sequences to improve phylogenetic inference among mushrooms (*Inocybe*, *Agaricales*). *Am. J. Bot.* 89, 688–698. doi: 10.3732/ajb.89.4.688

Minh, B. Q., Schmidt, H. A., Chernomor, O., Schrempf, D., Woodhams, M. D., von Haeseler, A., et al. (2020). IQ-TREE 2: new models and efficient methods for phylogenetic inference in the genomic era. *Mol. Biol. Evol.* 37, 1530–1534. doi: 10.1093/molbev/msaa015

Nelson, A., Vandegrift, R., Carroll, G. C., and Roy, B. A. (2020). Double lives: transfer of fungal endophytes from leaves to woody substrates. *PeerJ* 8:e9341. doi: 10.7717/peerj.9341

Rehner, S. A., and Samuels, G. J. (1995). Molecular systematics of the hypocreales - a teleomorph gene phylogeny and the status of their anamorphs. *Canad. J. Bot.* 73, 816–823. doi: 10.1139/b95-327

Rodriguez, R. J., White, J. J., Arnold, A. E., and Redman, R. S. (2009). Fungal endophytes: diversity and functional roles. *New Phytol.* 182, 314–330. doi: 10.1111/j.1469-8137.2009.02773.x

Schmitt, I., Crespo, A., Divakar, P. K., Fankhauser, J. D., Herman-Sackett, E., Kalb, K., et al. (2009). New primers for promising single-copy genes in fungal phylogenetics and systematics. *Persoonia* 23, 35–40. doi: 10.3767/003158509X470602

Sesma, A., and Osbourn, A. E. (2004). The rice leaf blast pathogen undergoes developmental processes typical of root-infecting fungi. *Nature* 431, 582–586. doi: 10.1038/nature02880

Shearer, C. A., Crane, J. L., and Chen, W. (1999). Freshwater ascomycetes: *Ophioceras* species. *Mycologia* 91, 145–156. doi: 10.1080/00275514.1999.12061004

Song, J., Liang, J., Mehrabi-Koushki, M., Krisai-Greilhuber, I., Ali, B., Bhatt, V. K., et al. (2019). Fungal systematics and evolution: FUSE 5. *Sydowia* 71, 141–245. doi: 10.12905/0380.sydowia71-2019-0141

Spanu, P. D. (2012). "The genomics of obligate (and Nonobligate) biotrophs. *Annu. Rev. Phytopathol.* 50, 91–109. doi: 10.1146/annurev-phyto-081211-173024

Thongkantha, S., Jeewon, R., Vijaykrishna, D., Lumyong, S., McKenzie, E., and Hyde, K. (2009). Molecular phylogeny of *Magnaporthaceae* (*Sordariomycetes*) with a new species *Ophioceras chiangdaoense* from *Dracaena loureiroi* in Thailand. *Fungal Divers.* 34, 157–173.

Vaidya, G., Lohman, D. J., and Meier, R. (2011). SequenceMatrix: concatenation software for the fast assembly of multi-gene datasets with character set and codon information. *Cladistics* 27, 171–180. doi: 10.1111/j.1096-0031.2010.00329.x

Valent, B. (1990). Rice blast as a model system for plant pathology. *Phytopathology* 80, 33–36. doi: 10.1094/Phyto-80-33

Vu, D., Groenewald, M., de Vries, M., Gehrmann, T., Stielow, B., Eberhardt, U., et al. (2019). Large-scale generation and analysis of filamentous fungal DNA barcodes boosts coverage for kingdom fungi and reveals thresholds for fungal species and higher taxon delimitation. *Stud. Mycol.* 92, 135–154. doi: 10.1016/j.simyco.2018.05.001

White, T. J., Bruns, S., Lee, S., and Taylor, J. (1990). "Amplification and direct sequencing of fungal genes for phylogenetics," in *PCR Protocols: A Guide to Methods and Applications*, eds M. Innis, D. H. Gelfand, J. J. Sninsky, and T. J. White (San Diego, CA: Academic Press), 315–322. doi: 10.1016/b978-0-12-372180-8.50042-1

Wijayawardene, N. N., Hyde, K. D., Al-Ani, L. K. T., Tedersoo, L., Haelewaters, D., Rajeshkumar, K. C., et al. (2020). Outline of fungi and fungus-like taxa. *Mycosphere* 11, 1060–1456. doi: 10.5943/mycosphere/11/1/8

Xu, X., Su, Z., Wang, C., Kubicek, C. P., Feng, X. X., Mao, L. J., et al. (2014). The rice endophyte *Harpophora* oryzae genome reveals evolution from a pathogen to a mutualistic endophyte. *Sci. Rep.* 4:5783. doi: 10.1038/srep05783

Xu, X., Wang, C., Li, S., Su, Z., Zhou, N. H., Mao, L. J., et al. (2015). Friend or foe: differential responses of rice to invasion by mutualistic or pathogenic fungi revealed by RNAseq and metabolite profiling. *Sci. Rep.* 5:13624. doi: 10.1038/srep13624

Yuan, Z. L., Lin, F. C., Zhang, C. L., and Kubicek, C. P. (2010). A new species of *Harpophora* (*Magnaporthaceae*) recovered from healthy wild rice (*Oryza granulata*) roots, representing a novel member of a beneficial dark septate endophyte. *FEMS Microbiol. Lett.* 307, 94–101. doi: 10.1111/j.1574-6968.2010.01963.x

Zhang, H., Zheng, X., and Zhang, Z. (2016). The *Magnaporthe grisea* species complex and plant pathogenesis. *Mol. Plant Pathol.* 17, 796–804. doi: 10.1111/mpp.12342

Zhang, N., Cai, G., Price, D. C., Crouch, J. A., Gladieux, P., Hillman, B., et al. (2018). Genome wide analysis of the transition to pathogenic lifestyles in magnaporthales fungi. *Sci. Rep.* 8:5862. doi: 10.1038/s41598-018-24301-6

Zhang, N., Zhao, S., and Shen, Q. (2011). A six-gene phylogeny reveals the evolution of mode of infection in the rice blast fungus and allied species. *Mycologia* 103, 1267–1276. doi: 10.3852/11-022

Conflict of Interest: The authors declare that the research was conducted in the absence of any commercial or financial relationships that could be construed as a potential conflict of interest.

Copyright © 2021 Feng, Liu, Chen and Zhang. This is an open-access article distributed under the terms of the Creative Commons Attribution License (CC BY). The use, distribution or reproduction in other forums is permitted, provided the original author(s) and the copyright owner(s) are credited and that the original publication in this journal is cited, in accordance with accepted academic practice. No use, distribution or reproduction is permitted which does not comply with these terms.

frontiers in Microbiology

ORIGINAL RESEARCH
published: 07 May 2021
doi: 10.3389/fmicb.2021.656235

Reappraisal of *Immotthia* in Dictyosporiaceae, Pleosporales: Introducing *Immotthia bambusae* sp. nov. and *Pseudocyclothyriella clematidis* comb. et gen. nov. Based on Morphology and Phylogeny

Hong-Bo Jiang[1,2,3], Rajesh Jeewon[4], Samantha C. Karunarathna[1,5,6,7,8], Chayanard Phukhamsakda[9], Mingkwan Doilom[5,10], Pattana Kakumyan[3], Nakarin Suwannarach[5,11], Rungtiwa Phookamsak[1,5,6,7,8] and Saisamorn Lumyong[5,11,12]**

[1] CAS Key Laboratory for Plant Diversity and Biogeography of East Asia, Kunming Institute of Botany, Chinese Academy of Sciences, Kunming, China, [2] Center of Excellence in Fungal Research, Mae Fah Luang University, Chiang Rai, Thailand, [3] School of Science, Mae Fah Luang University, Chiang Rai, Thailand, [4] Department of Health Sciences, Faculty of Medicine and Health Sciences, University of Mauritius, Réduit, Mauritius, [5] Research Center of Microbial Diversity and Sustainable Utilization, Faculty of Sciences, Chiang Mai University, Chiang Mai, Thailand, [6] CIFOR-ICRAF China Program, World Agroforestry (ICRAF), Kunming, China, [7] Honghe Center for Mountain Futures, Kunming Institute of Botany, Chinese Academy of Sciences, Honghe, China, [8] Centre for Mountain Futures (CMF), Kunming Institute of Botany, Kunming, China, [9] Engineering Research Center of Chinese Ministry of Education for Edible and Medicinal Fungi, Jilin Agricultural University, Changchun, China, [10] Innovative Institute of Plant Health, Zhongkai University of Agriculture and Engineering, Guangzhou, China, [11] Department of Biology, Faculty of Science, Chiang Mai University, Chiang Mai, Thailand, [12] Academy of Science, The Royal Society of Thailand, Bangkok, Thailand

Immotthia is a poorly known genus, and currently, no DNA sequence data are available to ascertain its proper phylogenetic placement and evolutionary relationships with other bitunicate fungi. To date, there are only two species accepted in the genus. During our ongoing research study of bambusicolous fungi in southwest China and Thailand, a fungus associated with stromata of *Hypoxylon* sp. was found on dead bamboo culms in Loei Province, Thailand. Preliminary morphological identification revealed that the fungal collection belongs to *Immotthia*. A novel species, *Immotthia bambusae*, is introduced herein based on a comparison of morphological characteristics with the type specimen of *I. hypoxylon* (≡ *Amphisphaeria hypoxylon* Ellis and Everh.), a synonym of *I. atrograna* (Cooke and Ellis) M. E. Barr. Phylogenetic analyses of a concatenated ITS, LSU, SSU, and TEF1-α DNA sequence matrix showed that *Immotthia* belongs to Dictyosporiaceae, Pleosporales. Despite *I. bambusae* strains constituting a supported subclade, they are nested with the genus *Pseudocoleophoma*. *Pseudocoleophoma clematidis* is morphologically different from all other *Pseudocoleophoma* species, while its conidial characteristics are similar to *Cyclothyriella*. Multigene phylogenetic analyses showed that *P. clematidis* formed a clade basal to *Immotthia*, separated from *Pseudocoleophoma* with strong statistical support. Therefore, we introduce a monotypic genus, *Pseudocyclothyriella* Phukhams. and Phookamsak, gen. nov. to

OPEN ACCESS

Edited by:
Jadson Diogo Pereira Bezerra, Universidade Federal de Goiás, Brazil

Reviewed by:
Sinang Hongsanan, Shenzhen University, China
Roger Melo, Federal University of Pernambuco, Brazil

***Correspondence:**
Rungtiwa Phookamsak
jomjam.rp2@gmail.com
Saisamorn Lumyong
scboi009@gmail.com

Specialty section:
This article was submitted to Evolutionary and Genomic Microbiology, a section of the journal Frontiers in Microbiology

Received: *20 January 2021*
Accepted: *22 March 2021*
Published: *07 May 2021*

Citation:
Jiang H-B, Jeewon R, Karunarathna SC, Phukhamsakda C, Doilom M, Kakumyan P, Suwannarach N, Phookamsak R and Lumyong S (2021) Reappraisal of Immotthia in Dictyosporiaceae, Pleosporales: Introducing Immotthia bambusae sp. nov. and Pseudocyclothyriella clematidis comb. et gen. nov. Based on Morphology and Phylogeny. Front. Microbiol. 12:656235. doi: 10.3389/fmicb.2021.656235

accommodate the single species, *Pseudocyclothyriella clematidis* (Phukhams. and K. D. Hyde) Phukhams. and Phookamsak, comb. nov. Detailed descriptions, color micrographs, and phylogenetic trees to show the placement of the new taxa are provided. In addition, an updated taxonomic treatment of the genera *Immotthia* and *Pseudocyclothyriella* is also provided based on the study of the type materials and phylogeny generated from DNA sequence data.

Keywords: bambusicolous fungi, Dothideomycetes, *Pseudocoleophoma*, taxonomy, two new taxa

INTRODUCTION

Immotthia was introduced by Barr (1987a) with *I. hypoxylon* (Ellis and Everh.) M. E. Barr (≡ *Amphisphaeria hypoxylon* Ellis and Everh.) as the type species. Through examinations of the type material of *I. hypoxylon* and Australian collections of *I. atrograna* (Cooke and Ellis) M. E. Barr (≡ *Sphaeria atrograna* Cooke and Ellis), Jaklitsch et al. (2002) concluded that these two taxa are conspecific. To date, two species are accepted in this genus, viz. *I. atrograna* and *I. atroseptata* (Piroz.) M. E. Barr (Species Fungorum, 2020) based on morphology, but no DNA sequence data are available to confirm their phylogenetic placement (Hyde et al., 2017; Doilom et al., 2018).

Immotthia is characterized by small- to medium-sized, globose to subglobose ascomata, forming on blackened hypostroma, bitunicate, fissitunicate, cylindrical asci, and brown to reddish brown, ellipsoidal to fusiform, 1-septate, smooth or slightly verrucose ascospores (Hyde et al., 2017; Hongsanan et al., 2020). The asexual morph of *Immotthia* has been reported as coelomycetous, identified as *Coniothyrium parasitans* (Berk. and Ravenel) Tassi which formed enteroblastic, phialidic, doliiform to ampulliform, or cylindrical, smooth, hyaline conidiogenous cells bearing brown, ellipsoidal, smooth, and aseptate conidia (Hyde et al., 2017; Hongsanan et al., 2020). However, the link between *Immotthia* and *C. parasitans* has not yet been proven based on DNA sequence analyses. *Immotthia* has been reported as hyperparasites on stromata of *Annulohypoxylon*, *Hypoxylon*, and *Pestalopezia*, or forms compressed ascostromata on decorticated wood (Cooke and Ellis, 1879; Ellis and Everhart, 1886; Pirozynski, 1973; Jaklitsch et al., 2002; Akulov and Hayova, 2016; Hyde et al., 2017; Hongsanan et al., 2020).

Immotthia was assigned to Dacampiaceae (Pleosporales, Dothideomycetes) by Barr (1987a,b) and this taxonomic treatment was followed by Akulov and Hayova (2016). Barr (2002) transferred non-lichenicolous genera from the Dacampiaceae to Teichosporaceae (Pleosporales, Dothideomycetes), where *Immotthia* was also included along and transferred to Teichosporaceae. Recently, *Immotthia* was tentatively placed in Roussoellaceae (Pleosporales, Dothideomycetes) based on similar morphological features of the asci, ascospores, and coelomycetous asexual morph which largely resemble taxa in Roussoellaceae (Hyde et al., 2017; Doilom et al., 2018; Hongsanan et al., 2020).

A well-studied genus *Pseudocoleophoma* Kaz. Tanaka and K. Hiray. was introduced by Tanaka et al. (2015) to accommodate two novel species having asexual morphology similar to *Coleophoma* from Japan. The genus is characterized by scattered to clustered, immersed to erumpent, globose to subglobose ascomata, with ostiolar neck, thin-walled peridium, composed of brown to dark brown, polygonal to rectangular cells, cylindrical to clavate, fissitunicate asci, with short-pedicellate, and hyaline, fusiform, 1-septate ascospores, with a conspicuous sheath (Tanaka et al., 2015; Jayasiri et al., 2019). *Pseudocoleophoma* has coelomycetous, coleophoma-like asexual morphs forming pycnidial, subglobose conidiomata, phialidic, doliiform to lageniform conidiogenous cells, and cylindrical or oblong, hyaline, aseptate, smooth-walled conidia (Tanaka et al., 2015). The genus belongs to Dictyosporiaceae based on phylogenetic evidence (Tanaka et al., 2015).

Two holomorphic species, *Pseudocoleophoma calamagrostidis* Kaz. Tanaka and K. Hiray. and *P. polygonicola* Kaz. Tanaka and K. Hiray., were initially accommodated in this genus (Tanaka et al., 2015). Later, six other species were accommodated based on morphological and phylogenetic support, viz. *P. bauhiniae* Jayasiri, E. B. G. Jones and K. D. Hyde (on *Bauhinia* sp., Thailand); *P. clematidis* Phukhams. and K. D. Hyde (on *Clematis vitalba*, Italy); *P. flavescens* (Gruyter, Noordel. and Boerema) W. J. Li and K. D. Hyde (from soil, rhizosphere of *Solanum tuberosum*, Netherlands); *P. rusci* W. J. Li, Camporesi and K. D. Hyde (on *Ruscus aculeatus*, Italy); *P. typhicola* Kamolhan, Banmai, Boonmee, E. B. G. Jones and K. D. Hyde (on decaying submerged *Typha latifolia*, Great Britain); and *P. zingiberacearum* Tennakoon, D. J. Bhat, C. H. Kuo and K. D. Hyde (on *Hedychium coronarium*, Taiwan) (Tanaka et al., 2015; Hyde et al., 2016; Jayasiri et al., 2019; Tennakoon et al., 2019; Li et al., 2020; Phukhamsakda et al., 2020).

Most of the *Pseudocoleophoma* species have been represented by their asexual morphs (Hyde et al., 2016; Tennakoon et al., 2019; Li et al., 2020; Phukhamsakda et al., 2020). Only three species have been reported for both sexual and asexual morphs, viz. *P. bauhiniae*, *P. calamagrostidis*, and *P. polygonicola* (Tanaka et al., 2015; Jayasiri et al., 2019). Currently, species of *Pseudocoleophoma* are only known from Europe (Great Britain, Italy, and Netherlands) and Asia (Taiwan and Thailand), and they were found as saprobes on various hosts and substrates from both terrestrial and freshwater habitats (Tanaka et al., 2015; Hyde et al., 2016; Jayasiri et al., 2019; Tennakoon et al., 2019; Li et al., 2020; Phukhamsakda et al., 2020).

In the present study, a fresh collection of *Immotthia* is examined and compared with other *Immotthia* species based on morphological characteristics. The new collection is described as a novel species in *Immotthia* and illustrated. Through

DNA sequencing of the fresh material, we also resolved the phylogenetic placement of *Immotthia* for the first time, based on maximum likelihood and Bayesian inference analyses. In addition, the novel genus *Pseudocyclothyriella* is also introduced to accommodate *Pseudocyclothyriella clematidis* comb. nov. (≡ *Pseudocoleophoma clematidis*) based on morphological distinctiveness and multigene phylogenetic analyses.

MATERIALS AND METHODS

Sample Collection, Specimen Examination, and Preservation

Dead bamboo culms were collected from Loei Province, Thailand, in 2020. The specimens were kept in a paper bag and returned to the laboratory for observation and examination. Fungal fruiting bodies on the host substrate were observed with a Motic SMZ 140 series dissecting stereoscope, and a centrum was mounted in sterilized distilled water for morphological examination and captured using a Nikon ECLIPSE Ni compound microscope connected with a Canon EOS 600D digital camera. Tarosoft (R) Image Frame Work version 0.9.7 was used to measure the size of ascomata, peridium, pseudoparaphyses, asci, and ascospores. In addition, holotypic specimens of *Immotthia atroseptata* [United States, North Carolina, behind N. C. Department of Agriculture, Nursery Inspection Station, 1 mile west of Linville, Avery Co., on apothecia of *Pestalopezia rhododendri* on the leaves of *Rhododendron maximum* L. (Ericaceae), March 21, 1972, Neli Lapp DAOM 139001], *I. hypoxylon* (United States, Louisiana, Plaquemines Parish, on decaying wood, December 30, 1885, A. B. Langlois 138, NY0083004), and *Pseudocoleophoma clematidis* (Italy, Arezzo Province, Badia Tega—Ortignano Raggiolo, on dead aerial branch of *Clematis vitalba*, March 9, 2013, E. Camporesi, IT 1110, MFLU 16-0280) were also re-examined and illustrated. Adobe Photoshop CS6 software (Adobe Systems Inc., United States) was used to edit and provide the photographic plates based on captured pictures of the fungal structures. Good practices for morphological examinations as outlined by Senanayake et al. (2020b) were followed for the morphological study, while phylogenetic methods as outlined by Dissanayake et al. (2020) were followed for phylogenetic analyses. The holotype is deposited in the herbarium of Cryptogams Kunming Institute of Botany Academia Sinica (KUN-HKAS), Yunnan, China. The isotype was stored in Herbarium Mycologicum Academiae Sinicae (HMAS), Beijing, China. The Facesoffungi and Index Fungorum numbers are registered for the newly described taxa (Jayasiri et al., 2015; Index Fungorum, 2020). New species are established based on the guidelines provided by Jeewon and Hyde (2016).

DNA Extraction, PCR Amplification, and Sequencing

Fungal genomic DNA was extracted from fruiting bodies using Forensic DNA Kit (Omega®, United States) following the manufacturer's instructions and protocols outlined by Doilom et al. (2017) and Zeng et al. (2018). DNA was extracted from five duplicates of different fruiting bodies on the holotypic specimen of *Immotthia bambusae* (KUN-HKAS 112012) to allow verification of correct DNA sequence data. DNA amplification was performed by polymerase chain reaction (PCR). The primer pairs ITS5/ITS4 (White et al., 1990), LR0R/LR5 (Vilgalys and Hester, 1990), NS1/NS4 (White et al., 1990), and EF1-983F/EF1-2218R (Rehner, 2001) were used to amplify the PCR fragments of the internal transcribed spacers (ITS1-5.8S-ITS2), the 28S large subunit rDNA (LSU), the 18S small subunit rDNA (SSU), and the translation elongation factor 1-alpha (TEF1-α), respectively. PCR reactions were conducted in 25 μl total volume containing 2 μl of fungal genomic DNA template, 1 μl of each forward and reverse primer, 12.5 μl of 2 × Power Taq PCR Master Mix (mixture of EasyTaq™ DNA Polymerase, dNTPs, and optimized buffer; Beijing BioTeke Corporation, China), and 8.5 μl of sterilized double-distilled water (ddH_2O). The PCR thermal cycle profiles for ITS, LSU, SSU, and TEF1-α gene were set up following Jiang H. B. et al. (2020). PCR products were sent to TsingKe Biological Technology (Beijing) Co., Ltd., China, for PCR purification and sequencing.

Alignment and Phylogenetic Analyses

The newly generated ITS, LSU, SSU and TEF1-α sequences of the new taxon were subjected to the BLASTn search tool[1] for initial verification and search of reference taxa for further analyses. Similarity indices based on BLASTn search showed that five new strains are closely related to *Pseudocoleophoma* Kaz. Tanaka and K. Hiray (Dictyosporiaceae, Pleosporales). In order to investigate the phylogenetic status of the new taxa, a combined dataset of taxa including members of the Dictyosporiaceae was analyzed based on DNA sequence data available in recent publications (Iturrieta-González et al., 2018; Yang et al., 2018; Hyde et al., 2020a,b; Phukhamsakda et al., 2020). DNA sequences of representative taxa used are shown in **Table 1**. Individual DNA sequence alignments were initially performed *via* the online platform MAFFT v. 7.474[2] (Katoh et al., 2019) and were improved manually using BioEdit v. 5.0.6 (Hall, 2001). Preliminary phylogenetic analyses of a concatenated LSU–SSU–TEF1-α–RPB2–ITS sequence matrix represented the relationships of *Immotthia* in Dictyosporiaceae with other families in Pleosporales (**Supplementary Figure 3**), and a concatenated ITS–LSU–TEF1-α sequence dataset (**Supplementary Figure 1**) was also analyzed by maximum-likelihood (ML) analysis *via* the web portal CIPRES Science Gateway v. 3.3 (Miller et al., 2010), with the help of the tool RAxML-HPC v.8 on XSEDE (8.2.12).

ML analysis using the GAMMA model of nucleotide substitution was performed *via* the web portal CIPRES Science Gateway v.3.3 (Miller et al., 2010), with the help of the tool RAxML-HPC v.8 on XSEDE (8.2.12). The evolutionary model of nucleotide substitution for Bayesian inference (BI) analysis was selected independently for each locus using MrModeltest 2.3 (Nylander, 2008). GTR + I + G is the best fit for ITS and LSU loci under the Akaike information criterion (AIC), while

[1]https://blast.ncbi.nlm.nih.gov/Blast.cgi

[2]https://mafft.cbrc.jp/alignment/server/

TABLE 1 | Taxa names, strain numbers, and GenBank accession numbers of taxa used for the present phylogenetic analyses.

Taxa names	Strain/voucher no.	GenBank accession numbers			
		ITS	LSU	SSU	TEF1-α
Aquadictyospora clematidis	**MFLUCC 17-2080**	MT310592	MT214545	NG_070646	MT394727
Aquadictyospora lignicola	**MFLU 17-1422**	NR_157487	NG_064471	/	MF953164
Aquaticheirospora lignicola	**HKUCC10304**	AY864770	AY736378	AY736377	/
Cheirosporium triseriale	**HMAS 180703**	EU413953	EU413954	/	/
Dendryphiella eucalyptorum	**CBS 137987**	KJ869139	KJ869196	/	/
Dendryphiella fasciculata	**MFLUCC 17-1074**	NR_154044	NG_059177	/	/
Dendryphiella paravinosa	**CPC 26176**	NR_154012	NG_059137	/	/
Dendryphiella phitsanulokensis	**MFLUCC 17-2513**	NR_159827	NG_064502	NG_065729	/
Dendryphiella variabilis	**CBS 584.96**	NR_160584	LT963454	/	/
Dictyocheirospora bannica	**KH 332**	NR_154039	NG_059061	NG_064841	AB808489
Dictyocheirospora garethjonesii	**MFLUCC 16-0909**	KY320509	KY320514	/	/
Dictyocheirospora garethjonesii	DLUCC 0848	MF948623	MF948631	/	MF953166
Dictyocheirospora indica	MFLUCC 15-0056	MH381763	MH381772	MH381757	MH388817
Dictyocheirospora pseudomusae	**yone 234**	LC014550	AB807520	AB797230	AB808496
Dictyocheirospora rotunda	MFLU 18-1041	MH381764	MH381773	MH381758	MH388818
Dictyocheirospora rotunda	**MFLUCC 14-0293**	KU179099	KU179100	KU179101	/
Dictyosporium appendiculatum	**MFLUCC 17-2259**	NR_168192	MH376715	/	/
Dictyosporium bulbosum	yone 221	LC014544	AB807511	AB797221	AB808487
Dictyosporium digitatum	KH 401	LC014545	AB807515	AB797225	AB808491
Dictyosporium digitatum	yone 280	LC014547	AB807512	AB797222	AB808488
Dictyosporium elegans	**NBRC 32502**	DQ018087	DQ018100	DQ018079	/
Dictyosporium meiosporum	**MFLUCC 10-0131**	KP710944	KP710945	KP710946	/
Dictyosporium olivaceosporum	**KH 375**	LC014542	AB807514	AB797224	AB808490
Dictyosporium tratense	**MFLUCC 17-2052**	MH381767	MH381776	MH381761	MH388820
Dictyosporium tubulatum	**MFLUCC 15-0631**	MH381769	MH381778	/	MH388822
Digitodesmium bambusicola	**CBS 110279**	DQ018091	DQ018103	/	/
Gregarithecium curvisporum	**KT 922**	NR_154049	NG_059394	NG_061002	AB808523
Immotthia bambusae	**KUN-HKAS 112012AI**	MW489455	MW489450	MW489461	MW504646
Immotthia bambusae	**KUN-HKAS 112012AII**	MW489456	MW489451	MW489462	MW504647
Immotthia bambusae	**KUN-HKAS 112012B**	MW489457	MW489452	/	/
Immotthia bambusae	**KUN-HKAS 112012C**	MW489458	MW489453	MW489463	MW504648
Immotthia bambusae	**KUN-HKAS 112012D**	MW489459	MW489454	MW489464	MW504649
Jalapriya pulchra	**MFLUCC 15-0348**	KU179108	KU179109	KU179110	/
Jalapriya pulchra	MFLUCC 17-1683	MF948628	MF948636	/	MF953171
Jalapriya toruloides	**CBS 209.65**	DQ018093	DQ018104	DQ018081	/
Neodendryphiella mali	FMR 17003	LT993734	LT993735	/	/
Neodendryphiella mali	**FMR 16561**	LT906655	LT906657	/	/
Neodendryphiella michoacanensis	**FMR 16098**	NR_160583	NG_066395	/	/
Neodendryphiella tarraconensis	**FMR 16234**	NR_160582	NG_066394	/	/
Periconia igniaria	CBS 845.96	LC014586	AB807567	AB797277	AB808543
Periconia igniaria	CBS 379.86	LC014585	AB807566	AB797276	AB808542
Pseudocoleophoma bauhiniae	**MFLUCC 17-2586**	MK347736	MK347953	MK347844	MK360076
Pseudocoleophoma calamagrostidis	**KT 3284**	NR_154375	NG_059804	NG_061264	LC014614
Pseudocoleophoma flavescens	CBS 178.93	/	GU238075	GU238216	/
Pseudocoleophoma polygonicola	**KT 731**	NR_154274	NG_059393	NG_064848	AB808522
Pseudocoleophoma rusci	**MFLUCC 16-1444**	NR_170045	MT183514	NG_070346	/
Pseudocoleophoma typhicola	**MFLUCC 16-0123**	NR_154350	KX576656	/	/
Pseudocoleophoma zingiberacearum	**NCYUCC 19-0052**	MN615939	MN616753	/	MN629281
Pseudoconiothyrium broussonetiae	**CBS 145036**	NR_163377	NG_066331	/	/

(Continued)

TABLE 1 | Continued

Taxa names	Strain/voucher no.	GenBank accession numbers			
		ITS	LSU	SSU	TEF1-α
Pseudocyclothyriella clematidis "*Pseudocoleophoma clematidis*"	**MFLU 16-0280**	MT310596	MT214549	/	/
Pseudocyclothyriella clematidis *"Pseudocoleophoma clematidis"*	**MFLUCC 17-2177A**	MT310595	MT214548	MT226667	MT394730
Pseudodictyosporium elegans	**CBS 688.93**	NR_137148	NG_057743	NG_062684	/
Pseudodictyosporium indicum	CBS 471.95	DQ018097	/	/	/
Pseudodictyosporium thailandica	**MFLUCC 16-0029**	NR_154347	NG_059688	NG_063611	KX259526
Pseudodictyosporium wauense	**DLUCC 0801**	MF948622	MF948630	/	MF953165
Vikalpa australiense	HKUCC 8797	DQ018092	/	/	/

CBS, Culture Collection of the Westerdijk Fungal Biodiversity Institute, Utrecht, Netherlands; CPC, Culture Collection of Pedro Crous, Netherlands; DLUCC, Dali University Culture collection, Yunnan, China; FMR, Facultat de Medicina, Universitat Rovira i Virgili, Reus, Spain; HKUCC, Hong Kong University Culture Collection, Hong Kong, China; HMAS, Herbarium Mycologicum Instituti Microbiologici, Academiae Sinicae, Beijing, China; KH, K. Hirayama; KUN-HKAS, Herbarium of Cryptogams Kunming Institute of Botany Academia Sinica, Yunnan, China; KT, K. Tanaka; MFLU, the Herbarium of Mae Fah Luang University, Chiang Rai, Thailand; MFLUCC, Mae Fah Luang University Culture Collection, Chiang Rai, Thailand; NBRC, Biological Resource Center, National Institute of Technology and Evaluation, Chiba, Japan; NCYUCC, National Chiayi University Culture Collection, Taiwan, China; yone, H. Yonezawa.
The newly generated sequences and the ex-type strains are in black bold.

the HKY + I substitution model is the best fit for SSU and TEF1-α loci. BI analysis was carried out by MrBayes v. 3.2.6 (Ronquist and Huelsenbeck, 2003). Markov chain Monte Carlo sampling (MCMC) was used to decide posterior probabilities (PP) (Rannala and Yang, 1996; Zhaxybayeva and Gogarten, 2002). Six simultaneous Markov chains were run for 1,000,000 generations and trees were sampled every 100th generation. The 0.15 "temperature" value was set in the MCMC heated chain. All sampled topologies beneath the asymptote (20%) were discarded as part of a burn-in procedure, and the remaining 8,000 trees were used for calculating posterior probabilities (PP) in the 50% majority rule consensus tree (when the split frequency was lower than 0.01). Tree topology of BI analysis is represented in **Supplementary Figure 2**.

Tree topologies generated in this study were visualized on FigTree v. 1.4.0[3], and Microsoft Office PowerPoint 2016 (Microsoft Inc., United States) was used to edit and redraw the phylogram. New sequences generated from the present study are deposited in GenBank (**Table 1**). The final alignment and phylogram were submitted in TreeBASE[4].

RESULTS

Taxonomy

Immotthia M. E. Barr, Mycotaxon 29: 504 (1987a), **Figure 1**.

Index Fungorum Number: IF 25106

Facesoffungi Number: FoF 08362

Hyperparasitic on *Annulohypoxylon*, *Hypoxylon*, and *Pestalopezia*, or *saprobic* on decorticated wood. *Sexual morph*: *Hypostroma* dark brown to black, crust under ascomata, patch-like, composed of thick-walled cells of *textura angularis*, covering the surface of host stromata, difficult to distinguished from the peridium of ascomata, sometimes forming dark brown hyphae at the lowest layer penetrated with the host of *Hypoxylon* which was interpreted to belong to the *Hypoxylon* host. *Ascomata* dark brown to black, subglobose to obpyriform, or inequilateral, gregarious to densely aggregated, superficial, uniloculate, or carbonaceous when dry, glabrous, surface rough with protruding cells, arising from a large hypostroma, usually with a pore-like, inconspicuous ostiole or minute papilla. *Peridium* thin- to thick-walled, of unequal thickness, composed of several layers, inner layers comprising hyaline to dark brown, pseudoparenchymatous cells, of *textura angularis*, outer layers composed of thick, dark brown to black cells, arranged in a *textura angularis*. *Hamathecium* composed of dense, septate, branched, anastomosing, cellular pseudoparaphyses embedded in a gelatinous matrix. *Asci* (4–) (6–)–8-spored, bitunicate, fissitunicate, cylindrical or cylindric-clavate, subsessile to short-pedicellate with obtuse knob-like or furcate pedicel, apically rounded with a well-developed ocular chamber. *Ascospores* overlapping 1–2-seriate, pale yellowish to brown, or reddish brown, ellipsoidal to fusiform, with rounded ends, 1-septate, asymmetrical, with the upper cell slightly larger than the lower cell, slightly constricted at the septum, smooth- to rough-walled, verrucose. *Asexual morph*: Coelomycetous, chaetophoma-, coniothyrium-, microsphaeropsis-, or pyrenochaeta-like, associated with the sexual morph on natural substrate. *Conidiomata* pycindial, similar to ascomata but differ in having a smaller size, black, carbonaceous, immersed to erumpent, becoming superficial, globose to obpyriform, uni- to multiloculate, glabrous, with indistinct ostiolate. *Pycnidial wall* thin- to thick-walled, composed of several layers of brown to dark brown pseudoparenchymatous cells, of *textura angularis*. *Conidiophores* reduced to conidiogenous cells. *Conidiogenous cells* enteroblastic, phialidic, discrete, determinate, ampulliform, or cylindric, smooth, hyaline, with minute collarette and conspicuous periclinal thickening. *Conidia* ellipsoidal, rounded at both ends, one-celled, at first hyaline, becoming brown at

[3]http://tree.bio.ed.ac.uk/software/figtree/

[4]https://www.treebase.org/, submission ID: 27606.

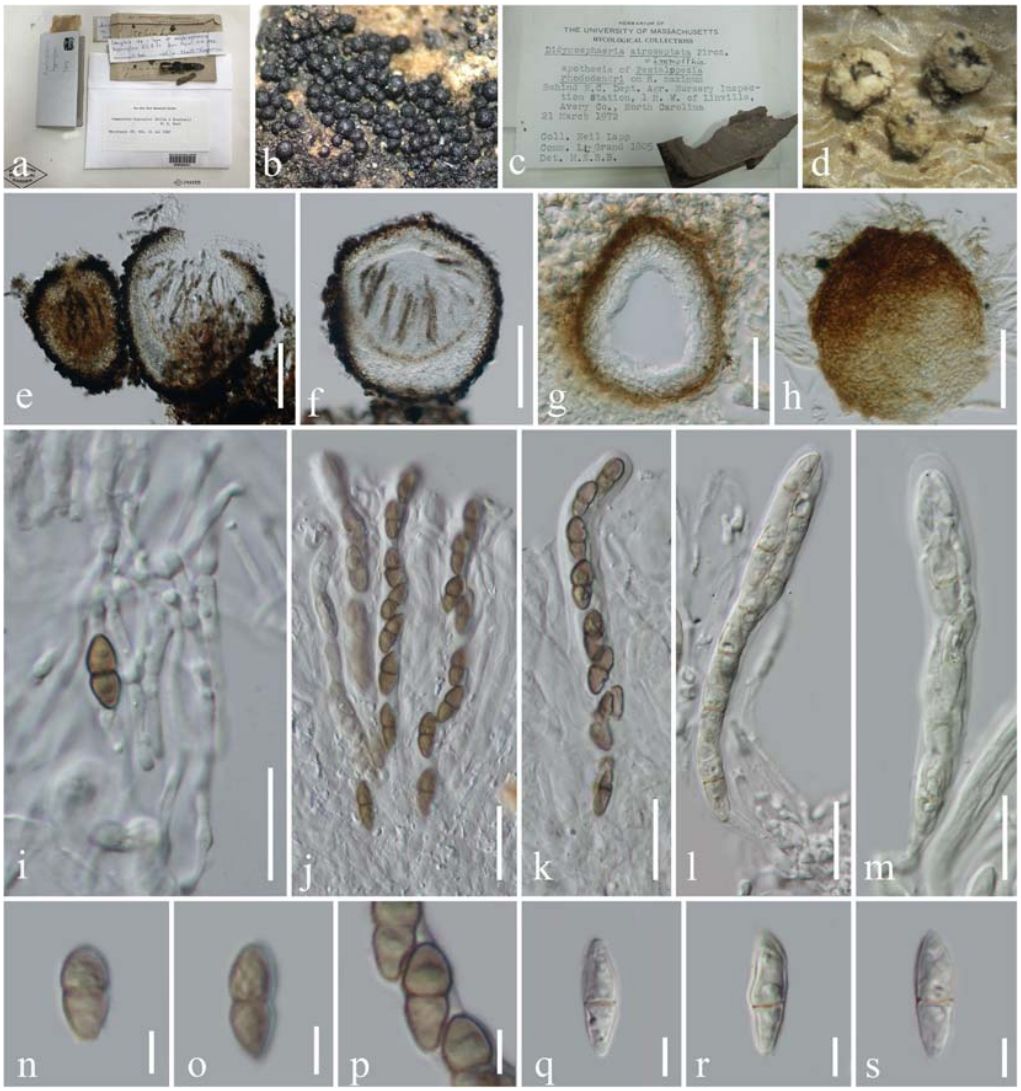


FIGURE 1 | Morphological characteristics of *Immotthia*. **(c,d,g,h,j,k,q–s)** *Immotthia atroseptata* (DAOM 13900; holotype of *Didymosphaeria atroseptata*). **(a,b,e,f,i–k,n–p)** *Immotthia hypoxylon* (NY00830041, holotype of *Amphisphaeria hypoxylon*). **(a,c)** Herbarium label and specimens. **(b,d)** Appearance of ascomata on host substrates. **(e–g)** Section through ascomata. **(h)** Exterior of ascoma. **(i)** Pseudoparaphyses. **(j–m)** Asci. **(n–s)** Ascospores. Scale bars: **(e,f)** = 100 μm, **(g,h)** = 30 μm, **(i–m)** = 20 μm, and **(n–s)** = 5 μm.

maturity, smooth-walled or finely verrucose (adapted from Jaklitsch et al., 2002; Akulov and Hayova, 2016; Hyde et al., 2017; Doilom et al., 2018).

Type Species: *Immotthia hypoxylon* (Ellis and Everh.) M. E. Barr, Mycotaxon 29: 504 (1987a).

≡ *Amphisphaeria hypoxylon* Ellis and Everh., J. Mycol. 2(4): 41 (1886).

Current Name: *Immotthia atrograna* (Cooke and Ellis) M. E. Barr (1993), Mycotaxon 46: 71.

≡ *Sphaeria atrograna* Cooke and Ellis, Grevillea 8(no. 45): 15 (1879).

Life Mode and Known Distribution: Hyperparasitic on *Annulohypoxylon*, *Hypoxylon*, and *Pestalopezia* on various host substrates and saprobic on decaying wood. *Immotthia* is presently known from Austria, Belgium, China, France, Lithuania, Norway, Poland, Puerto Rico, Russia, Sweden, Switzerland, Ukraine, United States, and Venezuela (Pirozynski, 1973; Jaklitsch et al., 2002; Akulov and Hayova, 2016; Hyde et al., 2017; Doilom et al., 2018; Farr and Rossman, 2020).

Notes: The phylogenetic affinities of *Immotthia* have never been investigated in previous studies, and the genus was accommodated in different families by different authors based only on morphological characteristics (Barr, 1987a, 2002; Jaklitsch et al., 2002; Akulov and Hayova, 2016; Hyde et al., 2017; Doilom et al., 2018). In the present study, *Immotthia* is phylogenetically close to *Pseudocoleophoma* in Dictyosporiaceae. The sexual morph of *Immotthia* differs from *Pseudocoleophoma* in morphology and habitat. *Immotthia* forms dense, superficial

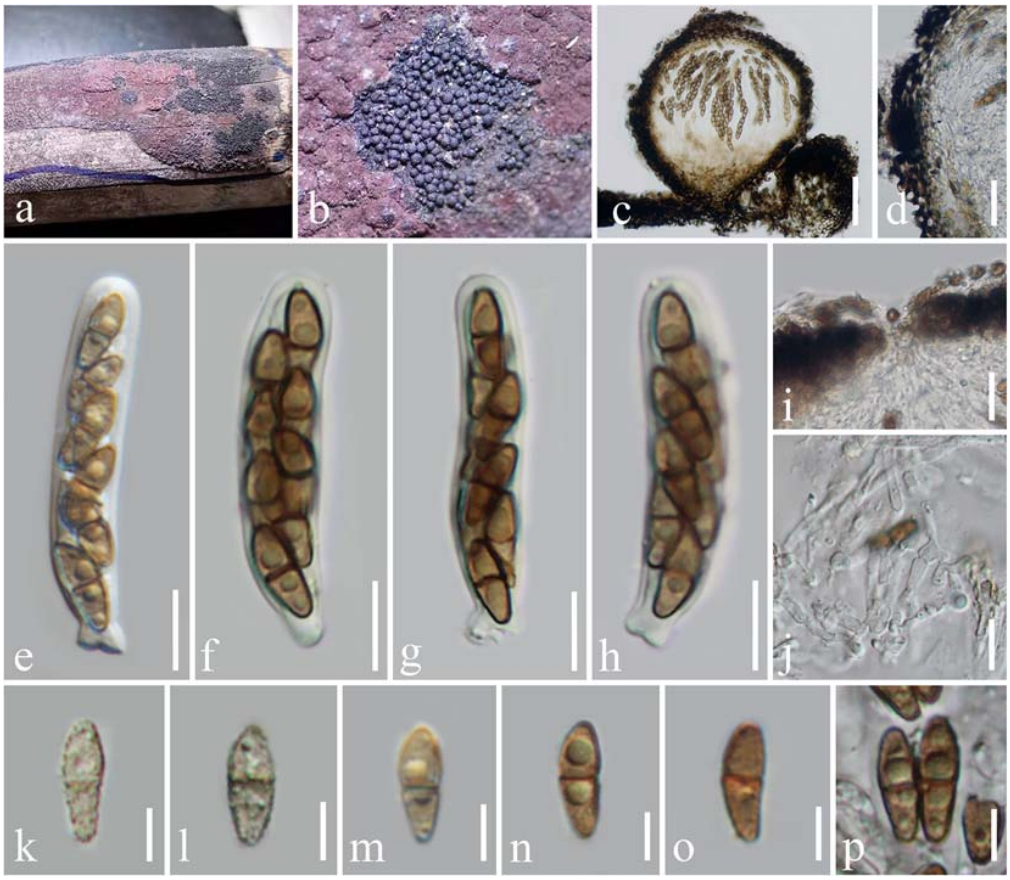


FIGURE 2 | *Immotthia bambusae* (KUN-HKAS 112012, holotype). **(a,b)** Appearance of hypostromata on *Hypoxylon* sp. associated with dead bamboo culms. **(c)** Vertical section of ascoma. **(d)** Peridium. **(e–h)** Asci. **(i)** Pore-like ostiole. **(j)** Pseudoparaphyses. **(k–p)** Ascospores. Scale bars: **(c)** = 50 μm, **(d)** = 20 μm, **(i)** = 15 μm, **(e–h,j)** = 10 μm, and **(k–p)** = 5 μm.

ascomata on hypostoma, with cylindrical to cylindric-clavate asci, ellipsoidal to fusiform, light brown to reddish brown, asymmetrical ascospores, lacking mucilaginous sheath and usually found as hyperparasites on hypoxylon-like stroma. On the other hand, *Pseudocoleophoma* forms scattered or in groups, immersed to erumpent ascomata, with cylindrical to clavate asci, fusiform, hyaline ascospores, surrounded by mucilaginous sheath, and mostly found as saprobes in a terrestrial environment (Tanaka et al., 2015; Jayasiri et al., 2019; Tennakoon et al., 2019; Li et al., 2020). The asexual morph of *Immotthia* differs from *Pseudocoleophoma* in having multiloculate, carbonaceous conidiomata and ellipsoidal, brown, aseptate conidia (Hyde et al., 2017), whereas *Pseudocoleophoma* has uniloculate conidiomata and cylindrical to subcylindrical or fusiform, hyaline, 0–1-septate conidia.

Immotthia bambusae H. B. Jiang and Phookamsak, **sp. nov., Figure 2**.

Index Fungorum Number: IF 557242

Facesoffungi Number: FoF 09538

Etymology: The specific epithet "*bambusae*" refers to the host, bamboo, of which the new species was collected.

Holotype: KUN-HKAS 112012

Hyperparasitic on *Hypoxylon* sp. on dead bamboo culms. *Sexual morph*: *Hypostroma* effuse, black, with numerous, superficial ascomata, composed of thin layered, of blackened, pseudoparenchymatous cells of *textura angularis*. *Ascomata* 130–210 μm high, 150–220 μm diam., dark brown to black, scattered, gregarious, globose to subglobose, or obpyriform, arising from the hypostroma, carbonaceous, brittle when dry, easily dispersed, uniloculate, glabrous, rough-walled, with a pore-like, inconspicuous ostiole. *Peridium* 15–30 μm wide, of unequal thickness, slightly thick at the base, composed of several layers of pseudoparenchymatous cells, outer layers composed of thick-walled, blackened cells, arranged in *textura angularis* to *textura globulosa*, inner layers composed of flattened, brown cells, of *textura angularis* to *textura prismatica*, paler toward the inner layers. *Hamathecium* composed of dense, 1.5–2 μm broad, cellular pseudoparaphyses, septate, branched, anastomosing among the asci, embedded in gelatinous matrix. *Asci* 45–60(–62) × 7.5–10 μm ($\bar{x}$ = 53 × 9 μm, n = 15), (6–)8-spored, bitunicate, fissitunicate, cylindrical, subsessile, with knob-like or furcate pedicel, apically rounded with well-developed ocular chamber. *Ascospores* 9–11 × 3–4.5 μm ($\bar{x}$ = 10 × 3.7 μm, n = 20), overlapping 1–2-seriate, light

brown to brown, ellipsoidal to fusiform, with rounded ends, lower cell slightly longer and narrower than the upper, 1-septate, rough-walled, finely verrucose, initially presented small to large guttules, disappeared when mature, without sheath. *Asexual morph*: Undetermined.

Material Examined: Thailand, Loei Province, a wild bamboo forest (17°15′44.68″N, 101°8′39.32″E, altitude 364.09 m), on *Hypoxylon* sp. associated with dead culms of bamboo, February 25, 2020, H. B. Jiang and R. Phookamsak, BBL07-2-1 (KUN-HKAS 112012, holotype; HMAS 249866, isotype).

Life Mode and Known Distribution: Hyperparasitic on *Hypoxylon* sp. associated with bamboo culms (Thailand).

Notes: The type specimens of all *Immotthia* species were compared; *I. bambusae* shows the most similarity to *I. hypoxylon*, a synonym of *I. atrograna*. However, the novel taxon differs from *I. atrograna* (= *I. hypoxylon*) in having a smaller size of ascomata, asci, and ascospores. The lower cell of ascospores of *I. bambusae* is longer and narrower than the upper cell, while in *I. atrograna* (= *I. hypoxylon*), the upper cell of ascospores is larger than the lower cell. *Immotthia bambusae* was collected on the stromata of *Hypoxylon* associated with bamboo in Thailand (tropical region), whereas the type specimen of *I. hypoxylon* was collected from *Hypoxylon truncatum* colonizing dead canes of *Rosa* in Louisiana, United States (subtropical region). The other different features between *I. bambusae* and the other *Immotthia* species are provided in **Table 2**. Therefore, *I. bambusae* is introduced as a new species in this study based on both morphology and multigene phylogeny.

In this study, we sequenced five different fruiting bodies and DNA sequence similarity (ITS regions) revealed that they have identical nucleotides (100% similarity). Even our phylogeny depicts a close relationship (100% support) among these five strains. This ensures the correctness of the new generated sequences from the direct DNA extraction of fruiting bodies.

Pseudocyclothyriella Phukhams. and Phookamsak, **gen. nov.**

Index Fungorum Number: IF 557441

Facesoffungi Number: FoF 09539

Etymology: The generic epithet "*Pseudocyclothyriella*" refers to the resemblance of conidial morphology of the new genus to the genus *Cyclothyriella*.

Saprobic on *Clematis vitalba* (Ranunculaceae). *Sexual morph*: Undetermined. *Asexual morph*: *Conidiomata* pycnidial, solitary to gregarious, uniloculate, immersed to erumpent, laterally becoming superficial, visible as black, shiny on host, subglobose to subconical, coriaceous, subcoriaceous at the outer layers, glabrous, dark brown to black, ostiolate, papillate. *Ostioles* central, ovoid, with minute papilla, filled with hyaline periphyses. *Pycnidial wall* thick-walled of equal thickness, composed of multilayered scleroplectenchymatous cells, outer layer composed of several layers of thick-walled, dark brown to black cells of *textura angularis* to *textura globulosa*, inner layer composed of hyaline to pale brown cells, bearing conidiogenous cells. *Conidiophores* reduced to conidiogenous cells. *Conidiogenous cells* holoblastic, phialidic, determinate, discrete, cylindrical to subcylindrical, or ampulliform, hyaline, aseptate, smooth-walled, arising from the inner layers of conidioma. *Conidia* oval to oblong, hyaline to yellowish brown, slightly curved toward the ends, aseptate, smooth-walled.

Type Species: *Pseudocyclothyriella clematidis* (Phukhams. and K. D. Hyde) Phukhams. and Phookamsak.

Life Mode and Known Distribution: *Pseudocyclothyriella* is reported as a saprobe on *Clematis vitalba* (Ranunculaceae). The genus is presently known from Italy (Phukhamsakda et al., 2020).

Notes: Based on morphological distinctiveness and multigene phylogenetic analyses, a monotypic genus *Pseudocyclothyriella* is introduced herein to accommodate a single coelomycetous species, *P. clematidis* which was previously described as *Pseudocoleophoma clematidis* by Phukhamsakda et al. (2020). *Pseudocyclothyriella* formed an independent clade basal to *Immotthia* and *Pseudocoleophoma* with strong statistical supports (92% ML, 0.98 PP). *Pseudocyclothyriella* is similar to *Cyclothyriella* in having cylindrical, oblong to ellipsoid, aseptate, hyaline to pigmented conidia (Jaklitsch and Voglmayr, 2016). However, *Pseudocyclothyriella* can be distinguished from *Cyclothyriella* based on the conidiomatal characteristics and phylogenetic evidence. *Pseudocyclothyriella* is characterized by solitary to gregarious, immersed to erumpent, black, shiny, subglobose to subconical conidiomata, with oval, papilla, ostiolar canal, and pycnidial wall composed of thick-walled, scleroplectenchymatous cells. On the other hand, *Cyclothyriella* has black, more or less globose pycnidia, clustered in valsoid configuration, with brightly colored, disc-like ostiole, and pycnidial wall composed of pseudoparenchymatous cells (Jaklitsch and Voglmayr, 2016). *Cyclothyriella* belongs to its own family Cyclothyriellaceae, whereas *Pseudocyclothyriella* belongs to Dictyosporiaceae.

Pseudocoleophoma differs from *Pseudocyclothyriella* in pycnidial wall composed of thin-walled, brown to dark brown pseudoparenchymatous cells and oblong, cylindrical to subcylindrical, or rod-shaped, 0–1-septate, smooth-walled conidia (Tanaka et al., 2015; Jayasiri et al., 2019; Tennakoon et al., 2019; Li et al., 2020). *Pseudocyclothyriella* is morphologically similar to a presumably coniothyrium-like asexual morph of *Immotthia* in having black, carbonaceous pycnidia, and pigmented, aseptate, smooth-walled conidia (Hyde et al., 2017). However, *Immotthia* forms pycnidia in groups, or multiloculate conidiostromata associated with the ascomata of *Immotthia* on natural host substrates and has ellipsoidal conidia as well as having hyperparasitic life mode (Hyde et al., 2017), while *Pseudocyclothyriella* forms solitary to gregarious, uniloculate pycidia and has oval to oblong conidia as well as having saprobic life mode (Phukhamsakda et al., 2020). The sexual morph of *Pseudocyclothyriella* is undetermined; thus, the sexual morphologies of *Pseudocyclothyriella* and *Immotthia* could not be compared.

Pseudocyclothyriella clematidis (Phukhams. and K. D. Hyde) Phukhams. and Phookamsak, **comb. nov., Figure 3**

Index Fungorum Number: IF 557442

Facesoffungi Number: FoF 09540

≡ *Pseudocoleophoma clematidis* Phukhams. and K. D. Hyde, in Phukhamsakda et al., Fungal Divers (102): 21 (2020).

Holotype Details: Italy, Arezzo Province, Badia Tega—Ortignano Raggiolo, on dead aerial branch of *Clematis vitalba*,

TABLE 2 | Synopsis of *Immotthia* species based on type studies (*I. hypoxylon* is listed separately from *I. atrograna* in this study for a better understanding).

Species name	Ascomata	Asci	Ascospores	Asexual morph	Host occurrences	References
Immotthia atrograna (= *I. hypoxylon*)	120–270 μm diam., 150–310 μm high, carbonaceous, glabrous, densely aggregated in large groups or loosely scattered, globose to obpyriform, with pore-like, cream to reddish brown, 30–50 diam., inconspicuous ostiole	60–86 × 6–10 μm, 8-spored, oblong to cylindrical, shortly pedicellate with knob-like or obtuse pedicel	(8–)9–14(–18) × 5–6 μm, 1-seriate, yellowish brown to reddish brown, ellipsoid to biconical, often upper cell slightly shorter and broader than the lower, ends rounded to subacute, 1-septate, constricted at the septum, smooth to slightly verrucose	*Coniothyrium parasitans*	Aceri-Fraxinetum, *Carya olivaeformis*, *Carya* sp., *Hypoxylon rubigmosum*, *H. rubiginosum* on *Fraxinus excelsior*, *H. rubigmosum* on *Fraxinus* sp., *H. rubigmosum* on *Salix alba*, *Hypoxylon* sp., *Hypoxylon* sp. on *Acer pseudoplatanus*, *Hypoxylon* sp. on *Fraxinus excelsior*, *Hypoxylon* sp. on *Fraxinus* sp., *Liquidambar* sp., *Robinia* sp.	Jaklitsch et al., 2002
Immotthia atroseptata	170–250 μm diam., 190–350 μm high, simple or aggregated, globose to obpyriform, with conical or truncate apex perforated by a small, inconspicuous ostiole	62–95 × 8–11 μm, 8-spored, clavate, with a short furcate pedicel	13–17.5 × 4.5–6 μm, 1–2-seriate, brown to reddish brown, ellipsoidal to fusiform with both rounded ends, the upper cell slightly larger than the lower, 1-septate, constricted at the septum, smooth-walled	Undetermined	Apothecia of *Pestalopezia rhododendri* on fallen leaves of *Rhododendron maximum*	Pirozynski, 1973; Doilom et al., 2018
Immotthia bambusae	150–220 μm diam., 130–210 μm high, carbonaceous, scattered, rarely solitary, gregarious, globose to subglobose, with rounded apex with a pore-like, inconspicuous ostiole	45–60(–62) × 7.5–10 μm, 6–8-spored, cylindrical, sessile to subsessile, with knob-like or furcate ends	9–11 × 2.8–4.5 μm, 1–2-seriate, light brown to brown, ellipsoidal to fusiform, with rounded ends, lower cell slightly longer and narrower than the upper, 1-septate, finely verrucose	Undetermined	*Hypoxylon* sp. on bamboo	This study
Immotthia hypoxylon	120–280 μm diam., 170–290 μm high, carbonaceous, glabrous, scattered to clustered, gregarious, subglobose to obpyriform, with pore-like ostiole	(67–)70–90(–108) × 8–11 μm, 8-spored, cylindrical, shortly pedicellate with a knob-like or obtuse end	10–13(–15) × 4–6 μm, 1-seriate, brown to reddish brown, ellipsoidal to fusiform, with round ends, 1-septate, slightly constricted at the septum, rough-walled	*Coniothyrium parasitans*	*Hypoxylon investiens* on *Quercus* sp., *Hypoxylon* sp. on *Fraxinus* sp., *H. truncatum* on dead canes of *Rosa* sp., *Tilia* sp., wood	Hyde et al., 2017

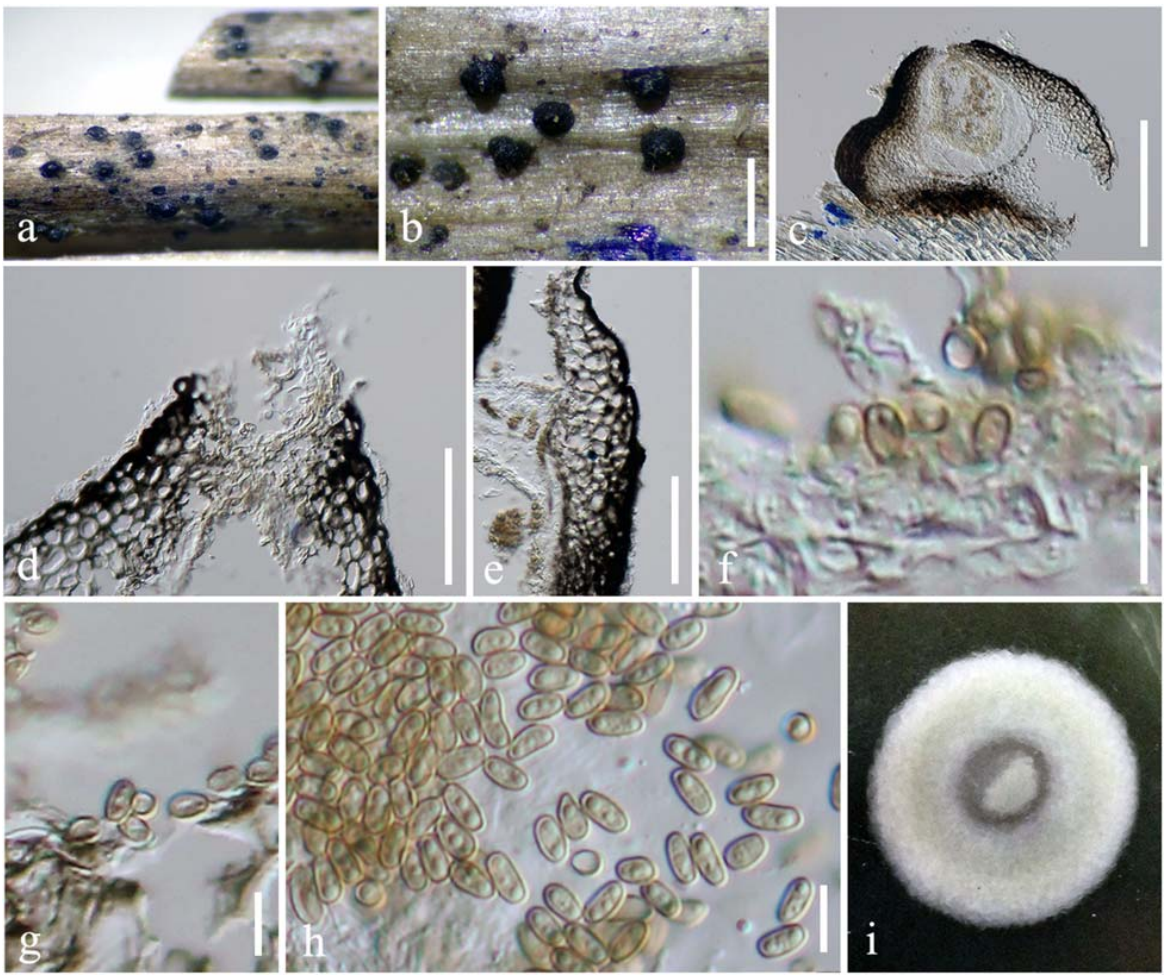


FIGURE 3 | *Pseudocyclothyriella clematidis* (MFLU 16-0280, holotype). **(a,b)** Appearance of pycnidial conidiomata on host substrates. **(c)** Vertical section of conidioma. **(d)** Ostiole. **(e)** Pycnidial wall. **(f,g)** Conidiogenous cells with attached conidia. **(h)** Conidia. **(i)** Culture colony on MEA (upper view). Scale bars: **(b)** = 500 μm, **(c)** = 200 μm, **(d,e)** = 20 μm, and **(f–h)** = 5 μm.

March 9, 2013, E. Camporesi, IT 1110 (MFLU 16-0280), ex-type living culture, MFLUCC 17-2177.

Description and Illustration: See Phukhamsakda et al. (2020).

Ecology and Known Distribution: As a saprobe, *Pseudocyclothyriella clematidis* has contributions in the cycle of the material. To date, the species is just reported in Italy (Phukhamsakda et al., 2020).

Notes: *Pseudocyclothyriella clematidis* was previously treated in *Pseudocoleophoma* based on phylogenetic evidence (Phukhamsakda et al., 2020). *Pseudocyclothyriella clematidis* differs from the other *Pseudocoleophoma* species in having yellowish brown, oval to oblong, aseptate conidia (Phukhamsakda et al., 2020). A morphological comparison of *P. clematidis* with other *Pseudocoleophoma* species is provided in **Table 3**. The two strains of *Pseudocyclothyriella clematidis* (MFLU 16-0280 and MFLUCC 17-2177A) formed a strongly supported clade in this study. Phukhamsakda et al. (2020) introduced *Pseudocoleophoma clematidis* based on phylogenetic evidence and reported the species was poorly supported in a subclade in between the main clade of *Pseudocoleophoma* and *P. typhicola* (MFLUCC 16-0123). However, in our multigene phylogeny, we recovered the same taxon as basal to *Pseudoconiothyrium broussonetiae*.

Crous et al. (2019) mentioned that the closest hits of *P. broussonetiae* using the ITS sequence had highest similarity to *Pseudocoleophoma typhicola* (MFLUCC 16-0123). However, *P. typhicola* is morphologically different from *P. broussonetiae*, but is typical of *Pseudocoleophoma*. We rechecked the BLASTn search result based on ITS and LSU sequences of *P. typhicola* (MFLUCC 16-0123) available in GenBank and noted that the DNA sequences from the ITS regions of *P. typhicola* are similar to the endophytic Pleosporales sp. isolate MBD_4078 (MK595603) and the uncultured fungus clone ITS_S7_clon2 (HQ873356) with 90.50% similarities and matches with *P. broussonetiae* strain CBS 145036 (NR_163377) with 90.23% similarity which is far away from *Pseudocoleophoma*. On the other hand, the BLASTn search result based on LSU sequence showed that the species is closely related with *Pseudocoleophoma*,

TABLE 3 | Synopsis of morphological characteristics of *Pseudocoleophoma* and *Pseudocyclothyriella*.

Species name	Sexual morph			Asexual morph			References
	Ascomata	Asci	Ascospores	Conidiomata	Conidiogenous cells	Conidia	
Pseudocoleophoma bauhiniae	100–120 × 125–145 μm, solitary or scattered, dark brown, subglobose to obpyriform, coriaceous	65–80 × 5–8 μm, clavate to cylindric-clavate	17–20 × 3.5–4.5 μm, hyaline, cylindric-fusiform, 1–3-septate, without sheath	130–150 × 90–115 μm, immersed to superficial, globose to subglobose, glabrous, multiloculate, ostiolate	2.5–5.5 × 2–3 μm, phialidic, hyaline, doliiform to lageniform	7.5–11 × 2–3 μm, hyaline, oblong to ellipsoidal, with rounded or obtuse ends, aseptate	Jayasiri et al., 2019
P. calamagrostidis	160–220 × 140–200 μm, scattered, dark brown, globose to depressed globose	62.5–80 × 7.5–10 μm, cylindrical	16–19 × 3–4.5 μm, hyaline, narrowly fusiform, 1-septate, with sheath	250–500 × 220–300 μm, immersed to erumpent, depressed globose, glabrous, uniloculate, ostiolate	5–9 × 2–4 μm, phialidic, hyaline, doliiform to subglobose	6–10 × 2–2.5 μm, hyaline, cylindrical, aseptate	Tanaka et al., 2015
P. flavescens	N/A	N/A	N/A	20–140 μm diam., solitary or confluent, globose, glabrous or covered by hyphae	4–6 × 3–6 μm, globose to doliiform	4–7 × 2–3.5 μm, hyaline, oblong to ellipsoidal with two very large polar guttules, aseptate	De Gruyter et al., 1993; Li et al., 2020
P. polygonicola	280–350 × 230–310 μm, scattered to 2–4-gregarious, brown to dark brown, globose to subglobose	74–90 × 9–12.5 μm, cylindrical to clavate	19–23 × 4–6 μm, hyaline, fusiform, 1-septate, with sheath	170–250 μm diam., superficial, ampulliform, glabrous, uniloculate, ostiolate	7–17 × 3.5–5 μm, phialidic, hyaline, doliiform to lageniform	11.5–18 × 3–4.5 μm, hyaline cylindrical, aseptate	Tanaka et al., 2015
P. rusci	N/A	N/A	N/A	130–200 × 250–330 μm, deeply immersed, globose, subglobose or ovoid, glabrous, uniloculate, ostiolate	4–9 × 3–7 μm, enteroblastic, phialidic, hyaline, doliiform, ampulliform to subcylindrical	8–14 × 3–6 μm, hyaline, cylindrical to subcylindrical or fusiform, aseptate	Li et al., 2020
P. typhicola	N/A	N/A	N/A	60–100 × 140–150 μm, semi-erumpent, subglobose, glabrous, uniloculate	2–5 × 2–5 μm, enteroblastic, hyaline, subcylindrical	9–11 × 2–3 μm, hyaline, oblong to cylindrical, 1-euseptate	Hyde et al., 2016
P. zingiberacearum	N/A	N/A	N/A	200–220 × 110–150 μm, immersed, depressed globose, glabrous, multiloculate, non-ostiolate	1.5–2.5 × 1–1.5 μm, phialidic, hyaline, doliiform to lageniform	12–14 × 2–3 μm, hyaline, oblong to ellipsoidal, aseptate	Tennakoon et al., 2019
Pseudocyclothyriella clematidis (≡ *Pseudocoleophoma clematidis*)	N/A	N/A	N/A	130–150 × 100–130 μm, immersed, globose to subglobose, glabrous, uniloculate, ostiolate	2–4 × 1.5–4 μm, holoblastic, phialidic, hyaline, cylindrical to subcylindrical	5–8 × 2–4 μm, yellowish brown, oval, aseptate	Phukhamsakda et al., 2020; This study

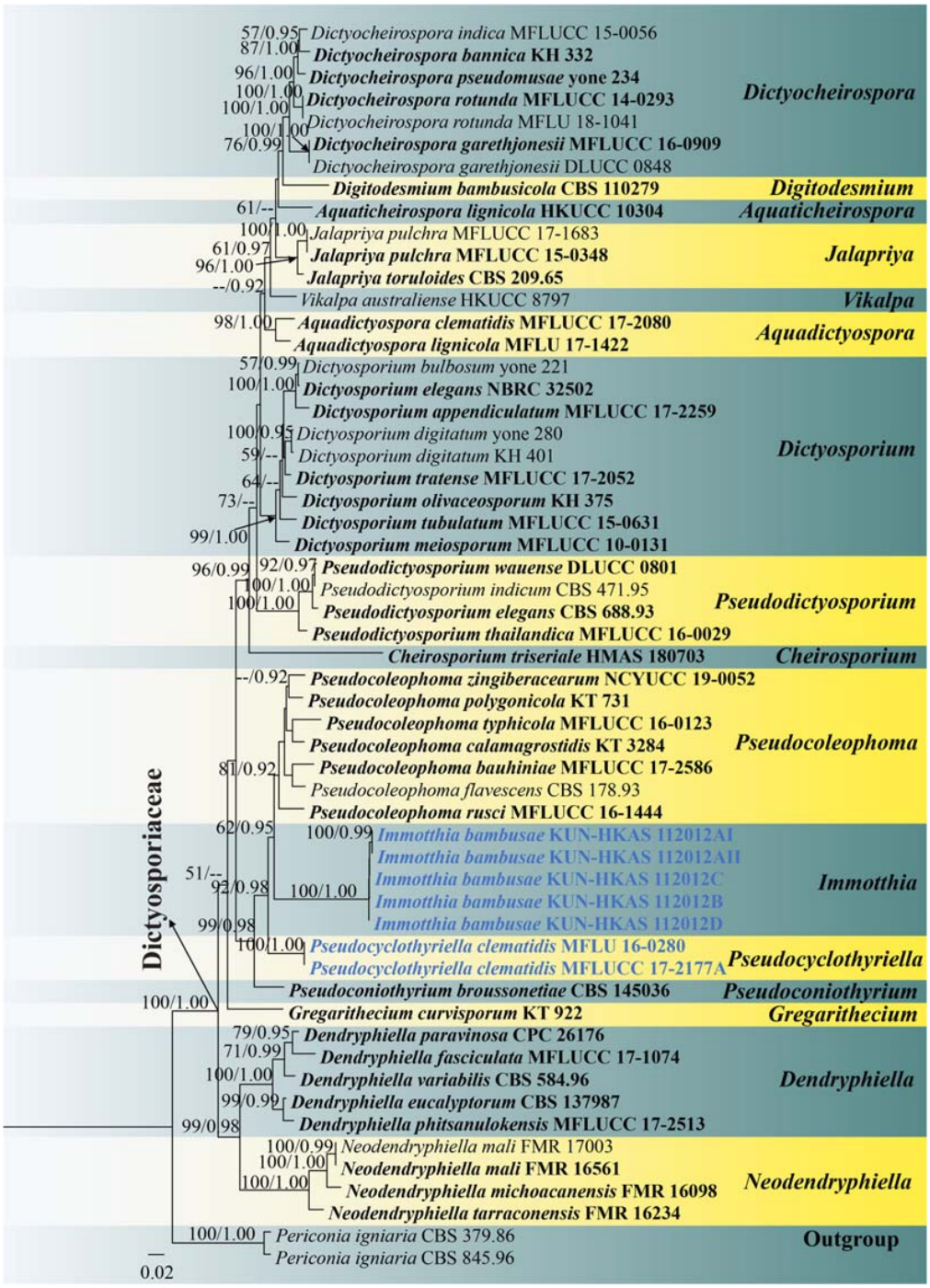


FIGURE 4 | RAxML tree based on a combined ITS, LSU, SSU, and TEF1-α sequence matrix represented the phylogenetic relationships of taxa in Dictyosporiaceae. The tree is rooted to *Periconia igniaria* (CBS 845.96 and CBS 379.86). Bootstrap support values for ML equal to or greater than 50% and the Bayesian posterior probabilities equal to or higher than 0.90 PP are indicated above the nodes as ML/PP. Ex-type strains are in black bold and the new species and new combinations are indicated in blue bold.

and hence, these may be erroneous. In this study, we therefore excluded the ITS sequence of *P. typhicola* from our aligned sequence dataset and the phylogenetic results showed that *P. typhicola* clusters within *Pseudocoleophoma* (**Figure 4**). However, *P. typhicola* needs to be resequenced as well as obtaining more reliable genes (only ITS and LSU are available in GenBank) for a better phylogenetic resolution is needed.

Phylogenetic Analyses

The closest query cover identification of five new strains (KUN-HKAS 112012AI, KUN-HKAS 112012AII, KUN-HKAS 112012B, KUN-HKAS 112012C, and KUN-HKAS 112012D) on BLASTn search tool indicated that our new *Immotthia* taxon is similar to *Pseudocoleophoma rusci* (MFLUCC 16-1444), *P. calamagrostidis* (KT 3284), *P. polygonicola* (KT 731), and *Dictyocheirospora pseudomusae* (yone 234) when DNA sequences (ITS, LSU, SSU, and TEF1-α) were compared.

Phylogenetic analyses of a combined ITS, LSU, SSU, and TEF1-α sequence matrix were performed based on 56 strains of taxa in Dictyosporiaceae and two strains of *Periconia igniaria* (CBS 845.96 and CBS 379.86) as outgroup. This dataset consists of 3,397 total characters including gaps (ITS: 1–585 bp, LSU: 586–1,445 bp, SSU: 1,446–2,473 bp, TEF1-α: 2,474–3,397 bp). The best scoring ML tree was selected to represent the phylogenetic relationships of the new taxon with other representative taxa in Dictyosporiaceae (**Figure 4**), with the final ML optimization likelihood value of −17,968.180137 (ln). All free model parameters were estimated by GTRGAMMA model, with 1,026 distinct alignment patterns and 33.65% of undetermined characters or gaps. Estimated base frequencies were as follows: $A = 0.240488$, $C = 0.242841$, $G = 0.269410$, and $T = 0.247261$, with substitution rates AC = 1.638750, AG = 3.305690, AT = 2.424291, CG = 0.898018, CT = 8.545431, and GT = 1.000000. The gamma distribution shape parameter alpha = 0.169318 and the Tree-Length = 1.822628. The final average standard deviation of split frequencies at the end of total MCMC generations was calculated as 0.009979 in BI analysis.

Preliminary phylogenetic analysis based on a concatenated LSU–SSU–TEF1-α–RPB2–ITS sequence matrix of representative families in Pleosporales depicts that *Immotthia* belongs to the family Dictyosporiaceae (**Supplementary Figure 3**). The phylograms from ML and BI analyses (**Figure 4** and **Supplementary Figure 2**) of a concatenated ITS–LSU–SSU–TEF1-α sequence matrix were similar in overall topologies and were also similar to the tree topology of a concatenated ITS–LSU–TEF1-α sequence dataset (**Supplementary Figure 1**). Our five new strains of *I. bambusae* constitute a strongly supported independent subclade basal to *Pseudocoleophoma* (62% ML, 0.95 PP). Two strains of *Pseudocyclothyriella clematidis* (≡ *Pseudocoleophoma clematidis*, MFLU 16-0280 and MFLUCC 17-2177A) formed an independent subclade basal to *Immotthia* with strong statistical supports (92% ML, 0.98 PP). Based on current phylogenetic status and morphological distinctiveness compared with the other *Pseudocoleophoma* species, *Pseudocoleophoma clematidis* is transferred to the novel genus *Pseudocyclothyriella* as *P. clematidis*.

DISCUSSION

An updated taxonomic treatment of bambusicolous fungi has been conducted since the last decade by Japanese mycologists (Tanaka et al., 2009, 2015) and followed by many Asian mycologists (Liu et al., 2011, 2012, 2014, 2015; Dai et al., 2012, 2014a,b,c, 2017, 2018, 2019; Phookamsak et al., 2014, 2015, 2018; Adamčík et al., 2015; Ariyawansa et al., 2015; Senanayake et al., 2015, 2020a; Jiang et al., 2018, 2019a,b,c; Sommai et al., 2019; Yang et al., 2019a,b; Jiang H. B. et al., 2020; Jiang N. et al., 2020; Hyde et al., 2020a,b; Monkai et al., 2020; Sun et al., 2020; Tang et al., 2020; Xie et al., 2020; Zhang et al., 2020). To date, more than 1,300 bambusicolous fungi have been reported consisting of 150 basidiomycetes and 1,150 ascomycetes. However, the taxonomic placements of many described species have yet to be verified based on DNA sequence phylogeny (Dai et al., 2018).

In this study, we collected a fungus associated with *Hypoxylon* stromata on bamboo from northeastern Thailand. Based on morphological examination comparable with the type specimens, the species is identified as a typical *Immotthia* but largely different to warrant the establishment of a new species. Thus, we introduce a novel species *I. bambusae* and this is also the first report of *Immotthia* associated with *Hypoxylon* stromata on bamboo in Thailand. Furthermore, it is the first time that DNA sequence data of *Immotthia* are obtained and its phylogenetic affinity within the Dictyosporiaceae was investigated. In addition, a novel genus *Pseudocyclothyriella* is introduced as a monotypic genus to accommodate *P. clematis* during the phylogenetic investigation of *Immotthia*.

Multigene phylogenetic analyses showed that *Immotthia* formed a well-resolved clade within Dictyosporiaceae in all analyses (**Figure 4** and **Supplementary Figures 1–3**). The genus clustered with *Pseudocoleophoma* in all analyses with significant support in BI analysis (0.95 PP; **Figure 4**), but low support in ML analysis (62% ML; **Figure 4**). However, *Immotthia* is also morphologically different from *Pseudocoleophoma* (see notes under generic description).

Immotthia is widely distributed from tropical to temperate regions including Austria, Belgium, China, France, Lithuania, Norway, Poland, Puerto Rico, Russia, Sweden, Switzerland, Ukraine, United States, and Venezuela (Pirozynski, 1973; Jaklitsch et al., 2002; Akulov and Hayova, 2016; Hyde et al., 2017; Doilom et al., 2018; Farr and Rossman, 2020). *Immotthia* does not seem to exhibit a hyperparasitic lifestyle on *Hypoxylon*, but species of this genus were also reported as saprobes on various decayed hardwoods (Jaklitsch et al., 2002). *Immotthia bambusae* did not germinate on potato dextrose agar (PDA) medium, suggesting that the species has possibly an obligate parasitic life mode, which is in agreement with Jaklitsch et al. (2002).

Jaklitsch et al. (2002) treated the type species of *Immotthia*, *I. hypoxylon*, as a synonym of *I. atrograna* after they examined the type materials of these two species. They found that the basionym of both *I. hypoxylon* and *I. atrograna* shared similar size range of ascomata, asci, and ascospores and it does not show any convincing difference on the ascomata, although these two species occurred on different hosts and habitats (Jaklitsch et al., 2002). Hyde et al. (2017) re-examined the type material of *I. hypoxylon* and compared it with other collections from North America and reported similar morphology, but the latter have larger ascomata and shorter asci than the type (Hyde et al., 2017). A comparison of the type examination between *I. hypoxylon* (Hyde et al., 2017) and *I. atrograna* (Jaklitsch et al., 2002) shows that *I. atrograna* has a larger ascomata, smaller asci, and overlapped size range of ascospores. However, these two species

still lack DNA sequence data, and hence, their taxonomic status with regards to whether they are conspecific warrants further investigation. Herein, we follow the treatment of Jaklitsch et al. (2002) until the epitypes of these two species are designated and their taxonomy is revisited.

Dictyosporiaceae comprises 17 genera, including *Immotthia* and *Pseudocyclothyriella*. Asexual morph of *Immotthia* is recognized as chaetophoma-, coniothyrium-, microsphaeropsis-, or pyrenochaeta-like (Jaklitsch et al., 2002; Akulov and Hayova, 2016; Hyde et al., 2017; Doilom et al., 2018), which is also similar to coelomycetous asexual morph of *Roussoella* (Hyde et al., 2017). Hyde et al. (2017) tentatively placed *Immotthia* in Roussoellaceae based on the morphological similarity to *Roussoella*. However, *Immotthia* is phylogenetically distinct from *Coniothyrium* (Coniothyriaceae) and *Roussoella* (Roussoellaceae). The genus is transferred from Roussoellaceae to Dictyosporiaceae in this study. The coelomycetous asexual morph of *Immotthia* was found on natural substrates associated with the sexual morph. However, the link between sexual and asexual morph of *Immotthia* has not yet been proven, although Jaklitsch et al. (2002) attempted to elucidate the connection based on cultural experiments. The ascospores of *Immotthia* do not germinate on artificial media due to its obligate parasitic life mode. The connection of the sexual–asexual morph needs to be confirmed based on DNA sequence data obtained from direct DNA extraction of fruiting bodies as well as on culture-based studies.

Asexual morphs of most genera in Dictyosporiaceae are hyphomycetes, except for *Immotthia*, *Pseudocoleophoma*, *Pseudocyclothyriella*, and *Pseudoconiothyrium* which are coelomycetous asexual morphs (Tanaka et al., 2015; Crous et al., 2019; Hongsanan et al., 2020). Based on morphological characteristics, *Immotthia* is most similar to *Pseudoconiothyrium* in having hyaline, smooth, doliiform to ampulliform, phialidic conidiogenous cells and ellipsoidal, brown conidia (Crous et al., 2019). However, the genus can be distinguished from *Pseudoconiothyrium* by multiloculate, smaller conidiomata, smooth-walled conidia, whereas *Pseudoconiothyrium* has uniloculate, larger conidiomata, verrucose conidia (Crous et al., 2019). Two strains of *Pseudocoleophoma clematidis* formed a stable clade basal to *Immotthia* and separated from the main clade of *Pseudocoleophoma* in all analyses (**Figure 4** and **Supplementary Figures 1–3**). We, therefore, re-examined the holotype specimen of *P. clematidis* and found that the species was morphologically different from the other *Pseudocoleophoma* (see **Table 3**). Thus, *Pseudocyclothyriella* is introduced herein based on the evidence from both morphology and phylogeny. *Pseudocyclothyriella* is also similar to *Pseudoconiothyrium* but differs in having thick-walled, scleroplectenchymatous cells of pycnidial wall. Based on our current phylogenetic results, *Immotthia* and *Pseudocyclothyriella* are clearly distinct from *Pseudoconiothyrium*.

Only four genera in Dictyosporiaceae have been reported for their sexual morphs, viz. *Dictyosporium* Corda, *Gregarithecium* Kaz. Tanaka and K. Hiray., *Immotthia*, and *Pseudocoleophoma*. *Immotthia* is morphologically different from these three genera in having ellipsoidal to fusiform, light brown to reddish brown, asymmetrical ascospores, lacks mucilaginous sheath, and exhibits a hyperparasitic life mode (Jaklitsch et al., 2002; Hyde et al., 2017). On the other hand, the other three genera have hyaline, fusiform to narrowly fusiform ascospores, with or without mucilaginous sheath and have been reported as saprobes in terrestrial and freshwater habitats (Tanaka et al., 2015; Boonmee et al., 2016). The familial descriptions for Dictyosporiaceae have previously been restricted to hyphomycetous asexual morphs (Boonmee et al., 2016; Hongsanan et al., 2020). We recommend that the descriptions and illustrations of Dictyosporiaceae should include both coelomycetous and hyphomycetous asexual morphs.

DATA AVAILABILITY STATEMENT

The datasets presented in this study can be found in online repositories. The names of the repository/repositories and accession number(s) can be found in the article/**Supplementary Material**.

AUTHOR CONTRIBUTIONS

H-BJ and RP: conceptualization, data curation, and formal analysis. SL, SCK, and RP: funding acquisition. H-BJ, RP, CP, and MD: investigation, methodology, and writing—original draft. RP and NS: project administration. SL, SCK, RJ, and PK: supervision. NS, PK, RJ, SL, and SCK: writing—review and editing. All authors contributed to the article and approved the submitted version.

FUNDING

This research was supported by the Key Research Project, Agroforestry Systems for Restoration and Bio-industry Technology Development (Grant No. 2017YFC0505101), Ministry of Sciences and Technology of China (Grant No. 2017YFC0505100), National Science Foundation of China (NSFC) project code 31850410489 (Grant No. Y81I982211), and Chiang Mai University. RP thanks CAS President's International Fellowship Initiative (PIFI) for young staff (Grant No. Y9215811Q1), the National Science Foundation of China (NSFC) project code 31850410489 (Grant No. Y81I982211), and Chiang Mai University for financial support. SCK thanks CAS President's International Fellowship Initiative (PIFI) young staff under the grant number: 2020FYC0002 and the National Science Foundation of China (NSFC) for funding this work under the project code 31851110759.

ACKNOWLEDGMENTS

We acknowledge the Biology Experimental Center, Germplasm Bank of Wild Species, Kunming Institute of Botany, Chinese Academy of Sciences for providing the facilities of molecular laboratory. Shaun Pennycook at Manaaki Whenua – Landcare Research is thanked for his help in naming the new fungal

species. Austin Smith at World Agroforestry (ICRAF), Kunming Institute of Botany, China, is thanked for English editing. Sinang Hongsanan at Guangdong Provincial Key Laboratory for Plant Epigenetics, Shenzhen Key Laboratory of Microbial Genetic Engineering, College of Life Science and Oceanography, Shenzhen University, is thanked for advising on phylogenetic analyses. H-BJ would like to thank Mae Fah Luang University for the Ph.D. scholarship. RJ would like to thank the University of Mauritius for research support.

SUPPLEMENTARY MATERIAL

The Supplementary Material for this article can be found online at: https://www.frontiersin.org/articles/10.3389/fmicb.2021.656235/full#supplementary-material

Supplementary Figure 1 | RAxML tree based on ITS, LSU and TEF1-α sequence matrix represented the phylogenetic relationships of taxa in Dictyosporiaceae. The tree is rooted to *Periconia igniaria* (CBS 845.96 and CBS 379.86). Bootstrap support values for ML are indicated above the nodes. Ex-type strains are in black bold and the new species and new combinations are indicated in blue bold.

Supplementary Figure 2 | Phylogram generated by Bayesian inference (BI) analysis based on a combined ITS, LSU, SSU and TEF1-α sequence matrix represented the phylogenetic relationships of taxa in Dictyosporiaceae. The tree is rooted to *Periconia igniaria* (CBS 845.96 and CBS 379.86). Bayesian posterior probabilities are indicated above the nodes. Ex-type strains are in black bold and the new species and new combinations are indicated in blue bold.

Supplementary Figure 3 | RAxML tree based on LSU, SSU, TEF1-α, RPB2 and ITS sequence matrix represented the phylogenetic relationships of *Immotthia* in Dictyosporiaceae with other families in Pleosporales. The tree is rooted to *Capondium coffeae* (CBS 147.52). Bootstrap support values for ML are indicated above the nodes. The placement of *Immotthia* in Dictyosporiaceae is indicated by yellow background.

REFERENCES

Adamčík, S., Cai, L., Chakraborty, D., Chen, X. H., Cotter, H. V. T., Dai, D. Q., et al. (2015). Fungal biodiversity profiles 1–10. *Cryptogam. Mycol.* 36, 121–166. doi: 10.7872/crym/v36.iss2.2015.121

Akulov, O. Y., and Hayova, V. P. (2016). *Immotthia atrograna* (Dacampiaceae, Ascomycota), a new for Ukraine fungicolous fungus from Carpathians. *Ukr. Bot. J.* 73, 84–89. doi: 10.15407/ukrbotj73.01.084

Ariyawansa, H. A., Hyde, K. D., Jayasiri, S. C., Buyck, B., Chethana, K. W. T., Dai, D. Q., et al. (2015). Fungal diversity notes 111–252—taxonomic and phylogenetic contributions to fungal taxa. *Fungal Divers.* 75, 27–274. doi: 10.1007/s13225-015-0346-5

Barr, M. E. (1987a). New taxa and combinations in the Loculoascomycetes. *Mycotaxon* 29, 501–505.

Barr, M. E. (1987b). *Prodromus to Class Loculoascomycetes*. Amherst, MA: Newell, Inc., 168.

Barr, M. E. (1993). Redisposition of some taxa described by J.B. Ellis. *Mycotaxon* 46, 45–76.

Barr, M. E. (2002). Teichosporaceae, another family in the Pleosporales. *Mycotaxon* 82, 373–389.

Boonmee, S., D'souza, M. J., Luo, Z., Pinruan, U., Tanaka, K., Su, H., et al. (2016). Dictyosporiaceae fam. nov. *Fungal Divers.* 80, 457–482. doi: 10.1007/s13225-016-0363-z

Cooke, M. C., and Ellis, J. B. (1879). New Jersey fungi. *Grevillea* 8, 11–16.

Crous, P. W., Schumacher, R. K., Akulov, A., Thangavel, R., Hernández-Restrepo, M., Carnegie, A. J., et al. (2019). New and interesting fungi. 2. *Fungal Syst. Evol.* 3, 57–134. doi: 10.3114/fuse.2019.03.06

Dai, D. Q., Bahkali, A. H., Li, Q. R., Bhat, D. J., Wijayawardene, N. N., Li, W. J., et al. (2014a). *Vamsapriya* (Xylariaceae) re-described, with two new species and molecular sequence data. *Cryptogam. Mycol.* 35, 339–357. doi: 10.7872/crym.v35.iss4.2014.339

Dai, D. Q., Bhat, D. J., Liu, J. K., Chukeatirote, E., Zhao, R. L., and Hyde, K. D. (2012). *Bambusicola*, a new genus from bamboo with asexual and sexual morphs. *Cryptogam. Mycol.* 33, 363–379. doi: 10.7872/crym.v33.iss3.2012.363

Dai, D. Q., Phookamsak, R., Wijayawardene, N. N., Li, W. J., Bhat, D. J., Xu, J. C., et al. (2017). Bambusicolous fungi. *Fungal Divers.* 82, 1–105. doi: 10.1007/s13225-016-0367-8

Dai, D. Q., Tang, L. Z., and Wang, H. B. (2018). "A review of bambusicolous ascomycetes," in *Bamboo: Current and Future Prospects*, ed. H. P. S. Abdul Khalil (London: IntechOpen). doi: 10.5772/intechopen.76463

Dai, D. Q., Wijayawardene, N. N., Bhat, D. J., Chukeatirote, E., Bahkali, A. H., Zhao, R. L., et al. (2014b). *Pustulomyces* gen. nov. accommodated in Diaporthaceae, Diaporthales, as revealed by morphology and molecular analyses. *Cryptogam. Mycol.* 35, 63–72. doi: 10.7872/crym.v35.iss1.2014.63

Dai, D. Q., Wijayawardene, N. N., Bhat, D. J., Chukeatirote, E., Zhao, R. L., Wang, Y., et al. (2014c). The phylogenetic placement of *Eriosporella bambusicola* sp. nov. in Capnodiales. *Cryptogam. Mycol.* 35, 41–49. doi: 10.7872/crym.v35.iss1.2014.41

Dai, D. Q., Wijayawardene, N. N., Tang, L. Z., Liu, C., Han, L. H., Chu, H. L., et al. (2019). *Rubroshiraia* gen. nov., a second hypocrellin-producing genus in Shiraiaceae (Pleosporales). *MycoKeys* 58, 1–26. doi: 10.3897/mycokeys.58.36723

De Gruyter, J., Noordeloos, M. E., and Boerema, G. H. (1993). Contributions towards a monograph of *Phoma* (Coelomycetes)—I. 2. Section *Phoma*: additional taxa with very small conidia and taxa with conidia up to 7 µm long. *Persoonia* 15, 369–400.

Dissanayake, A. J., Bhunjun, C. S., Maharachchikumbura, S. S. N., and Liu, J. K. (2020). Applied aspects of methods to infer phylogenetic relationships amongst fungi. *Mycosphere* 11, 2652–2676. doi: 10.5943/mycosphere/11/1/18

Doilom, M., Dissanayake, A. J., Wanasinghe, D. N., Boonmee, S., Liu, J. K., Bhat, D. J., et al. (2017). Microfungi on *Tectona grandis* (teak) in Northern Thailand. *Fungal Divers.* 82, 107–182. doi: 10.1007/s13225-016-0368-7

Doilom, M., Hyde, K. D., Phookamsak, R., Dai, D. Q., Tang, L. Z., Hongsanan, S., et al. (2018). Mycosphere notes 225–274: types and other specimens of some genera of Ascomycota. *Mycosphere* 9, 647–754. doi: 10.5943/mycosphere/9/4/3

Ellis, J. B., and Everhart, B. M. (1886). New species of fungi from various localities. *J. Mycol.* 2, 37–42.

Farr, D. F., and Rossman, A. Y. (2020). *Fungal Databases, U.S. National Fungus Collections, ARS, USDA*. Available online at: https://nt.ars-grin.gov/fungaldatabases/ (accessed November 1, 2020).

Hall, T. (2001). *BioEdit Version 5.0.6*. Raleigh, NC: North Carolina State University.

Hongsanan, S., Hyde, K. D., Phookamsak, R., Wanasinghe, D. N., McKenzie, E. H. C., Sarma, V. V., et al. (2020). Refined families of Dothideomycetes: Dothideomycetidae and Pleosporomycetidae. *Mycosphere* 11, 1553–2107. doi: 10.5943/mycosphere/11/1/13

Hyde, K. D., de Silva, N. I., Jeewon, R., Bhat, D. J., Phookamsak, R., Doilom, M., et al. (2020a). AJOM new records and collections of fungi: 1–100. *Asian J. Mycol.* 3, 22–294. doi: 10.5943/ajom/3/1/3

Hyde, K. D., Dong, Y., Phookamsak, R., Jeewon, R., Bhat, D. J., Jones, E. B. G., et al. (2020b). Fungal diversity notes 1151–1276: taxonomic and phylogenetic contributions on genera and species of fungal taxa. *Fungal Divers.* 100, 5–277. doi: 10.1007/s13225-020-00439-5

Hyde, K. D., Hongsanan, S., Jeewon, R., Bhat, D. J., McKenzie, E. H. C., Jones, E. B. G., et al. (2016). Fungal diversity notes 367–490: taxonomic and phylogenetic contributions to fungal taxa. *Fungal Divers.* 80, 1–270. doi: 10.1007/s13225-016-0373-x

Hyde, K. D., Norphanphoun, C., Abreu, V. P., Bazzicalupo, A., Chethana, K. W. T., Clericuzio, M., et al. (2017). Fungal diversity notes 603–708: taxonomic and phylogenetic notes on genera and species. *Fungal Divers.* 87, 1–235. doi: 10.1007/s13225-017-0391-3

Index Fungorum (2020). *Index Fungorum*. Available online at: http://www.indexfungorum.org/Names/Names.asp (accessed Oct 27, 2020)

Iturrieta-González, I., Gené, J., Guarro, J., Castañeda-Ruiz, R. F., and García, D. (2018). *Neodendryphiella*, a novel genus of the Dictyosporiaceae (Pleosporales). *MycoKeys* 37, 19–38. doi: 10.3897/mycokeys.37.27275

Jaklitsch, W. M., and Voglmayr, H. (2016). Hidden diversity in *Thyridaria* and a new circumscription of the Thyridariaceae. *Stud. Mycol.* 85, 35–64. doi: 10.1016/j.simyco.2016.09.002

Jaklitsch, W. M., Scheuer, C., and Voglmayr, H. (2002). Notes on the genus *Immotthia* (Pleosporales, Ascomycetes), including some type studies. *Osterr. Z. Pilzkd.* 11, 93–106.

Jayasiri, S. C., Hyde, K. D., Ariyawansa, H. A., Bhat, D. J., Buyck, B., Cai, L., et al. (2015). The faces of fungi database: fungal names linked with morphology, phylogeny and human impacts. *Fungal Divers.* 74, 3–18. doi: 10.1007/s13225-015-0351-8

Jayasiri, S. C., Hyde, K. D., Jones, E. B. G., McKenzie, E. H. C., Jeewon, R., Phillips, A. J. L., et al. (2019). Diversity, morphology and molecular phylogeny of Dothideomycetes on decaying wild seed pods and fruits. *Mycosphere* 10, 11–86. doi: 10.5943/mycosphere/10/1/1

Jeewon, R., and Hyde, K. D. (2016). Establishing species boundaries and new taxa among fungi: recommendations to resolve taxonomic ambiguities. *Mycosphere* 7, 1669–1677. doi: 10.5943/mycosphere/7/11/4

Jiang, H. B., Hyde, K. D., Doilom, M., Karunarathna, S. C., Xu, J. C., and Phookamsak, R. (2019a). *Arthrinium setostromum* (Apiosporaceae, Xylariales), a novel species associated with dead bamboo from Yunnan, China. *Asian J. Mycol.* 2, 254–268. doi: 10.5943/ajom/2/1/16

Jiang, H. B., Hyde, K. D., Jayawardena, R. S., Doilom, M., Xu, J., and Phookamsak, R. (2019b). Taxonomic and phylogenetic characterizations reveal two new species and two new records of *Roussoella* (Roussoellaceae, Pleosporales) from Yunnan, China. *Mycol. Prog.* 18, 577–591. doi: 10.1007/s11557-019-01471-9

Jiang, H. B., Phookamsak, R., Bhat, D. J., Khan, S., Bahkali, A., Elgorban, A. B., et al. (2018). *Vamsapriya yunnana*, a new species of *Vamsapriya* (Xylariaceae, Xylariales) associated with bamboo from Yunnan, China. *Phytotaxa* 356, 61–70. doi: 10.11646/phytotaxa.356.1.5

Jiang, H. B., Phookamsak, R., Doilom, M., Mortimer, P. E., Xu, J. C., Lumyong, S., et al. (2019c). Taxonomic and phylogenetic characterizations of *Keissleriella bambusicola* sp. nov. (Lentitheciaceae, Pleosporales) from Yunnan, China. *Phytotaxa* 423, 129–144. doi: 10.11646/phytotaxa.423.3.2

Jiang, H. B., Phookamsak, R., Xu, J. C., Karunarathna, S. C., Mortimer, P. E., and Hyde, K. D. (2020). Taxonomic and phylogenetic characterizations reveal three new species of *Mendogia* (Myriangiaceae, Myriangiales). *Mycol. Prog.* 19, 41–51. doi: 10.1007/s11557-019-01540-z

Jiang, N., Liang, Y. M., and Tian, C. M. (2020). A novel bambusicolous fungus from China, *Arthrinium chinense* (Xylariales). *Sydowia* 72, 77–83. doi: 10.12905/0380.sydowia72-2020-0077

Katoh, K., Rozewicki, J., and Yamada, K. D. (2019). Mafft online service: multiple sequence alignment, interactive sequence choice and visualization. *Brief. Bioinform.* 20, 1160–1166. doi: 10.1093/bib/bbx108

Li, W. J., McKenzie, E. H. C., Liu, J. K., Bhat, D. J., Dai, D. Q., Camporesi, E., et al. (2020). Taxonomy and phylogeny of hyaline-spored coelomycetes. *Fungal Divers.* 100, 279–801. doi: 10.1007/s13225-020-00440-y

Liu, J. K., Hyde, K. D., Gareth, E. B. G., Ariyawansa, H. A., Bhat, D. J., Boonmee, S., et al. (2015). Fungal diversity notes 1– 110: taxonomic and phylogenetic contributions to fungal species. *Fungal Divers.* 72, 1–197. doi: 10.1007/s13225-015-0324-y

Liu, J. K., Phookamsak, R., Dai, D. Q., Tanaka, K., Jones, E. B. G., Xu, J. C., et al. (2014). Roussoellaceae, a new pleosporalean family to accommodate the genera *Neoroussoella* gen. nov., *Roussoella* and *Roussoellopsis*. *Phytotaxa* 181, 1–33. doi: 10.11646/phytotaxa.181.1.1

Liu, J. K., Phookamsak, R., Jones, E. B. G., Zhang, Y., Ko-Ko, T. W., Hu, H. L., et al. (2011). *Astrosphaeriella* is polyphyletic, with species in *Fissuroma* gen. nov., and *Neoastrosphaeriella* gen. nov. *Fungal Divers.* 51, 135–154. doi: 10.1007/s13225-011-0142-9

Liu, Y., Liu, Z., and Wongkaew, S. (2012). Developing characteristics and relationships of *Shiraia bambusicola* with Bamboo. *Songklanakarin. J. Sci. Technol.* 34, 17–22.

Miller, M. A., Pfeiffer, W., and Schwartz, T. (2010). "Creating the CIPRES science gateway for inference of large phylogenetic trees," in *Proceedings of the Gateway Computing Environments Workshop (GCE)*, (New Orleans, LA), 1–8.

Monkai, J., Boonmee, S., Ren, G. C., Wei, D. P., Phookamsak, R., and Mortimer, P. E. (2020). *Distoseptispora hydei* sp. nov. (Distoseptisporaceae), a novel lignicolous fungus on decaying bamboo in Thailand. *Phytotaxa* 459, 93–107. doi: 10.11646/phytotaxa.459.2.1

Nylander, J. (2008). *MrModeltest2 v. 2.3 (Program for Selecting DNA Substitution Models using PAUP*)*. Uppsala: Evolutionary Biology Centre.

Phookamsak, R., Liu, J. K., Manamgoda, D. S., Wanasinghe, D. N., Ariyawansa, H., Mortimer, P. E., et al. (2014). Epitypification of two bambusicolous fungi from Thailand. *Cryptogam. Mycol.* 35, 239–256. doi: 10.7872/crym.v35.iss3.2014.239

Phookamsak, R., Lu, Y. Z., Hyde, K. D., Jeewon, R., Li, J., Doilom, M., et al. (2018). Phylogenetic characterization of two novel *Kamalomyces* species in Tubeufiaceae (Tubeufiales). *Mycol. Prog.* 17, 647–660. doi: 10.1007/s11557-017-1365-2

Phookamsak, R., Norphanphoun, C., Tanaka, K., Dai, D. Q., Luo, Z. L., Liu, J. K., et al. (2015). Towards a natural classification of *Astrosphaeriella*-like species; introducing Astrosphaeriellaceae and Pseudoastrosphaeriellaceae fam. nov and *Astrosphaeriellopsis*, gen. nov. *Fungal Divers.* 74, 143–197. doi: 10.1007/s13225-015-0352-7

Phukhamsakda, C., McKenzie, E. H. C., Phillips, A. J. L., Jones, E. B. G., Bhat, D. J., Stadler, M., et al. (2020). Microfungi associated with *Clematis* (Ranunculaceae) with an integrated approach to delimiting species boundaries. *Fungal Divers.* 102, 1–203. doi: 10.1007/s13225-020-00448-4

Pirozynski, K. A. (1973). Three hyperparasites of ascomycetes. *Mycologia* 65, 761–767. doi: 10.2307/3758515

Rannala, B., and Yang, Z. (1996). Probability distribution of molecular evolutionary trees: a new method of phylogenetic inference. *J. Mol. Evol.* 43, 304–311. doi: 10.1007/BF02338839

Rehner, S. (2001). *Primers for Elongation Factor 1-Alpha (EF1-Alpha)*. Available online at: http://ocid.NACSE.ORG/research/deephyphae/ EF1primer.pdf (accessed June 20, 2020)

Ronquist, F., and Huelsenbeck, J. P. (2003). MrBayes 3: bayesian phylogenetic inference under mixed models. *Bioinformatics* 19, 1572–1574. doi: 10.1093/bioinformatics/btg180

Senanayake, I. C., Bhat, D. J., Cheewangkoon, R., and Xie, N. (2020a). Bambusicolous *Arthrinium* species in Guangdong Province, China. *Front. Microbiol.* 11:602773. doi: 10.3389/fmicb.2020.602773

Senanayake, I. C., Maharachchikumbura, S. S. N., Hyde, K. D., Bhat, J. D., Jones, E. B. G., McKenzie, E. H. C., et al. (2015). Towards unraveling relationships in Xylariomycetidae (Sordariomycetes). *Fungal Divers.* 73, 73–144. doi: 10.1007/s13225-015-0340-y

Senanayake, I. C., Rathnayaka, A. R., Marasinghe, D. S., Calabon, M. S., Gentekaki, E., Lee, H. B., et al. (2020b). Morphological approaches in studying fungi: collection, examination, isolation, sporulation and preservation. *Mycosphere* 11, 2678–2754. doi: 10.5943/mycosphere/11/1/20

Sommai, S., Nuankaew, S., Khamsuntorn, P., Suetrong, S., and Pinruan, U. (2019). *Tamhinispora saraburiensis* sp. nov. (Tubeufiaceae, Dothideomycetes) on bamboo in Thailand based on morphology & phylogenetic analysis. *Phytotaxa* 402, 1–2. doi: 10.11646/phytotaxa.402.1.1

Species Fungorum (2020). *Species Fungorum*. Available online at: http://www.speciesfungorum.org/Names/Names.asp (assessed Oct 27, 2020)

Sun, Y., Goonasekara, I. D., Thambugala, K. M., Jayawardena, R. S., Wang, Y., and Hyde, K. D. (2020). *Distoseptispora bambusae* sp. nov. (Distoseptisporaceae) on bamboo from China and Thailand. *Biodivers. Data J.* 8:e53678. doi: 10.3897/BDJ.8.e53678

Tanaka, K., Hirayama, K., Yonezawa, H., Hatakeyama, S., Harada, Y., Sano, T., et al. (2009). Molecular taxonomy of bambusicolous fungi: tetraplosphaeriaceae, a new pleosporalean family with *Tetraploa*-like anamorphs. *Stud. Mycol.* 64, 175–209. doi: 10.3114/sim.2009.64.10

Tanaka, K., Hirayama, K., Yonezawa, H., Sato, G., Toriyabe, A., Kudo, H., et al. (2015). Revision of the Massarineae (Pleosporales, Dothideomycetes). *Stud. Mycol.* 82, 75–136. doi: 10.1016/j.simyco.2015.10.002

Tang, X., Goonasekara, I. D., Jayawardena, R. S., Jiang, H. B., Li, J. F., Hyde, K. D., et al. (2020). *Arthrinium bambusicola* (Fungi, Sordariomycetes), a new species from *Schizostachyum brachycladum* in northern Thailand. *Biodivers. Data J.* 8:e58755. doi: 10.3897/BDJ.8.e58755

Tennakoon, D. S., Bhat, D. J., Kuo, C. H., and Hyde, K. D. (2019). Leaf litter saprobic Dictyosporiaceae (Pleosporales, Dothideomycetes):

Pseudocoleophoma zingiberacearum sp. nov. from *Hedychium coronarium*. *Kavaka* 53, 1–7. doi: 10.36460/Kavaka/53/2019/1-7

Vilgalys, R., and Hester, M. (1990). Rapid genetic identification and mapping of enzymatically amplified ribosomal DNA from several *Cryptococcus* species. *J. Bacteriol.* 172, 4238–4246. doi: 10.1128/jb.172.8.4238-4246.1990

White, T. J., Bruns, T., Lee, S., and Taylor, J. (1990). "Amplification and direct sequencing of fungal ribosomal RNA genes for phylogenetics," in *PCR Protocols, A Guide to Methods and Applications*, eds M. A. Innis, D. H. Gelfand, J. J. Sninsky, and T. J. White (San Diego, CA: Academic), 315–322.

Xie, X., Liu, L. L., Shen, X. C., Kang, Y. Q., Hyde, K. D., Kang, J. C., et al. (2020). Contributions to species of Xylariales in China-3. *Collodiscula tubulosa* (Xylariaceae). *Phytotaxa* 428, 122–130. doi: 10.11646/phytotaxa.428.2.6

Yang, C. L., Baral, H. O., Xu, X., and Liu, Y. (2019a). *Parakarstenia phyllostachydis*, a new genus and species of non-lichenized Odontotremataceae (Ostropales, Ascomycota). *Mycol. Prog.* 18, 833–845. doi: 10.1007/s11557-019-01492-4

Yang, C. L., Xu, X. L., Wanasinghe, D. N., Jeewon, R., Phookamsak, R., Liu, Y. G., et al. (2019b). *Neostagonosporella sichuanensis* gen. et sp. nov. (Phaeosphaeriaceae, Pleosporales) on *Phyllostachys heteroclada* (Poaceae) from Sichuan Province, China. *MycoKeys* 46, 119–150. doi: 10.3897/mycokeys.46.32458

Yang, J., Liu, J. K., Hyde, K. D., Jones, E. B. G., and Liu, Z. Y. (2018). New species in *Dictyosporium*, new combinations in *Dictyocheirospora* and an updated backbone tree for Dictyosporiaceae. *MycoKeys* 36, 83–105. doi: 10.3897/mycokeys.36.27051

Zeng, X. Y., Jeewon, R., Wen, T. C., Hongsanan, S., Boonmee, S., and Hyde, K. D. (2018). Simplified and efficient DNA extraction protocol for Meliolaceae specimens. *Mycol. Prog.* 17, 403–415. doi: 10.1007/s11557-017-1361-6

Zhang, J. Y., Phookamsak, R., Boonmee, S., Hyde, K. D., Dai, D. Q., and Lu, Y. Z. (2020). *Roussoella guttulata* (Roussoellaceae, Pleosporales), a novel bambusicolous ascomycete from Thailand. *Phytotaxa* 471, 221–233. doi: 10.11646/phytotaxa.471.3.4

Zhaxybayeva, O., and Gogarten, J. P. (2002). Bootstrap, Bayesian probability and maximum likelihood mapping: exploring new tools for comparative genome analyses. *Genomics* 3, 1–15. doi: 10.1186/1471-2164-3-4

Conflict of Interest: The authors declare that the research was conducted in the absence of any commercial or financial relationships that could be construed as a potential conflict of interest.

Copyright © 2021 Jiang, Jeewon, Karunarathna, Phukhamsakda, Doilom, Kakumyan, Suwannarach, Phookamsak and Lumyong. This is an open-access article distributed under the terms of the Creative Commons Attribution License (CC BY). The use, distribution or reproduction in other forums is permitted, provided the original author(s) and the copyright owner(s) are credited and that the original publication in this journal is cited, in accordance with accepted academic practice. No use, distribution or reproduction is permitted which does not comply with these terms.

frontiers in Microbiology

ORIGINAL RESEARCH
published: 13 May 2021
doi: 10.3389/fmicb.2021.660261

The Plant Family Asteraceae Is a Cache for Novel Fungal Diversity: Novel Species and Genera With Remarkable Ascospores in Leptosphaeriaceae

*Mingkwan Doilom[1,2,3,4], Kevin D. Hyde[1,2,3,4], Wei Dong[1,5], Chun-Fang Liao[4], Nakarin Suwannarach[2,3] and Saisamorn Lumyong[2,3,6]**

[1] Innovative Institute for Plant Health, Zhongkai University of Agriculture and Engineering, Guangzhou, China, [2] Research Center of Microbial Diversity and Sustainable Utilization, Faculty of Science, Chiang Mai University, Chiang Mai, Thailand, [3] Department of Biology, Faculty of Science, Chiang Mai University, Chiang Mai, Thailand, [4] Center of Excellence in Fungal Research, Mae Fah Luang University, Chiang Rai, Thailand, [5] Department of Entomology and Plant Pathology, Faculty of Agriculture, Chiang Mai University, Chiang Mai, Thailand, [6] Academy of Science, The Royal Society of Thailand, Bangkok, Thailand

OPEN ACCESS

Edited by:
Jadson Diogo Pereira Bezerra, Universidade Federal de Goiás, Brazil

Reviewed by:
Ning Jiang, Beijing Forestry University, China
Xinlei Fan, Beijing Forestry University, China

***Correspondence:**
Saisamorn Lumyong
scboi009@gmail.com

Specialty section:
This article was submitted to Evolutionary and Genomic Microbiology, a section of the journal Frontiers in Microbiology

Received: 29 January 2021
Accepted: 19 March 2021
Published: 13 May 2021

Citation:
Doilom M, Hyde KD, Dong W, Liao C-F, Suwannarach N and Lumyong S (2021) The Plant Family Asteraceae Is a Cache for Novel Fungal Diversity: Novel Species and Genera With Remarkable Ascospores in Leptosphaeriaceae. Front. Microbiol. 12:660261. doi: 10.3389/fmicb.2021.660261

In a cursory survey of fungi on Asteraceae in Yunnan Province, China, we report fungal species belonging to the family Leptosphaeriaceae (Pleosporales, Dothideomycetes). Two novel species have remarkable ascospores that are unusual for sexual ascomycetes. Multilocus phylogeny of large subunit, small subunit, and internal transcribed spacer sequence data showed one to be a novel genus, while the other is a new species. *Praeclarispora artemisiae* gen. et sp. nov. is introduced and is typical of Leptosphaeriaceae, but has unusual fusiform, versicolor ascospores with a brown median cell. *Sphaerellopsis artemisiae* sp. nov. has scolecosporous ascospores with deeply constricted septa that split into two parts, which resembles *S. isthmospora* but differs by ascospore dimension and molecular data. In addition, *Plenodomus artemisiae* is reported as a new collection from dead stems of *Artemisia argyi* in Qujing City. *Plenodomus sinensis* is reported as a new host record from *Ageratina adenophora*. All taxa are illustrated and described based on evidence of taxonomy and phylogeny.

Keywords: *Ageratina adenophora*, *Artemisia argyi*, China, new record, phylogeny, *Sphaerellopsis artemisiae*, taxonomy

INTRODUCTION

The plant family Asteraceae (= Compositae) is the major and widespread family of Angiosperms (flowering plants). The family comprises over 1,900 genera with over 32,000 accepted species (The Plant List, 2013). Most members of Asteraceae are herbaceous plants, but a significant number are shrubs, climbers, and trees. The family has a cosmopolitan distribution ranging from subpolar to tropical regions. The largest proportion of species occurs in arid and semiarid regions of subtropical

and lower to middle temperate latitudes (Barkley et al., 2006). Several members of Asteraceae are economically important plants as food crops, including globe artichoke (*Cynara cardunculus* var. *scolymus*), lettuce (*Lactuca* spp.), safflower (*Carthamus tinctorius*), and sunflower (*Helianthus* spp.). Many genera are important in horticulture such as pot marigold (*Calendula officinalis*) and coneflowers (*Echinacea* spp.), and others are of herbal medicinal importance, including gumweed (*Grindelia* spp.), yarrow (*Achillea millefolium*), and silvery wormwood (*Artemisia argyi*). Many species in Asteraceae are also considered as invasive weeds including sticky snakeroot (*Ageratina adenophora*) and Siam weed (*Chromolaena odorata*).

Studying the fungi on Asteraceae will provide important information toward establishing the numbers of fungi (Hyde et al., 2020b), due to the fact that many species are herbaceous in arid and semi-arid areas, where we know little about fungal diversity. Several novel fungal species have been described from the plant family Asteraceae. For example, *Hermatomyces chromolaenae* from stems of *Chromolaena odorata*, *Torula chromolaenae* from a dead branch of *C. odorata*, and *Dendryphion hydei* from branch litter of *Bidens pilosa* were introduced by Li et al. (2017, 2020) and Tibpromma et al. (2017), respectively. A novel genus, *Neocochlearomyces* isolated from leaves of *C. odorata*, was described by Crous et al. (2018). Phookamsak et al. (2019) introduced novel fungal species from *Cirsium arvense* and *Artemisia* sp. Mapook et al. (2020) introduced 60 new taxa from Siam weed, including one new family Neomassarinaceae, 12 new genera, and 47 new species. Herein, fungal species belonging to the family Leptosphaeriaceae are reported from *Ageratina adenophora* and *Artemisia argyi* (Asteraceae).

Leptosphaeriaceae (Pleosporales, Dothideomycetes) was established by Barr (1987) and typified by *Leptosphaeria*. Leptosphaeriaceae is characterized by immersed, erumpent to superficial ascomata, scleroplectenchymatous peridium, cylindrical asci and hyaline to brown, transversely septate ascospores with coelomycetous or hyphomycetous asexual morphs (Alves et al., 2013; de Gruyter et al., 2013; Hyde et al., 2013; Ariyawansa et al., 2015). Historic reviews of Leptosphaeriaceae were detailedly provided by Hyde et al. (2013) and Ariyawansa et al. (2015). Species of Leptosphaeriaceae are widely distributed on various hosts and different regions (Dayarathne et al., 2015; Tennakoon et al., 2017; Phookamsak et al., 2019). They can be saprobic, hemibiotropic, pathogenic, or parasitic occurring on stems and leaves of herbaceous or woody plants in terrestrial and aquatic habitats (Alves et al., 2013; Hyde et al., 2013; Jones et al., 2015; Wanasinghe et al., 2016; Doilom et al., 2018). The early classification of taxa in Leptosphaeriaceae lacked DNA sequence data from ex-type strains. In addition, most strains in GenBank are named without a link to voucher specimens, which is not practical to verify their morphological characteristics to ensure accurate naming (Ariyawansa et al., 2015). Thus, phylogenetic analyses of taxa in Leptosphaeriaceae formed a paraphyletic clade (Dong et al., 1998; Zhang et al., 2012). Ariyawansa et al. (2015) provided a well-resolved backbone tree for Leptosphaeriaceae to resolve species and genera based on multilocus phylogeny with detailed morphology, and the results supported the monophyletic nature of 10 genera in Leptosphaeriaceae among the other families in Pleosporales. Currently, 14 genera are accepted in the family, *viz*., *Alloleptosphaeria*, *Alternariaster*, *Chaetoplea*, *Heterosporicola*, *Leptosphaeria*, *Neoleptosphaeria*, *Ochraceocephala*, *Paraleptosphaeria*, *Plenodomus*, *Pseudoleptosphaeria*, *Querciphoma*, *Sclerenchymomyces*, *Sphaerellopsis*, and *Subplenodomus* (Hongsanan et al., 2020a; Wijayawardene et al., 2020).

In this study, we introduce a new genus and two new species from *Artemisia argyi* that have remarkable ascospores. In addition, *Plenodomus sinensis* is reported as a new host record from *Ageratina adenophora*. Combined analyses of large subunit (LSU), small subunit (SSU), and internal transcribed spacer (ITS) sequence data with morphology supported the placement of our taxa in Leptosphaeriaceae.

MATERIALS AND METHODS

Sample Collection, Specimen Examination, and Fungal Isolation

The specimens of *Ageratina adenophora* and *Artemisia argyi* belonging in Asteraceae were collected from Yunnan Province, China. Specimens were placed in zip-lock plastic bags and returned to the laboratory for fungal observation and isolation. Fungal structures on the host substrates were observed using the Motic SMZ 161 stereomicroscope and their ascomata on substrates were captured with a digital camera fitted on to the stereomicroscope. Micro-morphological characteristics were observed and photographed with a Nikon ECLIPSE Ni compound microscope fitted with a Canon EOS 600D digital camera. Indian Ink was used to observe mucilaginous sheaths surrounding the ascospores. Micro-morphological characteristics were measured by the Tarosoft (R) Image Frame Work program. Images used for figures were edited with Adobe Photoshop CS6 software (Adobe Systems, United States).

Fungal isolation was made from single spore as detailed in Chomnunti et al. (2014). Germinating ascospores were observed using the Motic SMZ 161 stereomicroscope and single ascospore was transferred using sterile needle and grown on potato dextrose agar (PDA) at room temperature (25–30°C). Pure cultures were kept for further studies.

Fungal Preservation and Fungal Registration Numbers

The herbaria were deposited at the herbarium of Cryptogams, Kunming Institute of Botany Academia Sinica (HKAS), Kunming, Yunnan Province, China and Key Laboratory of Industrial Microbiology and Fermentation Technology of Yunnan (YMF), Kunming, Yunnan Province, China. Living cultures were deposited at the Kunming Institute of Botany Culture Collection (KMUCC), Kunming, Yunnan Province, China. Facesoffungi (FoF) numbers and Index Fungorum (IF) numbers were registered as described by Jayasiri et al. (2015) and Index Fungorum (2021), respectively.

DNA Extraction, PCR Amplification, and Sequencing

Fungi were grown on PDA for 1 week at room temperature (25–30°C). Fungal mycelia were then scraped off and transferred to 1.5 ml sterilized micro-centrifuge tubes. Biospin Fungus Genomic DNA Extraction Kit–BSC14S1 (BioFlux®, China) was used to extract genomic DNA following the manufacturer's protocol. The LSU 28S rRNA, the SSU 18S rRNA, the ITS, partial translation elongation factor 1-alpha (*tef1*-α) and partial RNA polymerase II second largest subunit (*rpb2*) were amplified and sequenced using primers LR0R/LR5 (Vilgalys and Hester, 1990; Rehner and Samuels, 1994), NS1/NS4, ITS5/ITS4 (White et al., 1990), EF1-983F/EF1-2218R (Rehner and Buckley, 2005), and fRPB2-5f/fRPB2-7cR (Liu et al., 1999), respectively.

The PCR amplification was performed in a total volume of 25 μl. PCR mixtures contained 12.5 μl of Easy Taq PCR Super Mix, 1 μl of dNTPs, 1 μl of each primer, and 9.5 μl of ddH_2O. The PCR thermal cycle program for LSU, SSU, and ITS amplification was provided as initially 94°C for 3 min, followed by 35 cycles of denaturation at 94°C for 30 s, annealing at 56°C for 50 s, elongation at 72°C for 90 s, and a final extension at 72°C for 10 min. The annealing was adjusted to 52°C and 55°C for *rpb2* and *tef1*-α, respectively. PCR products were purified and sequenced at Shanghai Sangon Biological Engineering Technology & Services Co., (Shanghai, China). GenBank accession numbers of *tef1*-α of our strains are provided in "Additional GenBank numbers."

Phylogenetic Analysis

Consensus sequences were generated using BioEdit v.7.2.5 (Hall, 1999). Sequences of each strain were blasted using the MegaBLAST search of GenBank's nucleotide database[1] to examine their closest taxa. A total 89 sequences were used in phylogenetic analyses (**Table 1**). *Didymella exigua* (CBS 183.55) was used as the outgroup taxon. Individual dataset of the LSU, SSU, and ITS was aligned online with MAFFT version v.7.471 (Katoh et al., 2019)[2] and manually edited where necessary using BioEdit v.7.2.5. Phylogenetic trees were inferred with maximum parsimony (MP), maximum likelihood (ML), and Bayesian inference (BI).

Maximum parsimony analysis was performed with PAUP v. 4.0b10, with the parameter setting as the method described in Wanasinghe et al. (2018). Descriptive tree statistics for parsimony [Tree Length (TL), Consistency Index (CI), Retention Index (RI), Relative Consistency Index (RC), and Homoplasy Index (HI)] were calculated for trees generated under different optimality criteria. ML analysis was calculated as the method described in Doilom et al. (2017). All free model parameters will be estimated by RAxML and ML estimate of 25 per site rate categories. The model selected for ML was GTRGAMMA. BI analysis was conducted using the Markov Chain Monte Carlo (MCMC) method with MrBayes v. 3.2.7 (Huelsenbeck and Ronquist, 2001). By using MrModeltest 2.2 (Nylander, 2004), the GTR + I + G was selected as the best-fit nucleotide substitution models under the Akaike information criterion (AIC) for LSU, SSU, and ITS sequence data. Six chains were run for the individual and combined datasets. The MCMC algorithm was started from a random tree topology. Five million generations were selected with a sampling frequency every 100 generations. The Tracer v.1.6 program (Rambaut et al., 2013) was used to check the effective sampling sizes (ESS) that should be above 200, the stable likelihood plateaus, and burn-in value. The results suggest that the first 5,000 generations should be excluded as burn-in. Phylogenetic trees were visualized using FigTree v.1.4.0 (Rambaut, 2009) and formatted using PowerPoint 2010 (Microsoft Corporation, WA, United States).

[1] http://blast.ncbi.nlm.nih.gov/

[2] http://mafft.cbrc.jp/alignment/server/index.html

RESULTS

Phylogenetic Analysis

The alignment comprised 90 strains including the outgroup taxon, which consisted of 3,286 characters including alignment gaps (1–1331 bp for LSU, 1332–2680 bp for SSU, and 2681–3286 bp for ITS). The MP analysis for the combined dataset had 325 parsimony informative, 2,840 constant, and 121 parsimony uninformative characters and yielded 18 most parsimonious trees (TL = 2158, CI = 0.342, RI = 0.729, HI = 0.658, and RC = 0.249). The RAxML analysis resulted in a best scoring likelihood tree selected with a final combined dataset = −15205.152646. The matrix had 620 distinct alignment patterns, with 36.47% of undetermined characters or gaps.

Phylogenetic analysis of combined LSU, SSU, and ITS sequence data (**Figure 1**) showed that *Praeclarispora artemisiae* (KUMCC 20-0201A and KUMCC 20-0201B) clustered with *Ochraceocephala* (MP/ML/BI = 61%/96%/1.00) in the family Leptosphaeriaceae. Two strains, KUMCC 20-0200A and KUMCC 20-0200B, grouped with the ex-type strain of *Plenodomus artemisiae* (KUMCC 18-0151) with high bootstrap support (MP/ML/BI = 96%/95%/1.00). The collection KUMCC 20-0204 clustered with MFLU 17-0757 (paratype) and other strains of *Plenodomus sinensis* (MP/ML/BI = 70%/85%/1.00). *Sphaerellopsis artemisiae* (KUMCC 20-0202A and KUMCC 20-0202B) grouped separately from its closest relative *Sphaerellopsis isthmospora* with strong bootstrap support (MP/ML/BI = 100%/100%/1.00) (**Figure 1**).

Taxonomy

Praeclarispora Doilom, W. Dong, K. D. Hyde & C. F. Liao, *gen. nov*.

Index Fungorum number: IF558142; FoF number: FoF 09225

Etymology: The generic epithet "*Praeclarispora*" refers to remarkable-spored.

Saprobic on dead twigs of *Artemisia argyi*. **Sexual morph:** *Ascomata* black, scattered to gregarious, breaking the epidermis in linear fissures, semi-immersed, becoming erumpent to superficial, subglobose, uni- to multi-loculate, coriaceous, with ostiolate papilla. *Peridium* unevenly relatively thick, composed of several layers of thick-walled cells of *textura angularis*, outer layer black, inner layer brown. *Hamathecium* comprising numerous,

TABLE 1 | GenBank accession numbers and culture collection numbers of species included in the present phylogenetic study.

Species	Culture collection/voucher no.	GenBank accession numbers		
		LSU	SSU	ITS
Alloleptosphaeria italica	MFLUCC 14-0934^{T}	KT454714	N/A	KT454722
Alternariaster bidentis	CBS 134021^{T}	KC609341	N/A	KC609333
Alternariaster centaureae-diffusae	MFLUCC 14-0992^{T}	KT454715	KT454730	KT454723
	MFLUCC 15-0009	KT454716	KT454731	KT454724
Alternariaster helianthi	CBS 327.69	KC584369	KC584627	KC609335
Didymella exigua	CBS 183.55^{NT}	EU754155	EU754056	GU237794
Heterosporicola chenopodii	CBS 115.96	EU754188	EU754089	JF740227
	CBS 448.68^{ET}	EU754187	EU754088	FJ427023
Heterosporicola dimorphospora	CBS 165.78	JF740281	JF740098	JF740204
	CBS 345.78^{ET}	GU238069	GU238213	NR111618
Leptosphaeria cichorii	MFLUCC 14-1063^{T}	KT454712	KT454728	KT454720
Leptosphaeria conoidea	CBS 616.75	MH872726	JF740099	MH860957
Leptosphaeria doliolum	MFLU 15-1875	KT454719	KT454734	KT454727
	CBS 155.94	JF740282	N/A	JF740207
	CBS 505.75^{IT}	GQ387576	GQ387515	JF740205
	CBS 541.66	JF740284	N/A	JF740206
Leptosphaeria slovacica	CBS 125975	JF740316	N/A	JF740248
	CBS 389.80	JF740315	JF740101	JF740247
Neoleptosphaeria rubefaciens	CBS 223.77	JF740312	N/A	JF740243
	CBS 387.80	JF740311	N/A	JF740242
Ochraceocephala foeniculi	CBS 145654^{T}	MN516774	MN516743	MN516753
Paraleptosphaeria dryadis	CBS 643.86	GU301828	KC584632	JF740213
Paraleptosphaeria macrospora	CBS 114198	MH874520	N/A	MH862957
Paraleptosphaeria nitschkei	CBS 306.51^{ET}	JF740308	N/A	JF740239
	MFLU 13-0688	KR025864	N/A	KR025860
Paraleptosphaeria orobanches	CBS 101638^{T}	JF740299	N/A	JF740230
Paraleptosphaeria praetermissa	CBS 114591	JF740310	N/A	JF740241
Paraleptosphaeria rubi	MFLUCC 14-0211^{T}	KT454718	KT454733	KT454726
Paraphoma radicina	CBS 111.79^{ET}	EU754191	EU754092	FJ427058
Phaeosphaeria oryzae	CBS 110110^{ET}	GQ387591	GQ387530	KF251186
Plenodomus agnitus	CBS 121.89	JF740271	N/A	JF740194
	CBS 126584	JF740272	N/A	JF740195
Plenodomus artemisiae	KUMCC 18-0151^{T}	MK387958	MK387928	MK387920
	KUMCC 20-0200A	**MT957055**	**MT957048**	**MT957062**
	KUMCC 20-0200B	**MT957056**	**MT957049**	**MT957063**
Plenodomus biglobosus	CBS 119951	JF740274	JF740102	JF740198
	CBS 127249	JF740275	N/A	JF740199
Plenodomus chrysanthemi	CBS 539.63^{T}	GU238151	GU238230	NR111622
Plenodomus collinsoniae	CBS 120227	JF740276	N/A	JF740200
Plenodomus confertus	CBS 375.64	JF740277	N/A	AF439459
Plenodomus congestus	CBS 244.64^{T}	JF740278	N/A	AF439460
Plenodomus deqinensis	CGMCC 3.18221^{T}	KY064031	N/A	KY064027
Plenodomus enteroleucus	CBS 142.84^{ET}	JF740287	N/A	JF740214
	CBS 831.84	JF740288	N/A	JF740215
Plenodomus fallaciosus	CBS 414.62	JF740292	N/A	JF740222
Plenodomus guttulatus	MFLU 15-1876^{T*}	KT454713	KT454729	KT454721
Plenodomus hendersoniae	CBS 113702	MH874506	N/A	MH862939
Plenodomus influorescens	CBS 143.84	JF740297	N/A	JF740228
Plenodomus libanotidis	CBS 113795	MH874508	N/A	MH862943
Plenodomus lijiangensis	KUMCC 18-0186^{T}	MK387959	MK387929	MK387921
Plenodomus lindquistii	CBS 386.80	JF740301	N/A	JF740232

Continued.

TABLE 1 | Continued

Species	Culture collection/ voucher no.	GenBank accession numbers		
		LSU	SSU	ITS
Plenodomus lingam	CBS 260.94	JF740307	N/A	JF740235
Plenodomus lupini	CBS 248.92	JF740303	N/A	JF740236
Plenodomus pimpinellae	CBS 101637^{T}	MH874352	N/A	JF740240
Plenodomus salviae	MFLUCC 13-0219^{T}	KT454717	KT454732	KT454725
Plenodomus sinensis	KUMCC 18-0152	MK387961	MK387931	MK387923
	KUMCC 18-0153	MK387960	MK387930	MK387922
	KUMCC 20-0204	**MT957057**	**MT957050**	**MT957064**
	KUN-HKAS 102227	MK387962	MK387932	MK387924
	MFLU 17-0757^{PT}*	MF072718	MF072720	MF072722
	MFLU 17-0767^{T}*	MF072717	MF072719	MF072721
Plenodomus tracheiphilus	CBS 127250	JF740318	N/A	JF740250
Plenodomus triseptatus	MFLUCC 17-1345^{T}	MN648451	MN648453	MN648452
Plenodomus visci	CBS 122783^{T}	EU754195	EU754096	NR119957
Plenodomus wasabiae	CBS 120119	JF740323	N/A	JF740257
Praeclarispora artemisiae	**KUMCC 20-0201A^{T}**	**MT957053**	**MT957046**	**MT957060**
	KUMCC 20-0201B^{T}	**MT957054**	**MT957047**	**MT957061**
Pseudoleptosphaeria etheridgei	CBS 125980^{T}	JF740291	N/A	JF740221
Querciphoma carteri	CBS 101633	GQ387593	GQ387532	KF251210
	CBS 105.91	GQ387594	GQ387533	KF251209
Sclerenchymomyces clematidis	MFLUCC 17–2180^{T}	MT214558	MT226675	MT310605
Sclerenchymomyces jonesii	MFLUCC 16-1442^{T}	KY211870	KY211871	KY211869
Sphaerellopsis artemisiae	**KUMCC 20-0202A^{T}**	**MT957058**	**MT957051**	**MT957065**
	KUMCC 20-0202B^{T}	**MT957059**	**MT957052**	**MT957066**
Sphaerellopsis filum	CBS 234.51	KP170723	N/A	KP170655
	CBS 235.51	KP170724	N/A	KP170656
	CBS 317.68^{NT}	KP170725	N/A	KP170657
Sphaerellopsis hakeae	CPC 29566^{T}	KY173555	N/A	KY173466
Sphaerellopsis isthmospora	HKAS 102225A^{T}*	MK387963	MK387933	MK387925
	HKAS 102225B^{T}*	MK387964	MK387934	MK387926
Sphaerellopsis macroconidialis	CBS 233.51	KP170726	N/A	KP170658
	CBS 658.78^{T}	KP170727	N/A	KP170659
	CPC 21113	KP170728	N/A	KP170660
Sphaerellopsis paraphysata	CPC 21841^{T}	KP170729	N/A	KP170662
	KUMCC 18-0195	MK387965	MK387935	MK387927
Subplenodomus apiicola	CBS 285.72	GU238040	GU238211	JF740196
Subplenodomus drobnjacensis	CBS 270.92	JF740286	N/A	JF740212
Subplenodomus valerianae	CBS 499.91	JF740319	N/A	JF740252
	CBS 630.68	GU238150	GU238229	JF740251
Subplenodomus violicola	CBS 306.68	GU238156	GU238231	FJ427083

CBS, Westerdijk Fungal Biodiversity Institute, Utrecht, The Netherlands; CGMCC, China General Microbiological Culture Collection Center, Beijing, China; CPC, Collection of Pedro Crous housed at CBS; HKAS, Herbarium of Cryptogams, Kunming Institute of Botany Academia Sinica, Yunnan, China; KUMCC, Kunming Institute of Botany Culture Collection, Chinese Science Academy, Kunming, China; MFLU, Mae Fah Luang University, Chiang Rai, Thailand.; MFLUCC, Mae Fah Luang University Culture Collection, Chiang Rai, Thailand.

^{ET}, ex-epitype; ^{IT}, ex-isotype; ^{NT}, ex-neotype; ^{PT}, paratype; ^{T}, ex-type; ^{T}*, holotype.*

The newly generated sequences are shown in bold.

filiform, septate, of cellular pseudoparaphyses embedded in a gelatinous matrix. *Asci* eight-spored, bitunicate, fissitunicate, narrowly obovoid, short pedicellate, apically rounded, with ocular chamber. *Ascospores* tri- to tetra-seriate, fusiform, curved, tapered toward the acute ends, versicolor, 0–1-septate when immature, becoming brown in median cell and hyaline to pale brown in other cells, middle cell larger than other cells, septate when mature, slightly constricted at the septa, thin- and smooth-walled. **Asexual morph:** Undetermined.

Type species*: P. artemisiae* Doilom, W. Dong, K. D. Hyde and C. F. Liao

Notes: Based on a blastn search of NCBIs GenBank, the closest hits using LSU sequence of *Praeclarispora artemisiae* matches with several genera in Leptosphaeriaceae and has highest

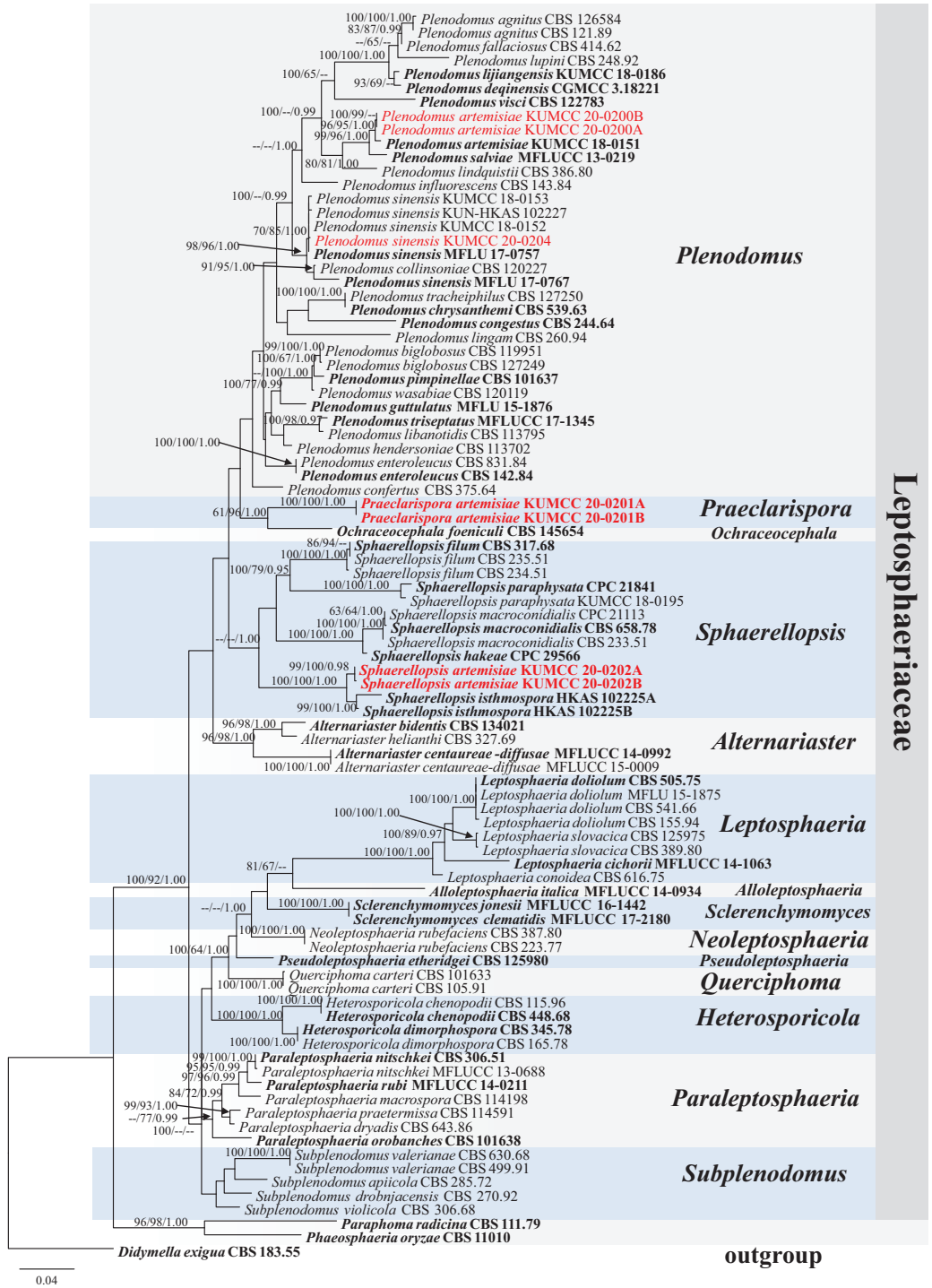


FIGURE 1 | Phylogenetic tree generated from maximum likelihood analysis (RAxML) based on a combined LSU, SSU, and ITS sequence data. The tree is rooted to *Didymella exigua* (CBS 183.55). Maximum parsimony and maximum likelihood bootstrap values ≥60% and Bayesian posterior probabilities ≥0.95 (MPBS/MLBS/BYPP) are indicated at the nodes. Ex-epitype, ex-isotype, ex-neotype, ex-type, holotype, and paratype are bolded black, and the new isolates are in red.

similarity to *Sphaerellopsis filum* (CBS 234.51, identities = 99.18%) and *S. paraphysata* (CPC 21841, identities = 99.05%), followed by *Ochraceocephala foeniculi* (CBS 145654, identities = 98.83%). The closest hits using SSU sequence are *Plenodomus lingam* (CBS 260.94, identities = 99.81%), *Pl. artemisiae* (KUMCC 20-0200A, identities = 99.81%), *Pl. biglobosus* (CBS

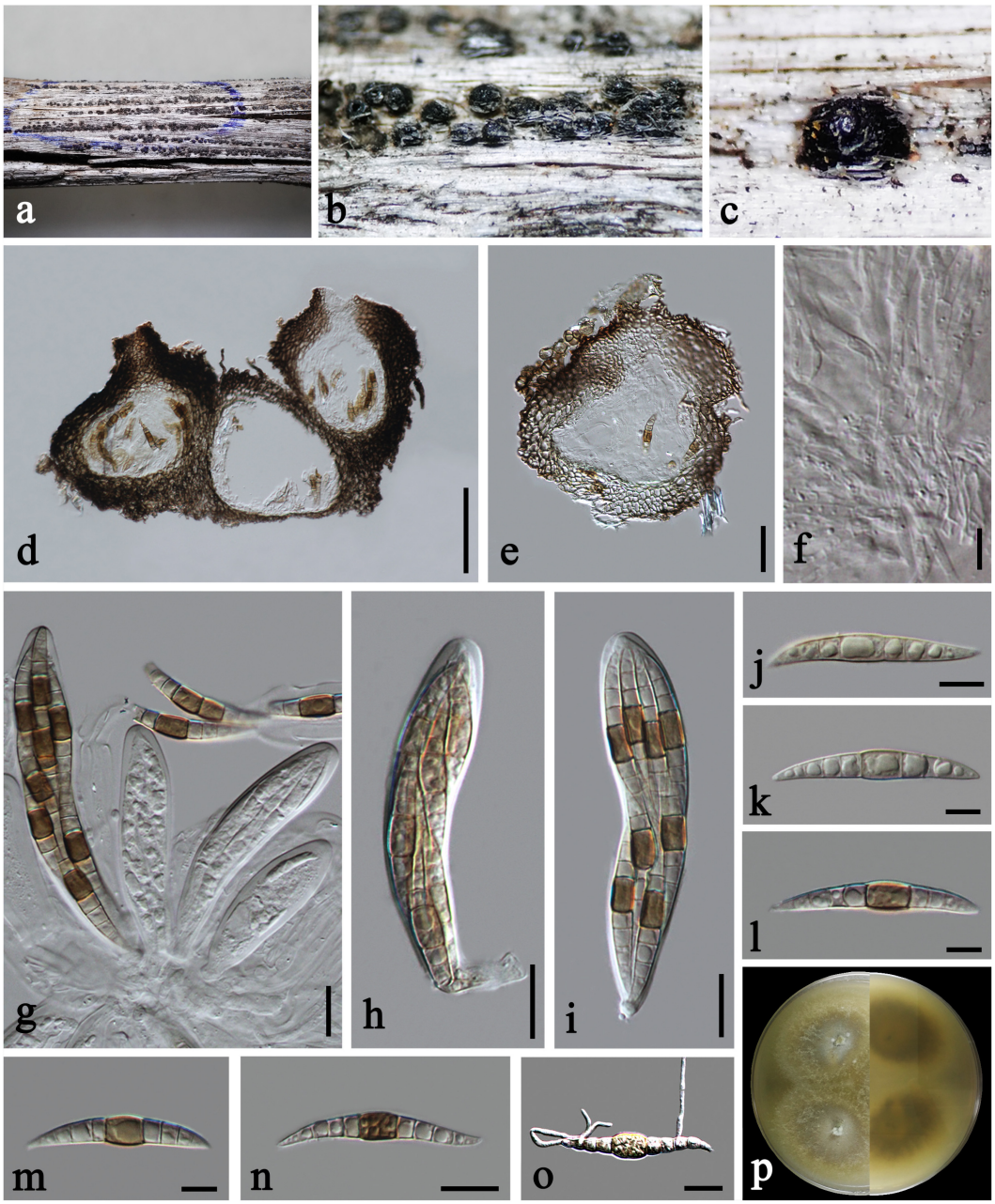


FIGURE 2 | *Praeclarispora artemisiae* (HKAS 112654, holotype). **(a–c)** Appearance of ascomata on host substrate. **(d,e)** Vertical sections through ascomata. **(f)** Pseudoparaphyses. **(g–i)** Asci. **(j–n)** Ascospores. **(o)** Germinated ascospore. **(p)** Colony on PDA after 15 days (above and below views). Scale bars: **(c)** = 250 μm, **(d)** = 50 μm, **(e)** = 30 μm, **(f,k–m)** = 10 μm, **(g–j,n,o)** = 20 μm.

119951, identities = 99.81%), and *O. foeniculi* (CBS 145654, identities = 99.71%). ITS sequence matches with published species *Pl. hendersoniae* (CBS 113702, identities = 92.14%), *Pl. biglobosus* (CBS 119951, identities = 89.66%), and *O. foeniculi* (CBS 145654, identities = 87.93%). However, in our multilocus analysis (**Figure 1**), *P. artemisiae* forms a sister branch with *O. foeniculi* with 96% ML and 1.00 BYPP but low MP bootstrap support, and separates from *Leptosphaeria*, *Plenodomus*, and *Sphaerellopsis*. The ITS phylogeny has similar results with the multilocus phylogeny (**Supplementary Figure 1**); LSU phylogenetic analysis clearly shows *Praeclarispora* separates from *O. foeniculi* as a distinct genus (**Supplementary Figure 2**). A single gene comparison between *P. artemisiae* and *O. foeniculi* shows that there are 1.17% (10/854), 0.29% (3/1029), and 13.81% (76/550) nucleotide difference in LSU, SSU, and ITS sequence data, respectively.

Ochraceocephala foeniculi is only known from its hyphomycetous asexual morph, which is characterized by

hyaline, loosely or densely branched conidiophores, phialidic conidiogenous cells, and hyaline to yellowish, globose to subglobose conidia, and isolated as plant pathogen from living *Foeniculum vulgare* (Aiello et al., 2020). *Praeclarispora artemisiae* is reported herein from only its ascomycetous sexual morph, characterized by black ascomata, narrowly obovoid asci, and fusiform ascospores with a larger, brown, median cell, and isolated as saprobe from decaying twigs of *Artemisia argyi*. Unfortunately, we could not obtain the asexual morph from the culture for further morphological assessments. Even though we observed them under different conditions as described in Phookamsak et al. (2015) and Senanayake et al. (2020), neither conidia nor conidiomatal structures were produced. Therefore, we believe that it is wise to keep *Ochraceocephala* and *Praeclarispora* as separate genera in Leptosphaeriaceae for now. A different scenario may occur with the discovery of similar fungi from both of their asexual and sexual morphs with more fresh sampling.

Praeclarispora artemisiae Doilom, W. Dong, K. D. Hyde & C. F. Liao, *sp. nov.*, **Figure 2**.

Index Fungorum number: IF558143; FoF number: FoF 09226

Etymology: The specific epithet "*artemisiae*" refers to the host genus *Artemisia*.

Holotype: HKAS 112654

Saprobic on dead twigs of *Artemisia argyi*. **Sexual morph:** *Ascomata* 170–245 μm high, 185–285 μm diam., black, scattered to gregarious, breaking the epidermis in linear fissures, semi-immersed, becoming erumpent to superficial, subglobose, uni- to multi-loculate, coriaceous, with ostiolate papilla. *Ostioles* 50–70 μm diam., central, brown, ostiolar canal filled with periphyses. *Peridium* 30–60 μm wide at the sides, unevenly thick, composed of scleroplectenchymatous cells, arrange in *textura angularis*, outer layer black, inner layer brown. *Hamathecium* 2–4.5 μm diam., numerous, filiform, septate, of cellular pseudoparaphyses embedded in a gelatinous matrix. *Asci* 100–140 × 19–27 μm ($\bar{x}$ = 120 × 23 μm, n = 15), eight-spored, bitunicate, fissitunicate, narrowly obovoid, short pedicellate, apically rounded, with ocular chamber. *Ascospores* 55–70 × 6–11 μm ($\bar{x}$ = 61 × 8.5 μm, n = 20), overlapping tri- to tetra-seriate, fusiform, curved, tapered to acute ends, versicolor, 0–1-septate when immature, becoming brown in median cell or occasionally two median cells, and hyaline to pale brown in other cells (**Figure 2g**), middle cell longer and slightly wider than the other cells, 8–10(–12)-euseptate when mature, slightly constricted at the septa, guttulate, thin- and smooth-walled. **Asexual morph:** Undetermined.

Culture characteristics: On PDA, colony circular, reaching 45 mm diam. in 15 days at room temperature (25–30°C), surface rough, with sparse mycelia on the surface, dry, umbonate from the side view, edge entire; from above, yellowish to cream at the margin, gray at the middle, white at the center; from below, yellowish at the margin, gray at the middle, yellowish brown at the center; producing yellowish pigmentation in culture.

Material examined: CHINA, Yunnan Province, Qujing City, dead twigs of *Artemisia argyi* (Asteraceae), October 1, 2019, C. F. Liao, (HKAS 112654, **holotype**); ex-type living culture KUMCC 20-0201; *ibid*., YMF 107390, **isotype**.

Additional GenBank numbers: *tef1*-α = MW396658 (KUMCC 20-0201A); MW396659 (KUMCC 20-0201B).

Plenodomus artemisiae A. Karunarathna, Phookamsak and K. D. Hyde, in Phookamsak et al., Fungal Diversity 95: 23 (2019), **Figures 3**, **4a**

Saprobic on dead stems of *Artemisia argyi*. **Sexual morph:** *Ascomata* 140–230 μm high, 210–260 μm diam., black, scattered, superficial with base seated in the substrate, compressed globose, uniloculate, glabrous, coriaceous, ostiolate, obscurely papillate. *Peridium* unevenly thick, 20–60 μm wide at the sides, with a poorly developed base, 10–15 μm wide, thinner toward the papilla, 12–15 μm wide, composed of several layers of thick-walled cells of *textura angularis*, outer layer black, inner layer brown. *Hamathecium* 2–2.5 μm diam., numerous, filiform, hyaline, septate, of cellular pseudoparaphyses embedded in a gelatinous matrix. *Asci* 60–80 × 9.5–11 μm ($\bar{x}$ = 68 × 10 μm, n = 15), eight-spored, bitunicate, fissitunicate, cylindric-clavate, short pedicellate, apically rounded. *Ascospores* 29–36 × 4.5–5.5 μm ($\bar{x}$ = 33 × 4.8 μm, n = 15), overlapping 2–3-seriate, narrowly fusiform, with tapering and rounded ends, hyaline, 1-septate, occasionally 5–7-septate when old, constricted at the median septum, guttulate, thin- and smooth-walled, without sheath or appendages. **Asexual morph:** Undetermined.

Culture characteristics: On PDA, colony irregular, reaching 40 mm diam. in 14 days at room temperature (25–30°C), surface rough, with dense mycelia, velvety and fluffy, dry, raised from the side view, edge undulate; from above, yellowish at the margin, cream to white at the center; from below, yellowish at the margin, orange brown at the middle, black at the center; producing yellowish pigmentation in culture.

Material examined: CHINA, Yunnan Province, Qujing City, dead stems of *Artemisia argyi* (Asteraceae), October 1, 2019, C. F. Liao, (HKAS 112653, **new collection**); living culture KUMCC 20-0200; *ibid*., YMF 112653, **new collection**.

Additional GenBank numbers: *tef1*-α = MW396660 (KUMCC 20-0200A); MW396661 (KUMCC 20-0200B).

Notes: Our collections KUMCC 20-0200A and KUMCC 20-0200B cluster with *Plenodomus artemisiae* (KUMCC 18-0151) with strong bootstrap support (MP/ML/BI = 99%/96%/1.00) (**Figure 1**). They have very similar morphological characteristics, except our collections have more septa (5–7-septate vs. only 5-septate) than the holotype (KUN-HKAS 102226) of *Pl. artemisiae* (Phookamsak et al., 2019). Our two collections have 99.65%, 99.90, 99.44, and 99.34% similarities with the ex-type strain (KUMCC 18-0151) of *Pl. artemisiae* in LSU, SSU, ITS, and *tef1*-α sequence data, respectively, which indicate them to be conspecific. We therefore identify our collections as *Pl. artemisiae* based on morphological and molecular evidences. *Plenodomus artemisiae* was initially reported from dead branches and stems of an unidentified *Artemisia* sp. in Yunnan Province, China (Phookamsak et al., 2019). Our new collection was collected from the same region, and we identify its host as *Artemisia argyi*.

Plenodomus sinensis Tennakoon, Phook. and K. D. Hyde, in Tennakoon et al., Phytotaxa 324(1): 76 (2017), **Figures 4b**, **5**

Saprobic on *Ageratina adenophora*. **Sexual morph:** *Ascomata* 220–325 μm high, 205–345 μm diam., black, scattered to gregarious, raised, superficial, subglobose to conical, with

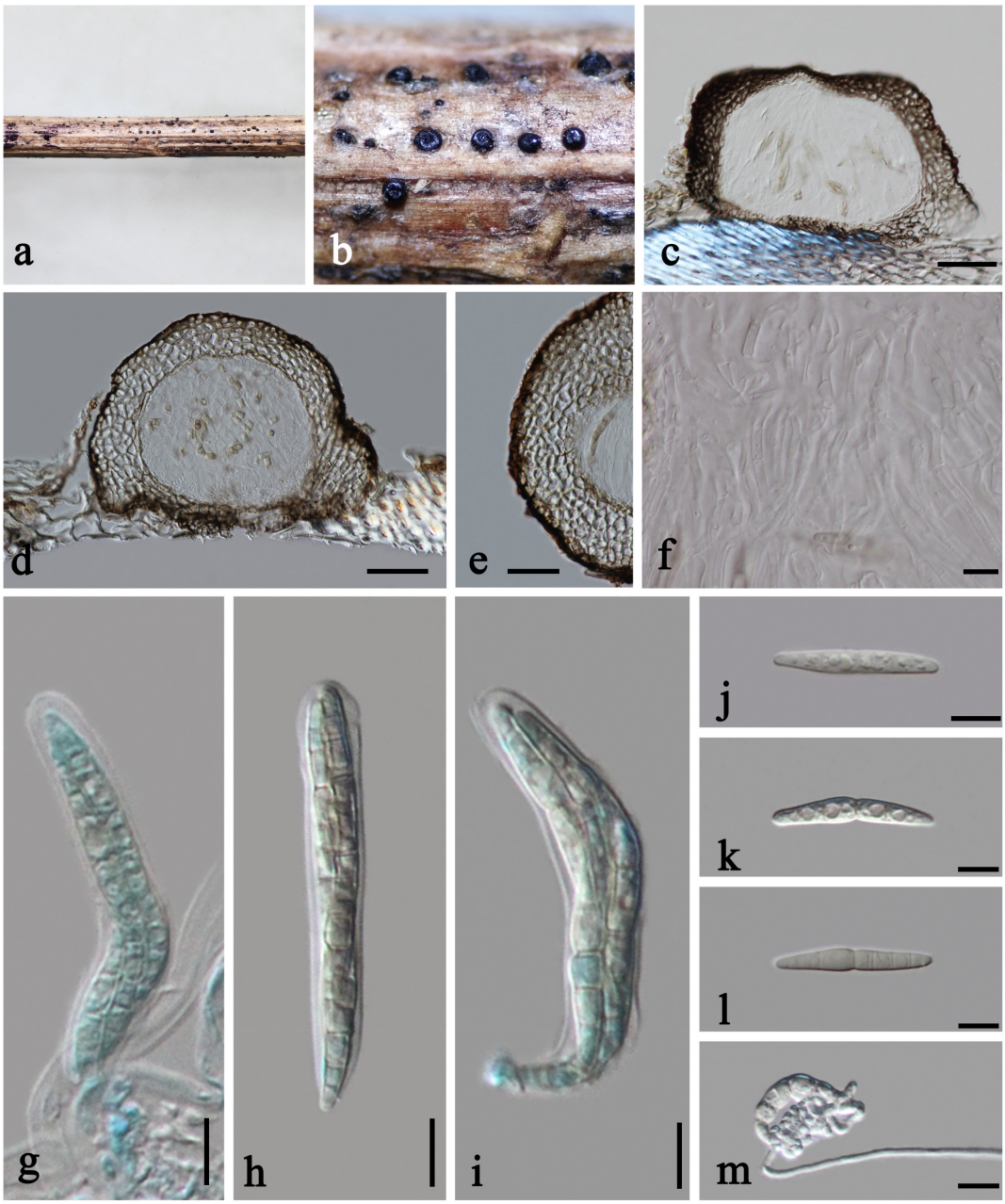


FIGURE 3 | *Plenodomus artemisiae* (HKAS 112653, new collection). **(a,b)** Ascomata on host substrate. **(c,d)** Vertical sections of ascomata. **(e)** Structure of peridium. **(f)** Pseudoparaphyses. **(g–i)** Asci. **(j–l)** Ascospores (l showing the old ascospore occasionally with 5–7 septa). **(m)** Germinated ascospore. Scale bars: **(c,d)** = 50 μm, **(e)** = 30 μm, **(f–m)** = 10 μm.

flattened and thickened base, uniloculate, glabrous, coriaceous, with minutely ostiolate papilla, easily removed from the host substrate. *Ostioles* 55–95 μm diam., central, brown, ostiolar canal filled with some periphyses. *Peridium* unevenly thick, 25–115 μm wide at the base, 30–70 μm wide at the sides, mostly thickened at the base and thinner at the sides, three-layered, outer layer composed of dark brown, thick-walled cells of *textura angularis*, middle layer composed of pale brown to subhyaline, thick-walled, large cells of *textura globulosa* or *textura angularis*, inner layer composed of light brown, thin-walled, compressed cells of *textura angularis*. *Hamathecium* 2–4.5 μm wide, septate, branched, of cellular pseudoparaphyses embedded in a gelatinous matrix, slightly constricted at the septa. *Asci* 80–115 × 10–13 μm ($\bar{x}$ = 98 × 11 μm, *n* = 20), eight-spored, bitunicate, fissitunicate, cylindrical, with short furcate pedicel, apically rounded, with a distinct ocular chamber. *Ascospores* 29–39 × 4–5.5 μm ($\bar{x}$ = 33 × 4.9 μm, *n* = 30), overlapping 2–3-seriate, hyaline, 0–1-septate when immature, becoming olivaceous to

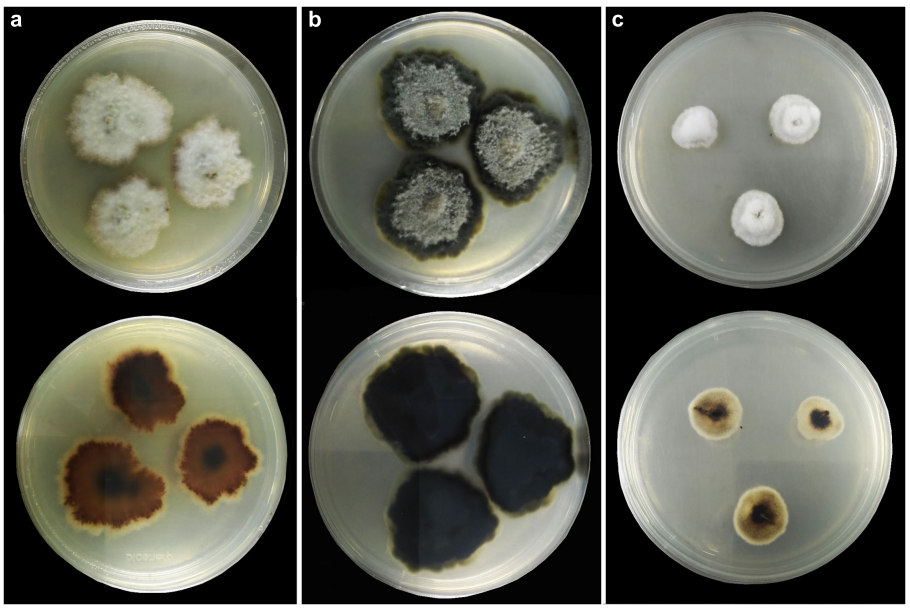


FIGURE 4 | Colonies on PDA (up-front, down-reverse). **(a)** *Plenodomus artemisiae* (HKAS 112653). **(b)** *Plenodomus sinensis* (HKAS 112657). **(c)** *Sphaerellopsis artemisiae* (HKAS 112655).

yellowish, fusiform, with obtuse ends, 6–7-septate, constricted at the middle septum, not or slightly constricted at each septum, cell above central septum slightly wider, guttulate, thick- and smooth-walled, with mucilaginous globoid-shaped appendages at both ends. **Asexual morph:** Undetermined.

Culture characteristics: On PDA, colony irregular, reaching 40 mm diam. in 30 days at room temperature (25–30°C), surface rough and dull, with dense mycelia mostly immersed in culture, dry, umbonate from the side view, edge undulate; from above, dark gray at the margin, gray at the center; from below, greenish at the margin, black at the center; not producing pigmentation in culture.

Material examined: CHINA, Yunnan Province, Chuxiong City, Daguokou Township, Biji Village, dead branches of *Ageratina adenophora* (Asteraceae), September 14, 2019, C. F. Liao, (HKAS 112657, **new host record**); living culture KUMCC 20-0204; *ibid*., YMF 107633, **new host record**.

Notes: Our specimen HKAS 112657 and the holotype of *Plenodomus sinensis* (MFLU 17-0767) have 6–7-septate ascospores with mucilaginous globoid-shaped appendages at both ends, but they are slightly different in ascomatal base. Tennakoon et al. (2017) described flattened ascomatal base in the holotype, in addition, we observed the thickened one in our collection. Multilocus phylogeny shows that our collection KUMCC 20-0204 clusters with four collections of *Pl. sinensis*, including paratype MFLU 17-0757, but separates from the holotype MFLU 17-0767. Although MFLU 17-0767 clusters with *Pl. collinsoniae* (**Figure 1**), it differs in having larger asci, longer ascospores with olivaceous to yellowish pigmentation as discussed in Tennakoon et al. (2017). Our collection must be *Pl. sinensis* as its morphological characteristics are more similar to *Pl. sinensis*. *Plenodomus sinensis* appears to have a wide host range, occurring on *Cirsium* sp., *Plukenetia volubilis*, *Tamarindus indica*, and ferns in China (Tennakoon et al., 2017; Phookamsak et al., 2019). This is the first report of *Pl. sinensis* on *Ageratina adenophora* in China.

Sphaerellopsis artemisiae Doilom, W. Dong, K. D. Hyde and C. F. Liao, *sp. nov*., **Figures 4c**, **6**

Index Fungorum number: IF557892; FoF number: FoF 09227

Etymology: The specific epithet "*artemisiae*" refers to the host genus *Artemisia*.

Holotype: HKAS 112655

Saprobic on dead stems of *Artemisia argyi*. **Sexual morph:** *Ascomata* 320–400 μm high, 230–300 μm diam., black, scattered or gregarious in small groups, superficial, subglobose, uniloculate, glabrous, coriaceous, with minutely ostiolate papilla. *Ostioles* 110–130 μm diam., central, dark brown to black, ostiolar canal filled with some periphyses. *Peridium* 30–55 μm at the sides, unevenly thick, thicker at the base, up to 70 μm wide, thinner at the ostiole, 13–18 μm wide, composed of several layers of brown to dark brown, thin-walled, large cells of *textura angularis*, inwardly compressed. *Hamathecium* 2–5.5 μm wide, sparse, hyaline, filamentous, septate, cellular pseudoparaphyses, constricted at the septa. *Asci* 105–170 × 17–25.5 μm ($\bar{x} = 122 \times 20.5$ μm, $n = 15$), eight-spored, bitunicate, fissitunicate, narrowly clavate, short pedicellate, apically rounded with a well-developed ocular chamber. *Ascospores* 80–117 × 5–7.5 μm ($\bar{x} = 92.5 \times 6.5$ μm, $n = 25$), overlapping 4–6-seriate, hyaline to yellowish, scolecosporous, bent at the fourth to fifth septum from the base, 10–13-septate, constricted at the septa, split into two part-spores at the bending point when old; upper part 45–75 μm long, cylindrical, 6–8-septate, with rounded apex and truncate base; lower part 30–42 μm long, subcylindric-clavate, 3–4-septate, with truncate apex and

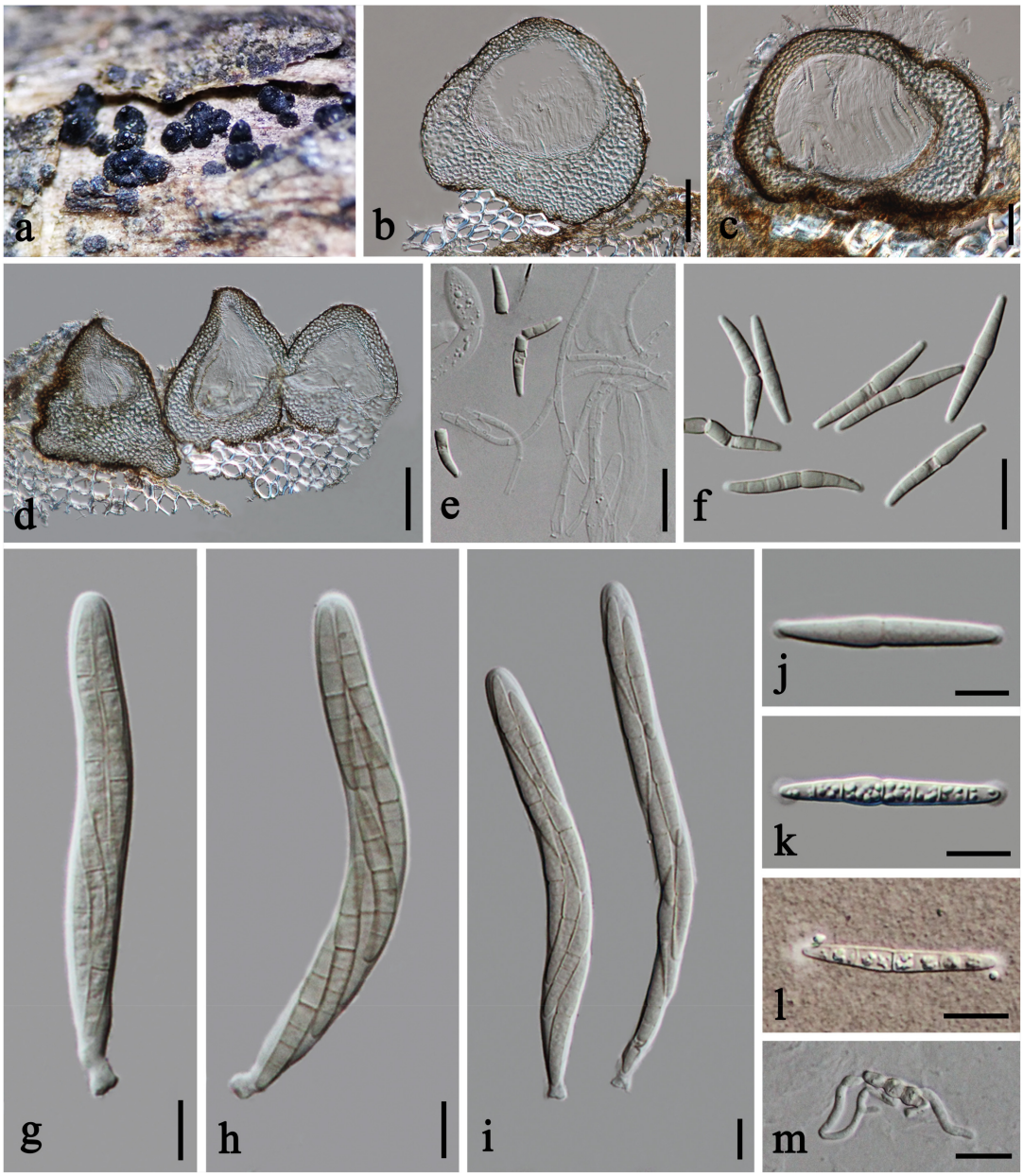


FIGURE 5 | *Plenodomus sinensis* (HKAS 112657, new host record). **(a)** Ascomata on host substrate. **(b–d)** Vertical section of ascomata. **(e)** Structure of peridium. **(g–i)** Asci. **(f,j–l)** Ascospores (l Ascospore in Indian Ink). **(m)** Germinated ascospore. Scale bars: **(b–d)** = 50 μm, **(e)** = 30 μm, **(f,m)** = 20 μm, **(g–l)** = 10 μm.

tapering or conical base, guttulate, without sheath or appendages. **Asexual morph:** Undetermined.

Culture characteristics: On PDA, colony circular, reaching 15 mm diam. in 7 days at room temperature (25–30°C), surface rough, with dense mycelia, velvety to fluffy, dry, raised from the side view, edge entire; from above, white to cream; from below, white at the margin, pale brown at the middle, black at the center; not producing pigmentation in culture.

Material examined: CHINA, Yunnan Province, Kunming City, dead stems of *Artemisia argyi* (Asteraceae), October 27, 2019, C. F. Liao, (HKAS 112655, **holotype**), ex-type living culture KUMCC 20-0202; *ibid*., YMF 107391, **isotype**.

Additional GenBank numbers: *tef1*-α = MW396662 (KUMCC 20-0202A); = MW396663 (KUMCC 20-0202B).

Notes: In our multilocus analysis, our collections *Sphaerellopsis artemisiae* (KUMCC 20-0202A and KUMCC 20-0202B) cluster with *Sphaerellopsis isthmospora* and separate from other *Sphaerellopsis* species with high bootstrap support (**Figure 1**). *Sphaerellopsis artemisiae* resembles *S. isthmospora* in having scolecosporous ascospores with deeply constricted septa that split into two parts at the fourth to fifth septum

from the base (Phookamsak et al., 2019), but it differs in having longer and wider ascospores (92.5 × 6.5 μm vs. 87.1 × 5.9 μm). Phylogenetic analysis of combined LSU, SSU, and ITS sequence data also supports the idea that they are different species (**Figure 1**). In addition, a comparison of *tef1*-α sequence data shows that *S. artemisiae* has 4.04% differences with *S. isthmospora*. Based on morphological difference and molecular data, we therefore introduce *S. artemisiae* as a novel species.

DISCUSSION

The members of the plant family Asteraceae are distributed throughout the world. Many novel fungal species have been reported from several genera in this family (Li et al., 2017; Tibpromma et al., 2017; Crous et al., 2018; Phookamsak et al., 2019; Mapook et al., 2020). Thus, Asteraceae is a promising cache of novel fungal species that warrant further study for

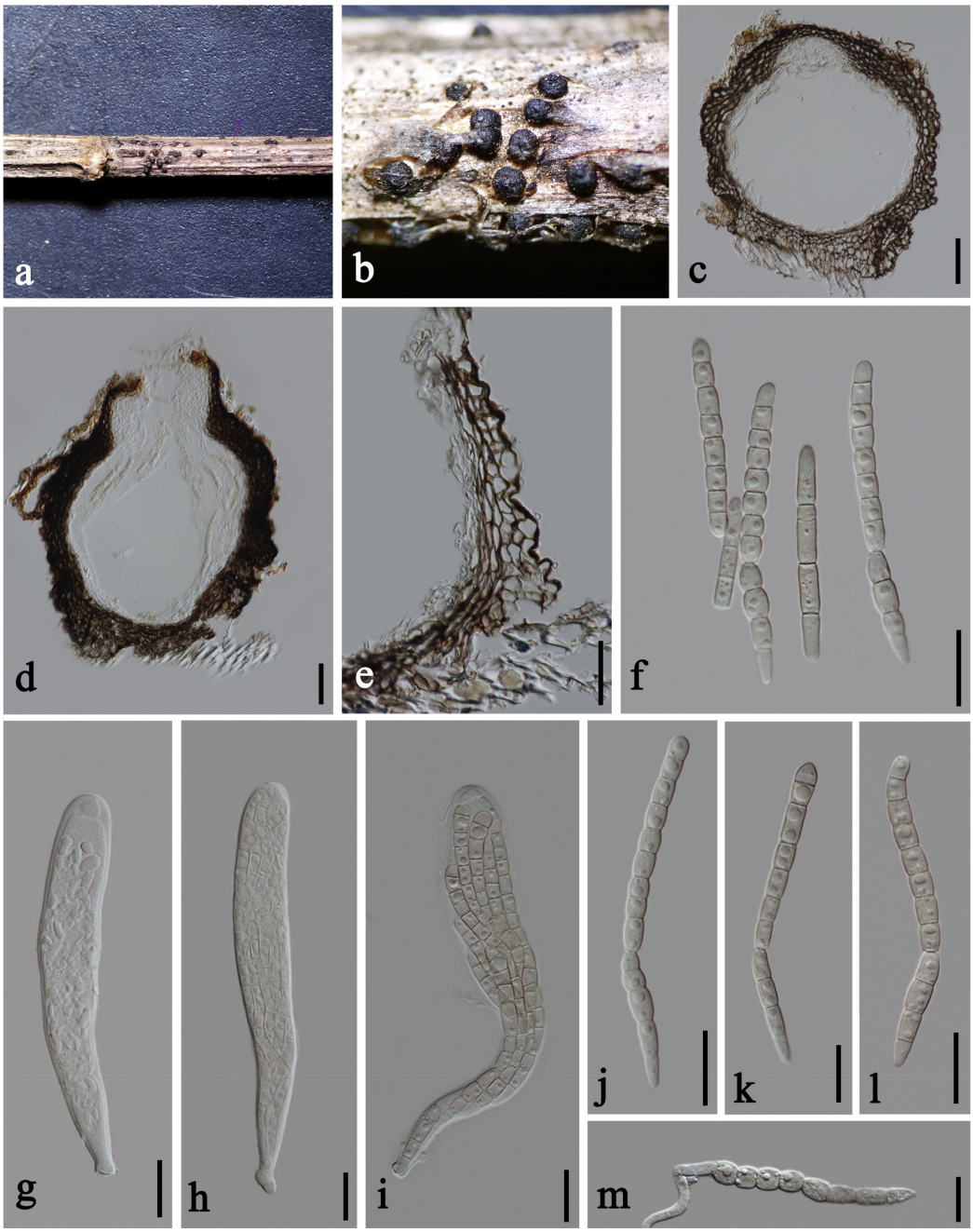


FIGURE 6 | *Sphaerellopsis artemisiae* (HKAS 112655, holotype). **(a, b)** Ascomata on host substrate. **(c,d)** Vertical sections of ascomata. **(e)** Structure of peridium. **(f)** Splitted ascospores. **(g–i)** Asci. **(j–l)** Ascospores. **(m)** Germinated ascospore. Scale bars: **(c,d)** = 50 μm, **(e)** = 30 μm, **(f–m)** = 20 μm.

basic science, use in biocontrol and biotechnology (Hyde et al., 2019). Our study reveals one new genus (*Praeclarispora*), two new species (*Praeclarispora artemisiae* and *Sphaerellopsis artemisiae*), one new collection of the sexual morph report (*Plenodomus artemisiae*), and one new host record (*Pl. sinensis*) on *Ageratina adenophora* in Yunnan Province, China. The two new species have remarkable ascospores that are unusual for sexual ascomycetes when compared with other genera (Doilom et al., 2018; Pem et al., 2019; Dong et al., 2020; Hongsanan et al., 2020a,b; Hyde et al., 2020c).

Praeclarispora has fusiform ascospores, with a larger median cell and tapering end cells which is slightly similar to *Heptameria*. However, *Praeclarispora* and *Heptameria* are different genera based on the distinct characteristics of ascomata, asci and ascospores. *Heptameria* has pseudothecial ascomata with rather thick pseudothecial wall (100–160 μm thick in *H. obesa*) (Lucas and Sutton, 1971), whereas *Praeclarispora* has euthecial ascomata with relatively thin peridium (30–60 μm thick in *P. artemisiae*). In addition, *Heptameria* often forms in several roundish groups on the substrate (Lucas and Sutton, 1971), while *Praeclarispora* mostly forms in linear fissures (never form in roundish groups). *Heptameria* has club-like asci (Lucas and Sutton, 1971), while they are narrowly obovoid in *Praeclarispora*. The ascospores of *Heptameria* are bi- or tri-seriate in the upper portion of the asci and uniseriate below (Lucas and Sutton, 1971), contrasting the tri- to tetra-seriate ascospores in *Praeclarispora*. *Heptameria* has distoseptate, rather thick-walled ascospores with a median, brown, rather large and muriform cell comprising of several transverse, longitudinal, and occasionally oblique septa (Lucas and Sutton, 1971), while *Praeclarispora* has euseptate, thin-walled ascospores and lacking the muriform median cell. Unfortunately, *Heptameria* cannot be incorporated in the phylogenetic tree as lacking sequence data and is referred to Dothideomycetes genera *incertae sedis* based on morphology (Lumbsch and Huhndorf, 2007, 2010; Zhang et al., 2012; Hyde et al., 2013; Wijayawardene et al., 2020). On the other hand, the available sequence data support *Praeclarispora* as a distinct genus within Leptosphaeriaceae (**Figure 1**).

Heptameria was introduced by Thümen with *H. elegans* as the type species (Thümen, 1879). However, *H. elegans* was considered as a synonym of an earlier proposed species *H. obesa* (≡ *Sphaeria obesa*) based on the examination of the holotype of *H. elegans* and *H. obesa* (Lucas and Sutton, 1971). Therefore, *H. obesa* is used as the type species. Although the current name of *H. obesa* is recorded as *Leptosphaeria obesa* in Index Fungorum (2021), *Heptameria* is not synonymized as *Leptosphaeria* and treated as a distinct genus by its cucurbitaria-like pseudothecia and characteristic ascospores (Petrak, 1951), which is also accepted by recent outline of fungi (Wijayawardene et al., 2020). However, sequence data derived from the type species *H. obesa* are indeed needed to confirm whether *Heptameria* is a valid genus, as most species of *Heptameria* have been transferred to other genera. Currently, only two species, i.e., *H. obesa* and *H. uncinata*, are accepted in the genus (Lucas and Sutton, 1971). It is very likely that the type species *H. obesa* will be extinct as it has been missing for nearly 150 years, especially in the increasingly serve climate change. Considering this circumstance and avoiding future confusion of *Heptameria*, *Praeclarispora* gen. nov. is introduced based on its distinct morphology.

One of the findings here is that *Plenodomus sinensis* has both flattened and thickened ascomatal bases, while the type that was studied by Tennakoon et al. (2017) has a flattened ascomatal base. The information of new collections and new records can be used to update fungal classification and improved identification of species (Hyde et al., 2020a). Our collection amends the morphology of *P. sinensis*, which is useful for fungal identification.

Additional protein-coding markers such as *rpb2* and *tef1*-α are necessary to improve the phylogenetic resolution of genera and families in Pleosporales (Jaklitsch et al., 2018). However, most species of Leptosphaeriaceae lack *tef1*-α sequence data and other protein-coding markers, and some known species were sequenced using different *tef1*-α primer pairs. Thus, the phylogenetic analysis was constructed based on combined LSU, SSU, and ITS sequence data as provided in Dayarathne et al. (2015); Wanasinghe et al. (2016), Tennakoon et al. (2017), and this study. Nevertheless, we provide *tef1*-α sequence data for *P. artemisiae*, *P. artemisiae*, and *S. artemisiae* to facilitate the future identification of species. The *rpb2* sequence data were unsuccessfully obtained even after several attempts.

DATA AVAILABILITY STATEMENT

The datasets presented in this study can be found in online repositories. The names of the repository/repositories and accession number(s) can be found in the article/**Supplementary Material**.

AUTHOR CONTRIBUTIONS

MD and WD designed the study. MD, WD, and KH wrote the manuscript. MD, WD, C-FL, and NS conducted the experiments, analyzed the data, and revised the manuscript. MD, NS, and SL contributed to research funds. All authors revised the manuscript.

FUNDING

This research work is partially supported by the Chiang Mai University. MD sincerely thanks the 5th batch of Postdoctoral Orientation Training Personnel in Yunnan Province (grant no. Y934283261) and the 64th batch of China Post-doctoral Science Foundation (grant no. Y913082271) for financial research support. KH thanks Chiang Mai University for the award of Visiting Professor, and the Foreign Experts Bureau of Yunnan Province, Foreign Talents Program (2018; grant no.

YNZ2018002), and Thailand Research grant entitled Impact of climate change on fungal diversity and biogeography in the Greater Mekong Subregion (grant no. RDG6130001).

ACKNOWLEDGMENTS

We gratefully thank Shaun Pennycook (Landcare Research, New Zealand) for assistance in new epithets.

SUPPLEMENTARY MATERIAL

The Supplementary Material for this article can be found online at: https://www.frontiersin.org/articles/10.3389/fmicb.2021.660261/full#supplementary-material

Supplementary Figure 1 | Phylogenetic tree generated from maximum likelihood analysis (RAxML) based on ITS sequence data.

Supplementary Figure 2 | Phylogenetic tree generated from maximum likelihood analysis (RAxML) based on LSU sequence data.

REFERENCES

Aiello, D., Vitale, A., Polizzi, G., and Voglmayr, H. (2020). *Ochraceocephala foeniculi* gen. et sp. nov., a new pathogen causing crown rot of fennel in Italy. *MycoKeys* 66, 1–22. doi: 10.3897/mycokeys.66.48389

Alves, J. L., Woudenberg, J. H. C., Duarte, L. L., Crous, P. W., and Barreto, R. W. (2013). Reappraisal of the genus *Alternariaster* (Dothideomycetes). *Persoonia* 31, 77–85. doi: 10.3767/003158513x669030

Ariyawansa, H. A., Phukhamsakda, C., Thambugala, K. M., Bulgakov, T. S., Wanasinghe, D. N., Perera, R. H., et al. (2015). Revision and phylogeny of Leptosphaeriaceae. *Fungal Divers.* 74, 19–51. doi: 10.1007/s13225-015-0349-2

Barkley, T. M., Brouillet, L., Strother, J. L., and Flora of North America Editorial Committee (eds) (2006). Asteraceae *Martinov Tribe Cardueae Cassini. Flora of North America North of Mexico, Vol. 19: Magnoliophyta: Asteridae (In Part):* Asteraceae*, Part 1, 3–12*. Available online at: http://www.efloras.org/florataxon.aspx?flora_id=1&taxon_id=10074 (accessed December 22, 2020)

Barr, M. E. (1987). New taxa and combinations in the Loculoascomycetes. *Mycotaxon* 29, 501–505. doi: 10.1127/0029-5035/2010/0091-0501

Chomnunti, P., Hongsanan, S., Aguirre-Hudson, B., Tian, Q., Peršoh, D., Dhami, M. K., et al. (2014). The sooty moulds. *Fungal Divers.* 66, 1–36. doi: 10.1007/s13225-014-0278-5

Crous, P. W., Luangsa-ard, J. J., Wingfield, M. J., Carnegie, A. J., Hernández-Restrepo, M., Lombard, L., et al. (2018). Fungal planet description sheets: 785–867. *Persoonia* 41, 238–417. doi: 10.3767/persoonia.2018.41.12

Dayarathne, M. C., Phookamsak, R., Ariyawansa, H. A., Jones, E. B. G., Camporesi, E., and Hyde, K. D. (2015). Phylogenetic and morphological appraisal of *Leptosphaeria italica* sp. nov. Leptosphaeriaceae, Pleosporales from Italy. *Mycosphere* 6, 634–642. doi: 10.5943/mycosphere/6/5/13

de Gruyter, J., Woudenberg, J. H. C., Aveskamp, M. M., Verkley, G. J. M., Groenewald, J. Z., and Crous, P. W. (2013). Redisposition of phoma-like anamorphs in Pleosporales. *Stud. Mycol.* 75, 1–36. doi: 10.3114/sim0004

Doilom, M., Dissanayake, A. J., Wanasinghe, D. N., Boonmee, S., Liu, J. K., Bhat, D. J., et al. (2017). Microfungi on *Tectona grandis* (teak) in Northern Thailand. *Fungal Divers.* 82, 107–182. doi: 10.1007/s13225-016-0368-7

Doilom, M., Hyde, K. D., Phookamsak, R., Dai, D. Q., Tang, L. Z., Hongsanan, S., et al. (2018). Mycosphere notes 225–274: types and other specimens of some genera of Ascomycota. *Mycosphere* 9, 647–754. doi: 10.5943/mycosphere/9/4/3

Dong, J., Chen, W., and Crane, J. L. (1998). Phylogenetic studies of the Leptosphaeriaceae, Pleosporaceae and some other Loculoascomycetes based on nuclear ribosomal DNA sequences. *Mycol. Res.* 102, 151–156. doi: 10.1017/s0953756297004826

Dong, W., Wang, B., Hyde, K. D., McKenzie, E. H. C., Raja, H. A., Tanaka, K., et al. (2020). Freshwater Dothideomycetes. *Fungal Divers.* 105, 319–575. doi: 10.1007/s13225-020-00463-5

Hall, T. (1999). BioEdit: a user-friendly biological sequence alignment editor and analysis program for windows 95/98/NT. *Nucleic Acids Symp. Ser.* 41, 95–98.

Hongsanan, S., Hyde, K. D., Phookamsak, R., Wanasinghe, D. N., McKenzie, E. H. C., Sarma, V. V., et al. (2020a). Refined families of Dothideomycetes: Dothideomycetidae and Pleosporomycetidae. *Mycosphere* 11, 1553–2107. doi: 10.5943/mycosphere/11/1/13

Hongsanan, S., Hyde, K. D., Phookamsak, R., Wanasinghe, D. N., McKenzie, E. H. C., Sarma, V. V., et al. (2020b). Refined families of Dothideomycetes: orders and families *incertae sedis* in Dothideomycetes. *Fungal Divers.* 105, 17–318. doi: 10.1007/s13225-020-00462-6

Huelsenbeck, J. P., and Ronquist, F. (2001). MRBAYES: bayesian inference of phylogeny. *Bioinformatics* 17, 754–755. doi: 10.1093/bioinformatics/17.8.754

Hyde, K. D., de Silva, N. I., Jeewon, R., Bhat, D. J., Phookamsak, R., Doilom, M., et al. (2020a). AJOM new records and collections of fungi: 1–100. *Asian J. Mycol.* 3, 22–294. doi: 10.5943/ajom/3/1/3

Hyde, K. D., Jeewon, R., Chen, Y. J., Bhunjun, C. S., Calabon, M. S., Jiang, H. B., et al. (2020b). The numbers of fungi: is the descriptive curve flattening? *Fungal Divers.* 103, 219–271. doi: 10.1007/s13225-020-00458-2

Hyde, K. D., Jones, E. B. G., Liu, J. K., Ariyawansa, H., Boehm, E., Boonmee, S., et al. (2013). Families of Dothideomycetes. *Fungal Divers.* 63, 1–313. doi: 10.1007/s13225-013-0263-4

Hyde, K. D., Norphanphoun, C., Maharachchikumbura, S. S. N., Bhat, D. J., Jones, E. B. G., Bundhun, D., et al. (2020c). Refined families of Sordariomycetes. *Mycosphere* 11, 305–1059. doi: 10.5943/mycosphere/11/1/7

Hyde, K. D., Xu, J. C., Rapior, S., Jeewon, R., Lumyong, S., Niego, A. G. T., et al. (2019). The amazing potential of fungi: 50 ways we can exploit fungi industrially. *Fungal Divers.* 97, 1–136. doi: 10.1007/s13225-019-00430-9

Index Fungorum (2021). *Index Fungorum*. Available online at: http://www.indexfungorum.org/names/names.asp (accessed January, 2021)

Jaklitsch, W. M., Checa, J., Blanco, M. N., Olariaga, I., Tello, S., and Voglmayr, H. (2018). A preliminary account of the Cucurbitariaceae. *Stud. Mycol.* 90, 71–118. doi: 10.1016/j.simyco.2017.11.002

Jayasiri, S. C., Hyde, K. D., Ariyawansa, H. A., Bhat, D. J., Buyck, B., Cai, L., et al. (2015). The faces of fungi database: fungal names linked with morphology, phylogeny and human impacts. *Fungal Divers.* 74, 3–18. doi: 10.1007/s13225-015-0351-8

Jones, E. B. G., Suetrong, S., Sakayaroj, J., Bahkali, A. H., Abdel-Wahab, M. A., Boekhout, T., et al. (2015). Classification of marine ascomycota, basidiomycota, blastocladiomycota and chytridiomycota. *Fungal Divers.* 73, 1–72. doi: 10.1007/s13225-015-0339-4

Katoh, K., Rozewicki, J., and Yamada, K. D. (2019). MAFFT online service: multiple sequence alignment, interactive sequence choice and visualization. *Brief. Bioinform.* 20, 1160–1166. doi: 10.1093/bib/bbx108

Li, J. F., Jeewon, R., Mortimer, P. E., Doilom, M., Phookamsak, R., and Promputtha, I. (2020). Multigene phylogeny and taxonomy of *Dendryphion hydei* and *Torula hydei* spp. nov. from herbaceous litter in northern Thailand. *PLoS One* 15:e0228067. doi: 10.1371/journal.pone.0228067

Li, J. F., Phookamsak, R., Jeewon, R., Bhat, D. J., Mapook, A., Camporesi, E., et al. (2017). Molecular taxonomy and morphological characterization reveal new species and new host records of *Torula* species (Torulaceae, Pleosporales). *Mycol. Prog.* 16, 447–461. doi: 10.1007/s11557-017-1292-2

Liu, Y. J., Whelen, S., and Hall, B. D. (1999). Phylogenetic relationships among ascomycetes: evidence from an RNA polymerse II subunit. *Mol. Biol. Evol.* 16, 1799–1808. doi: 10.1093/oxfordjournals.molbev.a026092

Lucas, M., and Sutton, B. (1971). *Heptameria* Rehm & Thüm. *Trans. Br. Mycol. Soc.* 57, 283–288. doi: 10.1016/S0007-1536(71)80010-4

Lumbsch, H. T., and Huhndorf, S. M. (2007). Outline of ascomycota–2007. *Myconet* 13, 1–58.

Lumbsch, H. T., and Huhndorf, S. M. (2010). Outline of ascomycota–2009. *Fieldiana Life Earth Sci.* 1, 1–60.

Mapook, A., Hyde, K. D., McKenzie, E. H. C., Jones, E. B. G., Bhat, D. J., Jeewon, R., et al. (2020). Taxonomic and phylogenetic contributions to fungi associated with the invasive weed *Chromolaena odorata* (Siam weed). *Fungal Divers.* 101, 1–175. doi: 10.1007/s13225-020-00444-8

Nylander, J. A. A. (2004). *MrModeltest v2.0. Program Distributed by the Author. Evolutionary Biology Centre, Uppsala University*. Available online at: https://github.com/nylander/MrModeltest2/releases. (accessed March 15, 2020).

Pem, D., Jeewon, R., Bhat, D. J., Doilom, M., Boonmee, S., Hongsanan, S., et al. (2019). Mycosphere notes 275–324: a morphotaxonomic revision and typification of obscure Dothideomycetes genera (*incertae sedis*). *Mycosphere* 10, 1115–1246. doi: 10.5943/mycosphere/10/1/22

Petrak, F. (1951). Uber die Gattung *Heptameria* Rehm & Thuemen. *Sydowia* 5, 423–425.

Phookamsak, R., Hyde, K. D., Jeewon, R., Bhat, D. J., Jones, E. B. G., Maharachchikumbura, S. S. N., et al. (2019). Fungal diversity notes 929–1035: taxonomic and phylogenetic contributions on genera and species of fungi. *Fungal Divers.* 95, 1–273. doi: 10.1007/s13225-019-00421-w

Phookamsak, R., Norphanphoun, C., Tanaka, K., Dai, D. Q., Luo, Z. L., Liu, J. K., et al. (2015). Towards a natural classification of Astrosphaeriella-like species; introducing Astrosphaeriellaceae and Pseudoastrosphaeriellaceae fam. nov. and *Astrosphaeriellopsis*, gen. nov. *Fungal Divers.* 74, 143–197. doi: 10.1007/s13225-015-0352-7

Rambaut, A. (2009). *FigTree v1.3.1 Released. Institute of Evolutionary Biology. Ashworth Laboratories, University of Edinburgh, Scotland*. Available online at: http://tree.bio.ed.ac.uk/software/figtree (accessed September 15, 2020)

Rambaut, A., Drummond, A. J., and Suchard, M. (2013). *Tracer [Computer Program]*. Available online at: http://tree.bio.ed.ac.uk/software/tracer/ (accessed September 20, 2020)

Rehner, S. A., and Buckley, E. (2005). A *Beauveria* phylogeny inferred from nuclear ITS and EF1-α sequences: evidence for cryptic diversification and links to *Cordyceps* teleomorphs. *Mycologia* 97, 84–98. doi: 10.1080/15572536.2006.11832842

Rehner, S. A., and Samuels, G. J. (1994). Taxonomy and phylogeny of *Gliocladium* analysed from nuclear large subunit ribosomal DNA sequences. *Mycol. Res.* 98, 625–634. doi: 10.1016/S0953-7562(09)80409-7

Senanayake, I. C., Rathnayake, A. R., Marasinghe, D. S., Calabon, M. S., Gentekaki, E., Lee, H. B., et al. (2020). Morphological approaches in studying fungi: collection, examination, isolation, sporulation and preservation. *Mycosphere* 11, 2678–2754. doi: 10.5943/mycosphere/11/1/20

Tennakoon, D. S., Phookamsak, R., Wanasinghe, D. N., Yang, J. B., Lumyong, S., and Hyde, K. D. (2017). Morphological and phylogenetic insights resolve *Plenodomus sinensis* (Leptosphaeriaceae) as a new species. *Phytotaxa* 324, 73–82. doi: 10.11646/phytotaxa.324.1.5

The Plant List (2013). *Compositae*. Available online at: http://www.theplantlist.org/ (accessed January 14, 2021)

Thümen, F. V. (1879). Contributiones ad floram mycologicam lusitanicam. Ser. II. *Inst. Coimbra* 27, 251–259.

Tibpromma, S., Hyde, K. D., Jeewon, R., Maharachchikumbura, S. S. N., Liu, J. K., Bhat, D. J., et al. (2017). Fungal diversity notes 491–602: taxonomic and phylogenetic contributions to fungal taxa. *Fungal Divers.* 83, 1–261. doi: 10.1007/s13225-017-0378-0

Vilgalys, R., and Hester, M. (1990). Rapid genetic identification and mapping of enzymatically amplified ribosomal DNA from several *Cryptococcus* species. *J. Bacteriol.* 172, 4238–4246. doi: 10.1128/jb.172.8.4238-4246.1990

Wanasinghe, D. N., Camporesi, E., and Hu, D. M. (2016). *Neoleptosphaeria jonesii* sp. nov., a novel saprobic sexual species, in Leptosphaeriaceae. *Mycosphere* 7, 1368–1377. doi: 10.5943/mycosphere/7/9/10

Wanasinghe, D. N., Phukhamsakda, C., Hyde, K. D., Jeewon, R., Lee, H. B., Jones, E. B. G., et al. (2018). Fungal diversity notes 709–839: taxonomic and phylogenetic contributions to fungal taxa with an emphasis on fungi on Rosaceae. *Fungal Divers.* 89, 1–236. doi: 10.1007/s13225-018-0395-7

White, T. J., Bruns, T., Lee, S., and Taylor, J. (1990). "Amplification and direct sequencing of fungal ribosomal RNA genes for phylogenetics," in *PCR Protocols: A Guide to Methods and Applications*, eds M. A. Innis, D. H. Gelfand, J. J. Sninsky, and T. J. White (New York: Academic Press), 315–322. doi: 10.1016/b978-0-12-372180-8.50042-1

Wijayawardene, N. N., Hyde, K. D., Al-Ani, L. K. T., Tedersoo, L., Haelewaters, D., Rajeshkumar, K. C., et al. (2020). Outline of fungi and fungus-like taxa. *Mycosphere* 11, 1060–1456. doi: 10.5943/mycosphere/11/1/8

Zhang, Y., Crous, P. W., Schoch, C. L., and Hyde, K. D. (2012). Pleosporales. *Fungal Divers.* 53, 1–221. doi: 10.1007/s13225-011-0117-x

Conflict of Interest: The authors declare that the research was conducted in the absence of any commercial or financial relationships that could be construed as a potential conflict of interest.

Copyright © 2021 Doilom, Hyde, Dong, Liao, Suwannarach and Lumyong. This is an open-access article distributed under the terms of the Creative Commons Attribution License (CC BY). The use, distribution or reproduction in other forums is permitted, provided the original author(s) and the copyright owner(s) are credited and that the original publication in this journal is cited, in accordance with accepted academic practice. No use, distribution or reproduction is permitted which does not comply with these terms.

frontiers in Microbiology

ORIGINAL RESEARCH
published: 21 June 2021
doi: 10.3389/fmicb.2021.650513

Multigene Phylogeny and Morphology Reveal Three Novel Species and a Novel Record of *Agaricus* From Northern Thailand

Chanyawat Jaichaliaw[1,2], *Jaturong Kumla*[2,3], *Santhiti Vadthanarat*[2,3], *Nakarin Suwannarach*[2,3]* *and Saisamorn Lumyong*[2,3,4]*

[1] *MS Degree Program in Applied Microbiology, Department of Biology, Faculty of Science, Chiang Mai University, Chiang Mai, Thailand,* [2] *Department of Biology, Faculty of Science, Chiang Mai University, Chiang Mai, Thailand,* [3] *Research Center of Microbial Diversity and Sustainable Utilization, Faculty of Science, Chiang Mai University, Chiang Mai, Thailand,* [4] *Academy of Science, The Royal Society of Thailand, Bangkok, Thailand*

OPEN ACCESS

Edited by:
Peter Edward Mortimer, Kunming Institute of Botany, Chinese Academy of Sciences, China

Reviewed by:
Philippe Callac, INRAE, MycSA, France
Samantha Chandranath Karunarathna, Key Laboratory for Plant Diversity and Biogeography of East Asia, Kunming Institute of Botany, Chinese Academy of Sciences, China

***Correspondence:**
Nakarin Suwannarach
suwan_461@hotmail.com
Saisamorn Lumyong
scboi009@gmail.ac.th

Specialty section:
This article was submitted to Evolutionary and Genomic Microbiology, a section of the journal Frontiers in Microbiology

Received: *07 January 2021*
Accepted: *19 April 2021*
Published: *21 June 2021*

Citation:
Jaichaliaw C, Kumla J, Vadthanarat S, Suwannarach N and Lumyong S (2021) Multigene Phylogeny and Morphology Reveal Three Novel Species and a Novel Record of Agaricus From Northern Thailand. Front. Microbiol. 12:650513. doi: 10.3389/fmicb.2021.650513

Agaricus is a saprophytic mushroom genus widely distributed throughout the world. In this study, a survey of the *Agaricus* species carried out around Chiang Mai University in northern Thailand from 2018 to 2019 yielded 12 collections. Morphological characteristics and phylogenic analyses based on the internal transcribed spacers (ITS) and a fragment of the large subunit (LSU) of the nuclear ribosomal DNA (rDNA), and a fragment of the translation elongation factor 1-alpha (*tef*1) genes were investigated. The results revealed that these collections belong to six species including *Agaricus erectosquamosus*, *Agaricus pallidobrunneus*, *Agaricus subrufescens,* and three new species. *Agaricus thailandensis* sp. nov. was found to belong to *Agaricus* sect. *Minores,* which is placed in *Agaricus* subg. *Minores. Aagricus pseudoerectosquamosus* sp. nov. was placed in *Agaricus* sect. *Brunneopicti* within *Agaricus* subg. *Pseudochitonia.* Furthermore, *Agaricus lannaensis* remains an incertae sedis in *Agaricus* subg. *Pseudochitonia*. Additionally, this study was proposed that *A. pallidobrunneus* was discovered in Thailand for the first time. Full descriptions, color photographs, illustrations, and phylogenetic trees are provided.

Keywords: Agaricales, new taxa, phylogeny, saprophytic mushroom, taxonomy

INTRODUCTION

The genus *Agaricus* L. with *Agaricus campestris* L. as the type species was first proposed by Donk (1962). This genus belongs to the family Agaricaceae of the order Agaricales. It is distributed worldwide and is commonly found in grasslands and forests (Kerrigan et al., 2005, Kerrigan, 2016; Parra, 2008, 2013; Zhao et al., 2012a, 2016; Chen et al., 2015; He et al., 2018a,b). *Agaricus* is a saprophytic fungal genus and is characterized by its white to pink free lamellae when young, which becomes brown at maturity, the presence of an annulus on the stipe, and brown to dark brown spore prints (Kerrigan et al., 2005; Zhao et al., 2016; He et al., 2017, 2018a). In the global market, *Agaricus bisporus* (J.E. Lange) Imbach (white bottom mushroom), and *Agaricus subrufescens* Peck (almond mushroom) are edible mushrooms that are commercially cultivated. Medicinal properties have been reported

for both species (He et al., 2017, 2018a; Zhang et al., 2017). Many other *Agaricus* species such as *Agaricus agrinferus* (Kerrigan and Callac), *Agaricus augustus* Fr., *Agaricus bitorquis* (Quél.) Sacc., *A. campestris, Agaricus flocculosipes* (Zhao, Desjardin, Guinb, and Hyde), *Agaricus sinodeliciosus* (Zhao, Wang, and Zhao), and *Agaricus taeniatus* (Sai, Li, Shao, Li, and Wen) have been reported as edible (Kerrigan et al., 2008; Zhao et al., 2012b; Li et al., 2014; Thongklang et al., 2014b; Wang et al., 2015; Karunarathna et al., 2016; Zhang et al., 2017). In contrast, *Agaricus* species in *Agaricus* sect. *Xanthodermatei* and *Agaricus* sect. *Hondenses* have been described as poisonous as they contain toxic phenolic compounds that can cause gastrointestinal symptoms (Kerrigan et al., 2005; Petrova et al., 2007; Parra, 2013; Asef et al., 2016).

There are approximately 6,000 records of *Agaricus* in the Species Fungorum (accessed in April 2021). However, these records have been found to include synonyms, some misidentifications, and a number of species that have not yet been well-documented. To date, a total of over 500 species of *Agaricus* are currently recognized. These include many new species from America, Asia, Australia, and Europe (Wang et al., 2015; Kerrigan, 2016; He et al., 2017; Callac and Chen, 2018) and few new species from Africa (Hama et al., 2010; Zhao et al., 2012b; Ling et al., 2021) and Oceania (Geml et al., 2007; Lebel and Syme, 2012; Lebel, 2013). Among the approximately 200 new species described since 2000, more than half have been reported to be from Asia, and a quarter have been reported in America (particularly North America) (Zhao et al., 2011, 2016; Thongklang et al., 2014a; Liu et al., 2015; Karunarathna et al., 2016; Kerrigan, 2016; Chen et al., 2017; Callac and Chen, 2018; Hyde et al., 2018). Morphological characteristics, odor, and the chemical reactions of Schäffer's reagent and KOH have mainly been used in the traditional identification of the *Agaricus* species (Parra, 2008; Karunarathna et al., 2014; Chen et al., 2015, 2017; Zhou et al., 2016). However, high variations of phenotypes, varying environmental factors, differing geographic conditions, and the separate developmental stages of basidiomata may influence the morphological identification process. This could make it difficult to distinguish this particular species from other closely related *Agaricus* species (Heinemann, 1978; Kerrigan, 1986; Singer, 1986; Callac et al., 1998a,b; Challen et al., 2003; Parra, 2008). Therefore, the application of molecular tools that are based on DNA analyses has proven to be essential in identifying the *Agaricus* species (Challen et al., 2003; Kerrigan et al., 2005, 2008; Zhao et al., 2011; Chen et al., 2015; Thongklang et al., 2016).

Zhao et al. (2016) classified *Agaricus* into five subgenera and 20 sections based on morphological characteristics, multigene molecular phylogeny (ITS, LSU, and *tef*1), and the divergence time. The revised classification of *Agaricus* by Chen et al. (2017), and Parra et al. (2018) resulted in six subgenera (*Agaricus* subg. *Agaricus*, *Agaricus* subg. *Flavoagaricus*, *Agaricus* subg. *Minores*, *Agaricus* subg. *Minoriosis*, *Agaricus* subg. *Pseudochitonia* and *Agaricus* subg. *Spissicaules*) with 23 sections. Subsequently, a new section of *Agaricus* subg. *Pseudochitonia* was introduced by He et al. (2018a). Therefore, *Agaricus* now contains six subgenera and 24 sections.

Over the last decade, the study of *Agaricus* has expanded rapidly, especially in tropical regions. Notably, Thailand is proving to be a hot spot for the discovery of novel species. This is evidenced by the discovery of many new species of macrofungi, 45 of which are new *Agaricus* species that have been discovered since 2011 (Zhao et al., 2011, 2012a, 2016; Karunarathna et al., 2014; Thongklang et al., 2014a,b; Ariyawansa et al., 2015; Chen et al., 2015, 2017; Liu et al., 2015; Li et al., 2016; Hyde et al., 2017, 2018; He et al., 2018a). This study outlines how we found twelve *Agaricus* specimens during the course of our investigation of macrofungi in northern Thailand. Among these, we describe three new species and one new record. This investigation introduces the taxa based on studies of morphology and multigene analyses of combined ITS, LSU, and *tef* 1 sequences. Additionally, this study included a mini-review of *Agaricus* species that are found in Thailand.

MATERIALS AND METHODS

Sample Collection

Agaricus were surveyed at Chiang Mai University, Chiang Mai Province, Thailand during the rainy seasons of the years 2018 and 2019. Photographs were immediately taken in the field. Basidiomata were collected and wrapped in aluminum foil and kept in plastic boxes while being transferred to the laboratory within 24 h of collection. Specimens were dried in a hot air oven at 45°C until they were completely dried. They were then kept in a plastic zip-locked bag and deposited in the Biology Department's Herbarium (CMUB) along with the Herbarium of Sustainable Development of Biological Resources (SDBR-CMU), Faculty of Science, Chiang Mai University, Thailand. Facesoffungi and MycoBank numbers have also been provided (Robert et al., 2013; Jayasiri et al., 2015).

Morphological Observation

Macroscopic descriptions were made based on fresh specimens. Color, name, and codes were given according to the methods employed by Kornerup and Wanscher (1978). Chemical reactions were determined following the methods described by Chen et al. (2015) and He et al. (2017) including Melzer's reagent, 10% potassium hydroxide (KOH) in water, and Schäffer's reaction. Microscopic characteristics, including basidiospores, basidia, cystidia, and pileipellis, were observed from dried specimens that had been rehydrated in 95% ethanol followed by distilled water, 5% aqueous KOH, or Melzer's reagent. A minimum of 50 basidiospores, 20 basidia, and cystidia were measured using a compound light microscope (Olympus CX31, Japan). Basidiospores are presented in the following format: (*a*)*b*–*c*–*d*(*e*), for which "*c*" represents the average, "*b*" and "*d*" represent the average + and - standard deviation (SD), respectively, and "*a*" and "*e*" represent the minimum and maximum values, respectively. For spore statistics, Q represents the ratio of length divided by the width of

the basidiospore, and Q_m represented the average Q of all specimens ± standard deviation.

DNA Extraction, PCR Amplification, and Sequencing

DNA was extracted from the fresh tissue of each specimen using the FAVOGEN Genomic DNA Extraction Mini Kit (Taiwan) by following the manufacturer's instructions. The ITS region of the rDNA was amplified using the ITS4/ITS5 primers (White et al., 1990) by polymerase chain reaction (PCR). The LSU of the rDNA gene was amplified with LR5/LROR primers (Vilgalys and Hester, 1990) and the *tef*1 gene was amplified with primers EF1-983F/EF1-1567R (Rehner and Buckley, 2005). The PCR programs of ITS, LSU, and *tef*1 genes were established by following the methods employed by He et al. (2017). PCR products were checked by electrophoresis on 1% agarose gels stained with ethidium bromide and observed under UV light. PCR products were purified using NucleoSpin Gel and a PCR Clean-up Kit (Macherey-Nagel, Germany). PCR products were then sent to a commercial sequencing provider (1^{ST} BASE Company, Kembangan, Malaysia). The obtained sequences were ultimately subjected to BLASTn search in GenBank.[1]

Sequence Alignment and Phylogenetic Analyses

Newly generated sequences were assembled using the Sequencher program. Details of the sequences used for phylogenetic analysis obtained from this study and previous other studies are provided in **Supplementary Table 1**. Two sequence datasets were prepared for phylogenetic analyses. The first dataset was comprised of sequences of two subgenera, namely *Agaricus* subg. *Flavoagaricus* and *Agaricus* subg. *Minores*. The second dataset contains sequences of six sections in *Agaricus* subg. *Pseudochitonia* namely, *Agaricus* sect. *Bohusia*, *Agaricus* sect. *Brunneopicti*, *Agaricus* sect. *Floculenti*, *Agaricus* sect. *Nigrobrunnescentes*, *Agaricus* sect. *Rubricosi*, and *Agaricus* sect. *Sanguinolenti*. The datasets were then aligned using MAFFT version 7 (Katoh and Standley, 2013). The first and second aligned datasets were deposited in TreeBASE under the numbers 27426 and 28087, respectively. Maximum Likelihood (ML) phylogenetic tree inference was performed for each dataset using RAxML-HPC2 version 8.2.10 (Stamatakis, 2006) on the CIPRES web portal (Miller et al., 2009). The phylogenetic tree was inferred from a four-partitions (ITS, LSU, *tef*1 exons, and *tef*1 introns) combined dataset using the GTRCAT model with 25 categories. *A. campestris* LAPAG370 was used as an outgroup for both datasets. Statistical support of the clades was obtained with 1,000 rapid bootstrap replicates. For Bayesian Inference (BI), the best-fit model of substitution amongst those implementable in MrBayes was estimated separately for each region using jModelTest 2 (Darriba et al., 2012) on the CIPRES portal based on the Bayesian Information Criterion (BIC). The selected models that are similar in both data sets, were HKY + I + G for ITS, SYM + G for *tef*1 exons, K80 + G for introns of *tef*1. While for LSU, were K80 + I + G in the first dataset, and K80 + I in the second dataset. Partitioned BI was performed with MrBayes 3.2.6 software for Windows (Ronquist et al., 2012). Two runs of five chains were conducted for eleven million (first dataset) and three hundred thousand generations (second dataset), which were sampled every 200 generations. At the end of the runs, the average deviations of split frequencies were 0.007058 (first dataset) and 0.009527 (second dataset). The potential scale reduction factor values of all parameters were close to 1. The burn-in phase (25%) was estimated by checking the stationarity in the plot generated by the sump command.

[1]http://blast.ncbi.nlm.nih.gov

RESULTS

Phylogenetic Analyses Results

A total of 36 sequences from 12 specimens were newly obtained from this study and deposited in GenBank (**Supplementary Table 1**). The combined ITS, LSU, *tef*1 exons, and *tef*1 introns sequence datasets consisted of 81 and 54 taxa in the first and second datasets, respectively. The first and second aligned datasets were comprised of 2257 (ITS: 1–778, LSU: 779–1674, *tef*1 exons: 1675–2140 and *tef*1 introns: 2141–2257) and 2204 (ITS: 1–784, LSU: 785–1689, *tef*1 exons: 1690–2093 and *tef*1 introns: 2094–2204) characters including gaps, respectively. ML and BI trees of both datasets revealed similar topologies without any supported conflict (BS ≥ 70% and PP ≥ 0.90). Phylogenetic results were based on the first dataset (**Figure 1**) which contained *Agaricus* subg. *Flavoagaricus* and *Agaricus* subg. *Minores*. Selected *Agaricus* species formed two main clades namely *Agaricus* subg. *Flavoagaricus* (BS = 100%, PP = 1) and *Agaricus* subg. *Minores* (BS = 87%, PP = 0.90). *Agaricus thailandensis* (vouchers SDBR-CMU-CJ118 and SDBR-CMU-CJ225) formed a monophyletic clade (BS = 100%, PP = 1) in *Agaricus* sect. *Minores* of *Agaricus* subg. *Minores* and closely related to *Agaricus* sp. voucher CA935 with the high support values (BS = 100%, PP = 1). Furthermore, they formed a sister clade to *Agaricus flammicolor* (Chen et al., 2017) and *A. badioniveus* (Chen et al., 2017) (BS = 71%, PP = 0.92). Another obtained specimen voucher SDBR-NK0079 was placed within the cluster of the known species clade of *A. subrufescens* (BS = 100%, PP = 1) in *Agaricus* sect. *Arvenses* of *Agaricus* subg. *Flavoagaricus*.

The second tree was based on sequences of six sections of *Agaricus* subg. *Pseudochitonia* (**Figure 2**). Six main clades were assigned including, *Agaricus* sect. *Bohusia* (BS = 92%, PP = 0.99), *Agaricus* sect. *Brunneopicti* (BS = 92%, PP = 1), *Agaricus* sect. *Floculenti* (BS = 62%, PP = 0.93), *Agaricus* sect. *Nigrobrunnescentes* (BS = 57%, PP = 0.93), *Agaricus* sect. *Rubricosi* (BS = 100%, PP = 1) and *Agaricus* sect. *Sanguinolenti* (BS = 100%, PP = 1). Two new species, namely *Agaricus lannaensis* and *Aagricus pseudoerectosquamosus* formed two different species clades within *Agaricus* subg. *Pseudochitonia*. *Agaricus lannaensis* (vouchers SDBR-CJ192, SDBR-NK0584, and SDBR-NK0564) formed a highly supported clade with *Agaricus* sp. voucher CA820 (BS = 100%, PP = 1) and they

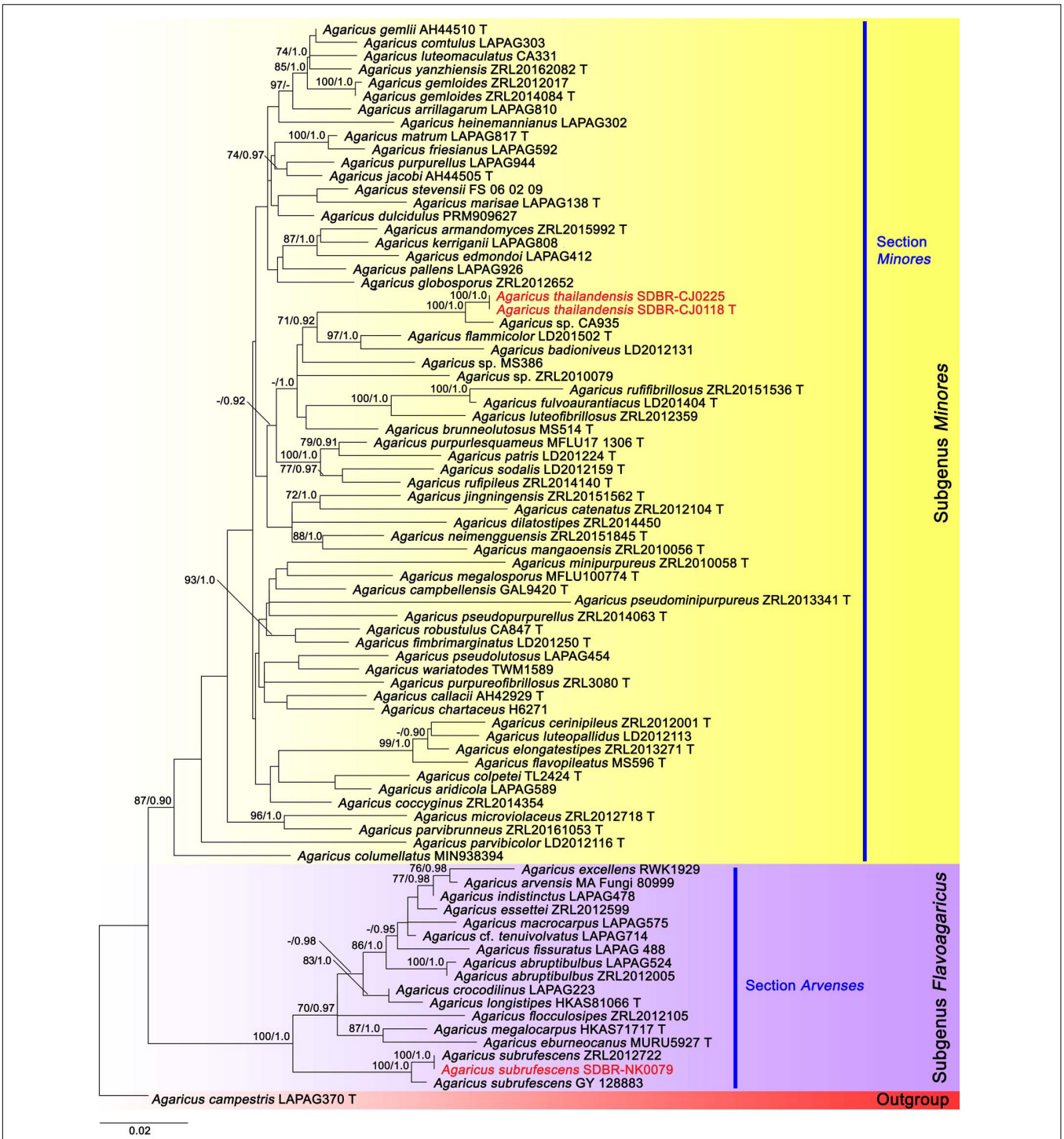


FIGURE 1 | Phylogenetic tree of the genus *Agaricus* generated from maximum likelihood based on multigene sequences (ITS, LSU, *tef*1 exons, and *tef*1 introns) of *Agaricus* subg. *Flavoagaricus* and *Agaricus* subg. *Minores*. *Agaricus campestris* was used as an outgroup. The vouchers from this study are in red and "T" means type specimen. Bootstrap support values (BS ≥ 70%) and posterior probabilities (PP ≥ 0.90) are presented above the supported branches.

formed a sister clade to unnamed species *Agaricus* voucher LD2012162 (BS = 92%, PP = 1). This clade was closely related to the clade of *Agaricus* sect. *Flocculenti*. Another new species, *A. pseudoerectosquamosus* (vouchers SDBR-CJ108 and SDBR-NK0064) formed a clade (BS = 100%, PP = 0.99) that was closely related to *Agaricus* sp. voucher NTT117 with the high support values (BS = 100%, PP = 1), in *Agaricus* sect. *Brunneopicti* (BS = 92%, PP = 1). Additionally, the other four

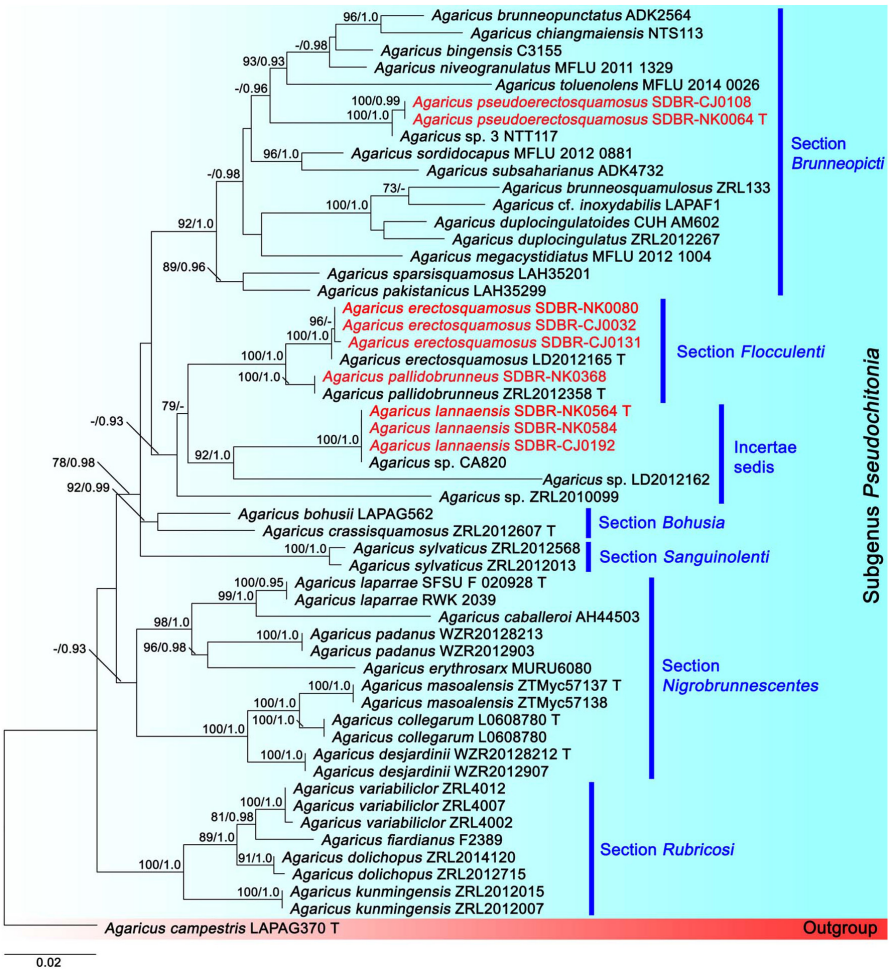


FIGURE 2 | Phylogenetic tree of the genus *Agaricus* generated from maximum likelihood based on multigene sequences (ITS, LSU, *tef*1 exons, and *tef*1 introns) of six sections in *Agaricus* subg. *Pseudochitonia* namely, *Agaricus* sect. *Bohusia*, *Agaricus* sect. *Brunneopicti*, *Agaricus* sect. *Floculenti*, *Agaricus* sect. *Nigrobrunnescentes*, *Agaricus* sect. *Rubricosi* and *Agaricus* sect. *Sanguinolenti*. *Agaricus campestris* was used as an outgroup. The vouchers from this study are in red and "T" means type specimen. Bootstrap support values (BS ≥ 70%) and posterior probabilities (PP ≥ 0.90) are presented above the supported branches.

Agaricus collections obtained in this study were clustered within two known species clades, in which *Agaricus* vouchers SDBR-NK0080, SDBR-CJ0032, and SDBR-CJ0131 were clustered with *Aagricus erectosquamosus* Linda J. Chen, K.D. Hyde & R.L. Zhao. *Agaricus* voucher SCBR-NK0368 formed a clade with *Agaricus pallidobrunneus* R.L. Zhao. with high value supports (BS = 100%, PP = 1).

Taxonomic Description of New Species

Agaricus lannaensis N. Suwannarach, J. Kumla & S. Lumyong sp. nov. **Figure 3**

MycoBank: MB 838052

Facesoffungi number: FoF 09468

Etymology: "*lannaensis*" referring to the Kingdom of Lanna, the historic name of northern Thailand, where the new species was found.

Holotype: THAILAND, Chiang Mai Province, Mueang Chiang Mai District, Chiang Mai University, 18°47′33.6″N 98°57′30.2″E, elevation 331 m, June 2, 2019 (N. Suwannarach and J. Kumla) SDBR-NK0564, CMUB 39945.

Description: *Basidiomata* medium-sized, stipitate-pileate with lamellate hymenophore. *Pileus* (2.4) 3.2–7.4 cm in diameter, at first spherical, campanulate, then subumbonate with straight margins, and whole cap covered by fibrils and broken into small squamules. The surface background is pale orange (6A3) at the center and turns gradually orange white (5A2) at the margins, covered by innate scales. The pileus is at first covered, then gradually sprayed, denser at pileus, partially at margins when aged, appressed innately scaled, brown (7E8) at the top of the pileus, and gradually brown (7E7) at margins, then grayish red (8C5) when cut or touched. *Pileus*

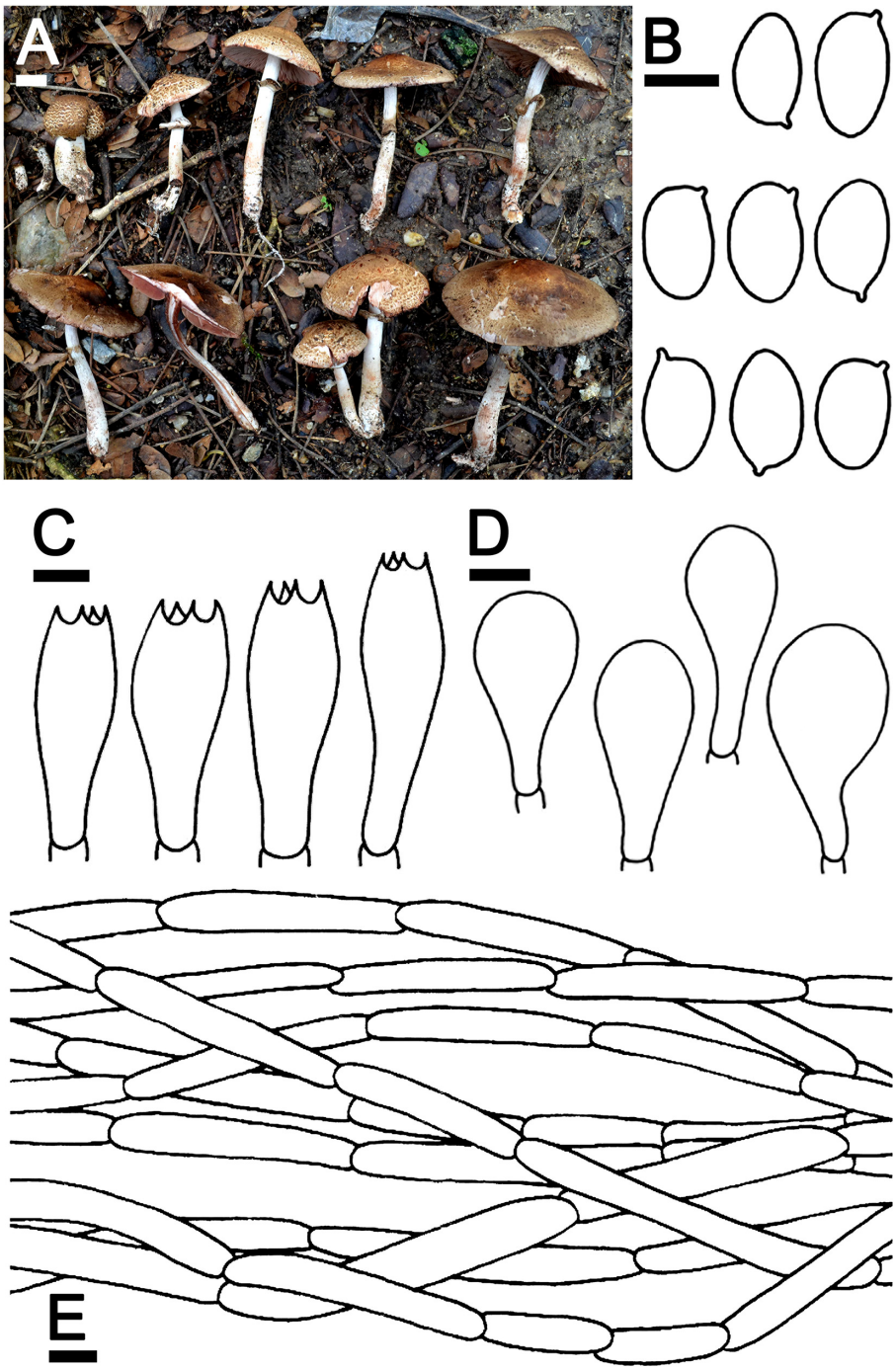


FIGURE 3 | *Agaricus lannaensis* SDBR-NK0564 (holotype). **(A)** Basidiomata on the field, **(B)** Basidospores, **(C)** Basidia, **(D)** Cheilocystidia, **(E)** Pileipellis. Scale bars **(A)** = 1 cm and **(B–E)** = 5 μm.

context soft white (1A1) then reddish brown (8E7) when cut, pluteoid. *Lamellae* emarginate, crowded, thin, regular, 3–4 different lengths of lamellae, at first pastel red (8A4), becoming dark brown (8F8). *Stipe* (4.3)4.6–8.8 × 0.6–1.2 cm, cylindrical, smooth above annulus until under lamellae, covered by small squamules which fibrilloses white (1A1) under annulus until the base, then grayish red (8C5) when cut or touched, scales reddish brown (8D5) at the base. *Stipe context* soft, fistulose, orange-white (6A2), then reddish brown (8E7) when cut. *Annulus* are membranous, thin, pendant, simple, stick above the middle of the stipe, at first white (1A1), dark brown (7F4) at edges, then light brown (7D5) when aged.

Spores print dark brown (8F5) and the *odor* is phenol-like. Macrochemical reactions; KOH reaction yellow and Schäffer's reactions negative.

Basidiospores (5.5)6.3–6.8–7.3(8.0) × (4.0)4.1–4.3–4.4(4.5) μm (n = 50), Q = 1.22–2.00, Q_m = 1.62 ± 0.19, broadly ellipsoid to elongate, smooth, thin-walled, brown in water and KOH, inamyloid. *Basidia* 19–26 × 5.5–8.5 μm, clavate, 4-spored, hyaline, sterigmata up to 2.5 μm long. *Cheilocystidia* 13–47 × 6.5–24 μm, clavate to broadly clavate, often with a short peduncle, hyaline. *Pleurocystidia* absent. *Pileipellis* composed of 3.8–7.5 μm wide cutis hyaline hyphae, smooth, cylindrical, occasionally branched. *Annulus* composed of 1–3 μm wide hyaline hyphae, cylindrical with rounded apex, branched. *Stipitipellis* composed of cutis hyphae wide up to 2–5 μm, cylindrical, occasionally branched, hyaline. *Clamp connections* absent.

Ecology and distribution: Fruiting solitary or gregarious on sandy loam soil during the rainy season (mid-May to October). Known only from Thailand.

Additional specimens examined: THAILAND, Chiang Mai Province, Mueang Chiang Mai District, Chiang Mai University, 18°47′33.6″N 98°57′30.2″E, elevation 331 m, June 2, 2019, J. Kumla, SDBR-NK0584; 18°47′45″N 98°57′2″E, elevation 340 m, October 9, 2019, C. Jaichaliaw, SDBR-CJ0192.

Note: In the field, *A. lannaensis* is morphologically similar to *Agaricus brunneopileatus* Callac & R.L. Zhao. However, *A. brunneopileatus* differs from *A. lannaensis* by the fact that it had a negative reaction in KOH and Schäffer's reactions, smaller basidiospores (4.9–5.8 × 2.5–3.6 μm) and shorter basidia (12.6–18 × 6.2–8.8 μm) (Zhao et al., 2016). The phylogeny also supports the determination that they are different species, for which *A. brunneopileatus* was assigned to *Agaricus* sect. *Subrutilescentes* in *Agaricus* subg. *Spissicaules* (Zhao et al., 2016). Phylogenetically, *A. lannaensis* formed a clade with the unnamed species *Agaricus* sp. voucher CA820 collected from Thailand, and they formed a sister clade to *Agarius* sect. *Flocculenti* comprised with *A. erectosquamosus* and *A. pallidobrunneus* (**Figure 2**). *Agaricus erectosquamosus* were clearly distinguished from *A. lannaensis* by the orange KOH reaction and the presence of erect squamules on the pileus that appeared dense at the disc and brown against a dirty white background (Zhao et al., 2016). *A. pallidobrunneus* has brownish orange to dark brown pileus, but *A. lannaensis* has a pale orange pileus (Zhao et al., 2016).

Agaricus pseudoerectosquamosus J. Kumla, N. Suwannarach, and S. Lumyong sp. nov. (**Figure 4**)

MycoBank: MB 838053

Facesoffungi number: FoF 09469

Etymology: "*pseudo*" = false, referring to the morphological characteristics that are easily mistaken for *A. erectosquamosus*

Holotype: THAILAND, Chiang Mai Province, Mueang Chiang Mai District, Chiang Mai University, 18°48′6.4″N 98°57′23″E, elevation 330 m, September 20, 2018, J. Kumla, SDBR-NK0064, CMUB 39944

Description: *Basidiomata* medium-sized, stipitate-pileate with lamellate hymenophore. *Pileus* (3)5.2–7.5 cm in diameter, at first umbonate, broadly conical, then hemispherical with inflexed margin, rimos; surface background white (1A1), innately squamulose, denser at the center, poor at the margins with depressed at the center, uplifted, brownish orange (5C4) at the center, pale to white (1A1) at the edges. *Pileus context* soft, white (1A1). *Lamellae* free, crowded, even, 4–5 different lengths of lamellullae, pale red (8A3). *Stipe* 6.7–10 × 1.2–2.1 cm, subclavate, inserted or caespitose, surface skin covered pale yellow near lamellae to dark brown (4A3 to 6F8) at the base by the fibrillose, denser, white (1A1). *Annulus* thick, double, stick above the middle of stipe, white (1A1), and often cogwheel-like. *Stipe context* fistulose, white (1A1). *Spores print* dark brown (8F5). *Odor* phenol-like. Macrochemical reactions; KOH reaction yellow and Schäffer's reactions negative.

Basidiospores (8.0)8.2–8.5–8.8(9.0) × (4.5)4.7–5.0–5.4(5.5) μm (n = 50), Q = 1.45–2.00, Q_m = 1.69 ± 0.14, ellipsoid to elongate, smooth, thin-walled, brown in water and KOH, inamyloid. *Basidia* 19.5–26 × 8–9.5 μm, clavate, 4-spored, hyaline, sterigmata up to 2 μm long. *Cheilocystidia* 19.5–40 × 11.5–22.5 μm, clavate to broadly clavate, often with a long peduncle, hyaline. *Pileipellis* composed of fibrilloses 5–20 × 4–5.6 μm hyaline hyphae, smooth, short cylindrical, occasionally branched, and cutis hyphae 2–5 μm, wide, occasionally branched, hyaline. *Annulus* composed of 2–4.5 μm wide hyaline hyphae, cylindrical with a rounded apex and branched. *Stipitipellis* composed of cutis hyphae up to 3–7 μm wide, cylindrical, occasionally branched, hyaline. *Clamp connections* absent.

Ecology and distribution: Fruiting solitary or gregarious on sandy loam soil during the rainy season (mid-May to October). Known only from Thailand.

Additional specimens examined: THAILAND, Chiang Mai Province, Mueang Chiang Mai District, Chiang Mai University, 18°48′17″N 98°57′13″E, elevation 340 m, September 22, 2019, C. Jaichaliaw, SDBR-CJ0108.

Note: Morphological characteristics and phylogenetic analysis assigned *A. pseudoerectosquamosus* to *Agaricus* sect. *Brunneopicti* in *Agaricus* subg. *Pseudochitonia*. Morphologically, *A. pseudoerectosquamosus* is similar to *A. erectosquamosus* (Zhao et al., 2016). However, the orange associated with the KOH reaction, the dark brown squamules on the surface of the pileus, the shorter basidiospores (6.6–7.6 × 4.1–5.0 μm) and the narrower basidia (15–22 × 6.5–7.5 μm) in *A. erectosquamosus* clearly distinguished it from *A. pseudoerectosquamosus*. Moreover, the phylogeny placed *A. erectosquamosus* within *Agaricus* sect. *Flocculenti* of *Agaicus* subg. *Pseudochitonia*, (Zhao et al., 2016). Phylogenetically, *A. pseudoerectosquamosus* is a monophyletic clade that formed a sister clade to the unnamed species *Agaricus* sp. 3 voucher NTT117 collected from Thailand, and they formed a sister clade to *A. bingensis* (Heinem., Bull. Jard. Bot. État Bruxelles), *A. brunneopunctatus* Linda (J. Chen, Callac, & Parra), *A. chiangmaiensis* (Karunarathna, Guinb. & Hyde), *A. niveogranulatus* (Linda J. Chen, R.L. Zhao, Callac & Hyde), and *A. toluenolens* (Callac, Linda J. Chen &

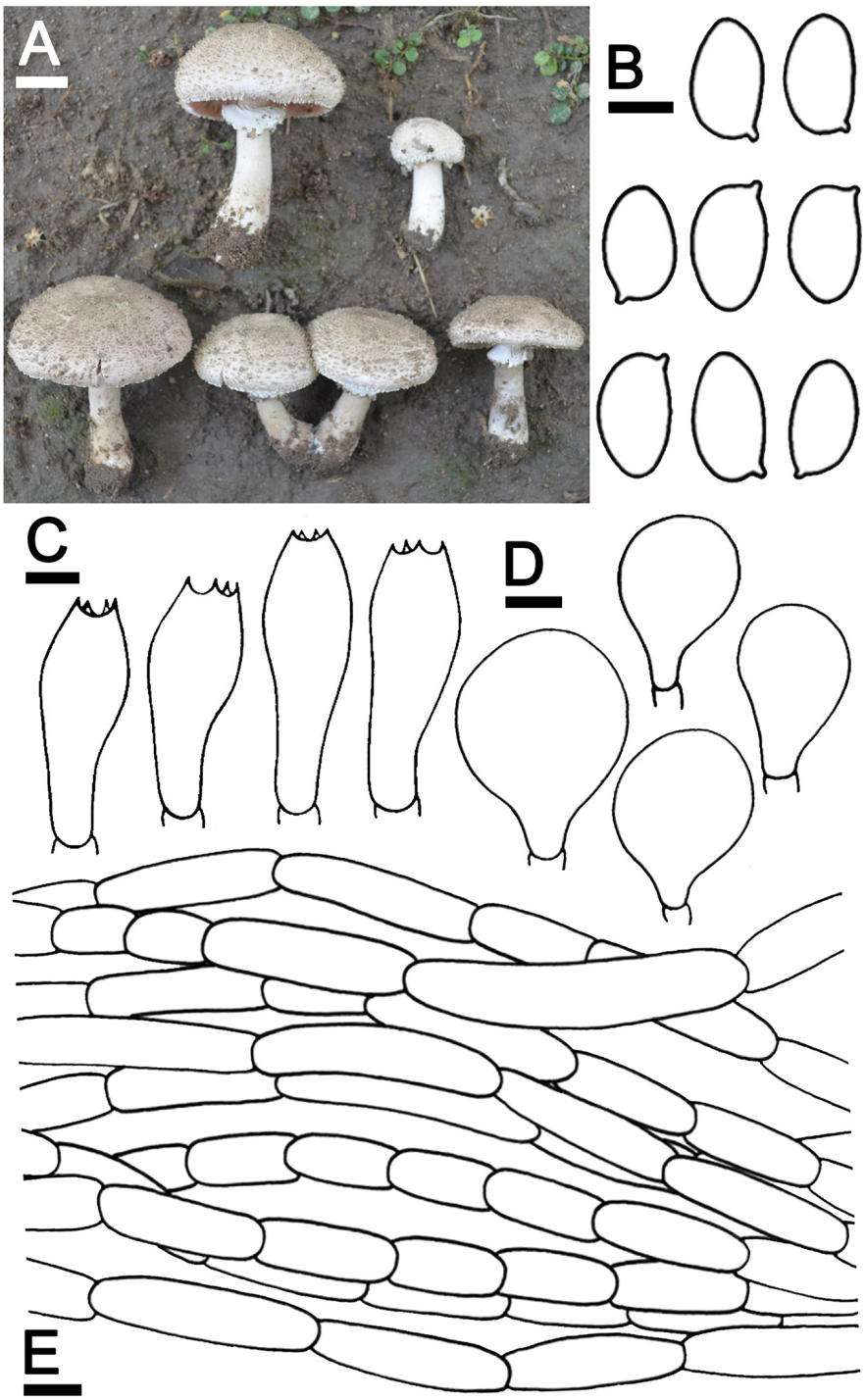


FIGURE 4 | *Agaricus pseudoerectosquamosus* SDBR-NK0064 (holotype). **(A)** Basidiomata on the field, **(B)** Basidiospores, **(C)** Basidia, **(D)** Cheilocystidia, **(E)** Pileipellis. Scale bars **(A)** = 2 cm and **(B–E)** = 5 μm.

K.D. Hyde) (**Figure 2**). Notably, these have all been found in Thailand except for *A. bingensis* and *A. brunneopunctatus*, which has been identified in Africa (Benin, Congo, Togo, and Uganda) (Pegler, 1977; Chen et al., 2015). However, *A. bingensis* has a larger pileus (8–25 cm in diameter), a longer stipe (11–20 × 1.2–4 cm), and the narrower basidia (16–21 × 5–6 μm) than *A. pseudoerectosquamosus* (Pegler, 1977; Chen et al., 2015). While, *A. brunneopunctatus* has mostly shorter basidiospores (7.3–8.45 μm) than *A. pseudoerectosquamosus* (Chen et al., 2015). *Agaricus chiangmaiensis* differs from *A.*

pseudoerectosquamosus by its larger pileus (10–17 cm in diameter), narrower basidiospores (7–8.5 × 3–4 μm), and smaller cheilocystidia (15–18 × 8–10 μm) (Karunarathna et al., 2014). The pileus (10–16 cm in diameter) and basidia (16–24 × 6.8–8.5 μm) of *A. niveogranulatus* were larger and mostly narrower than *A. pseudoerectosquamosus*, respectively (Chen et al., 2015). Additionally, *A. toluenolens* mostly has a narrower stipe (3.5 × 0.6–1 cm) and basidia (16–21 × 7–8.5 μm) than *A. pseudoerectosquamosus* (Chen et al., 2015).

Agaricus thailandensis Jaichliaw & S. Lumyong sp. nov. **Figure 5**

MycoBank: MB 838054

Facesoffungi number: FoF 09470

Etymology: "*thailandensis*" referring to Thailand, where the new species was found.

Holotype: THAILAND, Chiang Mai Province, Mueang Chiang Mai District, Chiang Mai University, 18°48′31″N 98°57′15″E, elevation 340 m, September 16, 2019, C. Jaichaliaw. SDBR-CJ0118, CMUB 39946

Description: *Basidiomata* medium-sized, stipitate-pileate with lamellate hymenophore. *Pileus* 2.6–5.8 cm in diameter, at first obtusely conical, then convex or plano-convex with straight margins; surface background white (1A1) to pinkish-white (13A2) at the center, covered by dark ruby (12F8) at the center, pale to grayish magenta (13D3) at the margins of the fibrillose scales, appressed, denser at the center of pileus and poor at the margin. *Pileus context* soft, white (1A1). *Lamellae* free, crowded, even, regular, thin, 2–3 different lengths of lamellae, concolorous, at first white (1A1), then reddish gray (12B2). *Stipe* 5.2–5.9 × 0.3–0.7 cm, cylindrical with subbulbous, inserted; surface smooth, background white (1A1) to dark yellow (4C8) at the base, covered by small fibrilloses, minutely, white (1A1). *Annulus* thin, simple, stick out above the middle of the stipe and at the margins of the pileus, pendant, white (1A1). *Stipe context* soft, fistulose, white (1A1). *Spores print* dark brown (7F8). The *odor* smells like almonds. Macrochemical reactions; KOH reaction yellow and Schäffer's reactions orange.

Basidiospores (6.0)6.1–6.3–6.4(6.5) × (3.5)3.7–4.0–4.3(4.5) μm (n = 50), Q = 1.44–1.86, Q_m = 1.58 ± 0.15, ellipsoid to elongate, smooth, thin-walled, brown in water and KOH, inamyloid. *Basidia* 13–20 × 6–8 μm, clavate, 4-spored, hyaline, sterigmata up to 4 μm long. *Cheilocystidia* 12.5–50 × 7–15.5 μm, clavate to broadly clavate, often with a long peduncle, hyaline. *Pleurocystidia* absent. *Pileipellis* cylindrical hyphae 1.5–8.5 μm wide, elongate, constricted, smooth, occasionally branched, hyaline. *Annulus* composed of 2.5–21.5 μm wide, cylindrical with rounded apex, branched hyaline hyphae. *Stipitipellis* composed of 2.5–22.5 μm wide, cylindrical with rounded apex, constricted, hyaline. *Clamp connections* absent.

Ecology and distribution: Fruiting solitary or gregarious on sandy loam soil during the rainy season (mid-May to October). Known only from Thailand.

Additional specimens examined: THAILAND, Chiang Mai Province, Mueang Chiang Mai District, Chiang Mai University, 18°47′45″N 98°57′2″E, elevation 340 m, September 27, 2019 (C. Jaichaliaw) SDBR-CJ0225.

Note: *Agaricus thailandensis* was placed within *Agaricus* sect. *Minores* of *Agaricus* subg. *Minores* based on the morphological and molecular data. The grayish magenta to dark ruby fibrils on the pileus surface and the reaction of KOH Schäffer's reactions of *A. thailandensis* are morphologically similar to those of *A. purpureofibrillosus* (Linda J. Chen, R.L. Zhao & K.D. Hyde) in *Agaricus* sect. *Minores* of *Agaricus* subg. *Minores* (Fr.) (Chen et al., 2017). In contrast, *A. purpureofibrillosus* has shorter basidiospores (4.5–5.3 × 2.7–3 μm) than *A. thailandensis* and their clear separation was supported by the phylogeny (Chen et al., 2017). Phylogenetically, *A. thailandensis* formed a sister clade to the unnamed species *Agaricus* sp. voucher CA935 collected from Thailand, and they formed a sister clade to *A. flammicolor* and *A. badioniveus* (**Figure 1**). Both species have been collected from China and Thailand (Chen et al., 2017). Morphologically, *A. flammicolor* differed from *A. thailandensis* by the presence of orange bright fibrils on the pileus, smaller basidiospores (4.4–6.2 × 2.5–3.2 μm) and narrower basidia (12–16 × 5–6 μm) (Chen et al., 2017). *Agaricus badioniveus* is different from *A. thailandensis* by the yellowish-brown fibrils on the pileus and the mostly smaller basidiospores (5–6.2 × 3.1–3.8 μm) (Chen et al., 2017).

Taxonomic Description of New Record

Agaricus pallidobrunneus R.L. Zhao., Fungal Divers.: 33, 2016 **Figure 6**

Description: *Basidiomata* medium-sized, stipitate-pileate with lamellate hymenophore. *Pileus* (2)3.6–8 cm in diameter, paraboloid with inflexed margins, becoming applanate to plano-concave, depressed at the center with reflexed margins; surface background white (1A1), partially or entirely covered by brownish orange (5C5) to dark brown to (7F7) scales, the scales at first appressed then uplifted and innately scaled with age. *Pileus context* soft, white (1A1) grayish red (10D5) when cut. *Lamellae* free, crowded, thin, regular, 4–5 different lengths of lamellae, 3–4 mm wide half-way to margins, at first grayish rose (12B6) then grayish brown (7F3) when aged. *Stipe* 9–10 × 0.7–1.3 cm, tapering upwards, covered with small brown scales at the base, moist, white (1A1) near the cap, gradually light brown (5D4) at the base. *Annulus* thin, double, sticking up above the middle of the stipe and at margins, pendant, white (8A1) becoming brownish orange (5C5) when aged. *Stipe context* soft, fistulose, white (1A1), grayish red (10D5) when cut. *Spores print* dark brown (7F5). *Odor* is pleasant. Macrochemical reactions; KOH reaction yellow and Schäffer's reactions negative.

Basidiospores (7)7.3–7.6–7.9(8.5) × (4.0)4.3–4.5–4.7(5.0) μm (n = 50), Q = 1.65–1.70, Q_m = 1.67 ± 0.08, ellipsoid to elongate, smooth, thin-walled, brown in water and KOH, inamyloid. *Basidia* 15–30 × 5–9 μm, clavate, 4-spored, hyaline, sterigmata up to 2.5 μm long. *Cheilocystidia* 18–29 × 10–17 μm, clavate to broadly clavate, hyaline. *Pleurocystidia* absent. *Pileipellis* composed of hyaline hyphae, smooth, short cylindrical, with occasionally branched and cutis hyphae 5–12.5 μm

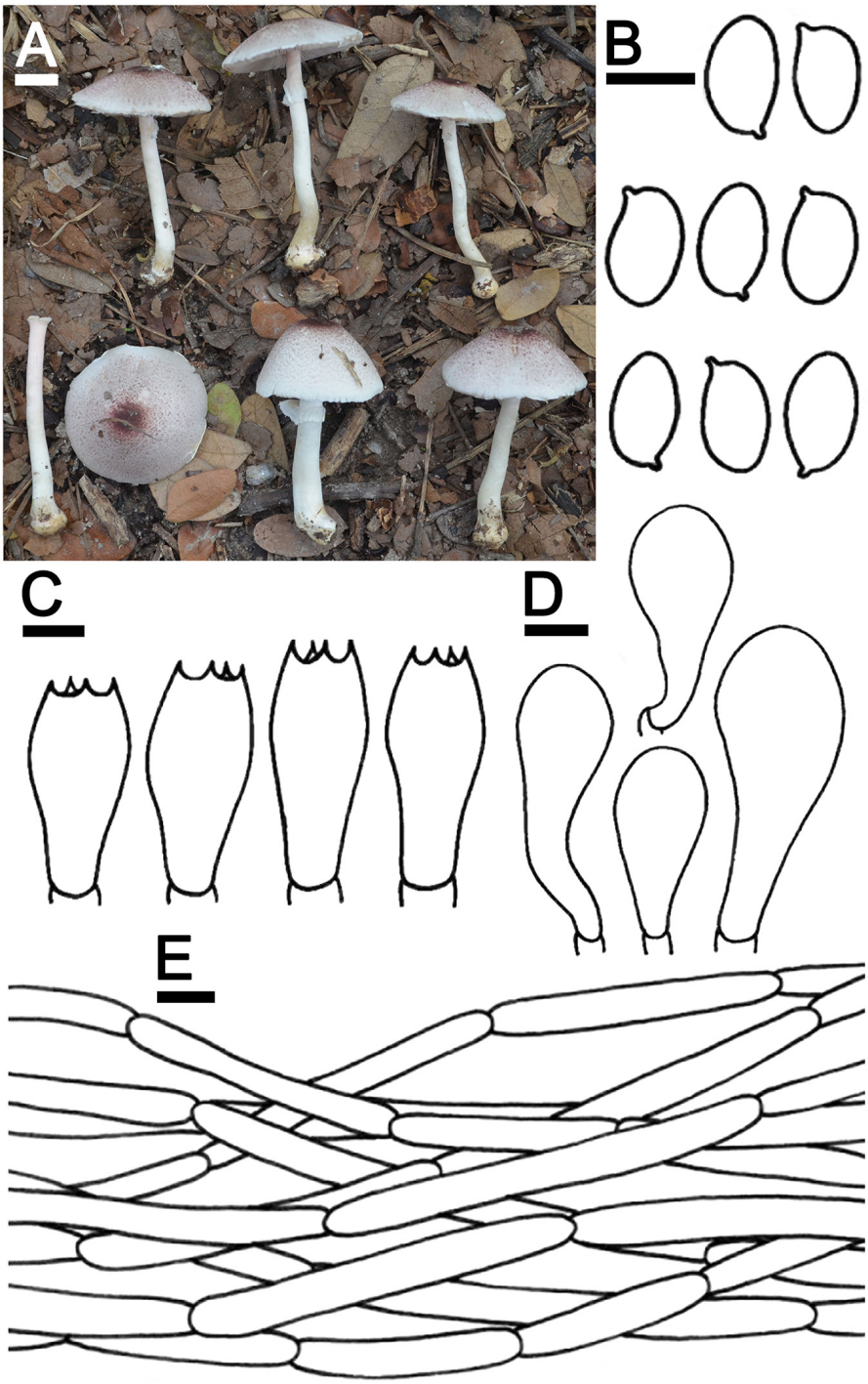


FIGURE 5 | *Agaricus thailandensis* SDBR-CJ0118A (holotype). **(A)** Basidiomata on the field, **(B)** Basidiospores, **(C)** Basidia, **(D)** Cheilocystidia, **(E)** Pileipellis. Scale bars **(A)** = 1 cm, **(B–D)** = 5 μm, and **(E)** = 10 μm.

wide, occasionally branched, hyaline. *Annulus* composed of 5–9.5 μm wide hyaline hyphae, cylindrical with rounded apex, branched. *Stipitipellis* composed of cutis hyphae wide up to 2.5–7 μm, cylindrical, occasionally branched, hyaline. *Clamp connections* absent.

Ecology and distribution: Fruiting solitary or gregarious on sandy loam soil during the rainy season (mid-May to October). Known from China and Thailand.

Material examined: THAILAND, Chiang Mai Province, Mueang Chiang Mai District, Chiang Mai University, 18°48′5″N

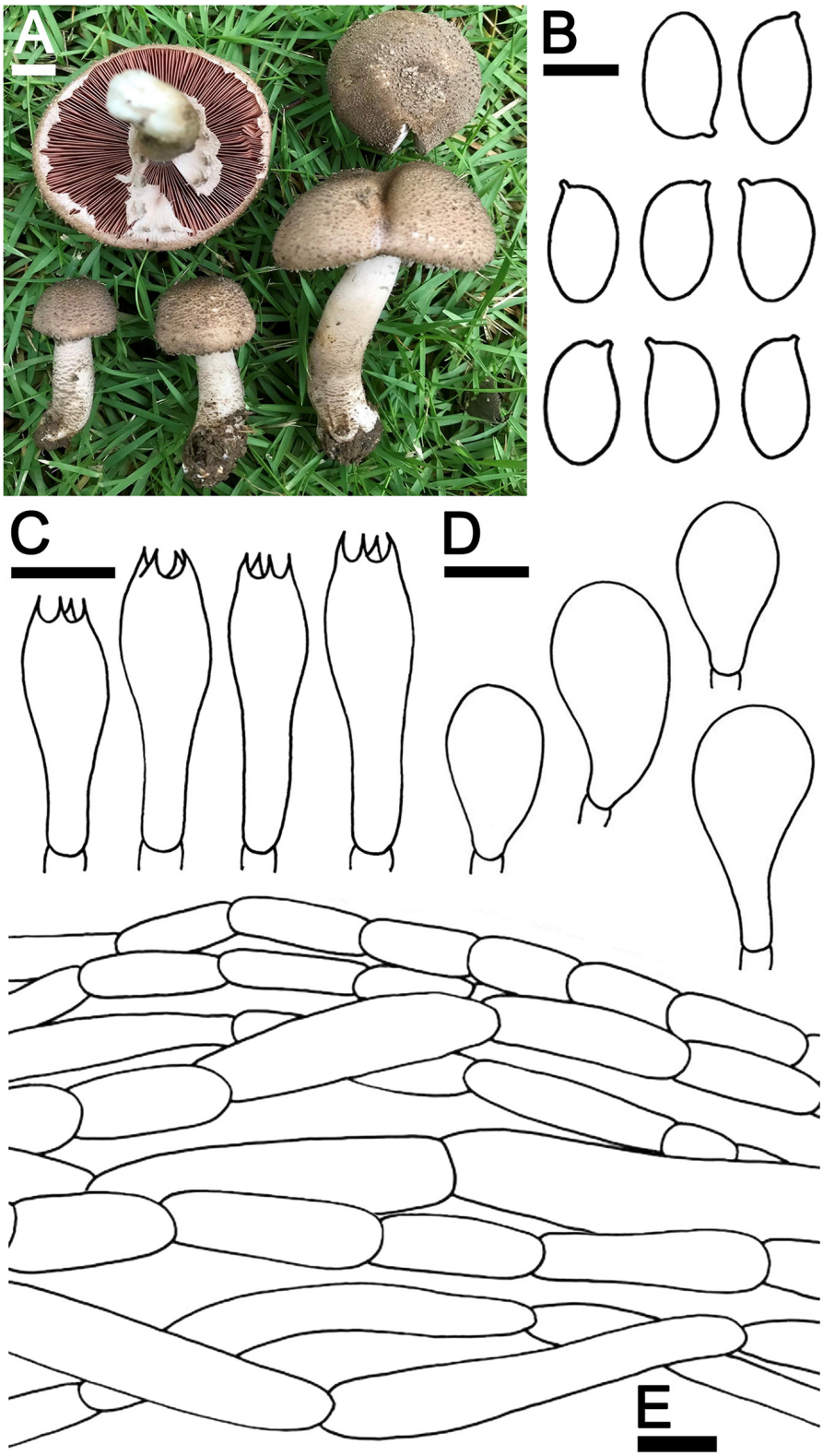


FIGURE 6 | *Agaricus pallidobrunneus* SDBR-NK0368. **(A)** Basidiomata on the field, **(B)** Basidiospores, **(C)** Basidia, **(D)** Cheilocystidia, **(E)** Pileipellis. Scale bars **(A)** = 1 cm, **(B)** = 5 μm, and **(C–E)** = 10 μm.

98°57′24″E, elevation 330 m, October 31, 2018, J. Kumla, SDBR-NK0368.

Note: Morphological characteristics and phylogenetic analysis of Thai specimens were used to assign *A. pallidobrunneus* to *Agaricus* sect. *Brunneopicti* in *Agaricus* subg. *Pseudochitonia*, according to Zhao et al. (2016). *Agaricus pallidobrunneus* is morphologically similar to *A. erectosquamosus*. However, *A. erectosquamosus* differs from *A. pallidobrunneus* by its erect, dark brown squamules on the pileus and stipe surface. The phylogeny also supports the determination that they are different species (Zhao et al., 2016).

DISCUSSION

Agaricus is widely distributed in both temperate and tropical areas throughout the world (Kerrigan et al., 2005, Kerrigan, 2016; Chen et al., 2015; Zhao et al., 2016; He et al., 2017, 2018a,b; Callac and Chen, 2018; Ling et al., 2021). Morphological characteristics have been traditionally used in the identification of specimens of the *Agaricus* species. However, identification can be difficult as some species have similar features. Thus, identification can be limited by the morphological characteristics as well as the different environmental conditions that affect those morphological characteristics (Heinemann, 1978; Kerrigan, 1986; Singer, 1986; Callac et al., 1998a,b; Parra, 2008). Over the last two decades, molecular phylogeny has been an essential tool in the identification of *Agaricus* (Challen et al., 2003; Kerrigan et al., 2005, 2008; Zhao et al., 2011; Parra, 2013; Chen et al., 2015). The current classification of the genus *Agaricus* consists of six subgenera and twenty-four sections based on the combined data of morphological characteristics, the multigene phylogenetic analysis, and an estimation of divergence times (Zhao et al., 2016; Chen et al., 2017; He et al., 2018a; Parra et al., 2018).

In Thailand, the fourteen *Agaricus* species that were recorded by Thai taxonomists were identified only by their morphological characteristics. Of these, most have previously been found in temperate areas. However, there has been a lack of available molecular data on this species (Chandrasrikul et al., 2011) and there may have been incidences of mis-classification because tropical microflora are poorly understood. Thus, we are not sure these fourteen species have been accurately identified, expect *A. subrufescens* (Wisitrassameewong et al., 2012). *Agaricus* species richness is high in Thailand but many species have not yet been described based on a single collection and some of them have not been confirmed by phylogenetic data. Zhao et al. (2011) classified *Agaricus* collected from temperate and tropical regions, while ten *Agaricus* species collected from Thailand have been described based on their morphological and molecular characteristics.

During the period of 2012 to 2014, seven new species and three new records of *Agaricus* were found in Thailand (Chen et al., 2012; Wisitrassameewong et al., 2012; Zhao et al., 2012a,b; Karunarathna et al., 2014; Thongklang et al., 2014a,b). Thirty-seven new species of *Agaricus* were described from 2015 to 2017 (Ariyawansa et al., 2015; Chen et al., 2015, 2017; Liu et al., 2015; Thongklang et al., 2016; Zhao et al., 2016; Zhou et al., 2016; Hyde et al., 2017). In 2018, a new species of Thai *Agaricus* was reported by He et al. (2018a). Prior to this study, *Agaricus* in Thailand were classified in five subgenera (*Agaricus* subg. *Agaricus*, *Agaricus* subg. *Flavoagaricus*, *Agaricus* subg. *Minores*, *Agaricus* subg. *Pseudochitonia* and *Agaricus* subg. *Spissicaules*), thirteen sections and fifty-eight species based on morphological and molecular data.

In this study, six species of *Agaricus* including three new species (*A. lannaensis*, *A. pseudoerectosquamosus,* and *A. thailandensis*), one new record (*A. pallidobrunneus*), and two previously known species (*A. erectosquamosus* and *A. subrufescens*) collected from Chiang Mai Province, Thailand were identified based on their morphological characteristics and a multigene phylogenetic analysis. *Agaricus lannaensis* and *A. pseudoerectosquamosus* belong to *Agaricus* subg. *Pseudochitonia* in an incertae sedis clade and *Agaricus* sect. *Brunneopicti*, respectively. *Agaricus thailandensis* has been placed in *Agaricus* sect. *Minores* of *Agaricus* subg. *Minores*. Based on the phylogenetic analyses, *A. lannaensis* (including *Agaricus* sp. CA820) formed a sister clade to unnamed species *Agaricus* voucher LD2012162 (**Figure 2**); however, they cannot be assigned to *Agaricus* sect. *Flocculenti* according to the classification system of *Agaricus* (Zhao et al., 2016). *Agaricus* sp. CA820 collected from Thailand should be recognized in *A. lannaensis*, however, its morphological characteristics should be further confirmed. *Agaricus pseudoerectosquamosus* and *A. thailandensis* are closely related to the unnamed species *Agaricus* sp. voucher NTT117 and CA935, respectively which have been collected in Thailand (**Figures 1**, **2**). However, there is a lack of available information on the morphological characteristics of these unnamed species. Thus, their species definition will be required in future studies. Notably, *A. subrufescens* and *A. erectosquamosus* have been previously reported to be from Thailand by Wisitrassameewong et al. (2012) and Zhao et al. (2016), respectively. *Agaricus pallidobrunneus* has been reported from China (Zhao et al., 2016), however, it has now been found for the first time in Thailand. Thus, to our knowledge, the *Agaricus* species recorded in Thailand has been raised to 62 species, 13 sections in five subgenera by the morphological and molecular evidence. Nevertheless, 13 *Agaricus* species listed by Chandrasrikul et al. (2011) require further confirmation by molecular data.

DATA AVAILABILITY STATEMENT

The datasets presented in this study can be found in online repositories. The names of the repository/repositories and accession number(s) can be found in the article/**Supplementary Material**.

AUTHOR CONTRIBUTIONS

CJ, JK, and NS: conceptualization and resources. CJ, JK, SV, and NS: methodology, formal analysis, and writing-review and editing. SV and CJ: software. NS and SL: validation. CJ, JK, and SV: investigation, data curation, and writing-original draft. NS

and SL: supervision. All authors read, revised, and approved the final manuscript.

FUNDING

This work was supported by Chiang Mai University, Thailand.

ACKNOWLEDGMENTS

We acknowledged the Department of Biology and Research Center of Microbial Diversity and Sustainable Utilization, Faculty of Science, Chiang Mai University for providing the laboratories and molecular work. We are grateful to Russell Kirk Hollis for assisting with English language editing of this manuscript.

SUPPLEMENTARY MATERIAL

The Supplementary Material for this article can be found online at: https://www.frontiersin.org/articles/10.3389/fmicb.2021.650513/full#supplementary-material

Supplementary Table 1 | Names, voucher numbers, countries and the corresponding GenBank accession numbers of the taxa used in the phylogenetic analyses. The sequences obtained in this study are in bold and superscript "T" refers to a type.

REFERENCES

Ariyawansa, H. A., Hyde, K. D., Jayasiri, S. C., Buyck, B., Chethana, K. T., Dai, D. Q., et al. (2015). Fungal diversity notes 111–252 taxonomic and phylogenetic contributions to fungal taxa. *Fungal Divers.* 75, 27–274. doi: 10.1007/s13225-015-0346-5

Asef, R., Hosseini, S. M. N., Callac, P., Goltapeh, E. M., Safaie, N., and Mahdizadeh, V. (2016). *Agaricus* section *Xanthodermatei* in Iran. *Phytotaxa* 247, 181–196. doi: 10.11646/phytotaxa.247.3.2

Bashir, H., Hussain, S., Khalid, A. N., Niazi, A. R. K., Parra, L. A., Callac, P., et al. (2018). First report of *Agaricus* sect. *Brunneopicti* from Pakistan with descriptions of two new species. *Phytotaxa* 357, 167–178. doi: 10.11646/phytotaxa.357.3.1

Bates, S. T., Chapman, R. M., Islam, M. B., Schwabe, A., Wardenaar, E. C., and Evenson, V. S. (2016). Phylogenetic placement of the secotioid fungus *Araneosa columellata* within *Agaricus*. *Mycotaxon* 131, 103–110. doi: 10.5248/131.103

Callac, P., and Chen, J. (2018). "Tropical species of *Agaricus*," in *Updates on Tropical Mushrooms. Basic and Applied Research*, eds J. E. Sánchez, G. Mata, and D. J. Royse, (San Cristobal de Las Casas: Chiapas), 25–38.

Callac, P., Hocquart, S., Imbernon, M., Desmerger, C., and Olivier, J. M. (1998a). Bsn–t alleles from French field strains of *Agaricus bisporus*. *Appl. Environ. Microbiol.* 64, 2105–2110. doi: 10.1128/AEM.64.6.2105-2110.1998

Callac, P., Moquet, F., Imbernon, M., Guedes-Lafargue, M. R., Mamoun, M., Olivier, J. M., et al. (1998b). Evidence for PPC1, a determinant of the Pilei–Pellis Color of *Agaricus bisporus* Fruitbodies. *Fungal Genet. Biol.* 23, 181–188. doi: 10.1006/fgbi.1998.1035

Challen, M. P., Kerrigan, R. W., and Callac, P. (2003). A phylogenetic reconstruction and emendation of *Agaricus* section *Duploannulatae*. *Mycologia* 95, 61–73. doi: 10.1080/15572536.2004.11833132

Chandrasrikul, A., Suwanarit, P., Sangwanit, U., Lumyong, S., Payapanon, A., Sanoamuang, N., et al. (2011). *Checklist of Mushrooms (Basidiomycetes) in Thailand*. Bangkok: Office of Natural Resources and Environmental Policy and Planning.

Chen, J., Callac, P., Parra, L. A., Karunarathna, S. C., He, M. Q., Moinard, M., et al. (2017). Study in *Agaricus* subgenus *Minores* and allied clades reveals a new American subgenus and contrasting phylogenetic patterns in Europe and Greater Mekong Subregion. *Persoonia* 38, 170–196. doi: 10.3767/003158517X695521

Chen, J., Zhao, R., Parra, L. A., Guelly, A. K., Kesel, D. A., Rapior, S., et al. (2015). *Agaricus* section *Brunneopicti*: a phylogenetic reconstruction with descriptions of four new taxa. *Phytotaxa* 192, 145–168. doi: 10.11646/phytotaxa.192.3.2

Chen, J., Zhao, R. L., Karunarathna, S. C., Callac, P., Raspé, O., Bahkali, A. H., et al. (2012). *Agaricus megalosporus*: a new species in section *Minores*. *Cryptogam. Mycol.* 33, 145–155. doi: 10.7872/crym.v33.iss2.2012.145

Darriba, D., Taboada, G. L., Doallo, R., and Posada, D. (2012). jModelTest 2: more models, new heuristics and parallel computing. *Nat. Methods* 9:772. doi: 10.1038/nmeth.2109

Donk, M. A. (1962). The generic names proposed for Agaricaceae. *Beiheifte Nova Hedwigia* 5, 1–320.

Dui, K. D. H., and Zhao, R. (2015). Edible species of *Agaricus* (Agaricaceae) from Xinjiang Province (Western China). *Phytotaxa* 202, 185–197. doi: 10.11646/phytotaxa.202.3.2

Foulongne-Oriol, M., Spataro, C., Moinard, M., Cabannes, D., Callac, P., and Savoie, J. M. (2012). Development of polymorphic microsatellite markers issued from pyrosequencing technology for the medicinal mushroom *Agaricus subrufescens*. *FEMS Microbiol. Lett.* 334, 119–126. doi: 10.1111/j.1574-6968.2012.02627.x

Geml, J., Geiser, D. M., and Royse, D. J. (2004). Molecular evolution of *Agaricus* species based on ITS and LSU rDNA sequences. *Mycol. Prog.* 3, 157–176. doi: 10.1007/s11557-006-0086-8

Geml, J., Laursen, G. A., Nusbaum, H. C., and Taylor, D. L. (2007). Two new species of *Agaricus* from the Subantarctic. *Mycotaxon* 100, 193–208.

Gui, Y., Zhu, G. S., Callac, P., Hyde, K. D., Parra, L. A., Chen, J., et al. (2015). *Agaricus* section *Arvenses*: three new species in highland subtropical Southwest China. *Fungal Biol.* 119, 79–94. doi: 10.1016/j.funbio.2014.10.005

Hama, O., Maes, E., Guissou, M. L., Ibrahim, D., Baragé, M., Parra, L. A., et al. (2010). *Agaricus subsaharianus*, une nouvelle espèce comestible et consommée au Niger, au Burkina Faso et en Tanzanie. *Cryptogam. Mycol.* 31, 221–234.

He, M. Q., Chen, J., Zhou, J. L., Ratchadawan, C., Hyde, K. D., and Zhao, R. L. (2017). Tropic origins, a dispersal model for saprotrophic mushrooms in *Agaricus* section *Minores* with descriptions of sixteen new species. *Sci. Rep.* 7, 1–31. doi: 10.1038/s41598-017-05203-5

He, M. Q., Chuankid, B., Hyde, K. D., Cheewangkoon, R., and Zhao, R. L. (2018a). A new section and species of *Agaricus* subgenus *Pseudochitonia* from Thailand. *MycoKeys* 40, 53–67. doi: 10.3897/mycokeys.40.26918

He, M. Q., Hyde, K. D., Wei, S. L., Xi, Y. L., Cheewangkoon, R., and Zhao, R. L. (2018b). Three new species of *Agaricus* section *Minores* from China. *Mycosphere* 9, 189–201. doi: 10.5943/mycosphere/9/2/3

He, M. Q., and Zhao, R. L. (2015). A new species of *Agaricus* section *Minores* from China. *Mycology* 6, 182–186. doi: 10.1080/21501203.2015.1121931

Heinemann, P. (1978). Essai d'une clé de determination des genres *Agaricus* et Micropsalliota. *Sydowia* 30, 6–37.

Hyde, K. D., Norphanphoun, C., Abreu, V. P., Bazzicalupo, A., Chethana, K. T., Clericuzio, M., et al. (2017). Fungal diversity notes 603–708: taxonomic and phylogenetic notes on genera and species. *Fungal Divers.* 87, 1–235. doi: 10.1007/s13225-017-0391-3

Hyde, K. D., Norphanphoun, C., Chen, J., Dissanayake, A. J., Doilom, M., Hongsanan, S., et al. (2018). Thailand's amazing diversity: up to 96% of fungi in northern Thailand may be novel. *Fungal Divers.* 93, 215–239. doi: 10.1007/s13225-018-0415-7

Ibrahim, D. M., Barage, M., Marafa, D. I., Sanchez, L. A. P., Raspe, O., Kesel, A. D., et al. (2010). *Agaricus subsaharianus*, une nouvelle espèce comestible et consommée au Niger, au Burkina Faso et en Tanzanie. *Cryptogam. Mycol.* 31, 221–234.

Jayasiri, S. C., Hyde, K. D., Ariyawansa, H. A., Bhat, J., Buyck, B., Cai, L. D., et al. (2015). The faces of fungi database: fungal names linked with morphology, phylogeny and human impacts. *Fungal Divers.* 74, 3–18. doi: 10.1007/s13225-015-0351-8

Karunarathna, S. C., Chen, J., Mortimer, P. E., Xu, J. C., Zhao, R. L., Callac, P., et al. (2016). Mycosphere essay 8: a review of genus *Agaricus* in tropical and humid subtropical regions of Asia. *Mycosphere* 7, 417–439. doi: 10.5943/mycosphere/7/4/3

Karunarathna, S. C., Guinberteau, J., Chen, J., Vellinga, E. C., Zhao, R. L., Chukeatirote, E., et al. (2014). Two new species in *Agaricus* tropical clade I. *Chiang Mai J. Sci.* 41, 771–780.

Katoh, K., and Standley, D. M. (2013). MAFFT multiple sequence alignment software version 7: improvements in performance and usability. *Mol. Biol. Evol.* 30, 772–780. doi: 10.1093/molbev/mst010

Kerrigan, R. W. (1986). *The Agaricales of California*, Vol. 6. ELureka: Mad River Press.

Kerrigan, R. W. (2016). *Agaricus* of North America. New York, NY: Botanical Garden.

Kerrigan, R. W., Callac, P., Guinberteau, J., Challen, M. P., and Parra, L. A. (2005). *Agaricus* section *Xanthodermatei*: a phylogenetic reconstruction with commentary on taxa. *Mycologia* 97, 1292–1315. doi: 10.1080/15572536.2006.11832737

Kerrigan, R. W., Callac, P., and Parra, L. A. (2008). New and rare taxa in *Agaricus* section *Bivelares* (Duploannulati). *Mycologia* 100, 876–892. doi: 10.3852/08-019

Kornerup, A., and Wanscher, J. H. (1978). *Methuen Handbook of Colour*. London: Eyre Methuen.

Lebel, T. (2013). Two new species of sequestrate *Agaricus* (section *Minores*) from Australia. *Mycol. Prog.* 12, 699–707. doi: 10.1007/s11557-012-0879-x

Lebel, T., and Syme, A. (2012). Sequestrate species of *Agaricus* and *Macrolepiota* from Australia: new species and combinations and their position in a calibrated phylogeny. *Mycologia* 104, 496–520. doi: 10.3852/11-092

Li, G. J., Hyde, K. D., Zhao, R. L., Hongsanan, S., Abdel-Aziz, F. A., Abdel-Wahab, M. A., et al. (2016). Fungal diversity notes 253–366: taxonomic and phylogenetic contributions to fungal taxa. *Fungal Divers.* 78, 1–237. doi: 10.1007/s13225-016-0366-9

Li, S. F., Xi, Y. L., Qi, C. X., Liang, Q. Q., Wei, S. L., Li, G. J., et al. (2014). *Agaricus taeniatus* sp. nov., a new member of *Agaricus* sect. *Bivelares* from northwest China. *Mycotaxon* 129, 187–196. doi: 10.5248/129.187

Ling, Z. L., Zhou, J. L., Parra, L. A., Kesel, A. D., Callac, P., Zhao, R. L., et al. (2021). Four new species of *Agaricus* subgenus *Spissicaules* from China. *Mycologia* 113, 476–491. doi: 10.1080/00275514.2020.1852808

Liu, J. K., Hyde, K. D., Jones, E. G., Ariyawansa, H. A., Bhat, D. J., Boonmee, S., et al. (2015). Fungal diversity notes 1–110: taxonomic and phylogenetic contributions to fungal species. *Fungal Divers.* 72, 1–197. doi: 10.1007/s13225-015-0324-y

Miller, M. A., Holder, M. T., Vos, R., Midford, P. E., Liebowitz, T., Chan, L., et al. (2009). *The CIPRES Portals. CIPRES*. Available online at: http://www.phylo.org/portal2/home (accessed October 10, 2020).

Parra, L. A. (2008). *Agaricus* L. Allopsalliota Nauta & Bas. I. Fungi Europaei, Vol. 1. Italy: Edizione Candusso.

Parra, L. A. (2013). *Fungi Europaei: Agaricus*: Allopsalliota, Nauta and Bas, Vol. 2. Italy: Edizione Candusso.

Parra, L. A., Angelini, C., Ortiz-Santana, B., Mata, G., Billette, C., Rojo, C., et al. (2018). The genus *Agaricus* in the Caribbean. nine new taxa mostly based on collections from the Dominican Republic. *Phytotaxa* 345, 219–271. doi: 10.11646/phytotaxa.345.3.2

Parra, L. A., Muñoz, G., and Callac, P. (2014). *Agaricus caballeroi* sp. nov., a new species of the section *Nigrobrunnescentes* collected in Spain. *Micol. Veget. Medit.* 29, 21–38.

Parra, L. A., Wisman, J., Guinberteau, J., Wilhelm, M., Weholt, Ø, and Musumeci, E. (2015). *Agaricus collegarum* and *Agaricus masoalensis*, two new taxa of the section *Nigrobrunnescentes* collected in Europe. *Micol. Vegetazione Mediterr.* 30, 3–26.

Pegler, D. N. (1977). *A Preliminary Agaric Flora of East Africa*. London: Her Majesty's Stationery Office.

Petrova, A., Alipieva, K., Kostadinova, E., Antonova, D., Lacheva, M., Gjosheva, M., et al. (2007). GC–MS studies of the chemical composition of two inedible mushrooms of the genus *Agaricus*. *Chem. Cent. J.* 1:33. doi: 10.1186/1752-153X-1-33

Rehner, S. A., and Buckley, E. (2005). A *Beauveria* phylogeny inferred from nuclear ITS and EF1–α sequences: evidence for cryptic diversification and links to *Cordyceps* teleomorphs. *Mycologia* 97, 84–98. doi: 10.1080/15572536.2006.11832842

Robert, V., Vu, D., Amor, A. B., Wiele, N. V. D., Brouwer, C., Jabas, B., et al. (2013). MycoBank gearing up for new horizons. *IMA Fungus* 4, 371–379. doi: 10.5598/imafungus.2013.04.02.16

Ronquist, F., Teslenko, M., Mark, V. D. P., Ayres, D. L., Darling, A., Höhna, S., et al. (2012). MrBayes 3.2: efficient Bayesian phylogenetic inference and model choice across a large model space. *Syst. Biol.* 61, 539–542. doi: 10.1093/sysbio/sys029

Schoch, C. L., Robbertse, B., Robert, V., Vu, D., Cardinali, G., Zhang, N., et al. (2014). Finding needles in haystacks: linking scientific names, reference specimens and molecular data for Fungi. *DataBase.* 2014, 1–21. doi: 10.1093/database/bau061

Singer, R. (1986). *The Agaricales in Modern Taxonomy*, 4th Edn. Koenigstein: Koeltz Scientific Books.

Stamatakis, A. (2006). RAxML–VI–HPC: maximum likelihood–based phylogenetic analyses with thousands of taxa and mixed models. *Bioinformatics* 22, 2688–2690. doi: 10.1093/bioinformatics/btl446

Tarafder, E. N. T. A. J., Dutta, A. K., Sarkar, J., and Acharya, K. (2018). A new species of *Agaricus* sect. *Brunneopicti* from Eastern India. *Phytotaxa* 374, 139–146. doi: 10.11646/phytotaxa.374.2.5

Thongklang, N., Chen, J., Bandara, A. R., Hyde, K. D., Raspé, O., Parra, L. A., et al. (2016). Studies on *Agaricus subtilipes*, a new cultivatable species from Thailand, incidentally, reveal the presence of *Agaricus subrufescens* in Africa. *Mycoscience* 57, 239–250. doi: 10.1016/j.myc.2016.02.003

Thongklang, N., Nawaz, R., Khalid, A. N., Chen, J., Hyde, K. D., Zhao, R. L., et al. (2014a). Morphological and molecular characterization of three *Agaricus* species from tropical Asia (Pakistan, Thailand) reveals a new group in section *Xanthodermatei*. *Mycologia* 106, 1220–1232. doi: 10.3852/14-076

Thongklang, N., Sysouphanthong, P., Callac, P., and Hyde, K. D. (2014b). First cultivation of *Agaricus flocculosipes* and a novel Thai strain of *A. subrufescens*. *Mycosphere* 5, 814–820. doi: 10.5943/mycosphere/5/6/11

Vilgalys, R., and Hester, M. (1990). Rapid genetic identification and mapping of enzymatically amplified ribosomal DNA from several *Cryptococcus* species. *J. Bacteriol. Res.* 172, 4238–4246. doi: 10.1128/jb.172.8.4238-4246.1990

Wang, Z. R., Parra, L., Callac, P., Zhou, J. L., Fu, W. J., Dui, S. H., et al. (2015). Edible species of *Agaricus* (Agaricaceae) from Xinjiang Province (Western China). *Phytotaxa* 202, 185–197. doi: 10.11646/phytotaxa.202.3.2

White, T. J., Burns, T., Lee, S., and Taylor, J. (1990). "Amplification and direct sequencing of fungal ribosomal RNA genes for phylogenetics," in *PCR Protocols, a Guide to Methods and Applications*, eds M. A. Innis, D. H. Gelfand, J. J. Sninsky, and T. J. Whitish, (San Diego, CA: Academic Press), 315–322. doi: 10.1016/b978-0-12-372180-8.50042-1

Wisitrassameewong, K., Karunarathna, S. C., Thongklang, N., Zhao, R. L., Callac, P., Chukeatirote, E., et al. (2012). *Agaricus subrufescens*: new to Thailand. *Chiang Mai J. Sci.* 39, 281–291.

Zhang, M. Z., Li, G. J., Dai, R. C., Xi, Y. L., Wei, S. L., and Zhao, R. L. (2017). The edible wide mushrooms of *Agaricus* section *Bivelares* from Western China. *Mycosphere* 8, 1640–1652. doi: 10.5943/mycosphere/8/10/4

Zhao, R. L., Desjardin, D. E., Callac, P., Parra, L. A., Guinberteau, J., Soytong, K., et al. (2012a). Two species of *Agaricus* sect. *Xanthodermatei* from Thailand. *Mycotaxon* 122, 187–195. doi: 10.5248/122.187

Zhao, R. L., Hyde, K. D., Karunarathna, S. C., Desjardin, D. E., Raspé, O., Soytong, K., et al. (2012b). *Agaricus flocculosipes* sp. nov., a new potentially cultivatable species from the palaeotropics. *Mycoscience* 53, 300–311. doi: 10.1007/s10267-011-0169-5

Zhao, R. L., Karunarathna, S., Raspé, O., Parra, L. A., Guinberteau, J., Moinard, M., et al. (2011). Major clades in tropical *Agaricus*. *Fungal Divers.* 51, 279–296. doi: 10.1007/s13225-011-0136-7

Zhao, R. L., Zhou, J. L., Chen, J., Margaritescu, S., Sánchez-Ramírez, S., Hyde, K. D., et al. (2016). Towards standardizing taxonomic ranks using divergence times–a case study for reconstruction of the *Agaricus* taxonomic system. *Fungal Divers.* 78, 239–292. doi: 10.1007/s13225-016-0357-x

Zhou, J. L., Su, S. Y., Su, H. Y., Wang, B., Callac, P., Guinberteau, J., et al. (2016). A description of eleven new species of *Agaricus* sections *Xanthodermatei* and *Hondenses* collected from Tibet and the surrounding areas. *Phytotaxa* 257, 99–121. doi: 10.11646/phytotaxa.257.2.1

Conflict of Interest: The authors declare that the research was conducted in the absence of any commercial or financial relationships that could be construed as a potential conflict of interest.

Copyright © 2021 Jaichaliaw, Kumla, Vadthanarat, Suwannarach and Lumyong. This is an open-access article distributed under the terms of the Creative Commons Attribution License (CC BY). The use, distribution or reproduction in other forums is permitted, provided the original author(s) and the copyright owner(s) are credited and that the original publication in this journal is cited, in accordance with accepted academic practice. No use, distribution or reproduction is permitted which does not comply with these terms.

frontiers in Microbiology

ORIGINAL RESEARCH
published: 01 July 2021
doi: 10.3389/fmicb.2021.652324

Genomic Analysis of *Sarcomyxa edulis* Reveals the Basis of Its Medicinal Properties and Evolutionary Relationships

Fenghua Tian[1,2], *Changtian Li*[2]* *and Yu Li*[2]*

[1] Department of Plant Pathology, College of Agriculture, Guizhou University, Guiyang, China, [2] Engineering Research Center of Chinese Ministry of Education for Edible and Medicinal Fungi, Jilin Agricultural University, Changchun, China

Yuanmo [*Sarcomyxa edulis* (Y.C. Dai, Niemelä & G.F. Qin) T. Saito, Tonouchi & T. Harada] is an important edible and medicinal mushroom endemic to Northeastern China. Here we report the *de novo* sequencing and assembly of the *S. edulis* genome using single-molecule real-time sequencing technology. The whole genome was approximately 35.65 Mb, with a G + C content of 48.31%. Genome assembly generated 41 contigs with an N50 length of 1,772,559 bp. The genome comprised 9,364 annotated protein-coding genes, many of which encoded enzymes involved in the modification, biosynthesis, and degradation of glycoconjugates and carbohydrates or enzymes predicted to be involved in the biosynthesis of secondary metabolites such as terpene, type I polyketide, siderophore, and fatty acids, which are responsible for the pharmacodynamic activities of *S. edulis*. We also identified genes encoding 1,3-β-glucan synthase and endo-1,3(4)-β-glucanase, which are involved in polysaccharide and uridine diphosphate glucose biosynthesis. Phylogenetic and comparative analyses of Basidiomycota fungi based on a single-copy orthologous protein indicated that the *Sarcomyxa* genus is an independent group that evolved from the Pleurotaceae family. The annotated whole-genome sequence of *S. edulis* can serve as a reference for investigations of bioactive compounds with medicinal value and the development and commercial production of superior *S. edulis* varieties.

Keywords: edible-medicinal mushroom, lignin-degrading peroxidases, phylogenetic analyses, *Sarcomyxa edulis*, secondary metabolism

OPEN ACCESS

Edited by:
Peter Edward Mortimer, Kunming Institute of Botany, Chinese Academy of Sciences, China

Reviewed by:
Shanshan Liu, The First Affiliated Hospital of Bengbu Medical College, China
Rajesh Jeewon, University of Mauritius, Mauritius

***Correspondence:**
Yu Li
fungi966@126.com
Changtian Li
lct@jlau.edu.cn

Specialty section:
This article was submitted to Evolutionary and Genomic Microbiology, a section of the journal Frontiers in Microbiology

Received: *12 January 2021*
Accepted: *26 May 2021*
Published: *01 July 2021*

Citation:
Tian F, Li C and Li Y (2021) Genomic Analysis of Sarcomyxa edulis Reveals the Basis of Its Medicinal Properties and Evolutionary Relationships. Front. Microbiol. 12:652324. doi: 10.3389/fmicb.2021.652324

INTRODUCTION

Sarcomyxa edulis (Y.C. Dai, Niemelä & G.F. Qin) T. Saito, Tonouchi & T. Harada is a fungus that is native to the temperate regions of Northeastern China, Northern Japan, United States, and Russian Far East (Jin et al., 2001; Dai et al., 2003; Saito et al., 2014). It is commonly known as the late oyster and is also called "Yuanmo," "Huangmo," or "Dongmo" in Chinese and "Mukitake" in Japanese. The fruiting body of *S. edulis* is fan-shaped, which is similar to *Ganoderma lucidum* ("Lingzhi"), but because of its yellow color, it is also known as "Huanglinggu" in China.

Sarcomyxa edulis is an edible and medicinal fungus (Imazeki et al., 1988; Li, 1991; Pan, 1995) that is prized for its nutritional value, unique aroma, delicate flavor, and meaty texture as well as

its medicinal properties (Li, 1991; Ma et al., 1991; Pan, 1995; Inafuku et al., 2012; Kim et al., 2012; Inoue et al., 2013; Li et al., 2013, 2016; Zhang et al., 2014). In traditional Chinese medicine, *S. edulis* is prepared as an alcohol decoction to treat stomachache and other ailments.

Sarcomyxa edulis was first described and assigned to the genus *Panellus* (Dai et al., 2003) through a comparison with the terribly bitter mushrooms from Finland to the specimens of China. *S. edulis* is under the same genus as *Sarcomyxa serotina*. As the type species, the taxonomic status of *S. serotina* has changed multiple times from the *Agaricus* genus to *Pleurotus*, *Sarcomyxa*, *Hohenbuehelia*, and finally *Panellus* (Dai et al., 2003). Phylogenetic studies have shown that *S. serotina* and *S. edulis* are excluded from the *Panellus* clade. A maximum likelihood (ML) tree constructed based on the D1/D2 region of the large subunit of the 28S ribosomal RNA gene showed that the *Sarcomyxa* genus formed a clade that was independent of *Mycena* and *Panellus* (Matheny et al., 2006; Saito et al., 2014). Thus, the classification of *Sarcomyxa* is controversial.

Sarcomyxa edulis was domesticated in the last decade in China; like *Hericium erinaceus*, it is an important specialty mushroom cultivated in Northern China, the largest production region. The commercial cultivation of *S. edulis* is profitable because of high demand. However, production has markedly declined in recent years as a result of diseases and the lack of resistant varieties.

Knowledge of the biology and evolution of *S. edulis* is limited because molecular-level information from the genome is lacking. The availability of a whole-genome sequence can clarify the taxonomy of *S. edulis* and aid future breeding efforts to improve this species for commercial cultivation. To this end, in the present study, we sequenced and annotated the genome of a monokaryotic strain of *S. edulis* and carried out a phylogenetic analysis that included 32 sequenced fungi, with the aim of establishing the taxonomic status of *S. edulis* and identifying secondary metabolites of medicinal importance.

MATERIALS AND METHODS

Sarcomyxa edulis Specimens

Sarcomyxa edulis basidiomes were collected from maple wood in Antu County, Jilin Province, China. Specimen 2016092521 was identified by morphologic and molecular analyses (Dai et al., 2003; Saito et al., 2014). The specimen was deposited in the herbarium of the Culture Center of Mycophyta in Jilin Agricultural University under accession number CCMJ18024 (**Figure 1**). The monokaryotic strain SE1 was germinated from one of the spores of specimen 2016092521 (Choi et al., 1999; Senanayake et al., 2020) and used for whole-genome sequencing. The mycelia of SE1 were cultured on an improved potato dextrose agar medium containing 5% wheat bran for 10 days at 24°C in the dark and collected for genome sequencing.

Whole-Genome Sequencing

Total DNA of *S. edulis* strain SE1 was extracted using the NuClear Plant Genomic DNA kit (Tiangen Biotech, Beijing, China). The DNA was detected by agarose gel electrophoresis and quantified with a Qubit fluorometer (Thermo Fisher Scientific, Waltham, MA, United States). The whole genome of SE1 was sequenced using PacBio RSII Single Molecule Real-Time (SMRT) technology, which generated 20-kb SMRTbell libraries. High-throughput sequencing on an HiSeq PE150 system (Illumina, San Diego, CA, United States) was carried out to polish the DNA sequence; additionally, paired-end read libraries were obtained by sequencing 350-bp inserts.

Custom Novogene pipelines (Beijing, China) were used to filter the PacBio RSII reads; those of low complexity and quality were filtered out with SMRT portal v3.2.0, with default parameters (Berlin et al., 2015; Koren and Phillippy, 2015), and the resultant clean reads were *de novo* assembled into a continuous contig with no gaps. Pilon v1.22 was used to polish the assembled long reads with the clean Illumina short reads (Walker et al., 2014). Genome completeness was assessed using Benchmarking Universal Single-Copy Orthologs (v4.1.4; Simão et al., 2015). RepeatMasker version open-4.0.5 was used to detect and annotate dispersed repeat sequences (Saha et al., 2008). Tandem repeat (TR) sequences were analyzed with Tandem Repeat Finder v4.07b (Benson, 1999). rRNA sequences were predicted with rRNAmmer v1.2 (Lagesen et al., 2007), and tRNA genes and tRNA secondary structures were predicted with tRNAscan-SE v1.3 (Lowe and Eddy, 1997). Non-coding RNAs including small (s)RNAs, micro (mi)RNAs, and small nuclear (sn)RNAs were annotated with Rfam (Gardner et al., 2009; Nawrocki et al., 2009) using default parameters (Cui et al., 2016). *Ab initio* and homology-based gene prediction methods were used to annotate the repeat masked SE1 genome assembly. For homolog-based gene prediction, the protein sequences of *Agaricus bisporus* (Morin et al., 2012), *Coprinopsis cinerea* (Stajich et al., 2010), *Pleurotus ostreatus* (Qu et al., 2016), and *Schizophyllum commune* (Ohm et al., 2010) were downloaded from the National Center for Biotechnology Information (NCBI) database and aligned using tBLASTn. Subsequently, mapping results were merged, and gene structures were predicted using GeneWise (v. 2.2.0; Birney et al., 2004). *Ab initio* genes were predicted using Augustus (Stanke et al., 2006), Genescan (Burge and Karlin, 1997), GlimmerHMM (Majoros et al., 2004), and SNAP (Korf, 2004). The protein-coding genes predicted from the *ab initio* and homology-based gene prediction methods were integrated using GLEAN (Elsik et al., 2007).

Gene Annotation and Functional Analysis

In order to determine the functions of the predicted genes, we compared homologous genes to protein and nucleotide sequences in the general functional BLAST databases. The basic steps of functional annotation were as follows: (1) the predicted gene protein sequences were compared with the functional databases by DIAMOND (with an *e*-value $\leq 10^{-5}$; Buchfink et al., 2014) and (2) filtering of alignment results: for the alignment results of each sequence, select the alignment result with the highest score (default identity $\geq$ 40%, coverage $\geq$ 40%) for annotation (Altschul et al., 1990).

Six gene and protein databases were used to predict gene functions including the NCBI Non-redundant Protein Database



FIGURE 1 | Fruiting body of *Sarcomyxa edulis*. **(a)** Developmental stages of *S. edulis*. **(b)** Mature *S. edulis*.

(nr; Li et al., 2002), Kyoto Encyclopedia of Genes and Genomes (KEGG; Kanehisa et al., 2004, 2006), Gene Ontology (GO; Ashburner et al., 2000), Eukaryotic Orthologous Groups (KOG; Tatusov et al., 2003), and Transporter Classification Database (TCDB; Saier et al., 2014).

Secondary metabolites were annotated using the antiSMASH (fungiSMASH option) database[1] and NaPDoS[2] (Ziemert et al., 2012; Weber et al., 2015; Blin et al., 2017). To validate the predicted results, the obtained gene clusters were manually verified. Each gene model within the database was searched with BLASTP and TBLASTN algorithms (Grigoriev et al., 2012). For polyketide synthase (PKS)/non-ribosomal peptide synthetase (NRPS) analysis, we selected a query type and entered the sequence data to identify ketosynthase KS and/or condensation C domains using the NaPDos pipeline[3]. Carbohydrate-active enzymes (CAZymes) were determined using the dbCAN 2 meta server (Zhang et al., 2018). Cytochrome P450 monooxygenase (P450) analysis was performed by searching a reference dataset[4] using the BLASTP program (Nelson, 2009).

Phylogenetic Tree Construction

In addition to *S. edulis*, 31 fungal species in the Basidiomycota and Ascomycota phyla were included in the phylogenetic analysis. Protein sequence data for four taxa were downloaded from the Joint Genome Institute genome database (Bao et al., 2013; Aronsen and Læssøe, 2016; Castanera et al., 2017), and sequences for the other 27 taxa were obtained from the NCBI database (**Supplementary Table 1**). BLASTP was used to compare the 32 species (Chen et al., 2016). OrthoMCL software (Li et al., 2003) and all-*versus*-all BLASTP were used with the parameters (*e*-value $\leq$ 1e-15, coverage $\geq$ 50%) to identify orthologous groups. Single-copy orthologs were extracted by Perl script (command line parameters of Gblocks: Gblocks proteins.fasta –b4 = 5 –b5 = h.), and sequence alignments were analyzed with MAFFT v7.158b (Katoh and Standley, 2013). ProTest was used to generate an optimal base substitution model with ML and neighbor-joining (NJ; Castresana, 2000; Miller et al., 2010). Several fossil calibration points fixed were used as references: the most recent common ancestor (MRCA) of *P. ostreatus*, *S. commune*, *Lentinula edodes*, *Panellus stipticus*, *Mycena albidolilacea*, *Termitomyces* sp., *Hypsizygus marmoreus*, *Volvariella volvacea*, *A. bisporus* var. *bisporus*, *A. bisporus* var. *burnettii*, *Leucoagaricus* sp., *C. cinerea*, *Laccaria bicolor*, *Hypholoma sublateritium*, *Hebeloma cylindrosporum*, *Gymnopilus dilepis*, and *Galerina marginata* diverged 123 million years ago (MYA), while the MRCAs of other taxonomic groups diverged at the following time points: *Serpula lacrymans* and *Coniophora olivacea*, 104 MYA; *Ganoderma sinens*, *Postia placenta*, *Wolfiporia cocos*, *Trametes versicolor*, and *Dichomitus squalens*, 122 MYA; *Tremella mesenterica* and *Cryptococcus neoformans*, 153 MYA; and *Ustilago maydis*, 273 MYA (Floudas et al., 2012). The final phylogenetic tree was constructed using RAxML (Stamatakis, 2014).

RESULTS

Identification of Specimen 2016092521

Specimen 2016092521 was identified as *S. edulis*. It is mild-tasting with ventricose cystidia, while the related species *S. serotina* is very bitter-tasting with hymenial cystidia. The basidiospores of the specimen are slightly longer than in *S. serotina*, 4.5–6.0 μm × 1.0–1.3 μm (**Supplementary Figure 1**). Maximum parsimony phylogenetic tree based on ITS gene sequences showed that specimen 2016092521 clusters with *S. edulis* and is distinct to *S. serotina* (**Supplementary Figure 2**).

Features of the *S. edulis* Genome

In total, 5,318 Mb of clean data were obtained, from which a 35.65-Mb assembly was obtained. The genome consisted of 41 contigs with N50 of 1,772,559 bp, N90 of 554,178 bp, and 48.31% G + C content (**Table 1**). A BLAST search of repeat sequences yielded 1,371,373 bp, covering 3.85% of the SE1 genome; meanwhile, interspersed nuclear elements and TRs accounted for 1.79 and 2.05% of the genome, respectively. Approximately 1.53% of the genome was long terminal repeats, 0.09% was DNA transposons, and 0.16% was long interspersed nuclear elements.

[1]http://antismash.secondarymetabolites.org
[2]http://napdos.ucsd.edu
[3]http://napdos.ucsd.edu/napdos_home.html
[4]http://drnelson.uthsc.edu/CytochromeP450.html

The proportion of TRs in the assembled genome was 1.36%, while minisatellite and microsatellite DNA accounted for 0.60 and 0.01% of the genome, respectively.

Functional Annotation

There were 9,364 gene models predicted in the different databases with a total sequence length of 15,135,900 bp, accounting for 42.45% of the whole genome with an average sequence length of 1,616 bp. We predicted 143 tRNAs (13,216 bp), 14 rRNAs (29,757 bp), 37 snRNAs (3,044 bp), 143 miRNAs (8,449 bp), and six sRNAs (359 bp; **Supplementary Table 2**). Among the 143 tRNAs, 21 were putative pseudogenes and 122 were anticodon tRNAs corresponding to the 20 common amino acid codons.

Annotation was performed with the NCBI nr, KEGG, KOG, TCDB, GO, P450, Secretory Protein, and CAZy databases (**Table 2** and **Supplementary Table 3**). In the nr database, 4,855 non-redundant proteins found in *S. edulis* had most matching with six fungi, accounting for 67.6% of total nr predicted proteins (**Figure 2**). These were similarly annotated in six species—namely, *G. marginata* (PRJNA207683), *L. bicolor* (PRJNA19043), *P. ostreatus* (PRJNA476433), *S. lacrymans* (PRJNA412961), *Moniliophthora roreri* (PRJNA279170), and *Jaapia argillacea* (PRJNA207685).

We assigned 1,760 proteins (18.80% of 9,364, the total annotated predicted proteins) to NCBI KOG categories (**Figure 3**). The "posttranslational modification, protein turnover, chaperones" category had the most enriched genes (230), followed by "general function prediction only" (190), "translation, ribosomal structure and biogenesis" (188), "energy production and conversion" (163), "amino acid transport and metabolism" (125), "RNA processing and modification" (124), "signal transduction mechanisms" (113), and "intracellular trafficking, secretion, and vesicular transport" (106). The representation of genes related to protein and energy metabolism could reflect the capacity of *S. edulis* to absorb and transform nutrients from a variety of substrates.

We mapped the predicted genes to the KEGG database and assigned functional classifications to 2,954 (31.55%, 9,364 gene models; **Figure 4**). Some categories related to metabolism and biosynthesis were highly enriched, including "purine metabolism," "oxidative phosphorylation," "butanoate metabolism," "fructose and mannose metabolism," "starch and sucrose metabolism," "amino sugar and nucleotide sugar metabolism," "arginine and proline metabolism," "pyrimidine metabolism," and "chloroalkane and chloroalkene degradation."

We used the TCDB to perform protein domain analysis and assigned 290 putative transport proteins to seven functional classes including "accessory factors involved in transport," "channels/pores," "electrochemical potential-driven transporters," "group translocators," "incompletely characterized transport systems," "primary active transporters," and "transmembrane electron carriers" (**Figure 5**). The top two enriched categories were "porters (uniporters, symporters, antiporters)" and "P–P bond hydrolysis-driven transporters."

In terms of GO functional classes, we predicted 5,884 proteins that accounted for 62.84% of the total predicted proteins. The most highly enriched GO terms in *S. edulis* were "cell," "cell part," "cellular process," "catalytic activity," "metabolic process," and "binding" (**Figure 6**).

Cytochrome P450 (CYP) is a superfamily of hemoproteins that use heme as a cofactor. CYPs have various substrates in different enzymatic reactions and are present in all kingdoms. We identified 83 putative CYP genes in *S. edulis* through a BLAST search and classified them into 34 families (**Supplementary Table 4**). The CYP5144 family had the highest number of enriched genes (14), followed by CYP5037 (13).

The CAZymes play important roles in the degradation of renewable lignocelluloses to provide carbohydrates for fungal growth, development, and reproduction (Xie et al., 2018). We determined CAZymes in the SE1 genome using the dbCAN 2 meta server. A total of 313 CAZyme-encoding gene models were assigned, including 93 superfamilies, *viz*., six carbohydrate esterases, 41 glycoside hydrolases, 23 glycosyltransferases, 11 carbohydrate-binding modules, eight auxiliary activities, and four polysaccharide lyases (**Table 3**). There were 63 AA (auxiliary activities) genes in the SE1 genome, including 13 AA1 (multicopper oxidase), 10 AA2 (lignin-modifying peroxidase),

TABLE 1 | General features of the *Sarcomyxa edulis* genome.

Characteristics	
Scaffold	
Total number	41
Total length (bp)	35,651,721
N50 (bp)	1,772,559
N90 (bp)	554,178
Max length (bp)	4,140,795
Genome coverage	150
GC content (%)	48.31
Genome	
Gene total length (bp)	15,135,900
Gene number	9,364
Gene length/genome (%)	42.45
Average gene length (bp)	1,616

TABLE 2 | Summary of *Sarcomyxa edulis* gene annotations.

Database used for gene/protein annotation	Number of genes
NR	7,183
GO	5,884
KEGG	2,954
KOG	1,760
Secretory protein	502
TCDB	290
CAZy	283
Annotated gene	
P450	162

CAZy, Carbohydrate-active Enzymes database; GO, Gene Ontology; KEGG, Kyoto Encyclopedia of Genes and Genomes; KOG, Eukaryotic Orthologous Groups; P450, cytochrome P450 monooxygenase; nr, National Center for Biotechnology Information non-redundant protein database; and TCDB, Transporter Classification Database.

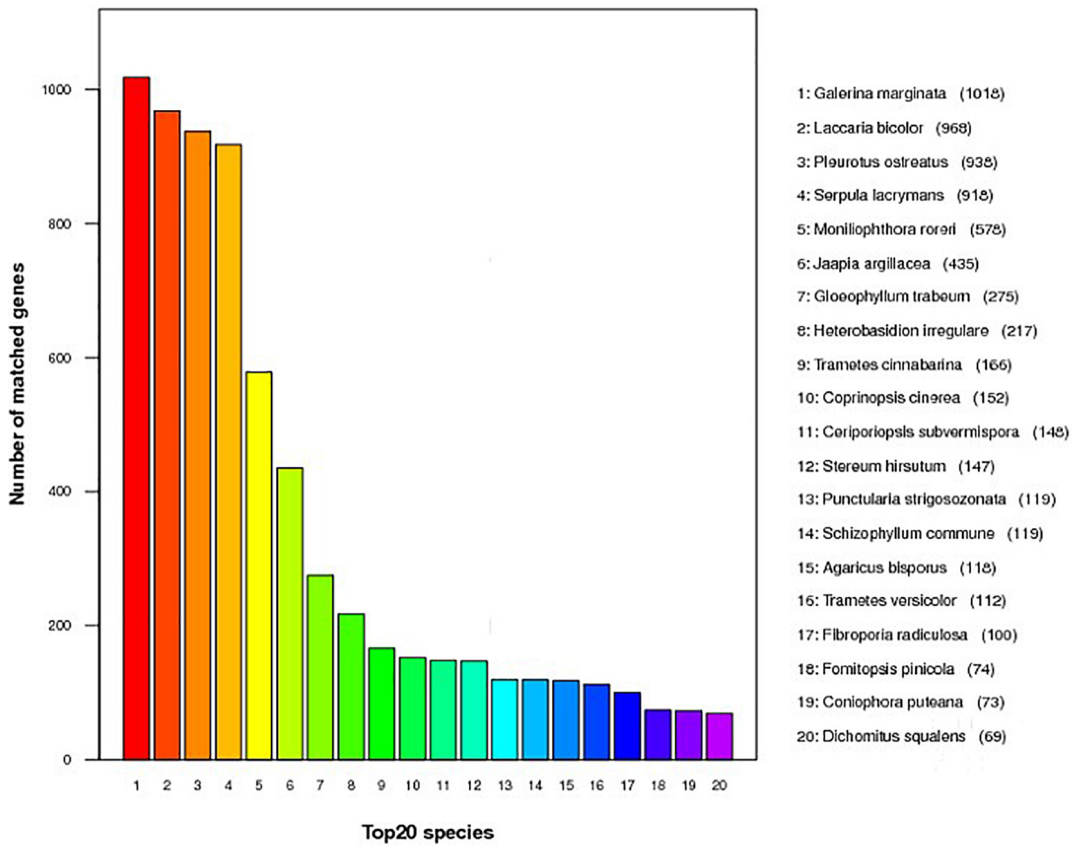


FIGURE 2 | Predicted proteins from *Sarcomyxa edulis* genome to the National Center for Biotechnology Information non-redundant protein database among different fungal species.

20 AA3 (glucose-methanol-choline oxidoreductase including cellobiose dehydrogenase, arylalcohol oxidase/glucose oxidase, alcohol oxidase, and pyranose oxidase), five AA5 (copper radical oxidase), two AA6 (1,4-benzoquinone reductase), one AA8 (cellobiose dehydrogenase), and 11 AA9 (lytic polysaccharide monooxygenase) genes.

We further investigated genes involved in the biosynthesis of secondary metabolites in *S. edulis* based on those identified in previous studies and found genes encoding fatty acid synthetases, NRPS, PKS, siderophore synthetases, and terpene synthases (Schwarzer et al., 2003; Finking and Marahiel, 2004; Sims and Schmidt, 2008; Chen et al., 2012; Lackner et al., 2012; Quin et al., 2014) that were often in contiguous gene clusters (Keller et al., 2006). Using the fungiSMASH database, we identified 39 secondary metabolite gene clusters in the SE1 genome, including four terpenes, one NRPS, one T1PKS, one siderophore, and one fatty acid gene cluster (**Supplementary Table 5**). Unlike primary metabolism, secondary metabolism does not participate in the growth and development of an organism but instead promotes its survival in a given environment, for example, by enhancing the defense response to pathogens. A Natural Product Domain Seeker analysis identified two C domains (C2 bacitracin_DCL and C1 cyclosporin_dual) and four KS domains (naphthopyrone_iterative, avermectin_modular, myxothiazol_modular, and epothilone_modular) in the SE1 genome.

Phylogenetic Analysis of *S. edulis*

A phylogenetic tree was constructed based on single-copy orthologous protein genes from 32 species of fungus, including 30 from the phylum Basidiomycota and two from the phylum Ascomycota serving as outgroups (**Figure 7**). The result showed that the *Sarcomyxa* genus formed a distinct clade to *Panellus* and *Mycena* in the *Mycenaceae* family. The topology suggested that *Sarcomyxa* was also independent of Pleurotaceae. Fungi in the Basidiomycota and Polyporales clades were clearly separated from those in the Agaricales clade, with Polyporales diverging before Agaricales. Notably, the Agaricales order followed a certain evolutionary pattern from "on log" to "on ground" growth.

DISCUSSION

CAZyme Analysis

GHs, GTs, PLs, CEs, and AAs—which catalyze the modification, biosynthesis, or degradation of glycoconjugates and carbohydrates—were the main CAZymes in the SE1 genome.

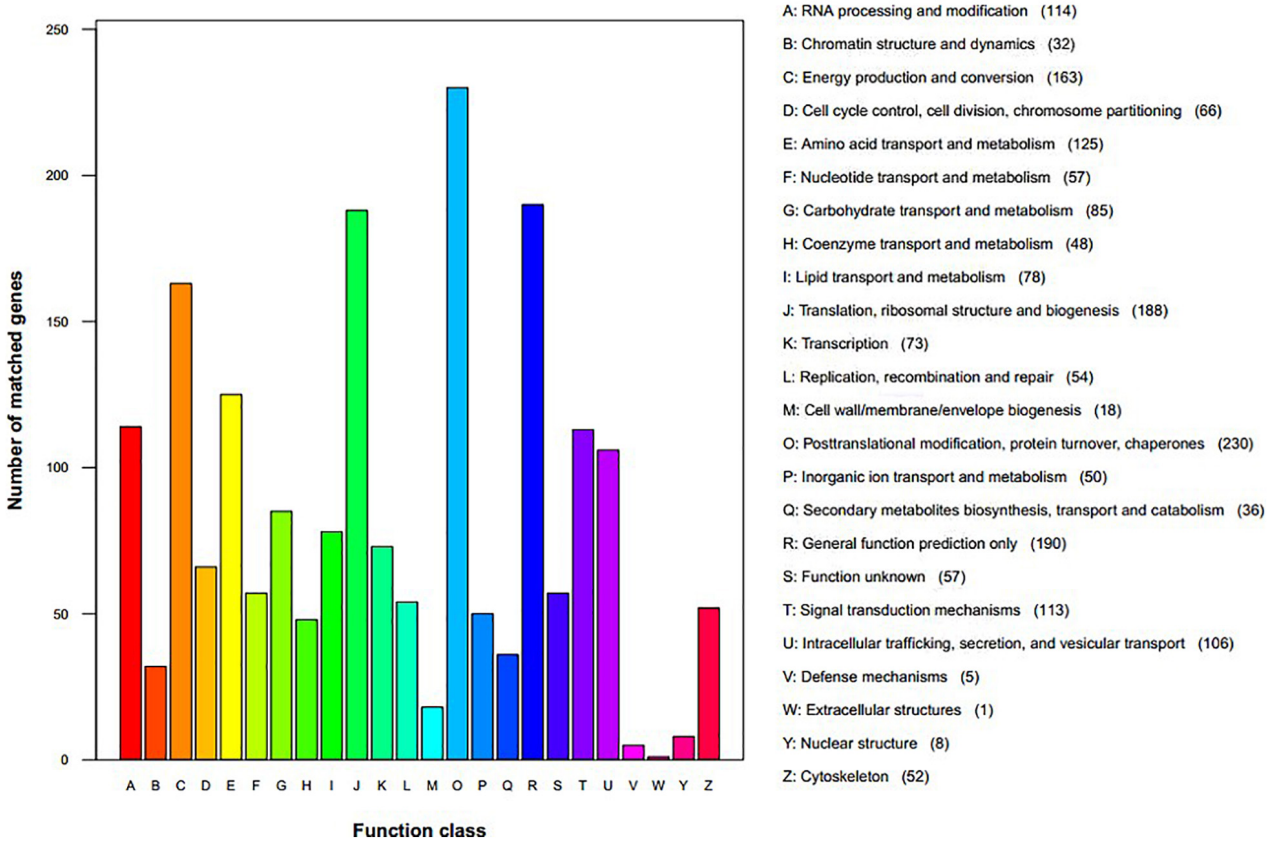


FIGURE 3 | Eukaryotic Orthologous Groups functional classification of *Sarcomyxa edulis* proteins.

CMBs were non-catalytic modules that appended to the enzymes stated above. There were twice as many GH genes as there were GT genes; this may be related to the lignocellulose degradation capacity of *S. edulis* that is necessary for its survival. Polysaccharide decomposition is more important for *S. edulis* than anabolism. *S. edulis* had fewer genes related to initial lignin degradation than the average number present in Basidiomycota fungi (**Supplementary Table 6**; Yuan et al., 2019). The protein products of CE, GH, and PL superfamilies are involved in the breakdown of the polysaccharide portion of plant cell walls, which mainly consists of pectin, cellulose, and hemicellulose and are known as cell wall-degrading enzymes (Ospina-Giraldo et al., 2010; Yap et al., 2014). *S. edulis* had fewer candidate CAZymes than other edible fungi, but it could make better use of hardwood. Therefore, the mechanism of substance degradation of *S. edulis* needs to be further explored.

Secondary Metabolite Analysis

Medicinal fungi have been the focus of many pharmacologic studies because of their secondary metabolites, which have antioxidant, antitumor, and antimicrobial properties. *S. edulis* has shown promising pharmacodynamic activities (Li, 1991; Inafuku et al., 2012; Kim et al., 2012; Inoue et al., 2013; Li et al., 2013, 2016; Zhang et al., 2014). Type I PKSs constitute a family of multifunctional proteins with high molecular weight and multiple catalytic domains that play an important role in the biosynthesis of reducing macrolide polyketides (Fujii et al., 2001). The chemical properties of predicted type I PKS genes in the SE1 genome have been characterized. Two C domains on contig 7—bacitracin and cyclosporine—were identified. Bacitracin is a branched cyclic peptide antibiotic active against Gram-positive bacteria and acts by binding to undecaprenyl pyrophosphate—a lipid carrier of cell wall precursors—and interfering with cell wall and peptidoglycan biosynthesis. Furthermore, bacitracin has been used for the prevention and treatment of skin and ophthalmic diseases (Ishihara et al., 2002; Hiron et al., 2011). As an immunosuppressant that is administered orally or *via* injection, cyclosporine is used to treat nephrotic syndrome (Cattran et al., 2007), psoriasis (Kumar et al., 2016), and keratoconjunctivitis sicca (dry eyes; Kasper et al., 2017). Four KS domains were also identified: naphthopyrone (KS4 on contig 12), avermectin (KS1 on contig 17), myxothiazol (KS2 on contig 17), and epothilone (KS3 on contig 17). Naphthopyrone prevents advanced glycation end product formation (Lee et al., 2006), while avermectin belongs to a family of macrocyclic lactones and functions as a biological pesticide that is highly active against a variety of nematodes. Avermectin has been widely used as an antiparasitic agent in aquaculture (Sheng et al., 2015). Myxothiazol is an antibiotic that inhibits ubiquinol. Epothilones are a class of water-soluble compounds similar to taxanes and

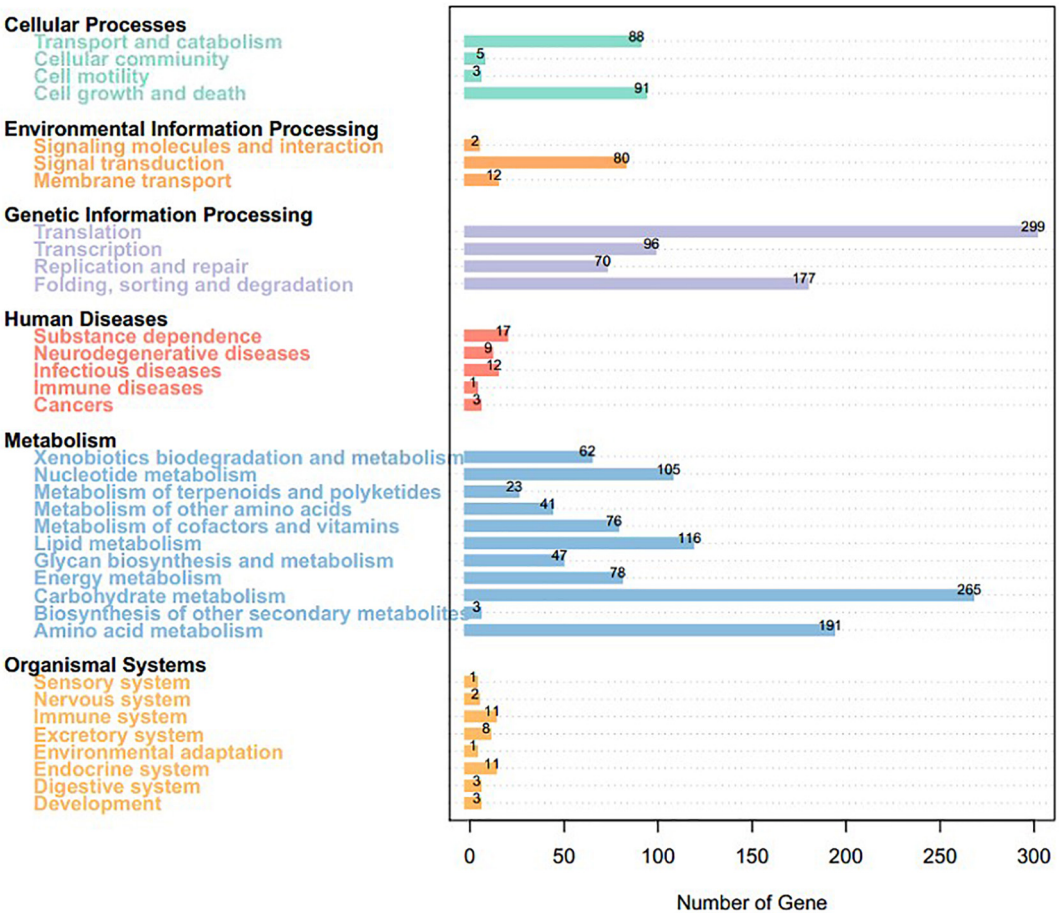


FIGURE 4 | Kyoto Encyclopedia of Genes and Genomes pathway annotation of *Sarcomyxa edulis* genes.

with anticancer potential that has shown greater efficacy than paclitaxel in P-glycoprotein-expressing multidrug-resistant cell lines (Kowalski et al., 1997). At present, research on the active components of *S. edulis* are mainly focused on polysaccharides and lipids. However, study on PKS has not been reported. Therefore, the active constituents of the mushroom are still waiting to be tapped.

Biosynthesis of Polysaccharides in *S. edulis*

The major types of bioactive compound with medicinal properties in *S. edulis* are polysaccharides such as β-D-glucan, (1→6)-β-D-glucose, and (1→3)-β-D-glucan, which have relatively high bioactivity (Ma et al., 1991). The biosynthesis of uridine diphosphate glucose—the precursor of these polysaccharides—is mediated by 1,3beta-glucan synthase and endo-1,3(4)-beta-glucanase. Two GT_{48} and 20 GH_{16} were annotated, which were present in *S. edulis* (**Supplementary Table 7**). The 20 GH_{16} genes were mainly predicted to be endo-1,3beta-glucanase (EC 3.2.1.39), endo-1,3(4)-beta-glucanase (EC 3.2.1.6), and endo-beta-1,3-galactanase (EC 3.2.1.181). Compared with edible and medicinal fungi, the number of GH_{16} in *S. edulis* is more than that in *Auricularia heimuer* and *W. cocos* but less than that in *Ganoderma lingzhi*. The two GT_{48} genes were predicted to be 1,3-beta-glucan synthase (EC 2.4.1.34). The same number of genes in GT_{48} was also reported in those mushrooms that contain high polysaccharide active components and have good medicinal value such as *A. heimuer*, *A. bisporus*, *G. lingzhi*, *P. ostreatus*, *V. volvacea*, and *W. cocos*.

Phylogenetic Analysis of *S. edulis*

Sarcomyxa edulis is an important edible and medicinal fungus that belongs to the order Agaricus, but the taxonomy of this genus is still controversial. In order to comprehensively analyze the relationship between *S. edulis* and related species and genera, 32 fungal species from Basidiomycota and Ascomycota were used in the phylogenetic analysis. The whole genome sequences of one to two representative species from different groups of edible and medicinal fungi and several adjacent genera of *Sarcomyxa* were analyzed to show the correctness of the analysis results.

Phylogenetic analyses of the concatenated dataset using ML methods resulted in an identical and well-supported topology in all alignment strategies compared to the study of Lin et al. (2013).

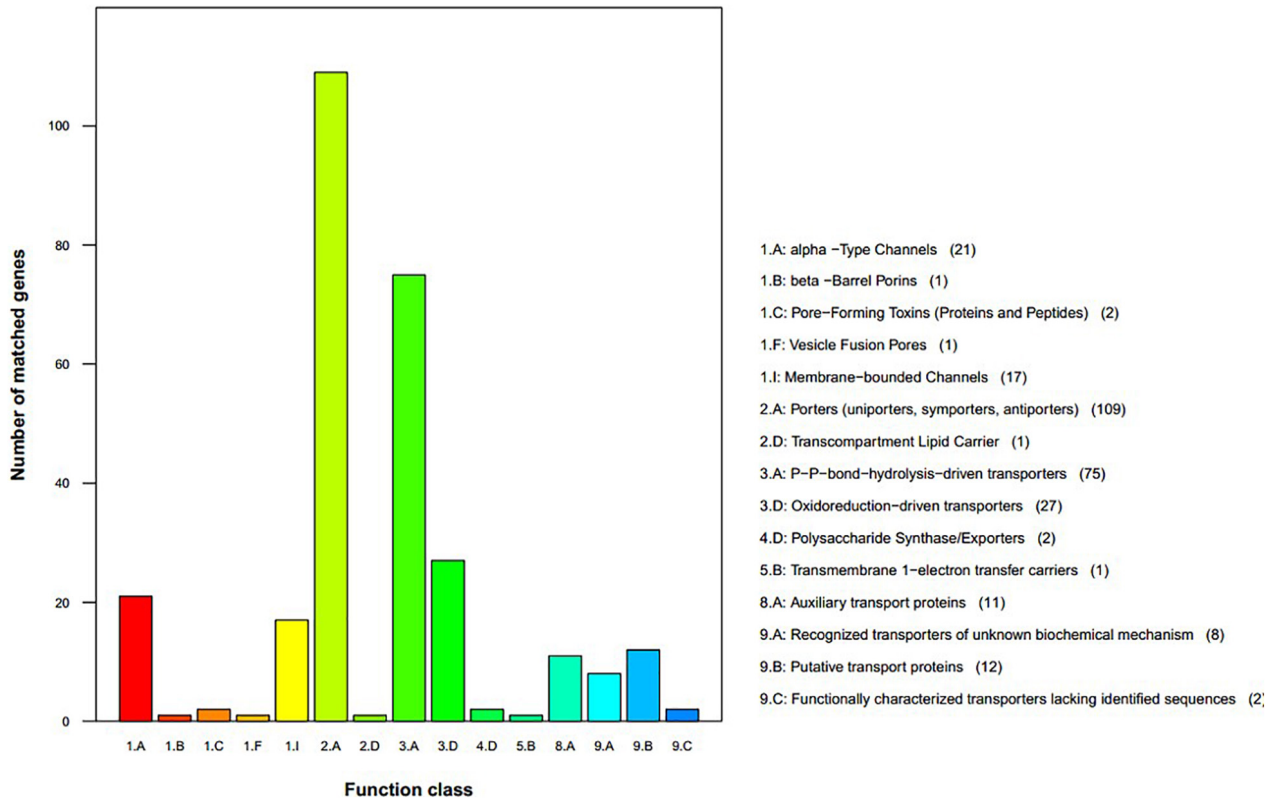


FIGURE 5 | Transporter Classification Database functional annotation of *Sarcomyxa edulis* genes.

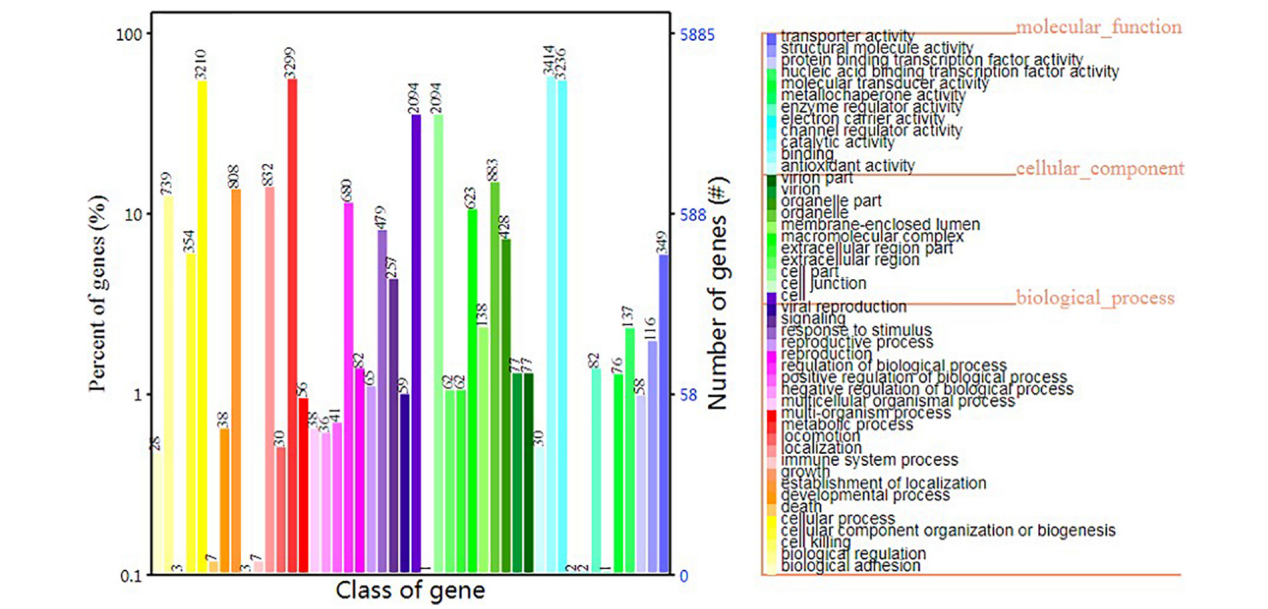


FIGURE 6 | Gene Ontology functional annotation of *Sarcomyxa edulis* genes.

It can reasonably model the large stochastic processes with lower variance. Even with very short sequences, it may outperform alternative methods such as parsimony or distance methods. It also has an explicit evolutionary model for data and better accounting for branch length (Mishler, 2006). For example, Li et al. (2021) and Xu et al. (2020) used the ML algorithm in

TABLE 3 | Carbohydrate-active enzyme annotation results.

Classification	Number	Number of superfamilies
Carbohydrate-binding module	55	11
Carbohydrate esterase	11	6
Glycoside hydrolase	140	41
Glycosyl transferase	37	23
Polysaccharide lyase	7	4
Auxiliary activities	63	8

RAxML to construct a genome-based phylogenetic tree. In this study, based on the ML/NJ phylogenetic analysis of *S. edulis* and 31 other species of fungus, it was shown that the *Sarcomyxa* genus is a distinct group. This is consistent with the previous classification of *Sarcomyxa* as a clade that is independent of and emerged before the *Mycena* and *Panellus* genera based on a ML tree constructed using the D1/D2 region of *S. edulis* comb. nov. and other species (Saito et al., 2014). A study of the major clades of the Agaricales order arrived at a similar conclusion based on a maximum probability tree that combined *rpb1*, *rpb1-intron2*, *rpb2*, 18S, 25S, and 5.8S nucleotide sequences (Matheny et al., 2006). Additionally, we found that Basidiomycota, Polyporales, and Agaricales constituted distinct clades. The evolution of the Agaricales order followed a trend from "on log" to "on ground" growth.

We also observed a transition from white rot to brown rot in the Polyporales clade over the course of evolution. This is in accordance with a previous analysis of lignin-degrading peroxidases in 31 fungal genomes, which showed that the lignin degradation mechanism of white rot fungi was retained in the early evolution of Agaricomycetes, while the loss of lignin peroxidases led to the emergence of brown rot fungi exhibiting a non-ligninolytic mode of wood decay (Floudas et al., 2012; **Supplementary Table 1**).

The comparative analyses of secondary metabolites revealed that *S. edulis* harbors terpene and PKS biosynthesis-associated genes. The annotated whole-genome sequence of *S. edulis* can serve as a reference for identifying genes related to the synthesis of bioactive compounds with medicinal or nutritional value

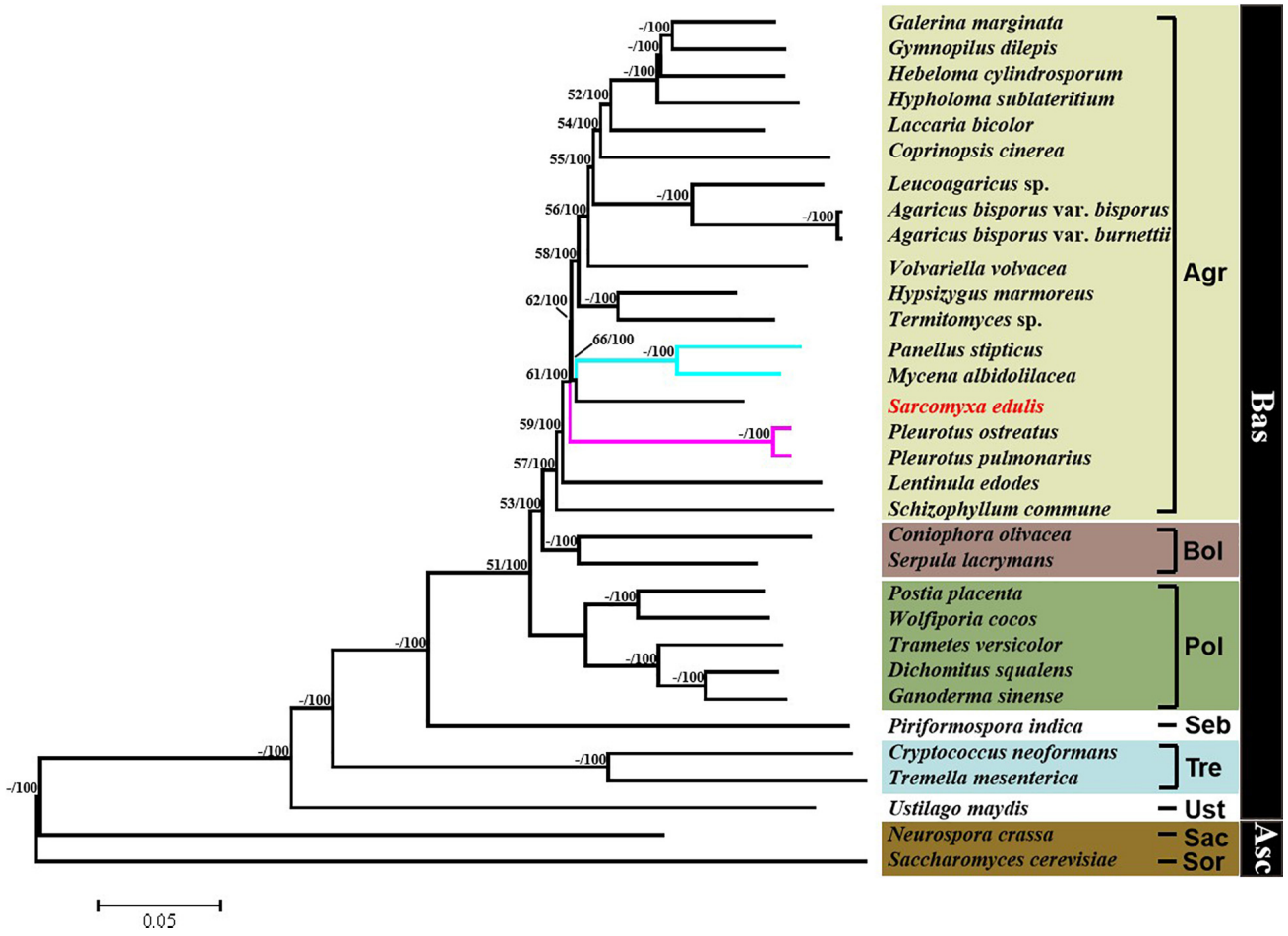


FIGURE 7 | Phylogenetic tree of *Sarcomyxa edulis* and 31 other fungal species. Maximum likelihood and neighbor-joining above 50% were placed close to topological nodes and separated by "/". The bootstrap values below 50% were labeled with "-". Asc, Ascomycota; Bas, Basidiomycota; Sor, Sordariales; Sac, Saccharomycetales; Ust, Ustilaginales; Tre, Tremellales; Seb, Sebacinales; Pol, Polyporales; Bol, Boletales; and Aga, Agaricales.

and the development and commercial production of superior *S. edulis* varieties.

DATA AVAILABILITY STATEMENT

The original contributions presented in the study are publicly available. This data can be found here: The genome sequence data and assembly reported in this paper are associated with NCBI BioProject: PRJNA483858 and BioSample: SAMN09748201 in GenBank. The Whole Genome Shotgun (WGS) number is INSDC: QUOL00000000.1).

AUTHOR CONTRIBUTIONS

FT contributed to conceptualization, methodology, software, data analysis, investigation, resources, data curation, and manuscript writing—original draft preparation. CL contributed to data validation, supervision, and project administration. CL and YL contributed to writing—review and editing. YL contributed to visualization and funding acquisition. All authors contributed to the article and approved the submitted version.

FUNDING

This research was funded by the National Natural Science Foundation of China (NSFC: 32000013), National Key Research and Development Program of China (2020YFD1000304), Program of Introducing Talents of Discipline to Universities (D17014), and National Key Research and Development Program of China Grant (2017YFD0601002).

ACKNOWLEDGMENTS

We are grateful to Francis Martin and Christoffer Bugge Harder and the 1000 Fungal Genome consortium for access to unpublished genome data. The genome sequence data were produced by the United States Department of Energy Joint Genome Institute in collaboration with the user community, and we would like to thank the National Center for Biotechnology Information for the genomic data provided. We thank the Mushroom Base of Jilin Agricultural University for assistance with cultivation.

SUPPLEMENTARY MATERIAL

The Supplementary Material for this article can be found online at: https://www.frontiersin.org/articles/10.3389/fmicb.2021.652324/full#supplementary-material

Supplementary Table 1 | Summary of fungi analyzed in this study and origin of their genomes.

Supplementary Table 2 | Genes predicted to be involved in non-coding RNA in *Sarcomyxa edulis*.

Supplementary Table 3 | *Sarcomyxa edulis* gene annotations.

Supplementary Table 4 | Putative CYP gene families of *Sarcomyxa edulis*.

Supplementary Table 5 | Genes predicted to be involved in the secondary metabolism of *Sarcomyxa edulis*.

Supplementary Table 6 | Distribution of the CAZyme family genes in different fungi.

Supplementary Table 7 | Genes predicted to be involved in polysaccharide biosynthesis in *Sarcomyxa edulis*.

REFERENCES

Altschul, S. F., Gish, W., Miller, W., Myers, E. W., and Lipman, D. J. (1990). Basic local alignment search tool. *J. Mol. Biol.* 215, 403–410. doi: 10.1016/S0022-2836(05)80360-2

Aronsen, A., and Læssøe, T. (2016). "The genus *Mycena* s.l," in *The Fungi of Northern Europe*, eds T. G. Frøslev, T. Læssøe, J. H. Petersen, and S. A. Elborne (Copenhagen, DK: Danish Mycological Society), 373.

Ashburner, M., Ball, C. A., Blake, J. A., Botstein, D., Butler, H., Cherry, J. M., et al. (2000). Gene ontology: tool for the unification of biology. *Nat. Genet.* 25, 25–29. doi: 10.1038/75556

Bao, D. P., Gong, M., Zheng, H. J., Chen, M. J., Zhang, L., Wang, H., et al. (2013). Sequencing and comparative analysis of the straw mushroom (*Volvariella volvacea*) genome. *PLoS One* 8:e58294. doi: 10.1371/journal.pone.0058294

Benson, G. (1999). Tandem repeats finder: a program to analyze DNA sequences. *Nucleic Acids Res.* 27, 573–580. doi: 10.1093/nar/27.2.573

Berlin, K., Koren, S., Chin, C. S., Drake, J., Landolin, J. M., and Phillippy, A. M. (2015). Assembling large genomes with single-molecule sequencing and locality sensitive hashing. *Nat. Biotechnol.* 33, 623–630. doi: 10.1038/nbt.3238

Birney, E., Clamp, M., and Durbin, R. (2004). Genewise and genomewise. *Genome Res.* 14, 988–995. doi: 10.1101/gr.1865504

Blin, K., Wolf, T., Chevrette, M. G., Lu, X., Schwalen, C. J., Kautsar, S. A., et al. (2017). AntiSMASH 4.0-improvements in chemistry prediction and gene cluster boundary identification. *Nucleic Acids Res.* 45, W36–W41. doi: 10.1093/nar/gkx319

Buchfink, B., Xie, C., and Huson, D. H. (2014). Fast and sensitive protein alignment using DIAMOND. *Nat. Methods* 12, 59–60. doi: 10.1038/nmeth.3176

Burge, C., and Karlin, S. (1997). Prediction of complete gene structures in human genomic DNA. *J. Mol. Biol.* 268, 78–94. doi: 10.1006/jmbi.1997.0951

Castanera, R., Pérez, G., López-Varas, L., Amselem, J., LaButti, K., Singan, V., et al. (2017). Comparative genomics of *Coniophora olivacea* reveals different patterns of genome expansion in Boletales. *BMC Genomics* 18:883. doi: 10.1186/s12864-017-4243-z

Castresana, J. (2000). Selection of conserved blocks from multiple alignments for their use in phylogenetic analysis. *Mol. Biol. Evol.* 17, 540–552. doi: 10.1093/oxfordjournals.molbev.a026334

Cattran, D. C., Alexopoulos, E., Heering, P., Hoyer, P. F., Johnston, A., Meyrier, A., et al. (2007). Cyclosporin in idiopathic glomerular disease associated with the nephrotic syndrome: workshop recommendations. *Kidney Int.* 72, 1429–1447. doi: 10.1038/sj.ki.5002553

Chen, L. F., Gong, Y. H., Cai, Y. L., Liu, W., Zhou, Y., Xiao, Y., et al. (2016). Genome sequence of the edible cultivated mushroom *Lentinula edodes* (Shiitake) reveals insights into lignocellulose degradation. *PLoS One* 11:e0160336. doi: 10.1371/journal.pone.0160336

Chen, W., Zhu, P., He, S., Jin, H., and Yan, X. (2012). Nonribosomal peptides synthetases gene clusters and core domain in *Pseudoalteromonas* sp. NJ631. *Acta Microbiol. Sin.* 52, 1531–1539.

Choi, Y. W., Hyde, K. D., and Ho, W. H. (1999). Single spore isolation of fungi. *Fungal Divers.* 3, 29–38.

Cui, X. F., Lu, Z. W., Wang, S., Wang, J. J. Y., and Gao, X. (2016). CMsearch: simultaneous exploration of protein sequence space and structure space improves not only protein homology detection but also protein structure prediction. *Bioinformatics* 32, 332–340. doi: 10.1093/bioinformatics/btw271

Dai, Y. C., Niemela, T., and Qin, G. F. (2003). Changbai wood-rotting fungi. a new pleurotoid species *Panellus edulis*. *Ann. Bot. Fenn.* 40, 107–112.

Elsik, C. G., Mackey, A. J., Reese, J. T., Milshina, N. V., Roos, D. S., and Weinstock, G. M. (2007). Creating a honey bee consensus gene set. *Genome Biol.* 8:R13. doi: 10.1186/gb-2007-8-1-r13

Finking, R., and Marahiel, M. A. (2004). Biosynthesis of nonribosomal peptides. *Annu. Rev. Microbiol.* 58, 453–488. doi: 10.1146/annurev.micro.58.030603.123615

Floudas, D., Binder, M., Riley, R., Barry, K., Blanchette, R. A., Henrissat, B., et al. (2012). The paleozoic origin of enzymatic lignin decomposition reconstructed from 31 fungal genomes. *Science* 336, 1715–1719. doi: 10.1126/science.1221748

Fujii, I., Watanabe, A., Sankawa, U., and Ebizuka, Y. (2001). Identification of claisen cyclase domain in fungal polyketide synthase WA, a naphthopyrone synthase of *Aspergillus nidulans*. *Chem. Biol.* 8, 189–197. doi: 10.1016/S1074-5521(00)90068-1

Gardner, P. P., Daub, J., Tate, J. G., Nawrocki, E. P., Kolbe, D. L., Lindgreen, S., et al. (2009). Rfam: updates to the RNA families database. *Nucleic Acids Res.* 37(suppl. 1), D136–D140. doi: 10.1093/nar/gkn766

Grigoriev, I. V., Nordberg, H. P., Shabalov, I., Aerts, A., Cantor, M., Goodstein, D., et al. (2012). The genome portal of the department of energy joint genome institute. *Nucleic Acids Res.* 40, D26–D32. doi: 10.1093/nar/gkr947

Hiron, A., Falord, M., Valle, J., Débarbouillé, M., and Msadek, T. (2011). Bacitracin and nisin resistance in *Staphylococcus* aureus: a novel pathway involving the BraS/BraR two-component system (SA2417/SA2418) and both the BraD/BraE and VraD/VraE ABC transporters. *Mol. Microbiol.* 81, 602–622. doi: 10.1111/j.1365-2958.2011.07735.x

Imazeki, R., Otani, Y., and Hongo, T. (1988). *Fungi of Japan*. Tokyo: Yama-Kei Publishers.

Inafuku, M., Nagao, K., Nomura, S., Shirouchi, B., Inoue, N., Nagamori, N., et al. (2012). Protective effects of fractional extracts from *Panellus serotinus* on non-alcoholic fatty liver disease in obese, diabetic db/db mice. *Br. J. Nutr.* 107, 639–646. doi: 10.1017/S0007114511003485

Inoue, N., Inafuku, M., Shirouchi, B., Nagao, K., and Yanagita, T. (2013). Effect of mukitake mushroom (*Panellus serotinus*) on the pathogenesis of lipid abnormalities in obese, diabetic ob/ob mice. *Lipids Health Dis.* 12:18. doi: 10.1186/1476-511X-12-18

Ishihara, H., Takoh, M., Nishibayashi, R., and Sato, A. (2002). Distribution and variation of bacitracin synthetase gene sequences in laboratory stock strains of *Bacillus licheniformis*. *Curr. Microbiol.* 45, 18–23. doi: 10.1007/s00284-001-0041-5

Jin, J., Hughes, K. W., and Petersen, R. H. (2001). Phylogenetic relationships of *Panellus* (Agaricales) and related species based on morphology and ribosomal large subunit DNA sequences. *Mycotaxon* 79, 7–21.

Kanehisa, M., Goto, S., Hattori, M., Aoki-Kinoshita, K. F., Itoh, M., Kawashima, S., et al. (2006). From genomics to chemical genomics: new developments in KEGG. *Nucleic Acids Res.* 34(suppl. 1), D354–D357. doi: 10.1093/nar/gkj102

Kanehisa, M., Goto, S., Kawashima, S., Okuno, Y., and Hattori, M. (2004). The KEGG resource for deciphering the genome. *Nucleic Acids Res.* 32(suppl .1), D277–D280. doi: 10.1093/nar/gkh063

Kasper, M. A. A. S. A., Farahat, H. G., Al-Morsy, O. A., and Alhagaa, A. A. (2017). Comparative study using cyclosporine a 0.05% eye drops, autologous serum 20% eye drops, and combined use of cyclosporine A 0.05% eye drops and autologous serum 20% eye drops in the treatment of moderate to severe dry eye. *Menoufia Med. J.* 2, 525–531. doi: 10.4103/1110-2098.215461

Katoh, K., and Standley, D. M. (2013). MAFFT multiple sequence alignment software version 7: improvements in performance and usability. *Mol. Biol. Evol.* 30, 772–780. doi: 10.1093/molbev/mst010

Keller, N. P., Turner, G., and Bennett, J. W. (2006). Fungal secondary metabolism-from biochemistry to genomics. *Nat. Rev. Microbiol.* 3, 937–947. doi: 10.1038/nrmicro1286

Kim, J. H., Lee, J. S., Lee, K. R., Shim, M. J., Lee, M. W., Shin, P. G., et al. (2012). Immunomodulating and antitumor activities of *Panellus serotinus* polysaccharides. *Mycobiology* 40, 181–188. doi: 10.5941/MYCO.2012.40.3.181

Koren, S., and Phillippy, A. M. (2015). One chromosome, one contig: complete microbial genomes from long-read sequencing and assembly. *Curr. Opin. Microbiol.* 23, 110–120. doi: 10.1016/j.mib.2014.11.014

Korf, I. (2004). Gene finding in novel genomes. *BMC Bioinformatics* 5:59. doi: 10.1186/1471-2105-5-59

Kowalski, R. J., Giannakakou, P., and Hamel, E. (1997). Activities of the microtubule-stabilizing agents epothilones A and B with purified tubulin and in cells resistant to paclitaxel (Taxol®). *J. Biol .Chem.* 272, 2534–2541. doi: 10.1074/jbc.272.4.2534

Kumar, R., Dogra, S., Amarji, B., Singh, B., Kumar, S., Vinay, K., et al. (2016). Efficacy of novel topical liposomal formulation of cyclosporine in mild to moderate stable plaque psoriasis: a randomized clinical trial. *JAMA Dermatol.* 152, 807–815. doi: 10.1001/jamadermatol.2016.0859

Lackner, G., Misiek, M., Braesel, J., and Hoffmeister, D. (2012). Genome mining reveals the evolutionary origin and biosynthetic potential of basidiomycete polyketide synthases. *Fungal Genet. Biol.* 49, 996–1003. doi: 10.1016/j.fgb.2012.09.009

Lagesen, K., Hallin, P. F., Rodland, E. A., Staerfeldt, H., Rognes, T., and Ussery, D. W. (2007). RNAmmer: consistent and rapid annotation of ribosomal RNA genes. *Nucleic Acids Res.* 35, 3100–3108. doi: 10.1093/nar/gkm160

Lee, G. Y., Jang, D. S., Lee, Y. M., Kim, J. M., and Kim, J. S. (2006). Naphthopyrone glucosides from the seeds of *Cassia tora* with inhibitory activity on advanced glycation end products (AGEs) formation. *Arch. Pharm. Res.* 29, 587–590. doi: 10.1007/BF02969270

Li, C., Guo, Z. J., Zhou, S. Y., Han, Y. Q., Zhang, M. M., Peng, Y., et al. (2021). Evolutionary and genomic comparisons of hybrid uninucleate and nonhybrid *Rhizoctonia* fungi. *Commun. Biol.* 4:201. doi: 10.1038/s42003-021-01724-y

Li, L., Stoeckert, C. J. Jr., and Roos, D. S. (2003). OrthoMCL: identification of ortholog groups for eukaryotic genomes. *Genome Res.* 13, 2178–2189. doi: 10.1101/gr.1224503

Li, R. G. (1991). *The Fungal Flora of Jilin Province*. Changchun: Northeastern Normal University Press.

Li, W. Z., Jaroszewski, L., and Godzik, A. (2002). Tolerating some redundancy significantly speeds up clustering of large protein databases. *Bioinformatics* 18, 77–82. doi: 10.1093/bioinformatics/18.1.77

Li, X. Y., Wang, L., Wang, Y., and Xiong, Z. H. (2016). Effect of drying method on physicochemical properties and antioxidant activities of *Hohenbuehelia serotina* polysaccharides. *Process Biochem.* 51, 1100–1108. doi: 10.1016/j.procbio.2016.05.006

Li, X. Y., Wang, Z. Y., and Wang, L. (2013). Polysaccharide of *Hohenbuehelia serotina* as a defense against damage by whole-body gamma irradiation of mice. *Carbohyd. Polym.* 94, 829–835. doi: 10.1016/j.carbpol.2013.02.015

Lin, Y., Hu, F., Tang, J. J., and Moret, B. M. E. (2013). Maximum likelihood phylogenetic reconstruction from high-resolution whole-genome data and a tree of 68 eukaryotes. *Pacific Symposium on Biocomputing*, Switzerland, 285–296. doi: 10.1142/97898144479730028

Lowe, T. M., and Eddy, S. R. (1997). tRNAscan-SE: a program for improved detection of transfer RNA genes in genomic sequence. *Nucleic Acids Res.* 25, 955–964. doi: 10.1093/nar/25.5.955

Ma, Y., Mizino, T., and Ito, H. (1991). Antitumor activity of some polysaccharides isolated from a Chinese mushroom, "Huangmo" the fruiting body of *Hohenbuehelia serotina*. *Agric. Biol. Chem.* 55, 2701–2710. doi: 10.1080/00021369.1991.10871044

Majoros, W. H., Pertea, M., and Salzberg, S. L. (2004). TigrScan and glimmerhmm: two open source ab initio eukaryotic gene-fifinders. *Bioinformatics* 20, 2878–2879. doi: 10.1093/bioinformatics/bth315

Matheny, P. B., Curtis, J. M., Hofstetter, V., Aime, M. C., Moncalvo, J. M., Ge, Z. W., et al. (2006). Major clades of Agaricales: a multilocus phylogenetic overview. *Mycologia* 98, 982–995. doi: 10.1080/15572536.2006.11832627

Miller, M. A., Pfeiffer, W., and Schwartz, T. (2010). "Creating the CIPRES science gateway for inference of large phylogenetic trees," in *Proceedings of the Gateway Computing Environments Workshop (GCE)*, (New Orleans, LA: IEEE Computer Society).

Mishler, B. D. (2006). *Integrative Biology 200A "Principles of Phylogenetics"*. Berkeley, CA: University of California.

Morin, E., Kohler, A., Baker, A. R., Foulongne-Oriol, M., Lombard, V., Nagy, L. G., et al. (2012). Genome sequence of the button mushroom *Agaricus bisporus* reveals mechanisms governing adaptation to a humic-rich ecological niche. *Proc. Natl. Acad. Sci. U.S.A.* 110, 4146–4148. doi: 10.1073/pnas.1206847109

Nawrocki, E. P., Kolbe, D. L., and Eddy, S. R. (2009). Infernal 1.0: inference of RNA alignments. *Bioinformatics* 25, 1335–1337. doi: 10.1093/bioinformatics/btp157

Nelson, D. R. (2009). The cytochrome P450 homepage. *Hum. Genomics* 4, 59–65. doi: 10.1186/1479-7364-4-1-59

Ohm, R. A., de Jong, J. F., Lugones, L. G., Aerts, A., Kothe, E., Stajich, J. E., et al. (2010). Genome sequence of the model mushroom *Schizophyllum commune*. *Nat. Biotechnol.* 28, 957–963. doi: 10.1038/nbt.1643

Ospina-Giraldo, M. D., Griffith, J. G., Laird, E. W., and Mingora, C. (2010). The CAZyome of *Phytophthora* spp.: a comprehensive analysis of the gene complement coding for carbohydrate-active enzymes in species of the genus *Phytophthora*. *BMC Genomics* 11:525. doi: 10.1186/1471-2164-11-525

Pan, X. R. (1995). *Macrofungi of the Xiaoxingan Mts*. Harbin: Northeastern Forestry University. Press.

Qu, J., Zhao, M., Hsiang, T., Feng, X., Zhang, J., and Huang, C. (2016). Identification and characterization of small noncoding RNAs in genome sequences of the edible fungus *Pleurotus ostreatus*. *BioMed. Res. Int.* 2016:2503023. doi: 10.1155/2016/2503023

Quin, M. B., Flynn, C. M., and Schmidt-Dannert, C. (2014). Traversing the fungal terpenome. *Nat. Prod. Rep.* 31, 1449–1473. doi: 10.1039/C4NP00075G

Saha, S., Bridges, S., Magbanua, Z. V., and Peterson, D. G. (2008). Empirical comparison of *ab initio* repeat finding programs. *Nucleic Acids Res.* 36, 2284–2294. doi: 10.1093/nar/gkn064

Saier, M. H. Jr., Reddy, V. S., Tamang, D. G., and Västermark, Å (2014). The transporter classification database. *Nucleic Acids Res.* 42, D251–D258. doi: 10.1093/nar/gkt1097

Saito, T., Tonouchi, A., and Harada, Y. (2014). Biological characteristics and molecular phylogeny of *Sarcomyxa edulis* comb. nov. and *S. serotina*. *Jap. J. Mycol.* 55, 19–28.

Schwarzer, D., Finking, R., and Marahiel, M. A. (2003). Nonribosomal peptides: from genes to products. *Nat. Prod. Rep.* 20, 275–287. doi: 10.1039/B111145K

Senanayake, I. C., Rathnayaka, A. R., Marasinghe, D. S., Calabon, M. S., Gentekaki, E., Lee, H. B., et al. (2020). Morphological approaches in studying fungi: collection, examination, isolation, sporulation and preservation. *Mycosphere* 11, 2678–2754. doi: 10.5943/mycosphere/11/1/20

Sheng, W. B., Li, W., Zhang, G. X., Tong, Y. B., Liu, Z. Y., and Jia, X. (2015). Study on the UV-shielding and controlled-release properties of a polydopamine coating for avermectin. *New J. Chem.* 39, 2752–2757. doi: 10.1039/C4NJ01744G

Simão, F. A., Waterhouse, R. M., Ioannidis, P., Kriventseva, E. V., and Zdobnov, E. M. (2015). BUSCO: assessing genome assembly and annotation completeness with singlecopy orthologs. *Bioinformatics* 31, 3210–3212. doi: 10.1093/bioinformatics/btv351

Sims, J. W., and Schmidt, E. W. (2008). Thioesterase-like role for fungal PKS-NRPS hybrid reductive domains. *J. Am. Chem. Soc.* 130, 11149–11155. doi: 10.1021/ja803078z

Stajich, J. E., Wilke, S. K., Ahrén, D., Au, C. H., Birren, B. W., Borodovsky, M., et al. (2010). Insights into evolution of multicellular fungi from the assembled chromosomes of the mushroom *Coprinopsis cinerea* (*Coprinus cinereus*). *Proc. Natl. Acad. Sci. U.S.A.* 107, 11889–11894. doi: 10.1073/pnas.1003391107

Stamatakis, A. (2014). RAxML version 8: a tool for phylogenetic analysis and post-analysis of large phylogenies. *Bioinformatics* 30, 1312–1313. doi: 10.1093/bioinformatics/btu033

Stanke, M., Keller, O., Gunduz, I., Hayes, A., Waack, S., and Morgenstern, B. (2006). AUGUSTUS: ab initio prediction of alternative transcripts. *Nucleic Acids Res.* 34, W435–W439. doi: 10.1093/nar/gkl200

Tatusov, R. L., Fedorova, N. D., Jackson, J. D., and Natale, D. A. (2003). The COG database: an updated version includes eukaryotes. *BMC bioinformatics* 4:41. doi: 10.1186/1471-2105-4-41

Walker, B. J., Abeel, T., Shea, T., Priest, M., and Earl, A. M. (2014). Pilon: an integrated tool for comprehensive microbial variant detection and genome assembly improvement. *PLoS One* 9:e112963. doi: 10.1371/journal.pone.0112963

Weber, T., Blin, K., Duddela, S., Krug, D., Kim, H. U., Bruccoleri, R. E., et al. (2015). Antismash 3.0-a comprehensive resource for the genome mining of biosynthetic gene clusters. *Nucleic Acids Res.* 43, W237–W243. doi: 10.1093/nar/gkv437

Xie, C. L., Gong, W. B., Zhu, Z. H., Li, Y., Hu, Z. X., and Peng, Y. D. (2018). Comparative transcriptomics of *Pleurotus eryngii* reveals blue-light regulation of carbohydrate-active enzymes (CAZymes) expression at primordium differentiated into fruiting body stage. *Genomics* 110, 201–209. doi: 10.1016/j.ygeno.2017.09.012

Xu, R., Liu, X. C., Peng, B., Liu, P. B., Li, Z., Dai, Y. T., et al. (2020). Genomic features of *Cladobotryum dendroides*, which causes cobweb disease in edible mushrooms, and identification of genes related to pathogenicity and mycoparasitism. *Pathogens* 9:232. doi: 10.3390/pathogens9030232

Yap, H. Y. Y., Chooi, Y. H., Firdaus-Raih, M., Fung, S. Y., Ng, S. T., Tan, C. S., et al. (2014). The genome of the tiger milk mushroom, *Lignosus rhinocerotis*, provides insights into the genetic basis of its medicinal properties. *BMC Genomics* 15:635. doi: 10.1186/1471-2164-15-635

Yuan, Y., Wu, F., Si, J., Zhao, Y. F., and Dai, Y. C. (2019). Whole genome sequence of *Auricularia heimuer* (Basidiomycota, Fungi), the third most important cultivated mushroom worldwide. *Genomics* 111, 50–58. doi: 10.1016/j.ygeno.2017.12.013

Zhang, H., Yohe, T., Huang, L., Entwistle, S., Wu, P., Yang, Z., et al. (2018). dbCAN2: a meta server for automated carbohydrate-active enzyme annotation. *Nucleic Acids Res.* 46, W95–W101. doi: 10.1093/nar/gky418

Zhang, R., Zhao, L. Y., Wang, H. X., and Ng, T. B. (2014). A novel ribonuclease with antiproliferative activity toward leukemia and lymphoma cells and HIV-1 reverse transcriptase inhibitory activity from the mushroom, *Hohenbuehelia serotina*. *Int. J. Mol. Med.* 33, 209–214. doi: 10.3892/ijmm.2013.1553

Ziemert, N., Podell, S., Penn, K., Badger, J. H., Allen, E., and Jensen, P. R. (2012). The natural product domain seeker NaPDoS: a phylogeny based bioinformatic tool to classify secondary metabolite gene diversity. *PLoS One* 7:e34064. doi: 10.1371/journal.pone.0034064

Conflict of Interest: The authors declare that the research was conducted in the absence of any commercial or financial relationships that could be construed as a potential conflict of interest.

Copyright © 2021 Tian, Li and Li. This is an open-access article distributed under the terms of the Creative Commons Attribution License (CC BY). The use, distribution or reproduction in other forums is permitted, provided the original author(s) and the copyright owner(s) are credited and that the original publication in this journal is cited, in accordance with accepted academic practice. No use, distribution or reproduction is permitted which does not comply with these terms.

frontiers in Microbiology

ORIGINAL RESEARCH
published: 09 July 2021
doi: 10.3389/fmicb.2021.689374

An Overview of 24 Years of Molecular Phylogenetic Studies in *Phallales* (*Basidiomycota*) With Notes on Systematics, Geographic Distribution, Lifestyle, and Edibility

Gislaine C. S. Melanda[1†], Alexandre G. S. Silva-Filho[2†], Alexandre Rafael Lenz[3], Nelson Menolli Jr.[4,5], Alexandro de Andrade de Lima[1], Renato Juciano Ferreira[6], Nathalia Mendonça de Assis[2], Tiara S. Cabral[7], María P. Martín[8] and Iuri Goulart Baseia[1,2]*

[1] Centro de Biociências, Departamento de Micologia, Programa de Pós-Graduação em Biologia de Fungos, Universidade Federal de Pernambuco (UFPE), Recife, Brazil, [2] Centro de Biociências, Departamento de Botânica e Zoologia, Programa de Pós-Graduação em Sistemática e Evolução, Universidade Federal do Rio Grande do Norte (UFRN), Natal, Brazil, [3] Departamento de Ciências Exatas e da Terra, Colegiado de Sistemas de Informação, Universidade do Estado da Bahia (UNEB), Salvador, Brazil, [4] Departamento de Ciências e Matemática, Subárea de Biologia, Instituto Federal de Educação, Ciência e Tecnologia de São Paulo (IFSP), São Paulo, Brazil, [5] Núcleo de Pesquisa em Micologia, Instituto de Botânica (IBt), São Paulo, Brazil, [6] Departamento de Ciências Biológicas, Universidade Regional do Cariri (URCA), Crato, Brazil, [7] Programa de Pós-Graduação em Genética, Conservação e Biologia Evolutiva, Instituto Nacional de Pesquisas da Amazônia (INPA), Manaus, Brazil, [8] Departamento de Micología, Real Jardín Botánico – CSIC, Madrid, Spain

OPEN ACCESS

Edited by:
Dhanushka Nadeeshan Wanasinghe, Chinese Academy of Sciences, China

Reviewed by:
Henrik R. Nilsson, University of Gothenburg, Sweden
Mario Amalfi, Botanic Garden Meise, Belgium

***Correspondence:**
Nelson Menolli Jr.
menollijr@yahoo.com.br

†These authors share first authorship

Specialty section:
This article was submitted to Fungi and Their Interactions, a section of the journal Frontiers in Microbiology

Received: *31 March 2021*
Accepted: *21 May 2021*
Published: *09 July 2021*

Citation:
Melanda GCS, Silva-Filho AGS, Lenz AR, Menolli N Jr, Lima AA, Ferreira RJ, Assis NM, Cabral TS, Martín MP and Baseia IG (2021) An Overview of 24 Years of Molecular Phylogenetic Studies in Phallales (Basidiomycota) With Notes on Systematics, Geographic Distribution, Lifestyle, and Edibility. Front. Microbiol. 12:689374. doi: 10.3389/fmicb.2021.689374

The order *Phallales* (*Basidiomycota*) is represented by gasteroid fungi with expanded and sequestrate basidiomata, known as stinkhorns and false truffles. In phalloids, the first DNA sequence was published in 1997, and after that, some studies aimed to resolve phylogenetic conflicts and propose new species based on DNA markers; however, the number of families and genera in the order still generates controversies among researchers. Thus, this work aims to provide an overview of *Phallales* diversity represented by selected DNA markers available in public databases. We retrieved *Phallales* sequences from DNA databases (GenBank and UNITE) of seven markers: ITS (internal transcribed spacer), nuc-LSU (nuclear large subunit rDNA), nuc-SSU (nuclear small subunit rDNA), mt-SSU (mitochondrial small subunit rDNA), *ATP*6 (ATPase subunit 6), *RPB*2 (nuclear protein-coding second largest subunit of RNA polymerase), and *TEF*1-α (translation elongation factor subunit 1α). To compose our final dataset, all ITS sequences retrieved were subjected to BLASTn searches to identify additional ITS sequences not classified as *Phallales*. Phylogenetic analyses based on Bayesian and maximum likelihood approaches using single and combined markers were conducted. All ITS sequences were clustered with a cutoff of 98% in order to maximize the number of species hypotheses. The geographic origin of sequences was retrieved, as well as additional information on species lifestyle and edibility. We obtained a total of 1,149 sequences, representing 664 individuals. Sequences of 41 individuals were unidentified at genus level and were assigned to five distinct families. We recognize seven families

and 22 genera in *Phallales*, although the delimitation of some genera must be further revisited in order to recognize only monophyletic groups. Many inconsistencies in species identification are discussed, and the positioning of genera in each family is shown. The clustering revealed 118 species hypotheses, meaning that approximately 20% of all described species in *Phallales* have DNA sequences available. Information related to geographic distribution represents 462 individuals distributed in 46 countries on all continents, except Antarctica. Most genera are saprotrophic with only one putative ectomycorrhizal genus, and 2.1% of the legitimate specific names recognized in *Phallales* are confirmed edible species. Great progress in the molecular analyses of phalloids has already been made over these years, but it is still necessary to solve some taxonomic inconsistencies, mainly at genus level, and generate new data to expand knowledge of the group.

Keywords: gasteroid fungi, GenBank, phylogeny, stinkhorns, UNITE

INTRODUCTION

The first molecular analyses including gasteroid fungi (Hibbett et al., 1997) showed that they represent a polyphyletic and artificial grouping of taxa that share a common ancestor with gilled and nongilled mushrooms that have active dispersion of the basidiospores. Hibbett et al. (1997) showed the gasteroid–phalloid fungi to group in a clade with other forms of gasteroid fungi, the *Geastraceae* Corda (earthstars) and *Sphaerobolaceae* J. Schröt. (cannonballs), all sharing a common ancestor with coralloid fungi. After that, Pine et al. (1999) confirmed the phylogenetic relationship between some cantharelloid, clavarioid, and phalloid fungi, naming all of them the gomphoid–phalloid clade, which was later confirmed as monophyletic (Hibbett and Thorn, 2001; Krüger et al., 2001; Binder and Hibbett, 2002; Hibbett and Binder, 2002) and designated as a subclass of *Agaricomycetes*: *Phallomycetidae* K. Hosaka, Castellano and Spatafora (Hosaka et al., 2006).

Phallales E. Fisch (*Agaricomycetes*, *Phallomycetidae*) includes representatives of gasteroid fungi with basidiospores that are passively dispersed mainly by insects and commonly named phalloid fungi, alien fungi, stinkhorns, and lattice or cage stinkhorns (Fischer, 1898; Cunningham, 1931; Miller and Miller, 1988; Pegler and Gomez, 1994). The phalloid fungi are mostly saprobic and characterized by hypogeous or epigeous immature basidiomata that are divided into chambers; thick white rhizomorphs are usually present; peridium with two or three layers, one of which is gelatinous; mature basidiomata that are usually epigeous or partially hypogeous, expanded, or sequestrate; pseudostipitate or sessile receptacle; receptacle carrying the green, olive to brown gleba; the usual presence of gelatinous to mucilaginous gleba that may be powdery at maturity, as in *Gastrosporium* Mattir.; and basidiospores mostly ellipsoid and smooth, with only a few genera with ornamentation on the basidiospore wall, as in *Gastrosporium*, *Kjeldsenia* Colgan, Castellano and Bougher, and *Phlebogaster* Fogel (Hosaka et al., 2006; Trierveiler-Pereira et al., 2014a).

Fischer (1898) grouped in *Phallales* the families *Clathraceae* Chevall. and *Phallaceae* Corda, which include specimens with expanded branched and unbranched basidiomata, respectively. *Lysuraceae* Corda was established in the same article as the establishment of *Phallaceae* (Corda, 1842); both families are characterized by basal pseudostipitate basidiomata, but unlike the morphology in *Phallaceae*, the apical part of the basidiomata in *Lysuraceae* is branched. *Lysuraceae* was not accepted by Fischer (1898) as an independent family in *Phallales*, and their species were considered by this author within *Clathraceae*, a view also adopted by a number of subsequent authors such as Cunningham (1944), Dring (1980), Jülich (1981), Miller and Miller (1988), Pegler and Gomez (1994), Hibbett and Thorn (2001), and Kirk et al. (2008). On the other hand, some authors (He et al., 2019; Wijayawardene et al., 2020) and well-known databases (Nilsson et al., 2019; Index Fungorum, 2020; MycoBank., 2020; Schoch et al., 2020) have placed in *Phallaceae* all the species traditionally classified as *Lysuraceae*. However, Hosaka et al. (2006), Degreef et al. (2013), Trierveiler-Pereira et al. (2014a), and Sulzbacher et al. (2016) consider these three families to be independent (**Table 1**).

Cunningham (1931) accepted in *Phallales* sequestrate (truffle-like) basidiomata classified in the genus *Claustula* K.M. Curtis and established this genus as a type of the new monogeneric family *Claustulaceae* G. Cunn. As mentioned by Cunningham (1931), this family shares with other phalloid fungi the gelatinous peridium, immature basidiomata divided into chambers, and elliptical smooth basidiospores. Zeller (1939) also studied sequestrate fungi and proposed two new families: *Gelopellaceae* Zeller and *Protophallaceae* Zeller. However, these two families, as well as *Hysterangiaceae* E. Fisch., have been consolidated within the order *Hysterangiales* K. Hosaka and Castellano, according to Zeller (1939). *Hysterangiales* was first proposed by Zeller (1939), but it was considered a *nomen nudum* because it was published without a description or diagnosis; it was later formally established in Hosaka et al. (2006).

Moreover, Hosaka et al. (2006) established the subclass *Phallomycetidae*, including the new order *Hysterangiales*

TABLE 1 | Family classification of *Phallales* and related orders according to published molecular studies and taxonomic and molecular databases.

Work	Families accepted in *Phallales*	Families accepted in *Hysterangiales*	Families accepted in *Boletales*
Hosaka et al. (2006), Degreef et al. (2013)	*Clathraceae*, *Claustulaceae* (=*Gelopellaceae*), *Lysuraceae*, *Phallaceae*, *Protophallaceae*, *Trappeaceae*		
Trierveiler-Pereira et al. (2014a)	*Clathraceae*, *Claustulaceae* (=*Gelopellaceae*), *Gastrosporiaceae*, *Lysuraceae*, *Phallaceae*, *Protophallaceae*, *Trappeaceae*		
Sulzbacher et al. (2016)	*Clathraceae*, *Claustulaceae* (=*Gelopellaceae*), *Lysuraceae*, *Phallaceae*, *Protophallaceae*, *Trappeaceae*		
He et al. (2019), Wijayawardene et al. (2020)	*Claustulaceae*, *Gastrosporiaceae*, *Phallaceae* (=*Clathraceae*; *Lysuraceae*)	*Trappeaceae*, *Phallogastraceae* (=*Protophallaceae*)	
Schoch et al. (2020)	*Clathraceae*, *Phallaceae* (=*Lysuraceae*; =*Protophallaceae*)	*Hysterangiaceae* (=*Trappeaceae*)	*Gastrosporiaceae*
Nilsson et al. (2019)	*Clathraceae*, *Claustulaceae*, *Gastrosporiaceae*, *Phallaceae* (=*Lysuraceae*)	*Hysterangiaceae* (=*Trappeaceae*)	
Index Fungorum (2020)	*Claustulaceae* (=*Gelopellaceae*), *Phallaceae* (=*Clathraceae*; =*Lysuraceae*)	*Phallogastraceae* (=*Protophallaceae*), *Trappeaceae*	*Gastrosporiaceae*
MycoBank. (2020)	*Claustulaceae* (=*Gelopellaceae*), *Gastrosporiaceae*, *Phallaceae* (=*Clathraceae*; =*Lysuraceae*), *Protophallaceae*	*Trappeaceae*	

mentioned previously and the new *Geastrales* K. Hosaka and Castellano. Thus, in the study by Hosaka et al. (2006), *Phallomycetidae* comprises *Geastrales*, *Gomphalles* Jülich., *Hysterangiales*, and *Phallales*, a classification that is also accepted in He et al. (2019). In this way, Hosaka et al. (2006) agreed with Cunningham (1931) in the definition of *Phallales* including families with expanded basidiomata (*Clathraceae*, *Lysuraceae*, *Phallaceae*), as well as with sequestrate ones (*Claustulaceae*, *Trappeaceae* P.M. Kirk, and *Protophallaceae*). Although *Trappeaceae* was provisionally proposed in *Phallales* by Hosaka et al. (2006) with the genera *Phallobata* G. Cunn. and *Trappea* Castellano, the family was formally proposed two years later by Kirk et al. (2008), who classified it as part of *Hysterangiales*. Later, Sulzbacher et al. (2016) proposed a new genus in *Trappeaceae* (*Restingomyces* Sulzbacher, T. Grebenc and Baseia) and also considered the family in *Phallales* as previously pointed out by Hosaka et al. (2006).

After these 24 years of molecular studies, the sampling of some genera and families within molecular phylogenies of *Phallales* is incomplete. For example, *Gastrosporium*, which is part of the monogeneric family *Gastrosporiaceae* Pilát, was first incorporated in a molecular phylogenetic work by Hibbett and Binder (2002), who considered it as a sequestrate member of *Phallales*. This was later confirmed by Trierveiler-Pereira et al. (2014a), He et al. (2019), Kasuya et al. (2020), and Wijayawardene et al. (2020). However, Hosaka et al. (2006) did not include *Gastrosporium* in their phylogeny because of the lack of a protein code gene in their dataset. In the study by Trierveiler-Pereira et al. (2014a), *Trappeaceae* representatives were not included, and they recognized seven families in *Phallales*, which include *Gastrosporiaceae* plus the six families recognized by Hosaka et al. (2006).

On the other hand, the acceptance in *Phallales* of families composed of species characterized by sequestrate basidiomata (*Claustulaceae*, *Gastrosporiaceae*, *Gelopellaceae*, *Trappeaceae*, and *Protophallaceae*) has also generated controversies. For instance, morphological studies conducted by Zeller (1939, 1948) and Jülich (1981) considered *Gelopellaceae* and *Protophallaceae* in *Hysterangiales*, whereas Miller and Miller (1988) considered these families and *Claustulaceae* in *Phallales*. The last edition of Dictionary of the Fungi (Kirk et al., 2008) recognized three families in *Phallales*: *Claustulaceae* (=*Gelopellaceae*), *Gastrosporiaceae*, and *Phallaceae* (=*Clathraceae*; =*Lysuraceae*; =*Protophallaceae*), with *Trappeaceae* placed in *Hysterangiales*. Additionally, recent works based on *Basidiomycota* and general fungal classification (He et al., 2019; Wijayawardene et al., 2020) also considered *Trappeaceae* in *Hysterangiales* and only three families in *Phallales*: *Claustulaceae*, *Gastrosporiaceae*, and *Phallaceae* (**Table 1**). Representatives of some families of *Phallales* are shown in **Figure 1**.

There is still no consensus in family level systematics of *Phallales*, based on a compilation of sources (**Table 1**), such as works of fungal classification (He et al., 2019; Wijayawardene et al., 2020), taxonomic (Index Fungorum, 2020; MycoBank., 2020) and molecular databases (Nilsson et al., 2019; Schoch et al., 2020), and phylogenetic studies focused on *Phallales* (Hosaka et al., 2006; Degreef et al., 2013; Trierveiler-Pereira et al., 2014a; Sulzbacher et al., 2016). Thus, based on the importance of molecular data for systematics and phylogenetic studies and the fact that DNA databases can be a good tool to assess the history behind the sequences generated over the years, as well as the geographic distribution of certain taxa, we have undertaken this study using *Phallales* as a target group to retrieve sequences in molecular databases and to provide an overview of *Phallales* diversity represented by selected DNA markers available in public databases. Moreover, we aim to test

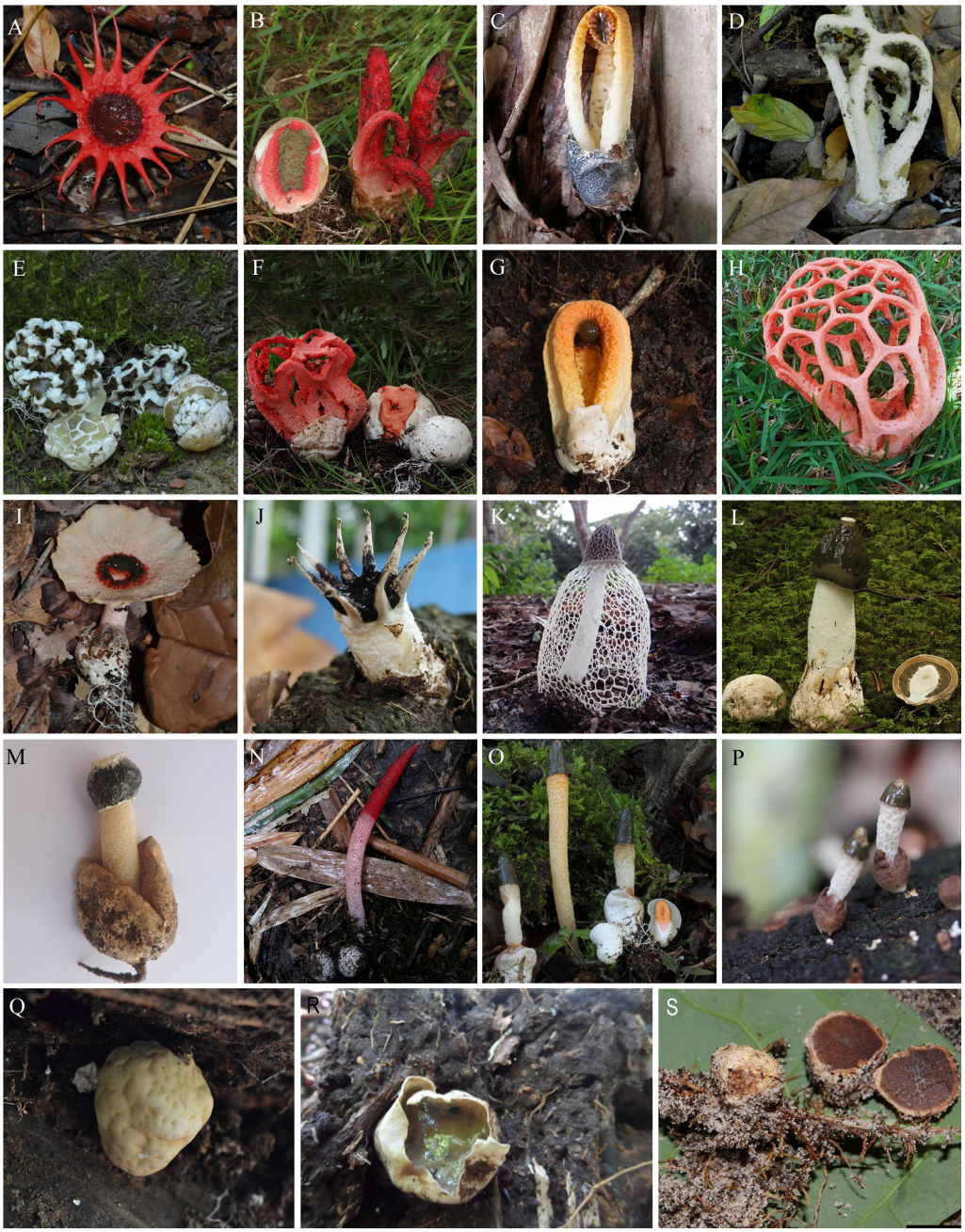


FIGURE 1 | Basidiomata of *Phallales*. *Clathraceae*: **(A)** *Aseroë rubra*; **(B)** *Clathrus archeri* MT13072101B (personal herbarium); **(C)** *Laternea dringii* (coll. AAL94); **(D)** *Blumenavia baturitensis* UFRN-Fungos 2868, holotype (coll. GCSM15); **(E)** *Ileodictyon gracile* MT141003001B (personal herbarium); **(F)** *Clathrus ruber* MT15100406B (personal herbarium); **(G)** *Clathrus columnatus* UFRN-Fungos 2912 (coll. AAL42); **(H)** *Clathrus natalensis* (coll. GSCM30); **(I)** *Abrachium floriforme* UFRN-Fungos 3271. *Lysuraceae*: **(J)** *Lysurus arachnoideus* INPA-Fungos 256537 (coll. TSC41). *Phallaceae*: **(K)** *Phallus indusiatus* INPA-Fungos 264931, neotype (coll. TSC148); **(L)** *Phallus impudicus*; **(M)** *Itajahya* sp. UFRN-Fungos 3342 (coll. AAL106); **(N)** *Mutinus bambusinus* UFRN-Fungos 3222 (coll. AAL100); **(O)** *Mutinus caninus*; **(P)** *Xylophallus clavatus* INPA-Fungos 271637 (coll. TSC237). *Protophallaceae*: **(Q,R)** *Protubera maracuja* (coll. GCSM18). *Trappeaceae*: **(S)** *Restingomyces reticulatus* UFRN-Fungos 1890, holotype (coll. MAS335). Photographs: **(A)** Clark L. Ovrebo; **(B,E,F,L,O)** Manuel Tabarés; **(C,G,M,N)** Alexandro de A. de Lima; **(D,H,Q,R)** Gislaine C. S. Melanda; **(I)** Alexandre G. S. Silva-Filho; **(J,K,P)** Tiara S. Cabral; **(S)** Marcelo A. Sulzbacher.

the phylogenetic positioning of named and unnamed sequences; to assess phylogenetic hypotheses using combined markers to recognize families and genera and to compare these data with the extant classification; to recognize the total number of species hypothesis (SH) represented in *Phallales* based on internal transcribed spacer (ITS) sequence clustering; and, finally, to record the global geographic distribution of their representative genera, their lifestyle, and edibility.

MATERIALS AND METHODS

Sequence Metadata

Our work used two databases to obtain *Phallales* sequences: NCBI GenBank[1] and UNITE[2]. All sequences were downloaded on August 7 to 9, 2020, from both databases. GenBank is part of the International Nucleotide Sequence Database Collaboration and contains the vast majority of phalloid sequences from published articles. The UNITE database automatically clusters ITS sequences of eukaryotic organisms to approximately the species level (called SHs), and to facilitate unambiguous scientific communication, a DOI is given to each SH.

According to the revised bibliography already mentioned (Hibbett et al., 1997; Hosaka et al., 2006; Trierveiler-Pereira et al., 2014a; Sulzbacher et al., 2016; Kasuya et al., 2020), seven markers were selected to retrieve sequences in GenBank using query strings (**Table 2**): nuclear ribosomal ITS, nuclear large subunit rDNA (nuc-LSU), nuclear small subunit rDNA (nuc-SSU); mitochondrial small subunit rDNA (mt-SSU), mitochondrial protein-coding ATPase subunit 6 (*ATP*6), and nuclear protein-coding second largest subunit of RNA polymerase (*RPB*2); and nuclear protein-coding translation elongation factor subunit 1α (*TEF*1-α). GenBank query results were downloaded in TinySeq_XML format, and single datasets of nucleotide sequences were created for each marker. One single dataset of all ribosomal markers from GenBank was downloaded, and in order to identify each marker, this single dataset was separated manually, based on the marker name in each sequence title. From the UNITE database, the sequences under *Phallales* (DOI: TH005985) not placed in GenBank were retrieved manually. Furthermore, manual checking was done for some genera, as they are not classified in *Phallales* in GenBank (*Gastrosporium*, *Kjeldsenia*, *Phallobata*, *Phlebogaster*, and *Trappea*) and UNITE (*Phlebogaster* and *Trappea*).

Sequence metadata were retrieved from GenBank qualifiers and UNITE annotations. GenBank qualifiers include[3]: *country*, *collection_date*, *culture_collection*, *environmental_sample*, *clone*, *isolate*, *isolation_source*, *lat_lon*, *organism*, *specimen_voucher*, *strain*, *tissue_type*, *type_material*, and *PCR_primers*, as well as information about authors, reference, title, and journal. UNITE annotations were obtained directly from the online database for each sequence; UNITE metadata include *sampling_area* (*country*), *sample_type* [Linked to (source)], and *collection_date*.

All ITS sequences obtained from GenBank and UNITE were used for additional Nucleotide BLAST searches in their respective database (NCBI BLAST, 2020; UNITE BLAST, 2020). These searches aimed to find ITS sequences of *Phallales* members that were deposited without being classified in this order. We retrieved unclassified sequences using the following cutoffs: query cover > 80%, identity > 70%, and e-value < e-1,000. The 80% sequence similarity represents the criterion to recognize the identity of sequences approximately at the order level (Tedersoo et al., 2014).

TABLE 2 | Query strings used to search for DNA sequences from phalloid fungi in GenBank.

Query	Query strings
Main query	txid68804[Organism] AND 300:10000[SLEN]
ITS; nuc-LSU; nuc-SSU; mt-SSU	rRNA[Title] OR ribosomal RNA[Title]
*ATP*6	ATP6[Title] OR ATPase6[Title] OR ATP synthase F0 subunit 6[Title] OR ATP synthase subunit 6[Title] OR MTATP synthase F0 subunit 6[Title] OR MT-ATP6[Title] OR MTATP6[Title] OR ATP-6[Title]
*RPB*2	rpb2[Title] OR rpbII[Title] OR RNA polymerase II second largest subunit[Title] OR RNA polymerase II second large subunit[Title] NOT rpb1
*TEF*1-α	TEF1[Title] OR EF1[Title] OR EF-1[Title] OR TEF-1[Title] OR TEF[Title] OR tef1a[Title] OR EF[Title] OR translation elongation factor 1[Title] OR EF1alpha[Title] OR EF1a[Title] OR EF1-alpha[Title] OR TEF1-alpha[Title]

All information from the sequences retrieved from both databases and the BLAST searches was merged manually and organized in **Supplementary Table 1** to better identify all markers of each individual based on their herbarium/culture accession number and/or other code given by whoever generated the sequences. An individual was considered repeated when it had more than one sequence of the same marker under different accession numbers or when it was indicated as a clone in the databases (individuals with "R" in the columns "R = repeated or duplicated voucher" of **Supplementary Table 1**). In these cases, two lines were created in **Supplementary Table 1** for the same individual. The names of genera and species present in our **Supplementary Table 1** are based on the qualifier *organism* in GenBank for each individual. In UNITE, the names adopted were according to the UNITE taxon name.

Phylogenetic Positioning of Sequences and Recognition of Families and Genera

Phylogenetic analyses were performed using seven datasets, the combined one and the other six with each individual marker: ITS, nuc-LSU, mt-SSU, *ATP*6, *RPB*2, and *TEF*1-α. The marker nuc-SSU was not considered in the analyses because of the few (1%) sequences available (**Supplementary Table 1**). Sequences of *Hysterangiales* species were used as outgroup for individual marker analyses, as seen in **Supplementary Table 2**. The combined dataset (ITS + nuc-LSU + mt-SSU + *ATP*6 + *RPB*2 + *TEF*1-α) was constructed to confirm the organization in families, and this also used members of *Hysterangiales* as outgroup (**Supplementary Table 3**). Specimens from almost all genera retrieved in *Phallales* and that had most markers sequenced were chosen for the combined dataset (**Supplementary Table 3**), which includes 139 sequences: 69 ITS, 114 nuc-LSU, 26 mt-SSU, 76 *ATP*6, 65 *RPB*2, and 41 *TEF*1-α.

All datasets were aligned using MAFFT v.7 (Katoh and Standley, 2013) under the E-INS-i criteria. Seaview v.4

[1]http://www.ncbi.nlm.nih.gov/

[2]https://unite.ut.ee/index.php

[3]http://www.insdc.org/documents/feature_table.html#7.3

(Gouy et al., 2010) was used to visualize and adjust the alignments. The *RPB2* alignment was partitioned into intron and exon, and *TEF*1-α alignment into intron 1/2/3 and exon 1/2 according to GenBank coding sequence notation. The best nucleotide substitution model was selected with BIC (Bayesian information criterion) using jModelTest 2v.1.6 (Darriba et al., 2012) for each individual dataset. Two strategies were used for phylogenetic reconstructions of each alignment: maximum likelihood and Bayesian inference. Maximum likelihood analyses were performed in RAxML v8.2.X (Stamatakis, 2006), combined with the rapid bootstrapping algorithm with 1,000 replicates under the GTRGAMMA option to obtain the maximum likelihood bootstrap (MLbs). Bayesian inferences were performed using MrBayes 3.2.6 (Ronquist et al., 2012) with two independent runs, each one beginning from random trees with four simultaneous independent chains, performing 2×10^7 Markov chain Monte Carlo (MCMC) generations, sampling one tree every 1×10^3 generation. The first 5×10^3 sampled trees were discarded as burn-in, whereas the remaining ones (all sampled after the average standard deviation of split frequencies reached < 0.01) were used to reconstruct a 50% majority-rule consensus tree and to calculate Bayesian posterior probabilities (PP) of the clades. The jModelTest 2v.1.6, RAxML v8.2.X, and MrBayes 3.2.6 were run from the CIPRES Science Gateway 176 3.1 (Miller et al., 2010). All final alignments and the resulting topologies were deposited in TreeBASE under the number 28016.

Species Hypotheses Recognition

The ITS sequences of *Phallales* retrieved were clustered using CD-HIT-EST (Huang et al., 2010) at 98.0% sequence similarity threshold (Tedersoo et al., 2014) to assess species hypotheses in *Phallales*.

Geographic Distribution, Lifestyle, and Edibility

The qualifiers *country* and *lat_lon* from GenBank and *sampling_area* from UNITE were used to organize the global geographic distribution map of *Phallales* and each genus. To construct the maps based on this global distribution, the locality of each individual identified at genus level was retrieved from the databases (**Supplementary Table 4**). When possible, the missing localities in DNA databases were double searched in their original article or in secondary articles that give this information (**Supplementary Table 4**). When the geographic coordinate information was missing, we made an effort to establish it through Google Maps[4] to complete the table. In the case of individuals for which the only origin information was the country, the geographic coordinates suggested by Google Maps were used based on the name of the respective country as a search keyword. One general map with all *Phallales* distribution was made, as well as separate maps according to genera.

To record the information related to lifestyle of each genus, we followed the FungalTraits database (Põlme et al., 2021) and additional data obtained from the qualifiers *environmental_sample* (GenBank), *isolation_source* (GenBank), and *sample_type* (UNITE). To complement and better explore the use of the phalloid species sampled with molecular data, the edibility status of the species was considered based on Li et al. (2021) and complementarily searched in the main text of the articles in which the sequences were generated.

[4]https://www.google.com.br/maps

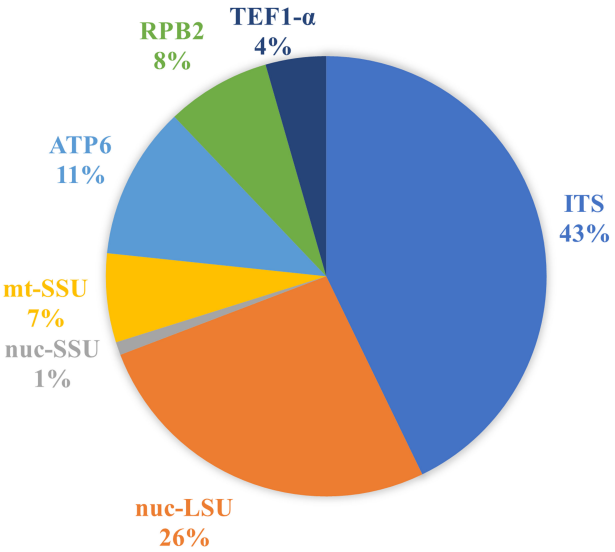


FIGURE 2 | Relative proportion of phalloid DNA sequences deposited in DNA databases (GenBank and UNITE) according to the molecular marker.

RESULTS

Sequence Metadata

Our final dataset led to a total of 1,149 DNA sequences of *Phallales* divided into 492 ITS, 303 nuc-LSU, 11 nuc-SSU, 75 mt-SSU, 129 *ATP*6, 88 *RPB*2, and 51 *TEF*1-α (**Figure 2**).

Based on the available records of collection date (**Figure 3**), the first uploaded sequences of *Phallales* individuals were the nuc-SSU sequences of *Pseudocolus fusiformis* (E. Fisch.) Lloyd, dated October 31, 1997 (AF026623), and November 5 of the same year (AF026666), both part of the work published by Hibbett et al. (1997). In 2006, there was a peak of deposited sequences, including new markers such as *ATP*6, *RPB*2, and *TEF*1-α (**Figure 3**), and in 2012, there was a higher constancy of deposited sequences, in which ITS and nuc-LSU are the most represented markers (**Figure 3**). Interestingly, the sequence obtained from the oldest phalloid individual belongs to *Colus hirudinosus* Cavalier and Séchier (voucher UC 955042, dated February 1, 1952) and was uploaded in GenBank on April 4, 2020 (nuc-LSU accession code MK607412, author of sequence: Kuo, M.).

The 1,149 sequences comprise 664 individuals, with 19 of them comprising repeated sequences for the same maker. A total of 58.7% of all individuals have only one sequenced marker, 23.9% have two sequenced markers, and 17.4% have three to five sequenced markers. There are 122 sequences representing 41 type collections (**Supplementary Table 5**).

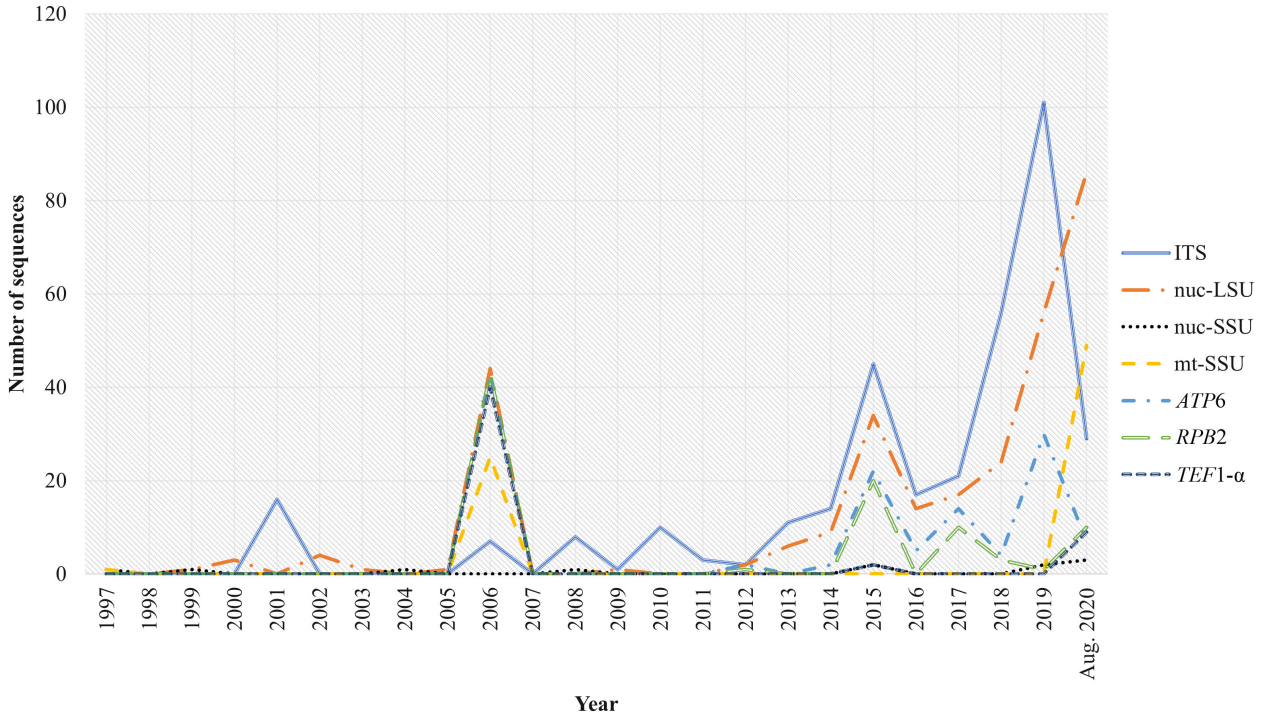


FIGURE 3 | Number of *Phallales* DNA sequences uploaded in DNA databases (GenBank and UNITE) along the years.

Sequences of 22 recognized genera were retrieved: *Abrachium* Baseia and T.S. Cabral, *Aseroë* Labill., *Blumenavia* Möller, *Clathrus* P. Micheli ex L., *Claustula*, *Colus* Cavalier and Séchier, *Gastrosporium*, *Gelopellis* Zeller, *Ileodictyon* Tul. and C. Tul., *Itajahya* Möller, *Kjeldsenia*, *Laternea* Turpin, *Lysurus* Fr., *Mutinus* Fr. (=*Jansia* Penz.), *Phallobata*, *Phallus* Junius ex L. (=*Dictyophora* Desv.), *Phlebogaster*, *Protubera* Möller, *Pseudocolus* Lloyd, *Restingomyces* (as *Phallales* sp.), *Trappea*, and *Xylophallus* (Schltdl.) E. Fisch. (**Table 3**). Sequences named *Gymnotelium* Syd. were retrieved as *Phallales*, but they are excluded from the present study because of their doubtful quality and because it is a genus classified in *Pucciniaceae* Chevall., *Pucciniales* Clem. and Shear (He et al., 2019). The genus *Calvarula* Zeller was not included in the combined analyses, because only one *TEF*1-α sequence is available and its placement at family level is questionable (see *Phylogenetic analyses*).

Phallus is the most highly represented genus, with 313 individuals and 471 sequences (**Table 3**). Forty-three unidentified *Phallales* individuals were not classified at genus level (see individuals with "NO" in genus columns in **Supplementary Table 1**); they are specified in **Table 3**. The possible classification of these individuals is discussed in *Phylogenetic analyses*.

Phylogenetic Analyses

The final aligned matrices for the analyses of each independent marker contain 481 sequences of ITS (1,210 positions), 306 nuc-LSU (1,245 positions), 77 mt-SSU (600 positions), 131 *ATP*6 (743 positions), 90 *RPB*2 (822 positions), and 53 *TEF*1-α (849 positions), and 139 of the combined matrix (4637 positions). The evolutionary models selected for the final dataset were as follows: ITS: TIM1 + I + G; nuc-LSU: TrN + I + G; mt-SSU: TPM3uf + G; *ATP*6: TVM + I + G; *RPB*2 Intron: TIM3 + I + G, *RPB*2 exon: TIM3 + I + G; *TEF*1-α intron 1: TrNef + G, *TEF*1-α exon 1: TrN + I + G, *TEF*1-α intron 2: TPM1 + G; *TEF*1-α exon 2: TPM1 + G, and *TEF*1-α intron 3: K80 + G.

The concatenated tree is shown in **Figure 4**, in which some names were changed according to the current name recognized by their phylogenetic positioning. The trees that resulted from the independent analyses of each marker are available in **Supplementary Figures 1–3**.

Phylogenetic Positioning of Unnamed and Doubtfully Named Sequences

Two ITS sequences of environmental samples retrieved from GenBank (EF218792 and MF487330) did not match any phalloid sequence in BLAST, and thus, they were eliminated from our data and not included in **Supplementary Tables 1**, **3**. Thirteen ITS sequences (MK518965, UDB015101 (JQ657782), MT644888, UDB018620, UDB0673787, UDB0317538, UDB0321542, UDB0215586, UDB0196057, UDB089976, MT512648, UDB0180761, and MH930315) and five nuc-LSU (MK518662, MH532563, MH532564, MH532565, and MH532566) were excluded from the dataset because they had many ambiguous bases and long gaps, possibly the result of poorly edited sequences. These sequences were also checked on NCBI BLAST, and they do not correspond to any species of *Phallales*. Six sequences were divided into ITS and nuc-LSU and incorporated

TABLE 3 | Total of individuals and number of sequences of each molecular marker for each taxon retrieved from GenBank and UNITE databases from phalloid fungi searches.

Genus or name in sequence	N° unrepeated individuals	N° sequences	ITS	nuc-LSU	nuc-SSU	mt-SSU	*ATP*6	*RPB*2	*TEF*1-α
Abrachium	1	4	0	2	0	0	1	1	0
Aseroë	9	17	3	6	2	1	1	3	1
Blumenavia	17	51	11	12	0	1	8	10	9
Calvarula ?	1	1	0	0	0	0	0	0	1
Clathrus	42	83	24	34	0	6	9	8	2
Claustula	2	5	0	0	0	1	0	2	2
Colus	1	1	0	1	0	0	0	0	0
"Dictyophora"	43	52	41	3	0	2	2	2	2
Gastrosporium	6	14	7	7	0	0	0	0	0
Gelopellis	5	16	0	4	0	2	4	3	3
Gymnotelium ?	1	3	1	1	1	0	0	0	0
Ileodictyon	8	25	1	8	0	4	5	4	3
Itajahya	10	13	9	2	0	0	2	0	0
"Jansia"	14	17	14	1	0	0	1	1	0
Kjeldsenia	1	3	0	1	0	0	0	1	1
Laternea	1	5	0	1	0	1	1	1	1
Lysurus	38	98	17	31	0	12	20	16	2
Mutinus	59	89	37	31	1	9	7	4	0
Phallobata	1	4	0	1	0	0	1	1	1
Phallus	313	471	274	115	4	27	40	6	5
Phlebogaster	1	2	1	1	0	0	0	0	1
Protubera	28	88	6	22	0	6	21	20	13
Pseudocolus	8	15	5	7	1	2	0	0	0
Trappea	5	15	2	4	0	1	3	3	2
Xylophallus	3	4	0	3	0	0	0	1	0
Basidiomycota sp.	3	3	3	0	0	0	0	0	0
Clathraceae sp.	2	4	2	0	2	0	0	0	2
Hysterangiales sp.	1	1	1	0	0	0	0	0	0
Phallaceae sp.	3	3	1	2	0	0	0	0	0
Phallales sp.	2	3	2	1	0	0	0	0	0
Phallales sp. (*Restingomyces*)	2	5	1	2	0	0	2	0	0
uncultured *Agaricomycetes*	1	1	1	0	0	0	0	0	0
uncultured fungus	25	25	25	0	0	0	0	0	0
uncultured *Phallaceae*	3	2	3	0	0	0	0	0	0
uncultured *Pleosporales*	1	1	1	5	2	0	2	0	0
Total	**664**	**1109**	**492**	**303**	**11**	**75**	**129**	**88**	**55**

Genus names followed by a question mark represent doubtful identification, and between quotes represent synonyms.

in both ITS and nuc-LSU alignments (see individuals with "YES" in the column "nuc-LSU sequence incorporated in phylogenetic analyses. . ." in **Supplementary Table 1**).

Among the sequences that need revision because of possible misidentification or doubtful positioning are those of the monospecific genus *Calvarula*, as *Calvarula excavata* Zeller (*TEF*1-α, DQ219293), which is positioned in *Lysuraceae* (**Supplementary Figure 1A**), although its classification was in *Protophallaceae* (Zeller, 1939). Sequences named *Protubera* sp. (T20068), *Protubera hautuensis* Castellano and Beever (OSC59673), *Protubera nothofagi* Castellano and Beever (OSC59699), *Trappea phillipsii* (Harkn.) Castellano (OSC56042), and *Trappea pinyonensis* States (AHF530) are grouped outside the *Phallales* core, in the outgroup of *Hysterangiales*. Thus, these sequences, as well as *Hysterangium* sequences, were used to root the trees as representative of *Hysterangiales*, and their identification must be further investigated. Sequences named *Protubera* sp. (vouchers FLAS-F60616 and FLAS-F 61859), *Protubera canescens* G.W. Beaton and Malajczuk, and *Protubera clathroidea* Dring also need to be investigated because they clustered in *Clathraceae* or *Lysuraceae* (**Supplementary Figures 1–3**), despite the classification of the genus in *Protophallaceae* (Hosaka et al., 2006; Trierveiler-Pereira et al., 2014a,b). Finally, some sequences of *Gelopellis* need further studies because they clustered out of the expected *Claustulaceae* (Hosaka et al., 2006; Trierveiler-Pereira et al., 2014a); *Gelopellis purpurascens* G.W. Beaton and Malajczuk (voucher H292) is grouped in *Phallaceae*

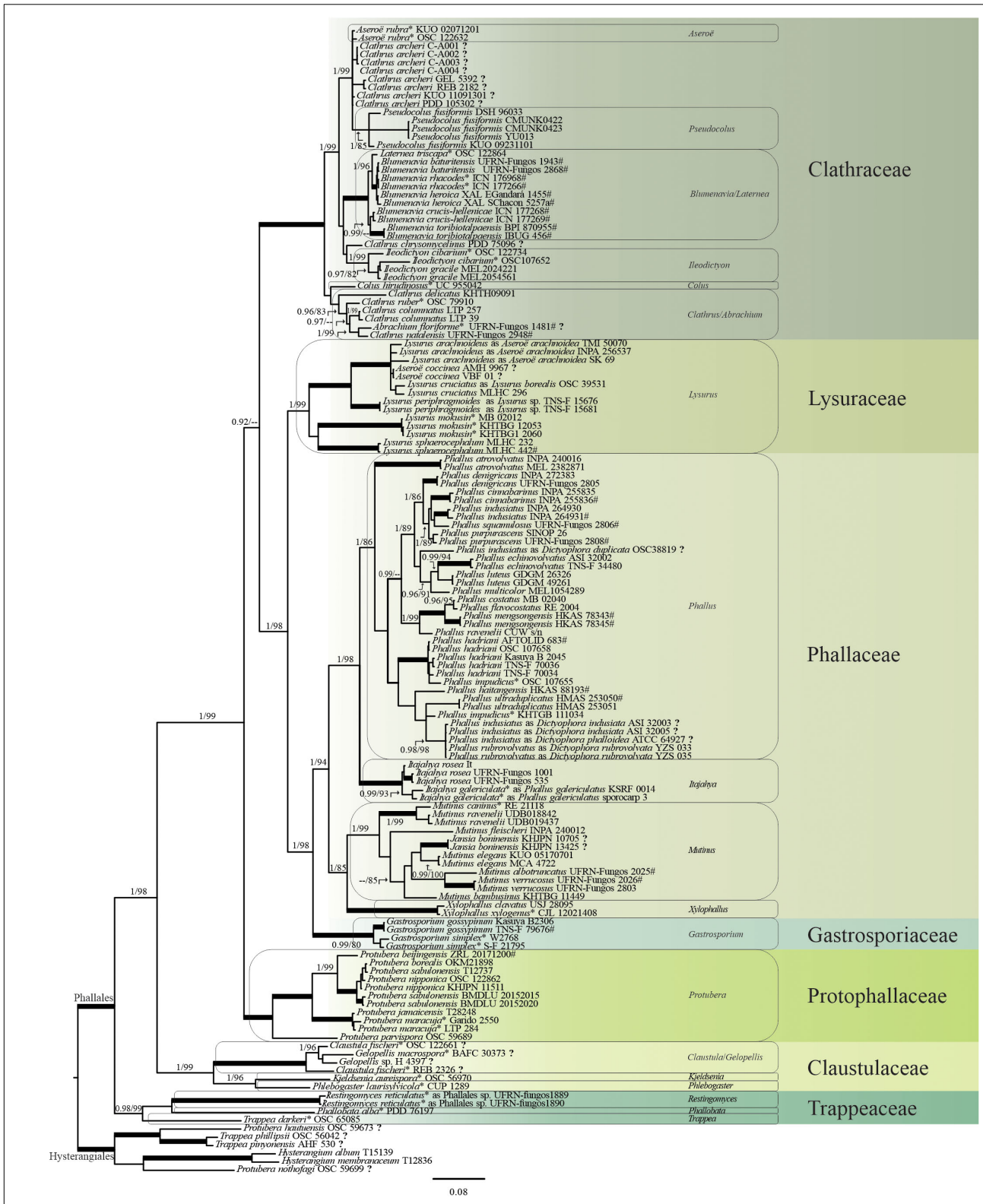


FIGURE 4 | Phylogenetic tree of the *Phallales* based on a combined dataset (ITS/nuc-LSU/mt-SSU/*ATP6*/*RPB2*/TEF1-α). Family clades are colored in green shades and named on the right. Names of recognized genera are highlighted in the boxes. (*) Type species. (?) Sequences that need review of their identity or generic status. (#) Type specimens. Tree topology is based on the Bayesian analyses. Numbers on branches are posterior probabilities (PP, before slash) and maximum likelihood bootstrap values (MLbs, after slash). Thickened branches in boldface indicate fully supported nodes (PP = 1, MLbs = 100). Scale bar indicates expected changes per site.

(**Supplementary Figure 3B**); *Gelopellis* sp. (voucher MEL 2063389) is in *Clathraceae* (**Supplementary Figures 2B**, **3A**) or external to *Phallaceae* (**Supplementary Figure 3B**).

For the total of 43 unidentified individuals not classified at genus level (**Table 3**), 39 were placed in five distinct families, two did not group with any family in *Phallales* (**Figure 5** and **Supplementary Table 6**), and the last two (*Hysterangiales* sp. UDB015101, and *Phallales* sp. UDB018620), as mentioned previously, were excluded from analyses. A total of 13 individuals were assigned to a specific genus: *Ileodictyon*, *Gastrosporium*, *Mutinus*, and *Phallus* (**Supplementary Table 6**). Fifteen individuals were identified to species level: *Blumenavia crucis-hellenicae* G. Coelho, Sulzbacher, Grebenc and Cortez, *Phallus impudicus* L., *Phallus hadriani* Vent., *Restingomyces reticulatus* Sulzbacher, B.T. Goto and Baseia (**Supplementary Table 6**). The identification of the sequences of *R. reticulatus* was possible by consulting the original article that proposed the new taxon (Sulzbacher et al., 2016). **Supplementary Figures 1A**, **2A,B**, **3B** show the phylogenetic positioning and the possible identification of some of the 41 unidentified individuals retrieved according to *TEF*1-α, ITS, nuc-LSU, and *ATP*6, respectively.

Recognition of Families and Genera

Based on the phylogenetic inferences using the concatenated data matrix (ITS + nuc-LSU + mt-SSU + *ATP*6 + *RPB*2 + *TEF*1-α), our results show *Phallales* as a strongly supported monophyletic order (PP = 1, MLbs = 100) and composed of seven families (**Figure 4**). We recognized 22 genera in *Phallales*, with *Dictyophora* and *Jansia* confirmed as synonyms of *Phallus* and *Mutinus*, respectively, although the recognition of some genera and the placement of their representatives deserve attention: *Abrachium*, *Aseroë*, *Blumenavia*, *Clathrus*, *Claustula*, *Gelopellis*, *Laternea*, *Protubera*, *Pseudocolus*, and *Trappea*.

The composition of each family based on our analyses is presented below.

Clathraceae

This family grouped the genera *Abrachium*, *Aseroë*, *Blumenavia*, *Clathrus*, *Ileodictyon*, *Laternea*, and *Pseudocolus* (**Figure 4**). In the combined analyses, *Aseroë* in the *Clathraceae* clade is represented by the type species *Aseroë rubra* Labill. but is not recognized as monophyletic and forms a paraphyletic group with other sequences named *Clathrus archeri* (Berk.) Dring. These sequences warrant further examination. *Pseudocolus*, represented by *P. fusiformis*, is within the well-supported clade formed by *A. rubra* and *C. archeri*.

Laternea, based on the type species *Laternea triscapa* Turpin, forms a monophyletic clade together with sequences of *Blumenavia*, which includes the epitype specimen *Blumenavia rhacodes* Möller (voucher ICN 177266).

Ileodictyon is recognized as monophyletic (PP = 1, MLbs = 99), including seven sequences of two individuals of the type species *Ileodictyon cibarium* Tul. and C. Tul and another eight sequences of two individuals of *I. gracile* Berk. The specific identity of OSC107652, named as *I. cibarium*, must be investigated because it is positioned closer to sequences identified as *I. gracile*. Although with no support, *Clathrus chrysomycelinus* Möller is external to *Ileodictyon*, and the identity or generic status of the individual PDD75096 must be investigated.

Colus is represented by one nuc-LSU sequence of the type species *C. hirudinosus* Cavalier and Séchier, and it is closer to *Clathrus*, although this relationship is not supported.

Clathrus is recovered as polyphyletic with representatives clustered in at least three clades (**Figure 4**). Its core is represented by the type species *Clathrus ruber* P. Micheli ex Pers. plus *Clathrus delicatus* Berk. and Broome, *Clathrus columnatus* Bosc, *Clathrus natalensis* G.S. Medeiros, Melanda, T.S. Cabral, B.D.B Silva and Baseia, and *Abrachium floriforme* (Baseia and Calonge) Baseia and T.S. Cabral. *Abrachium* is represented here by only one collection (holotype of the type species). Sequences of *C. archeri* and *C. chrysomycelinus* are related to species of *Aseroë* and *Ileodictyon*, respectively; as mentioned previously, these should be further investigated for a possible reannotation or recombination.

Lysuraceae

In the family *Lysuraceae*, sequences named under *Lysurus* and *Aseroë* are included, although the latter has been formally classified in *Clathraceae*. Sequences are distributed in four well-supported clades (**Figure 4**). The most well-sampled clade includes sequences of *Lysurus arachnoideus* (E. Fischer) Trierv.-Per. and Hosaka (=*Aseroë aracnoidea* E. Fisch.), *Aseroë coccinea* Imazeki and Yoshimi, and *Lysurus borealis* (Burt) Henn. (=*Lysurus cruciatus* Henn.). Our results confirm the synonymizing of *A. aracnoidea* in *Lysurus* (Trierveiler-Pereira et al., 2014a), and based on the individuals retrieved, *L. borealis* is the confirmed synonym of *L. cruciatus* (Dring, 1980). The other three clades represent the following three taxa: *Lysurus periphragmoides* (Klotzsch) Dring from Japan (Caffot et al., 2018), the type species *Lysurus mokusin* (L.) Fr., and *Lysurus sphaerocephalum* (Schltdl.) Hern. Caff., Urcelay, Hosaka and L.S. Domínguez., with the latter considered an invalid name (Index Fungorum, 2020; MycoBank., 2020) according to Art. F.5.1 (Shenzhen), due to the absence of an identifier-issued citation in a recognized repository.

Phallaceae

This family is composed of *Itajahya*, *Phallus* (=*Dictyophora*), *Mutinus* (=*Jansia*), and *Xylophallus* (**Figure 4**). The type species *P. impudicus* is represented by two individuals that are positioned in two different clades, although the collection OSC107655 is closer to other sequences of *P. hadriani* Vent. and most likely is misidentified as *P. impudicus*. Anyway, the identity and positioning of *P. impudicus* deserve further investigations. Sequences of *Phallus indusiatus* Vent. closer to *Phallus rubrovolvatus* (M. Zang, D.G. Ji and X.X. Liu) Kreisel also most likely represent misidentification.

Itajahya, recognized as monophyletic and sister to *Phallus*, is represented by sequences of *Itajahya rosea* (Delile) E. Fisch. and *Itajahya galericulata* Möller. Sister to *Itajahya* and *Phallus* is the clade formed by *Mutinus* and *Xylophallus*. *Mutinus* is represented by eight species, including the type species *Mutinus caninus* (Huds.) Fr. and *Jansia boninensis* Lloyd. *Xylophallus* is represented by

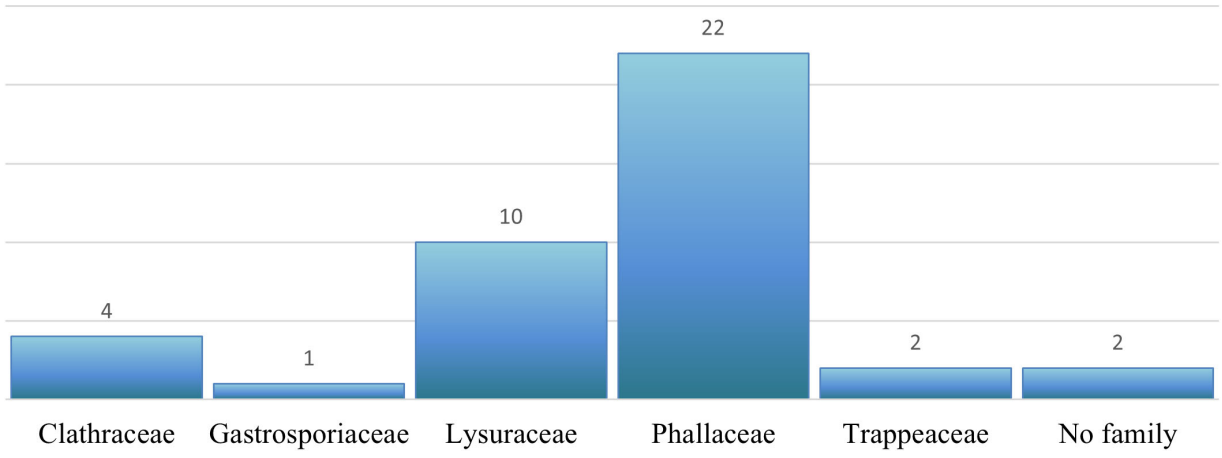


FIGURE 5 | Number of undetermined *Phallales* individuals and their putative family level classification according to the phylogenetic position of the sequences recovered.

Xylophallus clavatus T.S. Cabral, M.P. Martín, C.R. Clement, K. Hosaka and Baseia and the type species *Xylophallus xylogenus* (Mont.) E. Fisch.

Gastrosporiaceae

Gastrosporiaceae is delimited in our analysis with high support (PP = 0.98, MLbs = 80) and sharing a common ancestor with *Phallaceae*, with both families (*Gastrosporiaceae* and *Phallaceae*) as sister of *Lysuraceae* (**Figure 4**). This monogeneric family is here represented by sequences of *Gastrosporium gossypinum* T. Kasuya, S. Hanawa and K. Hosaka, and the type species *Gastrosporium simplex* Mattir.

Protophallaceae

Protophallaceae is represented by the genus *Protubera* with the type species *Protubera maracuja* Möller plus *Protubera beijingensis* G.J. Li and R.L. Zhao, *Protubera borealis* S. Imai, *Protubera jamaicensis* (Murrill) Zeller, *Protubera nipponica* Kobayasi, *Protubera sabulonensis* Malloch, and *Protubera parvispora* Castellano and Beever (**Figure 4**). *Protubera parvispora* (OSC59689) was not placed in the *Protophallaceae* clade in the *ATP*6 tree (**Supplementary Figure 3B**), but it was in *Protophallaceae* in the other analyses (combined, nuc-LSU, *RPB*2, and *TEF*1-α).

Claustulaceae

In the *Claustulaceae*, clustered sequences were named *Claustula*, *Gelopellis*, *Kjeldsenia*, and *Phlebogaster* (**Figure 4**). *Claustula* and *Gelopellis* formed a monophyletic clade represented by four individuals including their type species: *Claustula fischeri* K.M. Curtis (type country New Zealand) and *Gelopellis macrospora* Zeller (type country Chile). *Gelopellis macrospora* is represented by a sample from Argentina, whereas *C. fischeri* is represented by two individuals from New Zealand, but these did not cluster together in our analyses, which puts into doubt the identification of one or more of these individuals as *C. fischeri*. The other clade in *Claustulaceae* is formed by *Kjeldsenia* and *Phlebogaster* represented by their type species: *Kjeldsenia aureispora* W. Colgan, Castellano and Bougher and *Phlebogaster laurisylvicola* Fogel, respectively. We retrieved two sequences (nuc-LSU and *TEF*1-α) of one individual of *P. laurisylvicola* (CUP 1289), which appears close to *Hysterangium* species in the nuc-LSU analyses (**Supplementary Figure 2B**) but is in *Claustulaceae* in the *TEF*1-α (**Supplementary Figure 1A**) and the concatenated analyses (**Figure 4**), which support our classification of *Phlebogaster* in *Claustulaceae* (*Phallales*).

Trappeaceae

This family is represented as monophyletic (PP = 0.98, MLbs = 99) in the combined analyses by *Restingomyces*, *Phallobata*, and *Trappea* with their respective type species *R. reticulatus*, *Phallobata alba* G. Cunn., and *Trappea darkeri* (Zeller) Castellano, respectively (**Figure 4**). However, the sequences of these genera were not recovered as a single-family clade in some of the unique marker analyses: in *TEF*1-α (**Supplementary Figure 1A**) and *RPB*2 (**Supplementary Figure 3A**), *P. alba* and *T. darkeri* are recovered separately; in ITS (**Supplementary Figure 2A**), *R. reticulatus* and *T. darkeri* do not form a clade (although the individuals of *T. darkeri* in the ITS analyses are not the same as all the other analyses); in nuc-LSU (**Supplementary Figure 2B**) *T. darkeri* is external (PP = 0.96) to all *Phallales*, whereas *R. reticulatus* and *P. alba* clustered together but with no support.

Species Hypotheses Recognition

The clustering of the 479 sequences of ITS revealed 118 species hypotheses in *Phallales*, based on a sequence similarity threshold of 98.0%. In MycoBank. (2020), 576 legitimate specific names have already been deposited in *Phallales*. Our clustering shows that almost 20% of the total recognized species of *Phallales* have DNA sequences available, revealing that a lot of work remains to be done in this area.

Notes on Geographic Distribution, Lifestyle, and Edibility

Information on the country of origin included in DNA databases is available for 462 individuals (69.8%), from which 191 contain detailed information of the location but only 36 with the exact geographic coordinates. These individuals were distributed in 46 countries, which are concentrated in tropical and subtropical areas, with lower occurrence closer to the polar circles. Estonia is the source of the highest number of sequences (131) and individuals (131) deposited, all ITS. The United States is the second most sampled country, with 121 sequences of 79 individuals, and China is the third, with 108 sequences of 72 individuals. A map of global distribution of all phalloid individuals segregated by genera can be observed in **Figure 6**. For all 22 recognized genera, only *Phallobata* is not represented on the map, because there is no location information for the voucher. Individuals named under *Jansia* are represented as *Mutinus*, and those under *Dictyophora* as *Phallus* (**Supplementary Table 4**).

A total of 168 individuals (25.3%) are from environmental samples, including 148 individuals from soil, eight from roots of *Bouteloua gracilis* (Willd. ex Kunth) Lag. ex Griffiths (blue grama), two from air filters, three from seedling stem [two from *Hevea nitida* Mart. ex Müll. Arg and one from *Micrandra spruceana* (Baill.) R. E. Schult.], one from heavy metal–contaminated soil, one from marine subsurface sediments, and one from house dust. According to the FungalTraits database (Põlme et al., 2021), a total of 21 phalloid genera recognized in our work are soil saprotrophic, and only *Phlebogaster* is mentioned as ectomycorrhizal.

Among the *Phallales* sequences sampled in our work and their respective published references, only *Phallus dongsun* T.H. Li, T. Li, Chun Y. Deng, W.Q. Deng and Zhu L. Yang is reported by Li et al. (2020) as an edible species commercially cultivated in China. To complement the list of edible species of *Phallales* with molecular data available, according to edibility categories proposed Li et al. (2021), our study includes 11 confirmed edible species (E1): *Ileodictyon cibarium*, *Phallus echinovolvatus* (M. Zang, D.R. Zheng and Z.X. Hu) Kreisel, *Phallus fuscoechinovolvatus* T.H. Li, B. Song and T. Li, *P. hadriani*, *P. indusiatus*, *Phallus luteus* (Liou and L. Hwang) T. Kasuya, *Phallus merulinus* (Berk.) Cooke (as *Dictyophora merulina* Berk.), *P. rubrovolvatus*, *Phallus ultraduplicatus* X.D. Yu, W. Lv, S.X. Lv, Xu H. Chen and Qin Wang, *Protubera nipponica* [as *Kobayasia nipponica* (Kobayasi) S. Imai and A. Kawam.], and *Pseudocolus fusiformis*; three confirmed edible species, but with conditions (E2): *Clathrus archeri*, *Phallus impudicus*, and *Phallus multicolor* (Berk. and Broome) Cooke (as *Dictyophora multicolor* Berk. and Broome); six unconfirmed edible species (E3): *Clathrus columnatus*, *Ileodictyon gracile*, *Jansia boninensis*, *Lysurus mokusin*, *L. periphragmoides*, *Phallus rugulosus* (E. Fisch.) Lloyd; and three poisonous species (P): *Lysurus arachnoideus*, *Mutinus bambusinus* (Zoll.) E. Fisch., and *M. caninus*.

Molecular data are available for 81.5% of the *Phallales* species mentioned by Li et al. (2021) as having a known edibility status. Only *Mutinus borneensis* Ces., *Phallus armeniacus* Pat., *Phallus fragrans* M. Zang, and *Phallus tenuis* (E. Fisch.) Kuntze lack public sequence data. *Mutinus borneensis* and *P. armeniacus* are categorized by the authors as E3 (unconfirmed edible species), *P. fragrans* as E1 (confirmed edible species), and *P. tenuis* as P (poisonous species).

DISCUSSION

Phallales Molecular Data From the Past 24 Years

The year 2006 can be marked as a huge advance in *Phallales* taxonomy with the work of Hosaka et al. (2006), a study aided by the Deep Hypha initiative (Blackwell et al., 2006). Hosaka et al. (2006) were responsible for 68 phalloid sequences deposited in GenBank (**Figure 3**), as well as the introduction of new markers (*ATP*6, *RPB*2, and *TEF*1-α). Another important turning point observed in **Figure 3** is the increased use of molecular data in many works focused on *Phallales* diversity since 2013: nuc-LSU sequences – Degreef et al. (2013); ITS sequences – Moreno et al. (2013), Lu et al. (2014), Cabral et al. (2015), Kim et al. (2015), Elwess and Latourelle (2016), Patel et al. (2018), and Bobade and Dahanukar (2020); nuc-LSU and *ATP*6 sequences – Marincowitz et al. (2015); ITS and nuc-LSU sequences – Pietras et al. (2016); ITS, nuc-LSU, *RPB*1 and *ATP*6 sequences – Garnica et al. (2016). Trierveiler-Pereira et al. (2014a) also merit a spotlight because of their phylogenetic review of *Phallales* using nuc-LSU, *ATP*6, and *RPB*2 markers and by generating 53 sequences.

Recognition of Families and Genera

Clathraceae

Clathraceae is characterized by fungi with clathrate (branched) or pseudostipitate and clathrate basidiomata that are named cage or lattice stinkhorns (Pegler and Gomez, 1994; Melanda et al., 2020). Individuals with clathrate format belong to *Blumenavia*, *Clathrus*, *Ileodictyon*, and *Laternea*, whereas those with prominent pseudostipe and a clathrate part composed of arms, armless, or lattice belong to *Abrachium*, *Aseroë*, *Colus*, and *Pseudocolus*. Cabral et al. (2012) accepted in *Clathraceae* the genera *Abrachium*, *Aseroë*, *Blumenavia*, *Clathrus*, *Pseudocolus*, *Lysurus*, and *Ileodictyon*. Our phylogenetic analyses, in agreement with Hosaka et al. (2006) and Trierveiler-Pereira et al. (2014a), show *Lysurus* as part of *Lysuraceae*. Based on morphological taxonomy using as the main diagnostic feature the disposition of the gleba in the receptacle, Pegler and Gomez (1994) classified the following genera in the *Clathraceae* series Lysuroid: *Aseroë*, *Colus*, *Lysurus*, *Kalchbrennera* Berk., *Neolysurus* O.K. Mill., *Pseudocolus*, and *Simblum* Klotzsch ex Hook. According to Pegler and Gomez (1994), these genera share the receptacle composed of a tubular and sterile pseudostipe, with the gleba attached to the upper portion of the receptacle. For Dring (1980), *Kalchbrennera* and *Simblum* were considered synonyms of *Lysurus*. However, our phylogeny (**Figure 4**) does not confirm this morphological approach as a natural character, with representatives of *Clathraceae* series Lysuroid sensu Pegler and Gomez (1994) in both *Clathraceae* (*Aseroë* and *Colus*) and *Lysuraceae* (*Lysurus*).

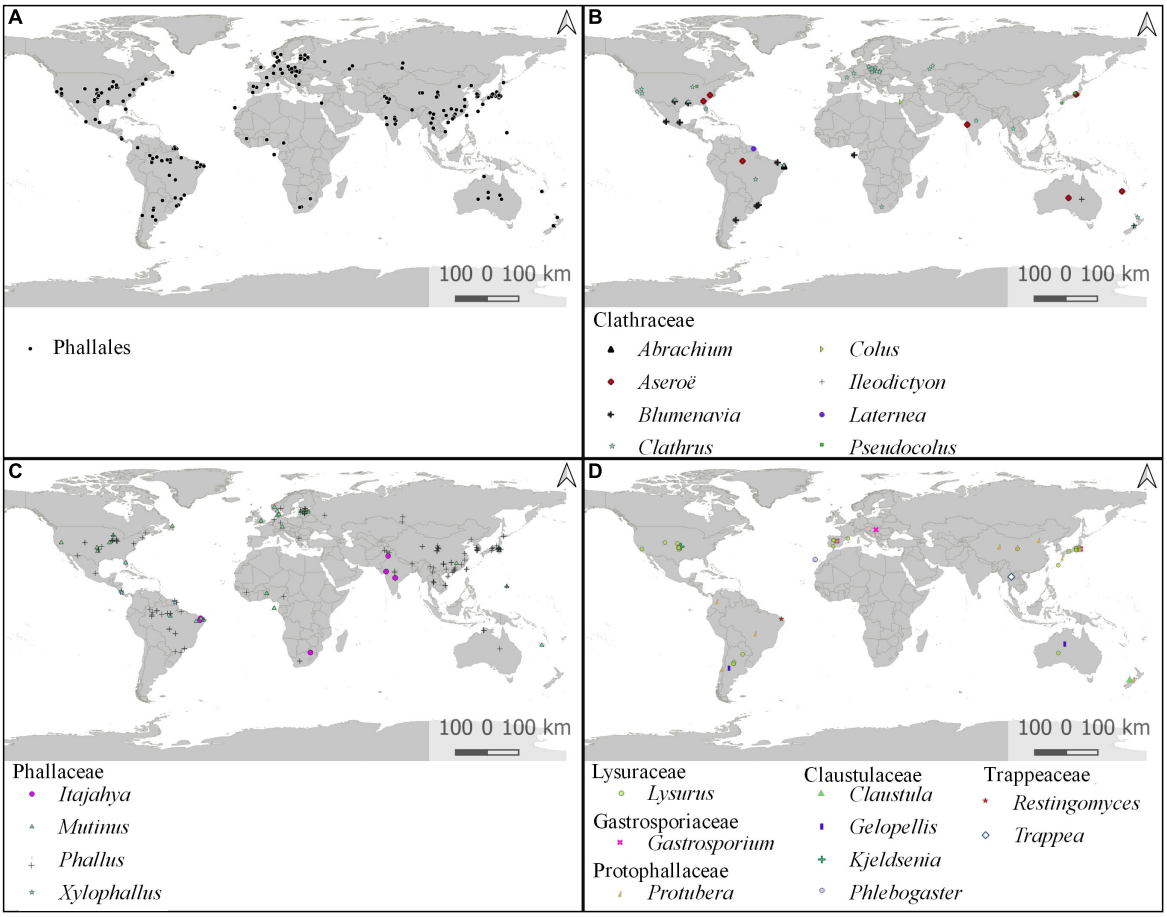


FIGURE 6 | Global geographic distribution of *Phallales* based on samples with molecular sequences available and locality information. **(A)** Global distribution of all *Phallales* samples. Global distribution of **(B)** *Clathraceae* genera; **(C)** *Phallaceae* genera; **(D)** *Lysuraceae*, *Gastrosporiaceae*, *Protophallaceae*, *Claustulaceae*, and *Trappeaceae* genera.

The relationship of the type species of *Aseroë*, *A. rubra* from Australia (type country), and *C. archeri* (**Figure 4**) has been previously shown by Hosaka et al. (2006), Degreef et al. (2013), and Trierveiler-Pereira et al. (2014a). The name *C. archeri* is a result of the combination of *Lysurus archeri* Berk. (Dring, 1980), which also has *Anthurus archeri* (Berk.) E. Fisch. as a synonym. The morphological research into *Clathraceae* performed by Dring (1980) considered *Anthurus* as a synonym of *Clathrus*. No other sequences of any other name previously treated as *Anthurus* are available. Considering that the type species of *Clathrus* is found in another clade, another generic name must be investigated for *C. archeri*, with *Anthurus* and *Aseroë* being two putative names, considering this taxonomic history and the relationship shown in our analyses.

The positions of *Laternea* and *Blumenavia* indicate that they may belong to the same genus, in which *Laternea* would have nomenclatural priority. *Blumenavia* and *Laternea* are also grouped in a monophyletic clade, as previously observed by Degreef et al. (2013) and Trierveiler-Pereira et al. (2014a), although both of these works performed their phylogenetic analyses with only one individual of each genus. Melanda et al. (2020) reviewed *Blumenavia* but did not present any *Laternea* species in the phylogeny. Considering that the molecular global sampling of *Laternea* is represented by only one representative, new molecular studies involving *Laternea* are encouraged, so as to better understand the relationship between *Laternea* and *Blumenavia*.

The genus *Colus* was considered as a member of the family *Clathraceae*, based on a morphological approach by Cunningham (1944), Dring (1980), and Pegler and Gomez (1994); here, we confirm this classification and also encourage the generation of more sequences of this genus.

Clathrus was shown to be polyphyletic by Hosaka et al. (2006) and Trierveiler-Pereira et al. (2014a). The relationship between *Abrachium* and *Clathrus* was observed by Trierveiler-Pereira et al. (2014a), who showed *A. floriforme* in an unsupported clade with *C. ruber* (type species) and *C. columnatus*. *Abrachium* is a monospecific genus proposed by Cabral et al. (2012), with the type species *A. floriforme* being a combination from *Aseroë floriformis* Baseia and Calonge. Cabral et al. (2012) emended the family *Clathraceae* to include the armless sunflower-shaped receptacle characteristic of *Abrachium*. Based

on the high morphological variation between *Abrachium* and *Clathrus*, we have to wait for more sequences of abrachinoid individuals to infer any synonymy among the two genera, with *Clathrus* having nomenclatural priority. *Abrachium* appears to be widely distributed in the Atlantic Forest and Caatinga Biomes[5], and additional studies may show unknown diversity.

Linderia G. Cunn, *Linderiella* G. Cunn., *Ligiella* J.A. Sáenz, and other possible representatives of *Clathraceae* do not have any sequences available and need to be included in further molecular phylogenetic studies. MycoBank. (2020) and Index Fungorum (2020) consider *Linderiella* and *Linderia* as synonyms of *Clathrus*, whereas He et al. (2019) consider only *Linderiella* as a synonym of *Clathrus*, but the inclusion of sequences of these genera in phylogenetic studies can confirm their relationships.

Lysuraceae

The positioning of the type species of *Lysurus* (*L. mokusin*, type country: China) from the United States and Japan has been previously shown by Trierveiler-Pereira et al. (2014a). *Simblum*, *Kalchbrennera*, and *Neolysurus*, other possible representatives of *Lysuraceae*, do not have any sequences available and need to be included in further studies. *Simblum* and *Kalchbrennera* are considered synonyms of *Lysurus* by Dring (1980), He et al. (2019), and in Index Fungorum (2020), whereas MycoBank. (2020) considers only *Kalchbrennera* to be a synonym of *Lysurus*, but the inclusion of sequences of these genera in phylogenetic studies can clarify their relationships. *Lysurus periphragmoides* and *L. sphaerocephalum* (nom. inval.) are names that have been previously placed in *Simblum,* and the phylogenetic placement of sequences under these names in our analyses could confirm the synonymizing between *Lysurus* and *Simblum*. *Simblum periphragmoides* Klotzsch and *S. sphaerocephalum* Schltdl. were considered as heterotypic synonyms by Dring (1980), who proposed the combination *L. periphragmoides*, but this synonymizing was not accepted by Caffot et al. (2018), and based on our analyses (**Figure 4**) it is also not confirmed. Considering the positioning of sequences named *A. coccinea* in the *Lysuraceae*, we encourage further studies to investigate the generic status of this taxon and the identity of the individuals under this name.

Phallaceae

Li et al. (2014, 2016) provided phylogenetic data to show that *Dictyophora* and *Phallus* should be treated as a single genus, *Phallus*. Cabral et al. (2019) described a high diversity in *Phallus indusiatus*, a species complex well-known for the presence of an indusium; however, *P. indusiatus* actually represents at least four phylogenetic species. Li et al. (2020) published the new species *P. dongsun*, which is not included in our concatenated tree, and mentioned that samples named *P. impudicus* from China represent *P. dongsun*, as *P. impudicus* is a species described from Europe (the type locality of *P. impudicus*). As previously mentioned, the identity of the sequences named *P. impudicus* recovered in our analyses needs further examination in order to obtain a robust view of the phylogenetic position of the species.

Kreisel (1996) accepted the genus *Itajahya* as *Phallus* subgenus *Itajahya*. In the same work, the type species of *Itajahya*, *I. galericulata*, originally described from South Brazil (Möller, 1895), was combined in *Phallus galericulatus* (Möller) Kreisel (Kreisel, 1996). However, based on our analyses (**Figure 4**), *I. galericulata* is clustered in a clade separate from *Phallus* and together with other *Itajahya* species, which does not justify the classification and the synonymizing proposed by Kreisel (1996). For *Mutinus* and *Jansia*, however, they are considered synonymous as previously pointed out by Crous et al. (2017). The positioning of *Xylophallus* as sister to *Mutinus* has been previously shown by Trierveiler-Pereira et al. (2014a) and Crous et al. (2018).

There are no molecular data for *Aporophallus* Möller, *Floccomutinus* Henn., and *Staheliomyces* E. Fisch., all genera also accepted in *Phallaceae* (Index Fungorum, 2020; MycoBank., 2020), although *Floccomutinus* is considered a synonym of *Mutinus* by He et al. (2019) and in MycoBank. (2020). *Aporophallus* and *Staheliomyces* are monospecific genera, and their revision will be highly relevant. Sequences of taxa dealt under *Floccomutinus* could be useful to better assess their relationships with *Mutinus*.

Gastrosporiaceae

The monogeneric family *Gastrosporiaceae* was confirmed as part of *Phallales* in our study and also by previous authors: Kirk et al. (2008), Trierveiler-Pereira et al. (2014a), He et al. (2019), Kasuya et al. (2020), and Wijayawardene et al. (2020). The genus *Gastrosporium* contains three described species: *G. simplex* (type species) from Italy, *G. asiaticum* Dörfelt and Bumžaa from Mongolia, and *G. gossypinum* from Japan (Honshu). The positioning of the family *Gastrosporiaceae* external to *Phallaceae* in our phylogeny (**Figure 4**) rejects the suggestion by Hosaka et al. (2006), who did not include *Gastrosporium* in their analyses and thus suggested that the ancestor of *Clathraceae*, *Phallaceae*, and *Lysuraceae* could be the point of transition from sequestrated to expanded basidiomata in *Phallales*.

Protophallaceae

Protophallaceae is represented in our analyses only by *Protubera* species, as also shown by Trierveiler-Pereira et al. (2014a,b). *Protophallaceae* was proposed by Zeller (1939) with species of *Calvarula*, *Protophallus* Murril, and *Protubera*. *Calvarula* is not included in our combined analyses (**Figure 4**), and the identity of the individual EF5-1 as *C. excavata* needs to be investigated. Additional individuals and sequences of *Calvarula* are needed to clarify its family level positioning. *Protophallus* is considered a synonym of *Protubera* (Malloch, 1989; He et al., 2019), and the positioning of *Protubera jamaicensis* (=*Protophallus jamaicensis* Murrill) in our analyses (**Figure 4**) confirms this synonymization.

Sanshi and Kawamura (1958) analyzed specimens of *Protubera* from Japan and proposed a new genus named *Kobayasia* S. Imai and A. Kawam. to accommodate *Protubera nipponica*. However, Hosaka et al. (2006) and Trierveiler-Pereira et al. (2014a,b) have shown sequences of

[5]https://www.gbif.org/occurrence/map?taxon_key=7812817

P. nipponica within the clade formed by other *Protubera*, as also shown in our analyses (**Figure 4**), which does not justify *Kobayasia* as a separate genus and confirms its synonymization under *Protubera*. *Kobayasia kunmingica* M. Zang, K. Tao and X.X. Liu is the only other species described in *Kobayasia,* and its phylogenetic positioning should be investigated to better understand the relationship between *Protubera* and *Kobayasia*.

The relationship of *Protubera borealis* (voucher OKM21898) and *P. sabulonensis* has been shown by Hosaka et al. (2006) and Cabral et al. (2012). Sanshi and Kawamura (1958) considered *Protubera borealis* under the genus *Protuberella* S. Imai and A. Kawam. as *Protuberella borealis* (S. Imai) S. Imai and A. Kawam. However, the recognition of *Protuberella* as a separate genus was not accepted by Hosaka et al. (2006), Cabral et al. (2012), and Li et al. (2018), and it is also not confirmed here (**Figure 4**), although it is still considered as a distinct genus by He et al. (2019) and in Index Fungorum (2020).

Besides the sequences of *Protubera* clustered in *Phallales*, some individuals (T20068, OSC59673, and OSC59699) named under *Protubera* (including *P. nothofagi* and *P. hautuensis*) clustered in *Hysterangiales* (our outgroup), in agreement with Hosaka et al. (2006) and Trierveiler-Pereira et al. (2014b), who classified *P. nothofagi* in *Gallaceae* and *P. hautuensis* in *Phallogastraceae*. However, based on the positioning of the type species *P. maracuja* in *Phallales*, this must be the best classification for *Protubera* and *Protophallaceae*. The positioning of the individuals named *Protubera canescens* and *P. clathroidea* in *Clathraceae* and *Lysuraceae*, respectively (**Supplementary Figures 1–3**), has been shown also by Hosaka et al. (2006), Degreef et al. (2013), and Trierveiler-Pereira et al. (2014b). According to May et al. (2010), *P. canescens* is an egg (immature) form of *Ileodictyon*, and for Trierveiler-Pereira et al. (2014b), these *Protubera* species out of *Protophallaceae* may be egg forms of expanded phalloid taxa or misidentification.

Claustulaceae

In this family clade, the four genera *Claustula*, *Gelopellis*, *Kjeldsenia*, and *Phlebogaster* clustered together as in Hosaka et al. (2006). In Trierveiler-Pereira et al. (2014a), the family clade was represented only by *Gelopellis* and *Claustula*. Although *Claustula* and *Gelopellis* clustered together, it would be important to have sequences of nondoubtful identification and more representatives of both genera to confirm whether they could be considered synonyms, of which *Claustula* has nomenclatural priority. Individuals of *Gelopellis* clustered out of *Claustulaceae*, in *Clathraceae* (**Supplementary Figures 2B**, **3A**), or external to *Phallaceae* (**Supplementary Figure 3B**), and they also need revision to confirm their identity or generic status, mainly because immature basidiomata can lead to misidentification of some expanded phalloids, as seen in individuals of *Protubera*.

Trappeaceae

The composition of *Trappeaceae* in our study by the three genera *Restingomyces*, *Phallobata*, and *Trappea* is in agreement with Sulzbacher et al. (2016). *Trappea* is the type genus of the family as established by Castellano (1990), in a study that mentioned that the genus represents a transition between *Clathraceae* and *Hysterangium*, and proposed the type species of *Trappea* based on *Hysterangium darkeri* Zeller. The positioning of *Trappea* in *Phallales* as a member of *Trappeaceae* is based on an individual of *T. darkeri* without information on the location, as also previously shown by Hosaka et al. (2006) and Sulzbacher et al. (2016). As in *Protubera*, some species of *Trappea* are also placed in *Hysterangiales*, but considering the positioning of its type species in *Phallales*, we confirm the classification of *Trappea* in *Phallales*. The positioning of some *Trappea* in *Hysterangiales* has also been observed by Hosaka et al. (2006) and Trierveiler-Pereira et al. (2014b), and both authors showed *T. phillipsii* and *T. pinyonensis* positioned in the *Phallogastraceae* (*Hysterangiales*) family. The identity or the generic status of these individuals of *Trappea* in *Hysterangiales* needs further revision.

Distribution, Lifestyle, and Edibility

The DNA databases contain many sequences of *Phallales* representatives without precise information on the collection location or even without any metadata. In addition, the sequences have a low representation across continents, which makes it impossible to draw any robust inferences about the biogeographical distribution of families, genera, species, and clades. Thus, we encourage the inclusion of DNA sequences from representatives of *Phallales* from underexplored locations, such as Africa and maritime Southeast Asia, as well as the sequencing of collections already deposited in herbaria around the world and of taxa not yet sequenced. These further data will contribute to a better understanding of the evolutionary processes and distribution patterns in *Phallales*.

The explanation for the high number of sequences from Estonia is the increase of studies of ITS using environmental samples and the high number of these sequences deposited in UNITE (see **Supplementary Table 1**). Other locations with a large number of *Phallales* records and DNA sequences are partly due to the proximity of the research centers and specialists in the group.

Studies of environmental biodiversity or other ecological approaches including phalloid species started in 2003 (Bidartondo et al., 2003) and has continued in a few works (Sato et al., 2012; Kellner et al., 2014; Skaltsas et al., 2019; Vu et al., 2019).

In the FungalTraits database (Põlme et al., 2021), all their genera in *Phallales* are classified as saprotrophic. The genera *Phallobata*, *Phlebogaster*, *Restingomyces*, and *Trappea* are classified as part of *Hysterangiales*, but we recognize them in *Phallales*. *Phlebogaster* is considered an ectomycorrhizal genus in FungalTraits. Thus, considering *Phlebogaster* in *Phallales*, as supported by our analyses, the *Phallales* lifestyle must be expanded to include both saprotrophic and ectomycorrhizal genera. The ectomycorrhizal habit of *Phlebogaster* is most likely based on Fogel (1980), who described *P. laurisylvicola* as a hypogeous taxon under the plant species *Laurus azorica* (Seub.) Franco (*Lauraceae* Lindley). Kreisel (2001), in a checklist of gasteroid fungi, also mentioned *P. laurisylvicola* in association with *L. azorica*. However, we did not find any confirmation and description of these associations as an ectomycorrhizal symbiosis.

We regard this species as putatively ectomycorrhizal, but further investigation is needed.

Hosaka et al. (2006) cited *Protubera canescens* as the only *Phallales* ectomycorrhizal, but according to May et al. (2010), this species is an immature form of *Ileodictyon*, as mentioned previously. In addition, Trierveiler-Pereira et al. (2014b) affirmed that all *Protubera* species are saprotrophic as reported in FungalTraits (Põlme et al., 2021). Therefore, we suggest further investigation to clarify the ectomycorrhizal association in this phalloid species.

Wild edible fungi are an important renewable natural resource in some regions, constituting important sources of income and nutrition. Despite their unpleasant odor, many representatives of *Phallales* are edible but are considered mushrooms with little culinary value. Stinkhorns are the most popular edible *Phallales* (Boa, 1988). The stinkhorn *Phallus* is the genus with the largest number of species with edible status (14: nine E1, two E2, two E3, and one P), followed by *Lysurus* (three E3 and one P) and *Mutinus* (one E3 and two P) that include only poisonous and unconfirmed edible species (Li et al., 2021). *Phallus* was reported by Li et al. (2021) as a genus with 43 described species, whereas He et al. (2019) reported 34 known species. Based on these numbers, the percentage of confirmed edible species in the genus represents 20.9 to 26.5%; however, the number of known species is probably underestimated because MycoBank. (2020) lists approximately 125 legitimate specific names for the genus. For *Phallales*, considering the 576 legitimate specific names recognized in MycoBank. (2020), the number of confirmed edible species in the order represents only 2.1%, whereas the number of poisonous species represents only 0.7%. The proportion of the number of confirmed edible and poisonous species in *Phallales* in relation to the 118 SHs that we found is 10.2 and 3.4%, respectively. This confirms that the edibility of *Phallales* species is poorly explored.

Many stinkhorns are consumed in the egg stage because of their tasty flavor (Phillips et al., 2018). In Germany and North America, the egg stage of *Phallus* is sold canned or fresh (Læssøe and Spooner, 1994). In China, *L. mokusin* and *P. rubrovolvatus* (as *Dictyophora rubrovolvata* M. Zang, D.G. Ji and X.X. Liu) are considered edible (Læssøe and Spooner, 1994). In addition, *P. indusiatus* and *P. dongsun* stand out in China for their flavor, where they are commercially cultivated (Boa, 1988; Li et al., 2020) and represent an important economic product. Despite the nutritional and commercial importance, the consumption of wild stinkhorns is not recommended unless their taxonomic affiliation is known with certainty because some of them are poisonous, such as species of *Lysurus* and *Mutinus*. Additionally, some species of the same genus are confirmed edible, whereas others are controversial, such as *P. tenuis*, which is considered poisonous (Li et al., 2021).

CONCLUSION

This work presents a summary of studies using molecular tools in *Phallales*. In general, as in other groups of fungi, these tools clarify results of previous studies based on morphology; also, the use of combined markers has allowed a clearer delimitation and positioning of the families and genera. Although we recognized seven families and 22 genera in *Phallales*, an extra effort is needed in taxonomic studies of the genera *Abrachium*, *Aseroë*, *Blumenavia*, *Clathrus*, *Claustula*, *Gelopellis*, *Laternea*, *Protubera*, *Pseudocolus*, and *Trappea*, because some inconsistencies in species identification and positioning of their representatives should be clarified. It is also necessary to include sequences of the genera *Aporophallus* (*Phallaceae*), *Floccomutinus* (*Phallaceae*), *Kalchbrennera* (*Lysuraceae*), *Ligiella* (*Clathraceae*), *Linderia* (*Clathraceae*), *Linderiella* (*Clathraceae*), *Neolysurus* (*Lysuraceae*), and *Staheliomyces* (*Phallaceae*). The DNA databases are an excellent source of molecular data, both when searching for sequences and in helping to understand the evolution of traits shown in previous studies, but missing metadata can be a stalemate for that. Therefore, it is vital to fill in the records in DNA databases correctly and accurately.

Since the inclusion of molecular tools for systematics studies, considerable progress has been achieved in the taxonomic and evolutionary study of fungi. Sequences of different markers deposited in databases represent a valuable repository that is still poorly exploited. The data we utilized have been shown to be a good, no-cost tool to clarify taxonomic and systematics problems, test phylogenetic position of misidentified sequences, examine the geographic distribution of groups, explore the ecology and use of phalloid species, and to visualize where our knowledge gaps are. We therefore encourage all mycologists to conduct extensive reviews of molecular data available for their particular fungal taxa of expertise.

DATA AVAILABILITY STATEMENT

The datasets presented in this study can be found in online repositories. The names of the repository/repositories and accession number(s) can be found in the article/**Supplementary Material**.

AUTHOR CONTRIBUTIONS

GM and NM designed the project. ALe, GM, and NM extracted the data. GM organized the metadata. ALi, AS-F, ALe, GM, NA, and RF analyzed the data. ALi and GM performed quantitative analyses. AS-F performed BLAST and phylogenetic analyses. ALe performed species hypothesis recognition. GM, MM, AS-F, ALi, ALe, TC, NM, and RF wrote the draft. IB, MM, and NM supervised the project. All authors reviewed and approved the manuscript.

FUNDING

This work was supported by 'Coordenação de Aperfeiçoamento de Pessoal de Nível Superior' (CAPES) – Finance code 001 (Process 23077.056677/2021-47), and for AS-F and NA's scholarships; 'Conselho Nacional de Desenvolvimento Científico e Tecnológico' (CNPq) for GM's scholarship (Process

140541/2018-7); 'Fundação de Amparo a Ciência e Tecnologia do Estado de Pernambuco' (FACEPE) for ALi's scholarship; Special Visiting Researcher – PVE/CNPq (Process 407474/2013–7) given to IB and MM; and 'Fundação de Amparo à Pesquisa do Estado de São Paulo' (FAPESP) Grant #2018/15677-0 given to NM.

ACKNOWLEDGMENTS

All authors thank the funding agency CAPES for paying the fees of publication. AS-F and NA thank the funding agency CAPES; GM thanks CNPq; and ALi thanks FACEPE, for the scholarships. IB and MM thank to PVE/CNPq; and NM thanks to FAPESP, for the researchers grants. The authors are grateful to Paul Kirk for giving data from Index Fungorum of *Phallales* in Excel format; and to Clark L. Ovrebo, Manuel Tabarés, and Marcelo A. Sulzbacher for some photographs of basidiomata included in **Figure 1**. Thanks to Susan Catherine Casement Moreira and Marian Glenn for English revision.

SUPPLEMENTARY MATERIAL

The Supplementary Material for this article can be found online at: https://www.frontiersin.org/articles/10.3389/fmicb.2021.689374/full#supplementary-material

Supplementary Figure 1 | Phylogenetic trees of the *Phallales* order obtained with *TEF*1-α **(A)** and mt-SSU **(B)**. Names in blue and question marks indicate individuals with uncertain position or that represent a misidentification. Individuals retrieved without a genus name are represented in red with the possible species name based on our analyses given first. Family clades are colored in green shades and named on the right. Tree topology is based on the Bayesian analyses. Numbers on branches are posterior probabilities (PP, before slash) and maximum likelihood bootstrap values (MLbs, after slash). Thickened branches in boldface indicate fully supported nodes (PP = 1, MLbs = 100). Scale bar indicates expected changes per site.

Supplementary Figure 2 | Phylogenetic trees of the *Phallales* order obtained with ITS **(A)** and nuc-LSU **(B)**. Names in blue and question marks indicate individuals with uncertain position or that represent a misidentification. Individuals retrieved without a genus name are represented in red with the possible species name based on our analyses given first. Family clades are colored in green shades and named on the right. Tree topology is based on the Bayesian analyses. Numbers on branches are posterior probabilities (PP, before slash) and maximum likelihood bootstrap values (MLbs, after slash). Thickened branches in boldface indicate fully supported nodes (PP = 1, MLbs = 100). Scale bar indicates expected changes per site.

Supplementary Figure 3 | Phylogenetic tree of the *Phallales* order obtained with *RPB2* **(A)** and *ATP6* **(B)**. Names in blue and question marks indicate individuals with uncertain position or that represent a misidentification. Individuals retrieved without a genus name are represented in red with the possible species name based on our analyses given first. Family clades are colored in green shades and named on the right. Tree topology is based on the Bayesian analyses. Numbers on branches are posterior probabilities (PP, before slash) and maximum likelihood bootstrap values (MLbs, after slash). Thickened branches in boldface indicate fully supported nodes (PP = 1, MLbs = 100). Scale bar indicates expected changes per site.

Supplementary Table 1 | General data compilation of all *Phallales* sequences recovered.

Supplementary Table 2 | GenBank accession numbers for the outgroup used in phylogenetic analyses for individual markers.

Supplementary Table 3 | Taxa, individuals, and accession numbers of sequences used in phylogenetic analyses from the combined dataset.

Supplementary Table 4 | Taxa, individuals, and their respective geographic location used for the global distribution map.

Supplementary Table 5 | Type collections and collections of reference (REF.) in *Phallales* with the respective GenBank accession numbers. When the status of the type is unknown, only "type" is indicated.

Supplementary Table 6 | Putative identification for the undetermined *Phallales* individuals recovered.

REFERENCES

Bidartondo, M. I., Bruns, T. D., Weiß, M., Sérgio, C., and Read, D. J. (2003). Specialized cheating of the ectomycorrhizal symbiosis by an epiparasitic liverwort. *Proc. R. Soc. B Biol. Sci.* 270, 835–842. doi: 10.1098/rspb.2002.2299

Binder, M., and Hibbett, D. S. (2002). Higher-level phylogenetic relationships of homobasidiomycetes (mushroom-forming fungi) inferred from four rDNA regions. *Mol. Phylogenet. Evol.* 22, 76–90. doi: 10.1006/mpev.2001.1043

Blackwell, M., Hibbett, D. S., Taylor, J. W., and Spatafora, J. W. (2006). Research coordination networks: a phylogeny for kingdom Fungi (Deep Hypha). *Mycologia* 98, 829–837. doi: 10.1080/15572536.2006.11832613

Boa, E. (1988). Edible stinkhorns? *Mycologist* 2, 107–108. doi: 10.1016/S0269-915X(88)80072-7

Bobade, V., and Dahanukar, N. (2020). Molecular characterization of stinkhorn fungus *Aseroë coccinea* Imazeki et Yoshimi ex Kasuya 2007 (Basidiomycota: Agaricomycetes: Phallales) from India. *J. Threat. Taxa* 12, 15530–15534. doi: 10.11609/jott.5091.12.4.15530-15534

Cabral, T. S., Clement, C. R., and Baseia, I. G. (2015). Amazonian phalloids: New records for Brazil and South America. *Mycotaxon* 130, 315–320. doi: 10.5248/130.315

Cabral, T. S., Marinho, P., Goto, T. B., and Baseia, I. G. (2012). *Abrachium*, a new genus in the Clathraceae, and *Itajahya* reassessed. *Mycotaxon* 119, 419–429. doi: 10.5248/119.419

Cabral, T. S., Silva, B. D. B., Martín, M. P., Clement, C. R., Hosaka, K., and Baseia, I. G. (2019). Behind the veil - exploring the diversity in *Phallus indusiatus* s.l. (Phallomycetidae, Basidiomycota). *MycoKeys* 58, 103–127. doi: 10.3897/mycokeys.58.35324

Caffot, M. L. H., Hosaka, K., Domínguez, L. S., and Urcelay, C. (2018). Molecular and morphological data validate the new combination of *Lysurus sphaerocephalum* from Argentina, with some additional records on Phallales (Agaricomycetes). *Mycologia* 110, 419–433. doi: 10.1080/00275514.2018.1456834

Castellano, M. A. (1990). The new genus *Trappea* (Basidiomycotina, Hysterangiaceae), a segregate from *Hysterangium*. *Mycotaxon* 38, 1–9.

Corda, A. C. J. (1842). *Icones fungorum hucusque cognitorum*. Prague: J.G. Calve, 92.

Crous, P. W., Wingfield, M. J., Burgess, T. I., Carnegie, A. J., Hardy, G. E. S. J., Smith, D., et al. (2017). Fungal Planet description sheets: 625–715. *Persoonia* 39, 270–467. doi: 10.3767/persoonia.2017.39.11

Crous, P. W., Wingfield, M. J., Burgess, T. I., Hardy, G. E. S. J., Gené, J., Guarro, J., et al. (2018). Fungal Planet description sheets: 716–784. *Persoonia* 40, 240–393. doi: 10.3767/persoonia.2018.40.10

Cunningham, G. H. (1931). The Gasteromycetes of Australasia. XI. The Phallales. Part II. *Proc. Linn. Soc. New South Wales* 56, 182–200.

Cunningham, G. H. (1944). *The Gasteromycetes of Australia and New Zealand*. New Zealand: Dunedin, J. Mclndoe, 236.

Darriba, D., Taboada, G. L., Doallo, R., and Posada, D. (2012). jModelTest 2: more models, new heuristics and high-performance computing Europe PMC Funders Group. *Nat. Methods* 9, 772. doi: 10.1038/nmeth.2109

Degreef, J., Amalfi, M., Decock, C., and Demoulin, V. (2013). Two rare Phallales recorded from São Tomé. *Cryptogam. Mycol.* 34, 3–13. doi: 10.7872/crym.v34.iss1.2013.3

Dring, D. M. (1980). Contributions towards a rational arrangement of the Clathraceae. *Kew Bull.* 35, 1–96. doi: 10.2307/4117008

Elwess, N. L., and Latourelle, S. M. (2016). DNA Barcoding and phylogenetic characterization of mushrooms with in the adirondack park. *J. Agric. Res.* 2, 28–43.

Fischer, E. (1898). "Phallineae," in *Die natürlichen Pflanzenfamilien, Teil. Abteilung. Leipzig*, eds A. Engler and K. Prantl 276–296.

Fogel, R. (1980). Additions to the hypogeous mycoflora of the Canary Islands and Madeira. *Contrib. Univ. Michigan Herb.* 14, 75–82.

Garnica, S., Riess, K., Schön, M. E., Oberwinkler, F., and Setaro, S. D. (2016). Divergence times and phylogenetic patterns of Sebacinales, a highly diverse and widespread fungal lineage. *PLoS One* 11:0149531. doi: 10.1371/journal.pone.0149531

Gouy, M., Guindon, S., and Gascuel, O. (2010). SeaView version 4: A multiplatform graphical user interface for sequence alignment and phylogenetic tree building. *Mol. Biol. Evol.* 27, 221–224. doi: 10.1093/molbev/msp259

He, M. Q., Zhao, R. L., Hyde, K. D., Begerow, D., Kemler, M., Yurkov, A., et al. (2019). Notes, outline and divergence times of Basidiomycota. *Fungal Divers.* 99, 105–367. doi: 10.1007/s13225-019-00435-4

Hibbett, D. S., and Binder, M. (2002). Evolution of complex fruiting-body morphologies in homobasidiomycetes. *Proc. R. Soc. B* 269, 1963–1969. doi: 10.1098/rspb.2002.2123

Hibbett, D. S., Pine, E. M., Langer, E., Langer, G., and Donoghue, M. J. (1997). Evolution of gilled mushrooms and puffballs inferrred from ribosomal DNA sequences. *Proc. Natl. Acad. Sci.* 94, 12002–12006. doi: 10.1073/pnas.94.22.12002

Hibbett, D. S., and Thorn, R. G. (2001). "Basidiomycota: Homobasidiomycetes," in *The Mycota VII Part B: Systematics and Evolution*, eds D. J. McLaughlin, E. G. McLaughlin, and P. A. Lemke (Berlin Heidelberg: Springer-Verlag), 121–168. doi: 10.1007/978-3-662-10189-6_5

Hosaka, K., Bates, S. T., Beever, R. E., Castellano, M. A., Colgan, W., Domínguez, L. S., et al. (2006). Molecular phylogenetics of the gomphoid-phalloid fungi with an establishment of the new subclass Phallomycetidae and two new orders. *Mycologia* 98, 949–959. doi: 10.3852/mycologia.98.6.949

Huang, Y., Niu, B., Gao, Y., Fu, L., and Li, W. (2010). CD-HIT Suite: A web server for clustering and comparing biological sequences. *Bioinformatics* 26, 680–682. doi: 10.1093/bioinformatics/btq003

Index Fungorum (2020). *Excel version of the list of Phallales present in Index Fungorum send by e-mail by Paul Kirk*. Available Online at: http://www.indexfungorum.org/ (accessed August 14, 2020).

Jülich, W. (1981). *Higher taxa of Basidiomycetes*. Vaduz: J. Cramer Verlog.

Kasuya, T., Hanawa, S., and Hosaka, K. (2020). A new species of *Gastrosporium* (Phallales) from coastal sand dunes of Ibaraki Prefecture, central Japan. *Truffology* 3, 9–16.

Katoh, K., and Standley, D. M. (2013). MAFFT multiple sequence alignment software version 7: Improvements in performance and usability. *Mol. Biol. Evol.* 30, 772–780. doi: 10.1093/molbev/mst010

Kellner, H., Luis, P., Pecyna, M. J., Barbi, F., Kapturska, D., Kruğer, D., et al. (2014). Widespread occurrence of expressed fungal secretory peroxidases in forest soils. *PLoS One* 9:e95557. doi: 10.1371/journal.pone.0095557

Kim, C. S., Jo, J. W., Kwag, Y. N., Sung, G. H., gee Lee, S., Kim, S. Y., et al. (2015). Mushroom flora of ulleung-gun and a newly recorded *Bovista* species in the Republic of Korea. *Mycobiology* 43, 239–257. doi: 10.5941/MYCO.2015.43.3.239

Kirk, P. M., Cannon, D. W., Minter, D. W., and Stalpers, J. A. (2008). *Dictionary of the Fungi*, 10th Edn. Switzerland: CABI Europe.

Kreisel, H. (1996). A preliminary survey of the genus *Phallus* sensu lato. *Czech Mycol.* 48, 273–281. doi: 10.33585/cmy.48407

Kreisel, H. (2001). Checklist of the gasteral and secotioid *Basidiomycetes* of Europe, Africa, and the Middle East. *Osterr. Z. Pilzkd.* 10, 213–313.

Krüger, D., Binder, M., Fischer, M., and Kreisel, H. (2001). The Lycoperdales. A molecular approach to the systematics of some gasteroid mushrooms. *Mycologia* 93, 947–957. doi: 10.2307/3761759

Li, G., Deng, D., Wei, J., Zhang, C., Zhao, R., and Lin, F. (2018). *Protubera beijingensis* sp. nov. (Protophallaceae, Phallales) from China. *Phytotaxa* 348, 133–140. doi: 10.11646/phytotaxa.348.2.8

Li, H., Ma, X., Mortimer, P. E., Karunarathna, S. C., Xu, J., and Hyde, K. D. (2016). *Phallus haitangensis*, a new species of stinkhorn from Yunnan province, China. *Phytotaxa* 280, 116–128. doi: 10.11646/phytotaxa.280.2.2

Li, H., Mortimer, P. E., Karunarathna, S. C., Xu, J., and Hyde, K. D. (2014). New species of *Phallus* from a subtropical forest in Xishuangbanna, China. *Phytotaxa* 163, 91–103. doi: 10.11646/phytotaxa.163.2.3

Li, H., Tian, Y., Menolli, N., Ye, L., Karunarathna, S. C., Perez-Moreno, J., et al. (2021). Reviewing the world's edible mushroom species: A new evidence-based classification system. *Compr. Rev. Food Sci. Food Saf.* 20, 1982–2014. doi: 10.1111/1541-4337.12708

Li, T., Li, T., Deng, W., Song, B., Deng, C., and Yang, Z. L. (2020). *Phallus dongsun* and *P. lutescens*, two new species of Phallaceae (Basidiomycota) from China. *Phytotaxa* 443, 19–37. doi: 10.11646/phytotaxa.443.1.3

Lu, Y., Gui, Y., Gong, G., Wei, S., and Zhu, G. (2014). Genetic diversity of 18 *Dictyophora rubrovolvata* germplasm resources from Guizhou. *Guizhou Agric. Sci.* 42, 17–20.

Læssøe, T., and Spooner, B. (1994). The uses of 'Gasteromycetes'. *Mycologist* 8, 154–159. doi: 10.1016/S0269-915X(09)80179-1

Malloch, D. (1989). Notes on the genus *Protubera* (Phallales). *Mycotaxon* 34, 133–151.

Marincowitz, S., Coetzee, M. P. A., Wilken, P. M., Wingfield, B. D., and Wingfield, M. J. (2015). Phylogenetic placement of *Itajahya*: An unusual Jacaranda fungal associate. *IMA Fungus* 6, 257–262. doi: 10.5598/imafungus.2015.06.02.01

May, T. W., Sinnott, N., and Sinnott, A. (2010). The truffle-like "*Protubera canescens*" is an early developmental stage of the cage fungus "*Ileodictyon*.". *Vic. Nat.* 127, 49–54.

Melanda, G. C. S., Accioly, T., Ferreira, R. J., Rodrigues, A. C. M., Cabral, T. S., Coelho, G., et al. (2020). Diversity trapped in cages: Revision of *Blumenavia* Möller (Clathraceae, Basidiomycota) reveals three hidden species. *PLoS One* 15:e0232467. doi: 10.1371/journal.pone.0232467

Miller, M. A., Pfeiffer, W., and Schwartz, T. (2010). Creating the CIPRES Science Gateway for inference of large phylogenetic trees. 2010 Gatew. *Comput. Environ. Work. GCE* 2010, 1–8. doi: 10.1109/GCE.2010.5676129

Miller, O. K., and Miller, H. H. (1988). *Gasteromycetes: Morphological and Development Features*. Eureka, CA: Mad Rivers Press.

Möller, A. (1895). *Brasilische Pilzblumen. Botanische Mitteilungen aus den Tropen 7*. Germen: Jena,G. Fischer.

Moreno, G., Khalid, A. N., Alvarado, P., and Kreisel, H. (2013). *Phallus hadriani* and *P. roseus* from Pakistan. *Mycotaxon* 125, 45–51. doi: 10.5248/125.45

MycoBank (2020). *Excel version of the list of taxa present in MycoBank*. Available Online at: https://www.mycobank.org/ (accessed August 11, 2020).

NCBI BLAST (2020). *NCBI Nucleotide BLAST*. Available Online at: https://blast.ncbi.nlm.nih.gov/Blast.cgi (accessed September 1, 2020).

Nilsson, R. H., Larsson, K. H., Taylor, A. F. S., Bengtsson-Palme, J., Jeppesen, T. S., Schigel, D., et al. (2019). The UNITE database for molecular identification of fungi: Handling dark taxa and parallel taxonomic classifications. *Nucleic Acids Res.* 47, D259–D264. doi: 10.1093/nar/gky1022

Patel, R. S., Vasava, A. M., and Rajput, K. S. (2018). Morphological and molecular evidence for the occurrence of *Itajahya galericulata* (Basidiomycota, Phallales) in India. *Plant Fungal Syst.* 63, 39–44. doi: 10.2478/pfs-2018-0006

Pegler, D. N., and Gomez, L. D. (1994). An unusual member of the cage fungus family. *Mycologist* 8, 54–59. doi: 10.1016/s0269-915x(09)80124-9

Phillips, E., Gillett-Kaufman, J. L., and Smith, M. E. (2018). Stinkhorn mushrooms (Agaricomycetes: Phallales: Phallaceae). *EDIS* 2018, 1–5. doi: 10.32473/edis-pp345-2018

Pietras, M., Rudawska, M., Iszkuło, G., Kujawa, A., and Leski, T. (2016). Distribution and molecular characterization of an alien fungus, *Clathrus archeri*, in Poland. *Polish J. Environ. Stud.* 25, 1197–1204. doi: 10.15244/pjoes/61230

Pine, E. M., Hibbett, D. S., and Donoghue, M. J. (1999). Phylogenetic relationships of cantharelloid and clavarioid Homobasidiomycetes based on mitochondrial and nuclear rDNA sequences. *Mycologia* 91, 944–963. doi: 10.2307/3761626

Põlme, S., Abarenkov, K., Henrik Nilsson, R., Lindahl, B. D., Clemmensen, K. E., Kauserud, H., et al. (2021). FungalTraits: a user-friendly traits database of fungi

and fungus-like stramenopiles. *Fungal Divers.* 105, 1–16. doi: 10.1007/s13225-020-00466-2

Ronquist, F., Teslenko, M., Van Der Mark, P., Ayres, D. L., Darling, A., Höhna, S., et al. (2012). MrBayes 3.2: Efficient bayesian phylogenetic inference and model choice across a large model space. *Syst. Biol.* 61, 539–542. doi: 10.1093/sysbio/sys029

Sanshi, I., and Kawamura, A. (1958). On the japanese species of *Protubera*. *Sci. reports Yokohama Natl. Univ. Sect. II Biol. Geol. Sci.* 7, 1–6.

Sato, H., Tsujino, R., Kurita, K., Yokoyama, K., and Agata, K. (2012). Modelling the global distribution of fungal species: New insights into microbial cosmopolitanism. *Mol. Ecol.* 21, 5599–5612. doi: 10.1111/mec.12053

Schoch, C. L., Ciufo, S., Domrachev, M., Hotton, C. L., Kannan, S., Khovanskaya, R., et al. (2020). NCBI Taxonomy: A comprehensive update on curation, resources and tools. *Database* 2020:baaa062. doi: 10.1093/database/baaa062

Skaltsas, D. N., Badotti, F., Vaz, A. B. M., da Silva, F. F., Gazis, R., Wurdack, K., et al. (2019). Exploration of stem endophytic communities revealed developmental stage as one of the drivers of fungal endophytic community assemblages in two Amazonian hardwood genera. *Sci. Rep.* 9:12685. doi: 10.1038/s41598-019-48943-2

Stamatakis, A. (2006). RAxML-VI-HPC: Maximum likelihood-based phylogenetic analyses with thousands of taxa and mixed models. *Bioinformatics* 22, 2688–2690. doi: 10.1093/bioinformatics/btl446

Sulzbacher, M. A., Grebenc, T., Cabral, T. S., Giachini, A. J., Goto, B. T., Smith, M. E., et al. (2016). *Restingomyces*, a new sequestrate genus from the Brazilian Atlantic rainforest that is phylogenetically related to early-diverging taxa in Trappeaceae (Phallales). *Mycologia* 108, 954–966. doi: 10.3852/15-265

Tedersoo, L., Bahram, M., Põlme, S., Kõljalg, U., Yorou, N. S., Wijesundera, R., et al. (2014). Global diversity and geography of soil fungi. *Science* 346:1256688. doi: 10.1126/science.1256688

Trierveiler-Pereira, L., da Silveira, R. M. B., and Hosaka, K. (2014a). Multigene phylogeny of the *Phallales* (*Phallomycetidae, Agaricomycetes*) focusing on some previously unrepresented genera. *Mycologia* 106, 904–911. doi: 10.3852/13-188

Trierveiler-Pereira, L., Meijer, A. A. R., Hosaka, K., and Silveira, R. M. B. (2014b). Updates on *Protubera* (Protophallaceae, Phallales) and additional notes on *P. maracuja*. *Mycoscience* 55, 35–42. doi: 10.1016/j.myc.2013.05.001

UNITE BLAST (2020). *UNITE BLAST*. Available Online at: https://unite.ut.ee/analysis.php (accessed September 1, 2020).

Vu, D., Groenewald, M., de Vries, M., Gehrmann, T., Stielow, B., Eberhardt, U., et al. (2019). Large-scale generation and analysis of filamentous fungal DNA barcodes boosts coverage for kingdom fungi and reveals thresholds for fungal species and higher taxon delimitation. *Stud. Mycol.* 92, 135–154. doi: 10.1016/j.simyco.2018.05.001

Wijayawardene, N. N., Hyde, K. D., Al-Ani, L. K. T., Tedersoo, L., Haelewaters, D., Rajeshkumar, K. C., et al. (2020). Outline of *Fungi* and fungus-like taxa. *Mycosphere* 11, 1060–1456. doi: 10.5943/mycosphere/11/1/8

Zeller, S. M. (1939). New and noteworthy Gasteromycetes. *Mycologia* 31, 1–32. doi: 10.2307/3754429

Zeller, S. M. (1948). Notes on certain Gasteromycetes, including two new orders. *Mycologia* 40, 639–668. doi: 10.2307/3755316

Conflict of Interest: The authors declare that the research was conducted in the absence of any commercial or financial relationships that could be construed as a potential conflict of interest.

Copyright © 2021 Melanda, Silva-Filho, Lenz, Menolli, Lima, Ferreira, Assis, Cabral, Martín and Baseia. This is an open-access article distributed under the terms of the Creative Commons Attribution License (CC BY). The use, distribution or reproduction in other forums is permitted, provided the original author(s) and the copyright owner(s) are credited and that the original publication in this journal is cited, in accordance with accepted academic practice. No use, distribution or reproduction is permitted which does not comply with these terms.

Advantages of publishing in Frontiers

OPEN ACCESS
Articles are free to read for greatest visibility and readership

FAST PUBLICATION
Around 90 days from submission to decision

HIGH QUALITY PEER-REVIEW
Rigorous, collaborative, and constructive peer-review

TRANSPARENT PEER-REVIEW
Editors and reviewers acknowledged by name on published articles

Frontiers
Avenue du Tribunal-Fédéral 34
1005 Lausanne | Switzerland

Visit us: www.frontiersin.org
Contact us: frontiersin.org/about/contact

REPRODUCIBILITY OF RESEARCH
Support open data and methods to enhance research reproducibility

DIGITAL PUBLISHING
Articles designed for optimal readership across devices

FOLLOW US
@frontiersin

IMPACT METRICS
Advanced article metrics track visibility across digital media

EXTENSIVE PROMOTION
Marketing and promotion of impactful research

LOOP RESEARCH NETWORK
Our network increases your article's readership